A conductometric method for measuring the diffusion coefficients of water in polymer films

P. A. SEWELL AND G. SKIRROW

A method is described in which electrical conductance is used to follow the transient state uptake of water by a polymer film. Since it lends itself readily to automatic monitoring, the method is suited to the study of diffusion processes which attain equilibrium rapidly. Diffusion coefficients obtained by the method for the transport of water in films of a modified cellulose between 70 and 120°C are compared with the corresponding values obtained by conventional (including steady state) methods.

MOST methods for the determination of diffusion coefficients of vapours in polymer films are usually based on either steady state or transient state measurements. In steady state measurements, a fixed vapour pressure differential is maintained across a film of known thickness and the steady state flux determined. Suitable combination of the observations with information obtained from the sorption isotherm enables the diffusion coefficient to be obtained[1, 2]. This method is unsuitable if the film suffers from cracks or pin-holes, and it is time consuming and tedious if the diffusion coefficient is low. In the transient state method, the normal practice is to suspend a film from a microbalance and to observe the rate of uptake by the film (or loss from the film) subsequent to a change of the ambient pressure of vapour. Unless a recording balance is used difficulties may be encountered when the rate of attainment of equilibrium is very rapid, and if the uptake of vapour by the film is small, it is necessary to use either a sensitive balance or a large sample.

The uptake of water by certain polymers is accompanied by a change in the electrical conductance[3]. This property can be used to provide a means of continuously following the uptake during transient experiments and, therefore, of obtaining values for the diffusion coefficient. This paper outlines a simple experimental approach and examines some results obtained for the diffusion of water in a modified cellulose.

EXPERIMENTAL

The measurements described here were restricted to a cellulose film of thickness 0·02 mm containing 4% hydroxyethyl cellulose supplied by British Cellophane Ltd. Glycerol used during manufacture as a plasticizer was removed by soaking the film in distilled water.

The conductometric apparatus is shown in *Figure 1*. The cell (A), immersed in a thermostat, contained a strip of the sample, B, (approximately 7·0 mm wide × 15·0 mm long) clamped between polished brass plate electrodes held in position by tungsten leads. These leads were connected to an
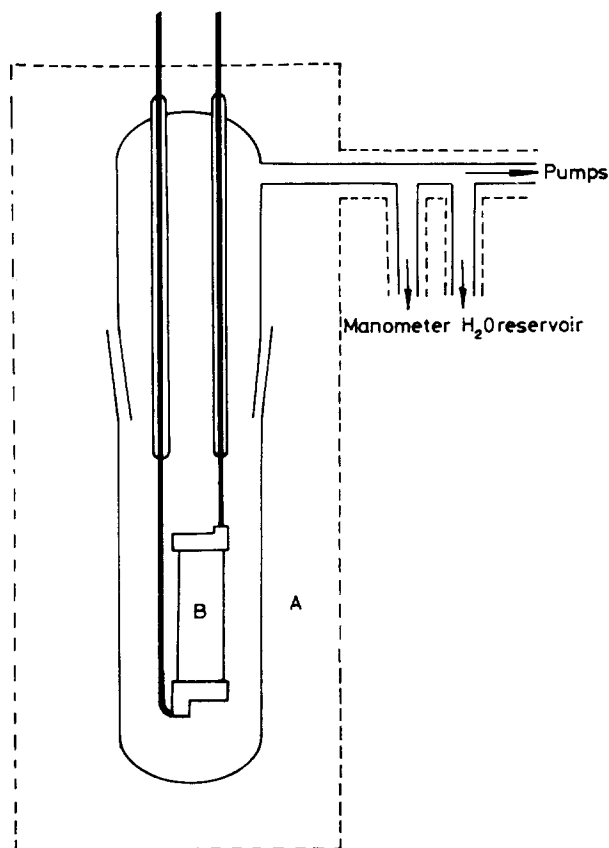
Figure 1. The conduction apparatus

impedance converter circuit, the output of which was fed to a potentiometric recorder. Water vapour was introduced to the degassed film from the reservoir, and changes in conductance with time, and the final equilibrium conductance obtained from the recorder plot. Absolute values of the conductance or specific conductance were not necessary for the present work, and in this account the conductance, σ, is given in units of recorder deflection when a 120 V D.C. potential was applied to the electrodes.

In order that the conductance could be related to the concentration of water in the film, separate experiments using a volumetric method were undertaken to determine the isotherms for water sorption. In this method a known amount of water vapour was brought into contact with a polymer film situated in a tube of known volume and temperature and the volume of water remaining in the vapour phase at equilibrium was accurately measured for different ambient pressures of vapour.

Gravimetrically determined diffusion coefficients were obtained in the conventional way using a spiral spring balance. Steady state determinations of the differential diffusion coefficients, D, were made by introducing a known pressure of water vapour to one side of a previously degassed film (area

3

approximately 3 cm²) cemented to a small glass funnel, the other side being continuously pumped. When the steady state was attained, the flux of water was determined by trapping the effluent vapour for a known time in a section cooled by liquid nitrogen. This water was distilled into a bulb of known volume and its pressure measured at 100°C.

RESULTS AND DISCUSSION

The results of a volumetric method for the determination of these isotherms are shown in *Figure 2*.
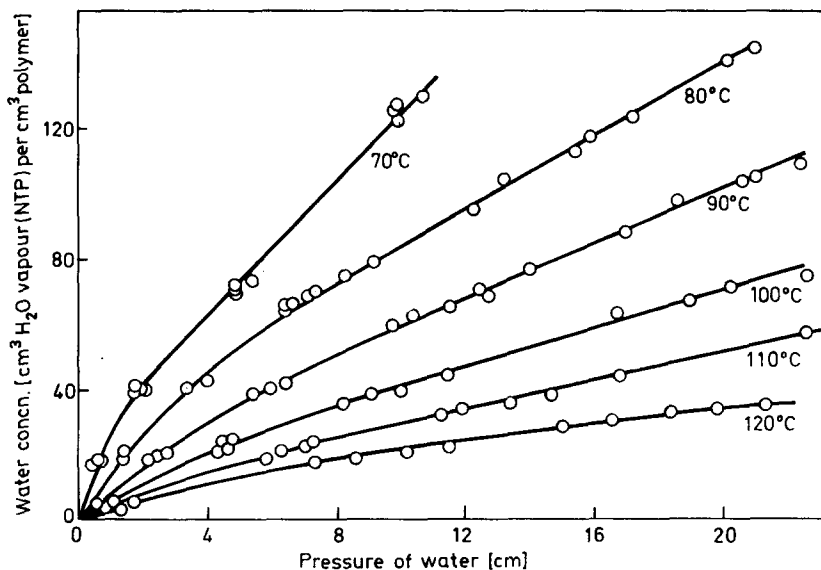

Figure 2. Sorption isotherms for water in modified cellulose

We are not going to discuss these equilibrium measurements in detail but, the following points may be briefly made. None of the isotherms were taken to saturation, but over the range of solute concentrations used, no hysteresis was detected, although isotherms determined over a greater range of humidities using a gravimetric method did show the hysteresis loop typical of water–cellulose systems. The isotherm shapes are characteristic of systems showing fairly pronounced penetrant–polymer interaction, and the partial molar enthalpies of mixing ($ca - 3$ kcal mole^{-1}) became less exothermic as the concentration increased.

The relationship between the conductance and the water concentration (c) (*Figure 3*) is given by

$$\sigma = \sigma' \exp (bc) \tag{1}$$

and that between conductance and temperature (*Figure 4*) by

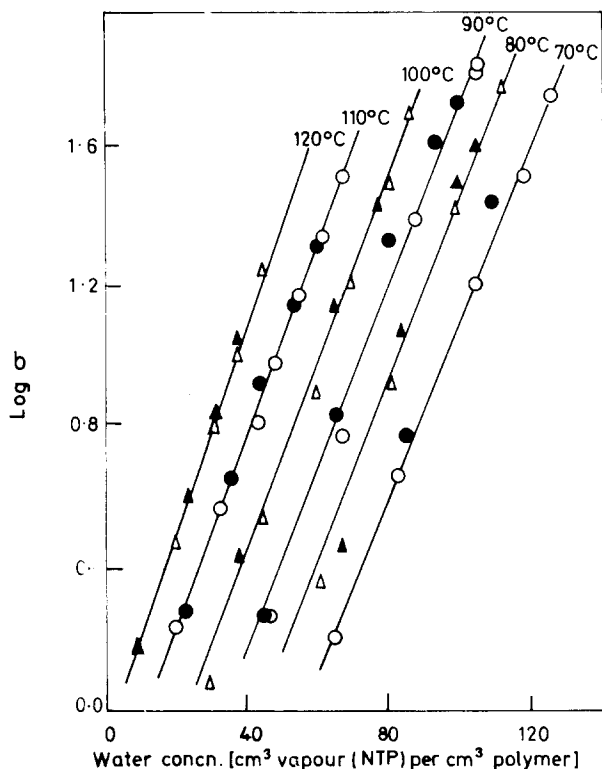$$\sigma = \sigma_0 \exp (- E_c/R\, T) \tag{2}$$

4

Figure 3. Equilibrium conductance measurements
○, △, sorption results; ●, ▲, desorption results.

where E_c is the energy of activation for conductance–approximately 20 kcal mole^{-1}. For equilibrium water uptake the conductance at fixed water vapour pressures was time-independent. Separate experiments showed that the conduction process obeyed Ohm's law, and that the conductance of the dry polymer was negligible compared with that observed when water was present.

Figure 5 shows conductance-time plots for large and for small pressure increments. Although, apart from a small perturbation at the start of the small incremental dose curve, this curve is apparently Fickian over most of its course, the curve corresponding to the large dose shows a marked anomolous early section. For this reason, most of the results described here were obtained by using small incremental doses.

The observed conductance at any time in a transient state experiment (σ_t) is given by

$$\sigma_t = (1/l) \int_0^l \sigma \, dx \tag{3}$$

where l is the thickness of the film.

However, because of the exponential relationship between conductance and concentration, the observed conductance depends not only on the amount of water taken up, but also on its distribution in the polymer. For
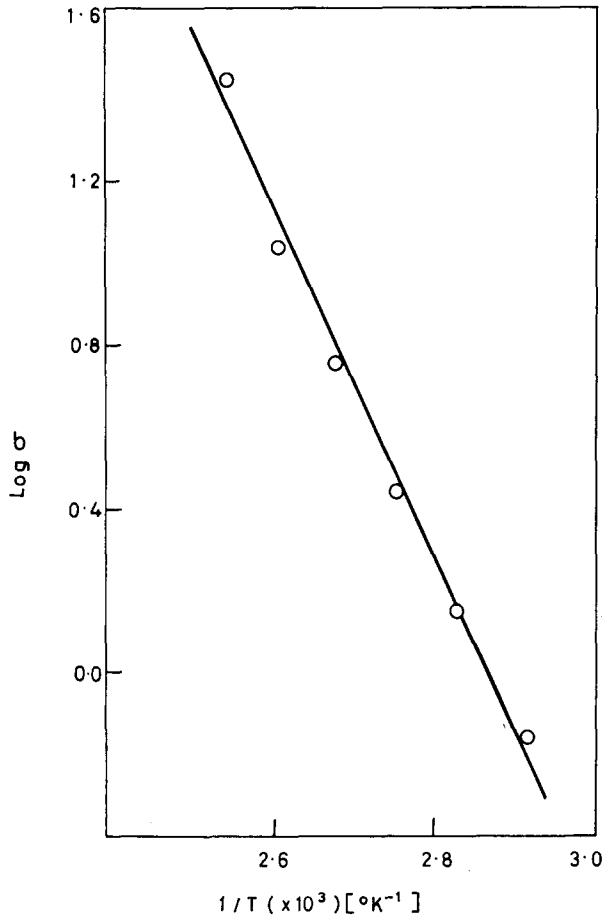
5

Figure 4. Activition plot for conduction (water concn. 50 cm², NTP, per cm³ dry polymer)

small concentration increments, a linear relationship can be assumed to hold between conductance and concentration over the concentration range of the increment i.e.

$$\sigma = mc + a \qquad (4)$$

where m and a are constants for the particular increments, and for a small incremental change the diffusion coefficient can be obtained by making use of equations analogous to those used in mass-time studies, namely

$$(\sigma_\infty - \sigma_t)/(\sigma_\infty - \sigma_i) = (8/\pi^2) \exp(-\pi^2 Dt/l^2) \qquad (5)$$

or

$$(\sigma_t - \sigma_i)/(\sigma_\infty - \sigma_i) = (16Dt/\pi l^2)^{\frac{1}{2}} \qquad (6)$$

where σ_i and σ_∞, are respectively the initial and final conductances and σ_t is the conductance at time t.
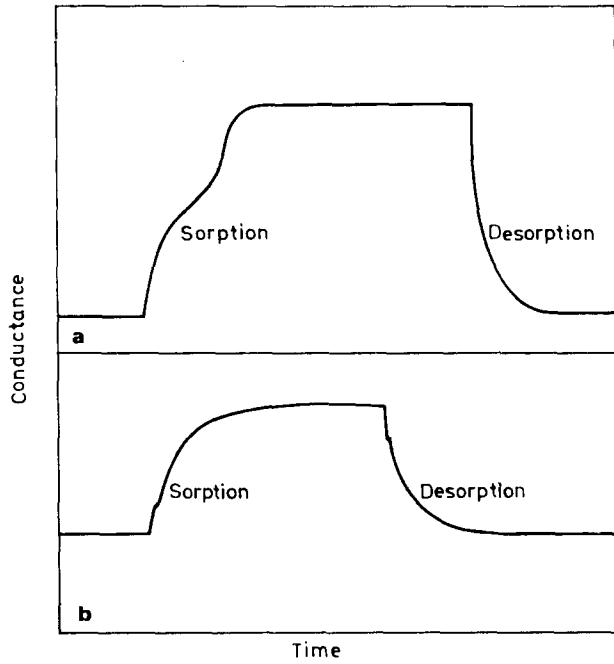
6

Figure 5. Change in conductance with time during transient state diffusion: (a), large increment; (b) small increment (Observed conductance in arbitrary units).
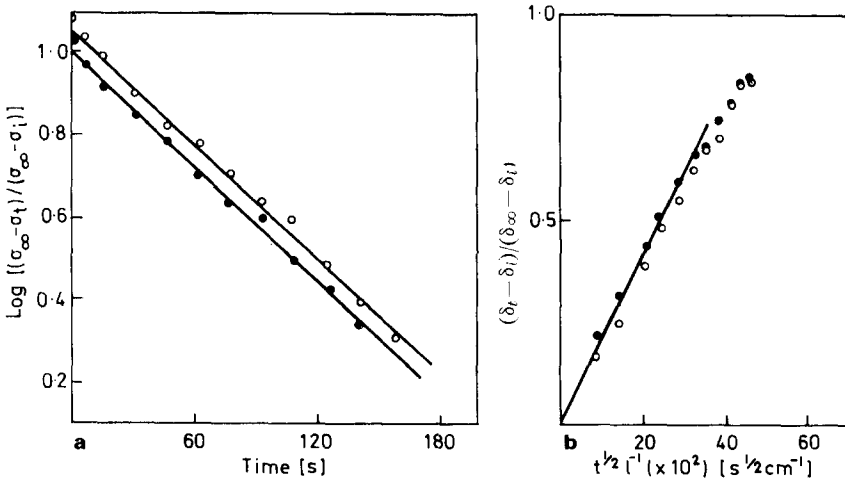

Figure 6. Sorption and desorption of water by modified cellulose ○, sorption; ●, desorption

Figures 6a and *6b* show typical plots from which diffusion coefficients were calculated. Since the diffusion coefficients are concentration dependent, coefficients derived by the above procedures were average or integral diffusion coefficients ($\bar{D}$). The concentration intervals of the experiments are small, however, and the diffusion coefficients may be assumed to be constant over each of these increments, and may be related to the mean concentration of the increment. The differential diffusion coefficient (D) was taken as the mean of values derived from sorption and desorption experiments over the same concentration increment: Diffusion coefficients were also calculated by a half-time procedure according to the equation

$$D = (0.049 l^2/2)(1/t_{S/2} + 1/t_{D/2}) \tag{7}$$

where $t_{S/2}$ and $t_{D/2}$ are the half-times for sorption and desorption respectively. Reasonable agreement was obtained between diffusion coefficients calculated from equations (5), (6) and (7). The results shown in *Figure 7*, which illustrates the exponential relationship between the diffusion coefficients and concentration, have been calculated by the half-time method.

From mass-time reverting sorption experiments (i.e. gravimetric sorption experiments commencing from the fully outgassed film but involving different concentration increments) at the lower end of the temperature range shown in *Figure 7*, integral diffusion coefficients were calculated using the equation

$$M_t/M_\infty = (16Dt/\pi l^2)^{\frac{1}{2}} \tag{8}$$
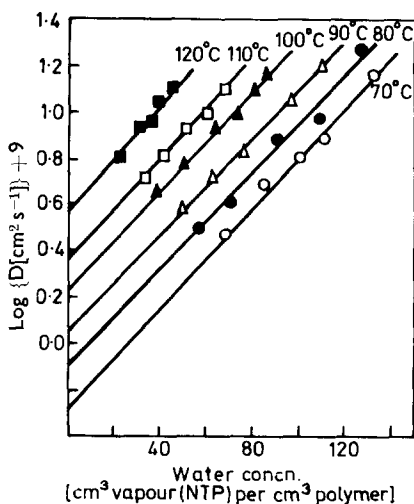
Figure 7. Concentration dependence of the diffusion coefficient
$\bigcirc$, 70°C; $\triangle$, 90°C; $\square$, 100°C;
$\bullet$, 80°C; $\blacktriangle$, 100°C; $\blacksquare$, 120°C.

Figure 8. Comparison of diffusion coefficients derived from steady state, conductance and gravimetric experiments at 80°C
$\Diamond$, conductance method; $\triangle$, gravimetric method; $\bigcirc$, steady state method

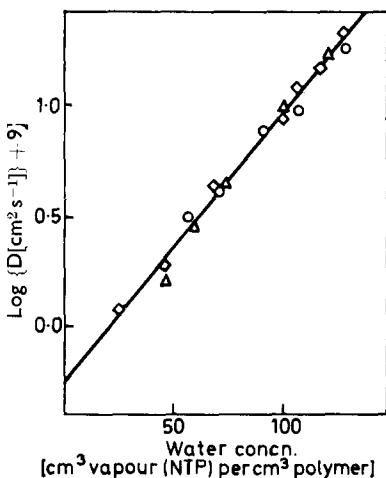where M_t and M_∞ are the changes in mass up to time t and infinity respectively. Differential diffusion coefficients were calculated from the intgeral diffusion coefficients by means of the approximation

$$\bar{D} = (1/c_0) \int_0^{c_0} \mathscr{D} \, dc \qquad (9)$$

where c_0 is the final uniform concentration of penetrant in the film. Thus, for the boundary conditions

$$c = 0, \ 0 < x < l, \ t = 0 \qquad (10)$$
$$c = c_0, \ x = 0, \ x = 1, \ t > 0$$

Equation (9) can be differentiated to give

$$D_{c_0} = \bar{D}_{c_0} [1 + c_0(d \ln \bar{D}_{c_0}/dc_0)] \qquad (11)$$

Since the plots of $\ln D_{c_0}$ *versus* c_0 are linear, values of D_{c_0} are readily derived. Diffusion coefficients at 80°C derived from steady state, conductance–time and mass–time experiments are compared in *Figure 8* where it can be seen that there is reasonable agreement between the methods.

Finally, some brief comments on the shape of the large increment sorption–time curves and on the conduction process can be made. The cause of the inflection in the conduction plot is not clear, although superficially the curve resembles the mass–time sorption curve of systems showing two-stage effects[4]. Two-stage effects in the water–regenerated cellulose system have been observed by Newns[5], although his experiments were made at temperatures around 15°C compared with 70°C in this work. The agreement shown here between diffusion coefficients determined by small increment conduction–time and mass–time as well as with steady state measurements and the additional observation that inflections shown by conduction–time plots are not evident on mass–time plots implies that two stage effects are not important in the present work. Possibly the effect is connected with the surface temperature changes which will be particularly noticeable when large doses of water are added to, or withdrawn from, the film. The relatively large activation energy for conduction compared with that for diffusion would make the perturbing effect on conduction–time plots more noticeable than that on mass–time plots. An experiment using a strip of film in the form of a hollow cylinder with thermocouple junctions inside and outside the cylinder showed qualitatively a distinct temperature rise inside the cylinder during sorption and a fall during desorption.

Although it has been suggested that the conduction processes for water in related polymers is electronic, it seems more likely that in the present system it is ionic. Presumably ionization of the sorbed water occurs, and protons migrate down the electrical potential gradient.

This migration is essentially a diffusion process, but the energy of activation associated with it will differ somewhat from that for the diffusional uptake of water since the ionic sizes will differ from the effective molecular size of water, the interactions between the ions and the polymer polar sites are likely to be stronger than those shown by water, and the orientation of the polymer chains will be different in the direction of electrical migration than

in the direction of diffusional water uptake. Furthermore the effective energy of activation for conduction involves not only the activation energy for diffusional migration of the ions but also the enthalpy or ionization of the sorbed water. Consequently, it is not surprising to find the activation energy for conduction (20 kcal mole^{-1}) considerably greater than that for the diffusional uptake (*ca* 11 kcal mole^{-1}).

ACKNOWLEDGEMENT

Donnan Laboratories,
University of Liverpool   *(Received 3 October 1969)*

REFERENCES

1 Crank, J., 'The Mathematics of Diffusion', Oxford Univ. Press, 1956
2 Meares, P. *J. Polym. Sci.* 1958, **27**, 391
3 Hearle, J. W. S. 'Moisture in Textiles' (Eds. J. W. S. Hearle, and R. H. Peters), Butterworths, London, 1960
4 Bagley, E , and Lond, F. A. *J. Amer. Chem. Soc.* 1955, **77**, 2172
5 Newns, A. C. *J. Polym. Sci.*, 1959, **41**, 425

The crystallization of fractions of partially isotactic poly(propylene oxide)

C. BOOTH, D. V. DODGSON and I. H. HILLIER

The crystallization kinetics of fractions of poly(propylene oxide) have been studied dilatometrically and microscopically. The dilatometric results have been successfully analyzed in terms of a model involving an increase in density within the outlines of the spherulites growing with a constant radial rate. Nucleation theory has been adapted to take account of the stereoregular nature of the polymer, and the rate constants from both techniques have been analyzed using values of the thermodynamic melting point and number average isotactic sequence lengths obtained from melting point data for the polymer.

STUDIES of the isothermal crystallization kinetics in bulk polymers are capable in principle of yielding information on the mechanism of crystallization, and its correlation with polymer morphology and the molecular structure of the polymer[1]. Dilatometric data are usually interpreted in terms of the growth of macroscopic entities of particular geometry, and yield rate constants, the temperature dependence of which is interpreted using classical nucleation theory. Because these rate constants may depend upon the particular model used to interpret the dilatometric data, independent measurements of the growth rate of the crystalline entities (spherulites) (usually by optical microscopy) allow a more unequivocal interpretation of their temperature dependence. Analyses of dilatometric data for a number of polymers have shown that the Avrami equation[2] with an exponent of 3 or 4, corresponding to the growth of spherulites, is rarely adhered to; this has led [3-6] to explanations of the deviations in terms of phenomenological theories involving secondary crystallization. The nature of this is discussed in terms of mechanisms such as the thickening of lamellar crystals[7], or the crystallization of interfibrillar low molecular weight, or other less readily crystallizable material[8].

The temperature dependence of the crystallization rate constants, used to obtain estimates of the interfacial free energies in the nucleation process, is most commonly analyzed using equations which are strictly applicable only to homopolymers of infinite molecular weight. A more complete analysis of the data requires a consideration of the finite molecular weights, the molecular weight distribution, and, in the case of copolymers, the finite lengths and distribution of lengths of the crystallizable sequences. Therefore to fully interpret dilatometric and microscopic data it is necessary to use well characterised polymers. To this end we have studied the crystallization of fractions of partially isotactic poly(propylene oxide).

The preparation of these fractions has already been described in detail[9]. Briefly, poly(propylene oxide) was prepared[10] using the zinc diethyl and water catalyst and fractionated[11] by precipitation from dilute solution in iso-octane to yield fractions having identical wide molecular weight distributions but with differing degrees of isotacticity.

The pertinent characteristics of the fractions are given in *Table 1*. The number-average degrees of polymerization (x_n) are obtained from the

Table 1 The characteristics of fractions of poly(propylene oxide)

Fraction	Weight %	x_n ($\times 10^{-3}$)	y_n	X
F1	6·4	5	55	0·98
F2	3·8	5	22	0·95
F3	2·5	5	15	0·93

viscosity-average molecular weights and distribution widths reported earlier[9]. The number-average isotactic sequence lengths (y_n) and the thermodynamic melting point of isotactic poly(propylene oxide) ($T_m{}^0 = 82°C$) are obtained from an analysis of the multiple melting transitions found in these fractions[9]. The mole fractions of isotactic diads (X) are calculated by assuming a random distribution of non-isotactic diads along the polymer chain. The true values of X cannot exceed these estimates, and our own and other[12] estimates of X by n.m.r. spectroscopy show that $X > 0.9$.

EXPERIMENTAL

Glass dilatometers were used. Small samples (< 100 mg), moulded in high vacuum, were placed in the dilatometers, outgassed and finally confined with mercury. The dilatometers were immersed in boiling water for 15 to 30 min and then quickly transferred to a thermostat ($\pm$ 0·01 °C). Thermal equilibrium was established within 2 min. The contraction (~ 40 mm) was followed by means of a cathetometer ($\pm$ 0·04 mm).

Spherulite growth rates were measured on a hot stage[13] of a polarizing microscope. Thin films of the sample on a microscope slide were heated to 120°C for 2 to 5 min and then quickly transferred to the hot stage which was kept at a constant temperature ($\pm$ 0·02°C) by a proportional controller. Melting at 100°C resulted in a high density of nuclei with consequent difficulty in the resolution of individual spherulites. Spherulite sizes were recorded photographically.

ANALYSIS OF RESULTS

Dilatometric data

The dilatometric data have been analyzed by means of the Avrami equation[2]

$$\frac{h_0 - h_t}{h_0 - h_\infty} = \frac{\chi(t)}{\chi(\infty)} = [1 - \exp(-zt^n)] \tag{1}$$

where h_t is the dilatometer meniscus height at time t, $\chi(t)$ the degree of crystallinity, and z and n the Avrami rate constant and exponent respectively. A value of $n = 3$ or 4 corresponds to the constant radial growth of instantaneously or sporadically nucleated spherulites growing with a constant density. The results of least squares computer fitting of equation (1) with

Table 2 Comparison of Avrami equation with crystallization isotherms

Fraction	Temperature (°C)	z	n	Standard deviation (%)
F1	46·0	$2·54 \times 10^{-3}$	2·0	5·9
	48·4	$3·29 \times 10^{-4}$	2·1	4·5
	50·1	$3·82 \times 10^{-5}$	2·3	4·1
	52·4	$3·44 \times 10^{-5}$	2·0	4·8
	55·0	$4·56 \times 10^{-7}$	2·4	3·8
F2	40·1	$7·39 \times 10^{-4}$	2·1	4·0
	43·8	$7·86 \times 10^{-5}$	2·2	3·6
	46·4	$3·44 \times 10^{-5}$	2·0	4·5
	49·9	$3·20 \times 10^{-6}$	2·0	3·7
	52·4	$6·78 \times 10^{-7}$	2·0	3·2
	54·8	$1·34 \times 10^{-7}$	2·0	4·7
F3	40·2	$3·30 \times 10^{-5}$	2·4	4·4
	42·7	$1·85 \times 10^{-6}$	2·6	3·5
	44·0	$2·16 \times 10^{-5}$	2·0	5·3
	45·4	$6·20 \times 10^{-6}$	2·0	4·7
	50·8	$1·46 \times 10^{-7}$	2·0	5·0

adjustable parameters n and z are given in Table 2. Theory and experiment are further compared in Figure 1.

Examination of the fit obtained reveals that the major contributions to the large standard deviation shown in Table 2 occurs towards the end of the crystallization, with approximately the first 60% of each isotherm being well fitted by the Avrami equation with an exponent of 3 (Figure 1). Furthermore, in our samples of poly(propylene oxide) we observe spherulites growing
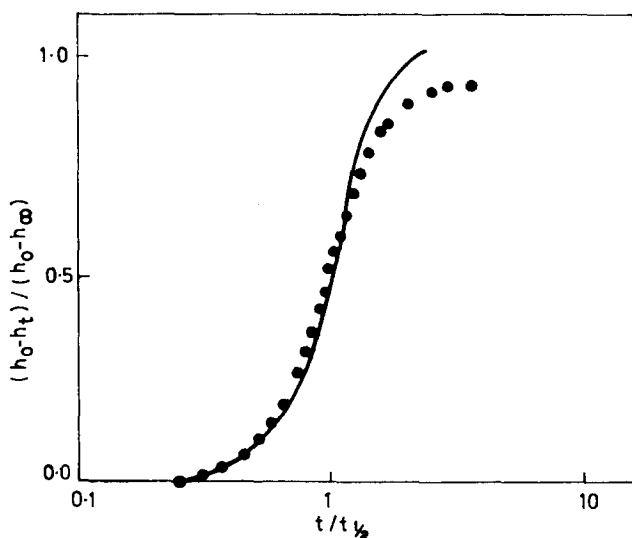

Figure 1 Crystallization isotherm for sample F2 at 43·8°C. The curve is calculated from equation (1) with n = 3.

13

with a constant radial rate. These considerations indicate that the large deviations from the Avrami equation, and the low exponent values, arise from an increasing density of the growing spherulites similar to that found experimentally for polypropylene[4]. To take account phenomenologically of this density increase we have assumed, as in previous analyses[3], that this secondary crystallization can be described by a first order process which leads to the equation

$$\frac{h_0 - h_t}{h_0 - h_\infty} = \frac{\chi(t)}{\chi(\infty)} = \frac{\chi(a, \infty)}{\chi(\infty)} \; [1 - \exp(- z_p t^3)]$$

$$+ \frac{\chi(s, \infty)}{\chi(\infty)} z_s \int_0^t \; [1 - \exp(- z_p \theta^3)] \exp[- z_s (t - \theta)] \; d\theta \quad (2)$$

where $\chi(a, \infty)$ and $\chi(s, \infty)$ are the degrees of crystallinity arising from the primary (Avrami) and secondary (first order) processes alone, the corresponding rate constants being z_p and z_s. The fit of our data to this equation is shown in *Table 3* and it can be seen that the inclusion of an additional

Table 3 Comparison of equation (2) with crystallization isotherms

Fraction	Temperature (°C)	z_p	z_s	Fraction of secondary crystallization	Standard deviation (%)
Fl	46·0	$2·17 \times 10^{-4}$	$7·08 \times 10^{-3}$	0·22	1·9
	48·4	$2·04 \times 10^{-5}$	$5·58 \times 10^{-3}$	0·21	0·9
	50·1	$3·28 \times 10^{-6}$	$3·30 \times 10^{-3}$	0·18	1·0
	52·4	$3·42 \times 10^{-7}$	$1·40 \times 10^{-3}$	0·19	1·0
	55·0	$1·81 \times 10^{-8}$	$4·45 \times 10^{-4}$	0·17	1·3
F2	40·1	$7·08 \times 10^{-5}$	$2·88 \times 10^{-2}$	0·32	1·2
	43·8	$3·75 \times 10^{-6}$	$9·47 \times 10^{-3}$	0·26	0·8
	46·4	$4·20 \times 10^{-7}$	$4·58 \times 10^{-3}$	0·29	0·8
	49·9	$1·67 \times 10^{-8}$	$1·20 \times 10^{-3}$	0·29	0·6
	52·4	$1·52 \times 10^{-9}$	$6·33 \times 10^{-4}$	0·32	0·9
	54·8	$9·41 \times 10^{-11}$	$2·44 \times 10^{-4}$	0·24	0·7
F3	40·2	$3·70 \times 10^{-6}$	$2·39 \times 10^{-3}$	0·19	1·1
	42·7	$3·64 \times 10^{-7}$	$4·87 \times 10^{-4}$	0·17	0·9
	44·0	$1·10 \times 10^{-7}$	$8·16 \times 10^{-4}$	0·19	0·8
	45·4	$2·62 \times 10^{-8}$	$3·78 \times 10^{-4}$	0·20	0·9
	50·8	$1·01 \times 10^{-10}$	$1·53 \times 10^{-4}$	0·24	0·9

parameter yields a much improved fit. This provides evidence that equation (2) is more appropriate than the simple Avrami picture of the crystallization process. We have also considered the possibility of a slow rate of formation of nuclei, as reported by Aggarwal *et al*[6]. The inclusion in the rate expression of this effect, with a first order rate constant for nucleus formation as an additional adjustable parameter, does not significantly improve the fit of

the data. We conclude that in our experiments the rate of nucleus formation is rapid compared with the rate of crystallization.

Microscopic data

The constant radial growth rates obtained for the three fractions of polymer are listed in *Table 4*. Analysis of the temperature dependence of the rate constants (*Tables 3* and *4*) follows the discussion of the effect of finite molecular weight, and partial isotacticity, on the nucleation of poly(propylene oxide).

Table 4 Spherulite growth rates

Fraction	Temperature (°C)	$(mm\ min^{-1} \times 10^3)$
F1	42·3	19·55
	46·3	7·95
	47·6	2·35
	51·0	1·0
F2	40·5	9·95
	42·3	6·25
	44·2	4·0
	46·3	4·4
F3	39·0	3·5
	40·5	2·4
	42·3	2·0
	44·2	1·1

NUCLEATION THEORY APPLIED TO PARTIALLY ISOTACTIC POLYMER

It is generally taken that at temperatures sufficiently far from the glass transition, the rate determining step in the linear spherulite growth rate is secondary nucleation. For such a model, the growth rate G is given[1] as

$$G = G_0 \exp\left(-\Delta F^*/RT\right) \tag{3}$$

where ΔF^* is the free energy of formation of a nucleus of critical dimensions. For a homopolymer of infinite molecular weight this is given by

$$\Delta F^* = 4\sigma_e\sigma_u/\Delta f_u \tag{4}$$

for a two-dimensional nucleus, and

$$\Delta F^* = 8\pi\sigma_e\sigma_u^2/\Delta f_u^2 \tag{5}$$

for a three-dimensional cylindrical nucleus[1]. Here σ_e and σ_u are the end and lateral interfacial free energies of the nucleus, and Δf_u is the free energy of fusion per chain unit, all energies being expressed in units of cal mole^{-1}.

For the polymer investigated here, equations (4) and (5) must be modified to take account of the finite molecular weights and lengths of the isotactic sequences. We consider a model for poly(propylene oxide) in which both the molecules and isotactic sequences vary in length according to the most probable distribution, with number-average degree of polymerization x_n and number-average isotactic sequence length y_n. For a homopolymer with a

15

most probable distribution, and degree of crystallinity $(1 - \lambda)$, the free energy of fusion ΔF_f at temperature T is given as[14]

$$\frac{\Delta F_f}{N x_n} = (1 - \lambda)\, \Delta f_u + RT \left\{ \frac{1}{x_n} \ln\lambda + \frac{(1 - \lambda)}{\zeta} \left[\ln D + (\zeta - 1) \ln p_x \right] \right\} \quad (6)$$

Here ζ is the length of the crystalline sequences, N the number of polymer molecules, and

$$\ln D = - 2\sigma_e / RT$$

$$p_x = [1 - (1/x_n)]$$

For a polymer with a most probable distribution of isotactic sequences an additional entropy term[14]

$$\Delta S = - R[(1 - \lambda)/\zeta] [\ln X + (\zeta - 1) \ln p_y] \quad (7)$$

must be included in equation (6). Here X is the mole fraction of isotactic diads and

$$p_y = [1 - (1/y_n)]$$

The free energy of formation of a cylindrical nucleus, ζ units long and ρ units in cross section becomes, using equations (6) and (7)

$$\Delta F = 2\pi^{\frac{1}{2}} \rho^{\frac{1}{2}} \zeta \sigma_u + 2\rho\sigma_e - \zeta\rho\Delta f_u$$

$$- RT \{N \ln[1 - (\rho\zeta/x_n N)] + \rho[\ln X + (\zeta - 1) \ln p_x p_y]\} \quad (8)$$

As x_n is large ($\sim 5\,000$) and y_n is of the order of 20 we may put $(1/x_n) \simeq 0$, and $\ln p_y \simeq - 1/y_n$. With these approximations, equation (8) becomes

$$\Delta F = 2\pi^{\frac{1}{2}} \rho^{\frac{1}{2}} \zeta \sigma_u + 2\rho\sigma_e - \zeta\rho\,\Delta f_u + RT\rho\,[(\zeta - 1)/y_n] - RT\rho \ln X \quad (9)$$

The dimensions ζ^*, ρ^*, of the critical nucleus may be obtained from equation (9) by setting

$$\left(\frac{\partial \Delta F}{\partial \rho} \right)_\zeta = 0 \text{ and } \left(\frac{\partial \Delta F}{\partial \zeta} \right)_\rho = 0$$

giving

$$\rho^{*\frac{1}{2}} = 2\pi^{\frac{1}{2}}\sigma_u/(\Delta f_u - RT/y_n) \quad (10)$$

$$\zeta^* = (4\sigma_e - 2RT\ln X - 2RT/y_n)/(\Delta f_u - RT/y_n) \quad (11)$$

and

$$\Delta F^* = \pi^{\frac{1}{2}}\rho^{*\frac{1}{2}}\zeta^*\sigma_u \quad (12)$$

For our polymer, X is near unity, and although a value of σ_e for poly-(propylene oxide) has not been reported, a value for poly(ethylene oxide) is $1\,500$ cal mole^{-1} [15] so that equation (11) may be approximated as

$$\zeta^* = 4\sigma_e/(\Delta f_u - RT/y_n)$$

giving

$$\Delta F^* = 8\pi\sigma_u^2\sigma_e/(\Delta f_u - RT/y_n)^2 \quad (13)$$

With the usual approximation

$$\Delta f_u = (T_m{}^0 - T)\Delta h_u/T_m{}^0 = \Delta T\Delta h_u/T_m{}^0$$

16

where $T_m{}^0$ is the thermodynamic melting point of the polymer and Δh_u the heat of fusion

$$\Delta F^* = 8\pi\sigma_u{}^2\sigma_e / \left(\frac{\Delta T \Delta h_u}{T_m{}^0} - \frac{RT}{y_n} \right)^2 \qquad (14)$$

For a two-dimensional nucleus, ζ units long and ρ sequences in breadth, a similar argument yields

$$\zeta^* = 2\sigma_e / (\Delta f_u - RT/y_n)$$

$$\rho^* = 2\sigma_u / (\Delta f_u - RT/y_n)$$

and

$$\Delta F^* = 4\sigma_u\sigma_e / \left(\frac{\Delta T \Delta h_u}{T_m{}^0} - \frac{RT}{y_n} \right) \qquad (15)$$

Thus, a plot of $\ln G$ vs $1/T \left(\frac{\Delta T \Delta h_u}{T_m{}^0} - \frac{RT}{y_n} \right)^m$

where $m = 1$ for two-dimensional and 2 for three-dimensional nucleation, should yield a single straight line for all three fractions if the pre-exponential factor in equation (3) remains unchanged.

In *Figure 2* we plot the rate constants (z_p and z_s) and the spherulite growth rates (G) in terms of the conventional two-dimensional nucleation theory
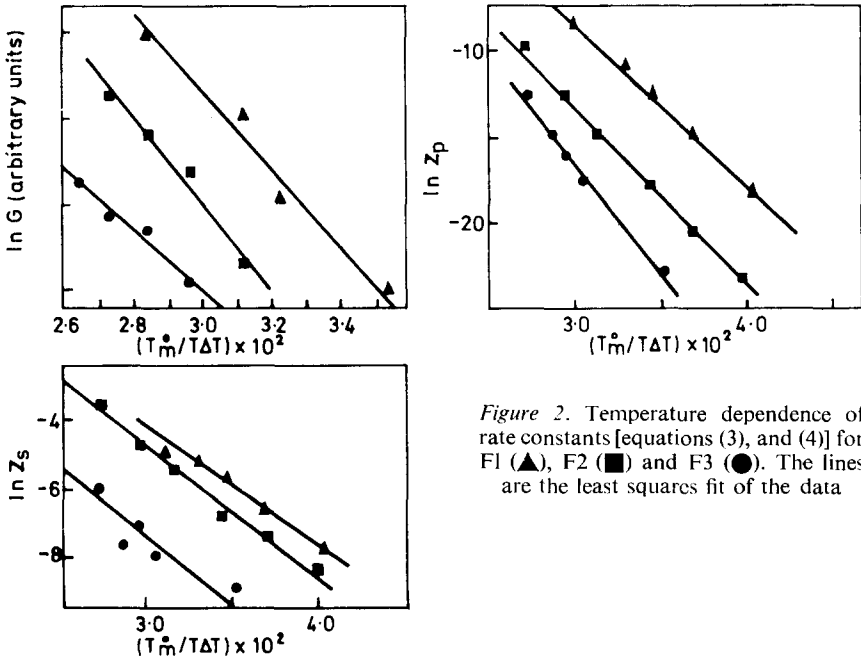
Figure 2. Temperature dependence of rate constants [equations (3), and (4)] for F1 (▲), F2 (■) and F3 (●). The lines are the least squares fit of the data

applicable to infinite molecular weight homopolymer [equations (3) and (4)]. For each fraction a distinct linear plot is obtained. In *Figures 3* and *4* the data are analyzed, with a value for Δh_u of 2 000 cals/mole[16], by means of the theory developed here [equations (3), (14) and (15)] to take account of the

17

variation in isotactic sequence lengths between the three fractions. Although the microscopic data are somewhat scattered, they can be satisfactorily represented for both two and three dimensional nucleation by single straight lines for all three fractions. A similar conclusion is reached for the rate constants obtained from the dilatometric data, although there is a tendency for the data for fraction F1 to be slightly displaced.
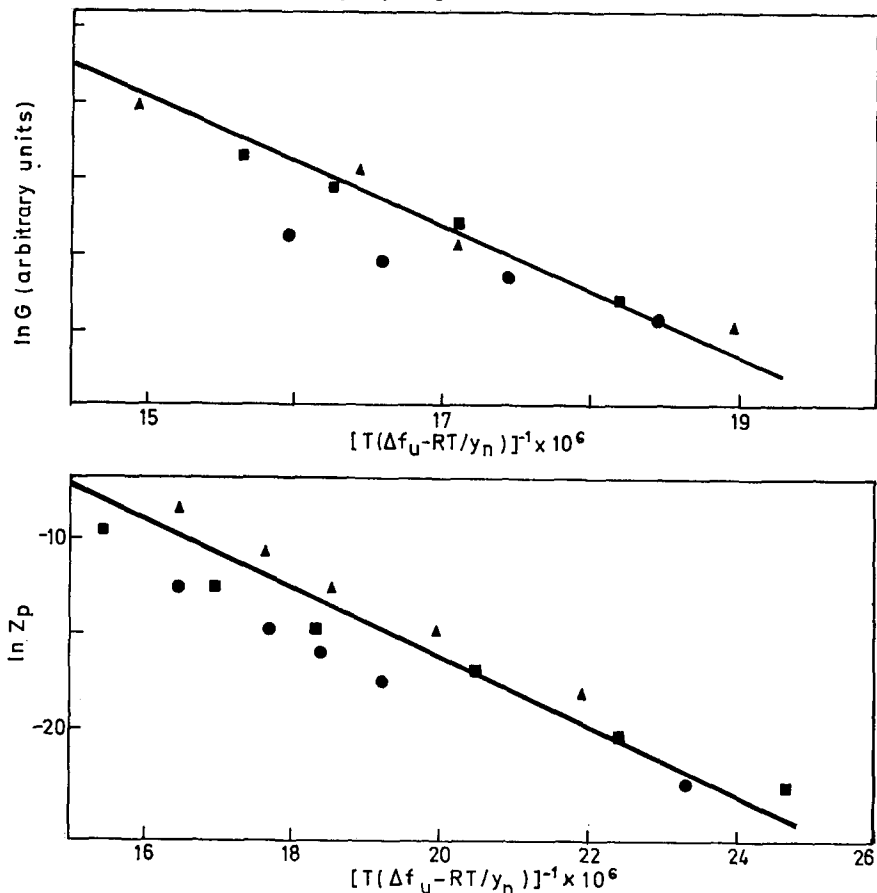

Figure 3 Temperature dependence of rate constants [equations (3), and (15)] for F1 (▲), F2 (■) and F3 (●)

DISCUSSION

The microscopic observations and the fit of the crystallization isotherms in the early stages by an Avrami equation with an exponent of 3 shows that crystallization proceeds by the constant radial growth of spherulites. The deviations from the Avrami description are postulated to be due to a slow increase in density (secondary crystallization) within the growing spherulites, which can be described by a first order process with rate constants given in *Table 3*. The extent of this secondary crystallization does not vary significantly with crystallization temperature or polymer fraction and accounts for 20 % of the total crystallinity developed.

18

The rate of secondary crystallization has a similar temperature dependence to the rate of primary crystallization indicating that it is controlled in rate by a similar nucleation act. A choice between the two explanations of the secondary crystallization – either a slow thickening of lamellae, or crystallization of interfibrillar (less isotactic) material – cannot be made from the results reported in this paper. However, we have reported elsewhere[9] that there is no significant change in the melting points of the fractions with increasing degree of crystallization. This suggests that the secondary crystallization is due to slow interfibrillar crystallization.

Table 5 Parameters for growth rates (units, cal and mole)

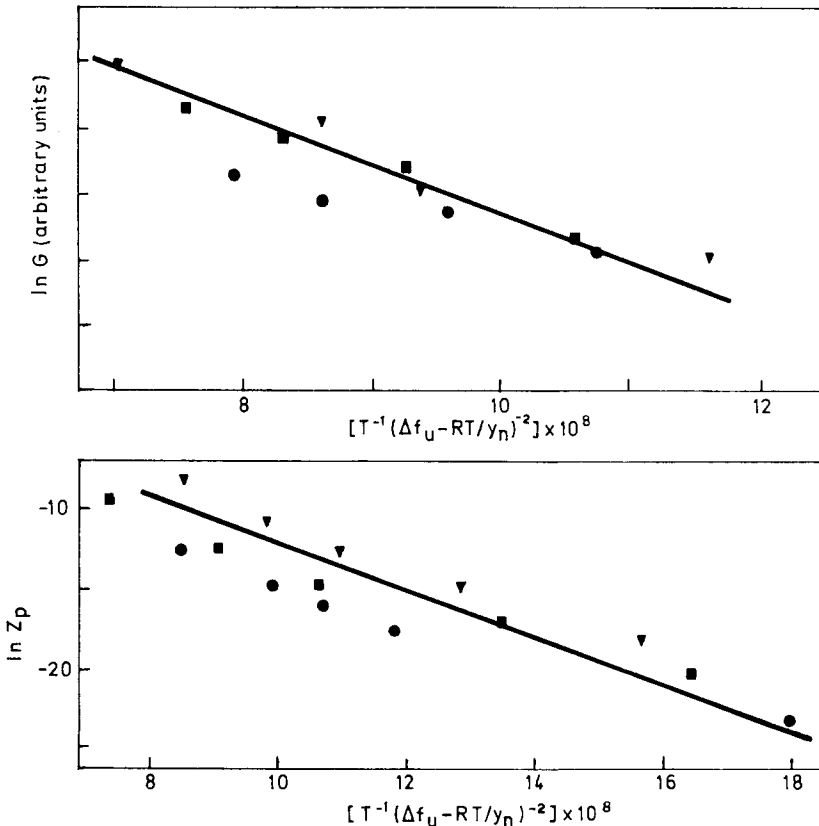|		$\sigma_e \sigma_u$	$\sigma_e \sigma_u^2$	σ_u
$\ln G \; vs \; 1/T \; \left(\dfrac{\Delta T \Delta h_u}{T_m^0} - \dfrac{RT}{y_n} \right)$	Microscopic	$3\cdot3 \times 10^5$		220
	Dilatometric	$2\cdot6 \times 10^5$		173
$\ln G \; vs \; 1/T \; \left(\dfrac{\Delta T \Delta h_u}{T_m^0} - \dfrac{RT}{y_n} \right)^2$	Microscopic		$4\cdot6 \times 10^6$	55
	Dilatometric		$3\cdot1 \times 10^6$	46

Figure 4 Temperature dependence of rate constants [equations (3), and (14)] for F1 (▼); F2 (■); and F3 (●)

The temperature dependence of the growth rates can be satisfactorily analyzed in terms of classical nucleation theory if account is taken of the length and distribution of isotactic sequences in the polymer. The values of the thermodynamic melting point of the isotactic polymer and the number-average isotactic sequence lengths of the partially isotactic fractions, obtained from melting data for the three fractions, thus provide a consistent set of parameters for the samples. In common with other workers we cannot distinguish between two and three dimensional nucleation from our data.

The parameters for growth rates from *Figures 3* and *4* are summarized in *Table 5*. The values are in agreement with the 'universal' parameters found by Mandelkern *et al*[17] from data for a number of polymers. The values for σ_u are calculated on the assumption that $\sigma_e = 1\ 500$ cal mole^{-1}. The value of σ_u for poly(propylene oxide) is unknown but, by comparison with the value for branched polyethylene[18], might be expected to lie in the range 100–200 cal mole^{-1}. The data thus suggest a two dimensional nucleation process. Our earlier analysis of the melting transitions in these fractions was based upon the predominance of three dimensional nucleation. This divergence between rate and melting data is not uncommon, and has been explained in terms of isothermal lamellar thickening[19] by a factor of two.

Department of Chemistry,
University of Manchester.

REFERENCES

1 Mandlekern, L., 'Crystallization of Polymers', McGraw Hill, 1964.
2 Avrami, M. *J. Chem. Phys.* 1939, 7, 1103; *J. Chem. Phys.*, 1940, **8**, 212; *J. Chem. Phys.* 1941, **9**, 177
3 Hillier, I. H., *J. Polym. Sci.*, (A) 1965, **3**, 3067
4 Hoshino, S., Meinecke. E., Powers, J., Stein R. S. and Newman S. *J. Polym. Sci.* (A) 1965, **3**, 3041
5 Price, F. P. *J. Polym. Sci.* (A) 1965, **3**, 3079
6 Aggarwal, S. L., Marker, L., Kollar, W. I. and Geroch, R., *J. Polym. Sci.* (A) 1966, **4**, 715
7 Fischer, E. W. and Schmidt, G. F., *Angew. Chem. (Int. Ed.)*, 1962, **1**, 448
8 Keith, H. D., *Kolloid Zeits.* 1969, **231**, 421
9 Booth, C., Devoy, C. J., Dodgson, D. V. and Hillier, I. H. *J. Polym. Sci.*, in press.
10 Booth, C., Higginson, W. C. E. and Powell, E., *Polymer, Lond.* 1964, **5**, 479
11 Allen G., Booth, C. and Jones, M. N., *Polymer, Lond.*, 1964, **5**, 257
12 Tani, H., Ogumi, N. and Watanabe, S. *J. Polym. Sci.* (B) 1968, **6**, 577
13 Hay, J. N. *J. Sci. Instrum.* 1964, **41**, 456
14 Flory, P. J. *J. Chem. Phys.* 1949, **17**, 223
15 Braun, W., Hellwege, K. H., and Knappe, W., *Kolloid Zeits.*, 1967, **215**, 10
16 Devoy, C. J., Ph.D. Thesis, University of Manchester, 1966
17 Mandelkern., K., Jain, N. L. and Kim, H., *J. Polym. Sci.*, (A), 1968, **6**, 165
18 Turnbull, D. and Cormia, R. L. *J. Chem. Phys.* 1961, **34**, 820
19 Hoffman, J. D. *SPE Trans.* 1964, **4**, number 4

The thermoelasticity of natural rubber in torsion

P. H. BOYCE and L. R. G. TRELOAR

Following a recent theoretical treatment of the thermoelasticity of rubber in torsion[1], an apparatus has been devised to measure the stress/temperature coefficients of elastomers in torsion.

The experiments carried out enable the temperature coefficient of the mean-square chain vector length $\overline{r_0^2}$ to be derived. For natural rubber a value for d ln $\overline{r_0^2}$/dT of 0·43 ± 0·05 × 10^{-3} deg^{-1} has been obtained; this compares favourably with values obtained by other workers from stress-temperature data for simple extension. No significant variation in this figure was obtained with variations of strain or crosslink density.

UP TO the present time most of the work that has been done on the thermo-elasticity of elastomers has been confined to the case of simple extension. On the basis of the Gaussian statistical theory, Flory[2] has derived the following relation for simple extension

$$f = (\nu k T / l_i) \, (\overline{r_i^2 / r_0^2}) \, (\alpha - \alpha^{-2}) \tag{1}$$

where f is the tensile force, ν is the total number of chains in the specimen, $l_i = V^{1/3}$, where V is the volume in the final strained state, α is the extension ratio referred to the length l_i, and k and T have their usual meaning. The mean-square vector length of network chains in the undistorted (isotropic) state of volume V is denoted by $\overline{r_i^2}$ whilst $\overline{r_0^2}$ is the mean-square chain vector length for the same set of chains in the absence of the constraints introduced by the crosslinks. A recent analysis by Treloar[1] for the case of the torsion of a rubber cylinder gives the corresponding relation

$$M = (\pi/2) \, (\nu k T / V_u) \, \overline{(r_i^2 / r_0^2)} \psi a_0^4 \tag{2}$$

In equation (2) M is the torsional couple, ψ is the torsion (expressed in radians per unit length of the strained axis), V_u is the volume in the unstrained (i.e. stress-free) state, a_0 is the unstrained radius and the remaining symbols have their previous meaning.

The stress/temperature coefficients at constant pressure can be found by differentiating equations (1) and (2), taking into account the changes in dimensions of the rubber with temperature. For simple extension the result obtained is[3]

$$[\partial \ln \, (f/T)/\partial T]_{p,l} = - \text{d} \ln \overline{r_0^2}/\text{d}T - \beta/(\alpha^3 - 1) \tag{3}$$

where β, the coefficient of volume expansion of the rubber, is $V^{-1}(\partial V/\partial T)_p$.

The corresponding relation in torsion[1] is*

$$[\partial \ln (M/T)/\partial T]_{p,l,\psi} = - \, \mathrm{d} \ln \overline{r_0^2}/\mathrm{d}T + \beta \tag{4}$$

which can be expressed in the alternative form

$$(\partial M/\partial T)_{p,l,\psi} = (M/T)(1 + \beta T - T \, \mathrm{d} \ln \overline{r_0^2}/\mathrm{d}\,T) \tag{4a}$$

In simple extension it is sometimes found convenient to express the internal energy component of the tensile stress at constant volume as f_{ev} which is defined as $(\partial E/\partial l)_{T,V}$. It can be shown[3] that

$$f_{ev}/f = - \, T[\partial \ln (f/T)/\partial T]_{V,l} = T \, \mathrm{d} \ln \overline{r_0^2}/\mathrm{d}\,T \tag{3a}$$

Similarly in the case of torsion we may introduce the quantity M_{ev}, representing the internal energy contribution to the couple at constant volume, given by

$$M_{ev}/M = - \, T[\partial \ln (M/T)/\partial T]_{V,l,\psi} = T \, \mathrm{d} \ln \overline{r_0^2}/\mathrm{d}\,T \tag{5}$$

The quantities M_{ev}/M and f_{ev}/f are thus seen to be strictly analogous.

By using equation (4a) in conjunction with equation (5) the relative contribution, M_{ev}/M, of the internal energy to the couple can be derived from stress–temperature experiments at constant pressure, and hence the quantity $\mathrm{d} \ln \overline{r_0^2}/\mathrm{d}\,T$ may be obtained. The aim of this work was to obtain a value of this quantity from torsional experiments on natural rubber, and to compare the value obtained with existing data for the case of simple extension.

EXPERIMENTAL

Materials

Natural rubber vulcanizates were made with various degrees of crosslinking by curing pale crêpe with 2·7–3·1 % by weight of dicumyl peroxide for 30–55 min at 140°C. Cylinders were moulded of approximately 185 mm length and 6·5 mm diameter. No treatment was given to extract any uncrosslinked material or excess vulcanizing reactants which might have been present.

Each cylinder was gripped at either end in a half-inch long cylindrical split clamp made from brass. Reference marks for the measurement of the axial extension ratio were made in ink on the surface of the cylinder. The length between the brass clamps, the diameter of the cylinder and the length between the reference marks were all measured with a travelling microscope.

Apparatus

The apparatus used for the measurement of the torsional stress (couple) as a function of temperature at constant pressure, length and twist, is shown in *Figure 1*. In the design of this apparatus close attention was paid to the

---

* In equation (4) β is defined as $V_u^{-1}(\partial V_u/\partial T)_p$. Since $(V - V_u)/V_u$ is very small ($\sim10^{-4}$), this does not differ significantly from β in equation (3).
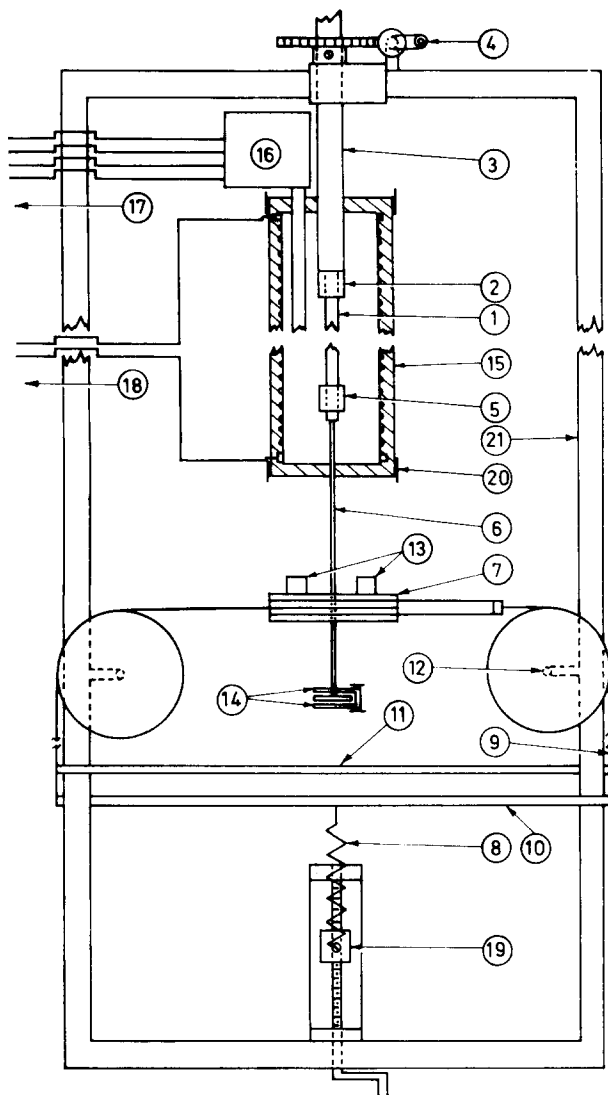
Figure 1. Schematic front view of apparatus

The numbered parts represent:

(1) sample (2) upper clamp (3) upper rod (4) worm gear (5) lower clamp (6) silver-steel rod (7) torsion drum (8) tension spring (9) threads (10) transmission bar (11) counterbalancing bar (12) ball-bearing pulleys (13) weights (14) stops (15) heating chamber (16) thermo-resistive probe (Type 5110 G. Sangamo-Weston) (17) temperature-indicator controller (Type 6003-2, Fielden) (18) variable a.c. transformer (Type V5HMTF, Variac) (19) low-pitch screw adjustment for tension spring (20) clamps attached to main frame (21) main frame.

necessity for accurate control of the axial and torsional strains to which the sample was subjected.

In carrying out the experiments, a given amount of twist was inserted into the sample by rotating the upper clamp *via* the upper rod which was connected to the worm gear. The lower clamp, which was rigidly attached by a silver-steel rod to the torsion drum, was prevented from rotating about its axis by adjustment of the spring by which the tension in the attached threads was controlled. This tension was transmitted *via* the transmission bar as shown
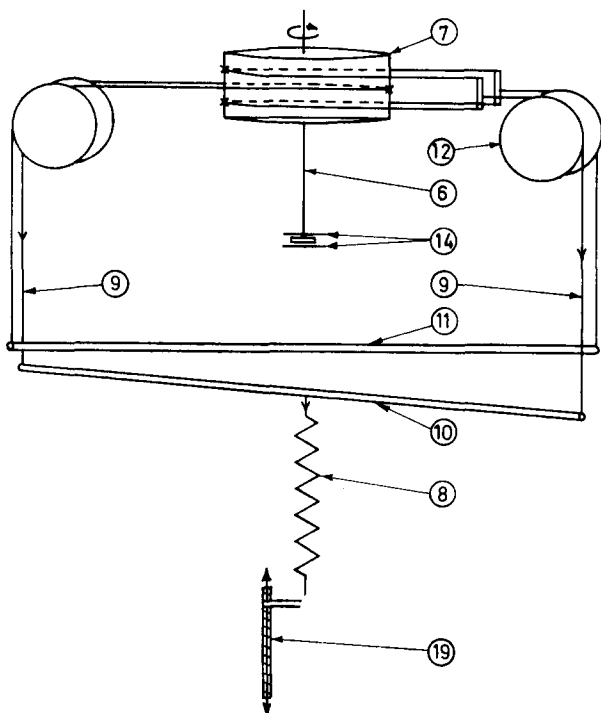
Figure 2. Schematic diagram of torsional system (The numbered parts are referred to in *Figure 1*)

in *Figure 2*; by maintaining the vertical position of this bar constant, the angular position of the drum was automatically fixed. The arrangement of the threads around the drum and their connection to the transmission bar and counterbalancing bar offered a stable torsional device in which the couple could be calculated from the measured extension of the spring. The frictional component of the stresses in the ball-bearing pulleys was found to be negligibly small. The angle of twist of the sample was controlled to within ± 0.5 degrees. The couple was measured to within ± 0.1 g cm in the range $10-200$ g cm.

The sample was also given a small axial extension sufficient to maintain a positive tension and to eliminate buckling in the twisted state. The extension was controlled by adjustment of the weights applied to the top of the torsion

drum. A guide to the vertical alignment and position of the drum was pro-
vided by the stops. The length of the sample was controlled to within ± 0.05
cm.

The heating chamber was constructed from a Pyrex glass tube which was
wound with standard electrical-resistance wire. The temperature of the
sample was controlled by an electronic temperature-indicator controller which
was connected to a variable transformer which supplied the appropriate
voltage to the resistance wire. The temperature at the centre of the sample
was controlled to within $\pm 0.5°C$, but a maximum temperature difference of
$2°C$ was detected along the length of the sample. However, this was not
sufficient to create appreciable errors in the resulting stress-temperature
data.

Procedure

The sample was allowed to relax at $100°C$ for 1 to $1\frac{1}{2}$ h under the maximum
torsional strain to be used in subsequent experiments. Stress–temperature
data were then recorded in the range $20 - 60°C$. Stress readings were taken
at 5 or $10°C$ intervals after sufficient time had been allowed for the attain-
ment of thermal equilibrium; from preliminary experiments this was found
to be about 10 min when, between each interval, the sample was heated or
cooled at the rate of $1-3°C$ per min. The decreasing/increasing temperature
cycle was repeated until effective reversibility was obtained. The procedure
was then repeated in a similar manner at different lower values of the strain.
but excluding the initial relaxation at $100°C$.

RESULTS AND CONCLUSIONS

Stress relaxation

The effects of stress relaxation are shown in *Figure 3*. The total reduction
in stress during the preliminary, high temperature relaxation and the two
subsequent temperature cycles was about 10%. The periods of time that are
shown at 30 and $60°C$ illustrate the difference between the rates of stress
relaxation at these two temperatures. The time taken to obtain the complete
curve illustrated was 4 days, compared with 10 h for each subsequent curve
for the same sample at a lower strain.

Analysis of stress-temperature data

A typical set of stress–temperature plots for one particular sample at
different strains is shown in *Figure 4*. In all cases a reversible, linear relation-
ship was found to exist between couple and temperature. The slope of any one
line was reproducible to within 2% for successive temperature cycles. It
should be noted that the broken line plot (at $\psi a_0 = 0.690$) was obtained from
a repeated run, after the curves at the lower strains had been recorded. The
small displacement of this plot from the bold line curve signified that, although
reversibility had been achieved within the time of one run, thermodynamic
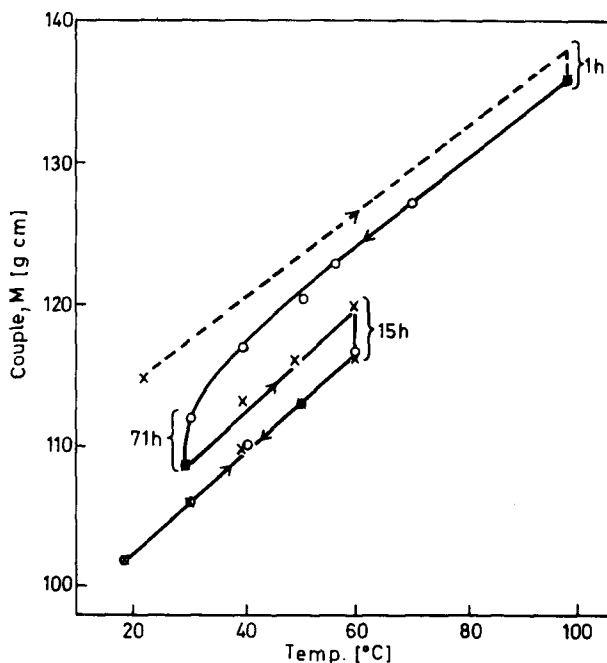reversibility had not been achieved over the total time of the experiment.

Figure 3. Typical stress-relaxation plot for natural rubber in torsion
○, decreasing temperature,   ×, increasing temperature

However, the value of the stress–temperature coefficient had not changed significantly.

The quantity $(T/M)\partial M/\partial T$ [equation (4a)] was calculated from relative stress–temperature data for a temperature of 293°K. The resulting data are included in *Table 1*.

Effects of strain and crosslink density upon M_{ev}/M

In *Table 1* the torsional strain is expressed in terms of the parameter ψa_0 corresponding to n turns of twist in the total length of the sample; a_0 and ψ are defined as in equation (2). The crosslinking density is expressed in terms of G, the shear modulus, which was calculated from the reversible stress–temperature data at 20°C by use of the equation

$$G = 2M/\pi\psi a_0{}^4$$

Both ψa_0 and λ, the extension ratio, were referred to the original, unstrained dimensions at 20°C. M_{ev}/M was calculated at 293°K from the $(T/M)\,\partial M/\partial T$ values using equations (4a) and (5). The coefficient of volume expansion, β, for natural rubber was taken as $6\cdot6 \times 10^{-4}$ deg^{-1}.

26
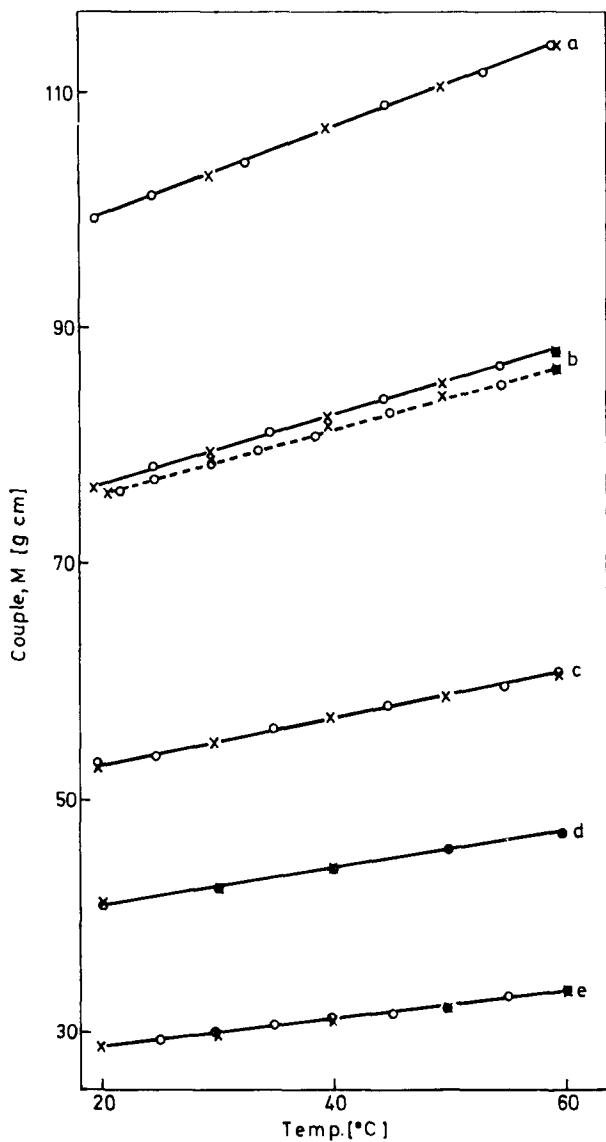
Figure 4. Stress-temperature plots at different torsional strains
○, decreasing temperature, ×, increasing temperature
Torsional strain parameter ψa_0 = (a) 0·888, (b) 0·690, (c) 0·492
(d) 0·393, (e) 0·297

Table 1 Thermoelastic data for natural rubber in torsion

G [kg cm^{-2}]	n turns	ψa_0 [rad]	$\dfrac{T}{M}\left(\dfrac{\partial M}{\partial T}\right)_{p,l,\psi}$	M_{ev}/M [%]
2·1	9	0·888	1·06	13·3
($\lambda = 1\cdot25$)	7	0·690	1·06	13·3
	5	0·492	1·07	12·3
	4	0·393	1·08	11·3
	3	0·297	1·09	10·3
3·0	7	0·683	1·04	15·3
($\lambda = 1\cdot19$)	6	0·586	1·07	12·3
	5	0·488	1·07	12·3
3·6	6	0·633	1·07	12·3
($\lambda = 1\cdot15$)	5·5	0·580	1·05	14·3
	5	0·526	1·06	13·3
3·7	6·5	0·696	1·05	14·3
($\lambda = 1\cdot13$)	6	0·642	1·07	12·3
	5·5	0·589	1·10	9·3

The average value of the quantity M_{ev}/M, obtained from the figures in *Table 1*, is 12·6 ± 1·6%. The relative error in M_{ev}/M is, of course, much larger than the relative error in $(T/M)\partial M/\partial T$ (eight times as large); there is, however, no indication of any significant dependence of M_{ev}/M on either the crosslink density or the amount of the torsional strain.

From the mean value of M_{ev}/M the resulting value of d ln $\overline{r_0^2}$/dT for natural rubber at 20°C is found to be 0·43 ± 0·05 × 10^{-3} deg^{-1}.

Comparison with simple extension data

Although there is no difficulty in principle in carrying out comparable thermoelastic measurements in simple extension, the accuracy of the values of d ln $\overline{r_0^2}$/dT determined from such experiments is generally lower, owing to the greater sensitivity of the stress–temperature coefficient in extension to volume changes, discussed in an earlier paper[1]. The presence of the term $-\beta/(\alpha^3 - 1)$ in equation (3) implies a sensitivity to the absolute value of the strain, and hence to the precision with which the unstrained length can be determined, which is absent in the corresponding equation (4) for torsion. As a result the errors in the determination of the internal energy contribution to the tensile force f_{ev}/f (and hence d ln $\overline{r_0^2}$/dT) increase progressively as the strain decreases. It is presumably for this reason that published results show no agreement on the question of whether or not the internal energy contribution to the stress, f_{ev}/f, is dependent upon the strain; some authors [7,10,13,14,15] have reported an increase in this quantity as the strain becomes smaller, while others[4,5,9,17,18] have found no significant change. In one case[16] a decrease has been reported. *Table 2* gives some of the published data obtained from simple extension experiments; in cases where the figures varied according to the strain the values quoted refer to the region of higher strains, where

the variations were generally reduced to a minimum. It is satisfactory to note that the present result for M_{ev}/M in torsion, namely 12·6%, is within the range covered by the data for the equivalent quantity f_{ev}/f.

Table 2 Published values of f_{ev}/f for natural rubber for thermoelastic measurements in simple extension.

f_{ev}/f [%]	Temperature [°C]	Authors	Method of determination
17	0 – 70	Ciferri[4]	Constant pressure, equation (3)
13	0 – 70	Ciferri, Hoeve and Flory[5]	Calculated from experimental data of Wood and Roth[6]
20	45	Roe and Krigbaum[7]	Constant pressure, equation (3)
20	30	Allen, Bianchi and Price[8]	Constant volume – direct measurement of $(\partial f/\partial T)_{V,l}$
12·5	20 – 60	Yamamoto, Kusamizu and Fujita[9]	Constant pressure, modified Mooney form of equation (3)
18	30	Shen, McQuarrie and Jackson[10]	Constant pressure, equation (3)
18	25 – 70	Barrie and Standen[11]	Constant pressure–length *v.* temperature measurements at constant load, equation (3)
15	30	Shen and Blatz[12]	Constant pressure, using $f_{ev}/f = 1 - T(d \ln G/dT) - \beta T/3$

It is concluded that the torsional method provides a convenient and accurate means of determining the quantity $d \ln \overline{r_0^2}/dT$ which possesses distinct experimental advantages over the more usual method of simple extension.

ACKNOWLEDGEMENTS

Department of Polymer and Fibre Science,

University of Manchester

Institute of Science and Technology

REFERENCES

1 Treloar, L. R. G. *Polymer Lond.*, 1969, **10**, 291
2 Flory, P. J. *J. Amer. Chem. Soc.* 1956, **78**, 5222
3 Flory, P. J. *Trans Faraday Soc.* 1961, **57**, 829
4 Ciferri, A. *Die Makromol. Chem.* 1961, **43**, 152
5 Ciferri, A., Hoeve, C. A. J. and Flory, P. J. *J. Amer. Chem. Soc.* 1961, **83**, 1015
6 Wood, L. A. and Roth, F. L. *J. appl. Physics* 1944, **15**, 781
7 Roe, R. J. and Krigbaum, W. R. *J. Polymer Sci.* 1962, **61**, 167
8 Allen, G., Bianchi, U. and Price, C. *Trans Faraday Soc.* 1963, **59**, 2493

9 Yamamoto, K., Kusamizu, S. and Fujita, H. *Die Makromol. Chem.* 1966, **99**, 212
10 Shen, M. C., McQuarrie, D. A. and Jackson, J. L. *J. appl. Physics* 1967, **38**, 791
11 Barrie, J. A. and Standen, J. *Polymer Lond.* 1967, **8**, 97
12 Shen, M. C. and Blatz, P. J. *J. appl. Physics* 1968, **39**, 4937
13 Roe, R. J. and Krigbaum, W. R. *J. Polym. Sci. (A)* 1963, **1**, 2049
14 Crespi, G. and Flisi, U. *Die Makromol. Chem* 1963, **60**, 191
15 Opschoor, A. and Prins, W. *J. Polym. Sci. (c)* 1967, **16**, 1095
16 Haly, A. R. *J. Polym. Sci. (A)* 1965, **3**, 3331
17 Ciferri, A. *Trans Faraday Soc.* 1961, **57**, 846
18 Mark, J. E. and Flory, P. J. *J. Amer. Chem. Soc.* 1964, **86**, 138

Polyphosphazenes: Part 1 Synthesis

G. ALLEN, C. J. LEWIS* and S. M. TODD

High molecular weight poly(dichlorophosphazene) has been prepared by various methods. The reaction between ammonium chloride and phosphorus pentachloride was found to give polymers of intrinsic viscosity $\leqslant 0.66$ dl/g. The thermal polymerization of hexachlorocyclotriphosphazene in the presence of hydrogen chloride gave polymers of low molecular weight whereas without the hydrogen chloride soluble polymers of intrinsic viscosity > 2 were obtained. The chlorine atoms have been replaced by alkoxy or aryl-oxy groups thus rendering the polymers stable to hydrolysis. Evidence is found for the re-equilibration of the trimer to give a range of cyclic and linear chlorophosphazenes.

THE THERMAL STABILITY of low molecular weight phosphazene compounds has led many investigators to prepare phosphazene polymers in the hope that these too would have good thermal stability. To date polyphosphazenes have been prepared by three methods.

(1) The reaction of ammonium chloride and phosphorus pentachloride both with[1] and without[2] solvent. High yields of linear polymers of degree of polymerization up to 20 were obtained.

(2) Copolymerization of the cyclic phosphazenes with other monomers to give polymers in which the phosphazene ring is retained. Some interesting crosslinked polymers have been prepared in this way but no linear polymer with molecular weight exceeding 15 000 has been reported.

(3) Ring opening polymerization of the lower cyclic homologues to form high polymers. The best known polymer prepared in this way is the poly-(dichlorphosphazene) rubber first reported by Stokes[3]. It was obtained by heating the hexachlorocyclotriphosphazene to 250–350°C. Polymer formed slowly at the lower temperature, rapidly at the higher temperature, and the product swelled in benzene but did not dissolve showing that it was a crosslinked network. The only cyclic phosphazenes which undergo ring opening polymerization are the halides and pseudohalides. These and the polymers formed from them are hydrolytically unstable[1].

The phosphazene ring may be made hydrolytically stable by replacing the halide by organic groups such as 2,2,2-trifluorethoxy. Hexa(trifluorethoxy) cyclotriphosphazene is reported as being resistant to acid and alkali while not degrading on distillation at 500°C.

Recently two publications[4, 5] have reported the preparation and properties of a limited number of soluble phosphazene polymers by the ring-opening

* On leave from I.C.I. Petrochemical and Polymer Laboratory, The Heath, Runcorn, Cheshire

polymerization of the cyclic chloride and effecting hydrolytic stability by organic substitution. We have been working along similar lines for several years and have prepared a range of polymers with different side groups to determine the effect of the side group on thermal stability and other physical properties.

POLYMER PREPARATION

The polymer preparation described in this work falls into two distinct reaction schemes. The first involves the formation of linear chlorophosphazenes stabilized by phosphorus pentachloride or hydrogen chloride and condensation of these into high polymers. The second concerns the thermal polymerization of cyclic phosphazenes to give linear high polymers. Initially all the polymers prepared were converted to the poly[*bis*(2,2,2-trifluorethoxy)phosphazene] so that characterization could be carried out without fear of hydrolysis. When the most suitable method of preparation had been decided upon, other groups were substituted into the poly(dichlorophosphazene).

REAGENTS

Because of the hydrolytic instability of the poly(dichlorophosphazene) all reagents used prior to replacement of the chlorine by organic groups were dried by conventional techniques.

Hexachlorocyclotriphosphazene, as obtained commercially, contained up to 10% of the tetramer. It was purified by recrystallization from 80/100 light petroleum and sublimation at 90°C, 0·1 mmHg. The purified material, melting point 113°C, was stored in dried glassware under vacuum.

PREPARATION AND CONDENSATION OF Cl-(-PCl$_2$=N-)-$_n$PCl$_4$

The preparation of these compounds by two methods has been reported[1, 6]; phosphorus pentachloride was reacted with either hexachlorocyclotriphosphazine or ammonium chloride. The actual structure of these compounds is thought to be as written above but has not yet been proved conclusively.

(a) *Reaction of phosphorus pentachloride with hexachlorocyclotriphosphazene*

The action of phosphorus pentachloride on hexachlorocyclotriphosphazene is reported to cause the ring to open to give a linear chain of low molecular weight[1]. The phosphorus pentachloride then adds on, thus stabilizing the molecule against recyclization. If the phosphorus pentachloride were not present at the temperature used for the reaction, the hexachlorocyclotriphosphazene would polymerize to give the crosslinked poly(dichlorophosphazene) rubber.

32

Lund[1] reacted the two reagents in proportions to yield final products of average composition $Cl-(-PCl_2=N-)-_nPCl_4$ where n was 2 to 20. He showed that the final product was free from unreacted cyclic material, being completely insoluble in light petroleum. If the reactant ratio could be varied so that the average value of n is much greater than 20 then this could be a convenient method of preparing linear polymers.

Hexachlorocyclotriphosphazene (0·029 mole) was placed in a pyrex tube with phosphorus pentachloride (0·0005 mole). The tube was quickly sealed and then heated to 360°C for 5 h, cooled, opened and placed in a flask with light petroleum. The product only swelled and did not dissolve showing that insufficient phosphorus pentachloride had been present to prevent the phosphazene crosslinking. If the product had been a linear polymer its average degree of polymerization would be expected to be 175. The preparation was repeated with reactant ratios required to give products with average D.P.s of 36 and 75. In these two reactions the product was completely soluble in light petroleum, indicating that sufficient phosphorus pentachloride was present to prevent crosslinking but insufficient to form the compound $Cl-(-PCl_2=N-)-_nPCl_4$.

(b) *Reaction of phosphorus pentachloride with ammonium chloride*

The action of phosphorus pentachloride on ammonium chloride in a refluxing solvent, such as *sym*-tetrachlorethane, gives a mixture of both cyclic and linear phosphazenes. By varying reaction conditions it can be arranged so that the reaction product is predominantly either the cyclic or linear phosphazenes. In this case the required product was the linear phosphorus pentachloride stabilized chlorophosphazene. The first reaction carried out was similar to that reported by Lund[1], the only difference being the solvent used. The higher the boiling point of the solvent the quicker the reaction proceeds so that *o*-dichlorobenzene (boiling point 179°C) was used in preference to the *sym*-tetrachloroethane (boiling point 147°C) used by Lund.

Phosphorus pentachloride (0·187 mole) and ammonium chloride (0·168 mole) were placed in a 1 litre flask with *o*-dichlorobenzene (100 ml). The flask was fitted with a stirrer and reflux condenser and then slowly warmed in an oil bath. Hydrogen chloride was given off and caused foaming; this was controlled by adjusting the temperature. As the evolution of gas decreased the flask was kept free of foam by slowly raising the temperature. Eventually it was possible to boil the solvent under reflux and this washed down sublimed phosphorus pentachloride from the walls of the flask and the condenser. The solution was heated under reflux for 5 h until no more hydrogen chloride was evolved, then the solvent was distilled off at 1 mmHg pressure. The product, a thick oily mass, was extracted with light petroleum, the insoluble linear material was separated and converted to the trifluorethoxy derivative as described later. The intrinsic viscosity of the polymer was determined in tetrahydrofuran at 25°C and found to be less than 0·05 dl/g.

The preparation was repeated but instead of adding all the ammonium chloride at the start only 7 g was added initially. After hydrogen chloride evolution had ceased, a further 1·5 g was added and eventually the remaining 0·5 g. After the evolution of gas had finally ceased the solution was treated as

33

c

in the previous experiment. By this means it was hoped that the following reaction scheme would be followed:

$$PCl_5 + NH_4Cl \rightarrow (1/n) Cl-(-PCl_2=N-)-_nPCl_4 + 4HCl$$

$$Cl-(-PCl_2=N-)-_nPCl_4 + NH_4Cl \rightarrow Cl-(-PCl_2=N-)-_nPCl_2=NH + 3HCl$$

$$Cl-(-PCl_2=N-)-_nPCl_2=NH + Cl-(-PCl_2=N-)-_nPCl_4$$
$$\rightarrow Cl-(-PCl_2=N-)-_{2n}PCl_4$$
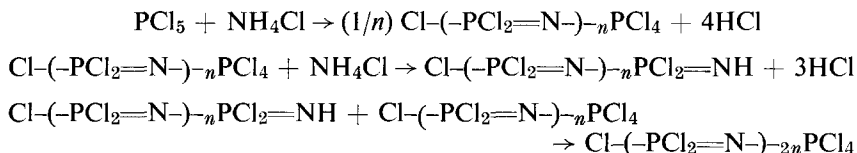
The intrinsic viscosity of the product after conversion to the trifluorethoxy derivative was less than 0·05 dl/g showing that the product was still of very low molecular weight. The latter preparation was repeated and the product subjected to thermal and vacuum treatment in an effort to raise the molecular weight. The efforts were unsuccessful. The volatiles from the treatment consisted of phosphorus pentachloride and cyclic chlorophosphazenes.

Another portion was heated under reflux with stirring in *o*-dichlorobenzene with 0·5 g of ammonium chloride. The product, after 4 h, was a swollen gelatinous mass which showed that crosslinking had occurred.

PREPARATION AND CONDENSATION OF $(PX_2=N)_n$ HX

Becke-Goehring[2] has prepared the above compound, where X is chlorine, by the bulk reaction of ammonium chloride and phosphorus pentachloride under pressure at elevated temperatures. The structure of these compounds is reported to be $Cl-(-PCl_2=N-)-_nH$. Since the phosphorus pentachloride-stabilized linear chlorophosphazene may be prepared by the ring opening of the cyclic trimeric chloride with phosphorus pentachloride, similar reactions were tried with anhydrous hydrogen halides and cyclic phosphazenes under pressure.

(a) *Bulk reaction of phosphorus pentachloride and ammonium chloride*
    The experiments were similar to those reported by Becke-Goehring[2]. Phosphorus pentachloride (417 g, 2 mole) and ammonium chloride (107 g, 2 mole) were reacted in a glass-lined autoclave at 180°C. Initially there was a surge of pressure up to 700 p.s.i., this was released and the release valve adjusted so that the pressure was maintained at 150–220 p.s.i. After 22 h the evolution of hydrogen chloride had practically ceased, the valve was closed and the sealed autoclave heated for a further 1 h at 180°C and 30 min at 200°C and then allowed to cool. The product was treated with light petroleum to extract the cyclic material and 86 g of cyclic oligomers were recovered. The linear material was heated at 100°C and 0·01 mmHg. pressure for 4 h to remove solvent and residual traces of cyclic material. The yield of linear material was 125 g, (59% of the total product). It had a molecular weight corresponding to $H(NPCl_2)_{15}Cl$. Some of the linear polymer was converted to the trifluorethoxy derivative. The product had an intrinsic viscosity of 0·18 dl/g.

During a repeated preparation the autoclave release valve blocked during the heating stage resulting in a pressure of above 1 000 p.s.i. being obtained before the bursting disc blew. The autoclave was cooled, the valve unblocked,

a new bursting disc fitted and the reaction continued. The yield from this reaction contained 30 g of unreacted ammonium chloride and 195 g of chlorophosphazenes of which 86% was linear material which, after conversion to the trifluorethoxy derivative had an intrinsic viscosity of 0·66 dl/g.

According to Becke-Goehring, the material prepared in this reaction may be condensed to soluble high molecular weight polymers, of D.P. about 90, by reaction with limited amounts of water.

$$Cl-(-PCl_2\!=\!\!=\!N-)-_nPCl_2\!=\!\!=\!NH + H_2O$$

$$\rightarrow Cl-(-PCl_2\!=\!\!=\!N-)-_{n-} \left[\begin{array}{c} Cl \\ | \\ -P-O-PCl_2\!=\!\!=\!N- \\ || \\ NH \end{array} \right]_x \!\!\!-H + 2HCl$$
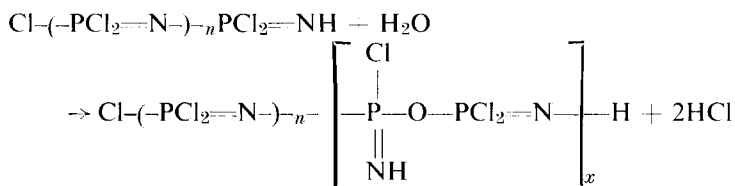
Some of the linear product from the first preparation was dissolved in wet benzene and allowed to stand for 20 h. The solution was refluxed for 1 h, 0·2 g water was added and reflux continued for a further $1\frac{1}{2}$ h. After cooling, the solution was used for the conversion of the polymer to the trifluorethoxy derivative. The product had an intrinsic viscosity of 0·25 dl/g.

The remainder of the linear product from the first preparation was heated in a flask at 100°C and 10^{-3} mmHg pressure for 67 h in an effort to condense the polymer to higher molecular weight. The product was shaken with benzene, the polymer in contact with the surface of the glass swelled but did not dissolve. The benzene solution of the remainder was decanted from the swollen gel and was converted to the trifluorethoxy derivative, the intrinsic viscosity was 0·20 dl/g.

(b) *Reaction of hydrogen chloride with hexachlorocyclotriphosphazene*

Hexachlorocyclotriphosphazene, (0·072 mole) xylene (50 ml) and hydrogen chloride (0·137 mole) were heated in a glass lined autoclave at 350°C for 17 h; the pressure was 190 p.s.i. After cooling, the solution was poured into a large excess of light petroleum. The insoluble linear material, 75% of the product, was separated and the solvent evaporated to yield the cyclic material. The dark brown coloured linear material was heated at 100°C and 10^{-3}mmHg pressure for 2 h, cooled, dissolved in benzene and converted to the trifluoroethoxy derivative. The product had an intrinsic viscosity of 0·15 dl/g. The cyclic material was distilled to yield 42% trimer, 21% tetramer, 6% pentamer and 31% of higher cyclics. A repeat preparation was carried out and the linear material dissolved in chloroform and mixed with 25 g hexachlorocyclotriphosphazene. The mixture was heated to remove the chloroform and then to 230°C for $1\frac{1}{2}$ h. After cooling, the mixture was extracted with light petroleum. The linear material was converted to the trifluoroethoxy derivative, the intrinsic viscosity of the product was 0·15 dl/g.

Repeat preparations with smaller amounts of hydrogen chloride only yielded less linear material without noticeably increasing the intrinsic viscosity, until, when less than 0·1 mole hydrogen chloride per mole $PNCl_2$ was used, a crosslinked insoluble gel was obtained.

Another linear polymer was prepared as in the first experiment and divided into two portions. The first was heated at 100°C and 10^{-3} mmHg pressure for 48 h before converting to the trifluoroethoxy derivative, it had an intrinsic viscosity of 0·20 dl/g. The second portion was dissolved in benzene and 1 ml of triethylamine added as an acid acceptor. The polymer formed a swollen gel in less than 24 h.

(c) *Reaction of hydrogen chloride with hexakis(2,2,2-trifluoroethoxy)-cyclotriphosphazene*

The *hexakis*(trifluoroethoxy)cyclotriphosphazene was prepared and then reacted with hydrogen chloride in an attempt to form the linear compound H–[–N=P(OCH$_2$CF$_3$)$_2$–]–$_n$Cl which would be expected to be less susceptible to crosslinking on condensation than the linear chlorophosphazenes.

Three-gram quantities of the product were treated, in xylene solution, with various amounts of hydrogen chloride under pressure. The reaction conditions were as used to prepare the H–(–N=PCl$_2$–)–$_n$Cl. The product from all of the reactions was the unchanged starting material showing that no ring opening occurred under these conditions.

(d) *Reaction of hydrogen bromide with hexachlorocyclotriphosphazene*

In a further attempt to prepare a linear low molecular weight phosphazene suitable for condensation to a high molecular weight polymer, hydrogen bromide was reacted with hexachlorocyclotriphosphazene. It was hoped that the linear compound H–(–N=PCl$_2$–)–$_n$Br would be formed which might condense without crosslinking because of the expected greater ease of removal of hydrogen bromide, in comparison with hydrogen chloride.

The reaction was carried out in exactly the same way as described for the similar reaction with hydrogen chloride. The product contained 80% of a material, insoluble in light petroleum, and of a similar appearance to the hydrogen chloride-stabilized linear material. Conversion to the trifluoroethoxy derivative yielded a polymer of intrinsic viscosity 0·06 dl/g. Attempts were made to condense the linear product from a repeat preparation by heating under vacuum at 120°C for 8 h. The material did not become more viscous and it was insoluble in benzene and showed no swelling. It contained some gritty particles and appeared to have degraded.

A further sample of the linear material was dissolved in benzene, 1 ml of triethylamine was added and the solution allowed to stand for 60 h. The solution was then used to convert the polymer to the trifluoroethoxy derivative. The intrinsic viscosity of the product was 0·05 dl/g.

THERMAL POLYMERIZATION OF HEXACHLOROCYCLOTRIPHOSPHAZENE

The thermal polymerization of hexachlorocyclotriphosphazene has been widely studied. The rate of polymerization may vary appreciably depending on the polymerization temperature and the possible impurities present in the starting material. The object of this investigation was not to study the kinetics of the polymerization but to use the polymerization to prepare phosphazene

polymers which could then be characterized. Thus the starting material was not subjected to more purification than already described and no catalysts were added.

(a) Thermal polymerization at 300°C

Polymerizations were done in tubes prepared from 10 mm internal diameter thick-walled pyrex tubing dried overnight at 120°C. Hexachlorocyclotriphosphazene (20 g) was weighed into the tube and it was then evacuated to 10^{-4} mmHg pressure for 1 h on a vacuum line. The tube was isolated from the vacuum, warmed carefully to melt the contents and allowed to cool. When the contents had solidified the tube was evacuated for 2h at a pressure of 10^{-4} mmHg and then sealed under vacuum. The sealed tube was heated at 300°C and inspected at 15 min intervals. The contents were initially mobile but after heating for 1 to $1\frac{1}{4}$ h they became a pale yellow rubbery mass. After $1\frac{1}{4}$ h the tube was allowed to cool, opened, quickly placed in a stoppered flask, and covered with light petroleum. The bulk of the product did not dissolve but the light petroleum extracted 1·1 g. of cyclic material. The main product did not dissolve in benzene, it merely swelled to several times its original volume. This indicated that crosslinking had taken place and, since it happened in such a short time, it was decided to try a lower temperature in an attempt to retard the crosslinking reaction.

(b) Thermal polymerization at 250°C

A tube and contents were prepared as in (a) and heated at 250°C. After about 12 h the contents of the tube had become noticeably more viscous. The gradual increase in viscosity continued until after 48 h the product was very viscous and pale yellow in colour. The tube was cooled, opened and left to stand overnight in light petroleum. The product did not dissolve so the light petroleum was replaced by benzene. Evaporation of the light petroleum yielded 7 g of starting material. Since the product was not completely soluble in benzene, some crosslinked material must have been formed.

The soluble portion was converted to the trifluoroethoxy derivative (intrinsic viscosity, 1·5 dl/g). Later experience showed that the insolubility in this preparation probably arose because the product was not dissolved immediately in benzene. On standing the product slowly begins to crosslink, the termination not being complete until the chloride polymer becomes highly crosslinked or is converted to an organo derivative.

Six tubes were prepared as above and heated at 250°C. Tubes were removed at various times so that a measure of the products of the polymerization as time progressed could be obtained. The tube was cooled, opened, immediately placed in a stoppered flask with 150 ml benzene and shaken until dissolution was complete. The solution was then poured into 2 l of stirred light petroleum to precipitate the polymer. The solution was decanted and the residual polymer left to stand overnight with light petroleum. The solvent-soluble material from the extracts consisted of cyclic material together with a little low molecular weight linear material not precipitated by the light petroleum. The cyclic material was separated from this linear material by redissolving in light petroleum and decanting.

37

The composition of the cyclic material was measured by analysis of its benzene solutions using a Varian Aerograph Model 700 gas-liquid chromatograph. The components were identified and measured by comparison with benzene solutions of known compositions of pure cyclic chlorides. The results are shown in *Table 1*.

Table 1. Percentage composition of polymerization mixture from hexachlorocyclotri-phosphazene at 250°C at various times

Time [h]	$P_3N_3Cl_6$	$P_4N_4Cl_8$	$P_5N_5Cl_{10}$	$P_6N_6Cl_{12}$	*Polymer*
0	97·4	2·6	nil	nil	nil
20	73·4	3·5	0·5	1·3	21·3
30	58·0	4·2	0·7	2·8	34·3
40	48·0	4·9	0·8	3·4	42·8
48	41·2	6·5	1·6	7·7	43·0
56	25·9	5·8	1·7	6·5	60·1
62	14·2	3·6	2·7	10·9	68·7

The 62 h polymerization was the only one to produce any heptamer, $P_7N_7Cl_{14}$ which was present at less than 1% concentration. The polymer figure in *Table 1* consists of soluble linear polymer with the exception of the 62 h polymerization which contained about 10% of insoluble crosslinked gel. This investigation showed that 48–56 h was the optimum time at 250°C for the polymerization to give soluble materials, at a yield of approximately 50%.

PREPARATION OF POLYMERS FOR CHARACTERISATION

The highest molecular weight soluble polymer prepared in this work was that from the thermal polymerization of the hexachlorocyclotriphosphazene. This method was used as a standard to prepare a chloride polymer into which other side groups could be introduced to give a range of polymers for characterization.

(a) *Standard preparations of chlorophosphazene high polymer*
    Polymerizations were carried out either on 20 g or 100 g scale. Twenty-gram quantities were reacted in 10 mm diameter tubes, and 100-g quantities in tubes prepared from 20 mm internal diameter thick-walled pyrex tubing. The procedure was as previously described. The heating/time cycle chosen was 250°C for 48 h and dissolution of the polymerized product was usually obtained after shaking for 6 h in benzene. Replacement of the chlorine in the polymer was performed immediately, since delays led to gelation.

(b) *Replacement of chlorine in the polymer by alkoxy or aryloxy groups*
    The chlorine in the chlorophosphazenes is easily replaced with alkoxy or aryloxy groups by reaction with the sodium salt of the alcohol or phenol.
    The benzene solution of the polymer obtained as above was slowly run into a well-stirred tetrahydrofuran solution of the sodium salt of the alcohol, or

phenol, which was present in 20% excess. The solution was stirred and heated under reflux, overnight for the smaller preparations and for 48 h for the larger preparations. The solution was then allowed to cool before being poured into a large excess of light petroleum. The precipitated material always contained the polymer in a finely divided form, contaminated with sodium chloride and the sodium salt of the alcohol or phenol; in some cases it also contained the cyclic organophosphazenes. It was filtered, dried under vacuum and then washed several times with water to remove the sodium salts. The cyclic and linear organophosphazenes were then separated by repeated extraction with a solvent which dissolved the cyclic material and not the linear polymers. In the case of the large-scale preparations the extraction with water and then with an organic solvent was carried out in a Soxhlet apparatus until a constant weight was obtained. The polymer was then dissolved in a solvent and precipitated by adding the solution to the solvent used for extracting the cyclic material; this ensured the final removal of cyclic material. After standing overnight the polymer was isolated and dried under vacuum to a constant weight.

The polymers prepared, together with their intrinsic viscosities and solvents are listed in *Table 2*.

Table 2 Polymers prepared of the type $[PN(OR)_2]_n$ with their intrinsic viscosities and solvents

Polymer R=	Intrinsic viscosity [dl/g]	Solvent for polymer	Solvent for cyclic material
$-CH_2CF_3$	0·82	THF	light petroleum
$-C_6H_4CF_3$ (*meta*)	1·5	THF	light petroleum
$-C_6H_4Cl$ (*para*)	1·42	THF	light petroleum
$-C_6H_3Cl_2$ (2,4)	12	THF	light petroleum
$-C_6H_4F$ (*para*)	9	THF	light petroleum
$-C_{10}H_7$ (β)	1·9	DMF	acetone
$-C_6H_4-C_6H_5$ (*para*)	1·2	DMF	acetone
$-CH_2(CF_2)_6CF_3$	–	none found	none found

ATTEMPTED PREPARATION OF ARYLPHOSPHAZENE POLYMERS

Following the successful preparations of alkoxy and aryloxyphosphazene polymers several attempts were made to prepare arylphosphazene polymers. The cyclic arylphosphazenes are usually prepared from the corresponding fluorophosphazenes so that the attempts to prepare the arylphosphazene polymers usually involved the intermediate preparation of the fluoro polymer.

(a) *Attempted aryl substitution in the poly(dichlorophosphazene)*

For the preparations the poly(dichlorophosphazene) polymer was prepared as already described.

(1) Fine lithium wire (10 g) was reacted with. bromobenzene (110 g) in benzene, the bromobenzene being added at a rate such that the solution

boiled steadily under reflux. When all the lithium had dissolved a benzene solution of poly(dichlorophosphazene) (10 g) was added slowly with stirring. The suspension was heated under reflux with stirring overnight, cooled and evaporated to dryness. The product was found to contain no polymeric material.

(2) Sodium wire (5 g) was made into a very fine suspension by melting in paraffin oil, agitating with a vibratory stirrer to give very fine globules and then cooling. The oil was replaced by dry n-heptane and chlorobenzene (15 g) slowly added with vigorous stirring. A benzene solution of poly(dichlorophosphazene) (10 g) was added slowly with vigorous stirring and the solution heated under reflux overnight. No polymeric material could be isolated from the product.

(3) Potassium fluorosulphite (KSO_2F) (20 g) was added to a solution of poly(dichlorophosphazene) (10 g) in benzene. The whole was heated until no more sulphur dioxide was evolved. A solution of phenyl lithium was prepared as in (1) and slowly added to the suspension of poly(difluorophosphazene) and potassium chloride. After heating under reflux overnight the suspension was cooled and evaporated to dryness. No polymeric material could be recovered from the product.

(b) *Preparation of poly(difluorophosphazene) and reaction with phenly lithium*

Decafluorocyclopentaphosphazene (10 g) was weighed into a tube prepared from 10 mm internal diameter thick walled pyrex tubing. The tube was connected to a vacuum line, immersed in liquid nitrogen, and when the contents had frozen the tube was evacuated to 10^{-4} mmHg pressure. After 1 h the tube was isolated from the vacuum and the contents allowed to melt. The contents were then re-frozen, evacuated to 10^{-4} mmHg pressure again and the tube sealed under vacuum. After warming to room temperature the tube was heated at 250°C and inspected at intervals. After 65 h the contents of the tube had become very viscous, but not immobile. The tube was cooled and opened and the contents placed in benzene. After shaking for 24 h it had not dissolved: it was also insoluble in light petroleum and chloroform. The starting material was very soluble in light petroleum.

A repeat polymerization was carried out and the polymerized product poured directly into a well-stirred solution of phenyl lithium in benzene, prepared from. lithium (7 g) and bromobenzene (50 g). A very vigorous reaction occurred and the suspension was heated under reflux with stirring overnight. The contents of the flask were evaporated to dryness and the product examined; no polymeric material was recovered.

DISCUSSION

It would appear therefore that elimination of the stabilizing end groups from the linear chlorophosphazenes could occur by one of two mechanisms, either intra- or intermolecular elimination. The former would yield a cyclic chlorophosphazene; the latter would lead to further polymerization. The attempted condensation of the low molecular weight $Cl-(-PCl_2=N-)-_nPCl_4$

by heating under vacuum shows that it loses phosphorus pentachloride by intramolecular elimination. The evidence for this is the large amount of cyclic material formed and the lack of any high polymer. The condensation of the same material with ammonium chloride formed the material stabilized with hydrogen chloride thus:

$$Cl\text{--}(\text{--}PCl_2\text{==}N\text{--})\text{--}_n PCl_4 + NH_4Cl \rightarrow$$
$$Cl\text{--}(\text{--}PCl_2\text{==}N\text{--})\text{--}_n PCl_2\text{==}NH + 3HCl$$
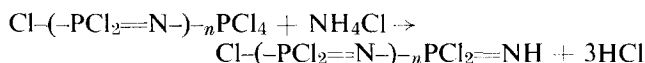
This must lose its stabilizing hydrogen chloride by intermolecular elimination since a high polymer is formed. In the $Cl\text{--}(\text{--}PCl_2\text{==}N\text{--})\text{--}_n PCl_4$ material reported by Lund[1] the average value of n was 11. The mechanism which has been proposed for the reaction of phosphorus pentachloride with ammonium chloride to form the cyclic chlorophosphazenes depends on an intramolecular elimination of hydrogen chloride. This elimination occurs when n is small since the bulk of the product is the hexachlorocyclotriphosphazene with lower yields of the higher cyclics. This would indicate therefore that the loss of hydrogen chloride occurs by an intramolecular process at low molecular weights with the intermolecular process becoming increasingly important as the molecular weight increases. This is not unexpected since as the length of the chain increases the probability of the two ends meeting becomes less.

The intermolecular elimination will occur initially by loss of end groups from neighbouring molecules but, as the molecular weight and hence the polymer viscosity increases, elimination between the end group of one molecule and a mid-chain unit of a second molecule can become increasingly important; this appears to happen when the polymer has an intrinsic viscosity of about 0·20 dl/g. This latter reaction will lead to branching as shown below and eventually to crosslinking.

$$2\ Cl\text{--}(\text{--}PCl_2\text{==}N\text{--})\text{--}_n H \xrightarrow{\text{linear}} Cl\text{--}(\text{--}PCl_2\text{--}N\text{--})\text{--}_{2n} H$$

$$\xrightarrow{\text{branched}} Cl\text{--}(\text{--}PCl_2\text{==}N\text{--})\text{--}_{n-1} \overset{\overset{\displaystyle Cl}{|}}{\underset{\underset{\displaystyle (N\text{==}PCl_2\text{--})\text{--}_{n-x}Cl}{|}}{P}}\text{==}N\text{--}(\text{--}PCl_2\text{==}N\text{--})\text{--}_x H$$
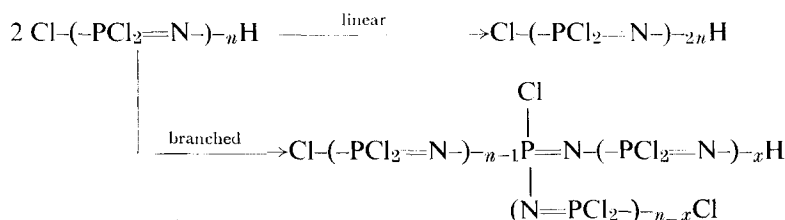
The reaction of hydrogen chloride with hexachlorocyclotriphosphazene has not been reported before. A most interesting result from this reaction was the composition of the cyclic material recovered from the reaction product. The presence of cyclic material other than the starting material would indicate the existence of an equilibrium occurring between the chlorophosphazenes. The reaction could have proceeded by ring opening followed by stabilization of the linear molecule with hydrogen chloride and then polymerization by reaction with more cyclic material. If this was the mechanism then the reaction attempted between the hydrogen chloride-stabilized material and hexachlorocyclotriphosphazene should have given a higher molecular weight product; no such product was found. Also the molecular weight was not noticeably affected by variation of the quantity of hydrogen chloride present

so long as more than a certain minimum amount was present. The temperature for the reaction was in the range in which thermal polymerization of the hexachlorocyclotriphosphazene occurs quickly to a crosslinked rubber. The role of the hydrogen chloride appears to be to inhibit branching and/or crosslinking.

The reaction of hydrogen chloride and *hexakis*(trifluoroethoxy)cyclotriphosphazene was attempted, because, if the linear compound had been formed and elimination had occurred by an intermolecular mechanism, only a linear polymer could have been formed. In the hydrogen bromide reaction, linear polymer would be formed by hydrogen bromide elimination and branching would occur by hydrogen chloride elimination. Consideration of the relative strength of the P—Br bond (65 kcal) and the P—Cl bond (79 kcal) suggests that a higher molecular weight polymer would be formed before branching occurred. This did not happen.

If the mechanisms of polymerization suggested[7] for the thermal polymerization of hexachlorocyclotriphosphazene are correct, with no depolymerization occurring, then the polymerization product would be expected to be a range of polymers of the type $(PNCl_2)_{3n}$ and the tetramer, pentamer and heptamer found in the product would not be expected. The only way these could be formed would be by depolymerization. A polymerization–depolymerization equilibrium would eventually be set up, the composition of the product depending on the relative stabilities of the components. If the ceiling temperature is in fact 600°C, as has been suggested[8], it would be expected that at 250°C the product would be predominantly polymeric.

A sample of poly(dichlorophosphazene) was heated in an evacuated tube at 250°C for 48 h. The product swelled in benzene but did not dissolve. It was extracted with benzene (4 × 48 h) and the combined extracts when evaporated to dryness were shown to contain no cyclic material. The linear high polymeric chlorophosphazene crosslinks readily once isolated, especially if heated. Thus it would appear that the depolymerization of the crosslinked rubber proceeds very slowly, if at all, at 250°C. Therefore the results suggest a depolymerization from the linear polymer to the cyclic chlorophosphazenes but, before a polymerization–depolymerization equilibrium is achieved, the linear polymer begins to crosslink thus constantly unbalancing the equilibrium.

Some preparations of substituted chlorophosphazenes were unsuccessful as the poly(dichlorophosphazene) used in their preparation had degraded. These occurred when the preparations involved 3-hydroxypentanol, 1,1,1,3,3,3-hexafluoropropan-2-ol and 2,4,6-trichlorophenol. A similar result was obtained for the attempted preparation of poly(diphenylphosphazene). The cause of this degradation was not investigated but it was possibly due to the bulky nature of the side groups.

It was known that catechol formed a spiro compound $N_3P_3(O_2C_6H_4)_3$ with hexachlorocyclotriphosphazene, one catechol molecule bonding twice to each phosphorus atom. The reaction of catechol with the linear chloro polymer did not produce a spiro derivative but a crosslinked product.

The polymerization of the cyclic fluorides to a crosslinked rubber has been reported elsewhere. From the reactions reported here it appears that the

42

formation of linear fluoro polymers occurs as a precursor of the crosslinked rubber, in a similar way to the chlorophosphazenes.

ACKNOWLEDGEMENT

Chemistry Department,
University of Manchester

REFERENCES

1 Lund, L. G., Paddock, N. L., Proctor, J. E. and Searle H. T. *J. Chem. Soc.* 1960, p 2542
2 Becke-Goehring, M. and Koch, G., *Chem. Ber.* 1959, **92**, 1188
3 Stokes, H. N. *J. Amer. Chem.* 1897, **19**, 782
4 Allcock, H. R., Kugel, R. L. and Valan, K. J. *Inorg. Chem.* 1966, **6**, 1709
5 Mirhej, M. E. and Henderson, J. F. *J. Macromol. Chem.* 1966, **1**, 187
6 Schenck R. and Römer, G. *Chem. Ber.* 1924, **57B**, 1343
7 Allcock, H. R. 'Heteroatom ring systems and polymers', Academic Press, 1967
8 Soulen, J. B. and Silverman, M. S. *J. Polym. Sci.* (*A*) 1963, **1**, 823

Polyphosphazenes:
Part 2. Characterization

G. ALLEN, C. J. LEWIS* and S. M. TODD

Thermal analysis of several phosphazene polymers,

$$\left[\begin{array}{c} OR \\ | \\ P{=}N \\ | \\ OR \end{array} \right]_n$$
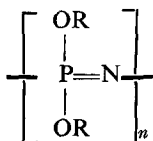
shows the effect of the substituent, R, on their thermal properties. Aryloxy-phazenes have higher transition temperatures than alkoxyphosphazenes and their thermal stability is superior. Fractionation and molecular weight studies are reported for three of the polymers, $R = -CH_2CF_3$, $-C_6H_4.C_6H_5$, and $-C_6H_5Cl$ and evidence for branched chains is obtained. Mechanical and dielectric properties are also reported for these three partially crystalline materials.

LITTLE characterization work has been carried out on the polyphosphazenes since, until recently, no soluble polymers had been reported, apart from small quantities of poly(dichlorophosphazene) extracted from the crosslinked rubber prepared from the polymerization of hexachlorocyclotriphosphazene. The study of chlorophosphazene polymers is complicated by the fact that in addition to their hydrolytic instability they crosslink to a gel in a few days in solution, and in a few hours when free of solvent.

There have been two reports[1,2] on the fractionation, molecular weight and intrinsic viscosity of poly(dichlorophosphazene). X-ray measurements have been made for poly(dichlorophosphazene)[3], poly[bis(trifluorethoxy)phosphazene][4] and poly(diphenoxyphosphazene)[4]; the repeat distances are reported as 0·492 nm (4·92 Å), 0·48 nm (4·8 Å) and 0·49 nm (4·8Å) respectively. Allcock[4] measured the transition temperatures of four polymers, $R = -CH_3$, $-C_2H_5$, $-CH_2CF_3$ and $-C_6H_5$.

In view of the lack of information on the phosphazene polymers we have undertaken some characterization of the phosphazene polymers prepared as described in Part 1 (pages 32–44).

THERMAL PROPERTIES

The glass transition and melting temperatures were determined using a DuPont D.T.A. Model 900 set at a heating rate of 20°C min^{-1}. Melting points were checked using a polarizing microscope, fitted with a hot stage, at a controlled rate of heating. The results summarised in *Table 1* show that most of the polymers have two first order transitions and that only the upper melting phenomenon leads to total disappearance of crystallinity.

* On leave from I.C.I. Petrochemical and Polymer Laboratory, The Heath, Runcorn, Cheshire.

Table 1 Glass and melting transition temperatures for some phosphazene polymers of the type $[PNR_2)_n$

Polymer R =	T_g [°C]	T_m [°C]	
		by D.T.A.	by microscopy
Cl	−64	−	−
1/1, Cl/OCH₂CF₃	−60	−	−
OCH₂CF₃	−70	83 and 240	238
OC₆H₄CF₃ (meta)	−35	−*	330
OC₆H₄Cl (para)	−12	165 and 405	> 350
OC₆H₃Cl₂ (2, 4)	2	195	210
OC₆H₄F (para)	−14	−	−
OC₁₀H₇ (β)	47	160*	> 350
OC₆H₄C₆H₅ (para)	43	160 and 398	> 350
OCH₂(CF₂)₆CF₃	−40	−	−

* The thermogram showed a strongly exothermic reaction above 300 C, probably degradation taking place which possibly masked the melting transition above 300°C

The glass transition temperatures range from −70 to 47°C and correlate roughly with the size of the substituent. Fluorination has a notable tendency to produce amorphous polymers with low T_gs. Considering the size of the side groups it is perhaps remarkable that high degrees of crystallinity are attained. However, models show that the flexible ether linkages enable the hydrocarbon side groups to pack efficiently. It is interesting to note that the corresponding alkyl and aryl phosphazenes are severely hindered and the preparation of these derivatives is particularly difficult.

THERMAL STABILITY

Thermogravimetric analysis was carried out on a modified DuPont D.T.A. Model 900 at a heating rate of 10°C min⁻¹ and under an atmosphere of dry nitrogen at a flow rate 40 ml min⁻¹. This technique overestimates the static performance of a polymer and so an isothermal method was also used. The intrinsic viscosity of a sample was redetermined after heating under vacuum for 8 h at 255°C. The results are shown in *Table 2*.

The thermal stability of the substituted phosphazene polymers depends markedly on the nature of the substituent group. During the course of this work Allcock[4] reported the stabilities of four alkoxy polyphosphazenes to be in the order:

$$R = —CH_2CF_3 > —C_6H_5 > —C_2H_5 > — CH_3$$
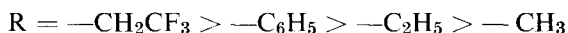
The last three were not prepared because of the known lack of stability of the corresponding hexa-substituted cyclotriphosphazenes (though Allcock's result was not known at the time). Our work shows that the aryloxy derivatives are more stable than the alkoxy. The latter are completely volatilized below 550°C whereas the aryloxy derivatives lose only 50% of their weight at 600°C. The volatiles evolved from the poly[di(*para*-phenylphenoxy)-phosphazene] contained *para*-phenylphenol, 4,4'-diphenyldiphenylether and

Table 2 Thermal stability of some phosphazene polymers of the type $(PNR_2)_n$

Polymer R =	Weight loss [%]	Temp. [°C]	Temp. of 10% loss, [°C]	Intrinsic viscosity	
				Initial	After 8 h at 255°C
Cl	100	550	410	–	–
Cl/OCH$_2$CF$_3$ (1:1)	68	500	380	–	–
OCH$_2$CF$_3$	100	500	410	0·82	0·2
OCH$_2$(CF$_2$)$_6$CF$_3$	100	540	425	–	–
OC$_6$H$_4$F (*para*)	75	500	385	–	–
OC$_6$H$_4$CF$_3$ (*meta*)	100	570	380	1·5	0·08
OC$_6$H$_4$Cl (*para*)	76	600	400	1·42	0·42
OC$_6$H$_3$Cl$_2$ (2, 4)	34	600	440	12	1·5*
OC$_6$H$_4$C$_6$H$_5$ (*para*)	45	600	470	1·2	0·72†
OC$_{10}$H$_7$ (β)	51	600	475	1·9	0·5‡
OC$_6$H$_4$C$_6$H$_5$ (*para*)	57	470	390	in moist nitrogen	
	35	450	370	in dry air	

* after 16 h at 255°C the intrinsic viscosity was 0·56 dl/g
† after 16 h at 255°C the intrinsic viscosity was 0·56 dl/g; after heating in air for 8h at 255°C the intrinsic viscosity was 0·19 dl/g
‡ after 16 h at 255°C the intrinsic viscosity was 0·45 dl/g

hexa(*para*-phenylphenol)cyclotriphosphazene. This suggests that the side groups interact forming crosslinks below the temperature at which the main chain degrades whereas in the alkoxy derivatives this does not occur and therefore complete volatilization is possible.

FRACTIONATION AND CHARACTERIZATION IN SOLUTION

With the exception of the —OCH$_2$(CF$_2$)$_6$CF$_3$ derivative, all the polymers were crystalline. Fractionation with respect to molecular weight was complicated by the fact that all polymers degraded in solution at the elevated temperatures at which liquid–liquid fractionation might have been attained. Thus we were forced to rely on liquid–crystal phase separation for the preparation of fractions. The amorphous fluorocarbon derivative was insoluble in all available solvents, so that the characterization of this polymer with respect to molecular weight was impossible.

Of the ten crystallizable polymers which were synthesized, three were chosen for further investigation on the basis of thermal properties. The solution properties of the 2,2,2-trifluorethoxy, *para*-chlorophenoxy and *para*-phenylphenoxy derivatives were studied in some detail. Only the intrinsic viscosities recorded in *Table 2* of Part 1 (page 40) were measured for the remaining soluble polymers. Gel permeation chromatography was possible only on the *para*-chlorophenoxy compound. No solvent could be found with a sufficiently large value of dn/dc to allow the other two polymers to be studied by g.p.c. Liquid–crystal fractionations were however conducted on all three samples and the solution properties of the fractions were investigated.

46

(1) Poly(2, 2, 2-trifluorethoxy)phosphazene

Two samples of this polymer were fractionated: sample A, intrinsic viscosity = 0·25 dl/g; and sample C, intrinsic viscosity = 0·66 dl/g. Three grams of sample A of this polymer were fractionated by cooling from 1 200 ml of methanol solution. A temperature of 55°C was maintained for 12 h to effect solution after which the temperature was lowered to 40°C and maintained for 2 days with slow stirring. The polymer which had precipitated was allowed to settle and the supernatant solution syphoned off through a glass plug. The solution was then cooled again and further fractions separated. The results obtained are shown in *Table 3*. Some degradation took place at this temperature. The first three fractions separated as crystalline solids and the fourth as a liquid and, as would be expected, the crystalline fractions did not separate with respect to molecular weight.

Table 3 Fractionation of trifluorethoxy sample A by cooling in methanol

Fraction	% wt.	$[\eta]$ dl/g in tetrahydrofuran at 25°C	Precipitation temperature [°C]
1A1	1·42	–	40
1A2	42·3	0·23	38
1A3	16·8	0·23	31
1A4	13·1	0·11	25
1A5	26·6	0·08	residue

Weight average $[\eta]$ = 0·17 dl/g; whole polymer $[\eta]$ = 0·25 dl/g

A further 3 g of sample A was fractionated by the addition of cyclohexane as non-solvent to a solution of the polymer in 1 200 ml acetone. The fractionation was carried out at 25°C, the non-solvent being added slowly until a second phase appeared. The second phase was allowed to equilibrate overnight and then separated. The results of the fractionation are shown in *Table 4*

Table 4 Fractionation of trifluorethoxy sample A by precipitation with cyclohexane from acetone solution

Fraction	% wt.	$[\eta]$ dl/g in tetrahydrofuran at 25°C	$\overline{M}_w$, light scattering in cyclohexanone at 25°C
2A1	2·4	0·43	–
2A2	10·2	0·37	–
2A3	31·1	0·49	55000
2A4	18·9	0·155	–
2A5	17·2	0·06	–
2A6	7·5	0·05	–
2A7	13·8	0·05	–

In this fractionation the weight average $[\eta]$ was 0·23 dl/g showing that negligible degradation had occurred. The first three fractions separated as crystalline solids but the remainder as liquids. The $\bar{M}_w$ measured for the highest viscosity fraction lay at the lower end of the range measurable by light scattering, due to the low value of dn/dc, and therefore only one fraction was studied.

Six grams of sample C were fractionated by precipitation with cyclohexane from acetone as described above for sample A. The results obtained are shown in *Table 5*. There was a little degradation and once again no separation with respect to molecular weight.

(2) *Poly[di(p-chlorphenoxy)phosphazene]*

Ten grams of this polymer were fractionated by cooling from 2 l of dimethylformamide. The experiment was carried out in a similar way to the fractionation of the trifluorethoxy polymer from methanol. The results are shown in *Table 6*. Little or no degradation took place in this experiment, probably because lower temperatures were used and the polymer had a higher thermal stability. The ratio of $\bar{M}_w/\bar{M}_n$ for the whole polymer obtained by gel permeation chromatography was 31.

(3) *Poly[di(p-phenylphenoxy) phosphazene]*

Fourteen grams of this polymer were fractionated by cooling from 3 l of dimethylformamide in a similar way as in (2) above. The results are shown in *Table 7*. Some degradation took place as a result of the higher temperature used for the crystallization.

SUMMARY OF SOLUTION PROPERTIES

Only in the low molecular weight part of the trifluorethoxy sample A has the fractionation proceeded with respect to molecular weight. Melting point determinations showed no variation between crystalline fractions of a given polymer. Thus it would appear that little or no fractionation occurred and this was confirmed for the *para*-chlorophenoxy polymer by obtaining the gel permeation chromatographs shown in *Figure 1* for the two fractions D4 and D6.

Inspection of the solution properties recorded in *Tables 3–7* reveals a random scatter of results with, for example, no correlation between $[\eta]$ and $\bar{M}_w$. We conclude that the polymer molecules are highly branched. The gel permeation curves (*Figure 1*) show an appreciable peak at low molecular weight. This is not removed by fractionation as might have been expected for linear material. It may well be due to branched material appearing with an effectively lower hydrodynamic volume. Such material could also account for the disparity in the ratio $\bar{M}_w/\bar{M}_n$ determined by the two different methods: i.e. (A) g.p.c. and (B) direct comparison of $\bar{M}_n$ from osmometry and $\bar{M}_w$ from light scattering.

Table 5 Fractionation of trifluorethoxy sample C by precipitation with cyclohexane from acetone solution

Fraction	% wt.	$[\eta]$ in T.H.F. at 25°C [dl/g]	$\bar{M}_w \times 10^{-5}$ *	$\bar{M}_n \times 10^{-5}$ †	$A_2 \times 10^4$ [cm³ gm⁻² mole] light scattering	osmometry	Heterogeneity ratio $\bar{M}_w/\bar{M}_n$
C1	19·63	0·59	4·62	0·65	0·35	Nil	7·1
C2	6·37	0·59	5·87	—	0·41	—	—
C3	6·08	0·71	3·77	1·32	0·34	0·73	2·25
C4	8·69	0·75	2·96	—	0·47	—	—
C5	19·19	0·67	4·24	—	0·41	—	—
C6	17·63	0·64	3·59	0·65	0·43	Nil	5·5
C7	22·42	0·42	5·69	—	0·89	—	—

* Light scattering in cyclohexanone at 25°C
† Osmometry in methyl ethyl ketone at 25°C
Weight average $[\eta] = 0.59$ dl/g; whole polymer $[\eta] = 0.66$ dl/g

Table 6 Fractionation of p-chlorphenoxy polymer by cooling in dimethylformamide

Fraction	% wt.	Crystallization temp. T_c [°C]	$[\eta]$ in cyclohexanone at 25 C [dl/g]	$\bar{M}_w \times 10^{-5}$ *	$\bar{M}_n \times 10^{-5}$ †	$A_2 \times 10^4$ [cm³/g⁻² mole] light scattering	osmometry	Heterogeneity ratio $\bar{M}_w/\bar{M}_n$ experimental	G.P.C.
D1	3·98	36·8	1·40	10·4	1·245	3·31	1·85	8·3	—
D2	7·84	36·1	1·39	6·26	0·947	2·87	3·54	6·6	—
D3	21·22	35·8	1·17	4·54	1·096	3·42	4·47	4·2	—
D4	7·17	31·5	1·46	6·72	0·923	4·85	3·21	7·3	17·3
D5	25·74	30·0	2·25	15·12	0·918	7·28	1·99	16·5	—
D6	13·81	26·2	2·22	7·10	1·016	4·85	2·18	6·9	15·7
D7	20·25	Residue	0·95	5·78	0·350	1·43	—	16·5	—

* Light scattering in cyclohexanone at 25°C
† Osmometry in cyclohexanone at 65°C
Weight average $[\eta] = 1.6$ dl/g; whole polymer $[\eta] = 1.42$ dl/g

49

D

Table 7 Fractionation of *p*-phenylphenoxy polymer by cooling in dimethylformamide

Fraction	% wt.	Crystalization temp., T_c [°C]	$[\eta]$ in cyclohexanone at 50°C [dl/g]
E1	9·27	48·0	0·60
E2	10·13	46·0	0·79
E3	34·9	45·4	0·73
E4	15·64	36·0	0·61
E5	5·42	34·0	0·58
E6	24·65	Residue	0·56

Weight average $[\eta] = 0·66$ dl/g; whole polymer $[\eta] = 0·84$ dl/g
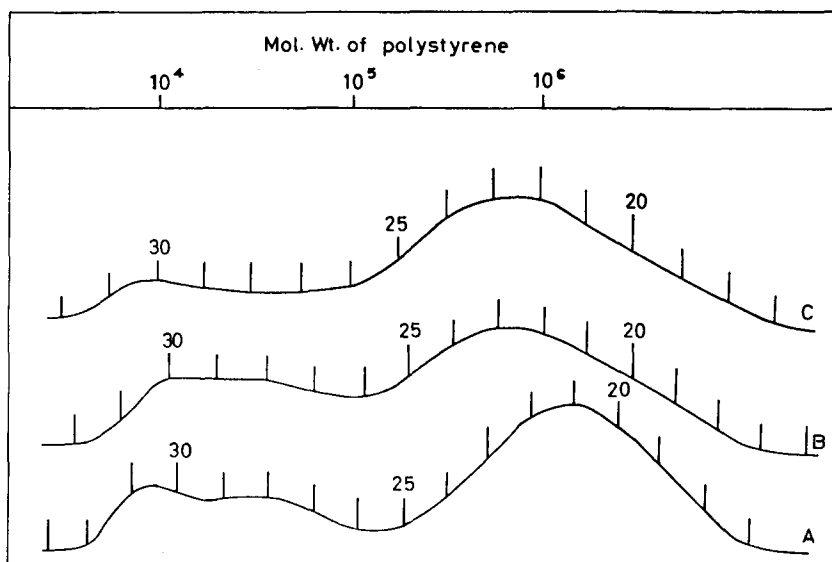
Figure 1 G.P.C. chromatograms for *p*-chlorphenoxy polymer:
A, whole polymer; B, fraction D4; C, fraction D6

Further evidence for branching comes from the light-scattering studies. In no case was the average radius of gyration of the polymer fraction large enough to be measured by light-scattering at $\lambda = 546·0$ nm (5 460 Å). For a freely rotating chain with two fixed valence angles:

$$S_0^2 = \frac{nl^2 (1 - \cos \theta_1) (1 - \cos \theta_2)}{6 (1 - \cos \theta_1 \cos \theta_2)}$$

where l is the bond length and θ_1 and θ_2 are the bond angles. Substituting

bond angles and lengths determined by Giglio on poly(dichlorophosphazene) gives $(\bar{S}_0^2)^{\frac{1}{2}} = 40\cdot0$ nm (400 Å) for the p-chlorophenoxy derivative linear chain of molecular weight 10^6. These calculated unperturbed dimensions are usually smaller than measured values and furthermore chain expansion would obtain in our experiments since theta-conditions were not used. Therefore, if the polymer chains were linear it should have been possible to determine the unperturbed dimensions of the polymer by light scattering.

We conclude that all our phosphazene polymers have branched chains and broad molecular weight distribution.

MECHANICAL AND DIELECTRIC PROPERTIES

The three polymers whose properties were discussed above were also ex-amined in the bulk state. Dynamic, mechanical, and dielectric loss measure-ments have been made over a range of frequencies and temperatures.

(a) Torsion pendulum

The sample was mounted in a torsion pendulum similar to that described by Nielsen[5,6]. The modulus and loss tangent of the sample were measured at temperatures from $-150°C$ to the temperature at which the sample became too soft for further measurement.

(b) Vibrating reed

The apparatus used for this determination was developed by Robinson[7]. The sample, in the form of a thin reed, was clamped at one end and its reson-ance frequency measured at a range of temperatures from $-150°C$ to the temperature at which the sample became too soft for further measurements.

(c) Dielectric measurements—low frequency

The measurements at frequencies 10^{-1} to 10^2 c/s were made using a bridge described by Scheiber[8]. The bridge is based on the Wheatstone bridge principle and uses a substitution technique. The detectors used were a general radio tuned amplifier, and null detector type 1232A for 30 to 100 c/s and a D.C. electrometer for the lower frequencies. The sample in the form of a disc 2 in diameter $\times \frac{1}{16}$ in thick with metal foil electrodes attached with a thin layer of grease was mounted in a three terminal cell to avoid fields and edge effects. The measurements were made at a range of temperatures near the β transition of the polymer.

(d) Dielectric measurement—audio frequency

The measurements at frequencies of 10^2 to 10^4 c/s were made using a general radio capacitance bridge type 1615A. This transformer ratio-arm bridge[9] was used in conjunction with the general radio tuned audio oscillator type 1317A and the detector used for 30–100 c/s in (c). The sample used was the same as in (c), the measurements being taken on both bridges simul-taneously. The measurements were taken at a range of temperatures from $-150°C$ to above the β transition of the polymer.

51
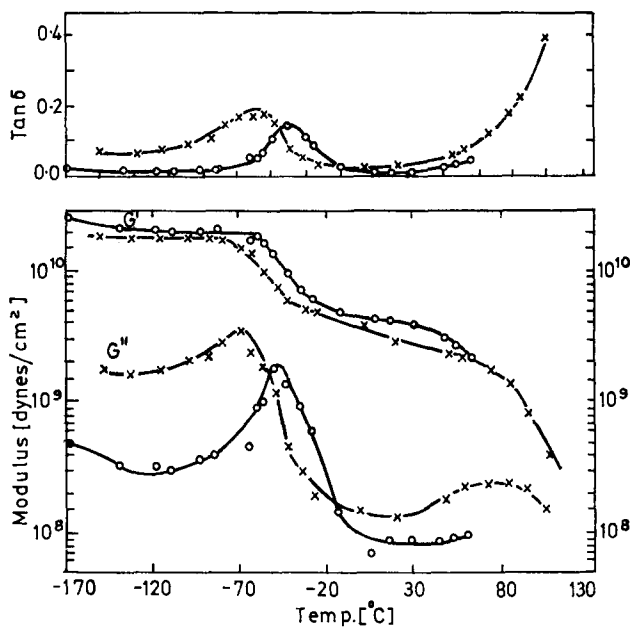
Figure 2 Dynamic mechanical measurements for trifluorethoxy
polymer:
×, torsion pendulum (∼1 c/s); ○, vibrating reed (∼300 c/s)
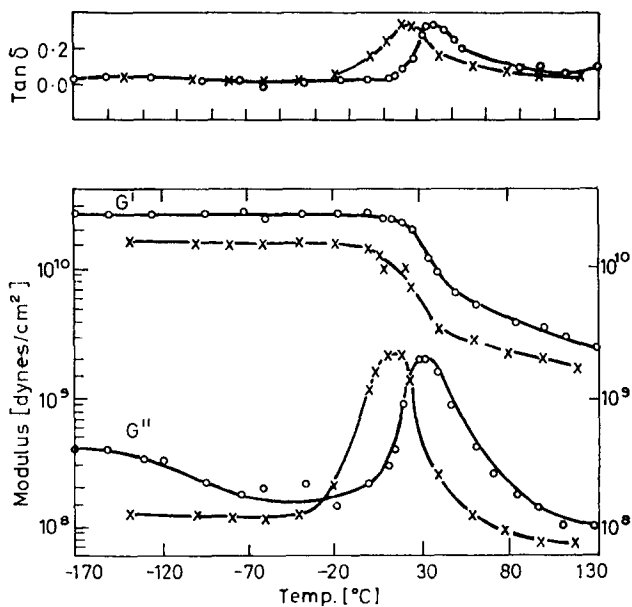
Figure 3 Dynamic mechanical measurements for *p*-chlorophenoxy
polymer:
×, torsion pendulum (∼1 c/s); ○, vibrating reed (∼300 c/s)
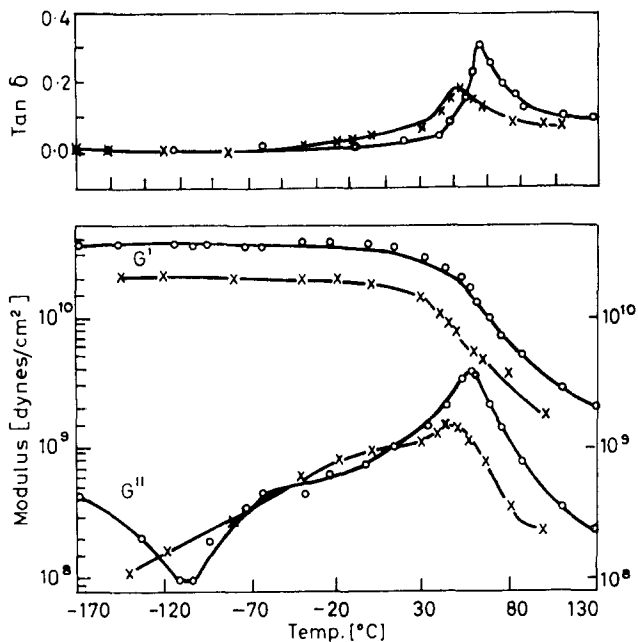
Figure 4 Dynamic mechanical measurements for *p*-phenylphenoxy
polymer:
×, torsion pendulum (~1 c/s); ○, vibrating reed (~300 c/s)

(e) *Results*

The results of the mechanical measurements are shown in *Figures 2, 3* and *4* and the dielectric measurements in *Figures 5, 6* and *7*. The loss process in polymers may be considered as an activated rate process. The measurement of the temperature dependence of this loss process can be used to evaluate the activation energy associated with the loss from the slope of the plot of $\log(f_m)$ against $1/T$. This plot is shown in *Figure 8* for the three polymers. The results obtained for the activation energies are shown in *Table 8*.

Table 8 Activation energy from mechanical and
dielectric loss measurements for the β dispersion

Polymer	Activation energy ΔH^* [kcal/mole]
Trifluorethoxy	47
p-Chlorphenoxy	102
p-Phenylphenoxy	81·5

53

For semi-crystalline polymers the loss process associated with the melting transition is termed the α loss region. The loss region of next lower temperature is termed β, the next the γ and so on. The same terminology is used for both mechanical and dielectric processes. The loss regions measured by the two techniques as shown by G'' and ϵ'' do not always coincide since the relaxation mechanism giving rise to the loss may be different for the two methods. There is a good agreement in the results reported here by the two techniques.
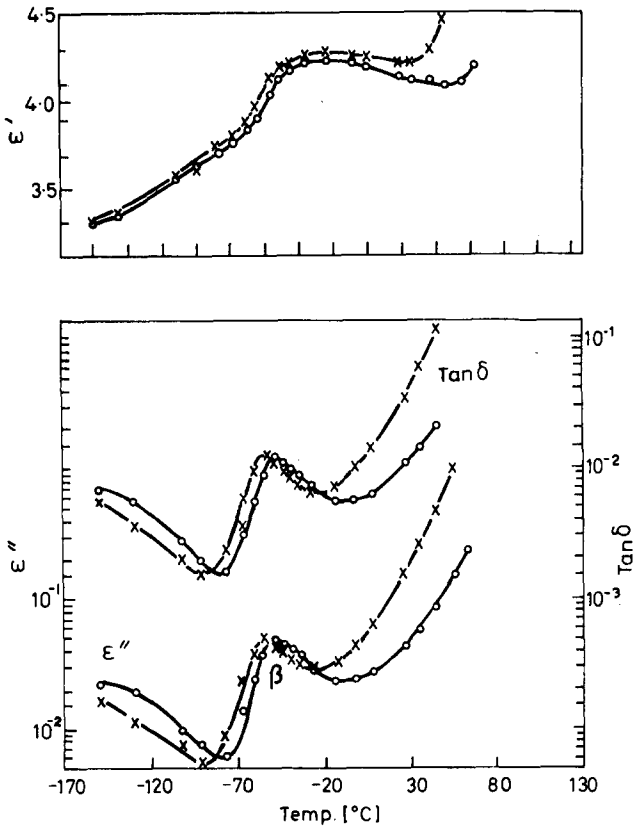
Figure 5 Dielectric measurements for trifluorethoxy polymer: $\times$, 1 kc/s; $\bigcirc$, 10 kc/s

The α loss associated with the melting transition may be seen for the trifluorethoxy in *Figures 2* and *5*, the loss begins at temperatures above 50°C. In the case of the other two polymers measurements could not be made at the appropriate temperatures so that the presence of an α loss could not be confirmed.

The β loss region for all three polymers coincides with the glass-rubber transition in the amorphous phase. The activation energy for the mechanical and dielectric loss processes are the same for the p-chlorphenoxy polymer,
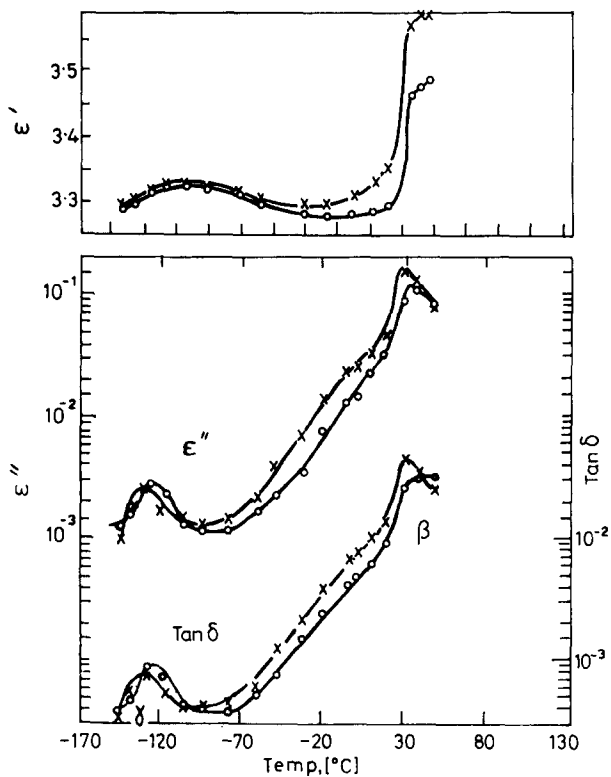
Figure 6 Dielectric measurements for p-chlorophenoxy polymer: ×, 1 kc/sec; ○, 10 kc/sec
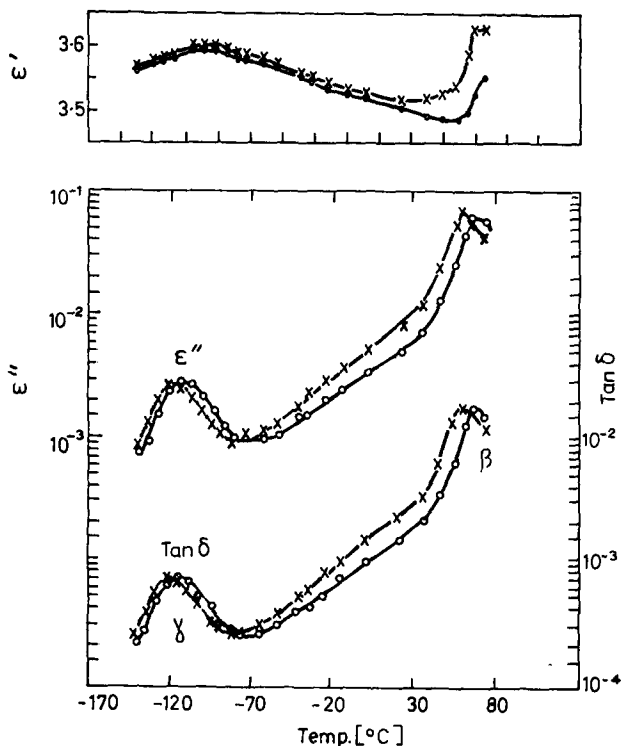
Figure 7 Dielectric measurements for *p*-phenylphenoxy polymer:
×, 1 kc/sec; ○, 10 kc/sec

the same is also true for the *p*-phenylphenoxy polymer. This suggests that the
mechanism for the loss is similar for the mechanical and dielectric processes
in these two polymers. For the trifluorethoxy polymer the activation energy
for the mechanical process is more strongly temperature dependent than for
the dielectric process, suggesting that the mechanism for the two processes
are different. The γ loss region in the case of the trifluorethoxy polymer
occurs at such a low temperature that only the high temperature side of the
peak can be seen in *Figures 2* and *5*. This loss probably lies in the region
$-160°C$ to $-200°C$ so that either lower temperatures or higher frequencies
than used here are required for its measurement. In the other two polymers
the size of the γ loss is much smaller than the β loss and the mechanical
techniques are not sensitive enough to detect it. The relaxation mechanism
giving rise to this loss is not known. The fact that the loss in the
p-chlorophenoxy and *p*-phenylphenoxy are of similar magnitude and position
would suggest that it arises from side-group rotation since these two groups

56
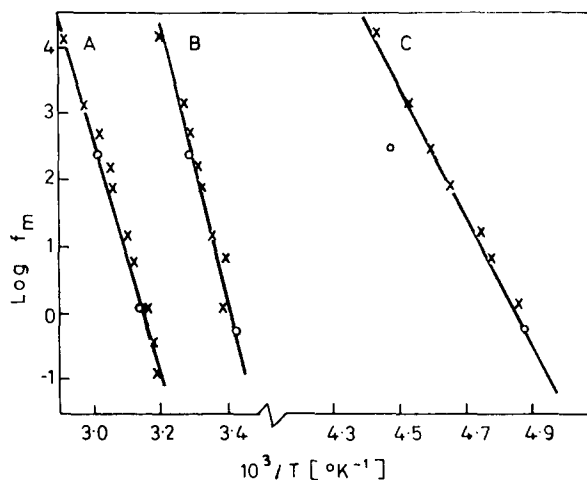
Figure 8 Location of loss maxima of dielectric (×) and mechanical
(○) measurements for the dispersion.
A, *p*-phenylphenoxy; B, *p*-chlorophenoxy; C, trifluorethoxy

are of similar size whereas the somewhat smaller trifluorethoxy side group
has a correspondingly lower temperature for the γ loss.

DIFFRACTION STUDIES

X-ray examination of these polymers showed them to give the typical
pattern exhibited by semi-crystalline polymers. Chain repeat distances for
the three polymers selected for further characterisation and also for the
β-naphthoxy polymer, were all between 0·48 and 0·49 nm (4·8 and 4·9 Å).
These values are in agreement with the values (0·48 and 0·49 nm) reported
by Allcock[4] for the trifluorethoxy and the phenoxy polymers respectively
and also with the value (0·492 nm) reported by Giglio *et al*[3] for the cross-
linked poly(dichlorophosphazene). Thus the size of the substituent has no
effect on the chain repeat distance. We conclude that the side-groups must
fit into the chain without causing undue steric hindrance, even in the case of
the β-naphthoxy derivative.

Heating the polymers to above their lower first order transition causes
a specimen to lose only part of its order. This is in keeping with the observa-
tion of two first order transitions. Order is still retained in the lateral dimen-
sion. This is shown in *Figure 9*. The upper figure shows the X-ray diffraction
pattern obtained for the trifluorethoxy at room temperature, the lower one
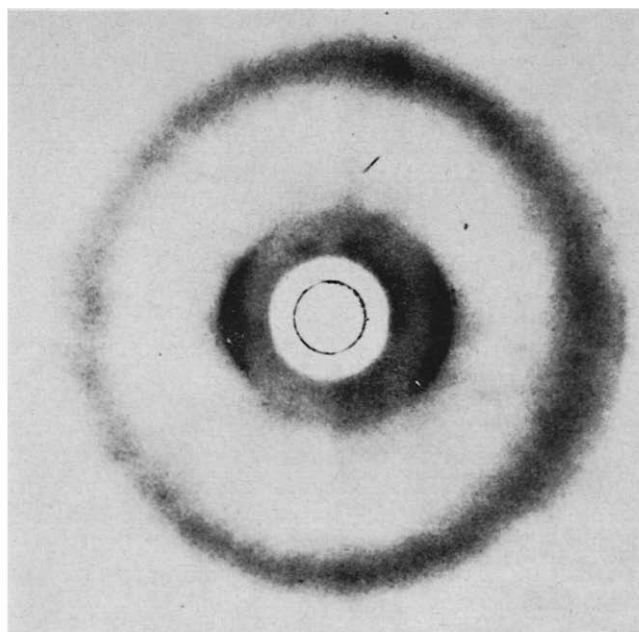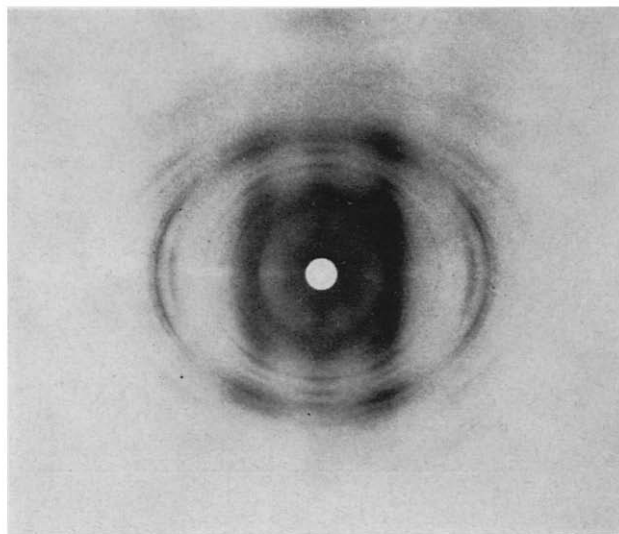
Figure 9 X-ray diffraction pattern obtained from the trifluorethoxy polymer
(a) at room temperature, (b) at 90°C

is of the same polymer sample heated at 90°C showing only a reflection corresponding to a lateral dimension of 1·1 nm (11 Å). The three dimensional order shown by the upper figure reappears on cooling to room temperature.

FIBRE AND FILM FORMING PROPERTIES

The p-phenylphenoxy polymer formed fibres quite readily from the melt. Unfortunately under the shear conditions required to form the fibre at 225°C the polymer degraded rather rapidly so that only a small quantity of fibre was prepared. The mono-filaments of diameter 50–60 μm, were submitted to tensile test. In the undrawn state the Young's Modulus was $2\cdot14 \times 10^{10}$ dyn/cm^2 ($2\cdot14 \times 10^9$ N/m^2) which is about the same as undrawn nylon. The other two polymers formed fibres at lower temperature but were brittle due to their high degree of crystallinity and were not tested further.

The p-chlorphenoxy polymer could be cast from tetrahydrofuran at room temperature into clear thin films (8–10 $\times$ 10^{-3} nm thick) which were similar in appearance to polyethylene. The p-phenylphenoxy and the trifluorethoxy polymers gave opaque brittle films and were not tested further. Samples of the p-chlorphenoxy film were immersed in water at room temperature for 68 h, other samples were boiled in water for 8 h to test for hydrolytic stability. The samples were then compared by tensile test, at a speed of 20 mm/min with untreated samples of the film. The results are shown in *Table 9*.

Table 9 Tensile test of poly[di(p-chlorphenoxy)phosphazene] films

Sample	Untreated film	After 68 h in water at 25°C	After 8 h in water at 100°C
Initial Modulus kg/cm^2	4700	3900	3400
Yield Stress kg/cm^2	210	220	180
Elongation %	100	83	108

The comparative tests suggests that water does have a slight reaction with the polymer thus causing the tensile modulus to drop. The tensile strength of the untreated film falls between polyethylene which has an initial modulus of approximately 10^3 kg/cm^2 (10^8 N/m^2) and polypropylene which has one of approximately 10^4 kg/cm^2 (10^9 N/m^2).

ELECTRICAL CONDUCTIVITY

The resistivity of the p-chlorphenoxy polymer has been measured by Professor D. Eley *et al* for compressed discs of thickness 0·07 mm. From the temperature dependence of the resistivity the energy gap can be estimated from the expression $\rho = \rho_0 \exp(\Delta\epsilon/2kT)$ where ρ is the resistivity in ohm cm. For poly (p-chlorphenoxyphosphazene)$\Delta\epsilon = 3\cdot2$ eV.

Thus the polymer has a very low conductivity when compared to the carbon polyene polymers, in fact the energy gap measured is so large that it may not represent the conductivity of the sample but the energy for charge injection by the electrode.

If the π bonds in the phosphazene chain were delocalized, as suggested for the cyclic oligomers, then the conductivity would be expected to be comparable to that of the carbon polyene polymers which have a similar type of chain i.e. —C=C—C=C—.

ACKNOWLEDGEMENT

Chemistry Department,
University of Manchester

REFERENCES

1 Patat, F. and Kollinsky, F. *Makromol. Chem.* 1951, 6, 292
2 Knoesel, R., Parrod, J. and Benoit, H. *Comp. Rend.* 1960, **251**, 2944
3 Giglio, E. Pompa F. and Ripamonti, A. *J. Polym. Sci.* 1962, **59**, 293
4 Allcock, H. R., Kugel, R. L. and Valan, K. J. *Inorg. Chem.* 1966, **5**, 1709
5 Nielson, L. E., 'Mechanical Properties of Polymers,' Reinhold, 1962
6 Nielsen, L. E. *A.S.T.M. Bull.*, 1950, 165, 48
7 Robinson, D. *J. Sci. Instr.* 1955, **32**, 2
8 Scheiber, D. J. *J. Res. Nat. Bur. Stand.* 1961, **65c**, 1
9 McCrum, N. G., Read, B. E. and Williams, G., 'Anelastic and dielectric effects in polymeric solids, Wiley, 1967

Notes and Communications

Radiolysis and photolysis of polyphenylvinylketone

C. DAVID, W. DEMARTEAU, F. DEROM and G. GEUSKENS

Valuable information concerning the mechanism of chain breaking or crosslinking under the effect of γ-irradiation can be obtained by the comparative study of the photolysis and radiolysis of polymers. The present work is concerned with the effect of γ-irradiation on polyphenylvinylketone (PPVK). Main chain scission was previously shown to occur when this polymer is irradiated with ultra-violet light of 366 nm[1]. Acetophenone and ethylene are formed during the photolysis and radiolysis of the model compound butyrophenone[2-4]. In this last case Norrish type 2 scission due to reaction of the first $n-\pi^*$ triplet state of the ketone has been shown to occur[2, 4, 5].

EXPERIMENTAL

Monomer and polymer synthesis and ultra-violet irradiation techniques have already been described[1]. Gamma irradiations were carried out in a Co^{60} Gammacell 200, the intensity of which was 0·53 Mr/h. The temperature in the source was 36 °C. The polymer was irradiated in sealed bulbs as a fine powder outgassed at room temperature under a pressure of 10^{-5} torr.

Molecular weights before and after irradiation were determined by viscosity measurements in benzene at 25 °C using the approximate equation:

$$[\eta] = 10^{-4} M_v^{0·7}$$

Naphthalene and diphenyldisulphide were added to the polymer solution before casting the films for u.v. irradiation.

For γ-irradiation, the additives were dissolved in a small amount of polymer precipitant which was added to the PPVK powder and slowly evaporated. The mole fraction of these additives in the polymer was determined by vapour phase chromatography after outgassing the samples.

RESULTS AND DISCUSSION

The molecular weight of the polymer was found to decrease under the influence of γ-irradiation. The infra-red spectra of the initial polymer[1] remains unchanged even after absorption of 50 Mr. Assuming $M_v = M_w$ and $M_n = M_w/2$, the number of main chain scissions $(M_{n_0}/M_n) - 1$ as a function of dose r is reported in *Figure 1*.

A straight line is obtained according to the equation:

$$\frac{M_{n_0}}{M_n} - 1 = \frac{G_s \times M_n \times r \times 6·24 \times 10^{11}}{6·02 \times 10^{23}}$$

where G_s, the number of main chain scission per 100 eV absorbed was found to be 0·35. The behaviour of PPVK under γ-irradiation is thus not in agreement with the empirical rule of Miller *et al*[6]. This states that crosslinking occurs when each carbon of the main chain of a vinyl polymer carry at
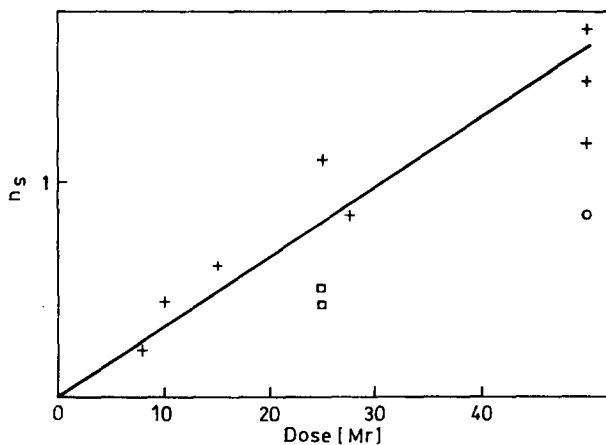
Figure 1 Number of scissions per chain of polyphenylvinylketone
($M_{n_0} = 87500$) *versus* irradiation dose (in Mrads)
+ PPVK without additive
○ PPVK containing 3 mole % naphtalene
□ PPVK containing 1·2 mole % diphenyldisulphide.

least one hydrogen atom; whereas if a tetra-substituted carbon atom is present in the main chain, a decrease in molecular weight occurs.

The photolysis of PPVK as solid films, or in solution, has been studied recently[1]. Main chain scission was also observed in that case and was explained by Norrish type 2 degradation. A quantum yield of 0·3 was obtained for the polymer irradiated in benzene solution.

A comparative study of the effect of specific radical scavengers or excited state quenchers on photochemical and radiochemical reactions is often useful in determining the nature of the active intermediates involved in the reaction. Diphenyldisulphide (Ph–S–S–Ph) is a free radical scavenger and naphthalene is known to be a quencher of the first excited n–π^* triplet state of many aromatic ketones, including butyrophenone[2, 7, 8]. Examination of *Table 1* and *Figure 1* shows that photochemical as well as radiochemical chain scissions of solid PPVK are inhibited to some extend by naphthalene and Ph–S–S–Ph. A strong inhibiting effect on the formation of acetophenone due to triplet energy transfer from the ketone to naphthalene had been observed previously during u.v. or γ-irradiation of butyrophenone in solution and in the present work for butyrophenone irradiated as a pure liquid.

Our results demonstrate the participation of radicals and of excited n–π^* triplet state of the ketone group during the radiolysis and photolysis of PPVK. The Norrish type 2 scission most probably occurs by reaction of this triplet state for PPVK as for butyrophenone. Some triplet participation has also been observed in the photoreduction of benzophenone induced by

62

Table 1 Effect of naphthalene and diphenyldisulphide on the photolysis and radiolysis of polyphenylvinylketone and butyrophenone

	Additive	Irradiation	X	$(X_0 - X)/X_0$ $\times 100$	Comments	Ref.
PPVK	$C_{10}H_8$ (3 mole %)	γ 50 Mr	0·86*	43*	Powder	This work
	Ph–S–S–Ph (1·2 mole %)	γ 25 Mr	0·43*	40*	Powder	This work
	$C_{10}H_8$ (3 mole %)	u.v. 1·8 $\times$ 10^{-5} E	0·44*	66*	Film	This work
	Ph–S–S–Ph (3 mole %)	u.v. 1·8 $\times$ 10^{-5} E	1·02*	15*	Film	This work
But	$C_{10}H_8$ (4·8 $\times$ 10^{-2} mole l^{-1})	γ 0·9 Mr	0·075†	>90†	4·9 $\times$ 10^{-2} mole l^{-1} in benzene solution	(4)
	$C_{10}H_8$ (10^{-2} mole l^{-1})	γ 25 Mr	—	>90†	Pure liquid	This work
	Ph–S–S–Ph (10^{-2} mole l^{-1})	γ 25 Mr	—	>90†	Pure liquid	This work
	$C_{10}H_8$ (10^{-3} mole $^{-1}$)	u.v.	0·14‡	67‡	10^{-1} mole l^{-1} in benzene solution	(2)

* X = Number of scissions per chain
† X = G value of acetophenone formation
‡ X = φ value of acetophenone formation
Subscript zero refers to the experiment without additive.

γ-rays in the presence of isopropanol[9] and during the radiolysis of cyclopentanone[10]. The radicals formed in the photolysis most probably are short-lived intermediates in the Norrish type 2 scission[11]. In the radiolysis, other scavengable radicals can also be formed that are responsible for other types of chain breaking involving no triplet state.

Service de Chimie Générale II,
Université Libre de Bruxelles,
Brussels, Belgium

REFERENCES

1 David, C., Demarteau, W. and Geuskens, G. *Polymer Lond.* 1967, **8**, 497
2 Baum, E. J. Thesis, University of California 1965
3 Coyle, D. J. *J. Phys. Chem.* 1963, **67**, 1800
4 Brown, W. G. *Chem. Communications* 1963, p 195
5 Wagner, P. J. and Hammond, G. S. *J. Amer. Chem. Soc.* 1966, **88**, 1245
6 Miller, A. A., Lawton, E. J. and Balwit, J. S. *J. Polym. Sci.* 1954, **14**, 503
7 Ermolaev, V. L. *Soviet Physics Uspekhi* 1963, **80**, 333
8 Moore, W. M. and Ketchum, M. *J. Amer. Chem. Soc.* 1962, **84**, 1369
9 von Sonntag, C., Lang, G. and Schulte-Frohlinde. D. 'The Chemistry of ionization and excitation' (G. R. A. Johnson and G. Scholes, Eds) Taylor and Francis, 1967
10 Dunion, P. and Tumbore, C. N. *J. Amer. Soc.* 1965, **87**, 4211
11 Wagner, P. J. *Tetrahedron Letters* 1967 p 1753

Gamma relaxation in epoxy resins and related polymers

G. A. Pogany

A torsion pendulum has been employed to investigate the low temperature (γ) relaxation in epoxy resins and in certain related rigid polymers. In epoxy resin cured with diethylene triamine the relaxation between $-80°C$ and $-40°C$ is caused by the crankshaft type rotation of the segment —CH_2—$CH(OH)$—CH_2—O—. The same is responsible for the lowering of the glassy modulus at $20°C$ as shown by the increase in the creep compliance of the resin with increasing cure. Low temperature relaxations of various magnitudes have been found in all the following polymers: epoxy resin cured with acid anhydride, phenoxy resin, polycarbonate, polysulfone, polyimide, polyphenylene oxide, Bakelite, and a Friedel-Crafts polymer. It is suggested that these relaxations are caused by some kind of non-rotational wriggling motion of segments containing benzene rings. The temperature of these relaxations may depend on the rigidity of links between the benzene rings.

Almost every known polymer has a low temperature relaxation, except where two bulky side groups are positioned regularly on every second carbon atom[1,2]. The exact nature of these relaxations is still uncertain, but in linear aliphatic polymers they have been attributed to some form of localised motion of groups, smaller than a single polymer molecule[3-11].

Schatzki[12] suggested that six carbon atoms in a diamond lattice can form a crankshaft if the two terminating atoms are co-linear, and the four central carbon atoms can then rotate without requiring cooperative motion from others. Andrews and Hammack[13] disagreeing with the crankshaft theory, suggest that intermolecular bond loosening is really responsible for all relaxation, because breaking down of intermolecular bonds makes the motion possible.

Heijboer[14] found that polymers with cyclohexyl groups show a relaxation at about $-80°C$ which is caused by the transformation between chair–chair configuration of the cyclohexyl group. Benzene rings cannot perform such relaxation, but Sinnott[15], Woodward[16], and Haberland and Carmichael[17] suggest that oscillation or wagging of the phenyl groups can cause low temperature relaxation, and their motion is influenced by steric or energy factors. Van Hoorn[19] examined a series of linear epoxy compounds (polyhydroxyethers) and observed three relaxations, the one with the lowest temperature, according to Van Hoorn, is caused by ring rotation.

The low temperature (γ) mechanical relaxation in crosslinked epoxy resin was first reported by Kline[20] who, using medium frequency measurements, found the peak at about $-30°C$. Kline noticed that the area under the peak increases with increasing cure temperature but failed to observe any corresponding changes in the modulus. Kline and Sauer[21] also found that water had little effect on the γ peak. This paper investigates the nature of the γ relaxation in crosslinked epoxy resins and in related polymers. A comparison is drawn between these relations and an hypothesis is presented to explain their cause.

EXPERIMENTAL

The modulus (G) and logarithmic decrement (δ) of the specimens were measured with a torsion pendulum in free vibration at 0·67 c/s frequency between $-180°C$ and $+250°C$. Creep measurements were carried out by converting a torsion pendulum into a creep apparatus. A torque was applied by passing an electric current through a coil in a magnetic field causing it to rotate. The techniques are well known and have been described in detail elsewhere[22, 23].

Epoxy resin specimens were cast in the laboratory from purified diglycidyl ether of *bis*phenol A and different amounts of diethylene triamine (DETA) curing agent. After curing for one week at 25°C the specimens of $100 \times 10 \times 1·5$ mm were machined out of the cast block. The amine cured epoxy resin is built up from the following units:
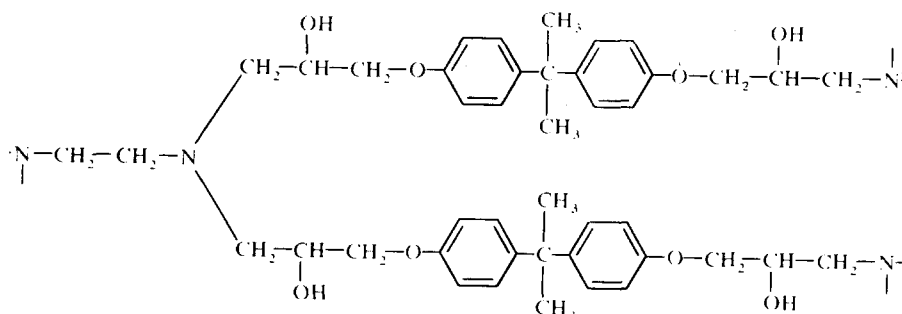
The acid anhydride cured epoxy resin was prepared from the commercial Epikote* 834 and methyl nadic anhydride (MNA). This resin contains ether and ester linkages[24].

MNA   *Typical link*
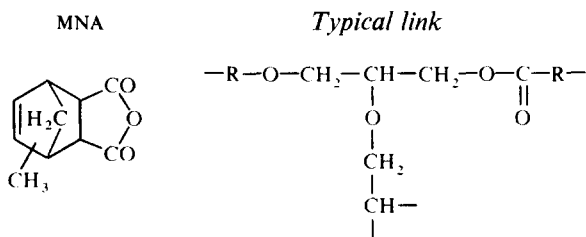
(where R represents a ring structure)

All other polymers have been provided by their manufacturer, and are listed below.

---

*Registered trade name of Shell Chemicals UK Ltd.

The *bis*phenol A group forms part of several commercial linear polymers:

Polycarbonate[25]
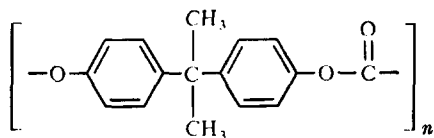
Polysulphone[26]
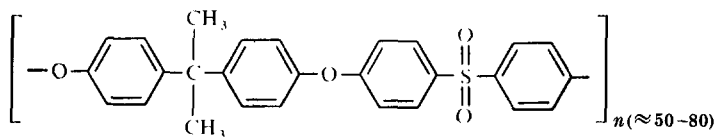
Phenoxy resin[27]
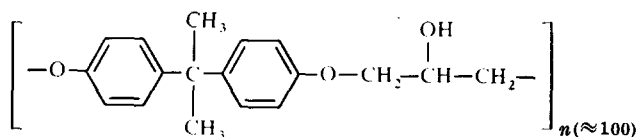
And there are some other polymers commercially available which also have ring-structures in their backbone:

Polyimide[28]
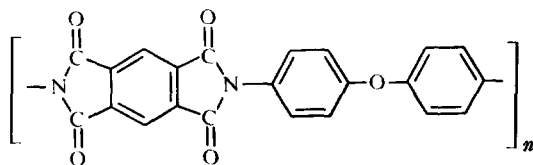
Poly(phenylene oxide)[29]
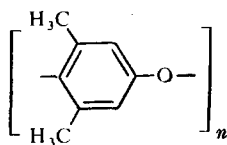
Friedel-Crafts polymer[30] (developed at R.A.E. Farnborough)
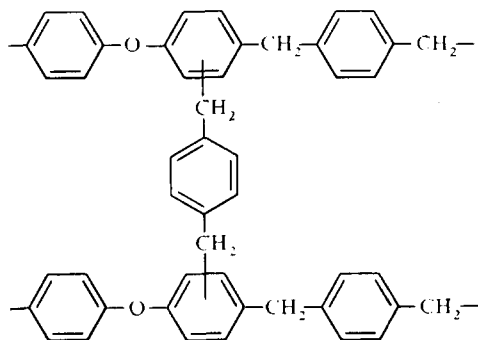
Bakelite[31]
  Novolak type:
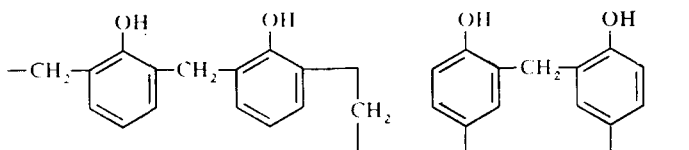
  Resole type:
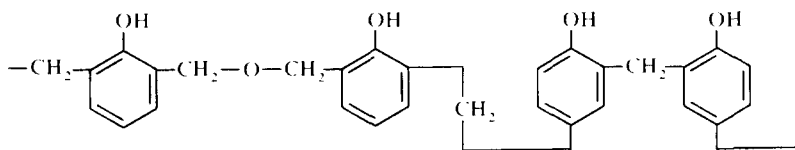
RESULTS AND DISCUSSION

The effect of cure on the γ peak

The effect of cure on the γ relaxation was investigated in two basic experiments. In the first experiment the effect of heating a specimen cured at room temperature only was examined. In the second experiment changes between the γ relation of specimens with different degrees of permanent undercure were established. All experiments were carried out in the torsion pendulum, in 10–15°C intervals, on cooling from room temperature to −180°C.

The effect of heating on the γ peak can be seen in *Figure 1*. A specimen prepared from the diglycidyl ether of *bis*phenol A with the stoichiometric amount of diethylene triamine (DETA), at 25°C without any high temperature post-cure was heated in steps of 40°C, and held at each new temperature for at least 5 h. After each step, the specimen was cooled and its γ peak measured. A continuous increase in the area under the peak, especially its broadening at higher temperatures, can be seen. There was little further change after the 100°C cure, apart from the surface effects which are discussed in a separate paper[32]. (For more precise measurements cf. *Figure 5*.)
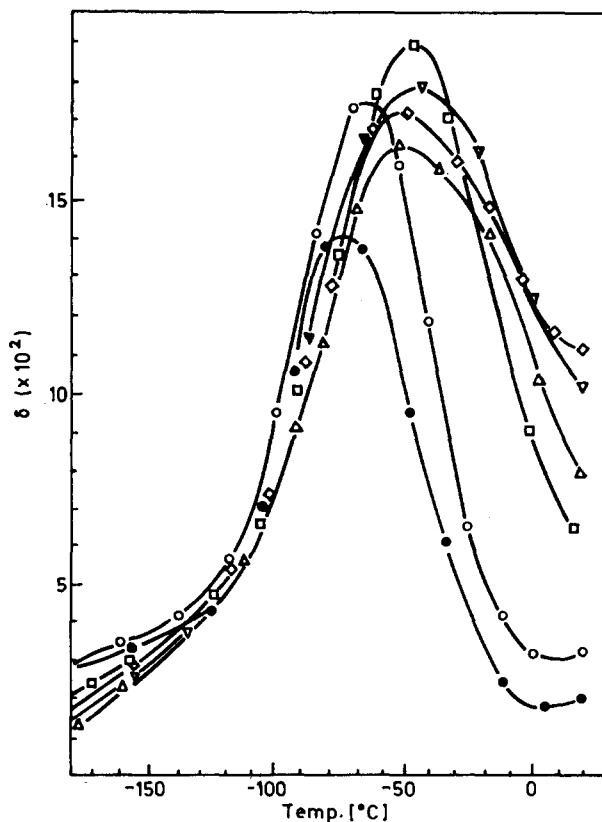
Figure 1 Changes in the γ peak with cure temperature
●, no heat treatment   ◇ , 5 h at 140°C N_2 purge
○, 8 h at 60°C N_2 purge   △, 5 h at 190°C no N_2
□, 6 h at 100°C N_2 purge   ▽, degraded surface removed

In the next experiment five samples made from the purified diglycidyl ether of *bis*phenol A cured with 4, 8, 12, 16 and 20 parts per hundred (p.h.r.) of diethylene triamine (DETA) were examined. Since the stoichiometric amount is 12 p.h.r., the experiment was expected to show the effect of varying composition on the mechanical damping. All samples have been fully cured at 50°C above their respective T_g prior to testing[22]. The results are shown in *Figure 2*.

As the amount of curing agent increases, the area under the peak increases, but only up to the stoichiometric amount (12 p.h.r. DETA). Excess amine in a fully cured sample has no effect on the γ peak.

It is interesting to compare the differences in the effect of different curing agent concentration on the α relaxation[33] and on the γ relaxation. The temperature of both the α and the γ peaks have been plotted against the curing agent concentration in *Figure 3*. The temperature of the α peak reaches a maximum at the stoichiometric amount of curing agent, and excess
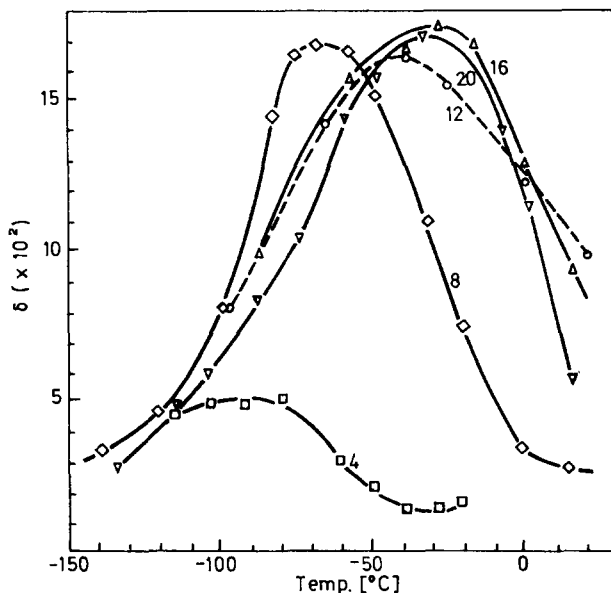
Figure 2 Changes in the γ peak with curing agent concentration for fully cured resins

DETA conc:	
□, 4 phr	○, 12 phr
◇, 8 phr	△, 16 phr
	▽, 20 phr

of either component causes it to decrease. The temperature of the γ relaxation also increases with increasing curing agent concentration up to the sotichiometric amount, but remains constant thereafter.

The possibility that absorbed water may be responsible for the γ relaxation in epoxy resin has been discarded after the following experiment. A sample was saturated with 2·4% wt. water at elevated temperatures. Its γ peak was measured and found to be identical to that which was obtained after the specimen has been degassed in vacuum to less than 0·1% wt. water. This confirms the results of Kline and Sauer[21].

The relation of the γ relaxation to chemical structure

It has been demonstrated that the area under the γ peak is proportional to the degree of cure, and that it is not influenced by absorbed water. Nor is the γ peak inherent in either the epoxy or the amine component. The most obvious cause of the γ peak is the chemical reaction between the epoxy and the amine molecules, which create flexible segments after the oxyrene ring opens. The links which develop, have been shown in the Experimental section.

71
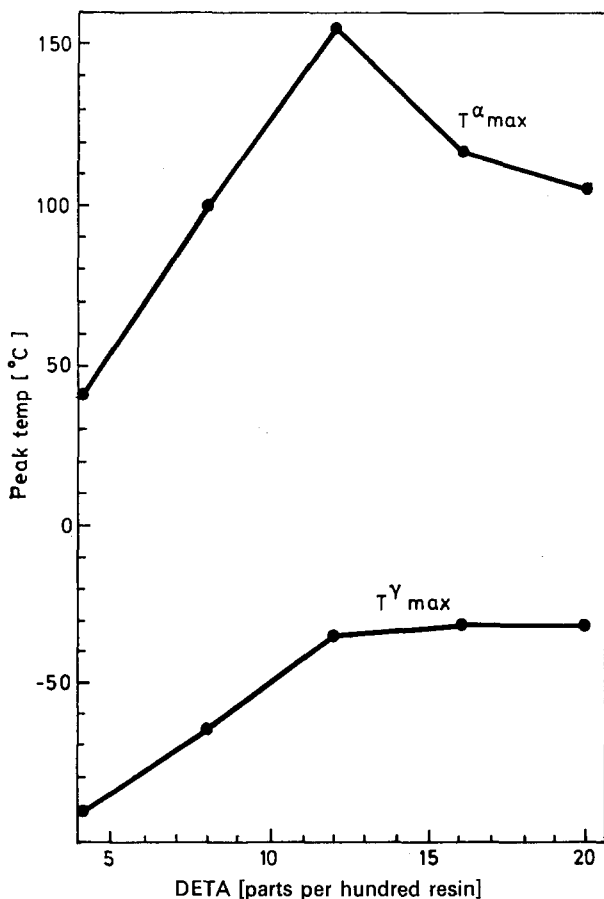
Figure 3 Changes in the α and γ peak temperatures with curing
agent concentration for fully cured resins

It has been suggested[20], and now it is conclusively proved, that the
—CH_2—$CH(OH)$—CH_2—O— group is responsible for the γ relaxation in
the amine cured epoxy resin at $-80°C$.

It is probable that the relaxation is caused by a crankshaft type rotation[12]
of the —CH_2—$CH(OH)$—CH_2—O— group. The bond angles of carbon
($109·5°$) and that of oxygen ($105·0°$) are very similar and the group could form
a crankshaft. The rotation is hindered by the pendant –OH group, which
is also capable of forming hydrogen-bonds. The hindrance of the –OH group
is probably responsible for the γ relaxation taking place at $-80°C$, instead
of possibly at $-120°C$ as in some other polymers.

To gain further information in addition to that from amine-cured epoxy
resin, other polymers, which contain the *bis*phenol A group, were also
examined. These were epoxy resin cured with acid anhydride (MNA), phenoxy
resin, polycarbonate and polysulphone. Their structures are given in the
Experimental section. All these polymers have some low temperature

72

relaxation, as shown in *Figure 4*, but only phenoxy resin has a large peak at −80°C.

In the acid anhydride cure, the –OH groups react with both epoxy and acid anhydride, creating ether and ester links of the type shown in the
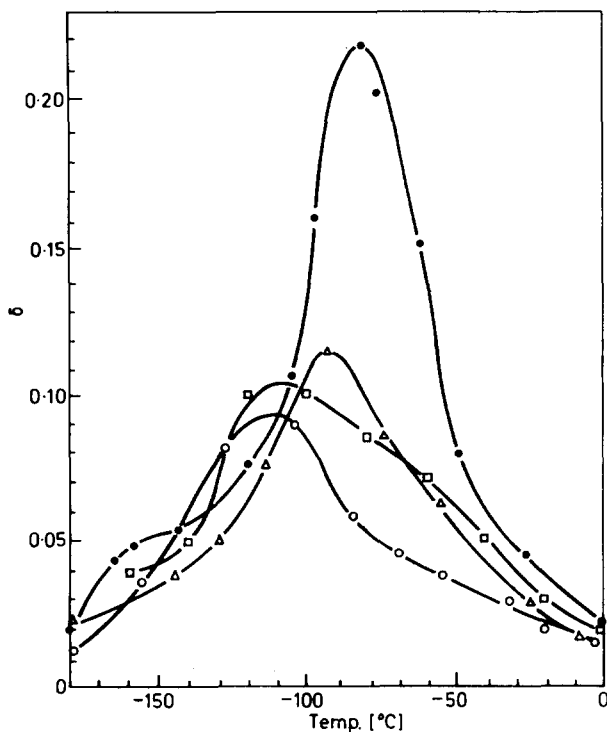
Figure 4 γ peaks for polymers containing *bis*phenol A groups
●, phenoxy resin   □, polycarbonate
△, MNA cured epoxy   ○, polysulphone

Experimental section. Here, and also in the polycarbonate and polysulphone, the flexible group is missing. In phenoxy resin, however, there is a group which is almost identical to the flexible group formed by the amine cure. This result therefore provides additional support for the hypothesis given above.

The shift of the γ peak to higher temperature

It can be observed from the previous experiments that increasing cure shifts the temperature of the peak to higher temperatures, i.e. from about −80°C to about −40°C. There are two possible explanations of this fact. It is possible that the γ relaxation as observed in a fully cured resin is a product of two separate relaxations. If so, the relaxations are so close, that they can not be detected separately. It is also possible that one is much

greater than the other and presumably the last stages of cure increase the one which is at the higher temperature. This could result in an apparent shift of the peak.

The following is an alternative explanation. As the viscosity of the resin increases on curing, the chances of the unreacted monomers meeting are reduced. Heating increases thermal motion and these segments can again come into contact with each other. Chemical reactions take place at their successful meetings and new permanent links develop. These links tie down the previously free segments, which are no longer able to return to their equilibrium position, and the increased steric hindrance could move the peak to higher temperatures.
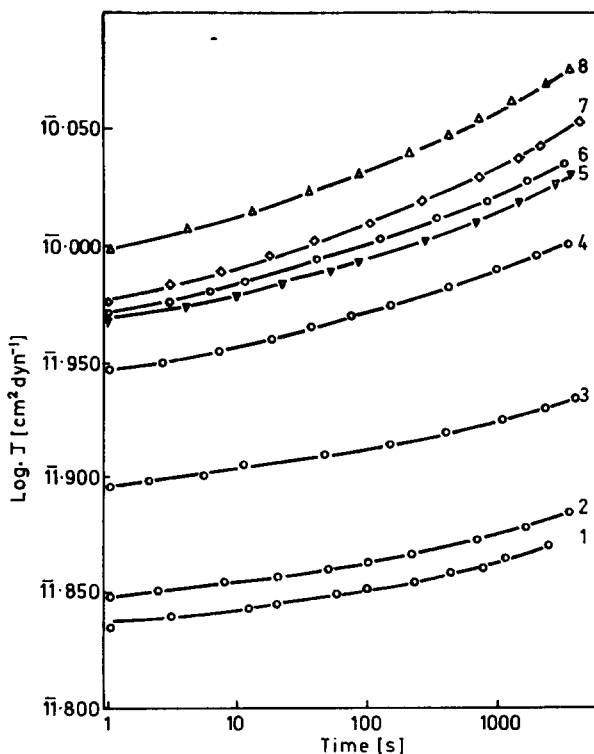
Figure 5 Effect of cure temperature on the creep compliance/time relationship

No.	T_{max}	No.	T_{max}
1	25°C in N_2	5	190°C in air
2	40°C in N_2	6	140°C in N_2
3	60°C in N_2	7	170°C in N_2
4	100°C in N_2	8	surface removed

(all measurements at 20°C)

The relationship between the γ relaxation and the glassy modulus

It is interesting to note the anomalous results observed in the modulus

curves at temperatures above the γ relaxation, that is the glassy modulus declines with increasing degree of cure. This phenomenon corresponds, of course, to the broadening of the γ peak.

Figure 5 shows the effect of progressing cure on the room temperature creep compliance of specimens cast with the stoichiometric amount of DETA. The dependence of log J_t on log t, after 25°C cure is shown by curve 1. The specimen was then heated at 40°C for 20 000 seconds, cooled to 20°C and the relation between log J_t and log t re-examined. The result is shown as curve 2 in *Figure 5*. The procedure was then repeated several times, but always higher and higher temperatures were used. The creep curves at 20°C after each successive step, up to a heat treatment of 190°C, are shown in *Figure 5*.

The shape of these creep curves is reasonably similar but the curves are displaced vertically. The lowest curve (1) is for the specimen which was cured at 25°C, and an increase in the temperature of cure increases the room temperature creep compliance. The only exception from this trend is curve 7, which was obtained after the specimen was exposed to air at 190°C and evidently this resulted in a reduction in the creep compliance. It was subsequently observed that this specimen acquired a dark brown surface during the oxidative heat treatment, and removal of this surface layer resulted in an increase in the creep compliance (curve 8).

It is inferred therefore that the formation of the dark brown surface is responsible for the lowering of the compliance, a phenomenon which will be examined fully in another publication[32]. The increase of the creep compliance with increased heat treatment is expected from the changes associated with the γ peak. A practical aspect of this observation was presented in a previous paper in connection with monitoring the state of cure[22].

LOW TEMPERATURE RELAXATION IN RELATED RIGID POLYMERS

To complete this investigation, other resins which contain benzene rings in their backbone, but not the *bis*phenol A group, were also examined. These resins were polyimide (linear), Bakelite, (Novolak and Resole types, crosslinked), a Friedel-Crafts polymer (crosslinked) and poly(phenylene oxide) (linear). The result on poly(phenylene oxide) was taken from the literature[29]. The effect of water and fillers on these relaxations has not been investigated.

The low temperature relaxation in polymers which contain the *bis*phenol A group was shown in *Figure 4*. The above polymers, with even more rigid structures, still have a low temperature relaxation as shown in *Figure 6*.

It is not easy to establish the cause of a relaxation in polymers with such rigid structures. Reding *et al*[6, 7] suggest that it is caused by the –O–CO–O– group, Hara and Okamoto[10] mention side chain motion. Bussink, and Heijboer[11] point out that the relaxation shifts to higher temperatures by the methyl substitution of the carbon atom in *ortho* position to the COO– link. Using atomic models it is difficult to see how the –O–CO–O– group could relax without some sort of motion of the benzene rings.
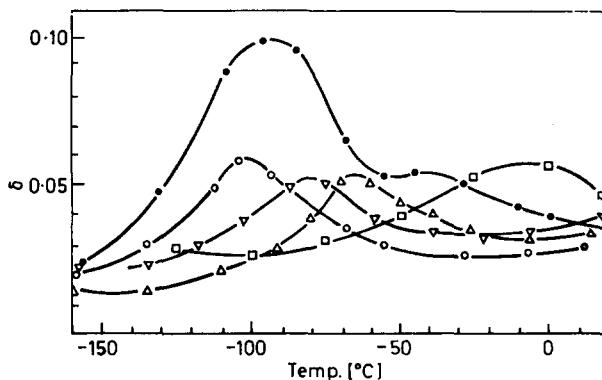
Figure 6 γ peaks in rigid polymers containing benzene rings in their backbone

●, polyimide   △, Bakelite—Novolak
○, Friedel-Crafts polymer   □, poly(phenylene oxide)
▽, Bakelite—Resol

The causing of low temperature relaxation by benzene rings in certain linear polymers has been discussed in the introduction[15]. This has been ascribed to a wag-type motion, which becomes possible in polystyrene at about 40°K. If the benzene rings form part of the backbone they can still cause a relaxation but because of the obvious restrictions[16], this relaxation shifts to about −100°C.

Now it has been demonstrated that similar low temperature relaxation exist also in crosslinked resins. The possibility of a crankshaft type motion is inconceivable in many of these polymers, as some of them are built almost exclusively from benzene rings. This experiment therefore suggests that a wriggle type motion of units containing benzene rings is causing the low temperature relaxation in these rigid (crosslinked) structures. The hypothesis would explain why motion in poly(phenylene oxide), where two methyl groups are attached to each benzene ring in *ortho* positions to the oxygen, seems to be more hindered than motion in the crosslinked Friedel-Crafts polymer. As the relaxation involves a small segment only the mere presence of crosslinks does not seem to make much difference to the temperature of these relaxations. It also seems plausible that because the benzene rings in the Resole type of Bakelite are connected by a longer, more flexible unit than in the Novolak type, it has its relaxation at a lower temperature.

It should be noted that in the amine-cured epoxy resin the γ relaxation at −80°C is much larger than that associated with the benzene rings. In this resin the existence of the −100°C relaxation can not be seen as a separate peak.

CONCLUSIONS

The −80°C (γ) relaxation in epoxy resins crosslinked with aliphatic polyamines, measured at 0·67 c/s is caused by the segment
$$-CH_2-CH(OH)-CH_2-O-.$$

With cure progressing the peak increases in size and shifts towards higher temperatures until it finally reaches about $-40°C$. Simultaneously the glassy modulus of the resin measured at $20°C$ decreases with increasing degree of cure. It is proposed that the drop in the modulus is associated with the development of the γ peak and that the shift of the peak is caused by steric hindrance, which increases with cure.

A similar relaxation exists in phenoxy resins, which contain identical structural units. Other polymers with ring units have low temperature (γ) relaxations at temperatures from $-100°C$ to $0°C$ depending on their chemical composition. Some of these polymers are composed almost entirely of benzene rings which are attached to the network with more than one link. A crankshaft type rotation of segments is inconceivable, and it is suggested that, in these polymers, this low temperature relaxation is caused by the motion (probably wriggling) of units containing benzene rings. Because the benzene rings are not pendant like in polystyrene their relaxation is shifted to considerably higher temperatures.

It may be concluded that the low temperature relaxation in polymers is caused by the localised motion of flexible segments or by the cooperative, non-rotational motion of larger groups. The greater the flexibility of the links between these groups, the greater their effect and the lower the temperature of the relaxation.

Shell Research Ltd.,
Carrington Plastics Laboratory,
Urmston, Manchester

REFERENCES

1 Schmieder, K., Wolf, K. *Koll. Zeit.* 1953, **134**, 157
2 Hoff, E. A. W., Robinson, D. W., Wilbourne, A. H. *J. Polym. Sci.* 1955, **18**, 161
3 Deutsch, K., Hoff, E. A. W., Reddish, W. *J. Polym. Sci.* 1954, **13**, 565
4 Illers, K. H. *Makromol. Chem.* 1960, **38**, 168
5 Willbourn, A. H. *Trans. Far. Soc.* 1958, **54**, 717
6 Reding, F. P., Faucher, J. A., Whitman, R. D. *J. Polym. Sci.* 1961, **54**, S56; 1962, **57**, 483
7 Stratta, J. J., Reding, F. P., Faucher, J. A. *J. Polym. Sci.* (*A*) 1964, **2**, 5017
8 Illers, K. H. *Z. Electrochem* 1961, **65**, 679
9 Heijboer, J. 'Physics of non-crystalline solids', (ed. J. A. Prins) North Holland Publishing Co., Amsterdam, 1965, p 238
10 Hara, T., Okamoto, S. *Japan J. appl. Phys.* 1964, **3**, 499
11 Bussink, J. and Heijboer, J., 'Physics of non-crystalline solids', (ed., A. W. Prins) North Holland Publishing Co., Amsterdam, 1965, p 388

12 Schatzki, T. F. *J. Polym. Sci.* 1962, **57**, 496
13 Andrews, R. D., Hammack, T. J. *J. Polym. Sci. (B)* 1965, **3**, 655, 659
14 Heijboer, J. *Koll. Z.* 1960, **171**, 7
15 Sinnott, K. M. *SPE, Trans.* 1962, **2**, 65
16 Woodward, A. E. *Amer. Chem. Soc. Polymer Preprints* 1965, **6**, 643
17 Haberland, G. G., Carmichael, J. B. *Amer. Chem. Soc. Polymer Preprints* 1965, **6**, 637
18 Baccaredda, M., Butta, E., Frosini, V., De Petris, S. *Mat. Sci. and Engineering* 1968, **3**, 157
19 Van Hoorn, A. *J. appl. Polym. Sci.* 1968, **12**, 871
20 Kline, D. E. *J. Polym. Sci.* 1960, **47**, 237
21 Kline, D. E., Sauer, J. A. *SPE Trans.* 1962 (Jan), p 21
22 Pogany, G. A. *J. Mat. Sci.* 1969, **4**, 405
23 McCrum, N. G., Pogany, G. A. *J. Macromol. Sci. (B)* 1970, **4**, 109
24 Lee, H., Neville, K. 'Epoxy Resins', McGraw-Hill, New York, 1957
25 Cristopher, W. F., Fox, D. W., 'Polycarbonate', Reinhold, New York, 1962
26 *Rubber and Plastics Age* 1965, p 690 (iii)
27 Bakelite Ltd., Product data sheet
28 Scala, L. C. and Hickman, W. M. *J. appl. Polym. Sci.* 1965, **9**, 245
29 Steinbuch, R. Th. *British Plastics* 1965 (Nov), p 666
30 Phillips, L. N. *Trans. Plast. Inst.* 1964 (Oct), p 298
31 Billmeyer, Jr., F. W., 'Textbook of Polymer Science', Interscience New York, 1964
32 Pogany, G. A. *British Polymer J.* 1969, **1**, 177
33 Pogany, G. A. *European Polymer J.* 1970, Vol. 6, to be published

Prediction of the glass transition temperature of polymers

H. G. WEYLAND, P. J. HOFTYZER AND D. W. VAN KREVELEN

A method is proposed for the prediction of the glass transition temperature of polymers from the chemical structure. The method uses increments for constitutional molecule groups. The found increments appear to correlate with the increments to the molar cohesion energy.

WHEN a series of polymers is compared, the correlation between the glass transition temperature and chemical structure is striking. This has been investigated for a long time, and numerous methods have been proposed for predicting the T_g of polymers from their chemical structure[1-5].

In general these methods are based on the assumption that the repeating unit of the polymer can be divided into molecule groups which have weighted additive contributions to the T_g, independently of their neighbours.

This can be expressed mathematically as follows:

$$\sum_i s_i T_{gi} = T_g \sum_i s_i \tag{1}$$

where T_{gi} and s_i are, respectively, the T_g contribution and the weight of the molecule groups i in the repeating unit of the polymer. The smallest polymer segment capable of independent torsional oscillation is usually taken to be a molecule group.

It should be noted that the form of equation (1) agrees with the well-known thermodynamic expression for thermal transitions, $\Delta H = T\Delta S$, on the assumption that the changes in enthalpy, ΔH, and entropy, ΔS, can be obtained from increments of constitutional molecule groups. Bondi[3], among others, has shown that in many cases, this type of model can be successfully used for the prediction of thermal properties of matter.

Published T_g structure relationships based on equation (1), generally make assumptions regarding s_i. Hayes[4] assumed the molar cohesion energy for $\Sigma s_i T_{gi}$, and derived from this, a number of rules to calculate s_i. Bondi[3] considered s_i a constant for rigid molecule groups, while Barton and Lee[5] suggested the weight or mole fraction of the molecule group for s_i.

In this paper the validity of this T_g structure model is examined using several assumptions for s_i. The best results are shown to be obtained with s_i proportional to the number of atom distances in the main chain of the polymer. The correlation between the constant T_{gi} and the increments of the molecule groups to the molar cohesion energy is also discussed.

STRUCTURE RELATIONSHIPS FOR UNBRANCHED CHAINS

Method

Efforts to determine the optimum values of the constants T_{gi} and s_i from the available polymer T_g data have been made primarily to find a workable

T_g structure relationship. Unfortunately, these attempts have failed because the computer programs used for calculating these values did not converge to stable end-values. One of the main reasons for this failure was that the system did not have a pronounced optimum with respect to s_i. Within a rather wide range it appeared that the values for s_i could be chosen arbitrarily.

Table 1 Types and numbers of polymers used for checking

Polyamides;	aliphatic	19
	aromatic	44
Polyesters;	aliphatic	20
	aromatic	32
Polyurethanes		12
Polycarbonates		7
Polyanhydrides		9
Polyethers		10
Polysulphones		4
Polyolefins		5
	Total	162

By adapting the constants of equation (1) to a number of selected well-known polymers, s_i could best be approximated by the number of atom distances of the molecule groups *in the main chain* of the polymer. Moreover it appeared that the methylene units in polyamides and in polyurethanes have to be considered separately from those in other polymers.

For a large number of polymers (*Table 1*), the validity of this T_g structure model has been investigated and compared with that of some T_g structure relationships found in the literature. These relationships are mentioned in *Table 2*.

Table 2 Validity of T_g structure relationship based on equation (1)

Assumption with respect to s_i	Standard deviation for 162 polymers investigated
$s_i = 1$	24·7°K
s_i, calculated according to Hayes	23·7°K
s_i, proportional to the molecular weight	20·4°K
$s_i = 1$ per atom distance in the main chain	17·8°K

Before discussing this work, some remarks should be made regarding the accuracy of the T_g data and the choice of polymers. The accuracy of published T_g values is generally not very great. Due to differences in measuring methods, conditions, and the molecular weight of the samples, differences of tens of degrees centigrade between published values are not exceptional. Hence, in the ideal case we may expect a standard deviation with respect to the measured T_gs which is somewhere between 10°K and 20°K.

Because the values of T_{gi} in the relationships are still unknown, it will be evident that in order to determine their validity for polymer T_g data, only

those polymers can be used that have molecule groups which are present in at least two polymers. This requirement excludes the major part of the addition polymers from this investigation. In the next section the validity of the model for some of these polymers–namely the polymers with linear aliphatic side chains–will be discussed.

The T_g data of the polymers used in this investigation have mainly been taken from the Polymer Handbook[6] and the work of Griffin Lewis[7]. The types and numbers of polymers used are shown in *Table 1*. The 162 polymers mentioned in this table contain 20 different molecule groups, which for each of the relationships yields 162 equations with 20 unknown quantities. From this set of equations the optimum values of T_{gi} and the standard deviation with respect to the measured T_g have been calculated with the aid of a computer, a standard program being used for linear regression analysis.

Results

The results of this work are shown in *Tables 2* and *3*. From *Table 2* it appears that the best results are obtained with the approximation of s_i by the number of atom distances in the main chain. In view of the accuracy to which the T_g data are known, the standard deviation found for this relationship can be considered to be rather good. Up to now, large differences between predicted and measured T_g have been found only for the polymers poly(p-phenyleneether) and poly(p-phenylenesulfide), using this relationship. For both polymers a T_g of 445°K is predicted, whereas a T_g has been measured
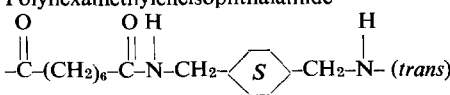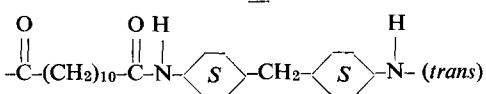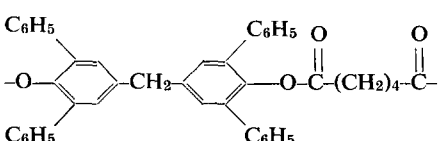
Table 3 Prediction of T_g of polymers according to $\sum_i s_i T_{gi} = T_g \sum_i s_i$

Molecule group	Relationship					
	$s_i = $ molecular weight (–CH_2– = 1)			$s_i = 1$ per atom distance in the main chain		
	s_i	$s_i T_{gi}$ (°K)	T_{gi} (°K)	s_i	$s_i T_{gi}$ (°K)	T_{gi} (°K)
–CH_2–	1	158	158	1	171	171
–CH_2– in polyamides and polyurethanes	1	245	245	1	263	263
–$CH(CH_3)$–	2	526	263	1	304	304
–$C(CH_3)_2$–	3	645	215	1	210	210
–$CH(phenyl)$–	6·4	2560	400	1	585	585
–$C(CH_3)(phenyl)$–	7·4	3560	481	1	716	716
–O–	1·1	255	232	1	220	220
–SO_2–	4·6	2150	467	1	743	743
p-phenylene	5·4	2820	521	4	2010	502
m-phenylene	5·4	2500	463	3	1371	457
o-phenylene	5·4	2420	448	2	934	467
1,4-cyclohexylene (*trans*)	5·7	2960	520	4	2080	520
2,6-dimethyl-1,4-phenylene	7·4	3740	506	4	2156	539
2,5-dimethyl-1,4-phenylene	7·4	2760	370	4	1500	375
2,6-diphenyl-1,4-phenylene	16·3	8030	493	4	2256	564
–NHCO–	3·1	1510	488	2	1068	534
–NHCOO–	4·2	1690	402	3	1224	408
–COO–	3·1	910	293	2	636	318
–O–CO–O–	4·3	1080	251	3	783	261
–CO–O–CO–	5·1	450	86	3	363	121

P—F

as $358\,^\circ$K. The second best relationship, with s_i proportional to the molecular weight of the molecule groups, also fits reasonably well. The constants T_{gi} and s_i found for the two relationships are mentioned in *Table 3*: some examples are given in *Table 4*. In many cases the two other relationships investigated appear to fail badly in predicting the T_g.

Table 4 Some examples of predicting the T_g of linear polymers.

Polyethyleneterephthalate: T_g (calculated) $= (2 \times 636 + 2010 + 2 \times 171)/(4 + 4 + 2)$
$= 362\,^\circ$K

Polymer	T_g (measured) (°K)	T_g (calculated)	
		$s_i = 1$ per atom distance (°K)	$s_i =$ molecular weight (°K)
Polyethylene	150	171	158
Polypropylene	253	237	241
Polyisobutylene	197	191	201
Polystyrene	373	378	367
Polyethyleneoxide	206	187	186
Polyethyleneadipate	223	230	226
Polyethyleneterephthalate	342	362	364
Polyethyleneisophthalate	324	332	340
Polyethylenephthalate	290	319	334
Nylon 66	330	338	338
Polyhexamethyleneterephthalamide	410	409	415
Polyhexamethyleneisophthalamide	403	391	397
$-\overset{O}{\overset{\|}{C}}-(CH_2)_6-\overset{O}{\overset{\|}{C}}-\overset{H}{\overset{\|}{N}}-CH_2-\langle S\rangle-CH_2-\overset{H}{\overset{\|}{N}}-$ *(trans)*	403	395	400
$-\overset{O}{\overset{\|}{C}}-(CH_2)_{10}-\overset{O}{\overset{\|}{C}}-\overset{H}{\overset{\|}{N}}-\langle S\rangle-CH_2-\langle S\rangle-\overset{H}{\overset{\|}{N}}-$ *(trans)*	407	407	416
$-O-\langle C_6H_5 \rangle -CH_2-\langle C_6H_5 \rangle-O-\overset{O}{\overset{\|}{C}}-(CH_2)_4-\overset{O}{\overset{\|}{C}}-$ (with C_6H_5, C_6H_5, C_6H_5, C_6H_5)	388*	391	425
Poly(p-2,6-dimethylphenylene ether)	488	475	471
Poly(p-2,6-diphenylphenylene ether)	498*	495	476
Poly(p-phenylene ether)	358*	445	472

*Our measurements

POLYMERS WITH LINEAR ALIPHATIC SIDE CHAINS

In the following the connection between T_g and the chemical structure of polymers with linear aliphatic side chains is considered.

Method

Following on from the last section, linear aliphatic side chains are taken into account in the same way as the main chain. Hence the weight $\sum_i s_i$ is

obtained by adding to $\sum_i s_i$ of the basic polymer, the number of methylene groups, n, in the side chain.

If the T_g-increment of the methylene groups in the side chain is written as $T_g(CH_2)$, the T_g of polymers with linear aliphatic side chains may be expressed according to equation (1) by:

$$T_g(n + \sum_i s_i) = [\sum_i s_i\, T_{gi}] \text{ (basic polymer)} + [\sum_n T_g\, (CH_2)] \text{ (side chain)}$$

This shows that, the T_g of the basic polymer, T_g (basic), satisfies the expression:

$$\sum_i s_i\, T_{gi} = T_g(\text{basic}) \sum_i s_i$$

Hence for the influence of the side chain on T_g we obtain the expression:

$$[\sum_n T_g\, (CH_2)] \text{ (side chain)} = T_g\, (n + \sum_i s_i) - T_g\, (\text{basic}) \sum_i s_i \quad (2)$$

Results

In *Figure 1* the quantity $[\sum_n T_g(CH_2)]$(side chain) calculated according to equation (2) from polymer T_g data, has been plotted for several series of polymers against the number of methylene units, n, in the side chain. This figure shows that the T_g of these polymers can be described with the T_g structure relationship if two values are used for the increment $T_g(CH_2)$ of the methylene units in the side chain. For the polyolefins and the polyacrylates up to $n = 6$, $T_g(CH_2)$ appears to be 170°K, whereas above this number a value of 410°K has to be taken for $T_g(CH_2)$. In the cases of the polystyrenes and the polymethacrylates the increment $T_g(CH_2)$ changes from 170°K to 410°K at $n = 10$. For another polymer series a turning-point at $n = 6$ has been found. Sometimes this turning-point could not be detected due to the lack of data about polymers with long side chains.

When these increments are used for calculating the T_g of polymers with linear aliphatic side chains, the calculated T_g appears to correlate with the measured T_g, with a mean deviation of about 10°K. The types and numbers of polymers used in this investigation are shown in *Table 5*, and some examples are given in *Table 6*.

As appears from *Figure 1*, nearly the same curve as that found for the polyolefins is obtained from the melting-points, T_m of the n-paraffins by plotting the product $(n + 2)T_m$ against the number of methylene groups, n, with ethane at the origin. This result suggests that there may be a certain connection between the melting-points of the n-paraffins and the T_g of polymers with linear aliphatic side chains.

It should also be noted that for these polymers the T_g structure relationship, with s_i proportional to the molecular weight of the molecule groups, fits reasonably well. Again, this relationship yields a somewhat lower value for $T_g(CH_2)$ (at $n < 6$, $T_g(CH_2) = 150°K$) and somewhat larger differences between the predicted and measured T_gs.

DISCUSSION

It will be evident that the relationship we have found should primarily be regarded as an empirical method for predicting the T_g of polymers. It has been shown that, for a large number of polymers, T_g can be estimated with
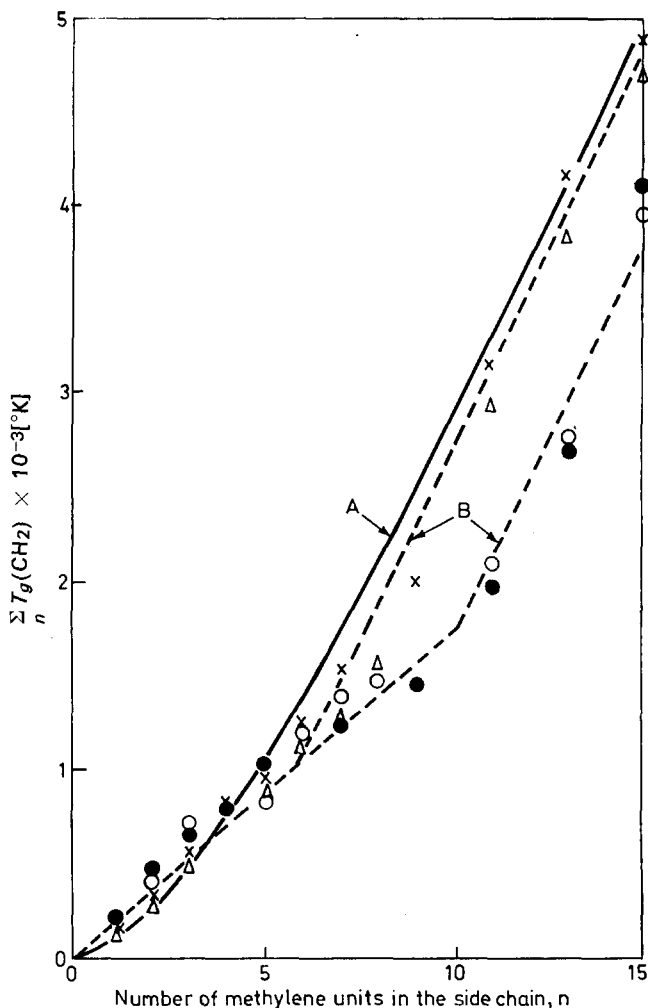
Figure 1 T_g of polymers with linear aliphatic side chains ×, Poly-olefins; △, Polyacrylates; ●, Polymethacrylates; ○, Polystyrenes; A (unbroken line), $(n + 2)T_m$ of the *n*-paraffins; B (broken line), approximation

an accuracy of about 20°K, while for series of polymers an even higher degree of accuracy can be obtained. The significance of the method is illust-rated by *Figure 2*, which shows that, with the exception of the –NHCO– group, the constants T_{gi} correlate rather well with the contributions of the molecule groups to the molar cohesion energy, c.e., (as mentioned by Hayes[4]). A connection between the molar cohesion energy, c.e., and the T_g of polymers is probable[3, 4] but Lee and Sewell[8] have shown that the correlation is poor, and they concluded that c.e. is not the only factor determining T_g. *Figure 2* shows that it is not T_g and c.e., but their increments that correlate well.

84

Table 5 Types and numbers of polymers with linear aliphatic side chains*

Polymer $X = -(CH_2)_n-$	Number	Basic polymer ($n = 0$)	
		T_g [$^\circ$K]	$\sum\limits_i s_i$

-CH$_2$-CH-
    |
   X-CH$_3$
	12	253	2

-O-CH-
  |
  X-CH$_3$
	4	243	2

-CH$_2$-C$=$CH-CH$_2$-
    |
   X-CH$_3$
	6	203	4

O   O
   || ||
-O-C-CH-C-O-(CH$_2$)$_2$-O-(CH$_2$)$_2$-
     |
    X-CH$_3$
	5	244	10

-CH$_2$-CH-
    |
   X—⟨phenyl⟩
	4	373	2

-CH$_2$-CH-
    |
   X—⟨S ring (thiophene 6)⟩
	4	363	2

-CH$_2$-CH-
    |
   X—⟨S ring (thiophene 5)⟩
	2	348	2

-CH$_2$-CH-
    |
   O-X-CH$_3$
	6	250	2

-CH$_2$-CH-
    |
   O—CO-X-CH$_3$
	5	301	2

-CH$_2$-CH-
    |
   CO-O-X-CH$_3$
	12	282	2

-CH$_2$-CH-
    |
   ⟨phenyl⟩-X-CH$_3$
	11	372	2

-CH$_2$-CH-
    |
   ⟨phenyl⟩-O—X-CH$_3$
	5	348	2

CH$_3$
   |
-CH$_2$-C-
   |
   CO-O-X-CH$_3$
	11	382	2

*The T$_g$ data have been taken mainly from refs. 6 and 7.

85

Table 6 Some examples of predicting the T_g of polymers with linear aliphatic side chains

Polymer	T_g (measured) [°K]	T_g (calculated) [°K]
-CH₂-CH- | (CH₂)₁₅-CH₃	314	307
-CH₂-C=CH-CH₂- | (CH₂)₉-CH₃	220	235
-O-CO-CH-CO-O-(CH₂)₂-O-(CH₂)₂- | (CH₂)₆-CH₃	215	216
-CH₂-CH- | CO-O-(CH₂)₁₅-CH₃	308	310
-CH₂-CH- | ⬡-(CH₂)₁₅-CH₃	278	265

Figure 2 Connection between T_g and c.e. increments

86

This, together with equation (1) indicates that the connection between T_g and c.e. is rather complex and also contains the increment s_i.

Summarizing, it may be concluded that the empirical model as given by equation (1) has turned out to be a workable basis for a quantitative description of the connection between T_g and chemical structure of polymers. However, because of the approximations made, there is still a certain chance of failure in predicting T_g. The influence of s_i on the model appears to be small, which permits a rather crude approximation of this constant, for example by simple rules based on the structure of the molecule groups. In this respect the number of atom distances and the molecular weight of the molecule groups have been found to fit well. In general, the approximation of s_i by the number of atom distances yields somewhat better results, though the difference is not great.

A somewhat more accurate relationship might be obtained by calculating the optimum values of both T_{gi} and s_i from a large number of polymer data. However, a much higher degree of accuracy is not to be expected. The main cause of failure is to be ascribed to the model. In the model the nature of the sequence of the molecule groups and their influence on one another have been neglected, when in fact, they do have a distinct influence on T_g, as appears from numerous examples. This leads to the conclusion that only by incorporating these factors into a much more complicated model a substantial improvement of accuracy in predicting T_g can be obtained.

AKZO Reseach and Engineering N.V.
Velperweg 76.
Arnhem,
The Netherlands   *(Received 30 September 1969)*

REFERENCES

1 Beaman, R. G. *J. appl. Polym. Sci.* 1965, 9, 3945
2 Barton, J. M. *R.A.E. Technical Report* 67187, 1967
3 Bondi, A. 'Physical Properties of Molecular Crystals, Liquids and Glasses,' John Wiley, New York, 1968
4 Hayes, R. A. *J. appl. Polym. Sci.* 1961, 5, 318
5 Barton, J. M. and Lee, W. A. *Polymer, Lond.* 1968, 9, 602
6 Brandrupp, J. and Immergut, E. H. 'Polymer Handbook', Interscience, New York, 1965
7 Griffin Lewis, O. 'Physical constants of linear homopolymers', Springer Verlag, 1968
8 Lee, W. A. and Sewell, J. H. *J. appl. Polym. Sci.* 1968, **12**, 1397

Synthesis of tertiary amine polymers

F. Danusso and P. Ferruti

Systematic work, in Italy, on the synthesis of polymers having tertiary amino groups as structural units is reported. The polymers carry amino groups, (a) situated in the molecular main chain; (b) directly bound to the main chain as side groups; or (c) situated on side groups. Type (a) were synthesized by poly-addition of mono- or diamines (or aminoacids) to a compound having two vinyl double bonds activated by adjacent electron attracting groups. These polymers have different chemical functions regularly arranged along the main chain. For (b), the synthesis of polymeric compounds using enamines as monomers is discussed; results of practical interest were obtained by copolymerizing enamines with acrylonitrile to give products which may reach an alternating disposition of the co-units along the chain. In type (c) polymers which are partially stereoregular could also be synthesized, using anionic catalysts at low temperatures.

UP TO NOW, macromolecular chemists have shown little interest in developing convenient methods for the synthesis of high polymers containing tertiary amino groups, either aliphatic or cycloaliphatic. However, such polymers may be extensively used in different applications, as materials or (more generally) as reagents.

Amino polymers have been described, particularly in the patent literature, although their structure and characterization is still uncertain. Such polymers are however extensively used in industry. Some tertiary polyamines and their N-oxides may also be used in pharmacology. For example, a number of these polymers have preventive properties against silicosis[1-3] and others are anti-heparinic[4]. Due to their basicity and chemical reactivity, amino polymers may interact with a number of biological macromolecular substances present in living organisms. Hence this sort of application may well increase.

In this paper we describe results obtained recently in the preparation of polymers containing tertiary amino groups (either aliphatic or cycloaliphatic) mostly by original methods of synthesis.

Classification of the polymers

In view of the purposes of this work, it may be useful to propose a classification scheme for polymers containing tertiary amino groups. Substances of this type may be grouped in three main classes:

(A) Polymers in which they are situated in the main chain.

(B) Polymers in which they are directly bound to the main chain as side groups. In this case they may, or may not, be the only side substituents present.

(C) Polymers in which the amino groups are not directly bound to the main chain, but which exist with other groups as constituents of side chains.

This paper is divided into three main sections according the above classification.

(A) POLYMERS CONTAINING AMINO GROUPS IN THE MAIN CHAIN:

polyamines by poly-additon of amines to compounds containing vinyl double bonds

The addition of primary or secondary amines to vinyl double bonds activated by electron attracting groups is well known. In this reaction, nitrogen is always bound to the carbon β to the activating group, whereas hydrogen migrates to the α-carbon[5].

Under suitable conditions and with the use of bifunctional compounds, this reaction may lead to new linear polymers. The only example previously known is described in a patent claim[6].

The polymers we obtained by this reaction have the character of saturated polyamines, often of high molecular weight. The amine groups form an integral part of the macromolecular chain, and are usually accompanied by other functional groups in the main chain according to predetermined regular sequences.

Polymers from disecondary diamines and bis-acrylamides

We have particularly studied the poly-addition of disecondary diamines to bis-acrylamides[7, 8].

$$x \; HN\!-\!R'\!-\!NH + x \; CH_2\!=\!CH\!-\!\underset{\underset{O}{\|}}{C}\!-\!\underset{\underset{R''}{|}}{N}\!-\!R'''\!-\!\underset{\underset{R''}{|}}{N}\!-\!\underset{\underset{O}{\|}}{C}\!-\!CH\!=\!CH_2 \rightarrow$$

with R on the diamine nitrogens.

$$\left[-\underset{\underset{R}{|}}{N}\!-\!R'\!-\!\underset{\underset{R}{|}}{N}\!-\!CH_2\!-\!CH_2\!-\!\underset{\underset{O}{\|}}{C}\!-\!\underset{\underset{R''}{|}}{N}\!-\!R'''\!-\!\underset{\underset{R''}{|}}{N}\!-\!\underset{\underset{O}{\|}}{C}\!-\!CH_2\!-\!CH_2\!- \right]_x$$
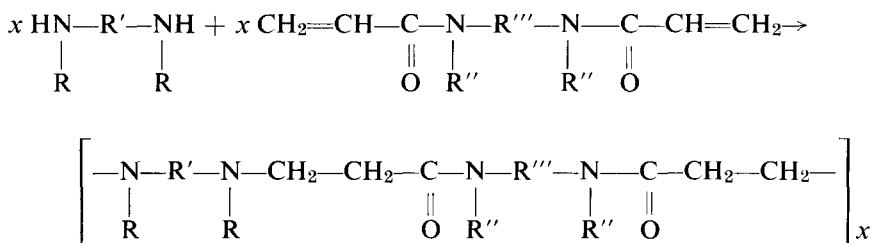
Poly-addition substantially takes place in the absence of secondary reactions; apart from the lack of elimination of a by-product, the reaction is similar to that of a bifunctional polycondensation (i.e. a branching scheme poly-addition)[9].

We confirmed[6] that this polymerization is a nucleophilic polyaddition, with an ionic mechanism. It is not influenced by the presence of the typical inhibitors of radical polymerization, and it does not require acidic or basic catalysts. Poly-addition takes place most easily in solution, and generally the choice of solvent is of great importance in determining the reaction rate.

Contrary to a previous paper[5], the dielectric constant of the solvent does not seem to play an important role; but the solvents that most rapidly lead to a high molecular weight are protic solvents, such as water or alcohols.

Table 1 gives the intrinsic viscosities (in chloroform at 30°C) of the products obtained by polyaddition of 2-methylpiperazine to 1,4-diacrylylpiperazine (*Table 2*, polymer II) in solvents with different dielectric constants; the monomer concentration, temperature and polymerization time are the same for each case.

Table 1 Poly-addition of 2-methylpiperazine to 1,4-diacrylylpiperazine in different solvents*

Dielectric constant	Solvent	% yield	$[\eta]$† (dl/g)
80·2 at 20°C	water	95	0·81
47 at 23°C	dimethylsulfoxide	80	0·13
36·1 at 20°C	nitrobenzene	90	0·11
24·3 at 25°C	anhydrous ethanol	95	0·33
12·5 at 20°C	pyridine	85	0·17

*Temp., 17°C; monomer concentration, 30%; polymerization time, 192 h
†Measured in chloroform at 30°C

Figure 1 shows the increase with time of the average molecular weight, as indicated by intrinsic viscosity (in chloroform at 30°C) for the polyaddition
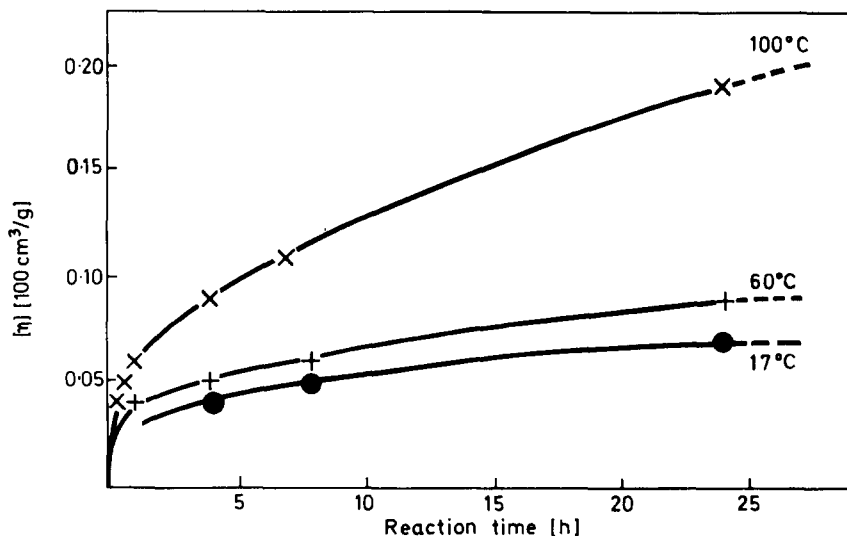
Figure 1 Molecular weight (as intrinsic viscosity in chloroform at 30°C) *versus* reaction time in poly-additions of 1,4-diacrylylpiperazine with 2-methylpiperazine, at different temperatures, in pyridine[7]

of 2-methylpiperazine to 1,4-diacrylylpiperazine in equimolar amounts, at different temperatures, in anhydrous pyridine. In this solvent, an increase in

molecular weight with time of reaction is always observed. On increasing the temperature, the polymerization rate increases, and for an equal polymerization time, the products obtained have higher molecular weights.

Figure 2 shows the results obtained under the same conditions using water as a reaction solvent. At 100°C the molecular weight, after a rapid initial increase, reaches a maximum and then decreases with time.
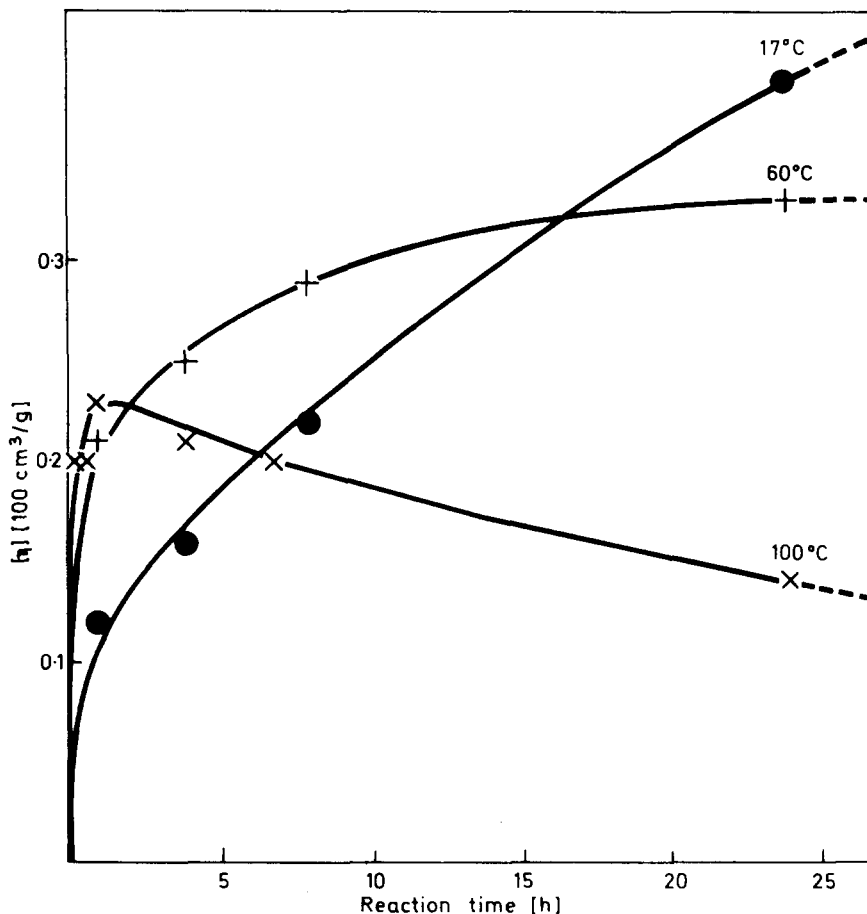
Figure 2 Molecular weight (as intrinsic viscosity in chloroform at 30°C) *versus* reaction time in polyadditions of 1,4-diacrylylpiperazine with 2-methylpiperazine, at different temperatures, in water[7]

At 60°C, after a short initial period in which it increases more slowly than at 100°C, the molecular weight reaches higher values, for an equal reaction time. Finally, at 17°C, the molecular weight first increases more slowly than at 60°C, then the increase is more rapid and far higher values are reached. This behaviour, which may seem anomalous, can be explained by the occurrence, in the aqueous solution, of simultaneous hydrolysis of the

amide link. The rate of polymerization, and of hydrolysis, increases on increasing the temperature; the rate of hydrolysis is greater at high temperatures for the reaction times we have used.

In agreement with the mechanism scheme of this type of polyaddition, if other conditions are the same, the molecular weight of the polymers depends on the relative concentrations of the two monomers and increases to a maximum which corresponds to equimolar proportions. *Figure 3* shows a typical example.
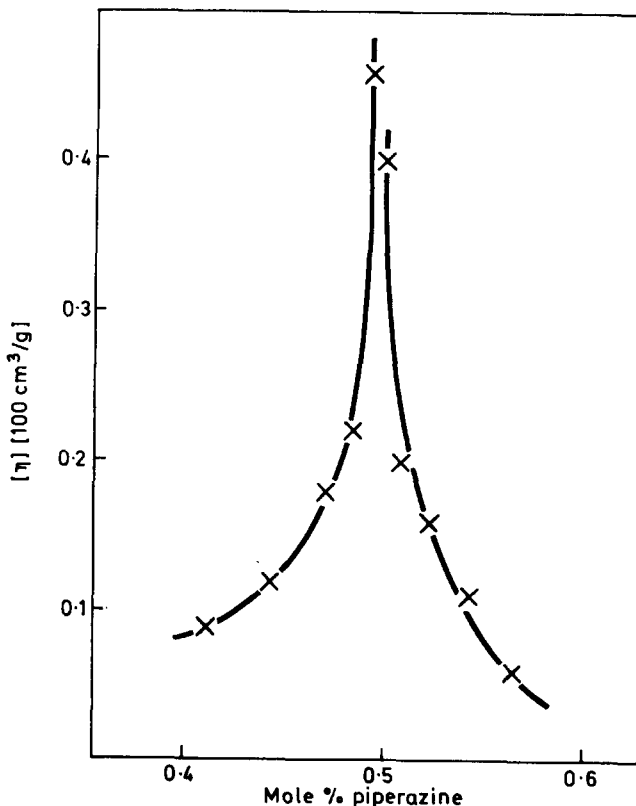
Figure 3 Polyaddition of 1,4-diacrylylpiperazine with piperazine: molecular weight (as intrinsic viscosity) versus initial ratio between the amounts of the two monomers ($[\eta]$ in 0·1 N HCl/1N NaCl aq. soln at 30°C)[7]

Table 2 shows the structure of some polymers obtained by polyaddition of di-secondary diamines to *bis*-acrylamides. On the basis of the experimental results mentioned above, their synthesis was generally accomplished in water or in alcohol, at temperatures ranging from 15°C to 60°C and for reaction times varying from a few hours to several days. Equimolecular amounts of the monomers were always used[6, 7].

Table 2 Polyamide amines from disecondary diamines and *bis*-acrylamides

Ref. no.	Unit	$[\eta]^*$ dl/g at 30°C	m.p. [°C]	Crystallinity
I	-N◯N-CH₂CH₂CO-N◯N-COCH₂CH₂-	0·46†	270 dec.	high
II	-N◯N-CH₂CH₂CO-N◯N-COCH₂CH₂- (CH₃)	0·81	218	low
III	-N-CH₂CH₂-N-CH₂CH₂CO-N◯N-COCH₂CH₂- (CH₃)(CH₃)	0·21	113	high
IV	-N-CH₂-CH₂-N-CH₂CH₂CO-N◯N-COCH₂CH₂- (CH(CH₃)₂)(CH(CH₃)₂)	0·12	97	high
V	-N◯N-CH₂CH₂CO-N◯N-COCH₂CH₂- (CH₃)	0·27	217	low
VI	-N◯N-CH₂CH₂CO-N◯N-COCH₂CH₂- (CH₃)(CH₃)	0·31	—	amorphous
VII	-N◯N-CH₂CH₂CO-N-CH₂CH₂-N-COCH₂CH₂- (CH(CH₃)₂)(CH(CH₃)₂)	0·55	210	high
VIII	-N-CH₂CH₂-N-CH₂CH₂CO-N-CH₂CH₂-N-COCH₂CH₂- (CH₃)(CH₃)(CH(CH₃)₂)(CH(CH₃)₂)	0·17	102	medium
IX	-N◯N-CH₂CH₂CO-N-CH₂CH₂-N-COCH₂CH₂- (C₂H₅)(C₂H₅)	0·35	—	amorphous
X	-N◯N-CH₂CH₂CO-NH-CH₂CH₂-NH-COCH₂CH₂-	0·12‡	231 dec.	high

*In chloroform were not otherwise indicated
†In aqueous 0·1 M hydrochloric acid/1 M sodium chloride
‡In aqueous 0·5 M acetic acid/1 M sodium acetate

The polymerization time required to reach a sufficiently high molecular weight product, other conditions being the same, depends on the nature of the monomer and in particular on the structure of the diamine. The following inverse scale of the reaction times has been observed: N,N'-diisopropyl-ethylendiamine ≪ N,N'-dimethylethylendiamine < 2-methylpiperazine ≤ piperazine. Such an order most likely reflects the order of reactivity of the diamines toward polyaddition; consequently one must conclude that the steric bulkiness of the secondary amino group is, in our case, determinant, for the following reasons.

When comparing the rates of addition to the activated double bonds of amines, such as piperidine and morpholine, where there is a practically identical steric bulkiness, it was found that a higher basicity of the amine is associated with a higher reactivity[5]. The basicities of the amines studied showed the following increasing order[10]: piperazine $\leqslant$ 2-methylpiperazine $<$ N,N'-dimethylethylenediamine $\leqslant$ N,N'-diisopropylethylenediamine. Such an order is the exact reverse of the order of reactivities found by us in the polyaddition; however, in this case, it also shows the effect of increasing steric bulkiness in the diamines.

Polyamide amines obtained by polyaddition of disecondary diamines to *bis*-acrylamides are generally soluble in water, alcohol, and chloroform, and insoluble in aliphatic hydrocarbons. They are often very hygroscopic.

The polymers reported in *Table 2* can be crystallized, except for polymers VI and IX; the latter is rubber-like at room temperature.

It may seem surprising that polymers I and V, although scarcely crystalline, are not completely amorphous. In these polymers, in fact, a structural irregularity should exist since the direction of the methyl group with respect to the polymer chain varies. Their partial crystallinity can be explained by considering that the methyl group has a relatively small dimension in comparison with the base unit.

The thermal stability of the polyamide amines described has been evaluated by thermogravimetric measurements under vacuum, under nitrogen, and in air, with heating rates of 150°C/h. Using this method, volatilization starts at about 200°C under vacuum, and a few tens of degrees higher under nitrogen and in air, without there being any large differences between the various polymers.

Polymers from primary amines and bisacrylamides

The above polyaddition of disecondary diamines to *bis*-acrylamides leads to polyamide amines in which the amine groups (a) and amide groups (b) are regularly arranged along the main chain according to the repeating sequence:

$$-a-a-b-b-a-a-b-b-$$
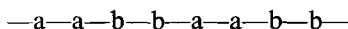
Contrary to previous work[11], we have also synthesized linear high polymers by polyaddition of primary amines to *bis*-acrylamides[12].

$$x\ RNH_2 + x\ CH_2{=}CH{-}CO{-}\underset{\underset{R'}{|}}{N}{-}R''{-}\underset{\underset{R'}{|}}{N}{-}CO{-}CH{=}CH_2$$

$$\longrightarrow \left[\underset{\underset{R}{|}}{N}{-}CH_2CH_2CON{-}\underset{\underset{R'}{|}}{R''}{-}\underset{\underset{R'}{|}}{N}COCH_2CH_2\right]_x$$
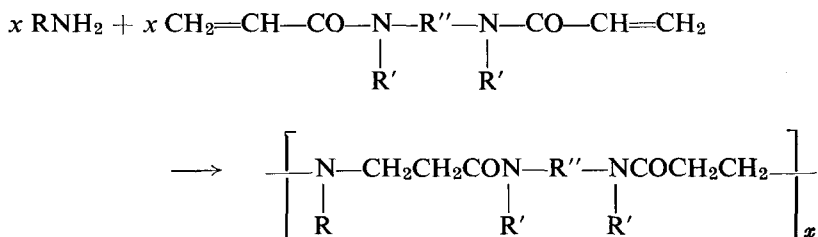
In this case, the product obtained from a first addition of a primary amine to an activated double bond is a secondary amine, which may be further added to a second double bond. Therefore, the primary amine must be considered as a bifunctional monomer, useful for the formation of linear high polymers, if cyclization reactions can be avoided.

The polyamide amines obtained in this way have amine and amide groups following one another along the main chain according to the repeat sequence:

$$—a—b—b—a—b—b—a—b—b—$$
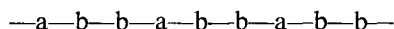
The structures of some polyamide amines obtained by this method are shown in *Table 3*. The operating conditions for polyaddition are analogous to those adopted for disecondary diamines.

Table 3 Polyamide amines from primary amines and *bis*-acrylamides

Ref. no.	Unit	$[\eta]^*$ $[dl/g]$
I	$-CH_2-CH_2-CO-N\langle\rangle N-CO-CH_2-CH_2-N-$ $\quad CH_3$	0·40
II	$-CH_2-CH_2-CO-N\langle\rangle N-CO-CH_2-CH_2-N-$ $\quad C_2H_5$	0·24
III	$-CH_2-CH_2-CO-N\langle\rangle N-CO-CH_2-CH_2-N-$ $\quad C_3H_{7-n}$	0·11
IV	$-CH_2-CH_2-CO-N\langle\rangle N-CO-CH_2-CH_2-N-$ $\quad CH(CH_3)_2$	0·11
V	$-CH_2-CH_2-CO-N\langle\rangle N-CO-CH_2-CH_2-N-$ $\quad C_4H_{9-n}$	0·27
VI	$-CH_2-CH_2-CO-N\langle\rangle N-CO-CH_2-CH_2-N-$ $\quad CH_2-\langle\rangle$	0·15
VII	CH_3 $-CH_2-CH_2-CO-N\langle\times\rangle N-CO-CH_2-CH_2-N-$ $\quad CH_3$	0·43
VIII	$-CH_2-CH_2-CO-N-CH_2-CH_2-N-CO-CH_2-CH_2-N-$ $\quad C_2H_5 \qquad C_2H_5 \qquad CH_3$	0·20
IX	$-CH_2-CH_2-CO-N-CH_2-CH_2-N-CO-CH_2-CH_2-N-$ $\quad CH(CH_3)_2 \quad CH(CH_3)_2 \quad CH_3$	0·54

*Measured in chloroform, at 30°C

95

From x-ray analysis all these new polymers are amorphous during preparation. Some of them, however, after crystallizing treatment with non-solvents, revealed considerable crystallinity (polymers I, VI, IX); however, crystallization could not be induced in others even though they possess regular structures.
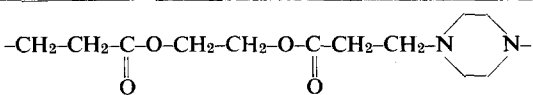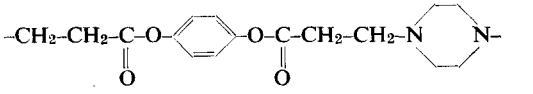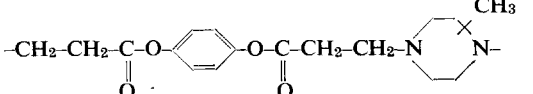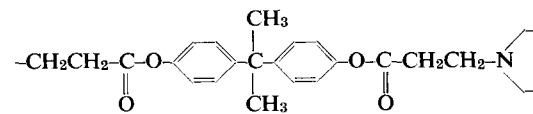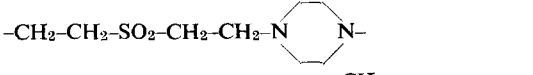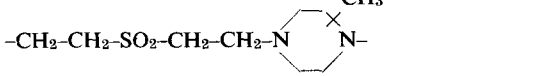
Several properties, including solubility and thermal stability, of polyamide amines obtained from primary amines are substantially similar to those from disecondary diamines.

Polymers from disecondary diamines and acrylic diesters or divinylsulphone

The poly-reaction that leads to the polyamide amines described up to now may also be accomplished with acrylic diesters or divinylsulphone instead of *bis*-acrylamides[13]. In this case, disecondary diamines could be used quite conveniently as co-monomers. Under the conditions we used, primary amines do not yield well defined products with acrylic diesters, whereas with divinylsulphone they yield cyclic dimeric products[14].

Some of the polymers obtained in this way are listed in *Table 4*. These

Table 4 Polymers from disecondary diamines and *bis*-acrylic esters or divinylsulphone

Ref. no.	Unit	$[\eta]^*$ at 30°C (dl/g)	m.p. [°C]	Crystallinity
I	$-CH_2-CH_2-C(=O)-O-CH_2-CH_2-O-C(=O)-CH_2-CH_2-N$⟨ ⟩$N-$	0·41	93	high
II	$-CH_2-CH_2-C(=O)-O-$⟨C₆H₄⟩$-O-C(=O)-CH_2-CH_2-N$⟨ ⟩$N-$	0·48†	189	high
III	$-CH_2-CH_2-C(=O)-O-$⟨C₆H₄⟩$-O-C(=O)-CH_2-CH_2-N$⟨CH₃⟩$N-$	0·25	164	high
IV	$-CH_2CH_2-C(=O)-O-$⟨C₆H₄⟩$-C(CH_3)_2-$⟨C₆H₄⟩$-O-C(=O)-CH_2CH_2-N$⟨ ⟩$N-$	0·23	145	high
V	$-CH_2-CH_2-SO_2-CH_2-CH_2-N$⟨ ⟩$N-$	0·60‡	200	high
VI	$-CH_2-CH_2-SO_2-CH_2-CH_2-N$⟨CH₃⟩$N-$	0·29	—	amorphous

* In chloroform, unless otherwise specified
† η sp/conc. (conc. = 0·5%) in glacial acetic acid
‡ In dimethylsulphoxide, at 100°C

polymers show the following repeating sequences along the main chain:

—a—a—c—c—a—a—c—c—

—a—a—d—a—a—d—
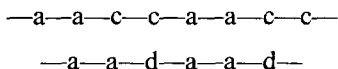
where a represents the tertiary amine group, c, the ester group, and d the sulphone group.

When examined by x-rays, all these polymers – except polymer VI – are seen to be highly crystalline. In spite of its apparent structural disorder, polymer III shows a very high crystallinity, which is higher than that of the earlier polyamide amines, which also contain one group derived from 2-methylpiperazine.

The polymers reported in *Table 4* show a behaviour towards solvents which is different from the polyamide amines previously described; in particular, except for polymer I, they show a lower affinity toward water and alcohols. Other properties, including thermal stability, are substantially the same.

Polymers from aminoacids and bis-acrylamides

Aminoacids may be used as the monomers for a polyaddition to give regular-structured polyampholites. By this route, it should also be possible to obtain water–soluble polymers showing optical activity by a simple method from fairly common and cheap substances, such as natural α-amino-acids.

The problem, however, is more complex than for disecondary diamines or primary monoamines. In fact – in agreement with predictions from the reaction mechanism – under the conditions we used, primary or secondary amine salts did not react with the double bonds of acrylamides or *bis*-acrylamides. In the same way, neutral aminoacids, which are in the form of internal salts, are not suitable monomers. Actually, on mixing aqueous solutions of 1,4-diacrylpiperazine and glycine or β-alanine, and by maintaining the mixture at 20°C for several days, no reaction occurs and the reagents can be recovered in practically quantitative amounts.

In addition, a great many aminoacids are not sufficiently soluble in the solvents which are suitable for poly-addition, except for water. However, the disadvantage of water lies in secondary reactions, such as the hydrolysis of the amide bond, which may occur when operating under severe temperature conditions or when long reaction times are used.

It should be theoretically possible to use aminoacids as monomers if the amine group is present in the polymerization system in the non-ionized state, and if side reactions are simultaneously prevented. A further important condition is the possibility of purifying the resulting polymer from added reagents.

We obtained[15] interesting results when we carried out poly-addition of some aminoacids with *bis*-acrylamides in an aqueous solution at room

97

temperature in the presence of a fairly volatile tertiary amine, such as triethylamine. It is well known that aminoacids do not form stable salts with ammonia and amines; however, in aqueous solution, the existence of the following equilibrium may be reasonably expected:

$$\overset{+}{H_3}N\text{--}R\text{--}COO^- + R_3'N \rightleftharpoons H_2N\text{--}R\text{--}COO^- + R_3\overset{+}{N}H$$
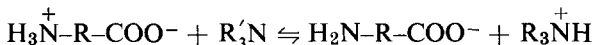
Once the polymer has been obtained, it may be substantially freed from triethylamine by prolonged high vacuum treatment. The use of hydroxides, or of alkaline carbonates, instead of triethylamine did not lead to satisfactory results. This method allowed the preparation of polymers with fairly high inherent viscosities (in water or methanol) from 1,4-diacrylylpiperazine and aminoacids such as glycine, β-alanine, taurine and others which do not contain substituents on the carbon atom adjacent to the amino nitrogen. Some of the polymers obtained are listed in *Table 5* (I to VI).

Table 5 Polymers from aminoacids and 1,4-diacryloylpiperazine

Ref. no.	Unit	η_{inh}^* at 30°C [dl/g]
I	–CH₂–CH₂–CO–N⬡N–CO–CH₂–CH₂–N– | CH₂–COOH	0·12†
II	–CH₂–CH₂–CO–N⬡N–CO–CH₂–CH₂–N– | (CH₂)₂–COOH	0·27
III	–CH₂–CH₂–CO–N⬡N–CO–CH₂–CH₂–N– | (CH₂)₃–COOH	0·18
IV	–CH₂–CH₂–CO–N⬡N–CO–CH₂–CH₂–N– | (CH₂)₄–COOH	0·12
V	–CH₂–CH₂–CO–N⬡N–CO–CH₂–CH₂–N– | (CH₂)₅COOH	0·12
VI	–CH₂–CH₂–CO–N⬡N–CO–CH₂–CH₂–N– | (CH₂)₂SO₃H	0·13
VII	–CH₂–CH₂–CO–N⬡N–CO–CH₂–CH₂–N⬡(COOH, ×)N–	0·28‡
VIII	–CH₂–CH₂–CO–N⬡N–CO–CH₂–CH₂–N⬡(HOOC, COOH)N–	0·30†

*In 90% methanol/10% water, were not otherwise specified (conc. = 0·5%)
†In water
‡In 80% methanol

Corresponding results were also obtained with cyclic aminoacids, such as piperazine-2-carboxylic acid and piperazine-2,3-dicarboxylic acid (*Table 5*, VII and VIII). In the former case, a polymer may be obtained without addition of triethylamine, but with a far lower polymerization rate.

Further difficulties are encountered when natural aminoacids, other than glycine are used as monomers; this is due to steric hindrance. In this case, even in the presence of equimolar amounts of triethylamine, only low molecular weight polymers were obtained in aqueous solution and at room temperature. It is also rather difficult to prepare high polymers from primary amines which are very sterically hindered (e.g. isopropylamine)[8]. The reaction rate cannot be increased by conducting the polymerization in water at higher temperatures since hydrolysis will occur.

We did succeed in obtaining polymers with fairly high intrinsic viscosities, and possessing optical activity, by using dipeptides such as glycyl- or β-alanyl derivatives of α-aminoacids[15]. Some results obtained by us with optical isomers of glycyl or β-alanyl alanine are listed in *Table 6*.

It is also theoretically possible to use tri- or polypeptides, as monomers, provided that the first residue is derived from glycine or β-alanine. In this case, polymers with a regular structure should be obtained, with peptide side chains arranged in a predetermined sequence.

Polymers from hydrazine (or 1,1-dimethylhydrazine) and bis-acrylamides

It may also be of interest to report the results obtained when monomers with a nucleophilic character different from amines are used.

For example, linear polyamide hydrazines may be obtained with hydrazine (or 1,1-dimethylhydrazine) and *bis*-acrylamides[16]. As far as we know, polymers of this type have not been described in the literature; their basicity, solubility and chemical reactivity make them interesting from a practical point of view.

Since hydrazine has four mobile hydrogens, it must be considered to be a polyfunctional monomer in the poly-addition under examination. However, as previously observed, in the poly-addition of disecondary diamines to *bis*-acrylamides, the steric bulkiness of the amino group exerts a dominant influence on the rate of polymerization. This can also be expected with hydrazine derivatives.

This may be the reason why hydrazine reacts with an equimolar amount of *bis*-acrylamide according to the equation:

$$x\ NH_2NH_2 + x\ CH_2{=}CH{-}CO{-}N{-}R'{-}N{-}CO{-}CH{=}CH_2$$
$$\underset{R}{|}\qquad\underset{R}{|}$$

$$\rightarrow \left[NH{-}NH{-}CH_2{-}CH_2{-}CO{-}\underset{\underset{R}{|}}{N}{-}R'{-}\underset{\underset{R}{|}}{N}{-}CO{-}CH_2{-}CH_2 \right]_x$$
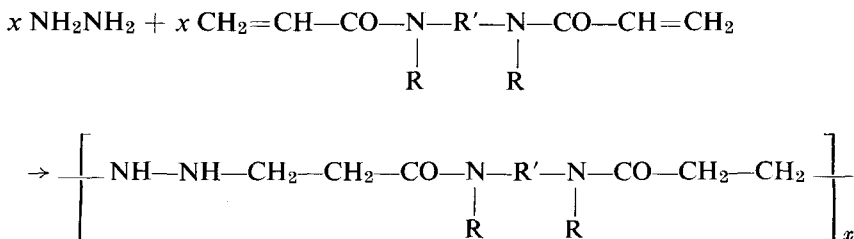
to give an essentially linear polymer.

Table 6 Polymers from dipeptides and 1,4-diacrylylpiperazine

Ref. no.	Unit	η_{inh} at 30°C [dl/g]*	$[\alpha]_D^{25}$†
I	-CH₂-CH₂-CO-N⟨ ⟩N-CO-CH₂-CH₂-N- | CH₂-CO-(L-Ala)	0·24†	-25·6°
II	-CH₂-CH₂-CO-N⟨ ⟩N-CO-CH₂-CH₂-N- | CH₂-CH₂-CO-(D,L-Ala)	0·16	—
III	-CH₂-CH₂-CO-N⟨ ⟩N-CO-CH₂-CH₂-N- | CH₂-CH₂-CO-(D-Ala)	0·25	+10·4°
IV	-CH₂-CH₂-CO-N⟨ ⟩N-CO-CH₂-CH₂-N- | CH₂-CH₂-CO-(L-Ala)	0·19	-9·8°

*In 90% methanol/10% water, were not otherwise specified (conc. = 0·5%)
†In water
‡In aqueous normal hydrochloric acid (conc. = 1%)

For the end-group

$$R-NH-NH_2$$
$$\text{(a)} \quad \text{(b)}$$
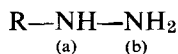
(where R is the growing polymeric chain), an addition to the nitrogen atom (a) is expected to be more difficult that an addition to the nitrogen atom (b) due to the steric hindrance of the growing polymer chain. Addition involving the —NH—NH groups present in the chain, with consequent crosslinking, is similarly improbable.

The experimental results were found to be in agreement with the data expected. The polymers obtained are shown in *Table 7* (from I to III).

Table 7 Polyamide hydrazines

Ref. no.	Unit	$[\eta]$ at $30°C*$ $[dl/g]$
I	-CH₂-CH₂-CO-N⟨⟩N-CO-CH₂-CH₂-NH-NH-	0·18
II	-CH₂-CH₂-CO-N⟨CH₃×⟩N-CO-CH₂-CH₂-NH-NH-	0·18
III	-CH₂-CH₂-CO-N-CH₂-CH₂-N-CO-CH₂-CH₂-NH-NH- │CH(CH₃)₂ │CH(CH₃)₂	0·16
IV	-CH₂-CH₂-CO-N⟨⟩N-CO-CH₂-CH₂-N- │N(CH₃)₂	0·10
V	-CH₂-CH₂-CO-N⟨⟩N-CO-CH₂-CH₂-N- │N(CH₃)₂	0·08

*In chloroform

The structure of linear polyamide hydrazines obtained from hydrazine and *bis*-acrylamides has been confirmed not only by elemental analysis, but also by spectroscopic data. It is interesting to observe that linear polymers are obtained from equimolar amounts of hydrazine and *bis*-acrylamide, whereas crosslinked polymers are obtained with higher amounts of *bis*-acrylamide, although fairly long reaction times are necessary. Hydrazine is fairly reactive in this type of poly-addition; polyamide hydrazines, like polyamide amines, are prepared in aqueous solution at room temperature. Under these conditions, the molecular weight of the product increases rapidly to a maximum, and then decreases. As mentioned above, this also occurs in the preparation of polyamide amines under similar experimental conditions. Again, this behaviour may be explained by the simultaneous hydrolysis of the amide link.

101

The presence of the —NH—NH— group in these polymers makes it possible to carry out modification reactions. In particular, a further reaction with monofunctional compounds containing activated double bonds, such as acrylonitrile or phenylisothiocyanate, is possible:

$$—NH—NH— + C_6H_5NCS \longrightarrow \quad \begin{matrix} —N—NH— \\ | \\ C=S \\ | \\ HN—C_6H_5 \end{matrix}$$
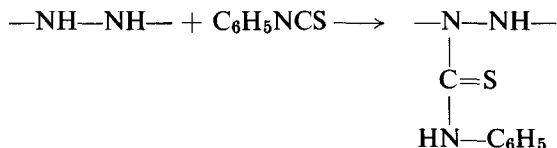
Under conditions corresponding to those described, linear polymers may also be obtained from *bis*-acrylamides and typical derivatives of hydrazine, such as 1,1-dimethylhydrazine. The polymers obtained are listed in *Table 7* (IV, V). The intrinsic viscosity values show that their molecular weight is not very high.

We may conclude that the poly-addition of dialkylhydrazine or, under suitable conditions, of hydrazine, to *bis*-acrylamides, must be considered as a particularly easy reaction and up to now the only route available for the synthesis of linear polymers with amide and hydrazine groups regularly arranged along the main chain.

Polymers from primary phosphines and bis-acrylamides

Good results were obtained when the above method of polymerization was applied to phosphines[17]. Polyphosphines obtained by radical catalysed poly-addition of primary phosphines to diolefins – such as diallyl or its derivatives – are described in patent literature[18]. However, these products have low molecular weights and their structure is still uncertain.

The polyamide phosphines obtained by us, however, were prepared in the absence of catalysts and in the presence of radical polymerization inhibitors, using a process similar to that used for the synthesis of polyamide amines. The reaction is carried out in a toluene–ethanol solution under nitrogen at about 40°C. Under such conditions, the time required to reach a satisfactory molecular weight varies from one to four days.

Some examples of polymers obtained from 1,4-diacrylylpiperazine or 1,4-diacrylyl-2-methylpiperazine and phenylphosphine or benzylphosphine, as monomers, are given in *Table 8*.
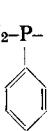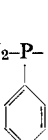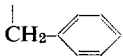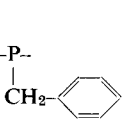
The thermal stability of these polymers is fairly good. As observed from the thermobalance under vacuum, weight loss starts above 360°C, whereas under the same conditions polyamide amines with similar structure start to decompose at about 200°C.

Conclusions

The foregoing remarks on the branching scheme poly-addition which we have used to synthesize polymers with a tertiary amine group (or related

102

groups) suggest that an extremely high number of variants is possible for this method of synthesis, since the number of substances that may be used as monomers is particularly high. This poly-reaction can be performed using mild conditions and in the presence of various other groups; these groups can be chosen so as to exclude interchange reactions, thus conferring a high stability to even very complex macromolecules.

Table 8 Polyamide phosphines

Ref. no.	Unit	$[\eta]^*$ at $30°C$ $[dl/g]$
I	$-CH_2-CH_2-CO-NN-CO-CH_2-CH_2-P-$ (piperazine ring; P bonded to phenyl with =O)	0·25
II	$-CH_2-CH_2-CO-NN-CO-CH_2-CH_2-P-$ (piperazine ring with CH$_3$ and ×; P bonded to phenyl with =O)	0·31
III	$-CH_2-CH_2-CO-NN-CO-CH_2-CH_2-P-$ (piperazine ring; P bonded to CH_2-phenyl)	0·90†
IV	$-CH_2-CH_2-CO-NN-CO-CH_2-CH_2-P-$ (piperazine ring with CH$_3$ and ×; P bonded to CH_2-phenyl)	0·23

*In chloroform were not otherwise specified
†η sp/conc. (conc. = 0·5 %) in glacial acetic acid

Furthermore, by using suitable reaction conditions one can synthesize polymers consisting of segments of different lengths, or polymers with an ordered structure from monomers of complex structure.

This poly-reaction could have important applications in the synthesis of very complex macromolecules such as biopolymers. It is a simple and spontaneous poly-reaction which occurs at normal temperatures, to give polymers containing base units of predetermined length with a number (possibly a large number) of different chemical groups regularly arranged along the main chain.

103

## (B) POLYMERS WITH AMINE GROUPS DIRECTLY BOUND TO THE
MAIN CHAIN:

homopolymers and copolymers of enamines

No significant reports on the polymerization of enamine compounds have appeared in the literature. However, the enamines isolated so far in the pure state are derived from aldehydes higher than acetaldehyde or from ketones higher than acetone. With regard to, for example, N-vinyl or isopropenyl amines, we can definitely say that apart from a few patent claims[19] the literature does not report any certain examples of isolation. The results described in patents do not seem to be reproducible.

For a vinyl homopolymerization, monomers of N-vinyl amine character are of greater interest than enamines of complex structure; the latter are more widely known at present. In fact, even apart from catalysis problems, enamines are expected to have little tendency to homopolymerize because monomers of the vinyl or vinylidene type with a highly hindered double bond generally give very poor yields of high polymers on homopolymerization.

The N-vinyl amines that have definitely been isolated have at least one aromatic substituent bonded to nitrogen. However, the presence of phenyl substituents substantially decreases the basicity of the amino group.

We examined the case of N-vinylmorpholine (I) in detail. By reacting acetaldehyde and excess morpholine, in the presence of basic dehydrating agents, we isolated 1,1-dimorpholinethane (II) in good yield[20]. This compound was shown to exist in equilibrium with morpholine and N-vinylmorpholine.

$$\text{(II)} \qquad\qquad \text{(I)} \qquad\qquad \text{(III)}$$
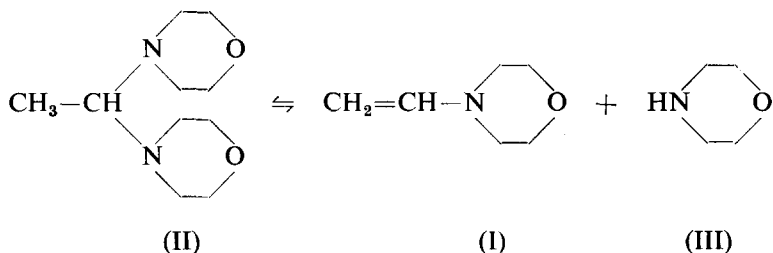
Such an equilibrium is displaced to the right by an increase in temperature, but it exists even at room temperature when the compound is liquid. Mannich and Davidsen[21], had previously suggested a similar dissociation of the analogous derivatives of piperidine, only at a higher temperature and in the vapour phase.

This equilibrium is responsible for some apparent anomalies in the behaviour of 1,1-dimorpholinethane. This compound, melting at about 25°C, may be distilled at 50–55°C and 20 mmHg. Surprisingly, the boiling point depends on the rate of heating and the distillate spontaneously gives off a large amount of heat in the collection vessel. By gradually decreasing the pressure, the distillation occurs at progressively higher temperatures; at 0·1 mmHg the temperature of the vapour reaches about 80°C. This may be

explained if distillation at 20 mmHg occurs after dissociation and co-distillation of the two products occurs. Under high vacuum, at least a part of the original compound may be distilled unchanged.

If the 20 mmHg distillate is collected in a vessel at $-78°C$ and the i.r. spectrum taken immediately, a sharp band due to the vinyl group is observed. If the distillate is heated to room temperature, heat is evolved and this band disappears. Finally, in the i.r. spectra run at different temperatures on the liquid compound, the bands of the vinyl double bond (e.g. at 6·05 μm) become evident and gradually become stronger on increasing the temperature; at 80°C a substantial amount of N-vinylmorpholine is present in the system.

The chemical behaviour of 1,1-dimorpholinethane is also in agreement with the existence of a dissociation equilibrium in morpholine and N-vinyl-morpholine[22]. Some typical reagents that form compounds with enamines, such as 4-nitrophenylazide or benzonitryloxide, give quite good yields of the corresponding derivatives of N-vinylmorpholine in the presence of 1,1-dimorpholinethane, and under mild reaction conditions.

$$II + Ar-N_3 \longrightarrow \qquad + III$$

$$[Ar = 4\text{-}NO_2\text{-}C_6H_5\text{-}]$$
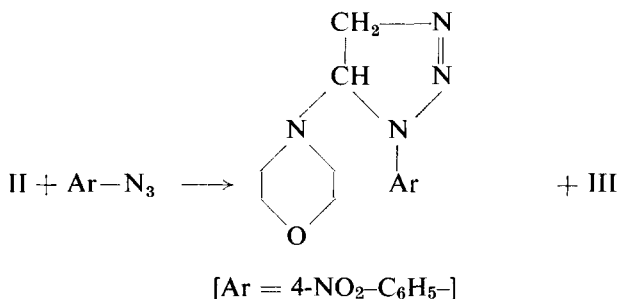
Other secondary amines introduced into the system may participate in the dissociation equilibrium. For example, derivatives of N-vinyldiethylamine are obtained in the presence of diethylamine[22]:

$$II + (C_2H_5)_2NH + Ar-N_3 \longrightarrow \qquad + III$$

$$[Ar = 4\text{-}NO_2\text{-}C_6H_4\text{-}]$$
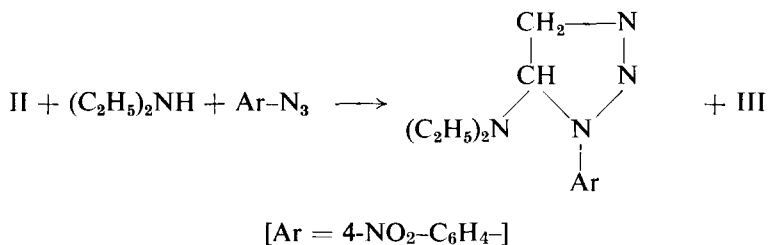
Two factors are important in these exchange reactions: the basicity of the added amine and its steric bulkiness. The other conditions being constant, amines with a higher basicity tend to displace morpholine; however, this does not occur if amines have a high basicity but are very hindered, (e.g. dicyclohexylamine).

P—H

All attempts to isolate pure N-vinylmorpholine by chemical or physical methods have been unsuccessful[20,22]. N-Vinylmorpholine is apparently unstable in the absence of morpholine, and decomposes during its isolation yielding brown polymeric products of a non-polyvinyl type.

However, a dilute solution of vinyl morpholine, which quickly decomposes to tars and morpholine, has been obtained[22]. By analogy with observations under suitable conditions, of enamines derived from acetone (N-isopropenylamines), or of methyl-*n*-alkylketones[23], we may suppose that free N-vinylmorpholine tends to give rise to oligomeric or polymeric self-condensation products with loss of morpholine, under the experimental conditions used.

It is difficult to obtain homopolymers of N-vinylmorpholine directly from 1,1-dimorpholinethane. The high electronic density on the vinyl double bond excludes the use of anionic and radical initiators. 1,1-Dimorpholinethane is actually inert to the action of initiators such as azo*bis*isobutyronitrile. The use of cationic-type initiators is, however, complicated because the system contains several chemical species capable of interacting with them. However, we succeeded in obtaining low molecular weight polymers from 1,1-dimorpholinethane using protonic acids (e.g. sulphuric, *p*-toluensulphonic or even acetic acid) in an alcoholic solution. Even hydroquinone and water can initiate the polymerization although they are very weak acids. The use of iodine or alkyl iodides gives identical results.

The polymers obtained have molecular weights not exceeding several thousands and they are yellow or light brown. As shown by i.r. and n.m.r. analyses, their structure is somewhat irregular, although reproducible, and only roughly corresponds to that of polyvinylmorpholine[20].

Enamines are known to react by an ionic mechanism, in the absence of catalysts, with acrylonitrile and with other compounds containing vinyl double bonds activated by electron-attracting groups in the α-position[25-28]; the reaction takes place under mild conditions. The first reaction products are cyclic products, such as:

$$C_2H_5-CH=CH-N\underset{\diagdown\!\diagup}{\overset{\diagup\!\diagdown}{}}O \; +CH_2=CHCN \longrightarrow$$
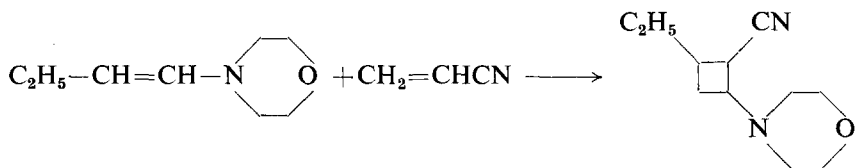
These products are thermally quite stable when they are obtained from enamines of aldehydes but, if they are derived from enamines of ketones, they decompose on heating, to give cyanethylated enamines with opening of the ring[27]:
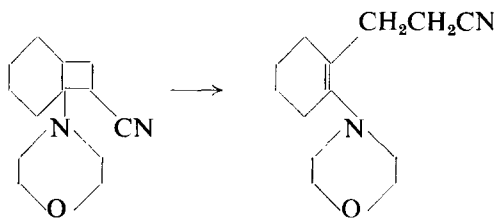
However, if acrylonitrile and enamine are allowed to react in the presence of radical initiators, copolymers of fairly high molecular weight are formed and copolymerization predominates over simple addition, or side reactions.

The best results are obtained using enamines of aldehydes; enamines of ketones, e.g. 1-morpholinocyclohexene or 1-morpholinocyclopentene also give copolymers with acrylonitrile, although high yields are seldom obtained. We particularly investigated the copolymerization with acrylonitrile of some enamines of butyraldehyde, especially 1-piperidinobutene and 1-morpholino-butene[24], to give the following copolymers:

$$[X = -CH_2-, \text{ or } -O-]$$
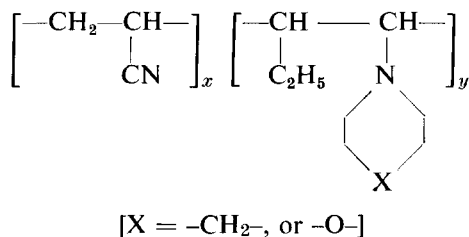
Azo compounds, and in particular azodiisobutyronitrile, were used as radical initiators. The copolymerization is best carried out in bulk with carefully purified monomers, in an inert atmosphere, at temperatures between 40°C and 70°C, and for times varying from a few hours to several days.

The curve of composition with 1-morpholinobutene, (*Figure 4*), is similar to that obtained for other enamines. The enamines being examined do not homopolymerize appreciably in the presence of radical initiators; consequently the enamine content of the copolymers increases with the concentrations of enamine in the monomer phase, but never rises above 50% (in moles).

It is interesting to observe, (e.g. in *Figure 4*), that the experimental results are best interpreted by considering an effect of the penultimate unit on the reactivity of the growing copolymeric radical. A radical ending with two acrylonitrile units reacts far more readily with the enamine than with acrylonitrile; however, this difference disappears if the penultimate unit is an enamino group.

The rate of copolymerization increases with increasing concentration of acrylonitrile in the monomer mixture as well as with temperature.
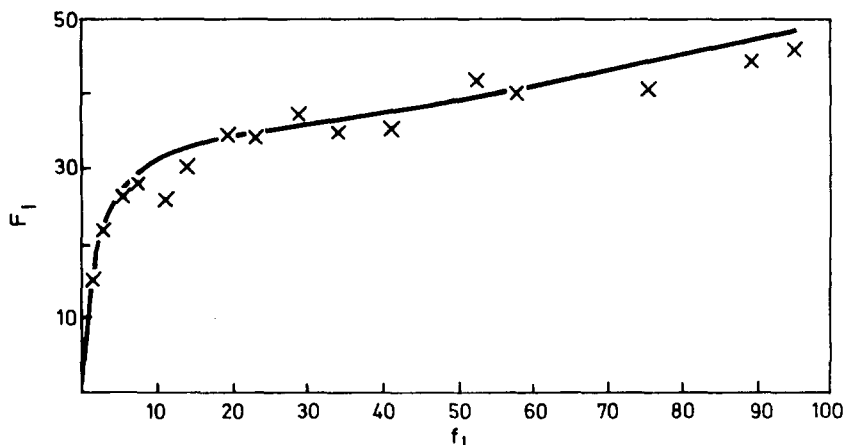
107

Figure 4 Composition curve of the copolymerization of acrylonitrile with 1-morpholino-butene (60°C; AzBN as initiator). [Incremental polymer composition (mole fraction F_1) *versus* the monomer composition (mole fraction f_1).]. The solid curve is calculated taking into account the penultimate effect [24]
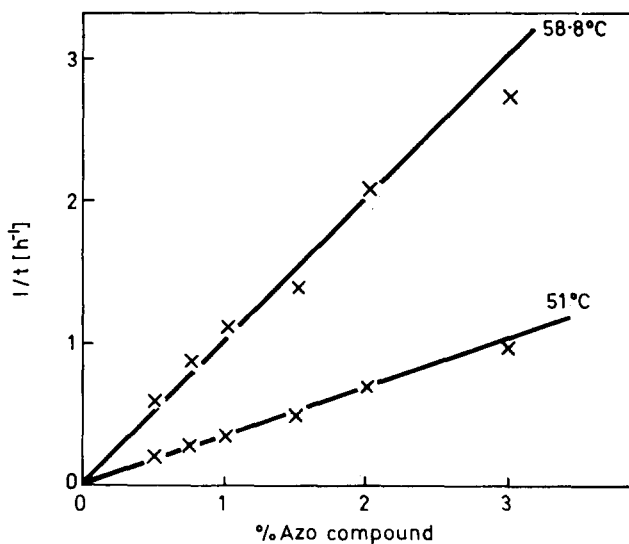

Figure 5 Copolymerization of acrylonitrile with 1-morpholino-butene: demonstration of the unitary overall reaction order with regard to the initiator

Further kinetic features have been found on studying the copolymerization of equimolar mixtures of monomers, and at low yields. The overall reaction rate is proportional to the concentration of the initiator (see, e.g. *Figure 5*) and has a fairly high energy of activation of about around 30 kcal mole^{-1}. Moreover, the molecular weight of the copolymer is not very high and it is

fairly insensitive to variations in the composition of the monomer phase, the concentration of the initiator, and the degree of conversion.

These observations suggest that an appreciable chain transfer with the monomer, particularly a degradation chain transfer with enamine, occur.

If the copolymerization is carried out at higher conversions, the reaction tends to stop at a fairly low degree of conversion. The threshold conversion, which we have determined, does not only depend on temperature but also on the amount of initiator used. This may be connected with the presence of a degradative transfer, which in this case predominates; the kinetic chain length is consequently rather short.

In the cases we considered, the intrinsic viscosities in acetone at 30°C of enamine–acrylonitrile copolymers varied from 0·09 to 0·14dl/g.

The copolymers are white powders, stable in the air, and amorphous by x-rays. They are generally soluble in chloroform, acetone, acetonitrile, dimethylformamide, pyridine and glacial acetic acid. They are mostly insoluble in alcohols, aliphatic hydrocarbons and water.

The copolymers having an enamine unit content above 7–8% dissolve in dilute aqueous acid and they may be reprecipitated unchanged from these solutions with alkalis, as shown by comparison of intrinsic viscosities and i.r. spectra.

Having demonstrated that it is possible to obtain acrylonitrile–enamine copolymers in the pure state, it was interesting to check whether N-vinyl morpholine copolymers could be obtained directly from 1,1-dimorpholinethane and acrylonitrile. Here the reaction system appears to be complex, in that the morpholine that is present in the dissociation equilibrium of 1,1-dimorpholinethane, in equimolar amounts to N-vinylmorpholine, may react with acrylonitrile to give a simple co-dimer as a by-product.

However, under suitable conditions and in the presence of radical initiators, good yields of the copolymers considered and substantial amounts of 4-(β-cyano)ethylmorpholine are obtained[24].
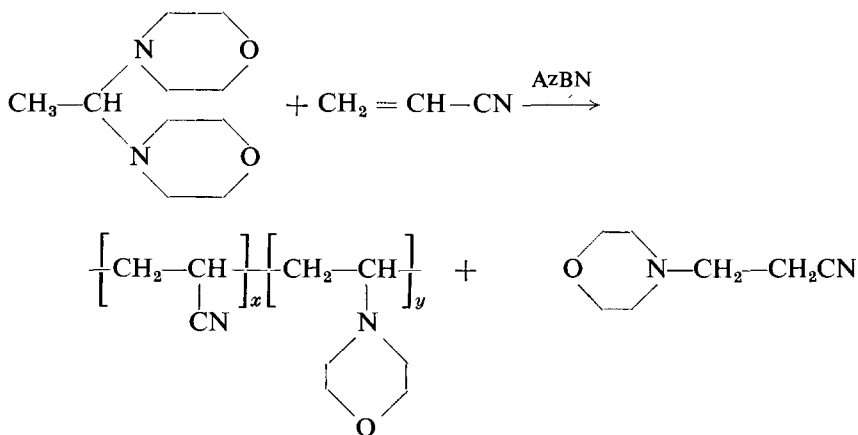
The composition of the copolymers varies on varying the ratio of the monomers; but the complexity of the system makes the use of the traditional equations of radical copolymerization complicated. However, contents of enamine units in the copolymer of about 30% may be obtained.

The molecular weight, solubility and chemical reactivity of the copolymers obtained are similar to those of the copolymers of acrylonitrile with more substituted enamines. On the contrary, their thermal stability is much higher. Using the Adamel CT 59 thermo-balance, Chevenard-Journier system, and heating rates of 105 °C/h, decomposition commences at about 320 °C with the copolymer of N-vinylmorpholine in air and at about 260 °C in the case of copolymers of enamines of higher aldehydes.

(C) POLYAMINES IN WHICH THE AMINE GROUPS ARE IN THE SIDE CHAIN

Polymers with the amine groups bound to the main chain by aliphatic hydrocarbon residues

Amino-olefins with the general formula

$$CH_2{=}CH{-}(CH_2)_n{-}NR_2 \quad (n \geqslant 2)$$
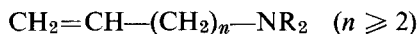
have been recently polymerized in the presence of conveniently modified Ziegler-Natta catalysts, to give stereoregular high polymers[29]. However, the polymerization of allyl amine monomers ($n = 1$) to high polymers has not so far been accomplished.

However, high molecular weight tertiary poly(allyl amines) may be synthesized by modification of other macromolecular substances, although this method is not always as easy as it might appear at first sight. The main difficulty is to find reactions which give quantitative transformations of the required chemical groups. In fact, at least in fundamental research, the aim is to prepare a homopolymer that formally corresponds to a well defined monomer.

There are relatively few methods of synthesizing tertiary amines and, therefore, there are few available polymers suitable for modification. For the reasons mentioned before, we reject reactions which are difficult to control and those (e.g. the Hoffman condensation) that usually lead to mixtures of products.

Satisfactory results were obtained by reducing the carbonyl groups of poly-N,N-dialkyl acrylamides[30]:
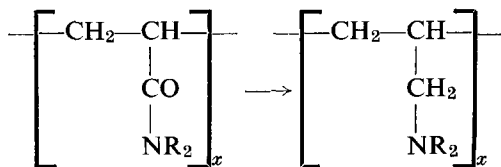
The reducing agent used was excess lithium aluminium hydride dissolved in dioxane, N-methylmorpholine or anisole, at a reaction temperature of

110

100°C to 150°C; this has been previously used with fairly good results for the reduction of other polymers[31].

From polyacrylamides we obtained poly(allyl amines) in yields ranging from 60% to 90%. Their intrinsic viscosities varied between 0·2 and 1 dl/g and we may assume therefore that the molecular weights of these polymers is high and of the same order of magnitude as that of the starting polyacrylamides. The high degree of reduction evidenced by the disappearance of the absorption band of amide C=O (6·1 μm), which was very intense in the starting polymers. Moreover, the elemental analysis of poly(allyl amines) is in excellent agreement with the calculated values.

Polyacrylamides often dissolve or swell in water, but the poly(allyl amines) obtained by us are insoluble in water, except for poly-N-allyl-morpholine which dissolves below 10°C, although they reprecipitate on heating. On the other hand, n-heptane acts as a precipitant for all the polyacrylamides considered, whereas it easily dissolves aliphatic or cycloaliphatic poly(allyl amines) (except for poly-N-allylmorpholine). All poly(allyl amines) considered dissolve easily in diluted aqueous acids (even in the weak acids like acetic acid) and reprecipitate on the addition of alkali.

Open chain aliphatic poly(allyl amines) like poly-N,N-diethylallylamines, are flexible, hard materials which resemble some polyhydrocarbons, such as polyethylene. The presence of cyclic structures, derived from pyrrolidine, piperidine and morpholine, makes these polymers hard and somewhat brittle when moulded in thin sheets.

All the poly(allyl amines) obtained by us were amorphous by x-rays, even the modified stereoregular polyacrylamines. This may be due to a lack of stereoregularity from racemization that occurred during modification. It is well known that stereoregular vinyl polymers, especially those containing a carbonyl group in the α-position at the tertiary carbon atom, may lose stereoregularity by heat treatment with basic catalysts[32].

Amine polymers of the type of poly(acrylic acid) derivatives

Most amine polymers previously known with a well defined structure fall into this present class. Well known examples are polyacrylates or polymethacrylates of amino alcohols.

In research carried out in an attempt to prepare polymers with pharmacological activity capable of preventing silicosis[1] we obtained interesting results[33] by preparing substituted polyacrylamides of the type

$$\left[\begin{array}{c} -CH_2-CH- \\ | \\ CO-N-CH_2-CH_2-N\diagup\diagdown O \\ | \\ R \end{array} \right]_x$$
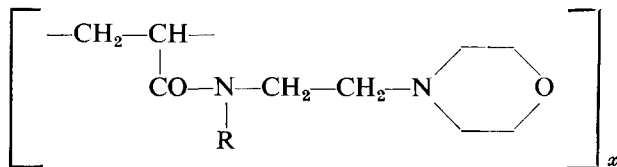
The behaviour of the monomers toward polymerization is substantially

111

the same as that of the usual N,N-dialkyl substituted acrylamides, when the initiator does not interact with the amino groups.

We obtained high polymers of these monomers both by radical polymerization in the presence of azo-*bis*isobutyronitrile and by anionic polymerization in the presence of butyl lithium or Grignard compounds.

The former method yielded polymers amorphous to x-rays. The latter (in a toluene solution at $-78\,°C$) gave different polymers. These are partially insoluble in solvents that dissolve radical polymers; their x-ray diffraction spectra exhibit broad crystallinity bands, which are absent from the spectra of the corresponding free radical produced polymers. These bands may be attributed to the presence of imperfect crystals, that is, to a paracrystalline arrangement, which might be due to substantially regular chains.

The presence of crystallinity was surprising since there are reports in the literature that the presence of tertiary amines hinders the corresponding stereospecific anionic polymerization of N,N-dialkyl substituted acrylamides[34]. In our work, the monomer itself had the character of a tertiary amine.

The polymerization of monomers like β-dialkyl(amino)ethyl methacrylates with various organometallic catalysts, such as phenyl magnesium bromide, which had been previously studied[35], gave amorphous polymers when the tertiary amino group present had an aliphatic or cycloaliphatic character. Under the same conditions, analogous nitrogenous monomers, in which the nitrogen atom is not basic but is present in a heterocyclic structure of the carbazole type, yielded crystallizable isotactic polymers[35].

At present, the acrylamides studied by us seem to be the only monomers with basic amino substituents that may be polymerized stereospecifically. This is apart from the amino olefins mentioned previously[29], since in this case the amino group must here be previously protected by complex formation.

REFERENCES

1 Natta, G., Vigliani, E. C., Danusso, F., Pernis, B., Ferruti, P. and Marchisio, M. A. *Rend. Accad Naz. Lincei* (VIII) 1966, **40**, 11
2 Ferruti, P. and Marchisio, M. A. *La Medicina del Lavoro* 1966, **57**, 481
3 Vigliani, E. C., Pernis, B., Marchisio, M. A., Ferruti, P. and Parazzi, E. 15th Congrés Inernat. de Médicine du Travail, Wien, Sept. 19–24, 1966, **2**, 665
4 Marchisio, M. A., Sbertoli, C. and Farina, G. *La Medicina del Lavoro* 1968, **59**, 136
5 Mallik, K. L. and Das, M. N. *Z. Phys. Chem.* 1960, **25**, 205
6 Hulse, G. E. *U.S. Patent* 2, 759, 913 (*C.A.* **50**, 17533)
7 Danusso, F., Ferruti, P. and Ferroni, G. *Chimica e Industria* (*Milan*) 1967, **49**, 271
8 Danusso, F., Ferruti, P. and Ferroni, G. *Chimica e Industria* (*Milan*) 1967, **49**, 453
9 Danusso, F. 'New trends in chemistry teaching, UNESCO, 1969, **2**, 172
10 Perrin, D. D., 'Dissociation Constants of Organic Bases in Aqueous Solution' Butterworth, London, 1965

11 Morgan, P. W. 'Condensation polymers: by interfacial and solution methods' Interscience New York 1965, p 423
12 Danusso, F., Ferruti, P. and Ferroni, G. *Chimica e Industria (Milan)* 1967, **49**, 587
13 Danusso, F., Ferruti, P. and Ferroni, G. *Chimica e Industria (Milan)* 1967, **49**, 826
14 Bellaart, A. C. *Rec. Trav. Chim.* 1962, **81**, 156
15 Danusso, F., Ferruti, P. Communication to the 10th Meeting of the Italian Chemical Society, Padova, June 19, 1968
16 Ferruti, P. and Brzozowski, Z. *Chimica e Industria (Milan)* 1968, **50**, 441
17 Ferruti, P. and Alimardanov, R. *Chimica e Industria (Milan)* 1967, **49**, 831
18 Garner, A. Y. *U.S. Patent* 3,010,946 (*C.A.* **56**, 61704)
   Niebergall, H. *German Patent* 1,086,897 (*C.A.* **55**, 14977)
   Gutweiler, K. and Niebergall, R. *German Patent* 1,103,590 (*C.A.* **55**, 24102)
   Gutwieler, K., Saüder, M., Schneider, G. *German Patent* 1,131,412 (*C.A.* **57**, 12722)
19 See for example: Geigy, A. G. *British Patent* 832,078 (*C.A.* **54**, 20877);
   Blumenkopf, N., Heicht, O. F. *U.S. Patent* 3,126,363 (*C.A.* **61**, 4368);
   and also Von Braun, J., Pinkernelle, W. *Ber.* 1927, **70**, 1230;
   Gardner, C., Kerrigan, V., De Rose, J., Weedon, B. C. L. *J. Chem. Soc.* 1949, p 789
20 Danusso, F., Ferruti, P. and Peruzzo, G. F. *Atti Accad Naz. Lincei* 1965, **39**, 498
21 Mannich, C., Davidson, H. *Ber.* 1936, **69**, 2016
22 Ferruti, P., Bianchetti, G. and Pocar, D. *Gazz. Chim. Ital.* 1967, **97**, 109
23 See for example: Bianchetti, G., Pocar, D., Dalla Croce, P., Gallo, G. G., Vigevani, A. *Tetrahedron Letters* 1966, p 1637;
   Bianchetti, G., Dalla Croce, P., Pocar, D. *Tetrahedron Letters* 1965, p 2039
24 Danusso, F., Ferruti, P., Feré, A: *European Polymer J.* in press
25 Stork, G., Brizzolara, A., Landesman, H., Szmuskovicz, J. and Terrel, R. *J. Amer. Chem. Soc.* 1963, **85**, 207
26 Brannock, K. C., Bell, A., Burpitt, R. D. and Kelly, C. A. *J. Org. Chem.* 1961, **26** 625
27 Fleming, I. and Harley-Mason, J. *J. Chem. Soc.* 1964, p 2165
28 Danusso, F. and Ferruti, P. unpublished results
29 Giannini, U., Brückner, G., Pellino, E. and Cassata, A. *J. Polym. Sci. (B)* 1967, **5**, 527
30 Danusso, F. and Ferruti, P. *Chimica e Industria (Milan)* 1968, **50**, 71
31 Petit, J. and Houel, B. *Compt Rend.* 1958, **246**, 1427
   Houel, B. *Compt Rend.* 1958, **246**, 2488
   Cohen, H. L. and Minsk, L. M. *J. Org. Chem.* 1959, **24**, 1404
   Cohen, H. L., Borden, D. G. and Minsk, L. M. *J. Org. Chem.* 1961, **26**, 1274
32 Veno, A. and Schuerch, C. *J. Polym. Sci., (B)* 1965, **3**, 53
33 Danusso, F., Ferruti, P., Peruzzo, G. F. and Natta, G. *Chimica e Industria (Milan)* 1966, **48**, 357
34 Butler, K., Thomas, P. R. and Tyler, G. J. *J. Polym. Science* 1960, **48**, 357
35 Natta, G., Longi, R. and Pellino, E. *Makromol. Chem.* 1964, **71**, 212

Notes and Communications

The temperature coefficient of the c lattice parameter of polyethylene; an example of thermal shrinkage along the chain direction

Y. KOBAYASHI* and A. KELLER

THE UNIT CELL parameters of polyethylene and their dependence on crystallization conditions and chemical composition (branch content) has been subject to numerous studies in the past. As a result of these it is generally established that the a and b parameters, are markedly dependent on the above variables (a more so than b) but c is invariant. As a and b relate to interchain separation and c to the periodicity along the chain[1], these findings have set a well established pattern in polymer crystallography: variability of the 'lateral' lattice parameters but constancy of the periodicity (and corresponding lattice parameter) along the chain, the latter being determined by the valence angles and bond distances involved

The most definitive work on lattice parameters in polyethylene is due to Swan[2] who among others determined the temperature coefficients over a wide temperature range. In the temperature range around 30°C he reports $\alpha_a = 22 \times 10^{-5}°C^{-1}$ for a and $\alpha_b = 3\cdot8 \times 10^{-5}°C^{-1}$ for b. As regards c the thermal coefficient obtained was $\alpha_c = (-3\cdot5 \pm 5) \times 10^{-6}°C^{-1}$. 'Whether α_c is significantly different from zero is rather hard to decide; the writer prefers the value zero' (quotation from ref. 2). This is the only, and as seen indecisive, hint of a possible variation of c, and that in a sense opposite to that of the other parameters.

We have conducted a detailed precision x-ray investigation of the 002 reflection of polyethylene single crystals as precipitated from solution. The main purpose was a study of the line profile to help solve the problem of the fold structure[3]; this will be covered in a separate publication. As part of this investigation the c lattice parameter was automatically determined leading to definitive information on its thermal behaviour. This will form the material of the present note.

EXPERIMENTAL

The experimental details will be described in our forthcoming comprehensive publication. Here only the bare outlines will be given. Except for one sample which was crystallized under 4 300 atm pressure from the melt (supplied by B. Wunderlich) the samples were single crystals grown from xylene at 70°C. They were used in the form of oriented mats 0·5 mm thick with the c axis

* Present address: Faculty of Technology, Tokyo Metropolitan University, Setagaya-ku, Tokyo, Japan

normal to the mat plane. The oriented nature of the mat was advantageous for obtaining adequate intensity concentration in case of the inherently weak 002 reflection. For the most definitive measurements the mats were annealed at 120–125°C. This stabilized the crystals against further textural changes during the main measurements themselves. These consisted of recording the 002, together with the nearby 112, reflection in the temperature range of 20–125°C.

The measurements were carried out with a Philips Horizontal x-ray goniometer and a scintillation counter using Cu-K α-radiation. Heating of the sample was achieved with a laboratory built oven surrounding the sample. The 2θ angles were calibrated by using elementary silicone. With this calibration specimen $K\alpha_1$ and $K\alpha_2$ was clearly resolved indicating the high degree of collimation achieved.

The spacings could be measured to the accuracy of one unit in the fifth figure. Spacing values could be reproduced with this accuracy when removing and repositioning the same specimen and of course variations with temperature could be followed with this precision. As the silicone used for calibration absorbs more strongly than the polymer the absolute spacing values may be subject to a small systematic calibration error. (No doubt this could be ascertained by suitably chosen calibration standard, if such exists: however, the ultimate accuracy of the absolute value was of no consequence to us).
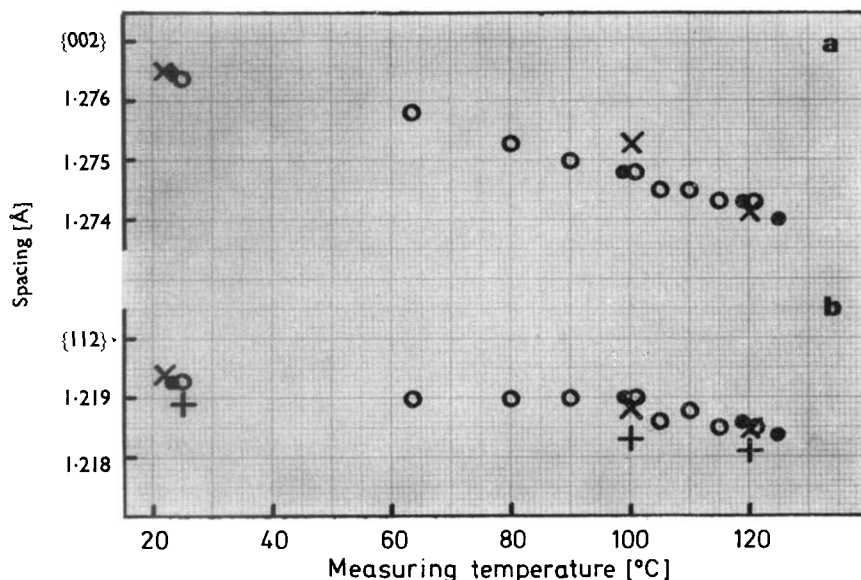

Figure 1 Variation of {002} and {112} interplanar spacings with temperature
○, Sample A: annealed at 120°C, 2 h; fold length, 139Å from x-ray small angle reflection
●, Sample B: annealed at 125°C, 1 day; fold length, 262Å from x-ray small angle reflection
×, Sample C: pressure crystallized sample; polymer A in ref. 5
+, The {112} spacing which was calculated from the observed {002} value and the expansion coefficients of the a and b axes by Swan.

RESULTS AND DISCUSSION

The results on three samples are shown by *Figure 1* for both 002 and 112 reflection. It is immediately apparent that the {002} spacing is reduced with increasing temperature, the effect in this case well exceeding experimental error. The spacings reverted to the starting value on cooling.

From the values at 20°C and 120°C an expansion coefficient of $\alpha_c = 18 - 10^{-6}°C^{-1}$ is calculated. However, it is apparent that the thermal change is more pronounced in the upper temperature range. From the most complete measurement series of sample A one could define $\alpha_c = -21 \times 10^{-6}°C^{-1}$ between 65°C and 120°C and $\alpha_c = -12 \times 10^{-6}°C^{-1}$ between 20°C and 65°C, (The spacings for sample C were subject to greater errors than the rest in view of the fact that this sample was unoriented, hence the intensity of the reflection was much lower).

The decrease of the {112} spacing with temperature is much smaller giving $\alpha^{\{112\}} = -6 \times 10^{-6}°C^{-1}$. This is to be expected as the effect of the positive expansion coefficient of a and b will be felt. This was tested quantitatively. As seen from *Figure 1b* agreement with calculation based on Swan's data for a and b is complete as regards variation with temperature. The actual calculated spacing values are lower by 4×10^{-5}Å, but this is likely to be due to a systematic difference between the actual values of a and b in our and Swan's samples, particularly as the absolute value of these lattice parameters can vary with sample type (e.g. ref. 4).

The thermal shrinkage of c, now definitely confirmed and accurately measured, is expected to be due to increased rotation around C–C bonds with increasing temperature. This will lead to a small configurational change of the chains, twisting the original planar zig-zag. The change in the average C–C bond angle would yield expansion but this effect is expected to be much smaller. In this respect the case of diamond with $a = 1·18 \times 10^{-6}°C^{-1}$ could be of guidance. Hence neglecting this possible small positive effect and attributing the whole measured decrease between 20°C and 120°C to rotation around single bonds, an average angle of 3° between consecutive planes defined by pairs of C—C bonds is obtained on the assumption that this twist is uniform throughout the crystal (this assumption is probably an approximation, the twist is likely to be larger close to the basal surface than in the interior). A twist of this magnitude is certainly feasible; it will be facilitated by the increased chain separation inherent in the positive expansion coefficient of a and b.

In conclusion, a negative temperature coefficient along c attributable to a shrinkage of the chains with increasing temperature has been established in the case of polyethylene. Other polymers with a nominally planar zig-zag configuration could be expected to follow the same pattern.

SUPPLEMENTARY OBSERVATIONS ON VARIATIONS WITH SAMPLE TYPES

In the course of the comprehensive work two runs were carried out on single crystal samples *not* previously annealed. Both of these showed lower c values at 20°C namely 1·2743 Å and 1·2755 Å compared with 1·2765 Å of the

annealed samples in *Figure 1*. However, both were found to give a value of 1·2765 Å after annealing treatment. The change was actually followed in the sample giving the 1·2743 Å originally. Here the {002} spacing against temperature curve decreased as in *Figure 1a* up to 100°C but increased beyond, this increase portion being irreversible; subsequent cooling yielded the higher 1·2765 Å value at room temperature. This examination was carried out immediately after the sample was prepared. An examination of the still unannealed portion of the same preparation 8 months later, however, gave the high value of 1·2765 Å. (In fact samples A and B in *Figure 1* were all stored samples). In view of accuracy in measurement and sample positioning we consider these effects as real. While further data would be desirable for any generalisation some comments will be made at this stage since we cannot, at present, continue this investigation.

In all cases the spacing has increased on heat treatment or storage which corresponds to better planarity of the zig-zag, and hence to greater crystal perfection. The notion that the chain configuration can improve its regularity on heat treatment and storage is perfectly reasonable, and the recent finding that also the a and b spacing can decrease on annealing[4] supports this. In fact if twists are built in the chain, this will need to be reduced as the adjacent chains come closer. The source of variable chain twist at the same temperature may lie in the crystallization conditions but could also be related to the long period. The constrained configuration of a fold could exert a torque on the straight stems within the lattice. This torque would have a smaller effect on the chain configuration if the stems are longer.

University of Bristol,
H. H. Wills Physics Laboratory,
Royal Fort, Tyndall Avenue,
Bristol BS8 1TL   *(Received 10 October 1969)*

REFERENCES

1 Bunn, C. W. *Trans. Faraday Soc.* 1939, **35**, 428
2 Swan, P. R. *J. Polym. Sci.* 1962, **56**, 403
3 Keller, A. *Reports on Progress in Physics* 1968, **31** (Pt 2), 623
4 Martin, G. M. and Eby, R. K. *J. Nat. Bur. Stand.* 1968, **72A**, 467
5 Arakaws, T. and Wunderlich, B. *J. Polym. Sci. (C)* 1967, **16** 653

Book Reviews

10th International Conference on Coordination Chemistry, plenary lectures presented at the conference held in Tokyo and Nikko, Japan, 12–16 September, 1967

Butterworth, London, 1969, 196 pp., 50s

This book comprises the plenary lectures presented at the 10th International Conference on Coordination Chemistry held in Tokyo and Nikko, Japan, in September, 1967.

The first paper (R. S. Nyholm) reviews the current position regarding magnetism, bonding, and structure of coordination compounds. In this area of chemistry it appears that the rather optimistic views concerning the value of magnetic susceptibility measurements for the study of chemical structure are not really being fulfilled. The appearance of this authoritative review is very timely.

The second contribution (Y. Saito) deals with a more limited area–notably the structures and absolute configurations of cobalt(III) complexes. Crystallographic data are presented, but there is also a brief discussion of the problem of absolute configuration and optical properties.

The third lecture (F. Basolo) deals with the substitution reactions of metal complexes The current views on substitution mechanisms in octahedral, square planar, and tetra hedral transition metal complexes are reviewed.

The paper by L. G. Sillen deals with the author's recent contribution to the study of hydrolytic equilibria, and much of the work presented in this paper represents unpublished work.

The contribution by O. A. Reutov deals with the importance of coordination in electrophilic substitution reactions of organometallic compounds. This lecture, like that by G. Wilke, entitled 'Über Nickelorganische Verbindungen', is a little different from the others in that the authors present their material largely from the standpoint of organic chemists. In Reutov's paper, the physical and mechanistic aspects are emphasised, whereas Wilke's lecture is mainly an elegant summary of work done on template effects in oligomerizing olefins.

The problem of five-coordination in $3d$ metal complexes is authoritatively reviewed by L. Sacconi, although this is a field in which there has been considerable development since 1967.

The essay by A. E. Martell entitled 'Catalytic effects of metal chelate compounds' provided especially interesting reading. Reactions are classified into four main groups: (1) those in which metal chelate rings are formed; (2) those in which the metal chelate rings are altered; (3) those in which the metal chelate rings are broken; and (4) those in which the metal chelate rings remain unaltered. A very wide scope of reactions is covered, many of biological interest.

M. F. Lappert

Introduction to plastics
by Lionel K. Arnold

George Allen and Unwin, London, 1969, 216 pp., 35s

This book, of American origin, is intended for readers with little or no knowledge of plastics and elastomers. It sets out to describe in a brief and elementary manner the synthesis, fabrication, and application of these materials. Polymerization reactions are illus-

trated, together with examples of production methods. Likewise, established fabrication processes are briefly described and include product manufacturing by casting, compression, injection, and blow-moulding, extrusion, sheeting processes, costing techniques, and cellular structures. There is little detail of other widely used processes such as spreading, calendering, and mill and internal mixing.

Thirteen of the seventeen chapters introduce readers to the important classes of plastics and rubbers, those described including natural resins, cellulosic plastics, phenolics and aminoplasts, thermoplastics (polyolefins, vinyl, styrene and acrylic polymers), polyesters and epoxy resins, polyamides, polyurethanes, and silicones. 'Engineering' or high performance plastics, e.g. polysulphones and polyacetals, are dealt with separately and the uninitiated reader may find this helpful.

Chapter 14 on rubbers, has a useful table of comparative properties. Included are natural rubber and its derivatives, SBR, nitrile, polybutadiene, polychloroprene, ethylene-propylene, chlorosulphonated polyethylene, polysulphide, acrylic, fluoroelastomers, urethane, silicone, and epichlorohydrin rubbers, although descriptive detail is very brief.

Fibres, films, and foams are dealt with separately in a short chapter.

Finally an attempt is made to indicate which physical properties are of importance in assessing polymeric materials for particular end uses, illustrated by examples of industrial markets successfully penetrated by plastics and rubbers. There is an index of American and equivalent British trade names and a sufficient bibliography gives a guide to specialised literature. Unfortunately the subject index is totally inadequate.

In general, the book does little more than provide a broad and mainly descriptive survey of polymer processes and products but will be useful to readers seeking such limited information. However, if it serves also to promote further enquiry much will have been accomplished by this book which is very readable, well produced and available at modest cost.

C. HEPBURN

Technical dictionary of high polymers
by W. DAWYDOFF and H. HOWORKA

Pergamon Press Ltd. London, 1969, 960 pp., £11, $28.00

All dictionaries are useful, but some are more useful than others. For polymer scientists, and, more especially, plastics technologists this is one of the more useful ones. It is an East German publication in all but name, containing some 10 000 terms each rendered in English, French, German and Russian. The terms range from high polymer science (chemistry, physics and physical chemistry) to production methods (polymerization, condensation etc.) and applications and fabrication methods. Like most linguistic dictionaries the main faults arise in pure science, for example, the classic translation hurdles of 'block and graft polymerization' are not cleared impeccably, and some important terms (e.g. 'reactivity ratio') are omitted. On the whole, technology is much better served, including related fields such as fibres, surface coatings, paper industry, plastizers, and glass fibre technology. In these areas, many modern terms are included, but much space is taken up by repetition of almost identical terms. A significant reduction in the number of words could be obtained by extensive pruning in this way.

The book is easy to use as each term is indexed four times, in separate sections for each language, with the equivalent in the other languages appearing alongside. The printing is good, and free from errors, but the paper is thin and rather poor. Because of this, the book may not stand up to the use which it will have in the departmental library where it belongs.

C. A. FINCH

Book Reviews

10th International Conference on Coordination Chemistry, plenary lectures presented at the conference held in Tokyo and Nikko, Japan, 12–16 September, 1967

Butterworth, London, 1969, 196 pp., 50s

This book comprises the plenary lectures presented at the 10th International Conference on Coordination Chemistry held in Tokyo and Nikko, Japan, in September, 1967.

The first paper (R. S. Nyholm) reviews the current position regarding magnetism, bonding, and structure of coordination compounds. In this area of chemistry it appears that the rather optimistic views concerning the value of magnetic susceptibility measurements for the study of chemical structure are not really being fulfilled. The appearance of this authoritative review is very timely.

The second contribution (Y. Saito) deals with a more limited area–notably the structures and absolute configurations of cobalt(III) complexes. Crystallographic data are presented, but there is also a brief discussion of the problem of absolute configuration and optical properties.

The third lecture (F. Basolo) deals with the substitution reactions of metal complexes The current views on substitution mechanisms in octahedral, square planar, and tetra hedral transition metal complexes are reviewed.

The paper by L. G. Sillen deals with the author's recent contribution to the study of hydrolytic equilibria, and much of the work presented in this paper represents unpublished work.

The contribution by O. A. Reutov deals with the importance of coordination in electrophilic substitution reactions of organometallic compounds. This lecture, like that by G. Wilke, entitled 'Über Nickelorganische Verbindungen', is a little different from the others in that the authors present their material largely from the standpoint of organic chemists. In Reutov's paper, the physical and mechanistic aspects are emphasised, whereas Wilke's lecture is mainly an elegant summary of work done on template effects in oligomerizing olefins.

The problem of five-coordination in $3d$ metal complexes is authoritatively reviewed by L. Sacconi, although this is a field in which there has been considerable development since 1967.

The essay by A. E. Martell entitled 'Catalytic effects of metal chelate compounds' provided especially interesting reading. Reactions are classified into four main groups: (1) those in which metal chelate rings are formed; (2) those in which the metal chelate rings are altered; (3) those in which the metal chelate rings are broken; and (4) those in which the metal chelate rings remain unaltered. A very wide scope of reactions is covered, many of biological interest.

M. F. Lappert

Introduction to plastics
by Lionel K. Arnold

George Allen and Unwin, London, 1969, 216 pp., 35s

This book, of American origin, is intended for readers with little or no knowledge of plastics and elastomers. It sets out to describe in a brief and elementary manner the synthesis, fabrication, and application of these materials. Polymerization reactions are illus-

118

trated, together with examples of production methods. Likewise, established fabrication processes are briefly described and include product manufacturing by casting, compression, injection, and blow-moulding, extrusion, sheeting processes, costing techniques, and cellular structures. There is little detail of other widely used processes such as spreading, calendering, and mill and internal mixing.

Thirteen of the seventeen chapters introduce readers to the important classes of plastics and rubbers, those described including natural resins, cellulosic plastics, phenolics and aminoplasts, thermoplastics (polyolefins, vinyl, styrene and acrylic polymers), polyesters and epoxy resins, polyamides, polyurethanes, and silicones. 'Engineering' or high performance plastics, e.g. polysulphones and polyacetals, are dealt with separately and the uninitiated reader may find this helpful.

Chapter 14 on rubbers, has a useful table of comparative properties. Included are natural rubber and its derivatives, SBR, nitrile, polybutadiene, polychloroprene, ethylene-propylene, chlorosulphonated polyethylene, polysulphide, acrylic, fluoroelastomers, urethane, silicone, and epichlorohydrin rubbers, although descriptive detail is very brief.

Fibres, films, and foams are dealt with separately in a short chapter.

Finally an attempt is made to indicate which physical properties are of importance in assessing polymeric materials for particular end uses, illustrated by examples of industrial markets successfully penetrated by plastics and rubbers. There is an index of American and equivalent British trade names and a sufficient bibliography gives a guide to specialised literature. Unfortunately the subject index is totally inadequate.

In general, the book does little more than provide a broad and mainly descriptive survey of polymer processes and products but will be useful to readers seeking such limited information. However, if it serves also to promote further enquiry much will have been accomplished by this book which is very readable, well produced and available at modest cost.

C. HEPBURN

Technical dictionary of high polymers
by W. DAWYDOFF and H. HOWORKA

Pergamon Press Ltd. London, 1969, 960 pp., £11, $28.00

All dictionaries are useful, but some are more useful than others. For polymer scientists, and, more especially, plastics technologists this is one of the more useful ones. It is an East German publication in all but name, containing some 10 000 terms each rendered in English, French, German and Russian. The terms range from high polymer science (chemistry, physics and physical chemistry) to production methods (polymerization, condensation etc.) and applications and fabrication methods. Like most linguistic dictionaries the main faults arise in pure science, for example, the classic translation hurdles of 'block and graft polymerization' are not cleared impeccably, and some important terms (e.g. 'reactivity ratio') are omitted. On the whole, technology is much better served, including related fields such as fibres, surface coatings, paper industry, plastizers, and glass fibre technology. In these areas, many modern terms are included, but much space is taken up by repetition of almost identical terms. A significant reduction in the number of words could be obtained by extensive pruning in this way.

The book is easy to use as each term is indexed four times, in separate sections for each language, with the equivalent in the other languages appearing alongside. The printing is good, and free from errors, but the paper is thin and rather poor. Because of this, the book may not stand up to the use which it will have in the departmental library where it belongs.

C. A. FINCH

The effect of pressure on ceiling-temperature in the polymerization of tetrahydrofuran

M. RAHMAN and K. E. WEALE

The ceiling-temperature for polymerization of tetrahydrofuran is found to increase with pressure by about 20°C/100 N/mm². The plot of log T_c versus pressure in the range 152·0–253·0 N/mm² is linear, and extrapolates to the known value of T_c at 0·1 N/mm². The coefficient d log T_c/dP, obtained from the results, is consistent with values of ΔH and ΔV determined at ordinary pressure.

PUBLISHED DATA on the equilibrium polymerization of tetrahydrofuran (THF) were reassessed by Ivin and Leonard[1], who concluded that the ceiling-temperature for the polymerization of pure THF, to monomer-soluble polymer, is 80 ± 3°C. Subsequently Dreyfuss and Dreyfuss[2] reported a value of 84°C. A study of the polymerization of THF at high pressures[3] (with boron trifluoride diethyletherate catalyst) suggested that the ceiling-temperature is strongly pressure-dependent, and we have investigated this aspect.

EXPERIMENTAL

THF which had been dried with calcium hydride, was heated under reflux (4 h) with lithium aluminium hydride, and then fractionated (b.p. 65°C). Redistilled boron trifluoride diethyletherate (b.p. 125°C) was used. Freshly-dried monomer was used for each run as moist THF gave a methanol-insoluble liquid polymer at the highest temperatures, while the dry monomer gave only solid polymer. Reaction mixtures were made up to contain 2% by volume of catalyst, and the reactions were carried out in a stainless-steel tube about 12 cm long and 1 cm in diameter. The tube was closed at one end by a steel screw, with a neoprene O-ring, and was fitted at the other end with a short steel piston, also carrying an O-ring, which could slide in the bore. No leak of monomer was detected in tests at 130°C and ordinary pressure. The reaction tube was immersed in oil inside a pressure vessel, and pressure was transmitted to the reactants by movement of the piston. The vessel temperature was constant to ± 0·05°C. After each run unreacted monomer was removed under vacuum, and the polymer was washed with methanol and dried under vacuum.

RESULTS AND DISCUSSION

Runs were carried out at three pressures, (152·0, 202·5 and 253·0 N/mm²),

and at a series of temperatures. The yields of polymer obtained are shown in *Table 1*. Considerably longer runs at the highest temperature (at each pressure) also yielded no polymer.

Table 1 Yields (wt. %) of polytetrahydrofuran at various pressures (*P*) and temperatures (*T*) (Conc. of BF$_3$ etherate = 2% v/v)

$P = 152 \cdot 0$ N/mm^2 Time = 18h		$P = 202 \cdot 5$ N/mm^2 Time = 10h		$P = 253 \cdot 0$ N/mm^2 Time = 6h	
T[°C]	*Yield*[%]	*T*[°C]	*Yield*[%]	*T*[°C]	*Yield*[%]
80	4·5	90	8·5	90	9·5
90	6·3	95	9·8	100	12·4
100	6·7	100	10·7	110	13·6
105	4·4	105	11·0	115	12·5
108	1·1	110	10·0	120	11·0
110	None	115	6·9	125	7·6
		118	3·1	127	4·5
		120	None	130	None
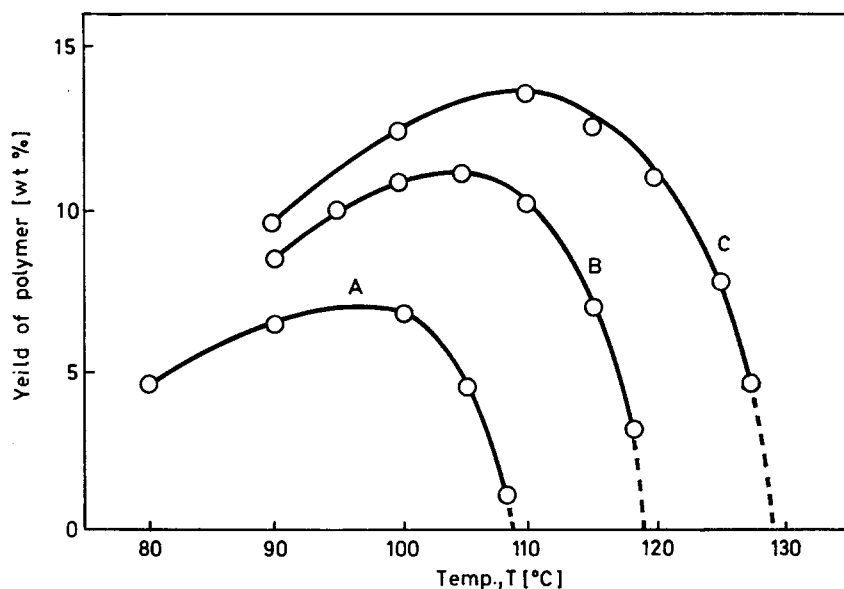
Figure 1 Yield of polytetrahydrofuran at three pressures and various temperatures. A, 152·0 N/mm^2 (18 h): B, 202·5 N/mm^2 (10 h): C, 253·0 N/mm^2 (6 h).

The results are plotted in *Figure 1* which shows that at each pressure the yield passes through a maximum with increasing temperature, and then falls rapidly to zero.

If the curves are interpreted as indicating the approach to the ceiling-

temperature at each pressure, and are used to estimate the ceiling-temperatures, the results obtained are:

P [N/mm^2]	152·0	202·5	253·0
T_c [°C]	109	119	129

The plot of log T_c[°K] versus pressure is linear, and when extrapolated to $P = 0·1$ N/mm^2 ($\sim$1 atm) gives a ceiling-temperature of about 81 °C, which is satisfactorily close to the values obtained at ordinary pressure. The dependence of T_c on pressure thus follows the Clapeyron-Clausius equation:

$$\frac{dT_c}{dP} = \frac{T_c \, \Delta V}{\Delta H}$$

as previously found[4] for α-methyl styrene. The slope d ln T_c/dP ($= \Delta V/\Delta H$) is 2·11 ml/kcal (0·0503 ml/kJ). Both ΔV and ΔH may vary with pressure, although their ratio is constant, but it is of interest to calculate ΔV using values of ΔH obtained at ordinary pressure. Sims[5] reports $\Delta H = -4·28$ kcal/mole, while Dreyfuss and Dreyfuss[2] found $\Delta H = -4·58$ kcal/mole. The corresponding values calculated for ΔV are $-9·1$ and $-9·7$ ml/mole, respectively. From measurements of the density of THF, and of a 20% solution of poly(THF) in the monomer, at 26°C and ordinary pressure, we derive

$$\Delta V = -9·5 \text{ ml/mole.}$$

The term $-\Delta V$ is appreciably smaller for THF than for α-methylstyrene, (14–15 ml/mole). In vinyl polymerization the decrease in volume which occurs when a monomer molecule adds to the chain is principally due to the formation of the new C—C bond; and there is a smaller opposing effect due to the lengthening of the C=C bond, which becomes a single bond. In the ring-opening polymerization of THF a new C—O bond is formed, but the decrease in volume due to this should be effectively balanced by the breaking of a C—O bond in the ring. The net decrease in volume, which appears to be about 9 ml/mole, may be largely due to the elimination of an excluded volume associated with the five-membered ring.

Department of Chemical Engineering and Chemical Technology,
Imperial College,
London, S.W.7.   *(Received 2 January 1970)*

REFERENCES

1 Ivin, K. J. and Leonard, J. *Polymer, Lond.* 1965, **6**, 621
2 Dreyfuss, M. P. and Dreyfuss, P. *J. Polym. Sci.* (*A*) 1966, **4**, 2179
3 Mehdi, S. A., Rahman, M. and Weale, K. E., to be published
4 Kilroe, J. G. and Weale, K. E. *J. Chem. Soc.* 1960, p 3849
5 Sims, D. *J. Chem. Soc.* 1964, p 864

Properties of polymer crystal aggregates.

(1) Comparison of polyethylene crystal aggregates with bulk crystallized polyethylene

D. A. BLACKADDER and P. A. LEWELL*

Although certain fundamental aspects of polymer single crystal physics are still under investigation and discussion, there is much to be gained by a direct approach to the problem of relating existing knowledge of single crystal behaviour to the description of bulk crystallized polymer. In this series of papers the experimental principle is quite simple: single crystals of polymer obtained from dilute solution are aggregated together to form macroscopic samples large enough for mechanical and physical testing. These aggregates or mats can be modified in various ways and compared with geometrically similar samples of bulk crystallized polymer. In this the first paper of the series, experiments are described in which mats of polyethylene crystals are compared directly with bulk crystallized polyethylene.

DURING the past twelve years a great deal of information has been acquired concerning polymer single crystals[1, 2]. Discoveries in this field have impinged to some extent on the much older study of bulk crystallized polymer, though some scientists appear disappointed that so much single crystal research has affected the problems of bulk polymer processing and texture control so little. At present some quite basic matters pertaining to single crystals are still under discussion, yet it seems desirable to try to establish direct bridges between the two bodies of knowledge concerning single crystals and bulk polymer respectively.

In recent years the fringed micelle model for bulk polyethylene has been replaced by a chain folding model involving lamellae. There is a considerable amount of experimental evidence for the existence of lamellae in bulk polymer including low angle x-ray diffraction, examination of replicas of fracture surfaces[3], study of the internal structure of spherulites[4], digestion of samples with fuming nitric acid[5, 6] and the preparation of very thin sections for electron microscopy[7]. The lamellae appear to act as building blocks in the formation of spherulites. As the stacks of lamellae radiate outwards they frequently twist, probably due to surface strain[8], to give the characteristic fine detail of the optical extinction patterns of spherulites.

It is very tempting to regard these lamellar units in bulk polymer as analogous to the lamellar single crystals obtainable from dilute solutions. The morphology of crystals obtained from solution has been investigated under conditions of increasing temperature of crystallization and concentration in an effort to approach the conditions of melt crystallization. When the crystallization temperature is increased it has been found[9, 10] that the crystals elongate along the *b* axis, progressing from simple lozenges to elongated hexagons. In view of these results it is significant that the lamellar entities observed in the debris remaining after nitric acid attack on bulk polymer are elongated and lath shaped, the long direction lying along the spherulite radius[6]. Increasing the polymer concentration up to 50% in xylene solution[11] revealed that lamellar crystallization is characteristic of the entire concentration range, though molecules crystallizing through several lamellae, and so binding them together, become increasingly important. The morphology of bulk crystallized material is therefore at least consistent with the trends established for crystallization from solution.

Density measurements, on the other hand, have provided some indication that the analogy between single crystals and the lamellar units in bulk polymer must not be pushed too far. Recently[12] the density of single crystals of polyethylene (and more complicated entities) has been confirmed as 0.972 g/cm^3, but the density of bulk polyethylene can be raised above this value by annealing. Densities as high as 0.986 g/cm^3 have been obtained in this laboratory. If the two-phase model applies to both single crystals and bulk polymer then the density measurements indicate that bulk polyethylene can have a degree of crystallinity greater than that of single crystals. (The two-phase model involves an amorphous phase of density[13] 0.852 g/cm^3 and a crystalline phase with a density[14] of the order of 1.00 g/cm^3 depending on the sample). Clearly this conclusion is not consistent with the view that bulk polymer is an assemblage of lamellae, similar to single crystals, associated with some less dense material.

The implications of this difficulty will be considered at length in the present series of papers, but one obvious explanation for the anomaly is that the simple two-phase model is not valid over the entire range of crystallinities even if it provides an acceptable description of samples which are not highly crystalline. In particular, the density of the non-crystalline material may be increased as a result of the compressive forces exerted upon it by the growing lamellae within the bulk material, especially at high degrees of crystallinity. Two very common terms must therefore be used with caution: *amorphous* will here denote simply non-crystalline, and samples will be characterized by their densities rather than by invoking the ambiguous *degree of crystallinity*.

Although there is little doubt that lamellae exist in bulk polymer and that they have certain morphological features in common with solution crystallized entities, it is evident that difficulties persist in relating properties of single crystals to properties of bulk polymer. The study of aggregated crystals, with the constituent lamellae in close proximity as in bulk polymer, might be expected to yield useful results. If bulk polymer is composed of lamellae which are indeed similar to single crystals then the properties of

crystal aggregates and of bulk polymer would be expected to have some features in common.

In the present work, aggregates of crystals have been prepared and some of their mechanical properties investigated. The aggregates are held together solely by van der Waals forces since tie-molecules between the individual entities are absent. In addition the amorphous material in an aggregate may be expected to differ in certain respects from the amorphous component of bulk crystallized polymer. Tensile testing would appear to be particularly appropriate for the study of crystal aggregates. Several parameters may be measured under different conditions and the results compared with those obtained using samples of bulk polymer.

The major aims of the investigation described in this paper are: (1) to establish the deformation mechanism in aggregates of crystals subjected to tensile stress, and (2) on the basis of a comparison, to obtain further information concerning the corresponding deformation mechanism in bulk polymer, thereby indicating the extent to which bulk crystallized polymer may be regarded as merely a complicated assemblage of crystals.

EXPERIMENTAL

Preparation of crystal aggregates or mats

Determination of the properties of aggregates of single crystals has been hindered in the past by the experimental difficulties inherent in assembling a uniform sample. Much of the work that has been done, for example by Lowell and McCrum[15] on the absorption of cyclopropane by mats of single crystals, has required a mat only a few thousandths of an inch thick. Such mats can readily be prepared, with lateral dimensions of the order of several centimetres, by pressing a concentrated slurry between two filter pads and drying. Such mats are too fragile for mechanical tests and too thin for accurate porosity determination.

The procedure used to make the mats employed in this investigation was similar to that described by Sinnott[16]. The polymer used was commercial Rigidex 50, having a weight average molecular weight of 8×10^4 and an $\bar{M}_w/\bar{M}_n$ ratio of about 5. In making 1 wt.% suspensions of crystals from p-xylene solution at 75°C it was convenient to use about 9 g of polymer per batch. For several mats the crystal suspensions were taken through the heating cycle described by Blundell et al[22] to produce uniform lamellae largely free of overgrowths. The suspensions were then diluted to a concentration of 0.1 wt.% and strained through a 70 mesh copper screen to remove any pieces of film that often form on the walls of the crystallizing vessel when crystallizing at such high concentrations. The crystals were then concentrated into a suspension of about 2 wt.% by filtering through filter paper in a funnel.

The filtering apparatus used to make the crystal mats consisted of a 2 in (50 mm) diameter glass tube, containing a 2 in (50 mm) diameter, porosity 3 sintered glass disc. A piece of filter paper was placed over the sintered disc

127

and the concentrated suspension was poured into the flanged filter. The suspension was allowed to settle under gravity for about 2h until a thick gel formed and solvent stopped dripping from the bottom of the filter. The height of this gel above the sintered disc was quite reproducible for suspensions prepared in identical fashions. Crystal suspensions that had been taken through the above mentioned heating cycle (type A crystals) settled to a gel containing about 3 wt. % polymer, whereas crystal suspensions that had not been taken through the heating cycle (type B crystals) settled into much more concentrated gels containing about 8% polymer. (This is consistent with the observed settling properties of the suspensions. When crystallized directly from a 1 wt. % solution the crystals readily settle into the bottom third of the crystallizing vessel, leaving supernatant liquid at the top. If the suspension is then taken through the heating cycle, however, the crystals do not settle on standing, even after several months).

A glass disc was then carefully placed on top of the gel, again with a piece of filter paper separating glass and polymer, and a 500g weight was laid on top of the disc. When the solvent again stopped dripping from the filter cake, a slight vacuum (less than 25 mmHg) was applied to allow an initial rate of solvent removal of about one drop per minute. Every twelve hours the vacuum was increased in order to return to this initial rate of solvent removal. At no time was the rate of solvent removal allowed to exceed one drop per minute. After two or three days the mat was observed to pull away from the walls of the filter funnel and shrink laterally. After about a week, the filter cake was no longer moist in appearance and solvent could not be seen dripping from the funnel no matter how high the vacuum. The mat was then placed in a vacuum oven at 70°C to withdraw the remainder of the solvent. It should be emphasized that the rate at which solvent is withdrawn from the compacted cake is critical if cracks are to be avoided. Once the mat reaches the state where it appears to be no longer moist the possibility of cracks developing is reduced and the quite severe conditions of a vacuum oven can be employed to withdraw the remaining traces.

Two types of mats were prepared in this manner, markedly different in their physical form, depending upon whether type A or B crystal suspensions were used. For the former type of crystals the cake formed by filtration under gravity (containing a relatively large amount of solvent) steadily grew more compact during filtration under vacuum, so that the final mat had a very low porosity (0.010 ± 0.002). The porosity was accurately determined in the following manner. First a fragment of the mat was placed in the density gradient column which gave a value of $0.972 \pm 0.002 \, g/cm^3$, in agreement with previously determined values for single crystals[12]. Inter-lamellar voids in the mat do not affect the density as measured in the gradient column, since they are penetrated and filled by the column liquid. The mat was then carefully machined into a rectangular block (approximate dimensions $0.75 \times 0.5 \times 0.2$ in; $19 \times 13 \times 5$ mm), the mass determined to ± 0.0001 g and the dimensions of the block measured to within ± 0.0002 in (0.005 mm) using a micrometer. The porosity of the mat could then be calculated to within 0.2%.

128

For type B crystals the relatively compact cake formed during gravity filtration did not compact much more during vacuum filtration. The solvent escaped more quickly, leaving a very friable mat with a high porosity (of the order of 0·4). Evidently the non-uniform crystallites cannot pack as closely as the more uniform crystals in type A suspensions, even though they initially have superior settling properties. The mats formed from type B suspensions were compressible and could be made suitable for mechanical tests. A steel die was used to mould the friable mats into thin discs at room temperature by applying a pressure of 7700 p.s.i.*. The resulting mat was similar in appearance to those formed without compression from type A suspensions, but still had a greater porosity (0·073 ± 0·005).

No special attempt was made to control the crystal orientation during mat-making. Although it is probable that a majority of crystals had their basal planes parallel to the basal plane of the mat it would not be realistic to assume that the mat was composed of successive parallel layers. In this respect, the mats have an important similarity to the rather confused orientation of lamellae in bulk polymer. Scanning electron micrographs of the mat surface revealed no definite orientation of the lamellae.

Irradiation of crystal mats

Crystal mats prepared from type B crystals and compacted at 7700 p.s.i. were machined into rectangular blocks, and the porosity accurately determined in the manner described previously. The mats were placed in glass tubes which were evacuated down to a pressure of 10^{-6} mmHg and sealed. They were then exposed to specified dosages of high energy γ-radiation in the TIG Pond, Atomic Energy Research Establishment, Harwell. Reliable temperature control was necessary, as thermal effects could completely mask the effect of irradiation. The temperature was kept constant at 22°C during irradiation and thermal spikes or hot spots were avoided since the large source provided uniform exposure.

The specimens were not removed from the glass tubes for several weeks following irradiation, to allow the free-radicals to decay. In every case measurements revealed that the density and porosity were unaffected by the procedure, indicating that oxidation and local heating had been successfully avoided.

Tensile testing apparatus

Tensile tests were performed on a modified Hounsfield W Type Tensometer in a constant temperature room held at 20°C. The crystal aggregate specimens were too small for conventional gripping techniques to be used, and metal bars were flued to either end of the specimen (*Figure 1*) and bolted directly to the chucks of the tensometer. The glue chosen for this application was Araldite epoxy resin, made by CIBA of Duxford, Cambs.. Normally,

*1 p.s.i. $= 1$ lbf/in^2 $= 7·03 \times 10^{-2}$ kgf/cm^2 $= 6·90 \times 10^3$ N/m^2.

epoxy resins do not adhere well to polyethylene, but by treating the surfaces to be bonded with chromic acid for 10 min at 35°C, a bond that would withstand a specimen tensile load of 2000 p.s.i. was formed. To ensure that the resin would not stretch under tension to the same extent as the polymer
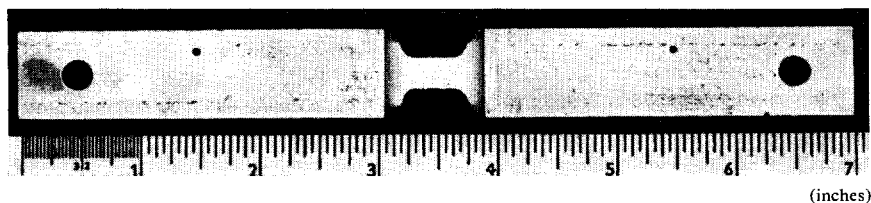

Figure 1 Tensile test specimen

(inches)

specimen two bars were glued together without a specimen between them and subjected to a tensile load. At 300 p.s.i. the extension was less than 10^{-5} in*, i.e. less than 0·25% of the extension that would be effected by applying a tensile load of 300 p.s.i. to a 1 in specimen of bulk polymer with a typical modulus of 7×10^4 p.s.i..

Experiment revealed the single crystal mats to be extremely brittle, thus confining tensile tests to the very small deformation region. To measure the correspondingly small loads applied to the specimen an exceptionally light beam was obtained with a full-scale deflection corresponding to a load of only 16 lb (7·3 kg). (Friction in the grip supports can lead to errors in measuring the applied load when using such a light beam. This source of error was eliminated by supporting the specimen assembly in a horizontal plane by very flexible coil springs attached to an overhead gallows). Specimen deformation was measured to within $\pm 10^{-5}$ in using a Hounsfield Extensometer clamped to the metal bars at either end of the specimen.

A steadily increasing small load was applied to the specimen and at frequent intervals, usually every one-quarter pound ($\sim \frac{1}{9}$ kg), the distance between the extensometer clamps was measured. The rate of strain was readily obtained by noting the time as well at each interval. A small zero load was usually applied (about 1 lb; 0·5 kg) to ensure that the specimen assembly was properly aligned along the screw axis.

At the completion of the test, a stress–strain curve was obtained by drawing a smooth curve through the series of points spaced at regular stress intervals. The accuracy of the curve depends upon the number of points available. Since the total load applied was necessarily limited by the fragile nature of the specimen, the only way to increase the number of points was to make the stress intervals between strain measurements as small as possible. Further, it required a finite amount of time to make a strain reading (about 20 s) and it was essential that the specimen strain occurring during the measurement time was very small compared to the specimen strain occurring during the interval between successive readings, in order to obtain a reliable strain reading for a given value of the stress. These conditions could only be met if the measure-

*1 in = 25·4 mm.

130

ments were performed at extremely small strain rates, much smaller than those employed for conventional tensile tests. Consequently, two gear boxes were used in series together with a modified belt and pulley drive to reduce the minimum speed of the apparatus by a factor of 1000.

Procedure

In order to place in perspective the region of the stress–strain relation investigated, conventional tensile tests were performed on specimens cut from bulk polymer. The polyethylene used was Rigidex Type 3, supplied by British Resin Products in the form of compression molded sheets $\frac{1}{4}$ in (6·4 mm) in thickness, with a density as measured in the density gradient column of 0·947 g/cm³, a weight average molecular weight of about 160000 and a $\bar{M}_w/\bar{M}_n$ ratio of about 20. Crystal aggregate specimens were then tested to failure using the modified tensometer.

Several tests were subsequently performed on given crystal aggregate specimens by applying, at various rates, a continuously increasing load up to a maximum of 133 p.s.i. Since the stress–strain characteristic was linear in this region, the constant strain rate resulted in a constant loading rate. The strain was also observed as the load was removed. (No evidence of strain hardening was apparent and early tests were frequently repeated to ensure that the tensile properties of the specimen had not changed. At least 12 h were allowed to elapse between tests, and the residual strain remaining after the load had been removed in the previous test was invariably recovered by the specimen during this interval). The strain rate was then kept constant at about $3 \times 10^{-6} \mathrm{s}^{-1}$ and tests were performed at various stress amplitudes up to a maximum of 403 p.s.i.

In order to compare the properties of single crystal mats to those of bulk polymer in the low strain region at low strain rates, the testing procedure used above for mats of types A and B was repeated using specimens identical in geometry to the mat specimens but cut from sheets of bulk polyethylene of various degrees of crystallinity. A new specimen was used for each test. The tensile properties of the following types of bulk polymer were investigated in the low strain region:

Rigidex Type 3: described previously.

Alkathene V14114: supplied by ICI Plastics Ltd, in the form of $\frac{3}{16}$ in (4·8 mm) thick sheets compression moulded at 160°C with a weight average molecular weight of $1·5 \times 10^6$ and a density of 0·927 g/cm³.

Vestolen A6016: supplied by BP Chemicals Ltd in the form of compression moulded sheets $\frac{3}{32}$ in (2·4 mm) in thickness with a very narrow molecular weight distribution and a density of 0·961 g/cm³.

Tests were also performed on samples of Rigidex Type 3 and Vestolen which had been annealed to alter their densities.

<div align="center">RESULTS AND DISCUSSION</div>

The tensile properties of samples of Rigidex Type 3 polyethylene (density

<div align="center">131</div>

0·947 g/cm³) are shown in *Figure 2*, in order to put subsequent measurements on single crystal mats in proper perspective. The portion of the stress–strain relation in the low stress region is nearly straight, and the tensile modulus, or slope of the stress–strain characteristic, can be measured. Although the characteristic is straight in this region it is not single-valued during a loading–unloading cycle. Even at very small stress amplitudes there is residual strain
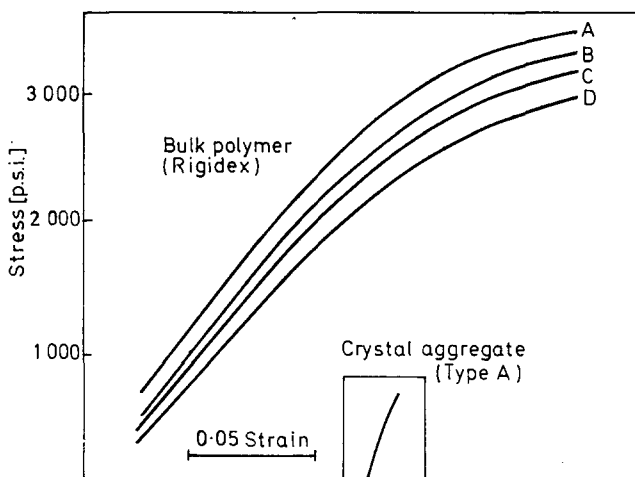

Figure 2 Comparison of stress–strain curves for bulk polymer and crystal aggregates

Initial slopes: A, 2·6 × 10⁴ p.s.i.;   B, 2·5 × 10⁴ p.s.i.;
C, 2·4 × 10⁴ p.s.i.   D, 2·2 × 10⁴ p.s.i.
Rates: A, 0·5 in/min;   B, 0·25 in/min;
C, 0·125 in/min;   D, 0·063 in/min

after removal of the applied load, though this is fully recoverable in time. The slope of the characteristic increases with increasing strain rate, and in the example shown the modulus increases from 2·2 × 10⁴ to 2·6 × 10⁴p.s.i. as the strain rate increases eightfold.

As the applied stress is increased, the slope of the stress–strain characteristic gradually decreases, reaching zero at about 3000p.s.i. where uniform elongation over the entire specimen length occurs at constant stress. Great changes in molecular arrangement are occurring in this region, and if the load is removed the specimen will never return to its original length.

The stress–strain characteristic of a single crystal mat tested to failure is also shown in *Figure 2*, plotted on the same scale as the above tests. It is immediately clear that such a mat is markedly different from bulk polymer in at least one important respect, the mat being subject to brittle fracture at a total elongation of only 1%. It is thus made clear at the outset that the mechanical properties of bulk crystallized polyethylene in the large strain region have no similarity whatever to those of a single crystal mat. At the structural level it implies that the tie molecules running through the amorphous material connecting neighbouring lamellae in bulk polymer have a

132

profound effect. What effect these tie molecules have on properties in the small strain region remains to be seen. The remainder of the experiments were therefore restricted to the very low strain region, necessitating the use of the sensitive strain resolution equipment described earlier, in an effort to discover similarities between bulk polymer and crystal aggregates.

In *Figure 3* the tensile test on a mat shown previously on *Figure 2* is re-plotted on magnified axes. A smooth curve has been drawn through a series of points spaced at intervals of $1 \cdot 5 \times 10^{-4}$ along the strain axis, showing that
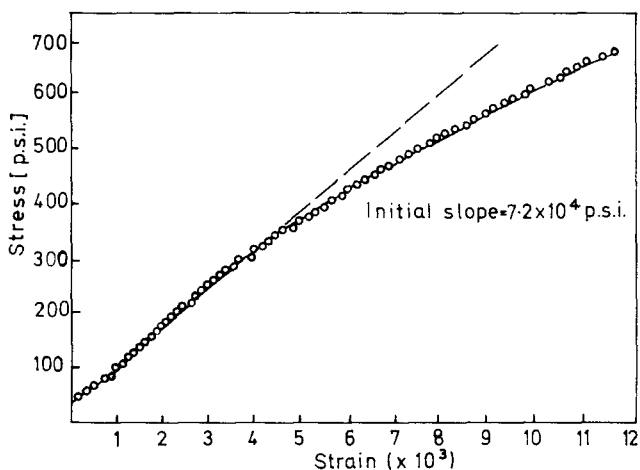
Figure 3 Stress–strain curve for crystal aggregate (same test as in *Figure 2*)

the equipment used was sensitive enough to provide a reliable characteristic in this low strain region. Fragments from the fracture surface were placed in the density gradient column and found to have a density identical to that of the unstretched mat. Scanning electron photomicrographs of the fracture surfaces revealed some fibrils superimposed on the lamellae, pre-sumably where some lattice destruction had occurred at fracture.

The fact that brittle fracture occurs suggests at once a possible deformation mechanism within the crystal mat. As for many granular materials, brittle fracture of the aggregates could be an inevitable result of the weakness of internal boundaries. Indeed earlier work[11, 17] on the deformation of layered lamellae has clearly shown that lamella–lamella adhesion is relatively weak, so that the boundaries between lamellae within the aggregate, being loci of low breaking strength, could provide routes for crack propagation resulting in brittle fracture. Deformation in mats preceding fracture could therefore involve inter-lamellar slip along these weak boundaries.

Irradiation provides a means of verifying that the deformation mechanism in the crystal aggregates involves inter-lamellar slip. Salovey and Keller[18] have shown by solubility measurements that inter-lamellar crosslinks are produced when crystal aggregates, in which the lamellae are in close contact, are irradiated. Such crosslinks would be expected to strengthen the weak

internal boundaries, thus resulting in altered tensile properties of mats if the deformation mechanism involves relative movement of the lamellae.

In *Figure 4*, the complete stress–strain curves for compacted type B mats are shown as a function of the radiation dose. The results indicate that increasing the radiation dose from 0 Mrad to 40 Mrad has two effects on the tensile properties of the aggregates: the strength of the mat is increased over
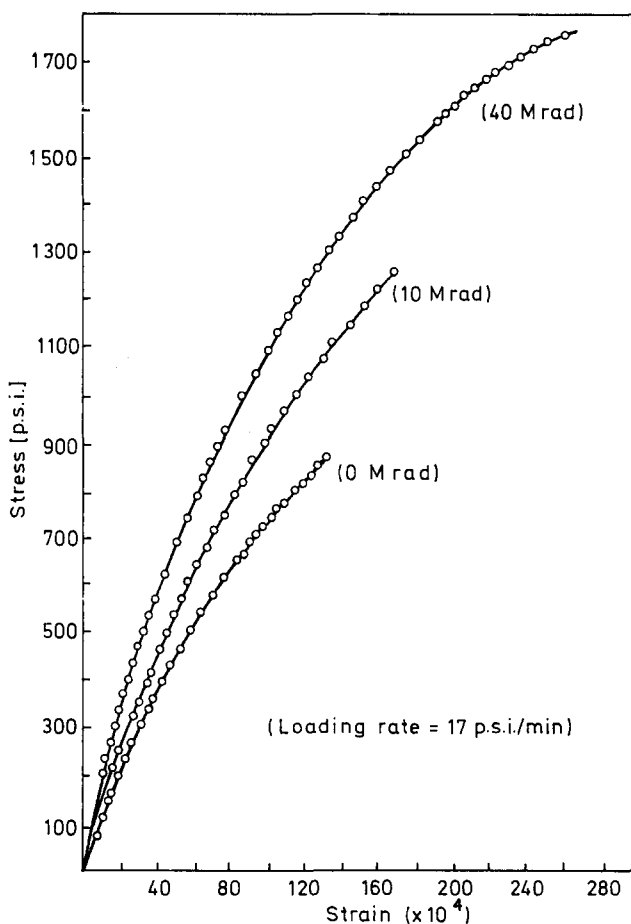
Figure 4 Stress–strain curves for irradiated crystal aggregates (type B)

the entire strain region and the extension at break is doubled. If it is assumed that radiation produces crosslinks between the lamellae, as concluded by Salovey and Keller[18], then these results indicate that deformation in the mats is due to inter-lamellar slip; strengthening the inter-lamellar boundaries increases the resistance to deformation. Further, the fact that the extensibility increases with radiation dose supports the original view that brittle fracture is a result of weak boundaries.

Figure 5 shows the stress–strain characteristic for a loading–unloading cycle on a single crystal mat composed of compacted type B crystals. These tests were performed at a constant rate with various stress amplitudes up to 400 p.s.i. As can be seen, the deformation was reversible and was completely recoverable with time. The area under the curve is proportional to the energy dissipated during the cycle and as for bulk polymer increases with
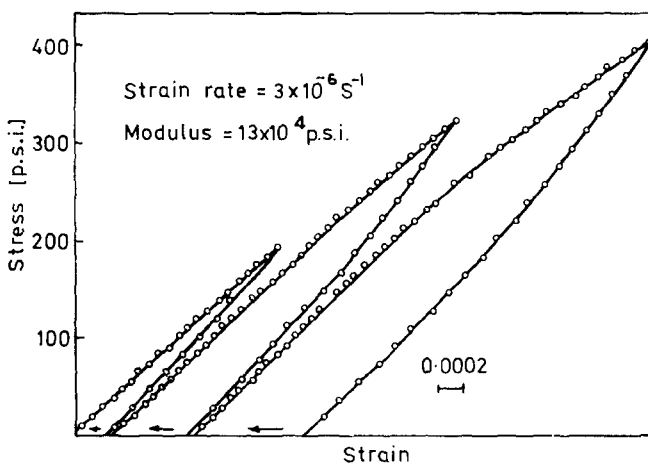
Figure 5 Loading–unloading cycles for crystal aggregates (type B)

stress amplitude. The slope of the characteristic was constant and reproducible up to a stress of about 250 p.s.i., in agreement with the characteristic shown in *Figure 3*. However, the characteristic was not single-valued during a loading–unloading experiment with stress amplitude below 250 p.s.i., indicating that non-elastic deformation occurs even at low stress levels. This is consistent with results reported by Rabinowitz and Brown[19] on highly crystalline bulk polyethylene, who found an open-loop effect at stress amplitudes as low as 18 p.s.i. They attributed this to the existence of 'non-crystalline deformation processes' as well as 'dislocation deformation processes' the former being more easily activated than the latter. For the case of single crystal mats it is difficult to conceive of inter-lamellar slip causing any serious deformation in the non-crystalline regions as explained in the introduction. Thus for single crystal mats, inter-lamellar slip without significant concomitant deformation of the amorphous material is responsible for the hysteresis effect in a load–unload cycle.

Some comment is required concerning the reversibility of the inter-lamellar slip process in crystal mats as it has been pointed out[19] that random slip usually produces permanent strain in non-polymeric materials. The tie point concept proposed by McCrum and Morris[20] could provide an explanation. According to this theory, when a load is applied the lamellae become stressed at points (such as sites of lamella branching) where they are restricted from moving in their slip direction. When the load is removed these tie points exert a backward stress causing the lamellae to return to their original

positions. Thus the reversibility of the above tests is not inconsistent with a deformation mechanism of inter-lamellar slip, nor does it require the presence of tie molecules between lamellae. If the applied load is increased without limit, as in a test to fracture, local failure of the lattice could occur at these tie points, accounting for the existence of some fibres at the fracture surface revealed by the photomicrographs.

It is of interest to compare the area under the stress–strain curves for crystal mats to the area under the curves for bulk polymer. In *Figure 6* tensile tests with common strain rate and stress amplitude are compared for a crystal mat and two types of bulk polymer. As the density of the bulk polymer (and hence the relative amount of crystalline material) increases, the area
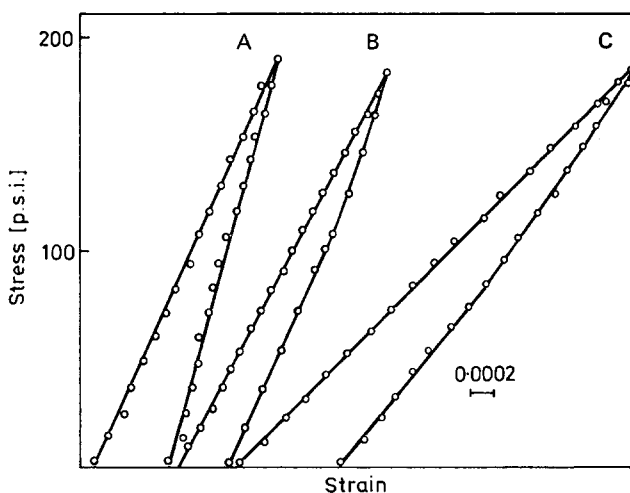
Figure 6 Loading–unloading cycles for crystal aggregates and two
types of bulk polymer.
A, Vestolen 0·978 g/cm³;
B, Mat 0·972 g/cm³;
C, Rigidex 0·947 g/cm³;

under the stress–strain curves decreases, consistent with the view[19] that noncrystalline deformation dissipates more energy. The area under *both* curves, however, is greater than the area under the crystal-mat curve, despite the fact that one of the bulk samples tested had a density greater than that of the crystal aggregate. Therefore it could be argued that deformation through inter-lamellar slip in crystal aggregates involves less of the simultaneous energy-dissipating deformation of amorphous material than occurs during the deformation of samples of bulk material of identical or higher density.

The slope of the initial portion of the stress–strain curve offers a useful means of characterizing a given polymer sample. As shown in *Figures 3, 5* and *6*, the stress–strain characteristics for crystal mats and bulk polymer are reasonably well approximated by a straight line up to stress amplitudes of the

order of 150p.s.i., or total strains of 100–200 $\times$ 10^{-5}. Since increments of strain could be detected as low as 2 $\times$ 10^{-5} with the apparatus employed, modulus values could be determined accurately and reproducibly in this very low strain region.

Figure 7 shows the modulus of the two types of crystal mats investigated as a function of the strain rate. The mat composed of compacted type B crystals had a higher modulus than the mat composed of type A crystals
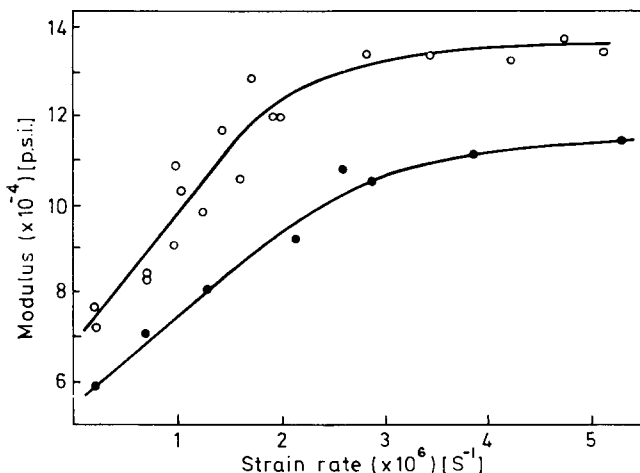

Figure 7 Tensile modulus versus strain rate for crystal aggregates. ●, type A; ○, type B
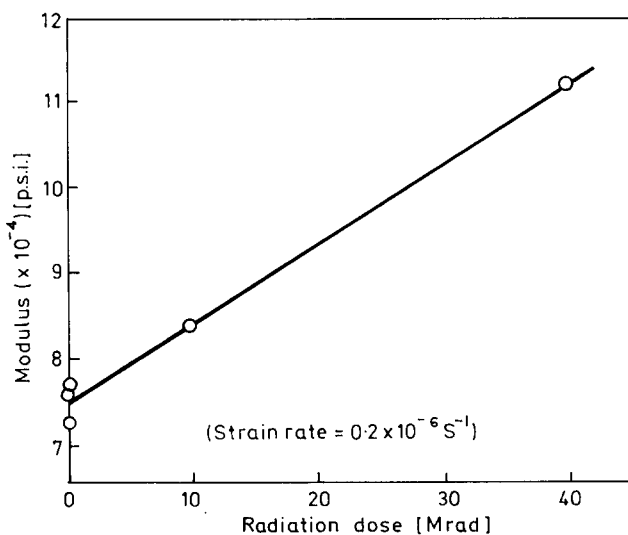
Figure 8 Tensile modulus of type B crystal aggregates versus radiation dose

137

over the entire range of strain rates investigated, despite the fact that the former had a void content of 7·3 vol.% and the latter about 1 vol.%. This behaviour is consistent with the view that the deformation mechanism in crystal mats involves inter-lamellar slip.

The voids in the less porous mat were probably concentrated in the regions between the large plane surfaces of the crystals, since the constituent crystals were monolayers with a large specific surface. Thus on application of a tensile stress the crystals could slide over one another with relative ease, since inter-lamellar contact is reduced by voids of this first type.
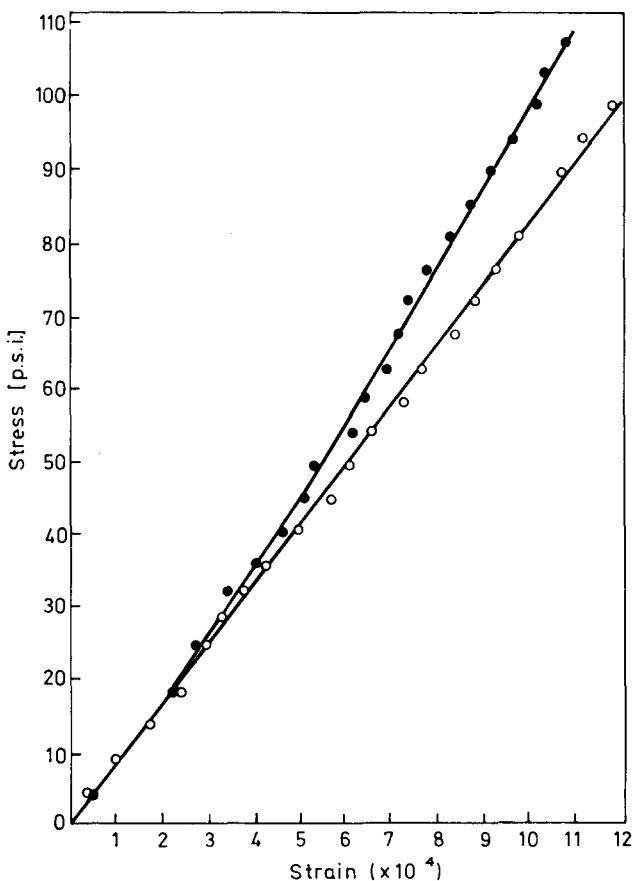
Figure 9 Successive tensile tests on a crystal aggregate irradiated at 10 Mrad. ○, first test; ●, second test (strain rate = 0·2 × 10⁻⁶ s⁻¹)

The voids in the mat of type B crystals, while occupying a greater volume, could well be largely of a different type. Due to the circumstances of preparation these crystals were mostly axialites of low specific surface containing lamellae assembled in a layered structure. Most of the lamellae were therefore already in good permanent contact with their neighbours in an axialite, and

the extent of contact between the outermost lamellae in different axialites would be further enhanced by the compression process which was probably very effective in eliminating voids between the plane surfaces of adjacent axialites. This higher degree of contact between units would result in a higher modulus. The irregular edges of axialites would seem a natural home for voids of a different type resistant to compaction. These voids would probably not have as much of an effect on the tensile properties of the mat in the very low strain region as would voids of the other type described above. It should be noted that voids need not provide the only explanation for the
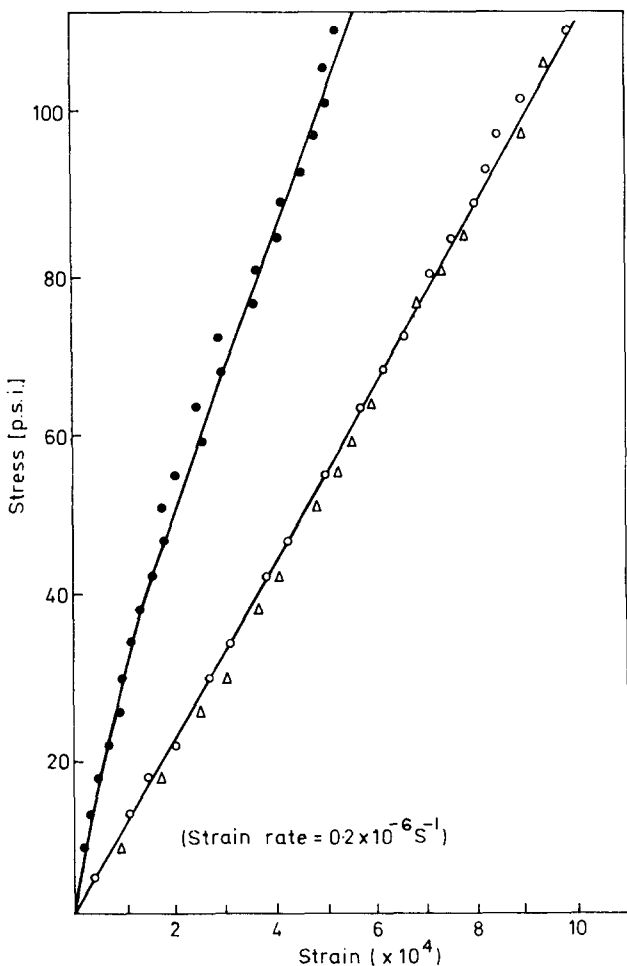
Figure 10 Successive tensile tests on a crystal aggregate irradiated at 40 Mrad. ◯, first test; ●, second test; △, third test. Aggregate was heated to 60°C between second and third tests

differences between type A and type B mats. The mat-making procedure undoubtedly results in anisotropic samples, and it is possible that the two

types of crystals lead to the formation of mats whose degrees of anisotropy are sufficiently different to explain some or all of the observed variations in properties.

Irradiation increases the modulus of type B crystal mats in the very low strain region, as shown in *Figure 8*. (This is consistent with the effect of irradiation over the entire strain region up to fracture, as shown previously in *Figure 4*). It is of interest to note, however, that difficulty was encountered in obtaining reproducible results for the modulus of a given irradiated
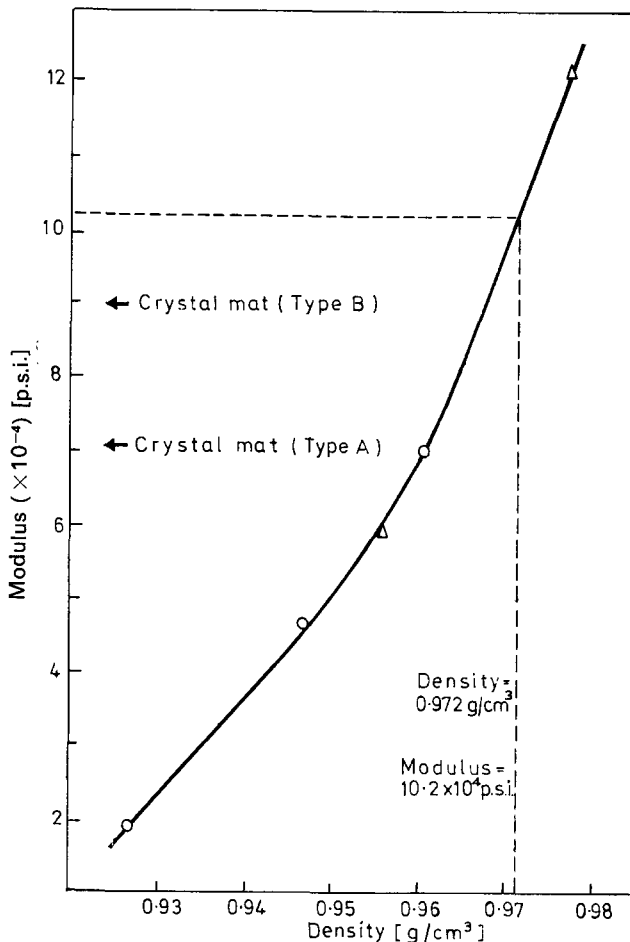
Figure 11 Tensile modulus versus density: ○, bulk polymer; △, annealed bulk polymer (strain rate = 0·75 × 10⁻⁶ s⁻¹)

specimen, whereas it was earlier emphasized that repeated tests on a given unirradiated specimen yielded identical modulus values. In *Figures 9* and *10* successive tests on 10 and 40 Mrad specimens respectively are plotted. It is apparent that some type of work-hardening occurs and that this is due to the introduction of crosslinks, for the magnitude of the effect appears to increase

with radiation dose. It seems likely that interlamellar slip causes tension in some of the crosslinks which is not relieved on removal of the load, even when all strain is recovered so that the slip process is hindered in subsequent tests. Thermal treatment might be expected to relieve residual tension in the crosslinks and the 40 Mrad specimen was held at 60°C for 12 h before performing a third test represented by the triangular points in *Figure 10*. The test was found to yield a modulus value nearly identical to that obtained in the first test, supporting the view that the work-hardening effect is caused by unrelieved tension in the crosslinks.

The tensile modulus is a convenient parameter with which to compare single crystal mats and bulk polymer. In *Figure 11*, the moduli for various samples of bulk polymer at a fixed strain rate are plotted against the density of the bulk material as measured in the gradient column. The moduli were determined in exactly the same fashion as were the moduli for crystal mats on identically shaped specimens. A triangle point indicates an annealed bulk sample whose original density was that of the circles immediately below on the curve. The samples of bulk material which had been annealed were found to have a void content of up to 2 vol. %. *Figure 11* indicates that the modulus values for these annealed bulk samples are perfectly consistent with the values for the unannealed samples, which had a negligible void content, since all points lie on the same curve. Therefore these voids have little, if any, effect on the modulus. The shape of the curve is similar to that obtained by Levene *et al*[21] who measured the dynamic modulus of bulk samples with various degrees of crystallinity.

It is clear from the curve that the tensile moduli of crystal mats are of the same order as the moduli of bulk material. This is an important similarity for it indicates that the concept of bulk material behaving as an aggregate of lamellae, with deformation occurring through a process of inter-lamellar slip, could well be correct for this strain region. For low density bulk material ($0.927 g/cm^3$) inter-lamellar slip in the crystalline regions would be accompanied by flow in the relatively extensive non-crystalline regions, resulting in a lower modulus. For high density material ($0.978 g/cm^3$) on the other hand, some of the tie molecules connecting the lamellae could be in tension, thus opposing inter-lamellar slip as well as inhibiting deformation in the non-crystalline regions and resulting in a modulus higher than that obtained for crystal mats.

The modulus values obtained for crystal aggregates may be compared with the value predicted from *Figure 11* for bulk material of equal density ($0.972 g/cm^3$). While both types of crystal mats have moduli below this particular value, the modulus of type B mats comes surprisingly close, being identical to the modulus of a bulk sample with density $0.968 g/cm^3$. This relatively small difference in modulus between type B aggregates and bulk polymer of equal density is not necessarily a consequence of voids in the former species (which are probably concentrated at the axialite edge boundaries), for although both samples contain an equal amount of non-crystalline material, the effect of this material on the deformation properties would differ.

In bulk polymer, relative movement between any two neighbouring lamellae

is opposed by the resistance to stretching offered by the material in the inter-
vening region which is intimately connected to both lamellae. In an aggregate,
however, the less dense material on the lamella surfaces is directly connected
to one crystalline domain only, and therefore would not necessarily be
deformed by slip at the lamellar boundaries. This would result in a lower
modulus for the crystal aggregate. In this connection, evidence has already
been presented (*Figure 6*) to support the view that deformation in crystal
mats dissipates less energy than does deformation in bulk polymer of equal
density. (*Figure 11* provides a precedent for the modulus being independent
of the presence of voids).
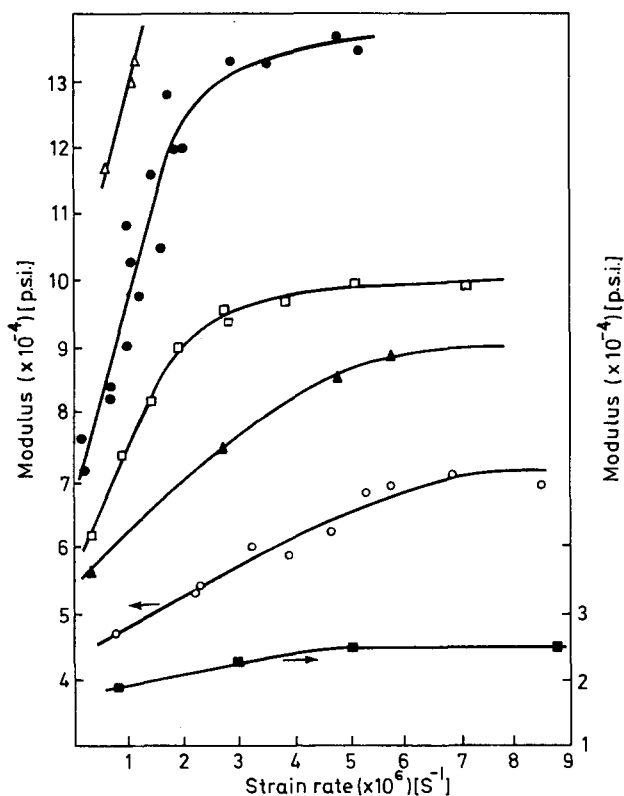
Figure 12 Tensile modulus versus strain rate for crystal aggregates
and various types of bulk polymer.
■, Alkathene (0·927 g/cm³);   □, Vestolen (0·961 g/cm³);
○, Rigidex (0·947 g/cm³);   ●, crystal aggregate, type B (0·972 g/cm³);
▲, annealed Rigidex (0·956 g/cm³);   △, annealed Vestolen (0·978 g/cm³).

Certainly the modulus of type B crystal aggregates would be affected by the
presence of voids if measurements were made in a higher strain region where
inter-axialite slip occurred. Also, if the voids were concentrated at the boun-
daries between lamellae, a very small void content would have a great effect

on the modulus, thus explaining why the modulus of type A aggregates is equal to that of a bulk sample with density as low as $0.961 \, g/cm^3$.

Evidence has been presented above which suggests that the resistance to deformation in the crystalline regions of bulk polymer, in the low strain region, is to a great extent determined by the ability of the lamellae to slide over one another. It is apparent from *Figure 7* that a characteristic feature of the inter-lamellar slip deformation process in crystal aggregates is its very strong dependence on strain rate in the low strain rate region. For both types of crystal mats the modulus increased sharply at first, and gradually levelled off at higher values of the strain rate. The slope of the curve was greater for type B mats in which inter-lamellar slip was believed to be more difficult, due to stronger inter-lamellar boundaries. An analogous effect would be expected for the case of bulk polymer if the deformation results from an inter-lamellar slip process as earlier results have indicated.

Figure 12 shows that the modulus of bulk material exhibits a strain rate dependence entirely consistent with that observed for crystal mats. (Note that the modulus dependence on strain rate is virtually confined to the very low strain rate region. Rigidex type 3 with a density of $0.947 \, g/cm^3$ is a good example. The modulus at first increases sharply in the low strain rate region and levels off at higher rates as shown in *Figure 13* which covers the high strain rate region. The moduli in *Figure 13* are lower than those of *Figure 12*
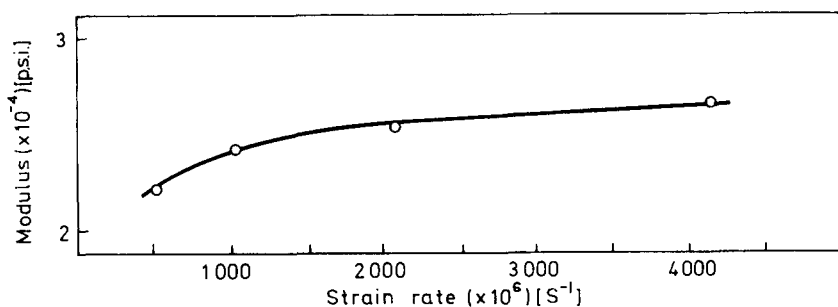
Figure 13 Tensile modulus versus strain rate for bulk polymer (Rigidex, $0.947 \, g/cm^3$) in the high strain rate region

since they were determined for strains greater than 1% to accommodate the high rates). The slope of the modulus versus strain rate curve in the low strain rate region increased with increasing crystallinity, with the result that the expected slope for a bulk sample of density $0.972 \, g/cm^3$ was about the same as that for type B crystal mats. This provides further support for the view that the deformation mechanism at low strains is much the same for a compacted crystal mat as for a sample of bulk crystallized polymer with an equal density. It is also consistent with the results of McCrum and Morris[20] who reported that inter-lamellar slip can occur in bulk polymer and that this is a strain rate dependent process.

Rabinowitz and Brown[19] have investigated the strain rate dependence of the modulus of a sample of bulk material of density nearly identical to that of

the crystal aggregates used in the present work. The absolute values of the modulus resulting from the separate investigations cannot be compared directly since the data for the bulk material was obtained using an apparatus a hundred times more sensitive than that employed for strain measurement in the present work, permitting the use of much lower stress amplitudes for modulus measurement. However, their measurements were made in the same strain rate region as that employed here so the results of the separate investigations can be plotted on a common strain rate axis (*Figure 14*). It is
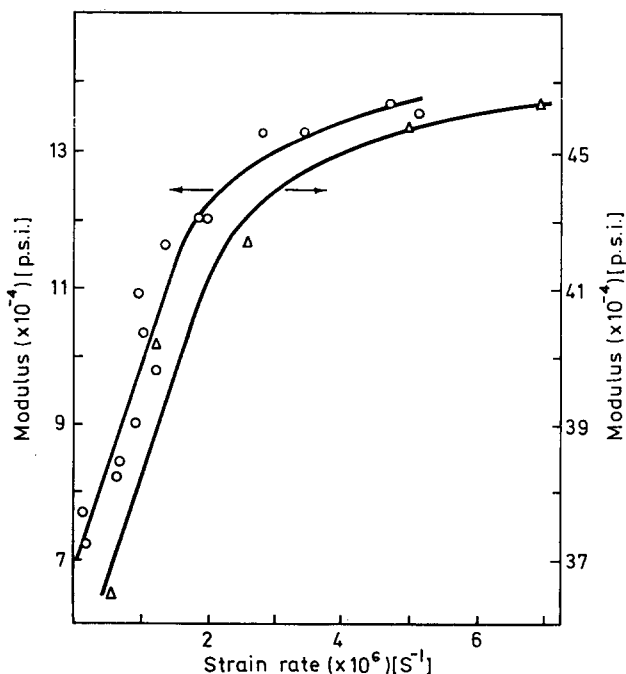
Figure 14 Comparison of modulus versus strain rate curves: $\bigcirc$, crystal aggregates (type B) at 20°C; $\triangle$, data of Rabinowitz and Brown[19] for bulk polymer (density = 0·973 g/cm³) in the micro-strain region at 23°C

interesting to note that the two curves in *Figure 14* are parallel for this could indicate a common deformation mechanism. This would support the view, developed above, that the deformation mechanism in type B crystal aggregates (inter-lamellar slip) is very similar to the deformation mechanism in a sample of bulk material of equal density. This conflicts with the interpretation of Rabinowitz and Brown[19]. By analogy perhaps to non-polymeric systems, they deduced that the strain rate dependence of any dislocation deformation mechanism (such as inter-lamellar slip) would be much smaller than that of

144

non-crystallographic shear or flow mechanisms, hence they attributed the observed time-dependent deformation to the non-crystalline regions.

CONCLUSIONS

(1) Crystal mats are subject to brittle fracture at low strains and their tensile properties therefore have nothing in common with the corresponding properties of bulk crystallized material in the large strain region ($> 1\%$).

(2) Deformation in crystal mats is believed to involve inter-lamellar slip, which has been found to be both a reversible and time dependent deformation mechanism.

(3) The tensile modulus of crystal aggregates in the low strain region has been found to be of the same order as the modulus for bulk polymer.

(4) The tensile modulus of a compacted mat with a high degree of inter-lamellar contact appears to be only slightly smaller than the tensile modulus of a sample of bulk polymer of equal density. The difference could be due to amorphous material in bulk polymer acting as an inter-lamellar link, rather than to the existence of voids in the aggregate.

(5) The strain rate dependence of the tensile modulus of crystal aggregates is similar to the strain rate dependence of the modulus of bulk material in the low strain region. The similarities become more obvious as the density of the bulk approaches that of a crystal aggregate. This together with the similarity of the moduli, suggests that inter-lamellar slip occurs in bulk polymer as well.

These conclusions may be summarized by saying that in the low strain region the tensile properties of an aggregate of polyethylene crystals are very similar to those of bulk crystallized polymer with the same density as individual single crystals. This concordance lends support to the view that lamellar crystalline regions are indeed the fundamental building blocks in the structure of bulk crystallized polymer though they are disguised to such an extent that the resemblance to an aggregate of single crystals is not manifest under all conditions.

In the next paper of this series, which follows on page 147, the properties of polyethylene crystal aggregates are shown to be worthy of study in their own right.

University of Cambridge,
Department of Chemical Engineering,
Pembroke Street, Cambridge

REFERENCES

1 Keller, A. *Rep. Progr. Phys.* 1968, **31**, 623
2 Blackadder, D. A. *J. Macromol. Sci. (Revs)* 1967, **C1**, 297
3 Anderson, F. R. *J. appl. Phys.* 1964, **35**, 64
4 Fujiwara, Y. *J. appl. Polym. Sci.* 1960, **4**, 10
5 Palmer, R. P. and Cobbold, A. J. *Makromolek. Chem.* 1964, **74**, 174
6 Keller, A. and Sawada, S. *Makromolek. Chem.* 1964, **74**, 190
7 Andrews, E. H. *J. Polym. Sci. (B)* 1965, **3**, 353
8 Hoffman, J. D. and Lauritzen, J. I. *J. Res. Nat. Bur. Stand.* 1961, **65A**, 297
9 Bassett, D. C. and Keller, A. *Phil. Mag.*, 1962, **7**, 1553
10 Keith, H. D. *J. Polym. Sci. (A)* 1964, **2**, 4339
11 Bassett, D. C., Keller, A. and Mitsuhashi, S. *J. Polym. Sci. (A)* 1963, **1**, 763
12 Blackadder, D. A. and Lewell, P. A. *Polymer, Lond.* 1968, **9**, 249
13 Richardson, M. J., Flory, P. J. and Jackson, J. B. *Polymer, Lond.* 1963, **4**, 221
14 Swan, P. R. *J. Polym. Sci.* 1962, **56**, 403
15 Lowell, P. N. and McCrum, N. G. *J. Polym. Sci. (B)* 1967, **5**, 1145
16 Sinnott, K. M. *J. appl. Phys.* 1966, **37**, 3385
17 Geil, P. H. *J. Polym. Sci. (A)* 1964, **2**, 3813
18 Salovey, R. and Keller, A. *Bell Systems Technical Journal*, 1961, **40**, 1409
19 Rabinowitz, S. and Brown, N. *J. Polym. Sci. (A-2)* 1967, **5**, 143
20 McCrum, N. G. and Morris, E. L. *Proc. R. Soc. (A)* 1966, **292**, 506
21 Levene, A., Pullen, W. and Roberts, J. *J. Polym. Sci. (A)* 1965, **3**, 697
22 Blundell, D. J., Keller, A. and Kovacs, A. J. *J. Polym. Sci. (B)* 1966, **4**, 481

Properties of polymer crystal aggregates. (2) Annealing of polyethylene crystal aggregates

D. A. BLACKADDER and P.A. LEWELL*

As described in an earlier paper, crystals of polyethylene prepared from dilute solution may be aggregated to form macroscopic specimens or mats, large enough for physical and mechanical properties to be measured. Three such properties, density, tensile modulus, and solvent swelling, have been investigated as functions of annealing temperature. Although the properties converge on those values appropriate to bulk polymer as the annealing temperature approaches the melting point, this convergence is not monotonic. On the contrary there is strong evidence for two quite distinct annealing processes, each dominant over a particular temperature range. These mechanisms, *in situ* crystal thickening and partial melting respectively, have been further investigated using irradiated specimens.

POLYETHYLENE crystals prepared from dilute solution may be dried and agglomerated to form macroscopic samples or mats, large enough for physical and mechanical testing by normal methods. In Part 1[1] (page 125) the tensile properties of mats and bulk crystallized polyethylene were compared, the experiments being confined to the low strain region by the fact that mats fracture at strains of only 1%. A mechanism for mat deformation involving inter-lamellar slip was proposed and certain deductions were made concerning the corresponding behaviour of bulk crystallized polymer.

It is obvious that mat behaviour must be dominated by inter-lamellar interactions since they determine the cohesion of the mat. Processes which alter the behaviour of the mat must therefore be susceptible to description in terms of modifications to these interactions consequent upon changes in the conditions such as increase of pressure or temperature. One such process is annealing, in which the mat is held for a known time at a temperature above that at which the constituent crystals were prepared but below the expected melting point. It was noted previously[1] that annealing bulk polymer is a convenient method of raising its density and tensile modulus. That something similar should occur when mats are annealed seems reasonable, and the problem of interpreting the mat process is simpler. So far this area has received little attention though a considerable amount of information is available concerning the annealing of single crystals. It has been well established that such annealing results in an increased fold length, but the precise mechanism is still a matter for debate[2,3]. The small amount of data concerning mats must now be reviewed.

Statton[4] has shown that the properties of a crystal mat can be drastically altered by annealing at temperatures between 120 and 137°C. Crystal mats several millimetres thick and possessing a layered structure were found to

*Present address: New Brunswick Research and Productivity Council, Fredericton, New Brunswick, Canada

exhibit remarkable changes in extensibility after annealing. Electron micrographs revealed that the layered structure was absent after annealing although the molecules still showed an orientation perpendicular to the base of the mat. It was proposed that the process of lamellar thickening obliterated the boundaries between crystals, as the vacated space in each lamella provided the growing room for the refolding of chains in adjacent platelets. Thus the mat became one large para-crystal, with its sites of weakness homogeneously distributed resulting in improved mechanical properties. Some years previously Geil[5] had developed somewhat similar ideas for the annealing of a few overlapping lamellae. Lowell and McCrum[6] have investigated the effect of annealing on the quantity of gas absorbed by bulk polyethylene and by polyethylene crystal mats. The results obtained were surprising because the solubility coefficient and, by inference, the amorphous content, were found to decrease with increasing annealing temperature for bulk polyethylene, but to increase with annealing temperature for crystal mats. This behaviour is consistent with the variation of the γ-relaxation[7] (caused by the relaxation of the CH_2 groups in the amorphous material) with annealing temperature for both bulk polymer and mats. A conflict appears to exist, however, between these findings and the results quoted earlier where the fold period and the density of single crystals were found to increase on annealing.

The present investigation was designed to document the effects of annealing on some physical properties of crystal mats with a view to relating these effects to morphological changes in the constituent lamellae.

EXPERIMENTAL

In an effort to corroborate the results of the gas solubility investigation[6] it was decided to measure initially the volumetric change accompanying the penetration of a liquid into a crystal mat. A solvent, p-xylene, was chosen as penetrant because of its high affinity for polyethylene. The assumption inherent in this procedure is that the solvent readily penetrates the amorphous material, causing extensive swelling, but is restricted from entering the crystalline regions because the internal crystal forces oppose distortion of the lattice. The experiments involved measuring the swelling over a given time interval for a variety of specimens, the time interval being sufficiently long to allow the rate of expansion to decay from an initially high value to very near zero. Subsequent expansion, if any, would be due to slow penetration into the crystalline regions. The expansion observed was proportional to the amount of amorphous material and could be used to detect changes in the amount of such material on annealing a crystal mat. The detailed procedure was as follows.

A mat, prepared from type B crystals formed from 1 wt.% solution at 75°C and compacted as described in Part 1[1], was machined into a rectangular block of approximate dimensions $19 \times 13 \times 6$ mm $(0.75 \times 0.50 \times 0.25$ in). The volume was determined by micrometer measurement of each dimension to ± 0.01 mm $(\pm 0.0005$ in). The swelling experiments were performed at

70°C, elevated temperature being required to increase the rate of solvent penetration. To allow for ordinary thermal expansion the rectangular mat was first placed in an air oven at 70°C and allowed to reach thermal equilibrium. The volume at 70°C was determined by removing the mat from the oven for a series of three very brief intervals (of the order of 5 s) and measuring by micrometer a different dimension during each interval, before significant cooling could occur. This seemingly crude technique yielded consistently reproducible results for the thermal expansion of the mat. The mat was then placed in a glass tube containing p-xylene which was mounted in an oil bath at 70°C. The volume was determined at intervals of several hours by rapid micrometer measurement in the manner described above. After 36 h the rate of expansion had decreased from an initially high value to a barely detectable level. After 42 h volume measurements were terminated and the expansion due to solvent penetration at 70°C was calculated using the equation below:

$$\Delta V = \frac{(V_s - V_a)}{M} \rho \times 100\%$$

where ΔV = percent expansion due to solvent penetration at 70°C, relative to the volume of polymer at 25°C
V_s = volume of mat after 42 h in solvent bath at 70°C
V_a = volume of dry mat at 70°C
M = mass of specimen
ρ = density of specimen at 25°C as measured in the density gradient column.

In all cases, at least 90% of the total change in volume, ΔV, occurred during the first 24 h.

This procedure was repeated using specimens cut from various sheets of bulk polyethylene differing in density, to verify that ΔV is a function of the density, as well as to determine the expansion to be expected for a sample of bulk material of density equal to that of the crystal mats. The experiment was then repeated using crystal mats annealed at various temperatures. A standard annealing procedure was adopted in which the specimen was placed in a steel die and heated slowly to a particular temperature in an air oven. The temperature, measured by a thermometer extending through the top of the oven with its bulb in the die, was maintained constant to within ± 0.01°C for 18 h before cooling at 5°C/h to room temperature. The density of crystal mats was also measured as a function of annealing temperature in order to correlate the swelling data with morphological changes in the constituent crystals. Small cubes of type B aggregates (about 2·5mm, 0·1in, along one edge) were placed in glass tubes which were subsequently evacuated down to a pressure of about 10^{-3}mmHg. Oxygen-free nitrogen was introduced and, after six purges, the tubes were sealed. Annealing was accomplished by heating the tubes in an air oven to a particular temperature and maintaining the temperature constant for 18 h before cooling at 5°C/h to room temperature as above. Fragments from these annealed specimens were then placed in a density gradient column at 25°C and their density determined.

149

RESULTS AND DISCUSSION

Solvent swelling and density measurements

The swelling of bulk polyethylene due to solvent penetration at 70°C is shown in *Figure 1* as a function of the weight fraction of amorphous material. (The weight fraction of amorphous material was chosen for this plot to be consistent with the gas solubility investigation[6], and was calculated using the density measured at 25°C together with the literature values of 0·854 and
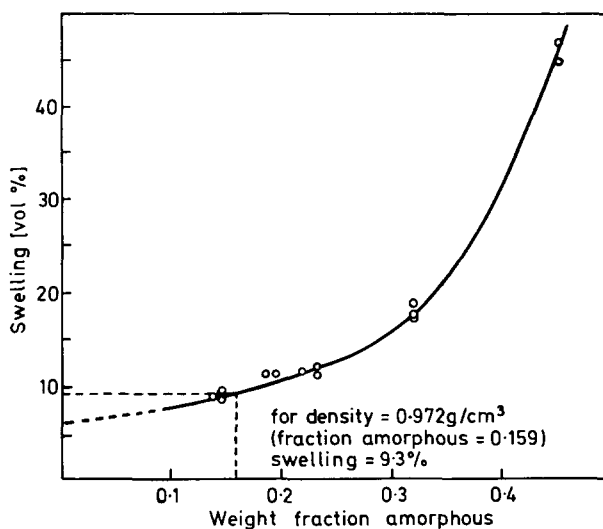

for density = 0·972g/cm³
(fraction amorphous = 0·159)
swelling = 9·3%

Figure 1 Swelling of bulk polymer due to solvent penetration at 70°C versus weight fraction of amorphous material

0·999 g/cm³ for the densities of amorphous and perfectly crystalline polyethylene respectively[8,9]. It must be emphasised that in the present paper amorphous simply means non-crystalline, it should not be taken to imply complete disorder. Each point represents an experiment on a separate specimen and the results are seen to be very consistent. Extrapolation to zero weight fraction of amorphous material reveals an intercept on the expansion axis, indicating that, for a given sample of bulk material, part of the observed expansion is due to solvent penetrating the crystalline regions. This is not surprising in view of the procedure of recording the total expansion after an arbitrary time interval, the time interval being long enough to allow the rate of expansion to decay to near zero. It is apparent, however, that the amount of swelling increases as the weight fraction of amorphous material is increased. The measurement of solvent swelling is therefore a means of detecting changes in the amorphous content, and is capable of yielding useful information on the effects of annealing crystal mats. Apart from producing small changes in the amount of non-crystalline material it seems quite likely that some molecular configurations in this material may also be modified by annealing.

In *Figure 2*, the expansion of type B crystal mats due to solvent penetration at 70°C is plotted as a function of the annealing temperature. The curve has a surprising shape with a minimum occurring at an annealing temperature of about 117°C. Unannealed mats, as well as mats annealed at the crystallization temperature of 75°C, exhibited a relatively large amount of solvent
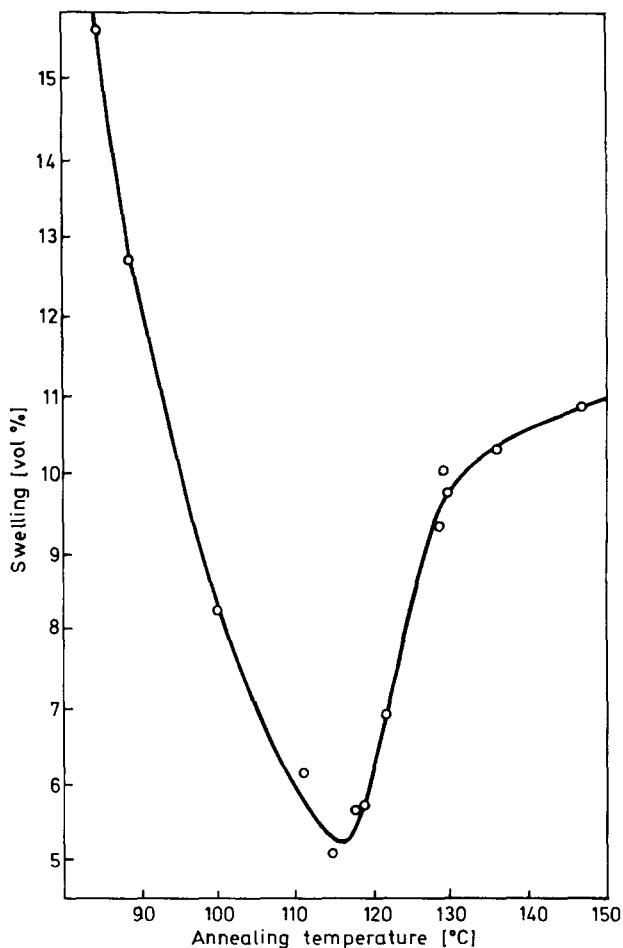

Figure 2 Swelling of crystal mats due to solvent penetration at 70°C versus annealing temperature. (swelling of unannealed mats = 22%)

swelling (of the order of 22%), and in fact appeared to be breaking up in the solvent with the formation of large cracks throughout. The mats annealed at 117°C, however, expanded less than any sample of *bulk* material (*Figure 1*). Mats annealed at temperatures above 130°C appeared to have melted and they resembled paraffin wax. They no longer possessed the chalky appearance characteristic both of unannealed samples and samples annealed at temperatures up to and including 129°C. There is a sharp change in the slope of the

curve at about 130°C, where this visible melting occurred, and the corresponding value of the solvent swelling is very close to the value expected for a sample of bulk polyethylene of density 0·972 g/cm³, as determined from *Figure 1*.

The results shown in *Figure 2* have some features in common with the gas solubility results of Lowell and McCrum[6]. In both cases a minimum is evident in the plot of a crystallinity–sensitive property against annealing temperature for single crystal mats. No significance was attached to this minimum in the solubility investigation, and its position was not determined precisely though it appears to be somewhere in the range 110–115°C. The solubility coefficient, like the expansion ΔV, steadily increased after passing through a minimum until, at an annealing temperature of 130°C, it reached a value very close to that expected for a sample of bulk material of density 0·972 g/m³. There are also some notable dissimilarities between the results of the two investigations and these concern the region below the temperature at which the minimum occurs. In this temperature range the solubility coefficient did not exhibit the very strong dependence upon annealing temperature observed here for solvent swelling. Also, the minimum value of the solubility coefficient of the crystal mats corresponds to an amorphous fraction of about 0·12 (or a density of 0·979 g/cm³) while the minimum expansion in *Figure 2* is significantly less than the value expected for a bulk sample with density 0·979 g/cm³, according to *Figure 1*.

The variation of the density (as determined in the gradient column) with annealing temperature is shown in *Figure 3* for type B crystal mats. The
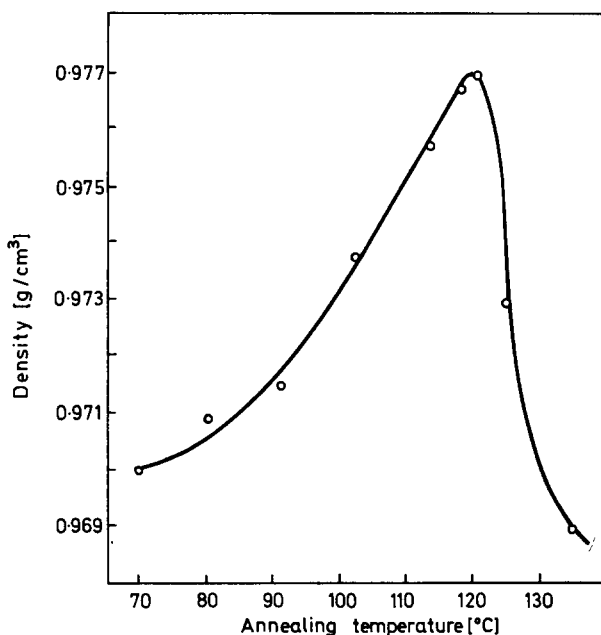
Figure 3 Density of crystal mats versus annealing temperature

density increased from an initial value[10] of about 0.970 g/cm^3 to a maximum of 0.977 g/cm^3 at an annealing temperature of about $120°C$. At higher annealing temperatures the density decreased sharply, even falling below the initial value at temperatures in excess of $130°C$. These results are in general agreement with the variation of the two other crystallinity–sensitive properties with annealing temperature described above.

It is apparent that the processes responsible for the sharp reduction in the solvent swelling of type B crystal mats over the range of annealing temperatures up to $117°C$, as well as the processes responsible for the much less abrupt reduction of the solubility coefficient over a similar temperature range, are associated with an overall increase in the density, and hence the crystallinity, of the mats. Similarly, in the temperature range above $117°C$, the processes which cause both the swelling and solubility coefficient to increase with increasing annealing temperature are associated with an overall decrease in the crystallinity of the mats.

It is not obvious why annealing at temperatures up to $117°C$ should have such a drastic effect on the expansion due to solvent penetration of type B crystal mats. The density increases only slightly over this annealing temperature range, and it is inconceivable that the entire reduction in swelling could be due to this. *Figure 1*, for example, indicates that raising the density to 0.977 from 0.970 g/cm^3 would be expected to reduce the solvent swelling from 10% to about 8%, while in fact the swelling decreased from 22% to 5% (*Figure 2*). For the unannealed mats, especially in view of the cracks which developed, it seems much more plausible to suppose that the main effect is due to a weakening of the Van der Waals forces between crystals by the solvent, resulting in physical separation of the lamellae. The resulting swelling would then be far in excess of the amount expected for bulk material of equal density where the effect was due simply to solvent entering and swelling the amorphous material.

It follows that annealing at temperatures up to $117°C$ must result in some sort of inter-lamellar link being formed to resist the action of the solvent in separating the lamellae, and thus cause the observed dramatic reduction in swelling. Indeed there is evidence to suggest that these links are even more effective in preventing inter-lamellar movement than the tie-molecules known to be present between the lamellae in bulk polymer; the solvent induced expansion of a mat annealed at $117°C$ is significantly less than the corresponding expansion of a sample of bulk material of density equal to that of the mat. Annealing at temperatures above $117°C$ would appear to result in the destruction of these unique inter-lamellar links as the behaviour of the mat gradually reverts to what would be expected for a sample of bulk material of equal density.

Clearly, an understanding of how these links are formed at low annealing temperatures and how they are eventually destroyed at higher temperatures is essential to an understanding of the whole annealing process in crystal mats. Another experimental approach was therefore required.

Tensile measurements

The solvent–swelling study has indicated that annealing crystal mats at

153

moderate temperatures (up to about 117°C) might well result in the formation of some sort of inter-lamellar link, with simultaneous increase in the overall crystallinity of the mat. Previous results[1] have indicated that the tensile properties of crystal mats are consistent with a deformation mechanism involving inter-lamellar slip, so that a network of inter-lamellar links would be expected to resist deformation and result in a higher tensile modulus. The tensile properties of crystal mats were therefore investigated as a function of the annealing temperature to verify the existence of annealing-induced inter-lamellar links.

The tensile modulus of single crystal mats (see Part 1[1] for experimental details) is plotted in *Figure 4* as a function of the annealing temperature.
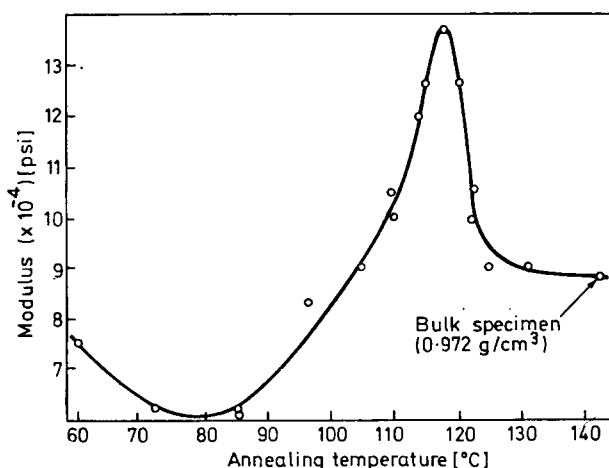
Figure 4 Tensile modulus versus annealing temperature for crystal mats

Each point represents a test performed on a new specimen using the same rate of loading and total stress amplitude. A comparison of this curve with that resulting from the solvent-swelling study in *Figure 2* reveals some interesting similarities. Annealing at temperatures between 85°C and 117°C for example, results in a progressive increase in the modulus and a reduction in the extent of solvent-induced swelling. The maximum in *Figure 4* occurs at the same annealing temperature as the minimum in *Figure 2*, and after passing through these values both the modulus and solvent swelling approach the value expected for a sample of bulk material of density $0·972 \, g/cm^3$. In both cases this limiting value is reached at an annealing temperature of 130°C. The minimum that occurs in the modulus at very low annealing temperatures (of the order of 80°C) is without a counterpart in the solvent-swelling results where the expansion decreased steadily over the annealing temperature range between 75°C and 117°C.

If it is assumed that the deformation mechanism in crystal mats involves inter-lamellar slip, as previous results[1] have indicated, it follows that the steady increase in modulus over the annealing temperature range between 80°C and 117°C could well be due to the formation of a network of inter-

154

lamellar links, which oppose relative movement of the lamellae. The fact that the extraordinary reduction in solvent-swelling up to 117°C is accompanied by an increase in the tensile modulus gives strong support to the view that annealing in this moderate temperature range causes interactions between neighbouring lamellae with simultaneous increase in the overall crystallinity of the mat. Further the increase in the swelling at annealing temperatures above 117°C was attributed in part to the reduction in the crystallinity of the mat and in part to the destruction of the unique network of links between lamellae. The fact that the tensile modulus decreases in this temperature range as well, supports the view that the interactions are indeed weakened or destroyed.

Having established that the implications of the tensile modulus experiments are consistent with those of the solvent-swelling study, it remains to explain how annealing at moderate temperatures could give rise to interactions between lamellae, and how annealing at higher temperatures could cause them to be destroyed. There can be little doubt that the increase in the density of the mats caused by annealing at temperatures up to about 120°C is due to an increase in the fold length of the constituent lamellae. The plot of density versus annealing temperature in *Figure 3* indicates that the increase in crystallinity occurs over the same range of annealing temperature as the increase in tensile modulus and decrease in solvent-swelling. Hence it seems very likely that inter-lamellar links are formed as a direct consequence of the thickening process.

A mechanism whereby crystal thickening could give rise to inter-lamellar links has already been proposed independently by Statton[4] and by Geil[5], and it is consistent with the present experimental results. The inter-lamellar links formed by annealing at moderate temperatures could result from a cooperative interlocking between lamellae, as the holes formed in a crystal as a consequence of its molecules adopting a new fold length are filled by refolding chains from neighbouring platelets. Certainly the mechanism could readily account for the observed changes in the tensile modulus and solvent-induced swelling, for these properties are particularly sensitive to the existence of weak boundaries between the constituent crystals. By eliminating or obscuring these boundaries, interlocking would have a dramatic effect on such properties. A specimen in which the lamellae are bound together by mutual interlocking of folds would be expected to have properties different from a sample of bulk polymer of equal density, in which the lamellae are bound together by amorphous material. Consider a crystal aggregate annealed at 117°C. It has a density of 0.978 ± 0.001 g/cm^3 and yet its tensile modulus from *Figure 4* is nearly 40% greater than the value for bulk polyethylene of equal density. (The modulus of a sample of bulk polyethylene of density 0.978 g/cm^3 at a strain rate of the order 0.2×10^{-6} s^{-1} can be estimated from *Figure 12* of Part 1[1] to be about 10×10^4 psi). Further, according to *Figures 1* and *2*, the solvent-induced swelling of an aggregate annealed at 117°C is significantly less than the corresponding swelling for a sample of bulk material of equal density. This observed departure from bulk polymer behaviour is consistent with the formation of unique inter-lamellar links in the mat, such as could arise from mutual interlocking.

Annealing at temperatures between 117°C and 130°C results in a departure from the trend established by annealing at lower temperatures. A mat annealed at 130°C, quite apart from having a density lower than a mat annealed at 117°C, is much more like a sample of bulk polymer of equal density. As mentioned previously, the modulus and swelling measured for aggregates annealed at 130°C are very close to those values expected for samples of bulk polyethylene of density 0·972 g/cm³. It appears that annealing at temperatures between 117°C and 130°C results in a progressively more complete destruction of the unique inter-lamellar links which hitherto endowed the annealed crystal aggregates with properties distinct from bulk polymer. Partial melting followed by recrystallization in bulk form could account for these observations. If the molecules in a region of the mat were to achieve an intermediate state of disorder so that the lattice structure in this region were disrupted, it would not be re-established in its original form on recrystallization. Rather, subsequent recrystallization would be analogous to crystallization from the melt, the new lamellae being separated by amorphous material and connected by tie molecules. Partial destruction of the unique interlocking network would result in a decrease in the tensile modulus. In fact, as the annealing temperature is increased the modulus of the mat would gradually approach the value expected for a sample of bulk material of equal density since progressively more partial melting would occur.

It is not surprising that this partial melting process is accompanied by a decrease in crystallinity, for the proportion of non-crystalline material in the melt-crystallized product would be expected to be greater than in the crystal aggregates annealed at 117°C. It may well be asked, however, why annealing at 130°C results in a density of 0·972 g/cm³, the original density of the un-annealed aggregate. This is probably simply fortuitous, as experiments have shown that the density of material recrystallized from the melt in bulk is dependent upon the molecular properties of the particular sample of polyethylene. Here, the polyethylene used to make the solution-grown crystals for the aggregates was Rigidex 50. Annealing a bulk sample of Rigidex 50 at 130°C followed by slow cooling results in a density of 0·972 g/cm³. A different polyethylene would presumably yield a different density value for crystal aggregates annealed at 130°C.

So far as the tensile modulus and solvent-swelling are concerned, it is of interest that the change from typical crystal mat behaviour to bulk polymer behaviour is accomplished at annealing temperatures below that at which a change occurs in the appearance of the mats. An aggregate annealed at 129°C, for example, still had the chalky appearance typical of crystal mats, although it had become very similar to bulk material in these other respects. Annealing at 131°C caused a remarkable change in appearance (the specimen had obviously melted) but with little change evident in the modulus or swelling. This gives support to the idea of partial melting occurring at lower annealing temperatures.

It should be noted that the refolding of chains to produce interlocking between adjacent lamellae evidently continues to occur, although to a progressively smaller extent, at annealing temperatures above 117°C,

despite the fact that partial melting occurs as well. This follows from the fact that each point in *Figure 4* represents a test performed on a new specimen. Clearly, if only partial melting occurred at an annealing temperature of 120°C for example, the resulting modulus would be expected to be somewhere between the values obtained for the unannealed aggregate and bulk polymer of density 0·972 g/cm³. (It was confirmed that the properties of an aggregate annealed at a given temperature were not affected by previous annealing at lower temperatures. Several solvent-swelling experiments were performed on a given specimen, taking care to remove all traces of solvent by prolonged drying in a vacuum oven before annealing again at a higher temperature. The results obtained were entirely consistent with results from specimens which had been annealed only once).

It must now be explained why a minimum occurs in *Figure 4* at an annealing temperature of about 80°C. The temperature is certainly too low to cause any morphological changes in the crystal lattice and the effect appears to be peculiar to tensile modulus measurements. Temperature-induced changes in the degree of compaction of the mats might provide an explanation, for inter-lamellar slip would be facilitated by any increase in the spacing between lamellae. To detect such changes, the volume of each aggregate was accurately determined by micrometer immediately before and after each annealing treatment, yielding the results shown below in *Table 1*.

Table 1 Volume changes on annealing

Type of mat [1]	Annealing temperature [°C]	Increase in volume on annealing [%]
B	60	0
B	73·8	3·2
B	85	3·8
B	105	3·4
B	110·6	3·4
B	114·1	3·5
B	117·7	4·3
B	122·6	4·0
B	124·8	3·1
B	129·5	3·0
B	131·5	−3·0
B	137	−6·0
A	112·4	−1·0

It is clear that annealing compacted type B mats at temperatures of the order of 70°C causes a significant increase in the volume of the aggregate which does not occur on annealing at 60°C. The magnitude of this volume change appears to remain reasonably constant up to an annealing temperature of 129°C. The volume decrease on annealing at temperatures above 129·5°C is a result of extensive melting followed by recrystallization in bulk form. The volume increase appears to be peculiar to compacted (type B) mats, for annealing a type A mat at 112·4°C resulted in a volume decrease.

These results are consistent with the view that the reduction in tensile modulus caused by annealing at temperatures between 70 and 80°C is due to temperature-induced changes in the degree of compaction. When no compaction has occurred the effect is naturally absent, as in type A mats.

Reinforcement of inter-lamellar boundaries, with concomitant increase in the density, can be detected at annealing temperatures as low as 85°C (i.e. 10°C above the crystallization temperature) according to *Figures 2, 3* and *4*). If, as has been assumed, such boundary reinforcement results from the refolding of molecular chains in adjacent platelets, then these results imply that lamella thickening can occur at surprisingly low temperatures. This evidence for some sort of morphological change occurring at low annealing temperatures is not without precedent. Accurate calorimetry[11] using crystals prepared at various temperatures has revealed a significant rate of heat release, thought to be related to increases in the fold length, at temperatures 10°C above the original crystallization temperature. Also, it has been observed[12] that the rate of nitric acid attack increases sharply in the region of 80°C, and this has been attributed to changes in the crystals under attack rather than to increased acid reactivity. It has been proposed that the lattice itself becomes susceptible to acid attack due to suddenly increased 'thermal motions' of the molecular chains. Direct measurement of the x-ray long spacing for annealed crystals has not as yet firmly established a lower limit for chain thickening. Statton and Geil[13] have concluded that 110°C represents the threshold annealing temperature, below which no change in the x-ray long spacing is apparent, although their results for prolonged annealing experiments (15 h) were inconclusive. Baltá Callejá, *et al*[14] have subsequently found that 110°C is not a unique lower limit, since annealing a specimen with an original thickness of 9·8 nm for 30 min at 102°C caused the thickness to increase to 10·5 nm. Annealing for longer periods (such as 18 h as in the present work) at even lower temperatures might well be expected to cause detectable changes in the long spacing.

In the present work experiment revealed that annealing crystal mats at temperatures up to and including 130°C, the temperature at which visible melting occurred, had no significant effect on the extension at break. Brittle fracture occurred at a strain of 0·014 ± 0·001 for all specimens, in agreement with the experiments on unannealed aggregates[1]. In contrast the mats described by Statton[4] became very extensible after annealing at temperatures above 120°C yet his interpretation made no mention of partial melting. The reasons for the differences are being pursued, but it seems certain that they are due to fundamental differences in the mats which were not prepared from identical polymer crystals in the two investigations.

Testing the proposed annealing mechanism

The above results have indicated that the reinforcement of internal boundaries on annealing crystal aggregates at temperatures up to about 117°C is a consequence of *in situ* lamellar thickening. One means of testing this hypothesis is to impose restraints on the thickening process in an effort to detect subsequent changes in the annealing behaviour of the aggregates.

An earlier study[14] has shown that the original crystal fold length, and therefore the crystallization temperature, affect the thickening process in that the temperature at which thickening begins is higher for crystals with an initially greater fold length. One type of restraint on the thickening process may thus be imposed simply by raising the crystallization temperature of the crystals used to make the mats.

Irradiation would appear to offer another means of restraining crystal thickening on annealing. It has been shown[15] that the deformation of single crystals on an extensible substrate can be progressively inhibited by irradiation. Such behaviour suggests the formation of a strong network of intralamellar links which oppose the relative movement of molecular chains within the crystal. Hence, if thickening is normally accomplished *in situ* by the relative movement of chains in the direction of the chain axes, the network would inhibit the thickening process. In their work on the fusion of irradiated and unirradiated polyethylene crystals Bair *et al*[16] found evidence for the inhibition of thickening by irradiation. Kawai and Keller[17] also found that the increase in long spacing on annealing was significantly smaller for crystal samples which had been pre-irradiated, implying an inhibition of the thickening process by crosslinks. Inter-lamellar crosslinks were judged to be more effective than intra-lamellar links since irradiation had a greater influence on specimens with a high degree of inter-lamellar contact. Experiments were also performed on samples which had been annealed prior to irradiation. The number of inter-lamellar ties formed by a given dose of irradiation could be remarkably increased in this way, presumably because annealing increases the degree of inter-lamellar contact in agreement with previous work[18]. It was proposed that this increased contact was due to the intermeshing of folds in adjacent lamellae on thickening, a view entirely consistent with the present results.

In this work the thickening process was restrained by raising the crystallization temperature from 75°C to 85°C for some specimens, and by irradiating others, using the procedures described previously[1]. The solvent-swelling of both types of specimens was measured as a function of annealing temperature and the results compared with similar measurements on unirradiated samples composed of crystals formed at 75°C.

In *Figure 5* the swelling due to solvent penetration is plotted as a function of the annealing temperature for aggregates composed of crystals grown at 75 and 85°C respectively. The curves are of similar shape, but do not superimpose, the curve for the 85°C crystals being consistently displaced to the right along the temperature axis. Consider first the range up to 115°C. The fact that the curves are parallel over this range indicates that the same process is responsible for the progressive reduction in swelling. However, at a given annealing temperature, the swelling is less for the mat composed of crystals with the lower crystallization temperature. Since the onset of thickening is known to occur at lower annealing temperatures for crystals prepared at lower crystallization temperatures, more thickening and hence more boundary reinforcement will have occurred at a given annealing temperature for mats composed of the latter type of crystals.

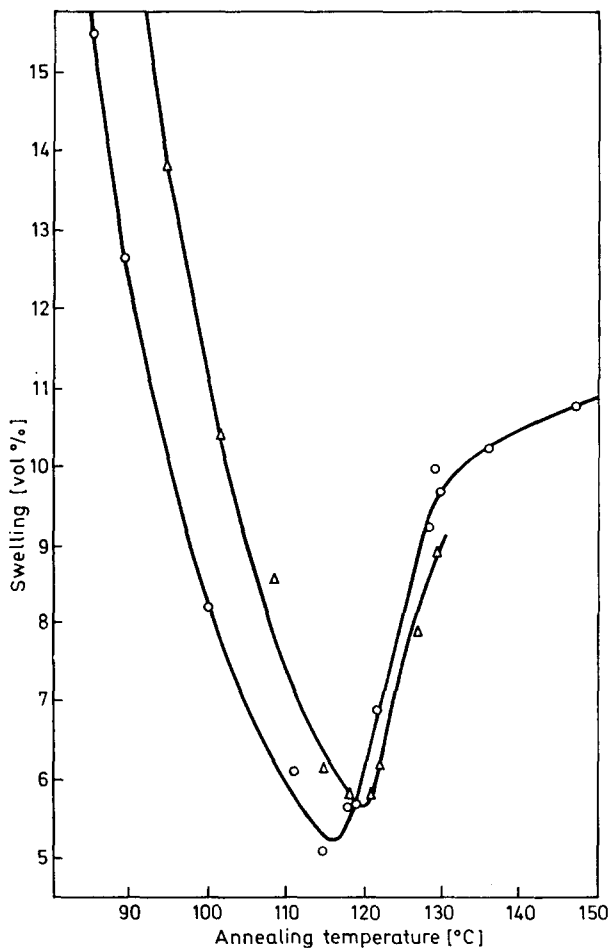The fact that the curves in *Figure 5* are again of similar shape above 115°C

159

Figure 5 Swelling of crystal mats due to solvent penetration at 70°C
versus annealing temperature
○, 75°C crystal mats; △, 85°C crystal mats

indicates that the same competing process occurs in both specimens but the process becomes dominant at a higher annealing temperature for the 85°C crystal aggregates. At any given annealing temperature above about 120°C the solvent-swelling of these aggregates is lower than for the 75°C aggregates. It has been well established[2,3] that the temperature at which melting or partial melting begins is a function of the fold length, hence the displacement of the minimum to a higher temperature for the mat of 85°C crystals is probably due to these crystals having a greater initial fold length.

Bair *et al*[16] have measured the heat of fusion of annealed polyethylene crystals, grown at 85°C, and their results have some features in common with those of the present investigation. Samples which were annealed at

118°C for 1 000 min (the annealing period used in the present study) had a heat of fusion greater than that of the unannealed crystals, in agreement with the above hypothesis that annealing at this temperature causes *in situ* lamellar thickening. Further, samples which were annealed at 123°C had a heat of fusion significantly lower than that of samples annealed at 118°C indicating the onset of a competing process.

Measurements performed on samples annealed for various time intervals revealed that annealing at temperatures above 118°C results in an initial decrease in the heat of fusion, followed by a gradual increase, indicating that the competing process could be partial melting with subsequent slow recrystallization, again in agreement with the present work. When mats of crystals prepared at 85°C were annealed at temperatures below 114°C and then melted, the heat of fusion curves had two main features: the actual heat of fusion did not change measurably but the shape of the curves changed a good deal even at 102°C. Bair *et al* chose to interpret the results in terms of improved inter-lamellar packing without any thickening or density increase. It is clear from the present results, however, that a large change in inter-lamellar adhesion may result from very small changes in density, undetectable by heat of fusion studies, but manifest in other ways including direct density measurement of high precision.

In *Figure 6* the swelling due to solvent penetration is plotted as a function of the annealing temperature for mats of crystals formed at 75°C which had previously been irradiated at 10, 20 and 40 Mrad. For purposes of comparison, the corresponding curve for unirradiated 75°C aggregates has again been plotted in this figure. Annealing at temperatures up to 80°C did not affect the swelling of irradiated or unirradiated specimens, so that the swelling values plotted for an annealing temperature of 80°C correspond to the values for the unannealed specimens as well. It is clear that irradiation progressively reduces the extent of swelling which can occur in the unannealed aggregates; a dose of 40 Mrad for example, being sufficient to reduce the swelling from 22% to 8·25%. This is entirely consistent with the effect of irradiation on the tensile properties of the unannealed aggregates[1] and it is believed to be due to the strengthening of the boundaries within the aggregate by the formation of inter-lamellar crosslinks. The action of the solvent in separating the lamellae is therefore inhibited.

It is also clear from *Figure 6* that prior irradiation causes extensive changes in the shape of the swelling versus annealing temperature curve. Consider first the range of annealing temperatures up to about 115°C. If the appropriate swelling at 80°C is regarded as the datum for each curve corresponding to a particular dosage, it can be seen that the reduction in swelling, caused by annealing at a higher temperature (up to 115°C), becomes progressively smaller as the radiation dose is increased. As a result, at an annealing temperature of about 115°C the swelling of each irradiated specimen is significantly greater than the swelling of an unirradiated specimen, in sharp contrast to the behaviour of the unannealed mats. These results firmly support the view that the reduction in swelling, caused by annealing within this temperature range, is due to the reinforcement of internal boundaries as a result of lamellar thickening, for the introduction of cross-
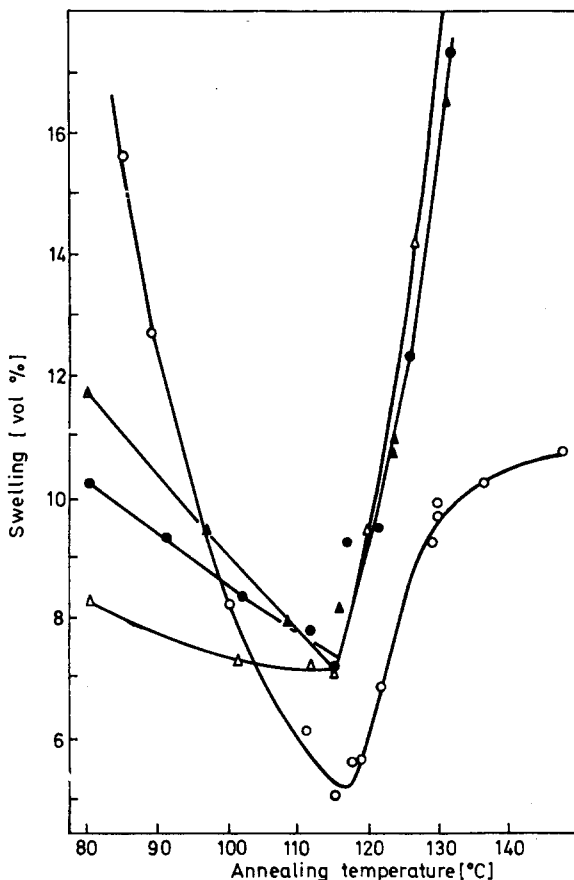
161

Figure 6 Swelling of crystal mats due to solvent penetration at 70°C
versus annealing temperature
○, unirradiated   ●, 20 Mrad
▲, 10 Mrad   △, 40 Mrad

links, known to inhibit the thickening of lamellae, results in less boundary reinforcement within the aggregate.

Annealing irradiated and unirradiated specimens at temperatures above 115°C results in a marked departure from the trend established on annealing at lower temperatures. In both cases a minimum is obtained after which the swelling steadily increases with annealing temperature until at 130°C melting occurs causing a sudden change in the physical appearance of the specimens. However, whereas the swelling of an unirradiated specimen approaches the value appropriate for a bulk sample with density 0·972 g/cm³ as the annealing temperature approaches 130°C, the swelling of an irradiated sample approaches a value appropriate to a bulk sample of much lower density. Indeed, at 130°C where visible melting occurs, the swelling of the 10 and 20 Mrad specimens corresponds to a bulk sample with density 0·952 g/cm³

(as determined from *Figure 1*) while that for the 40 Mrad specimen corresponds to a bulk sample of density $0.947 \, g/cm^3$. This behaviour provides further very strong support for the occurrence of partial melting. If, in this higher temperature range, an intermediate state of disorder is achieved on annealing crystal mats, subsequent recrystallization will be analogous to crystallization from the melt, the density of the resulting material normally depending upon the molecular properties of the polyethylene used to make the original crystals. Irradiation of the mats, however, alters the molecular properties of the polyethylene by increasing the chain branching, so that, once melted, a smaller proportion of the material is able to recrystallize. Therefore after melting and recrystallization of the crystal mats has occurred, the density will be lower and the solvent-swelling greater for those specimens which had been irradiated beforehand. If crystal aggregates are annealed at successively higher temperatures in the range where partial melting occurs, the swelling increase with annealing temperature would be expected to be greater for irradiated samples, and the swelling would approach the value expected for a bulk sample with a density much lower than $0.972 \, g/cm^3$, the value obtained for the unirradiated sample. The curves in *Figure 6* are therefore consistent with the occurrence of partial melting on annealing at temperatures above about 116°C.

The effect of irradiation on the annealing of crystal aggregates has been investigated previously, and it is of interest to compare the earlier results with those from the present study. According to the results of Kawai and Keller[17] a high degree of inter-lamellar contact would encourage the formation of inter-lamellar rather than intra-lamellar links on irradiation, the former being most effective in preventing thickening. In the present work where compaction presumably brought about very good inter-lamellar contact a dose of only 40 Mrad sufficed to suppress thickening almost completely.

In another investigation, Bair *et al*[16] have annealed irradiated samples of 85°C crystals at 121°C. The heats of fusion of the annealed irradiated samples were significantly lower than the heat of fusion of the annealed unirradiated samples, and decreased with increasing radiation dose. It was proposed that annealing 85°C crystals at temperatures between 118 and 127°C involved only lamellar thickening. However, in view of the fact that the heat of fusion of the unannealed 85°C crystals was greater than the heats of fusion obtained for the annealed irradiated samples, it seems more reasonable to suppose that partial melting occurs as well on annealing at 121°C. As in the present experiments, recrystallization after partial melting would be inhibited in the irradiated specimens as a consequence of the altered molecular properties of the polymer, resulting in the observed lower heats of fusion.

CONCLUSIONS

It has been shown that the study of the physical and mechanical properties of crystal aggregates can yield useful information on the properties of the constituent crystals. In particular, the annealing mechanism within polyethylene crystals has been clarified. It appears that annealing can give rise to both *in situ* thickening and partial melting, the onset of the former process

occurring at temperatures only 10°C above the crystallization temperature. The temperature at which partial melting begins will depend on the original fold length and on the amount of thickening that has occurred *via* the former process. In the present work, where the degree of compaction of the lamellae imposed limits on the extent of *in situ* thickening, partial melting became dominant at temperatures of the order of 117°C. When partial melting occurs the subsequent recrystallization of the affected regions resembles bulk crystallization and results in a solid of lower density than before. The extent to which this effect operates is dependent upon the molecular properties of any given sample. The results of the present investigation are therefore consistent with those from an earlier gas solubility study[6] and serve to resolve the conflict which existed hitherto between annealing studies on crystal mats[6] on the one hand, and individual lamellae[13] and bulk polymer on the other. Also, it has become apparent that the inter-lamellar boundaries within crystal aggregates can be remarkably strengthened by annealing at temperatures at which *in situ* thickening occurs. The evidence suggests that the increased contact between the lamellae is a consequence of a cooperative intermeshing of folds. Such behaviour would appear to be consistent with a certain regularity in the fold pattern. A new model for the surface structure recently proposed by Blackadder and Roberts[19] has shown that such regularity could well be compatible with the low crystal density values reported earlier[10].

REFERENCES

1 Blackadder, D. A. and Lewell, P. A. *Polymer, Lond.* 1970, **11**, 125
2 Keller, A. *Rep. Progr. Phys.* 1968, **31**, 623
3 Blackadder, D. A. *J. Macromol. Sci. (Revs)* 1967, **C1**(2), 297
4 Statton, W. O. *J. appl. Phys.* 1967, **38**, 4149
5 Geil, P. H., 'Polymer single crystals', Interscience, New York, 1963
6 Lowell, P. N. and McCrum, N. G. *J. Polym. Sci. (B)* 1967, **5**, 1145
7 Sinnott, K. M. *J. appl. Phys.* 1966, **37**, 3385
8 Richardson, M. J., Flory, P. J. and Jackson, J. B. *Polymer, Lond.* 1963, **4**, 221
9 Swan, P. R. *J. Polym. Sci.* 1962, **56**, 403
10 Blackadder, D. A. and Lewell, P. A. *Polymer Lond.* 1968, **9**, 249
11 Karasz, F. E. and Hamblin, D. J. *National Physical Laboratory Report* 1963, BP R 15
12 Blundell, D. J., Keller, A. and Connor, T. M. *J. Polym. Sci. (A-2)* 1967, **5**, 991
13 Statton, W. O. and Geil, P. H. *J. appl. Polym. Sci.* 1960, **3**, 357
14 Baltá Callejá, F. J., Bassett, D. C. and Keller, A. *Polymer, Lond.* 1963, **4**, 269
15 Martin-Voigt, I. and Andrews, E. H., Paper presented at International Meeting 'Microstructure of Materials', Oxford, September, 1968
16 Bair, H. E., Salovey, R. and Huseby, T. W. *Polymer, Lond.* 1967, **8**, 9
17 Kawai, T. and Keller, A. *Phil. Mag.* 1965, **12**, 687
18 Salovey, R. and Bassett, D. C. *J. appl. Phys.* 1964, **35**, 3216
19 Blackadder, D. A. and Roberts, T. L. *Makromolek. Chem.* 1969, **126**, 116

Solution properties of
poly-N-vinylcarbazole

GULLAPALLI SITARAMAIAH and DARRYL JACOBS

Poly-N-vinylcarbazole, polymerized by free radical initiation, was fractionated and the fractions were characterized by gel permeation chromatography, viscometry, light scattering and osmometry. Fractions obtained were in the 8 000–450 000 M_w range with polydispersities of 1·1–1·2. Intrinsic viscosities were obtained in five solvents at 25°C and increased in the order cyclohexanone < benzene < tetrahydrofuran < chloroform < tetrachloroethane. The universal calibration method of Benoit was found to be applicable for the g.p.c. data of PVK. The Mark-Howinck relations suggested that benzene ($a = 0·58$) is a poor solvent and tetrachloroethane ($a = 0·68$) a good solvent for PVK. Flory-Fox-Schaefgen, Kurata-Stockmayer, Stockmayer-Fixman relationships were used to evaluate the unperturbed dimension of the chain. A K_0 value of $6·8 \times 10^{-4}$ and a$(\bar{R}_0^2/M)^{1/2}$ value of $6·19 \times 10^{-9}$ have been obtained. The steric factor, σ, has been obtained as 2·8 for PVK, compared to a value of 2·2 for polystyrene, which suggests that the bulky carbazole group exerts increased hindrance to free rotation of the polymer chain.

THE RELATIONSHIP between chemical structure and photoconductivity of organic compounds and polymers has received considerable attention. The discovery fo the photoconductive properties of poly-N-vinylcarbazole (PVK) by Hoegl[1] led to detailed studies of the photodischarge characteristics of this polymer doped with a variety of sensitizers[2]. Recently such studies were reported by Lardon et al[3]. The mechanism of charge transfer of PVK-iodine complex was investigated by Herman and Rembaum[4]. In view of this interest in PVK as a photoconductor it has been considered important to investigate its molecular properties such as molecular size and conformation. The bulky carbazole group on the vinyl chain of this polymer may confer special steric effects and modify the conformational behavior.

The present study has been concerned with the fractionation of poly-N-vinylcarbazole and a study of the characteristics of the fractions, in a wide molecular weight range of 10000–500000, by techniques of viscometry, light scattering, osmometry and gel permeation chromatography (g.p.c.). Viscosity molecular weight data obtained in different solvents have been used to evaluate the viscosity molecular weight relationships and unperturbed dimension of the PVK chain. Also, interaction of the polymer in solution has been interpreted in terms of the current theories of the polymer solutions.

EXPERIMENTAL

Materials

Poly-N-vinylcarbazole (PVK) was obtained from Dr D. R. Wilson of this

laboratory. The polymer was prepared by polymerizing a 25% (w/v) vinyl-carbazole solution in benzene at 85°C for 24 h using azo*bis*isobutyronitrile (0·3% of monomer) as initiator. High purity vinylcarbazole was obtained by precipitating commercial vinylcarbazole from methanol followed by further purification by sublimation. This polymer had a molecular weight (M_w) of 162 000 and a polydispersity (M_w/M_n) of 3·8. Fractions of this polymer were obtained by stepwise precipitation at room temperature from 1% benzene solution using methanol as precipitant. The precipitated fractions were redissolved in benzene and isolated in the presence of excess methanol in a Waring blender. The individual fractions were then dried in vacuum at 60°C for 18 h. Eleven fractions (labelled 1–11) were obtained and used in the present study.

All solutions were made in Baker Reagent or Spectra Grade solvents.

Characterization

(a) *Gel permeation chromatography.* The Waters, Model 200, gel permeation chromatograph was used for characterizing the molecular weight distribution of the fractions with tetrahydrofuran (THF) as solvent. The instrument was operated at the ambient temperature. Columns used were inert cross-linked polystyrene gels with pore sizes of 10^5 nm (10^6Å), 3×10^4 nm, 10^3 nm and 10^2 nm. A plate count using 1% toluene/THF (v/v), showed 950 plates/ft ($\sim$3 170 plates/m). The elution volume was 1 ml/min. The instrument was calibrated using Pressure Chemical standard polystyrenes ranging in molecular weights from 5×10^3 to 1×10^6. Each sample was injected at a 1/4%w/v concentration. All solutions before injection were filtered with a 0·45 μm α-metricel Gelman membrane to eliminate gel and other debris which might decrease the column efficiency.

(b) *Viscometry.* Dilute solution viscosities were measured in five solvents: benzene, chloroform, tetrachloroethane, cyclohexanone and tetrahydrofuran using Cannon-Ubbelohde viscometers for which kinetic energy corrections were negligible. All solutions were filtered through a 0·45μm α-metricel Gelman filter and viscosity data measured at $25 \pm 0·01$°C, were used to evaluate the intrinsic viscosities by means of the Huggins relationship:

$$\eta_{sp}/c = [\eta] + k'[\eta]^2 c \qquad (1)$$

where k' is the Huggins coefficient and $[\eta]$ is the intrinsic viscosity.

(c) *Light Scattering:* Weight-average molecular weights were obtained from light scattering measurements at 25°C using a Sofica photometer. Scattered light intensities were measured at a wavelength of 546·1nm (5461Å) and at angles 45°, 90° and 135° to the incident beam. All solutions were made using spectral grade benzene and each sample was filtered through a 0·20 μm α-metricel Gelman filter to eliminate any gel or debris present in the solution. Molecular weights were computed by Debye's dissymmetry method[5].

The dn/dc measurements were made on a Brice-Phoenix differential refractometer at the wavelengths of 546·1nm and 436·1nm, with benzene, chloroform, tetrahydrofuran and tetrachloroethane as solvents. Potassium chloride, sucrose and polystyrene solutions were used to obtain the calibration constant. The dn/dc values obtained for PVK in four solvents are shown in *Table 1*.

Table 1 Values of dn/dc in different solvents at 25 °C

Solvent	546·1 *nm*	436·1 *nm*
Benzene	0·190	0·210
Chloroform	0·232	0·268
Tetrahydrofuran	0·262	0·282
Tetrachloroethane	0·185	0·214

(d) *Osmometry.* A Hewlett-Packard 502 High Speed Membrane Osmometer was used for the determination of number average molecular weights. Osmotic pressures were measured at 37°C in reagent grade chlorobenzene. Gel Cellophane membranes (450-D and 600-D) obtained from Arro Labs were conditioned to the solvent and used to give reliable osmotic data for each fraction.

Permeation was not detected and osmotic pressures were completely reproducible. The number average molecular weights were obtained by use of the relationship:

$$\pi/c = RT/M_n + A_2 c \tag{2}$$

where π is the osmotic pressure and A_2 is the virial coefficient of polymer-solvent interaction.

RESULTS AND DISCUSSION

Characteristics of the Fractions

The molecular weights of the fractions measured by light scattering and membrane osmometry are recorded in *Table 2*. M_w values cover a wide range of molecular weight, 7900 – 443000. The molecular weight distribution of the fractions as expressed by M_w/M_n ranged betweeen 1·1–1·2, suggesting that fractionation was efficient resulting in fractions of narrow distribution. The integral distribution of PVK is shown in *Figure 1*. The polydispersity values obtained by gel permeation chromatography were higher and varied between 1·2–1·4. Efficiency of column elution and resolution was explained by earlier workers as the source of increased polydispersity from g.p.c.[6,7]

Intrinsic viscosities of the fractions measured in five solvents at 25°C are shown in *Table 3*. The viscosities increased in the order of cyclohexanone < benzene < tetrahydrofuran < chloroform < tetrachloroethane. For a fifty-fold increase in molecular weight in the range of 7900 – 443000, the viscosity increase in the best solvent, tetrachloroethane was observed to be ten-fold.

167

For the fraction (M_w=443000), a [η] value of 0·925 dl g^{-1} was observed in tetrachloroethane as compared to a value of 0·595 dl g^{-1} in benzene. Values of Huggins coefficient generally varied within the usual range of 0·3–0·5.

Table 2 Molecular weights and polydispersity of PVK fractions

Fraction	$\bar{M}_w$	$\bar{M}_n$	$\dfrac{\bar{M}_w}{\bar{M}_n}$	$\dfrac{\bar{M}_w}{\bar{M}_n}$ (g.p.c.)
1	442900	358000	1·2	1·4
2	285700	242100	1·2	1·4
3	166700	161400	1·1	1·4
4	137500	134500	1·1	1·4
5	110500	96850	1·1	1·3
6	85800	78100	1·1	1·3
7	61300	53800	1·1	1·3
8	36900	33100	1·1	1·3
9	20400	18900	1·1	1·2
10	13100	11900	1·1	1·2
11	7880	7200	1·1	1·2
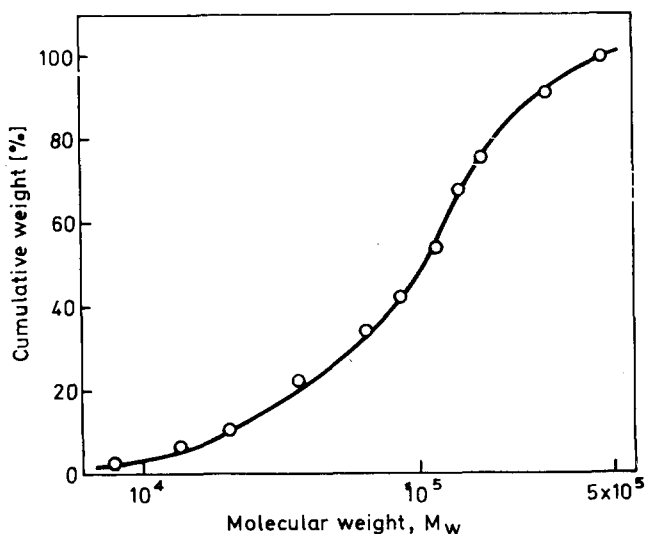
Figure 1 Integral distribution curve for PVK

Intrinsic viscosity: molecular weight relationships

The intrinsic viscosity is a measure of the hydrodynamic volume of a polymer in solution, and, therefore, increases with molecular weight. The variation of intrinsic viscosity with molecular weight expressed by the Mark-Howinck relationship[8]

$$[\eta] = KM^a \tag{3}$$

168

where the exponent, a is a measure of the chain extension which is influenced by the permeability of the molecular chain to solvent and its configuration. For many synthetic polymers a varies between 0·5–0·8. However, when a polymer acquires a highly extended configuration higher values of a may be obtained and for rigid rods, it approaches a value of 2. A typical Mark-Howinck plot for PVK in TCE is shown in *Figure 1*. The K and a values for

Table 3 Intrinsic viscosities of PVK fractions at 25 C

Fraction	$\bar{M}_w$	$[\eta] [dl\,g^{-1}]$				
		Benzene	Chloroform	Tetrachloro-ethane	Tetrahydro-furan	Cyclo-hexanone
1	442 900	0·595	0·868	0·925	0·740	0·550
2	285 700	0·426	0·546	0·625	0·490	0·418
3	166 700	0·359	0·451	0·503	0·396	0·305
4	137 500	0·310	0·390	0·429	0·345	0·290
5	110 500	0·255	0·321	0·350	0·285	0·235
6	85 800	0·222	0·258	0·297	0·218	0·202
7	61 300	0·177	0·223	0·261	0·192	0·153
8	36 900	0·125	0·165	0·176	0·130	0·110
9	20 400	0·090	—	0·116	0·095	0·075
10	13 100	0·075	—	—	0·076	—
11	7 880	0·073	—	—	—	—
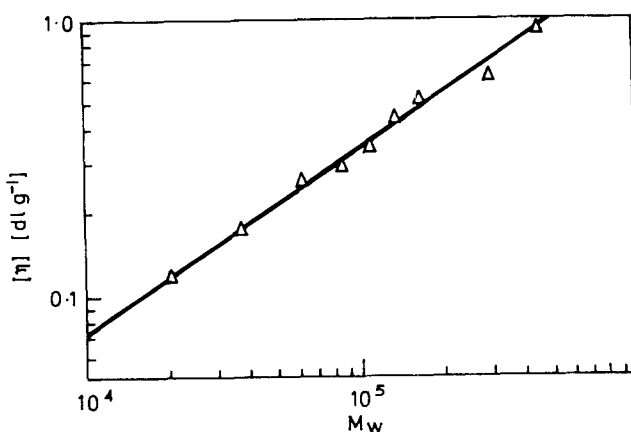
Figure 2 Intrinsic viscosity versus molecular weight ($\bar{M}_w$) for PVK in tetrachloroethane at 25°C

PVK fractions in different solvents are presented in *Table* 4. The lowest values of a in benzene and cyclohexanone suggest that these are poor solvents for PVK. Although benzene is a poor solvent for PVK, it was found to be a good solvent for polystyrene[9-11] with an exponent of 0·74. The K and a values for benzene agree well with those obtained by Ueberreiter and Springer[12]. The exponent has a maximum value of 0·68 in TCE which suggests that this is the

best solvent for PVK. The Mark-Howinck exponents fall within the range of 0·5–0·8. This indicates that the polymer conforms to a random coil configuration in these solvents.

Analysis of g.p.c. data

A universal calibration method of interpreting g.p.c. data was suggested by Benoit and coworkers[13]. In this treatment it was proposed that $[\eta]M_w$, which is a measure of the hydrodynamic volume, governs the retention in the chromatographic column. The Flory relation given below in equation (3), on

Table 4 K and a values in $[\eta] = KM^a$ at 25°C

Solvent	$K(\times 10^4)$	a
Benzene	3·05	0·58
Cyclohexanone	2·00	0·61
Tetrahydrofuran	1·44	0·65
Chloroform	1·36	0·67
Tetrachloroethane	1·29	0·68
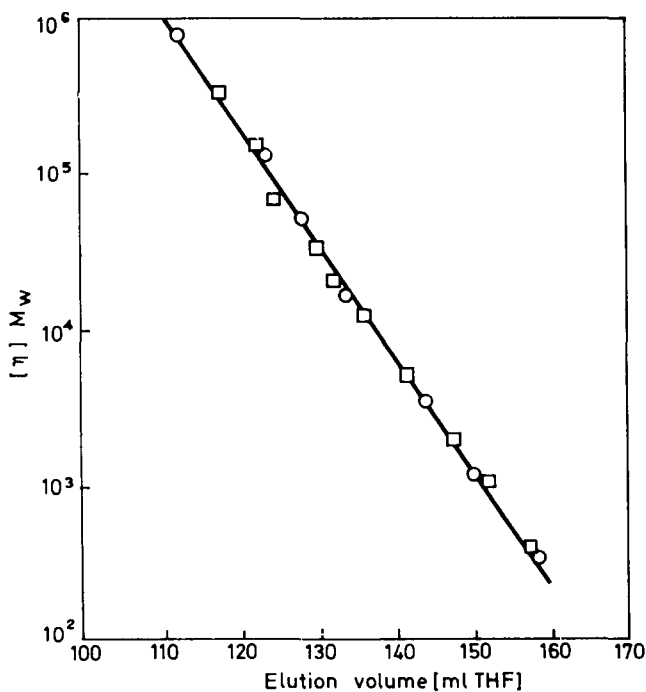
Figure 3 $[\eta]$ $\bar{M}_w$ versus elution volume for PVK and polystyrene; □, PVK; ○, polystyrene

170

which Benoit's proposal is based, is applicable for random coil polymers which yield Mark-Howinck exponents of 0·5–0·8. In the present work it is shown that the exponents for PVK fall in this range. Intrinsic viscosities of PVK obtained in THF have been used to obtain $[\eta]M_w$ values. A plot of $[\eta]M_w$ versus elution volume (e.v.) is shown in *Figure 3*. Also $[\eta]M_w$ data for a series of narrow distribution polystyrenes are plotted on the same graph. It may be noted that good correlation has been obtained for these polymers. *Figure 3* may be conveniently used for obtaining PVK molecular weight from $[\eta]$ and e.v. values.

GPC data have also been analyzed by the method of Meyerhoff[14]. However, the plots of log M or $(\bar{R}^2)^{1/2}$ or $M^{1/2}[\eta]^{1/3}$ vs elution volume showed a linear relation for each polymer series but no universal calibration graph was obtained. Therefore, it is concluded that Benoits' technique is superior to the method of calibration described by Meyerhoff.

Molecular dimension

The end-to-end length $(\bar{R}^2)^{1/2}$ may be obtained by the use of the Flory relationship[8]:

$$[\eta] = \Phi \, (\bar{R}^2)^{3/2}/M \qquad (4)$$

for flexible random coil polymers in solution. Ptitsyn and Eizner[15], in their discussion of excluded volume effects of polymer solutions, suggested a method for the use of the right Φ value in equation (4) for each solvent to get the molecular dimension. This is based on the use of the Mark-Howinck exponent as follows:

$$\Phi' = 2·87 \times 10^{21}(1 - 2·63 \, \epsilon + 2·86 \, \epsilon^2) \; [\text{dl cm}^{-3}\text{mole}^{-1}]$$

where $\epsilon = (2a - 1)/3$ and Φ' is the corrected Φ for excluded volume effects.

Double logarithmic plots of $(\bar{R}^2)^{1/2}$ versus M for PVK in benzene and tetrachloroethane are shown in *Figure 5*. The following $(\bar{R}^2)^{1/2}$ versus M relationships at 25°C have been obtained for PVK.

$$(\bar{R}^2)^{1/2} = 0·703 \, M^{0·515} \text{ for benzene} \qquad (5)$$

$$= 0·814 \, M^{0·536} \text{ for tetrahydrofuran} \qquad (6)$$

$$= 0·493 \, M^{0·541} \text{ for chloroform} \qquad (7)$$

$$= 0·912 \, M^{0·554} \text{ for tetrachloroethane} \qquad (8)$$

The dimensions were found to be practically identical in benzene and cyclohexanone and therefore, the $(\bar{R}^2)^{1/2}$ versus M relationship for benzene has been found applicable to cyclohexanone. The exponent of 0·515 for benzene and 0·554 for tetrachloroethane suggest that the former is a poor solvent and the latter a good solvent for PVK. The molecular dimensions of PVK in benzene determined by light scattering by Ueberreiter and Springer[12] compare well with ±10% of our values. This can be considered to be good agreement when the uncertainties in the two methods are examined.
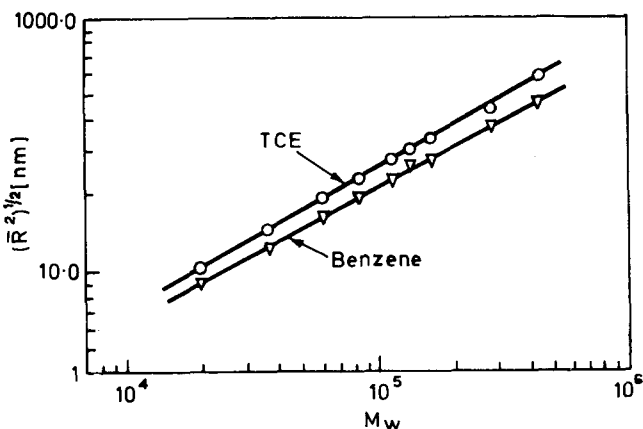
Figure 4 $(\bar{R}^2)^{1/2}$ versus $\bar{M}_w$ for PVK in benzene and TCE at 25°C
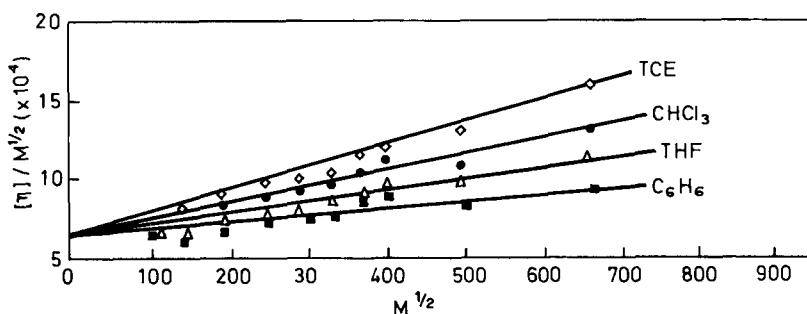
Figure 5 Stockmayer and Fixman graph for K_0 evaluation

Evaluation of unperturbed dimensions

In the Flory-Fox theory[8,16,17] the intrinsic viscosity is related to the molecular weight by

$$[\eta] = \Phi \, (\bar{R}_0^2/M)^{3/2} \, M^{1/2} a^3 \tag{9}$$

where $\bar{R}_0^2$ is the mean square end-to-end length in the unperturbed state and α is the expansion factor which arises due to polymer–solvent interactions. Since $\bar{R}_0^2/M$ is generally independent of molecular weight, equation (9) may be written as:

$$[\eta] = K_0 M^{1/2} a^3 \tag{10}$$

where K_0 is a constant independent of polymer molecular weight and solvent. The determination of unperturbed dimension, therefore, involves evaluation of K_0. Among the methods for obtaining K_0 from intrinsic viscosity/molecular weight data, the graphical procedures described by Flory, Fox and Schaefgen (F.F.S.)[18,19], Kurata and Stockmayer (K.S.)[21], and Stockmayer and Fixman

172

(S.F.)[22] are usually employed. However, the F.F.S. method was found inadequate in good solvents[20,21]. The K.S. and S.F. methods were observed to give the same K_0 value and were equally applicable for good and poor solvents [21,23]. The S.F. method is more attractive because of its simplicity. Further, Cowie[24] has shown that this method gives reliable K_0 values when the molecular weights of the fractions are $< 1 \times 10^6$ and the Mark-Howinck exponent is < 0.7. These considerations apply in the present work and therefore the Stockmayer-Fixman relation

$$\frac{[\eta]}{M^{1/2}} = K_0 + 0.51 \quad \Phi_0 B M^{1/2} \tag{11}$$

was employed. From the graphs of $[\eta]/M^{1/2}$ versus $M^{1/2}$ (*Figure 5*) a K_0 value of $6.8 \pm 0.2 \times 10^{-4}$ was obtained as the ordinate intercept. Using this result, a value of 6.19×10^{-9} was obtained for $(\bar{R}^2_0/M)^{1/2}$.

The conformational parameter of PVK chain

This parameter, σ, is defined as:

$$\sigma^2 = (\bar{R}_0{}^2)/(\bar{R}^2_{0f}) \tag{12}$$

where $\bar{R}^2_{0f}$ is the mean square end-to-end distance of a hypothetical chain with free internal rotation. The conformational factor, σ, has been computed as 2.82 for PVK. This value is much higher than 2.2 ± 0.2 recorded for polystyrene and lower than 3.1 reported for poly-2-vinylnaphthalene. This suggests that the bulky carbazole group exerts a steric effect which results in considerable hindrance to the free rotation of PVK chain .

Molecular expansion of PVK

Having obtained a proper value of K_0 (6.8×10^{-4}) in equation (10) the values of the expansion factor, α, were computed on the basis of the relationship suggested by Kurata and Yamakawa[27]:

$$[\eta] = K_0 M^{1/2} \alpha^{2.43} \tag{13}$$

This is, in fact, a modification of the Flory equation (9) and takes into consideration the non-Gaussian character of the chains with excluded volume.

The α-values were used to interpret the molecular expansion on the basis of the Flory relation

$$\alpha^5 - \alpha^3 = 2c_M \left(\tfrac{1}{2} - \chi\right) M^{1/2} \tag{14}$$

Linear plots of $(\alpha^5 - \alpha^3)$ versus $M^{1/2}$ in *Figure 6* do not pass through the origin, but give an abscissa intercept of 6 000 molecular weight. This anomalous result is due to the fact that the Flory theory, as noted by Kurata and Stockmayer[21], does not rigorously estimate the excluded volume effects of polymers in solution.

The molecular expansion was also interpreted in terms of the Kurata,
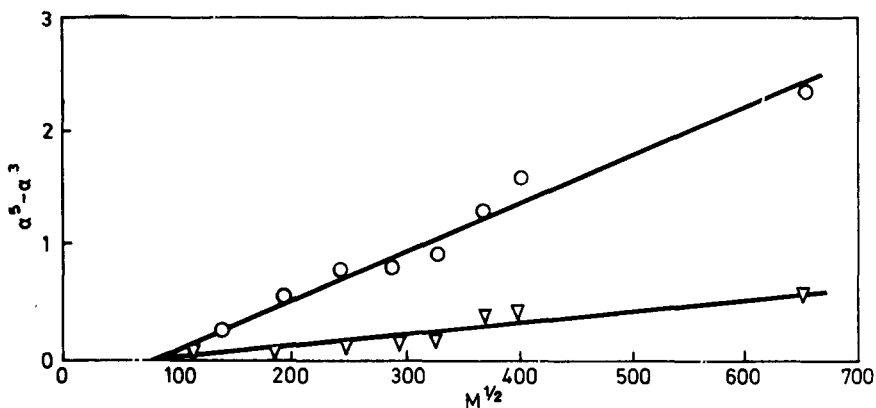
Figure 6 $(a^5 - a^3)$ versus $M^{1/2}$ graph according to Flory
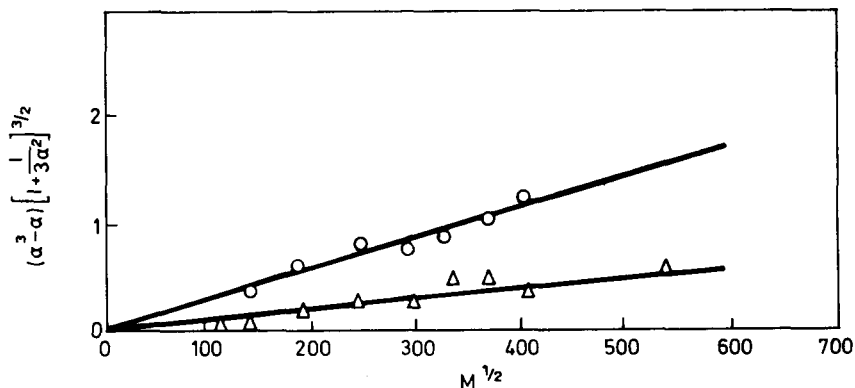
Figure 7 $(a^3 - a)\left[1 + \dfrac{1}{3a^2}\right]^{3/2}$ versus $M^{1/2}$ in K.S.R. treatment; $\bigcirc$, TCE; $\triangle$, benzene

Stockmayer and Roig theory of excluded volume effect in which this relation is given:

$$\frac{a^3 - \alpha}{N^{1/2}} = \frac{1}{(1 + 1/3a^2)^{3/2}} \left(\frac{4}{3}\right)^{5/2} \left(\frac{3}{2\pi}\right) \left(\frac{\beta}{b^3}\right) \tag{15}$$

where b is the effective bond length, β is the binary cluster integral and N is the number of segments in the polymer chain. As seen from *Figure 7*, linear graphs passing through the origin were obtained when interpreted in terms of equation (15). This indicates that the molecular expansion of PVK agrees with the K.S.R. theory.

CONCLUSIONS

(1) Benzene and cyclohexanone are thermodynamically poor solvents for poly-n-vinylcarbazole and tetrachloroethane is the best solvent. The value

of 0·58 for benzene obtained for the Mark-Howinck exponent a is identical with that obtained by Ueberreiter and Springer. The a value was found to be higher in other solvents and a maximum value of 0·68 was obtained in tetrachloroethane.

(2) The universal calibration technique based on hydrodynamic volume, used for interpreting gel permeation data, may be used to predict PVK molecular weights.

(3) The unperturbed dimension of PVK corresponds to a $(\bar{R}_0{}^2/M)^{1/2}$ value of $6\cdot19 \times 10^{-9}$.

(4) The steric factor of 2·8 for PVK suggests that considerable hindrance to free rotation is exerted by the carbazole group. This value is much higher than 2·2 for polystyrene.

(5) The molecular expansion conforms to the excluded volume treatment of Kurata, Stockmayer and Roig.

Xerox Research Laboratories,
800 Phillips Road, W-114
Webster, New York 14580

REFERENCES

1 Hoegl, H., Sus, O. and Neugebauer, W. *German Patent* 1957, 1068, 115
2 Hoegl, H., *J. Phys. Chem.* 1965, **69**, 755
3 Lardon, M., Lell-Doller, E. and Weigl, J. W. *Molecular Crystals* 1967, **2**, 241
4 Hermann, A. M. and Rembaum, A. *J. Polym. Sci. (C)* 1967, **17**, 107
5 Stacey, K. A. 'Light-scattering in physical chemistry', Butterworths, London, 1956, pp 27–34
6 Brierly-Jones, K. E., Patel, J. M. and Peaker, F. W. Third international g.p.c. seminar, Geneva, May, 1966
7 Alliet, D. F. and Pacco, J. M., Sixth international g.p.c. seminar, Florida, October, 1968
8 Flory, P. J. 'Principles of polymer chemistry', Cornell University Press, Ithaca, New York 1953
9 Krigbaum, W. R. and Flory, P. J. *J. Polym. Sci.* 1953, **11**, 37
10 Orfino, T. A. and Wenger, F. *J. Phys Chem.*, 1963, **67**, 566
11 Natta, G., Danusso, F. and Moraglio, G. *Makromol. Chem.* 1956, **20**, 37
12 Ueberreiter, K. and Springer, J. *Z. Phys. Chem. (Leipzig)* 1963, **36**, 299
13 Grubisic, Z., Remp, P. and Benoit, H. *J. Polym. Sci. (B)*, 1967, **5**, 753
14 Meyerhoff, G. *Makromol. Chem.* 1965, **89**, 282
15 Ptitsyn, O. B. and Eizner, Y. E. *Soviet Phys. (English Translation)* 1960, **4**, 1020
16 Flory, P. J. *J. Phys. Chem.* 1949, **17**, 303
17 Fox, T. G. Jr. and Flory, P. J. *J. Amer. Chem. Soc.* 1951, **73**, 1909
18 Flory, P. J. and Fox, T. G. Jr. *J. Amer. Chem. Soc.* 1951, **73**, 1904
19 Schaefgen, J. R. and Flory, P. J. *J. Amer. Chem. Soc.* 1948, **70**, 2709
20 Chinai, S. N. and Samuels, R. J. *J. Polym. Sci.* 1956, **19**, 463

21 Kurata, M. and Stockmayer, W. H. *Fortschr. Hochpolymer Forsch.* 1963, **3**, 196
22 Stockmayer, W. H. and Fixman, M. *J. Polym. Sci. (C)* 1963, **1**, 137
23 Sitaramaiah, G. *J. Polym. Sci., (A)* 1965, **3**, 2743
24 Cowie, J. M. G. *Polymer, Lond.* 1966, **7**, 487
25 Bandrup, J. and Immergut, E. H. *Polymer Handbook* Interscience Publishers, 1965
26 Kurata, M. and Yamakawa, H. *J. Chem. Phys.* 1958, **29**, 311
27 Kurata, M., Stockmayer, W. H. and Roig, A. *J. Chem. Phys.* 1960, **33** 151

The effect of ionizing radiation on the thermal properties of linear high polymers:
Part 1. Vinyl polymers

D. R. Gee and T. P. Melia

A differential scanning calorimeter has been used to measure the heat capacities (over the temperature range 200–500°K) of polyethylene single crystals and melt crystallized samples of polyethylene and isotactic polypropylene, which had been subjected to different doses (0–1000 Mrads) of cobalt-60 gamma radiation at 298°K and 425°K, respectively. Melting temperatures, heats and entropies of fusion of the irradiated samples are listed. Changes in these parameters with radiation dose are interpreted in terms of ordering processes in the liquid and solid phases, which result from the radiation induced formation of intermolecular crosslinks.

A NUMBER of techniques, such as infra-red[1, 2] and electron spin resonance spectroscopy[3], x-ray[4] and electron diffraction[5], gel permeation chromatography[6], volume dilatometry[7], and viscometry[8], have been used to assess the changes produced in vinyl polymers by ionizing radiation, but few[9, 10] calorimetric studies have been reported. In this work we present the results of heat capacity measurements (over the temperature range 200°K to 500°K) on polyethylene single crystals and melt crystallized samples of polyethylene and isotactic polypropylene, which had been irradiated with gamma rays. These experiments had as their initial aim the assessment of the effect of gamma radiation on the thermal properties of vinyl polymers and as their ultimate aim the provision of a more profound understanding of the nature of the crosslinking processes which radiation induces.

EXPERIMENTAL

Material

The linear polyethylene sample (coded 337/173) was supplied by Dr G. Boocock of the Shell Chemical Company Ltd, Carrington, Manchester, England. Prior to use it was melted, annealed *in vacuo* at 408°K for 48h and then slowly cooled (5°K/h) to room temperature. The annealed sample had a density of $0.978 \pm 0.001 \, \mathrm{g \, cm^{-3}}$, a melt flow index of $31 \, \mathrm{mg \, min^{-1}}$ and an intrinsic viscosity of $2.0 \, \mathrm{dl \, g^{-1}}$. Gel permeation chromatography analysis on the annealed sample yielded the values $\bar{M}_w = 1.38 \times 10^5$ and $\bar{M}_n = 2.33 \times 10^4$. Infra-red analysis[11] showed that the degree of chain branching

178

was less than 0·1%, A weight fraction crystallinity of 0·88 was estimated from the density using the values 0·999 ± 0·001 and 0·853 ± 0·002 gcm^{-3} for the density of crystalline[12] and amorphous[13] polyethylene, respectively.

Single crystals of polyethylene were prepared as follows[14, 15]. A 0·1% solution of the linear polyethylene in p-xylene was refluxed for 2h, cooled to 348°K and allowed to stand for a further 2h at this temperature. During this time crystallization occurred. The crystal suspension was heated at 10°K/h to 373°K and maintained at this temperature for 30 min. The clear solution was placed in a thermostat at 348°K and allowed to stand for 16h. It was then cooled to room temperature and stored for several days. The crystals were removed by filtration, washed with ether and dried *in vacuo*. Microscopic examination with a Gillett and Sibert microscope (Type M36690) showed the crystals to be well defined and of uniform size. The dry crystals had a density of 0·973 ± 0·001 gcm^{-3}.

The isotactic polypropylene sample (coded 128/64) was kindly given by Dr G. Boocock (Shell Chemical Company). Prior to use atactic polymer was removed by Soxhlet extraction with n-heptane. The polymer was then melted, annealed *in vacuo* at 435°K for 48h and slowly cooled (5°K/h) to room temperature. The sample had a melt flow index of 50 mg min^{-1} and on combustion 0·02% ash remained. The intrinsic viscosity measured in tetralin at 408°K was 1·205 dl g^{-1}. This was used to calculate the viscosity average molecular weight[16]. The value obtained is 135000 ± 1000. Infra-red[17] and n.m.r.[18] analysis showed no evidence for atactic or syndiotactic sequences. The sample had a density[19] of 0·898 ± 0·001 gcm^{-3}. Assuming a unit cell density[20] of 0·935 ± 0·002 g cm^{-3} and a value of 0·853 ± 0·001 g cm^{-3} for the density of the amorphous phase[20], a value of 0·58 was calculated for the weight fraction crystallinity.

Sample irradiation

Samples were irradiated in the 10000 curie cobalt-60 gamma radiation source (Nuclear Engineering Ltd, Model N.E.L.9) at the University of Salford. Prior to irradiation the samples were placed in glass tubes, evacuated to a pressure of 0·13 N m^{-2} and then sealed. These tubes were placed in a thermostat, situated near to the source, whose temperature could be controlled to ±0·5°K. The gamma ray intensity was measured with a ferrous-cupric dosimeter[21].

Calorimetry

The differential scanning calorimeter[22] (DSC) used in the heat capacity and heat of fusion measurements has been described previously.

Density measurements

Sample densities at 298°K were measured by a flotation method using ethanol–water mixtures[19].

Molecular weight measurements

Molecular weight determinations were carried out using a gel permeation chromatograph (Model 100) supplied by Waters Associates[23]. o-Dichlorobenzene was the solvent and a column temperature of 401 °K was employed. Calibration was effected with narrow molecular weight distribution polystyrene samples[24].

RESULTS

Molecular weight distribution curves for both the original and irradiated (25 Mrads) solution and melt-crystallized polyethylene samples were obtained by gel permeation chromatography. For the solution-crystallized polyethylene no marked difference in molecular weight distribution is observed at doses up to 25 Mrads. The cumulative distribution curves for the melt-crystallized polyethylene samples are presented in *Figure 1*. At doses above 25 Mrads insufficient polymer could be dissolved in p-xylene to make molecular weight distribution studies above this dose worthwhile.
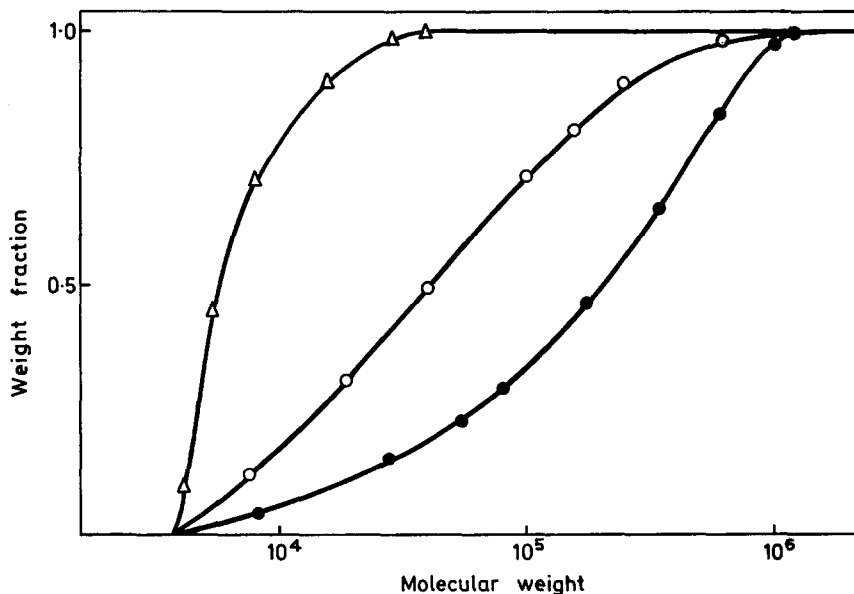
Figure 1 Cumulative molecular weight distribution plots for melt-crystallized polyethylene. ○, original sample; ●, sample irradiated with a dose of 25 Mrads at 298 °K; △, sample irradiated with a dose of 25 Mrads at 425 °K

Typical heat capacity/temperature curves for the three polymer samples after irradiation with gamma radiation at 298 °K and 425 °K (melt-crystallized polyethylene only at this temperature) are presented in *Figure 2*. Detailed results are given in *Tables 1–6*. In deriving the enthalpy and entropy values given in columns 5 and 7 of these tables the assumption was made that the
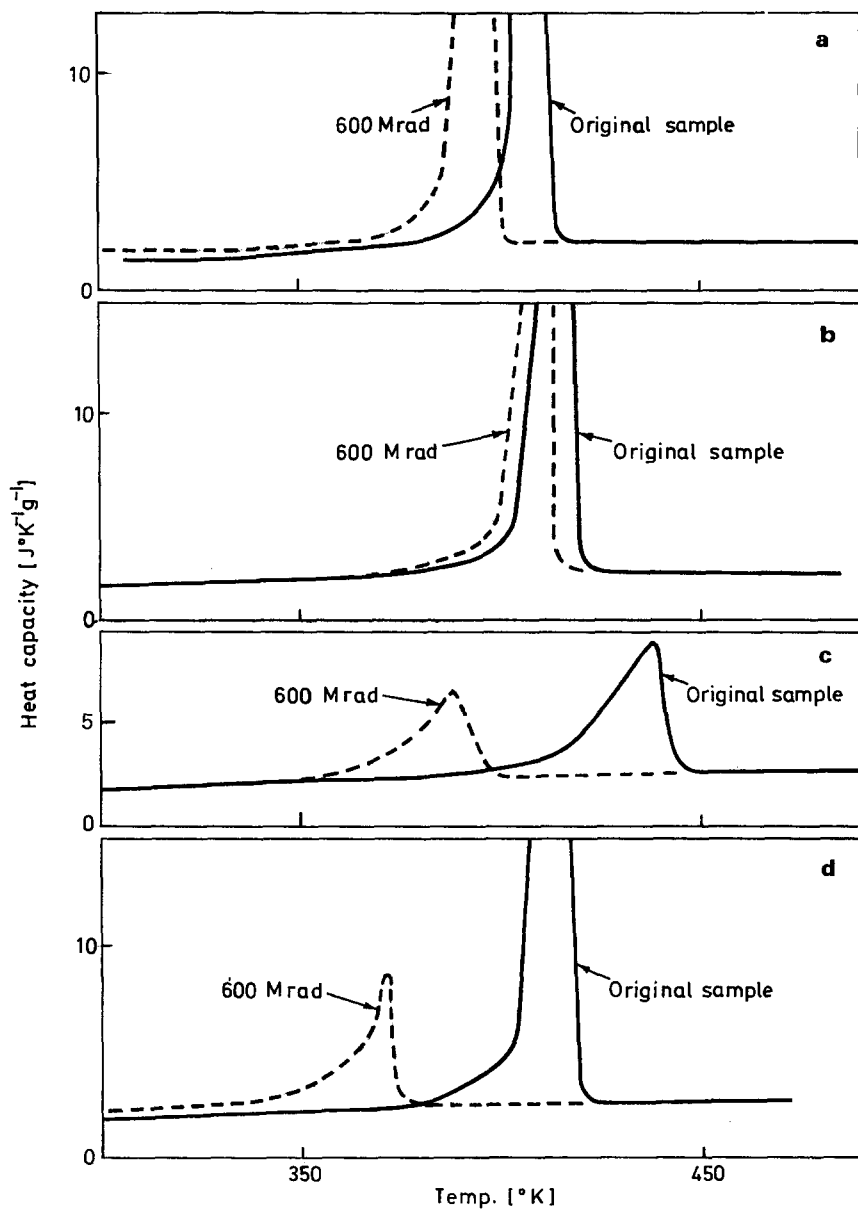
Figure 2 Typical heat capacity *versus* temperature curves for irradiated polymers.
    (a) Polyethylene single crystals after irradiation at 298°K;
    (b) Melt-crystallized polyethylene after irradiation at 298°K;
    (c) Melt-crystallized isotactic polypropylene after irradiation at 298°K;
    (d) Melt-crystallized polyethylene after irradiation at 425°K

heat capacities of the irradiated samples were identical with those of the unirradiated polymer below 200°K. This assumption has been justified previously[25]. The enthalpy and entropy of fusion values given in the tables were calculated from the heat capacity results using equations 6 and 7 of reference 26. The data of Wunderlich[27], for polyethylene single crystals, Broadhurst[28], for crystalline and amorphous polyethylene, and Gee and Melia[29], for crystalline and amorphous isotactic polypropylene were used to evaluate the integrals which appear in these equations.

DISCUSSION

The general expression of Lyons and Fox[30] for random crosslinking between polymer chains (equation 5 of reference 30) has been used to derive the relationship

$$\log \left[\frac{\{W_i\}_0}{s\{W_i\}_r} \right] = \frac{q_0 r Q A}{2 \cdot 303 \, m} \tag{1}$$

where $\{W_i\}_0$ and $\{W_i\}_r$ are the weight fractions of the molecules of the ith species at zero dose and dose r, respectively;

s is the weight fraction of polymer soluble in p-xylene after irradiation with a dose r;

q_0 is the crosslinking probability;

Q the molecular weight per micrometre length of polymer;

A is the chain length of the extended polymer;

and m is the molecular weight of the polymer repeat unit.

This equation forms the basis for the plots of *Figure 3* which were constructed from the data presented in *Figure 1*. The expected linear relationships between log $[\{W_i\}_0/s\{W_i\}_r]$ and A are found but in neither case does the line pass through the origin. The low value of the intercept (0·04) for the polyethylene sample irradiated at 425°K suggests that random crosslinking conditions were approached in this experiment. A possible explanation of the relatively high intercept value (0·64) obtained with the sample irradiated at 298°K is that end-linking of molecules[31, 32] is the predominant intermolecular bonding process induced by gamma radiation in melt crystallized polyethylene at these doses (25 Mrads). For the sample irradiated at 425°K the G value for the crosslinking reaction may be calculated from the data of *Figure 3* using the method of Lyons and Fox[30]. The value obtained $G = 2 \cdot 1 \pm 0 \cdot 2$ crosslinks per 100 eV compares with that of 2·0 $\pm$ 0·4 crosslinks per 100 eV calculated from swelling[33, 34] and solution measurements[2, 35].

During the irradiation of polyethylene single crystals both intermolecular and intramolecular crosslinking reactions may be induced[36]. Density measurements show that polyethylene single crystals have a considerable amorphous content[37]. Flory[38] suggests that this may be associated with slack chain folds at the crystal surface. Since it is well established that crosslinking reactions occur preferentially in the amorphous regions, it follows that the slack chain
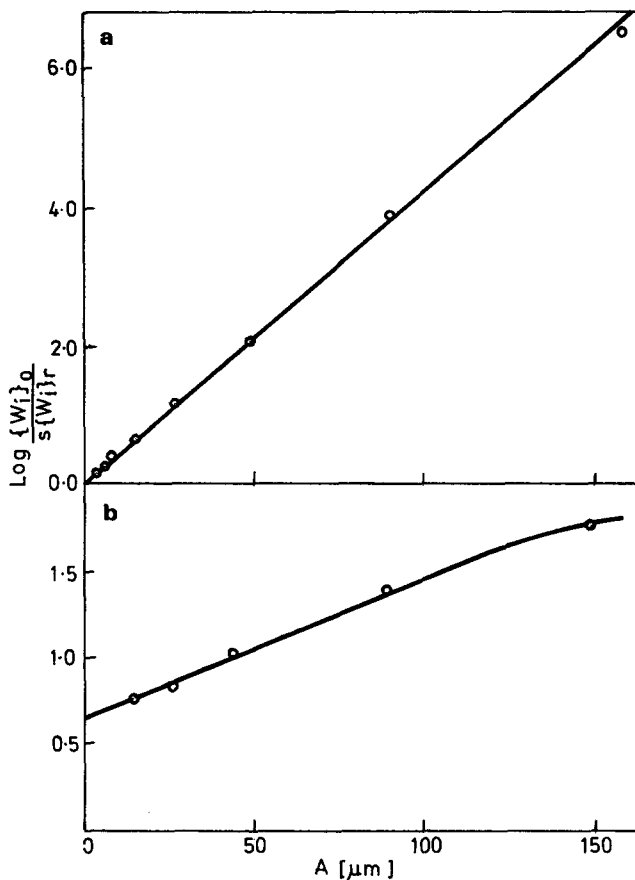
Figure 3 Plot of log $\left[\dfrac{\{W_i\}_0}{s\{W_i\}_r}\right]$ *versus* A [see equation (1)]:

(a) sample irradiated with a dose of 25 Mrads at 425° K;

(b) sample irradiated with a dose of 25 Mrads at 298° K

folds provide the most favourable sites for crosslinking. Kawai *et al*[39] have interpreted the gelation properties of irradiated polyethylene single crystals in terms of the predominance of intramolecular crosslinking at low doses followed by a progressive build-up of intermolecular crosslinks at higher doses.

The dose independence of the densities of irradiated polyethylene single crystals (*Table 1*) indicates that crosslinking has no significant effect on molecular order over the dose range studied in this work (0–1 000 Mrads). This fact, coupled with the dose independence of the entropy of fusion below 600 Mrads, suggests that at doses below this value crosslinking has little effect on liquid state order. Above this dose the entropy of fusion decreases rapidly indicating an increase in liquid state order.

A possible explanation of these results is that at doses below 600 Mrads intramolecular crosslinking between slack chain folds predominates and these do not alter the solid and liquid structures significantly. At doses above 600 Mrads intermolecular crosslinking becomes more important and these linkages prevent the breakdown of the lattice structure above the melting point. The decreased entropies of fusion observed reflect the increase in liquid order. Similarly, the decrease in the heats of fusion at higher dose levels reflects the restrictions on molecular motions imposed by these cross-links.

In the present heat capacity measurements in the differential scanning calorimeter the peak in the heat capacity versus temperature plot in the melting region has been taken as the melting point of the particular sample under investigation. For polyethylene single crystals the melting point first decreases with dose (*Table 1*) then, between 75 and 400 Mrads, no change occurs and, finally, at doses above 400 Mrads, a decrease in melting temperature with dose is observed. Comparable melting point depressions have been

Table 1 Thermodynamic properties of polyethylene single crystals irradiated at 298 °K

Dose [Mrads]	Density [g cm⁻³]	Weight fraction crystallinity	T_m [°K]	$H^0_{420} - H^0_0$ [J g⁻¹]	ΔH_f^* [J g⁻¹]	$S^0_{420} - S^0_0$ [J °K⁻¹ g⁻¹]	ΔS_f^* [J °K⁻¹ g⁻¹]
0	0·973	0·84	408	761·0	246·4	3·022	0·600
25	0·975	0·84	404	762·3	247·7	3·015	0·594
50	0·974	0·84	401	760·6	246·0	3·015	0·594
75	0·972	0·84	399	766·0	251·4	3·030	0·608
100	0·973	0·84	398	758·9	244·4	3·023	0·601
200	0·973	0·84	398	764·9	250·3	3·012	0·590
300	0·974	0·84	398	759·7	245·1	3·026	0·604
400	0·973	0·84	397	762·1	247·5	3·023	0·602
500	0·974	0·84	396	750·2	235·6	3·011	0·589
600	0·973	0·84	395	743·4	228·8	3·023	0·601
800	0·976	0·86	395	729·2	216·3	2·966	0·545
1000	0·978	0·88	391	724·4	214·5	2·936	0·414

observed with irradiated polyethylene single crystals by Salovey and Keller[40] and Bair et al[10]. In both cases heating rates of 5–10°K/min were employed. Salovey et al[40] studied the melting process in irradiated polyethylene single crystals over a period of seven days using a precision dilatometric technique. They found no change in melting temperature with dose, at low dose, provided heating rates sufficiently slow to allow the establishment of equilibrium during the dilatometric experiments were employed. It would thus appear that the fall in melting temperature with dose, at low dose, observed in this work is a direct result of the finite heating rate employed during the calorimetric measurements. This dependence of melting temperature on heating rate may be associated with changes in the surface free energy of the polymer crystals as a result of the presence of crosslinks between the slack folds on the crystal surface. Above doses of 75 Mrads the melting temperature/dose behaviour is that expected from the nature of the heat and entropy of fusion/dose relationship (*Table 1*).

The heat and entropy of fusion and melting temperature versus dose relationships (*Table 2*) for the irradiated samples after fusion and melt

Table 2 Thermodynamic properties of polyethylene single crystals after irradiation at 298°K fusion and melt crystallization

Dose [Mrads]	T_m [°K]	$H_{420}^0 - H_0^0$ [J g^{-1}]	ΔH_f^* [J g^{-1}]	$S_T^0 - S_0^0$ [J K^{-1} g^{-1}]	ΔS_f^* [J K^{-1} g^{-1}]
0	409	741·7	197·4	3·005	0·453
25	405	729·8	185·5	2·981	0·429
50	404	726·7	182·4	2·968	0·416
75	399	727·2	182·9	2·953	0·401
100	396	724·2	180·0	2·965	0·413
200	395	723·3	179·0	2·969	0·417
300	394	718·6	174·4	2·967	0·415
400	394	718·3	174·0	2·957	0·405
500	390	712·5	168·2	2·951	0·399
600	389	708·0	163·7	2·942	0·390
800	389	693·3	149·9	2·887	0·335
1 000	386	680·9	136·6	2·853	0·301

crystallization are of similar form, but not identical with, those of the original samples. The lower values observed probably result from crystallization difficulties associated with the presence of crosslinks.

Inspection of *Table 3* reveals that the entropy and enthalpy of fusion of the

Table 3 Thermodynamic properties of polyethylene irradiated at 298°K

Dose [Mrads]	Density [g cm^{-3}]	Weight fraction crystallinity	T_m [°K]	$H_{420}^0 - H_0^0$ [J g^{-1}]	ΔH_f^* [J g^{-1}]	$S_{420}^0 - S_0^0$ [J °K^{-1} g^{-1}]	ΔS_f^* [J °K^{-1} g^{-1}]
0	0·979	0·88	413	791·5	259·8	3·101	0·625
25	0·987	0·93	415	804·6	278·1	3·134	0·677
50	0·990	0·95	414	808·5	284·0	3·141	0·691
75	0·995	0·98	414	814·8	293·5	3·151	0·715
100	0·994	0·98	414	804·8	283·2	3·133	0·694
200	0·995	0·98	415	795·7	274·4	3·108	0·669
300	0·996	0·98	415	781·9	260·6	3·074	0·635
400	0·995	0·98	415	777·7	256·4	3·050	0·611
500	0·995	0·98	412	766·2	244·9	3·023	0·584
600	0·994	0·98	410	761·6	239·3	3·009	0·570
800	0·995	0·98	406	720·5	199·2	2·948	0·509
1 000	0·995	0·98	398	710·5	189·2	2·925	0·486

semi-crystalline, melt-crystallized polyethylene, irradiated at 298°K, increase with dose up to 75 Mrads and then begin to decrease. A clue to the probable cause of this behaviour is provided by the density data shown in the same table. The sample density increases with dose up to 75 Mrads, above which it remains constant at 0·995 gcm^{-3}. This value approaches that of a com-

185

pletely crystalline polyethylene[2] (0·999 g cm^{-3}). This suggests that molecular order in the solid state is increased by irradiation with gamma rays up to a dose of 75 Mrads, but after this point little further change is possible. Such an increase in molecular order in the solid phase would account for the increased heat and entropy of fusion provided the effect was not compensated for by an equivalent increase in order in the liquid phase. Above 75 Mrads the density of intermolecular crosslinks increases and, although this has little effect on the order in the solid phase, these impose restraints on the polymer molecules in the liquid phase which are reflected in the decreased heats and entropies of fusion. This interpretation is supported by the density data of Charlesby and Ross[7] which reveal a decrease in the liquid phase density with dose for samples of melt crystallized polyethylene irradiated below the melting temperature.

Table 4 Thermodynamic properties of polyethylene irradiated at 425°K

Dose [Mrads]	T_m [°K]	$H^0_{420} - H^0_0$ [J g^{-1}]	ΔH_f^* [J g^{-1}]	$S^0_{420} - S^0_0$ [J °K^{-1} g^{-1}]	ΔS_f^* [J °K^{-1} g^{-1}]
0	413	791·4	259·8	3·101	0·625
25	408	761·5	214·8	3·009	0·476
50	402	735·4	177·1	2·945	0·370
75	389	714·8	146·2	2·901	0·288
100	383	696·8	118·2	2·874	0·224
200	375	678·6	95·7	2·863	0·196
300	364	662·3	75·2	2·847	0·166
400	345	653·1	58·9	2·822	0·113
500	356	641·2	50·1	2·801	0·104
600	371	629·2	44·2	2·744	0·071

For the samples irradiated at 425°K a steady decrease of heat and entropy of fusion with dose is observed (*Table 4*). The explanation of this behaviour is as follows. Crosslinks introduced during irradiation of the liquid polymer at 425°K lead to the retention of some of the disorder characteristic of the liquid state when the polyethylene crystallizes. The extent of this effect will depend upon the density of crosslinks which in turn will depend upon the gamma radiation dose applied. Thus, a gradual decrease in the heat and entropy of fusion with dose would be expected. A melting point minimum is observed with these samples after irradiation with a dose of 450 Mrads. Charlesby[43] has reported similar behaviour with irradiated *n*-paraffins. He suggests that this dose corresponds to the point at which an infinite network of polymer chains is formed.

According to Flory[41] the melting point, T_m, of a network formed from randomly coiled chains is related to the fraction of crosslinked units, p, by the expression

$$\frac{T_m^0 - T_m}{T_m} = \frac{RT_m^0}{\Delta H_f} p \qquad (2)$$

where T_m^0 is the equilibrium melting temperature of the pure polymer, ΔH_f is its heat of fusion and R is the gas constant. For polyethylene samples irradiated at 425°K, with doses less than 450 Mrads, $(T_m^0 - T_m)/T_m$ is plotted against p in *Figure 4*. Values of p were calculated from the G value for cross-linking (2.1 ± 0.2 crosslinks per 100 eV) by assuming that there are 30 eV per ion pair and 1.51×10^{18} ion pairs/Mrad g[42]. The variation of p with
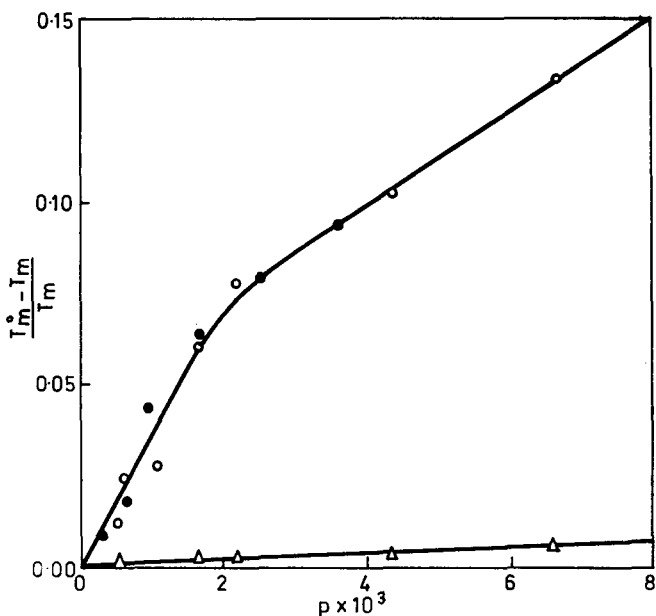
Figure 4 Plot of $\dfrac{T_m^0 - T_m}{T_m}$ *versus* p [equation (2)] for melt crystallized

polyethylene samples irradiated at 425°K:
○, this work; ● reference 42; △, predicted by equation (2)

$(T_m^0 - T_m)/T_m$ predicted by equation (2) is also shown in *Figure 4*. Comparison of these two plots reveals that the observed melting point depressions are many times greater than those predicted by equation (2). Since the melting point depressions observed in this work compare with those determined dilatometrically[42] it appears that equation (2) has limited validity when applied to real systems. Equation (2) is derived on the basis that crystallinity is allowed to develop in an ideal fashion in directions lateral to the chain direction; no imperfections are allowed and no restrictions are placed on the size of crystallites that develop[41]. However, Mandelkern *et al*[42, 43], using x-ray diffraction techniques, have shown that a decrease in crystallite size occurs after irradiation of polyethylene above its melting point. This suggests that the introduction of crosslinks by irradiation prevents the formation of the more perfect crystallites which are required by the Flory equilibrium melting theory[41]. The present results are consistent with this viewpoint.

The polymer formed by irradiation of highly crystalline polyethylene at

298°K approximates to a network of perfectly ordered polymer chains. Flory[41] and Mandelkern[42] have related the melting point of such a network to the number of crosslinks. This relationship may be expressed in the form

$$\frac{1}{T_m^0} - \frac{1}{T_m} = \frac{Rp}{\Delta H_f}\left(\frac{9}{4} - \frac{3}{4}\ln pK\right) \tag{3}$$

where K is the number of chemical repeat units that can be identified with a statistical element.

According to this equation the melting point of the network should be greater than that of the non-crosslinked polymer. Such an increase is observed with polyethylene at low doses (*Figure 5*). Although it is not possible to estimate accurately the fraction of units crosslinked from the plot of
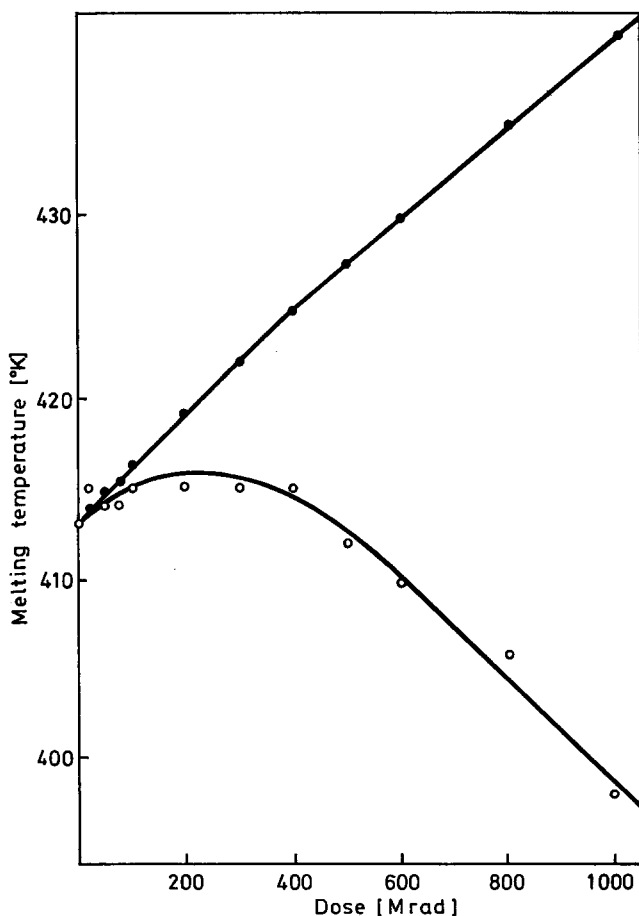
Figure 5 Melting temperature *versus* dose plots for melt-crystallized polyethylene samples irradiated at 298°K:
○, this work; ●, predicted by equation (3)

Figure 3 an estimate of this parameter may be made from recently published infra-red[31, 32] and solubility data[31] for a polyethylene sample having a crystallinity of 0·85. These data have been used in conjunction with equation (3) to construct the plot of *Figure 5*. Below 100 Mrads the observed and calculated melting points agree to within ±1°K. At higher doses the plots diverge. This may result from either a change in the fusion parameters or the introduction of crystal imperfections during the crosslinking process.

It has been shown[6, 8] that chain scission is the predominant radiation-induced change which occurs in isotactic polypropylene at doses less than 40 Mrads, whilst at higher doses the crosslinking reaction becomes more important. The irregular entropy and enthalpy of fusion/dose relationships observed (*Tables 5* and *6*) when isotactic polypropylene is irradiated with cobalt-60 gamma radiation at 298°K may be explained in terms of these two

Table 5 Thermodynamic properties of isotactic polypropylene irradiated at 298 K

Dose [Mrad]	Density [g cm^{-3}]	Weight fraction crystallinity	T_m [°K]	$H_{450}^0 - H_0^0$ [J g^{-1}]	ΔH_f^* [J g^{-1}]	$S_{450}^0 - S_0^0$ [J °K^{-1} g^{-1}]	ΔS_f^* [J°K^{-1} g^{-1}]
0	0·898	0·58	439	713·0	117·7	2·889	0·278
25	0·888	0·48	423	703·6	100·7	2·861	0·225
50	0·897	0·58	416	709·0	113·7	2·877	0·266
100	0·897	0·58	411	704·5	109·2	2·877	0·266
200	0·899	0·58	407	695·0	99·7	2·862	0·251
300	0·900	0·59	402	691·4	96·1	2·852	0·240
400	0·897	0·58	396	686·4	91·1	2·845	0·234
500	0·898	0·58	391	679·8	84·5	2·831	0·220
600	0·898	0·58	388	671·5	76·2	2·829	0·218
800	0·898	0·58	376	664·6	69·3	2·806	0·195
1 000	0·898	0·58	369	657·6	62·3	2·774	0·163

Table 6 Thermodynamic properties of isotactic polypropylene after irradiation at 298°K, fusion and melt crystallization

Dose [Mrad]	T_m [°K]	$H_{450}^0 - H_0^0$ [J g^{-1}]	ΔH_f^* [J g^{-1}]	$S_{450}^0 - S_0^0$ [J °K^{-1} g^{-1}]	ΔS_f^* [J °K^{-1} g^{-1}]
0	437	713·4	118·1	2·889	0·278
25	421	692·9	90·0	2·826	0·190
50	412	689·6	94·3	2·824	0·213
100	408	685·0	89·7	2·827	0·216
200	405	682·5	87·2	2·832	0·220
300	399	676·3	81·0	2·821	0·210
400	392	673·2	77·9	2·809	0·197
500	385	669·5	74·2	2·808	0·196
600	381	667·1	71·8	2·795	0·184
800	367	656·3	61·0	2·779	0·167
1 000	360	655·5	60·2	2·771	0·160

processes. The scission of polymer chains at low doses leads to a decrease, not only in the molecular weight, but also in the ordering of the polymer chains in the solid phase. This is reflected in the lower densities (*Tables 5* and *6*) and heats and entropies of fusion observed with samples irradiated with doses of 25 Mrads. Above 25 Mrads the crosslinking reaction predominates and the behaviour of the fusion parameters parallels that of melt crystallized polyethylene.

ACKNOWLEDGEMENTS

Department of Chemistry and Applied Chemistry
University of Salford

REFERENCES

1 Dole, M., Matsuo, H. and Williams, T. F. *J. Amer. Chem. Soc.* 1958, **80**, 2595
2 Charlesby, A. and Pinner, S. H. *Proc. Roy. Soc. (Lond.)* 1959, **A249**, 367
3 Iwasaki, M., Ichikawa, T. and Tomyama, K. *J. Polym. Sci. (B)* 1967, **5**, 423
4 Charlesby, A. *J. Polym. Sci.* 1953, **10**, 201
5 Karpov, V. L. and Zverev, B. I., 'Sbornik Rabotpo Radiatsionnoi Khim', Moscow, 1958
6 Lyon, B. J. and Fox, A. S. *J. Polym. Sci. (C)* 1968, **21**, 159
7 Charlesby, A. and Ross, M. *Proc. Roy. Soc. (Lond.)* 1953, **A217**, 122
8 Black, R. M. and Lyons, B. J. *Proc. Roy. Soc. (Lond.)* 1959, **A253**, 322
9 Dole, M. and Howard, W. H. *J. Phys. Chem.* 1957, **61**, 137
10 Bair, H. E., Salovey, R. and Huseby, T. W. *Polymer, Lond.* 1967, **8**, 9
11 Rugg, F. M., Smith, J. J. and Wartman, L. H. *J. Polym. Sci.* 1953, **9**, 1
12 Swann, P. R. *J. Polym. Sci.* 1962, **56**, 403
13 Grubler, M. G. and Kovacs, A. J. *J. Polym. Sci.* 1959, **34**, 551
14 Blackadder, D. A. and Lewell, P. A. *Polymer, Lond.* 1968, **9**, 249
15 Blundell, D. J. and Keller, A. *J. Polym. Sci. (B)* 1966, **4**, 481
16 Moraglio, G. *Chim. e. Ind. (Milan)* 1959, **41**, 879
17 Natta, G., Pasquon, I. *et al, Atti. Accad. Nazl. Lincei. Rend. Classe. Sci. Fis. Mat. Nat.* 1960, **28**, 539
18 Natta, G., Lombardi, E., Segre, A. L. and Zambelli, A. *Chim. e. Ind. (Milan)* 1965, **47**, 378
19 Jackson, J. B., Flory, P. J. and Chiang, R. *Trans. Faraday Soc.* 1963, **59**, 1906
20 Danusso, F. and Moraglio, G. *Chim. e. Ind. (Milan)* 1959, **41**, 748
21 Hart, E. J., Ramler, W. J. and Rocklin, S. R. *Radiation Res.* 1956, **4**, 378
22 O'Neill, M. J. *Anal. Chem.* 1964, **36**, 1238
    O'Neill, M. J., Justin, J. and Brenner, N. *Anal. Chem.* 1964, **36**, 1233
23 Maley, L. E. *J. Polym. Sci. (C)* 1965, **8**, 253
24 Williams, T. and Ward, I. M. *J. Polym. Sci. (B)* 1968, **6**, 621
25 Gee, D. R. and Melia, T. P. *Polymer, Lond.* 1969, **10**, 239
26 Gee, D. R. and Melia, T. P. *Makromol. Chem.* 1968, **116**, 122
27 Wunderlich, B. *J. Phys. Chem.* 1965, **69**, 2078
28 Broadhurst, M. G. *J. Res. Nat. Bur. Stand.* 1963, **67A**, 233
29 Gee, D. R. and Melia, T. P. *Makromol. Chem.*, in press

30 Lyons, B. J. and Fox, A. S. *J. Polym. Sci. (C)* 1968, **21**, 159
31 Dole, M., Milner, D. C. and Williams, T. F. *J. Amer. Chem. Soc.* 1958, **80**, 1580
32 Crook, M. and Lyons, B. J. *Trans. Faraday Soc.* 1963, **59**, 2334
33 Waddington, F. B. *J. Polym. Sci.* 1958, **31**, 221
34 Charlesby, A. and Davison, W. H. *Chem. and Ind.* 1957, p 232
35 Dole, M., Kang, H. Y. and Saito, O. *J. Amer. Chem. Soc.* 1967, **89**, 1980
36 Salovey, R. *J. Polym. Sci.* 1962, **61**, 163
37 Okada, T. and Mandelkern, L. *J. Polym. Sci. (B)* 1966, **4**, 1043
38 Flory, P. J. *J. Amer. Chem. Soc.* 1962, **84**, 2857
39 Kawai, T., Keller, A., Charlesby, A. and Ormerod, M. G. *Phil. Mag.* 1965, **12**, 657
40 Salovey, R. and Keller, A. *Bell Syst. Tech. J.* 1961, **40**, 1397
41 Flory, P. J. *J. Amer. Chem. Soc.* 1956, **78**, 5222
42 Mandelkern, L., Roberts, D. E., Halpin, J. C. and Price, F. P. *J. Amer. Chem. Soc.* 1960, **82**, 46
43 Kitamaru, R. and Mandelkern, L. *J. Amer. Chem. Soc.* 1964, **86**, 3529

The effect of ionizing radiation on the thermal properties of linear high polymers:

Part 2. Nylon-6

D. R. GEE and T. P. MELIA

A differential scanning calorimeter has been used to measure the heat capacities of nylon-6 samples, which had been subjected to different doses (0–1000 Mrads) of cobalt-60 gamma radiation at 298°K, over the temperature range 200–550°K. At doses up to 200 Mrads the melting temperature decreases steadily with dose whilst the heat and entropy of fusion steadily increase. Above this dose a second peak appears in the heat capacity versus temperature plot. With increasing dose this low temperature peak becomes more apparent whilst the melting transition becomes less so. Possible explanations of these effects are proposed.

THIS IS the second paper[1] in a series concerned with the effect of ionizing radiation on the thermal properties of linear high polymers. In this paper the results of heat capacity measurements (over the temperature range 200–550°K) on nylon-6 samples, which had been subjected to different doses of gamma radiation at 298°K, are described.

EXPERIMENTAL

Materials

The nylon-6 sample was supplied by Dr M. B. Huglin, University of Salford. The sample, which was in film form (0·5mm thick), was extracted with methanol to remove monomer and moisture and dried at 350°K *in vacuo*. The intrinsic viscosity of the polymer in *meta*-cresol solution at 303°K was 0·202 ± 0·002 lg⁻¹. This yields a value of 46000 for the viscosity average molecular weight[2]. The sample density was $1·125 \pm 0·005 \mathrm{g\,cm^{-3}}$ at 298°K[3].

Sample irradiation

The method used has been described previously[1].

Calorimetry

The differential scanning calorimeter used in the heat capacity measurements has been described previously[4, 5].

RESULTS

Typical heat capacity versus temperature plots for irradiated nylon-6 samples are shown in *Figure 1*. The heat capacity of all samples between 180°K and the glass transition temperature may be represented by the linear expression

$$C = 0 \cdot 179 + 4 \cdot 27 \times 10^{-3} T \qquad [\text{J } °K^{-1} g^{-1}] \qquad (1)$$

whilst the equations

$$C_m = 1 \cdot 331 + 2 \cdot 73 \times 10^{-3} T \qquad [\text{J } °K^{-1} g^{-1}] \qquad (2)$$

and

$$C_m(\text{irradiated}) = 1 \cdot 236 + 2 \cdot 73 \times 10^{-3} T \qquad [\text{J } °K^{-1} g^{-1}] \qquad (3)$$

represent the heat capacities of the original sample and the irradiated ones above the melting temperature.

The crystallinities, melting and glass transition temperatures and some derived thermodynamic properties of these samples are shown in *Tables 1* and *2*. The weight fraction crystallinities of the various samples were estimated from the heat capacity results using the method of Dole[6]. The glass transition temperature is taken as the half-height in the upward sweep in the heat capacity versus temperature plot. The melting temperature is taken as the maximum in the heat capacity versus temperature curve. In deriving the entropy and enthalpy values shown in columns 6 and 8 of *Tables 1* and *2* the assumption was made that the heat capacities of the irradiated samples were identical with those of unirradiated nylon-6 below 200°K[7]. This assumption has been justified previously[8]. The enthalpy and entropy of fusion values were calculated from the present heat capacity results using equations 6 and 7 of reference 9.

DISCUSSION

The melting behaviour of irradiated nylon-6 is complex (*Figure 1*). At doses up to 200 Mrads there is a steady decrease in melting temperature with dose. Above 200 Mrads a second peak appears in the heat capacity versus temperature plot. With increasing dose this low temperature peak becomes more apparent whilst the high temperature one becomes less so. For the same samples after fusion and melt crystallization only a single melting peak is observed. This peak occurs at a temperature between those observed for the two peaks in the original samples at doses below 800 Mrads; above this dose it has the same value as the low temperature peak. A possible explanation of these effects is that the introduction of intermolecular crosslinks during irradiation causes a change in the crystal structure of the nylon-6 and that the new crystal form melts at a lower temperature (about 460°K). Thus, the two melting peaks observed are associated with the presence of both crystal forms in the irradiated samples. Similar melting behaviour has been observed in these laboratories with syndiotactic polypropylene which exists in the helical and *trans* planar zig-zag forms[9, 10]. On this basis the single fusion

193

Table 1 Thermodynamic properties of nylon-6 irradiated at 298°K

Dose [Mrads]	Weight fraction crystallinity	T_g [°K]	T_m (1) [°K]	T_m (2) [°K]	$H^0_{504} - H^0_0$ [J g^{-1}]	ΔH_f^* [J g^{-1}]	$S^0_{504} - S^0_0$ [J °K^{-1} g^{-1}]	ΔS_f^* [J °K^{-1} g^{-1}]
0	0·64	325	498	—	768·4	112·9	2·843	0·237
25	0·66	325	494	—	772·2	124·9	2·861	0·272
50	0·66	325	494	—	779·2	131·9	2·874	0·285
75	0·67	326	494	—	782·9	136·4	2·884	0·297
100	0·69	326	492	—	785·7	140·6	2·894	0·310
200	0·69	326	491	474	776·2	131·1	2·881	0·297
300	0·68	327	487	470	772·6	126·7	2·872	0·287
400	0·67	327	486	469	766·3	119·8	2·867	0·280
500	0·69	328	486	469	768·2	123·1	2·859	0·275
600	0·68	328	472	462	762·5	116·7	2·850	0·264
800	0·67	329	—	457	752·1	105·5	2·832	0·245
1000	0·67	330	—	453	750·3	103·7	2·825	0·238

Table 2 Thermodynamic properties of nylon-6 after irradiation at 298°K, fusion and melt crystallization

Dose [Mrads]	Weight fraction crystallinity	T_g [°K]	T_m [°K]	$H^0_{504} - H^0_0$ [J g^{-1}]	ΔH_f^* [J g^{-1}]	$S^0_{504} - S^0_0$ [J°K^{-1} g^{-1}]	ΔS_f^* [J°K^{-1} g^{-1}]
0	0·63	323	497	765·0	108·4	2·839	0·233
25	0·63	324	494	763·1	113·5	2·863	0·268
50	0·64	324	494	768·1	119·3	2·866	0·273
75	0·63	325	494	772·1	122·5	2·873	0·278
100	0·63	325	491	775·7	126·1	2·877	0·282
200	0·63	325	490	764·9	115·3	2·867	0·272
300	0·63	326	486	764·1	114·5	2·852	0·257
400	0·63	326	483	751·2	101·6	2·841	0·246
500	0·63	326	482	750·1	100·5	2·829	0·234
600	0·63	327	468	746·8	97·2	2·818	0·223
800	0·63	328	457	740·9	91·3	2·797	0·202
1000	0·63	329	453	735·3	85·7	2·789	0·194

195

peak observed after fusion and melt crystallization is probably associated with the melting of a crystal form having a conformation intermediate between those existing in the two crystal forms observed in the original samples.

Since the two melting transitions (*Figure 1*) coalesce in all the irradiated samples no attempt has been made to assign values to their separate latent
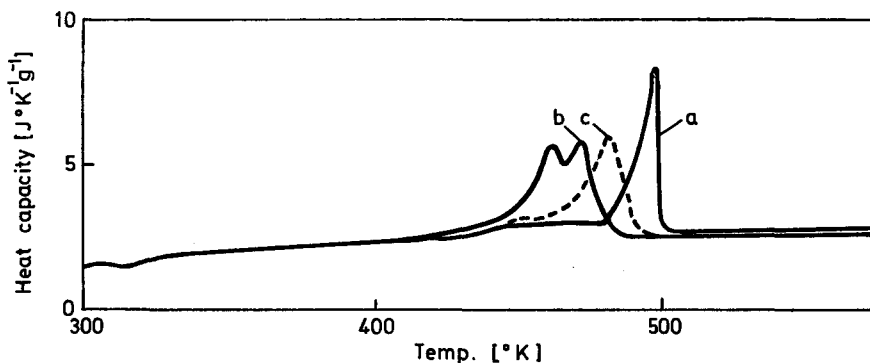
Figure 1 Heat capacity *versus* temperature plots for nylon-6: (a) original sample, (b) after irradiation (600 Mrads) at 298°K, (c) after irradiation (500 Mrads), fusion and recrystallization

heats and entropies. Both contributions are included in the ΔH_f^* and ΔS_f^* values of *Table 1*. For nylon-6 these two parameters show an initial increase with dose up to 200 Mrads. Above this dose a steady decrease occurs. Similar behaviour has been observed with melt-crystallized polyethylene[1], which showed a maximum in the heat and entropy of fusion versus dose plots at 75 Mrads, after irradiation at 298°K. These features were explained in terms of ordering processes in the liquid and solid phases, which resulted from the introduction of intermolecular crosslinks. Similar reasoning can be applied to explain the data obtained with nylon-6. At doses up to 200 Mrads intermolecular crosslinking causes an increase in solid state order which is not compensated for by an equivalent ordering in the liquid phase. Above 200 Mrads the density of intermolecular crosslinks is such that not only is the crystal form of the nylon-6 changed but also restraints are imposed on the polymer molecules in the liquid phase. These are reflected in decreased heats and entropies of fusion and lower liquid state heat capacities.

The glass transition temperature of irradiated nylon-6 increases with dose (*Tables 1* and *2*). This increase is consistent with the viewpoint that intermolecular crosslinks are introduced during irradiation[11].

For the original nylon-6 sample the observed value of the glass transition temperature (325°K) and the calculated values of the melting temperature (498°K), heat (176·4 ± 3·5 J g⁻¹) and entropy (0·354 ± 0·006 J °K⁻¹g⁻¹) of fusion compare with previously published values[12–16].

196

ACKNOWLEDGEMENTS

Department of Chemistry and Applied Chemistry,
University of Salford

REFERENCES

1 Gee, D. R. and Melia, T. P. *Polymer, Lond* 1970, **11**, 178
2 Hoshino, K. and Watanabe, M. *J. Chem. Soc. (Japan)* 1949, **10**, 24
3 Jackson, J. B., Flory, P. J. and Chiang, R. *Trans. Faraday Soc.* 1963, **59**, 1906
4 O'Neill, M. J. *Anal. Chem.* 1964, **36**, 1238
5 O'Neill, M. J., Justin, J. and Brenner, N. *Anal. Chem.* 1964, **36**, 1233
6 Dole, M. *J. Polym. Sci. (C)* 1967, **18**, 57
7 Kolesov, V. P., Paukov, I. E. and Skuratov, S. M. *Russian J. Phys. Chem.* 1962, **36**, 400
8 Dainton, F. S., Evans, D. M., Hoare, F. E. and Melia, T. P. *Polymer, Lond.* 1962, **3**, 277
9 Gee, D. R. and Melia, T. P. *Makromol. Chem.* 1968, **116**, 122
10 Gee, D. R. and Melia, T. P. *Polymer (Lond.)* 1969, **10**, 239
11 Fox, T. G. and Loshaek, S. *J. Polym. Sci.* 1955, **15**, 371
12 Marx, P., Smith, C. W., Worthington, A. E. and Dole, M. *J. Phys. Chem.* 1955, **59**, 1015
13 Gechele, G. B. and Crescentini, L. *J. appl. Polym. Sci.* 1963, **7**, 1349
14 Rybnikar, F. *Chem. Listy* 1958, **52**, 1042
15 Inove, M. *J. Polym. Sci. (A)* 1963, **1**, 2697
16 Ke, B. and Sisko, A. W. *J. Polym. Sci.* 1961, **50**, 87

Dispersions of polymeric acrylic soaps. (2) An investigation of physico-chemical properties

N. B. GRAHAM* and H. W. HOLDEN

A study has been made of viscosity, pH and surface tension effects in aqueous dispersions of copolymers containing acrylic acid which is partially to completely neutralized. The description of these self-emulsified systems appears to account for the experimental facts obtained thus far. The disperse phase consists of polymer particles stabilized at the interface by carboxylate ions in compact complexes, with the neutralizing base providing the counter-ions. Excess base over that required for the interfacial layer can diffuse freely and rapidly across the interface; under quasi-equilibrium conditions virtually all of it forms a salt with the acid in the polymeric phase. The partially neutralized polymer is more hydrophilic than the original copolymer and therefore the disperse phase is swollen by water to a much higher partial volume than would be calculated on the basis of polymer alone. When fully neutralized, the same copolymers appear to form true solutions at very low concentrations and at higher concentrations show evidence for aggregation similar to the micelle formation of conventional soaps. A number of time-dependent phenomena have been observed with these systems which may be related to polymer diffusion and relaxation processes.

IN A previous paper[1], the preparation of aqueous dispersions of random copolymers, containing up to 20% acrylic acid and partially neutralized with a variety of bases, was described. Many examples were found which formed stable emulsion systems without additional surface-active materials. The present paper summarizes the results of experiments undertaken to gain a fuller understanding of the physical chemistry of the dispersions.

EXPERIMENTAL SECTION

Procedures

The polymerization and emulsification procedures were followed, with specific variations, as described previously[1]. Various viscosity measurements were carried out with a Gardner-Holdt Bubble Viscometer, Cannon-Fenske capillary viscometer and Bendix Ultraviscoson as required. The pH studies at various times made use of Leeds and Northrup, Phillips, and Radiometer pH meters with glass pH electrode conditioned in 0·1 N HCl solution and standardized with buffer at pH 6·0. Surface tension measurements were made with a Cenco/du Nouy ring tensiometer.

---

* Present Address: ICI Ltd, Petrochemical and Polymer Laboratory, PO Box 11, The Heath, Runcorn, Cheshire, England

Results of viscosity studies

As described previously, the preparation of aqueous dispersions by the direct addition of water to the partially neutralized acrylic acid copolymers often resulted in a sudden drop in viscosity within narrow concentration limits. Very large differences were also encountered in the preparation of dispersions of a single copolymer at one concentration, where the only variables were the choice and amount of base. One dispersion showed very

Table 1 Emulsion samples used in constructing Figure 1

Dispersion	Curve in Figure 1	Copolymer* (ref. 1)	Base used; neutralization	Wt. PrOH† Wt. copolymer	Emulsification Procedure‡ and notes
1	D	13	Et₃N 60%	0·023	No heating; optimum neutralization
2	C	15	NaOH 32%	0·0012	60°C, steam bath
3	E	13	Et₃N 50%	∼0·0	No heating; both procedures used (see note for dispersion 6)
4	F	16	Et₃N 35%	∼0·0	Heated with steam bath
5	G	13	Et₃N 35%	∼0·0	No heating
6	H	13	Et₃N 35%	∼0·0	Base mixed first with polymer; some heat generated
7	A	15	Me₂NCH₂CH₂OH 60%	0·045	Heated with steam bath
8	B	15	Me₂NCH₂CH₂OH 45%	0·039	Heated with steam bath

* Copolymer 13: butyl acrylate/acrylic acid, 90/10% (weight basis)
      15: styrene/2-ethylhexyl acrylate/ethyl acrylate/methyl methacrylate/acrylic acid, 10/50/5/20/15%
      16: styrene/ethyl acrylate/acrylic acid, 40/40/20%
† PrOH: residual isopropanol from copolymerization stage
‡ Except where noted, the emulsification was carried out by the longer procedure in reference 1: all the base and water were added together and stirred in the presence of the copolymer until dispersion was complete

large reversible variations in viscosity with temperature. While some of the viscosity changes could have been caused by phase inversion, others appeared to be the result of close packing of the disperse phase particles.

The effect of dilution on the viscosity of a number of self-dispersed acrylic emulsions was studied, with the results shown in Figure 1. The detailed composition of the systems is given in Table 1. Curves 1–6 were obtained using Bendix Ultraviscoson measurements, while curves 7 and 8 were derived from Gardner-Holdt comparator measurements. The representation of the data employs the partial volume ϕ_p of copolymer; for this approximate calculation the specific volume of the copolymer is derived from those of the corresponding homopolymers on the assumption of additivity of partial volumes[2]. The calculation of the specific volume of the emulsion assumes no volume change on mixing of the constituents and ignores the effects of

ionization; for simplicity the residual isopropanol and neutralizing base are not included in ϕ_p.

The experimental curves may be compared with Sibree's empirical modification[3] of Hatschek's equation[4] for paraffin-in-water emulsions: $\eta/\eta_0 = [1 - (1 \cdot 3\phi)^{1/3}]^{-1}$, and with the theoretical curve of Guth and Simha[5] for low phase volumes. It may be seen that although there are very large
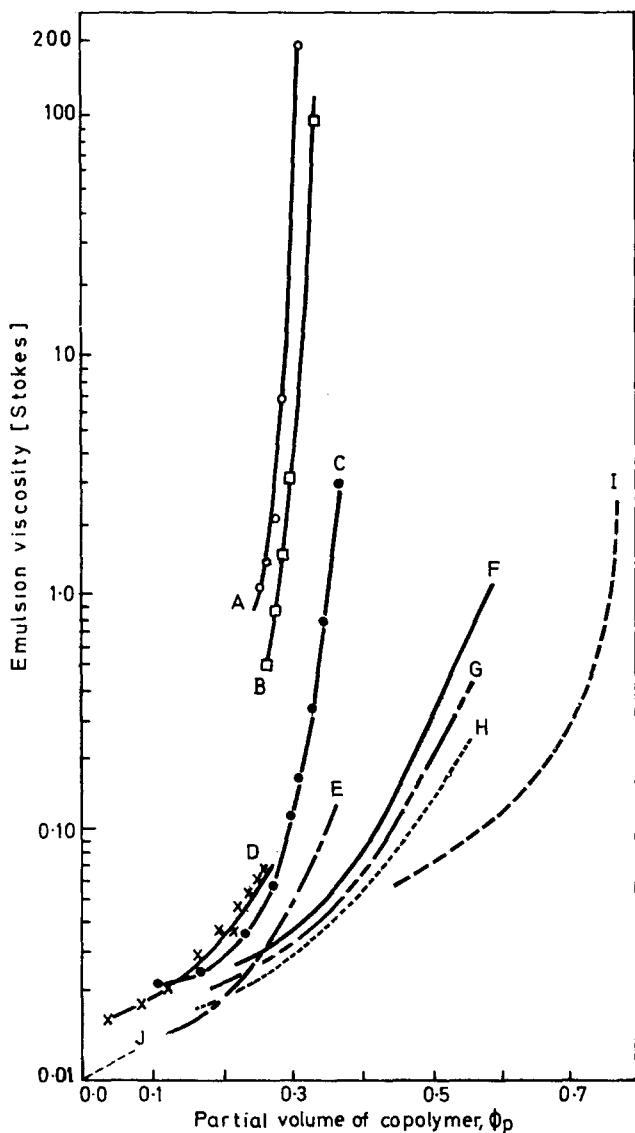
Figure 1 Variation in viscosity of selected dispersions with polymer concentration: J, equation of Guth and Simha[5]; I, equation of Sibree[3]; for identification of experimental dispersions of present work, refer to Table 1

changes in the viscosity, there are no discontinuities in the curves to suggest phase inversion. The self-dispersed acrylic emulsions behave as though the partial volume of the disperse phase is much greater than the partial volume of the polymer itself.

The points which for clarity have been omitted from the curves for dispersions 3–6 show rather more experimental scatter than those of curves 1 and 2. The two emulsions of identical composition represented by curve 3 behave identically, within experimental error, even though the emulsions were prepared by different procedures. On the other hand differences between systems 5 and 6 exceeded the scatter of the experimental points, either because of slight discrepancies in composition or because of slight differences in the final state resulting from the different emulsification routes.
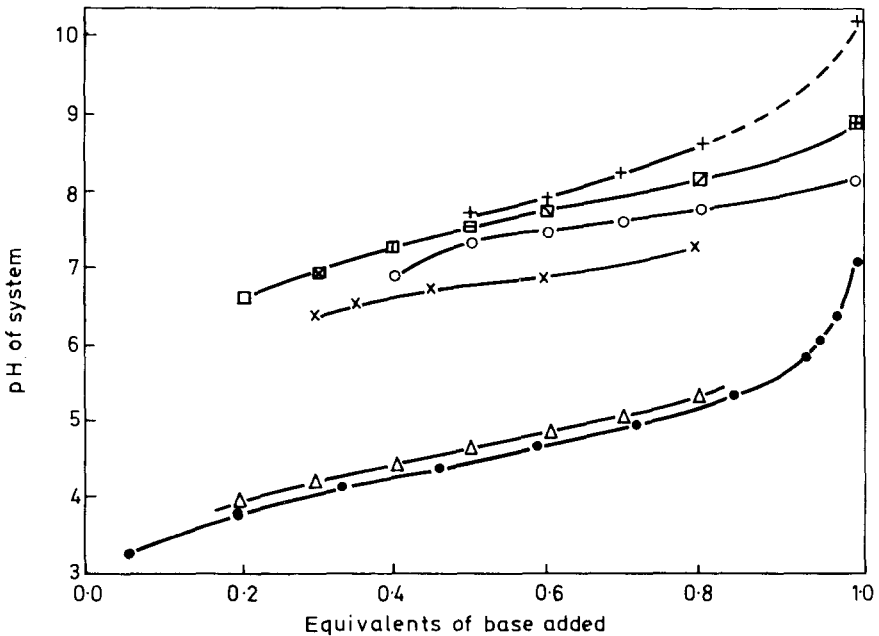
Figure 2 Variation in pH of selected dispersions with degree of neutralization of polymeric acid

⁺, copolymer 37: styrene/ethyl acrylate/acrylic acid, weight ratio 45/45/10%, with triethylamine as the neutralizing base; polymer content of dispersions 25%.
○, the same copolymer with triethanolamine as the neutralizing base; 25% polymer.
□, copolymer 13: butyl acrylate/acrylic acid 90/10%, with triethylamine; 29·3% polymer. (Various modifications of square symbol are for cross-referencing with *Figure 3*).
×, copolymer 15: styrene/2-ethylhexyl acrylate/ethyl acrylate/methyl methacrylate/acrylic acid, 10/50/5/20/15%, with dimethylaminoethanol; 39·2% polymer.
●, acetic acid solution, titrated with dimethylaminoethanol.
△, soluble copolymer[6]: acrylamide/acrylic acid, 73·5/26·5%, titrated with sodium hydroxide

The results presented here indicate that the dispersed, partially-neutralized polymer phase is substantially swollen by water. The water swelling effect differs greatly with the base used; of those studied, ammonia gave the

greatest effect, followed closely by sodium hydroxide and dimethylamino-
ethanol; triethylamine gave by far the smallest effect. This observation
suggests that the water in the polymer is directly involved in the solvation
of the various ionic species.

Results of pH studies

An interesting feature of these systems is the fact that the pH of dispersions
of widely differing composition falls within narrow limits near neutrality, in
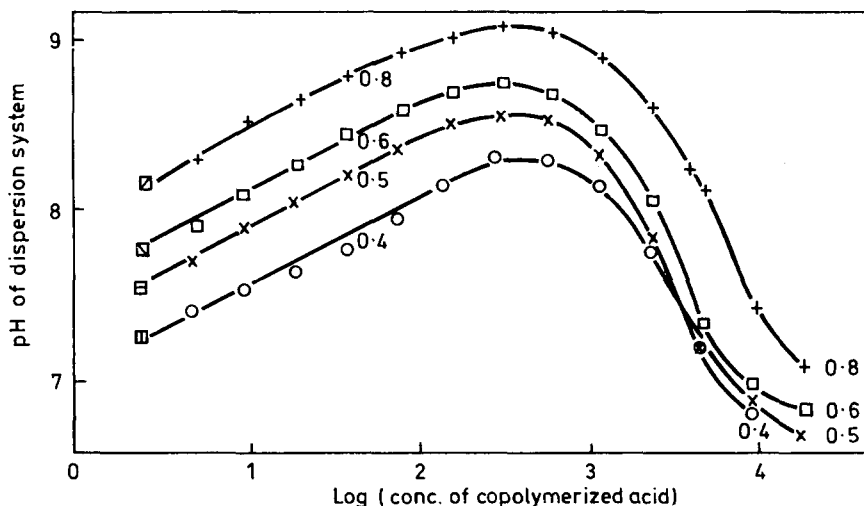
Figure 3 Variation in pH of dispersions of butyl acrylate/acrylic acid 90/10%, copolymer
with dilution. Degree of neutralization with triethylamine: ☐, 40%; ◨, 50%; ◪, 60%;
◩ 80%. (Symbols for systems at start of experiment correspond to those used in *Figure 2*).

spite of the fact that they all contain acrylic acid in excess of the neutralizing
base added. *Figure 2* illustrates the measured pH values of several series of
dispersions at different levels of partial neutralization. The systems prepared
from a common copolymer generate smooth curves, which may be compared
with the neutralization curves of acetic acid with dimethylaminoethanol
and of a water-soluble random copolymer[6] (acrylamide, 73·5%, acrylic acid,
26·5%) with sodium hydroxide, also shown in *Figure 2*.

Since the pH measurement in the two-phase systems may be presumed to
characterize only the aqueous phase, it is clear that the excess acid remains
in the disperse phase. Since the curves of *Figure 2* are similar in shape to the
neutralization curve for a weak acid, the systems were tested for buffering
properties. Simple dilution of the systems with water, however, was found to
have a marked effect on pH.

In *Figure 3*, a family of curves is shown which was obtained by measurement
of pH of dispersions with consecutive volume-for-volume dilutions with
distilled water. The abscissa of the figure is defined, by analogy with the pH
scale, as the negative of log(concentration in mole/l of copolymerized acrylic

acid). The first points correspond to the systems identified by the correspondingly coded symbols in *Figure 2*. It may be seen that the pH increases linearly for dilutions of about 200 fold; eventually, however, the pH of the boiled distilled water (6·4 to 6·5 for this set of experiments) begins to predominate and the pH of the dilute system falls after the polymer concentration has been reduced below 0·1 %. The slope of the linear portions was virtually constant (0·53 $\pm$ 0·02) for these examples, but exhibited other values in the range 0·35–0·85 for different copolymers and neutralizing bases studied.

A few experiments were carried out with the 60% neutralized system in which the diluent contained 0·1 % to 1 % neutral salt. Since the change in pH with dilution was strongly suppressed, the presence of the salt must shift the partition equilibrium; thus, virtually all of the added base remains combined with the polymeric acid.
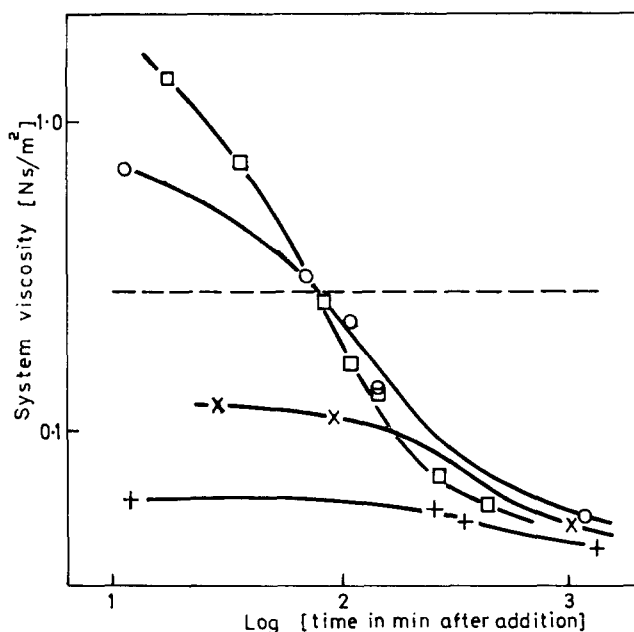
Figure 4 Changes in viscosity with time after small increases in water and base content of a stable emulsion. Copolymer of styrene/2-ethylhexyl acrylate/methyl methacrylate/acrylic acid/acrylamide, 10/55/20/11/4%, originally emulsified with 0·25 equivalents of dimethylaminoethanol.

Symbol	Aqueous Base Added	Resulting % neutralization of acrylic acid	Calculated % non-aqueous content
. . . .	None (original emulsion)	25·0	39·4
–·–	Blank (water only)	25·0	35·8
⨯	Ammonia	28·0	35·8
○	Sodium hydroxide	28·0	35·8
▢	Dimethylaminoethanol	28·6	35·9

203

Effect of adding aqueous base to a stable emulsion

The following experiment deomonstrated complex interactions in the system when the level of neutralization and dilution are altered. The stable emulsion was prepared from copolymer 35 of reference 1 (styrene/2-ethylhexyl acrylate/methyl methacrylate/acrylic acid/acrylamide, 10/55/20/11/4%), 25% neutralized with dimethylaminoethanol. Small amounts of bases were added with vigorous mixing to the original preparation, as indicated in the caption of *Figure 4*; the mixtures were quickly transferred to Gardner-Holdt tubes for viscosity measurements. In each case there was an instantaneous increase in viscosity, followed by a slower decrease to a viscosity slightly greater than that obtained by the simple dilution (blank) experiment, as shown in *Figure 4*.

Increases in viscosity of copolymer lattices containing acid, upon addition of base, are well known[7-9] and are attributable to the formation of an ionic salt within the polymer; this in turn brings about a swelling of the particle by absorption of water. It appears likely that the variations in viscosity shown in *Figure 4* can be accounted for by changes in the relative volume fraction of the continuous and disperse phases.

The time-dependence of the viscosity appears to be peculiar to these self-emulsified systems. The amount of shearing required to make the few viscosity measurements may be considered a negligible contributing factor; however the absolute magnitudes of the viscosities shortly after mixing are probably not significant. The addition of a small amount of rather concentrated solution to the emulsion could not be carried out homogeneously even with vigorous stirring, and temporary gelation of part of the system with ammonia and sodium hydroxide was unavoidable; subsequent reworking to a uniform consistency occurred during the strongly time-dependent phase of the experiment and probably accelerated the slow process by disrupting swollen structures.

Swelling effects observed by microscopy

Direct visual evidence for the swelling and reorganization processes has been obtained. An example of the former is given in the three micrographs of *Figure 5*. For this illustration, a coarse but reasonably stable emulsion was selected, although the same effects have been observed in finer emulsions where particle populations and Brownian motion make photographic records less satisfactory. A sample of the emulsion was placed on a slide under a cover glass and focused at 2000 magnification under phase-contrast conditions. A drop of concentrated ammonia solution was then brought into contact with the system at the edge of the cover glass; it eventually gave rise to a concentration boundary moving by diffusion across the field of view. The boundary of increasing ammonia concentration may be seen moving from left to right, causing the particles to swell and actually be moved by the change in the phase relations. Measurements on the particles show that they increase in volume by a factor of about 2·5. The consecutive micrographs were obtained about 15 sec apart.

In dispersions of uniform fine particle size it is observed that the system
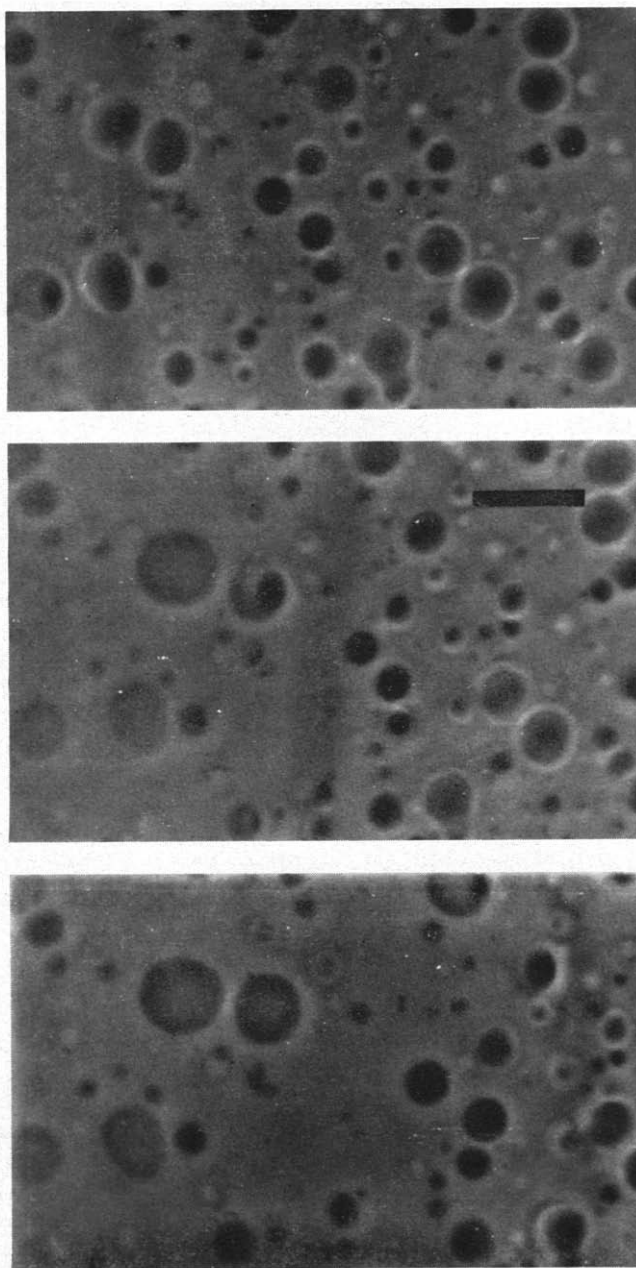
Figure 5 Consecutive photomicrographs showing the passage of a diffusion front of ammonia through an emulsion, with resultant swelling of disperse phase particles. Oil immersion, phase contrast optics; the marker indicates 10 μm

stiffens up completely because of the imbibing of virtually all the water. After a few hours, however, aggregation of particles can be observed, and contraction inferred by the occurrence of intervening spaces containing clear aqueous solution.

Surface tension effects

Although the pH was observed to change on dilution and although the polymers are not homogeneous in monomer distribution or in molecular weight, it was considered worthwhile to carry out a brief study of surface tension of the emulsions.

The emulsions, as prepared, exhibited predictably low surface tensions around 30 dyn/cm (30 mN/m). Measurements with successive dilutions were made on four of the dispersions of the butyl acrylate/acrylic acid, 90/10%, copolymer containing 0·3, 0·6, 0·8 and 1·0 equivalent of triethylamine (the same system as used in *Figures 2* and *3*). The results, shown in *Figure 6*, generate curves similar to those obtained with conventional soaps. In this representation the concentration at which, upon further dilution, a sharp increase in surface tension is noted, depends on the size of the particular concentration scale used. (See inset graph in which the low concentration data for the 80% and 100% neutralized copolymer are continued on a concentration scale expanded approximately seventeen-fold). If the critical concentration for the fully neutralized copolymer be taken at 0·5%, this composition corresponds to an acrylate salt content of $3·6 \times 10^{-3}$ mole/l. The result may be compared with critical micelle concentrations of $3·3 \times 10^{-3}$ mole/l for sodium myristate and $4·4 \times 10^{-4}$ mole/l for sodium stearate[10].

For the partially neutralized copolymers, the critical concentration, for the systems containing 0·6 and 0·8 equivalents of base, appears to lie between 1% and 2%. For the 0·3 equivalents example it lay nearer 8%, and the surface tension measurement became quite erratic below about 6%. In these cases only a very small portion of the ionized polymeric material can participate as a dissolved constituent of the aqueous phase where its influence on the surface tension can be observed.

DISCUSSION

One of the questions which these experiments sought to answer was whether or not there was any fundamental difference in emulsions prepared by the two quite different procedures described in the first paper and in *Table 1*. In the formation of emulsions by the partial neutralization of the polymer, followed by the vigorous mixing of polymer and water, the mechanically-created interface must be stabilized by the migration of amphiphilic species to the interface.

In the formation of emulsions by the stirring of all the water and base in contact with the original polymer, the base diffuses into the surface of the polymer producing ionizable salts which make the polymer much more hydrophilic. This layer becomes swollen with water and in this softened state
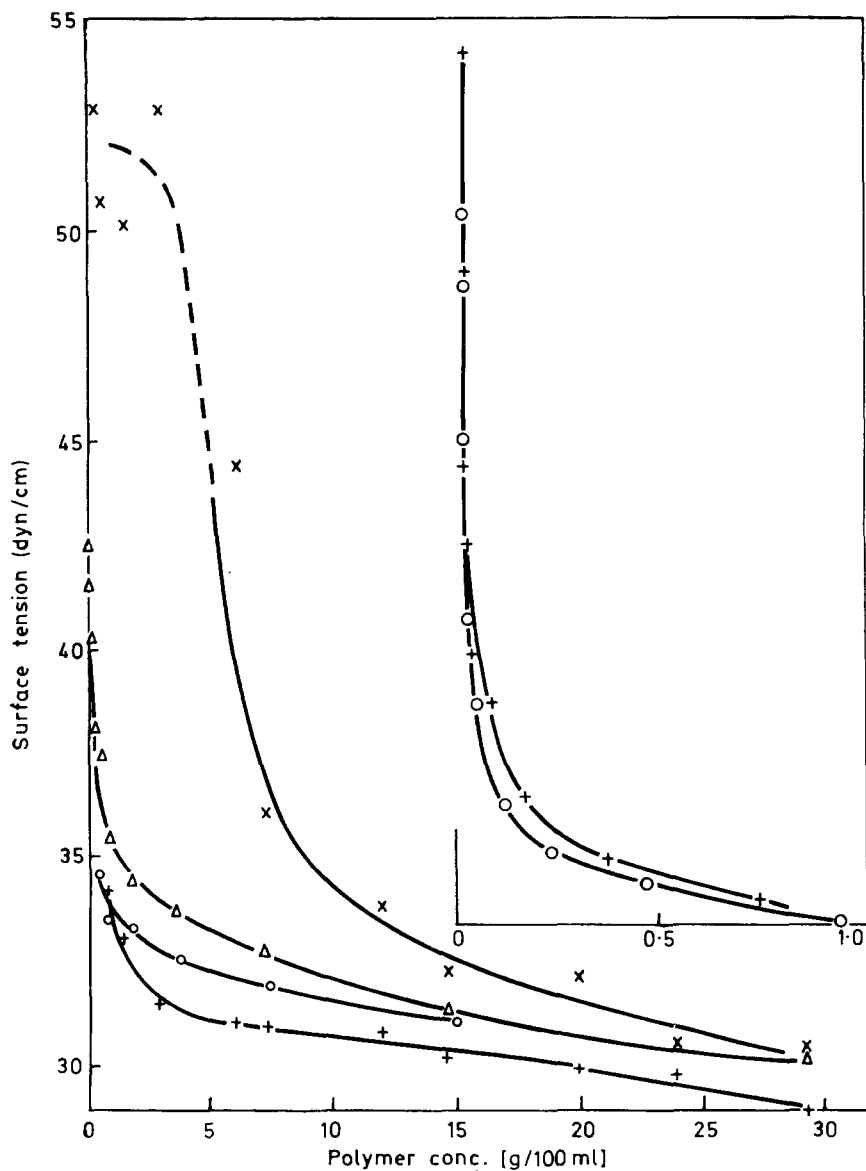
Figure 6 Variations in surface tension* of dispersions with dilution (copolymer of butylacrylate/acrylic acid 90/10 neutralized to various degrees with triethylamine): ×, 30%; △, 60%; +, 80%; ○, 100%. Inset shows continuation of curves at low concentrations

---

*Units of surface tension: 1 dyn/cm ≡ 1 mN/m.

it is much more readily swept into the aqueous phase by the relatively mild shear conditions. Since the first copolymer taken up in this way would be fully neutralized and dispersed as individual molecules or micelles, the solution froths and behaves like a typical soap solution. The interesting point is that when the composition is suitably chosen, instead of producing a saturated solution or dissolving only that polymer equivalent to the amount of base added, a portion of the base continues to diffuse into the copolymer until all the copolymer is softened and emulsified. During the whole process a rapid redistribution of stabilizing species occurs so that the final emulsion is quite uniform. Exceptions to this rule occurred when the stirring was stopped as soon as all the polymer was taken up from the walls of the vessel; in this case one frequently observed an emulsion of exceedingly fine and uniform particles with a small population of larger, irregularly shaped particles.

With either type of emulsification procedure, it may be postulated that the only steps required to obtain a stabilizing layer at the interface are (1) the migration of the small base molecules or basic cations to the interface and (2) the formation of ionic complexes at the interface with rearrangement of the stabilizing copolymer chains in the lowest energy configuration. Repartition of the other non-polymeric constituents between the phases will proceed more or less concurrently and, as is apparent in many disperse system phenomena, quite rapidly.

It is not possible to say at this stage whether a thermodynamically stable or metastable state is reached by these procedures. It may be concluded however, from the viscosity experiments reported in *Table 1* and *Figure 1* that emulsions of the same composition prepared by different routes are substantially identical, provided agitation is continued for some time after dispersion is achieved. Earlier gross differences observed were caused by the presence of larger proportions of isopropanol (from the copolymerization step) which altered the phase volumes by its own partition equilibrium.

Excessively hydrophilic copolymers cannot self-emulsify because, even if two phases are formed, they would not differ sufficiently in character for the copolymer to function as an amphiphilic interfacial stabilizer for a very large area. Of those copolymers which do self-emulsify, the less hydrophilic ones can form emulsions at consistently higher polymer concentrations than their more hydrophilic analogues. These copolymers are less swollen by water and therefore form a disperse phase of smaller partial volume. Such systems will only be stable if enough copolymerized carboxyl groups are present to give adequate interfacial stabilization. The present work indicates that a minimum of 4% by weight of copolymerized acrylic acid is required for the more tractable systems, and perhaps more for marginal cases.

Many particularities modify the foregoing generalization. For example, the choice of base used can alter the hydrophilic nature of the copolymer. Furthermore, emulsions can be prepared at lower viscosity and higher polymer levels if the propanol solvent is removed to keep the volume fraction of the disperse phase as low as possible. In another example, a copolymer (styrene/2-ethylhexylacrylate/methyl meth acrylate/acrylic acid/acrylamide, 10/55/20/22/4%) emulsified with 0·40 equivalents of ammonia at 40·4%

polymer content, exhibited apparently reversible changes in viscosity of over 100 fold over a relatively short temperature interval. This effect originates in changes caused by a temperature-sensitive equilibrium partition of water between the phases. This conclusion is supported by the observation that the phenomenon is greatly suppressed by a reduction in the polymer concentration of the system.

In the case of the copolymers which are hydrophobic even when partially neutralized, contact with water will not lead to significant swelling or softening of the polymer; any residual isopropanol may be extracted into the aqueous phase. Thus, it will be difficult to disperse the polymer mechanically, and there will be very little mobility of the copolymer chains within particles which could permit the formation of a stable charged interface. This situation arises with most of the hydrophobic styrene copolymers studied in this work, where the copolymers are in a glassy state during normal emulsification procedures. Dispersions of such copolymers can be obtained by softening them with a water-insoluble solvent such as xylene. Polymers containing a high proportion of styrene sometimes give rise to apparently stable emulsions in which many particles are elongated or even dumbell shaped; these result from hardening of the polymeric phase when the system is cooled down while stirring is continued.

The experiments described here pay little attention to the important question of emulsion stability, and to the fact that the emulsions preparable at highest polymer content are always associated with a partial neutralization of the polymer. A study of the copolymeric acrylic soaps by means of a Langmuir balance (to be reported separately[11]) gave evidence for complex-formation when the pH of the substrate was near 7. It is very significant, that, in all the emulsion systems studied, the pH of the aqueous phase finds a level in the range 6·5–8·5 which should favour the attainment of a stable ionic layer at the interface.

By direct calculation, it may be shown that there is usually more surface-active material available than is actually necessary for self-emulsification, and therefore that there is a reserve capacity for emulsification of additional non-aqueous material. Consider the following actual case, which produced an extremely stable emulsion of very fine particles and thus a very large interfacial area: the particles have a diameter of $0·1\,\mu$m, a density of $1·04\,\mathrm{g\,cm^{-3}}$ and a composition of approximately equal parts by weight of water and polymer, containing 11% by weight of acrylic acid. The copolymer contains $9·1 \times 10^{20}$ carboxyl groups per gram, the volume per particle is $5·2 \times 10^{-16}$ cm^3 and the surface area per particle is $3·1 \times 10^{-10}$ cm^2, the weight of polymer per particle is $2·7 \times 10^{-16}$ g and includes $2·5 \times 10^5$ carboxyl groups. If we assign a value of $20\,\text{Å}^2$ ($0·2\,\text{nm}^2$) for the area occupied by a carboxyl group at the end of a normal paraffin chain[12], then a maximum of 60% of the groups could be accommodated at the interface. In practice, steric effects, ionic repulsion and possibly solvation will result in a larger area (perhaps $60–100\,\text{Å}^2$)[11] and only about 12–20% of the groups would be involved.

On the basis of the pH behaviour of systematically varied dispersion compositions (*Figure 2*), it is concluded that the excess acid and virtually all the base are contained in the disperse phase. This result is quite in-

POL—P

dependent of the stability of the dispersions. In addition it is reasonable to conclude that the disperse phase continues to exist in substantially the same form, in many cases even at a high degree of neutralization, where the systems are virtually transparent or show a marked Tyndall effect. If this were not the case, and outright dissolution of the polymer occurred, the pH curves should eventually coincide with the conventional neutralization curves of soluble acids shown in *Figure 2*.

The effect of dilution on the pH of the emulsions gives support for the idea of a partition equilibrium of the base between the phases with most of the base in the polymer phase. The response of pH to dilution was immediate, and no time-effect could be observed which could not have been attributed equally to the measuring instrument. Passage of base between the phases appears to be unimpeded by the slow processes typical of polymeric systems.

It is important to note that the examples in *Figure 3* were all two-phase systems, but differed widely in the stability of the initial dispersions. At 80% neutralization, dispersion was easy but coagulation took place within 24h; at 40% and 50% neutralization settling occurred but with negligible coagulation, and in the 60% case settling was virtually absent after 10 months. No attempt was made to assess the effect of dilution on stability; since the uniform increase in pH of all the dispersions with dilution does not correlate with the variations of stability of the starting emulsions, it appears unlikely that the configuration of the ionic interfacial layer is significantly altered during the relatively short duration of these experiments.

Evidence has been produced (*Figure 4*) for additional slow spontaneous processes occurring in these systems after an alteration of some parameter. These presumably are the result of a slow accommodation by the polymeric constituents to sudden alterations of phase relationships caused by migration of the more mobile species. The later stages of the experiments illustrated by *Figure 4* appear to indicate a genuine reorganization of the systems. The amount of water absorbed by the particles (which depends on the base used) determines the mobility of the polymer, and hence the rate of attainment of a new steady state. Even the water-diluted system showed a decrease in viscosity with time, which would indicate a slow repartition of constituents. These results serve to show that many of the effects described earlier might be subject to revision if the time scale of the experiments were greatly extended.

The surface tension measurements on these systems show that when copolymers of this type are fully neutralized, their behaviour is apparently analogous to a conventional soap. They greatly lower the surface tension of water. They can emulsify or solubilize other water-insoluble liquids. It is probable that they form simple aqueous solutions only at extremely low concentrations, and form irregular, water-swollen micelles above 0·5–1%, which tend to aggregate or precipitate as a separate phase at somewhat higher concentrations.

In the partially neutralized condition, these copolymers function both as insoluble material to be dispersed and as surface-active stabilizer for the dispersion. Only a much smaller proportion of the copolymer is dissolved in

the aqueous phase; nearly all of it is part of the disperse phase in one of its two roles. While micelles can act in dilution experiments as reservoirs from which simply dissolved molecules can be supplied to maintain low surface tension, the comparatively large droplets of the disperse polymer phase can release single polymer molecules only by much slower and more complicated processes.

Acrylic copolymeric soaps form an interesting class of materials including a large number which are self-dispersible as stable emulsions. Further study should concentrate on those processes taking place in the systems which are associated with the long relaxation times of the polymer molecules.

ACKNOWLEDGEMENT

REFERENCES

1 Graham, N. B. and Holden, H. W. *Polymer, Lond.* 1969, **10**, 633
2 Murdock, J. D. and Nelan, N. Unpublished work, this laboratory
3 Sibree, J. O. *Trans. Faraday Soc.* 1930, **26**, 26, as quoted in 'Emulsions: Theory and Practice', by P. Becher, Chapter 3, Reinhold, New York, 1957
4 Hatschek, E. *Kolloid-Z.* 1911, **8**, 34, as quoted in Becher reference 3
5 Guth, E. and Simha, R. *Kolloid-Z.* 1936, **74**, 266, as quoted in Becher reference 3
6 Miller, M. L. and Rauhut, C. E. *J. Colloid Sci.* 1959, **14**, 524
7 Fordyce, D. B., Dupre, J. and Toy, W. *Official Digest* 1959, **31**, 284
8 Wesslau, H. *Makromol. Chem.* 1963, **69**, 220
9 Berke, E. A. and Jahn, R. G. *U.S. Patent* 2,973,285
10 Brandrup, J. and Immergut, E. H. (Eds.) *Polymer Handbook* Interscience Publishers, New York, 1966
11 Graham, N. B., Holden, H. W. and Raymond, F. L. Accepted for publication in *British Polymer Journal*
12 Adam, N. K. 'The Physics and Chemistry of Surfaces', 3rd edit. Oxford Univ. Press, London, 1941, pp 50–51

Effect of structure on the glass transition temperatures of some perfluoroalkylene-linked aromatic polyimides

J. M. BARTON and J. P. CRITCHLEY

The preparation of a series of high molecular weight aromatic polyimides by the reaction of di(4-aminophenyl)ether with 1,3-*bis*(3,4-dicarboxyphenyl) hexafluoropropane dianhydride, and pyromellitic dianhydride is described. The glass transition temperatures (T_g) of these polymers were measured by differential scanning calorimetry at heating rates of 8–64°K/min on samples of controlled thermal history, and T_gs at a dilatometric heating rate (0·06°K/min) were estimated. The values provide a good fit to a simple molar additive relationship between T_g and copolyimide composition from which the T_g of poly{[5,7-dihydro-1,3,5,7-tetraoxobenzo(1,2-*c*:4,5-*c'*)-dipyrrole-2,6(1*H*,3*H*)-diyl]-*p*-phenyleneoxy-*p*-phenylene} (Kapton) is estimated to be 598°K. The reason why this predicted T_g is difficult to observe experimentally may be that only limited molecular motion can occur at the T_g because many of the polymer segments are tied into a network by strong intermolecular forces.

AROMATIC POLYIMIDES of high thermal stability and good mechanical properties such as poly{[5,7-dihydro-1,3,5,7-tetraoxobenzo(1,2-c:4,5-c')-dipyrrole-2,6(1H,3H)-diyl]-*p*-phenylenecxy-*p*-phenylene} marketed by du Pont under the name Kapton, are well known[1]. A characteristic of these polyimides is the apparent absence of a T_g below the temperature at which degradation or crosslinking occurs[2]. Consequently, the polymers are not fusible or mouldable. Recently, higher molecular weight, thermally stable perfluoroalkylene-linked aromatic polyimides have been developed[3,4] which show measurable T_gs and which exhibit viscous flow at higher temperatures, enabling them to be compression moulded.

Copolymerization of an aromatic diamine such as di(4-aminophenyl)ether with pyromellitic dianhydride and perfluoroalkylene-linked aromatic dianhydrides allows the preparation of polyimides with T_gs over a wide temperature range; the dependence of the T_g of such copolymers on their structure is the subject of the present paper.

The polyimides being considered are linear copolymers of assumed general structure —[—(A)$_x$(B)$_y$—]—[—(A)$_x$(B)$_y$—]—$_n$

where A is
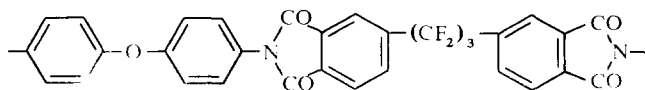
and B is
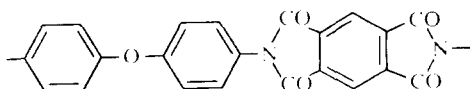
and the values of x and y may vary.

The homopolymers of A and B, and three copolymers of differing molar composition, were investigated. The general method for the preparation of aromatic polyimides was followed; this involved the synthesis at room temperature in dimethylacetamide of a soluble poly(amic acid) which, after being cast as a film, was converted into the corresponding polyimide:
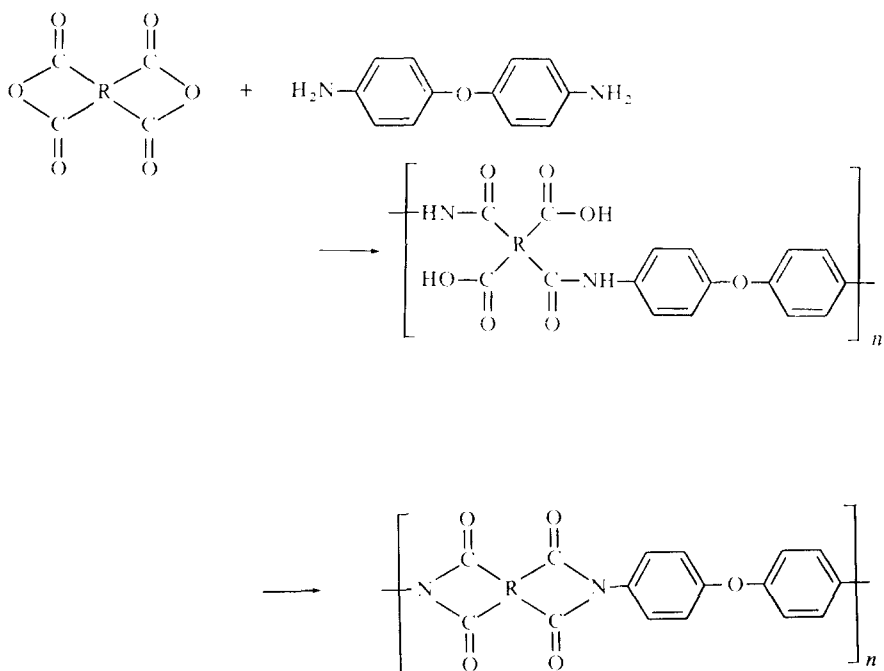
EXPERIMENTAL

Reagents

Dimethylacetamide. Technical grade material was distilled from phosphorus pentoxide at 20–30 mmHg, and stored over molecular sieve (Type 5a).

Di(4-aminophenyl) ether. Laboratory grade material was purified by several sublimations (170°C/0·1 mmHg), m.p. 186–187°C.

213

Pyromellitic dianhydride. Laboratory grade material was purified by recrystallisation from acetic anhydride/acetic acid mixture and subsequently sublimed three times (220°C/10⁻⁴mmHg), m.p. 286°C.

1,3-Bis(3,4-dicarboxyphenyl)hexafluoropropane dianhydride. This reagent[3,4,5] was purified by recrystallisation from acetic anhydride, followed by three sublimations (185°C/10⁻⁴mmHg), m.p. 173–174°C.

Polymerizations

Typical preparation of a co-poly(amic acid) A 100ml flask, fitted with mercury-sealed stirrer, nitrogen inlet, and drying tube was flame-dried. Under these anhydrous conditions, di(4-aminophenyl)ether (2·00g, 0·01 mole) was dissolved in dimethylacetamide (40·0g) to give a clear, colourless solution. 1,3-*Bis*(3,4-dicarboxyphenyl)hexafluoropropane dianhydride (3·99g, 0·009 mole) and pyromellitic dianhydride (0·218g, 0·001 mole) were intimately mixed in powder form in a dry-box and added in portions over 5min with vigorous stirring. The last traces of dianhydride were washed in with a further quantity of dimethylacetamide (5·6g), giving a total solids content of 12%. A slightly exothermic reaction occurred initially and the solution rapidly became viscous and very pale yellow in colour; stirring was continued for approximately 3h although maximum inherent viscosities were normally attained after only 1h.

Formation of poly(amic acid) film. The poly(amic acid) solution was cast on to clean, dry, glass plates and spread by means of a glass rod to give an evenly thin layer. Most of the solvent was removed at 80°C under a stream of nitrogen, and the films carefully peeled from the plates.

Conversion of poly(amic acid) to polyimide film. Films of the poly(amic acids) were clamped in metal frames and heated in a forced draft oven from room temperature to 240°C over 1h, and at 240°C for an additional hour, by which time all the amic acid groups had been converted to imide units, according to infra-red spectral evidence.

Properties

The polyimides and their corresponding poly(amic acids) are listed in *Table 1*. The poly(amic acids) were soluble in dimethylacetamide, in which solvent their inherent viscosities (0·5% solution) were determined. With the exception of polyimide I (*Table 1*), and in contrast to those aromatic polyimides with perfluoroalkylene-links in both the diamine and dianhydride moieties[3-5], these polyimide films were insoluble in dimethylacetamide. Polyimides II–VI were soluble in concentrated sulphuric acid, but in this solvent a decrease in inherent viscosity with time was observed, due presumably to chemical degradation[6] of the polymer. The polyimides of this series were all yellow coloured, the intensity increasing as the mole proportion of (B) units increased.

214

Table 1 Elemental analyses and solution viscosities of poly(amic acids) and polyimides

Polymer no.	Molar ratio		ηinh		Analyses of polyimides							
					Required				Found			
	A	B	Poly(amic acid)	Polyimide	C[%]	H[%]	F[%]	N[%]	C[%]	H[%]	F[%]	N[%]
I	1·00	0	1·38*	1·31*†	61·2	2·3	18·7	4·6	61·4	2·6	18·3	4·7
II	0·9	0·1	1·36*	--	61·7	2·3	17·5	4·8	61·7	2·5	17·9	5·0
III	0·75	0·25	1·57*	--	62·6	2·4	15·5	5·1	62·3	2·6	15·2	4·7
IV	0·5	0·5	1·62*	--	64·2	2·6	11·5	5·7	64·2	2·6	11·8	5·6
V	0·4	0·6	1·90*	--	65·0	2·5	9·6	5·9	64·8	2·5	9·6	6·0
VI	0	1·00	2·7*	--	69·1	2·6	..	7·3	68·9	2·9	--	7·4

* 0·5% solution in dimethylacetamide
† polymer dissolved on warming and stirring for 3 days

Both elemental (*Table 1*) and infra-red spectral analyses fully supported the expected structures of the polyimides. The course of dehydration of the poly(amic acid) films was followed by the disappearance of the broad absorption bands at $3400–2200 cm^{-1}$ and the appearance of a characteristic doublet at about $1780 cm^{-1}$ and $1725 cm^{-1}$ assigned to the imide ring. However, the absorption band at about $730 cm^{-1}$, often quoted as characteristic of the imide ring, seems to feature only in systems containing the pyromellitimide ring[5].

Measurement of T_g

T_g measurements at heating rates in the range $8–64°K/min$ were made by differential scanning calorimetry (DSC) using the Perkin-Elmer instrument, model DSC-1B. The temperature scale of the instrument was calibrated at different heating rates with tin, indium, benzoic acid, stearic acid, diphenyl, and octane as melting point standards. Samples of the polymers ($\sim 20 mg$), comprising discs cut from film, were encapsulated in aluminium pans and scanned at different heating rates under a nitrogen atmosphere. The samples were preconditioned before each scan by heating for about 30min at a temperature about $50°K$ above the T_g and then either quickly cooled, or cooled slowly at a constant rate of either $0·5$ or $2°K/min$, to a temperature about $100°K$ below the T_g. The quickly cooled samples gave a typical discontinuity in the heat capacity/temperature plot, while the slowly cooled samples gave a peak in the heat capacity curve on subsequent fast heating. These phenomena are frequently observed in polymers and are associated with the time dependence of the glass transition[7,8]. At a given heating rate, the 'T_g' was taken to be the point of inflection, T_i, in the plot of differential heat capacity against temperature.

From the DSC data obtained at relatively high heating rates the T_g corresponding to a heating rate of $0·06°K/min$, which is generally acceptable as a suitably low rate for reliable T_g measurements by dilatometry, was estimated[8] from a linear extrapolation of the plot of log(*heating rate*) against $1/T_i$; also, by using an experimentally determined activation energy, E, and the equation:

$$\ln[(\phi/\phi_g)(T_g/T_i)^2] = (E/R)[(1/T_g) - (1/T_i)] \qquad (1)$$

215

where T_i is the 'apparent T_g' corresponding to the heating rate ϕ, T_g corresponds to a standard heating rate ϕ_g (in this case 0·06°K/min), and R is the gas constant. These methods are based on a kinetic analysis of the glass transition process and have been found to give good agreement with experiment for a number of polymers[9]. The activation energy, E, was determined for each of the polymers by scanning the slowly cooled samples at 32°K/min and analysing the peak in the heat capacity/temperature curve by the method of Ellerstein[8].

RESULTS AND DISCUSSION

Glass transition temperatures

Typical DSC curves, from scans at 32°K/min, for polyimide I are shown
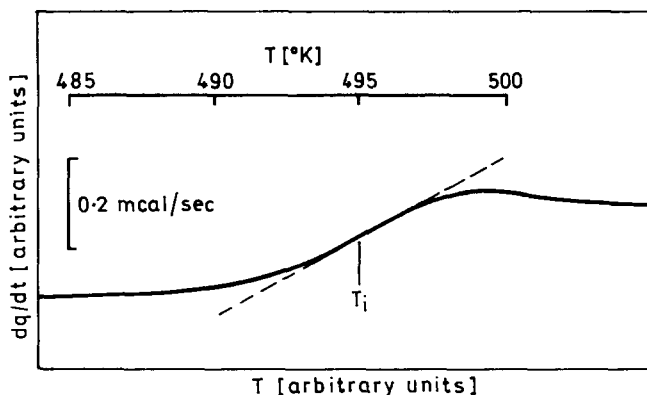
Figure 1 DSC trace for polyimide I scanned at 32°K/min after rapid cooling from above T_g

for a quickly cooled sample in *Figure 1*, and for a slowly cooled (2°K/min) sample in *Figure 2*.

The results of the DSC measurements at different heating rates on quickly cooled samples of polyimides I–IV are illustrated in *Figure 3* as plots of log(*heating rate*) against $10^3/T_i$, where T_i is the inflection temperature from the DSC traces. The linear extrapolations to obtain the T_g at a 'dilatometric' heating rate of 0·06°K/min are shown.

The activation energy, E, was estimated from an analysis of the peak in the plot of the rate of differential heat flow, dq/dt, against T, obtained in a scan of a slowly cooled sample, using the following method[8]. The base lines, drawn as dotted lines in *Figure 2*, were constructed by extrapolation of the trace from above and below the transition region, and the ordinate (h) corresponding to any given temperature (T) within the peak area was drawn as illustrated in *Figure 2*. If the change in heat capacity of the sample follows first-order kinetics then, at a given temperature (T), the ratio of h to the peak

216

area (A) remaining between the upper baseline and the ordinate through T is proportional to the rate constant (k) for the process[8,10]. The Arrhenius activation energy (E) is then given by a plot of $\log(h/A)$ versus $1/T$, which should be linear with a slope of $-E/2.303\,R$. A typical plot of $\log(h/A)$ against $10^3/T$ is shown in *Figure 4*, for polyimide 1, derived from the trace illustrated in *Figure 2*.

In *Table 2* data are presented for E, T_i from scans at $32°$K/min on quickly cooled samples, and T_g estimated both by extrapolation of the plot of
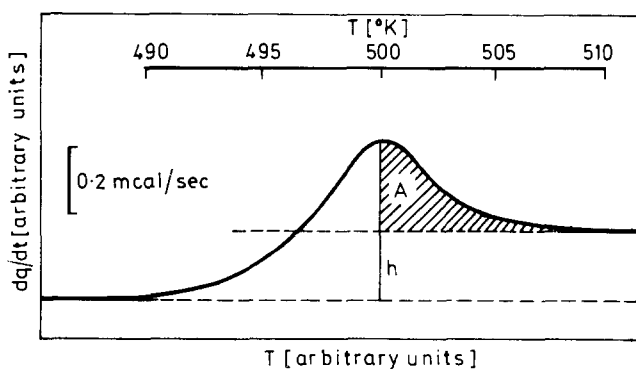
Figure 2 DSC trace for polyimide 1 scanned at $32°$K/min after cooling from above T_g at $0.2°$K/min

Table 2 Summary of transition temperature data

Polyimide number*	E [kcal mole]	(a)	$T[°K]$ (b)	(c)
I	197	495	486	483
II	193	506	492	491
III	204 198†	516 –	500 –	500 503†
IV	118†	550	524	524†
V	–	~573	–	–

(a) T_i at $32°$K/min for quickly cooled sample
(b) T_g at $0.06°$K/min extrapolated from plot of $\log(heating\ rate)$ against $1/T_i$ for quickly cooled samples
(c) T_g at $0.06°$K/min calculated from E and equation (1)

* See Table 1
† For sample cooled at 0.5 °K/min.

217
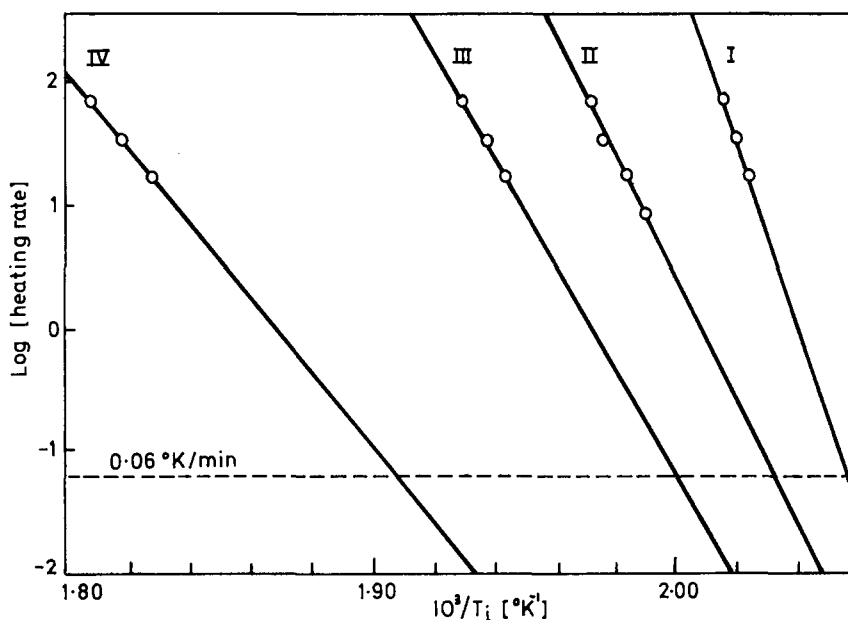
Figure 3 Plots of log(*heating rate*) against $10^3/T_i$ for quickly cooled samples of polyimides I to IV

log(*heating rate*) versus $1/T_i$, and from equation (1) for results on slowly cooled samples. There is very good agreement between the T_gs estimated by the two methods.

For polyimide V the transition was slight and difficult to observe and, although an inflection temperature was found in a scan at 32°K/min on a quickly cooled sample, no transition was observed in scans at 16°K/min, and no peak was observed on scanning the slowly cooled sample. These observations fit a general trend through the series of copolyimides, of decreasing magnitude of the specific heat change at T_g with increasing pyromellitimide content. In fact no transition at all could be detected in polyimide VI (Kapton) by DSC measurements.

Dependence of T_g on structure

By treating a wide range of homopolymers as ideal copolymers in which the 'monomer' units are the structural groups (as defined below) of the homopolymer repeating unit, it was found[11,12] that the following equation could be used to relate T_g to structure

$$T_g = \sum n_i T_i / \sum n_i \qquad (2)$$

The number of groups of the *i*th type in the repeating unit is n_i, and T_i is an invariant additive temperature parameter associated with the *i*th group. A structural group, in general, is considered to be the smallest group capable

218
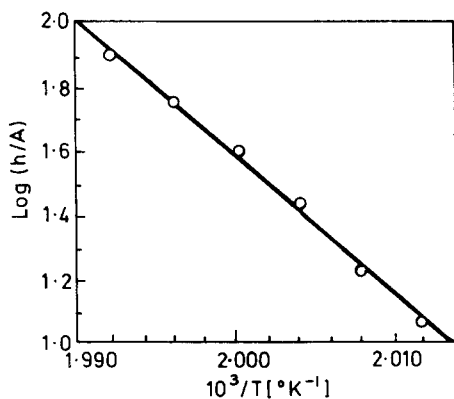
Figure 4 Activation energy plot for polyimide I scanned at 32°K/min after cooling at 2°K/min from above T_g
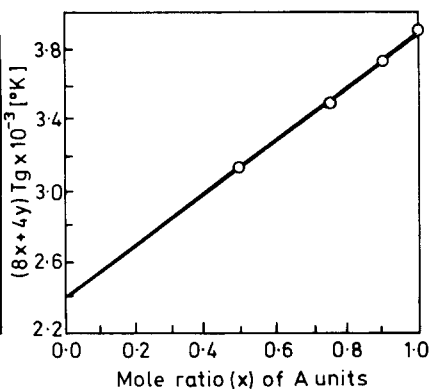
Figure 5 Fit of the T_g data to equation (4)

of independent torsional oscillation with respect to its nearest neighbours and for groups to be identical they must have the same nearest neighbours. For an alternating copolymer equation (2) gives

$$T_g = (xT_A + yT_B)/(x\alpha_A + y\alpha_B) \qquad (3)$$

where x and y are the mole fractions of A and B in the copolymer, α is the number of groups in a repeating unit, and $T_{gA(B)} = T_{gA(B)}/\alpha_{A(B)}$. This is of the same form as the Dimarzio and Gibbs[13] copolymer T_g equation but the latter is applied to bonds rather than groups. It is possible to allow for the effect of fine structure (sequence distribution) in non-random copolymers and obtain good agreement with experimental T_g data[14], but the present series of copolymers were formed by polycondensation from co-monomers of the same order of reactivity, so it is reasonable to expect them to approach the ideal alternating type of structure.

For the present copolyimides, $\alpha_A = 8$, $\alpha_B = 4$ (assuming rotation occurs about the ether linkage) and equation (3) can be written in the linear form,

$$(8x + 4y)T_g = T_B + (T_A - T_B)x \qquad (4)$$

Using the estimated T_gs from column (b) of *Table 2*, a plot of $(8x + 4y)T_g$ against x is shown in *Figure 5*. A very good fit of the experimental points to a straight line is obtained. The slope of the line obtained by linear squares regression is $T_A - T_B = 1492·2°K$ and the intercept is $T_B = 2392·7°K$. Since $T_B = 4T_{gB}$, the intercept value for T_B gives $T_{gB} = 598°K$, which agrees well with $T_{gB} = 599°K$ from the slope. Thus a theoretical T_g of 598–599°K is predicted for polyimide VI (Kapton).

From *Figure 5* a T_g of 535°K is predicted for the copolymer of composition $x = 0·4$ (polyimide V). Only the quickly cooled sample of this copolymer scanned at 32°K/min gave an observable T_i at $\simeq 573°K$. For the other

219

four polymers, a plot of T_i(32°K/min) against extrapolated T_g(0·06°K/min) is linear, and from this plot the T_g for polyimide V is 539°K; this agrees fairly well with the prediction from equation (4). As also reported by Sroog et al[2], and in conformity with the fact that the material does not fuse or flow on heating, no definite transitions were observed for polyimide VI. Similarly, Cooper et al[15], found no definite glass transition up to 500°C from shear modulus/temperature measurements (although there is a small inflection in their modulus curve at about 670°K). However, they quote data of Freeman et al[16], which indicate a transition at 658°K by electrical dissipation factor measurements at 1 kHz. In dynamic mechanical measurements of transitions, for example by the torsion pendulum method, a frequency of 1 Hz usually gives T_gs in the same region as dilatometric measurements. For the dielectric transition at 1 kHz to correspond to our predicted T_g of 598°K at 1 Hz, an activation energy of about 80 kcal/mole would be required, which is a reasonable value.

Bernier and Kline[17] using dynamic mechanical measurements at about 500Hz found a major relaxation process giving rise to a loss maximum at about 675°K. This result would correspond to our predicted T_g at 598°K if the activation energy were 65 kcal/mole, which again is a reasonable value.

One possible explanation of why the T_g is difficult to observe in polyimide VI is that it may be in a temperature region where crosslinking occurs, so that the T_g increases during the experiment. With the perfluoroalkylene-linked copolymers there was, however, no evidence that heating around the T_g caused rapid crosslinking: solubility in sulphuric acid, and fusibility were maintained. An alternative explanation for the failure to observe a clear T_g in polyimide VI by all the usual methods is that the pyromellitimide units are bound into a network structure by strong interchain forces. There is evidence that pyromellitimide units do tend to form strong intermolecular bonds consistent with the presence of charge transfer complexes[18], and the increasing intensity of yellow colouration up the series from polyimide I to VI is consistent with an increasing concentration of such complexes. The observed decreasing specific heat change at T_g with increasing pyromellitimide content could be explained by an increasing number of polymer segments being tied into a network, leaving only uncomplexed regions free to participate in the glass transition. The fact that a major transition in the predicted T_g region in Kapton is observed by mechanical and dielectric loss measurements but not by DSC measurement on polyimide VI implies that the latter method is not sufficiently sensitive to detect the limited molecular motion occurring at T_g in the polymer.

Materials Department,
Ministry of Technology,
Royal Aircraft Establishment,
Farnborough, Hampshire.

REFERENCES

1 Sroog, C. E. *J. Polym. Sci.* (*C*) 1967, **16**, 1191
2 Sroog, C. E., Endrey, A. L., Abramo, S. V., Beer, C. E., Edwards, W. M. and Olivier, K. L. *J. Polym. Sci.* (*A*) 1965, **3**, 1373
3 Critchley, J. P., McLoughlin, V. C. R., Thrower, J. and White, I. M. *Chem. and Ind.* 1969, **28**, 934
4 Critchley, J. P., Pippett, J. S. and White, M. A. Paper presented at the 5th International Symposium on Fluorine Chemistry, Moscow, U.S.S.R., 21–26 July 1969
5 Critchley, J. P., Pippett, J. S. and White, M. A. Forthcoming publication
6 Wallach, M. L. *Polymer Preprints* 1967, **8**, 1170
7 Wunderlich, B., Bodily, D. M. and Kaplan, M. H. *J. appl. Phys.* 1964, **35**, 95
8 Ellerstein, S. M. *Applied Polymer Symposia*, 1966, **2**, 111
9 Barton, J. M. *Polymer, Lond.* 1969, **10**, 151; and unpublished work
10 Borchhardt, H. J. and Daniels, F. *J. Amer. Chem. Soc.* 1957, **79**, 41
11 Lee, W. A. and O'Mahony, D. Ministry of Technology, Royal Aircraft Establishment, *Tech. Rep.* No. 66292, 1966
12 Barton, J. M. and Lee, W. A. *Polymer, Lond.* 1968, **9**, 603
13 Dimarzio, E. A. and Gibbs, J. H. *J. Polym. Sci.* 1959, **40**, 121
14 Barton, J. M., I.U.P.A.C. International Symposium on Macromolecular Chemistry, Toronto, September 1968, *Preprint A.12.7*
15 Cooper, S. L., Mair, A. D. and Tobolsky, A. V. *Textile Res. J.* 1965, **35**, 1110
16 Freeman, J. H., Frost, L. W., Bower, G. M. and Traynor, E. J. Westinghouse Report – Paper presented at the Conference on Structural Plastics, Adhesives, and Filament Wound Composites, Wright-Patterson Air Force Base, Dayton, Ohio, December 1962
17 Bernier, G. A. and Kline, D. E. *J. appl. Polym. Sci.* 1968, **12**, 593
18 Dine-Hart, R. A. Private communication

221

Radiation effects in homopolymers and dilute copolymers of vinyl acetate

KAORU YONETANI and WILLIAM W. GRAESSLEY

The effects of small doses of gamma radiation on linear and branched poly(vinyl acetate) were investigated. When irradiated in vacuum at ambient temperature and then heated to 60°C after irradiation, the linear polymer increases in molecular weight with dose as expected for a random cross-linking process. The branched polymer undergoes an additional reaction which appears to involve rapid, preferential scission at approximately one sixth of the branch locations and which goes to completion well before the gel point. Copolymers with trace amounts of α-methyl groups (0·1–10 groups per 1000 main chain carbon atoms) were prepared to simulate branching. These materials were highly sensitive to post-irradiation heat treatment compared with the homopolymers, although the numbers of trapped radicals were the same in all samples according to e.s.r. measurements. Crosslinking rate increases with α-methyl content as judged by gel point values on annealed samples, reaching a maximum near three α-methyl groups per 1000 vinyl acetate units and decreasing again at high α-methyl contents.

POLYMERS in the solid state undergo a number of chemical changes when exposed to high energy radiation. In many systems the major reactions affecting molecular weight are random crosslinking and chain scission, both reactions involving only the repeating units in the chain and both occurring in direct proportion to the total radiation dose up to very large doses. Depending on the relative rates of the crosslinking and scission processes the polymer either forms a gel and develops an increasingly complete network as the radiation proceeds or continually decreases in molecular weight without gel formation. Some systems undergo other reactions as well, and these not only proceed rapidly to completion but they also appear to be associated with specific types of irregularities in the structure. Examples are the rapid disappearance of vinyl groups in polyethylene[1], the high initial rates of chain scission in polypropylene[2], and the rapid scission processes in branched poly(vinyl acetate)[3]. Such reactions are interesting because of their possible importance in radiation damage to biological systems and because they may yield information on the relative contributions of intramolecular and intermolecular energy transfer in solid polymeric systems. The present article reports further studies on radiation sensitivity of branch points in poly(vinyl acetate). Unlike the earlier work, measurements are made at very low dose levels, i.e. in the region prior to the gel point.

In the earlier study a series of poly(vinyl acetate) samples of various branching densities (0·13–1·74 branch points per molecule) were irradiated beyond the gel point, and gel curves were prepared from solvent extraction. Behavior near the gel point suggested that preferential scission of approximately 13% of the branch points had occurred in each of the samples prior

222

to the gel point. Independent analysis of the behavior at high doses yielded 19% preferential scission at the branch points.

The branch points of the experimental polymers had been formed by transfer reactions during the polymerization process. Three types of branch structure can result from polymer transfer reactions:
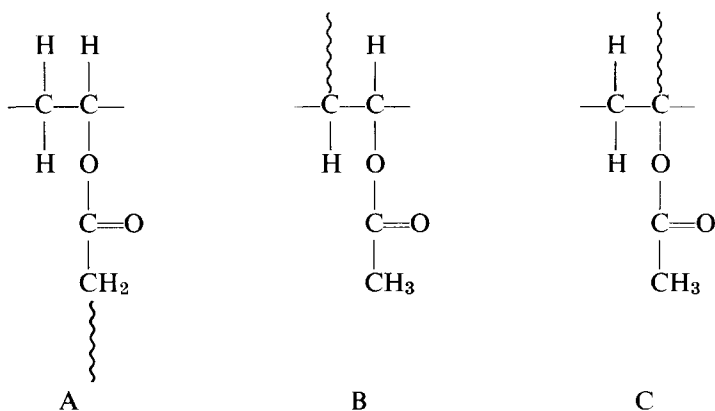
Structures A and B would not be expected to be especially sensitive to radiation. Moreover, saponification and re-acetylation indicate that approximately 70% of the branches have structure A[4], eliminating it as a candidate in view of the observed sensitive fraction of only 0·13–0·19. Structure C was suggested to be the most likely candidate because the central carbon lacks a hydrogen atom, and polymers containing main chain carbon atoms without hydrogen tend to undergo chain scission almost exclusively[5].

In the present work molecular weight measurements on linear and branched homopolymers were made in the pre-gel region in an effort to observe the rapid scission process directly. The studies were also extended to another type of branch point, the α-methyl group. Copolymers of vinyl acetate with trace quantities of isopropenyl acetate were prepared to simulate structure C.

EXPERIMENTAL

A. Preparation of samples

Vinyl acetate supplied by Union Carbide Chemical Corporation and isopropenyl acetate supplied by J. T. Baker Chemical Company were distilled at approximately 50°C under vacuum in an argon atmosphere to remove inhibitor.

Poly(vinyl acetate) was prepared by free radical polymerization in bulk, with azo*bis*isobutyronitrile as initiator. The polymer was isolated by precipitation with hexane and freeze-dried from benzene solution. Polymerization and structural data on the two homopolymers used are recorded in *Table 1*. The molecular weight distribution and the long chain branching density

were controlled by the extent of conversion. Characterization and analysis of this system are described elsewhere[6].

Two groups of copolymer samples were prepared, one group to determine the reactivity ratios (see below), the other for the radiation study (*Table 1*). All samples in the second group had very low isopropenyl acetate concentrations, and all were prepared to maintain the same molecular weight as nearly as possible.

Table 1 Homopolymerization and copolymerization data

Homopolymerization data

Polymerization conversion [%]	M_w	b*	Initiator concn. (AIBN)† [moles/l]	Polymerization temperature [°C]
20	9.63×10^5	0·2	3×10^{-5}	60
71	3.06×10^6	1·7	3×10^{-5}	72

*Number-average number of branch points per molecule.
†Azobisisobutyronitrile.

Copolymerization of vinyl acetate (VAc) with isopropenyl acetate (IPAc)

VAc/IPAc [mole/ratio]	Initiator, % by weight of monomer (benzoyl peroxide)	Polymerization time [h]	Polymerization temperature [°C]	Polymerization conversion [%]
0/1	5·0	40·0	70	20·0
1/1	0·5	15·0	60	9·3
2/1	0·5	3·5	60	7·4
3/1	0·5	6·3	60	9·0
4/1	0·25	1·75	60	10·2
5/1	0·25	2·0	60	4·3
10/1	0·25	1·2	60	10·5
20/1	0·25	0·5	60	8·2
80/1	0·25	0·5	60	10·0

VAc/IPAc [mole ratio]	M_w ($\times 10^{-5}$)	Initiator concn. (AIBN) [moles/l] ($\times 10^5$)	Polymerization temperature [°C]	Polymerization conversion [%]
50/1	9·46	3	50	18·8
385/1	8·72	3	60	21·1
1350/1	8·72	3	60	19·0
5775/1	9·61	3	60	20·2

Monomer reactivity ratios for the vinyl acetate/isopropenyl acetate (VAc–IPAc) system must be known in order to prepare copolymers with a known number of isopropenyl acetate units in the polymeric chain. Composition of a series of copolymers made at low conversions were measured by nuclear

magnetic resonance (Varian A60 and T60). Spectra of the VAc–IPAc co-
polymers and IPAc homopolymer are shown in *Figure 1*. Peaks for the
copolymer were assigned tentatively as follows:

```
 (b) (a)      (d)
  H  CH3 H   H   H
  |   |   |   |   |
 —C — C — C — C — C—
  |   |   |   |   |
  H   |   H   |   H
      O       O
      |       |
      C=O     C=O
      |       |
      CH3     CH3
     (c)
```
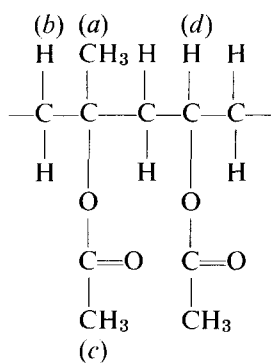
(a) 1·40, (b) 1·75,
(c) 1·95, (d)4·80 p.p.m.
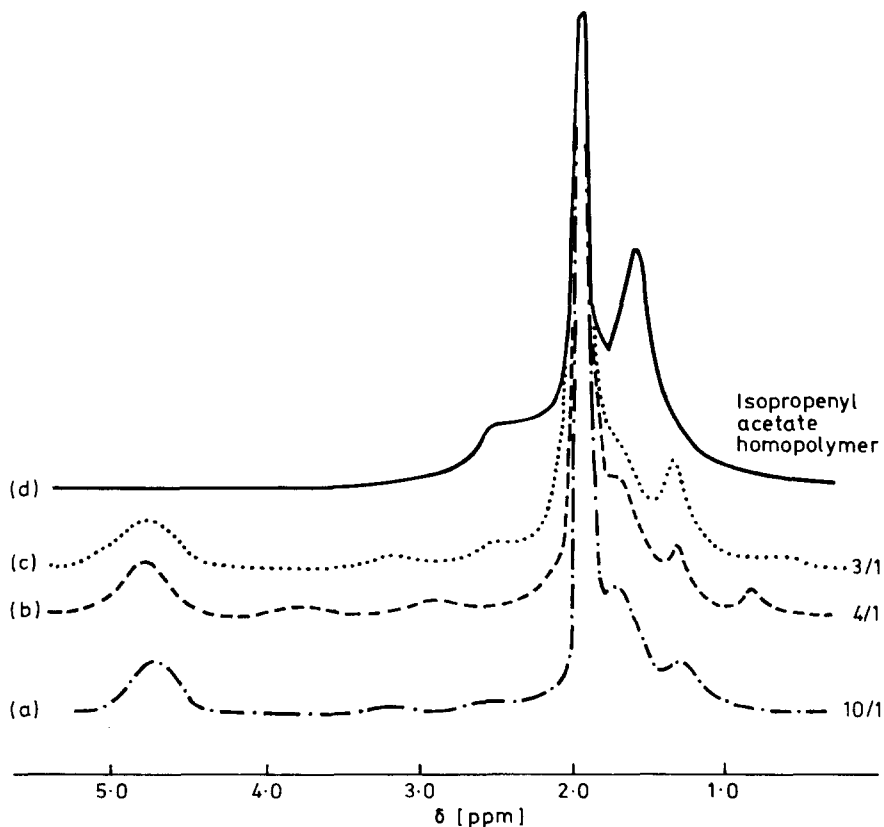
Figure 1 N.M.R. spectra
(a) 10/1 VAc/IPAc copolymer; (b) 4/1 VAc/IPAc copolymer; (c) 3/1 VAc/IPAc copolymer;
(d) IPAc homopolymer

225

The values above apply to dilute copolymers only. At high IPAc contents the peaks shifted slightly, especially peak *b*, due to the changing environment of the protons. The resonance peaks in the high field region are considerably overlapped. Therefore, the compositions of the copolymers were calculated from the ratio of adsorption intensities:

$$\frac{\delta(d)}{\delta(a) + \delta(b) + \delta(c)}$$

The data are listed in *Table 2*. Composition of copolymer was found to be nearly the same as the initial monomer composition, in good agreement with reactivity ratios of $r_1 = 1$ and $r_2 = 1$ reported by Smets and Hart[7].

Table 2 Copolymerization of VAc (M_1) with IPAc (M_2)

Mole ratio in monomer M_2/M_1	Mole ratio in polymer M_2/M_1
1/1	1/1·22
1/2	1/2·12
1/3	1/2·85
1/4	1/4·55
1/5	1/4·75
1/10	1/12·3
1/20	1/22·3
1/80	Undetectable

B. Irradiation and molecular weight measurement

Samples of freeze-dried polymer were heated at 70°C for a few minutes to collapse them into a more compact state. All samples were then evacuated at $1–5 \times 10^{-5}$ mmHg for 50h in pyrex tubes and sealed under vacuum. All samples were irradiated at ambient temperature ($\sim$35°C) in a Co^{60} gamma source. The dose rate was 0·43 Mrad/h. No changes in the infra-red spectrum were detectable at these dose levels. Depending on the experiment the irradiated samples were subjected to various treatments before exposure to air. Post-irradiation annealing conditions were found to be especially important in some polymers and are specified with each set of results.

The molecular weights of irradiated but completely soluble samples were measured in the Brice-Phoenix light scattering photometer with methanol as the solvent. Each solution was warmed to 60°C, and the presence or absence of gel was determined visually. Great care was necessary in filtering the solutions prior to the scattering measurements in order to avoid removing high molecular weight components. As expected, Zimm plots of the scattering data became increasingly distorted as the gel point was approached, reflecting an increasing complexity of structure. Molecular weights were evaluated as described elsewhere[4].

C. Gas analysis

The gas evolved during irradiation was analysed in a mass spectrometer

(Consolidated Electrodynamic Corporation 21-104). Rather large doses were required to produce enough products for analysis. Each polymer was sealed in a break-seal tube under the vacuum of $1-5 \times 10^{-5}$ mmHg and irradiated to the extent of 20 Mrad. After irradiation the break-seal tubes were joined to the gas-sampling system of the spectrometer which was then evacuated. The tubes were warmed to 70°C for 10 min, the seal was broken, the total pressure in the system was measured, and the analysis was performed. No acetic acid was detected in any of the samples reported here. Very high doses, approximately 100 Mrads, did produce a detectable odour of acetic acid however.

D. Electron spin resonance (e.s.r.) measurements

The e.s.r. measurements were carried out to evaluate trapped radical concentrations in the irradiated samples. Absorption peaks were measured in a Varian Spectrometer with field modulation at 100kHz. Samples for measuring e.s.r. spectra were sealed in quartz tubes under the vacuum of $1-5 \times 10^{-5}$ mmHg and irradiated. The measurements were carried out at room temperature (~ 25°C). In the initial experiments the irradiated samples were cooled to liquid nitrogen temperature immediately after irradiation, and the e.s.r. measurements were made at that temperature. However, no difference in the trapped radical concentration (up to 2·0 Mrad irradiation) was found when measurements were made at room temperature without cooling the sample. The radicals appeared to be stable more or less indefinitely at 35°C in vacuum, although disappearing rapidly at 50°C or upon exposure to air.

RESULTS AND DISCUSSION

A. Molecular weight changes

If only random crosslinking and random chain scission take place during irradiation, and the extent of both processes is directly proportional to the radiation dose, then the weight-average molecular weight M_w should change with radiation dose R according to:

$$\frac{1}{M_w} = \frac{1}{(M_w)_0}\left(1 - \frac{R}{R_g}\right) \tag{1}$$

The initial molecular weight is $(M_w)_0$, and the gel-point dosage is R_g. Furthermore, R_g should be inversely proportional to $(M_w)_0$ for different samples of the same polymer. Thus, plots of $1/M_w$ versus R for samples with different initial molecular weight should yield a series of parallel straight lines, extending in each case from $1/M_w = 1/(M_w)_0$ at $R = 0$ to $1/M_w = 0$ at $R = R_g$. In the presence of random chain scission these properties are strictly true only for systems of linear chains with most probable molecular weight distributions. However, deviations are known to be very small even for quite different distributions[9].

Molecular weights of the irradiated homopolymers are plotted in *Figures 2*

and *3*. The data on the linear polymer (*Figure 2*) conform rather well to equation (1), indicating a system in which random crosslinking and scission are indeed the dominant processes. The gel point dosage R_g is 2·9 Mrad. On the other hand, the data for the branched polymer (*Figure 3*) differs significantly from random behavior. The molecular weight remains almost constant until a dose of 0·5–0·7 Mrad. Beyond that point the molecular weight increases at approximately the rate expected for random crosslinking, based on the behaviour of the linear polymer. The gel point dosage is 1·5 Mrad, which is substantially larger than the value of 0·9 Mrad predicted from the data on the linear polymer on the assumption of random crosslinking and scission alone. Branching density is the only known difference in structure between the two homopolymers, so the explanation must somehow lie in the response of isolated branch points to irradiation. The constancy of molecular weight in the initial stages is striking (*Figure 3*), and of course could be explained if the presence of branch points somehow suppressed all reactions which alter molecular weight during the first 0·6 Mrad of irradiation. This seems highly unlikely in view of the small numbers of branch points in the system. Also, the fact that the *G* values for trapped radical formation (radicals per 100 eV of energy deposited) were the same in the branched and linear
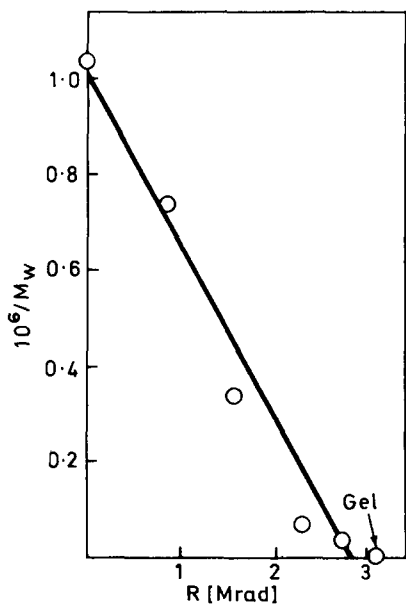
Figure 2 The reciprocal of weight average molecular weight versus dose for linear poly(vinyl acetate) (20% conversion). Irradiated samples were annealed at 60°C for 2 days before exposure to air
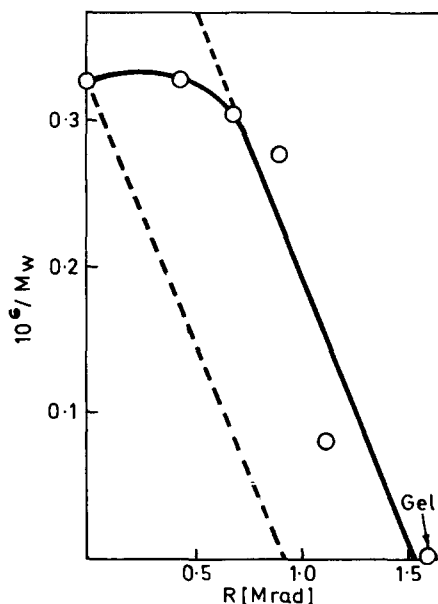
Figure 3 The reciprocal of weight average molecular weight versus dose for branched poly(vinyl acetate) (71% conversion). Irradiated samples were annealed at 60°C for 2 days before exposure to air. The dotted line indicates the predicted curve of molecular weight as a function of dose

homopolymer (see below) implies the lack of any such protective effect. A more plausible explanation is the rapid scission process postulated earlier[10], competing with random scission and crosslinking at the very early stages of irradiation and going to completion during the first 0·6 Mrad of dose.

The number of preferential scission reactions necessary to account for the behavior of the branched polymer can be estimated from the displacement of the gel point. The relation of the initial weight average molecular weight $(M_w)_0$ of the sample to a modified value $(M_w)'$ can be expressed by[10]:

$$(M_w)' = (M_w)_0/(1 + mb)^2 \qquad (2)$$

where $(M_w)'$ indicates the extrapolated value of molecular weight to $R = 0$ from the random behavior range in the *Figure 3*, b is the initial number of branches per molecule and m is the fraction which undergoes preferential scission.

The value of b for the branched sample is 1·7 and the gel point ratio R_g(random)/R_g(observed) is 0·9/1·5, so $(M_w)_0/(M_w)'$ is 1·67 yielding $m = 0·17$ from equation (2). This value agrees well with values obtained from the post-gelation study[10]. The reaction cross-section of the branch points is remarkably large. A simple calculation shows that, in order to consume all susceptible branch points in the system during the first 0·6 Mrads of irradiation, approximately five scissions must occur at the branch points for each crosslink formed anywhere on the system. Such a rate would also suffice to maintain a nearly constant value of M_w during the initial stages of irradiation.

Table 3 Gel point data in copolymers*

	$M_w \times 10^{-5}$	Observed gel point† [Mrad]	$G(x)$*
20% PVAc homopolymer	9·63	3·0 + 0·1	0·163
5775/1 copolymer	9·61	2·3 ± 0·1	0·218
1350/1 copolymer	8·72	1·9 ± 0·1	0·291
385/1 copolymer	8·72	1·3 ± 0·1	0·425
50/1 copolymer	9·46	1·3 ± 0·1	0·392

*Crosslinks per 100 eV of absorbed energy, calculated by neglecting the influence of random chain scission on the dosage to reach the gel point
†Annealed at 70°C for 10 h

The effect of frequency of isopropenyl acetate units along the chain on the gel point dosage was examined. All copolymer samples were annealed for 10 h at 70°C after irradiation, then the sealed tubes were broken and samples dissolved in methanol by shaking for 2 days at room temperature. Observations were made on samples irradiated at intervals of 0·2 Mrad near the gel point. The gel point was determined as the minimum dosage to give rise to visually observable gel.

The presence of occasional α-methyl groups along the molecule lowers the dose to the gel point rather substantially (*Table 3*). It has been expected that the lack of α-hydrogen would favour chain scission at that point in the

chain, but *Table 3* shows that trace amounts can more than double the apparent crosslinking efficiency. Scission does appear to dominate at high α-methyl contents, however. The 1/1 copolymer was irradiated in vacuum with a dose of 10 Mrad at room temperature and heated to 70°C after irradiation. A large number of bubbles were formed, and the polymer transformed into a foam, similar to the behavior of irradiated poly(methyl methacrylate). The irradiated 1/1 copolymer was partly soluble in methanol and
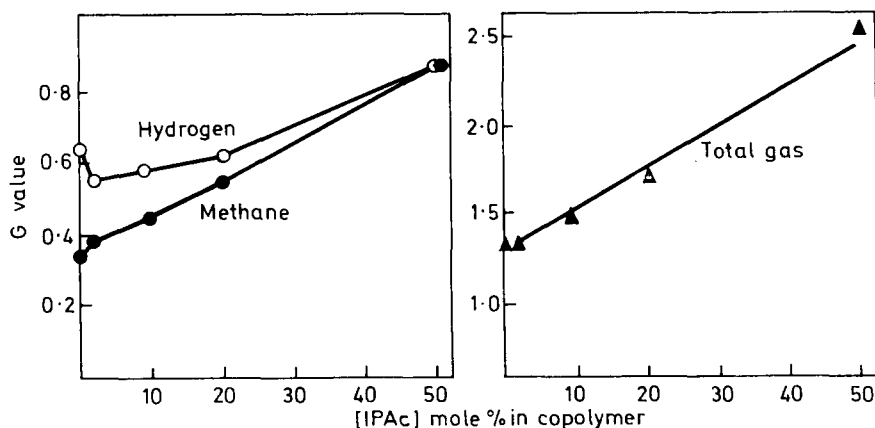
Figure 4 G value (molecules of gas per 100 eV of absorbed radiation) versus isopropenyl acetate content in the copolymers. All samples received 20 Mrad of irradiation, and all were held at 70°C for 10 min after irradiation
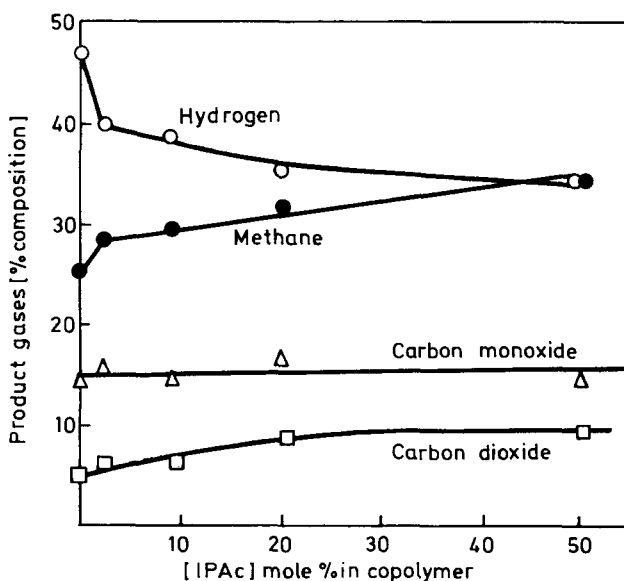
Figure 5 Composition of the evolved gas as a function of isopropenyl acetate content in the copolymer. (Same sample treatment as in *Figure 4*)

230

completely soluble in toluene. The intrinsic viscosity in toluene – 0·24 dl/g before irradiation – was reduced to 0·19 dl/g by 10 Mrad irradiation.

Gas evolution

Figure 4 shows that the *G* value for total gas (molecules evolved per 100 eV of deposited energy) increases smoothly with the amount of isopropenyl acetate in the copolymer. However, the fraction of methane and hydrogen in the gas changes almost discontinuously with the introduction of isopropenyl acetate units (*Figure 5*). It appears that isolated α-methyl groups are sites of abnormal susceptibility to radiation-induced reactions. Since the carbon monoxide and carbon dioxide contributions are practically unaltered by copolymerization the additional methane likely comes from the α-methyl groups themselves and not from adjacent acetate groups.
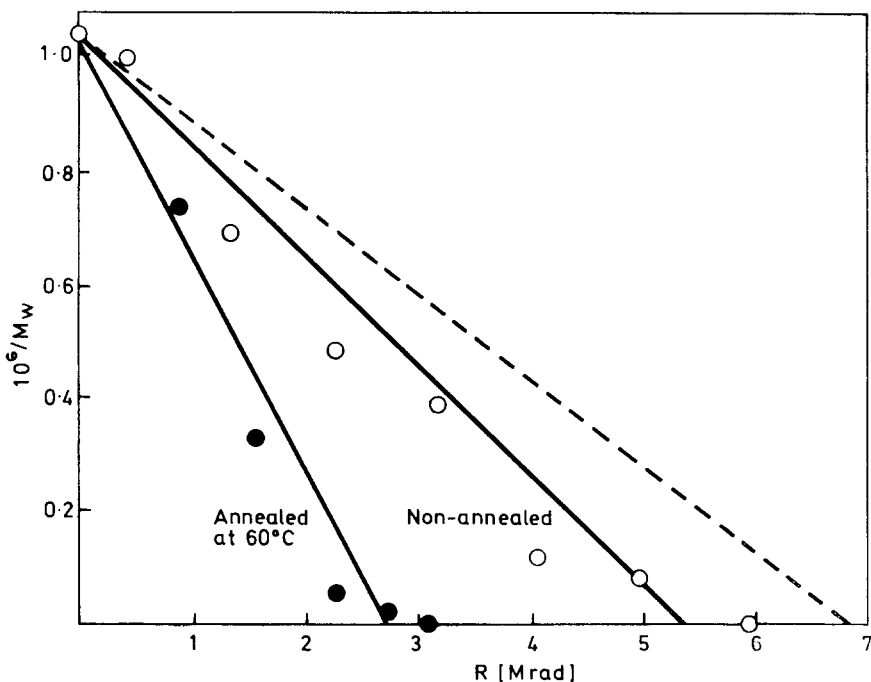
Figure 6 Effect of annealing on molecular weight in the irradiated linear poly(vinyl acetate). The open circles (○) designate the non-annealed samples withoutpost-irradiation heat treatment; the solid circles (●) designate samples held at 60°C for 2 days after irradiation

Post-irradiation effects

Trapped radicals are formed when polymers are irradiated in the solid state. Further reactions involving these trapped radicals are possible, e.g., crosslinking and oxidation, depending on the subsequent treatment. Annealing allows mutual deactivation of radicals, which may result in either additional crosslinking or simply radical disproportionation with no molecular

weight change. The effects of annealing have been extensively investigated in the case of polyethylene[11]. Without annealing trapped radicals may react with oxygen, and the products in some cases lead to chain scission. Chapiro[5] pointed out the necessity of elimination of free radicals to avoid post-irradiation oxidation. Sears and Parkinson[12] discovered a marked post-irradiation oxidation in high density polyethylene and deproteinized natural
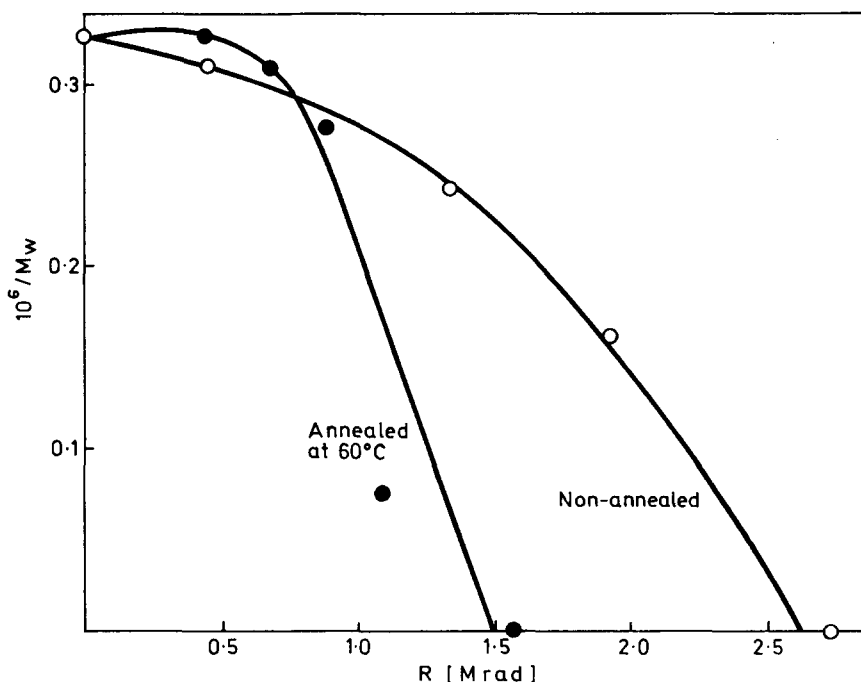
Figure 7 Effect of annealing on molecular weight in the irradiated branched poly(vinyl acetate). (Symbols and sample treatment are as in *Figure 6*)

rubber, but only minor effects in low density polyethylene, polybutadiene and poly(vinyl chloride). Oxidation through the trapped radicals in polypropylene causes considerable chain scission[13-15]. Geymer[16] was able to avoid post-irradiation oxidation in polypropylene by a preliminary exposure to methyl mercaptan after irradiation. A simple radical transfer reaction was assumed to occur through which the polymer radicals are removed with no change in polymer molecular weight.

The effect of several post-irradiation treatments on molecular weight was investigated. In both the branched and linear homopolymers moderate differences were found in the molecular weight of samples with and without heating to 60°C after irradiation (*Figures 6* and *7*). Similar but more marked annealing effects were found in the 50/1 copolymer (*Figure 8*). The 50/1 copolymer was also examined by methyl mercaptan treatment at room temperature after irradiation. Trapped radicals were undetectable by e.s.r.
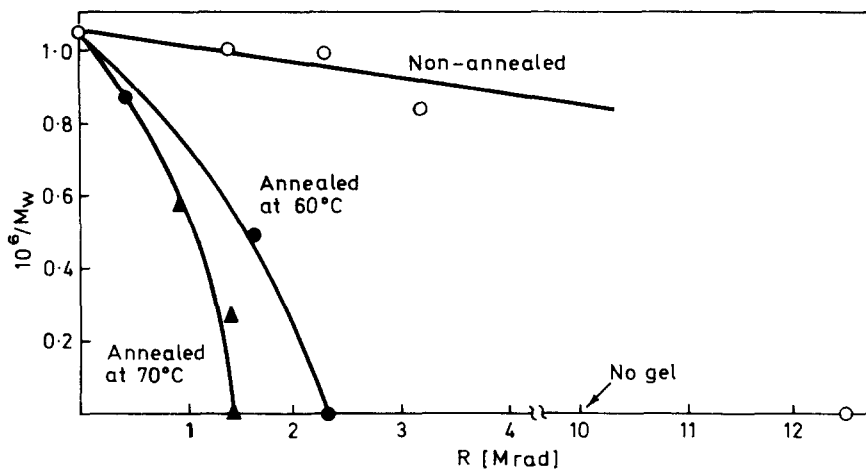
Figure 8 Effect of post-irradiation treatment on molecular weight in the 50/1 VAc/IPAc copolymer. The triangles designate the samples annealed at 70°C for 10 h; other symbols are the same as in the *Figure 6*
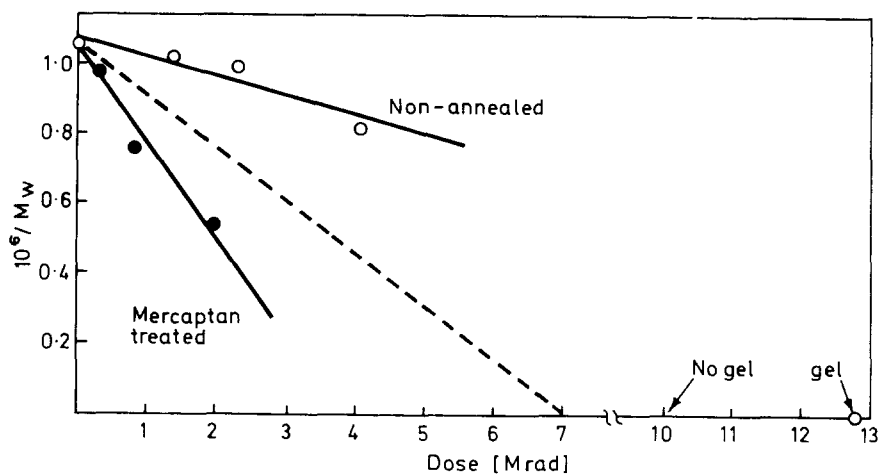
Figure 9 Effect of mercaptan treatment on molecular weight in the 50/1 copolymer. The open circles (○) designate samples with no post-irradiation treatment. The closed circles (●) designate samples treated with methyl mercaptan before exposure to air

after 1 h of exposure to mercaptan vapours. at one atmosphere. Molecular weights in irradiated 50/1 copolymer after mercaptan treatment are shown in *Figure 9*.

The e.s.r. experiments showed the same radical concentration for both homopolymers and the 50/1 copolymer. Radical concentration was proportional to dose up to 1·5 Mrad in all samples and levelled off with further irradiation. The value for all samples at 1·0 Mrad irradiation was $2·5 \times 10^{17}$

radicals per gram of polymer [$G(R\cdot) = 0\cdot4$]. Some differences in the shape of the e.s.r. spectrum between homopolymer and copolymer were noted, although these differences tended to disappear at higher radiation doses. The signal was too broad and diffuse to establish the structures of the radical species involved however.

The effects of post-irradiation treatment can be explained in part by the fate of the trapped free radicals. Consider first the 50/1 copolymer in which annealing has the greatest effect. With annealing, $G(x)$ is increased by copolymerization (*Table 3*) while without annealing the apparent $G(x)$ is much reduced. Considered alone, the differences between annealed and non-annealed samples could be explained either by the formation of new bonds by the trapped radicals during the annealing process, or by the avoidance of fracture of already existing bonds by radical oxidation reactions. In the latter case, the mercaptan-treated samples would follow the annealed curve; in the former they would follow the non-annealed curve. *Figure 9* shows that mercaptan treatment gives intermediate molecular weights which tend to lie somewhat closer to the annealed curves. The function of annealing in the copolymer is therefore both the avoidance of post-irradiation degradation and the formation of new bonds. The mercaptan treatment gives a gel point close to the gel point for annealed and non-annealed linear homopolymer. It therefore seems likely that the $G(x)$ enhancement in annealed copolymer samples comes from the formation of new crosslinks during annealing. The important conclusion from these results is that, because of the marked differences in annealing sensitivity, the radicals in the homopolymer and copolymer must have different structures.

If it is assumed that each trapped radical gives one random chain scission on exposure to oxygen, then one should be able to calculate the differences in molecular weight caused by radical oxidation from the trapped radical concentration. Consider first the linear homopolymer, which follows random crosslinking theory both with and without annealing (*Figure 6*). The molecular weight changes produced by random crosslinking and random scission are given by[8]:

$$\frac{1}{M_w} = \frac{1}{(M_w)_0} - \left(q_0 - \frac{p_0}{2}\right)\frac{R}{w_0} \tag{3}$$

$$q = q_0 R \tag{4}$$

$$p = p_0 R \tag{5}$$

in which w_0 is the molecular weight of the mer, q and p are the fractions of mers participating in crosslinks and chain scission respectively, and q_0 and p_0 are proportionality constants. If equation (3) is taken to apply to the annealed polymer, then the non-annealed polymer will obey:

$$\frac{1}{M_w} = \frac{1}{(M_w)_0} - \left(q_0 - \frac{p_0 + p_0'}{2}\right)\frac{R}{w_0} \tag{6}$$

where p_0' is the proportionality constant relating p', the number of trapped radicals per mer in the system and the radiation dose R. From the annealed

results on the linear homopolymers, $(q_0 - p_0)/2 = 3\cdot1 \times 10^{-5}$. From the trapped radical concentration reported above $p' = 3\cdot6 \times 10^{-5}$. The dotted line in *Figure 6* was calculated with equation (6) and these values. Data on the branched homopolymer shows a shift with annealing in about the same ratio as the linear homopolymer, so we conclude that trapped radicals in both produce random scission upon exposure to air approximately on a 1:1 basis (actually 80 scissons per 100 trapped radicals would fit the data best for the non-annealed sample in *Figure 6*).

A similar calculation was made for the 50/1 copolymer, using the data on the mercaptan-treated samples to evaluate $q_0 - p_0/2$. The dotted line in *Figure 9* is the result, showing that the effects of oxidation are much too large to be accounted for by a simple 1:1 replacement of trapped radicals by random scissions. One possibility is that many more oxidative scissions are produced by each trapped radical in the 50/1 copolymer than in the homopolymers. Another possibility is that oxidative degradation of a sizeable portion of the trapped radicals results in fracture of radiation-induced crosslinks on approximately a 1:1 basis rather than simple random scission. Such an outcome would be feasible if the radicals were preferentially located adjacent to crosslinking sites, rather than randomly distributed throughout the system.

CONCLUSIONS

Radiation-induced fracture of approximately one sixth of the branch points in poly(vinyl acetate) prior to the gel point has been confirmed by molecular weight measurements. The radiation behaviour of dilute vinyl acetate/isopropenyl acetate copolymers substantiates the apparently high sensitivity towards radiation of isolated branched points. Maximum differences occur with approximately three α-methyl groups per 1 000 vinyl acetate units. In contrast to the homopolymers the copolymers show appreciable affects of post-irradiation treatment. Significant amounts of new crosslinks are produced upon annealing at 70°C, while if the samples are exposed to air without annealing, considerable amounts of scission occur. Gas yields, e.s.r. results, and post-irradiation changes all suggest that the concentration of trapped radicals is unaffected by copolymerization, but that the structure and reactivity of the radicals is considerably different in homopolymer and copolymer.

Material Science Department and
Materials Research Center,
Northwestern University,
Evanston, Illinois 60201

REFERENCES

1 Dole, M., 'Crystalline olefin polymers', Part I (Eds. R. A. V. Raff and K. W. Doak), Interscience, New York, 1965, pp 845–927
2 Keyser, R. W., Clegg, B. and Dole, M. *J. Phys. Chem.* 1963, **67**, 300
3 Graessley, W. W., Alberino, L. M. and Mittelhauser, H. M. *Polymer Preprints* 1966, Amer. Chem. Soc. Meeting, New York, 1966, **7**, 1018
4 Graessley, W. W., Hartung, R. D. and Uy, W. C. *J. Polym. Sci.* (*A-2*) 1969, **7**, 1919
5 Chapiro, A., 'Radiation chemistry of polymeric systems', Interscience, New York, 1962
6 Graessley, W. W. and Mittelhauser, H. M. *J. Polym. Sci.* (*A-2*) 1967, **5**, 421
7 Hart, R. and Smets, G. *J. Polym. Sci.* 1960, **5**, 55
8 Charlesby, A., 'Atomic radiation and polymers', Pergamon Press, London, 1960
9 Inokuchi, M. and Dole, M. *J. Chem. Phys.* 1963, **38**, 3006
10 Mittelhauser, H. M. and Graessley, W. W. *Polymer, Lond.* 1969, **10**, 439
11 Kang, H. Y., Saito, O. and Dole, M. *J. Amer. Chem. Soc.* 1967, **89**, 1980
12 Sears, W. C. and Parkinson, Jr., W. W. *J. Polym. Sci.* 1956, **21**, 325
13 Fisher, H., Hellwege, K. H. and Neudorfl, P. *J. Polym. Sci.* (*A*) 1963, **1**, 2109
14 Veselovskii, R. A., Leshchenko, S. S. and Karpov, V. L. *Polymer Sci.* (*U.S.S.R.*) 1968, **10**, 881
15 Mizutani, H., Yamamoto, K., Matuoka, H. and Ihara, H. *Kobunshi Kagaku* 1965, **22**, 97
16 Geymer, D. O. *Macromol. Chem.* 1966, **99**, 152

Note on: 'Oxidative coupling of some 2,6-disubstituted phenols' by J. M. Bruce and S. E. Paulley. (*Polymer* 1969, **10**, 701)

In the paper cited above several references to earlier work have been omitted. The greater part of the experiments described by Bruce and Paulley have already been published by van Dort, de Jonge and Mijs (*J. Polym. Sci.* (*C*) 1968, **22**, 431). Manganese dioxide oxidation of 2,6-dimethylphenol has been extensively investigated by McNelis (*J. Org. Chem.* 1966, **31**, 1255), but his work is not quoted. Hay's paper on cuprous chloride/pyridine/oxygen oxidations of several disubstituted phenols is cited wrongly in connection with manganese dioxide (*J. Polym. Sci.* 1962, **58**, 581).

The paper by Bacon and Izzat (*J. Chem. Soc.* 1966, p 791) comparing the relative efficiency of 2,6-dimethylphenol oxidants is not mentioned. In connection with redistribution and C—O coupling mechanisms, the work of Mijs, van Lohuizen Bussink and Vollbracht (*Tetrahedron* 1967, **23**, 2253) could have been cited.

W. J. MIJS

AKZO Research and Engineering N.V.
Arnhem, The Netherlands

REFERENCES

1 Dole, M., 'Crystalline olefin polymers', Part I (Eds. R. A. V. Raff and K. W. Doak), Interscience, New York, 1965, pp 845–927
2 Keyser, R. W., Clegg, B. and Dole, M. *J. Phys. Chem.* 1963, **67**, 300
3 Graessley, W. W., Alberino, L. M. and Mittelhauser, H. M. *Polymer Preprints* 1966, Amer. Chem. Soc. Meeting, New York, 1966, 7, 1018
4 Graessley, W. W., Hartung, R. D. and Uy, W. C. *J. Polym. Sci. (A-2)* 1969, **7**, 1919
5 Chapiro, A., 'Radiation chemistry of polymeric systems', Interscience, New York, 1962
6 Graessley, W. W. and Mittelhauser, H. M. *J. Polym. Sci. (A-2)* 1967, **5**, 421
7 Hart, R. and Smets, G. *J. Polym. Sci.* 1960, **5**, 55
8 Charlesby, A., 'Atomic radiation and polymers', Pergamon Press, London, 1960
9 Inokuchi, M. and Dole, M. *J. Chem. Phys.* 1963, **38**, 3006
10 Mittelhauser, H. M. and Graessley, W. W. *Polymer, Lond.* 1969, **10**, 439
11 Kang, H. Y., Saito, O. and Dole, M. *J. Amer. Chem. Soc.* 1967, **89**, 1980
12 Sears, W. C. and Parkinson, Jr., W. W. *J. Polym. Sci.* 1956, **21**, 325
13 Fisher, H., Hellwege, K. H. and Neudorfl, P. *J. Polym. Sci. (A)* 1963, **1**, 2109
14 Veselovskii, R. A., Leshchenko, S. S. and Karpov, V. L. *Polymer Sci. (U.S.S.R.)* 1968, **10**, 881
15 Mizutani, H., Yamamoto, K., Matuoka, H. and Ihara, H. *Kobunshi Kagaku* 1965, **22**, 97
16 Geymer, D. O. *Macromol. Chem.* 1966, **99**, 152

Note on: 'Oxidative coupling of some 2,6-disubstituted phenols' by J. M. Bruce and S. E. Paulley. (Polymer 1969, 10, 701)

In the paper cited above several references to earlier work have been omitted. The greater part of the experiments described by Bruce and Paulley have already been published by van Dort, de Jonge and Mijs (*J. Polym. Sci. (C)* 1968, **22**, 431). Manganese dioxide oxidation of 2,6-dimethylphenol has been extensively investigated by McNelis (*J. Org. Chem.* 1966, **31**, 1255), but his work is not quoted. Hay's paper on cuprous chloride/pyridine/oxygen oxidations of several disubstituted phenols is cited wrongly in connection with manganese dioxide (*J. Polym. Sci.* 1962, **58**, 581).

The paper by Bacon and Izzat (*J. Chem. Soc.* 1966, p 791) comparing the relative efficiency of 2,6-dimethylphenol oxidants is not mentioned. In connection with redistribution and C—O coupling mechanisms, the work of Mijs, van Lohuizen Bussink and Vollbracht (*Tetrahedron* 1967, **23**, 2253) could have been cited.

W. J. Mijs

AKZO Research and Engineering N.V.
Arnhem, The Netherlands   (Received 21 January 1970)

Viscosity, molecular weight and chain entanglement

M. M. CROSS

Literature data relating zero shear viscosity (η_0) to weight-average molecular weight (M_w) in different polymer systems are re-examined. In all cases viscosity appears to be a continuous function of molecular weight with no evidence of a discontinuity at a critical value of M_w. In general a single equation of the form $\eta_0 = K_1 M_w + K_2 M_w^{3\cdot4}$ gives a much better representation of data than the two separate relations $\eta_0 = K_1 M_w$ and $\eta_0 = K_2 M_w^{3\cdot4}$. However, at higher molecular weights the viscosity increase is often more abrupt than the 3·4 power law. A simple treatment of chain entanglement based on probability theory leads to a more general equation of the form
$$\eta_0 = a_0 + a_1 M_w + a_2 M_w^3 + a_3 M_w^5 + \ldots\ldots$$

THE CONCEPT of a critical molecular weight for chain entanglement stems from a consideration of the zero shear viscosity (η_0) of a polymer as a function of the weight-average molecular weight (M_w). Following the empirical approach of Fox, Gratch and Loshaek,[1] and the theoretical treatment of Bueche[2-4] it is widely accepted that the η_0/M_w relationship exhibits a discontinuity at the critical molecular weight M_c, with equations of the form

$$\eta_0 = K_1 M_w (M_w < M_c) \tag{1a}$$

$$\text{and} \quad \eta_0 = K_2 M_w^{3\cdot4}\ (M_w > M_c) \tag{1b}$$

However, recent studies, for example by Boyce, Bauer and Collins[5] on polybutadiene melts and by Gupta and Forsman[6] on concentrated polystyrene solutions, indicate that there is no real discontinuity at M_c and that equations (1a) and (1b) are effectively asymptotes to a continuous curve. This suggests that it may be possible to represent the whole range of molecular weight by a single equation of the form

$$\eta_0 = K_1 M_w + K_2 M_w^{3\cdot4} \tag{2}$$

Evidence analysed below shows that in general equation (2) gives a much better representation of experimental data than the two separate equations (1a) and (1b).

Non-Newtonian flow is commonly attributed to chain entanglement and it had been postulated that at the critical molecular weight M_c there is also a transition from Newtonian to non-Newtonian flow.[7, 8] Here again there is evidence that the transition cannot be abrupt, for non-Newtonian flow has been observed[5] at molecular weights significantly lower than the recognised value of M_c.

If equation (2) is valid it is still possible to define a molecular weight M_c, given by $K_1 M_c = K_2 M_c^{3\cdot4}$. This molecular weight will be characteristic of the system but will not be in any sense critical. A possible interpretation is to regard $K_1 M$ as a Newtonian contribution to the viscosity, involving chains which are not entangled, while $K_2 M^{3\cdot4}$ is a non-Newtonian contribution arising from chain entanglement. At M_c the two terms are equal and, consistent with experimental observations, there will still be a detectable non-Newtonian contribution at significantly lower molecular weights.

Equation (2) gives a good approximation to the theoretical predictions of Bueche. Assuming that entanglements exist at uniform intervals along each chain, i.e. that there is a fixed molecular weight (M_e) between entanglement points, Bueche[4] derives a rather complex relationship between η and M which is essentially continuous, but which approximates to $\eta = K_1 M$ for $M \ll 2 M_e$ and to $\eta = K_2 M^{3\cdot5}$ for $M \gg 2M_e$.

The only limitation which has been found with equation (2) is at higher molecular weights, where slopes are often considerably higher than 3·4, e.g. data by Porter and Johnson[7] on polyethylene glycol show a slope of approximately 7. In such cases there is obviously a deviation from Bueche's theory.

GENERAL FORM OF VISCOSITY—MOLECULAR WEIGHT RELATIONSHIP

Consider the interaction of two neighbouring chains of molecular weight M. The probability of entanglement will be proportional to the product of the chain lengths, i.e. to M^2. The number of primary entanglements associated with a given chain A can thus be expressed by kM^2. Again, each chain which is attached to A will have kM^2 entanglements with its neighbours. Accordingly the number of effective secondary entanglements with chain A will be proportional to M^4. Similarly there will be tertiary entanglements involving M^6.

For unit velocity gradient the viscous drag on molecule A can be obtained by summing the contributions due to primary, secondary and higher order entanglements. It can thus be expressed in the form of a series, $f = A_1 M^2 + A_2 M^4 + A_3 M^6 + \ldots$. In addition there will be a frictional term $A_0 M$ to represent the force required to drag the molecule through its surroundings in the absence of entanglement. Hence the total drag is given by

$$F = A_0 M + A_1 M^2 + A_2 M^4 + A_3 M^6 + \ldots\ldots \tag{3}$$

At zero rate of shear the molecules will be in the entangled state and the viscosity (η_0) will be given by the product FN, where N is the number of molecules in unit volume. Since N is inversely proportional to M this leads to a general relationship of the form

$$\eta_0 = a_0 + a_1 M + a_2 M^3 + a_3 M^5 + \ldots\ldots \tag{4}$$

In practice experimental data can usually be represented quite adequately by reducing the equation to three terms in the form

$$\eta_0 = a_1 M + a_2 M^3 + a_3 M^5 \tag{5}$$

239

and evaluating the three coefficients by the solution of simultaneous equations at three suitable values of M.

EVIDENCE FROM THE LITERATURE

In order to avoid any errors associated with reading from graphs this analysis has been restricted to data published in tabular form.

Figures 1 and *2* show data published by Flory[9] on poly(decamethylene adipate) and re-examined by Fox *et al*[1]. In accordance with the Flory equation a plot of log η_0 against $M_w^{\frac{1}{2}}$ (*Figure 1*) gives an excellent straight line and there
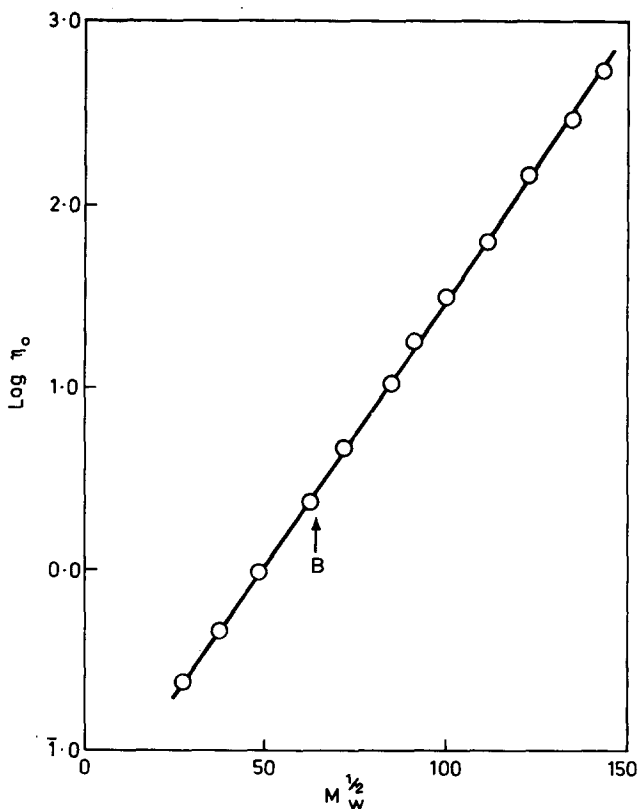
Figure 1 Log η_0 versus $M_w^{\frac{1}{2}}$ plot for decamethylene adipate[9] at 109 °C

is no suggestion of a transition at a critical molecular weight. The point B corresponds to the value of M_c quoted by Fox. The log η_0 versus log M_w plot,

240

represented by Fox with two straight lines, is shown in *Figure 2* as a continuous curve. There is no reason to regard this behaviour as anomalous and other examples of continuous curves are shown in the literature. An excellent example is the curve for polyethylene glycol shown by Porter and Johnson[7].

The dotted lines in *Figure 2* and subsequent figures are tangents with slopes of 1 and 3·4. A rapid check on the validity of equation (2) is provided by the
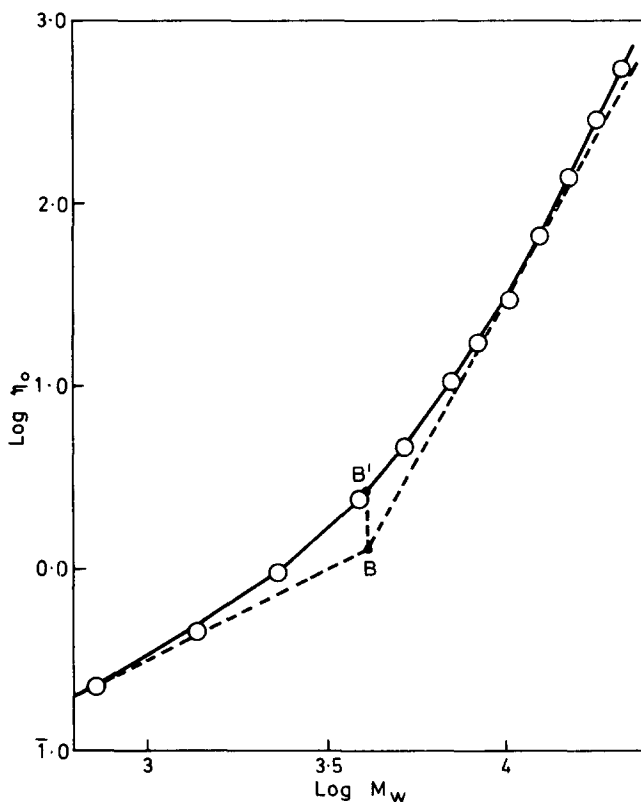
Figure 2   Log η_0 versus log M_w plot for decamethylene adipate[9]. Curve computed from equation (5)

consideration that the point of intersection B defines a molecular weight where $K_1 M = K_2 M^{3\cdot4}$ and hence where the viscosity calculated from equation (2) will be twice the value given by equation (1a) or (1b). Thus if a vertical line is drawn from B to meet the curve in B' the distance BB' should equal log 2, i.e. 0·3. In *Figure 2* the measured distance BB' is approximately 0·29. At higher molecular weights the slope becomes significantly greater than 3·4 and there is a corresponding deviation from equation (2).

Equation (2) gives a very adequate representation of the data of Allen and Fox[10] on anionic polystyrenes, shown in *Figure 3*. It is equally satisfactory

241

for the data of Gruver and Kraus[11] and of Boyce *et al*[5] on polybutadienes, and the data of Gupta and Forsman[6] on concentrated polystyrene solutions.

Figure 4 shows data by Ninomiya, Ferry and Oyanagi[12] on poly(vinyl acetate). Again equation (2) is much better than equation (1) but there is deviation at higher molecular weights, where the slope reaches approximately 4·5. A similar slope is shown in data by Bueche[13] on 14% polystyrene solutions. In each case equation (5) gives a good representation. In *Figures 2, 3* and *4* the experimental points are shown in relation to the curve computed from equation (5).
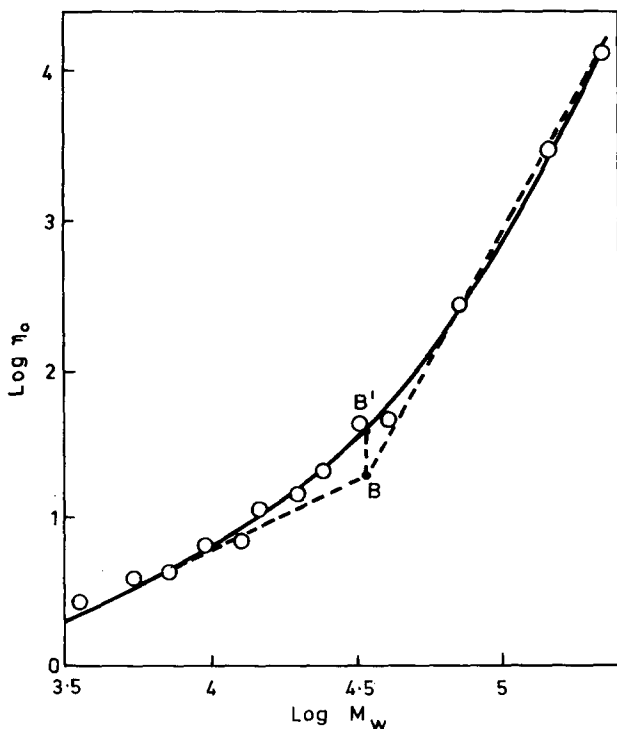
Figure 3 Data for anionic polystyrene[10] at 217°C in relation to curve computed from equation (5)

The analysis emphasises the essentially continuous nature of the η_0/M_w relationship. In all cases equation (2) gives a much better representation of the data than the widely used equations (1a) and (1b), and this gives a different interpretation to the significance of M_c. It is clear that equation (4) is a more general relationship with a very wide application.
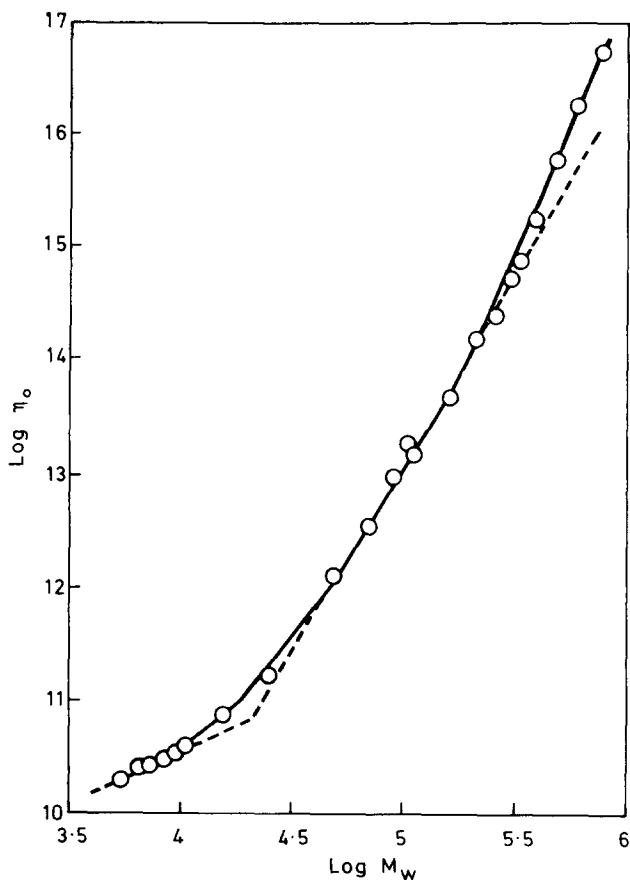
Figure 4 Data for poly(vinyl acetate)[12] at 40 °C in relation to curve
computed from equation (5)

ACKNOWLEDGEMENT

REFERENCES

1 Fox, T. G., Gratch, S. and Loshaek, S. 'Rheology', (ed. F. R. Eirich) Vol. 1, p 431,
  Academic Press, New York, 1956

2 Bueche, F., *J. Chem. Phys.* 1952, **20**, 1959
3 Bueche, F., *J. Chem. Phys.* 1956, **25**, 599
4 Bueche, F., 'Physical Properties of Polymers', pp 67–83, Interscience Publishers, New York, London, 1962
5 Boyce, R. J., Bauer, W. H. and Collins, E. A. *Trans. Soc. Rheol.* 1966, **10**, 545
6 Gupta, D. and Forsman, W. C. *Macromolecules* 1969, **2**, 304
7 Porter, R. S. and Johnson, J. F. *Trans. Soc. Rheol.* 1962, **6**, 107
8 Schreiber, H. P., Bagley, E. B. and West, D. C. *Polymer, Lond.* 1963, **3**, 355
9 Flory, P. J., *J. Amer. Chem. Soc.* 1940, **62**, 1057
10. Allen, V. R. and Fox, T. G., *J. Chem. Phys.* 1964, **41**, 337
11 Gruver, J. T. and Kraus, G. *J. Polym. Sci. (A)* 1965, **2**, 797
12 Ninomiya, K., Ferry, J. D. and Oyanagi, Y., *J. Phys. Chem.* 1963, **67**, 2297
13 Bueche, F. *J. appl. Phys.* 1953, **24**, 423

244

Thermodynamics of polymerization of heterocyclic compounds:
Part 6. The heat capacity, entropy, enthalpy and free energy of 1,3-dioxepan and poly-1,3-dioxepan

G. A. CLEGG AND T. P. MELIA

An adiabatic vacuum calorimeter and a differential scanning calorimeter have been used to measure the heat capacities of 1,3-dioxepan and poly-1,3-dioxepan from 80°K to 360°K. An estimate has been made of heat capacity values below 80°K for both monomer and polymer. Entropy, enthalpy and free energy values have been derived and are listed at 10°K intervals for the monomer and 50% crystalline polymer. For 1,3-dioxepan the melting temperature and heat of fusion were found to be 197·60 ± 0·05°K and 96·78 ± 0·30Jg^{-1}, respectively. For the poly-1,3-dioxepan the glass transition temperature, melting point and heat of fusion were found to be 189°K, 296 ± 1°K and 140·3 ± 2·8Jg^{-1}, respectively. Estimates have been made of the heat capacities of 100% crystalline and completely amorphous poly-1,3-dioxepan. The increase in heat capacity of the amorphous polymer at the glass transistion temperature, $10·7J°K^{-1}$ mole bead^{-1}, is in agreement with that predicted on the basis of the hole theory of melting. The entropy of polymerization $\Delta S^0_{gc'}$ has been calculated as $-181·5 \pm 6·4J°K^{-1}$ mole^{-1}.

THIS PAPER is the sixth in a series[1-5] concerned with the thermodynamics of polymerization of oxygen-containing heterocyclic compounds. Heat capacity measurements on 1,3-dioxepan and poly-1,3-dioxepan over the temperature range 80–360°K are described. The results have been used to estimate the entropy of the monomer and polymer and to derive the Third Law values of $\Delta S^0_{1c'}$ and $\Delta S^0_{gc'}$.

EXPERIMENTAL

Calorimetry

Two calorimeters were employed. A precision, adiabatic, vacuum calorimeter, which has been described previously[1], and a Perkin Elmer differential scanning calorimeter[6] (DSC). The weights of 1,3-dioxepan and poly-1,3-dioxepan used in the adiabatic vacuum calorimeter were 24·904g and 17·213g, respectively. The weights of polymer used in the DSC varied between 35 and 45mg. A heating rate of 4°K/min was employed in the DSC measurements.

Materials

1,3-Dioxepan. Prior to sealing in the adiabatic vacuum calorimeter 1,3-dioxepan was distilled on a 90cm column and the fraction of boiling point

393°K (753 mmHg) was collected. The reagent was then stirred over lithium aluminium hydride *in vacuo*, before being distilled into the calorimeter.

Poly-1,3-dioxepan. The polymerization of 1,3-dioxepan was carried out *in vacuo* under anhydrous conditions. Monomer (26 ml) and methylene dichloride (64 ml) were distilled into a 150 ml reaction vessel containing a phial of perchloric acid initiator (10^{-4} molar) in methylene dichloride solution. The vessel was cooled to 228°K and the phial broken. Polymerization was allowed to proceed for 2 h and termination was brought about by introducing dry ammonia into the reaction vessel. The methylene dichloride was removed from the polymer by evaporation on a water bath and the polymer was then heated in a vacuum oven at 320°K for about 24 h and finally allowed to cool to room temperature. The molecular weight of the polymer was determined on a Mecrolab vapour pressure osmometer (Model 301 A) and yielded a value of $\bar{M}_n = 72000$. The polymer is thought to be cyclic[7].

RESULTS

1,3-Dioxepan

The observed values of the heat capacity are presented in *Figure 1*. Smoothed values of the heat capacity, together with derived values of the entropy, enthalpy and free energy are presented in *Table 1*. The heat capacity data below 80°K were obtained using the extrapolation procedure of Kelley, Parks and Huffmann[8]. Cycloheptane, for which reliable heat capacity data are available, was chosen as the standard substance for this extrapolation. Since a considerable amount of pre-melting occurs in the monomer at temperatures above 160°K the smoothed values of the heat capacity shown in *Table 1* were corrected for pre-melting by extrapolating the data for the solid from below 160°K to the melting point (197·6°K). It is necessary to correct the measured heat capacity, C, to the quantity, C_{sat}. This correction, which makes allowance for the fact that the measured heat capacity includes some heat of vaporization, may be effected by means of equation 3 of reference 3. The term dP/dT in this equation was evaluated from the relationship

$$\log P[\text{mmHg}] = 8\cdot372 - (2\,142/T) \qquad (1)$$

which was obtained from previously published data[10]. The heat capacity of liquid 1,3-dioxepan (C_m) may be represented by

$$C_m = 1\cdot021 + 2\cdot595 \times 10^{-3}T \,[\text{J}°\text{K}^{-1}\text{g}^{-1}] \qquad (2)$$

The melting of 1,3-dioxepan has been studied under equilibrium conditions in order to determine its true melting temperature and to assess its purity. The method used has been described previously[5]. The melting point and total impurity present were $197\cdot60 \pm 0\cdot05$°K and $0\cdot09 \pm 0\cdot05$ mole %, respectively. The results of three determinations of the heat of fusion in the adiabatic, vacuum calorimeter were 96·73, 96·82 and 96·77 J g^{-1}. These yield the value $96\cdot78 \pm 0\cdot30$ J g^{-1} for the heat of fusion.

The results obtained in the present investigation, together with vapour pressure data derived from equation (1), have been used to calculate the

Table 1 Smoothed values of the heat capacity, entropy, enthalpy and Gibbs free energy for 1,3-dioxepan

Temperature [$^\circ$K]	C [$J^\circ K^{-1}g^{-1}$]	$S_T^0 - S_0^0$ [$J^\circ K^{-1}g^{-1}$]	$H_T^0 - H_0^0$ [Jg^{-1}]	$-(G_T^0 - G_0^0)$ [Jg^{-1}]
0	0·0	0·0	0·0	0·0
10	0·017	0·008	0·05	0·03
20	0·105	0·042	0·60	0·25
30	0·215	0·105	2·19	0·97
40	0·298	0·179	4·76	2·38
50	0·367	0·253	8·09	4·54
60	0·424	0·325	12·06	7·43
70	0·474	0·394	16·56	11·03
80	0·522	0·461	21·55	15·30
90	0·565	0·525	26·98	20·23
100	0·607	0·586	32·84	25·79
110	0·648	0·646	39·12	31·95
120	0·690	0·704	45·81	38·70
130	0·731	0·761	52·91	46·03
140	0·771	0·817	60·42	53·92
150	0·812	0·871	68·34	62·36
160	0·852	0·925	76·65	71·34

Extrapolated data for the solid

170	0·891	0·978	85·36	80·86
180	0·930	1·030	94·47	90·89
190	0·969	1·081	103·7	101·45
197·57	0·995	1·120	111·6	109·86

Liquid

197·57	1·533	1·609	208·4	109·86
200	1·539	1·624	211·5	113·4
210	1·565	1·700	227·0	130·1
220	1·591	1·774	242·8	147·4
230	1·617	1·845	258·8	165·5
240	1·643	1·914	275·1	184·3
250	1·669	1·982	291·7	203·8
260	1·695	2·048	308·5	223·9
270	1·721	2·112	325·6	244·8
273·16	1·729	2·132	331·1	251·3
280	1·747	2·175	342·9	266·2
290	1·773	2·237	360·5	288·3
298·16	1·794	2·287	375·1	306·8
300	1·799	2·300	378·4	310·9
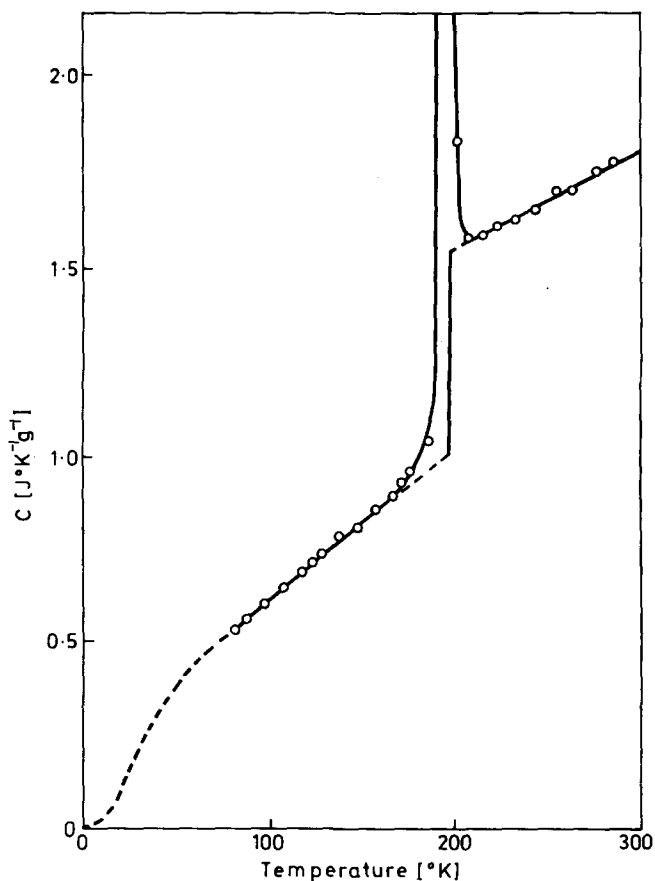
Figure 1 Observed values of the heat capacity for 1,3-dioxepan

entropy of 1,3-dioxepan gas at 1 atm and 298·16°K. The results of this calculation are presented in *Table 2*.

Poly-1,3-dioxepan

The observed values of the heat capacity are presented in *Figure 2*. Smoothed values of the heat capacity, together with derived values of the entropy, enthalpy and free energy are presented in *Table 3*. The heat capacity data below 80°K were obtained using the Kelley, Parks and Huffmann extrapolation procedure. Polyoxymethylene[11] (Delrin) was chosen as the

248

Table 2 Entropy of 1,3-dioxepan gas at 1 atm pressure and 298·16 K

Source of data	Entropy contribution [J K^{-1} mole^{-1}]
$S_{80}^0 - S_0^0$ (Kelley, Parks and Huffman extrapolation)	47·1 ± 2·4
$\int_{80}^{197·57} (C/T)dT$	67·3 ± 0·2
ΔS(fusion)	49·9 ± 0·3
$\int_{197·57}^{298·16} (C/T)dT$	69·2 ± 0·2
$\Delta S_{298·16}$ (vaporization)	137·5 ± 1·4
$\Delta S = -R \ln(15·5/760)$	32·4 ± 0·3
Entropy of gas at 298·16 K	338·6 ± 4·8
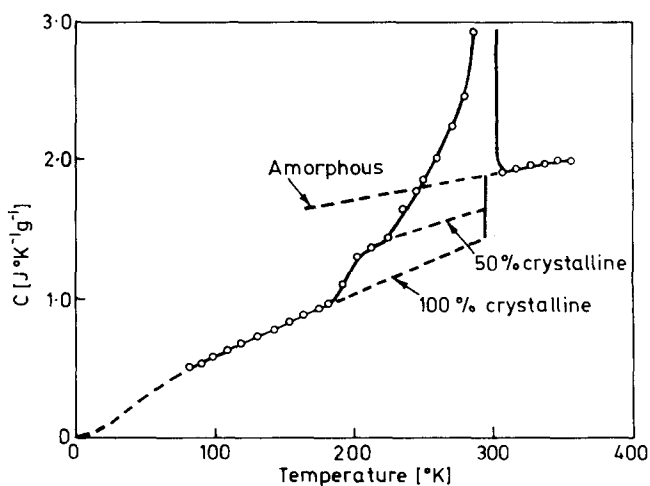
Figure 2 Observed heat capacities of 50% crystalline poly-1,3-dioxepan

Table 3 Smoothed values of the heat capacity, entropy, enthalpy and free energy for poly-1,3-dioxepan (50% crystalline)

Temperature [°K]	C [J°K^{-1}g^{-1}]	$S_T^0 - S_0^0$ [J°K^{-1}g^{-1}]	$H_T^0 - H_0^0$ [Jg^{-1}]	$-(G_T^0 - G_0^0)$ [Jg^{-1}]
0	0·0	0·0	0·0	0·0
20	0·072	0·026	0·39	0·14
40	0·243	0·130	3·59	1·62
60	0·381	0·256	9·89	5·47
80	0·496	0·381	18·65	11·86
90	0·544	0·443	23·85	15·98
100	0·592	0·502	29·53	20·70
110	0·639	0·561	35·69	26·02
120	0·686	0·619	42·32	31·92
130	0·732	0·675	49·41	38·39
140	0·777	0·731	56·96	45·42
150	0·820	0·786	64·94	53·01
160	0·861	0·841	73·34	61·15
170	0·905	0·894	82·15	69·82
180	0·950	0·947	91·44	79·02
190	1·070	1·001	101·4	88·79
200	1·291	1·061	113·1	99·10
210	1·401	1·127	126·7	109·9
215	1·418	1·160	133·8	115·6

Extrapolated data for the solid

220	1·434	1·193	140·9	121·5
230	1·464	1·257	155·4	133·7
240	1·494	1·320	170·2	146·6
250	1·525	1·382	185·3	160·1
260	1·555	1·442	200·7	174·3
270	1·585	1·501	216·4	188·9
273·16	1·595	1·520	221·5	193·7
280	1·616	1·560	232·4	204·3
290	1·646	1·617	248·7	220·2
296	1·664	1·651	258·6	230·1

Liquid

296	1·898	1·888	328·8	230·1
298·16	1·902	1·902	332·9	234·2
300	1·905	1·914	336·4	237·7
310	1·923	1·976	355·5	257·1
320	1·940	2·038	374·9	277·2
330	1·958	2·098	394·3	297·8
340	1·975	2·156	414·0	319·1
350	1·993	2·214	433·9	340·9
360	2·010	2·270	453·9	363·4

standard substance for this extrapolation. Between 220°K and 296°K the heat capacity data represented by the broken line (50% crystalline) in *Figure 2* are tabulated. This is necessary because of the large amount of pre-melting which occurs in the polymer. The heat capacities of the 100% crystalline (C_c) and amorphous (C_a) polymer between the glass transition temperature (189°K) and the melting point (296°K) have been estimated using the method described previously[2]. The relevant equations are:

$$C_a = 1·380 + 1·76 \times 10^{-3}T \, [\text{J°K}^{-1}\text{g}^{-1}] \qquad (3)$$

$$C_c = 0.189 + 4.20 \times 10^{-3}T \, [\text{J}^\circ\text{K}^{-1}\text{g}^{-1}] \tag{4}$$

The crystallinity of the polymer was estimated using equation 11 of reference 5. The value obtained for the weight fraction crystallinity is 0.50.

The heat of fusion of the semi-crystalline polymer was calculated using equation 6 of reference 12. This was used in conjunction with equation 3 of reference 12 to calculate the heat of fusion of the 100% crystalline polymer. The value obtained is $140.3 \pm 2.8 \, \text{Jg}^{-1}$.

DISCUSSION

The increase in heat capacity $(C_a - C_c)$ for poly-1,3-dioxepan at the glass transition temperature $(10.7 \, \text{J}^\circ\text{K}^{-1}$ mole bead$^{-1})$ is in agreement with the findings of Wunderlich[13].

The entropy changes associated with the polymerization of gaseous (1 atm, 298.16°K) and liquid (15.5 mmHg, 298.16°K) 1,3-dioxepan to the crystalline and the amorphous polymer, respectively, are shown in *Table 4*. The $\Delta S_{gc}'$ value obtained in this work $(-181.5 \, \text{J}^\circ\text{K}^{-1}\text{mole}^{-1})$ compares with that of $-181.3 \, \text{J}^\circ\text{K}^{-1}\text{mole}^{-1}$ obtained for the polymerization of cyclo-heptane[9] to polyethylene[14].

Table 4 Entropies of polymerization of 1,3-dioxepan at 298.16 K

State of monomer	State of polymer	Monomer entropy [J K^{-1} mole^{-1}]	Polymer entropy [J K^{-1} mole^{-1}]	Entropy of polymerization [J K^{-1} mole^{-1}]
Gas (1 atm)	crystalline	338.6 ± 4.8	157.1 ± 1.6	−181.5 ± 6.4
Gas (1 atm)	amorphous	338.6 ± 4.8	194.2 ± 2.4	−144.4 ± 7.2
Liquid (15.5 mmHg)	crystalline	233.5 ± 3.1	157.1 ± 1.6	−76.4 ± 4.7
Liquid (15.5 mmHg)	amorphous	233.5 ± 3.1	194.2 ± 2.4	−39.3 ± 5.5

ACKNOWLEDGEMENTS

*Department of Chemistry
and Applied Chemistry,
University of Salford*

(Received 26 September 1969)
(Revised 30 January 1970)

REFERENCES

1 Clegg, G. A., Melia, T. P. and Tyson, A. *Polymer, Lond.* 1968, **9**, 75
2 Clegg, G. A., Gee, D. R., Melia, T. P. and Tyson, A. *Polymer, Lond.* 1968, **9**, 501
3 Clegg, G. A. and Melia, T. P. *Makromol. Chem.* 1969, **123**, 184

4 Clegg, G. A. and Melia, T. P. *Makromol. Chem.* 1969, **123**, 194
5 Clegg, G. A. and Melia, T. P. *Polymer, Lond.* 1969, **10**, 912
6 O'Neill, M. J. *Analyt. Chem* 1964, **36**, 1238
  O'Neill, M. J., Justin, J. and Brenner, N. *Analyt. Chem.* 1964, **36**, 1233
7 Plesch, P. H. and Westermann, P. H. *Polymer, Lond.* 1969, **10**, 105
8 Kelley, K. K., Parks, G. S. and Huffman, H. M. *J. phys. Chem.* 1929, **33**, 1802
9 Finke, H. L., Scott, D. W., Gross, M. E., Messerley, J. F. and Waddington, G. *J. Amer. Chem. Soc.* 1956, **78**, 5469
10 Skuratov, S. M., Strepikeev, A. A., Shtekher, S. M. and Volokhina, S. V. *Dokl. Akad. Nauk SSSR* 1957, **117**, 263
11 Dainton, F. S., Evans, D. M., Hoare, F. E. and Melia, T. P. *Polymer, Lond.* 1962, **3**, 263
12 Gee, D. R. and Melia, T. P. *Makromol. Chem.* 1968, **116**, 122
13 Wunderlich, B. *J. phys. Chem.* 1960, **64**, 1052
14 Dainton, F. S., Evans, D. M., Hoare, F. E. and Melia, T. P. *Polymer, Lond.* 1962, **3**, 277

Heterogeneous nucleation in the crystallization of polyolefins:
Part 1. Chemical and physical nature of nucleating agents*

F. L. BINSBERGEN

Nucleating agents for polyolefins are insoluble in the polymer melt and are probably always crystalline substances. The great majority of these agents expose a surface consisting of hydrocarbon groups resembling moderate to good solvents for the polymers, their insolubility being due to a layer-like arrangement of their strongly polar parts. Increasing the solubility by changing the structure, by mixing, or by addition of other substances results in a reduced nucleating effect. Epitaxy is ruled out as a mechanism for the nucleating effect. The nucleating surfaces are rather low energy surfaces. Alignment of polymer molecules along the rows of hydrocarbon groups in the exposed surface is suggested as the cause of the effect.

THE VARIOUS types of nucleation occurring in the crystallization of polymers are known to be[1] spontaneous, heterogeneous and orientation-induced nucleation and recrystallization after incomplete melting. We now want to present a study of one of these types – namely heterogeneous nucleation – in a series of papers. The present one deals with the nature of nucleating substances, a second with the crystallization kinetics of a polymer containing purposely added nucleating agents and a third with the theory of heterogeneous nucleation in relation with the phenomena observed.

Crystallizing polymers, when cooled down from the unoriented melt, generally crystallize on heterogeneities such as catalyst remnants, dust particles and the like[1,2]. However, the exact nature of these particles is largely unknown. Moreover, the nucleation is a rather uncontrolled phenomenon in practice, the nucleation density being frequently inhomogeneous in a polymer sample while considerable variations have been found between batches of the same polymer from different sources.

Certain substances, when incorporated in a polymer melt, promote abundant nucleation. These substances are then called nucleating agents. A large number of nucleating agents for polyolefins have been discovered by Wijga[3,4], Wales[5], the author[4,6], and several other investigators[7-9].

These agents make good control of the nucleation density and its homogeneity possible[10]. This leads to an improvement in several product properties, such as a greater transparency and surface gloss, less void formation in injection-moulded objects and a marked improvement in impact strength. The rate of crystallization is also increased, leading to shorter processing cycles.

---

* This paper is largely based on a part of the author's doctoral thesis[1]

P—S

The present investigation is aimed at finding a possible common feature in the chemical structure of the nucleating agents and defining their physical state. We then hope that we will be able to apply our conclusions to hetero-geneous nucleation in general with the reservation that the nucleating agents which are added on purpose may differ from the nucleating impurities present in the plain polymer.

To this end we tested about 2000 substances for their possible nucleating effect on the crystallization of polyolefins. The testing was mainly done in polypropylene, but substances active in polypropylene invariably showed a similar effect in other polyolefins, such as polyethylene and poly-4-methylpentene-1, as well as in isotactic polystyrene.

The nucleating effect is observed as a considerable decrease in the spherulite size with respect to the base polymer and as an increase in crystal-lization temperature at a constant cooling rate. It is considerably influenced by the degree of dispersion of the nucleating agent. Since the degree of dispersion was different for the various substances and also for the various methods of incorporation in the polymer, we restricted ourselves mainly to rather qualitative observations.

The disperson was sometimes so effective – especially after *in situ* formation of a nucleating agent by reaction of soluble reagents – that on microscopic examination no particulate matter could be found in the polymer melt, thus suggesting a possible dissolution of the agent. The question then arose as to whether molecularly dispersed material could have nucleating ability, e.g. as a counterpart of the condensation of supersaturated water vapour at ions; or whether the nucleating species could be in a state of micellar dissolution, a state actually observed for several organic metal salts having a large hydrocarbon part in the molecule. Many nucleating agents are indeed found among metal carboxylates, sulphonates, etc. Several experiments were carried out to determine the possible solubility of nucleating agents and chemically related compounds as well as to study the solubilization of nucleating agents by addition of either nucleating or non-nucleating substances to the polymer.

Epitaxial nucleation excepted, little is known about the mechanism of heterogeneous nucleation and about the requirements for a nucleating agent to be an effective one. The basic idea underlying most pictures of hetero-geneous nucleation is that the total interfacial free energy of the crystalline embryo is reduced by a foreign phase which already provides part of the interface to be formed; this brings about a reduction in the activation free energy for nucleation and thereby a decrease in the degree of supercooling required for nucleation. The higher the preference of the crystalline phase to adsorb at the foreign material rather than the liquid phase, the lower the activation free energy for nucleation will be.

The amount of reduction in interfacial free energy is dependent on both the geometrical form of the foreign phase and its chemical nature. Here the question arises as to whether the nucleating species has to be a solid – either an amorphous or a crystalline solid – or whether it can also be a liquid. We have devoted several experiments to this problem. In the case of a liquid there is little discussion on geometry of the surface. The effects of different shapes

of crystalline surfaces have been indicated previously[1]. Porosity of amorphous solid materials may be important as regards their nucleating properties.

Special treatments of the nucleating material, such as grinding or milling it in the presence of a contact liquid, had often an important influence on the nucleating effect, probably as a result of modification of the surface of the particles.

Certain non-nucleating substances showed a detrimental influence on the nucleating effect when mixed with the polymer containing a nucleating agent. We will try to interpret the effects of both mixtures and special treatments.

There is no point in classifying the nucleating agents with respect to the degree of activity, since little is known about the factors governing the activity of each substance (such as degree of dispersion and purity). Moreover, it was often possible for a weak or a moderate nucleating effect of a certain additive to be upgraded by purification of the substance or by a grinding treatment in the presence of a contact liquid.

<div align="center">EXPERIMENTAL</div>

(A) *Samples*

Several of the polypropylene samples used were from pilot-plant or from commercial production. Most of them were in the range of injection-moulding grades. The Shell materials used contained catalyst remnants of a level of roughly 20 ppm aluminium and 20 ppm titanium. One BASF sample was virtually free of catalyst remnants and will be denoted by 'ash-free' polypropylene.

The polyethylene samples used were Carlona grades from Shell Chemical Co., Carrington, U.K. and Hostalen grades from Farbwerke Hoechst, West Germany. These samples were Ziegler-type polyethylenes.

Poly-4-methylpentene-1 and isotactic polystyrene were prepared in laboratory-scale polymerizations by Dr van Amerongen.

The substances to be tested for their nucleating effect were for the larger part obtained from stock. Several metal salts or organic acids were prepared either by titration in aqueous or in alcoholic solution or by aqueous metathesis resulting in precipitation of the salt (see below). The pigments tested were purchased from various firms.

(B) *Incorporation of nucleating agents into the polymers*

Method 1. For quick testing the following procedure was used. Quantities of 1 to 2 mg of additive and 200 mg of polymer fluff were mixed for 5 min in a high-speed vibration ball mill (Unicam V.M. Mark II). This tiny ball mill has both a mixing action and a strong grinding action. In most cases the dispersed additive – when not dissolved in the polymer – showed a wide range of particle sizes up to several micrometres.

Method 2. Very fine dispersions could be obtained by dissolving an additive in 10 to 20 ml of a low-boiling-point liquid (water, ethanol, acetone or

hexane), adding this solution to 10 to 20g of polymer fluff in a shallow bowl and evaporating until almost dry on a steam bath while stirring with a spatula. If water was the solvent, 10 vol. % ethanol was added for wetting the polymer and during evaporation some more ethanol was added in order to expel the water. After this treatment the polymer was dried for several hours at 60°C under nitrogen at a reduced pressure (approximately 100 mmHg).

Then 0·15 to 0·3 wt. % of an antioxidant, Ionox 330*, was added, the sample was milled on a two-roll mill for 5 min at 180°C and subsequently pressed to a sheet of 0·5 or 1 mm thickness at 270°C.

Method 3. Various insoluble metal salts of carboxylic acids could be finely dispersed into the polymer by precipitating them onto the polymer fluff. The salts were prepared by aqueous metathesis in a slurry of polymer fluff in water containing 10 vol. % ethanol. The alcohol was added in order to ensure wetting of the polymer fluff.

The reaction schemes for bivalent metals are:

$$MSO_4[or\ M(NO_3)_2] + 2\ NaZ \rightarrow MZ_2 \downarrow + Na_2SO_4 \qquad (1a)$$
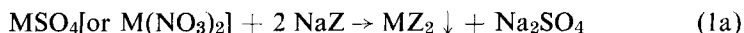
in which HZ is the carboxylic acid in question, or:

$$MSO_4 + NaZ + NaOH \rightarrow M(OH)Z \downarrow + Na_2SO_4 \qquad (1b)$$

Salts of trivalent metals were prepared according to:

$$M_2(SO_4)_3 + 4\ NaZ + 2\ NaOH \rightarrow 2\ M(OH)Z_2 \downarrow + 3\ Na_2SO_4 \qquad (2a)$$

or:

$$M_2(SO_4)_3 + 2\ NaZ + 4\ NaOH \rightarrow 2\ M(OH)_2Z \downarrow + 3\ Na_2SO_4 \qquad (2b)$$
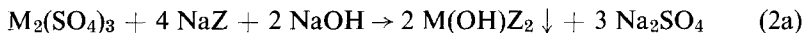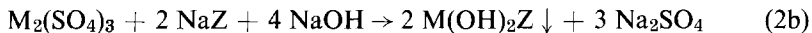
The preparation of tricarboxylates in aqueous environment is not possible for aluminium, gallium or indium[11-13]. Attempts in this direction invariably result in an intimate mixture of the basic salt and the free acid, from which the acid can easily be extracted or evaporated:

$$M_2(SO_4)_3 + 6\ NaZ + 2\ H_2O \rightarrow 2\ M(OH)Z_2.HZ \downarrow + 3\ Na_2SO_4$$
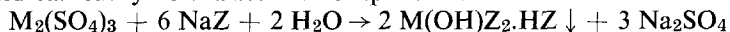
After the polymer containing the salts had been filtered off and washed with water and with acetone, it was dried, milled and compression-moulded as by Method 2.

Method 4. Dispersions invisible through the optical microscope using phase contrast optics at highest magnification (1 000 ×) were obtained by *in situ* preparation from reagents soluble in the polymer melt. Dry, powdered aluminium isopropoxide and *p*-tertiary-butylbenzoic acid in the ratio required for the dicarboxylate were blended with polymer fluff under nitrogen and either milled or extruded from a small extruder. The content of resulting nucleating agent was ill-defined, however, owing to incomplete reaction and to evaporation of reagents.

---

* Registered trade mark of Shell Chemical Co.

(C) *Assessment of nucleating effect*

The larger part of the testing was done by visual microscopy. A microscope specimen of $30-60\mu m$ thickness was obtained by pressing about 5 mg of a powder mixture or a piece of about 2 mg cut from a compression-moulded sheet between a slide and a cover glass at about $220°C$. The specimen was then kept at $240°C$ for approximately 1 min in order to allow strains induced by the pressing to relax, which was generally sufficient to avoid orientation-induced nucleation. Subsequently, the specimen was allowed to cool in air – when it crystallized – at a cooling rate of roughly $100°C/min$ (in the case of polypropylene and of polyethylene).

The spherulite size in the specimen was compared with that of plain polymer crystallized in the same way. A good nucleating effect was noted when the linear size of the spherulites in the test specimen was smaller than a certain fraction of the sizes in the control. This fraction was about $\frac{1}{10}$ for polypropylene and $\frac{1}{5}$ for polyethylene.

A number of polypropylene specimens were subjected to a somewhat less subjective method of testing: the depolarization of plane-polarized light was measured by means of a photomultiplier inserted into the microscope in place of the eyepiece.

This depolarization is defined as:

$$\Delta = (I - I_c)/I_p$$

in which I_p is the intensity measured with a bare slide between parallel polarizers, I_c the same between crossed polarizers and I the intensity measured with the specimen between crossed polarizers.

The discriminating power in the measurement of Δ is thus roughly a factor of 2 owing to the variations in sample thickness. Plain polypropylene showed a Δ of $5-10\%$. A good nucleating effect was noted for specimens of $\Delta < 1\%$.

(D) *Solubility tests*

The polymer melt itself is an inconvenient medium for testing the possible solubility of nucleating agents especially at the concentrations in which the latter are used. If a substance dissolves in the molten polymer at a certain elevated temperature and can separate out at a lower temperature it will supposedly be a long time before the phase separation can be observed because of the slow diffusion in the viscous melt. Aggregation of formed particles due to polar forces, as is often found in a low-molecular solvent, or precipitation due to gravity will not be observed at all.

Most solubility tests were therefore carried out with 1–5 wt. % dispersions of finely powdered substances in squalane (2,6,10,15,19,23-hexamethyl-tetracosane) up to its boiling point, $330°C$, or in molten paraffin wax up to $380°C$.

(E) *Solubilization tests*

By solubilization we mean a considerable increase in the solubility of an otherwise sparingly soluble substance in a given solvent owing to the addition

257

of (a small amount of) a third substance – without a noticeable chemical reaction taking place.

Metal stearates, not being nucleating agents, were tested for a possible solubilizing effect on salt-type nucleating agents, because they had an adverse influence on the nucleating effect of these agents.

Mixtures of nucleating agents sometimes showed a smaller nucleating effect than the individual substances.

Moreover, it is known that the solubility of alkali carboxylates, each of which is sparingly soluble in a hydrocarbon solvent, can be enhanced by mixing several of them together[14]. This might be termed mutual solubilization.

The mixtures were prepared in several ways:

(1) The components were powdered together in a mortar; a contact liquid was added if necessary.

(2) Intimate mixtures of aluminium salts of carboxylic acids were prepared by aqueous metathesis of aluminium sulphate, sodium hydroxide and a mixture of sodium salts of the acids wanted, according to reaction scheme (2a) (Section B).

(3) Intimate mixtures of sodium salts of carboxylic acids were made either by titrating a hot solution of the acids in ethanol with alcoholic sodium hydroxide or by reacting a solution of the acids in a hydrocarbon solvent with the stoichiometric quantity of a 50wt. % sodium suspension in paraffin wax.

(4) Similar mixtures of lithium salts were made by reacting a solution of the acids in a hydrocarbon solvent with a dilute solution of sec-butyl lithium, moisture and oxygen being excluded.

In a test tube, 5wt. % of the salt mixture was stirred in squalane. The temperature at which complete dissolution occurred was noted. Subsequent cooling often caused formation of a gel. Then the test tube was heated again until the gel became liquid; the corresponding temperature was called *gel point*.

The mixtures of alkali salts showed a long range of melting. This range was estimated and the highest melting temperature of the mixture was noted.

(F) *Grinding treatments of salts with various contact liquids*

Several aluminium carboxylates, prepared in water and subsequently dried, are difficult to disperse in the polymer melt. The particles, often of sizes up to 100μm, are believed to be aggregates of much smaller particles. Mechanical treatment together with the action of a dispersing liquid might break the aggregates into very small particles. Two different treatments were tried with some success:

(a) The salt was ball-milled with a contact liquid for 1 to 4 days.

(b) The salt was soaked with squalane and milled to a paste on a 3-roll paint mill. After repeated milling, addition of dry salt was necessary

to maintain the consistency of the paste. The ultimate solids content after 5 to 10 passages over the paint mill varied from 40 to 50%.

After ball-milling, the salt was mixed with polypropylene powder in a powder blender and the mixture was milled on a two-roller mill at 180°C. The paste produced by the paint mill was added to polypropylene while the latter was on the two-roll mill. A powder blend of the original salt and polypropylene subsequently milled at 180°C served as a blank.

RESULTS

(A) *Groups of nucleating agents*
Without trying to produce a complete list, we want to give an impression of what kinds of substances were found to be nucleating agents:

(1) *Aluminium salts of*:
   aromatic and cyclo-aliphatic mono- and dicarboxylic acids, aliphatic
      a,ω-dicarboxylic acids,

   aliphatic monocarboxylic acids bearing aromatic or cyclo-aliphatic
      substituents,

   aromatic phosphonic acids,

   phosphoric and phosphorous acid, partially esterified to aromatic esters.

The hydrocarbon part of the molecule generally did not carry any polar substituents other than the acid group(s) mentioned. If in the hydrocarbon part one or more hydrogens had been replaced by polar groups such as $-NH_2$, $-OH$, $-NO_2$, $-OCH_3$, $-(CO)-O-CH_3$, etc., the nucleating effect was often negligible. Exceptions to this rule were the aluminium salts of e.g. p-hydroxy- and p-nitrobenzoic acid.

(2) *Alkali salts of*:
   all the acids mentioned under (1), together with various of these acids
      carrying one polar substituent, except aliphatic a,ω-dicarboxylic acids,

   short, branched-chain aliphatic monocarboxylic acids,

   aromatic, cyclo-aliphatic and branched-chain aliphatic sulphonic acids.

(3) *Several salts of divalent metals*, such as Ca, Ba, Cu and Co; of *trivalent metals*, Ga and In; and of *tetravalent metals*, Ti and V (in the form of the titanyl and vanadyl ions, respectively)
      with a number of the acids mentioned above.

(4) *Various organic pigments*, such as:
   copper phthalocyanine and chlorinated copper phthalocyanine,

   anthraquinone type pigments of condensed aromatic structure, such as
      flavanthrone,

   quinacridones[15],

perylene[15] type pigments,

some azo-pigments carrying sodium, calcium or barium sulphonate groups.

(5) *Colloidal silver and gold.*

(6) *Hydrazones.* The only non-salt, non-pigment type organic substances found to show nucleating activity were hydrazones, made by reaction of salicyl hydrazide with either benzaldehyde or salicylaldehyde.

Inorganic salts (e.g. NaCl, PbI_2, $BaSO_4$) and oxides (e.g. pyrogene or hydrated silica) were invariably found to be inactive, contrary to what has been claimed in several patents. Several alkali halogenides have been reported to act as epitaxial nucleating agents for polyethylene crystallizing from dilute solution[16-18]. In bulk polyethylene, however, they have only a weak effect, the degree of supercooling at which they become active[19] being larger than that either for the substances listed above or even for the impurities naturally present in plain polyethylene.

(B) *Solubility as a limiting factor for nucleating effect*

A large number of nucleating substances were tested for solubility. Nearly all of them proved to be insoluble in squalane up to its boiling point and/or in paraffin wax up to 380°C.

Exceptions were the sodium salts of cyclopentane carboxylic acid and of cyclopentyl acetic acid and the salicylhydrazones of benzaldehyde and salicylaldehyde. However, examination of a polypropylene melt containing one of these four substances showed that they precipitated upon cooling before the polymer itself started to crystallize. Keeping the polypropylene melt at a temperature somewhere between 190 and 270°C caused coarsening of the precipitated substance, which led to a substantial decrease in nucleating effect owing to the decrease in number of the nucleating particles.

On the other hand, fine dispersions of Na(PTBB) or Al(OH)(PTBB)$_2$ (PTBB = p-tert-butylbenzoate) in polypropylene did not coarsen when kept at 190°C for 4 days or when the polymer was swollen in decalin at 150°C for ½ h, and the nucleating effect did not change. This indicates that these salts are virtually insoluble because even a slow transport of salt molecules would have caused coarsening.

The nucleating effect of sodium and aluminium salts of the homologous series of p-n-alkylbenzoic acids was found to decrease with increasing length of the alkyl chain. The aluminium salts of p-methyl- and p-ethylbenzoic acid were good nucleators, those of p-n-propylbenzoic acid moderate ones and those of p-n-butylbenzoic acid weak ones, while those of p-n-heptylbenzoic acid did not show any nucleating effect. The last-mentioned salt dissolved in paraffin wax at 215°C. On the other hand, aluminium salts of p-t-butyl- and of p-neopentylbenzoic acid were very good nucleating agents. The substitution of a branched-alkyl chain is supposed to enhance the solubility to a smaller extent than does substitution of a normal alkyl chain.

With sodium salts of *n*-alkylbenzoic acids the nucleating effect disappears at a longer chain length than in the case of aluminium salts. The sodium salt of *p-n*-heptylbenzoic acid is still a moderate nucleating agent, but that of *n*-decylmandelic acid was not a nucleator and dissolved in paraffin wax at 275°C.

A similar effect of alkyl chain length on solubility and nucleating effect was found for sodium salts of a few *p-n*-alkylbenzene sulphonic acids.

(C) *Solubilization*

The results of the experiments on solubilization of two nucleating salts by stearates are given in *Table 1*.

It is seen from *Table 1* that stearates cause a salt-type nucleating agent to dissolve and thereby destroy its nucleating effect. For this effect to disappear,

Table 1 Dissolving temperature and gel point of stearate-nucleating agent mixtures in squalane

Salts	Molar proportions	Mixing method	Dissolves at [°C]	Gel point* [°C]
AlOH(ST)₂			200	70
AlOH(ST)₂ + AlOH(PTBB)₂	10:1	precipitation	200	70
AlOH(ST)₂ + AlOH(PTBB)₂	3:1	powder mixing	300	?
AlOH(ST)₂ + AlOH(PTBB)₂	3:1	precipitation	250	70
AlOH(ST)₂ + AlOH(PTBB)₂	1:1	precipitation	no dissolution	--
AlOH(PTBB)₂			no dissolution	--
Na(ST)			180	160
Na(ST) + Na(PTBB)	1:1	powder mixing	320	300
Na(ST) + Na(PTBB)	1:1	precipitation	200	200
Na(ST) + Na(PTBB)	1:3	precipitation	incomplete dissolution	310
Na PTBB			no dissolution	—

ST = stearate; PTBB = *p*-tert-butylbenzoate
* Gel point = temperature at which mixture becomes liquid on reheating

complete dissolution of the nucleating agent is not necessary, as we have often observed. The stearate probably adsorbs at the surface of the particles of the agent and changes their surface properties, or the particles are covered with a skin of a concentrated solution of stearate plus solubilized nucleating agent.

Several mixtures of nucleating salts showed a considerably smaller nucleating effect than the pure substances. For a few of these mixtures we tried to find a possible correlation with increased solubility (see *Table 2*).

The observed melting ranges were large. The initial melting temperature was difficult to determine, but was probably 100–150°C lower than the highest melting point. The same will be true of the temperature of initial dissolution. The absence of nucleating effect in the first three mixtures is most probably due to the formation of a skin of dissolved salt around the salt particles.

261

Table 2 Dissolving temperature in molten paraffin, highest point of melting range and nucleating effect in polypropylene of mixtures of alkali-carboxylates

Salt mixture	Dissolving temperature [°C]	Highest point of melting range [°C]	Nucleating effect
Li salt of pivalic acid β,β-dimethylbutyric acid cyclohexanecaroxylic acid cyclopentanecaroxylic acid cyclopentylacetic acid	230	240	none
Na salt of - pivalic acid β β-dimethylbutyric acid cyclohexanecarboxylic acid	320	350 (decomp.)	none
Na salt of pivalic acid β,β-dimethylbutyric acid cyclohexanecarboxylic acid p-tert-butylbenzoic acid	350 (decomp.)	350 (decomp.)	none
Na salt of p-isopropylbenzoic acid o-tert-butylbenzoic acid p-tert-butylbenzoic acid p-neopentylbenzoic acid o-hydroxybenzoic acid o-acetoxybenzoic acid p-chlorobenzoic acid	> 370	> 370	good

In the benzoate mixture no melting was observed. The melting points of the individual benzoates are 100–200°C higher than those of the aliphatic carboxylates and therefore we assume that the benzoate mixture is wholly crystalline when in the polypropylene melt, producing a nucleating effect comparable to that of the individual salts.

(D) *Physical state.of nucleating particles*

Once it had become clear that the dispersed nucleating agents do not dissolve in the polymer melt we investigated whether they might be in a crystalline, a solid amorphous or possibly a liquid state. Most of the nucleating agents are clearly crystalline materials, such as the sodium, calcium and copper salts of organic acids and the organic pigments.

However, nucleating aluminium carboxylates show considerably diffuse scattering in x-ray diffraction patterns, while some, e.g. aluminium salts of aliphatic dibasic carboxylic acids do not give any crystalline reflections. Basic aluminium carboxylates (tricarboxylates exist in completely anhydrous environment only) are association polymers containing $-Al-O-Al-O-$ | | H H

chains[20-23] while crosslinking over carboxylate groups is probable. The formation of such a structure during precipitation from water may hinder orderly crystalline packing, especially in the case of salts of dibasic acids. Moreover, in the preparation of an aluminium salt of a mixture of acids, a random placing of carboxylate groups may completely prevent crystallization in cases where the pure salts are semi-crystalline.

Thus, nucleating aluminium salts of benzoic-type acids are semi-crystalline, whereas an aluminium salt of an equimolar mixture of p-isopropyl, p-t-butyl-, p-neopentyl-, o-hydroxy-, o-acetoxy-, and p-chlorobenzoic acids, prepared by aqueous metathesis, was amorphous according to x-ray diffraction. This mixed salt did not show any nucleating effect in polypropylene, although it did not dissolve in the polymer melt.

Nucleating aluminium salts of several aliphatic dibasic carboxylic acids, prepared in water, are non-crystalline from their x-ray pattern. Yet it is not certain that they are truly amorphous substances, for two reasons:

(1) The monobasic aluminium salts of succinic, glutaric and adipic acids are all good nucleating agents. But comparable salts prepared from equimolar mixtures of two or three sodium carboxylates show hardly any nucleating ability at the same degree of dispersion in the polymer as the pure salts.

(2) Absence of clear x-ray reflections is not always a proof of non-crystallinity, as was demonstrated for freshly precipitated ferric hydroxide, which electron microscopy and electron diffraction showed to consist of extremely small lozenge-type crystals*. Moreover, aluminium adipate prepared in hot xylene from aluminium tri-isopropoxide and adipic acid showed some faint x-ray reflections and, unlike the salt prepared by aqueous metathesis, was birefringent while both had an about equivalent nucleating effect.

Liquids have not been found to nucleate polyolefin crystallization. As regards the nucleating effect claimed for glycerol in polypropylene[24], we have to make a clear distinction between the overwhelming nucleation caused by a finely dispersed material and relatively large droplets acting as crystallization centres without bringing about fine crystallization. The droplets of glycerol were so large that they might easily contain enough solid impurities for the observed low level[24] of nucleation of polypropylene.

Polypropylene finely divided in high-density polyethylene is a good nucleating agent for the latter[25], provided that, after blending and cooling, the polymer mixture is not heated above the melting point of polypropylene during reprocessing. However, if the mixture is cooled directly from a temperature above the melting point of polypropylene, the normal crystallization of straight polyethylene is found, because polypropylene crystallizes at such a high degree of supercooling that it is still molten at a temperature where polyethylene starts to crystallize. In other words: crystallized polypropylene nucleates high-density polyethylene, molten (and supercooled) polypropylene does not.

* Private communication from Dr J. de Jonge, N.V. Philips, Eindhoven, Netherlands

(E) *Adsorption compounds*

All organic acids whose aluminium salts were nucleating agents acted as nucleating agents themselves. However, they did not show any nucleating effect in ash-free polypropylene; they were active only in polymers containing an appreciable amount of remnants of the Al/Ti catalyst, say, more than 5 ppm of aluminium. Therefore, these acids are not nucleating substances themselves but the nucleating species is some reaction product with the catalyst remnants.

The optimum nucleating effect upon incorporation of *p*-tert-butylbenzoic acid in polypropylene was observed at a content of about 0·3 wt. % of this acid, while the polymer had an ash content of about 20 ppm Al and 16 ppm Ti. The complete conversion into AlOH(PTBB)$_2$* and TiO(PTBB)$_2$ would require only 0·038 wt. % of acid. Nevertheless, the nucleating effect decreased upon the acid evaporating from the polymer, e.g. during continued milling at 180°C. Thorough extraction of the acid-containing polymer with carbon disulphide removed the larger part of the incorporated acid; this diminished the nucleating effect to some extent but not completely.

Similarly, the nucleating effect of 0·05 wt. % of AlOH(PTBB)$_2$ incorporated in an essentially ash-free polypropylene was increased by the addition of 0·45 wt. % of acid and decreased again on evaporation of the acid.

Both incorporated aluminium salts and the reaction products of catalyst remnants and acids are believed to adsorb an appreciable amount of acid, which increases the nucleating capability of the particles. Addition compounds of carboxylic salts with their acids are well known. The existence of such compounds has been demonstrated by the fact that their solubility in a given solvent is lower than that of the individual components[26].

Since the acid dissolves in the molten polymer there will be a partition equilibrium between adsorbed and free acid, the amount adsorbed decreasing proportionately as acid evaporates from the polymer.

(F) *Grinding treatments of aluminium carboxylates with various contact liquids*

Ball milling, using hydrocarbons, chlorinated hydrocarbons, alcohols or ketones did not improve the poor nucleating behaviour of dried salts, such as aluminium benzoate, aluminium succinate and aluminium adipate. However, pyridine had a beneficial influence on the nucleating effect, although not visibly on the degree of dispersion of the salt in the polymer. This liquid probably modifies the surface of the particles by acting as a terminal group of an aluminium-oxygen chain, thus superficially breaking the network of chains in the salts[27,28].

Freshly prepared aluminium benzoate, freed from benzoic acid by extraction and dried at 120°C, does not show any nucleating effect in polypropylene. It proved possible, however, to break the salt particles by paint milling the salt to a paste in squalane in 5 to 10 passages over the paint mill. After this treatment, the salt showed a good nucleating effect in polypropylene.

* PTBB = *p*-tert-butylbenzoate

STRUCTURAL CHARACTERISTICS OF THE NUCLEATING AGENTS

From the experimental observations we conclude that the nucleating agents in the polymer are not in the liquid state, are not dissolved, and most probably are not amorphous substances. The only possibility left is that the physical state of good nucleating agents is a fine dispersion of small crystals, or a thin crystalline layer adsorbed at dispersed particles of another substance.

Epitaxy as a mechanism for the nucleating effect can be ruled out, since the nucleating agents are active in all polyolefins tested and occur in homologous series suggesting gradually increasing lattice dimensions.

A number of crystal structure determinations have been reported for metal salts of organic acids of chemical structures resembling those of nucleating agents. The crystals are built up of polar (p) and non-polar (n) layers. The polar layers contain the carboxylate, sulphonate, phosphonate, etc., groups and the non-polar ones the hydrocarbon groups of the substance.

Sandwich structures (n–p–n–n–p–n) are found when the cross-section of the hydrocarbon group is equal to, or larger than, that of the polar group, e.g. in potassium hydrogen phenylacetate[29] [$(C_6H_5CH_2COO)_2KH$], in ammonium hydrogen phthalate[30], in potassium hydrogen benzoate[31], and in potassium hydrogen p-chlorobenzoate[32] [$(ClC_6H_4COO)_2KH$].

Alternating layer structures (n–p–n–p–n–p) are found for hydrated substances, such as hydrated potassium hydrogen salicylate[33] [$(HOC_6H_4COO)_2$-$KH.H_2O$] and hydrated magnesium benzenesulphonate[34] [$(C_6H_5SO_3)_2Mg.$ $6H_2O$]. Here, the expansion of the polar layer by the water molecules is compensated for by the hydrocarbon groups of adjacent layers meshing together like the teeth of gears. Probably, however, little water of hydration will be left after a salt has been heated in the polymer melt, so that alternating layer structures may be converted into sandwich structures by the inevitable heat production on the incorporation of the salt into the polymer.

For some aluminium salts, sandwich structures have been proposed[35]. In an x-ray powder diffractogram of aluminium mono-hydroxy di-(p-t-butylbenzoate) we found a relatively strong reflection at a d-value of 14Å (1·4nm). This might indicate – on analogy with the proposed structure of aluminium monohydroxy di-stearate – a sandwich structure in which the hydrocarbon part is somewhat inclined to the normal on the sandwich plane.

Condensed aromatic compounds, such as flavanthrone[36], violanthrone[37], and copper phthalocyanine[38] – all good nucleating agents – show a regular packing of parallel stacks of the flat ring systems.

The evidence suggests that the nucleating agents have the following features in common:

(1) The crystals of the nucleating agents expose faces of hydrocarbon groups. These groups resemble moderate to good solvents for polyolefins, i.e. aromatic, chlorinated aromatic, cycloaliphatic and branched-chain aliphatic hydrocarbons.

(2) The nucleating agents are, nevertheless, insoluble in the polymer melt due to a polar group attached to the hydrocarbon group or to a condensed aromatic structure.

265

The only substances to which these rules do not apply so clearly are the aluminium salts of dibasic aliphatic carboxylic acids.

The change in the activity of aluminium monohydroxy-dibenzoate on milling in squalane (see experimental section, item F) is probably due to the change of the exposed surface. The salt, when prepared by precipitation in water, may expose a polar surface containing adsorbed water, while on milling in a hydrocarbon liquid the non-polar part of the molecule turns to the surface or the particles are broken up into smaller ones exposing a non-polar surface.

The nucleating effect is probably linked up with a general feature of the crystal structure of the nucleating agents since the crystals of nucleating agents expose faces of hydrocarbon groups, the latter being arranged in rows or stacks parallel to the faces. As a result, the faces show shallow ditches in which adsorbed polymer molecules can be forced to assume a stretched conformation over some distance, making crystallization much easier. This picture is in agreement with:

(a) the close similarity of the birefringence pattern of a polypropylene melt containing oriented needles of Na(PTBB) with the birefringence pattern of the same specimen after crystallization[1];

(b) the highly oriented crystallization in injection-moulded polyethylene nucleated by copper phthalocyanine needles, which have been oriented during the flow in the die and the mould, while otherwise considerably less oriented crystallization is observed, or no orientation at all.

CONCLUSIONS

We summarize the presented experimental evidence in the following conclusions:

(a) As regards their physical state, nucleating agents for polyolefins are crystalline. Most of the agents are insoluble in the polymer melt. The soluble ones, upon cooling, crystallize from the polymer melt before the polymer starts to crystallize.

(b) As regards their chemical nature, the agents – with very few exceptions – consist of both hydrocarbon groups (resembling good solvents for the polymers) and either polar groups or a condensed aromatic structure (rendering the agents insoluble in the polymer melt).

(c) On the strength of a comparison with known crystal structures of related substence, we suggest that most agents consist either of parallel layers or of parallel rows of molecules. The layers expose the hydrocarbon groups while the polar groups are confined in the centre. The rows are stacks of flat, condensed aromatic molecules. Crystals of either structure have shallow ditches in their surfaces.

(d) Orientation of the nucleating particles in the polymer melt causes oriented crystallization of the polymer.

(e) The activity of the agents is strongly dependent on the degree and sometimes on the method of dispersion.

(f) Added stearates attenuate the nucleating activity of salt-type agents, but do not affect that of non-salt-type ones.

Koninklijke Shell-Laboratorium, Amsterdam
(Shell Research N.V.)

REFERENCES

1 Binsbergen, F. L. *PhD Thesis*, Groningen, Netherlands, 1969 (in English).
2 Price, F. P. *J. Polym. Sci. (C)* 1963, **3**, 117
3 Wijga, P. W. O. *US Pat.* 3,207,735; -6; -8 (1960)
4 Wijga, P. W. O. and Binsbergen, F. L. *US Pat.* 3,299,029 (1961)
5 Wales, M. *US Pat.* 3,207,737; -9 (1961–62)
6 Binsbergen, F. L. *US Pat.* 3,326,880; 3,327,020; -1 (1963)
7 Kargin, V. A. *et al, Dokl. Akad. Nauk. SSSR* 1964, **156**, 1156 (transl.: *Dokl. Phys. Chem.* 1964, **156**, 612, 644)
8 Döring, C. and Schmidt, H. *German Pat. (Federal Rep.)* 1,188,279 (1963)
9 Vonk, G. C. *Kolloid Z.* 1965, **206**, 121
10 Kuhre, C. J., Wales, M. and Doyle, M. E. *S.P.E. Journal* 1964, **20**, 1113
11 McBain, J. W. and McClatchie, W. L. *J. Amer. Chem. Soc.* 1932, **54**, 3266
12 Gilmour, A., Jobling, A. and Nelson, S. M. *J. Chem. Soc.* 1956, p 1972
13 Mehrotra, R. C. *J. Indian Chem. Soc.* 1961, **38**, 509
14 Kissa, E. *J. Colloid Sci.* 1962, **17**, 857; 1963, **18**, 147; 1964, **19**, 279
15 see Gaertner, H. *J. Oil Colour Chem. Ass.* 1963, **46**, 13
16 Willems, J. *Disc. Faraday Soc.* 1958, **25**, 111
17 Fischer, E. W. *Disc. Faraday Soc.* 1958, **25**, 204; *Kolloid Z.* 1958, **159**, 103
18 Koutsky, J. A., Walton, A. G. and Baer, E. *J. Polym. Sci. (A-2* 1966, **4**, 611; *J. Polym. Sci. (B)* 1967, **5**, 177
19 Koutsky, J. A., Walton, A. G. and Baer, E. *J. Polym. Sci. (B)* 1967, **5**, 185
20 Leger, A. F., Haines, R. L., Hubley, C. E., Hyde, J. C. and Sheffer, H. *Can. J. Chem.* 1957, **35**, 799
21 Sheffer, H. *Can. J. Res. (B)* 1948, **26**, 481
22 Scott, F. A., Goldenson, J., Wiberley, S. E. and Bauer, W. H. *J. Chem. Phys.* 1954, **58**, 61
23 Friberg, S. *Acta Chem. Scand.* 1965, **19**, 2267
24 Kargin, V. A., Sogolova, T. I. and Rapoport, N. Ya. *J. Polym. Sci. (C)* 1967, **16**, 1609
25 Last, A. G. M. *J. Polym. Sci.* 1959, **39**, 543
26 De Jong, A. W. K. *Berichte* 1923, **56**, 822
27 Gray, V. R. and Alexander, A. E. *J. Phys. Chem.* 1949, **53**, 9, 23
28 McGee, C. G. *J. Amer. Chem. Soc.* 1949, **71**, 278
29 Speakman, J. C. *J. Chem. Soc.* 1949, p 3357
30 Okaya, Y. and Pepinsky, R. *Acta Cryst.* 1957, **10**, 324
31 Skinner, J. M., Stewart, G. M. D. and Speakman, J. C. *J. Chem. Soc.* 1954, p 180
32 Mills, H. H. and Speakman, J. C. *J. Chem. Soc.* 1963, p 4350
33 Downie, T. C. and Speakman, J. C. *J. Chem. Soc.* 1954, p 787
34 Broomhead, J. M. and Nicol, A. D. I. *Acta Cryst.* 1948, **1**, 88
35 Ross, S. and McBain, J. W. *J. Amer. Oil Chemists' Soc.* 1946, **23**, 214
36 Stadler, H. P. *Acta Cryst.* 1953, **6**, 540
37 Bolton, W. and Stadler, H. P. *Acta Cryst.* 1964, **17**, 1015, 1020
38 Honigmann, B., Lenné, H. U. and Schrödel, R. *Z. Krist.* 1965, **122**, 185

Morphology of styrene-butadiene-styrene block copolymers

UMBERTO BIANCHI, ENRICO PEDEMONTE and ANTORNIO TURTURRO

A statistical thermodynamic treatment of phase separation in three-block copolymers (styrene–butadiene–styrene) is given; the formation of polystyrene islands is favoured by surface energy terms and opposed by entropic terms. For a given system, the average equilibrium size of an island appears to be an inverse function of temperature. Comparison between theoretically expected island dimensions and experimental results from electron microscopy is encouraging.

STYRENE (S)–BUTADIENE (B) copolymers of the type S–B–S are among the copolymers forming the new class of thermoelastic materials[1, 2]. They show rubber-like elastic behaviour at temperatures below the glass transition temperature (T_g) of polystyrene and, when heated above T_g, they behave like a thermoplastic and can be moulded or extruded very easily.

This peculiar combination of properties has been attributed to the formation of a two-phase system where S chain sections tend to separate from the elastic matrix B thus providing a van der Waals kind of crosslinking based on the cohesion forces inside each S island. On heating above T_g, polystyrene will acquire liquid-like mobility and the whole material behaves like a liquid.

Recent papers[3-5] have generally confirmed this interpretation, without giving, however, a quantitative interpretation of the morphology and properties shown by these copolymers.

We have recently given[6] a statistical-thermodynamical approach to the morphology of three-block copolymers in which polystyrene is the minor component dispersed in the polybutadiene matrix, and in this paper we will compare theoretical expectations with experimental results.

THEORY

We have recently formulated[6] the free energy change occurring when ν copolymer chains are changing from a state of complete mixing to a state in which the 2ν polystyrene ends are grouped into n islands. The calculation can be summarized as follows. Let V be the total volume of the system $V = v_B + v_S$ (where v_B and v_S are polybutadiene and polystyrene volumes respectively) containing n polystyrene islands. For simplicity of reasoning, it is convenient to divide the ν copolymer chains in groups of ν_i chains with the same end-to-end distance r_i; then

$$\nu_i = \nu W(r_i)\, dr \tag{1}$$

where $W(r_i)\, dr$ is the probability of a polybutadiene chain of having an end-to-end distance between r_i and $r_i + dr$; the assumption leading to

equation (3) will make unnecessary an explicit expression for $W(r_i)$. On placing one end in one of the n islands, the second end can explore a volume dV, given by $dV = 4\pi r_i \, dr$, in which it will have the opportunity of meeting $n_i = (n/v) \, dV$ islands.

From this it follows that each of the v chains can be placed in $2 \, n_i \, n/2$ distinguishable ways (the 2 in the numerator takes into account a possible difference between the two S terminal blocks, but treating them as identical will not affect the final result) and the set of v_i in $(n_i n)^{v_i}$ different ways. For v chains we therefore have

$$\Omega = \frac{v!}{\prod\limits_i v_i!} \prod_i (n_i n)^{v_i} \tag{2}$$

where $v!/\prod_i v_i!$ is the number of permutations of the chains over the initial distribution in sets of v_i chains.

By assuming as a reference state that one characterized by $n = 2v$, and that end-to-end distribution of butadiene chains is independent of the number of islands n, at least for large n, we have:

$$\Omega_0 = \frac{v!}{\prod\limits_i v_i!} \prod_i (n_i \times 2v)^{v_i} \tag{3}$$

(where $n_i = (2v/v) \, dV$) and for the configurational entropy change ΔS:

$$\Delta S = 2kv \ln (n/2v) \tag{4}$$

By putting $(2v/n) = \langle i \rangle$, where $\langle i \rangle$ is the average number of polystyrene end blocks per island and referring ΔS to a system containing one mole of S chains ($2v = N_A$ Avogadro number), we have

$$\Delta S = - R \ln \langle i \rangle \tag{5}$$

on the assumption that there is no change in the configurational entropy of B chains upon formation of n polystyrene islands.

The change from the reference state to any other state must obviously be accompanied by a change in internal energy too. We shall assume that ΔE contains a main surface energy contribution connected with the change in the amount of S–B surface of interaction as we change the amount of S ends aggregation, i.e. the number $\langle i \rangle$ or n. It is easy to see that, assuming for simplicity a spherical shape for S islands, the total surface of interaction s is given by:

$$s = (4\pi)^{1/3} (3v_S)^{2/3} \left(\frac{2v}{\langle i \rangle} \right)^{1/3} \tag{6}$$

where v_S is the colume occupied by polystyrene ends. On writing a similar expression for s in the reference state, we arrive at the energy change per mole of S chains:

$$\Delta E = B(\langle i \rangle^{-1/3} - 1) \tag{7}$$

where $B = (4\pi)^{1/3} \times (3v_S)^{2/3} \times (N_A)^{1/3} \times \sigma_{SB}$; and σ_{SB} is the surface

energy at the interface of S and B homopolymers. This amounts to ignoring the fact that the interface in a real system will contain some covalent bonds between S and B chains.

Assuming that the free energy change ΔF on going from the reference state ($\langle i \rangle = 1$) to a state characterized by $\langle i \rangle$ polystyrene ends blocks per island is mainly given by the terms in equations (5) and (7) we have:

$$\Delta F = B (\langle i \rangle^{-1/3} - 1) + RT \ln \langle i \rangle \qquad (8)$$

referred again to a mole of polystyrene ends.

Equation (8) gives a very simple picture of the situation; demixing of the system, i.e. an increase in $\langle i \rangle$, is opposed by the entropic term and favoured by the energetic term, which depends on σ_{SB}: the higher the interfacial energy, the stronger the tendency to aggregation.

The equilibrium value i_{eq} of $\langle i \rangle$ can be derived from equation (8) by equating the derivative $(\partial \Delta F/\partial \langle i \rangle)_T$ to zero; the result is:

$$i_{eq} = \left(\frac{B}{3\,RT} \right)^3 = \frac{4\pi\,(3v_S)^2\,N_A\sigma_{SB}^3}{(3\,RT)^3} \qquad (9)$$

Equation (9) shows that the equilibrium number of S chain ends in each island will depend on polystyrene molecular weight through v_S; i_{eq} is predicted to decrease strongly by increasing the temperature (mixing is favoured by high temperatures) and to be a strong function of σ_{SB}, increasing with the cube power of it.

On planning a comparison between these expectations and experimental facts, it is immediately obvious that whereas the molar volume of polystyrene chain ends ($v_S = (MW)_S/\rho_S$) is easily derived from a characterization of the copolymer, the evaluation of the interfacial energy σ_{SB} poses a difficult problem. In order to give a quantitative basis to equation (9), we have treated σ_{SB} as an interfacial tension which, according to Fowkes[7], can be written as:

$$\sigma_{SB} = \sigma_S + \sigma_B - 2(\sigma_S\sigma_B)^{1/2} \qquad (10)$$

where σ_S and σ_B are surface tensions of S and B respectively. Equation (10) is expected to be a good approximation to σ_{SB} when the interactions at the interface are mainly due to London dispersion forces, as it is in our case.

Due to the high exponent with which σ_{SB} enters equation (9), it is important to see if its temperature coefficient can be significant in calculating the dependence of i_{eq} on T. From equation (10) it is easy to see that:

$$\frac{d\sigma_{SB}}{dT} = \left[1 - \left(\frac{\sigma_S}{\sigma_B} \right)^{1/2} \right] \frac{d\sigma_B}{dT} + \left[1 - \left(\frac{\sigma_B}{\sigma_S} \right)^{1/2} \right] \frac{d\sigma_S}{dT} \qquad (11)$$

The two terms on the right hand side of equation (11) have opposite signs and, provided $d\sigma_B/dT \approx d\sigma_S/dT$, we can expect $d\sigma_{SB}/dT$ to be approximately zero.

The literature does not report direct determinations of σ_S or σ_B at any temperature; on looking for an indirect evaluation, Schonhorn[8] has recently discussed a correlation between σ and polymer cohesive energy density

(c.e.d.) or internal pressure, (P_i). His equation, for n-hydrocarbons liquids, is

$$\sigma = 0.31\, m\, \frac{\Delta E_{\text{vap}}}{V} \left(\frac{V}{nN_{\text{A}}} \right)^{1/3} \tag{12}$$

where m is the ratio between P_i and c.e.d., ΔE_{vap} is the molar energy of vapor-ization, V is the molar volume, n is the number of carbon atoms in the chain and N_{A} is the Avogadro number. As discussed by Ryong-Joon Roe[9], ex-tension of equation (12) to high polymers requires an assignment of a suitable value to the ratio V/n; we have formulated equation (12) as follows:

$$\sigma = 0.31\, P_i \left(\frac{v_u}{2N_{\text{A}}} \right)^{1/3} \tag{13}$$

where $P_i = m\,(\Delta E_{\text{vap}}/V)$ is the internal pressure and v_u is the molar volume of the repeating unit so that $v_u/2$ is the 'average' molar volume per chain element in vinyl polymers.

Equation (13) has been tested by comparing calculated σ values (in dyn/cm*) with those recently measured by Ryon-Joon Roe[9] for polydimethylsiloxane at 20°C ($\sigma_{\text{calc}} = 27$, $\sigma_{\text{exp}} = 21$) polyisobutene at 20°C ($\sigma_{\text{calc}} = 36.8$, $\sigma_{\text{exp}} = 34$) and polyethylene at 120°C ($\sigma_{\text{calc}} = 31.5$, $\sigma_{\text{exp}} = 31$); P_i values to be used with equation (13) have been derived from the work of Gee et al[10]. The agree-ment found is fair and extension of equation (13) to polystyrene and poly-butadiene gives, for σ at 100°C, a temperature at which both homopolymers are liquid, $\sigma_{\text{S}} = 53.5$ dyn/cm and $\sigma_{\text{B}} = 31.2$ dyn/cm; P_i values at 100°C were, respectively, 92 cal/cm³†(ref. 10) and 83 cal/cm³(ref. 11). Introducing these values into equation (10), we derive $\sigma_{\text{SB}} = 3$ dyn/cm. Turning back to equation (9) and taking $v_{\text{S}} = (MW)_{\text{S}}/\rho_{\text{S}}$, where $(MW)_{\text{S}} = 10^4$ is the molecular weight of polystyrene chain ends (see the following), we have all the necessary data to calculate i_{eq} numerically as a function of T. *Figure 1* is a plot of this function.
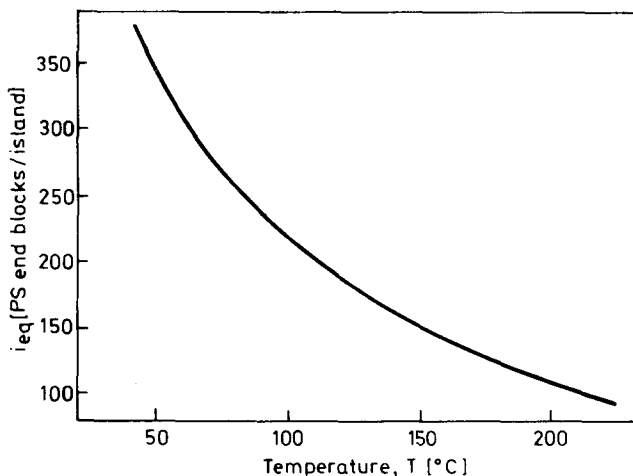
Figure 1 Equilibrium number of polystyrene end blocks per island against temperature. ($\sigma_{\text{SB}} = 3$ dyn/cm).

* 1 dyn/cm = 1 mN/m; † 1 cal/cm³ = 4.187 J/cm³

The average, equilibrium number of S chain ends per island is predicted to be, for our copolymer, of the order of 220 at 100°C; it is shown to increase greatly with decreasing temperature. At 70°C, i_{eq} becomes equal to 280 and, assuming for simplicity a density of 1 g/cm³, the size of S islands is expected to be around 200 Å (20 nm).

<center>EXPERIMENTAL</center>

Characterization

We used a commecial styrene–butadiene block copolymer (S–B–S) from Shell (Kraton 102)[1].

Infra-red spectroscopy

Infra-red analysis has been used to confirm the block structure of Kraton 102 and to reveal the configurational composition of the polybutadiene section; thin polymer films have been obtained from benzene solutions and observed at 25°C with a Perkin Elmer 225 spectrophotometer. The spectrum shows a very strong absorption at 18·5 μm compared with the absorption at 17·9 μm, with a ratio between optical densities of 1·88 which, according to Kraus *et al*[3], is an indication of an almost ideal block structure.

The method suggested by Silas *et al*[12] has been used to determine poly-butadiene configurations, taking into account that S absorptions at 13·2 μm and 14·3 μm are interfering with 1,4-*cis*-butadiene band (12·0–15·75 μm). From this analysis we derived a steric composition of 48% 1,4-*trans*, 44% 1,4-*cis*, and 8% 1,2.

NMR spectroscopy

Carbon tetrachloride solutions of our copolymer at a concentration of 10% and at 20°C have been examined with a Varian 100 MHz spectrometer, using tetramethylsilane as internal standard. Well resolved peaks, attributable to aromatic protons[13], confirm the block structure. From the interpretation of these peaks, we derive the molar fraction of styrene x_S according to the equation:

$$x_S = \frac{6\,[\text{aromatic H}]}{5\,[\text{total H}] - 2\,[\text{aromatic H}]}$$

The result is $x_S = 15\cdot7\%$, which corresponds to 26% by weight.

Molecular weights (MW)

An attempt to fractionate the starting material by addition of methanol to a benzene solution has revealed a very small molecular weight dispersion; the material has therefore been used as received in all subsequent measurements.

The number average MW (M_n) has been measured by a high speed Hewlett Packard membrane osmometer, using toluene solutions at 37°C; M_n is $(80 \pm 5) \times 10^3$. The method suggested by Bushuk and Benoit[14] has been applied to get weight average MW (M_w) of the whole copolymer as well as of the separate components.

<center>272</center>

To this purpose, light scattering measurements have been performed on various polymer solutions in different solvents (at least three) with different refractive index increments dn/dc. We have used as solvents cyclohexane, benzene and toluene. Light scattering and dn/dc values have been measured at room temperature with a Sofica single beam apparatus and a Zeiss interferometer, respectively.

Table 1 collects dn/dc values measured for the copolymer and the two homopolymers in the three solvents; the last column gives, for the same systems, the apparent molecular weight M_{ap} of the copolymer.

Table 1 dn/dc values for two homopolymers and the copolymer in the three solvents. (M_{ap}, apparent molecular weight of the copolymer)

Solvent	$(dn/dc)_S$ [cm³/g]	$(dn/dc)_B$ [cm³/g]	$(dn/dc)_{copol}$ [cm³/g]	M_{ap}
Cyclohexane	0·170	0·125	0·140	70 000
Benzene	0·106	0·0116	0·0364	120 000
Toluene	0·100	0·0321	0·0485	77 000

The two homopolymers used in this study were a polystyrene fraction from Pressure Chemical Company with $M_n = 19\cdot8 \times 10^3$ and $M_w/M_n = 1\cdot06$, and a polybutadiene fraction with $M_w = 2 \times 10^5$ and a 1,4-*cis* content of 97%, i.e. much higher than that of our copolymer. It has been shown, however, that the *cis* content does not seriously affect the dn/dc values; a sample with 79% 1,4-*trans* and 21% 1,2 gives, in cyclohexane, $dn/dc = 0\cdot118$ (ref. 15), compared with our value of $dn/dc = 0\cdot125$.

From the data in *Table 1*, we derive $M_w = (70 \pm 7) \times 10^3$: the good agreement with M_n confirms the sharpness of molecular weight distribution in our sample.

An accurate evaluation of the molecular weight of the S and B sections is unfortunately impossible, since it would require the use of solvents for which the difference in dn/dc of the two homopolymers is as high as possible, in any case higher than that given by benzene and toluene, for instance. We have not been able to find such solvents nor a solvent for the copolymer in which dn/dc for one of the two homopolymers is close to zero.

Refractive index increments in *Table 1* can, however, be used to calculate the weight percent of S by assuming that, also for copolymers, they depend only on the homopolymer concentration in weight:

$$\left(\frac{dn}{dc}\right)_{copolymer} = w_S \left(\frac{dn}{dc}\right)_S + (1 - w_S) \left(\frac{dn}{dc}\right)_B$$

where w_S is the percentage by weight of polystyrene. Introducing the figures of *Table 1*, w_S is calculated to be 25%, in good agreement with n.m.r. results; assuming an average total MW of $7\cdot5 \times 10^4$, for each S terminal chain MW $= 10^4$ and for the central B chain MW $= 5\cdot5 \times 10^4$.

273

Morphology and discussion

Copolymer solutions in cyclohexane at a concentration of 0·03 % have been evaporated on carbon films, treated with osmium tetroxide vapours[16] and subsequently observed with a Hitachi HU 11 electron microscope. *Figure 2* shows a picture of the sample, which reveals a two-phases system with the white representing S islands immersed in a dark B matrix.
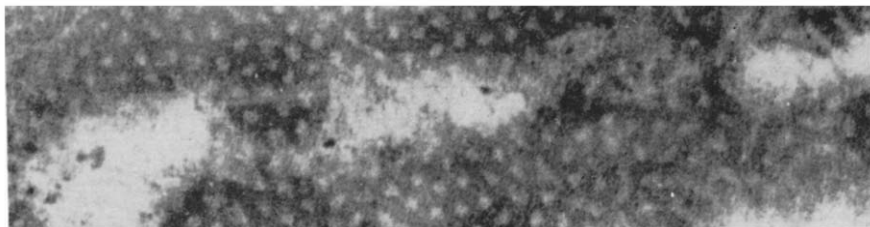
Figure 2 Electron micrograph of a film of S-B-S (S/B = 25/75) from cyclohexane solution. (0·1 μm $=$ 11 mm)

The results are similar to those obtained by Matsuo[4] and by Fischer[5]. Matsuo has worked on copolymers with a higher S content (S/B molar ratio, 80/20 to 40/60) and has shown a dependence of the morphology on the solvent from which the film is obtained. This result can probably be explained in terms of solvent effect on the interfacial energy parameter σ_{SB}, such that the dry film can retain a memory of the previous situation. Fischer[5] has worked with a copolymer with a S content of 38 % by weight and a molecular weight of S chains of $2·5 \times 10^4$; he has shown the existence of very regularly spaced, spherical S islands of approximately 300 Å (30 nm) in diameter, corresponding to $i_{eq} \approx 400$ styrene chains/island.

Comparison with the theoretical expectations given in *Figure 1* must take into account that the glass transition temperature for polystyrene in our copolymer is around 70°C (see the following for a discussion on this point); we would therefore expect that rearrangements in the number of S chain ends per island are going to be very slow at temperatures below 70°C. It follows that copolymer samples, even examined at room temperature, are probably showing a morphology characteristic of a temperature in the vicinity of T_g for polystyrene islands. If this is the case, i_{eq} found in *Figure 2* is in very good agreement with the value calculated at 70°C through equation (9). Moreover, i_{eq} from Fischer's work[5] ($i_{eq} \approx 400$) is much larger than in our case, thus confirming, at least qualitatively, the dependence of i_{eq} on polystyrene molecular weight given in equation (9).

Some preliminary results can also confirm the expected strong dependence of i_{eq} on T. If we take a film of the copolymer and heat it in vacuum, at high temperature, the size of S islands should reach an equilibrium value, the smaller the higher the temperature. After a period of standing at high temperature, the sample is quenched in water-ice mixture and then kept at room temperature: with time, S islands should collapse together increasing in size and therefore increasing the turbidity of the film.

Figure 3 shows the result of such an experiment, performed on films 0·2–0·3 mm in thickness, heated at 150°C and then quenched at 0°C; their trans-

parency have then been followed with a Zeiss spectrophotometer, at $\lambda = 400$ nm.

Even if it is difficult to derive quantitative data, *Figure 3* indeed shows an increase in turbidity with time at constant temperature as a result of the increase in size of the S islands. The long time over which these changes take place can be explained by remembering that S islands are in the glassy state
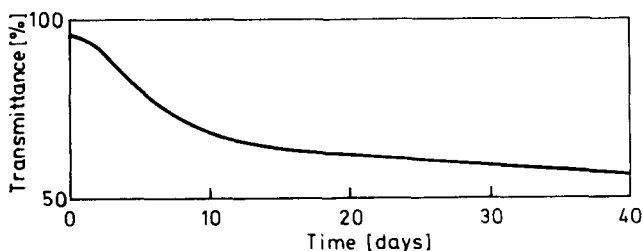
Figure 3 Film transparency followed with a Zeiss spectrophotometer, as a function of time ($\lambda = 400$ nm; $T = 155 \rightarrow 25$ C).

at room temperature, making fast molecular rearrangements impossible. For this reason, we would expect that more quantitative measurements of i_{eq} as a function of T will reveal negative deviations from the theoretical curve in *Figure 1* for temperatures below the glass transition temperature T_g of S islands. In connection with this problem, it is of interest the fact that polystyrene T_g in S–B–S copolymers has been shown to be definitively lower than that of a pure polystyrene sample having the same molecular weight.

Our dilatometric measurements[17], performed on samples extruded at 150°C, have given $(T_g)_S = 71$°C which has to be compared with $T_g = 89$°C, the glass transition temperature of pure S with $M \approx 10^4$ (ref. 18).

We believe that a collection of a few hundred S chains, forming an island of colloidal dimensions, can hardly be expected to have the same T_g as the pure, bulk polymer. Surface effects can no longer be ignored, especially with reference to the degree of mobility that the presence of polybutadiene, a rubbery liquid, will confer to the adjacent S chains. In terms of Gibbs and Di Marzio[19] theory, this is equivalent to saying that cooperative restrictions to the packing of i_{eq} polystyrene chains are progressively decreased by decreasing the number of chains.

It follows that S chains in an island should have greater mobility and therefore should be able to pack better, with a resulting specific volume smaller than that of bulk polymer.

Implications of these ideas about a difference in thermodynamic properties between styrene islands and bulk polymer are currently under investigation

Istituto di Chimica Industriale,
Università di Genova,
Via Pastore 3,
Genova, Italy

275

REFERENCES

1 Giacchero, A. and Goretti, G., *L'Industria della Gomma* 1967 (September), N. 126
2 Deanin, R. D., *SPE Journal* 1967, **23**, 1
3 Kraus, G., Childers, C. W. and Gruver, J. J., *J. appl. Polym. Sci.*, 1967, **11**, 1581
4 Matsuo, M. *Japan Plastics* 1968 (July)
5 Fischer, E., *J. Macromol. Sci. (A-2)* 1968, **6**, 1285
6 Bianchi, U., Pedemonte, E. and Turturro, A. *J. Polym. Sci. (B)*, 1969, **7**, 785
7 Fowkes, F. M. *Ind. and Eng. Chem.* 1964, **56**, 40
8 Schonhorn, H. *J. Chem. Phys.* 1965, **43**, 2041
9 Roe Ryong-Joon *J. Phys. Chem.* 1968, **72**, 2013
10 Allen, G., Gee, G., Mangaraja, D., Sims, D. and Wilson, G. J. *Polymer, Lond*, 1960. **1**, 467
11 Bianchi, U. and Bianchi, E. *Chim. Ind. (Milan)* 1962, **44**, 1362
12 Silas, R. S., Yates, J. and Thornton, V. *Anal. Chem.* 1959, **31**, 529
13 Bovey, F. A., Tares, G. V. D. and Fillipovich, G. J. *J. Polym. Sci.* 1959, **38**, 73
14 Bushuk, W. and Benoit, H. *Can. J. Chem.* 1958, **36**, 1616
15 Ribeyrolles, Ph., Guyot, A. and Benoit, H. *J. Chem. Phys.* 1959, **36**, 377
16 Kato, K. *J. Polym. Sci.* 1966, **4**, 35
17 Turturro, A., unpublished results
18 Fox, T. G. and Soshaek, S. *J. Polym. Sci.* 1955, **15**, 371
19 Gibbs, J. H. and Di Marzio, E. Z. *J. Chem. Phys.* 1958, **28**, 383

High resolution n.m.r. studies of poly-γ-benzyl-L-glutamate: effect of polydispersity and molecular weight

E. M. BRADBURY, C. CRANE-ROBINSON and H. W. E. RATTLE

The nuclear magnetic resonance peaks of the α-carbon protons of different synthetic polypeptide samples show differences in behaviour as the material is taken through a helix–coil transition; these differences have hitherto been ascribed to variations in helix–coil interconversion rates. The work here described, which was carried out on several samples of poly-γ-benzyl-L-glutamate, indicates that the observed differences in behaviour may be explained on the basis of differing molecular weights and polydispersity of the materials observed rather than on an exchange phenomenon.

FROM a proton magnetic resonance study of the helix → coil transition of poly-L-alanine and a comparison with other homopolypeptides, it has been concluded by Ferretti and Paolillo[1] that the 'observation of separate helix and random coil peaks (i.e. for the polypeptide backbone protons) is a completely general phenomenon which permits lower limits to the lifetime of the helix and random coil portions of the polypeptide to be evaluated'. It is further suggested that the effect is independent of the molecular weight of the sample, and the spectra shown appear to support this view. Our nuclear magnetic resonance studies of the helix → coil transition of polypeptides of differing molecular weights do not lend support to this general conclusion[2–4]. It has been shown for different polypeptides of high molecular weight, including poly-L-alanine[4], that the backbone protons give rise to single resonance peaks. On going through the coil → helix transition these peaks shift from the chemical shift value characteristic of the coil towards that characteristic of the helical form. In these high molecular weight polypeptides the single backbone proton resonances are time averaged between the helix and coil environment and, as has been pointed out[5], the chemical shift value can be related to the helix content. Such observations would be expected from the kinetics of the helix → coil transition in polypeptides where it has been shown both for water-soluble polypeptides in aqueous systems[6, 7] and poly-γ-benzyl-L-glutamate in dichloracetic acid/ethylene dichloride that the mean relaxation time of the transition is of the order $10^{-7}–10^{-8}$ s.

For certain polypeptides it has been observed that the width of the αC$\underline{\text{H}}$ resonance peak passed through a maximum on going through the helix → coil transition[5]. This effect was attributed to exchange broadening and the lifetime of a residue in either the helical or random coil form was estimated to be of the order of 6×10^{-3} s. The first observation of double peaks for the resonances of the backbone protons of polypeptides was made by Ferretti[9] for poly-L-leucine and poly-β-methyl-L-aspartate. They were attributed

also to slow chemical exchange of residues between helical and random coil forms and the lifetime was estimated as of the order of 10^{-2}s. The molecular weights of the polymers mentioned were not given. Observations made in this laboratory of clearly resolved double resonance peaks for the αC$\underline{H}$ and amide N$\underline{H}$ of polypeptides in the region of the helix $\rightarrow$ coil transition have been confined to polypeptides known to be of low molecular weight and dissolved in organic acid/chloroform solvent systems[2, 4]. Although we have also interpreted the observation of double peaks as resulting from slow chemical exchange, it is clear that this is contrary to the now well established results from kinetic studies of the helix $\rightarrow$ coil transition and that some other explanation has to be sought for the observation of multi-component resonance peaks. In this respect Jardetzky[10] has suggested that the separate peaks may result from polydispersity of the sample.

In this paper we should like to discuss the effects of molecular weight and polydispersity on the n.m.r. spectra of poly-γ-benzyl-L-glutamate (PBLG).

EXPERIMENTAL

Polypeptides

All of the samples of PBLG except for PBLG PC12 were synthesized by W. E. Hanby at the Courtaulds Research Laboratory, Maidenhead. The molecular weights $(\bar{M}_w)$ were determined from their viscosities measured in dichloracetic acid and compared with the curve of viscosity against molecular weight obtained by Doty, Bradbury and Holtzer[11]. The values are given in *Table 1*. Sedimentation studies of both PBLG R10 and PBLG S416 in dimethyl formamide were made by Dr K. Cammack of MRE Porton, Salisbury. The S values were 1·58 and 1·67 respectively. Since two samples, R10 and S416, of similar $\bar{M}_w$ and S values were found to exhibit different behaviour in the n.m.r. spectra on going through the helix $\rightarrow$ coil transition their $\bar{M}_n$ values were determined. The $\bar{M}_n$ determinations were carried out in *m*-cresol/chlorobenzene (1:1 v/v) at 37°C using an SS-08 membrane in a Mechrolab high speed membrane osmometer, model 502. Five solutions were used, ranging from 0·2 to 1·0% w/v concentration. Osmotic pressure versus time graphs were drawn and extrapolated to zero time in an attempt to correct for diffusion effects. As can be seen from *Table 1*, similar $\bar{M}_n$ values were also obtained for these two samples and it was thought necessary therefore to obtain their molecular weight profiles.

The two samples were analysed by gel permeation chromatography (g.p.c.) using 1:1 v/v *m*-cresol/chlorobenzene containing 0·25% w/v of benzoic acid as a solvent with a flow rate of 0·5 ml/min. One-ml samples of a 1% w/v solution were injected on a three column sequence of 3×10^4 Å, 3×10^4 Å and 2×10^4 Å nominal porosities; the columns were packed with the normal crosslinked polystyrene gel sold by Waters Associates under the trade name Styragel. Injections from two separate solutions of each sample were made in order to check uniformity of the sample and reproducibility of the results. The chromatograms were not corrected for diffusion spread within the g.p.c.

columns. The calibration which is given in arbitrary units, is based on the elution of narrow fractions of polystyrene and polyglycol of known length. From the molecular weight profiles it is possible to obtain the number average $\bar{A}_n$ and the weight average $\bar{A}_w$ based on these arbitrary units. If these figures are compared with the $\bar{M}_n$ values obtained for these samples

Table 1 Molecular weights and S values for various PBLG samples

Sample number	Viscosity η_{sp}/c (l mole^{-1}) in dichloracetic acid	$\bar{M}_w$	Average degree of polymerization	$(\pi/c)_0$	$\bar{M}_n$	$\bar{M}_w/\bar{M}_n$	S values
PBLG S416	3·92	24000	110	19·30	13510	1·95	1·67
PBLG R10	4·07	25100	114	18·43	12900	1·78	1·58
PBLG 314	8·8	59000	268				
PBLG 413	9·46	66000	300				
PBLG 373(7)	10·9	77000	353				
PBLG AS106	14·9	110000	502				
PBLG SP18·4	18·4	141000	640				
PBLG PG12	29·5	716500	3270				

from osmometry, it is found that an approximately linear conversion exists: the average of four determinations of $\bar{M}_n/\bar{A}_n$ for the two samples is 26·1, all values of the ratios falling within 10% of this value. The ratio of $\bar{M}_w/\bar{A}_w$ for the sample S416 is 23·1 and is close to the ratios of $\bar{M}_n/\bar{A}_n$. There is, however, a large difference for sample R10 where $\bar{M}_w/\bar{A}_w$ was found to be 15·6 and this is attributed to the assymetric distribution and the very wide spread of molecular weights found for this sample.

Solvents and solutions

Deuterochloroform (99·8%D) was obtained from Stohler Isotope Chemicals and was used without further purification. The trifluoracetic acid obtained from Ralph N. Emanuel Ltd was distilled before use. Some samples of trifluoracetic acid needed extensive distillation to remove impurities which gave spurious peaks in the n.m.r. spectrum. The solutions were made up to a concentration of 2·5% w/v in the solvent mixture containing about 1% of tetramethylsilane.

Spectroscopy

High resolution n.m.r. spectra were recorded on the JEOL JNM-4H 100 MHz spectrometer and on the Varian HR 220 MHz spectrometer. Chemical shifts were determined relative to tetramethylsilane as an internal reference.

Optical rotatory dispersion curves were recorded in the range 250–500 nm

on a Bendix Polarmatic 62 spectropolarimeter. The solutions were contained in water-jacketed fused silica cells made by the Optical Cell Company.

RESULTS

For the samples of highest molecular weight PBLG PC12 and PBLG SP18.4 in 25% trifluoracetic acid (TFA)/75% deuterochloroform (CDCl₃) inverted helix–coil transitions with increasing temperature were studied. A high TFA content was chosen in order to obtain a high transition temperature and thus sharper resonance peaks. The changes in the envelope of the αCH resonance peak at 100 MHz of PBLG SP18.4 on going through a partial coil → helix
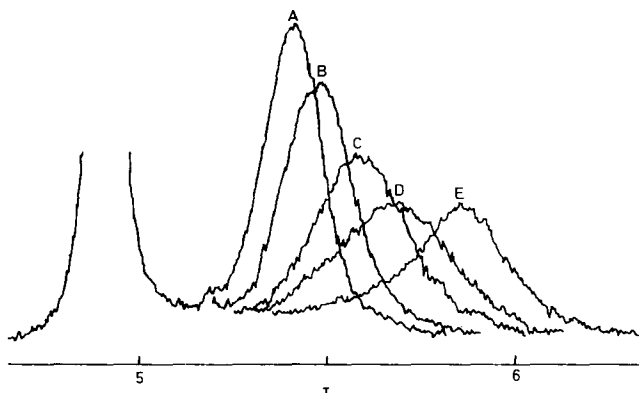
Figure 1 αCH resonance peak at 100 MHz of poly-γ-benzyl-L-glutamate SP18.4
$\bar{M}_w$ 140 000 in 30% TFA/70% CDCl₃
A, 36°C; B, 66·5°C; C, 70°C; D, 74°C; and E 87°C
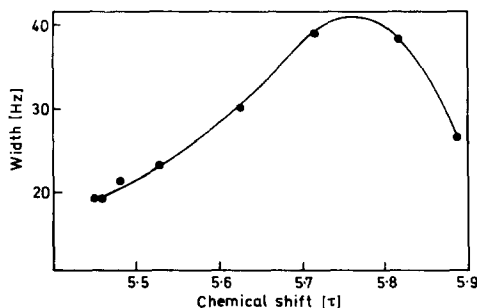
Figure 2 αCH line widths of PBLG SP18.4 spectra
shown in Figure 1

transition are shown in *Figure 1*. Identical results were obtained for PBLG PC12 of $\bar{M}_w$ 716 500 and this behaviour may be typical of very high molecular weight PBLG. In *Figure 1*, it can be seen that the chemical shift of the αCH peak for the random coil form is 5·40τ; on raising the temperature the peak shifts to higher field values and broadens until a temperature of 74°C is reached. Above this temperature although the peak continues to shift upfield, it becomes narrower. This behaviour is summarized in *Figure 2* and

similar behaviour has been commented on for this and other polypeptides in a 60 MHz study[5]. To confirm the presence of a single peak the experiment was repeated at 220 MHz. The spectra are given in *Figure 3* and show a single peak which shifts upfield with increasing helicity and which is broader at intermediate helix contents.

For the samples of intermediate molecular weights; PBLG 314, 413 and 373(7) of $\bar{M}_w$ from 59 000 to 77 000, a different behaviour was observed to that found for the highest molecular weight samples. The changes in the envelope of the αC$\underline{\text{H}}$ peak of PBLG 314 in 25% TFA/75% CDCl$_3$ on going through a partial inverted helix coil transition are shown in *Figure 4*. There
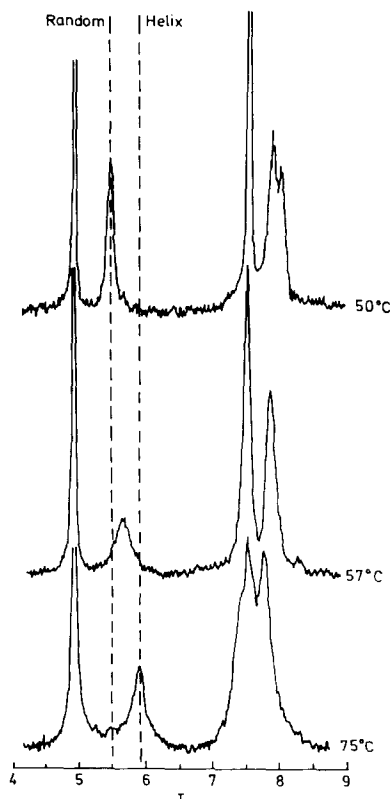
Figure 3 220 MHz spectrum of poly-γ-benzyl-L-glutamate SP18·4 $\bar{M}_w$ 140 000 in 25% TFA/75% CDCl$_3$

it is quite clear that at intermediate helix contents the αC$\underline{\text{H}}$ has more than one component. At intermediate helix contents (72°C and 75°C) the chemical shifts of the two apparent components to the αC$\underline{\text{H}}$ peak are closer together than the purely helical form at 5·90τ and the random coil form at 5·45τ and moreover vary in position. It was hoped that the components of this peak might be more clearly resolved at higher magnetic fields. Spectra recorded at 220 MHz are shown in *Figure 5* and it is striking that no increase in separation
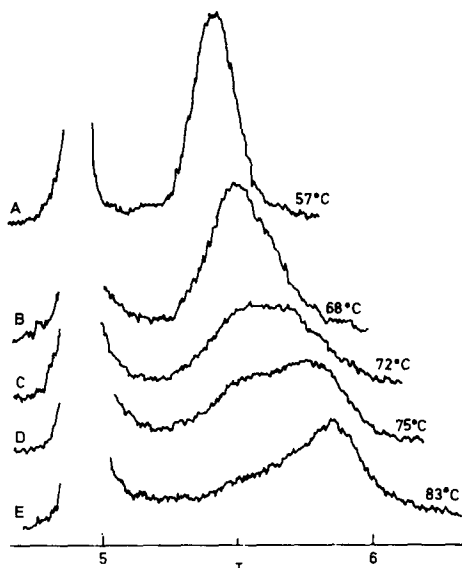
Figure 4 100 MHz spectra of poly-γ-benzyl-L-glutamate 314
$\bar{M}_w$ 59 400 in 30 % TFA/70 % CDCl$_3$
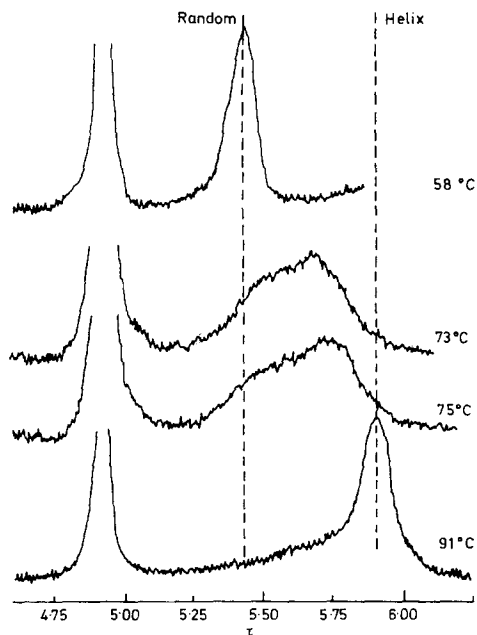
Figure 5 220 MHz spectra of poly-γ-benzyl-L-glutamate 314
$\bar{M}_w$ 59 400 in 25 % TFA/75 % CDCl$_3$

of the components is observed and that the spectra are virtually identical with those obtained at 100 MHz. This unexpected result suggests that the envelope of the αCH peak contains a large number of resonance components from protons in many different chemical environments.

As can be seen from *Table 1*, the two samples of lowest molecular weight, PBLG R10 and PBLG S416 have very similar S, $\bar{M}_w$ and $\bar{M}_n$ values. It was expected that similar n.m.r. spectra would be obtained on taking them through inverted helix → coil transitions. This was not the case and the spectra obtained at 100 MHz are shown in *Figures 6a* and *6b*. For PLBG R10 the full transition at 100 MHz has been published previously[4]. For half helical PBLG R10 at 60°C two components are clearly resolved for the αCH
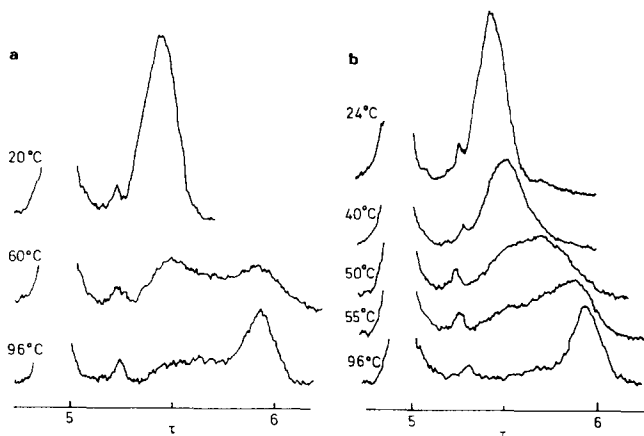
Figure 6 100 MHz spectra: (a) poly-γ-benzyl-L-glutamate R10 $\bar{M}_w$ 25100 in 20% TFA/80% CDCl$_3$; (b) poly-γ-benzyl-L-glutamate S416 in 20% TFA/80% CDCl$_3$
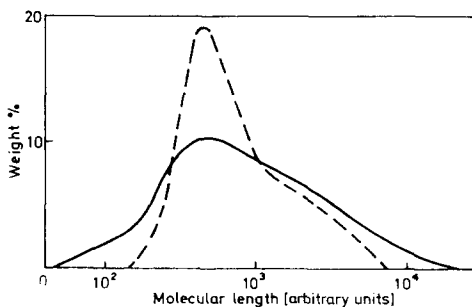
Figure 7 Molecular weight profiles of poly-γ-benzyl-L-glutamate R10 (solid line) and S416 (broken line)

resonance while for the half helical state of PBLG S416 at 50°C a multi-component envelope is obtained which may contain more than two components. It is clear, however, that none of the components of S416 are at the extreme positions of the two peaks obtained for the R10 polymer at all helix contents. Because of the similarity of the $\bar{M}_n$ and $\bar{M}_w$ values of these samples, the molecular weight profiles were obtained as described earlier. These are given in *Figure 7* and it can be seen that the molecular weight

spread of PBLG R10 is considerably broader and more assymetrical than for PBLG S416. The differences in the n.m.r. behaviour of these two polymers must therefore be related to differences in polydispersity.

The n.m.r. spectra of PBLG R10 were also recorded at 220 MHz and these are given in *Figure 8*. When compared to the 100 MHz spectra of *Figure 6*,
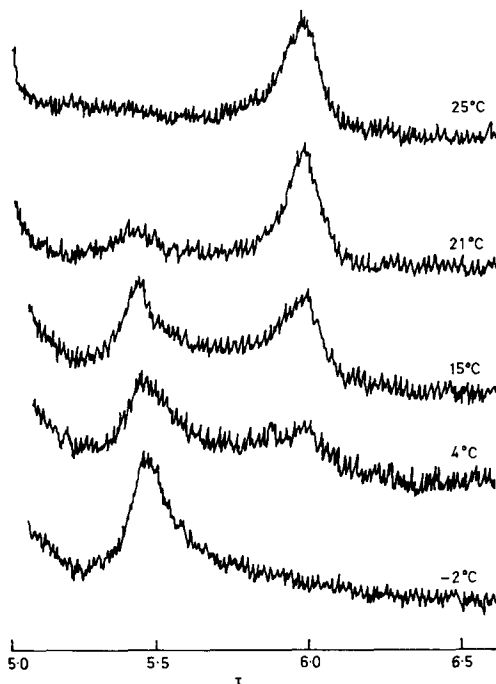
Figure 8 220 MHz spectra of poly-γ-benzyl-L-glutamate R10 in 8 % TFA/92 % CDCl₃

it is clear that the components of the αC$\underline{H}$ peak are more clearly resolved at the higher magnetic fields. This behaviour contrasts with that observed for the PBLG samples of intermediate molecular weight for which no increased separation of the components was observed on going to higher fields. In the case of the PBLG R10 sample, the two components of the αC$\underline{H}$ peak correspond therefore to two virtually homogeneous chemical environments, the mainly helical form and the mainly random coil form.

DISCUSSION

Previously published spectra of PBLG of different molecular weights together with certain of the spectra presented here seem to suggest that a double αC$\underline{H}$ peak is observed for low molecular weight materials while a single peak is characteristic of high molecular weights, i.e. the peak shape appears to depend on the chain length. Two facts, however, indicate that the poly-dispersity of the sample plays an important role: (1) the similarity of the

100 MHz and 220 MHz spectra of PBLG 314 demonstrates that in the middle of the helix coil transition the sample contains a considerable range of αC$\underline{H}$ environments, that is a considerable range of helix contents, if rapid helix–coil interconversion is assumed; (2) very marked differences are observed between PBLG R10 and PBLG S416, the lowest molecular weight samples which have very similar $\bar{M}_w$ and $\bar{M}_n$ values but very different molecular weight profiles.

The spectra presented here may be explained on the basis of polydispersity as follows. Any PBLG sample showing an average helical content of 50% under some solution condition could be constituted from either (a) one half fully helical and one half random coil molecules, or (b) each molecule being 50% helical on a time scale large compared to the relaxation time of helix → coil interconversion (10^{-7} to 10^{-8}s). A perfectly homodisperse sample would be in state (b), and real samples must lie in between the two extremes. If the rapid helix–coil interconversion demonstrated by the kinetic measurements involves all the residues in a single molecule to an equivalent extent then the αC$\underline{H}$ resonance position for a particular molecule depends precisely on its helix content and a homodisperse sample of whatever molecular weight will thus show a *single* αC$\underline{H}$ peak, the shift of which at 50% helix content will be midway between that for the fully helical and the completely random coil forms.

For a polydisperse sample, however, the dependence of helix content on chain length will result in a distribution of helix contents in the sample. This would lead to a spread of αC$\underline{H}$ environments under solution conditions giving 50% average helicity and thus to spectra of the type seen in *Figure 4* for PBLG 314. If the sample contains a *very wide* range of molecular weights then at 50% average helicity the sample might be constituted much as in state (a) and give rise to spectra of the type shown in *Figure 8* for PBLG R10. This implies that at all solution conditions the vast majority of the molecules are either mainly helical or mainly random coil and relatively few have partly helical conformations. An explanation of polypeptide double-peak spectra in terms of sample partition has been previously advanced by Jardetzky[10]. Such a situation could only be obtained in the low molecular weight range since at high molecular weights there is a much lower dependence of helicity on chain length under given solution conditions. In some cases (see e.g. ref. 13) where double peaks appear for a high molecular weight sample, it would be necessary to postulate that the sample was highly polydisperse.

It has been shown above that PBLG R10 contains a very wide range of molecular weights and the double peak observed for this sample may be due solely to polydispersity. Such an explanation of αC$\underline{H}$ peak shapes in terms of polydispersity implies that transition from a double peak spectrum to a single peak spectrum by way of a multiple peak situation is obtained both by increasing the molecular weight for a fixed polydispersity and by decreasing the polydispersity for a given molecular weight. Neither postulate is in disagreement with the spectra shown here and polydispersity could therefore account for all the phenomena so far observed, including the increased peak width at intermediate helicities for the high molecular weight sample PBLG

SP18·4. Whether polydispersity is indeed the sole cause of the differences in αC$\underline{H}$ peak shapes and there is no dependence on chain length can only be decided by studying very sharp molecular weight fractions. A comprehensive theory of αC$\underline{H}$ peak shapes and multiplicities based both on polydispersity and on chain length effects has been developed by Ullman[12]. In this theory it has been shown that the shapes of the αC$\underline{H}$ resonance peaks are dependent on chain length, the 'end effects' in short chains resulting in assymmetric peaks. However, in order to generate multiplicity of the αC$\underline{H}$ peak it was found necessary to introduce effects due to sample polydispersity. The results given above lend considerable support to Ullman's theory and his resolution of the controversy of 'fast' (by kinetic methods) and 'slow' (by n.m.r. methods) helix $\rightarrow$ coil exchange in homopolypeptides. We received a copy of Dr Ullman's manuscript in the course of the above work and gratefully acknowledge the catalytic effect of his ideas.

Department of Physics,
Portsmouth Polytechnic,
Park Road, Portsmouth, Hants.

REFERENCES

1 Ferretti, J. A. and Paolillo, L. *Biopolymers* 1969, **7**, 155
2 Bradbury, E. M., Crane-Robinson, C. and Rattle, H. W. E. *Nature* 1967, **216**, 862
3 Bradbury, E. M. and Rattle, H. W. E. *Polymer, Lond.* 1968, **9**, 201
4 Bradbury, E. M., Crane-Robinson, C., Goldman, H. and Rattle, H. W. E. *Nature* 1968, **217**, 812
5 Markley, J. L., Meadows, D. H. and Jardetzky, O. *J. Mol. Biol.* 1967, **27**, 25
6 Saksema, K., Michels, B. and Zana, R. *J. Chim. Phys.* 1968, **65**, 597
7 Hammes, G. G. and Roberts, P. B. *J. Amer. Chem. Soc.* 1969, **91**, 1812
8 Schwarz, G. and Sellig, J. *Biopolymers* 1968, **6**, 1263
9 Ferretti, J. A. *Chem. Commun.* 1967, p 1030
10 Jardetzky, O., 3rd International Conference on Magnetic Resonance in Biological Systems, Warrenton, Virginia, 1968
11 Doty, P., Bradbury, J. H. and Holtzer, A. M. *J. Amer. Chem. Soc.* 1956, **78**, 947
12 Ullman, R., Personal communication (1969)
13 Haylock, J. C. and Rydon, H. N., 'Peptides 1968', North Holland Publishing Co. Amsterdam, 1968 p 19

Note to the Editor

On a common misunderstanding in the measurement of thermal diffusivity

B. MARTIN

Some workers who are engaged in the accurate determination of physical properties for polymeric materials claim to present results for the variation of thermal diffusivity with temperature (for example see Shoulberg[1] 1963; Westover[2] 1960; Steere[3] 1966; Harmathy[4] 1964).

I should like to point out that the thermal diffusivity is a useful quantity only when it is constant and that what has actually been reported by these and many other authors is a function of temperature, $a(T)$ say, the meaning of which is obscure. It will be shown below that the thermal diffusivity can only legitimately be expressed as a function of temperature in the degenerate case when the thermal conductivity is constant.

The trouble arises from a failure to appreciate the difference between linear and non-linear differential equations and in noting the way in which the structure of the heat conduction equation enters into the definition of thermal diffusivity.

In one dimension the defining relation for thermal conductivity k in an isotropic material is

$$q_x = -k\frac{\partial T}{\partial x} \tag{1}$$

where q_x is the local heat flux and $\partial T/\partial x$ the temperature gradient. Note that in equation (1) k may depend on position x, temperature T, or both.

The differential equation governing non-steady heat transfer in one dimension is

$$\rho c_p \frac{\partial T}{\partial t} = -\frac{\partial q_x}{\partial x} \tag{2}$$

where t denotes time, ρ the density and c_p the specific heat per unit mass at constant pressure.

Substituting for q_x in equation (2) yields

$$\rho c_p \frac{\partial T}{\partial t} = \frac{\partial}{\partial x}\left(k\frac{\partial T}{\partial x}\right) \tag{3}$$

Now if k is independent of position and temperature it may be taken through the differential operator $\frac{\partial}{\partial x}$ to give the familiar equation

$$\frac{\partial T}{\partial t} = \frac{k}{\rho c_p}\frac{\partial^2 T}{\partial x^2} \tag{4}$$

287

and it is the group $k/(\rho c_p)$ which is defined to be the thermal diffusivity κ. Note particularly that the mere formation of this quantity from the differential equation requires the assumption that k is constant. Provided that the product ρc_p is sensibly constant κ is a very useful number and invaluable in simple heat transfer calculations. Clearly this definition of κ allows it to depend on temperature but any variation would only reflect changes in $1/(\rho c_p)$. It is important to observe that even in this case equation (4) is non-linear.

It is of course possible to determine the functions $\rho(T)$, $c_p(T)$ and $k(T)$ separately and use them to form the compound function

$$\theta(T) = \frac{k(T)}{\rho(T)c_p(T)} \tag{5}$$

defining this as the thermal diffusivity. However, no useful purpose would be served because the function $\theta(T)$ could not be employed in the heat conduction equation.

The function $\alpha(T)$ which appears in the literature is difficult to interpret because it is supposed to portray the variation of a quantity with temperature, when in the method of calculation it is implicitly assumed that the quantity is constant.

The diffusivity κ is first taken to be constant so that equation (4) becomes linear and hence amenable, in many cases, to analytical solution. The solution is either rearranged or approximated so that κ may be expressed explicitly in terms of temperature, position and time. Non-steady-state experiments are then conducted over different (narrow) temperature ranges and the results used in the formula for κ – ostensibly giving its value at the mid-point of the temperature range.

However, if ρc_p or k or both do vary significantly (if they do not the results will give a near constant value of $\alpha = \kappa$ anyway) then equation (3) is essentially non-linear and the first step in the calculation procedure cannot be carried out.

For those of us who wish to make use of published data in order to study genuinely non-linear heat transfer problems – for example close to the melting point where polymer properties can be very sensitive to small changes in temperature – the available curves of $\alpha(T)$ are of no value.

The reason usually quoted for obtaining $\alpha(T)$ is that only one relatively simple experiment need be done, whereas ordinarily three more elaborate experiments are required. It is suggested that in future more effort be devoted to the separate (admittedly difficult) determination of the meaningful functions ρ, c_p and k.

University of Cambridge,
Department of Chemical Engineering

REFERENCES

1 Shoulberg, R. H. *J. appl. Polym. Sci.* 1963, 7, 1597
2 Westover, R. F. 'Processing of thermoplastics', (Ed. Bernhardt) Rheinhold, 1960
3 Steere, R. C. *J. appl. Polym. Sci.* 1966, **10**, 1673
4 Harmathy, T. Z. *J. appl. Phys.* 1964, **35**, 1190

Molecular motion in chlorinated ethylene-propylene copolymer

A. ROMANOV and K. MARCINČIN

The molecular motion in solid chlorinated ethylene–propylene copolymer (EPc) (0–66 wt. % Cl) has been studied by the dynamical-mechanical method. It has been found that the damping maximum ascribed to the motion of groups from $-(CH_2)_2-$ to $-(CH_2)_4-$ shifts to higher temperatures with increasing chlorine content. The dependence of T_g on the chlorine content has an exponential character. The mixtures of EPc pairs with a low content of chlorine show a limited compatibility but the copolymers are not compatible at the higher contents of chlorine.

STATISTICAL ethylene-propylene copolymers (EPc) show four typical relaxation regions[1]: (1) the motion of chains as a whole with relaxation maximums at about 25°C; (2) the motion of chain segments containing 50–100 carbon atoms with relaxation maximums at about T_g; (3) the motion of the groups from $-(CH_2)_2-$ to $-(CH_2)_4-$ at about -120°C; (4) the motion of side groups such as $-CH_3$ in the polypropylene unit.

One of the ways of influencing the motion of molecules or segments is by chlorination. With EPc this has been studied, up to now, mainly from the point of view of reaction mechanism[2]. It has been found that the rate of EPc chlorination increases in the order—primary < secondary < tertiary carbon atoms. Competitive reactions therefore occur between tertiary and secondary carbons while reactions involving the primary carbon are unimportant. This mechanism was proved by infra-red spectroscopy and the chemical substitution should also be reflected in a change of molecular motion. In this study, EPc of various chlorine contents have been investigated by the method of dynamical-mechanical testing. Furthermore, this method has been used for studying the compatibility of EPc mixtures with different chlorine content and of mixtures of chlorinated EPc with polyvinylchloride.

EXPERIMENTAL

The starting ethylene-propylene copolymer Dutral was characterised as follows: content of propylene = 43 mole %; $[\eta] = 1.58$ dl/g determined in toluene at 30°C; density = 0.86 g/cm³; it was completely soluble in n-heptane and toluene at room temperature.

The chlorination of EPc was carried out in carbon tetrachloride at 50°C and it took 0.3–5 h. A 500 W bulb was used to initiate the reaction. After the chlorination the solution was diluted with diethyl ether and the polymer precipitated by methanol.

The product was washed several times in methanol, firstly at room temperature and then at the boiling point. After filtration it was dried *in vacuo* at 40–50°C. The content of chlorine was determined by the Schroninger method[3] modified for polymer systems[4].

The pairs of differently chlorinated EPc for the study of compatibility were prepared from a 1% solution in chlorobenzene by precipation with methanol.

The dynamical-mechanical tests were performed by means of a torsion pendulum at the frequency 1 c/s and temperature gradient of approximately 1 °C/min.

RESULTS AND DISCUSSION

A. Chlorinated ethylene-propylene copolymer

In the *Figures 1–3* the temperature dependance of modulus (G') and logarithmic decrement (λ) of ethylene-propylene copolymers with different chlorine contents are presented. The chlorine content varies over the range 0–66·6% which corresponds to 0–1·81 chlorine atoms for 2-carbon units in the main chain. *Figure 1* shows that with EPc there is a secondary maximum
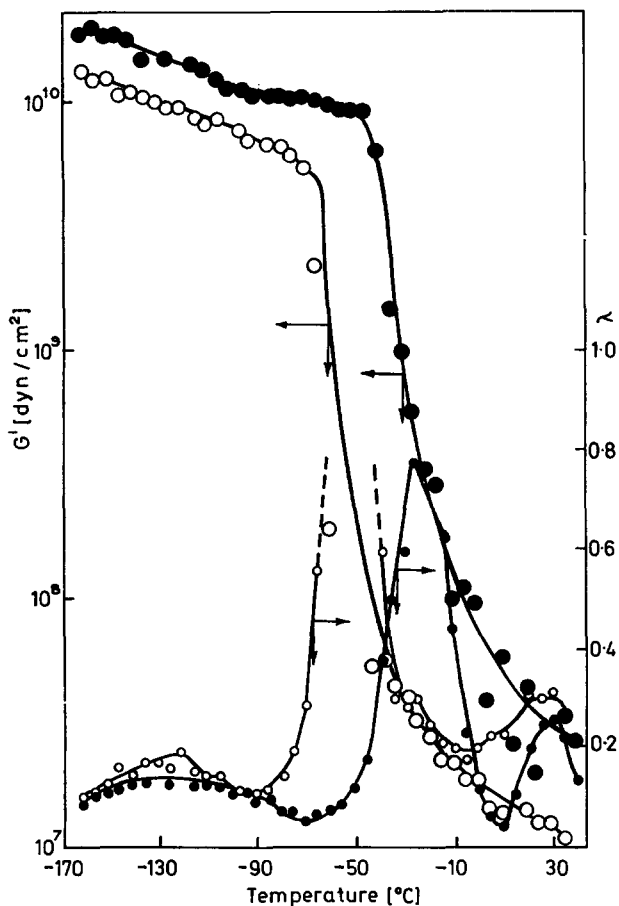
Figure 1 Dependence of G' and λ on temperature for
○, EPc; ●, Cl–EPc (19% Cl)

291

in the damping at nearly $-120\,^{\circ}$C, which is ascribed to the motion of the groups $-(CH_2)_n-$, where $n = 2$ to 4. The copolymer is amorphous and the influence of crystallinity need not be considered. From the figure it can be seen that the secondary maximum gets broader with increasing chlorine content in EPc and at the higher chlorine contents there are signs of peak-splitting. This can be ascribed to the influence of competitive reactions
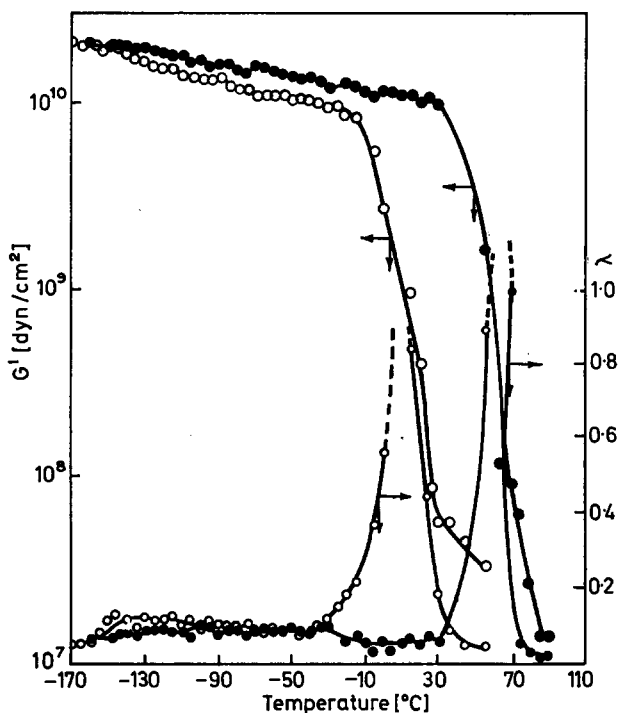
Figure 2 Dependence of G' and λ on temperature for ◯, Cl–EPc (32% Cl); ●, Cl–EPc (46·6% Cl)

between tertiary and secondary carbons. There is a low probability that the substitution of hydrogen atoms by chlorine at tertiary carbons of propylene units can influence the transformations of the secondary maximum. At the higher contents of chlorine (about 45%) the secondary maximum shifts to $-30\,^{\circ}$C. This maximum may have the same origin as the secondary maximum[9] in PVC, which appears at $-20\,^{\circ}$C and below[5]. In the case where hydrogens on secondary carbons are mostly substituted, the maximum ascribed to the groups from $-(CH_2)_2-$ to $-(CH_2)_4-$ decays as a result of the disappearance of these groups.

The dependence of the T_g change on the chlorine density in the EPc chain is represented in *Figure 4*. The rise of T_g is relatively higher at the lower
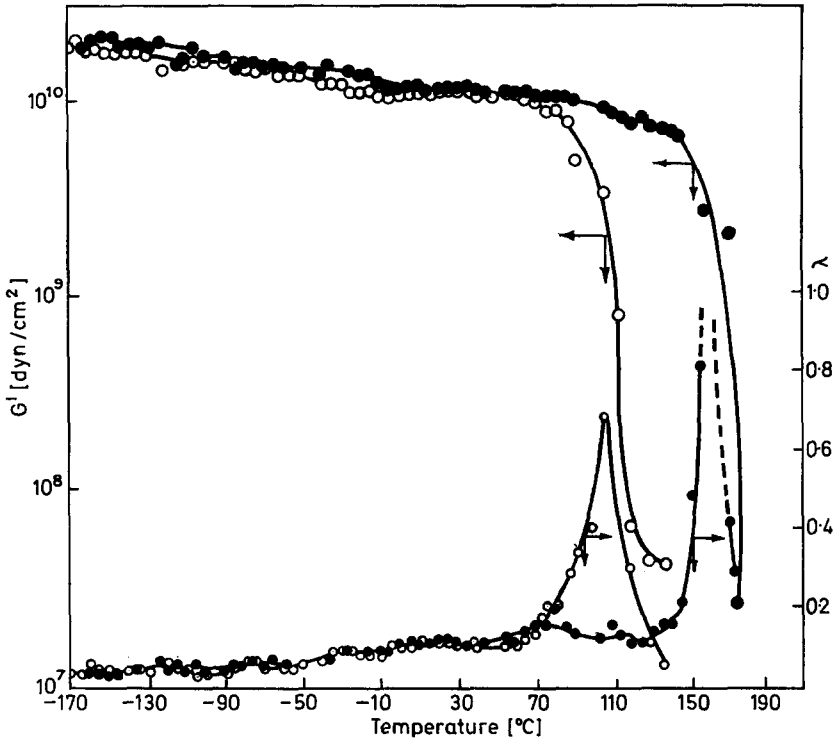
Figure 3 Dependence of G' and λ on temperature for
○, Cl–EPc (57% Cl); ●, Cl–EPc (66·6% Cl)
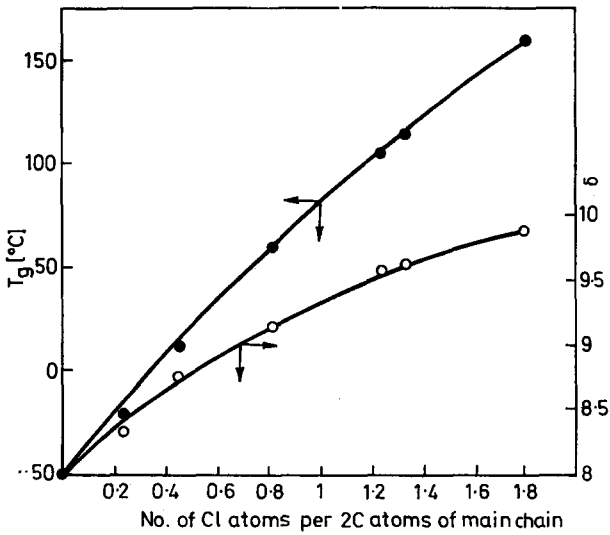
Figure 4 Dependence of T_g (●) and δ (○) on chlorine density in
ethylene-propylene copolymer (EPc)

293

chlorine contents. In our opinion, it is not a specific property of tertiary carbon atoms with substituted chlorine atoms, but it is an effect of changed interaction forces which have been changed by the presence of polar chlorine atoms in the polymer matrix. For instance, with chlorination of polyethylene there is also a positive deviation of T_g from linearity[6].

The change of solubility parameter (δ) calculated according to Small[7] is a measure of interaction forces and has a course which is analogous to that of T_g (*Figure 4*).

B. Mixtures of various chlorinated ethylene-propylene copolymers and mixtures of Cl-EPc with PVC

More than 250 pairs of polymers have been studied by various methods to date and only in a few cases was mutual compatibility found. With regard to compatibility, it was interesting to investigate the mixture of chlorinated EPc with various chlorine contents. An advantage in the investigation of these mixtures is the possibility of detecting low differences in the structures of pairs according to chlorine content. On the other hand, however, the small differences between chlorine contents lead to small differences between the T_gs of the components forming a mixture and the damping maxima of polymer pairs may be combined without regard to their compatibility or non-compatibility.
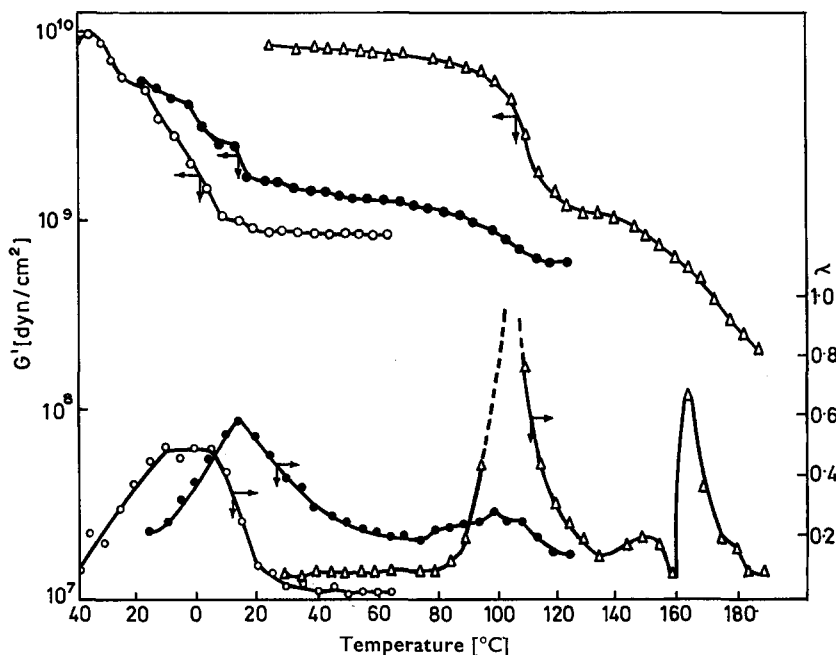
Figure 5 Dependence of G' and λ on temperature for mixtures of various chlorinated ethylene-propylene copolymers

$\bigcirc$, A — Cl–EPc (32% Cl) + Cl–EPc (19% Cl)
$\bullet$, B — Cl–EPc (57% Cl) + Cl–EPc (66·6% Cl)
$\triangle$, C — Cl–EPc (32% Cl) + Cl–EPc (59% Cl)

Table 1 gives a summary of the pairs used according the chlorine content and ΔT_g components. The differences in the values of the solubility parameters $\Delta\delta$ can be considered as the measure of the difference in the intermolecular forces (cohesive energies).

Table 1 Data for copolymer mixtures

Copolymer pairs	Label for mixture	Weight % of Cl compd. 1	compd. 2	ΔT_g [°C]	$\Delta\delta$
Cl·EPc–Cl·EPc	A	19	32	38	0·41
Cl·EPc–Cl·EPc	B	57	66·6	45	0·30
Cl·EPc–Cl·EPc	C	32	59	100	0·87
Cl·EPc–PVC	D	57	56	10	—
Cl·EPc–PVC	E	59	56	20	—
Cl·EPc–PVC	F	66·6	56	65	—

In *Figure 5* the courses of the modulus G' and λ for the mixtures A, B, C are shown. With the mixture A, one wide-spread maximum of damping and one region of modulus change occur. This could be ascribed to the compatibility of both components. Considering the relatively broad maximum it is more correct to take this as limited compatibility. Regarding the differences between components the mixture A may be compared with B. This mixture (B), however, shows two discrete maxima. The explanation could be found
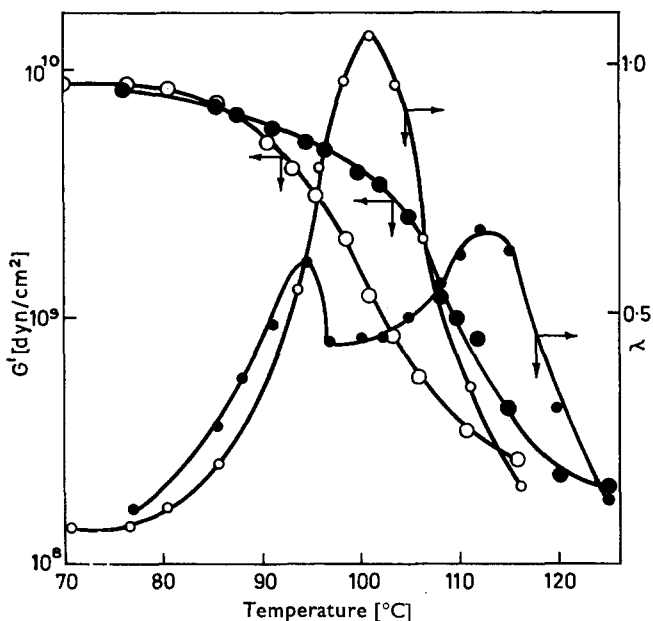
Figure 6 Dependence of G' and λ on temperature for the mixtures of polyvinylchloride, chlorinated ethylene-propylene copolymer
○, D — PVC + Cl–EPc (57% Cl)
●, E — PVC + Cl–EPc (59% Cl)

in the large steric effect of chlorine atoms and the enhancement of differences in chain flexibility. From this point of view the pair A is of higher compatibility than B. The pair C shows two discrete maxima and two regions of modulus change. However, the difference between the properties of components is higher and the compatibility is low.

The *Figures 6–7* show data for mixtures of chlorinated EPc with PVC. With the mixture D the chlorine content of the both components is very
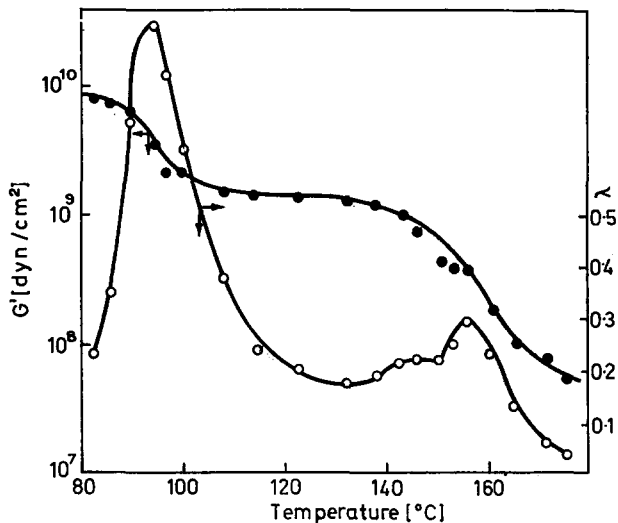
Figure 7 Dependence of *G'* and λ on temperature for the mixture
F— PVC + Cl–EPc (66·6% Cl)

similar and ΔT_g is 10°C. Although one damping maximum and one drop in modulus occurs here, it is very difficult to consider the mutual compatibility owing to the proximity of the T_g of both. The pairs E and F each show two discrete maxima which also correspond to the maxima of the particular components.

REFERENCES

1 Turley, S. G. and Keskkula, H. *J. Polym. Sci.* (*C*) 1966, **14**, 69
2 Portjanskij, A. E. and Nasberg, C. M. *Vysokomol. Soedinenija* 1968, **6**, 1394
3 Schroninger, N. *Microchimica Acta* 1955, **1**, 123
4 Sokolova, N. V., Orestova, V. A. and Mikolaeva, N. A. *Z. Analit. Chimii* 1959, **14**, 472
5 Nielsen, Lawrence E. 'Mechanical Properties of Polymers,' Reinhold Publishing Corporation, London, 1962, p 179
6 Jenkins, R. K., Byrd, N. R. and Lister, J. L. *J. appl. Polym. Sci.* 1968, **12**, 2059
7 Small, P. A. *J. appl. Chem.* 1953, **3**, 71

Preparation and properties of polyoxazoles

R. HIROHASHI, Y. HISHIKI and S. ISHIKAWA

Polyoxazoles were prepared by the polycondensation of 2,6-diamino-phenylene p-benz*bis*oxazole as monomer with terephthalaldehyde, iso-phthalaldehyde, glyoxal, tetrachloro-p-benzoquinone, terephthaloyl chloride, isophthaloyl chloride and p-xylylene dibromide in various polar solvents. Infra-red spectra, visible spectra and elemental analyses support the presence of an oxazole ring in a main polymer chain. Specific resistivities were in the range 10^{12}–10^{14} ohm cm at room temperature. The value of the energy gap was 0·3–3·1 eV. A link was observed in the temperature dependence curve of specific resistivity. These polymers are insoluble in organic solvents and they were found to be extremely thermally stable under oxidative conditions up to about 400°C.

SEMICONDUCTING polymers have attracted increasing attention in recent years. A number of these exhibit relatively high resistivities (10^9–10^{15} ohm cm) at room temperature[1]. If the relationship between structure and electronic properties could be accurately defined, materials with desired properties could be designed. Several structural factors have been shown to affect conductivity.

Previously, semiconducting polymers with hetero-rings in the main polymer chain had been investigated for polybenzimidazole[2], polyquino-quizarine[3] and polypyrrole[4]. The specific resistivities and energy gaps had values in the ranges 10^{12}–10^{14} ohm cm and 1·56–2·56 eV respectively.

In general, the more fused benzene rings and hetero-rings there are in the monomer, the better the electrical conductivity of the polymer. It has been reported many times that polycondensed aromatic hydrocarbons and hetero-cyclic aromatic compounds have electrical semiconducting properties.

This paper presents preparations and measurements of polymers containing oxazole rings in a main polymer chain. Various polyoxazoles were prepared in the hope of improved electrical conductivity. The semiconductive behaviour of compressed discs of various polyoxazoles has been examined.

Values of specific resistivities were in the range 10^{12}–10^{14} ohm cm at room temperature. The value of the energy gap showed 0·5–3·1 eV. Some of the polymers were extremely thermally stable under oxidative conditions up to about 400°C.

EXPERIMENTAL

Syntheses of model compounds

2-(p-*Aminophenyl*)*benzoxazole* (*MA*). A mixture of o-aminophenol (7·64 g, 0·07 mole), p-aminobenzoic acid (9·59 g, 0·07 mole), polyphosphoric acid

297

(PPA) (200 ml) was heated at 230°C for 4 h with stirring and then poured into water. The precipitate was washed with a 5% sodium carbonate solution and water, and recrystallized three times from methanol–water. The infrared spectrum of potassium bromide discs showed main absorptions at 1605, 1505, 1315 and 925 cm^{-1}. Analysis: calculated for $C_{13}H_{10}N_2O$ (mol. wt. 210·25) N,13·13%; found, N,13·19%.

2-(p-*Benzylidene aminophenyl*)*benzoxazole* (*MB*). A mixture of MA (1·05 g, 5 × 10^{-3} mole), benzaldehyde (0·64 g, 6·0 × 10^{-3} mole) and ethanol (20 ml) was heated for 2 h under reflux and then poured into water. The product obtained was recrystallized three times from ethanol and 1·18 g of powder was obtained (m.p. 161–163°C; yield 79·1%). Infra-red spectra showed absorption bands at 1610, 1250 and 922 cm^{-1}. Analysis: calculated for $C_{20}H_{14}N_2O$ (mol. wt. 298·36) N, 9·39%; found, N, 8·99%.

2-(p-*Benzamido*)*phenylbenzoxazole* (*MC*). A solution of benzoyl chloride (0·70 g, 5·0 × 10^{-3} mole) in ethanol (20 ml) was added to a mixture of MA (1·05 g, 5·0 × 10^{-3} mole) and ethanol (30 ml) and then poured into water. A powder (1·34 g, m.p. 225–227°C) was obtained in 85·3% yield; this was recrystallized from aqueous acetone.

The infra-red spectra showed peaks at 1658, 1530, 1412, 1327 and 925 cm^{-1}; the peaks at 922–925 cm^{-1} are characteristic of the oxazole ring. Analysis: calculated for $C_{20}H_{14}N_2O_2$ (mol. wt. 314·36) C, 76·41; H, 4·50; N, 8·91%; found C, 75·56; H, 4·89; N, 8·34%.

Synthesis of monomer

Two routes have been tried for the synthesis of the monomer 2,6-diamino phenylene benz*bis*oxazole (DBO) starting from 2,5-diamino-p-benzoquinone (DAQ). This was prepared by the reaction scheme shown on the next page.

Osman[5] has prepared 2,6-di(p-acetamido phenyl)benz*bis*oxazole (DAO) from 2,6-diallyl benz*bis*oxazole by heating under reflux in ethanol in the presence of piperidine. We did not use this method but instead we prepared 2,5-di(p-acetamidobenzylidene amino)-p-benzoquinone (DABQ) as the intermediate compound in yields as high as 85·2%. The infra-red studies showed peaks at 1662, 1608, 1526 and 1165 cm^{-1}.

2,6-Diamino phenylene benz*bis*oxazole (DBO) which was used as monomer was prepared by the route A, because the nitrogen analysis of DBO obtained by the route B did not agree with the calculated value.

Route A. DABQ (42·8 g, 0·1 mole), lead tetracetate 48·8 g (0·11 mole) and acetic acid (500 ml) were heated for 2 h under reflux, and then poured into water. The crude DAO was washed successively with hot water, dimethylformamide (DMF), hot water again, and finally, ethanol. A powder (40·8 g, m.p. 392–395°C) was obtained in 95·8% yield. Recrystallization from DMF three times gave a white solid. DAO (21·3 g, 0·05 mole), obtained as above,
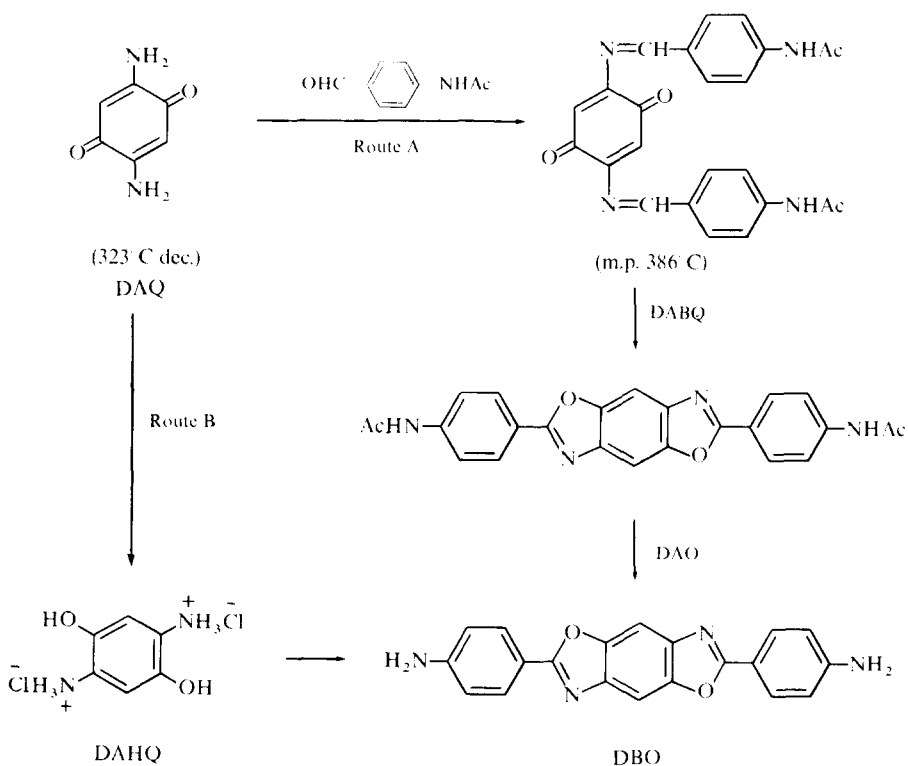
and aqueous hydroxide (400 ml) were heated at 140°C for 10 h. The deacetylated product was washed successively with aqueous 10% acetic acid, hot water and hot alcohol.

Analysis: calculated for $C_{20}H_{14}N_4O_2$ (mol. wt. 342·38) C, 70·16; H, 4·13; N, 16·37%; found C, 68·63; H, 4·26; N, 16·37%.

Route B. DAHQ (2·13 g 0·01 mole) and *p*-aminobenzoic acid (2·57 g, 0·02 mole) were heated in polyphosphoric acid (30 ml) at 150°C for 5 h with stirring, and then poured into water. The precipitate was washed successively with a 5% sodium bicarbonate solution, water, and ethanol. A powder (2·80 g, m.p. 353–356°C) was obtained in 81·8% yield.

Analysis: found N, 13·88%.

Syntheses of polymers

The reactions of polycondensation of DBO with TPA was carried out under the conditions shown in *Table 1*. A change of reaction solvents had little effect on the inherent viscosities of the polymers obtained.

A number of polyoxazoles are listed in *Table 2* along with reaction conditions and physical properties.

Typical examples of preparations of polybenzoxazoles are described below.

299

Table 1 Effects of reaction solvents in the syntheses of polyoxazoles:* polycondensation of 2,6-diamino phenylene benz*bis*oxazole (DBO) and terephthalaldehyde.

No.	Solvent	Catalyst	Temp. (°C)	Time (h)	Yield (%)	η_{inh}†
1	DMF	Py	Reflux	5·0	94·5	0·10
2	DMF	TEA	Reflux	5·0	95·2	0·10
3	DMF	MOR	Reflux	5·0	97·7	0·10
4	H₂SO₄	None	150	5·5	26·1	0·10
5	PPA‡	None	180	5·5	54·6	0·15
6	NMP	Py	180	5·0	80·2	0·20

*Reaction conditions: DBO = 0·005M; terephthaldehyde, 0·005M; solvent, 10 ml; catalyst, 3 drops
†Inherent viscosity; measured at a concentration of 0·2 g in conc. sulphuric acid (100 ml) at 30°C
‡The mixture of phosphorus pentoxide (124 g) and phosphoric acid (80 ml) was heated for 6 h on a water bath

DMF—dimethyl formamide   NMP—N-methyl pyrrolidone   TEA—triethylamine
PPA—polyphosphoric acid   Py —pyridine   MOR—morphorine

Table 2 Reaction conditions and physical properties of polyoxazoles:* polycondensation reaction products of 2,6-diamino phenylene benz*bis*oxazole and other reagents

Polymer	Reagent	Solvent	Catalyst	Temp. (°C)	Time (h)	Yield (%)	η_{inh}‡
A	TPA	DMF	Py	Reflux	5·0	86·2	0·10
B	IPA	DMF	Py	Reflux	5·0	68·5	0·10
C	GO	DMF	Py	Reflux	5·0	99·1†	0·10
D	TPC	HMPA	TEA	25	0·1	93·9	0·34
E	IPC	HMPA	TEA	25	0·5	96·0	0·43
F	CA	DMF	Py	Reflux	5·0	90·3	0·15
G	XDB	DMF	Py	Reflux	5·0	75·4	0·15

*Conditions: DBO monomer, 0·005 M; solvent, 10 ml; catalyst, 3 drops
†Following the method of J. Danhauser[6] using 2,7-diaminofluorene and glyoxal
‡Inherent viscosity: measured at a concentration of 0·2 g in 100 ml conc. sulphuric acid at 30°C
TPA, terephthalaldehyde; IPA, isophthalaldehyde; GO, glyoxal; TPC, terephthaloyl chloride; IPC, isophthaloyl chloride; CA, tetrachloro-*p*-benzoquinone; XDB, *p*-xylylene dibromide

Polycondensation of DBO *with terephthaldehyde, tetrachloro-p-benzoquinone or p-xylylenedibromide.* Polymerization was carried out in a 100 ml three-necked flask equipped with a stirrer, nitrogen gas inlet, and calcium chloride drying tube. The highly polar solvents – DMF, dimethyl acetamide (DMAC) and N-methyl pyrrolidone (NMP) – were used and the polymer precipitated during the reaction. The reaction mixture was poured into ethanol, the precipitated polymer filtered, washed with alcohol, and dried at 100°C under vacuum.

Polycondensation of DBO *with an acid chloride.* A hexamethyl phosphoric amide (HMPA) solution of DBO was cooled to 10°C. A solution of terephthaloyl chloride in HMPA was added to the magnetically stirred solution over a period of time. Stirring was continued for 30 min at the same temperature. The mixture was poured into ethanol and the precipitated polymer filtered, washed with alcohol, and dried at 100°C in vacuum.

Inorganic catalysts were not used, since inorganic impurities can obviously affect the conductivity. Pyridine (Py), triethylamine (TEA) and morphorine (MOR) were used as catalysts in the polycondensation reaction.
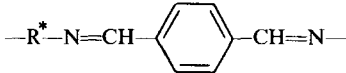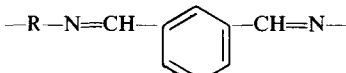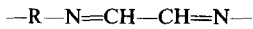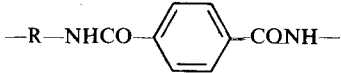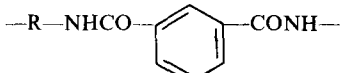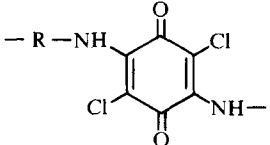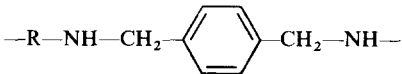
The powders were purified by extraction with water, and then ethanol, in a Soxhlet extractor and finally, dried at 100°C under vacuum, and stored over a dessicant. The polymer was found to have no ash content.

The structures and the nitrogen analyses for the polymers obtained from DBO and various monomers are shown in *Table 3*.

Polyoxazoles were soluble only in concentrated sulphuric acid and insoluble even in dimethylsulphoxide (DMSO), DMF, DMAC and NMP. On the other hand, model compounds were soluble in these solvents at room temperature.

Table 3 Structures and nitrogen analyses of polyoxazoles

Polymer	Structure	Nitrogen analyses Calc. (%)	Found (%)	Appearance of polymer
A	—R*—N=CH—⟨ ⟩—CH=N—	12·72	14·00	Yellow
B	—R—N=CH—⟨ ⟩—CH=N—	12·72	11·98	Yellow
C	—R—N=CH—CH=N—	15·38	13·55	Brown
D	—R—NHCO—⟨ ⟩—CONH—	11·86	10·74	Yellow–brown
E	—R—NHCO—⟨ ⟩—CONH—	11·86	10·42	Yellow-brown
F	—R—NH ... Cl ... Cl ... NH—	10·87	10·48	Brown
G	—R—NH—CH_2—⟨ ⟩—CH_2—NH—	12·66	12·40	Yellow

* R = DBO

Specific resistivity

Finely powdered polymer was compressed to form a disc (12·8 mm in diameter, 0·6–0·8 mm thickness) under a pressure of about 20 MN/m² (~200 atm), with suction to remove air and moisture.

The disc mounted in a cylinder was placed between stainless steel electrodes and compressed to about 4·0 MN/m² before the measurement. Temperature was measured using a chromel–alumel thermocouple embedded in Teflon, within 2 mm of the sample. The electrical conductivities of polymers were measured at various temperatures between room temperature and about 150°C under a pressure of 4·0 MN/m². All measurements were taken as the

temperature increased to lower the effects of the hysteresis of polymer. The thickness of the specimens was measured with a dial gauge type of cylinder after measuring the conductivity. Various voltages up to 100 V were applied across the sample from batteries in the d.c. measurement and the currents were measured with a Hewlett-Packard model 425A electrometer.

Thermal stability

Thermogravimetric analysis (TGA) and differential thermal analysis (DTA) were performed on about 50–100 mg samples in air or nitrogen at a constant heating rate of 5°C/min using an automatic recording differential thermal balance (Agne TGD-C4). The weight loss was automatically recorded.

RESULTS AND DISCUSSION

Absorption bands of poylmers

The characteristic absorption band of the benzoxazole ring at 242–244 nm of all model compounds, monomers and polymers, was measured in concentrated sulphuric acid. *Table 4* shows their ultra-violet and infra-red absorptions.

Table 4 Ultra-violet spectra and infra-red absorption spectra of monomers, model compounds and polymers

Compound	λ_{max}* (nm)	Wave number of oxazole ring absorption (cm^{-1})
DBO	242	920
MA	242	925
MB	242	922
MC	244	922
PA	245	915
PB	243	917
PC	243	916
PD	244	914
PE	242	915
PF	243	916
PG	243	914

*λ_{max}–absorption maximum (nm) in conc. sulphuric acid
†Wave number of infra-red absorption by KBr method
DBO— 2,6-diaminophenylene benz*bis*oxazole
MA— 2-(*p*-aminophenyl)benzoxazole
MB— 2-(*p*-benzylidene aminophenyl)benzoxazole
MC— 2-(*p*-benzamido)phenylbenzoxazole
PA—PG refers to polymers A —G (see *Table 2*)
TPA—terephthalaldehyde   IPC —isophthaloyl chloride
IPA —isophthalaldehyde   CA —tetrachloro-*p*-benzoquinone
GO —glyoxal   XDB—*p*-xylylene dibromide
TPC—terephthaloyl chloride

In all these polymers, the characteristic absorption band of the benzoxazole ring appeared near 920–922 cm^{-1}. The product obtained from the complete ring closure of DABQ gave the absorption band at 920–922 cm^{-1}; this may correspond to the oxazole ring. The spectra of the polyoxazoles were unchanged after warming (up to 100°C) in concentrated sulphuric acid for 5 h. We conclude from this that polyoxazoles are not decomposed by sulphuric acid.

Electrical conductivity

The specific resistivity of polyoxazole at room temperature was in the range 10^{12}–10^{14} ohm cm. For most of the polymers the current is directly proportional to the applied voltage according to the following equation: $I = kV^{\alpha}$ (I current, V applied charged voltage, α slope). The value of each slope in the relationship between current and voltage was in the range 0·76–1·50. A typical set of results is given in *Figure 1* and *Table 5*. In particular, a relationship not obeying Ohm's law was found for polymer F and polymer E.
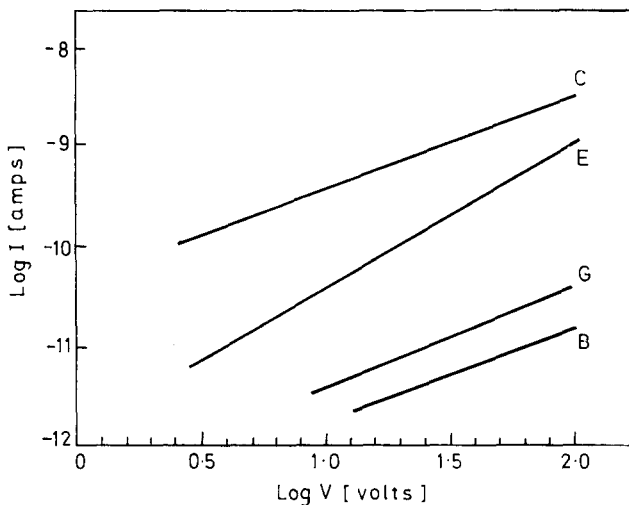
Figure 1 Ohm's law plots for polyoxazoles

Table 5 Values of slope calculated for polyoxazoles

Polymer	Slope (α)*
A	—
B	0·76
C	0·92
D	1·10
E	1·50
F	0·18
	(6·4–23·4 V)
	1·10
	(48·3–92·0 V)
G	1·10

* α was calculated from the equation $I = kV^{\alpha}$
where I = electrical current (A) and V = applied voltage (V)

These departures from Ohm's law are probably to be associated with a barrier set up at the electrode and polymer interface. When the voltage is charged continuously, the current decreases in the case of polarized samples and space charge effects. The voltage was measured $\frac{1}{2}$–1 h after charging.

The temperature-resistivity behaviour of the samples are shown in *Figure 2*.

The energy gap values of the polymers were calculated from the observed slope with the aid of the relationship $\rho = \rho_0 \exp \Delta E_g / 2kT$ (ρ is specific resistivity, ΔE_g is the energy gap for conduction, k is the Boltzmann constant T is the absolute temperature). A kink was observed in the temperature dependence curve of specific resistivity. This behaviour may depend on local segmental motions in the amorphous parts of the semi-crystalline regions of the polymer[7]. The logarithm of the resistivity of some polyoxazoles are plotted against the inverse of the absolute temperature in *Figure 2*.
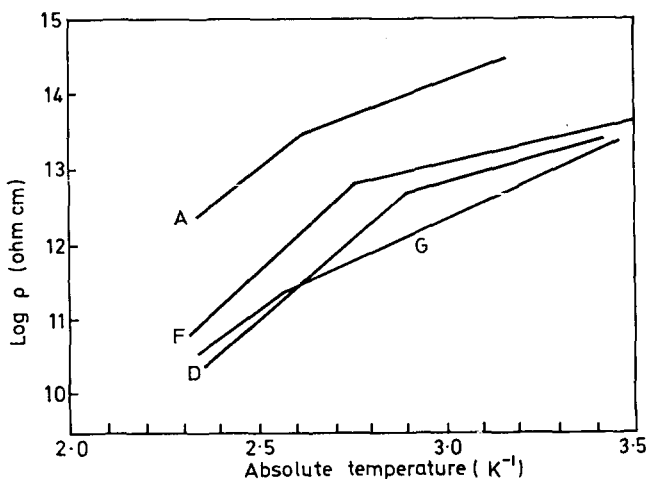
Figure 2 Relationships between log ρ and $1/T$

Because these polymers are infusible and insoluble in organic solvents, it was not possible to use extensive purification procedures. Bearing in mind the difficulties of handling infusible powders, the analytical data give a reasonable indication of purity. It has been suggested that impurity effects play a relatively unimportant part in semiconduction in organic polymers[8].

The specific resistivities of polyoxazoles are shown in *Table 6*. The values of the energy gap and the kink temperature in the temperature dependence curve of specific resistivity are shown in *Table 7*.

Polyoxazoles containing the aliphatic —N=CH— linkage (polymer C) showed higher conductivity than those containing an aromatic group (polymers A and B). An approximate order of conductivity for the linkages studied was polymer C > polymer A = polymer B. Polyoxazoles (D and E) with amide linkages have specific resistivities in the range 10^{12}–10^{13} ohm cm.

This fact may be explained by (a) tautomerism of amide group, i.e.

$$\begin{matrix} H & O \\ | & \| \\ -N-C- \end{matrix} \rightleftharpoons \begin{matrix} OH \\ | \\ -N=C- \end{matrix}$$
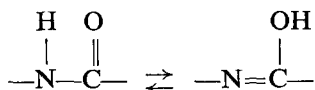
or (b) hydrogen bonding between molecules.

304

Table 6 Values of energy gap and specific properties of polyoxazoles

Polymer A A.V.* = 92·0 V		Polymer B A.V. = 9·73 V		Polymer C A.V. = 3·05 V		Polymer D A.V. = 23·4 V		Polymer E A.V. = 6·40 V		Polymer F A.V. = 15·9 V		Polymer G A.V. = 23·4 V	
Temp. (°C)	Specific resistivity† (ohm cm)	Temp. (°C)	Specific resistivity (ohm cm)	Temp. (°C)	Specific resistivity (ohm cm)	Temp. (°C)	Specific resistivity (ohm cm)	Temp. (°C)	Specific resistivity (ohm cm)	Temp. (°C)	Specific resistivity (ohm cm)	Temp. (°C)	Specific resistivity (ohm cm)
50	2.56×10^{14}	19	2.61×10^{13}	61	2.02×10^{12}	19	3.80×10^{13}	19	6.51×10^{13}	19	1.82×10^{13}	19	2.09×10^{13}
67	1.48×10^{14}	35	1.19×10^{13}	71	1.16×10^{12}	31	1.58×10^{13}	87	8.80×10^{12}	56	1.20×10^{13}	35	9.06×10^{12}
83	7.68×10^{13}	48	8.84×10^{12}	81	7.47×10^{11}	43	1.27×10^{13}	100	3.17×10^{12}	70	1.19×10^{13}	50	3.93×10^{12}
95	5.13×10^{13}	68	5.91×10^{12}	97	2.83×10^{11}	53	1.03×10^{13}	109	2.01×10^{12}	82	7.52×10^{12}	63	2.18×10^{12}
109	3.03×10^{13}	82	3.64×10^{12}	111	1.26×10^{11}	66	6.58×10^{12}	120	9.36×10^{11}	97	4.02×10^{12}	79	1.20×10^{12}
120	1.70×10^{13}	99	1.52×10^{12}	123	6.22×10^{10}	79	2.92×10^{12}	136	3.35×10^{11}	111	1.40×10^{12}	97	5.79×10^{11}
130	1.06×10^{13}	111	8.56×10^{11}	130	3.14×10^{10}	92	1.11×10^{12}	146	1.79×10^{11}	125	5.73×10^{11}	110	3.35×10^{11}
141	5.45×10^{12}	127	1.83×10^{11}	141	1.81×10^{10}	102	5.77×10^{11}			138	2.40×10^{11}	128	1.32×10^{11}
149	3.31×10^{12}	139	3.76×10^{10}	149	1.45×10^{10}	115	2.35×10^{11}			150	1.15×10^{11}	141	7.05×10^{10}
		149	8.95×10^{9}			130	8.57×10^{10}						
						145	3.65×10^{10}						

*A.V. = Applied voltage: various applied voltages were charged since a battery was used instead of a regulated voltage supply
†The polymers were compressed into discs under a pressure of 20MN/m² with suction to remove air and moisture
‡Dimensions of discs: diameter, 12·8 mm; thickness 0·6–0·8 mm

Table 7 Semiconducting properties of polymers.* The values of ΔE_g and kink temperature of polyoxazoles

Polymer A	Temp. range (°C)	ΔE_g (eV)	Kink temp.† (°C)
A	50–109	0·7	109
	109–141	0·5	
B	19–104	0·6	104
	104–149	3·1	
C	61–149	2·3	——
D	19–72	0·5	72
	72–145	1·7	
E	87–146	1·7	——
F	19–82	0·3	82
	82–150	1·6	
G	19–110	0·9	110
	110–141	1·4	

*ΔE_g was calculated from linear relationship between log ρ and $1/T$ by the equation: $\rho = \rho_0 \exp(\Delta E_v/2kT)$
†Kink temperature means the curve point for the region of high temperature and low temperature in the temperature dependence curve of specific resistivity

The polycondensation product F obtained from DBO and tetrachloro-*p*-benzoquinone may show increased electrical conductivity because of inter-molecular charge transfer by the interaction of halogen and the oxazole ring. The good electrical conductivity of polymer G having methylene linkages may be explained by the eka-conjugation structure proposed by Pohl[9].

It has been shown earlier that the structure of the monomer is an important factor in determining the resistivity of the polymer[12]. The number of fused aromatic rings in the monomer gives an indication of the extent of conjugation. The structure of the hetero-rings in the polymer is an important parameter in the study of the effect of structure on conductivity.

Thermal stability

Thermal stability of ordered polyoxazoles has been previously studied by Preston *et al*. They suggested that the benzoxazoles and benzothiazole units are thermally stable in air, up to about 550°C[11]. The thermal stability was determined by thermogravimetric analysis. Polyoxazoles A, B, D and E are extremely thermally stable under oxidative conditions up to about 400°C. As is shown in *Figure 3*, polymer G decomposes more easily than either polymer A or polymer D.

The oxidative thermal stability of the polymers are also dependent on the stability of the aromatic rings in the polymer. The thermal stability of polymer with methylene linkages will be lower than that of other polyoxazoles, since the methylene linkage is thermally weak. The results of differential thermal analysis of DBO and some polymers are shown in *Figure 4*.

The temperature of decomposition of the oxazole ring in DBO was seen to be about 395°C in air. The differential thermal analysis data suggest that the benzoxazole ring is of comparable thermal stability. The initial tempera-

ture of weight loss, the temperature at 50 wt. % loss, and the peaks of the temperature exotherm of polyoxazole are summarized in *Table 8*.
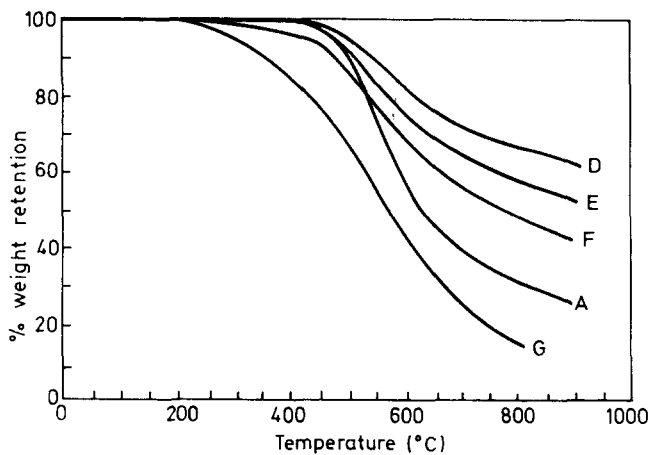
Figure 3 Thermogram plots of polyoxazoles in air
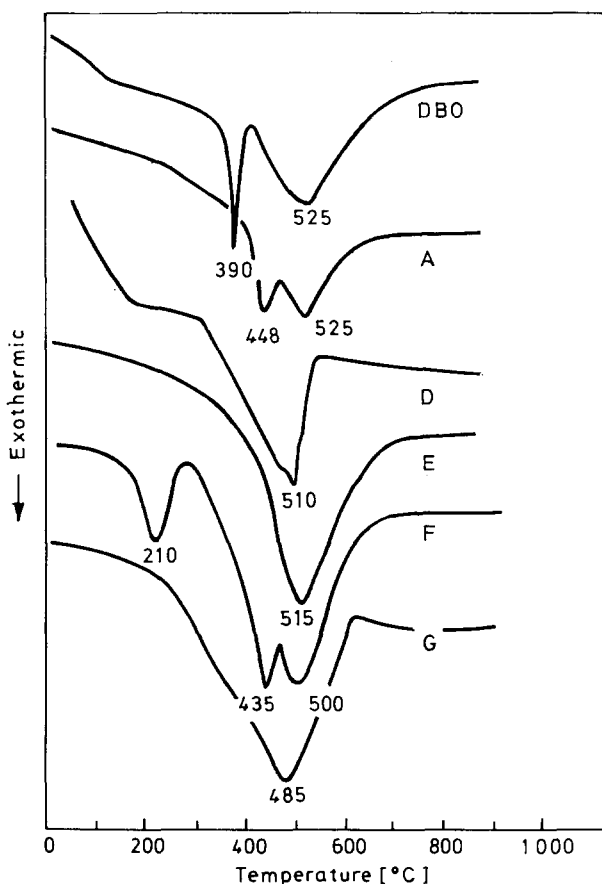
Figure 4 Differential thermal analysis curves of DBO and polyoxazoles

307

Table 8 Thermal properties of polyoxazoles

Polymer	Initial temp. of wt. loss* (°C)	Temp. at 50 wt.% loss† (°C)	Peak temp. of exothermic‡ (°C)
A	395	640	448, 525
B	352	713	365, 445, 548
C	300	620	430, 510
D	380	900	485, 510
E	390	900	515
F	190	790	210, 435, 500
G	200	570	485

*Initial Temperature of weight loss observed by TGA in air, rate 5°C/min. The temperatures given are those at the start point of weight loss in the TGA curve
†The weight loss is 50% of the original weight
‡Exothermic point observed by differential thermal analysis in air

Polyoxazoles with amide linkages were found to be stable thermally as shown by their constant weight on heating.

LIST OF ABBREVIATIONS

DAQ – 2,5-diamino-*p*-benzoquinone
DABQ – 2,5-di(*p*-acetamidobenzylidene amino)-*p*-benzoquinone
DAO – 2,6-di(*p*-acetamidophenyl)benz*bis*oxazole
DBO – 2,6-diaminophenylene benz*bis*oxazole

MA – 2-(*p*-aminophenyl)benzoxazole (*model compound A*)
MB – 2-(*p*-benzylidene aminophenyl)benzoxazole (*model compound B*)
MC – 2-(*p*-benzamido)phenylbenzoxazole (*model compound C*)

DMF – dimethyl formamide
PPA – polyphosphoric acid
NMP – N-methyl pyrrolidone
Py – pyridine
TEA – triethylamine
MOR – morphorine
DMAC – dimethyl acetamide
TPA – terephthalaldehyde
IPA – isophthalaldehyde
GO – glyoxal
TPC – terephthaloyl chloride
IPC – isophthaloylchloride
CA – tetrachloro-*p*-benzoquinone
XDB – *p*-xylylene dibromide
HMPA – hexamethyl phosphoric amide

Faculty of Engineering, Chiba University,
Yayoi-cho, Chiba, Japan

REFERENCES

1 Kho, J. H. T. and Pohl, H. A. *J. Polym. Sci. (A-1)* 1969, 7, 139
2 Pohl, H. A. *J. Polym. Sci. (A-2)* 1964, **2**, 2787
3 Inoue, H. *Bulletin of the University of Osaka Prefecture* 1961, **10**, 61
4 Botto, H. A. and Weiss, D. W. *Australian J. Chem.* 1963, **16**, 1076
5 Osman, A. N. *J. Amer. Chem. Soc.* 1957, **79**, 966
6 Danhauser, J. and Manecke, G. *Makromol. Chem.* 1965, **84**, 238
7 Binks, A. E. and Sharples, A. *J. Polym. Sci. (A-2)* 1968, **6**, 407
8 Brown, C. J. and Farthing, A. C. *J. Chem. Soc.* 1953, p 3270
9 Pohl, H. A. *J. Polym. Sci. (C)* 1967, **17**, 13
10 Mason, J. W., Hartman, R. D. and Pohl, H. A. *J. Polym. Sci. (C)* 1962, **17**, 187
11 Preston, J., Dewinter, W. F. and Black, W. B. *J. Polym. Sci. (A-1)* 1969, 7, 283

Heterogeneous nucleation in the crystallization of polyolefins:
Part 2. Kinetics of crystallization of nucleated polypropylene*

F. L. BINSBERGEN and B. G. M. DE LANGE

The kinetics of isothermal crystallization of nucleated polypropylene has been determined by depolarization measurement or dilatometry. The depolarization measurement was preferred, being faster and more reliable than dilatometry. For the evaluation of the recorded crystallization curves a non-linear regression analysis program was used fitting the data into the Avrami equation. An indication is given of some limitations in the applicability of this equation. Various experimental conditions may cause deviations in the crystallization kinetics from this equation. It is shown that in the analysis according to Avrami induction times become irrelevant. The nucleation density is highly dependent on the temperature of crystallization. Although the nucleation is for the larger part instantaneous, the density increases roughly by a factor of 10 at an increase in the degree of supercooling of 4°C. The temperature of melting prior to crystallization has no influence on the nucleation density, provided orientations in the melt have been relaxed. The nucleation density found was not proportional to the content of nucleating agent in the concentration series used, probably owing to the methods of preparation.

IN POLYPROPYLENE and several other polyolefins, the nucleation is generally of the predetermined type. This means that in an isothermal crystallization experiment all nucleating particles that are active at the temperature of crystallization act right from the start of the experiment.

In plain polypropylene, the number of crystallization centres shows an approximately stepwise dependence on the degree of supercooling. We suggested elsewhere[1] that this is due to the presence of small amounts of different types of nucleating species becoming active at different degrees of supercooling.

After the incorporation of a finely dispersed nucleating agent[2] an overwhelming amount of a single nucleating species is present. This might suggest that all the nucleating particles act as crystallization centres simultaneously and that they would do so from a certain degree of supercooling onwards. A few qualitative experiments clearly showed, however, that the number of crystallization centres is highly dependent on the temperature of crystallization. (Rybnikar[3] recently published similar experiments using weakly nucleated polypropylene.)

This phenomenon called for quantitative measurements of the nucleation

---

behaviour. Moreover, such measurements might enable us to determine the mechanism of nucleation, i.e. to develop an adequate theory.

Since in well-nucleated specimens the number of crystallization centres is far too large to be counted even in a microscopic specimen, we tried to calculate the nucleation density from the measurement of the overall crystallization kinetics. The kinetics of crystallization is governed by the course of the nucleation – instantaneous, time-dependent or something in between – and by the rate of growth of the spherulites. Consequently, separate measurement of the latter is necessary.

Assessing the exact course of the nucleation is difficult in fast crystallization experiments involving a large number of crystallization centres. Visual observations in the microscope showed that, in nucleated polypropylene too, the nucleation was mainly of the predetermined type.

In a few cases computed nucleation densities were checked by electron microscopy of the crystallized specimens.

METHODS OF MEASUREMENT

The temperature dependence of the nucleation density is best determined in isothermal crystallization experiments. The rate of growth of the spherulites is then essentially constant, and this rate can be determined separately. With a known rate of growth, the nucleation density (or frequency) can then be calculated from the bulk crystallization kinetics according to the well-known Avrami equation (see below).

On the other hand, the temperature dependences of nucleation and growth rates are difficult to separate in constant-cooling-rate experiments, and are heavily obscured by small time delays in nucleation.

In the general course of an isothermal crystallization experiment, the specimen is heated from room temperature to a temperature, T_1, above the melting point of the polymer, kept there for some time, and subsequently cooled to the temperature of crystallization, T_2.

Up to now, the type of measurement most frequently employed for the study of the kinetics of crystallization in bulk has been dilatometry. However, dilatometry as a means of measuring crystallization kinetics has a number of drawbacks[4]:

(1) It requires a relatively long time for temperature equilibration and thus does not permit accurate measurement of fast recrystallizations;

(2) Polymer samples often show a non-uniform nucleation density, which leads to different crystallization kinetics for different regions of the sample. This affects the overall crystallization kinetics to a considerable degree (see Appendix), but it is a phenomenon that cannot be observed separately in the dilatometer.

We have tried to avoid these difficulties by employing the measurement of depolarization of plane-polarized light by a microscope specimen[4, 5]. To this end, microscope specimens were inserted into a specially designed double heating stage, allowing short times for temperature equilibration. Since in a

microscope a small part of the specimen is observed, any non-uniformity in nucleation density or in temperature history in the investigated part of the specimen is ruled out.

To compare the two techniques, a few slow recrystallization experiments were carried out with the aid of both.

<div align="center">EXPERIMENTAL PART</div>

(1) *Samples*

(a) *Polymer*. In the quantitative measurements we used polypropylene from a single commercial batch (Shell Chemical Company). We removed stearate and potential stearic acid[2] by extracting the polymer powder in boiling acetone containing about 1 wt.% of concentrated hydrochloric acid for $\frac{1}{2}$ h. Subsequently, the powder was filtered off, washed with acetone, filtered and rinsed several times with acetone on the filter. Afterwards it was dried overnight at 50°C in a vacuum of about 1 mmHg pressure.

The analysis of this polymer was:
   intrinsic viscosity 2·9 dl/g (decalin, 135°C);
   metal content 11 ppm Al, 18 ppm Ti, 3 ppm Ca, 7 ppm Na.

If all calcium present were calcium stearate and all sodium present sodium stearate (which is not to be expected) the stearate content would be 140 ppm. Infra-red spectroscopy could not detect any carboxylate, however, so we assumed the calcium and sodium to be present as chlorides.

(b) *Preparation of nucleated samples*. The nucleating agents used in this investigation were the sodium salt of *para*-tert-butylbenzoic acid [Na(PTBB)] and the aluminium mono-hydroxy salt of the same acid [AlOH(PTBB)₂].

The *para*-tert-butyl-benzoic acid used in the preparation of nucleating agents was purified either by zone-melting or by sublimation. The melting point of the purified product was 161°C.

Na(PTBB) was prepared by dissolving the acid in an equimolar amount of aqueous sodium hydroxide to give an approximately 30 wt.% solution. It was precipitated by addition of acetone, filtered off and dried.

Fine dispersions of this salt in polypropylene were prepared according to reference 2 method 2.

Fine dispersions of AlOH(PTBB)₂ in polypropylene were prepared according to reference 2 method 3. Because this method uses rather large amounts of water in the washing of the precipitate we analysed the nucleated polypropylene for content and composition of the salt. The aluminium content in the ultimate sheets was determined by x-ray emission spectroscopy. The amount of carboxylate was determined by infra-red spectroscopy (with the blank in the reference beam) from the absorptions at 1560 cm⁻¹ (carboxylate) and at 717 cm⁻¹ (aromatic C—H). Both the aluminium and the carboxylate content were in reasonable agreement with the expected value for the whole

<div align="center">311</div>

range of concentrations used. Free carboxylic acid was not present, as was evidenced by the absence of absorption at $1695\,cm^{-1}$.

For an accurate analysis of the AlOH(PTBB)$_2$ used we prepared it separately according to method 3, but this time in the absence of the polymer. The salt was precipitated and filtered off, washed several times with water and dried. Aluminium analysis by oxidative decomposition in water and colorimetric determination of the complex with 8-hydroxyquinoline showed an aluminium content of $6\cdot8\,wt.\%$ (theory $6\cdot78$). Extraction with acetone in a Soxhlet for 6h showed that less than $0\cdot1\,wt.\%$ free acid was present. Infra-red analysis of the salt in potassium bromide pellets showed the presence of free hydroxyl ($3700\,cm^{-1}$) and absence of hydrogen bonding ($3400\,cm^{-1}$, broad absorption band).

This analysis confirms the monobasic nature of the salt, since the dibasic salt shows hydrogen bonding[6-8].

A concentration series both of Na(PTBB) and of AlOH(PTBB)$_2$ in polypropylene was prepared.

(2) Specimen preparation

Microscope specimens were made according to reference 2, the thickness of the polymer film in the specimen was taken between $0\cdot1\,mm$ and $0\cdot2\,mm$.

Disc-shaped specimens for dilatometry were cut from a $1\cdot5\,mm$ thick compression-moulded sheet (see reference 2).

(3) Apparatus and procedure

(a) *Rate of linear growth of spherulites.* The specimen was crystallized on a Kofler hot stage, mounted in the microscope (Reichert Zetopan-Pol), whose temperature was kept constant within $0\cdot5\,°C$. The sizes of several spherulites were measured from photographs taken at regular intervals, and were plotted against time.

(b) *Bulk crystallization rate by depolarization measurement.* Microscopic specimens were inserted in the clamp of a double-heating stage fitted in the microscope (*Figure 1*). Each oven consists of a copper block having a 'slot' just large enough to accommodate the specimen. In oven number 1 the polymer was melted and in oven number 2 it was allowed to crystallize. In the latter, the specimen intersects the optical axis of the microscope. The specimen can be moved by screws V and H (*Figure 1*) in order to change the place of observation. The temperature of oven number 2 was kept constant within $0\cdot5\,°C$, that of oven number 1 was $220 \pm 4\,°C$.

The rate of heat transfer of oven number 2 to the specimen was measured by cementing an ultra-thin Pt–Pt/Rh thermocouple in the polymer film. The temperature was found to be:

$$T = T_2 + (T_1 - T_2)\exp{(-0\cdot12t)} \qquad (1)$$

t being the time in seconds elapsed since insertion in oven number 2, and the indices 1 and 2 indicating the ovens.

During measurement the polarizers of the microscope were crossed. The light source, a 6 V, 5 A bulb, was stabilized by a voltage stabilizer. The light output of the optical system was measured by a photomultiplier inserted in the eyepiece tube, and recorded both by a writing chart recorder and by a digital recorder. The photomultiplier was operated in its linear range. (The photomultiplier and amplifier were supplied by PhotoVolt Company.)
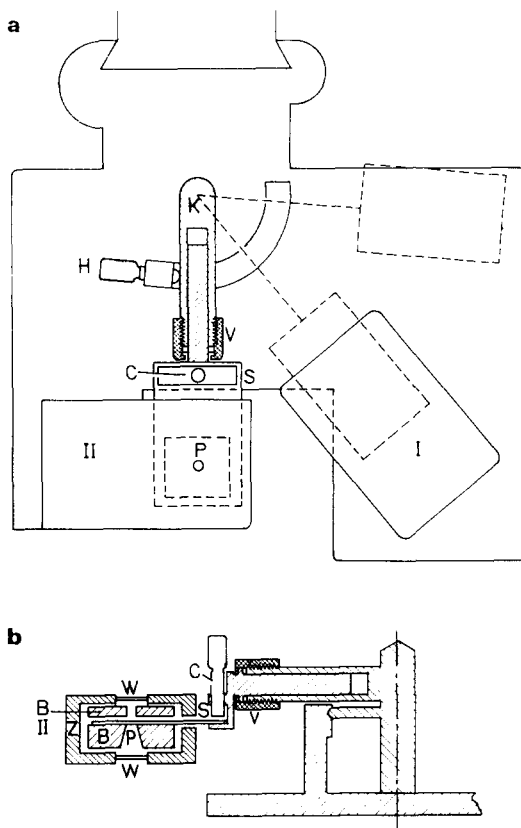
Figure 1 Double heating stage: (a) Top view; (b) Vertical cross section through swing arm and oven no. 2

I,	Oven No. 1	P,	Hole through which the light passes
II,	Oven No. 2	B,	Copper block
H, V,	Positioning screws	Z,	Heat insulation
S,	Slide	W,	Glass window
C,	Clamp for slide	K,	Swing arm

(c) *Bulk crystallization rate measurement by dilatometry.* The dilatometers described in the literature frequently have a bulky shape. Since the time necessary for temperature equilibration will be shorter for a thin than for a thick specimen, we used a disc-shaped dilatometer having an inner diameter

of 20 mm and an inner thickness of 2 mm. The dimensions of the specimens inserted were somewhat smaller.

For further improvement of the heat transfer between sample and bath the dilatometer was not made of glass but of stainless steel, type AISI 430, a mercury-resisting material (*Figure 2a*). The inner diameter of the capillary of the dilatometer is 0·4 mm, so that the correction necessary for mercury moving into the heated part of the dilatometer during the experiment will be only small.
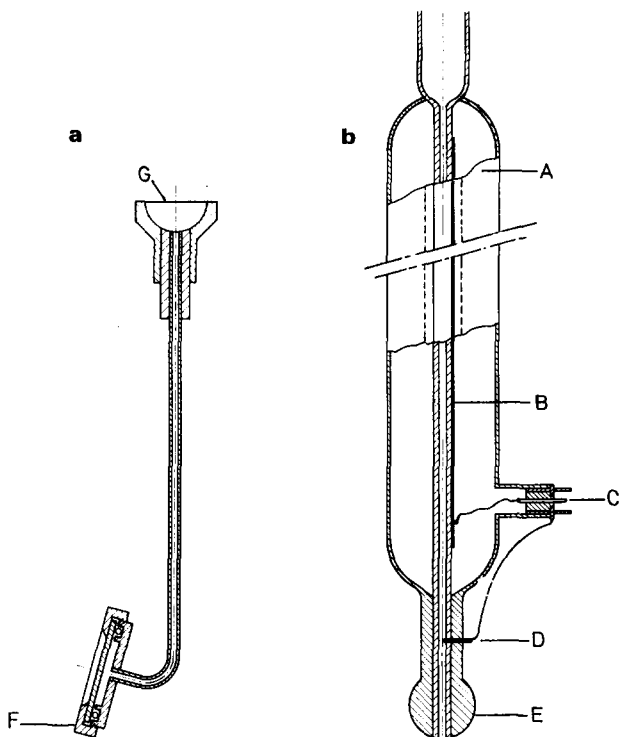
Figure 2 Dilatometer: (a) Dilatometer vessel; (b) Measuring vessel

A, Outer shielding partly silvered; capillary is visible through slits
B, Metal strip glued to capillary
C, Connection to capacitance bridge
D, Platinum point providing contact with mercury
E, Ball-joint connection with dilatometer vessel
F, Sample chamber
G, Ball joint to measuring capillary

The removable bottom plate fitted by a screw cap allows easy insertion of the specimen. Vacuum-tight sealing is provided by a rubber O-ring capable of withstanding temperatures up to 210°C.

The change in volume was determined via a precision glass capillary of 1·0 mm bore coated with silver (*Figure 2b*), allowing capacitive measurement of the height in the capillary.

Before measurement, the specimen was inserted in the dilatometer, which was then connected to the measuring capillary; the system was filled with a predetermined amount of mercury under a reduced pressure of 10^{-3} mmHg.

The dilatometer was then preheated at about 210°C in a thermostatted bath for about 15 min and quickly transferred to a second bath maintained at the crystallization temperature within 0·05°C.

(d) *Electron microscopy*. Free surfaces for replication were obtained by either

(1) lifting the cover glass from crystallized microscope preparations after cooling to room temperature, or

(2) crystallizing without cover glass, under nitrogen, in a closed vessel suspended in a thermostatted bath.

Replicas were made by carbon/platinum shadowing of the polypropylene surface, backing with poly(vinyl alcohol), dissolving the polypropylene at 150°C in decalin and subsequently dissolving the poly(vinyl alcohol) in water. The swelling of polypropylene in decalin sometimes caused fracture of the replicas. Therefore one of the following methods was also used: platinum-shadowing; backing with poly(vinyl alcohol); pulling off the poly(vinyl alcohol) film to which the metal adhered; depositing the carbon and dissolving the poly(vinyl alcohol) in water[9].

Electron micrographs were taken by means of a Siemens Elmiskop I.

EVALUATION OF THE KINETICS OF CRYSTALLIZATION

(1) *Avrami equation*

The general equation concerning the kinetics of isothermal crystallization named after Avrami[10]:

$$\alpha = 1 - \exp\left(-Kt^n\right) \tag{2}$$

(α being the fraction crystallized, t the time and K and n being adjustable parameters) has been derived in several ways[11, 12]. Here, we summarize the interpretation of this equation for the case of either instantaneous nucleation with a nucleation density (per unit volume), N, or a constant nucleation frequency (per unit time and unit volume), I, combined with the spherulitic mode of growth.

Instantaneous nucleation:

$$n = 3 \tag{3a}$$

$$K = \tfrac{4}{3}\pi N v^3 \tag{3b}$$

v being the linear rate of spherulitic growth.
Constant nucleation frequency:

$$n = 4 \tag{4a}$$

$$K = \tfrac{1}{3}\pi I v^4 \tag{4b}$$

The experimental crystallization curves were evaluated by non-linear regression analysis according to an adapted Avrami equation (see Appendix). This method was preferred to log–log plotting of the measured data because of the uncertainty in the exact starting time of the crystallization[13] and for several other reasons (see Appendix).

(2) Dilatometric measurement

In the dilatometer the decrease in volume of the sample brought about by crystallization is measured:

$$a_v = \frac{V_0 - V}{V_0 - V_\infty} \tag{5}$$

where V is the volume of the sample and V_0 and V_∞ are the initial and final volumes, respectively.

(3) Kinetic measurement of depolarization

Magill[14] showed that the depolarization Δ of incident plane-polarized light by crystallizing polypropylene often follows an Avrami equation fairly well:

$$\Delta = \Delta_\infty[1 - \exp(-Kt^n)] \tag{6}$$

in which Δ_∞ is the depolarization measured at the end of the experiment. At moderate supercooling he found mostly $n = 3$, indicating predetermined nucleation. It is not seen at once why this should be so.

It can be shown[15] by hypothetically subdividing a polycrystalline specimen into a very large number of equal piles, each containing F small, uniaxially birefringent, randomly oriented crystals of thickness w, that the depolarization is:

$$\Delta = \frac{4\pi^2 F w^2 (\Delta n)^2}{15\lambda^2}, \tag{7}$$

Δn being the birefringence and λ the wavelength of the light used.

Let us assume that a number of N birefringent cubes per unit volume grow in the melt. We imagine the crystallizing mass to be subdivided into a very large number of piles (N_p) per unit area.

The volume fraction (V_c) of the crystallized mass initially increases with the third power of the time:

$$V_c = Nw^3 = 8Nv^3t^3 = \sum_{k=1}^{N_p} F_k w / N_p D \tag{8}$$

for $w = 2vt$, v being the linear rate of growth and D the thickness of the specimen. The depolarization then follows:

$$\Delta = \frac{4\pi^2(\Delta n)^2}{15\lambda^2} \times w^2 \times \frac{\Sigma F_k}{N_p} = \frac{4\pi^2(\Delta n)^2}{15\lambda^2} \times 16Nv^4t^4 D, \tag{9}$$

in other words, the depolarization increases with the fourth power of the time. For other types of particles, too, uniform growth will be the cause that $V_c \sim t^3$ and $\Delta \sim t^4$.

We can clearly observe three-dimensional growth when an Avrami $n = 3$ is found in depolarization measurements of bulk crystallization. However, we must assume that there is no increase in thickness of birefringent entities – after an early stage of crystallization – but that the crystallizing regions are aggregates of birefringent entities of constant thickness increasing in number of length within the aggregates. This is consistent with the fibrous morphology of spherulites, the fibrils being stacks of lamellae that frequently branch[16] during growth.

There is another feature, especially in the crystallization of polypropylene, that may cause a depolarization-time curve to correspond more closely to $n = 3$ than to $n = 4$. This is the fact that the initial stage of crystallization shows a considerably higher birefringence than fully developed spherulites, thus causing the initial portion of the curve to be somewhat too high.

RESULTS

(1) Linear rate of growth of spherulites

Plots of the size of growing spherulites versus time were always linear and did not show an appreciable induction time. From these plots the radial rate of growth (v) was calculated. The results are given in Table 1.

A plot of $\log v$ versus $1/T\Delta T$ was linear (Figure 3) according to the theory of crystal growth by secondary nucleation but needed adaptation of the melting point (T_m) as a function of crystallization temperature, as has been indicated by von Falkai[17]. The adaptation used is given in Table 1.

Table 1 Radial rate of growth of polypropylene spherulites

$v \times 10^6$ (cm/s)	T (°C)	Assumed T_m (°C)
28	125	168
16	128	168
8·0	131	168
3·65	134	168
2·35	137	169
1·25	140	170·5
0·82	143	172
0·465	146	173·5
0·305	149	175

This adaptation is a peculiar feature of the crystallization of polypropylene, while something similar is not necessary for most other crystallizing polymers. Its potential incorrectness does not affect our evaluation of kinetic data, however.

317
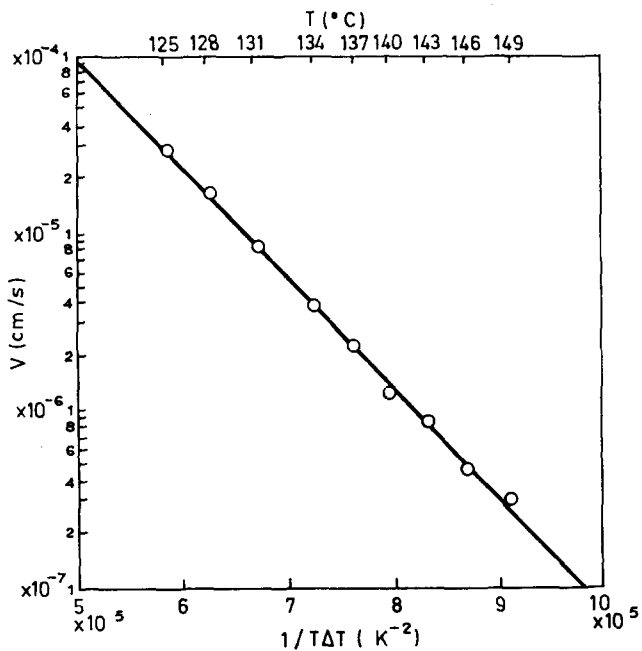
Figure 3 Radial rate of growth of polypropylene spherulites
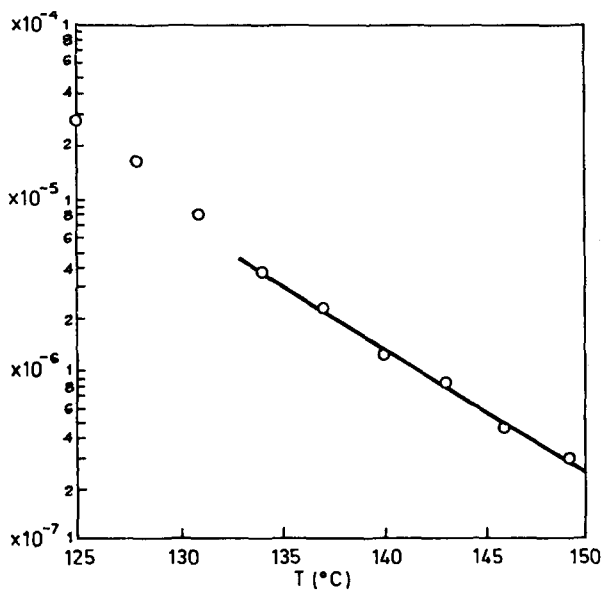
Figure 4 Radial rate of growth of polypropylene spherulites

318

Within a limited temperature region, a linear plot of log v versus T was obtained (*Figure 4*). This provides a convenient relation for purposes of calculus (as used further on):

$$v = 1.33 \times 10^{-6} \exp\left[-0.225\,(T - 140)\right] \qquad (10)$$

$$\text{for } 134 < T < 150$$

$$(v \text{ in cm/s, } T \text{ in } °\text{C})$$

Measurement of the rate of growth in nucleated polypropylene gave the same values as in non-nucleated polymer (within the limits of accuracy).

(2) *Kinetics of crystallization induced by nucleating agents*

The kinetics of crystallization induced by nucleating agents were mainly recorded by measuring the depolarization. Dilatometry was used as a check for these measurements. For the slower crystallizations the two methods generally yielded exactly the same kinetics. In crystallization experiments with half-times less than 15 min the results of the two methods often differed; this can be ascribed to too slow a temperature equilibration in the case of the dilatometer. Below we will present only the results of depolarization measurements.

Regression analysis of very slow crystallizations generally showed an Avrami exponent n of somewhat less than 3, while for fast ones it tended to give values considerably higher than 3, sometimes even 5 to 6. Many experiments of intermediate rate nicely followed the Avrami equation with $n = 3$, however. We cannot give a firm rule for what is 'slow' and what is 'fast' with respect to the deviation of n from 3.

For the fast crystallizations having $n > 3$ the regression analysis gave t_0 values that were too low, often indicating that the crystallization would have started long before the specimen was placed in oven number 2. By fixing the value of n at 3 the regression analysis gave the correct value of t_0. Therefore, this was done as a rule.

Duplication of a measurement by using the same specimen and place of observation resulted in the same crystallization curve. A new specimen from the same sample often displayed some differences in kinetics, except for the lowest temperature of a series where the differences were large owing to the fact that the crystallization half-time approached the time for temperature equilibration.

Often some orientation was present in the birefringence of the observed part of the specimen. The ultimate depolarization by the specimen was much lower when this orientation was placed parallel to either the polarizer or the analyser than when it was in a 45° postion. Yet, in both cases the same crystallization curve was recorded when the amplification of the photo-multiplier was adjusted to the same ultimate output voltage.

The nucleation densities calculated from the K values (resulting from regression analyses of the curves for fixed $n = 3$) have been plotted versus the crystallization temperature in *Figures 5* and *6*. Qualitatively, these numbers

319

were in accordance with the grain size observed in the specimens after the measurement. For both the nucleating agents used the number of crystallization centres increased by a factor of ten at an increase in supercooling of approximately 4°C. The concentration of nucleating agent was not linearly proportional to the nucleation density. In samples nucleated with $AlOH(PTBB)_2$ an ultimate level of nucleation seemed to have been reached at a concentration of roughly 1 wt.%.
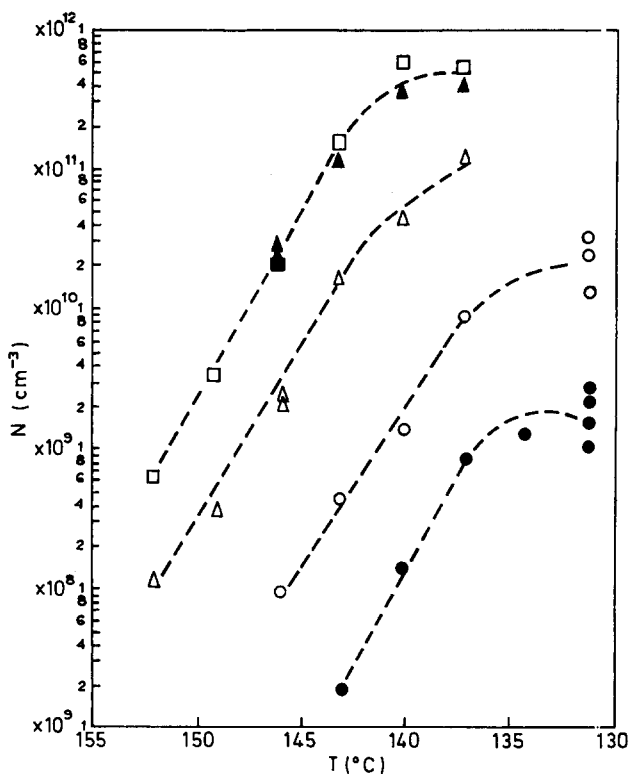
Figure 5 Number of crystallization centres versus temperature of crystallization for polypropylene containing various amounts of $AlOH(PTBB)_2$

●, 0·03 wt.%;   △, 0·3 wt.%;   □, 3 wt.%
○, 0·1 wt.%;   ▲, 1 wt.%;

Variation of the premelting temperature, T_1, between 175°C and 280°C had no influence on the crystallization kinetics of well-nucleated specimens. When a specimen of polypropylene containing 0·3 wt.% Na(PTBB) was melted at 240°C, crystallized at 143°C, remelted at 175°C and then recrystallized at 143°C, two identical crystallization curves were found, both when remelting was done directly and when the specimen had intermediately been cooled to room temperature.

The almost instantaneous character of the nucleation was demonstrated

by keeping a specimen for a short time at a temperature T_3, somewhat below T_2, prior to crystallization at T_2 (*Figure 7*). In such experiments the number of crystallization centres did not correspond to temperature T_2 (see *Figures 6* and *7*) but was very close to the number otherwise observed at T_3.
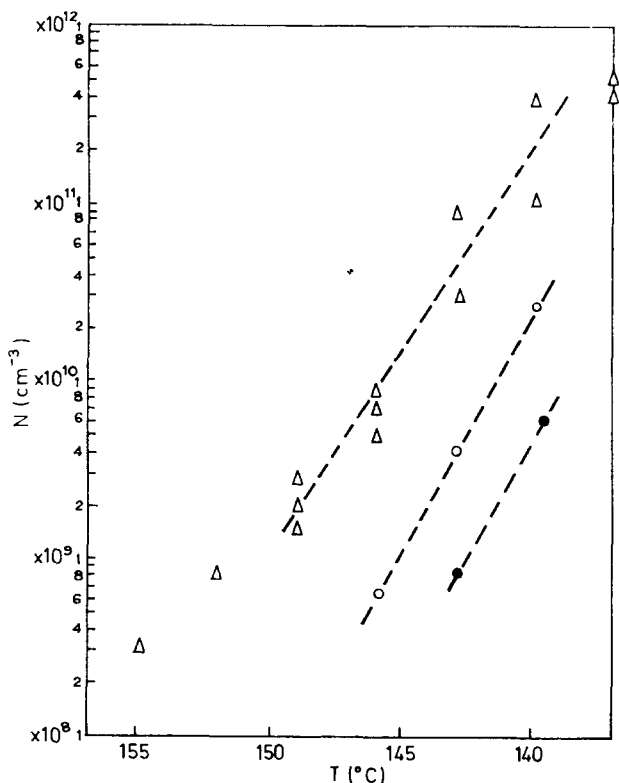
Figure 6 Number of crystallization centres versus temperature of crystallization for polypropylene containing various amounts of Na(PTBB)
●, 0·03 wt.%;   ○, 0·1 wt.%;   △, 0·3 wt.%
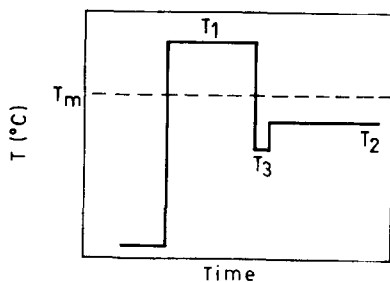
Figure 7 Special temperature programme

(3) *Nucleation density measured by electron microscopy*

Specimens of a concentration series of AlOH(PTBB)$_2$ were crystallized at 143°C and at 137°C. The size of the quadrites[18] – the crystalline aggregates that are the precursors of spherulites – were measured from a number of electron micrographs (like *Figure 8*) taken from each specimen. The number
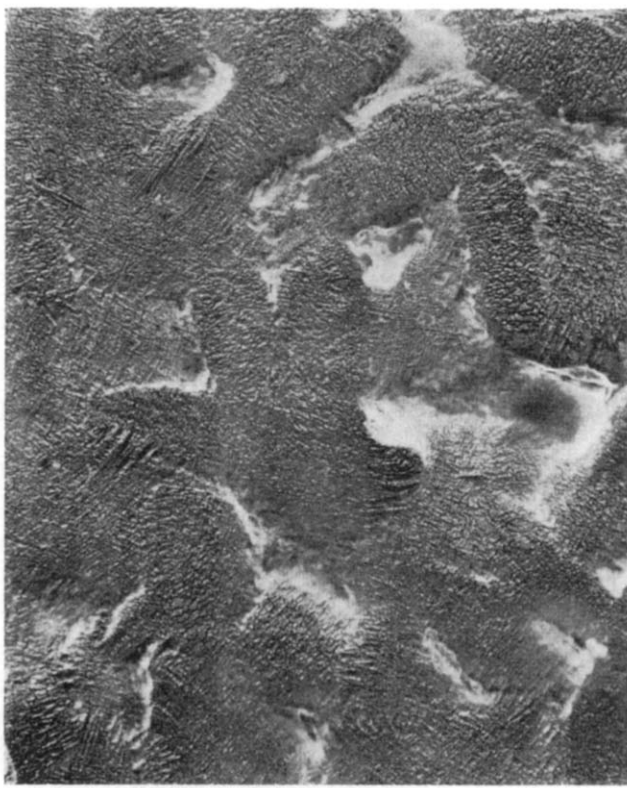
Figure 8 Polypropylene containing 0·5 wt.% AlOH(PTBB)$_2$ crystal-lized at 137°C with free surface (quadrites mainly seen edge-on): (×17 000)

of crystallization centres was calculated from the mean size assuming the volume of the quadrite to be roughly $0\cdot4z \times z \times z$, z being the larger dimension of the aggregate (see *Table 2*).

These values fit into the plots of *Figure 6* reasonably well if we assume that the downward curvature of the plots is an artefact caused by cooling being less rapid than required to maintain a constant temperature throughout the crystallization.

A specimen of polypropylene containing 1 wt.% AlOH(PTBB)$_2$ quenched from 220°C in cold water showed – very faintly – quadrites of a larger dimension of about $0\cdot5\mu m$, corresponding to a nucleation density of roughly 2×10^{13} cm^{-3}.

Table 2 Number of crystallization centres per cm³ (*N*) in polypropylene nucleated by AlOH(PTBB)₂

Concentration of nucleating agent (%)	Crystallization temperature (°C)	Mean larger dimension of quadrites (μm)	Number of crystallization centres (cm⁻³)
1·0	143	2·5	2×10^{11}
0·5	143	4	4×10^{10}
0·25	143	6	1×10^{10}
1·0	137	1·3	1×10^{12}
0·5	137	2	3×10^{11}

DISCUSSION

(1) *Evaluation of crystallization kinetics**

(a) *Avrami exponent.* The evaluation of crystallization kinetics recorded by measurement of depolarization generally gives an Avrami exponent, *n*, of 3, or needs this value to obtain the correct value of the time of starting the crystallization. Several of the slower crystallization experiments showed the same kinetics by depolarization measurement and by dilatometry. Moreover, the number of crystallization centres calculated from the evaluation using $n = 3$ were – within the reproducibility of the experiments – confirmed by electron microscopy for high nucleation density and by optical microscopical observation for low nucleation density.

Calculations of the number of crystallization centres from an evaluation using $n = 4$, assuming a constant nucleation frequency:

$$N = \int_0^\infty I(1 - \alpha)\, dt \tag{11}$$

led to values of *N* several orders too small.

Table 3 compares numbers of crystallization centres calculated from regression analysis with $n = 3$ and with $n = 4$. The values of $n = 3$ were in accordance with microscopic observation throughout the range of crystallization temperatures.

(b) *Induction time.* According to the results of the regression analysis there is no detectable induction time for the crystallization in agreement with the observations during measurement of linear growth rates. Assumption of an induction time would cause a value for *n* less than 3 to result from the kinetic data.

There may indeed be a relatively large time lapse between the start of crystal growth and the first detection of crystallization in an instrument that has a recording sensitivity of about $\frac{1}{2}\%$ of the full scale. We were able to show that the induction time is indeed only apparent in this sense, since by

---

*See Appendix.

Y*

Table 3 Number of effective crystallization centres, N, calculated assuming either instantaneous nucleation ($n = 3$) or constant nucleation frequency, I, ($n = 4$). Experiments with polypropylene containing 0·3 wt.% $AlOH(PTBB)_2$ at various crystallization temperatures, T_2

	$n = 3$	$n = 4$	
T_2	N (cm^{-3})	N (cm^{-3})	I (cm^{-3} s^{-1})
137	$1·2 \times 10^{11}$	$4·2 \times 10^{11}$	$8·7 \times 10^9$
140	$4·4 \times 10^{10}$	$4·6 \times 10^{10}$	$2·2 \times 10^8$
143	$1·7 \times 10^{10}$	$6·5 \times 10^9$	$1·15 \times 10^7$
146	$2·4 \times 10^9$	$2·7 \times 10^8$	$9·2 \times 10^4$
149	$3·8 \times 10^8$	$1·4 \times 10^7$	$1·14 \times 10^3$
152	$1·1 \times 10^8$	$4·3 \times 10^5$	$1·2 \times 10$

using an amplification for the photomultiplier in the first stage of crystallization 100 times as large as in the later stages we found a correspondingly earlier time of first detectable crystallization.

(c) *Fast crystallizations.* The limited reliability of the curved parts of the plots in *Figure 6* can be understood qualitatively by calculating the radii of spherulites initiated before thermal equilibrium is obtained. The radii at t_2 seconds after insertion of the specimen into oven number 2 for spherulites initiated at t_1 can be calculated by numerical integration using equations (1) and (10):

$$\int_{t_1}^{t_2} v \, dt = \int_{t_1}^{t_2} 1·33 \times 10^{-6} \exp \{-0·225 [T_2 - 140 + $$
$$+ (220 - T_2) \exp (-0·12t)]\} \, dt \qquad (12)$$

Table 4 Radii at t_2 of spherulites initiated at t_1 seconds after insertion of specimen in oven number 2, in μm

T_2	$t_1 = 20$ $t_2 = 40$	$t_1 = 20$ $t_2 = 50$	$t_1 = 40$ $t_2 = 50$
146	0·056	0·098	0·042
143	0·099	0·17	0·070
140	0·15	0·26	0·11
137	0·28	0·49	0·21
134	0·44	0·77	0·33

The kinetic evaluation becomes unreliable when before the actual temperature of crystallization and before its corresponding nucleation density is attained some crystallization takes place. The consequences are that t_0 is pushed to low values and simultaneously n is found to be larger than 3. Moreover, the early-started spherulites already cover an area that otherwise would crystallize much more finely, thus causing the nucleation density to be lower than in a truly isothermal experiment.

(2) *Dependence of nucleation density on temperature and on time*

The strong dependence of the nucleating effect on the degree of super-cooling combined with its almost perfectly instantaneous character is difficult to reconcile with the classical theory of heterogeneous nucleation on a flat or curved plane[20-23] since such a theory is able to explain either a strong temperature dependence of a nucleation *frequency* or an instantaneous nucleation character, but not the two together. The latter may still be the result of a nucleation frequency, being measurable at a (very) small degree of supercooling but being so large at the supercooling applied in this experiment that all particles nucleate the crystallization almost instantaneously. However, this effect should then be present with all nucleating particles and it therefore offers no explanation for the temperature dependence of the nucleation density.

The nucleating effect is not due to superheating of crystalline material enclosed in voids of the nucleating particles[24] since, at 173°C and above, the melting temperature does not influence the nucleation density. This fact was well established by showing both the dependence on crystallization tempera-ture mentioned and a very good reproducibility of the nucleation density at a single recrystallization temperature by up to twenty successive recrystalliza-tion measurements (with complete melting in between) on a single spot of the same specimen.

In the third paper of this series we will try to provide an explanatory mechanism of heterogeneous nucleation that covers all the effects men-tioned.

(3) *Relation between concentration of nucleating agent and number of crystallization centres*

The large deviation from proportionality in the relation between concen-tration of nucleating agent and nucleation density at one crystallization temperature is not well understood. The deviation may be ascribed to dif-ferences in dilution during preparation of the aluminium salt and to differences in humidity of the polypropylene powder at the beginning of the crystalliza-tion of the sodium salt onto the powder. It can hardly be imagined that at a higher concentration a progressively higher number of particles is formed. Hence, the particles in the nucleated specimen should, on average, have a higher activity as the concentration of the nucleating agent is higher.

As for the sodium salts, we have no further evidence on this point. A polypropylene melt containing 0·3 wt. % AlOH(PTBB)$_2$ seems almost optically clean (in dark field); at a concentration of 2 wt. % a faint structure was seen, and at 10 wt. % a very clear one. In the latter case the salt was seen as strings of droplets causing the melt to be hazy. The salt was less effective when a 10 wt. % master batch was diluted to 1 wt. % by powder mixing than in the case of direct preparation of a 1 wt. % sample. Thus we see that a slight variation in conditions of preparation may cause an appreciable change in nucleating effect.

REFERENCES

1 Binsbergen, F. L. *Dissertation* Groningen, Netherlands, 1969
2 Binsbergen, F. L. *Polymer, Lond.* 1970, **11**, 253
3 Rybnikar, F. *Kunststoffe* 1968, **58**, 515
4 Magill, J. H. *Polymer, Lond.* 1961, **2**, 221
5 Hock, C. W. and Arbogast, J. F. *Anal. Chem.* 1961, **33**, 462
6 Harple, W. W., Wiberley, S. E. and Bauer, W. H. *Anal. Chem.* 1952, **24**, 635
7 Scott, F. A., Goldenson, J., Wiberley, S. E. and Bauer, W. H. *J. Chem. Phys.* 1954, **58**, 61
8 Gilmour, A., Jobling, A. and Nelson, S. M. *J. Chem. Soc.* 1956, p 1972
9 Geil, P. H., 'Polymer single crystals', Interscience, New York, 1963, p 68 ff
10 Avrami, M. *J. Chem. Phys.* 1939, **7**, 1103; 1940, **8**, 212; 1941, **9**, 177
11 Evans, U. R. *Trans. Faraday Soc.* 1945, **41**, 365
12 Mandelkern, L., 'Crystallization in polymers', McGraw Hill, New York, 1964, chapter 8
13 Tomka, J. *European Polymer J.* 1968, **4**, 237
14 Magill, J. H. *Polymer Lond.* 1962, **3**, 35
15 Binsbergen, F. L. *J. Macromol. Sci. (B)* (submitted for publication).
16 Keith, H. D. and Padden, F. J. *J. applied Phys.* 1963, **34**, 2409; 1964, **35**, 1270
17 Von Falkai, B. *Makromol. Chem.* 1960, **41**, 86
18 Binsbergen, F. L. and de Lange, B. G. M. *Polymer, Lond.* 1968, **9**, 23
19 Mandelkern, L., Quinn, F. A. and Flory, P. J. *J. applied Phys.* 1954, **25**, 830
20 Volmer, M., 'Die Kinetik der Phasenbildung', Th. Steinkopf, Dresden, 1939
21 Lacmann, R. *Z. Kristallographie* 1961, **116**, 13
22 Fletcher, N. H. *J. Chem. Phys.* 1958, **29**, 572; 1963, **38**, 237
23 Edwards, G. R., Evans, L. F. and LaMer, V. K. *J. Colloid Sci.* 1962, **17**, 749
24 Turnbull, D. *J. Chem. Phys.* 1950, **18**, 198
25 Rohleder, J. and Stuart, H. A. *Makromol. Chem.* 1961, **41**, 110
26 Banks, W., Gordon, M., Roe, R. J. and Sharples, A. *Polymer, Lond.* 1963, **4**, 61
27 Sharples, A. and Swinton, F. L. *Polymer, Lond.* 1963, **4**, 119
28 Banks, W. and Sharples, A. *Makromol. Chem.* 1963, **59**, 233
29 Banks, W., Gordon, M. and Sharples, A. *Polymer, Lond.* 1963, **4**, 289
30 Rabesiaka, J. and Kovacs, A. J. *J. applied Phys.* 1961, **32**, 2314
31 Peterlin, A. *J. applied Phys.* 1964, **35**, 75
32 Hoshino, S., Meinecke, E., Powers, J., Stein, R. S. and Newman, S. *J. Polym. Sci. (A* 1965, **3**, 3041
33 Hillier, I. H. *J. Polym. Sci. (A)* 1965, **3**, 3067
34 Price, F. P. *J. Polym. Sci. (A)* 1965, **3**, 3079
35 Sharples, A. *Polymer, Lond.* 1962, **3**, 250
36 Boon, J., Challa, G. and Van Krevelen, D. W. *J. Polym. Sci. (A-2)* 1968, **6**, 1835
37 Gordon, M. and Hillier, I. H. *Trans. Faraday Soc.* 1964, **60**, 763
38 Hillier, I. H. *J. Polym. Sci. (A-2)* 1966, **4**, 1
39 Binsbergen, F. L. *Nature* 1966, **211**, 516
40 Magill, J. H. *Polymer, Lond.* 1961, **2**, 221

APPENDIX:

RELIABILITY OF THE EVALUATION OF THE KINETICS OF CRYSTALLIZATION ACCORDING TO THE AVRAMI EQUATION

The fitting of an experimental crystallization curve to the Avrami equation (2) has frequently resulted in a value for the 'exponent', n, that deviated considerably from integers or gave the wrong number[25-29]. In such cases the 'kinetic constant', K, is difficult to interpret, since the 'exponent' has a physical meaning for integral values only [see equations (3) and (4)].

The observed deviations have been attributed to various possible causes related to the nature of polymer crystallization processes, such as:

(1) secondary crystallization in already crystallized regions[30-34];
(2) an initial but ceasing time-dependent nucleation[35, 36];
(3) non-constant growth of lamellae of constant density[37, 38].

While these causes may be active in some crystallizing polymers, we want to discuss a number of causes lying either in experimental difficulties (such as inhomogeneous nucleation density, non-uniform thermal history of the sample and uncertainty about the exact starting time of the crystallization) or in the evaluation of the experimental data rather than in the nature of the crystallization of polymers.

EVALUATION OF RECORDED CRYSTALLIZATION

The evaluation of the crystallization kinetics can be carried out in several ways:

(1) Plotting log α versus log t for the initial part of the crystallization is supposed to give, according to equation (2), a straight line with slope n and intercept log K.

(2) Plotting log $[-\log(1 - \alpha)]$ versus log t should give a straight line with slope n and intercept log $0.4343 K$.
The fact that time $t = 0$, i.e. the start of the crystallization, is not exactly known gives some uncertainty in the slope and a considerable uncertainty in the intercept, especially in those experiments where the crystallization half-time (time at which $\alpha = \frac{1}{2}$) is less than, say, 10 times the time required for temperature equilibration. Moreover, the large relative inaccuracy of small values of α brings about a large uncertainty in the lower part of the log plots. Therefore we preferred a third method.

(3) The recording of a crystallization experiment by a strip chart recorder generally produces a sigmoidal curve (*Figure 9*). This curve is a plot of the deflection, y, versus the time, x. From *Figure 9* we see that we need a knowledge of the initial value of the deflection, y_0, the difference between the initial and the final one, y_1, and the starting time of the experiment, t_0, before K and n can be computed.

The Avrami equation in terms of *Figure 9* is:

$$y = y_0 + y_1\{1 - \exp[-K(x - t_0)^n]\}. \tag{13}$$

327

This means that in practice we have to fit the experimental data to a five-parameter equation (with y_0, y_1, K, t_0 and n) rather than to a two-parameter one like equation (2).

Generally, it is possible to make an accurate estimate of y_0, while a fairly good estimate of y_1 could be made, since the secondary crystallization of polypropylene causing the deflection y to exceed $(y_0 + y_1)$ (see *Figure 9*)
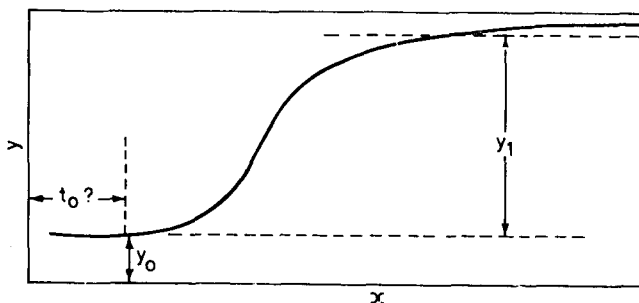
Figure 9 Recording of depolarization versus time

appeared to be slow compared with the primary one. Nevertheless, because of some uncertainty in the data points for α values close to 1, we generally used only data points for α values up to 0·6 or 0·7.

We want to know how accurately K and n can be determined from a curve like the one in *Figure 9* and to what extent these parameters are influenced by the uncertainty in the other three. For this purpose we used a computer program of non-linear regression analysis to fit equation (13) to the measured data.

The computer program used gives estimates of the accuracy of the determined values of the parameters and of the degree of their mutual correlation. We can summarize the method in the following way:

We require a function:

$$y = f(x;\ \beta_1,\ \beta_2,\ \ldots,\ \beta_n) + \epsilon \qquad (14)$$

to fit a set of data (x_i, y_i). The β_j are the various parameters to be adapted.

The sum $\sum_i (y_i - f_i)^2$ is to be minimized, in which f_i are values calculated from the x_i by means of a truncated Taylor expansion:

$$f_i = f(x_i;\ b_1, b_2, \ldots b_n) + \frac{\partial f}{\partial b_1}\Delta b_1 + \frac{\partial f}{\partial b_2}\Delta b_2 + \ldots \frac{\partial f}{\partial b_n}\Delta b_n \qquad (15)$$

in which the b_j are estimates for the β_j, and Δb_j are small variations in b_j. This leads to new estimates for the β_j, which are now $b_j + \Delta b_j$, using the Δb_j values for which the sum was minimum. Then the process is repeated, and so on until there is no significant improvement in the sum of squared differences.

If two derivatives, $\partial f/\partial b_j$ and $\partial f/\partial b_k$ when plotted against each other for the region of x values occurring in the experiment, appear to be nearly

linear functions of each other, it is seen from equation (15) that only a linear combination of Δb_j and Δb_k can be determined by minimizing the sum of squares, but not their individual values. In that case we say that the parameters β_j and β_k are highly correlated.

The program provides for a parameter correlation matrix giving the correlation coefficients for all pairs of derivatives $\partial f/\partial b_j$ and $\partial f/\partial b_k$. In *Table 5* we give such a parameter correlation matrix, obtained after a non-linear regression analysis for equation (13) with as input data (x_i, y_i) calculated using the equation:

$$y = 1 - \exp\left(-0.001x^3\right) \tag{16}$$

in the region $x = 0.2$ to $x = 14$, the y values given in five numbers.

From this table we see that the parameters K, t_0 and n, as they occur in equation (13) are strongly correlated. This means that the parameters, after some correlated variation δK, δt, δn, still allow a reasonable fit of the measured y and x data. For example, if we shift the point $t = 0$ we find a change in n and in K but we may still find a reasonable fit of measured data.

Consequently, the estimation of n and K by either of the log–log plotting methods is rather fortuitous since these methods presuppose an exact knowledge of the starting time of the crystallization, which is necessary for the calculation of log(*time*). Moreover, these methods attach a heavy weight

Table 5 Parameter correlation matrix for non-linear regression analysis according to equation (13) on data calculated from equation (16)

	y_0	y_1	K	t_0	n
y_0	1·0	0·134	0·680	0·744	−0·650
y_1	0·134	1·0	0·657	0·578	−0·704
K	0·680	0·657	1·0	0·992	−0·998
t_0	0·744	0·578	0·992	1·0	−0·981
n	−0·650	−0·704	−0·998	−0·981	1·0

to the first points of the crystallization curve while the accuracy of these points in a log–log plot is very poor.

As a matter of fact, the high degree of correlation between K, t_0 and n does not occur in the regression analysis only, but also in the evaluation by log–log plotting. In other words, this degree of correlation is an *inherent property* of the Avrami equation.

Another consequence of this correlation is that the estimation of induction times for the crystallization becomes meaningless if the 'induction time' is less than, say, 0·3 times the crystallization half-time.

The apparent induction time, i.e. the time lapse between supposed time of thermal equilibrium and time of the first detectable trace of crystallization, has already been shown by Mandelkern[19] and others not to be the incubation time for nucleation, since the latter would be much shorter, if detectable at all. This can be concluded from the superposability of all α–log$t$ plots.

In the analysis of Magill[14, 40] the 'induction times' appear to be only a

fraction of crystallization half-times; moreover, his specimens of plain polypropylene were up to 0·2 mm thick, which gives rise to optical retardations much larger than $\pi/4$, so that the recorded light output in the later stages of the crystallization is less than proportional to the fraction of crystallized material[15]. This causes a positive value of t_0, which may easily be interpreted as an induction time. In the papers mentioned, however, a definition of the induction time was not given.

Effects of experimental circumstances

(1) *Time for temperature equilibration.* Especially in bulky dilatometers, the temperature equilibration is slow owing to the low heat conductivity of most polymers. During cooling to the required crystallization temperature some nucleation and crystal growth takes place, thus obscuring the true starting time, t_0, of the crystallization.

(2) *Non-simultaneous start of crystallization in different areas of the specimen.* That crystallization does not set in at once throughout the specimen may easily happen in dilatometric measurements when the temperature equilibration is not yet complete. Actually, this will always be the case – if we neglect induction times – but an appreciable deviation from the Avrami equation will occur only when the crystallization half-time is shorter than, say, ten times the time for temperature equilibration.

Overlap of crystallization curves tends to give larger crystallization half-times than a single curve, giving values for K that are too low. For example, this is demonstrated by a log $[-\log (1 - \alpha)]$ versus log t plot for:

$$\alpha = \sum_{i=0}^{9} 0 \cdot 1 \, \beta_i \tag{17}$$

where $\beta_i = 1 - \exp \{-0 \cdot 001(t - i)^3\}$ for $t - i \geqslant 0$

and $\beta_i = 0$ for $t - i < 0$

(see *Figure 10a*)

This is equivalent to a plot of $\alpha = 1 - \exp(-0 \cdot 00005t^{3 \cdot 4})$. So the actual plot obtained has a slope that is slightly too high and a value of K that is a factor of about 20 too low.

(3) *Inhomogeneous nucleation density.* Polymer samples often show a non-uniform nucleation density, which leads to different crystallization kinetics for different regions of the sample. This affects the overall crystallization kinetics to a considerable degree, but it is a phenomenon that cannot be observed separately when use is made of dilatometry or differential thermal analysis.

A log $\{-\log (1 - \alpha)\}$ versus log t plot of:

$$\alpha = \tfrac{1}{2}[1 - \exp(-0 \cdot 001t^3)] + \tfrac{1}{2}[1 - \exp(-0 \cdot 008t^3)] \tag{18}$$

(*Figure 10b*) requires for at least approximate straightness the time to be shifted to lower values, giving a value for *n* even less than 2, and a value of *K* considerably higher than the arithmetic mean of 0·001 and 0·008. The ratio of *K* values used in this example is small compared with what is sometimes observed in different parts of one microscope specimen often separated by less than 1 mm.
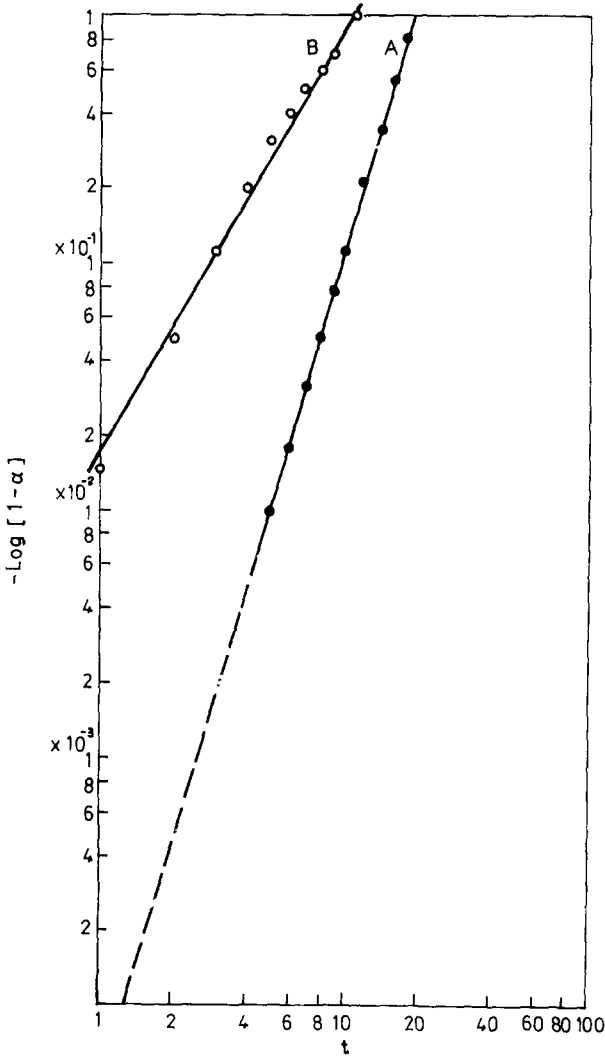
Figure 10 A. Plot for $\sum\limits_{i=0}^{9} 0\cdot1 \{1 - \exp[-0\cdot001 (t - i)^3]\}$,

see eq. (17)

B. Plot for $a = \frac{1}{2}\{1 - \exp[-0\cdot001 (t + 1)^3]\} + \frac{1}{2}\{1 - \exp[-0\cdot008(t + 1)^3]\}$

331

(4) *Non-randomless of distribution of nucleating particles.* We have considered the case where the nucleation density is homogeneous, i.e. with all imaginary cubes containing, say, 100 nucleating particles about equally large, but in fact, there is some special order in the mutual distance of nearest nucleating particles. We find hardly any deviation from the expected Avrami equation for particles distributed as the lattice points of a primitive cubic lattice. If the particles were found in rows, however, the distances within a row being smaller than the distances between rows, we may find the kinetics to incline to an Avrami exponent $n = 2$. This will especially be the case for orientation-induced nucleation, which occurs if the moulded-in orientation in the specimen has not been completely relaxed by heating the melt at a suitably high temperature[1, 39], since cylindrical growth after predetermined nucleation leads to this value[11, 12].

Notes to the Editor

Examination of oil-modified alkyds and urethanes by nuclear magnetic resonance spectroscopy

R. J. W. REYNOLDS, K. R. WALKER and G. W. KIRBY

Nuclear magnetic resonance (n.m.r.) spectroscopy can provide a method for the rapid preliminary analytical examination of small quantities of polymers sufficiently soluble in the usual solvents, for example, deutero-chloroform and hexadeuterodimethylsulphoxide. The method has been applied to a variety of drying oil and related esters. Solutions of the polymers (*ca* 50 mg) in deuterochloroform (0·5 ml) were used throughout.

The spectrum of a commercially available alkyd (A) based on castor oil, phthalic anhydride and glycerol, is shown in *Figure 1a*. Absorption in the region τ 7·4–9·4 is attributable to methylene and methyl groups in the ricinoleic units. Methylene groups not adjacent to either a double bond or a carbonyl group produce a strong, broad band centred at τ 8·75 and the methyl groups a distorted triplet at τ 9·13. Absorption between τ 7·4 and 8·2 originates from methylene groups adjacent to double bonds and carbonyl groups. Protons of the type H—C—O absorb between τ 4·8 and 6·4, the main band τ 5·6, arising from methylene groups in glycerol units. Olefinic absorption appears at *ca* τ 4·6. When the deuterochloroform solution was shaken with deuterium oxide the band at τ 4·17 disappeared and can therefore be assigned to hydroxylic protons. Finally, the aromatic protons of the phthaloyl residues produce a characteristic, partially resolved multiplet at τ 2·40.

Integration of the areas of various bands gave a semi-quantitative measure of the polymer composition. Comparison of the low and high field band areas indicated a phthalate/castor oil molar ratio of 6:1. The amount of glycerol used in condensation was deduced from the area from τ 4·8 to 6·4 after subtraction of an amount corresponding to the castor oil content. The resulting castor oil/glycerol ratio was 1:4. In the original polymer formulation the corresponding molar ratios, castor oil/phthalic anhydride/glycerol, were stated to be 1:5·5:3·7. The n.m.r. method thus provides a useful approximate guide to polymer composition.

The spectrum (*Figure 1b*) of a commercial drying-oil alkyd (B) (stated to be based on linseed oil/phthalic anhydride/pentaerythritol, 1:1·65:0·83) illustrates at once the lower phthalate content. The presence of two double bonds in the linoleic units accounts for the increased intensity of the olefinic proton, band at τ 4·6 and a new band at τ 7·27 can be assigned to methylene groups of the type, C=C—CH$_2$—C=C. Integration of the spectrum gave a composition, linseed oil/phthalic anhydride/pentaerythritol, of 1:1·5:1.

In another commercial alkyd (C), stated to be based on dehydrated castor oil/phthalic anhydride/glycerol (1:1·2:0·8), the dehydrated castor oil units
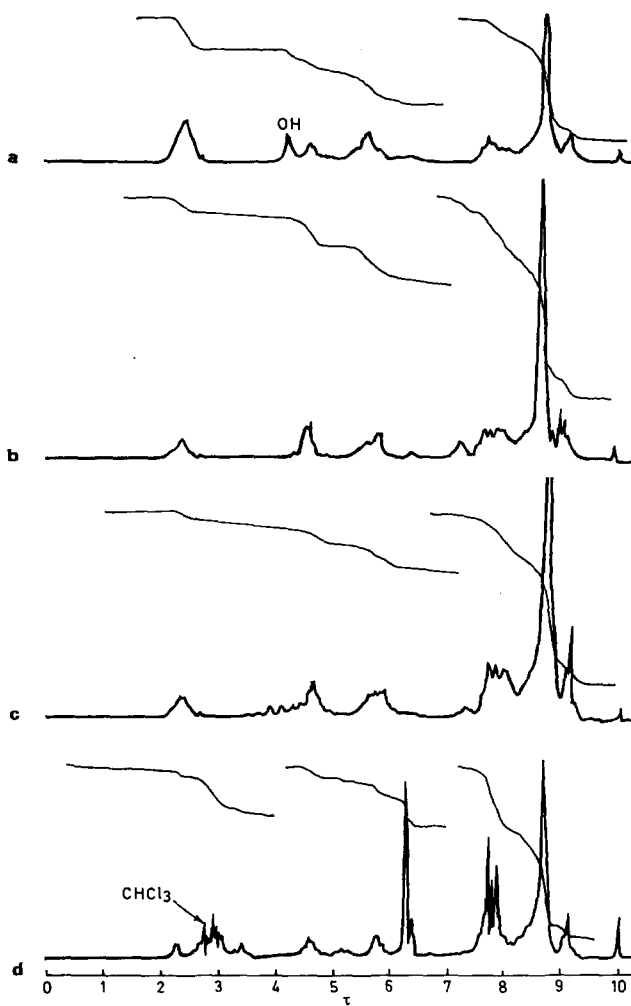
Figure 1 NMR spectra

produce a complex olefinic absorption (*Figure 1c*) due to a mixture of conjugated and non-conjugated double bonds. The methylene absorption, τ 7·25, arises from the non-conjugated components and is considerably weaker than the corresponding band in the linseed oil alkyd B. The corresponding ratio of components, calculated from the integrated spectrum, was 1:1·2:1.

An example of the practical use of the method has been in an examination of a film-forming urethane (D) pre-polymer made available to us as a xylene solution. An infra-red spectrum showed an intense band at 2275 cm $^{-1}$ indicating the presence of isocyanate groups. Evaporation of the xylene in the presence of moisture induced cross-linking and gave a polymer insoluble in convenient solvents. The xylene solution was therefore heated with methanol to convert the isocyanates into urethanes. Evaporation of the solvent then gave a gum which was examined in deuterochloroform (see *Figure 1d*). The high-field bands in the n.m.r. spectrum clearly showed presence of a fatty oil-based polymer. The shape and intensity of the olefinic band, *ca* τ 4·6, indicated one double bond per fatty acid unit suggesting an oleic or castor oil base. The presence of castor oil was suspected from preliminary examination. Comparison with a spectrum of castor oil itself reinforced this conclusion.

The sharp methoxyl singlet at τ 6·28 arose from urethanes formed by the methanol treatment and, possibly, from some transesterification. When the original xylene solution was treated with ethanol, ethoxyl signals and no methoxyl signals were observed from the resulting product. Three methyl signals were observed at *ca* τ 7·8 superimposed on the broad methylene bands. The two low-field signals varied in intensity from sample to sample and were attributed to residual xylene. The high-field signal suggested an aryl methyl group derived from toluene di-isocyanates used in the original mixture. The aromatic region, τ 2·2–3·5, was too complex for complete analysis. Certain bands could be attributed to aryl urethanes and residual xylenes; there was no indication of significant amounts of lower aliphatic esters or phthalates. The main conclusions were confirmed by conventional chemical analysis involving saponification of the ethanol-treated prepolymer and isolation of ricinoleic acid.

University of Technology,
Loughborough, Leicestershire.

Institute of Polymer Technology   R. J. W. REYNOLDS and K. R. WALKER
Department of Chemistry   G. W. KIRBY

Interpretation of the heat of dilution of polymer solutions

G. Lewis and A. F. Johnson*

By making the usual assumption that the number of nearest-neighbour interactions between polymer segments and solvent molecules are proportional to the volume fractions of the components in solution, it can be shown[1,2] that

$$\Delta H_d = RT\phi_1\phi_2\Delta n \chi_H \tag{1}$$

where ΔH_d is the integral heat of dilution, i.e. the enthalpy change on diluting a polymer solution containing a known concentration of polymer to a solution of lower finite concentration by addition of solvent; ϕ_1 and ϕ_2 are the volume fractions of polymer before and after dilution respectively; Δn is the number of moles of solvent added and χ_H the apparent enthalpy parameter.

Experimental data have been interpreted[3-5] using equation (1). Smooth curves have been obtained on plotting ΔH_d against $RT\phi_1\phi_2 \Delta n$ leading to the conclusion that χ_H is concentration dependent. The results of the present authors (*Table 1*) for the heat of dilution of the polystyrene–toluene system, when interpreted in a similar manner, in general appear to confirm the usefulness of equation (1) for observing the concentration dependence of χ_H. However, should χ_H vary with concentration and if the assumption is made that χ_H depends solely on the initial and final volume fractions of polymer in solution, then it does not follow that plotting ΔH_d against $RT\phi_1\phi_2\Delta n$ will yield a smooth curve.

If we consider a series of dilutions from ϕ_1 to ϕ_2 in which only the total volume of the system is varied, then ΔH_d against $RT\phi_1\phi_2\Delta n$ must give a straight line passing through the origin. If χ_H is concentration dependent then a similar series of dilutions from ϕ_1' to ϕ_2' and ϕ_1'' to ϕ_2'' will give different straight lines. Hence a plot of ΔH_d against $RT\phi_1\phi_2\Delta n$ for a series of dilutions with varying initial and final volume fractions of polymer will only produce a smooth curve if there has been a fortuitous choice of sample size or perhaps if systematic repeated dilutions are made on a solution.

It has been found that the heat of dilution for the polystyrene–toluene system (*Table 1*) and for the polar poly(methyl methacrylate)–chloroform system[6] can be represented, at least approximately, by smooth curves when $\Delta H_d \Delta n^{-1}$ is plotted against $RT\phi_1\phi_2$, i.e. when both abscissa and ordinate are intensive properties of the system. If the general series expansion for χ_H in terms of ϕ is considered (equation 2) where ϕ is the volume fraction of polymer in solution,

$$\chi_H = \chi_1 + \chi_2\phi + \chi_3\phi^2 + \ldots \ldots \tag{2}$$

it can be seen that when $\phi_1 \gg \phi_2$ and $\chi_2 \gg \chi_1$ one may not expect a smooth curve even when $\Delta H_d \Delta n^{-1}$ is plotted against $RT\phi_1\phi_2$. However, these conditions are outside the range of the experimental data presented here.

Inspection of *Table 1* shows that for polymer A, when $\Delta H_d \Delta n^{-1}$ is plotted against $RT\phi_1\phi_2$, the points lie on a straight line through the origin. For

---

*To whom requests for reprints should be sent.

Table 1 Heats of dilution for the system polystyrene + toluene at 303·15 K (W_1 and W_2 are the weights of polymer solution and solvent respectively.)

M_n	W_1(g)	W_2(g)	ϕ_1	ϕ_2	ΔH_d(J)	$RT\phi_1\phi_2$ (J mole^{-1})	$-\Delta H_d \Delta n^{-1}$ (J mole^{-1})
900	0·9408	1·2628	0·4063	0·1662	−0·3862	169·33	28·18
(A)	1·2037	0·8967	0·2255	0·1394	−0·1104	68·20	11·34
	0·2299	1·2663	0·2255	0·0335	−0·0355	19·02	2·58
	0·5667	1·3422	0·1145	0·0693	−0·0295	12·50	2·03
	0·3713	1·2122	0·1051	0·0243	−0·0201	6·44	1·53
	0·4617	1·1315	0·1051	0·0300	−0·0203	7·96	1·65
	0·2428	1·2579	0·4063	0·0618	−0·1375	63·30	10·07
4 600	1·1701	0·4864	0·1785	0·1250	−0·0368	56·41	6·97
(B)	0·1387	1·3842	0·1785	0·0158	−0·0126	7·12	0·84
	0·5579	1·1864	0·3837	0·1167	−0·2360	112·88	18·33
	0·2552	1·2418	0·3837	0·0616	−0·0842	59·54	6·25
	0·6311	1·1907	0·3837	0·1267	−0·2362	122·51	18·28
	0·5779	1·4313	0·1048	0·0401	−0·0159	9·31	1·02
10 900	0·8451	1·0156	0·1465	0·0652	−0·0216	24·06	1·96
(C)	0·4523	1·2492	0·1465	0·0410	−0·0202	15·16	1·49
	1·2802	0·4585	0·1465	0·1157	−0·0193	42·75	3·88
	0·2717	1·2970	0·1465	0·0267	−0·0107	9·85	0·76
	1·0685	0·7811	0·0776	0·0444	−0·0084	11·96	0·99
	0·4727	1·2556	0·0776	0·0209	−0·0054	4·09	0·40
19 650	0·9217	1·2385	0·3924	0·1601	−0·2845	158·36	21·17
(D)	0·2213	1·3200	0·3924	0·0527	−0·0631	52·14	3·01
	0·9853	1·2894	0·2590	0·1079	−0·1037	72·46	7·41
	0·8387	1·4238	0·1373	0·0493	−0·0146	17·06	0·95
	0·2873	1·4132	0·2590	0·0811	−0·0261	27·00	1·70
96 200	0·4544	1·3372	0·3284	0·0791	−0·0748	65·47	5·15
(E)	0·8393	0·2576	0·3284	0·2471	−0·0837	204·53	29·93
	1·0481	1·3761	0·2216	0·0929	−0·0526	51·89	3·52
	0·9229	1·3756	0·1217	0·0526	−0·0049	16·14	0·33
	1·0797	0·9765	0·0817	0·0425	−0·0032	8·75	0·30
164 000	0·8806	1·1651	0·3092	0·1272	−0·1544	99·13	12·29
(F)	0·5336	1·2002	0·1165	0·0351	−0·0085	10·31	0·65
	1·0242	0·8794	0·1165	0·0648	−0·0221	19·03	2·32
	0·2284	1·1609	0·3092	0·0491	−0·0161	38·27	1·28
	0·2371	1·2736	0·1165	0·0178	−0·0136	5·23	0·98
	0·7151	1·1206	0·1165	0·0445	−0·0362	13·07	2·98

higher molecular weight polymers, smooth curves are obtained showing the concentration dependence of χ_H. The scatter of points for polymer F is thought to indicate the limitation of the calorimetric technique employed for the measurements, i.e. the viscosity of polymer solution where $\bar{M}_n \sim$ 150 000 and $\phi \sim 0.2$ are too high to enable the rapid attainment of equilibrium conditions after dilution.

Department of Chemistry,
University of Manchester,
Manchester   G. LEWIS

School of Polymer Science,
University of Bradford,
Bradford, Yorkshire, BD7 1DP   A. F. JOHNSON

REFERENCES

1 Amaya, K. and Fujishiro R. *Bull. Chem. Soc. Japan* 1956, **29**, 361
2 Flory, P. J., 'Principles of Polymer Chemistry', Cornell University Press, New York, 1953
3 Kagemoto, A. and Fujishiro, R. *Bull. Chem. Soc. Japan* 1968, **41**, 2201
4 Kagemoto, A. Murakami, S. Fujishiro, R. *Bull. Chem. Soc. Japan* 1966, **39**, 15, 1814; 1967, **40**, 11; *Makromol, Chem.* 1967, **105**, 154
5 Lewis, G. and Johnson, A. F. *J. Chem. Soc (A)* 1969, p 1816
6 Lewis, G. and Johnson, A. F., to be published

338

Book Reviews

Application of nuclear magnetic resonance spectroscopy in organic chemistry (2nd edition)

by L. M. JACKMAN and S. STERNHELL
Pergamon Press, Oxford, 1969, 456 pp, 84s

The second edition of this well-known book is a completely new version of the original edition. Professor Jackman has been joined by Dr Sternhell in this task of revision. The book is more than three times as long as the original and contains about thirteen times as many literature references. It appears that the authors have not been well served by their publishers because relatively few references relate to 1966 or later and yet the book was not published until August 1969.

The large increase in size has brought about a change in character: the first edition has achieved popularity as a short introductory text (particularly for organic chemists); however, the new version is a full-scale monograph not intended for reading from cover to cover. An important change has been made, the tau chemical shift scale has been abandoned in favour of a delta scale – one in which delta increases positively to low fields. This is likely to be the agreed system for the future. Unfortunately, both editions define this particular delta incorrectly; a sign change has been introduced, possibly because the authors have not realized that frequencies *increase* towards *low* fields. Since ν_S is greater than ν_{TMS} equation (1-2-4) should read

$$\delta = (\nu_S - \nu_{TMS}) \times 10^6 / (\text{spectrometer frequency})$$

Luckily, this error does not affect the signs of chemical shifts quoted in the tables.

The numbering of equations, tables and diagrams is clumsy due to an unnecessary division of the book into parts as well as chapters. I can see no point in introducing such a complication. Because of the large number of literature references it would have been preferable to put the reference lists at the end of chapters thereby avoiding four-figure superscripts. The organization of subject matter runs as follows: Part 1 – Introduction to the theory and practice of n.m.r. spectroscopy (54 pages); Part 2 – Theory of chemical shifts in n.m.r. spectroscopy (103 pages); Part 3 – Applications of the chemical shift (109 pages); Part 4 – Spin-spin coupling (87 pages); Part 5 – Applications of time-dependent phenomena (28 pages).

There are many good things to be found in this second edition and at such a reasonable price it can be commended to all who are concerned with high resolution n.m.r. spectroscopy. There now remains a gap for a small introductory book similar to the first edition.

L. H. SUTCLIFFE

Structural design with plastics

by B. S. BENJAMIN
Van Nostrand/Reinhold, London, SPE Polymer Science and Engineering Series, 259 pp, £7

The modern trend to the use of plastics in load-bearing engineering structures is clearly of great importance to the plastics industry. Indeed many people in various branches of that industry are looking to this trend, particularly in civil engineering, as a potential large market for plastics. Dr Benjamin's book is an attempt to introduce civil engineers to the potentialities and problems of design with plastics, especially fibre reinforced thermosets, and as such it is very timely.

Approximately the first half of the book is devoted to a review of the relevant engineering properties of those plastics which have potential in civil engineering. This is followed by a

brief discussion of sandwich constructions leading into the second half which is a discussion of folded-plate, shell and other structures which the author regards as of special interest for plastics. The appeal throughout is to the practising engineer, emphasis being given to practical engineering aspects.

The discussion of materials is essentially a description of properties. There is no discussion of the nature of the materials in either chemical or physical terms (indeed there is not a chemical formula in the book, perhaps a record for books on plastics) and there is no attempt to inform the reader of the existence of the very substantial scientific understanding of properties even by the inclusion of references to suitable texts.

The discussion on the behaviour of structures focusses on those which are considered to be of particular application to plastics. The results of the applications of standard classical elasticity theory to these structures are presented and discussed in some detail but the particular problems associated with the special properties of plastics are not explicitly discussed in any significant detail. In places the author makes recommendations on how plastics should be used but neglects to give the appropriate discussion and thus avoids the really cogent problem. This omission is a disappointment but perhaps understandable in the current state of the subject.

The author describes some of his own work in designing, constructing and testing various structures in fibre reinforced plastics but does not discuss them in sufficient detail to make the presentation really useful. The reader is left asking a lot of questions, presumably reference to the original papers will provide answers.

The book is fairly well presented and is commendably free from typographical errors. The use of space for diagrams is lavish; simple graphs are often allowed to occupy complete pages and data which would best be presented as several lines on one graph frequently appears as several individual graphs making comparisons difficult. Both figures and tables are presented without titles or captions and can only be understood by reference to the relevant portion of the text which may well be several pages away. This will inevitably make reference to the substantial amount of data tedious. A list of symbols and a more careful definition of symbols would be useful.

The book will clearly have a greater appeal to the engineer than to the scientist although the latter will find much of interest in the discussion of particular structures. If it is instrumental in bringing engineers to a greater interest in, and appreciation of, plastics it will have succeeded.

D. W. SAUNDERS

ERRATUM

Polymer Volume 11, Number 4 (April)
'Effect of structure on the glass transition temperatures of some perfluoroalkylene aromatic polyimides' by J. M. Barton and J. P. Critchley

Page 21 The two lines following equation (3) should read as follows:
    'where x and y are the mole fractions of A and B in the copolymer, α is the number of groups in the repeating unit and $T_{gA(B)} = T_{A(B)}/\alpha_{A(B)}$'

Book Reviews

Application of nuclear magnetic resonance spectroscopy in organic chemistry (2nd edition)

by L. M. JACKMAN and S. STERNHELL
Pergamon Press, Oxford, 1969, 456 pp, 84s

The second edition of this well-known book is a completely new version of the original edition. Professor Jackman has been joined by Dr Sternhell in this task of revision. The book is more than three times as long as the original and contains about thirteen times as many literature references. It appears that the authors have not been well served by their publishers because relatively few references relate to 1966 or later and yet the book was not published until August 1969.

The large increase in size has brought about a change in character: the first edition has achieved popularity as a short introductory text (particularly for organic chemists); however, the new version is a full-scale monograph not intended for reading from cover to cover. An important change has been made, the tau chemical shift scale has been abandoned in favour of a delta scale – one in which delta increases positively to low fields. This is likely to be the agreed system for the future. Unfortunately, both editions define this particular delta incorrectly; a sign change has been introduced, possibly because the authors have not realized that frequencies *increase* towards *low* fields. Since ν_S is greater than ν_{TMS} equation (1-2-4) should read

$$\delta = (\nu_S - \nu_{TMS}) \times 10^6/\text{(spectrometer frequency)}$$

Luckily, this error does not affect the signs of chemical shifts quoted in the tables.

The numbering of equations, tables and diagrams is clumsy due to an unnecessary division of the book into parts as well as chapters. I can see no point in introducing such a complication. Because of the large number of literature references it would have been preferable to put the reference lists at the end of chapters thereby avoiding four-figure superscripts. The organization of subject matter runs as follows: Part 1 – Introduction to the theory and practice of n.m.r. spectroscopy (54 pages); Part 2 – Theory of chemical shifts in n.m.r. spectroscopy (103 pages); Part 3 – Applications of the chemical shift (109 pages); Part 4 – Spin-spin coupling (87 pages); Part 5 – Applications of time-dependent phenomena (28 pages).

There are many good things to be found in this second edition and at such a reasonable price it can be commended to all who are concerned with high resolution n.m.r. spectroscopy. There now remains a gap for a small introductory book similar to the first edition.

L. H. SUTCLIFFE

Structural design with plastics

by B. S. BENJAMIN
Van Nostrand/Reinhold, London, SPE Polymer Science and
Engineering Series, 259 pp, £7

The modern trend to the use of plastics in load-bearing engineering structures is clearly of great importance to the plastics industry. Indeed many people in various branches of that industry are looking to this trend, particularly in civil engineering, as a potential large market for plastics. Dr Benjamin's book is an attempt to introduce civil engineers to the potentialities and problems of design with plastics, especially fibre reinforced thermosets, and as such it is very timely.

Approximately the first half of the book is devoted to a review of the relevant engineering properties of those plastics which have potential in civil engineering. This is followed by a

brief discussion of sandwich constructions leading into the second half which is a discussion of folded-plate, shell and other structures which the author regards as of special interest for plastics. The appeal throughout is to the practising engineer, emphasis being given to practical engineering aspects.

The discussion of materials is essentially a description of properties. There is no discussion of the nature of the materials in either chemical or physical terms (indeed there is not a chemical formula in the book, perhaps a record for books on plastics) and there is no attempt to inform the reader of the existence of the very substantial scientific understanding of properties even by the inclusion of references to suitable texts.

The discussion on the behaviour of structures focusses on those which are considered to be of particular application to plastics. The results of the applications of standard classical elasticity theory to these structures are presented and discussed in some detail but the particular problems associated with the special properties of plastics are not explicitly discussed in any significant detail. In places the author makes recommendations on how plastics should be used but neglects to give the appropriate discussion and thus avoids the really cogent problem. This omission is a disappointment but perhaps understandable in the current state of the subject.

The author describes some of his own work in designing, constructing and testing various structures in fibre reinforced plastics but does not discuss them in sufficient detail to make the presentation really useful. The reader is left asking a lot of questions, presumably reference to the original papers will provide answers.

The book is fairly well presented and is commendably free from typographical errors. The use of space for diagrams is lavish; simple graphs are often allowed to occupy complete pages and data which would best be presented as several lines on one graph frequently appears as several individual graphs making comparisons difficult. Both figures and tables are presented without titles or captions and can only be understood by reference to the relevant portion of the text which may well be several pages away. This will inevitably make reference to the substantial amount of data tedious. A list of symbols and a more careful definition of symbols would be useful.

The book will clearly have a greater appeal to the engineer than to the scientist although the latter will find much of interest in the discussion of particular structures. If it is instrumental in bringing engineers to a greater interest in, and appreciation of, plastics it will have succeeded.

D. W. SAUNDERS

ERRATUM

Polymer Volume 11, Number 4 (April)
'Effect of structure on the glass transition temperatures of some perfluoroalkylene aromatic polyimides' by J. M. Barton and J. P. Critchley

Page 21 The two lines following equation (3) should read as follows:
'where x and y are the mole fractions of A and B in the copolymer, α is the number of groups in the repeating unit and $T_{gA(B)} = T_{A(B)}/\alpha_{A(B)}$'

Radioactivation analysis studies of polymerization reactions:
(1) Solution polymerization of styrene by radical catalysis

T. Maekawa, M. Matsuo, H. Yoshida*,

K. Hayashi* and S. Okamura

Radioactivation analysis was used to detect trace amounts of solvent frag-
ments attached to polymer chain ends in a study of the mechanism of chain
transfer to solvent in the polymerization of styrene in chloroform, methylene
dichloride, ethylene dichloride and bromobenzene. The polymerization was
carried out at 60°C with α,α'-azobisisobutylonitrile as initiator. It was con-
firmed that the fragments of solvent molecule, even with bromobenzene as
solvent, became attached to the polymer during the course of the transfer
reaction. This is in accordance with the generally accepted mechanisms of the
transfer reaction.

MANY studies of chain transfer reactions in solution polymerization have
been reported. The generally accepted mechanism involves the transference
of the activity of the growing radical to a solvent molecule, thus yielding a
solvent radical which may initiate further polymerization[1-6]. According to
this mechanism, fragments of solvent molecule should be incorporated into
polymer molecules as end groups. The presence of such solvent fragments
has been shown by chemical analysis of the polymer[5, 7, 8].

In the case of monohalobenzenes, however, although reduction in mole-
cular weight caused by the transfer reaction is observed, there is little evi-
dence of halogen in the polymer formed[9, 10]. As the resulting polymer was
analysed using conventional elemental analysis techniques, investigations
were restricted to low molecular weight polymer obtained from monomer of
low concentration.

In this work radioactivation analysis was used to detect fragments of low
concentration in high molecular weight polymer which was obtained under
the usual conditions of radical polymerization. Polymerization of styrene
by radical catalysis was studied in halo-alkyl and halo-benzene solvents.
The sensitivity of radioactivation analysis is 10^{-8} g for chlorine or 10^{-9} g
for bromine, which is higher than that of ordinary chemical methods by
3 or 4 orders of magnitude.

THEORY

According to the generally accepted mechanism of the chain-transfer reac-

---

* Faculty of Engineering, Hokkaido University, Sapporo, Japan

tion, fragments of solvent are incorporated into polymer as end groups in the following processes:

$$M_n \cdot + SX \rightarrow M_nX + S \cdot \tag{1}$$

$$S \cdot + nM \rightarrow SM_n \cdot \xrightarrow{SX} SM_nX + S \cdot \tag{2}$$
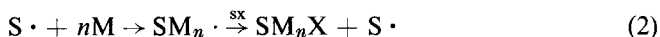
where M is a monomer molecule and SX is a solvent molecule. From the above mechanism, the expected number of solvent fragments (number of halogen atoms in the present investigation) combined to a polymer chain is derived in the following way.

For a constant concentration of initiator, assuming steady state and a constancy of the rate of initiation and $k_p/k_t^{\frac{1}{2}}$, the number, n, of solvent molecules in one polymer chain is defined as

$$n = k_{fs}[R \cdot][S]/\{k_t[R \cdot]^2 + k_{fs}[R \cdot][S] + k_{fm}[R \cdot][M]\}$$

$$n = C_s\frac{[S]}{[M]}\bigg/\left(\frac{k_t[R \cdot]}{k_p[M]} + C_s\frac{[S]}{[M]} + C_m\right) \tag{3}$$

where $[R \cdot]$ is the total polymer radical concentration and $[M]$ and $[S]$ are monomer and solvent concentration. k_p, k_t, k_{fm} and k_{fs} are rate constants for propagation, termination, transfer to monomer and to solvent, respectively and $C_s = k_{fs}/k_p$, $C_m = k_{fm}/k_p$. In the equation, the fact that the termination reaction in polymerization of styrene proceeds predominantly by recombination,[11, 12] is taken into account. The degree of polymerization in bulk, $\overline{DP}_0$, is expressed[13] as

$$1/\overline{DP}_0 = k_t[R \cdot]/k_p[M]_0 + C_m \tag{4}$$

The relation between n and the mole fraction of monomer in the polymerization system, equation (5), is obtained by applying equation (4) to equation (3).

$$n = C_s\frac{[S]}{[M]}\bigg/\left[C_m + C_s\frac{[S]}{[M]} + \left(\frac{1}{\overline{DP}_0} - C_m\right)\frac{[M]_0}{[M]}\right] \tag{5}$$

EXPERIMENTAL

Materials

Chloroform, methylene dichloride and ethylene dichloride were dried over anhydrous sodium sulphate and distilled twice. Bromobenzene was purified by washing with 10% aqueous sodium hydroxide, cold concentrated sulphuric acid and water, drying over anhydrous sodium sulphate and fractionally distilling. Styrene was washed with 5% aqueous sodium hydroxide and water, dried over anhydrous sodium sulphate and distilled twice just before use.

Polymerization and purification of polymer

Polymerization was carried out in vacuum at 60°C with 5×10^{-3} mole 1^{-1} of α,α'-azobisisobutylonitrile (AIBN) as an initiator. The polymerization was limited to less than 5% conversion and the polymer formed was precipitated by the addition of methanol. The polymer obtained was dissolved

in benzene and then reprecipitated in methanol so that the remaining chain transfer agent was removed. Five cycles of this dissolving–precipitating procedure were made to purify polymers effectively.

Activation analysis

Each polymer sample (20–100 mg) was sealed in polyethylene film. The samples were packed in a polyethylene capsule and irradiated with neutrons. The induced activity of the samples due to chlorine-38 and bromine-82 resulted from nuclear transmutation of $Cl^{37}(n,\gamma)Cl^{38}$ and $Br^{81}(n,\gamma)Br^{82}$ was counted with a multi-channel pulse height analyser. In order to measure absolute value of chlorine or bromine content, standard weighed samples of ammonium chloride or ammonium bromide contained in filter paper were irradiated in the capsule together with the polymer samples, and the induced activity of the latter was compared with that of the former. Before counting the activity, the irradiated samples were cooled for about one hour and one day, respectively, so that the chlorine and bromine content could be measured without interference from short-lived radioactive nuclei, as chlorine-38 and bromine-82 decay with half-lives of 37·3 min and 35·9 h, respectively.

Representative spectra of γ-rays emitted from polymer samples are shown in *Figure 1*. The activity of the samples was determined from peak height of 1·64 Mev for chlorine-38 and that of 0·554 Mev for bromine-82. *Figure 2*
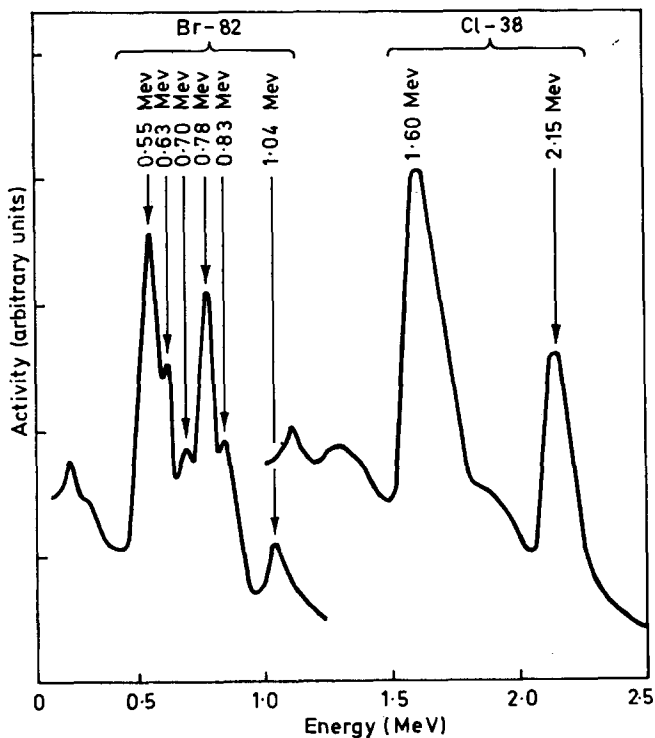
Figure 1 γ-ray spectra of chlorine-38 and bromine-82 contained in neutron-irradiated polymer samples
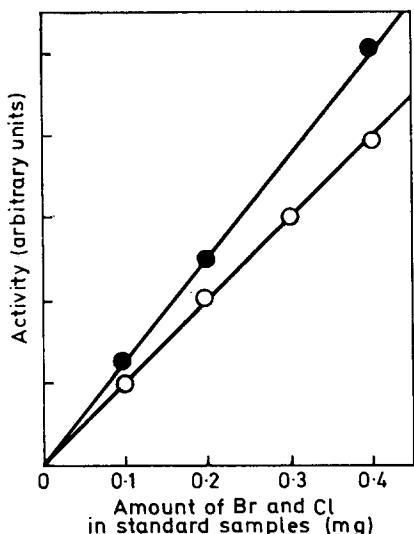
Figure 2 Calibration lines for quantitative measurement of chlorine and bromine by radioactivation analysis method: ○, chlorine; ●, bromine

shows the linear relation between the induced activity and the amount of standard samples.

The neutron irradiations were carried out with a JRR-2 reactor at the Japan Atomic Energy Research Institute (irradiation time 5 min, thermal neutron flux of 5×10^{13} n cm^{-2}s^{-1}) or a KRR-1 reactor at Kyoto University (20 min, 4×10^{12} n cm^{-2}s^{-1}).

In order to justify this analytical method, the mixture of polyvinylchloride with polystyrene was irradiated. The results shown in *Figure 3* indicate that
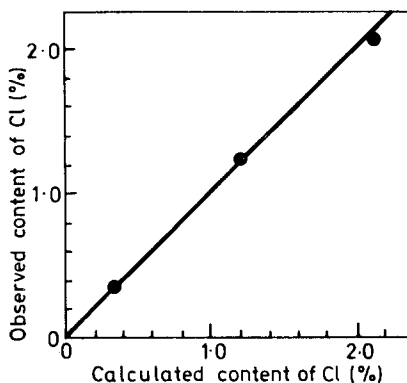
Figure 3 Relation between the chlorine content in polystyrene–polyvinylchloride films calculated from the mixture composition and that observed with the activation analysis method

chlorine atoms originally attached to the polymer do not escape from samples during irradiation in the reactor. Pfann et al[14] also confirmed this fact for bromine combined with polystyrene and Guinn and Wagner[15] obtained very close agreement between chlorine content values using both the activation analysis method and the conventional elemental analysis method.

345

RESULTS AND DISCUSSION

The halogen content and the number average molecular weight of polystyrene obtained from polymerization in chloroform, methylene dichloride, ethylene dichloride and bromobenzene solution are summarized in *Tables 1, 2, 3 and 4*. The number average molecular weight, $\overline{M}_n$ was calculated from the intrinsic viscosity using the following equation,[16] assuming a normal molecular weight distribution.

$$[\eta] = 2 \cdot 7 \times 10^{-4}(1 \cdot 80\overline{M}_n)^{0 \cdot 66} \tag{12}$$

Table 1 Observed chlorine contents in polymers obtained by solution polymerization of styrene in chloroform at 60°C with AIBN

[M]	[S]	Polymer		
		$\overline{M}_n$ $\times 10^{-4}$	% Cl in polymer $\times 10^2$	Cl atoms in a chain N_{Cl} $\times 10^2$
(mole 1⁻¹)				
8·68	0	6·12	0·876	—
8·46	0·304	5·85	0·978	1·65
8·27	0·594	5·75	0·996	1·94
7·89	1·13	5·43	0·947	1·84
7·23	2·08	4·05	1·02	1·65
5·78	4·16	3·62	0·890	2·41
4·34	6·24	2·35	0·910	3·11
3·04	8·11	1·55	1·81	4·07
2·17	9·37	1·07	2·41	4·62
1·13	10·8	0·74	2·64	3·64

Table 2 Observed chlorine contents in polymers obtained by solution polymerization of styrene in methylene dichloride at 60°C with AIBN

[M]	[S]	Polymer		
		$\overline{M}_n$ $\times 10^{-4}$	% Cl in polymer $\times 10^2$	Cl atoms in a chain N_{Cl} $\times 10^2$
(mole 1⁻¹)				
8·68	0	6·60	0·600	—
8·47	0·383	6·33	0·606	0·11
8·27	0·748	5·97	0·662	1·05
7·89	1·43	5·85	0·806	3·40
7·23	2·62	5·05	0·768	2·39
6·68	3·62	4·68	0·883	3·73
5·78	5·23	3·67	1·00	4·14
4·34	7·85	2·34	1·32	4·75
3·04	10·2	1·39	2·49	7·39
1·13	13·6	0·67	4·56	7·47

Table 3 Observed chlorine contents in polymers obtained by solution polymerization of styrene in ethylene dichloride at 60°C with AIBN

[M]	[S]	Polymer		
		$\overline{M}_n$ $\times 10^{-4}$	% Cl in polymer $\times 10^2$	Cl *atoms in a chain* N_{Cl} $\times 10^2$
(mole 1^{-1})				
8·68	0	6·60	0·633	—
8·47	0·309	6·49	0·741	1·97
8·27	0·602	6·12	0·752	2·06
7·89	1·15	5·80	0·763	2·13
7·23	2·11	5·74	0·842	3·45
6·68	2·91	4·09	0·820	2·75
5·78	4·22	3·56	1·01	3·51
4·34	6·33	2·29	1·22	3·72
3·03	8·22	1·66	1·60	4·17
2·17	9·48	1·02	3·60	7·70
1·13	11·0	0·54	11·1	14·4

Table 4 Observed bromine contents in polymers obtained by solution polymerization of styrene in bromobenzene at 60°C with AIBN

[M]	[S]	Polymer		
		$\overline{M}_n$ $\times 10^{-5}$	% Br in polymer $\times 10^3$	Br *atoms in a chain* N_{Br} $\times 10^2$
(mole 1^{-1})				
7·97	0·850	4·34	0·913	3·82
7·57	1·59	4·29	0·887	3·44
4·55	4·76	2·58	1·69	4·43
3·03	6·35	1·43	3·36	5·39
2·27	7·14	1·15	3·14	3·59

The viscosity was measured at 25°C in benzene solution. It should be noted that polystyrene synthesized under careful experimental conditions in bulk polymerization was still contaminated with 0·006–0·009% of chlorine from unknown sources. Therefore, to obtain the true content, this value should be subtracted from the chlorine content for each sample. The average number of chlorine or bromine atoms in a polymer chain, N_{Cl} or N_{Br}, calculated from the observed molecular weight and the content of the atoms is given in the third column of *Tables 1, 2. 3* and *4*.

According to equation (5), the theoretically expected value of N_{Cl} and N_{Br} is calculated from C_s, C_m and $\overline{DP}_0$. For chloroform, for example, N_{Cl} was calculated from the reported values of $C_s = 5 \times 10^{-5}$ (ref. 17), $C_m = 5 \times$

347

10^{-5} (refs. 18–20), $\overline{DP}_0 = 5.9 \times 10^2$ and $N_{Cl} = 3n^*$ (see *Figure 4*). The observed values of N_{Cl} were also plotted in *Figure 4*. Deviations of the observed values are insignificant. Although subtraction of a 'background' value of the chlorine content found in bulk polymerization might cause an uncertainty in the values of N_{Cl} listed in *Tables 1–3*, this is affected less at smaller mole fractions of monomer. It is obvious that the observed values
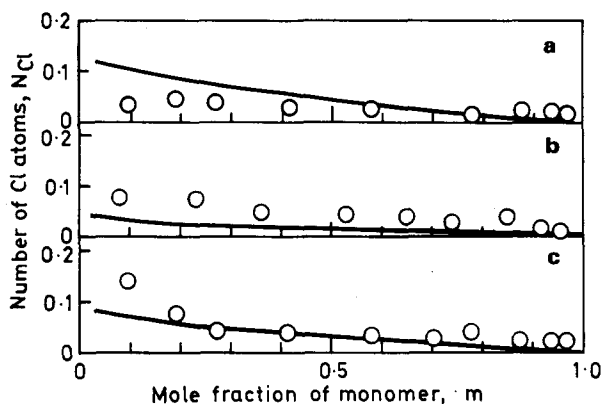
Figure 4 Number of chlorine atoms, N_{Cl}, attached to a polymer chain plotted as a function of mole fraction of styrene:
(a) Polymerization in chloroform at 60°C with AIBN. The line is the theoretical curve calculated from equation (5), with $C_s = 5 \times 10^{-5}$ (refs 17, 22), $C_m = 5 \times 10^{-5}$ and $N_{Cl} = 3n$; $\bigcirc$, experimental points
(b) Polymerization in methylene dichloride, $C_s = 1.8 \times 10^{-5}$ (refs 17, 23) and $N_{Cl} = 2n$
(c) Polymerization in ethylene dichloride. $C_s = 4 \times 10^{-5}$ (refs 22–24) and $N_{Cl} = 2n$

are in accordance with those expected from the generally accepted mechanism as illustrated in reactions 1 and 2. Similar results were obtained for the polymerizations in methylene dichloride and ethylene dichloride.

For bromobenzene, N_{Br} is calculated from $C_s = 1.3 \times 10^{-5}$; a comparison with experimental values is shown in *Figure 5*. In this case discretion must be used in choosing a C_s value. Bromobenzene may behave much like chlorobenzene in transfer. The transfer constants of chlorobenzene at 155°C and 60°C are 3.1×10^{-4} (ref. 9) and 1.33×10^{-5} (ref. 22), respectively, and the transfer constant of bromobenzene at 155°C is 3×10^{-4} (ref. 9). Since the transfer constant of bromobenzene at 155°C is 0.97 that of chlorobenzene, the transfer constant of bromobenzene at 60°C should be 1.3×10^{-5}. Kapur *et al*[21] have reported $C_s = 1.775 \times 10^{-4}$ for bromobenzene at 60°C. However, their data seem to be systematically higher than other data by

* Obviously $N_{Cl} = 2n$ for methylene dichloride and ethylene dichloride

about one order of magnitude. In our data at 60°C, C_s lies in the range 2–7×10^{-5}, most probably 2–4×10^{-5}. The observed N_{Br} values are in good agreement with those estimated from the normal transfer mechanism using $C_s = 1.3 \times 10^{-5}$. But considering the reliability of the chosen C_s value, partial occurrence is not excluded of a transfer mechanism suggested by
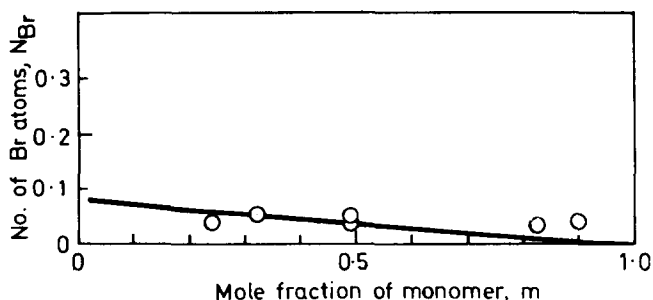
Figure 5 Number of bromide atoms, N_{Br}, attached to a polymer chain plotted as a function of mole fraction of styrene. Polymerization in bromobenzene at 60°C with AIBN. The line is the theoretical curve calculated from equation (5) with $C_s = 1.3 \times 10^{-5}$, $C_m = 5 \times 10^{-5}$ and $N_{Br} = n$; ○, experimental points

Mayo[9] in which the solvent molecules are not attached to polymer during the chain transfer to reaction solvent.

It is concluded that activation analysis is useful for the analysis of trace amounts of chemical components in polymers and it is therefore applicable to the kinetic study of solution polymerization. Compared with conventional chemical analysis which can detect only high concentrations of solvent fragments attached to very low molecular weight polymers, this method is more suitable for analysing high molecular weight polymers obtained under the usual conditions of polymerization.

Department of Polymer Chemistry,
Kyoto University,
Kyoto, Japan

REFERENCES

1 Smith, W. V. *J. Amer. Chem. Soc.* 1946, **68**, 2059
2 Mayo, F. R. *Discuss. Faraday. Soc.* 1947, **2**, 328
3 Mayo, F. R. *J. Amer. Chem. Soc.* 1948, **70**, 2373, 3689
4 Gregg, R. A., Alderman, D. M. and Mayo, F. R. *J. Amer. Chem. Soc.* 1948, **70**, 3740
5 Walling, C. *J. Amer. Chem. Soc.* 1948, **70**, 2561
6 Mayo, F. R. and Lewis, F. M. *J. Amer. Chem. Soc.* 1954, **76**, 457
7 Breitenbach, J. W. and Maschin, A. *Z. physik. Chem.* 1940, **A187**, 175
8 Bamford, C. H. and Dewar, M. J. S. *Proc. Roy. Soc.* 1948, **A192**, 329
9 Mayo, F. R. *J. Amer. Chem. Soc.* 1953, **75**, 6133

10 Breitenbach, J. W. and Schindler, A. *Monatshelfte für Chemie*, 1957, **88**, 810
11 Bevington, J. L. *et al*, *J. Polym. Sci.* 1954, **12**, 449; 1954, **14**, 463
12 Kolthoff, I. M. *et al*, *J. Polym. Sci.* 1955, **15**, 459
13 Mayo, F. R. *J. Amer. Chem. Soc.* 1943, **65**, 2324
14 Pfann, H. F., Salley, D. J., and Mark, H. *J. Amer. Chem. Soc.* 1944, **66**, 983
15 Guinn, V. P. and Wagner, C. D. *Anal. Chem.* 1960, **32**, 317
16 Pepper, D. C. *J. Polym. Sci.* 1952, **7**, 347
17 Gregg, R. A. and Mayo, F. R. *J. Amer. Chem. Soc.* 1953, **75**, 3530
18 Baysal, B. and Tobolsky, A. V. *J. Polym. Sci.* 1952, **7**, 529
19 Smith, W. V. *J. Amer. Chem. Soc.* 1949, **71**, 4077
20 Mayo, F. R., Gregg, R. A. and Matheson, M. S. *J. Amer. Chem. Soc.* 1951, **73**, 1691
21 Kapur, S. L. *J. Polym. Sci.* 1953, **11**, 399; 1954, **14**, 489
22 Misra, G. S. and Chadha, R. N. *Makromol. Chem.* 1947, **23**, 134
23 Our data
24 Bamford, C. H. and Dewar, M. J. S. *Discuss. Faraday Soc.* 1947, **2**, 314

Radioactivation analysis studies of polymerization reactions: (2) Initiation mechanism in radiation-induced radical polymerization of styrene

T. Maekawa, M. Matsuo, H. Yoshida,* K. Hayashi* and S. Okamura

The structure of the free radicals, formed by radiolysis, which initiate the radiation-induced polymerization of styrene in chloroform, methylene dichloride, ethylene dichloride and bromobenzene, was determined by radio activation analysis of the polystyrene formed. The initiation efficiency of the free radicals is discussed. Polymerization was initiated mainly by free radicals formed from solvent molecules, except when the mole fraction of the solvent was very low. With chloroform and ethylene dichloride as solvents, the polymerization was partly initiated by the secondary radicals; these were formed by the primary radicals generated during radiolysis abstracting hydrogen from solvent molecules.

IN THE study of radiation-induced free radical polymerization, it is difficult to identify which free radical initiates the polymerization, although the yield of the initiating free radical can be evaluated from the measured rate of polymerization. In the present investigation, the free radicals initiating the polymerization of styrene in halo-alkyl and halo-benzene solvents were studied by radioactivation analysis of the polymer formed.

The investigation was based on the following theory. Suppose that the free radicals formed by radiolysis from halogen containing solvent molecules initiate the polymerization, halogen atoms should then become attached to polymer chain ends. By analysing the halogen atoms in the end group, the initiating free radicals could be identified. Although the content of the halogen atoms is very small in a high molecular weight polymer, the content may be measured quantitatively using radioactivation analysis. As reported in the previous paper,[1] the activation analysis method was proved to be useful to estimate the small halogen content in polymer.

<div align="center">EXPERIMENTAL</div>

Materials

Purification of styrene, chloroform, methylene dichloride, ethylene dichloride and bromobenzene was described in the previous paper[1].

Polymerization

Solutions of monomer were degassed and, after three freeze–thaw cycles, sealed under vacuum (10^{-3} mmHg) in glass tubes. Polymerization was

---

* Faculty of Engineering, Hokkaido University, Sapporo, Japan

carried out at 60°C under γ-radiation from a Co-60 source ($8\cdot8 \times 10^3$ r/h, mostly 5×10^4 r). After the irradiation, polymer was precipitated in methanol. The polymer obtained was purified as described in the previous paper[1].

The number average molecular weight of the polymer was calculated from intrinsic viscosity using the relation[2]

$$[\eta] = 2\cdot7 \times 10^{-4}(1\cdot80 \, \overline{M}_n)^{0\cdot66} \tag{1}$$

assuming a normal molecular weight distribution. The viscosity was measured at 25°C in benzene solution.

Activation analysis

Chlorine and bromine in the polymer were quantitatively measured using activation analysis; this method was described in detail in the previous paper[1].

RESULTS AND DISCUSSION

The ratio of rates of polymerization in solution (R_p) with respect to the rate in bulk (R_{p0}) is calculated from the polymerization kinetics data. According to Nikitina and Bagdasaryan's treatment of energy transfer between monomer and solvent[3], the ratio is expressed as follows:

$$\frac{R_p}{R_{p0}} = \left[\frac{1 + \phi_{\mathrm{rel}}P_{\mathrm{rel}}(1 - m)/m}{1 + P_{\mathrm{rel}}(1 - m)/m} \right]^{\frac{1}{2}} \times m \tag{2}$$

Here ϕ_{rel} is the ratio of the rate constants of free radical formation from solvent molecules in pure state with respect to that from monomer molecules, P_{rel} is the relative probability of energy transfer from monomer to solvent rather than from solvent to monomer and m is mole fraction of monomer. The most probable values of ϕ_{rel} and P_{rel} are obtained by fitting the experimental data on curves defined by equation (2). The ratio, a, of the initiating free radicals formed from solvent molecules with respect to total initiating free radicals (those from solvent molecules and monomer molecules in the mixture), is expressed as follows:

$$a = \frac{\phi_{\mathrm{rel}}P_{\mathrm{rel}}(1 - m)/m}{1 + \phi_{\mathrm{rel}}P_{\mathrm{rel}}(1 - m)/m} \tag{3}$$

The a values calculated from equation (3) are compared with the observed numbers of chlorine and bromine atoms in a polymer chain, N_{Cl} and N_{Br}, in *Table 1*.

Polymerization in chloroform

Experimental results of the polymerization kinetics and the number of chlorine atoms are summarized in *Table 1*. *Table 1b* shows that the N_{Cl} value is not affected by the polymerization conversion within the range $1\cdot36$–$8\cdot77\%$. It was shown that the combination of chlorine atoms with the polymer by chlorination reactions occurs much less frequently under the influence of radiation.

The ratio of the rates of polymerization is plotted as a function of mole

Table 1 Experimental data for the radiation-induced polymerization of styrene in chloroform at 60°C and number of Cl atoms in a polymer chain (N_{Cl}) measured by activation analysis.

(a) Effect of mole fraction of monomer

m	$\dfrac{R_p}{R_{p0}}$	α	$\bar{M}_n$ $\times 10^{-5}$	Cl *atoms in polymer chain*, N_{Cl}	
				observed	*corrected**
1·00	1·00	0	8·68		
0·99	1·48	0·242	8·23	1·5	1·5
0·97	2·33	0·847	5·33	2·2	2·2
0·94	2·54	0·915	4·33	2·9	2·9
0·88	2·66	0·958	3·56	3·3	3·2
0·78	2·16	0·979	3·00	3·6	3·3
0·69	2·65	0·985	2·50	3·8	3·4
0·58	1·62	0·992	2·11	3·6	3·0
0·41	1·27	0·996	1·37	3·5	2·7
0·27	1·13	0·998	0·808	2·9	1·8
0·19	0·24	0·999	0·142	2·1	0·9
0·15	0·55	0·999	0·192	1·4	
0·10	0·35	0·999	0·097	1·2	

* To calculate the true contribution of initiation to the N_{Cl} value, correction of observed values was made by subtracting an estimated N_{Cl} value for the transfer reaction (based on equation 4) from an observed N_{Cl} value.

(b) Effect of polymerization conversion

m	*Conversion* (%)	α	$\bar{M}_n$ $\times 10^{-5}$	N_{Cl} *observed*
0·69	1·36	0·985	2·68	3·8
0·69	2·93	0·985	2·61	3·8
0·69	8·77	0·985	2·48	3·8

fraction of monomer, in *Figure 1*. The plotted points fitted the curve best when equation (2) had $\phi_{rel} = 16$ and $P_{rel} = 10$; these values are in good agreement with $\phi_{rel} = 17$ and $P_{rel} = 10$ obtained by Chapiro *et al*[4].

The radiolysis of chloroform was studied by Chen[5], and Cronheim and Günther[6]. Dichloromethyl radicals and chlorine atoms are the main radiation products. If free radicals from monomer molecules and dichloromethyl radicals and chlorine atoms from solvent molecules initiate polymerization, then the fraction of initiating free radicals is described as—

$$\text{monomer radical (or H} \cdot)/\cdot\text{CHCl}_2/\text{Cl} \cdot = (1 - \alpha)/\tfrac{1}{2}\alpha/\tfrac{1}{2}\alpha$$

As the termination reaction in styrene polymerization is predominantly due to recombination[7], a polymer chain is formed with the fragments of the initiating free radicals at both chain ends. Accordingly, the number of chlorine atoms in a polymer chain (depending on the structure of chain ends) and the probability of the occurrence of the structures can be calculated
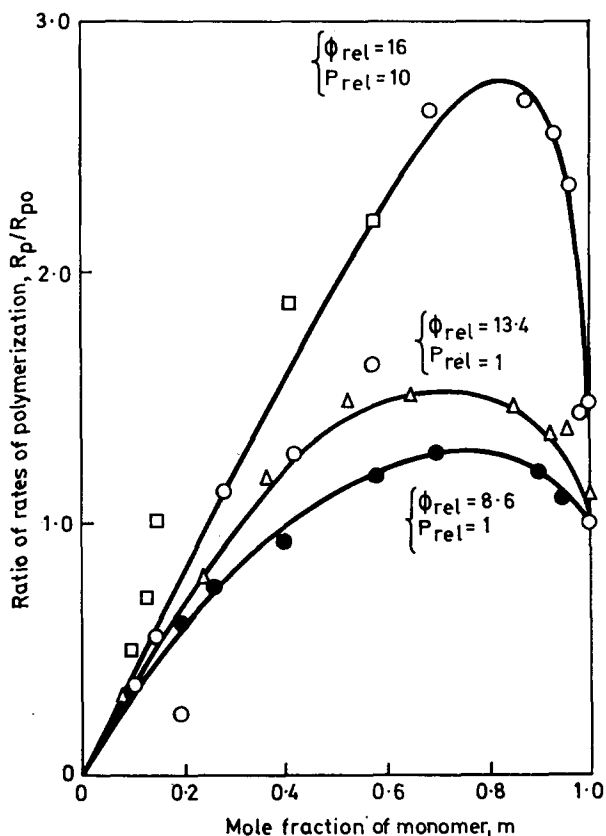
Figure 1 Relation between the rate of polymerization and the mole fraction of monomer in radiation-induced polymerization of styrene in solutions at 60°C. Solid curves are derived from equation (2) with the values of ϕ_{rel} and P_{rel} shown in the figure:

   ○, polymerization in chloroform,

   □, polymerization in chloroform (data obtained from polymers including methanol soluble part);

   △, polymerization in methylene dichloride;

   ●, polymerization in ethylene dichloride.

as shown in *Table 2*. Then the average number of chlorine atoms in a polymer chain, N_{Cl} ($=3\alpha$), is calculated without consideration of chain transfer reactions.

As shown in the previous paper[1] the solvent molecules combine with the polymer in the course of the transfer reaction. Since the degree of polymerization by radiation in bulk is rather high, the effect of solvent transfer is not negligible, in contrast to the case of radical catalysis polymerization. In order to draw the true contribution of initiation to the N_{Cl} value, correction of observed values was made by subtracting an estimated N'_{Cl} value

354

Table 2 Procedure of calculating the number of chlorine atoms, N_{Cl}, in a chain of polymer obtained from radiation-induced polymerization in chloroform

Structure of chain ends	Total number of Cl in a chain, A	Probability of structure occurring, B	A × B
Cl_2—Cl_2	4	$(a/2)^2$	a^2
Cl_1—Cl_1	2	$(a/2)^2$	$\frac{1}{2}a^2$
Cl_0—Cl_0	0	$(1-a)^2$	0
Cl_2—Cl_1	3	$2(a/2)^2$	$\frac{3}{2}a^2$
Cl_2—Cl_0	2	$2(1-a)a/2$	$2a - 2a^2$
Cl_1—Cl_0	1	$2(1-a)a/2$	$a - a^2$

Sum of A × B, $N_{Cl} = 3a$

due to transfer reaction, this being based on equation (4)[1], for an observed N_{Cl} value.

$$\tfrac{1}{3}N'_{Cl} = n = C_s\frac{[S]}{[M]}\bigg/\left[C_m + C_s\frac{[S]}{[M]} + \left(\frac{1}{\overline{DP}_0} - C_m\right)\frac{[M]_0}{[M]}\right] \qquad (4)$$

The corrected N_{Cl} values do not follow equation (3) when $N_{Cl} = 3a$. Instead they agree with the curve calculated from equation (3) with $N_{Cl} = 3\cdot4a$, in the region of large m (see *Figure 2*). This indicates that, even at a small mole fraction of solvent ($m = 0\cdot8$) the polymerization is initiated mostly by free radicals formed from solvent molecules by radiolysis.

One of the reasons for the difference between the corrected value, $N_{Cl} = 3\cdot4a$, and the theoretically expected value, $N_{Cl} = 3a$, may be that tri-chloromethyl radicals secondarily formed by hydrogen abstraction of chlorine atoms in the following mechanism also initiate the polymerization.

$$Cl\cdot + CHCl_3 \rightarrow \cdot CCl_3 + HCl$$
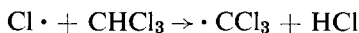
If 80% of chlorine atoms initiate the polymerization directly and 20% of the atoms abstract hydrogen from chloroform to give trichloromethyl radicals, then the value $N_{Cl} = 3\cdot4a$, is accounted for. For example, in the polymerization at $m = 0\cdot8$, 49% of the initiation reaction is due to $\cdot$CHCl$_2$, 10% to $\cdot$CCl$_3$, 39% to Cl$\cdot$, and 2% to free radicals formed from monomer molecules by radiolysis.

One of the reasons for the deviation of observed N_{Cl} values from the theoretically expected curve at low monomer fractions may arise from the invalidity of the kinetic theory of energy transfer which the calculated P_{rel} and ϕ_{rel} are based on. The discrepancy is not attributed to the chlorine atoms combined to low molecular weight polymer because the polymerization products soluble in methanol were examined occasionally and they showed no remarkable contribution as shown in *Figure 2*.

Polymerization in methylene dichloride

The experimental data of polymerization kinetics and of the chlorine content of the polymer are plotted in *Figures 1* and *2*. The curve of R_p/R_{p0}

355
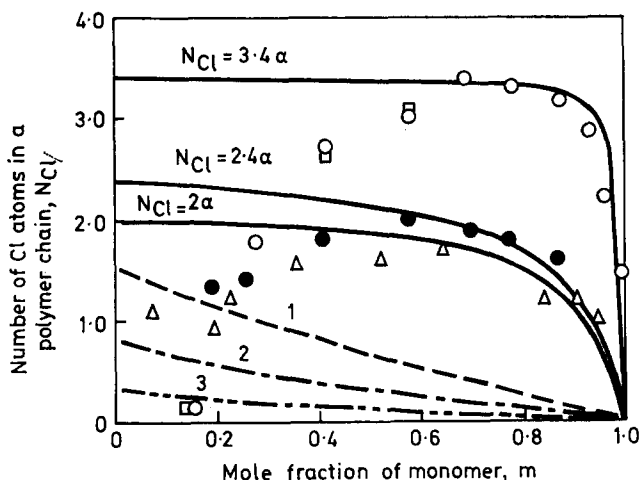
Figure 2 Relation between the number of chlorine atoms in a polymer chain and mole fraction in radiation-induced polymerization of styrene in solutions at 60°C. Solid curves are derived from equation (3). Observed N_{Cl} values were corrected to eliminate the chain transfer effect on N_{Cl} values according to the broken lines based on equation (4) and plotted:
Broken line 1 and the points ○—polymerization in chloroform;
□, polymerization in chloroform (data obtained from polymers including the methanol soluble part);
Broken line 2 and the points ●—polymerization in ethylene dichloride;
Broken line 3 and the points △—polymerization in methylene dichloride.

versus *m* in *Figure 1* gives the values of $\phi_{rel} = 13\cdot4$ and $P_{rel} = 1$. The corrected N_{Cl} values fit to the curve calculated from equation (3) with the relation of $N_{Cl} = 2a$, except for low fractions of monomer (see *Figure 2*).

The formation of free radicals by radiolysis from methylene dichloride was studied[8], which is

$$CH_2Cl_2 \xrightarrow{\;\;\text{MMM}\;\;} \cdot CH_2Cl + Cl \cdot$$
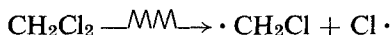
The radical formation mechanism gives $N_{Cl} = 2a$ using a similar calculation to that shown in *Table 2*. Therefore, the polymerization is initiated by the free radicals primarily formed by radiolysis from solvent molecules but not by the secondary ones such as those formed by hydrogen abstraction from methylene dichloride.

It is estimated that 39%, 39% and 22% of the initiation reaction may be due to monochloromethyl radicals, chlorine atoms and free radicals from monomer molecules, respectively, at the monomer fraction $m = 0\cdot8$.

Polymerization in ethylene dichloride
The relation between R_p/R_{p0} and *m* in *Figure 1* gives the values of $\phi_{rel} = 8\cdot6$

and $P_{rel} = 1$. The corrected values of N_{Cl} fit the curve calculated from equation (3) with $N_{Cl} = 2 \cdot 4a$, except for low fractions of monomer (*Figure 2*). However, the known mechanism of free radical formation from ethylene dichloride [8] gives the theoretically expected value of $N_{Cl} = 2a$.

$$C_2H_4Cl_2 \xrightarrow{\text{MM}} \cdot C_2H_4Cl + Cl \cdot$$
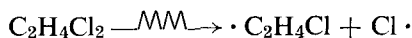
The deviation of the corrected N_{Cl} from the expected one at high monomer fractions is presumably due to the fact that primarily formed chlorine atoms abstract hydrogen from ethylene dichloride to form secondary radicals, $\cdot C_2H_3Cl_2$, which also initiate the polymerization. It is estimated that 60% of all chlorine atoms initiate the polymerization, while the rest of the atoms abstract hydrogen from ethylene dichloride. It is also estimated that when $m = 0 \cdot 8$, 34%, 20%, 14% and 32% of the initiation reaction is due to $\cdot C_2H_4Cl$, $Cl \cdot$, $\cdot C_2H_3Cl_2$ and free radicals from monomer, respectively.

Polymerization in bromobenzene (see Table 3)

The observed data give the values of $\phi_{rel} = 31$, $P_{rel} = 1$ and $N_{Br} = a$. The last result agrees with the theoretically expected value of $N_{Br} = a$ which is derived from the known mechanism of free radical formation[8, 9]:

$$C_6H_5Br \xrightarrow{\text{MM}} \cdot C_6H_5 + Br \cdot$$

At $m = 0 \cdot 8$, 44%, 44% and 12% of initiation reaction are due to phenyl radicals, bromine atoms and free radicals from monomer, respectively.

Table 3 Experimental data of radiation induced polymerization of styrene in bromobenzene at 60°C and number of Br atoms in a polymer chain observed by activation analysis method

m	$\dfrac{R_p}{R_{p0}}$	a	$\overline{M}_n$ $\times 10^{-5}$	Br, *atoms in a chain*, N_{Br} *observed*	*corrected**
1·00	1·00	0	5·33		
0·903	1·60	0·769	2·58	0·700	0·693
0·697	2·25	0·932	1·92	0·766	0·744
0·480	2·14	0·972	0·788	0·646	0·606
0·377	1·72	0·982	0·543	0·555	0·503

* Correction was made in a similar way to the chloroform case

CONCLUSIONS

In the radiation-induced polymerization of styrene in chloroform, methylene dichloride, ethylene dichloride and bromobenzene, the polymerization is initiated mainly by free radicals formed from solvent molecules by radiolysis except when the mole fraction of solvent is very low. In *Table 4* types of initiating free radicals and the proportion of their number at the mole fraction of monomer, $m = 0 \cdot 8$ are summarized.

In the case of alkyl chlorides, the ease with which hydrogen can be abstracted from them (per hydrogen atom) by chlorine atoms primarily formed

357

Table 4 The structure of initiating free radicals in radiation-induced polymerization of styrene in solution and their relative concentrations when the mole fraction of monomer, $m = 0.8$. Polymerization was carried out at 60°C using γ-radiations (8.8×10^3 r/h)

Solvent	ϕ_{rel}	P_{rel}	α at $m = 0.8$	Radicals*			
$CHCl_3$	16	10	0.976	$\cdot CHCl_2$ 49%	$Cl\cdot$ 39%	$\cdot CCl_3$ 10%	$St\cdot$ 2%
CH_2Cl_2	13.4	1	0.770	$\cdot CH_2Cl$ 39%	$Cl\cdot$ 39%		$St\cdot$ 22%
$(CH_2Cl)_2$	8.6	1	0.683	$\cdot C_2H_4Cl$ 34%	$Cl\cdot$ 20%	$\cdot C_2H_3Cl_2$ 14%	$St\cdot$ 32%
C_6H_5Br	31	1	0.887	$\cdot C_6H_5$ 44%	$Br\cdot$ 44%		$St\cdot$ 12%

* $St\cdot$ = styrene radical

by radiolysis is in the order: chloroform > ethylene dichloride > methylene dichloride. This order is the reverse of the order of C—H bond dissociation energies, 89, 93 and 93.2 kcal/mole (ref. 10) (21.2, 22.1 and 22.2 kJ/mole), respectively.

Department of Polymer Chemistry
Kyoto University,
Kyoto, Japan

REFERENCES

1 Maekawa, T., Matsuo, M., Yoshida, H., Hayashi, K. and Okamura S. *Polymer, Lond.* 1970, **11**, 342, this issue (Part 1 in this series)
2 Pepper, D. C. *J. Polym. Sci.* 1952, **7** 347
3 Nikitina, T. S. and Bagdasaryan, Kh. S., 'Sbornik Rabot po Radiatsionnoi Khimii', Academy of Sciences of USSR, Moscow 1955, p 183
4 Chapiro, A. *J. chim. phys.* 1960, **47**, 747; 1960, **47**, 764
5 Chen, T. H., Wong, K. Y. and Johnston, F. J. *J. Phys. Chem.* 1960, **64**, 1023
6 Cronhein, G. and Günther P. *Z. physik. Chem.* 1930, **B9**, 201
7 Bevington, J. C., Melville, H. W. and Taylor, R. P. *J. Polym. Sci.* 1954, **12**, 449; Bevington, J. C., Melville, H. W., and Taylor, R. P. *J. Polym. Sci.* 1954, **14**, 463; Henrici-Olive, G. and Olive, S. *J. Polym. Sci.* 1960, **48**, 329
8 Swallow, A. J., 'Radiation chemistry of organic compounds', Pergamon Press, Oxford, 1960, p 94
9 Haissinsky, M., 'Nuclear chemistry and its applications', Addison-Wesley Publishing Co., Reading, Massachusetts, 1964, p. 412
10 Semenov, N. N., 'Some problems on chemical kinetics and reactivity', Academy of Nauka, USSR, Moscow, 1958, chapter 1

Thermodynamic studies on poly(α-olefin)–solvent systems

P. J. T. TAIT and and P. J. LIVESEY*

This paper reports a study of the thermodynamic properties of concentrated solutions of tactic poly(α-olefins), prepared by means of Ziegler-Natta catalysts, and studied by means of the reduction in vapour pressure of solvent with increase in polymer concentration at constant temperature. The results obtained for the polymers polyheptene-1, polydecene-1, polydodecene-1 and polyoctadecene-1 in toluene are analysed in terms of various theories of polymer solutions. The lattice theory of Flory in its original form was found to explain well the behaviour of solutions of polyheptene-1, and when correction was made for size of repeat unit the theory then accounted satisfactorily for the behaviour of polydecene-1 with values of the interaction parameter close to 0·5. The Maron theory was also applied to these systems and produced similar results. The different characteristics shown by the systems toluene/polydodecene-1 and toluene/polyoctadecene-1 are discussed with reference to the theories of Sakurada and Szwarc, which consider the bulk polymer to be similar to a crosslinked network with the crystalline regions acting as the crosslinks, and in the region of high concentration of polymer these theories predict with some success the variations of the interaction parameters.

INTRODUCTION

THE AIM of the present work was twofold: firstly to obtain experimental data for the sorption behaviour of a series of α-olefinic polymers towards toluene, and secondly to determine to what extent current theories of polymer sorption and solution could account for the observed behaviour. Szwarc[1] and Sakurada[2] have shown that the solubility characteristics of amorphous and crystalline regions of polymers are different, the latter being physically inaccessible to solvent molecules at low concentrations, and so the solubility isotherms at temperatures below the polymer melting point will not follow the behaviour predicted by theories of solution such as those of Flory[3] and Maron[4].

Selection of polyheptene-1, polydecene-1, polydodecene-1 and polyoctadecene-1 afforded a convenient variation in crystallinity, and at the same time provided polymer systems in which the size of the pendant side groups was varied. Thus a concurrent study was carried out on pendant side group size effects in relation to solution theory. This is necessary due to the acceptance of the basic concepts of the Flory theory for the behaviour of the non-ordered regions of the poly(α-olefin) samples.

---

* President address: Department of Chemistry, Renesselaer Polytechnic Institute, Troy, New York. 12181, USA

The variety of physical properties exhibited by the series of poly(α-olefins) may be described in terms of their physical structures as elucidated by Turner Jones[5]. Whilst the lower members, for example polypropylene and poly-butene-1, are able to crystallize with the main chains in a helical conformation, a critical length of side chain is reached which renders this impossible, resulting in an essentially amorphous polymer which is soft, tacky and transparent at room temperature (e.g. polyheptene-1).

As the side chains are further lengthened their influence on the crystallization behaviour is increased, when they tend to align side-by-side as in the higher paraffin hydrocarbons, whilst at the same time accommodating a distorted main chain which may also become ordered with respect to other backbone chains. This increasing tendency to crystallize is maintained even as the length of the side chain is further increased and eventually the melting point of the polymer approximates closely to that of the corresponding paraffin, as in the case of polyoctadecene-1.

<div align="center">EXPERIMENTAL</div>

Materials

Polymers. These were obtained from the appropriate α-olefins, purified by drying over magnesium sulphate and subsequent distillation, using typical Ziegler-Natta catalysts[6]. Polyheptene-1 was prepared under an atmosphere of dry nitrogen using a $TiCl_3$–$Al(isoBu)_3$ catalyst system (Ti/Al mole ratio 1:8; monomer/$TiCl_3$ mole ratio 10:1) in toluene as solvent. A high vacuum technique was employed for the other three polymers with VCl_3–$Al(Et)_3$ or VCl_3–$Al(isoBu)_3$ catalysts in similar concentrations as before, again with toluene as solvent. After polymerization at room temperature (generally for about 30 h) the polymer was separated by pouring the reaction mixture into a large excess of cooled methanol containing hydrogen chloride to remove catalyst particles. Reprecipitation from warm chloroform was followed by evacuation to constant weight.

Solvent. Toluene was used in all runs and was purified in the following manner. Analar quality liquid was dried by refluxing over fresh sodium wire for about 5 h and then distilled from the sodium at a slow rate using a specially constructed adiabatic column. The middle fraction boiling at the appropriate temperature was retained. The refractive index was checked and samples analysed with a Perkin-Elmer F11 gas chromatograph. This analysis showed the middle fraction to be at least 99·8% pure, the majority of the impurity being benzene.

Vapour pressure apparatus

The system consisted of a sample bulb suspended from a quartz spring accessible to a simple mercury manometer. The somewhat complex apparatus of certain workers[7–9] was greatly simplified by the use of greaseless stopcocks instead of mercury cut-off valves. Solution compositions were determined from the spring extension, measured using a cathetometer, reading to ± 0·01 mm, which was also used to measure manometer pressures.

<div align="center">360</div>
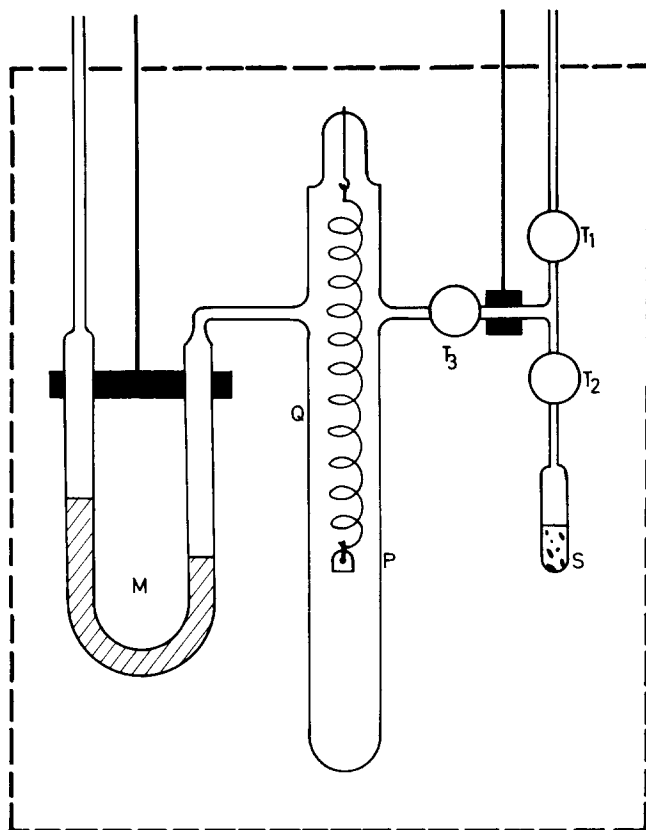
Figure 1 Vapour pressure apparatus M; mercury manometer of wide bore tubing to obviate meniscus corrections S; solvent reservoir P; glass bulb (wt. ∼ 0·25 g) containing the polymer sample attached to the quartz spring, Q

The apparatus is suspended from two brass rods attached to alloy blocks clamped to the manometer and to the side tube near T_3, facilitating easy removal from the constant temperature bath.

The greaseless stopcocks (J. H. Springham Ltd, Harlow, Essex) have a Viton A (fluorocarbon rubber) diaphragm which was found to be impervious to toluene over long periods of time. As a slight modification a small hole was drilled in the metal casing to allow water to escape from between the case and the diaphragm when the tap was opened.

Unlike a normal stopcock, the two sides are not equivalent in maintaining a vacuum; on one side leaks can only occur from an orifice of diameter 4 mm, sealed by the centre of the diaphragm, whilst the other side is open to the periphery of the barrel, being sealed by the outer edge of the diaphragm. Consequently the outlet from the centre of the diaphragm was always connected to the pressure vessel and solvent reservoir.

A vacuum of better than 10^{-2} mmHg could easily be held by these taps for a number of days under water.

Quartz springs. The quartz springs were supplied by UKAEA (Harwell) and had the following specifications:

Extension per gram	11 cm
Coil diameter	2 cm
Fibre thickness	0·023 cm
Number of coils per cm	10
Unloaded length	5·8 cm
Average maximum load carried	0·9 g

These springs were calibrated using standard weights and a cathetometer, linear relationships with load being found.

Thermostat bath. Since runs were likely to last 2–3 weeks, constancy of temperature was important. An efficient relay system was incorporated into the heater circuit, together with a very senstive mercury–toluene regulator having a high surface-to-volume ratio. A variable heating current was used and adjusted so that the heater was in and out of circuit for approximately the same time.

Constancy of temperature was checked using a Beckmann thermometer and a chromel–alumel thermocouple in conjunction with a potentiometric recorder. Maximum fluctuations in bath temperature were found to be $\pm 0.025°C$.

Procedure. To gain access to the pressure vessel a cut was made in the neck portion. The polymer sample (0·10–0·15 g) was placed in the bulb and the apparatus reconstructed and evacuated to 10^{-6} cmHg. The reliability of the stopcocks was checked by closing all three, raising the bath, and leaving overnight; any leakage was then detected by expanding each section of the apparatus into a McLeod gauge. Meanwhile the spring extension was measured to give a reference value. With T_3 shut, pure degassed toluene was distilled into S. T_1 was closed and T_3 carefully opened to admit the requisite amount of solvent vapour. After closing T_3, the bath was raised and the system allowed to equilibrate, keeping a high vacuum on the left-hand side of the mercury manometer. The pressure difference and spring extension were noted and the manipulations repeated after quickly evacuating the centre vessel and degassing the solvent. As the solution became more dilute, transfer of solvent was assisted by cooling the centre vessel and, in the final stages of dilution, warming the solvent reservoir S. Whereas in the majority of cases equilibration was reached within 15 h, with dilute solutions as long as 4 days was required. In case any leakage had occurred through T_3, T_1 and T_3 were quickly opened to vacuum, removing the vapour but very little liquid. Equilibrium was again attained on leaving overnight.

Hysteresis was checked by partially evaporating solutions and allowing the system to equilibrate: none was observed.

The effect of the upthrust of solvent vapour on the bulbs was determined by measuring the extension due to a known load of small glass beads for different solvent pressures. Any difference observed was within experimental error.

The vapour pressure of pure solvent at the experimental temperature (P_1^0) was obtained from the Antoine equation[10], the values of the constants used[11] being

$$A = 6 \cdot 953\,34$$
$$B = 1343 \cdot 94$$
$$C = 219 \cdot 377$$

Densities of polymers

Densities were determined at 30°C by a flotation method. The sample was degassed under high vacuum (the rubbery polymers, polyheptene-1, poly-decene-1, and polydodecene-1 were heated under vacuum to a temperature above the melting point) and pure ethanol distilled onto it. Air-free water was added until the sample just floated and the liquid density was then determined in the normal manner.

Molecular weights

The osmotic pressure method was used to determine number average molecular weights.

RESULTS

Table 1 lists densities and molecular weights for the polymers used. In *Table 2* representative experimental data for the four poly(α-olefin)–toluene systems studied are recorded.

Table 1 Densities and molecular weights (Temperature 30°C)

Polymer	Density (g cm^{-3})	$\overline{M}_n$ $\times$ 10^{-5}
Polyheptene-1	0·863	2·241
Polydecene-1	0·847	2·139
Polydodecene-1	0·856	0·949
Polyoctadecene-1(A)	0.881	2·208
Polyoctadecene-1(B)	0·888	1·935

THERMODYNAMIC CONSIDERATIONS

The simple lattice theory of Flory[5] expresses the chemical potential of the solvent in the solution as

$$\mu_1 - \mu_1^0 = RT[\ln(1 - v_2) + (1 - 1/x)\,v_2 + \chi_1\, v_2^2] \tag{1}$$
$$= RT \ln (P_1/P_1^0)$$

assuming the solvent vapour to be ideal. The volume fraction of polymer, v_2, is given by

$$v_2 = \frac{w_2}{(M_0/M_1)w_1 + w_2} \tag{2}$$

363

Table 2 Vapour pressure results (Temperature 30°C)

Polyoctadecene-1

Run 8 Sample A		Run 4 Sample B		Run 5 Fraction 5		Run 7 Fraction 5	
$P_1^0 = 3.650$ cmHg		$P_1^0 = 3.664$ cmHg		$P_1^0 = 3.690$ cmHg		$P_1^0 = 3.664$ cmHg	
$W_2 = 0.1379$ g		$W_2 = 0.1398$ g		$W_2 = 0.1223$ g		$W_2 = 0.0925$ g	
W_1	P_1	W_1	P_1	W_1	P_1	W_1	P_1
0.0012	0.444	0.0025	0.592	0.0023	0.668	0.0009	0.402
0.0035	0.972	0.0087	1.356	0.0037	1.062	0.0031	1.037
0.0095	1.708	0.0125	1.747	0.0150	2.148	0.0061	1.717
0.0171	2.180	0.0764	3.161	0.0494	3.146	0.0104	2.177
0.0428	2.860	0.4334	3.651	0.1292	3.588	0.0117	2.204
0.0518	3.027	0.6694	3.652	0.4652	3.684	0.0165	2.556
0.0615	3.151			0.8098	3.687	0.0248	2.930
0.1237	3.463					0.0458	3.355
0.1495	3.507					0.0466	3.401
0.2514	3.593					0.1945	3.648
0.2968	3.600						
0.4417	3.627						
0.7393	3.645						

Polyheptene-1

Run 1		Run 3		*Polydodecene-1* Run 1		Run 3 (Fractionated)	
$P_1^0 = 3.686$ cmHg		$P_1^0 = 3.670$ cmHg		$P_1^0 = 3.680$ cmHg		$P_0^1 = 3.670$ cmHg	
$W_2 = 0.1378$ g		$W_2 = 0.1016$ g		$W_2 = 0.1379$ g		$W_2 = 0.1245$ g	
W_1	P_1	W_1	P_1	W_1	P_1	W_1	P_1
0.0002	0.043	0.0022	0.340	0.0019	0.366	0.0033	0.539
0.0012	0.124	0.0042	0.602	0.0071	0.994	0.0053	0.708
0.0048	0.506	0.0069	0.932	0.0130	1.498	0.0069	1.004
0.0077	0.716	0.0111	1.379	0.0361	2.307	0.0097	1.263
0.0133	1.308	0.0188	1.931	0.0604	2.817	0.0109	1.416
0.0279	2.085	0.0654	3.207	0.1144	3.327	0.0211	2.022
0.0579	2.893	0.0852	3.366	0.1981	3.554	0.0257	2.179
0.1239	3.400	0.1634	3.587	0.2759	3.600	0.0863	3.218
0.3153	3.640	0.3147	3.639	0.5422	3.659	0.2373	3.588
0.6978	3.672	0.3290	3.649			0.4221	3.648
		0.4086	3.659			0.4936	3.659

Polydecene-1

Run 1		Run 3	
$P_1^0 = 3.664$ cmHg		$P_1^0 = 3.670$ cmHg	
$W_2 = 0.1340$ g		$W_2 = 0.1340$ g	
W_1	P_1	W_1	P_1
0.0031	0.280	0.0044	0.515
0.0084	0.814	0.0054	0.561
0.0169	1.419	0.0092	0.913
0.0235	1.757	0.0164	1.429
0.0528	2.681	0.0253	1.885
0.0990	3.262	0.0666	2.957
0.1982	3.545	0.0960	3.233
0.8348	3.661	0.1817	3.527
		0.2927	3.614

M_0 and M_1 being the molecular weights of polymer repeat unit and solvent respectively.

In this case the number of lattice sites, r, occupied by a single polymer molecule is equal to the degree of polymerization of the polymer (M_2/M_1), but in the majority of cases the repeat unit is different in size to that of the solvent molecule and must be redefined as the ratio of the molar volumes of polymer to solvent, i.e.

$$r = \frac{M_2}{M_1} \times \frac{\rho_1}{\rho_2} \tag{3}$$

and so
$$v_2 = \frac{w_2}{(\rho_2/\rho_1)w_1 + w_2} \tag{4}$$

The general theory of non-electrolyte solutions developed by Maron[4] is not based on statistical considerations, and gives for the total free energy of mixing, provided volume change upon mixing are small

$$\overline{\Delta G}_1 = RT[X_1 + (\chi_1 - \sigma v_1)\, v_2^2] \tag{5}$$

where $\quad X_1 = \ln v_1 + (1 - \epsilon/\epsilon_0 x)\, v_2$

and $\quad \epsilon/\epsilon_0 = 1/[1 + (\epsilon_0 - \epsilon_\infty)]v_2$

ϵ_0 the effective volume factor for the polymer at $v_2 = 0$, is equal to $100[\eta]\rho_2/2$ when $[\eta]$ is in dl g^{-1}. The term ϵ_∞, the effective volume factor for the polymer at tightest packing in solution, may be taken as 4·0 (ref. 12), while σ is given by the expression

$$\sigma = \left(\frac{\partial \chi_1}{\partial v_2} \right)_T$$

The presence of ordered regions in the solid polymer resulting in different solubility characteristics would indicate that the volume fractions should be computed on the basis of amorphous content, and further, if the solvent does not penetrate these regions, they will act as crosslinks leading to an unfavourable entropy effect. To explain the sorption patterns of partially crystalline poly(vinyl alcohol)/water systems Sakurada[2] used the relationship

$$\ln a_1 = \ln(1 - v_{2a}) + (1 - 1/x_a)\, v_{2a} + \chi_1\, v_{2a}^2 + 1/x_a\, (v_{2a}^{\frac{1}{3}} - \tfrac{1}{2}v_{2a}) \tag{6}$$

where x_a is the mean chain length in the amorphous regions and v_{2a} is the volume fraction of the amorphous region of polymer.

Szwarc, Rogers and Stannett[1] modified the Flory equation to study the sorption of organic vapours of polyethylene. For polymers with moderate to high degrees of crystallinity they obtained the relationships

$$\overline{\Delta G}_1 = RT[\ln v_{1a} + v_{2a} + \mu v_{2a}^2 + \rho_a V_1 v_{2a}^{\frac{1}{3}}/M_c] \tag{7}$$

and $\quad \chi_1 = \mu + \rho_a\, V_1\, v_{2a}^{-5/3}/M_c$

$\qquad = [\ln(a_1/v_{1a}) - v_{2a}]/v_{2a}^2$

where χ_1 is the value of μ calculated for the system disregarding the effect of crystalline links, M_c is the molecular weight of crosslinked chain and ρ_a the density of unswollen amorphous regions. A plot of χ_1 versus $v_{2a}^{-5/3}$ should thus be linear with a slope of $(\rho_a V_1/M_c)$ and intercept μ if M_c is constant.

DISCUSSION

The plots of P_1/P_1^0 against weight fraction of solvent (*Figures 2* and *3*) derived from the results in *Table 2* offer an immediate qualitative comparison between the polymers. Thus polyheptene-1 and polydecene-1 are more soluble than the two higher members of the series, having smooth curves with negligible scatter. Polydodecene-1 shows a higher value of P_1/P_1^0 in the weight fraction range (0–0·15), than might be expected from the remainder of the curve.

In the case of polyoctadecene-1, the plots have steeper initial gradients than those for the lower members of the series. It is also apparent from *Figure 3* that different fractions of polyoctadecene-1 give slightly different plots. These differences can be ascribed to the crystalline contents of the polyolefins which is appreciably large with polyoctadecene-1. Two first-order transitions were observed by differential thermal analysis measurements on the samples of polyoctadecene-1, in agreement with the finding of Aubrey and Barnatt[13].
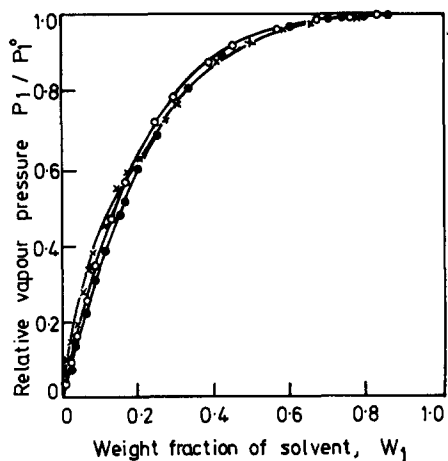
Figure 2 Relative vapour pressure of toluene solutions of poly(α-olefins) at 30°C
○, polyheptene-1
●, polydecene-1
×, polydodecene-1
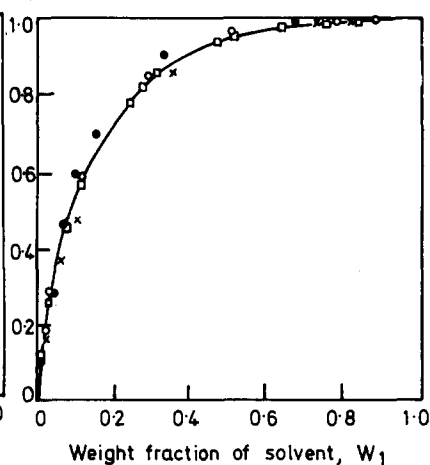
Figure 3 Relative vapour pressure of toluene solutions of polyoctadecene-1 at 30°C
×, B, unfractionated
○, B, fraction 5, run 5
●, B, fraction 5, run 7
□, A, unfractionated

The simple Flory theory

The simple Flory theory (equation 1) was used with the volume fraction expressed by equation (2). The resulting plots of the function

$$[\ln P_1/P_1^0 - \ln(1 - v_2) - (1 - 1/x)v_2] \text{ versus } v_2^2$$

show that the theory is obeyed to a good approximation by polyheptene-1 which exhibits a virtually constant value of $\chi_1 = 0·49$ over the entire con-

centration range (*Figure 4*). The similarity to the rubber-benzene system[7, 14] may be noted.

Polydecene-1 shows an almost linear increase in χ_1 with decrease in v_2, approaching the limiting value of 0·5 for polymer–solvent systems miscible in all proportions–a phenomenon observed in a number of systems[3]–whilst polydodecene-1 and polyoctadecene-1 show no comprehensive correlation with theory, both positive and negative values of χ being found. Included in *Figure 4* is the result for a control sample of atactic polystyrene which gives a value of $\chi_1 = 0\cdot46$ comparing favourably with that obtained by Bawn[15]. No adjustment for size of repeat unit has been made in this case since the repeat unit in polystyrene and the toluene molecule have similar sizes.
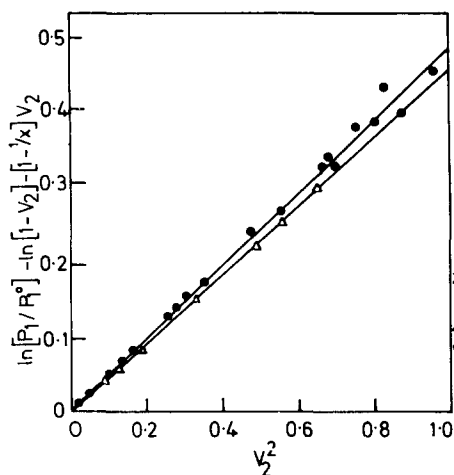
Figure 4 Application of the simple Flory theory to solutions of polyheptene-1 and polystyrene in toluene at 30°C
●, polyheptene-1
△, polystyrene
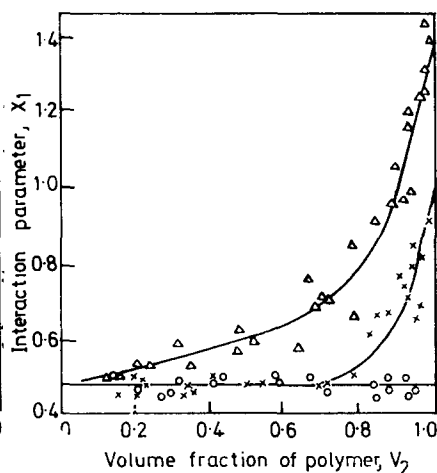
Figure 5 Interaction parameters from the extended Flory theory
○, polydecene-1
×, polydodecene-1
△, polyoctadecene-1

When the parameter r is incorporated and equation (4) applied, the interaction parameter is constant for polydecene-1 over the entire concentration range (*Figure 5*) showing excellent agreement with theory.

Polydodecene-1 presents a constant value of χ_1 with little spread of experimental points up to $v_2 \approx 0\cdot8$ whereupon a rapid increase in χ_1 occurs. The plot for polyoctadecene-1 shows no true linear portion and χ_1 approaches the axis $v_2 = 0$ almost asymptotically. Plots of $F(P_1, v_2)$ versus v_2^2 give $\chi_1 = 0\cdot48$ for polydedecene-1 whilst in the case of polydodecene the linear portion corresponds to $\chi_1 = 0\cdot47$. For the polyoctadecene/toluene system only the initial portion of the plot shows the expected linear dependence on v_2^2 giving $\chi_1 = 0\cdot60$ followed by a curve of increasing gradient which may be differentiated into distinct curves corresponding to the varying crystalline contents of each sample.

Apart from a spread of points in different samples due to variations in crystallinity a degree of scatter is evident in, for example, *Figures 5* and *6*. Due to the sensitivity of the quartz spring, errors in v_1 and v_2 are very small except in the cases of the most highly concentrated systems, but even here, with values of v_2 as high as 0·96, the errors involved in v_1 and v_2 are only 1·1% and 0·8% respectively. Errors in P_1/P_1^0 are small throughout the whole range, and only reach a value of 0·3% at high values of v_2 ($v_2 = 0·96$). Incidentally, errors due to the non-ideal behaviour of toluene vapour in the pressure range investigated are very small, i.e.

$$[(-BP/RT) < 4 \times 10^{-4}].$$

Although the errors in P_1/P_1^0, v_1 and v_2 are small, these can give rise to significant errors in the term

$$[\ln P_1/P_1^0 - \ln (1 - v_2) - (1 - 1/x) v_2]$$

For the polydecene-1/toluene system, when $v_2 = 0·96$, $\chi_1, = 0·456 \pm 0·037$, the error is $\pm 8\%$. Here the term

$$[\ln (P_1/P_1^0) - \ln(1 - v_2) - (1 - 1/x) v_2]$$

is comparatively large leading to a fairly small error in χ_1. On the other hand when $v_2 = 0·186$, $\chi_1 = 0·551 \pm 0·107$, the error is $\pm 19·5\%$. Nevertheless the error in the above term will be less than $\pm 10\%$ for v_2^2 greater than 0·10.
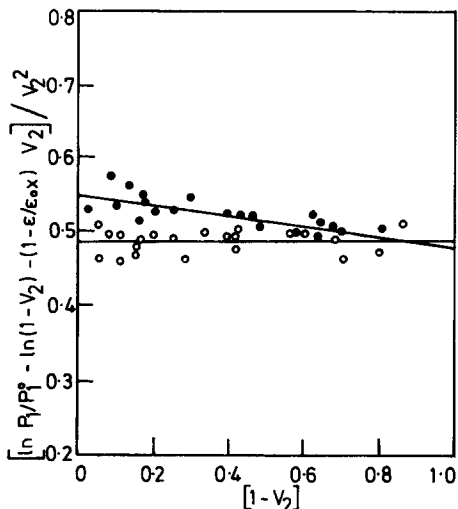
Figure 6 Application of the Maron theory to the system poly(α-olefin)/toluene at 30°C
●, polyheptene-1
○, polydecene-1
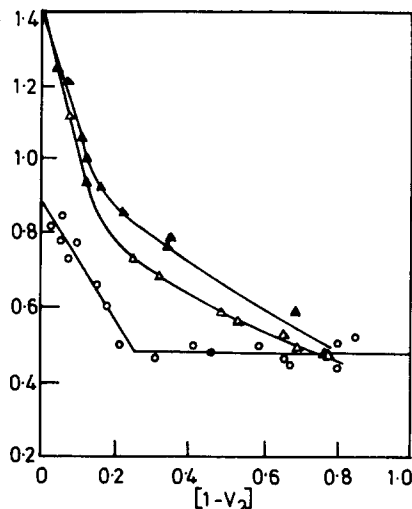
Figure 7 Application of the Maron theory to the system poly(α-olefin)/toluene at 30°C
○, polydodecene-1
●, polyoctadecene-1, sample B, fraction 5
△, polyoctadecene-1, sample A, unfractionated

The Maron theory

The close similarity between the extended Flory theory and the Maron theory can be seen; the main differences are in the term correcting the volume fraction of polymer, $[1 - (\epsilon/\epsilon_0 x)]v_2$, and the inclusion of a term expressing the concentration dependence of the interaction parameter χ_1. The former is small, but the latter assumes importance when χ_1 varies linearly with v_2. Application of the theory to experimental values gives similar results to the extended Flory theory since χ_1 in the latter is almost equivalent to $(\chi_1 - \sigma v_1)$ in the Maron theory.

The term $[\ln(P_1/P_1^0) - \ln(1 - v_2) - (1 - \epsilon/\epsilon_0 x)v_2]/v_2^2$ may be plotted against v_1 to obtain χ_1 as intercept and $\sigma = (\partial \chi_1/\partial v_2)_T$ as gradient.

For polyheptene-1 a linear dependence on v_1 is found corresponding to $\chi_1 = 0.55$ and $\sigma = -0.75$. With polydecene-1 the plot is parallel to the concentration axis and χ_1 has a constant value of ~ 0.48, the σv_1 term being zero. In the case of polydodecene-1, $(\chi_1 - \sigma v_1)$ is constant at ~ 0.48 down to a value of $v_1 = 0.25$, whereupon an apparently linear increase is found corresponding to $\sigma = -1.6$. The polyoctadecene-1 plot is rather more difficult to interpret and can be split into two distinct curves representing different runs.

It is apparent that as the length of the side chain increases in these polymers so does the extent of deviation from, firstly the simple Flory theory due to size of repeat unit, and secondly, from the modified Flory and Maron theories, due to the semi-crystalline nature of the higher α-olefin polymers. However, even with these latter samples the interaction parameter is tending towards a constant value with increasing solvent concentration and in the case of polydodecene-1 χ_1 does become constant when a true solution of both components is achieved. In highly concentrated solutions the theories considered previously do not take into account the preferential absorption of the solvent on the amorphous or 'least ordered' parts of the sample, which leads to an incorrect estimate of concentration.

However, both the Sakurada and Szwarc theories involve an expression for the volume fraction of polymer based on the fraction of the sample in the amorphous state, λ. Thus,

$$v_{2a} = \frac{w_2}{(\rho_2/\rho_1\lambda)\, w_1 + w_2}$$

It is necessary therefore to determine the crystallinity or degree of order which may not be the same for different samples of the same polymer since it is dependent upon the catalyst and polymerization conditions, together with any treatment subsequent to preparation. The crystalline content was estimated from the relationship[16]

$$\text{Weight per cent crystallinity} = \frac{\rho_c\,(\rho_2 - \rho_a)}{\rho_2\,(\rho_c - \rho_a)}$$

where ρ_c, ρ_a and ρ_2 are the densities of pure crystalline, pure amorphous and sample polymer respectively. For polyoctadecene-1, ρ_c may be taken as 0.95 g cm^{-3} and ρ_a assumed to be 0.85 g cm^{-3} at room temperature; for a

partly crystalline sample ρ_2 was found[17] to be 0·909 g cm^{-3}. Values of ρ_2 determined in this work were 0·88 and 0·89 g cm^{-3}.

It is thus evident that a wide range of crystallinities is possible, the above values of ρ_2 corresponding to 35–65%. Estimates of the degree of crystallinity in polydodecene prepared under similar conditions were 10–15%[17]. Due to these variations it is necessary to examine the effect of changing λ in both the Sakurada and the Szwarc theories.

The Sakurada theory

For the Sakurada theory to be applicable a plot of

$$\ln P_1/P_1^0 - \ln (1 - v_{2a}) - (1 - 1/x_a)\, v_{2a} - 1/x_a\, (v_{2a}^{1/3} - v_{2a}/2)$$

versus v_{2a}^2 should be linear with gradient χ_1. The term x_a which will be large for all except very highly crystalline samples, was set as the mean average chain length, equal to $(M_2/M_1)\,(\rho_1/\rho_2)$. The two systems studied showed an approximately linear plot at high v_{2a}^2 values, although for polyoctadecene-1 this was only apparent at the highest polymer concentrations, showing that, at least initially, the semi-crystalline polymer acts as a lattice structure which is deformed elastically on penetration by solvent.
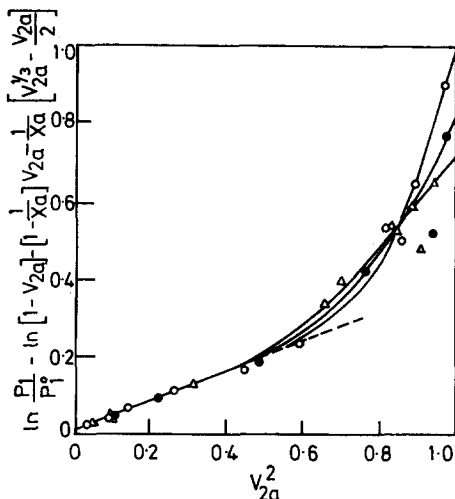
Figure 8 Application of the Sakurada equation to the system polydodecene-1/toluene at 30°C, assuming an amorphous content, $\lambda = 0\cdot875$

○, unfractionated sample, run 1
●, unfractionated sample, run 2
△, fraction 2
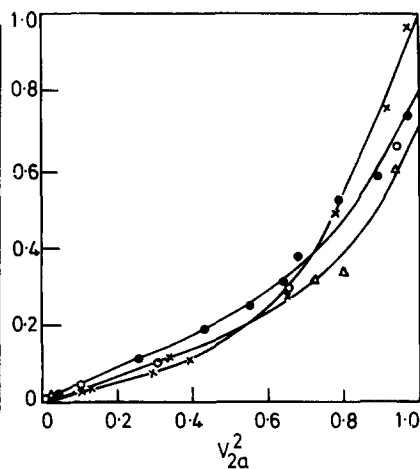
Figure 9 Application of the Sakurada equation to the system polyoctadecene-1/toluene at 30°C, assuming an amorphous content, $\lambda = 0\cdot525$

△, unfractionated, sample B
○, sample B, fraction 5, run 5
●, sample B, fraction 5, run 7
×, unfractionated, sample A

The separation of plots for different samples shown for polyoctadecene-1 in *Figure 9*, is, of course, due to variations in crystalline content. The more linear portions of the plots in dilute solution regions reflects the tendency of the system to become miscible in all proportions, although the numerical

370

values of the interaction parameter will be erroneous due to an under-estimate of the polymer concentration. In the intervening section the 'lattice' is breaking down after the amorphous regions are fully swollen with solvent, and the crystalline regions are taking part in the solution process. The sensitivity of the plots to changes in λ is shown in *Figure 10* where the vapour pressure results from one particular fraction of polyoctadecene-1 have been used and λ varied. The increase in linearity of the plots with amorphous content does not imply that if λ is increased further the plots (constructed using our experimental data) would be linear, since as $\lambda \to 1{\cdot}0$, $v_{2a} \to v_2$ and the Flory theory is the result: data obtained from the Flory theory demonstrate this point.
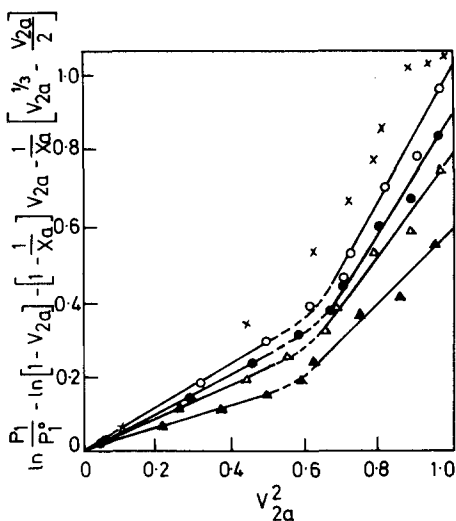
Figure 10 Application of the Sakurada equation to the system polyoctadecene-1/toluene at 30°C, using a single sample (B, fraction 5, run 7) and varying the amorphous content

○, $\lambda = 0{\cdot}650$
●, $\lambda = 0{\cdot}575$
△, $\lambda = 0{\cdot}525$
▲, $\lambda = 0{\cdot}425$
×, extended Flory theory, $\lambda = 1{\cdot}0$
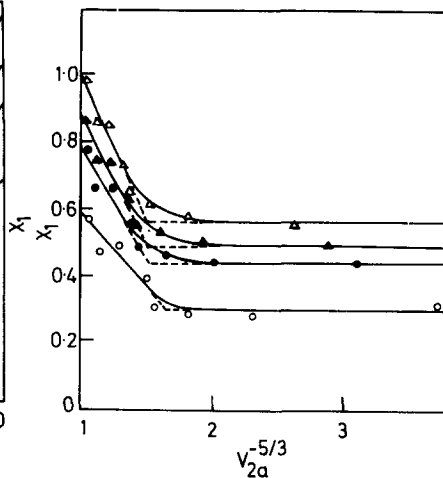
Figure 11 Application of the Szwarc treatment for crystalline polymers to the system polyoctadecene-1/toluene assuming an amorphous content. $\lambda = 0{\cdot}525$

×, unfractionated, sample B
○, sample B, fraction 5, run 5
●, sample B, fraction 5, run 7
□, unfractionated sample A

It is concluded that the Sakurada theory is of value only at high values of v_{2a} where λ can be assumed to be constant and therefore the theory cannot represent the system over the entire concentration range. It would also ap-pear that a relationship in which λ is proportional to a concentration term and consequently varies with the volume fraction of polymer, becoming $1{\cdot}0$ at low polymer concentration, should therefore be applied to the results.

371

The Szwarc theory

Since equation (7) derived using the Szwarc theory is applicable only to polymers containing an appreciable degree of crystallinity, the results for polyoctadecene-1/toluene system for various fractions are shown in *Figure 11*. As before these plots show distinct regions.

At high polymer concentrations the slope, given by $\rho_a v_1 / M_c$, is constant, indicating that the molecular weight of the 'crosslinked lattice' is constant, and that the latter is expanding elastically as more solvent molecules are
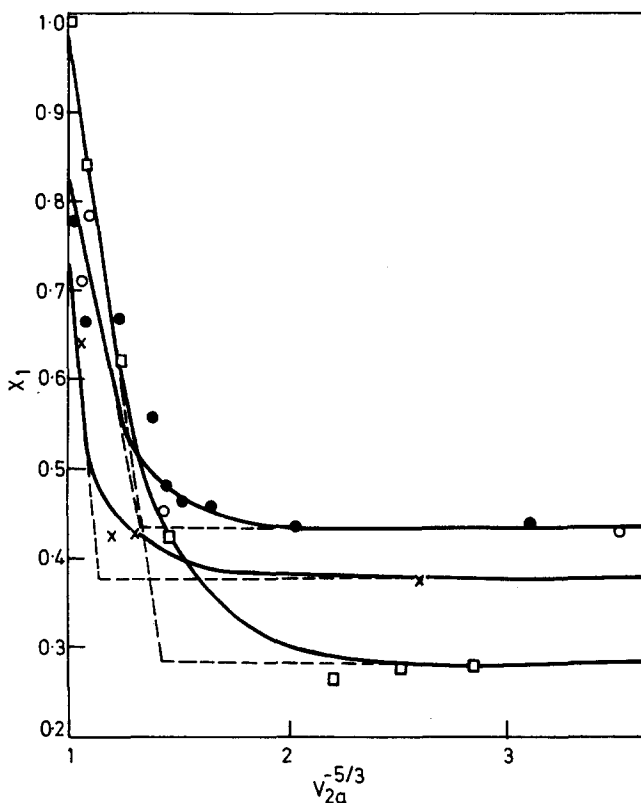
Figure 12 Application of the Swzarc treatment for crystalline polymers to the system polyoctadecene-1 toluene, using a single sample, B, fraction 5, run 7, and varying amorphous content

$\bigcirc$, $\lambda = 0.425$ $\triangle$, $\lambda = 0.575$
$\bullet$, $\lambda = 0.525$ $\bullet$, $\lambda = 0.650$

absorbed. From *Figure 12*, if an amorphous density, $\rho_a = 0.85$ is assumed and $v_1 = 107$ cm³ at 30°C, a value of $M_c \sim 100$ is obtained for $\lambda = 0.425$, and a value of $M_c \sim 200$ for $\lambda = 0.65$. These values are of the order found by Szwarc[1] for Ziegler polymerized polyethylene.

For values of $v_{2a}^{-5/3}$ greater than 2, χ_1 is constant and equal to μ and the plot has zero slope. This means that M_c must be ∞, or so high as to be considered infinity with, of course, the limiting value being the primary molecular weight

of the polymer. The slope is negligible when $M_c \sim 10000$ for the values of ρ_a and v_1 given above.

In the region between $v_{2a}^{-5/3} = 1\cdot5 - 2\cdot2$ the lattice is breaking down and the value of M_c increasing rapidly. The breakpoint region in this curve corresponds to that in the Sakurada plots, i.e., for $\lambda = 0\cdot65$ the Szwarc curve breaks at $v_{2a}^{-5/3} \sim 1\cdot5$ (*Figure 12*) corresponding to $v_{2a} \sim 0\cdot75$, and thus $v_{2a}^2 \sim 0\cdot6$ (*Figure 10*). In more dilute solutions for the same value of λ, both theories give $\chi_1 = 0\cdot55$, again showing good agreement. It should however be noted that the χ_1 values from these treatments will not normally agree with those from the Flory and Maron theories due to the different definitions of volume fraction.

In the region of high concentration of polymer whilst both theories predict with some success the variations of the interaction parameters, they are still incapable of representing adequately the system over the entire concentration range, especially at the period when the more ordered regions in the polymer are dissolving and the concentration is varying in a more complex manner than expected from mere addition of solvent. In a subsequent paper the polyolefin/toluene system will be considered with reference to recent developments in the Maron theory, when it will be shown that the degree of 'order' existing in the polymer at any time during the solution process may be evaluated from a combination of the vapour pressure and dilute solution measurements.

Department of Chemistry,
University of Manchester Institute of
Science and Technology

REFERENCES

1 Szwarc. M., Rogers, C. E., and Stannett, V. *J. Phys. Chem.* 1959, **63**, 1406
2 Sakurada, I., Nakajima, A. and Fujiwara, H. *J. Polym. Sci.* 1959, **35**, 497
3 Flory, P. J., 'Principles of Polymer Chemistry', Cornell University Press, Ithaca, New York, 1953, Chapter 12; *J. Chem. Phys.* 1942, **10**, 51
4 Maron, S. H. *J. Polym. Sci.* 1959, **38**, 329
5 Turner Jones, A. *Makromol. Chem.* 1964, **71**, 1
6 Anderson, I. H., Burnett, G. M. and Tait, P. J. T. *J. Polym. Sci.* 1962, **56**, 391
7 Gee, G. and Orr, W. J. C. *Trans. Far. Soc.* 1946, **42**, 507
8 Prager, S., Bagley, E., and Long, F. A. *J. Amer. Chem. Soc.* 1953, **75**, 2742
9 Nakajima, A., Sakurada, I. and Yamakawa, H. *J. Polym. Sci.* 1959, **35**, 489, 497
10 Antoine, G. *Compt. Rend.* 1888, **107**, 681, 836
11 Dreisbach, R. R., 'Physical Properties of Chemical Compounds', *Advances in Chemistry* Volume 15, Amer. Chem. Soc., 1955
12 Maron, S. H. and Nakajima, N. *J. Polym. Sci.* 1959, **40**, 59
13 Aubrey, D. W., and Barnatt, A. *J. Polym. Sci. (A–2)* 1968, **6**, 241
14 Gee, G. and Treloar, L. R. G. *Trans. Far. Soc.* 1942, **38**, 147
15 Bawn, C. E. H., Freeman, R. F. J. and Kamaliddin, A. R. *Trans. Far. Soc.* 1950, **46**, 677
16 Faucher, J. A. and Reding, F. P. *High Polymers* 1965, **20**, 677 (Eds. R.A.V. Raff and K.W. Doakes), Interscience, New York)
17 Turner Jones, A., ICI Plastics Division, Welwyn Garden City, Herts., private communication April, 1966

P—2A

Determination of macromolecular sizes in solution by light scattering Doppler spectrometry

D. B. Sellen

An apparatus for measuring the Doppler effect in the light scattered by solutions of macromolecules is described. The spectral broadening is measured by means of an optical homodyne technique, the theory of which is discussed together with practical considerations involved in its application. A brief statement of the results of the theory of Doppler broadening is made, and some experimental results are presented for Ludox (an aqueous suspension of silica). The variation in the spectral broadening with angle of scatter is shown to agree with theoretical predictions and a particle diameter of 170 Å (17 nm) deduced.

INTRODUCTION

LIGHT SCATTERING has been used as a method for finding molecular weights and determining size and shape of macromolecules in solution for the past twenty five years. However, experimental difficulties in investigating the frequency shifts in the scattered light relative to the incident beam were insuperable until the advent of the laser, and the first measurements were made on an aqueous suspension of polystyrene spheres by Cummins et al[1] in 1964. Since then several investigations have been reported[2-6]. The theory for Doppler shifts in light scattered by solutions has been investigated in some depth by Pecora[7-9].

The present paper describes an apparatus for making this type of measurement using an optical homodyne technique. The theory of its operation is given and some results for a colloidal dispersion of silica are presented.

Theory of Doppler broadening in light scattered by macromolecular solutions

The Doppler shift in the frequency of light scattered by a particle moving with velocity v is given by

$$\Delta v = vs/\lambda \qquad (1)$$

where s is the difference between unit vectors in the incident and scattered directions and has the magnitude $2 \sin \theta/2$ where θ is the scattering angle relative to the incident beam.

Equation (1) however assumes that the velocity v is maintained over a distance large compared with the wavelength. For a solution of macromolecules the mean free path is short compared with the wavelength due to the presence of the solvent so that this simple concept of a Doppler shift

does not apply. The broadening actually arises from the fact that, due to the random thermal motion of the molecules, the amplitude of light scattered in any given phase decays with time. The amplitude of the scattered light therefore consists of a random series of transients and the resultant spectrum is given by the square of the Fourier transform of these transients.

Consider a given molecule which is small compared with the wavelength at the origin of a spherical polar coordinate system at time $t = 0$. At a subsequent time t the molecule will be at a position r given by the probability function:

$$P(r) = \frac{1}{(2Dt)^{3/2}} \left(\frac{2}{\pi}\right)^{\frac{1}{2}} r^2 \exp \frac{-r^2}{4Dt} \qquad (2)$$

where D is the translational diffusion constant. At time t we may consider the light to be scattered according to the above probability function. The resultant scattered amplitude may be calculated by a process identical with the Rayleigh Gans Debye[10-12] method of finding the particle scattering factor for a large molecule. The amplitude A is given by:

$$A = \frac{1}{(2Dt)^{3/2}} \left(\frac{2}{\pi}\right)^{\frac{1}{2}} \int_0^\infty r^2 \exp \frac{-r^2}{4Dt} < \exp ik\, sr > dr$$

where $k = 2\pi/\lambda$, λ is the wavelength *in the solution*, $< \epsilon\, iksr >$ is the mean value averaged over all directions, and

$$< \exp iksr > = \sin ksr/ksr \qquad (5)$$

$$\text{Thus} \quad A = \exp - K^2 Dt \qquad (6)$$

$$\text{where} \quad K = ks \qquad (7)$$

The scattered light therefore consists of a random succession of exponentially damped oscillations and the spectrum consists of a Lorentzian distribution about the centre frequency:

$$I_\omega = \frac{IK^2 D}{\pi(\omega^2 + K^4 D^2)} \qquad (8)$$

where $I_\omega\, d\omega$ is the intensity of light having angular frequency shifted by an amount between ω and $\omega + d\omega$, and I is the total scattered intensity. A rigorous derivation of equation (8) has been given by Pecora[7].

If the molecules are not small compared with the wavelength then there will be transient changes in scattered amplitude due to rotational diffusion (except in the case of a spherical molecule), and due to random changes in configuration in the case of flexible molecules. These arise from the corresponding fluctuations in particle scattering factor. Only partial broadening occurs, however, as the transients do not decay to zero. These effects have been fully discussed by Pecora[7, 8].

In addition, if the molecules are optically anisotropic whatever their size, partial broadening results from rotational variation in polarizability[1, 9].

Theory of the optical homodyne

The frequency shifts to be measured are of the order of 100 Hz. This is equivalent to wavelength shifts of the order of 10^{-9}Å (10^{-8}nm), so that investigation by conventional spectroscopic methods is impossible and an optical heterodyne or homodyne technique must be used.

As the spectral broadening arises from phase-amplitude modulation of the scattered light, it will, in all cases, be symmetrical about the incident light frequency. Consider the arbitrary symmetrical distribution shown in *Figure 1*.
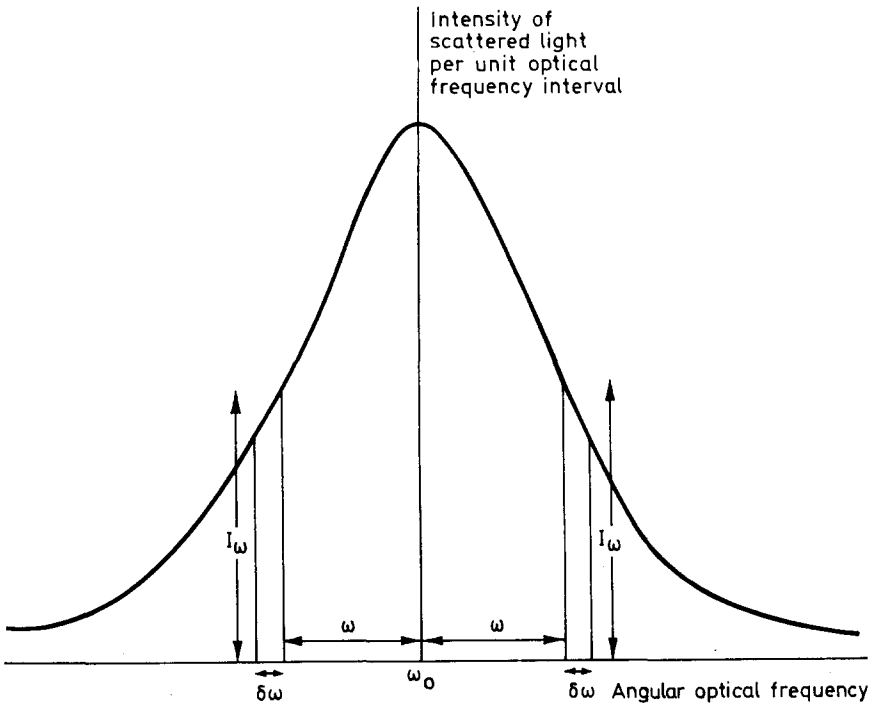
Figure 1 The optical homodyne (see text)

The scattered amplitude resulting from the two elementary areas is

$$2(2I_\omega \delta\omega)^{1/2} \cos \omega_0 t \cos (\omega t + a_\omega t) \qquad (9)$$

where $a_\omega t$ is the phase difference and varies at random with both ω and t. Thus homodyne beats occur between symmetrically displaced components.

From (9) the total scattered light intensity is:

$$[\sum_\omega 2(I_\omega \delta\omega)^{\frac{1}{2}} \cos (\omega t + a_\omega t)]^2 \qquad (10)$$

The summation consists of sum and difference frequencies together with a constant term and may be written:

$$I + \sum_{\omega_n} \sum_{\omega_n} 2(I_n \delta\omega_n I_m \delta\omega_m)^{1/2} \{\cos [(\omega_n - \omega_m)t + a_{nmt}] + \\ +\cos [(\omega_n + \omega_m)t + \beta_{nmt}]\} \qquad (11)$$

376

where I is the total unmodulated light intensity and α_{nmt}, β_{nmt} are randomly varying phases. The mean square signal due to the modulated component will be equal to the square of the overall photosensitivity, c^2, of the detector, times the sum of the squares of the intensity of each frequency component. If we write

$$\omega_n - \omega_m = B \qquad \Omega = (\omega_n + \omega_m)/2 \tag{12}$$

then the mean square signal due to the difference frequencies becomes

$$2c^2 \int_0^\infty dB \int_{\frac{1}{2}B}^\infty I_{\Omega-\frac{1}{2}B} I_{\Omega+\frac{1}{2}B} \, d\Omega \tag{13}$$

Similarly if we write $\qquad \omega_n + \omega_m = B \qquad \Omega = (\omega_n - \omega_m)/2 \tag{14}$

the mean square signal due to the addition frequencies becomes

$$2c^2 \int_0^\infty dB \int_0^{\frac{1}{2}B} I_{\frac{1}{2}B-\Omega} I_{\frac{1}{2}B+\Omega} \, d\Omega \tag{15}$$

and as $\qquad\qquad\qquad I_{\Omega-\frac{1}{2}B} = I_{\frac{1}{2}B-\Omega}$

the total mean square signal $\bar{s}^2$ is

$$\bar{s}^2 = 2c^2 \int_0^\infty dB \int_0^\infty I_{\frac{1}{2}B-\Omega} I_{\frac{1}{2}B+\Omega} \, d\Omega = c^2 I^2/2 \tag{16}$$

where B is the angular beat frequency.

In practice

$$\bar{s}^2 = c^2 \gamma^2 I^2/2 \tag{17}$$

where γ is a coherence factor which will be discussed later. If the signal is analysed with a wave analyser of bandwidth ΔB then the signal s_B within the bandwidth is given by

$$\bar{s}_B{}^2 = 2c^2 \gamma^2 \Delta B \int_0^\infty I_{\frac{1}{4}\frac{1}{2}B-\Omega} I_{\frac{1}{2}B+\Omega} \, d\Omega \tag{18}$$

and

$$\bar{s}^2 = \int_0^\infty \frac{\bar{s}_B{}^2 \, dB}{\Delta B} \tag{19}$$

Thus for the particular case of broadening due to translational diffusion, substitution of equation (8) in equation (18) gives

$$\bar{s}_B{}^2 = \frac{c^2 \gamma^2 \Delta B}{2} \frac{I^2 K^2 D}{\pi(\frac{1}{4}B^2 + K^4 D^2)} \tag{20}$$

It should be noted that (20) may be obtained from (6) directly. The transient intensity is

$$I_t = \exp - 2K^2 Dt \tag{21}$$

and (20) is the square of the Fourier transform of (21). Thus homodyne detection is simply a direct measure of intensity fluctuations.

Practical considerations in the use of an optical homodyne

(a) *Noise.* The beat signal to be analysed consists of a continuous distribution of frequencies and the signal measured is proportional to the square root of the bandwidth in accordance with equation(18). A photoelectric signal however arises from the random emission of photoelectrons from a photocathode and even in the absence of any modulation of the light intensity consists of a continuous distribution of frequencies normally referred to as photoelectric shot noise. This noise is given by s_n where

$$\bar{s}_n^2 = kIeG^2\Delta B \tag{22}$$

e is the charge on the electron, G the overall gain and $k = c/G$, the photocathode sensitivity

From (20) and (22)

$$\frac{\bar{s}_B^2}{\bar{s}_n^2} = \frac{\gamma^2 kI}{2e} \frac{K^2 D}{\pi(\frac{1}{4}B^2 + K^4 D^2)} \tag{23}$$

Thus it is advantageous to have both the photocathode sensitivity and the light intensity as high as possible. Neither the gain nor the bandwidth affect the beat to noise ratio.

The overall measured signal s_T is given by

$$\bar{s}_T^2 = \bar{s}_n^2 + \bar{s}_B^2 \tag{24}$$

so that it is necessary to measure $\bar{s}_n^2$ to find $\bar{s}_B^2$. This may be done by allowing part of the incident beam to fall independently on the same part of the photocathode as the scattered light and attenuating it so that the unmodulated component of the photoelectric signal is the same. The modulated component of this signal is then s_n.

The design of the apparatus could be simplified by using an external unmodulated light source for this purpose (see ref. 4) However, by using part of the incident beam any spurious modulation which it contains will be included in s_n.

(b) *Integration of beat signal.* The tuned signal rectified by the wave analyser constitutes a secondary homodyne system as the beats within the bandwidth beat with each other to produce a system of secondary beats. Thus the output from the wave analyser consists of an unmodulated component equal to the beat signal plus the secondary beats. The ratio of the two components will depend upon the type of rectification employed but will be of the order of unity if the time constant of the output meter is less than the reciprocal of the bandwidth. In order to obtain reasonable precision it is necessary to increase the time constant. If the precision p is defined as the ratio of the rectified beat signal to the secondary beats then

$$p \sim (t\Delta f)^{\frac{1}{2}} \tag{25}$$

where t is the time constant and

$$\Delta B = 2\pi\Delta f \tag{26}$$

(c) *Coherence*. In order to measure frequency shifts with an optical homodyne, it is necessary that at a given instant all the light received by the detector has the same centre frequency. This means that the coherence length of the incident light must be large compared with the dimensions of the illuminated volume, and large compared with optical path differences within the scattered beam. This is readily achieved with a laser without any undue restrictions on the geometry of the apparatus.

However, the illuminated volume is necessarily large compared with the wavelength so that the scattered light is spacially incoherent and complete phase cancellation of the beats occurs unless coherence is restored by stopping down the receiver system. Ideally the resolving power of the receiver should be of the same order as the dimensions of the illuminated volume (see for instance Gabor[13]). Under these conditions different parts of the illuminated volume become indistinguishable. However, although stopping down the receiver increases the coherence factor, γ, it also decreases the light intensity. The design is therefore necessarily a compromise to optimise the beat to noise ratio given by equation(23).

APPARATUS

The apparatus is shown in *Figure 2*. A lightproof box contains the light scattering cell which is of the semi-cylindrical type. The laser beam is focused at the centre of the cell by the lens L_1 where it has a diameter of about 0·1 mm due to the diffraction limitation. The scattered light receiver system containing the prisms P_1, P_2, P_3, rotates about a vertical axis and its position can be read from the circular scale which protrudes through the front of the box below the false bottom. A high density filter moves into the laser beam as the receiver moves into the zero angle position. S_1 is a stop 2 mm high by 4 mm wide giving a resolution of about 0·01 mm at the centre of the cell. S_2 is a vertical slit 4 mm wide. The angular discrimination is therefore $\pm 4°$ and the length of laser beam observed about 4 mm. Thus the dimensions of the illuminated volume of solution are 4 mm long by 0·1 mm high. These are considerably greater than the resolution of the receiver system. The effective length of the beam can be reduced by focusing an image of the centre of the cell on to the photocathode with the lens L_2 and stopping down. The resolution can also be decreased by reducing the size of S_1 but it is found that in both cases the beat-to-noise ratio is made worse. In practice, L_2 is adjusted to give a spot of light of convenient size on the photocathode.

Part of the incident beam is conveyed to the photomultiplier by the prisms P_4, P_5, P_6, and plane pieces of glass G_1 and G_2 (note that G_2 does not rotate with the scattered light receiver system). This reference beam facilitates the possible eventual use of the apparatus as a heterodyne system, but in the present work it has been used solely to determine the photoelectric noise s_n. The beam is made to diverge over the photocathode by the lens L_3 where it is stopped down to the dimensions of the scattered light beam by the rotating stop. Thus both beams illuminate the same part of the photocathode. The intensity of the reference beam is adjusted to match that of the scattered beam
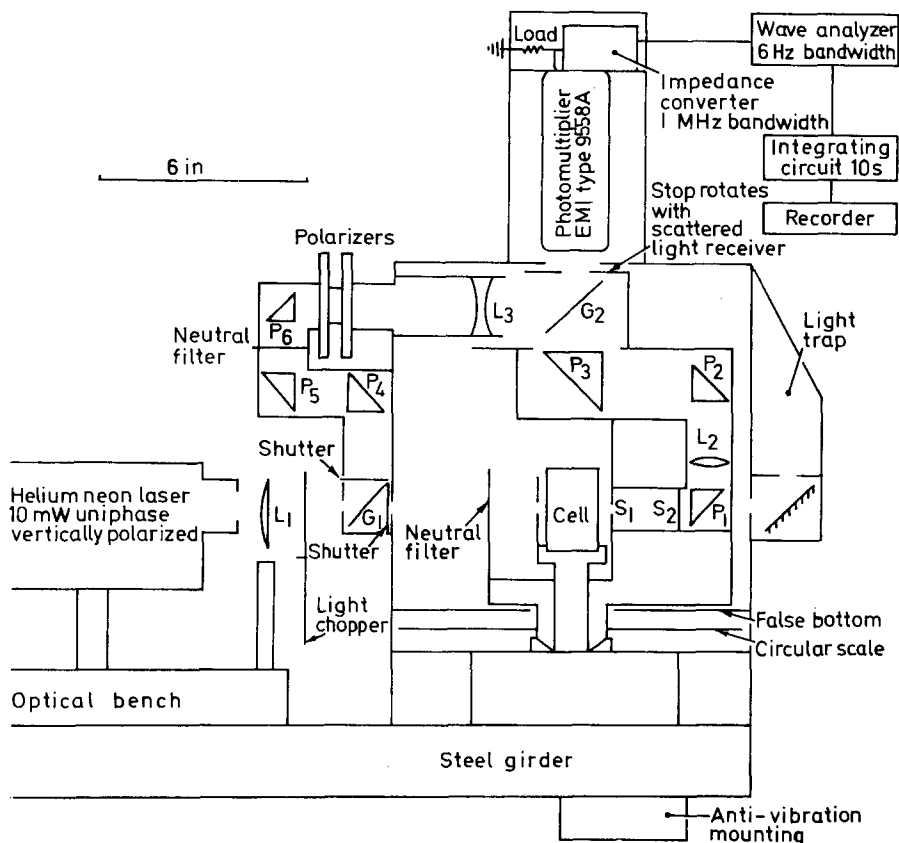
Figure 2 Light scattering Doppler spectrometer for macromolecular solutions

by the neutral filter and two rotatable polarizers. Two shutters are provided so that the beams can be measured independently.

The photoelectric signal passes through the electronic system as shown and is finally recorded for about five minutes on a slow speed pen recorder. A visual average of the signal is then taken to give a precision of about 3 % in accordance with equation(25). As AC electronics are used the signal due to the overall light intensity, i.e. cI is not detected. A light chopper is therefore included as shown which produces a square wave modulation of frequency 200 Hz. The fundamental frequency of this is then measured to give a signal S given by:

$$S = \frac{\sqrt{2}}{\pi} cI \qquad (27)$$

S is made the same for the two beams. The light chopper is then removed from the system and s_T and s_n measured at various frequencies.

380

RESULTS FOR LUDOX*

Ludox is an aqueous dispersion of approximately spherical particles of silica, and is sometimes used for calibrating conventional light scattering apparatus. Although not monodisperse the particle sizes are all small compared with optical wavelengths, and the high particle density results in a large scatter for a small concentration. These properties make Ludox suitable for the present investigation.

As with conventional light scattering measurements it is necessary to remove dust from solutions, but for a somewhat different reason. Dust particles move very slowly and so do not contribute as such to the broadening. However, as they move in and out of the very narrow beam they give rise to transient changes in scattered intensity which results in spasmodic spurious increases in the signal at low frequencies. This is especially troublesome when the coherence factor, γ, is low as is the case here.

A Ludox solution was made up at a concentration of $0 \cdot 5 \%$ and clarified by centrifuging for 1 h at 15000 g and passing through a millipore filter of pore size $1 \cdot 2 \ \mu m$. No dissymmetry of scatter was observed. Beat spectra were obtained for angles of scatter between $40°$ and $105°$. *Figure 3* shows the
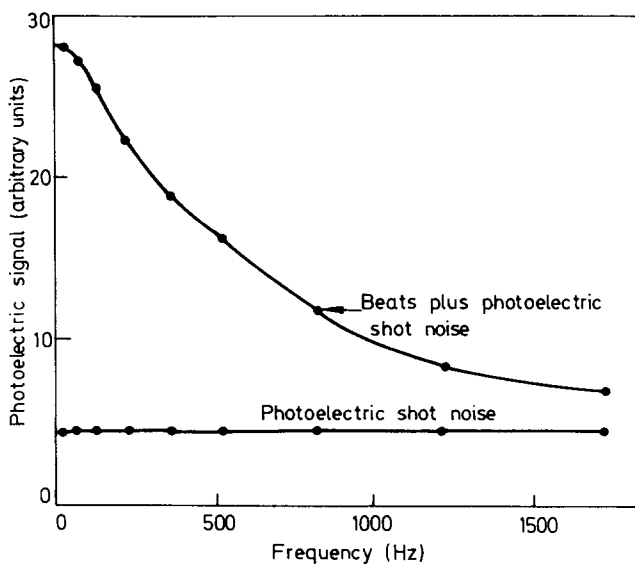
Figure 3 Instrument readings for an aqueous suspension of Ludox: angle of scatter $40°$

signals obtained at $\theta = 40°$ for the scattered light and the reference beam, each having the same intensity. The beat signals were calculated using equation(24).

---

*Du Pont Ltd, Du Pont House, 88 Breams Buildings, London, E.C.4

Equation(20) may be written in the form:

$$\frac{\bar{s}_B{}^2}{\bar{s}_0{}^2} = \frac{1}{(B^2/4K^4D^2) + 1} \tag{28}$$

where s_0 is the value of s_B extrapolated to zero frequency. Thus s_B/s_0 is a function of B/K^2 and therefore of $f/\sin^2\frac{1}{2}\theta$. This applies even when the material is polydisperse. In this case equation(21) is replaced by the summation of terms corresponding to each component but it is still a function of K^2t and therefore the Fourier transform a function of B/K^2. This assumes that the contribution of each component is not a function of angle of scatter, i.e. the molecules are all small compared with the wavelength. It will not apply if the molecules have a strong optical anisotropy but it is otherwise independent of the molecular shape.

Figure 4 shows the relation of s_B/s_0 to $f/\sin^2\frac{1}{2}\theta$ and it can be seen that all the data fall on the same line as expected. The solid line corresponds to that
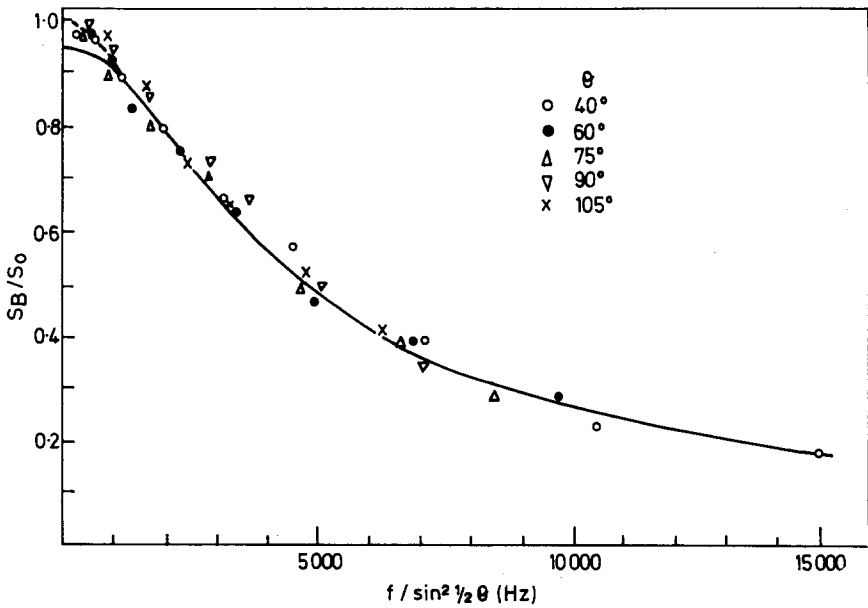
Figure 4 Homodyne beat spectrum for an aqueous suspension of Ludox

expected for molecules having an equivalent hydrodynamic diameter of 170 Å (17 nm). This was found by fitting the best straight line to a plot of $f^2/\sin^4\frac{1}{2}\theta$ against $s_0{}^2/s_B{}^2$. The hydrodynamic diameter, d, is related to the translational diffusion constant by

$$D = \frac{kT}{3\pi\eta d} \tag{29}$$

where k is Boltzmann's constant, T absolute temperature and η the viscosity of water. The deviation of the data at low angles is due to the polydispersity of the material. A sample, clarified by filtration only, gave curves of even more 'pointed' shape due to the presence of larger particles.

It is of interest to assess the performance of the apparatus by calculating γ, the coherence factor. This may be done by finding the total beat signal s^2 given by equation(19), calculating cI with equation(27) and using equation(17) to find γ. However, the range of beat frequencies measured was not wide enough to perform the complete integration in equation(19) empirically. Instead the frequency distribution was assumed to be given by equation (20); γ is then given by

$$\gamma = \frac{s_0}{S} \left(\frac{2 \times \text{half power width}}{\pi \Delta f} \right)^{\frac{1}{2}} \tag{30}$$

Table 1 shows that γ is low (about 1%) as expected and remains approximately constant with angle of scatter. This is also to be expected as the

Table 1 Coherence factor γ, as a
function of the angle of scatter θ

θ	γ
40°	0·0122
60°	0·0113
75°	0·0116
90°	0·0108
105°	0·0115

dimensions of the scattering volume remain approximately constant when projected perpendicular to the line of observation.

DISCUSSION AND CONCLUSION

The apparatus as it stands enables translational diffusion constants of macromolecules, which are small compared with optical wavelengths, to be determined with fair precision. This should be particularly useful for the study of such macromolecules as globular proteins which are generally thought to be monodisperse. The presence of aggregates should be readily detectable from the shapes of the beat frequency distributions at low frequencies and it should therefore be possible to obtain reliable data for the unaggregated molecules.

More sophisticated measurements such as rotational diffusion constants, optical anisotropy and distributions of relaxation times for flexible polymers will, however, require considerable improvements, particularly when all the spectral broadening effects are present simultaneously. The two major shortcomings of the apparatus are the low coherence factor and the spurious effects due to the movement of dust particles at the edges of the beam. It should be possible to improve the dust situation by using a signal limitation

technique. Also it may be preferable in some cases to increase the coherence factor at the expense of a slightly worse beat-to-noise ratio. The ultimate solution to both problems, however, is to increase the coherence factor by two orders of magnitude. This will only be made possible by a considerable increase in the scattered light intensity, so that very small stops may be used in the receiver system whilst still retaining a reasonable beat to noise ratio. The argon-ion lasers available at present give 700 mW at 4880 Å (488 nm) so that compared with the 10 mW at 6328 Å used here some two hundred times more scattered light should be available. Argon-ion lasers do not have such a large coherence length and are subject to low frequency instabilities[14], but as laser technology progresses high precision measurements should become possible.

In conclusion it may be said that the technique of light scattering Doppler spectrometry should be a useful tool for measuring translational diffusion constants of macromolecules which are small compared with optical wavelengths. With advances in laser technology it should be possible to extend the technique to rotational diffusion, optical anisotropy and distributions of relaxation times for flexible polymers.

ACKNOWLEDGEMENT

Astbury Department of Biophysics,
University of Leeds

REFERENCES

1 Cummins, H. Z., Knable, N., Yeh, Y. *Phys. Rev. Letters* 1964, **12**, 150
2 Dubin, S. B., Lunacek, J. H., Benedek, G. B. *Proc. Nat. Acad. Sci. US* 1967, **57**, 1164
3 Arecchi, F. T., Giglio, M., Tartari, U. *Phys. Rev.* 1967, **163**, 186
4 Cummins, H. Z., Carlson, F. D., Herbert, T. J., Woods, G. *Biophysical J.* 1969, **9**, 518
5 Ford, N. C., Lee, W., Karasz, F. C. *J. Chem. Phys.* 1969, **50**, 3098
6 Wada, A., Suda, N., Tsuda, T., Sada, K. *J. Chem. Phys.* 1969, **50**, 31
7 Pecora, R. *J. Chem. Phys.* 1964, **40**, 1604
8 Pecora, R. *J. Chem. Phys.* 1965, **43**, 1562
9 Pecora, R. *J. Chem. Phys.* 1968, **49**, 1036
10 Lord Rayleigh *Phil. Mag.* 1881, **12**, 81
11 Gans, R. *Ann. Physik* 1925, **76**, 29
12 Debye, P. *Ann. Physik* 1915, **46**, 809
13 Gabor, D. *Proc. Roy. Soc. (A)* 1949, **197**, 454
14 Jackson, D. A., Paul, D. M. *J. Sci. Instr. (Ser. 2)* 1969, **2**, 1077

Note to the Editor

Polymers from aromatic nitriles and diaminopyridine

D. I. PACKHAM and J. C. HAYDON

In an earlier publication we described the preparation and properties of a new class of polymers the macrocyclic polymers[1] obtained by the condensation of suitable tetranitriles with appropriate diamines. Some differences in the rates of reaction of the various diamines were observed. In particular the rate of reaction of pyromellitonitrile with 2,6-diaminopyridine was considerably slower than its reaction with *m*- or *p*-phenylene diamine or 4,4'-diaminodiphenyl ether. A closer examination of the condensation of 2,6-diaminopyridine with phthalonitrile and with pyromellitonitrile has revealed the existence of other macrocyclic structures and linear polymeric products.

Condensation of phthalonitrile with 2,6-diaminopyridine

The reaction of di-imino*iso*indoline with diamines, including 2,6-diaminopyridine, to give macrocyclic compounds was described by Elvidge and Linstead[2]. They suggested that where the diamines were sterically unfavourable for ring closure, linear polymeric products would result (*Reaction scheme 1*).

Reaction scheme 1

385
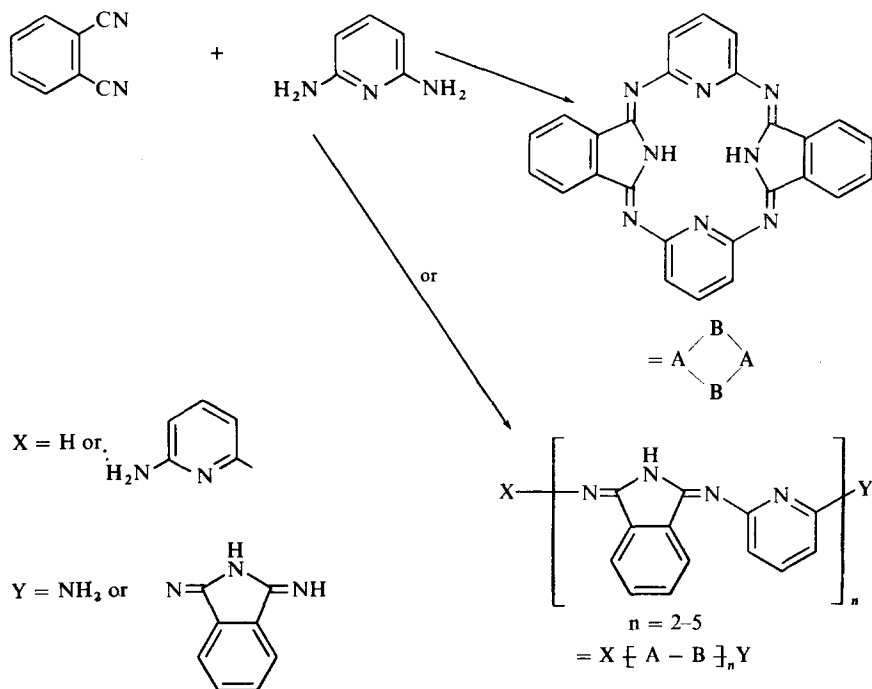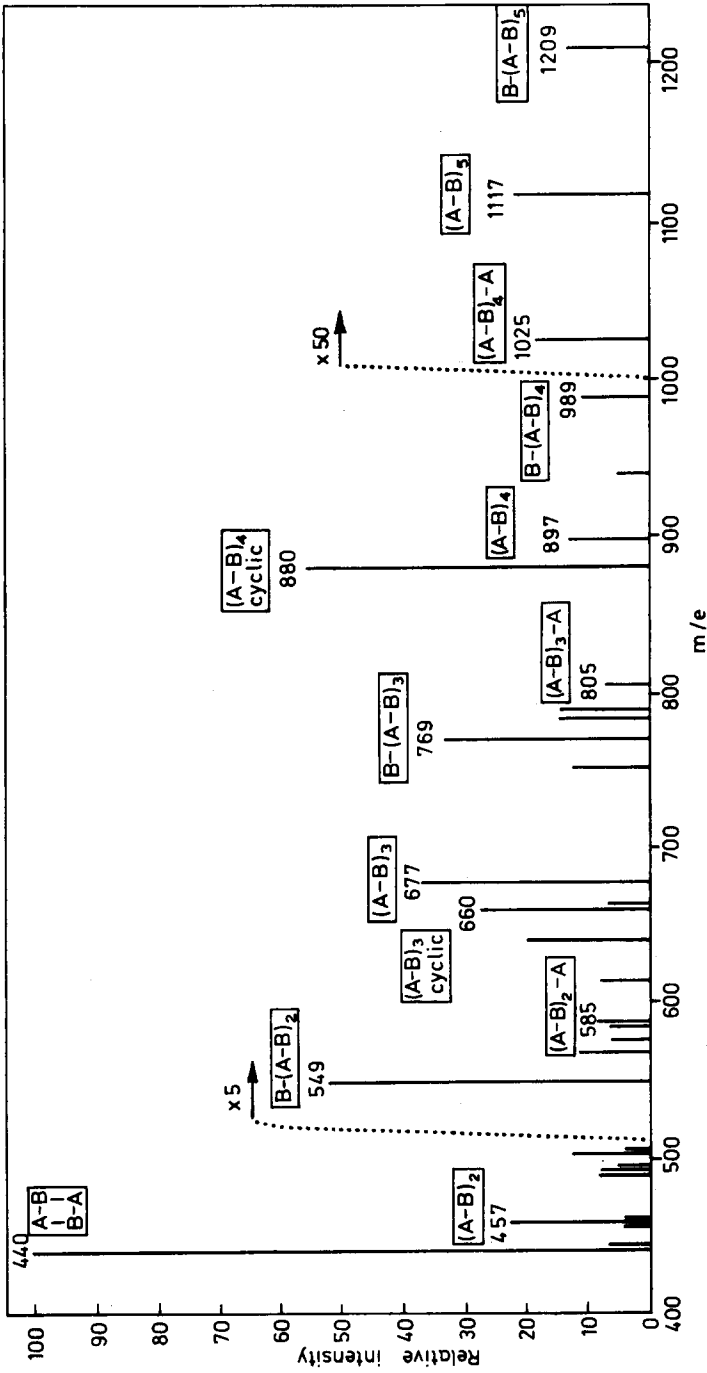
Figure 1 Mass spectral analysis of the products from the condensation of phthalonitrile with 2,6-diaminopyridine

Our experiments have shown that macrocyclic compounds can be obtained in good yield ($>90\%$) by the condensation of *m*- or *p*-phenylene diamine or 4,4'-diaminodiphenyl ether with phthalonitrile in 2-methoxyethanol or *n*-butanol containing sodium alkoxide as catalyst. Under the same conditions a much poorer yield of macrocyclic compound (*ca* 60%) was isolated from the reaction of 2,6-diaminopyridine with phthalonitrile. Examination of the other products from this reaction, by mass spectrographic analysis (m.s.a.) gave the results shown in *Figure 1*. The components of the mixture are conveniently represented by the combination of di-imino*iso*indolyl units (A) and the 2,6-disubstituted pyridine nucleus (B), thus the macrocyclic units are denoted (A—B)$_2$ cyclic, (A—B)^7 cyclic etc., and the linear products (A—B)$_n$, B—(A—B)$_n$, (A—B)$_n$B etc. The principal component of this fraction, representing a further 20% of the total products, was the simplest macrocyclic compound (A—B)$_2$ cyclic. The other products that were evident range from the linear open chain (A—B)$_2$ to the linear oligomer B(A—B)$_5$ of molecular weight 1209. Whilst products with even higher molecular weights may be formed they were not identified by our procedure.

Condensation of pyromellitonitrile with 2,6-diaminopyridine

The condensation of pyromellitonitrile with 2,6-diaminopyridine in 2-methoxyethanol containing sodium 2-methoxyethanolate afforded polymeric products in high yields. Condensation of the two components in equimolar ratio gave polymers where the structure should be analogous to the poly-[benzo*bis*(aminoiminopyrrolenines)] previously reported[3]. The reaction of diaminopyridine with pyromellitonitrile in a 2:1 molar ratio appeared to be very slow. During 5 days reaction only 50% of the calculated quantity of ammonia was evolved. Although a polymeric product was obtained in nearly theoretical yield its structure must consist of both macrocyclic and open chain units. The precise structure would be difficult to determine, but judged by the ammonia evolved in the reaction, the polymer should contain approximately 50% macrocyclic units. Increased reaction temperature, using *n*-butoxyethanol as solvent, had little effect on the extent or rate of the reaction. In view of the difficulties previously reported[1] when alcohols of high boiling point ($>180°C$) were used, we restricted our study to the use of 2-methoxyethanol or *n*-butanol as solvents.

Metal derivatives

Our interest in polymers of these types containing the pyridine nucleus has been in their capacities to combine with metal ions. Both the linear polymers and the macrocyclic type polymers were found to react with copper and nickel in solution. It was established that products containing almost the theoretical quantity of nickel could be obtained by treatment of the polymers with a solution of nickel acetate in pyridine. Similar products were prepared containing copper. Other metal derivatives should likewise be possible.

The electrical conductivity of the macrocyclic polymers and the poly-[benzo*bis*(aminoiminopyrrolenines)] has been reported[4]. As expected the

introduction of the metal ion into the polymer had a pronounced effect on the electrical conductivity of these materials. In particular the linear polymer containing nickel showed a drop in resistivity to approximately $10^8\Omega$ m (ref. 5).

The thermal and oxidative stabilities of the polymers in nitrogen and air were measured in the usual manner with du Pont thermogravimetric analysis equipment. The introduction of the metal ion into the polymer made little difference to the thermal stability of the products.

EXPERIMENTAL

Phthalonitrile and 2,6-diaminopyridine

A solution of phthalonitrile (5·4 g) and 2,6-diaminopyridine (4·6 g) in *n*-butanol (40 ml) containing sodium butoxide catalyst (0·1 g) was refluxed with stirring in a stream of nitrogen for 18 h. During this period ammonia (30 mequiv.) was evolved. The mixture was filtered hot to yield a light brown solid (2·3 g): a further quantity of the product (4·24 g) was obtained from the mother liquors. The total yield of impure macrocyclic compound was 65%. The product was recrystallized from nitrobenzene.

Analysis: found, N, 24·8%; calculated for $C_{26}H_{16}N_8$, N, 25·4%. M.S.A.: found, m/e 440·148; calculated for $C_{26}H_{16}N_8$, m/e 440·150. Mass spectral analysis of the residue gave the spectrum shown in *Figure 1*.

Pyromellitonitrile and 2,6-diaminopyridine

A solution of pyromellitonitrile (12·24 g, 0·08 mole) and 2,6-diamino-pyridine (17·44 g, 0·16 mole) in 2-methoxyethanol (300 ml) containing sodium methoxyethanolate (0·1 g) as catalyst was refluxed with stirring in a stream of nitrogen for 4 days. The ammonia evolved (90 mequiv.) was titrated with standard acid. The insoluble product was filtered off and extracted with 2-methoxyethanol, methanol and then dried to give a brown polymer (30·64 g, 96·5%).

Analysis: found, N, 28·6%; calculated, N, 30·9%. The infra-red spectrum was consistent with the proposed structure. A polymeric product was obtained in a similar manner from the condensation of pyromellitonitrile and 2,6-diaminopyridine in equimolar ratio.

Metal derivatives

A sample of polymer (6·5 g) prepared as described above was refluxed with stirring for 3 h with a solution of nickel acetate (8·65 g) in pyridine (80 ml). The mixture was filtered hot. The procedure was repeated and the insoluble product extracted with pyridine and then methanol and dried. The product contained nickel, 11·9% (Calculated for $C_{20}H_8N_8Ni)_n$, Ni, 14·1%.)

ACKNOWLEDGEMENTS

Division of Molecular Science,
National Physical Laboratory,
Teddington, Middlesex, UK

REFERENCES

1 Packham, D. I. and Rackley, F. A. *Chem. and Ind.* 1967, p 1254 *Polymer, Lond.* 1969, **10**, 559
2 Elvidge, J. A. and Linstead, R. P. *J. Chem. Soc.* 1952, p 5008
3 Packham, D. I. and Rackley, F. A. *Chem. and Ind.* 1967, p 1566
4 Graham, J. and Packham, D. I. *Polymer, Lond.* 1969, **10**, 645
5 Graham, J., personal communication

Book Reviews

Advances in polymer science (Volume 6)

Springer-Verlag, Berlin, 1969, 574 pp, DM 172

This volume raises some important questions. Is it a *book* or a *journal*? We are accustomed to the unbound periodical *Fortschritte* appearing regularly in our libraries as a reputable review journal, but how far will this custom of binding a whole year's output spread? Will we soon see journals like *Polymer* for sale or review? Do authors know they may be submitting manuscripts for a book? Let me be candid. No private individual (unless much more wealthy than this reviewer) will pay £17 for a very mixed bag of topics. Publishers justify the practice by claiming that certain libraries prefer to buy selected journal issues fully bound, rather than to collect the whole series of regular unbound periodicals. This may be so; then only such libraries need pay much attention to the remainder of this review.

This volume is supposed to contain twelve reviews. In fact one (pp 401–420) is missing. Two are in German. Four (counting the missing article) are based on papers presented to the first Kyoto Polymer Seminar in 1967. The length, standard and orientation of the articles all vary enormously.

Three articles are very detailed and particularly impressive. Dušek and Prins present a review of structure and elasticity of non-crystalline networks which explains practically every aspect of modern theory from elementary concepts of rubber elasticity to consequences of structuring in networks. Equally comprehensive is the article by Janeschitz-Kriegl on flow birefringence of elastico-viscous systems. This review works from theory to experimental techniques, and covers in passing just about every aspect of the hydrodynamic behaviour of polymer molecules. Phenomenological theories, molecular theories, 'stiff' chains, 'flexible' chains, all are covered. Equally comprehensive is the coverage of solution properties of oligomers (Sotobayashi and Springer in German).

Two short reviews seem particularly timely. An article by Hendra on laser-Raman spectra of polymers sets the field for what, in the opinion of the reviewer, is about to become a growth area in polymer analysis. Tobolsky and Du Pre present their torsional oscillator model for dynamic behaviour of molecules. This approach has not yet been taken up by workers in polymer dynamics, but does suggest a way in which some of the conceptual difficulties inherent in Gaussian ball and spring models of a polymer chain might be overcome.

The review articles mentioned above are physico-theoretical in orientation, and together do form a useful source book. The remaining articles concentrate more on kinetics and mechanisms. Coordinated ionic polymerization is with us again with molecular orbital theory lending respectability to the complexes (real and imaginary). An article on photo-sensitized charge transfer polymerization turns out to be mainly Japanese work on N-vinyl carbazole and, after a non-polymer introduction, never mentions dye-sensitized or bio-synthetic polymerizations at all. Polymerization in an electric field covers ionic polymerization but not electro-initiation which is dealt with in a separate article (kinetic schemes abound here). Once again we are reminded what radio-tracers can do to speculative reaction mechanisms. All good symposium material, pleasant reading, and a guide to what is going on in the world. But not a £17 text book.

Almost nobody will read all this book. Persons like this reviewer whose theoretical background is weak or rusty will turn to certain articles for reference. Workers who have not been to a general conference for two years will read and appreciate the less mathematical reviews. But why didn't the editors select the best third and give us a cheaper book that I could recommend?

A. M. NORTH

Inorganic macromolecules reviews (*Volume 1, Number 1*)

(Editors: E. G. R. GIMBLETT and K. A. HODD) Elsevier, 1970 88pp,
Annual subscription $25

The editors state that the purpose of this new quarterly journal is to provide review articles covering all aspects of the science and technology of inorganic molecules. The articles in this first issue are in fact some of the plenary lectures given at the international symposium on Inorganic Polymers in London in 1969. In an admittedly speculative introductory lecture, L. Holliday emphasizes the need for polymer structures intermediate between the naturally-occurring condensed inorganic networks and the present synthetic polymers. Margot Becke-Goehring reviews the chemistry of the nitrogen-sulphur compounds, and indicates the potential value of these ring systems for the synthesis of melamine-type polymers. The synthesis, structures and physical properties of poly-elemento-organo-siloxanes are ably reviewed by K. A. Andrianov, and H. A. Schroeder's article on the polymer chemistry of boron cluster compounds (especially the icosahedral carboranes) opens up interesting possibilities for a group of compounds whose unusual structure and properties have so far found little practical application. The final review by A. Eisenberg discusses the viscoelastic properties of a range of inorganic polymers, with special reference to the phenomenon of bond interchange in the softening region.

The diversity of these reviews indicates very well the nature of the essential problem in inorganic polymer chemistry. At one end of the scale, the desirable properties of potential inorganic polymers are reasonably well defined in terms of thermal stability, flexibility and so on; at the other end, there is an enormous variety of monomers which *might* polymerize to produce the desired properties. It is in the intermediate region – the control of structure and its relationship to the desired properties – where the greatest problems remain to be solved. It is to be hoped that the justification for yet another polymer journal may be found in the help which it might give in the attack on these problems.

A. K. HOLLIDAY

Characterization and analysis of polymers by gas chromatography

by M. P. STEVENS
Marcel Dekker, New York and London, 1969, 198 pp, $12·75, £6·10

The idea of producing a book with the above title is one that has considerable merit. Unfortunately, however, the volume under review amounts to little more than a competent but uncritical survey of the published literature. It is well known, of course, that publications in primary journals are often some way behind current practice and this is especially true in the industrial polymer field where the progress in analysis has been very rapid in recent years. As a result, there are in this book, a number of conspicuous omissions which are no fault of the author as a reviewer of the literature but someone more conversant with the activities of analysts in industrial laboratories would not have let them pass without comment; for example, apart from passing mention of a few pyrograms, there is no reference to the use of gas chromatography in fluorocarbon chemistry!

The Introduction makes an unfortunate start to the book. The first paragraph suggests that gas chromatography has been useful for problems which '. . . would otherwise require analytical techniques that are long and tedious. . . .' In my experience, the polymer chemist without gas chromatography would have been unaware of many of his present problems and, of those he had, some would have been insoluble! Furthermore, the next paragraph begins 'Because the full potential of gas chromatography may not be obvious to many workers in the chemical industry, particularly those in the polymer field, a few introductory remarks about this technique are in order'. While some brief introductory remarks about the nature of gas chromatography are to be expected in a book of this kind, to have such a reason for giving them in 1969 is surely naive.

391

The book begins with the analysis of volatile materials in polymers, mainly monomers and residual solvents. There is no mention whatever of the determination of traces of water, a very important problem which is often being dealt with by gas chromatographic methods. While it is right to record the sporadic efforts that are made to determine anti-oxidants, antistatic agents and plasticizers by gas chromatography, the reader ought to be told quite firmly that there are much better methods which use other techniques; because methods are reported in the literature it does not necessarily imply that they are useful in real life situations. Characterization of polymers by chemical degradation followed by gas chromatographic examination of the degradation products is then dealt with briefly but the major part of the book is devoted to characterization by thermal degradation, i.e. pyrolysis-gas chromatography. The factually correct record here does not highlight the pioneers of this technique; for example, I would like to have seen more credit given to Professor Robb's school at Birmingham. The Curie-point method is dismissed in two and a half lines, hardly in keeping with the interest in it during the last few years. Also, I would have liked to see a little more emphasis placed on the possibilities of stepwise pyrolysis. Finally, the author discusses the purity of monomers; nothing here about ethylene or propylene.

In the book as a whole there are other surprising omissions which should have been dealt with. Thus, nothing at all about on-line gas chromatography, which has been of importance in the polymer industry for many years. Four lines in the Introduction grudgingly admit that 'Spectroscopic methods are available for the characterization of certain polymers' so that the reader is left in ignorance of the fact that infra-red spectro-photometry is the major technique for the characterization of polymeric materials with pyrolysis-gas chromatography playing a minor but important complementary role. No emphasis is placed on the use of combinations of analytical techniques which are such an important feature of our diagnostic work in organic chemistry today and which are especially important for the polymer chemists; here I mean combinations of gas chro-matography (with preliminary pyrolysis where required) with mass spectrometry, infra-red spectroscopy or nuclear magnetic resonance spectroscopy. I have indicated the many omissions in this book because to me the title implies the promise of more than is given. It is not a book which I can recommend unreservedly to my colleagues in the polymer industry.

A. G. JONES

Conference Announcement

Structural aspects common to synthetic and biological macromolecules

Queen Elizabeth College, London

25 September 1970

This is a one day meeting of the British Biophysical Society and the British Polymer Physics Group. The meeting will be concerned with the general properties of filiform molecules, with experimental methods of investigation and with details of specific materials which demonstrate interesting behaviour. Short contributions are invited.

Offers of papers, together with a brief statement of the field of interest of the work, should be sent to either Dr B. R. Jennings of Queen Elizabeth College or Professor A. Keller of Bristol University.

Inorganic macromolecules reviews (Volume 1, Number 1)

(Editors: E. G. R. GIMBLETT and K. A. HODD) Elsevier, 1970 88pp,
Annual subscription $25

The editors state that the purpose of this new quarterly journal is to provide review articles covering all aspects of the science and technology of inorganic molecules. The articles in this first issue are in fact some of the plenary lectures given at the international symposium on Inorganic Polymers in London in 1969. In an admittedly speculative introductory lecture, L. Holliday emphasizes the need for polymer structures intermediate between the naturally-occurring condensed inorganic networks and the present synthetic polymers. Margot Becke-Goehring reviews the chemistry of the nitrogen-sulphur compounds, and indicates the potential value of these ring systems for the synthesis of melamine-type polymers. The synthesis, structures and physical properties of poly-elemento-organo-siloxanes are ably reviewed by K. A. Andrianov, and H. A. Schroeder's article on the polymer chemistry of boron cluster compounds (especially the icosahedral carboranes) opens up interesting possibilities for a group of compounds whose unusual structure and properties have so far found little practical application. The final review by A. Eisenberg discusses the viscoelastic properties of a range of inorganic polymers, with special reference to the phenomenon of bond interchange in the softening region.

The diversity of these reviews indicates very well the nature of the essential problem in inorganic polymer chemistry. At one end of the scale, the desirable properties of potential inorganic polymers are reasonably well defined in terms of thermal stability, flexibility and so on; at the other end, there is an enormous variety of monomers which *might* polymerize to produce the desired properties. It is in the intermediate region – the control of structure and its relationship to the desired properties – where the greatest problems remain to be solved. It is to be hoped that the justification for yet another polymer journal may be found in the help which it might give in the attack on these problems.

A. K. HOLLIDAY

Characterization and analysis of polymers by gas chromatography

by M. P. STEVENS
Marcel Dekker, New York and London, 1969, 198 pp, $12·75, £6·10

The idea of producing a book with the above title is one that has considerable merit. Unfortunately, however, the volume under review amounts to little more than a competent but uncritical survey of the published literature. It is well known, of course, that publications in primary journals are often some way behind current practice and this is especially true in the industrial polymer field where the progress in analysis has been very rapid in recent years. As a result, there are in this book, a number of conspicuous omissions which are no fault of the author as a reviewer of the literature but someone more conversant with the activities of analysts in industrial laboratories would not have let them pass without comment; for example, apart from passing mention of a few pyrograms, there is no reference to the use of gas chromatography in fluorocarbon chemistry!

The Introduction makes an unfortunate start to the book. The first paragraph suggests that gas chromatography has been useful for problems which '. . . would otherwise require analytical techniques that are long and tedious. . . .' In my experience, the polymer chemist without gas chromatography would have been unaware of many of his present problems and, of those he had, some would have been insoluble! Furthermore, the next paragraph begins 'Because the full potential of gas chromatography may not be obvious to many workers in the chemical industry, particularly those in the polymer field, a few introductory remarks about this technique are in order'. While some brief introductory remarks about the nature of gas chromatography are to be expected in a book of this kind, to have such a reason for giving them in 1969 is surely naive.

The book begins with the analysis of volatile materials in polymers, mainly monomers and residual solvents. There is no mention whatever of the determination of traces of water, a very important problem which is often being dealt with by gas chromatographic methods. While it is right to record the sporadic efforts that are made to determine anti-oxidants, antistatic agents and plasticizers by gas chromatography, the reader ought to be told quite firmly that there are much better methods which use other techniques; because methods are reported in the literature it does not necessarily imply that they are useful in real life situations. Characterization of polymers by chemical degradation followed by gas chromatographic examination of the degradation products is then dealt with briefly but the major part of the book is devoted to characterization by thermal degradation, i.e. pyrolysis-gas chromatography. The factually correct record here does not highlight the pioneers of this technique; for example, I would like to have seen more credit given to Professor Robb's school at Birmingham. The Curie-point method is dismissed in two and a half lines, hardly in keeping with the interest in it during the last few years. Also, I would have liked to see a little more emphasis placed on the possibilities of stepwise pyrolysis. Finally, the author discusses the purity of monomers; nothing here about ethylene or propylene.

In the book as a whole there are other surprising omissions which should have been dealt with. Thus, nothing at all about on-line gas chromatography, which has been of importance in the polymer industry for many years. Four lines in the Introduction grudgingly admit that 'Spectroscopic methods are available for the characterization of certain polymers' so that the reader is left in ignorance of the fact that infra-red spectro-photometry is the major technique for the characterization of polymeric materials with pyrolysis-gas chromatography playing a minor but important complementary role. No emphasis is placed on the use of combinations of analytical techniques which are such an important feature of our diagnostic work in organic chemistry today and which are especially important for the polymer chemists; here I mean combinations of gas chro-matography (with preliminary pyrolysis where required) with mass spectrometry, infra-red spectroscopy or nuclear magnetic resonance spectroscopy. I have indicated the many omissions in this book because to me the title implies the promise of more than is given. It is not a book which I can recommend unreservedly to my colleagues in the polymer industry.

A. G. JONES

Conference Announcement

Structural aspects common to synthetic and biological macromolecules

Queen Elizabeth College, London

25 September 1970

This is a one day meeting of the British Biophysical Society and the British Polymer Physics Group. The meeting will be concerned with the general properties of filiform molecules, with experimental methods of investigation and with details of specific materials which demonstrate interesting behaviour. Short contributions are invited.

Offers of papers, together with a brief statement of the field of interest of the work, should be sent to either Dr B. R. Jennings of Queen Elizabeth College or Professor A. Keller of Bristol University.

Synthesis of branched polystyrene

W. A. J. BRYCE, G. McGIBBON* and I. G. MELDRUM†

A new experimental technique for anionic polymerization has been devised and successfully used for the investigation of the coupling reaction between living polystyryl anions and 1,3,5-trichloromethyl benzene. This reaction was complicated by a dimerization reaction involving living polymer molecules.

INTRODUCTION

THE TECHNIQUES of anionic polymerization first introduced by Swarc[1] are now well established, and such techniques have since been employed in the preparation of regularly branched polymers of predetermined molecular weight and molecular weight distribution. By coupling living polymers with suitable low molecular weight compounds, trifunctional[2-4] and tetrafunctional[2,4,5] star branched polymers have been prepared and the coupling reaction has also been used to prepare polymers having six[6] or more[7] branches. The use of such model polymers allows careful investigation of the effect of branching on dilute solution behaviour[2,3], mechanical and flow properties of polymers[8,9].

This report describes a novel technique for the preparation of living polymers, and the method is adopted in preparing trichain star polystyrene by reaction of living polystyryl anions with 1,3,5-trichloromethyl benzene. The dilute solution properties of these polymers have been investigated, and will be described in later publications.

EXPERIMENTAL

Materials

Since the successful production of monodisperse polymers by anionic techniques requires careful elimination of impurities, rigorous precautions were taken to remove impurities from all solvents and monomers.

(a) *Solvent*. Tetrahydrofuran, (THF), was used as polymerization solvent throughout the investigation. Reagent grade THF was treated with potassium hydroxide pellets to remove inhibitors and distilled from sodium wire in an atmosphere of nitrogen. The solvent was then outgassed under vacuum and dried over a sodium film. Distillation onto a fresh sodium film, and the addition of a small amount of α-methyl styrene resulted in the formation of α-methyl styryl sodium, the red colour of which served as an indication of the

---

*Present address: Arthur D. Little Research Institute, Inveresk, nr. Musselburgh, Midlothian
†Present address: BP Research Centre, Chertsey Road, Sunbury-on-Thames, Middlesex

absence of reactive impurities. THF was distilled from this solution as required.

(b) *Monomer.* Styrene, washed with 10% sodium hydroxide solution to remove inhibitors, was partially dried over calcium chloride and distilled under reduced pressure. A centre fraction was stored over calcium hydride under vacuum. Further reduction of reactive impurities was achieved by storing the monomer, under vacuum, over the reactive anion mono-sodium benzophenone, which does not polymerize styrene[10], but should be reactive enough to reduce the water content further. Mono-sodium benzophenone is sufficiently soluble in styrene to give a pale green colour, which serves as an indication of the absence of reactive impurities. Styrene was distilled from this solution as required.

(c) *Catalysts.* Benzyl sodium and cumyl potassium have been shown to be efficient anionic polymerisation initiators[11], and both were used in this work.

Benzyl sodium was prepared by allowing a solution of dibenzyl mercury in THF to react for 3 h with a sodium film. The problem of isomerisation[11] was overcome by addition of a small quantity of α-methyl styrene.

A THF solution of cumyl potassium, prepared by reaction of cumyl ethyl ether with a potassium film was used as a polymerization initiator in the early stages of this work. Although it has been claimed[12] that quantitative yields of cumyl potassium can be prepared by this method, it was found by titration with palmitic acid that yields greater than 80% were never obtained, even in the presence of a large excess of potassium. In some cases, the yield was as low as 50%, despite the rigorous precautions taken to remove impurities. Thin layer chromatography, on a 'killed' catalyst sample showed the presence of unreacted cumyl ethyl ether. In later work, a commercial sample in heptane suspension, supplied by K. and K. Laboratories, Inc., was used.

Catalyst solutions were filtered under vacuum into glass ampoules which were stored under liquid nitrogen until required. The catalyst solutions were standardized against known weights of palmitic acid.

(d) *Coupling Compounds.* The low molecular weight materials used for coupling the living polystyryl anions to form trichain polystyrene were 1,3,5-tribromomethyl benzene and 1,3,5-trichloromethyl benzene. Their preparations are described below.

(1) *1,3,5-tribromomethyl benzene.* Mesitylene was brominated with dibromodimethyl hydantoin[13] using carbon tetrachloride as solvent, and benzoyl peroxide as catalyst. Recrystallization of the product from petroleum ether gave pale yellow needles, m.p. 98°C (lit. 97–99°C[14]) and bromine content 69% (calc. 67%).

(2) *1,3,5-trichloromethyl benzene.* As far as is known, the preparation of this compound has not previously been reported and is described here in some detail.

Mesitylene, (30 g), was refluxed with 1,3-dichloro-5,5-dimethyl hydantoin (74 g) and benzoyl peroxide (0·5 g) in carbon tetrachloride (500 ml) for

110h. The mixture was filtered hot to remove the insoluble dimethyl hydantoin and removal of the solvent left a yellow oil and a white solid, which proved to be unreacted dichlorodimethyl hydantoin.

The yellow oil was split into six fractions by vacuum distillation, and n.m.r. spectra showed the fifth fraction, boiling at 127°C, to be nearest the spectrum expected for 1,3,5-trichloromethyl benzene. After a further vacuum distillation, the oil crystallized slowly on standing, and the solid product was twice recrystallized from ethanol and petroleum ether, to give white needles, m.p. 57°C. The chlorine content, 46%, agreed well with the calculated values of 47·6%.

The n.m.r. spectrum of 1,3,5-trichloromethyl benzene is shown in *Figure 1*.
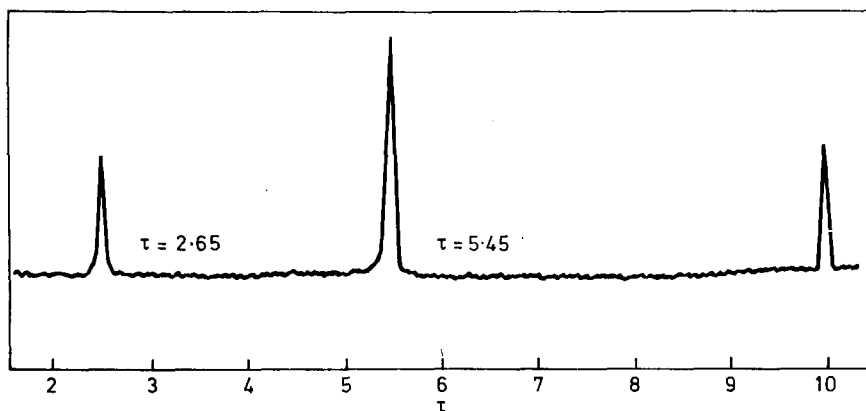
Figure 1 N.M.R. spectrum of 1,3,5-trichloromethyl benzene

Techniques associated with anion solutions

All work involving anion solutions, i.e. solvent and monomer purification, catalyst preparation and monomer polymerization, was carried out under high vacuum. Break-seals were used rather than stop-cocks, and fragile glass bulbs were found to be particularly useful for introducing small quantities of materials.

(a) *Polymerization apparatus.* A problem often encountered in anionic polymerization is that truly monodisperse polymers are not always obtained because of inefficient mixing of monomer and catalyst. This problem of mixing is not completely overcome by dropwise addition of monomer to the catalyst solution[15], and monomer distillation techniques have the disadvantage that local condensation of monomer may occur on the walls of the reaction vessel[16]. The distillation technique of Cowie, Worsfold and Bywater[17] overcomes the problem of local condensation of monomer by incorporating a heating element, but this apparatus is not particularly suitable for manipulation of solutions.

A satisfactory technique which has been devised to overcome these problems involved condensation of both solvent, from the initiator solution, and

monomer, from an ampoule, onto a cold finger, so that a dilute monomer solution was slowly added to the initiator solution.

The polymerization vessel, which is constructed from a 500ml flask, is shown in *Figure 2*. Stirring is effected by a conventional glass stirrer in the
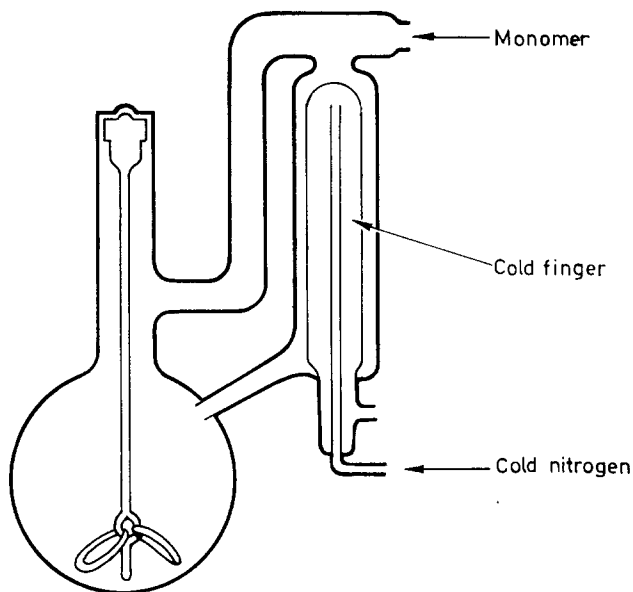
Figure 2 Polymerization apparatus

top of which is a small permanent magnet. The stirrer is driven externally by a large permanent magnet, and mixing is further improved by indentations in the sides of the vessel.

The cold finger is designed such that both monomer and solvent condense on the top, and it is cooled by gaseous nitrogen or air which has been passed through a long coiled tube immersed in liquid nitrogen. The temperature, and hence distillation rate may be adjusted by altering the gas flow rate. The rate of evaporation of solvent is sufficient to reduce the temperature of the initiator solution to about $-20°C$, thus decreasing the probability of side reactions. In practice, the use of this technique permitted a two hundred fold dilution of monomer while increasing the volume of solution only by the volume of monomer added.

(b) *Polymerization procedure.* Ampoules of catalyst (cumyl potassium in THF), solvent (THF stored over sodium di-α-methyl styrene tetramer), monomer (styrene distilled from mono-sodium benzophenone), and a fragile glass bulb containing the coupling agent (1,3,5-trichloromethyl benzene), were attached to the polymerization vessel shown in *Figure 2*. The apparatus was evacuated at 10^{-4}mmHg. for several hours and gently heated with a large flame to remove any remaining moisture.

397

After sealing from the vacuum line, a filtered solution of α-methyl styryl sodium was used to rinse the apparatus, and this solution was returned to the solvent ampoule. Remaining α-methyl styryl sodium anions were removed by repeated solvent distillation until the rinsing solution was colourless, when all the solvent, (250 ml), was distilled from the ampoule and used as the solvent for polymerization. The empty ampoule was removed from the apparatus.

Initiator was added and the refluxing system put into operation. When the temperature of the initiator solution had decreased to about −20°C, the break-seal of the styrene ampoule was opened, and the monomer, (6 ml), was allowed to distil onto the cold finger and into the initiator solution, over a period of 6 h.

After addition of all the monomer, the solution was warmed and a portion of the polymer solution was removed in an ampoule and terminated with methanol. This sample constituted the linear precursor. To the remainder, the coupling agent was added to form the branched star polystyrene. Polymers were precipitated from solution by pouring into a large excess of methanol, and dried in vacuo for 72 h at 40°C.

PHYSICAL MEASUREMENTS

Weight and number average molecular weights of linear and branched polymers prepared by the above technique have been determined by methods of light scattering and osmometry. Dilute solution viscosities have also been determined, the results of which will be described in a later paper. The techniques of gel permeation chromatography and ultracentrifugation gave a measure of the monodispersity of the samples. The latter techniques were particularly useful in identification of the species produced by the coupling reaction, and also in following progress of fractionations.

(1) *Light scattering*

Weight average molecular weights ($\bar{M}_w$) were obtained from light scattering measurements performed on a Sofica Photo Gonio Diffusometer. Benzene was used as a solvent and scattering intensities were determined at nine angles, between 30° and 150°. Zimm plots were constructed and molecular weights determined by extrapolation to zero angle and zero concentration.

(2) *Osmometry*

Number average molecular weights ($\bar{M}_n$) were determined from osmotic pressure measurements performed on a Mechrolab 501 high speed membrane osmometer. The instrument was operated at a temperature of 37°C with toluene as solvent. Measurements were carried out on solutions of different concentration and molecular weights were determined from the zero concentration osmotic pressure.

(3) *Gel permeation chromatography (g.p.c.)*

Molecular weight distributions were determined using a Waters Associates Gel Permeation Chromatograph Unit, Model 200. Toluene was used as solvent throughout, at a temperature of 80°C and a flow rate of 1 ml/min. Polymer samples were injected at a solution concentration of 0·25% over a period of 2 min.

The instrument was calibrated by means of a series of narrow molecular weight distribution polystyrenes of known molecular weight and the calibration curve is shown in *Figure 3*. The use of narrow molecular weight distribution polystyrenes as calibration standards proved particularly useful in
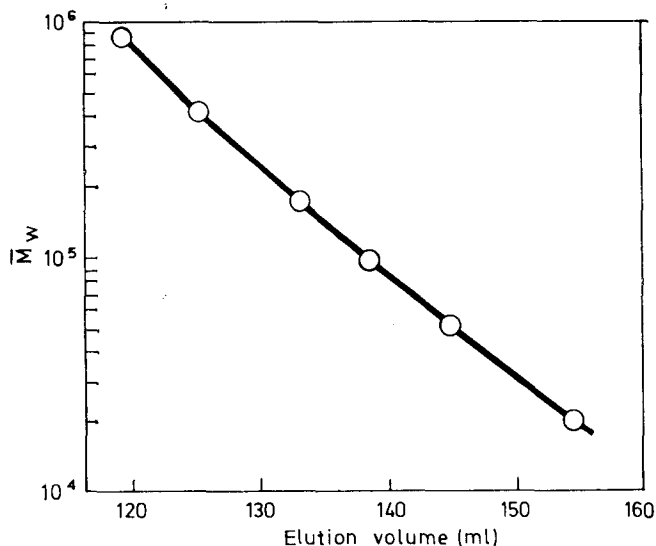
Figure 3 G.P.C. calibration curve

this study, since peak molecular weights of the anionic polymers prepared could be rapidly derived from the calibration curve.

(4) *Ultracentrifugation*

Sedimentation patterns of the polymers were obtained using a Beckman Model E Ultracentrifuge. Measurements were made at −7°C using *n*-butyl formate as solvent. This constitutes a theta-solvent for polystyrene at −9°C[18] and the low theta temperature was convenient in that solutions could be prepared at room temperature. Polymer concentrations were 0·6% and runs were carried out at 60000 revs. per min.

RESULTS AND DISCUSSION

Using the techniques described above, a series of linear polystyrenes has been prepared and the reaction between living polystyryl anions and suitable

low molecular weight coupling compounds has been investigated. The symbols L and Y are used here to describe the linear and branched polymers respectively and subscripts are used to differentiate polymers within each group. The linear polymers described here are not necessarily the precursors of corresponding branched polymers.

(1) Linear polymers

In preparing the linear polymers, an interesting phenomenon was discovered which has not hitherto been reported. It was found that a 'dimerization' reaction occurred between the living polystyryl anions if termination was not effected immediately after addition of all the monomer to the catalyst solution.

Figure 4a shows the molecular weight distribution as determined by g.p.c.

a   b
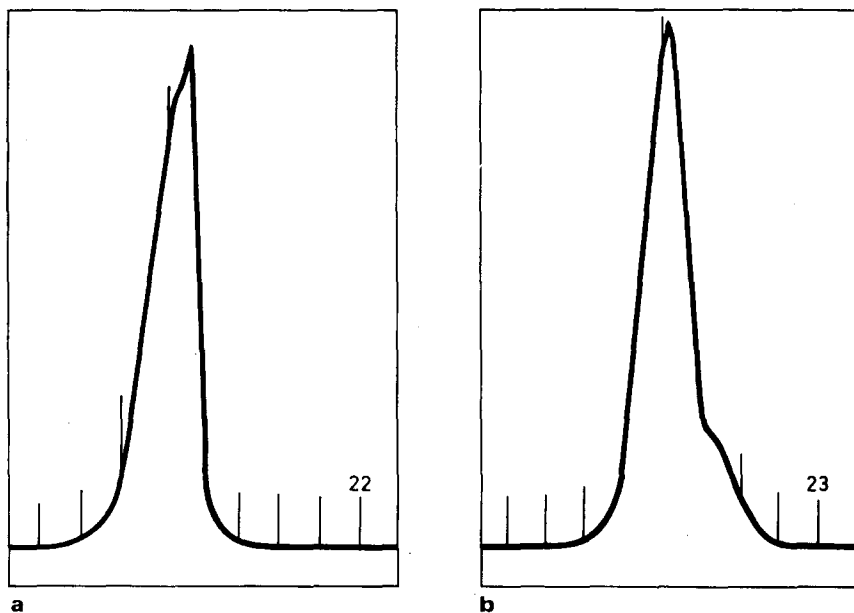
Figure 4 G.P.C. of linear polymers: (a) polymer terminated immediately after addition of all monomer; (b) polymer terminated after 17 h

of a typical linear polymer which was terminated immediately after addition of all the monomer, and *Figure 4b* shows the chromatograph of a sample of the same living polymer, which was terminated 17h after the end of the polymerization. A high molecular weight shoulder is obvious, and from the g.p.c. calibration curve shown in *Figure 3*, it may be seen that the peak molecular weight of the polymer represented by this shoulder is approximately twice that of the polymer represented by the main peak. The difference between the two polymer samples is particularly well defined in the sedimentation patterns shown in *Figure 5a* and *Figure 5b*,

400

Figure 5 Traces of schlieren patterns: (a) polymer terminated immediately after addition of monomer; (b) polymer terminated after 17 h

In view of the precautions taken to eliminate impurities it is unlikely that the high molecular weight material results from the coupling of the living polystyrene with a difunctional impurity.

Das, Feld and Szwarc[19] reported that living polystyryl lithium/THF solutions became more viscous on standing. They attributed this to association. In an article, Cubbon and Margerison[20] report that later work suggested that the increase in viscosity was due to alcoholates. (The authors would like to thank the referee for this information). Fetters[21] reported that the association was due to lithium alkoxide chain-ends.

Spach, Levy and Szwarc[22] gave evidence for the following reactions occurring

$$-\text{\small WW}-CH_2-CHPh^-Na^+ \longrightarrow -\text{\small WW}-CH=CHPh + NaH$$

$$-\text{\small WW}-CH_2-CHPh^-Na^+ + -\text{\small WW}-CH=CHPh \longrightarrow$$

$$-\text{\small WW}-CH_2-CH_2Ph + Na^+CHPh=CH-CPh^--CH_2-\text{\small WW}-$$

Neither of the above reactions would give a large increase in molecular weight. The formation of an alcoholate destroys the activity of a carbanion with only a small increase in molecular weight[23]. Since our evidence (*Figure 4* and *Figure 5*) shows a large increase in molecular weight it is suggested that the following reactions may be responsible.

After hydride abstraction:

$$-\text{\small WW}-CH_2-CHPh^-Na^+ + -\text{\small WW}-CHPh-CH=CHPh$$

$$\longrightarrow -\text{\small WW}-CH_2-CHPh-CHPh-CH^-Na^+$$
$$| $$
$$CHPh-\text{\small WW}-$$

$$-\text{\small WW}-CH_2-CHPh-CH-CHPh^-Na^+$$
$$|$$
$$CHPh-\text{\small WW}-$$

Both reactions would double the molecular weight in one step.

The production of the dichain polymer was obviously undesirable and in

order to suppress its formation, linear polymers were terminated as quickly as possible after addition of all the styrene. Termination was effected by addition of either methanol or the trifunctional coupling agent.

The molecular weights of the linear polymers used in solution property measurements were determined as previously described and are shown in *Table 1*. Molecular weight distributions determined by g.p.c. showed that the polymers listed in *Table 1* did not contain any dichain polymer.

Table 1 Molecular weights data for linear polymers

Polymer	$\bar{M}_n \times 10^{-5}$	$\bar{M}_w \times 10^{-5}$	$\bar{M}_w/\bar{M}_n$
1L	0·744	0·795	1·07
2L	1·283	1·374	1·07
3L	2·29	2·55	1·11
4L	5·30	5·84	1·10

(2) *Branched polymers*

A series of trifunctionally branched polymers, suitable for investigation of solution properties, has been prepared, but initial experiments were carried out in order to determine the optimum conditions for obtaining the maximum yield of star polymer.

In early experiments, the coupling reaction between polystyryl anions and 1,3,5-tribromomethyl benzene was investigated, and the sedimentation pattern of a typical product of the reaction is shown in *Figure 6*. It may be seen from
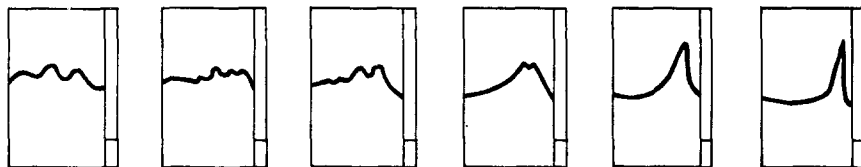
Figure 6 Traces of schlieren patterns of Y$_{7.1}$

this figure that the yield of trifunctional star polymer is very small, and the main products are mono- and dichain polymer. It is also obvious from the sedimentation pattern that high molecular weight, possibly tetrachain, polystyrene is a product of the reaction. Since metalation reactions are considered to be unlikely to occur[5] when potassium is used as a gegen-ion, it is probable that the 'dimerization' reaction described above produces living dichain polymer, and reaction of the latter with the coupling agent is responsible for the polymer species represented by the fourth peak in the sedimentation pattern.

In the reaction between living polystyrene and 1,3,5-tribromomethyl benzene as the coupling agent. The technique was fully investigated and two conditions were found necessary for the production of maximum yields of

trifunctional star polymer:

(a) The coupling agent should be added as quickly as possible after addition of all the monomer, otherwise the 'dimerization' reaction described above is competitive.

(b) Sufficient coupling agent must be added to the linear polymer to terminate *all* chains, as evidenced by the complete disappearance of the red colour due to the polystyryl anions. If a longer time is allowed for reaction of a slight excess of polystyryl anions with the coupling agent, the yield of star polymer is decreased, rather than increased.

Under these conditions a series of four polymers has been prepared in which the yield of trifunctional star polymer is high, and sedimentation patterns of these polymers are shown in *Figure 7*. The number average
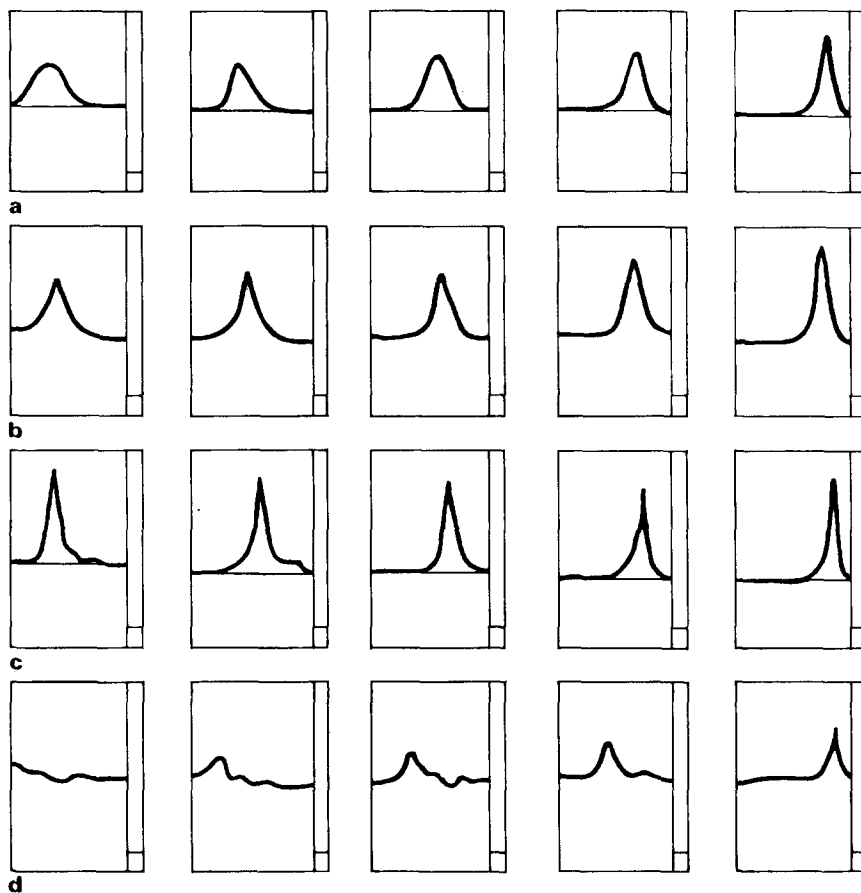
Figure 7 Traces of schlieren patterns (a) 1Y, (b) 2Y, (c) 3Y, (d) 4Y

molecular weights of the linear precursors are listed in *Table 2*, and it may be seen that the yield of star polymer is decreased as the molecular

weight of the linear precursor is increased. This is undoubtedly due to increased shielding of both living ends and reactive coupling groups by the larger polymer chains.

Figure 8 shows the gel permeation chromatogram of one of the products of the coupling reaction (4Y) and it may be seen that the three species indicated in the sedimentation pattern (*Figure 7d*), are not obvious in the chromatogram. Due to the smaller size in solution of the branched polymer,
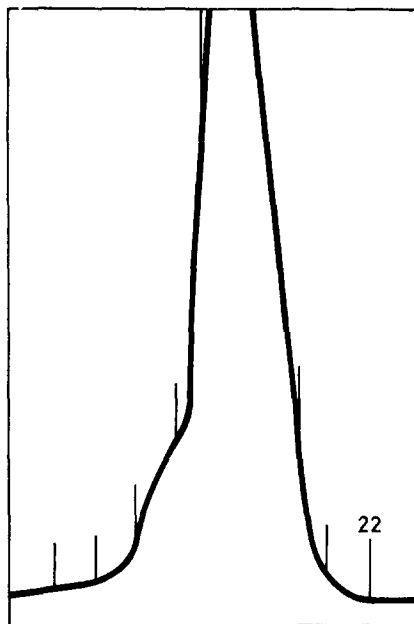
Figure 8 G.P.C. of 4Y (0·5%)

complete separation of the latter and the dichain polymer has not been possible. From *Figure 3*, it is estimated that the low molecular weight shoulder in the chromatogram corresponds to monochain polystyrene.

The presence of species other than trichain polymer required that before any investigation of the properties of the branched polymers could be made, it was necessary to isolate monodisperse samples of the trifunctional poly-styrenes from the parent mixtures, by fractionation.

Fractionations were carried out by precipitation from butanone solution using ethanol as non-solvent, and it was found convenient to follow the progress of the fractionations by ultracentrifugation of the centre fractions, and by gel permeation chromatography of all fractions. Although somewhat complicated by the fact that the dichain and trichain species were eluted together, the latter technique was useful in providing a rapid estimate of the efficiency of the fractionation. This is demonstrated in *Figure 9* which shows a gel permeation chromatogram of a typical product (3Y) of a coupling reaction, and the chromatograms of the three fractions obtained by precipita-
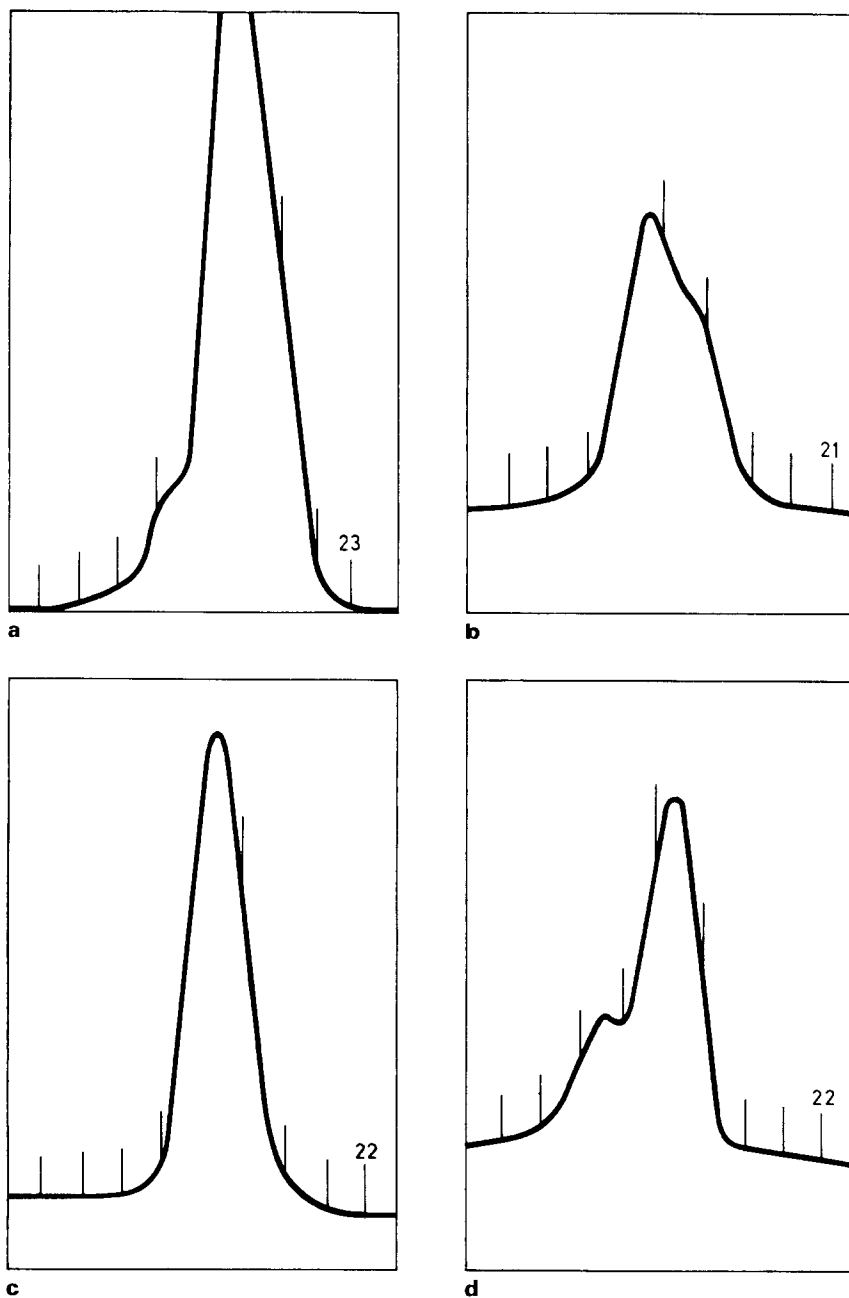
Figure 9 G.P.C.: (a) 3Y (0·5%); (b) high M.W. fraction of 3Y; (c) centre fraction of 3Y (i.e. 3Y₁); (d) low M.W. fraction of 3Y

tion from butanone solution. It is obvious that the fractionation procedure has been successful in removing high and low molecular weight material.

In the case of the low molecular weight branched polymers (1Y, 2Y and 3Y) sedimentation patterns and chromatograms indicated that only one fractionation was required to yield pure trichain polymers (1Y$_1$, 2Y$_1$ and 3Y$_1$) but the higher molecular weight polymer 4Y was subjected to two fractionations to yield star polymer 4Y$_2$.

The sedimentation patterns of the four truly trifunctional star polymers are shown in *Figure 10* and number and weight average molecular weights of these polymers are shown in *Table 2*.
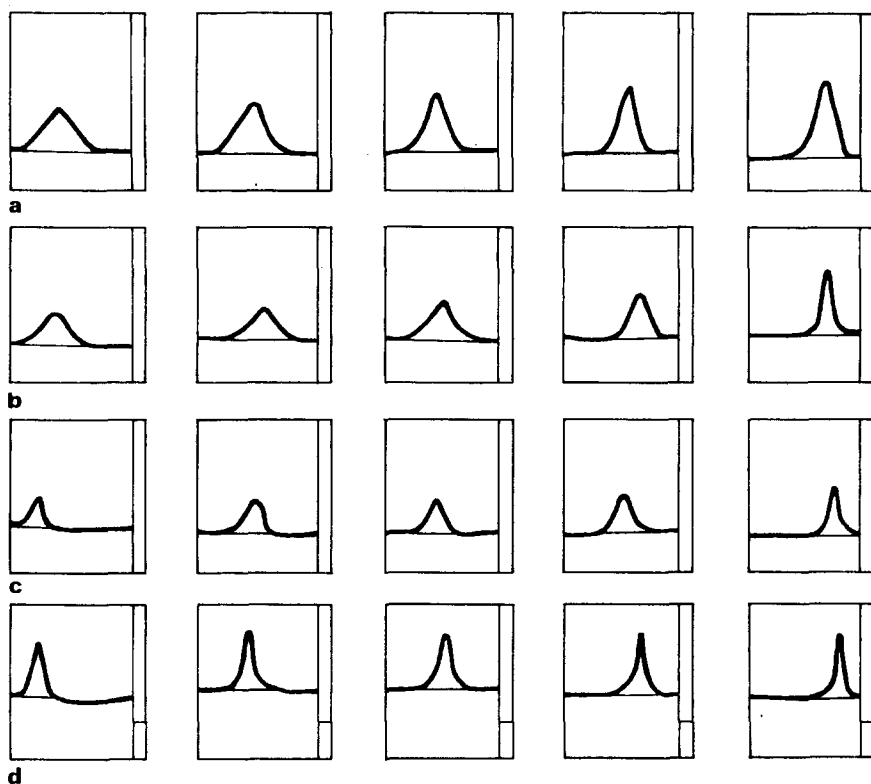
Figure 10 Traces of schlieren patterns: (a) 1Y$_1$, (b) 2Y$_1$, (c) 3Y$_1$ (0·3 %), (d) 4Y$_2$ (0·3 %)

Table 2 Molecular weight data for star polymers

Polymer	$\bar{M}_n \times 10^{-5}$	$\bar{M}_w \times 10^{-5}$	$\bar{M}_w/\bar{M}_n$	Precursor $\bar{M}_n \times 10^{-5}$	Linking ratio
1Y$_1$	0·797	0·925	1·16	0·315	2·53
2Y$_1$	1·445	1·48	1·02	0·48	3·01
3Y$_1$	2·84	3·26	1·15	1·02	2·78
4Y$_2$	3·51	4·10	1·17	1·31	2·68

Also shown in *Table 2* are the number average molecular weights of the linear precursors of the branched polymers described, and from this, the 'linking ratio' $M_n(Y)/\bar{M}_n(L)$ has been determined. Differences between the experimental value of this parameter and the theoretical value of three were expected, due to changes in molecular weight resulting from the fractionation procedure.

CONCLUSIONS

A new experimental technique for anionic polymerization has been devised and successfully used for the investigation of the coupling reaction between living polystyryl anions and 1,3,5-trichloromethyl benzene. This reaction was complicated by a dimerization reaction involving living polymer molecules, but this complication has been overcome and coupling reaction products consisted largely of trichain polystyrene. By fractionation of these products, a series of pure trichain polymers of narrow molecular weight distribution has been produced, properties of which will be reported in later publications.

Chemistry Department,
University of Aberdeen,
Old Aberdeen, AB9 2UE,
Scotland

REFERENCES

1 Swarc, M. *Nature* 1956, **178**, 1168
2 Morton, M., Helminiak, T. E., Gaudkary, S. D. and Beuche, F. *J. Polym. Sci.* 1962, **57**, 471
3 Orofino, T. A. and Wenger, F. *J. Phys. Chem.* 1963, **67**, 566
4 Zerlinsky, R. P. and Wofford, C. F. *J. Polym. Sci. (A)* 1965, **3**, 93
5 Yen, S. S. *Makromol. Chem.* 1965, **81**, 152
6 Gervasi, J. A. and Gosnell, A. B. *J. Polym. Sci. (A-1)* 1966, **4**, 1391
7 Altares, T., Wyman, D. P., Allen, V. R. and Meyerson, K. *J. Polym. Sci. (A)* 1965, **3**, 4131
8 Wyman, D. P., Elyash, L. J. and Frazer, W. J. *J. Polym. Sci. (A)* 1965, **3**, 681
9 Kraus, G. and Gruver, J. T. *J. Polym. Sci. (A)* 1965, **3**, 105
10 Invoe, S., Tsuruta, T. and Furukawa, J. *Makromol. Chem.* 1960, **42**, 12
11 Asami, R., Levy, M. and Swarc, M. *J. Chem. Soc.* 1962, p 361
12 Bhattacharyya, D. N., Lee, C. L., Smid, J. and Swarc, M. *J. Amer. Chem. Soc.* 1963, **85**, 533
13 Reed, R. A. *Chem. Prods.* 1960, **23**, 299
14 Reppe, W., Schlichting, O. and Meister, H. *Ann.* 1948, **560**, 93
15 Litt, M. *J. Polym. Sci.* 1962, **58**, 429
16 Wenger, F. *Makromol. Chem.* 1963, **64**, 151
17 Cowie, J. M. G., Worsfold, D. G. and Bywater, S. *Trans. Faraday Soc.* 1961, **57**, 705
18 Schulz, G. V. and Baumann, H. *Makromol. Chem.* 1963, **60**, 120
19 Das, K. S., Feld, M. and Szwarc, M. *J. Amer. Chem. Soc.* 1960, **82**, 1506
20 Cubbon, R. C. P. and Margerison, D. *Progress in Reaction Kinetics* Pergamon Press, 1965, Vol 3, p 419
21 Fetters, L. J. *J. Polym. Sci. (B)* 1964, **2**, 425
22 Spach, G., Levy, M. and Szwarc, M. *J. Chem. Soc.* 1962, p 355
23 Szwarc, M., 'Carbanions, living polymers and electron transfer processes', Interscience Publishers, 1968, p 658

Effects of temperature on a polycondensation in the melt

E. Turska and A. M. Wróbel

The effect of temperature on the transesterification process of the melt of 4,4'-dihydroxy-diphenyl-2,2-propane with diphenyl carbonate has been investigated. A series of polycondensations of these monomers has been carried out in the temperature range 200–250°C in the presence of zinc oxide as catalyst. It has been found that the character of the process depends on temperature. Below 230°C anomalies have been observed in the course of the process, but above this temperature the reaction follows the equilibrium mechanism.

KINETIC STUDIES of the preparation of polycarbonates by transesterification of 4,4'-dihydroxy-diphenyl-2,2-propane with diphenyl carbonate in the melt have been carried out and published by Losev and co-workers[1]. These authors, however, found definite anomalies when they attempted to elucidate the kinetic characteristics of the process, but these were not explained. The shape of their kinetic curves illustrating the relation between the viscosity-average molecular weight and time is distinctly different from that found by other authors for similar reversible reactions. In our opinion, the explanation of this phenomenon is connected with the non-typical course of the process over a part of the temperature range.

The aim of the present work is to determine whether polycondensation in the melt can resemble the precipitation encountered in solution as far as dependence on temperature is concerned. If so, the anomalous shape of curves and the difficulties in finding kinetic characteristics would be confined to quite a narrow range of temperature. Detailed kinetic investigations cannot be undertaken until this is elucidated.

EXPERIMENTAL

Starting materials

4,4-Dihydroxy-diphenyl-2,2-propane, supplied by Schuchardt GMBH, München, Germany, was purified by crystallizing from chlorobenzene solution, washing with trichloroethylene and drying in a vacuum desiccator over calcium chloride. The melting point of the purified 4,4'-dihydroxy-diphenyl-2,2-propane was 158°C, in agreement with the literature[2].

Diphenyl carbonate, supplied by the Fluka AG, Switzerland was crystallized from absolute ethanol and dried in a vacuum desiccator over calcium chloride. The melting point of the purified diphenyl carbonate was 78°C, in agreement with the literature[3].

Zinc oxide of annalar purity, supplied by Zakłady Bieli Cynkowej 'Oława', Poland, was used as catalyst.

Polycondensation reaction conditions

The polycondensation was carried out at 200, 210, 220, 230, 240 and 250°C under a pressure of 60 mmHg of nitrogen, samples of the reaction mixture being removed at definite intervals. The sampling was carried out by means of a special adaptor[4] which makes this operation possible without interrupting the process. The catalyst concentration was 0·27% (on the weight of monomers).

Molecular weight determination

Molecular weights of the polycarbonate samples were determined by the viscometric method. Intrinsic viscosities, $[\eta,]$ were determined at 20°C in methylene dichloride by means of an Ubbelohde dilution viscometer of capillary diameter 0·3 mm. Viscosity-average molecular weights $(\bar{M}_v)$ were calculated from the Schulz-Horbach equation[5]:

$$[\eta] = 1·11 \times 10^{-2}\bar{M}_v^{0·82} \tag{1}$$

Fractionation

The samples of polycarbonate were fractionated by the column extraction method [6] with methylene dichloride as solvent and n-heptane as non-solvent. The results were treated by the method of Tung[7].

Melting point determination

Measurements of the melting points of polycarbonate fractions were carried out by means of a microscope provided with a heated stage (Franz Küstner Nachf. KG, Dresden).

RESULTS AND DISCUSSIONS

According to the procedure described above, a series of polycondensations of 4,4'-dihydroxy-diphenyl-2,2-propane with diphenyl carbonate was performed at various temperatures, namely 200, 210, 220, 230, 240 and 250°C. Curves were plotted illustrating the relation between the viscosity-average molecular weight and time of the reaction. These curves are shown in *Figures 1* and *2*. As is seen, the shapes of the curves change markedly with temperature. Below a temperature of about 230°C the curves are more or less similar to the anomalous curves obtained by Losev and co-workers[1]. Above this temperature, the kinetic curves correspond in their character to a typical course of a reversible polycondensation reaction. In order to confirm the similarity between our curves for the lower range of temperatures and those of Losev *et al*, the two sets of results for a similar temperature are compared in *Figure 3*. As can be seen, the shapes of the curves are almost identical.

409
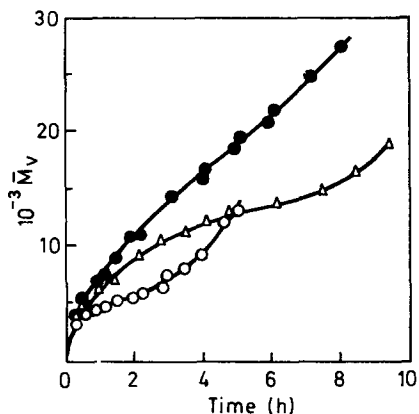
Figure 1 Dependence of viscosity-average molecular weight on time of the polycondensation at 200°C (O), 210°C (△), and 220°C (●)
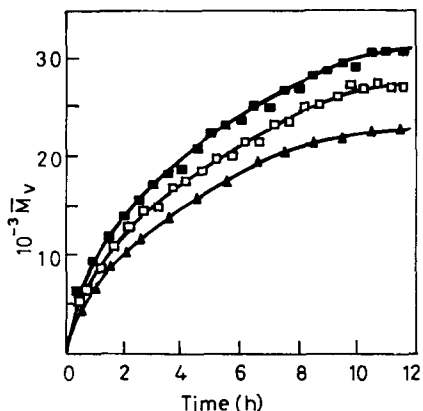
Figure 2 Dependence of viscosity-average molecular weight on time of the polycondensation at 230°C (▲), 240°C (□) and 250°C (■)

The following considerations may help in interpreting the phenomena observed. According to the work of Turska and Dems[8], in a polycondensation in solution it is possible to disturb the equilibrium under definite conditions and make the polycondensation continue further by precipitation of the higher fractions of polymer from solution. Further production of insoluble macromolecules and their subsequent precipitation then occur, thus causing a spontaneous continuation of the process. This type of mechanism for the polycondensation process gives a kinetic curve of $\bar{M}_v$ against time with shapes analogous to those obtained by Losev and by us.

It remains to consider whether in the case of polycondensation in the melt a similar process of precipitation of high-molecular-weight fractions is
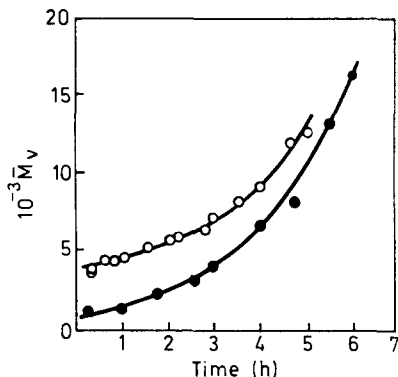
Figure 3 Experimental kinetic curve at 200°C (○) and the curve obtained by Losev at 198°C (●)

possible. We must take into account the fact that the melting temperature of a polymer is a function of its molecular weight. From melting point measurements of polycarbonate fractions, we obtained a curve illustrating the dependence of melting temperature on molecular weight (*Figure 4*).
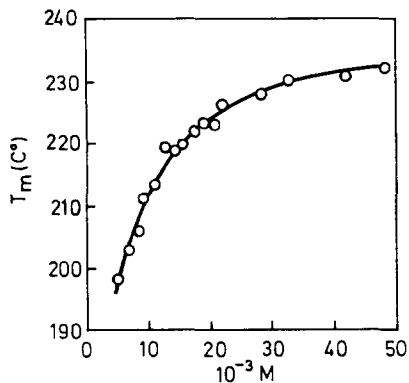
Figure 4 Dependence of melting temperature of polycarbonate fractions on molecular weight

As is seen from the figure, the melting temperature rises with the molecular weight, the differences between the melting temperatures of low and high fractions being considerable.

In a polydisperse polycarbonate at a temperature above the melting point of low fractions but below the melting point of high fractions, it is possible that the system is not homogenous. It might be assumed that, under definite conditions of temperature, the higher fractions of polycarbonate become insoluble in the melt and a phenomenon similar to that of precipitation from

411

solution takes place. If this reasoning applies to polycondensation reactions in the melt, one may suppose that under these conditions the higher fractions of macromolecules become inaccessible to the reaction, or, at least, their accessibility is considerably reduced. The course of the process should then be analogous to that of precipitation polycondensation, resulting in a continuous increase of the average molecular weight without possibility of reaching an equilibrium state. But if the same process is carried out, at a temperature above the melting point of the highest fractions, then the course of the process should lead to equilibrium.

Thus there is a possibility of a precipitation-type of reaction under the reaction conditions we used which would help to explain the anomalies in the shapes of the kinetic curves.

We decided to verify this hypothesis by further experiments. The products obtained at a temperature below 230°C (non-typical course of reaction) and those obtained above 230°C were fractionated. *Figures 5* and *6* show a comparison of the theoretical curves of Flory with the experimental distribution curves obtained for the products prepared at 240°C and 200°C, respectively. Theoretical distribution curves were calculated in each case from the
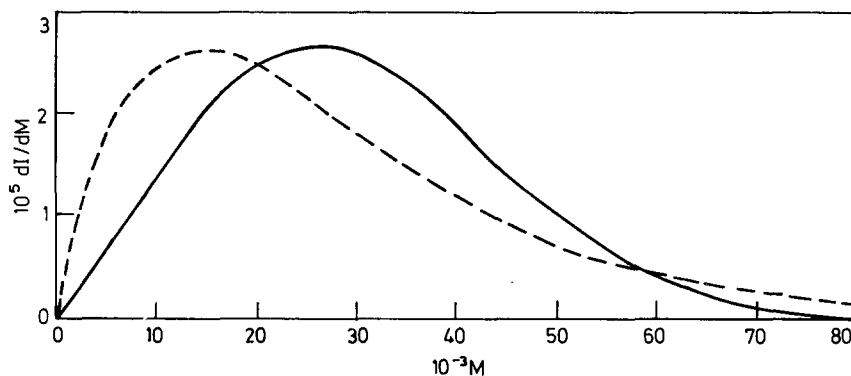
Figure 5 Experimental differential curve of distribution (unbroken line) and theoretical curve of Flory (broken line) for polycarbonate prepared at 240°C

extent of reaction, estimated from the number-average molecular weight. In the 200°C experiments the extent of reaction is that estimated for a polycarbonate of the observed number-average molecular weight with the most probable distribution. The product of polycondensation in the melt in a homogeneous system should have a distribution corresponding to the most probable distribution of Flory. Our results, shown in *Figure 5*, are consistent with this. As may be seen, the divergence of the experimental and theoretical curves is not large, and is within the limits of experimental error. However, a different picture is obtained in the case of the polycarbonate prepared at a lower temperature, which we must consider in terms of the precipitation mechanism.

Earlier work[8] on the solution-precipitation polycondensation showed that the product obtained by this method has a characteristic molecular weight distribution function, completely different from the most probable
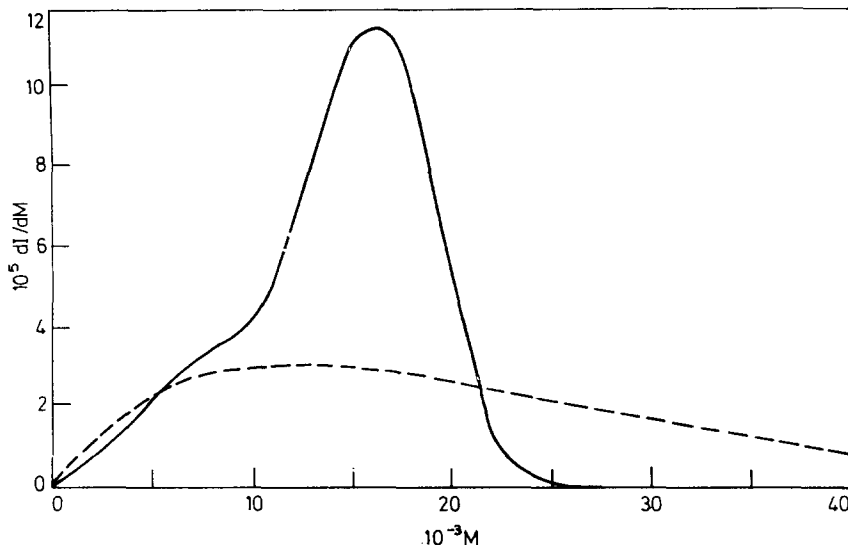
Figure 6 Experimental differential curve of distribution (unbroken line) and theoretical curve of Flory (broken line) for polycarbonate prepared at 200°C

distribution of Flory. It has a narrow range of molecular weight (depending on the reaction conditions)–a distinct maximum–the height of which is related to the duration of the process. The maximum probably corresponds to the distribution in the precipitated polymer, and the curve for the product as a whole is a superimposition of the most probable distribution curve for the product from the liquid phase and the distribution curve for the precipitated phase. The experimental distribution curve obtained for the polycarbonate produced at 200°C (*Figure 6*) clearly departs from the calculated curve, showing a sharp and high maximum within the range of molecular weights from 12 000 to 24 000. Taking into account the fact that polymers with molecular weights exceeding 12 000 have melting points above 200°C (*Figure 4*), we believe that the fractionation results confirm our considerations.

The observed dependence of the shape of the kinetic curves on the temperature of the process and the different distribution curves obtained showed that the process may proceed in different ways according to the temperature. Up to about 230°C the process is of a precipitation type and, therefore, kinetic observations cannot be interpreted on the basis of relationships valid for homogeneous systems. Above this temperature the process is of an equilibrium type and follows classical kinetics.

Institute of Polymers,
Ministry of Education and
Polish Academy of Sciences
116 Żeromski Street,
Łódź 40, Poland

REFERENCES

1 Losev, I. P., Smirnova, O. V. and Smurova, E. V. *Vysokomolekul. Soedin.* 1963, **5**, 57
2 Timmermans,   'Physicochemical constants of pure organic compounds' Interscience, New York, 1959
3 Bischoff, C. A. and Hedenstroem, A. *Ber.*, 1902, **35**, 3431
4 Wróbel, A. M. *Polimery* 1968, **3**, 127
5 Schulz, G. V. and Horbach, A. *Makromolek. Chem.*, 1959, **29**, 93
6 Turska, E., Dems, A. and Siniarska, M. *Bull. Acad. Polon. Sci. Ser. Sci. Chim.* 1965, **13**, 189
7 Tung, L. H. *J. Polym. Sci.* 1956, **20**, 495
8 Turska, E. and Dems, A. *J. Polym. Sci. (C)* 1968, **22**, 407

414

Kinetics of polycondensation in the melt of 4,4-dihydroxy-diphenyl-2,2-propane with diphenyl carbonate

E. Turska and A. M. Wróbel

The transesterification reaction in the melt of 4,4-dihydroxy-diphenyl-2,2-propane with diphenyl carbonate proceeds in a homogenous system without anomalous phenomena above 230°C. Consequently, the kinetics of the reaction were studied at the temperatures 230, 240, and 250°C. From the results obtained the reaction was found to be third order in agreement with work on other transesterification reactions. However, there is no likely mechanism to explain these kinetics. Treating the results in a formal way, values of kinetic constants and activation energy were calculated. The activation energy was found to be 14·5 kcal/mol. The dependence of the reaction rate constant on the catalyst concentration is linear.

IN THE PREVIOUS PAPER[1] we have shown that polycondensation in the melt of 4,4'-dihydroxy-diphenyl-2,2-propane with diphenyl carbonate proceeds homogenously above a temperature of 230°C. Consequently, kinetic investigations of this process with the application of formal kinetics are meaningful only above this temperature. Below 230°C sharp anomalies were observed and these were elucidated in the previous paper.

The purpose of the present work is to examine the kinetics of polycondensation in the melt of 4,4'-dihydroxy-diphenyl-2,2-propane with diphenyl carbonate and to characterize the process in terms of formal kinetics.

Kinetic investigations were made at the temperatures 230, 240 and 250°C. *Figure 1* shows our experimental kinetic curves relating the viscosity-average molecular weight ($\bar{M}_v$) and the duration of the process at the temperatures 230, 240 and 250°C. As is seen, the shape of the kinetic curves is characteristic of a reversible polycondensation reaction leading to the equilibrium state.

Since for kinetic purposes values of the number-average molecular weights are needed, these were calculated from the viscosity-average molecular weights by means of the Flory-Schaefgen equation[2]. Since we have shown in the previous paper that the molecular weight distribution function of polycarbonates obtained at these temperatures is in agreement with the most probable distribution by Flory, this procedure may be accepted as correct, although it gives only approximate values. Further kinetic considerations were based on the results obtained in this way.

To find the order of reaction, plots were made showing the dependence of $\bar{P}_n$, the number-average degree of polymerization, $\bar{P}^2_n$ and $\ln \bar{P}_n$ on the reaction time. These relationships were found to be similar for all three temperatures. *Figure 2* shows typical plots for a temperature of 240°C; non-linear relationships are obtained for $\bar{P}_n$ and $\ln \bar{P}_n$, but for $\bar{P}^2_n$ the relationship
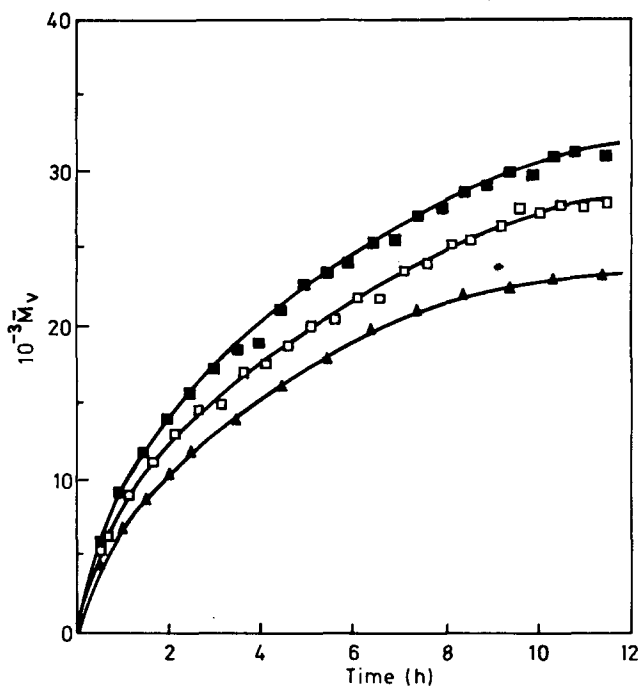
Figure 1 Experimental kinetic curves of relationship between viscosity-average molecular weight and duration of the polycondensation at 230°C (▲), 240°C (□) and 250°C(■)

is linear. Since the observed dependence of $\bar{P}_n^2$ is linear for all temperatures under investigation (*Figure 3*) the reaction was estimated to be of third order.

According to third-order kinetics

$$2C_0^2 kt = \bar{P}_n^2 - 1 \tag{1}$$

where $C_0 = $ the initial concentration of functional groups

$k = $ the reaction rate constant

and $t = $ the duration of reaction.

Rate coefficients were calculated from equation (1) for the three temperatures and a zinc oxide catalyst concentration of 0.27% (based on the weight of monomers): they were constant within the limits of experimental error. The average values of the rate constants are given in *Table 1*.

Table 1 Rate constants for various temperatures

Temperature (°C)	Rate constant $(\text{mmol}^{-2}\,\text{g}^2\,\text{min}^{-1})$
230	0·461
240	0·621
250	0·804
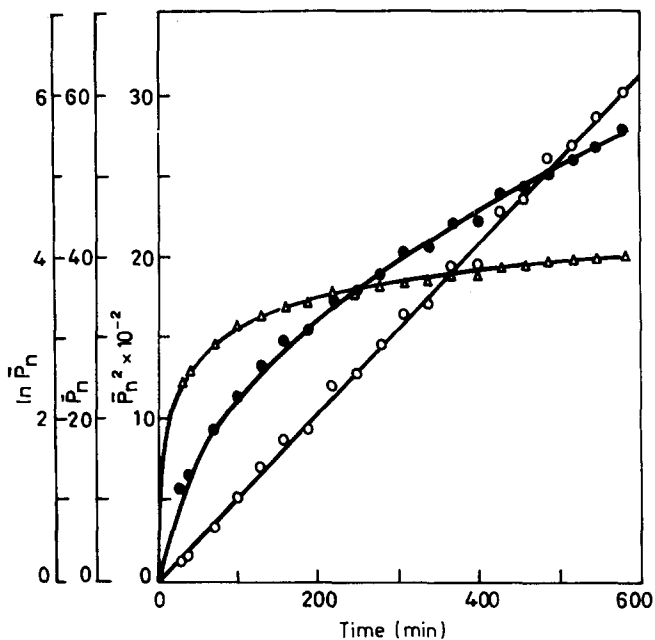
Figure 2 Dependence of number-average degree of polymerization $\overline{P}_n$ (●), $\ln \overline{P}_n$ (△) and $\overline{P}_n^2$ (○) on time of the polycondensation at 240°C
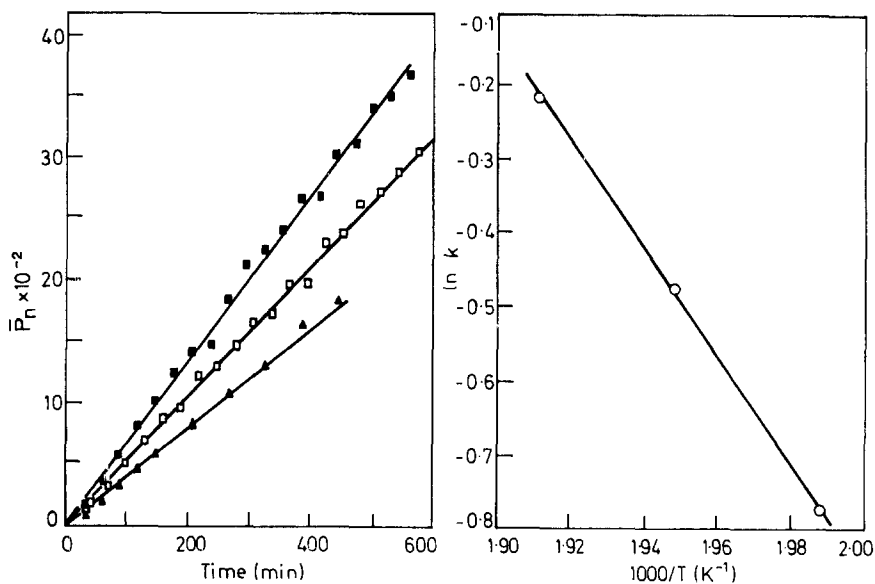
Figure 3 Dependence of number-average degree of polymerization on time of the the polycondensation for 230°C (▲), 240°C (□) and 250°C (■)
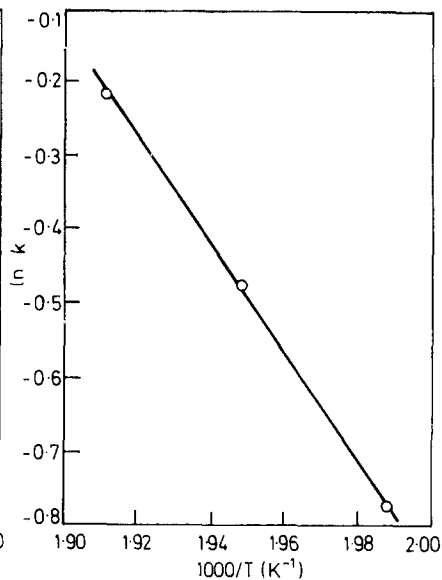
Figure 4 Dependence of the natural logarithm of the reaction rate constant on the inverse of the absolute temperature

417

The applicability of the Arrhenius equation was shown by the linearity of the plot of $\ln k$ against the inverse of the absolute temperature (T^{-1}) (*Figure 4*). The activation energy calculated for the given catalyst concentration is 14·5 kcal/mol.

In order to examine the effect of the catalyst concentration on the course of the reaction, a series of polycondensations was carried out at 240°C under a pressure of 60 mmHg for various concentrations in the range 0·05 — 0·37% (based on the weight of monomers). *Figure 5* shows the experimental results
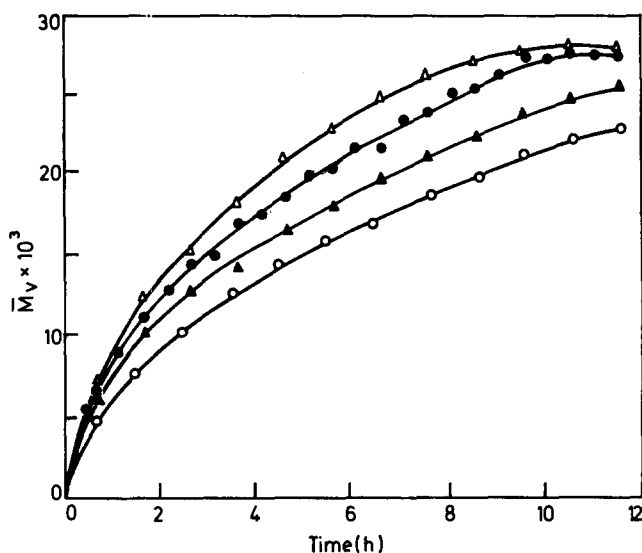
Figure 5 Experimental curves of relationship between viscosity-average molecular weight and duration of the polycondensation for 0·05% (○), 0·27% (●) and 0·37% (△) catalyst concentration

for the catalyst concentrations: 0·05, 0·16, 0·27 and 0·37%. Calculated values of the corresponding reaction rate constants are shown in *Table 2*.

Table 2 Reaction rate constants for various concentrations of catalyst

Catalyst concentration (%)	Rate constant $(\mathrm{mmol}^{-2}\,\mathrm{g}^2\,\mathrm{min}^{-1})$
0·05	0·371
0·16	0·489
0·27	0·621
0·37	0·770

The dependence of the reaction rate constant on the catalyst concentration is shown in *Figure 6*. Due to linear character of the plot, this relationship may be expressed by the equation:

$$k = 0.3 + 1.2\,C_{cat} \tag{2}$$

where C_{cat} is the catalyst concentration.
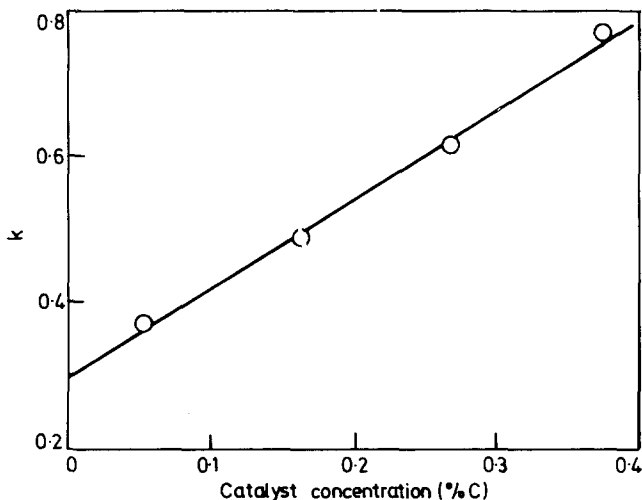
Figure 6 Dependence of reaction rate constant on catalyst concen-centration (%C)

On the basis of the present results the reaction under investigation proceeds formerly according to the kinetics of a reaction of the third order. Analogous results were obtained by other authors[3,4] investigating other transesterification reactions in the melt. In spite of the conformity of results obtained by different authors, it should be stated that there is no likely reaction mechanism to explain the kinetics. In our opinion, the third order of reaction has to be treated as a purely formal result. The equations used for the calculations are, in principle, derived for considerably simpler systems, and their application to the reactions under consideration required several simplifying assumptions. We believe that elucidation of the reaction mechanism may be possible by developing new procedures of calculations with a reduced number of simplifying assumptions. Investigations of this problem are now in progress in our laboratory.

Institute of Polymers,
Ministry of Education
and Polish Academy of Science,
116 Żeromski Street,
Łódź 40, Poland

REFERENCES

1 Turska, E. and Wróbel, A. M. *Polymer Lond.* 1970, **11**, 408
2 Schaefgen, J. R. and Flory, P. J. *J. Amer. Chem. Soc.* 1948, **70**, 2709
3 Skwarski, T. *Zeszyty Naukowe Politechn. Łódź. Chem.* 1956, **4** 41
4 Fontana, C. M. *J. Polym. Sci.* 1968, **6**, 2343

Solubility and transport of gases in Nylon and polyethylene

R. ASH, R. M. BARRER AND D. G. PALMER

Solubility isotherms for He, H_2, Ne, N_2, Ar and CO_2 have been determined over the temperature range 273·2K to 333·2K in Nylon 11 and polyethylene both indirectly, from time-lags and permeabilities, and also directly. For the 100% amorphous polymer at 298·2K solubility coefficients, σ, approximate to the relations:

$$\log \sigma = -2\cdot0_3 + 0\cdot0093 \ \varepsilon/k \ \text{(polyethylene)}$$
$$\log \sigma = -2\cdot4_1 + 0\cdot0111 \ \varepsilon/k \ \text{(Nylon 11)}$$

where ε/k is the Lennard-Jones interaction parameter for the gas. Heats of solution in polyethylene were endothermic for all the gases except CO_2 and in Nylon 11 for all except Ar and CO_2. Nylon was considerably more permselective to helium than polyethylene and energies of activation for diffusion were somewhat larger and more sensitive to molecular dimensions than in polyethylene.

INTRODUCTION

THE SOLUBILITIES of permanent gases in polymers are small and therefore not easily measured. Nevertheless, as a limiting case of polymer solutions, they have attracted considerable attention [1-4]. One method of measuring small solubility coefficients, σ, is based on membrane permeabilities P, and time-lags, L, and uses the relations $P = D\sigma$ and $D = A/L$, where D is the diffusion coefficient and A depends upon the geometry of the membrane. For a sheet of thickness l, $A = \frac{1}{6}l^2$. σ can also be determined by direct measurements of gas solubility [5,6]. If accurate measurements can be made using both procedures any disagreement must indicate that diffusion is non-ideal in that D depends on one or more of the following: distance x, time t and concentration c. For gases giving very dilute solutions however, any concentration dependence of D can be ruled out.

It is of considerable interest to develop the direct method of measurement and to investigate the solubility of gases in polymers of different hardness by both methods. Accordingly sorption, diffusion and permeation of gases have been investigated in Nylon 11 and polyethylene. Solubilities in other polyethylenes are available for comparision [7], but in Nylon our measurements are among the first to be made for gases. In partially crystalline polyethylene evidence of non-ideal diffusion has already been presented which may indicate time-dependence of D associated with some blind pore character in the heterogeneous medium [8].

EXPERIMENTAL

The hollow cylindrical membranes of Nylon 11 and polyethylene were the separated components of laminated tubing made by Messrs. Griflex Ltd,

London. The internal and external radii of the sheaths were 0·139 cm and 0·238 cm respectively for the Nylon, and 0·236 cm and 0·338 cm respectively for the polyethylene. Gases used were spectrally pure grades of helium, neon, argon, hydrogen, nitrogen and carbon dioxide supplied by the British Oxygen Company.

Flow measurement of solubility

Within the diffusion cell a 110 cm length of membrane had one end closed with a sealed glass tube while the other end was joined to an extended cone. Both joints were made using push-fit glass tubing with Araldite completing the seal. The Nylon and the polyethylene samples were contained in similar cells immersed in a water bath which was controlled to within $\pm$ 0·1 K. Experiments were conducted over the temperature range 283·2 – 333·2 K.

At time $t = 0$ the outer face of the evacuated membrane was subjected to a gas pressure p_{in} which was then kept constant throughout the experiment. This pressure was in the range $(4·0 – 21·3) \times 10^3$ N m^{-2} $(3 – 16$ cmHg). The gas pressure developed at the inner face, p_2, which was always much less than p_{in}, was measured with a McLeod gauge and plotted as a function of time. From this plot, L and dp_2/dt were obtained. With helium the time lags were small and a least squares calculation was used to obtain them.

The conductance Y, defined as the steady state flux per unit length of cylinder divided by p_{in}, was calculated using the formula[8]:

$$Y = \frac{V_0}{60} \times \frac{273}{(273 + T_a)\, p_{in}} \times \left(\frac{dp_2}{dt}\right) \quad \text{cm}^3 \text{ STP (cm s atm)}^{-1} \qquad (1)$$

The permeability coefficient, P, was calculated from

$$P = \frac{\ln (R_1/R_0)}{2\pi} \times Y \qquad (2)$$

and the diffusion coefficient, D_L, from the time-lag using

$$D_L = \frac{A}{L} = \frac{(R_1^2 + R_0^2) \ln (R_1/R_0) - (R_1^2 - R_0^2)}{4\, L \ln (R_1/R_0)} \quad \text{cm}^2 \text{ s}^{-1} \qquad (3)$$

where L is in seconds. Other symbols and units used in this paper are:

V_0 Volume of reservoir on the outgoing side   (cm^3)

T_a Ambient temperature   (°C)

η Length of sample   (cm)

$\dfrac{dp_2}{dt}$ slope of the linear portion of p_2 vs t plot   (cmHg min^{-1})

p_{in} ingoing pressure   (cmHg)

R_0 and R_1 internal and external radii of membrance   (cm)

The Henry's law solubility constant, σ_L, was calculated from the quotient:
$$\sigma_L = P/D_L \qquad (4)$$

where σ_L is in cm³ STP (cm⁻³ of polymer) atm⁻¹.

(1 cmHg = 1333 N m⁻²; 1 atm = 1·0133 × 10⁵ N m⁻²).

Static measurement of solubility

In the static method, equilibrium is first established between the polymer sample and a gas phase of known temperature and pressure; the gas is then swept away by surrounding the sample with mercury and finally the dissolved gas is permitted to desorb into a known volume where its pressure and temperature are measured. The solubility apparatus is shown in *Figure 1*.
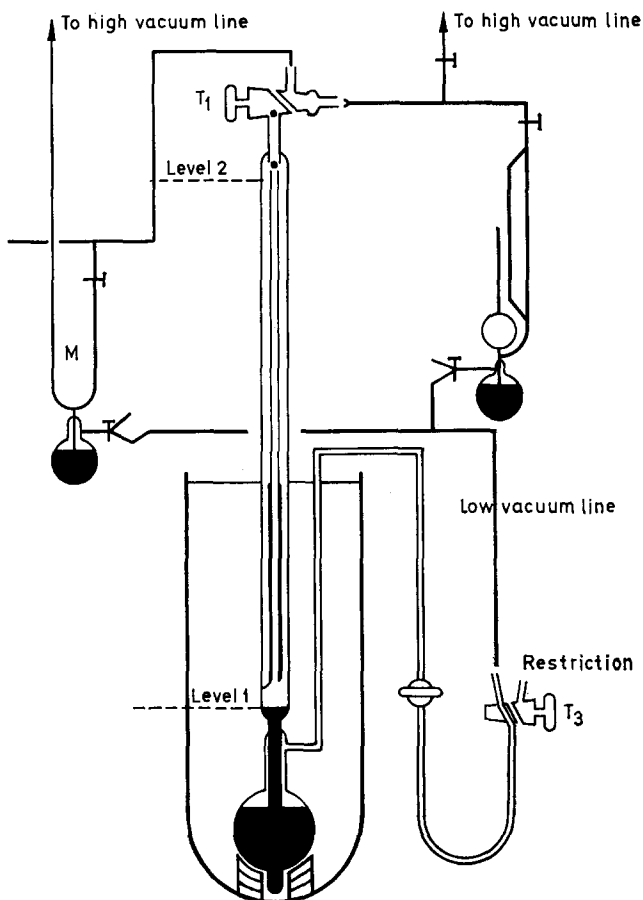
Figure 1 Apparatus for solubility measurements

The top of the polymer tube was mounted on a piece of glass tubing using Araldite while the bottom was kept in a central position with a glass spike. The cell was immersed in a water bath fitted with a thermostat, which controlled the temperature to better than ± 0·1 K. Solubilities were measured for the same series of temperatures as in the permeation studies.

423

With the sample outgassed, tap T_1 (*Figure 1*) was opened to the gas line and the system left for equilibrium to be established between the polymer and the gas at a pressure indicated by the mercury manometer M. Once equilibrium had been established, the mercury was raised to level 2 and tap T_1 opened to the pumps. Small holes below the internal seal allowed the entire volume above the mercury to be evacuated. Initial experiments confirmed that at this stage bubbles of gas at the equilibrating pressure were trapped in pockets on the surface of the glass and the polymer. Following Meares[5] these were removed by flushing the sample, i.e., with T_1 still opened to the pumps the mercury was rapidly lowered to level 1 and then returned to level 2. This was achieved by fully opening tap T_3 to the low vacuum line which caused the mercury to be lowered rapidly. As it passed the bottom of the membrane a stop-watch was started and tap T_3 turned to admit air at a rate controlled by a restriction in the supply arm. The watch was stopped as the rising mercury passed the bottom of the membrane. Once the desorption volume had been re-evacuated it was isolated from the pumps and the mercury lowered to level 1. A McLeod gauge was used to measure the final gas pressure, p'_∞, in the desorption volume.

It was found necessary to have level 2 a distance above the top of the sample not less than the maximum equilibrating pressure used; otherwise gas was desorbed from the sample even when it was surrounded by mercury. This gas escaped to the surface and was pumped away while the desorption volume was being re-evacuated after the flushing process. Initial isotherms obtained with level 2 just above the sample showed a pronounced curvature towards the equilibrating pressure axis.

To improve the method further, the final desorption pressure p'_∞, was corrected for loss of gas by desorption during the flushing process. The pressure corresponding to the total quantity of gas equilibrated in the membrane is then given by

$$p_\infty = p'_\infty/f \qquad (5)$$

where f is a factor which has been calculated in Appendix 1. The Henry's law solubility constant, σ_s, is finally given by

$$\sigma_s = \frac{V_0}{v} \times \frac{273}{273 + T_a} \times \frac{p_\infty}{p_1} \quad \text{cm}^3 \text{ STP (cm}^{-3} \text{ of polymer) atm}^{-1} \qquad (6)$$

where symbol and units not already given are

$V_0 =$ desorption volume		(cm³)
v = sample volume		(cm³)
p_1 = equilibrium pressure		(cmHg)
p_∞ = corrected final desorption pressure		(cmHg)

Accuracy

Based on the reproducibility of the results, the maximum errors in the experimental values of L and Y were $\pm 2\%$ and $\pm 1\%$ respectively. The uncertainty in P, D_L and σ_L is further dependent on the uniformity of the

membrane radii. The maximum variation in $(R_1 - R_0)$ was $\pm 2\%$ for Nylon and $\pm 4\%$ for polyethylene. Over the length of the membrane (110 cm) variations in the internal and external radii will average out, and no sensible error is introduced by taking the mean values.

Uncertainty in σ_S is associated with the volume calibrations, pressure measurements and the flushing process. In the derivation of f (Appendix 1) it was assumed that D_L determined from the time-lag could be used for desorption at the earliest times (i.e. during flushing). It was also reasonably assumed that the sheath and the slab of the same thickness had identical early-time solutions. However, even if the factor $(1 - f)$ as given in Appendix 1 were in error by 15%, the error in f is less than $\pm 2\%$ because in almost all cases $(1 - f) < 0\cdot1$. The total uncertainty in σ_S was estimated to be $\pm 2\%$.

RESULTS

Solubility measurements

The directly determined solubility isotherms obeyed Henry's law. *Figures 2* and *3* which illustrate this for gases in polyethylene also show that there is very little scatter of the experimental points. Accordingly, in each polymer accurate values of σ_S were derived, and these are summarised, together
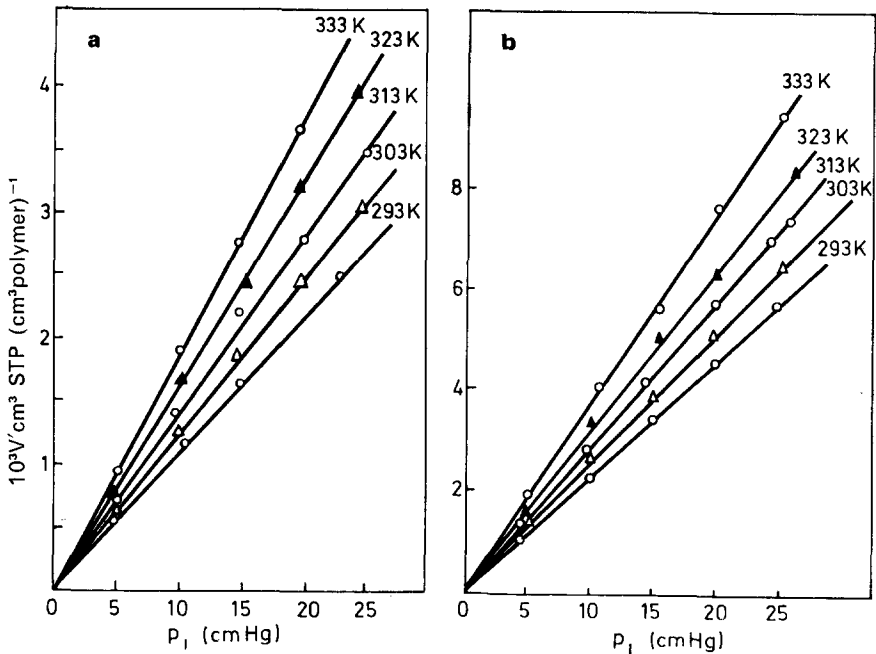
Figure 2 Solubility isotherms in polyethylene over a range of temperatures for (a) neon and (b) hydrogen

425
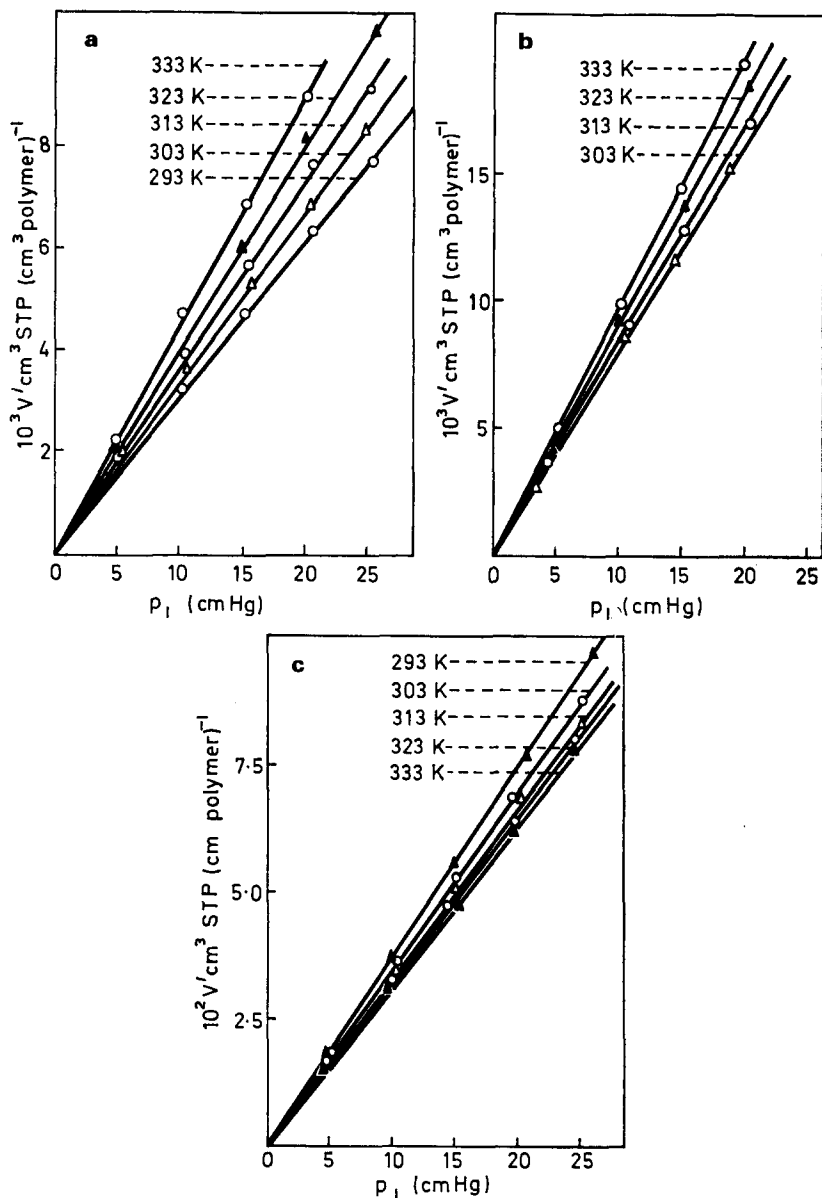
Figure 3 Solubility isotherms in polyethylene for (a) nitrogen (b) argon and (c) carbon dioxide

with values for σ_L obtained as the quotient P/D_L (equation 4), in *Tables 1* and *2*. σ_S and σ_L are in excellent agreement for Nylon 11 but for polyethylene σ_S/σ_L is consistently greater than unity. In this polymer, therefore, there is evidence of anomalous diffusion (cf. ref. 8). As the boiling points of the gases increase the temperature coefficients of the solubilities change from

Table 1 Values of P, D_L, σ_L and σ_s for Nylon 11

Gas	T/K	$D_L \times 10^7$	$P \times 10^9$	σ_L	σ_S	σ_S/σ_L	P_{He}/P_{gas} at 313·2 K
He	283·2	18·5	7·00	0·0038	—	—	—
	293·2	25·5	10·1	0·0040	—	—	
	303·2	35·0	14·8	0·0043	—	—	
	313·2	46·7	21·4	0·0045	—	—	
	323·2	59·1	30·8	0·0052	—	—	
Ne	293·2	—	—	—	0·0054	—	
	303·2	4·37	2·63	0·0060	0·0056	0·93	
	313·2	6·66	4·09	0·0062	0·0062	1·00	5·2
	323·2	9·55	6·04	0·0063	0·0065	1·03	
	333·2	14·2	9·62	0·0068	0·0066	0·97	
Ar	313·2	0·372	1·45	0·039	0·039$_1$	1·00	14·8
	323·2	0·618	2·30	0·037	0·038$_8$	1·05	
	333·2	1·05	3·78	0·036	0·037$_7$	1·05	
H₂	293·2	6·50	9·19	0·0141	0·0145	1·03	
	303·2	9·84	13·6	0·0138	0·0148	1·07	
	313·2	14·9	20·1	0·0135	0·0150	1·11	1·06
	323·2	19·7	29·7	0·0151	0·0158	1·05	
	333·2	28·6	43·6	0·0152	0·0163	1·07	
CO₂	313·2	0·191	7·64	0·40	0·368	0·92	2·8
	323·2	0·347	10·8	0·31	0·314	1·01	
	333·2	0·633	16·3	0·257	0·280	1·09	

positive (He, Ne, H₂, N₂ and Ar in polyethylene; and He, Ne and H₂ in Nylon 11) to negative (CO₂ in polyethylene; Ar and CO₂ in Nylon 11).

In both polymers log σ was a linear function of reciprocal temperature for each gas. From these straight lines heats of solution ΔH_{σ_S} were obtained and are included in *Tables 3* and *4*. In Nylon 11 there is the expected reasonable agreement between ΔH_{σ_S} and ΔH_{σ_L}. This is also true of polyethylene for most of the gases despite the anomalous diffusion which can make σ_L less accurate when determined from the time-lags and permeability coefficients. Values of ΔH given in brackets in *Table 4* are heats of solution reported Michaels by and Bixler[7].

Diffusion and permeability

Diffusion and permeability coefficients are summarised in *Table 1* for Nylon 11 and in *Table 2* for polyethylene. Plots of log D_L against K/T and similar plots of log P, were good straight lines with little scatter of experimental points. From them were obtained activation energies E_D and E_P for diffusion and permeation (*Tables 3* and *4*). E_D for polyethylene agrees well with the values of Michaels and Bixler[7] given in brackets in *Table 4*.

Table 2 Values of P, D_L, σ_L and σ_S for polyethylene

Gas	T/K	$D_L \times 10^6$	$P \times 10^8$	σ_L	σ_S	σ_S/σ_L	P_{He}/P_{gas} at 313·2 K
He	283·2	6·1	2·24	0·0037	—	—	
	293·2	8·2	3·60	0·0044	—	—	
	303·2	10·8	5·78	0·0053	—	—	
	313·2	13·8	8·99	0·0065	—	—	
	323·2	18·2	13·4	0·0075	—	—	
Ne	293·2	2·16	1·42	0·0066	0·0087	1·32	
	303·2	2·96	2·34	0·0079	0·0097	1·23	
	313·2	4·41	3·80	0·0087	0·0111	1·28	2·4
	323·2	5·75	5·72	0·0100	0·0126	1·26	
	333·2	8·1	9·40	0·0116	0·0144	1·24	
Ar	293·2	0·351	1·74	0·0496	—	—	
	303·2	0·624	3·29	0·0528	0·0615	1·16	
	313·2	1·02	5·78	0·0566	0·0640	1·13	1·6
	323·2	1·59	9·38	0·0591	0·0690	1·17	
	333·2	2·40	14·8	0·0615	0·0734	1·19	
H_2	293·2	3·87	5·55	0·0143	0·0181	1·27	
	303·2	5·67	9·09	0·0160	0·0200	1·25	
	313·2	8·51	14·6	0·0171	0·0223	1·30	C·62
	323·2	10·6	22·1	0·0209	0·0249	1·19	
	333·2	15·6	33·3	0·0214	0·0291	1·36	
N_2	293·2	0·317	0·599	0·0189	0·0239	1·26	
	303·2	0·545	1·200	0·0220	0·0262	1·19	
	313·2	0·910	2·20	0·0241	0·0287	1·19	4·1
	323·2	1·48	3·76	0·0255	0 0310	1·22	
	333·2	2·21	6·21	0·0281	0·0350	1·25	
CO_2	293·2	0·328	9·15	0·279	0·321	1·15	
	303·2	0·573	15·2	0·264	0·301	1·14	
	313·2	C·968	24·0	0·248	0·289	1·17	0·38
	323·2	1·52	34·4	0·227	0·283	1·26	
	333·2	2·34	51·4	0·219	0·273	1·25	

Table 3 Apparent activation energies and heats of solution in kcal mol^{-1} for Nylon 11 (1 kcal mol^{-1} = 4·18 kJ mol^{-1})

Gas	E_P	E_D	$\triangle H_{\sigma_L}$	$\triangle H_{\sigma_S}$
He	6·6$_9$	5·3$_1$	1·3$_8$	—
Ne	8·4$_7$	7·8$_7$	0·6$_0$	1·0
Ar	10·0	10·7	−0·7	−0·4
H_2	7·5$_5$	7·1$_8$	0·3$_7$	0·5
CO_2	8·1	12·4	−4·3	−3·2

Table 4 Apparent activation energies and heats of solution in kcal mol^{-1} for polyethylene (1 kcal mol^{-1} = 4·18 kJ mol^{-1}. The figures in brackets are from Michaels and Bixler[7]

Gas	E_P	E_D	ΔH_{σ_L}	ΔH_{σ_S}
He	8·1$_6$ (8·3)	4·9$_2$ (5·9)	3·2$_4$ (2·5)	—
Ne	9·0$_0$ —	6·4$_6$ —	2·5$_4$ —	2·5
Ar	10·2$_4$ (10·8)	9·3$_6$ (9·9)	0·8$_8$ (0·1)	1·1
H_2	8·6$_5$ —	6·7$_1$ —	1·9$_4$ —	2·2
N_2	11·3$_2$ (11·8)	9·4$_0$ (10·1)	1·9$_2$ (1·9)	1·8
CO_2	8·2$_6$ (9·3)	9·6$_0$ (9·2)	−1·3$_4$ (0·1)	−0·7

428

DISCUSSION

Solubility

Both Nylon 11 and polyethylene are partially crystalline, so that values of ΔH will include a contribution from possible melting of crystals as the temperature rises. According to the manufacturers, the volume fraction of amorphous polymer in the Nylon was $\sim 80\%$. For the polyethylene, from its specific volume and from the specific volumes of amorphous and fully crystalline polymer[7], the amorphous volume fraction was estimated to be $\sim 56\%$. Accepting these figures, one may correct the solubility coefficients to correspond with the 100% amorphous Nylon 11 and polyethylene. This neglects any temperature dependence of the crystalline fractions which may also influence the isotherms and hence the heats, because gases dissolve only in the amorphous regions of the polymers. The corrected values of σ at 298·2 K are given in *Table 5*, the figures in brackets included for comparison,

Table 5 σ at 298·2 K for 100% amorphous Nylon 11 and polyethylene and at 273·2 K for silicone elastomer

| Gas | σ | | Silicone Rubber |
	Nylon 11	Polyethylene	SiR-I[4]
He	0·0051*	0·0088* (0·012*)	0·043*
Ne	0·0069	0·016	0·090*
Ar	0·050	0·108 (0·103*)	0·34$_2$*
H$_2$	0·0175	0·034	0·074*
N$_2$	—	0·045 (0·014*)	0·203*
CO$_2$	0·59$_5$	0·557 (0·451*)	—

* These figures are values of σ_L

being those obtained by Michaels and Bixler[7]. Values for silicone rubber[4] at 273·2 K are also included. Except for the polar CO_2 molecule, *Table 5* indicates the order of solubility coefficients for a given gas to be: amorphous Nylon 11 < amorphous polyethylene < silicone SiR-I. This sequence is reasonable since uptake is expected to increase the smaller the difference in cohesive energy density between the liquefied gas and the elastomer. It is also seen that part of the very high permeability[4] of silicone elastomers relative to the other polymers arises from the higher solubility of gases in it.

In *Figures 4a* and *4b*, log σ for 100% amorphous polymer is plotted against the Lennard-Jones parameter, ϵ/k, (ref. 9) of the gases, in polyethylene and in Nylon 11. There are clear but not exact correlations which approximate to the form

$$\log \sigma = A + B\epsilon/k \tag{7}$$

where A and B are constants at any one temperature. The equations of the straight lines in *Figure 4* are:

$$\log \sigma = -2 \cdot 03 + 0 \cdot 0093 \ \epsilon/k \text{ (polyethylene at 298·2 K)}$$
$$\log \sigma = -2 \cdot 41 + 0 \cdot 0111 \ \epsilon/k \text{ (Nylon 11 at 298·2 K)}.$$

These relations may be compared with that obtained by Barrer and Chio[4] for the silicone rubber:

$$\log \sigma = -1 \cdot 44 + 0 \cdot 0089 \ \epsilon/k \text{ (SiR-I at 273·2 K)}$$
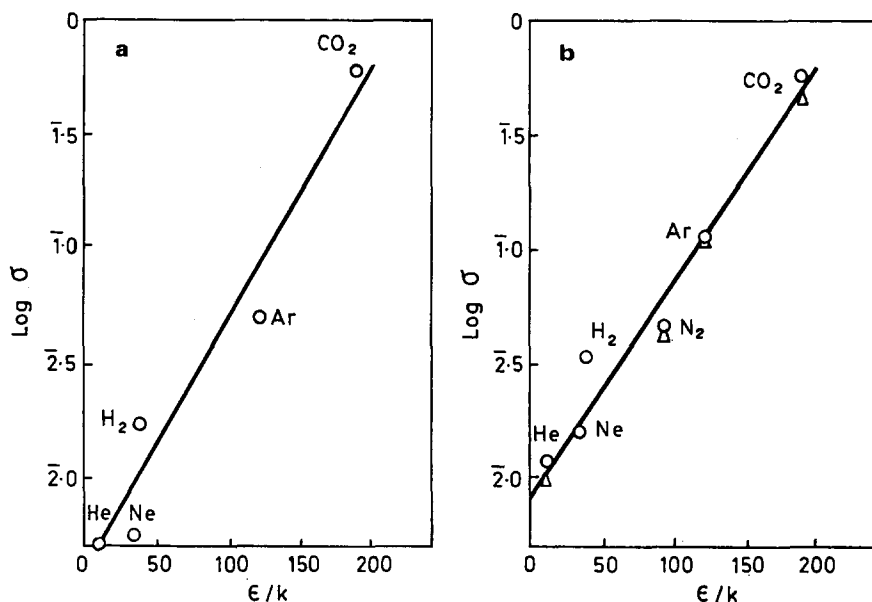
Figure 4 Relationship between log σ and the Lennard-Jones parameter ϵ/k for (a) Nylon 11 and (b) polyethylene.
$\bigcirc$, this work; $\triangle$, Michaels and Bixler[7]

In *Figure 4b* are included points obtained by Michaels and Bixler[7] for amorphous polyethylene. Their linear correlation differed only slightly from the equation given above. Such equations serve to give a first approximation to σ for any simple gas or vapour for which ϵ/k is known.

Permselectivities

In *Tables 1* and *2* are given the ratios of the permeability of helium to that of each of the other gases. These ratios are the steady-state separation factors for helium in the binary gas mixtures. Permeability coefficients for polyethylene are an order of magnitude greater than those of the harder Nylon polymer but the separation factors in polyethylene are correspondingly lower. High permselectivity is associated with low permeability [10] and is maximized in the case of the very rigid tightly crosslinked network of silica glass[11]. Changes in selectivity for a given helium+gas pair, on going from Nylon to polyethylene result more from changes in diffusion than solubility coefficients. For example D_{He}/D_{Ar} is 125 for Nylon 11 and 13·5 for polyethylene at 312·2 K.

Activation energies and molecular dimensions

In order to see how far E_D, and hence possibly D, may be related to simple molecular properties, E_D is plotted as a function of the van der Waals cross-sectional diameters, cross-sectional areas and molecular volumes of the diffusants in Nylon 11, polyethylene and two silicone elastomers[4] (*Figures 5a, b* and *c*). In the calculations the van der Waals molecular dimensions
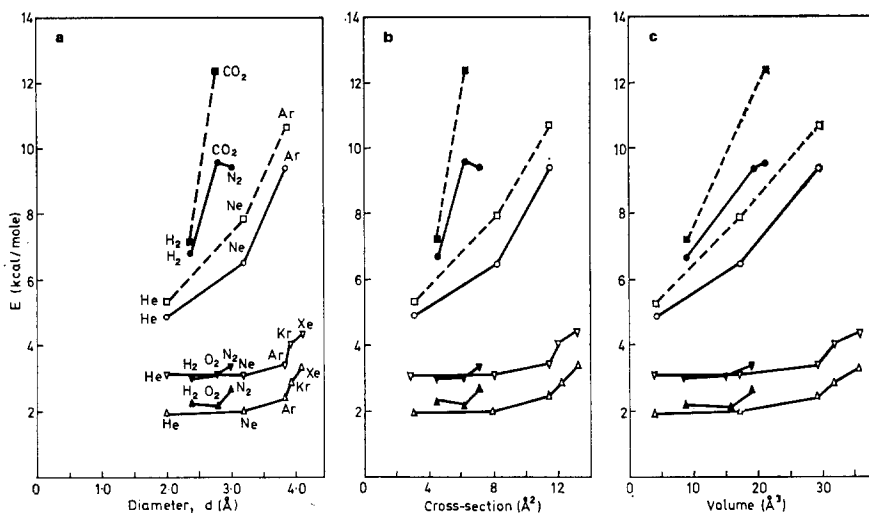
Figure 5 Energies of activation for diffusion as a function of (a) cross-sectional diameter; (b) cross-sectional area; and (c) volume of simple penetrant molecules, in several polymeric media.
□, ■ Nylon 11; ○, ● Polyethylene;
△, ▲ SiR-I; ▽, ▼ SiR-M

l_1, l_2, and l_3 (measured in metres $\times 10^{10}$) in three directions at right angles (one chosen to lie along the axis of dumbbell-shaped molecules) were:

Gas	He	Ne	Ar	Kr	Xe	H_2	O_2	N_2	CO_2
$l_1 = l_2$	~ 2·0	3·2	3·83	3·94	4·1	2·4	2·8	3·0	2·8
l_3	~ 2·0	3·2	3·83	3·94	4·1	3·0	3·8	4·08	5·2

The volume was expressed as the volume of the ellipsoid for the dumbbell-shaped molecules. From *Figure 5* it is seen that:

(1) the most nearly linear relationships arise when the abcissa is the molecule volume;

(2) the dumbbell-shaped molecules appear to be differentiated from the spherically symmetrical ones in that E_D lies on a different curve. The difference is minimal however for the most liquid-like silicone elastomers;

(3) the magnitude of E_D, as well as its variation with molecular dimensions, is greatest for the most rigid of the polymers, Nylon 11, and is least for the most liquid-like silicones.

Relations between E_D and molecular dimensions are evidently not simple and this led to the further examination shown in *Figures 6a* and *6b* for a butyl rubber[12], variously crosslinked natural rubbers[13] and for silicone rubbers[4, 14] in all of which studies the values of E_D for hydrocarbons were included. The van der Waals dimensions used for the hydrocarbons were, (in metres $\times 10^{10}$):

431

Hydro-carbon	CH_4	C_2H_6	C_3H_8	n-C_4H_{10}	n-C_5H_{12}	iso-C_4H_{10}	iso-C_5H_{12}	neo-C_5H_{12}
l_1	4·0	4·0	4·0	4·0	4·0	4·51	4·51	5·78
l_2	4·0	4·0	4·89	4·89	4·89	6·18	6·18	5·78
l_3	4·0	5·54	6·52	7·77	9·04	6·51	7·77	5·78

The assumption of the ellipsoid of revolution for n-paraffins C_4 and C_5 may underestimate the molecular volumes; also the calculation of cross-sectional area and of molecular volume assumes that these two species diffuse in a stretched configuration. Irregularities in the results in *Figures 6a* and *6b*
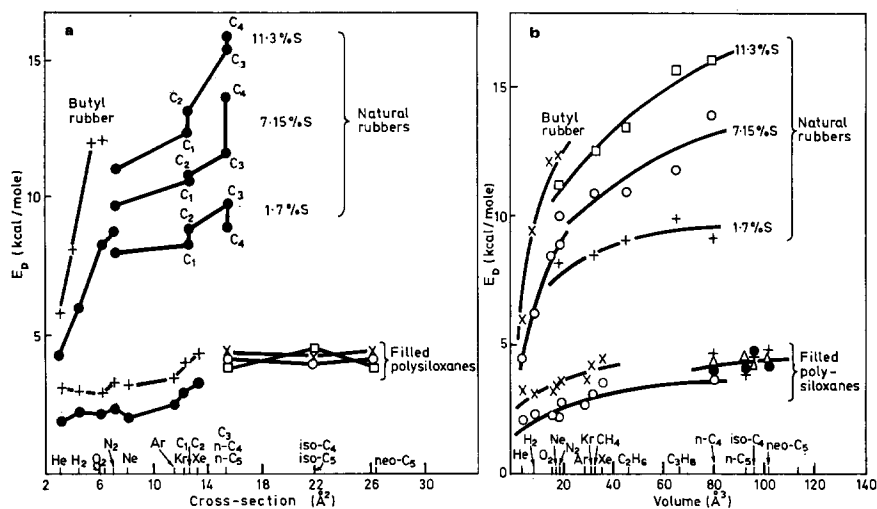
Figure 6 Energies of activation for diffusion as a function of (a) cross-section and (b) volume of molecules including hydrocarbons in variously crosslinked natural rubbers and in butyl and poly(siloxane) elastomers

show that E_D depends to some extent upon molecular shape of the paraffins. In confirmation of the results in *Figure 5*, therefore, correlations between E_D and overall molecular dimensions are likely to be satisfactory only when sequences of diffusants of similar shape or symmetry are being compared (e.g. CH_4, CF_4, CCl_4, CBr_4). There is, moreover, a tendency, especially when molecular volume is the abcissa, for the curves to flatten so that, despite the contrary appearance of the more restricted series of *Figure 5a* and *5b*, E_D may at least for chain molecules in elastomers become less sensitive to molecular volume as this volume increases.

CONCLUSION

Direct measurements of the low solubilities of gases in polymers can now be made with considerable accuracy if corrections are applied to allow for the

loss of gas during the flushing procedure. An exception arises in the case of helium which dissolves in the pyrex glass walls of the apparatus[15]. For this reason no direct measurements of solubility of helium were made in the present work and the most reliable procedure would still appear to be the flow method ($P = D\sigma$; and, for a slab, $D = l^2/6L$). However, anomalous diffusion effects can make the time-lag relationship $D = l^2/6L$ inaccurate. Such effects may arise from partial crystallization of the polymer, which can, for example, introduce blind pore character in the polymer, making D time-dependent[16]. There is evidence of such effects in the polyethylene but not the Nylon 11[8].

Physical Chemistry Laboratories,
Chemistry Department,
Imperial College,   *(Received 5 March 1970)*
London S.W.7   *(Revised 7 May 1970)*

REFERENCES

1 Barrer, R. M. *Trans. Faraday Soc.* 1947, **42**, 3
2 Michaels, A. S. and Bixler, H. J. in 'Progress in separation and purification' (ed. E. S. Perry), Interscience, New York, 1968, p 143
3 Stannett, V., 'Diffusion in polymers', (eds. J. Crank and G. S. Park), Academic Press, London, 1968, chap. 2
4 Barrer, R. M. and Chio, H. T. *J. Polym. Sci. (C)* 1965, **10**, 111
5 Meares, P. *Trans. Faraday Soc.* 1958, **54**, 40
6 Draisbach, H., Jeschke, D. and Stuart, H. A. *Zeit. Naturforsch.* 1962, **17a**, 447
7 Michaels, A. S. and Bixler, H. J. *J. Polym. Sci.* 1961, **50**, 393 and 413
8 Ash, R., Barrer, R. M. and Palmer, D. G. *Trans. Faraday Soc.* 1969, **65**, 121
9 Jolley, J. E. and Hildebrand, J. H. *J. Amer. Chem. Soc.* 1958, **80**, 1050
10 Barrer, R. M., Barrie, J. A. and Wong, P. S-L. *Polymer, Lond.* 1968, **9**, 609
11 Norton F. J. 'Transactions of the 8th Vacuum Symposium and 2nd International Congress', Pergamon, New York, 1962, p 8
12 van Amerongen, G. J. *J. Polym. Sci.* 1950, **5**, 307
13 Barrer, R. M. and Skirrow, G. *J. Polym. Sci.* 1948, **3**, 549
14 Barrer, R. M., Barrie, J. A. and Raman, N. K. *Polymer, Lond.* 1962, **3**, 595
15 Ash, R., Barrer, R. M., Barrie, J. A., Palmer, D. G. and Wong, P. S-L. *Chem. Comm* 1966, p 334
16 Ash, R., Baker, R. W. and Barrer, R. M. *Proc. Roy. Soc.* 1968, **304A**, 407

433

APPENDIX

Calculation of the gas lost during flushing

The sequence of events during flushing can be represented by the following diagram.
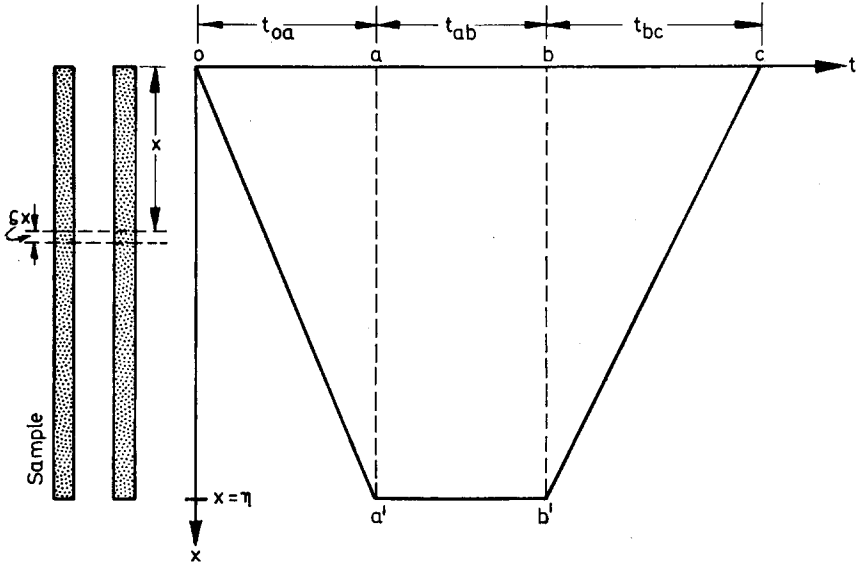
Figure 7 Explanatory diagram for calculating the gas lost during flushing:
oa′—mercury lowered at a constant rate; a′b′—entire sample exposed;
b′c—mercury raised at a constant rate

Let m_t be the quantity of gas lost from unit length of the sample in a time t and m_∞ the corresponding quantity in infinite time. Assuming that diffusion is radial only and that the longest time for which part of the sample is exposed t_{oc}, is sufficiently short for the 'short-time' solution of the diffusion equation to be valid, we write

$$\frac{m_t}{m_\infty} = 4 \left(\frac{Dt}{\pi l^2} \right)^{\frac{1}{2}} = \frac{0.92}{L^{\frac{1}{2}}} \times t^{\frac{1}{2}} \tag{8}$$

where we have substituted $D/l^2 = 1/6L$
The small segment δx is exposed for a time t given by

$$t = (t_{oa} + t_{bc}) (1 - x/\eta) + t_{ab} \tag{9}$$

and in this time it will have lost an amount of gas

$$m_t \, \delta x = \frac{0.92}{L^{\frac{1}{2}}} \times m_\infty \times t^{\frac{1}{2}} \, \delta x$$

434

The total quantity lost during flushing, $M_{t_{oc}}$, is obtained by summing δx from $x = 0$ to $x = \eta$. i.e.

$$M_{t_{oc}} = \frac{0 \cdot 92}{L^{\frac{1}{2}}} \times m_\infty \int_0^\eta t^{\frac{1}{2}} \, dx \qquad (10)$$

The total quantity lost from the whole membrane in infinite time M_{t_∞} is given by $M_{t_\infty} = m_\infty \times \eta$.

Substituting for t from equation (9) and integrating yields

$$1 - \frac{M_{t_{oc}}}{M_{t_\infty}} = 1 - \frac{0 \cdot 92}{L^{\frac{1}{2}}} \times \frac{2}{3} \left[\frac{t^{\frac{3}{2}}_{oc} - t^{\frac{3}{2}}_{ab}}{t_{oc} - t_{ab}} \right] = \frac{p'_\infty}{p_\infty} = f \qquad (11)$$

Notes to the Editor

The effects of pressure and temperature on the densities of liquid polymers

J. C. McGowan

Relationships between the volume, pressure and temperature of polymeric and other liquids have been put forward in two previous papers[1,2]. In these relationships, the volume was divided by a characteristic volume and the temperature by a characteristic temperature. However, since the pressure was not divided by a characteristic pressure, the relationships did not conform to the principle of corresponding states. For example equation (1) was used:

$$\frac{21 V_p (\rho_{l_0} - \rho_g)}{M} = \frac{1}{\kappa_0^{\frac{1}{6}}} \tag{1}$$

where in c.g.s. units V_p is the parachor

M is the molecular weight

ρ_{l_0} is the density of the liquid and

κ_0 its isothermal compressibility under negligible pressure and

ρ_g is the vapour density

It is now proposed to rewrite equation (1) as (2)

$$\frac{\phi (\rho_{l_0} - \rho_g)}{M} = \left(\frac{1}{\pi \kappa_0} \right)^{\frac{1}{6}} \tag{2}$$

where ϕ is a characteristic volume and π is a characteristic pressure. The equation is now correct dimensionally. In c.g.s. units ϕ, which is now a volume, equals the parachor as before and π equals 21^6 or $8 \cdot 58 \times 10^7$ dyn cm^{-2}. In SI units ϕ, m^3 mol^{-1}, equals the parachor (calculated as before) $\times 10^{-6}$, M in kg mol^{-1} will be one thousandth the c.g.s. units; ρ in kg m^{-3} will be a thousand times the c.g.s. units; π equals $8 \cdot 58 \times 10^6$ N m^{-2} and κ_0 will be in m^2 N^{-1}. The other equations can be modified in the same way. The characteristic temperature which was called T_c' was shown[2] to equal θ which was used earlier by Bondi and Simkin[3] and it is proposed now to use θ. The equations put forward previously[1,2] can now be modified and the general equation relating density ρ_1, pressure P and temperature T of a liquid can for example be written as (3).

$$\frac{9P}{\pi} \left[32 \cdot 25 - 32 \cdot 25 \frac{T}{\theta} \right]^{0.9} = \left[\frac{\phi (\rho_l - \rho_g)}{M} \right]^{9} - \left[32 \cdot 25 - 32 \cdot 25 \frac{T}{\theta} \right]^{2.7} \tag{3}$$

It is of interest that from equation (3), the pressure in liquids produced by temperature changes at constant volume can be estimated. Some results are shown in *Figure 1*. The pressure was taken as zero at 298·15 K and the curves were calculated for some values of θ in the range which includes many of the common polymers. These curves may be useful in studies on the extrusion of polymers. The pressure changes can be high. For example, for a liquid with $\theta = 800$ K, a change in temperature from 298 K to 373 K at a constant volume should give a pressure of $8·77 \times 10^7$ N m^{-2} (or 866 atm).

Since M equals the molar volume V and ρ_g can usually be neglected compared with ρ_l, the isothermal work $\int P\delta V$ for change of volume of a liquid can often be calculated. In forthcoming publications, it is proposed to discuss the relationship of this work to the viscosity of the liquid and miscibility of liquids.
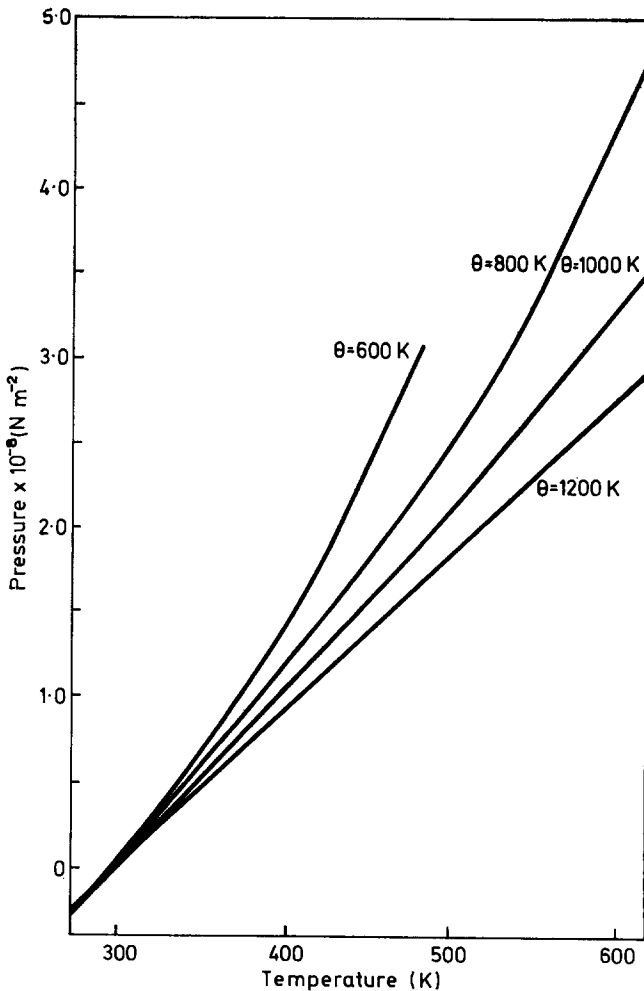
Figure 1 Pressure from rise of temperature

Imperial Chemical Industries Limited,
Research Department,
Bessemer Road,
Welwyn Garden City,
Hertfordshire

REFERENCES

1 McGowan, J. C. *Polymer, Lond.* 1967, **8**, 57
2 McGowan, J. C. *Polymer, Lond.* 1969, **10**, 841
3 Bondi, A. and Simkin, D. J. *Amer. Inst. Chem. Engineers' J.* 1960, **6**, 191

Mechanism of enviromental stress cracking in high impact polystyrene

P. J. CORBETT and D. C. BOWN

High impact polystyrene is a composite material containing a rubbery phase of particle size around 2–5μm dispersed in a polystyrene matrix[1]. We have studied the fracture surfaces obtained by rupture in a number of hostile environments. The fracture surfaces were vacuum metallized with a gold-palladium alloy to render them conducting and examined with a scanning electron microscope. The study reveals that the adhesion between the phases is greatly reduced by a number of organic liquids which are poor solvents for polystyrene; these liquids cause desocketing of the rubber particles.

In air at room temperature, the fracture surface does not reflect the rubber particle features, except in some cases at the point of initiation of a crack. For example, the fracture surface of an ASTM tensile specimen, which has been compression moulded and then ruptured according to ASTM Test No. D638-64T, exhibits the well-known sequence of initiation at a flaw at the interior, or more commonly, at the edge of the specimen[2]. The crack grows around this point to give a circular or fan-shaped area which then gives way to a rougher area which occupies the remainder of the fracture surface. These areas correspond to the 'mist and hackle' regions as defined by Andrews[3]. Neither of these regions have a structure which resembles the rubbery phase. From this it is inferred that the fracture path passes through the rubbery phase undeflected.

In contrast, when the specimen is ruptured in a hostile environment (e.g. *n*-heptane) the rubber particles are clearly seen to have been detached from their sockets. The fine detail of yielding and nodule formation of the matrix is also clearly visible. This matrix structure is similar to that obtained by the fracture of unmodified polystyrene in air[4, 5].

Imperial Chemical Industries Limited,
Research Department,
Bessemer Road,
Welwyn Garden City,
Hertfordshire

REFERENCES

1 McGowan, J. C. *Polymer, Lond.* 1967, **8**, 57
2 McGowan, J. C. *Polymer, Lond.* 1969, **10**, 841
3 Bondi, A. and Simkin, D. *J. Amer. Inst. Chem. Engineers' J.* 1960, **6**, 191

Mechanism of enviromental stress cracking in high impact polystyrene

P. J. CORBETT and D. C. BOWN

High impact polystyrene is a composite material containing a rubbery phase of particle size around 2–5μm dispersed in a polystyrene matrix[1]. We have studied the fracture surfaces obtained by rupture in a number of hostile environments. The fracture surfaces were vacuum metallized with a gold-palladium alloy to render them conducting and examined with a scanning electron microscope. The study reveals that the adhesion between the phases is greatly reduced by a number of organic liquids which are poor solvents for polystyrene; these liquids cause desocketing of the rubber particles.

In air at room temperature, the fracture surface does not reflect the rubber particle features, except in some cases at the point of initiation of a crack. For example, the fracture surface of an ASTM tensile specimen, which has been compression moulded and then ruptured according to ASTM Test No. D638-64T, exhibits the well-known sequence of initiation at a flaw at the interior, or more commonly, at the edge of the specimen[2]. The crack grows around this point to give a circular or fan-shaped area which then gives way to a rougher area which occupies the remainder of the fracture surface. These areas correspond to the 'mist and hackle' regions as defined by Andrews[3]. Neither of these regions have a structure which resembles the rubbery phase. From this it is inferred that the fracture path passes through the rubbery phase undeflected.

In contrast, when the specimen is ruptured in a hostile environment (e.g. *n*-heptane) the rubber particles are clearly seen to have been detached from their sockets. The fine detail of yielding and nodule formation of the matrix is also clearly visible. This matrix structure is similar to that obtained by the fracture of unmodified polystyrene in air[4, 5].

438

Figure 1 Electron micrograph of fracture surface of high impact
polystyrene ruptured in *n*-heptane
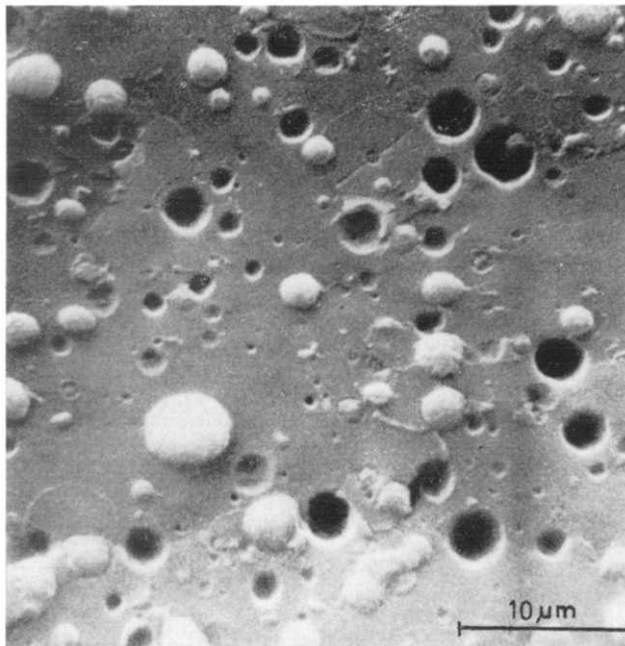
Figure 2 Electron micrograph of fracture surface of high impact
polystyrene ruptured in white spirit

The fracture surface obtained in white spirit (b.p. 150–200°C) gives rise to a finer matrix structure which could not be resolved with the scanning electron microscope.

Acetone produced a similar phenomenon of desocketing but with considerable blurring of the detail in the matrix, since acetone does have a solvation effect upon polystyrene.

It is worth noting that the edible oils and fats produce fracture surfaces which are similar to those produced by the organic liquids mentioned above. Thus the in service failure of high impact polystyrene in those applications in which it meets a hostile oil or fat environment, (e.g. in foodstuff packaging) may be one in which the rubber modification produces a smaller contribution to the 'toughness' of the material than is usually the case.

ACKNOWLEDGEMENTS

Research and Development Department,
Dow Chemical Company Limited,
Hayes Road, Sully, Nr. Penarth,
Glamorgan, Wales

REFERENCES

1 Molau, G. E. and Keskkula, H. *J. Polym. Sci. (A-1)* 1966, **4**, 1595
2 Murray, J. and Hull, D. *Polymer, Lond.* 1969, **10**, 451
3 Andrews, E. H., 'Fracture in Polymers', Oliver and Boyd, Edinburgh and London, 1968 p 184
4 Bird, R. J., Mann, J., Pogany, G. and Rooney, G. *Polymer, Lond.* 1966, **7**, 307
5 Haward, R. N. and Brough, I. *Polymer, Lond.* 1968, **10**, 724

Snarl splitting in polyethylene

R. Greer and J. W. S. Hearle

We have observed a novel form of fibre fracture in studies of fibre twisting. When a fibre is highly twisted it will, unless there is a large enough tensile load, snarl. Two forms of snarl occur: the commonest is a two-ply snarl at right angles to the original fibre axis (*Figure 1a*) but sometimes the fibre forms a single tight helix, like a coiled spring, on its own axis (*Figure 1b*). The onset of snarling normally occurs spontaneously when the torque reaches the critical level required to promote buckling, but it can also be induced by reducing the tensile load on a highly twisted fibre.
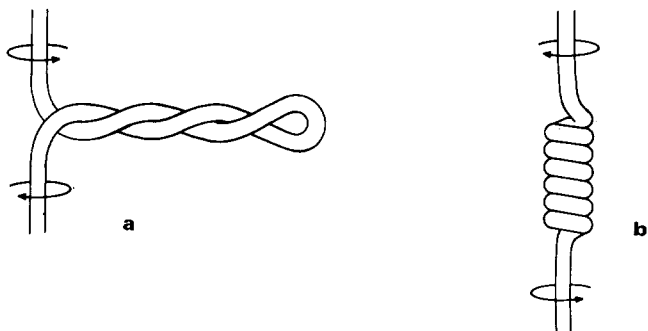
Figure 1 Snarls: (a) perpendicular; (b) parallel

By proper control of tensioning, we obtained the coil-spring snarling in a twisted polyethylene monofilament, and the resultant splitting may be a useful way of disrupting the fibre for structural studies. The appearance in a scanning electron microscope is shown in *Figures 2a* and *2b*. The fibre has split, with many fibrils peeling off, lying across the split and linking its two sides. This bursting of the surface is a consequence of the stress distribution in the system.
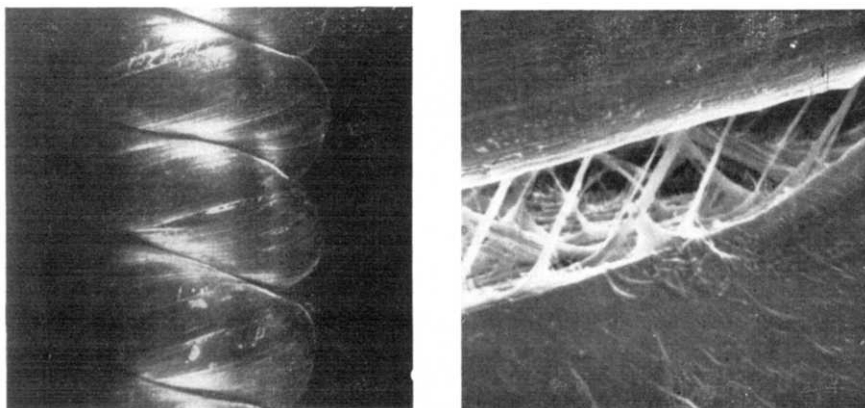
Figure 2 (a) Snarled polyethylene showing split; (b) enlarged view of region of split

The twisting gives rise to shear stress along the lines of twist, shown in *Figures 3a* and *3b* before and after snarling. However, the snarl involves a bending of the fibre with a resultant stretching of the outer surface of the bend. The split then occurs in the tensioned fibre surface along lines which are already under high shear stress. The linking of the two surfaces by fibrils will be due to the split starting in several places and following different lines.
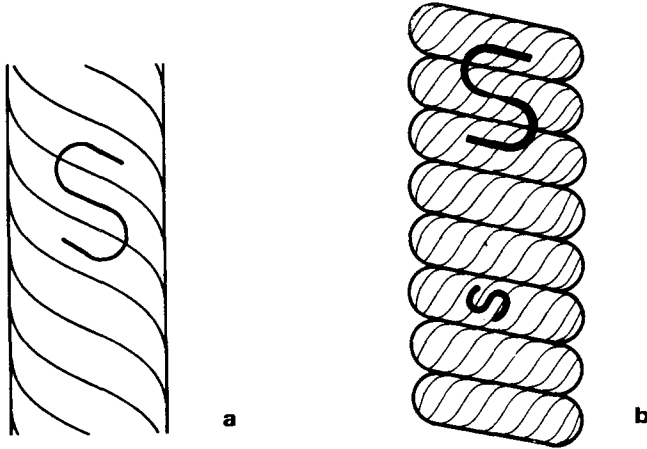
Figure 3 Lines of twist: (a) before snarl; (b) in snarl

One interesting feature of the split, shown in the enlarged view in *Figure 2b* is that on one side of the split the surface is little changed, and still shows the helical wrap lines; but that these lines have been obliterated on the other side, where the surface is covered with rather irregular short ridges.

The fibrils linking the two surfaces have thickness between 900 and 2600Å (90 and 260 nm), and the network which they form gives some insight into the internal structure of the material.

Department of Textile Technology,
University of Manchester Institute of Science and Technology,
Manchester, UK   *(Received 14 May 1970)*

Book Reviews

Hochtemperatur-beständige Kunststoffe

by ERICH BEHR

Carl Hanswer Verlag, Munich, 1969, 140pp., 30 DM

Considerable effort has been devoted during the past ten to twenty years to the synthesis of polymers of improved thermal stability and numerous review articles on the subject have now appeared in the literature. *Hochtemperatur-beständige Kunststoffe* is one of the first books on the topic. It is important in assessing this book to consider the stated aims of the author in writing it; these are to describe briefly new high temperature plastics, their formulae, preparation, properties and possible uses, to outline significant progress for the non-chemist, and to stimulate interest, specifically in Germany, in these materials. 'New polymers' are defined as those developed during the past five to ten years and 'heat–resistant plastics' as those having capabilities of use above 150°C. As a consequence of these aims, the treatment has been selective both in respect of the polymers detailed and the literature references cited. Greatest progress in producing useful thermally stable materials has been made with those polymers containing aromatic or heterocyclic groups in the backbone and most of the book is devoted to these, particular attention being given to those polymers which have reached commercial production.

The book is divided into two parts, the first (up to page 46) considering various parameters, which are important in determining the maximum temperature of utilization of plastics e.g. softening point, heat distortion point, glass transition temperature, weight loss, oxygen absorption, change in mechanical properties. This section also mentions ways of improving high temperature resistance e.g. by the addition of stabilizers, reinforcing fillers, crosslinking agents and by synthetic variations such as improved order, fluorination, co-ordination, or use of inorganic backbones. Finally the approach to thermally stable polymers via bond dissociation energy values, or the stability of model compounds is briefly considered.

The second and larger part of the book is devoted to aromatic and heterocyclic polymers, these being subdivided into those in which the rings are linked by single bonds and the so-called 'step-ladder' and 'ladder' polymers. As mentioned earlier emphasis has been very much laid on those polymers, which are commercially available e.g. no less than fourteen pages of this section are devoted to the polyimides, details being given of trade names, manufacturers and prices, as well as of typical properties. In comparison, other polymers are given very cursory treatment.

How far have the aims of the book been achieved? Certainly a good birds-eye view has been given of developments in one particular area of the thermally stable polymer field and the non-chemist would readily appreciate which of the developments are at present commercially significant. Possible stimulation of interest is more difficult to assess. Certainly those working in the field would not be satisfied as they now require detailed critical assessments of the vast amount of published literature. Possible users of the materials, on the other hand, would want more data on properties and fabrication procedures.

The setting and format of the book are very pleasant indeed, but at a cost of approximately 70s, it is probable that those in this country seeking the information it contains will turn in preference to one of the existing reviews in English.

W. W. WRIGHT

Gaps in Technology—Plastics

This publication is a useful collection of statistical information on the plastics industry particularly in Europe and the USA. It is a handy reference book for those who wish to search out such data at present widely scattered. It does not, unfortunately, as the title implies, really point out the gaps in technology for the hopeful technical man who might expect to read how he can enter some rewarding field to fill a gap.

The book is essentially an objective study of information which is already well known but has been brought together.

The progress of OECD member countries is examined on a comparative basis. The main concern of the study is not with so much the gaps in technology as the continued development of the markets in the context of technological innovation in recent years. An important distinction is drawn between the large-tonnage plastics, where no general technological or production gap exists between the USA and the rest, and the specialised plastics where the USA has a lead over Europe.

A great deal of comparative data is included on turnover, manpower, investment, research, training and the general structure of the plastics industry in each country. There are also useful sections covering taxation, tariff barriers, and patent legislation.

The growth of the industry historically is well explained with reference to the forces which have resulted in rapid development and technical innovation in some countries while others experienced relatively slow growth. To illustrate this point, Freeman's table 'Chronology of the Discovery and Development of Synthetic Resins' and Hufbaur's 'First Commercial Production of Various Plastics Materials' are reproduced. A number of case histories demonstrate development of production processes for polyolefins, PVC, polystyrene, and some of the newer materials.

In general, the study is a useful general guide to the plastics industry in relation to economic conditions in OECD countries. However, the statistics are usually based on official returns and these are generally grossly out of date.

In essence, this is a useful book on the library shelves for reference rather than one for reading from beginning to end.

W. F. WATSON

Polymer Journal, 1970, Volume 1, Number 1

In view of the very high level of activity in all areas of polymer science in Japan we should not be surprised by the advent of this new journal, published by the Society of Polymer Science of Japan. The board of editors have set out the scope and objects of *Polymer Journal* as being a forum for contributions on the chemistry, physics and biology of polymers. Topics will include the physics of properties and structure of polymers, the chemistry of synthesis of macromolecules and the biophysical and biochemical concepts of polymers.

The journal will appear in alternate months and is published in English.

The first issue (received in February 1970) has 135 pages, and carries fifteen papers and two short communications which cover a wide variety of topics; a random selection might include anionic and cationic copolymerization, solution properties of synthetic polypeptides, conformation of poly(N-methyl glycine) random chains, spherulitic growth rate of isotactic polystyrene, polymer electrets and methyl group relaxations. Most of the communications were received between mid-July and the end of September, one as recently as early November last. The standard of production of the first issue is very high; the format is attractive, equations, diagrams and tables are clearly printed and the papers are presented in

excellent English with a virtual absence of misprints. If, in the future, the publishers are able to realise their intention of speedy publication (a *sine qua non* for success) and to maintain the standard of the first issue, Polymer Journal will be assured of a place, as the major Japanese publication, and will be a 'must' for the research worker in polymer science.

C. H. BAMFORD

Vinyl and Allied Polymers:
Volume 1. Aliphatic polyolefins and polydienes:
Fluoro-olefin polymers

Edited by P. D. RITCHIE

Iliffe Books Ltd., London, 1968, 280 pp., 65s

This book, the first of three volumes on vinyl and allied polymers, is devoted almost exclusively to aliphatic polyolefins and aliphatic polydienes. The volume begins with a general classification of addition polymerization and goes on to discuss the chemistry, physics and technology of this important group of polymers. The broad and well balanced range of topics dealt with have been treated in a clear and concise fashion, with sufficient detail to enable the reader to grasp the fundamentals involved. Six authors have contributed and overlap has been kept to a minimum, although the section giving an historical introduction to polyolefins could probably have been better incorporated with the chemistry and industrial preparation of polyolefins where much has been duplicated.

The two chapters on the structure (both molecular and crystalline) and physical properties of polyolefins are particularly well written and present an excellent unified summary covering polyethylenes, substituted polyethylenes, polypropylene, ethylene copolymers, polybutene-1, poly-4-methylpentene-1, ionomers and the various olefin elastomers. Where possible the relationship between structure and properties has been clearly brought out. However, on page 128 it is erroneously stated that long chain branching has the effect of lowering melt viscosity at a given molecular weight. Other chapters concerning polyolefins cover their preparation (including most of the commercially important routes), fabrication, uses and limitations. There is also a chapter on the preparation of lower olefins. Thus the overall treatment of polyolefins is an extremely comprehensive and useful one. An attempt has been made to present a similar coverage of polydienes, with chapters on the relevent raw materials (extremely brief), the preparation of the polymers and the properties of the polymers. The overall treatment of polydienes is considerably less comprehensive than that of polyolefins.

It is important in an introductory book of this type which does not treat any topic in great detail to provide a comprehensive set of references. On the whole the book is adequate in this respect although there are instances where the reader would find it difficult to pursue certain topics further. In some cases specific references are required, whilst in others references to recent review articles would increase the value of the book. An instance of the latter is in the chemistry of coordination polymerization where the amount of published work is so large that the material presented in a book of this size is necessarily selective. The book was first published in 1968 and one of its stated aims is to provide an up-to-date account of this fast moving field. To criticise the book in 1970 may be unfair but it must be pointed out that several recent developments are not covered or are covered only very briefly. For example, the new generation of high mileage catalysts recently introduced for high density polyethylene to cut monomer to polymer conversion costs (unfortunately a factor not discussed) have not been mentioned.

The main virtue of the book is that it collects together in one volume the diverse aspects of the chemistry, physics and technology of polyolefins and polydienes, with the treatment of polyolefins being particularly comprehensive. The book is especially suitable for newcomers to the field who are presented with a well organised account of the fundamentals of the subject.

J. C. PADGET and R. J. WYATT

445

Gaps in Technology—Plastics

This publication is a useful collection of statistical information on the plastics industry particularly in Europe and the USA. It is a handy reference book for those who wish to search out such data at present widely scattered. It does not, unfortunately, as the title implies, really point out the gaps in technology for the hopeful technical man who might expect to read how he can enter some rewarding field to fill a gap.

The book is essentially an objective study of information which is already well known but has been brought together.

The progress of OECD member countries is examined on a comparative basis. The main concern of the study is not with so much the gaps in technology as the continued development of the markets in the context of technological innovation in recent years. An important distinction is drawn between the large-tonnage plastics, where no general technological or production gap exists between the USA and the rest, and the specialised plastics where the USA has a lead over Europe.

A great deal of comparative data is included on turnover, manpower, investment, research, training and the general structure of the plastics industry in each country. There are also useful sections covering taxation, tariff barriers, and patent legislation.

The growth of the industry historically is well explained with reference to the forces which have resulted in rapid development and technical innovation in some countries while others experienced relatively slow growth. To illustrate this point, Freeman's table 'Chronology of the Discovery and Development of Synthetic Resins' and Hufbaur's 'First Commercial Production of Various Plastics Materials' are reproduced. A number of case histories demonstrate development of production processes for polyolefins, PVC, polystyrene, and some of the newer materials.

In general, the study is a useful general guide to the plastics industry in relation to economic conditions in OECD countries. However, the statistics are usually based on official returns and these are generally grossly out of date.

In essence, this is a useful book on the library shelves for reference rather than one for reading from beginning to end.

W. F. WATSON

Polymer Journal, 1970, Volume 1, Number 1

In view of the very high level of activity in all areas of polymer science in Japan we should not be surprised by the advent of this new journal, published by the Society of Polymer Science of Japan. The board of editors have set out the scope and objects of *Polymer Journal* as being a forum for contributions on the chemistry, physics and biology of polymers. Topics will include the physics of properties and structure of polymers, the chemistry of synthesis of macromolecules and the biophysical and biochemical concepts of polymers.

The journal will appear in alternate months and is published in English.

The first issue (received in February 1970) has 135 pages, and carries fifteen papers and two short communications which cover a wide variety of topics; a random selection might include anionic and cationic copolymerization, solution properties of synthetic polypeptides, conformation of poly(N-methyl glycine) random chains, spherulitic growth rate of isotactic polystyrene, polymer electrets and methyl group relaxations. Most of the communications were received between mid-July and the end of September, one as recently as early November last. The standard of production of the first issue is very high; the format is attractive, equations, diagrams and tables are clearly printed and the papers are presented in

excellent English with a virtual absence of misprints. If, in the future, the publishers are able to realise their intention of speedy publication (a *sine qua non* for success) and to maintain the standard of the first issue, Polymer Journal will be assured of a place, as the major Japanese publication, and will be a 'must' for the research worker in polymer science.

C. H. BAMFORD

Vinyl and Allied Polymers:
Volume 1. Aliphatic polyolefins and polydienes:
Fluoro-olefin polymers
Edited by P. D. RITCHIE

Iliffe Books Ltd., London, 1968, 280 pp., 65s

This book, the first of three volumes on vinyl and allied polymers, is devoted almost exclusively to aliphatic polyolefins and aliphatic polydienes. The volume begins with a general classification of addition polymerization and goes on to discuss the chemistry, physics and technology of this important group of polymers. The broad and well balanced range of topics dealt with have been treated in a clear and concise fashion, with sufficient detail to enable the reader to grasp the fundamentals involved. Six authors have contributed and overlap has been kept to a minimum, although the section giving an historical introduction to polyolefins could probably have been better incorporated with the chemistry and industrial preparation of polyolefins where much has been duplicated.

The two chapters on the structure (both molecular and crystalline) and physical properties of polyolefins are particularly well written and present an excellent unified summary covering polyethylenes, substituted polyethylenes, polypropylene, ethylene copolymers, polybutene-1, poly-4-methylpentene-1, ionomers and the various olefin elastomers. Where possible the relationship between structure and properties has been clearly brought out. However, on page 128 it is erroneously stated that long chain branching has the effect of lowering melt viscosity at a given molecular weight. Other chapters concerning polyolefins cover their preparation (including most of the commercially important routes), fabrication, uses and limitations. There is also a chapter on the preparation of lower olefins. Thus the overall treatment of polyolefins is an extremely comprehensive and useful one. An attempt has been made to present a similar coverage of polydienes, with chapters on the relevent raw materials (extremely brief), the preparation of the polymers and the properties of the polymers. The overall treatment of polydienes is considerably less comprehensive than that of polyolefins.

It is important in an introductory book of this type which does not treat any topic in great detail to provide a comprehensive set of references. On the whole the book is adequate in this respect although there are instances where the reader would find it difficult to pursue certain topics further. In some cases specific references are required, whilst in others references to recent review articles would increase the value of the book. An instance of the latter is in the chemistry of coordination polymerization where the amount of published work is so large that the material presented in a book of this size is necessarily selective. The book was first published in 1968 and one of its stated aims is to provide an up-to-date account of this fast moving field. To criticise the book in 1970 may be unfair but it must be pointed out that several recent developments are not covered or are covered only very briefly. For example, the new generation of high mileage catalysts recently introduced for high density polyethylene to cut monomer to polymer conversion costs (unfortunately a factor not discussed) have not been mentioned.

The main virtue of the book is that it collects together in one volume the diverse aspects of the chemistry, physics and technology of polyolefins and polydienes, with the treatment of polyolefins being particularly comprehensive. The book is especially suitable for newcomers to the field who are presented with a well organised account of the fundamentals of the subject.

J. C. PADGET and R. J. WYATT

Acetylenes and Allenes

by THOMAS F. RUTLEDGE

Reinhold Book Corporation, 1968, 360 pp., $20

This book is a worthwhile review of the subject. Acetylenes and allenes are interconvertible and both structures exist in equilibrium in many compounds. A discussion of both groups in one volume is, therefore, necessary.

Most of the preliminary discussion on the nature of the acetylenic and allenic bonds is contained in what is essentially Part 1, 'Acetylenic compounds, preparation and substitution reactions', Thomas F. Rutledge, Reinhold Book Corporation, 1968. It could be considered that the present book under review is perhaps the exploitation of acetylenic and allenic compounds, although only a quarter of the book deals with the important processes of vinylation, cyclization, oligomerization and polymerization. The remainder of the book is concerned with the basic chemistry of acetylene, allenes and higher cumulenes in which their preparation and reactions are discussed at length.

It would have been worthwhile to mention the changing position of acetylene in the industrial chemical field. Ten years ago the art of vinylation, using acetylene, was the basis of manufacture of monomers such as vinyl chloride, acrylonitrile, vinyl acetate etc. Very little acrylonitrile is now made from acetylene and new routes from ethylene are progressively replacing those from acetylene for the other monomers mentioned. In fact the position of acetylene in the industrial field is being challenged vigorously by alternative processes based on cheaper ethylene and propylene.

Several types of reactions of acetylene compounds can be adopted to yield polymeric products but many of these are of academic interest only. A possible exception is poly-pentyne-1 which may have uses as a semi-conductor. Some of the polymers formed are highly unstable particularly those derived from m-or p-diethynyl benzene.

In conclusion we would like to point out that $Ru_2(CO)_9$ (p 86) does not exist and should be written $Ru_3(CO)_{12}$. Also copper *is* a transition metal (p 394). The book is rather expensive but it reads well and has an excellent bibliography.

D. G. H. BALLARD and J. P. CANDLIN

The NMR of Polymers

by I. YA. SLONIM and A. N. LYUBIMOV

Translated by C. N. TURTON and T. I. TURTON
Plenum Press, New York, 1970, 365 pp., 185s, $19.50

It must have caused the authors of this book some disappointment that four years have elapsed between the appearance of the original Russian version and this translation. During that interval high resolution n.m.r. of polymers in solution has made such considerable advances that the book, which is heavily weighted on the side of 'broad-line' n.m.r. applications (i.e. situations wherein the line shape is dominated by dipolar coupling) is out-of-date in many respects, and will be of very limited value to those polymer chemists who look to n.m.r. as a means of studying chemical structure. To this extent the title, preface and dust-jacket summary are misleading, a situation that could have been remedied in the English edition.

Part 1, written by A. N. Lyubimov, deals in 145 pages with the physical basis and instrumentation of n.m.r. The theoretical treatment of nuclear spin systems is uncompromisingly quantum-mechanical; it will be heavy going for anyone without a strong mathematical bent, and although an admirable and useful piece of work in itself, it seems out of place in a book of this kind. The discussion of experimental techniques and instrumentation contains many passages that will seem quaint to users of modern spectrometers, and reveals the rather elementary state of development of Russian spectrometers when the book was written, roughly equivalent to that reached in the USA in 1957.

Part 2, by I. Ya Slonim (161 pages of text, plus bibliography), covers polymer applications up to 1965 fairly exhaustively, though it is a severe shortcoming that only 33 pages of text are devoted to high resolution measurements. Separate sections deal with measurements of crystallinity, oriented polymers, study of molecular motion, and chemical processes such as polymerization, crosslinking, irradiation effects, and breakdown. Spin-echo measurements are discussed as well as the more conventional line-shape measurements. The bulk of the work reviewed is, of course, on synthetic polymers, but references to proteins, natural rubber and cellulose also appear. Where appropriate, n.m.r. results are compared with those from other techniques such as x-ray methods and mechanical relaxation. The bibliography of over 1000 references includes a supplement (added for this edition) covering work published up to early 1967, and all the references are classified according to topics and polymers in a subject index.

The translators have done an excellent job, and I noted only a few very minor errors, mainly of printing. The book should be of value to chemists and physicists interested in using n.m.r. to study structure and motion in solid polymers, and the bibliography is a useful reference source for all polymer applications up to 1967. The book is very expensive, however, even for a translation, and for material that is already considerably outdated it is not worth the price.

<div align="right">J. K. Becconsall</div>

Structure of Organic Solids
Main Lectures-IUPAC Microsymposium, Prague, 1968

Butterworths, London, 1969, 86 pp., 58s

If one accepts as a truism that our knowledge of the structure of organic solids is no more sophisticated than the techniques used in their study, then it follows that in order to extend our present understanding, it is necessary either to refine existing equipment and analytical approaches or to develop new methods of investigation. Adopting classical x-ray electron diffraction procedures as the yardstick, elements of all these aspects are to be found in this book.

The publishers bring together four main papers read at the Prague microsymposium in September, 1968, and published separately elsewhere. (*Pure and Applied Chem.* 1969, Vol. 18, No. 4). The first, by W. Hoppe and collaborators, describes new developments in the determination of the structure of complex organic molecules by outlining the use of a four-circle x-ray diffractometer, which has the ability to measure the full three-dimensional array of reflections with one crystal setting of complex organic molecules. A second paper by W. Ruland reviews the interpretation of scattering diagrams of, for example, glass polymers, which leads to an understanding of the structure of amorphous solids, a field of great current interest, despite the apparent anomaly of title. The third author, G. E. Bacon, discusses the subject of neutron diffraction studies of organic molecules and, like the other writers, illustrates his paper partly by reference to his own work. He stresses, also, the main advantage of this technique in locating hydrogen atoms in organic crystals. Finally, C. A. Taylor emphasizes the resurgence of interest, occasioned by the use of laser beams, in optical diffraction analogues under the heading 'Optical methods as an aid in structure determination'. The application of these in studies of paracrystallinity and order in fibres is mentioned.

It would not be expected that such a collection of papers in this well printed and attractively produced publication should constitute a textbook; nevertheless, whether as a reflection of the style of presentation which allows for ease of reading, or the individual authority of each account, there is more than a semblance of such a book. Thus, although the active worker in the field of structure determination will find little of which he is unaware, (some work is more recent than the date of the microsymposium) the reader with a more general interest or the advanced course student will undoubtedly benefit by reference to this collection. Approached in this light, and without easy access to the separate publications, the price of 58s will not seem unreasonable.

<div align="right">R. P. Sheldon</div>

Acetylenes and Allenes

by THOMAS F. RUTLEDGE

Reinhold Book Corporation, 1968, 360 pp., $20

This book is a worthwhile review of the subject. Acetylenes and allenes are interconvertible and both structures exist in equilibrium in many compounds. A discussion of both groups in one volume is, therefore, necessary.

Most of the preliminary discussion on the nature of the acetylenic and allenic bonds is contained in what is essentially Part 1, 'Acetylenic compounds, preparation and substitution reactions', Thomas F. Rutledge, Reinhold Book Corporation, 1968. It could be considered that the present book under review is perhaps the exploitation of acetylenic and allenic compounds, although only a quarter of the book deals with the important processes of vinylation, cyclization, oligomerization and polymerization. The remainder of the book is concerned with the basic chemistry of acetylene, allenes and higher cumulenes in which their preparation and reactions are discussed at length.

It would have been worthwhile to mention the changing position of acetylene in the industrial chemical field. Ten years ago the art of vinylation, using acetylene, was the basis of manufacture of monomers such as vinyl chloride, acrylonitrile, vinyl acetate etc. Very little acrylonitrile is now made from acetylene and new routes from ethylene are progressively replacing those from acetylene for the other monomers mentioned. In fact the position of acetylene in the industrial field is being challenged vigorously by alternative processes based on cheaper ethylene and propylene.

Several types of reactions of acetylene compounds can be adopted to yield polymeric products but many of these are of academic interest only. A possible exception is poly-pentyne-1 which may have uses as a semi-conductor. Some of the polymers formed are highly unstable particularly those derived from m-or p-diethynyl benzene.

In conclusion we would like to point out that $Ru_2(CO)_9$ (p 86) does not exist and should be written $Ru_3(CO)_{12}$. Also copper *is* a transition metal (p 394). The book is rather expensive but it reads well and has an excellent bibliography.

D. G. H. BALLARD and J. P. CANDLIN

The NMR of Polymers

by I. YA. SLONIM and A. N. LYUBIMOV

Translated by C. N. TURTON and T. I. TURTON
Plenum Press, New York, 1970, 365 pp., 185s, $19.50

It must have caused the authors of this book some disappointment that four years have elapsed between the appearance of the original Russian version and this translation. During that interval high resolution n.m.r. of polymers in solution has made such considerable advances that the book, which is heavily weighted on the side of 'broad-line' n.m.r. applications (i.e. situations wherein the line shape is dominated by dipolar coupling) is out-of-date in many respects, and will be of very limited value to those polymer chemists who look to n.m.r. as a means of studying chemical structure. To this extent the title, preface and dust-jacket summary are misleading, a situation that could have been remedied in the English edition.

Part 1, written by A. N. Lyubimov, deals in 145 pages with the physical basis and instru-mentation of n.m.r. The theoretical treatment of nuclear spin systems is uncompromisingly quantum-mechanical; it will be heavy going for anyone without a strong mathematical bent, and although an admirable and useful piece of work in itself, it seems out of place in a book of this kind. The discussion of experimental techniques and instrumentation contains many passages that will seem quaint to users of modern spectrometers, and reveals the rather elementary state of development of Russian spectrometers when the book was written, roughly equivalent to that reached in the USA in 1957.

Part 2, by I. Ya Slonim (161 pages of text, plus bibliography), covers polymer applications up to 1965 fairly exhaustively, though it is a severe shortcoming that only 33 pages of text are devoted to high resolution measurements. Separate sections deal with measurements of crystallinity, oriented polymers, study of molecular motion, and chemical processes such as polymerization, crosslinking, irradiation effects, and breakdown. Spin-echo measurements are discussed as well as the more conventional line-shape measurements. The bulk of the work reviewed is, of course, on synthetic polymers, but references to proteins, natural rubber and cellulose also appear. Where appropriate, n.m.r. results are compared with those from other techniques such as x-ray methods and mechanical relaxation. The bibliography of over 1000 references includes a supplement (added for this edition) covering work published up to early 1967, and all the references are classified according to topics and polymers in a subject index.

The translators have done an excellent job, and I noted only a few very minor errors, mainly of printing. The book should be of value to chemists and physicists interested in using n.m.r. to study structure and motion in solid polymers, and the bibliography is a useful reference source for all polymer applications up to 1967. The book is very expensive, however, even for a translation, and for material that is already considerably outdated it is not worth the price.

<div align="right">J. K. Becconsall</div>

Structure of Organic Solids
Main Lectures-IUPAC Microsymposium, Prague, 1968

Butterworths, London, 1969, 86 pp., 58s

If one accepts as a truism that our knowledge of the structure of organic solids is no more sophisticated than the techniques used in their study, then it follows that in order to extend our present understanding, it is necessary either to refine existing equipment and analytical approaches or to develop new methods of investigation. Adopting classical x-ray electron diffraction procedures as the yardstick, elements of all these aspects are to be found in this book.

The publishers bring together four main papers read at the Prague microsymposium in September, 1968, and published separately elsewhere. (*Pure and Applied Chem.* 1969, Vol. 18, No. 4). The first, by W. Hoppe and collaborators, describes new developments in the determination of the structure of complex organic molecules by outlining the use of a four-circle x-ray diffractometer, which has the ability to measure the full three-dimensional array of reflections with one crystal setting of complex organic molecules. A second paper by W. Ruland reviews the interpretation of scattering diagrams of, for example, glass polymers, which leads to an understanding of the structure of amorphous solids, a field of great current interest, despite the apparent anomaly of title. The third author, G. E. Bacon, discusses the subject of neutron diffraction studies of organic molecules and, like the other writers, illustrates his paper partly by reference to his own work. He stresses, also, the main advantage of this technique in locating hydrogen atoms in organic crystals. Finally, C. A. Taylor emphasizes the resurgence of interest, occasioned by the use of laser beams, in optical diffraction analogues under the heading 'Optical methods as an aid in structure determination'. The application of these in studies of paracrystallinity and order in fibres is mentioned.

It would not be expected that such a collection of papers in this well printed and attractively produced publication should constitute a textbook; nevertheless, whether as a reflection of the style of presentation which allows for ease of reading, or the individual authority of each account, there is more than a semblance of such a book. Thus, although the active worker in the field of structure determination will find little of which he is unaware, (some work is more recent than the date of the microsymposium) the reader with a more general interest or the advanced course student will undoubtedly benefit by reference to this collection. Approached in this light, and without easy access to the separate publications, the price of 58s will not seem unreasonable.

<div align="right">R. P. Sheldon</div>

Application of superposition principles to the viscometric changes during association in polyacrylonitrile solutions

R. B. BEEVERS*

An analysis has been made of the viscometric measurements obtained during the association of polyacrylonitrile solutions in dimethylformamide and in dimethylacetamide at 25°C to which benzene has been added. It is shown that a reduction scheme can be applied to the data taking the benzene concentration as the adjustable parameter to yield a single curve made up from the superposed data. Results for the two solvent systems are found to be almost identical apart from a shift to lower benzene concentrations in the case of solutions in dimethylacetamide.

DYNAMIC MECHANICAL properties of concentrated polymer solutions can be described by the use of a system of reduced variables[1], the real part of the reduced dynamic rigidity being given by[2]

$$G_{red} = (T_r c_r / T \, c) \, G \qquad (1)$$

where the subscript r denotes the reference state and the temperature and concentration of the polymer solution are denoted by T and c respectively. It will be shown here that the viscometric data obtained for polyacrylonitrile solutions during association, which has been brought about by addition of non-solvent, can also be described by a simple reduction scheme. In this case a reduction of the data is made adopting the non-solvent volume concentration as the adjustable parameter.

In order to examine the generality of the reduction scheme measurements have been made with dimethylacetamide as the solvent in addition to the results for solutions in dimethylformamide which have already been reported[3]. The polymer concentration has been kept below 1 g dl^{-1} in order to avoid macrogel formation. At higher polymer concentrations solutions of polyacrylonitrile in these two solvents show reversible viscoelastic properties[4].

Measurements of the viscosity number Φ_1 $(= \eta_{sp}/c_1)$ for solutions in dimethylformamide using benzene concentrations between 31·0 and 40·0% and at 25·0°C have been given in figure 5 of reference 3. Similar results may be obtained with dimethylacetamide if the benzene concentration is reduced to the range 24·0–29·0%. Before proceeding to analyse the data, the observed values of Φ_1 have been corrected to compensate for the slight differences in polymer concentration brought about by the dilution of the starting solution with varying amounts of non-solvent. In dimethylformamide, dilution of the initial stock solution of concentration 0·467 ± 0·002 g dl^{-1} yielded solutions varying in concentration (c_1) from 0·324 to 0·297 g dl^{-1}. Similarly solutions in dimethylacetamide, initially of 0·400 ± 0·002 g dl^{-1} varied between 0·304 and 0·284 g dl^{-1} on dilution. In both sets of data,

---

* Present address: CSIRO, Division of Textile Physics, 338 Blaxland Road, Ryde, Sydney, N.S.W., Australia.

correction has been made to a polymer concentration of 0.300 g dl^{-1}, and the corrected values of the viscosity number have been calculated from

$$\Phi_c = 0.300 \ \Phi_1/c_1 \tag{2}$$

This correction has the effect of reducing the spread in viscosity number by, at most, 2%.

A superposition of this corrected data has been made by a shift of the time-dependent curves along the abscissa following the usual procedures[1]. This has been made with respect to an approximate midpoint in the data; that is the reference state is 35.0% benzene for solutions in dimethylformamide and 27.0% benzene for the dimethylacetamide results. In superposing the data it was generally found that a small vertical shift was also required. Once the horizontal and small vertical shifts had been made, as summarized in *Table 1*,

Table 1 Values of the shift factor K and of the adjustment made in Φ_c in order to obtain a superposition of the viscosity data at $25°C$

Benzene ($\%$v/v)	Correction to Φ_c (dl g^{-1})	K
N,N'-dimethylformamide		
31·0	−0·20	74·1
32·0	−0·12	37·0
33·0	−0·08	6·67
34·0	−0·04	4·17
35·0	0·00	1·00
35·5	0·06	0·53
36·0	0·09	0·22
36·5	0·11	0·11
37·0	0·14	0·045
38·0	0·18	0·024
39·0	0·22	0·012
40·0	0·26	0·003
N,N'-dimethylacetamide		
24·0	−0·20	117·7
25·0	−0·15	20·0
26·0	−0·10	3·85
27·0	0·00	1·00
28·0	0·10	0·27
29·0	0·16	0·11

there was little doubt about the satisfactory nature of the fit. The whole process could be recommenced with substantially the same result to within 10%. The correction to Φ_c is greater for solutions in dimethylacetamide and shows a regular dependence on the benzene concentration. The parameters given in *Table 1* have been used to reduce the data to give Φ_{red} and t/K which are now shown plotted in *Figures 1* and *2*. A great deal of the original data has necessarily been excluded from these plots.

The reduced plots for the two solvent systems are remarkably similar both in respect of the 'time-scale' covered and in the magnitude of the change in Φ_{red} occurring through association. A more effective comparison is given in
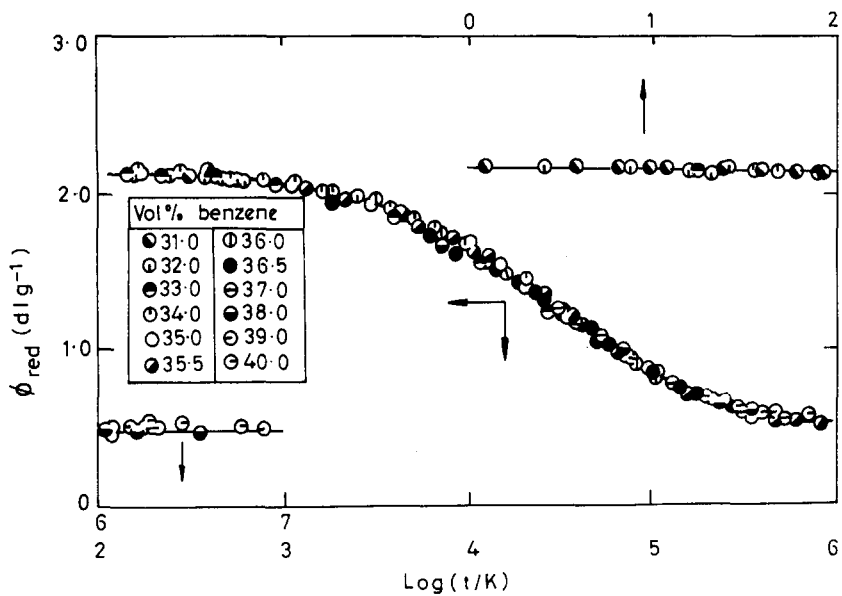
Figure 1 Superposed data for the association in dimethylformamide solutions at 25°C
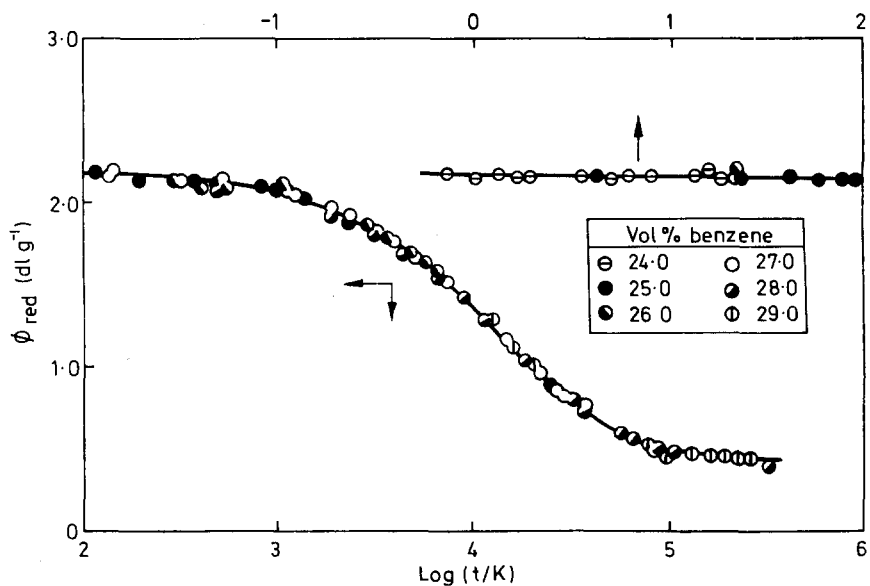
Figure 2 Superposed data for the association in dimethylacetamide solutions at 25°C
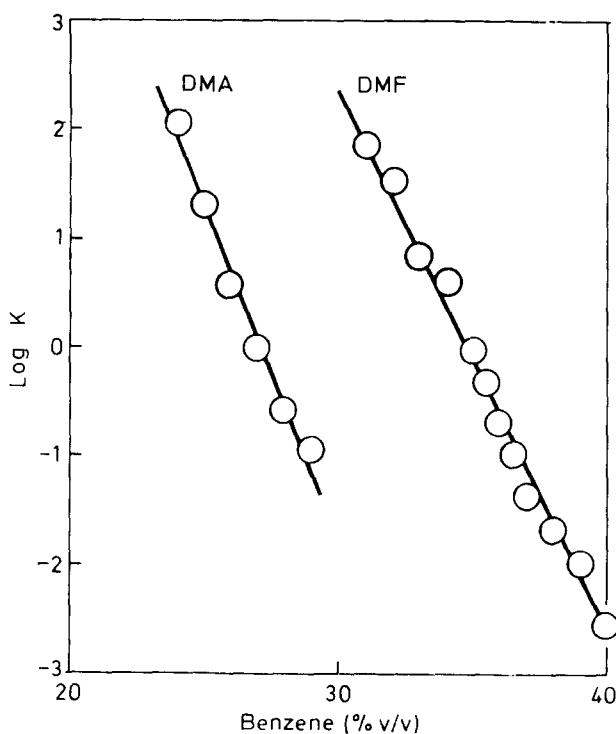
Figure 3 The dependence of the superposition shift factor on the benzene concentration for solutions of polyacrylonitrile in dimethyl-formamide (DMF) and dimethylacetamide (DMA)

Figure 3 which shows the dependence of the shift factor on the benzene concentration for both solvent systems. The similarity of these two solvent systems has been noted previously[5] when it was shown that the temperature dependence of the kinetic constants for association involved almost the same activation energy.

University of Bradford
Bradford, 7, Yorkshire

REFERENCES

1 Ferry, J. D. '*Viscoelastic Properties of Polymers*', Wiley, New York, 1961
2 Ferry, J. D. *J. Amer. Chem. Soc.* 1950, **72**, 3746
3 Beevers, R. B. *Polymer, Lond.* 1967, **8**, 419
4 Beevers, R. B. *Macromolecular Reviews* 1968, **3**, 113
5 Beevers, R. B. *Polymer, Lond.* 1969, **10**, 791

Low temperature mechanical relaxation in poly-p-xylylenes*

C. CHUNG† and J. A. SAUER‡

The mechanical relaxation behaviour of poly-p-xylylene, poly(chloro-p-xylylene) and poly(dichloro-p-xylylene) has been investigated by means of an inverted torsion pendulum apparatus. Values are given for the shear modulus and loss for each of these three polymers at various temperatures from 80 K to room temperature. It is found that the unsubstituted poly-p-xylylene, even though it contains only two CH_2 sequences in its chain between phenylene units, exhibits a strong, low temperature relaxation process with a loss maximum at 159 K (0·54 Hz). The mono-substituted polymer, poly(chloro-p-xylylene), shows no loss peak in the 150 K region but does exhibit a damping maximum at 254 K (0·40 Hz). For the di-substituted polymer, poly(dichloro-p-xylylene), the loss modulus peak is again found in the low temperature region, being situated at 150 K (0·34 Hz). The data, together with other experimental observations, suggest that local reorientational motions of the phenyl, or substituted phenyl units, are involved in these secondary relaxation processes.

INTRODUCTION

IT IS WELL established that linear polymers which contain a sequence of $-CH_2-$ units in the backbone chain will exhibit a relaxation process which, at a frequency of 1 Hz, occurs at a temperature of about 150 K[1–3]. This process has been observed in polyethylene in both melt polymer and in single crystal mats[4, 5]. It is generally referred to as the γ-relaxation to distinguish it from two higher temperature relaxations (called β- and α-relaxations). The molecular motions involved in the γ-process are considered to occur in the amorphous phase[3, 6, 7, 8] or in defect regions of the crystals[9, 10]. The molecular mechanism of the relaxation is not precisely known. It has been attributed to the onset of the glass transition of $-CH_2-$ sequences[2]; to diffusional motion of chain segments in the amorphous phase[3, 11]; to local mode oscillation of chain segments in the backbone chain[12, 13]; to loosening of intermolecular van der Waals bonding between gauche conformations of adjacent chains[14]; and to such specific types of mechanisms as the 'double kink' motion[15, 16] and the 4-atom 'crankshaft' motion[17, 18].

Despite the differing interpretations given to this low temperature relaxation process, there is general agreement that it is associated with stress-biased, thermally-activated, reorientational motions of a small number of

chain units. A similar process, but one that occurs at a temperature of about 100–120 K at 1 Hz, can also arise from hindered reorientational motion of pendant side chains. It is not known what the minimum number of $-CH_2-$, or equivalent, segments is in order for this process to be present. Some of the proposed mechanisms, such as the 'double kink' or 'crankshaft' models, would seem to require four such units. Willbourn[2] suggested that the γ-relaxation would arise whenever three or more such sequences were present. It has, for example, been observed in linear polymers with three $-CH_2-$ sequences as well as in polymers with three, or more, carbon atoms in the side chain. Examples of the first class are polypyrrolidone[19] and polyoxetane[20] and examples of the second class are the poly(vinyl ethers)[1] and the poly(alkyl methacrylates)[21]. However, at least for the branched polymers, a low temperature relaxation can occur even if there are only two carbon atoms in sequence on the pendant side chain. An example is polybutene where a relaxation process has been found at 130 K at about 10 Hz[22] and about 150 K at 3160 Hz[23].

In the present communication, it will be shown that linear polymers with fewer than three adjacent $-CH_2-$ units in the main backbone chain may also show relaxation in the 150 K temperature region. This will be demonstrated, for example, for several linear polymers of the poly-*p*-xylylene (PPX) type. PPX is prepared from purified di-*p*-xylylene, by cleaving *in vacuo* at 600°C and subsequent condensation of the vapour onto a cold substrate. Under these conditions, there is spontaneous polymerization and the resulting

polymer $\left(CH_2-\underset{}{\langle\bigcirc\rangle}-CH_2\right)_n$ is free of branches, crystalline, and of high

molecular weight[24]. Extensive studies have been made by Niegisch[25, 26] of the crystal structure of vapour-deposited films, as well as of single crystals grown from dilute solution in α-chloronaphthalene. These results show that two crystalline modifications can occur in PPX. The films obtained by deposition of the vapour onto a substrate at room temperature crystallize initially in an orthorhombic lattice. Upon subsequent annealing at about 220°C, the orthorhombic, or α-modification, converts to a hexagonal or β-modification.

EXPERIMENTAL

In the present study, we have investigated the low temperature mechanical relaxation behaviour of three different vapour-deposited and polymerized poly-*p*-xylylenes. One of these is the unmodified poly-*p*-xylylene prepared as described above; the other two materials are the chlorine-substituted polymers, poly(monochloro-*p*-xylylene) (PCPX) and poly(dichloro-*p*-xylylene) (PDCPX).

The two chlorine-substituted polymers are prepared by a similar process to that used for preparation of PPX from di-*p*-xylylene[27]. The mono-substituted polymer, PCPX, is prepared from purified dichloro-di-*p*-xylylene and

the di-substituted polymer, PDCPX, is prepared from chlorinated dimer that contains various isomers. It is thought[28] that about 85% of the phenylene groups in PDCPX have two chlorine atoms per ring, while some 10% have three chlorine atoms per two phenylene units and 5% have five per two phenylene groups (See note on p 461). Also it is not known whether the chlorine atoms in the di-substituted rings are in the 2, 3 or 2, 5 or 2, 6 positions.

The density, the estimated degree of crystallinity, and the reported glass transition temperatures for the three vapour deposited films are given in *Table 1* along with the thickness of the test specimens.

Table 1 Sample characteristics

Material	Thickness (cm)	Density (g/cm³)	Crystallinity* (%)	T_g* (°C)	T_m* (°C)
PPX	0·0053	1·11	50–70	60–70	420
PCPX	0·0075	1·283	50–70	80–100	290
PDCPX	0·0038	1·41	50–70	110	> 300

*Data kindly supplied by Union Carbide Chemical Company

All tests were carried out in a torsion pendulum apparatus which was designed and constructed to provide data on shear modulus and loss of thin samples[28]. The pendulum is of the inverted type, with the specimen in the form of a thin strip suspended between two clamps, the lower of which is the fixed end of the pendulum. The upper clamp is connected to an adjustable moment arm that is supported by a constantan wire. A counter balancing weight is used to compensate for the weight of the moment arm or to apply a known amount of axial tension to the specimen. The specimen is given an initial torsional deflection of up to 4° and the oscillation amplitude is monitored as a function of time by means of a Rotary Variable differential transformer. Sample length between clamps is about 6 cm and sample width is about 0·60 cm. A tape heater wrapped around the specimen chamber is used to control the heating rate. Most tests were made between liquid nitrogen temperatures and room temperature at a heating rate of about 1 °C/min. Measurements were made of the torsional oscillations every few degrees. To obtain the desired G', G'', and tan δ values for the specimen itself, corrections had to be made for the stiffness and internal friction of the supporting wire and also for the applied tensile load. Because of the extremely small thicknesses of some of the test samples (see *Table 1*), the contribution of the support wire to the measured quantities could become appreciable. The calculated modulus and loss values for the thinnest films are believed to be reliable ±7%. The test data becomes more reliable as the thickness of the samples increase.

RESULTS AND DISCUSSION

The real and imaginary parts of the shear modulus and loss for the PPX sample are given as a function of temperature in *Figure 1*. The shear modulus

456
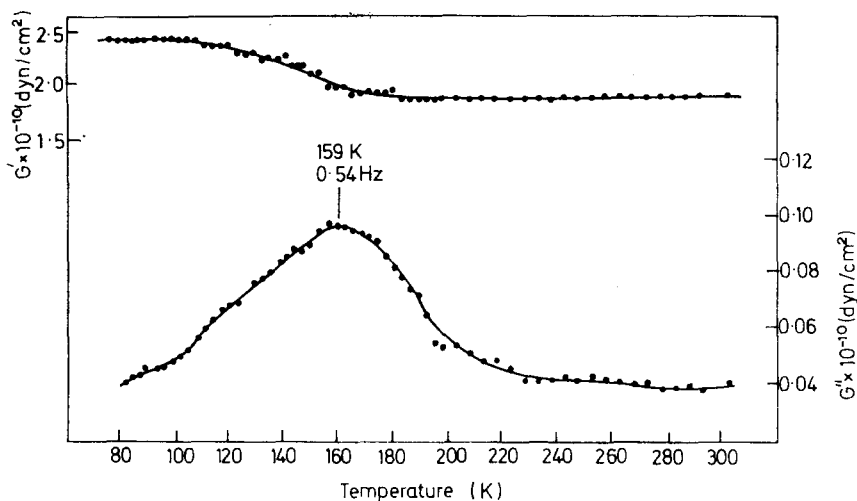
Figure 1 Shear modulus, G', and loss modulus, G'', against temperature for poly-*p*-xylylene (PPX)

has a value at 80 K of $2 \cdot 4 \times 10^{10}$ dyn/cm^2. In the temperature range 100–200 K, it falls to a value of about $1 \cdot 8 \times 10^{10}$ dyn/cm^2 and then is essentially insensitive to temperature changes up to 300 K. Accompanying the drop in shear modulus is a loss peak with maximum value at 159 K (0·54 Hz). Thus this polymer shows a distinct γ-relaxation process and the tan δ value near 160 K, is quite large ($\sim 5 \times 10^{-2}$).

The results for the monochloro-substituted polymer, PCPX, are shown in *Figure 2*. This material shows no relaxation in the region of 150 K. It does
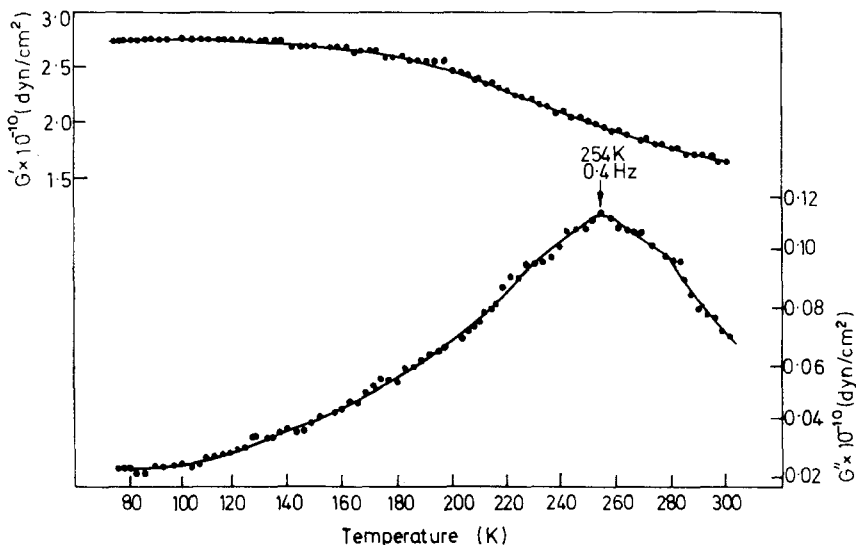
Figure 2 Shear modulus, G', and loss modulus, G'', against temperature for poly-chloro-*p*-xylylene (PCPX)

457

undergo a relaxation at higher temperatures marked both by a loss maximum and a modulus drop. The loss maximum is located at 254 K (0·40 Hz) and the value of tan δ at this maximum is about 6×10^{-2}.

Figure 3 gives the test results on the dichloro-substituted sample, PDCPX.
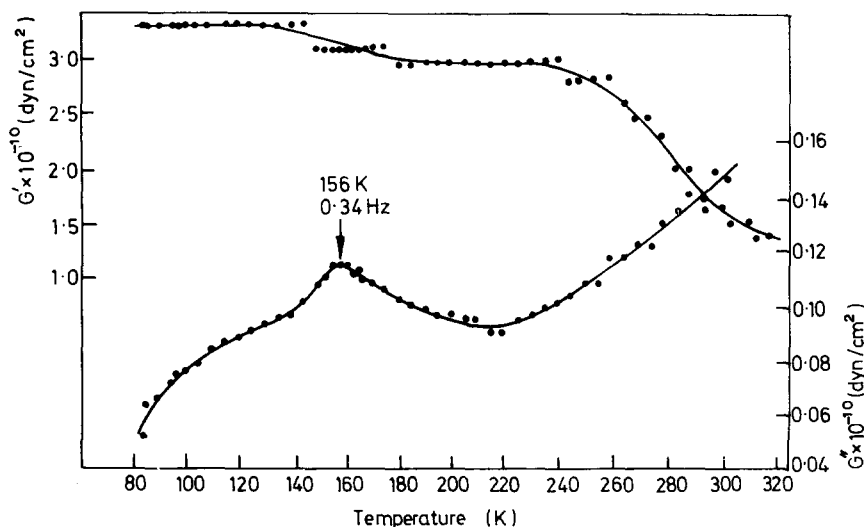
Figure 3 Shear modulus, G', and loss modulus, G'', against temperature for poly-dichloro-p-xylylene (PDCPX)

In the low temperature region, this polymer exhibits a relaxation process in the usual range for γ-type relaxations. The loss maximum is located at 156 K (0·34 Hz) and the value of tan δ at the peak (0·038) is slightly less than that for PPX. It also appears that a second relaxation may occur in this polymer in the 250–300 K range. Although there is no loss peak in this region, there is a modulus drop and a rise in loss value. These effects are not thought to be related to onset of the glass transition as they are not evident in the data of *Figure 1* for PPX and yet it is known (see *Table 1*) that the T_g of PPX is a lower temperature than for the dichloro-substituted polymer PDCPX.

The data presented in *Figures 1* and *3* for PPX and PDCPX provide definite evidence that at a frequency of $\sim$1 Hz, a low temperature relaxation in the 150–160 K range can occur in highly linear, crystalline polymers which contain only two CH$_2$ units in sequence. It is also clear that these relaxations are not due to impurities. Firstly, the poly-p-xylylenes prepared by the vapour-deposition process are of very high purity[24, 27] and secondly, the relaxation strength, as measured by the modulus drop or by the maximum value of tan δ (0·04–0·06), is high and comparable in magnitude and temperature position to that found in the polyamides, or polyethylene[3, 6].

Although the data of *Figures 1* and *3* constitute the most striking evidence of a significant low temperature relaxation in polymers containing only two CH$_2$ units in sequence, small loss peaks and shoulders in this same temperature range have been reported in samples of polystyrene and substituted

*Units of shear modulus: 1 dyn/cm^2 $=$ 10^{-1} N/m^2

polystyrenes[29, 30] and attributed to structural irregularities of the CH_2—CH_2 type arising from occasional head-to-head or tail-to-tail addition of monomer units. A study of poly(ethylene terephthalate) also gives some indication that a low temperature loss peak shoulder may be present in this polymer and it has been conjectured that this feature may arise from motion of the two CH_2 units in the chain[31].

The presence of a low temperature γ-relaxation in PPX, or PDCPX, does not, however, imply that it arises solely from motions of the CH_2 groups. In fact, this is quite unlikely. We prefer to associate it with hindered reorientational motions of the phenylene units, probably accompanied by local motions of the nearby CH_2 groups. The reasons for this assignment are as follows. Firstly, it is readily evident from studies with Fischer-Hirschfelder models that with only two methylene units in sequence, one cannot induce conformational changes of the CH_2 units without co-operative motion of the phenylene units. However, the phenyl rings themselves can readily undergo reorientational or 'crankshaft' type motions. Secondly, in many polymers where only a small number of CH_2 units occur in the backbone chain, as for example in poly-tetra- or trimethylene oxide, polyamides, and poly(ethylene terephthalate), the low temperature γ-process is observed in dielectric measurements as well as mechanical ones[6]. Thus the local motion involved must be associated not only with the methylene sequence but also with adjacent polar units (amide groups and oxygen atoms in the examples cited), to which the CH_2 sequences are attached. Thirdly, a number of other polymers which include phenyl rings, but have no methylene units, in their backbone chains also show an appreciable low temperature relaxation in the 100 K to 200 K range. We have detected such relaxations in polysulphone at 162 K (0·67 Hz), in poly(2,6-dimethyl-p-phenylene oxide) at 125 K (1·4 Hz) and in poly(bisphenol-A-carbonate) at 165 K (1·24 Hz)[32].Other observations of low temperature relaxations in polymers containing phenyl rings in the main chain have been reported[33, 34].

The test results on the substituted poly-p-xylylenes also seem to favour the interpretation that the γ-relaxation in these polymers is a local mode motion that involves torsional oscillations or reorientations of the phenyl rings. With a single asymmetric polar substituent in one of the hydrogen ring positions, the barrier hindering reorientations would be considerably increased due to dipolar interactions, as well as steric hindrance. One would thus expect, in PCPX, that the loss maximum, at a given frequency of measurement, would be shifted to higher temperatures and this is what has happened as *Figure 2* reveals. On the other hand, if two hydrogen atoms are replaced by chlorine atoms and if these two are on opposite sides of the phenyl rings, then the dipole moments will largely cancel one another. In addition, the symmetry present when only one hydrogen atom is substituted will be modified. As a result, the intermolecular interactions will be reduced and the relaxation process for the di-substituted polymer will occur at lower temperatures than for the mono-substituted one. *Figure 3* shows that the relaxation has been shifted back to the 150 K range.

The mechanical measurements also provide information concerning the position of the chlorine atoms in the di-substituted polymer, PDCPX. Firstly,

459

the 2,3-position does not agree with the data since in these positions the chlorine atoms would provide both dipolar and steric contributions to the rotational barrier, and the loss peak arising from reorientational motions of the phenyl rings would be shifted to higher temperatures instead of occurring at approximately the same temperature as for the unsubstituted polymer. The 2,5-position, where the chlorine dipoles effectively cancel, or the 2,6-position where only a component parallel to the rotation axis is present are thus more likely. Secondly, the apparent presence of a second relaxation in PDCPX in the 250–300 K region may result from reorientational motion of those polar phenyl rings that are asymmetrically substituted, i.e. which have one, or three, chlorine atoms on the ring. As noted earlier, it is thought that some 15% of the phenyls in PDCPX do not have the expected two chlorine atoms on the ring.

ACKNOWLEDGEMENTS

Rutgers University,
New Brunswick,
New Jersey, USA

REFERENCES

1 Schmeider, K. and Wolf, K. *Kolloid Z.* 1953, **134**, 157
2 Willbourn, A. H. *Trans. Far. Soc.* 1958, **54**, 717
3 Woodward, A. E. and Sauer, J. A. *Advances in High Polymers* 1958, **1**, 114
4 Sinnott, K. N. *J. appl. Phys.* 1966, **37**, 3385
5 Takayanagi, M. and Matsuo, T. *J. Macromol. Sci. (B)* 1967, **1**, 407
6 McCrum, N. G., Read, B. and Williams, G., 'Anelastic and dielectric effects in polymeric solids', J. Wiley and Sons, London, 1967
7 Gray, R. W. and McCrum, N. G. *J. Polym. Sci. (A-2)* 1969, **7**, 1329
8 Stehling, F. C. and Mandelkern, L. *J. Polym. Sci. (B)* 1969, **7**, 255
9 Takayanagi, M. *Mem. Faculty of Engineering, Kyushu Univ.* 1963, **23**, 41
10 Hoffmann, J. D., Williams, G. and Passaglio, E. *J. Polym. Sci. (C)* 1966, **14**, 173
11 Deeley, C. W., Kline, D. E., Sauer, J. A. and Woodward, A. E. *J. Polym. Sci.* 1958, **28**, 109
12 Yamafuji, K. and Ishida, Y. *Kolloid Z.* 1962, **183**, 15
13 Saito, N., O'Kano, K., Iwayanagi, S. and Hideshima, T. *Solid State Physics* 1963, **14**, 343
14 Andrews, R. D. and Hammack, T. J. *J. Polym. Sci. (B)* 1965, **3**, 659
15 Pechhold, W., Blasenberg, S. and Woerner, S. *Kolloid. Z.* 1963, **196**, 27
16 Pechhold, W., Eisele, U. and Knauss, G. *Kolloid. Z.* 1964, **196**, 27
17 Schatski, T. F. *J. Polym. Sci.* 1962, **57**, 496
18 Schatski, T. F. *J. Polym. Sci. (C)* 1966, **14**, 139
19 Lawson, K. D., Sauer, J. A. and Woodward, A. E. *J. appl. Phys.* 1963, **34**, 2492
20 Stratta, J. J., Reding, F. P. and Faucher, J. A. *J. Polym. Sci. (A)* 1964, **2**, 5017
21 Deutsch, K., Hoff, E. A. W. and Reddish, W. *J. Polym. Sci.* 1954, **13**, 565

22 Wolf, K. A. *Electrochem. Technol.* 1961, **65**, 604
23 Woodward, A. E., Sauer, J. A. and Wall, R. A. *J. Chem. Phys.* 1959, **30**, 854
24 Gorham, W. F. *J. Polym. Sci. (A-1)* 1966, **4**, 3027
25 Niegisch, W. D. *J. Polym. Sci. (B)* 1966, **4**, 531
26 Niegisch, W. D. *J. appl. Phys.* 1966, **37**, 4041
27 Gorham, W. F. and Niegisch, W. D., 'Xylylene Polymers', Encyclopedia of Polymer Science and Technology, Interscience, New York (to be published)
28 Chung, C., PhD Dissertation, Rutgers University, 1969
29 Illers, K. H. and Jenckel, E. *J. Polym. Sci.* 1959, **41**, 528
30 Fielding-Russell, G. S. and Wetton, R. E. *Chem. Soc. Spec. Publ.* 1966, No. 20, p 95
31 Illers, K. H. and Breuer, H. *J. Colloid. Sci.* 1963, **18**, 1
32 Chung, C. and Sauer, J. A. (to be published)
33 Baccarreda, M., Butta, E., Frosini, V. and de Petris, S. *Mat. Sci. and Eng.* 1968/69, **3**, 157
34 de Petris, S., Frosini, V., Butta, E. and Baccarreda, M. *Die Makromol. Chem.* 1967, **109**, 54

NOTE ADDED IN PROOF

The supposition that about 85% of the phenylene groups in PDCPX have 2 Cl atoms per ring, while some 10% have 3 Cl per two phenylene units and 5% have 5 Cl per two phenylene groups is in reasonable accord with a gas chromatographic analysis of the tetrachloro-*p*-xylene dimer conducted by D. D. Stewart (0·6%, 3 Cl; 7%, 5 Cl; and 92%, 4 Cl).

Equilibrium ring concentrations and the statistical conformations of polymer chains: Part 3. Substituent effects in polysiloxane systems

P. V. WRIGHT and J. A. SEMLYEN

The molar cyclization equilibrium constants K_x for cyclics $[R(CH_3)SiO]_x$, where R = H ($x = 4$–15), R = CH_3CH_2 ($x = 4$–20), R = $CH_3CH_2CH_2$ ($x = 4$–8) and R = $CF_3CH_2CH_2$ ($x = 4$–20), have been measured in some undiluted and solution equilibrates with an accuracy of $\pm 10\%$. K_4 and K_5 increase along the series R = H $<$ CH_3CH_2 $<$ $CH_3CH_2CH_2$ $<$ $CF_3CH_2CH_2$, whereas the K_x values for large cyclics ($x > 10$) decrease with increasing size of the substituent group R. The limiting proportionality between K_x and $x^{-5/2}$ predicted for macrocyclics by the Jacobson and Stockmayer theory is found for values of $x > ca$ 12 when R = H and for $x > ca$ 15 when R = CH_3CH_2 but only for values of $x > ca$ 25 when R = $CF_3CH_2CH_2$. The weight fractions of cyclics in high molecular weight poly(hydrogenmethylsiloxane), poly-(ethylmethylsiloxane) and poly(3,3,3-trifluoropropylmethylsiloxane) equilibrates increase with solvent dilution up to critical points corresponding to complete conversion of siloxane to ring molecules. The amounts of solvent required to attain these critical dilution points are ca 10% by volume of cyclohexanone at 383 K when R = $CF_3CH_2CH_2$, ca 60% by volume of toluene at 383 K when R = CH_3CH_2 and ca 80% by volume of toluene at 273 K when R = H. As in the poly(dimethylsiloxane) system, K_x values for the low molecular weight cyclics in poly(hydrogenmethylsiloxane) and poly(ethylmethylsiloxane) equilibrates increase with solvent dilution, whereas those for larger cyclics remain constant.

INTRODUCTION

MANY POLYSILOXANES based on the monomeric unit $R(CH_3)SiO$ equilibrate under the influence of catalysts to produce a thermodynamically-controlled distribution of ring and chain molecules. Poly(dimethylsiloxane) (R = CH_3) is the most important commercial polysiloxane and there have been several detailed investigations of the distribution of cyclic and linear molecules in the equilibrated polymer[1–5]. As part of a general study of the relationship between ring concentrations in polymeric systems and the statistical conformations of the corresponding chain molecules, we have determined the concentrations of cyclics in undiluted and solution equilibrates of some siloxanes that are closely related structurally to poly(dimethylsiloxane). The siloxanes chosen for this investigation were poly(hydrogenmethylsiloxane) (R = H), poly(ethylmethylsiloxane) (R = CH_3CH_2), poly(n-propylmethyl-siloxane) (R = $CH_3CH_2CH_2$) and poly(3,3,3-trifluoropropylmethylsiloxane)

($R = CF_3CH_2CH_2$). The results of this investigation are presented in this paper.

EXPERIMENTAL

Starting materials

Cyclic oligomers [$H(CH_3)SiO$]$_4$, [$CH_3CH_2(CH_3)SiO$]$_3$, [$CH_3CH_2CH_2(CH_3)$-SiO]$_3$ and [$CF_3CH_2CH_2(CH_3)SiO$]$_3$ were a gift from the Research Department of Midland Silicones Limited. The cyclics and all the solvents used in the work (dichlorethane, toluene, methanol, acetone, cyclohexanone, ethyl acetate, tetrahydrofuran, diethylene glycol dimethylether) were fractionally distilled before use, and their purities were checked by gas–liquid chromatography.

Equilibrations

[$H(CH_3)SiO$]$_4$ was equilibrated in bulk and in toluene solution at 273 K using *n*-butyl lithium as catalyst and *ca* 2% tetrahydrofuran as promoter[6, 7].

[$CH_3CH_2(CH_3)SiO$]$_3$ and [$CH_3CH_2CH_2(CH_3)SiO$]$_3$ were equilibrated in bulk at 383 K in sealed glass ampoules using potassium as catalyst. Solution equilibrates of [$CH_3CH_2 (CH_3)SiO$]$_3$ were carried out in toluene at 383 K using potassium hydroxide as catalyst and diethylene glycol dimethylether as promoter.

[$CF_3CH_2CH_2(CH_3)SiO$]$_3$ was equilibrated in the bulk and in cyclohexanone at 383 K using potassium hydroxide as catalyst[8].

Each equilibration was carried out using 100–300 g of cyclic siloxane. Gas-liquid chromatography and gel permeation chromatography were used to monitor the course of the reactions and establish whether equilibrium had been attained. The equilibria were quenched by adding small amounts of glacial acetic acid, and the densities of the mixtures were determined separately by weighing known volumes of the equilibrates at the appropriate temperatures.

Separation of cyclics from linear polymers

The cyclic fractions of many of the polysiloxane equilibrates were separated from linear polymer prior to fractional distillation.

Following treatment with glacial acetic acid, the undiluted poly(ethylmethylsiloxane) and poly(*n*-propylmethylsiloxane) equilibrates were dissolved in sufficient toluene to give linear polymer concentrations of *ca* 10% by weight. These solutions were washed with distilled water so as to remove dissolved salts, which were found to catalyse re-equilibrations at elevated temperatures. Cyclics were separated from linear polymers by a number of fractional precipitations with acetone.

The undiluted poly(3,3,3-trifluoropropylmethylsiloxane) equilibrate was treated similarly using ethyl acetate as solvent and toluene as precipitant.

The poly(hydrogenmethylsiloxane) system was found to be experimentally

463

less tractable than the others, and equilibrations had to be carried out at low temperatures with exclusion of moisture and oxygen in order to prevent crosslinking of the chains. Cyclics and linear polymer were not separated for. the undiluted poly(hydrogenmethylsiloxane) equilibrate. This equilibrate was quenched, dissolved in toluene and analysed directly by gas-liquid chromatography and gel permeation chromatography. Cyclic concentrations were determined by calibrating the chromatographic instruments using fractions of cyclic and linear hydrogenmethylsiloxanes obtained from solution equilibrates carried out in toluene.

The molecular weights of the chain polymers were estimated viscometrically or from gel permeation chromatographic elution volumes. A most probable distribution of chain lengths was assumed for each linear polymer and the extents of reaction of functional groups in the chain fractions p calculated from the molecular weights using Flory's equations[9]. In all cases but one, values of p exceeded 0·99 so that molar cyclization equilibrium constants of the low molecular weight cyclics corresponded closely to their molar concentrations

Fractional distillation of cyclics

Following the removal of linear polymer, cyclics were distilled into 10–20 liquid fractions covering progressively higher cyclics. Efforts were made to keep these fractions as sharp as possible by the use of fractionating columns and careful control of temperature and pressure. Final fractions were obtained using a molecular still with a cooled glass probe at pressures down to 10^{-2} mmHg and temperatures up to 473 K. The fractions and the residues were analysed by gas-liquid chromatography and gel permeation chromatography.

Gas-liquid chromatography

A Pye 104 gas-liquid chromatograph with a katharometer detector was used to analyse the cyclic fractions. Response factors were estimated using either weighed mixtures of pure components or sharp fractions. Embacel (treated for the removal of polar groups by the method of Bohemen et al[10]) was used as the solid support and OV17 (supplied by the Field Instrument Co.) as the stationary liquid phase at loadings of ca 8% by weight. Temperature programming was carried out in the range 303–673 K.

Gel permeation chromatography

The gel permeation chromatograph was fitted with a Waters Model R4 differential refractometer detector and the crosslinked polystyrene columns were obtained from Waters Associates Ltd. Columns with gel of the following porosities were employed: 60,1000,250,10000 and 3000 Å*.

Analysis of total equilibrates and higher cyclic fractions were carried out by appropriate combinations of these columns and the column systems were

*1Å $\equiv$ 0·1nm.

calibrated against weighted fractions of cyclic and linear siloxanes of the systems studied.

RESULTS AND DISCUSSIONS

Theoretical molar cyclization equilibrium constants

The equilibrium between ring and chain molecules in a polysiloxane equilibrate may be represented as follows

$$\text{+R(CH}_3\text{)SiO+}_y \rightleftharpoons \text{+R(CH}_3\text{)SiO+}_{y-x} + [\text{R(CH}_3\text{)SiO}]_x \qquad (1)$$
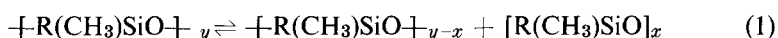
The nature of the termini of the chain molecules containing y and $y-x$ monomeric units depends on the catalyst used to establish equilibrium but the termini do not affect the position of equilibrium and hence many remain unspecified.

For a most probable distribution of chain lengths in the acyclic fraction, the molar cyclization equilibrium constants K_x are related to the extent of reaction of functional groups in the linear polymer, p, by

$$K_x = [\text{R(CH}_3\text{)SiO}]_x / p^x \qquad (2)$$

The Jacobson and Stockmayer[11] theory of cyclization provides a theoretical expression for K_x for large cyclic siloxanes formed by the forward reaction of equation (1) with zero enthalpy change, thus

$$K_x = [3/2 \pi \langle r_x^2 \rangle]^{3/2}(1/2N_A x) \qquad (3)$$

where $\langle r_x^2 \rangle$ is the mean-square distance between the ends of x-meric chains and N_A is the Avogadro constant. Equation (3) is based on the premise that the x-meric chains are of sufficient length and flexibility to obey the Gaussian expression for the density $W_x(0)$ of their end-to-end vectors $\mathbf{r}$ in the region corresponding to the close approach of chain ends ($\mathbf{r} = \mathbf{0}$), and further that these ends are randomly oriented[12].

Excluded volume effects should be negligible for siloxane chains in equilibrates containing a large fraction of high molecular weight polymer,[9,13] so that values of $\langle r_x^2 \rangle$ in such equilibrates may be identified with their unperturbed values $\langle r_x^2 \rangle_0$ as found under theta-point conditions. Furthermore, since values of $\langle r_x^2 \rangle_0$ for very long chains will be approximately proportional to the number of monomeric units, the Jacobson and Stockmayer theory predicts that in the limit of large x

$$K_x \propto x^{-2.5} \qquad (4)$$

This proportionality has been found to apply to large cyclics in the poly-(dimethylsiloxane) system, where a plot of log K_x values against log x yields the limiting slope of -2.5 for $x > ca$ 15 (ref. 12). Experimental molar cyclization equilibrium constants for large cyclic dimethylsiloxanes were found to be in excellent agreement with those calculated using values of $\langle r_x^2 \rangle_0$ computed

465

from Flory, Crescenzi and Mark's[14] rotational isomeric state model of poly-(dimethylsiloxane). In the discussion to follow, molar cyclization equilibrium constants of methylsiloxanes $[R(CH_3)SiO]_x$ containing other substituent groups R will be compared with values found for the dimethylsiloxanes and with predictions of the Jacobson-Stockmayer theory.

Effect of substituents on molar cyclization equilibrium constants in undiluted polysiloxane equilibrates

Experimental molar cyclization equilibrium constants K_x (in mol l^{-1}) for cyclics in undiluted poly(hydrogenmethylsiloxane), poly(dimethylsiloxane)[5], poly(ethylmethylsiloxane), poly(n-propylmethylsiloxane) and poly-(3,3,3-trifluoropropylmethylsiloxane) equilibrates are shown in *Figure 1*. The K_x values are accurate to within $\pm 10\%$ in all cases and to within $\pm 5\%$ for most of the low molecular weight cyclics. Molar cyclization equilibrium constants for the poly(hydrogenmethylsiloxane) system at 273 K will be compared with those of the other systems at 383 K despite the difference in the equilibration temperatures. Temperature changes of 110 K have little effect on cyclic concentrations in poly(dimethylsiloxane) equilibrates[2, 5] provided $x \geqslant 4$ and the same should be true for the poly(hydrogenmethylsiloxane) system. Cyclic trimers $[R(CH_3)SiO]_3$ were found to be present in all the equilibrates, but their concentrations were low and temperature-dependent and K_x values for these strained cyclics will not be considered here.

There is a striking correlation between the molar cyclization equilibrium constants K_x and the size of the substituent group R for the polysiloxane equilibrates. The K_x values for the smallest unstrained rings ($x = 4$ or 5) *increase* along the series $R = H < CH_3 < CH_3CH_2 < CH_3CH_2CH_2 < CF_3$-$CH_2CH_2$, so that K_4 and K_5 for $[H(CH_3)SiO]_4$ and $[H(CH_3)SiO]_5$ are lower by factors of seven and six than K_4 and K_5 for $[CF_3CH_2CH_2(CH_3)SiO]_4$ and $[CF_3CH_2CH_2(CH_3)SiO]_5$; by contrast, the K_x values for the larger cyclics *decrease* with increasing size of the substituent group R and, for example, K_{12} for $[H(CH_3)SiO]_{12}$ is ten times larger than K_{12} for $[CF_3CH_2CH_2(CH_3)SiO]_{12}$.

The experimental result presented in *Figure 1* show that the molar cyclization equilibrium constants for cyclic siloxanes $[R(CH_3)SiO]_x$ are highly sensitive to the nature of the substituent group R. Differences in K_x values must reflect differences in the conformational properties of the corresponding open chain molecules, and the latter can be interpreted in terms of the steric influences of the group R. The cyclic tetramers $[R(CH_3)SiO]_4$ and pentamers $[R(CH_3)SiO]_5$ can adopt a number of conformations free of unfavourable steric interactions whether R = H or $CF_3CH_2CH_2$. As the group R increases in size, the number of low-energy conformations which may be adopted by the corresponding linear chains must be drastically reduced so that K_4 and K_5 increase along the series $R = H < CH_3 < CH_3CH_2 < CH_3CH_2CH_2 < CF_3CH_2$-$CH_2$.

As shown in *Figure 1*, there are well-defined minima in the K_x values for cyclic ethylmethylsiloxanes and 3,3,3-trifluoropropylmethylsiloxanes at $x = 12$ which parallel that first observed by Brown and Slusarczuk[4] for the cyclic dimethylsiloxanes. No such minimum is found in the log K_x versus

466
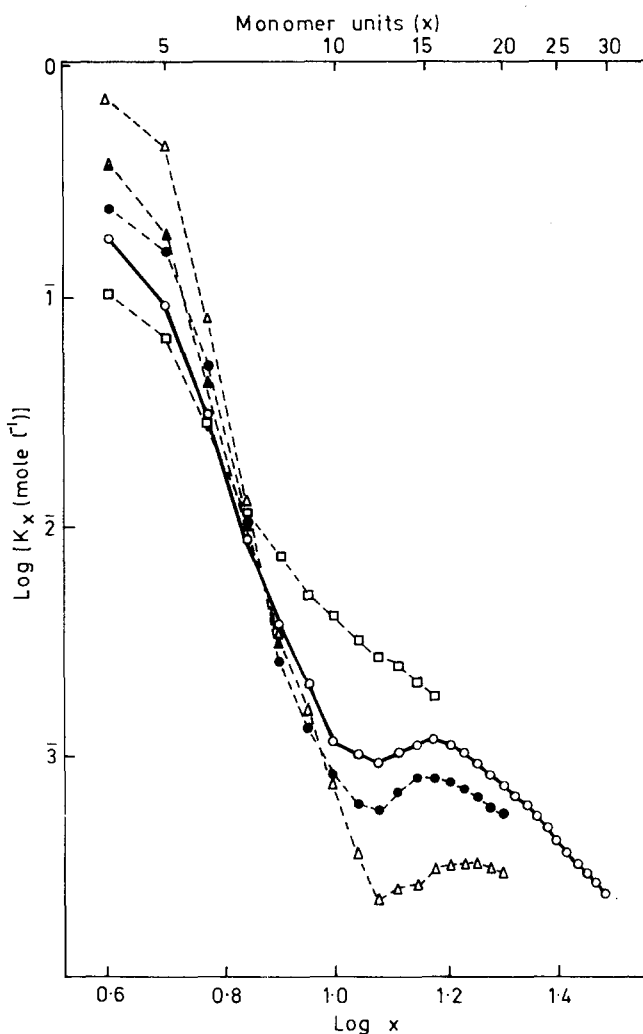
Figure 1 Experimental molar cyclization equilibrium constants
K_x for siloxanes $[R(CH_3)SiO]_x$ in undiluted equilibrates at
273 K (R = H) and 383 K (R = CH_3, CH_3CH_2, $CH_3CH_2CH_2$,
$CF_3CH_2CH_2$). K_x values are denoted by: □ for R = H; ○ for
R = CH_3; ● for R = CH_3CH_2; ▲ for R = $CH_3CH_2CH_2$;
△ for R = $CF_3CH_2CH_2$

log x plot for hydrogenmethylsiloxanes but there is a slight point of inflection
at $x \simeq 12$. Now, molar cyclization equilibrium constants K_x are directly
proportional to the densities $W_x(0)$ of end-to-end vectors **r** at **r** = **0**,[11, 12] so
there is a decrease in the 'flexibilities' of siloxane chains $+R(CH_3)SiO+_{12}$
along the series R = H $\rangle$ CH_3 $\rangle$ CH_3CH_2 $\rangle$ CF_3CH_2CH_2 in the sense that the
corresponding $W_{12}(0)$ values decrease, and $W_{12}(0)$ for chains with R = H
are ten-fold larger than $W_{12}(0)$ for chains with R = $CF_3CH_2CH_2$.

467

The hydrogenmethylsiloxane and ethylmethylsiloxane systems show limiting slopes close to $-2 \cdot 5$ in the log K_x versus log x plots at $x > ca$ 12 and $x > ca$ 15 respectively. This limiting slope is predicted for unstrained macrocyclics by the Jacobson-Stockmayer theory (equation 4) and is found for values of $x > ca$ 15 in the dimethylsiloxane system[5, 12]. By contrast, K_x values for cyclic 3,3,3-trifluoropropylmethylsiloxanes actually *increase* from $x = 15$ to a maximum at $x = 18$, there is then a slow decrease in K_x up to K_{25} and it is only for $x > ca$ 25 that the limiting slope of $-2 \cdot 5$ is approached.

The dimensions of oligomeric hydrogenmethylsiloxane and ethylmethylsiloxane chains in the undiluted equilibrates can be estimated by application of the Jacobson-Stockmayer expression (equation 3) to K_x values in the regions which exhibit the limiting log K_x versus log x slope of $-2 \cdot 5$. The dimensions of linear siloxanes $-[R(CH_3)SiO]-_x$ estimated in this way are found to increase along the series $R = H < CH_3 < CH_3CH_2$. The ratio $\langle r_{18}^2 \rangle / 36 l^2$ of the mean square end-to-end length $\langle r_{18}^2 \rangle$ of siloxane chains $-[R(CH_3)SiO]-_{18}$ containing 36 silicon-oxygen bonds (each of length $l = 1 \cdot 64 \text{Å}$[14]) to $2xl^2$ is $5 \cdot 4$ for $R = H$ at 273 K, $6 \cdot 8$ for $R = CH_3$ at 383 K and $8 \cdot 6$ for $R = CH_3CH_2$ at 383 K.

Effect of dilution on cyclic content of polysiloxane equilibrates

The total weight fractions of cyclics $[R(CH_3)SiO]_x$ ($x = 3-\infty$) in undiluted high molecular weight polysiloxane equilibrates are listed in *Table 1*. One of

Table 1 Cyclic contents of undiluted polysiloxane equilibrates

Substituent group R of monomeric unit [R(CH₃)SiO]	Temperature T (K)	Weight per cent cyclics in high molecular weight equilibrates ($p = 1$)			
		$x = 3-5$	$x = 6-18$	$x = 19-\infty$ †	Total
H	273	4·5	3·4	4·6	12·5
CH₃	383	10·0	3·6	4·7	18·3
CH₃CH₂	383	17·0	4·9	3·9	25·8
CH₃CH₃CH₂	383	27·0	*	−	−
CF₃CH₂CH₂	383	71·1	8·9	2·7	82·7

*31·0% for [CH₃CH₂CH₂(CH₃)SiO]ₓ with $x = 3-8$
†These values have been computed by extrapolation of experimental K_{18} values assuming that K_x is proportional to $x^{-2 \cdot 5}$ (equation 4)

the predictions of the Jacobson and Stockmayer theory is that if a ring–chain equilibration is carried out in the presence of an inert diluent, the weight fraction of material in the form of cyclics should increase with increasing dilution up to a critical point beyond which linear polymer will be effectively absent. The effects of dilution on the cyclic contents of four polysiloxane equilibrates are shown in *Figure 2*. The volume per cent of solvent required to attain the critical dilution point is *ca* 10% cyclohexanone at 383 K when $R = CF_3CH_2$- CH_2, *ca* 60% toluene at 383 K when $R = CH_3CH_2$, *ca* 75% toluene at 383 K when $R = CH_3$ (ref. 5) and *ca* 80% toluene at 273 K when $R = H$.

If the molar cyclization equilibrium constants for the cyclic siloxanes were to remain constant with dilution, the critical dilution points would correspond
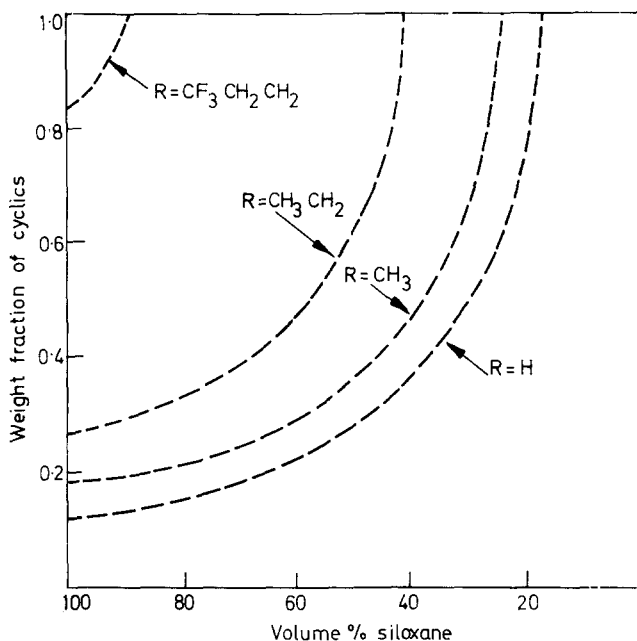
Figure 2 Weight fractions of cyclics $[R(CH_3)SiO]_x$ in high molecular weight ($p \cong 1$) polysiloxane equilibrates at 383 K ($R = CH_3, CH_3CH_2, CF_3CH_2CH_2$) and 273 K ($R = H$) as a function of the volume per cent siloxane in cyclohexanone ($R = CF_3CH_2CH_2$) and toluene ($R = H, CH_3, CH_3CH_2$)

to the addition of sufficient inert diluent to lower the molar concentrations of the siloxanes to the molar concentrations of the cyclics in the bulk equilibrates (i.e. *ca* 15% by volume for $R = CF_3CH_2CH_2$, *ca* 75% for $R = CH_3CH_2$, *ca* 85% for $R = CH_3$ and *ca* 90% for $R = H$). In practice, however, the molar cyclization equilibrium constants for the smaller cyclics in the poly(hydrogen-methylsiloxane) and poly(ethylmethylsiloxane) systems have been found to increase with dilution and the critical dilution points are lower than those predicted by simple application of the Jacobson-Stockmayer theory. As in the poly(dimethylsiloxane) system[5], K_4 and K_5 increase by *ca* 50–100% over the dilution range from the undiluted polymers to the critical dilution points, and K_6–K_8 show marked though smaller increases. Only the K_x values for the larger cyclics remain constant within experimental error. The effects of dilution on the molar cyclization equilibrium constants for $[H(CH_3)SiO]_x$ and $[CH_3CH_2(CH_3)SiO]_x$ ($x = 4$–8) are shown in *Figure 3*. In the poly(3,3,3-trifluoropropylmethylsiloxane) system, dilution with only *ca* 10% by volume cyclohexanone at 383 K results in virtually complete conversion to cyclics and no appreciable changes in the K_x values were observed over this limited dilution range.

It is noted that there are similar increases in the molar cyclization equilibrium constants for low molecular weight cyclics with solvent dilution in other ring–chain and ring–ring equilibria (e.g. ε-caprolactam in equilibrium with

469
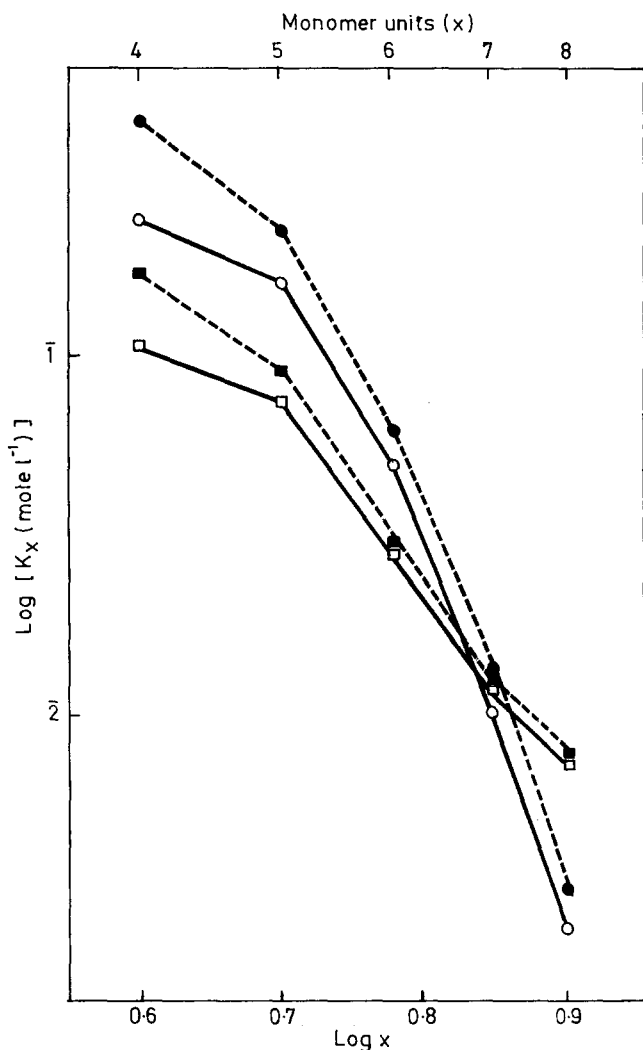
Figure 3 Experimental molar cyclization equilibrium constants
K_x for [H(CH$_3$)SiO]$_x$ at 273 K (denoted by □ and ■) and for
[CH$_3$CH$_2$(CH$_3$)SiO]$_x$ at 383 K (denoted by ○ and ●). K_x values
in undiluted equilibrates are denoted by □ and ○, and those
measured in toluene solution close to the critical dilution points
points are denoted by ■ and ●

nylon 6 and water;[15] 1,3-dioxolane in equilibrium with cyclic polymer and
various solvents[16]). These changes in K_x are believed to result from increases
in the activities of the monomers with decreasing polymer concentration.
High concentrations of linear polymer are present in the undiluted poly-
(hydrogenmethylsiloxane), poly(dimethylsiloxane) and poly(ethylmethyl-
siloxane) equilibrates. At the critical dilution points, the weight fractions of
linear polymers are reduced to zero and the molar concentrations of the low
molecular weight cyclics correspondingly increase.

ACKNOWLEDGEMENTS

Department of Chemistry,
University of York,
Heslington, York,
YO1 5DD, England   *(Received 8 May 1970)*

REFERENCES

1 Scott, D. W. *J. Amer. Chem. Soc.* 1946, **68**, 2294
2 Carmichael, J. B. and Winger, R. *J. Polym. Sci. (A)* 1965, **3**, 971
3 Hartung, H. A. and Camiolo, S. M., Papers presented to Division of Polymer Chemistry, American Chemical Society Meeting, Washington, March 1962
4 Brown, J. F. and Slusarczuk, G. M. J. *J. Amer. Chem. Soc.* 1965, **87**, 931
5 Semlyen, J. A. and Wright, P. V. *Polymer, Lond.* 1969, **10**, 543
6 Lee, C. L. *J. Organometal. Chem.* 1966, **6**, 620
7 We thank Dr W. G. Davies of Midland Silicones Ltd for suggesting this equilibration reaction and for outlining experimental details
8 Brown, E. D. and Carmichael, J. B. *J. Polym. Sci. (B)* 1965, **3**, 473
9 Flory, P. J. 'Principles of Polymer Chemistry' Cornell University Press, Ithaca, New York, 1953
10 Bohemen, J., Langer, S. H., Perrett, R. H. and Purnell, J. J. *J. Chem. Soc.* 1960, p 2444
11 Jacobson, H. and Stockmayer, W. H. *J. Chem. Phys.* 1950, **18**, 1600
12 Flory, P. J. and Semlyen, J. A. *J. Amer. Chem. Soc.* 1966, **88**, 3209
13 Flory, P. J. 'Statistical mechanics of Chain Molecules,' Interscience, New York, 1969
14 Flory, P. J., Crescenzi, V. and Mark, J. E. *J. Amer. Chem. Soc.* 1964, **86**, 146
15 Giori, G. and Hayes, B. T. *J. Polym. Sci. (A-1)* 1970, **8**, 351
16 Kuzub, L. I., Markevich, M. A., Berlin, A. A. and Yenikolopyan, N. S. *Polym. Sci., USSR (A-10)* 1968, **9**, 2332

Equilibrium ring concentrations and the statistical conformations of polymer chains:
Part 4. Calculation of cyclic trimer content of poly(ethylene terephthalate)

G. R. WALKER and J. A. SEMLYEN

The equilibrium concentration of cyclic trimer in poly(ethylene terephthalate) (PET) melts is calculated by the Jacobson and Stockmayer theory using rotational isomeric state models to describe the conformational statistics of the corresponding linear chains. The Williams and Flory rotational isomeric state model of PET is used for the calculations, together with a model which incorporates structural information made available by a recent study of internal rotation in ethyl formate. This latter model takes into account all the intramolecular interactions within monomeric units by considering interactions that depend on rotations about monads, diads and triads of skeletal bonds. The models define 26 244 discrete conformations for the acyclic trimer $(CO.C_6H_4.CO.O.CH_2.CH_2.O)_3$. The probability that such a chain will intramolecularly cyclize is calculated by computing the total number of conformations that have terminal atoms in close proximity for ring closure, each conformation being accorded a statistical weight based on molecular structural information relating to low molecular weight analogues and on estimates of the steric and electrostatic attractions and repulsions between non-bonded atoms of the chain. The rotational isomeric state models predict the cyclic trimer content of PET melts at 570 K to be 0·1–0·5% by weight (compared with the experimental value of 1·4%) and they give values of the ratio $[\langle r^2 \rangle_0/M]_\infty$ of the unperturbed mean-square end-to-end distance of PET to its molecular weight of 0·9–0·6Å²(g mol.wt.)$^{-1}$ at 303K (compared with the experimental value of 1·0).

INTRODUCTION

The Jacobson and Stockmayer theory relates the concentrations of cyclics in condensation polymers, or in polymers produced by reversible ring-to-chain equilibrations, to the probabilities of coincidence of the ends of the corresponding open chain molecules[1]. Recently, the theory has been applied to calculate macrocyclic concentrations in poly(dimethylsiloxane)[2, 3] and nylon-6[4] equilibrates. Chains undergoing intramolecular cyclization were assumed to obey the Gaussian relationship for the densities $W_x(\mathbf{r})$ of their end-to-end vectors $\mathbf{r}$ in the region $\mathbf{r} = \mathbf{0}$, so that

$$W_x(0) = (3/2\pi \langle r_x^2 \rangle)^{3/2} \tag{1}$$

where $\langle r_x^2 \rangle$ represents the mean-square end-to-end distance of a chain consisting of x monomeric units. Values of $\langle r_x^2 \rangle$ for chains in polymeric

melts were identified with those found under theta-point conditions, and computed by the mathematical methods of Flory and Jernigan[5, 6] using rotational isomeric state models[7, 8] to describe the conformational statistics of the linear chains. There was good agreement between the experimentally-determined concentrations of large rings in bulk and solution equilibrates and those calculated using the Jacobson and Stockmayer theory[2-4].

There are no exact analytic expressions available to calculate values of $W_x(0)$ for real polymeric chains of finite length and limited flexibility. Yet, in principle, it should still be possible to calculate values of $W_x(0)$ for such chains provided their conformational statistics can be adequately described by a rotational isomeric state model. The distances between the ends of the chains can be determined for each discrete conformation defined by the rotational isomeric state model and the number of conformations with their ends in close proximity found, each conformation being appropriately weighted so as to make due allowance for differences in their energies[9]. This method is applied here to calculate the equilibrium concentration of cyclic trimer in poly(ethylene terephthalate) (PET) melts (see references 10, 11 for closely related studies). A general rotational isomeric state model of PET is set up and used for the calculations. The model incorporates statistical weight parameters that take account of all the intramolecular attractions and repulsions between nonbonded atoms of the chain. It is based on the analysis by Williams and Flory[12, 13], of the structure of PET, and incorporates structural information made available by a recent study of internal rotation in ethyl formate[14]. The relationship of this general model to that set up by Williams and Flory[12, 13] is described, and both models are used for the calculations to follow.

A GENERAL ROTATIONAL ISOMERIC STATE MODEL FOR PET

Rotational isomeric states of skeletal bonds

A section of PET containing three monomeric units is shown in *Figure 1*. Values of bond lengths and bond angles to be used throughout are those assigned by Williams and Flory[12]; they are listed in the legend to *Figure 1*. There is molecular structural evidence to support assignment of the ester groups in PET to planar *trans* conformations and the terephthaloyl groups to *trans* ($\phi_2 = 0°$) and *cis* ($\phi_2 = 180°$) conformations with approximately equal probability[12]. Skeletal bonds of the $O.CO.C_6H_4.CO.O$ residues have high energy barriers restricting internal rotation, but the triads of bonds in the ethylene glycol residues do not. Using the rotational isomeric state approximation, the distribution of rotational states about the $O–CH_2$, $CH_2–CH_2$, $CH_2–O$ bonds will be assumed to be represented by choice of three discrete rotational isomeric states corresponding to minima in their torsional rotational potentials[13].

Riveros and Bright Wilson[14] have shown recently that the potential function for internal rotation about the $CH_2–O$ bond in ethyl formate has minima at
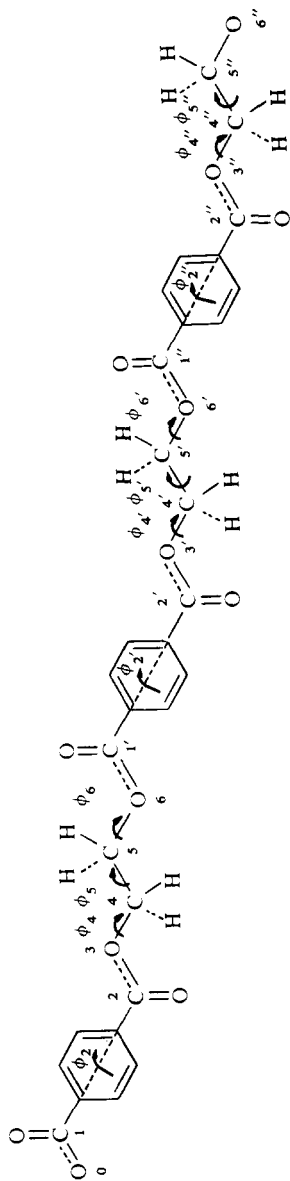
Figure 1 Section of PET in the all-*trans* conformation. Atoms of the repeat units are numbered 1–6, 1′–6′, 1″–6″. Angles of rotation about bonds 2, 4, 5, 6 are labelled ϕ_2, ϕ_4, ϕ_5, ϕ_6. $l_2 = 5 \cdot 74$ Å, $l_1 = l_3 = 1 \cdot 34$ Å, $l_4 = l_6 = 1 \cdot 44$ Å, $l_5 = 1 \cdot 53$ Å, $l_{C-H} = 1 \cdot 09$ Å, $l_{C=O} = 1 \cdot 22$ Å, $\theta_1 = \theta_2 = 66°$, $\theta_3 = \theta_6 = 67°$, $\theta_4 = \theta_5 = 70°$, $\widehat{CCH} = 109°$, $\widehat{OCO} = 55°$ (ref. 12)

474

$0°$, $\pm 95°$ (see *Figure 2*). A very similar potential function must be expected for the corresponding bonds in PET. Hence ϕ_4 and ϕ_6 are assigned to $0°$ [*trans* (t)], $+95°$ [*gauche*+ (g^+)] and $-95°$ (*gauche*− g^-)] positions. In the absence of similar detailed information relating to internal rotation about CH_2—CH_2 bonds in esters of ethylene glycol, rotational isomeric states at $\phi_5 = 0°(t)$, $+120°$ (g^+), $-120°$ (g^-) are chosen for the CH_2—CH_2 bonds in PET. The appropriateness of this choice receives support from studies of
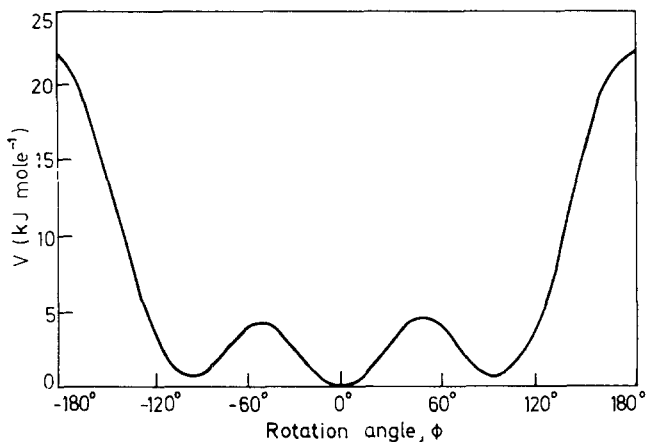
Figure 2 Torsional rotational potential $V(\phi)$ for internal rotation about the O—CH_2 bond in ethyl formate (ref. 14)

internal rotation about the CH_2—CH_2 bonds in a number of 1,2-disubstituted ethanes[15].

The special structural features of PET ensure the complete independence of rotations about bonds of different monomeric units, because the long, inflexible terephthaloyl groups prevent atoms of neighbouring units being brought into close range[12, 13]. Thus, PET consists of triads of skeletal bonds about which there is relatively free rotation, each triad being well-separated from the others by terephthaloyl units, within which internal rotation is highly restricted. Hence, all the short-range intramolecular interactions between non-bonded atoms of the chain can be taken into account by the introduction of a set of statistical weight parameters as will now be described.

Statistical weight parameters

Following the accepted procedure for assessing the energies of different conformations of polymeric chains, a statistical weight of unity is associated with the planar, all-*trans* conformation. Statistical weight parameters (defined in *Table 1*) are introduced to take account of the energies of other conformations relative to it. Each parameter is related to the difference in energy ΔE between its associated conformation and the all-*trans* conformation by the Boltzmann expression $\exp(-\Delta E/RT)$, where ΔE and R are in units of $J\,mol^{-1}$.

475

Table 1 Statistical weight parameters

Rotation angles	Interacting atoms or groups	Bond conformations	Statistical weight parameters
Interactions arising from rotations about one skeletal bond			
ϕ_4	$C=O \ldots CH_2$	$g^+(g^-)$	σ_1
ϕ_5	$-O- \ldots -O-$	$g^+(g^-)$	σ_2
ϕ_6	$CH_2 \ldots C=O$	$g^+(g^-)$	σ_1
Interactions arising from rotations about pairs of skeletal bonds			
ϕ_4, ϕ_5	$C=O \ldots -O-$	$tg^+(tg^-)$	ω_1
		$g^+t(g^-t)$	ω_2
		$g^+g^+(g^-g^-)$	ω_3
		$g^+g^-(g^-g^+)$	ω_4
ϕ_5, ϕ_6	$-O- \ldots C=O$	$tg^+(tg^-)$	ω_2
		$g^+t(g^-t)$	ω_1
		$g^+g^+(g^-g^-)$	ω_3
		$g^+g^-(g^-g^+)$	ω_4
Interactions arising from rotations about triads of skeletal bonds			
ϕ_4, ϕ_5, ϕ_6	$C=O \ldots C=O^*$	$ttg^+(ttg^-, g^+tt, g^-tt)$	δ_1
		$tg^+t(tg^-t)$	δ_2
		$tg^+g^+(tg^-g^-, g^+g^+t, g^-g^-t)$	δ_3
		$tg^+g^-(tg^-g^+, g^+g^-t, g^-g^+t)$	δ_4
		$g^+tg^+(g^-tg^-)$	δ_5
		$g^+tg^-(g^-tg^+)$	δ_6
		$g^+g^+g^+(g^-g^-g^-)$	δ_7
		$g^+g^+g^-(g^-g^-g^+, g^+g^-g^-, g^-g^+g^+)$	δ_8
		$g^+g^-g^+(g^-g^+g^-)$	δ_9

*Atoms of neighbouring phenylene groups $-C_6H_4-$ are well separated for all conformations and do not contribute appreciably to $\delta_1-\delta_9$.

The statistical weight parameter γ weighs the *cis* conformation of the terephthaloyl group relative to the *trans*. Williams and Flory[12] cite evidence to support a value of unity for γ and this is the value used here.

The parameter σ_1 is accorded the experimental value of $\exp(-778/RT)$ found by Riveros and Bright Wilson[14] for the corresponding $O-CH_2$ bond

in ethyl formate (see *Figure 2*). The difference of 778 $J\,mol^{-1}$ between the energies of the *gauche* and *trans* states of the $O—CH_2$ bond takes account of contributions from the intrinsic torsional rotational potential as well as from intramolecular steric and electrostatic interactions.

The parameter σ_2 weights a *gauche* state of the $CH_2—CH_2$ bond relative to the *trans* state and depends on the potential function for internal rotation about this bond as well as on the magnitude of intramolecular interactions between oxygen atoms separated by three skeletal bonds (see *Table 1*). In the absence of structural information relating to internal rotation about $CH_2—CH_2$ bonds in low molecular weight structural analogues, σ_2 is assigned the value given to it by Williams and Flory[12] (namely $\sigma_2 = 1.5$ at $303\,K$). This value is based on the energy difference between *gauche* and *trans* states found for $CH_2—CH_2$ bonds in polyoxyethylene[16, 17].

The statistical weight parameters $\omega_1 - \omega_4$ and $\delta_1 - \delta_9$ (defined in *Table 1*) are assigned values based on estimates of the steric and electrostatic attractions and repulsions between the nonbonded carbon and oxygen atoms of the polar ester groups. These estimates were made using semi-empirical equations that have been widely used for such purposes[18-20]. The methods recommended by Scott and Scheraga[21, 22] and by Brant and Flory[23, 24] and their respective coworkers were used to calculate nonbonded interaction energies, thereby yielding two sets of values for the parameters $\omega_1 - \omega_4$ and $\delta_1 - \delta_9$. A Buckingham expression was chosen to describe the van der Waals repulsions arising from the overlap of nonbonded atoms and an r_{ij}^{-6} attractive component was assumed to represent London dispersion attractions[18, 19], so that the steric interaction energy E_{ij} between atoms i and j separated by r_{ij} Å is given by

$$E_{ij} = a_{ij}\exp\left(-b_{ij}r_{ij}\right) - c_{ij}/r_{ij}^6 \qquad (2)$$

The parameters b_{ij} were taken as $4.6\,Å^{-1}$ for all atom pairs and values of c_{ij} were obtained from the polarizabilities of the atoms and the effective number of valence electrons using the Slater-Kirkwood equation[21-24]. The energy E_{ij} was minimized at the sum of the crystallographic van der Waals radii of the non-bonded atoms (the method recommended by Scott and Scheraga[21, 22]) and at a distance of separation 0.2 Å greater than this (the method recommended by Brant and Flory[23, 24]). Assuming van der Waals radii of 1.7 Å and 1.5 Å for carbon and oxygen atoms respectively[25], these procedures gave the a_{ij} values listed in *Table 2*. Electrostatic interactions were calculated using the point monopole approximation[22-24]. Partial electronic charges were assigned to the atoms of the ester groups as described in references 22 and 24, giving the two sets of values listed in *Table 2*. The electrostatic energy Q_{ij} between atoms i and j carrying partial charges q_i and q_j was calculated using the equation

$$Q_{ij} = 1389\,q_iq_j/\epsilon r_{ij} \qquad (3)$$

where r_{ij} is in Å, Q_{ij} is in $kJ\,mol^{-1}$ and ϵ is the dielectric constant. It has been concluded that a dielectric constant in the range $2.5–4.0$ should be used for calculating electrostatic interactions between nonbonded atoms at close

Table 2 Parameters required for the estimation of interaction energies

Atom pair i and j*	c_{ij} (kJ mol^{-1} Å^{-6})	$a_{ij} \times 10^{-5}$ (kJ mol^{-1})	
		methods of Scott and Scheraga	methods of Brant and Flory
C ... C	2301	35·44	59·58
C ...—O—	1598	14·98	24·60
C ... O=	1849	17·36	28·49
—O—...—O—	1167	6·86	10·96
—O—... O=	1339	7·87	12·55
O=... O=	1536	9·04	14·39

*Carbonyl oxygen atoms are denoted O=, the other oxygen atoms of the ester groups are denoted —O—.
Partial charge assignments (in units of electronic charge) are as follows:
Scott and Scheraga: $+0·517$ for C; $-0·417$ for O=; $-0·202$ for —O—
Brant and Flory: $+0·350$ for C; $-0·350$ for O=; $-0·109$ for —O—

range in polypeptide and polyester chains[22-24]. Hence the literature value for solid PET (namely $\epsilon = 3·0$) was adopted[26]. Values of $\omega_1 - \omega_4$ and $\delta_1 - \delta_9$ at 303 K and 570 K, which were obtained by calculating interaction energies using the procedures of Scott and Scheraga[21, 22] and Brant and Flory[23, 24], are listed in *Table 3*.

Table 3 Statistical weight parameters $\omega_1-\omega_4$ and $\delta_1-\delta_9$

	Values calculated using methods recommended by			
	Scott and Scheraga[21, 22]		Brant and Flory[23, 24]	
	303K	570K	303K	570K
ω_1	1·82	1·36	1·30	1·15
ω_2	0·92	0·96	0·98	0·99
ω_3	2·10	1·48	1·42	1·21
ω_4	0·64	0·79	0·08	0·27
δ_1	1·17	1·09	1·06	1·03
δ_2	0·60	0·76	0·82	0·90
δ_3	0·57	0·75	0·79	0·89
δ_4	1·62	1·30	1·82	1·38
δ_5	1·12	1·06	0·91	0·95
δ_6	1·35	1·17	1·22	1·11
δ_7	0·63	0·78	0·87	0·92
δ_8	2·72	1·70	0·45	0·65
δ_9	0·04	0·18	3×10^{-5}	4×10^{-3}

Williams and Flory's rotational isomeric state model

The Williams and Flory model [12, 13] assigns O—CH$_2$, CH$_2$—O bonds of PET to rotational isomeric states at $0°$, $\pm120°$. Their values for the statistical weight parameters at 303 K are as follows: $\gamma = 1$, $\sigma_1 = 0·7$, $\sigma_2 = 1·5$, $\omega_1 - \omega_3 = 1$ and $\omega_4 = 0·1$. Their model only considers interactions arising

from rotations about single or adjacent pairs of skeletal bonds so that the parameters $\delta_1 - \delta_9$ were not introduced. It gives similar values for the cyclic trimer content of PET and the unperturbed dimensions of the linear polymer to those obtained using the more general rotational isomeric state model described above, when the parameters $\omega_1 - \omega_4$ and $\delta_1 - \delta_9$ of the latter are calculated by the methods of Brant and Flory[23, 24] (see later).

CYCLIC TRIMER CONCENTRATION

Theoretical expression for cyclic trimer concentration

Goodman and Nesbitt[27] have established that there is a thermodynamic equilibrium between ring and chain molecules in PET melts in the presence of catalysts at 548–583 K. Cyclic dimer is absent, but cyclic trimer is present as $1 \cdot 4\%$ by weight together with smaller quantities of cyclic tetramer and pentamer.

The equilibrium between cyclic trimer $\llcorner M_3 \lrcorner$ and linear polymer in PET melts may be represented as follows

$$-M_y- \rightleftharpoons -M_{y-3}- + \llcorner M_3 \lrcorner \tag{4}$$
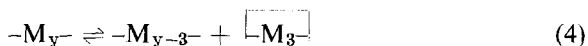
For the viscous, fibre-yielding melts analysed by Goodman and Nesbitt[27] there is a most probable distribution of chain lengths and the extent of reaction of functional groups in the chain fraction $p \simeq 1^*$. Thus, to a good approximation, the molar cyclization equilibrium constant

$$K_3 = \left[\llcorner M_3 \lrcorner \right] \tag{5}$$

Assuming zero enthalpy change for the forward and back reactions of equation (4) (see later), the Jacobson and Stockmayer theory[1, 2] yields the following expression for K_3 (in mol l^{-1})

$$K_3 = \frac{W_3(0)}{6N_A} \tag{6}$$

where $W_3(0)$ is the density of end-to-end vectors r for trimeric chains in the vicinity $r = 0$ (in molecules l^{-1}), N_A is Avogadro's constant and the correlations between the directions of terminal bonds expected for finite chains

---

*Dr G. Shaw of I.C.I. Fibres Ltd, Harrogate, England has used gel permeation chromatography to confirm that there is a most probable distribution of chain lengths in melt equilibrates of PET. His analyses of such melts also indicate a cyclic trimer concentration in agreement with Goodman and Nesbitt's published value. We are indebted to Dr Shaw for helpful discussions.

undergoing intramolecular cyclization are neglected (see below). Combination of equations (5) and (6) gives the percentage by weight w_3 of cyclic trimer in PET equilibrates as

$$w_3 = \frac{W_3(0)M_0}{20N_A\rho} \tag{7}$$

where M_0 is the molecular weight of a repeat unit and ρ is the density of the melt at the temperature of equilibration ($\rho = 1\cdot22\,\mathrm{g\,ml^{-1}}$ at 570 K)[26].

Numerical results and discussion

The rotational isomeric state models define 26 244 discrete conformations for the acyclic trimer extending from carbon atom 1 to oxygen atom 6″ in *Figure 1**. The number of conformations with the centres of terminal atoms separated by 0–2, 0–3, 0–4, 0–5 Å are 58, 186, 406, 762 for the model with ϕ_4, ϕ_6 at 0°, $\pm95°$ and 38, 120, 258, 538 for the Williams and Flory model where ϕ_4, ϕ_6 are at 0°, $\pm120°$. Some of these highly-coiled conformations are calculated to be of low energy with no large steric repulsions between non-bonded atoms and many favourable steric and electrostatic interactions. The cyclic trimer should be able to adopt these low-energy conformations. Hence, it should be an unstrained ring and this is the basis for the assumption of zero enthalpy change for the forward and back reactions of equation (4) (see above). The percentage by weight of cyclic trimer at 570 K was calculated from equation (7) by computing values for the density of end-to-end vectors $W_3(0)$ as follows. The sum of the statistical weights associated with each conformation of the acyclic trimer having terminal atoms within r Å was found and divided by the volume $(4/3)\pi r^3$ and by the total sum of the statistical weights of all 26 244 conformations. This sum is the conformational partition function of the chain and is given by equations (8′)–(16′) in the Appendix below.

Values of the cyclic trimer content of PET at 570 K and the unperturbed dimensions of the linear polymer at 303 K (calculated using both the general rotational isomeric state model described above and the Williams and Flory[12, 13] model) are compared with the corresponding experimental values in *Table 4*. The general rotational isomeric state model with values of $\omega_1 - \omega_4$ and $\delta_1 - \delta_9$ calculated by the methods of Brant and Flory[23, 24] give unperturbed dimensions of PET in close agreement with the experimental value, but predict a cyclic trimer content somewhat lower than that found experimentally. The methods of Scott and Scheraga[21, 22] give better agreement for the cyclic trimer content, but unperturbed chain dimensions substantially lower than those observed experimentally. It should be noted that the calculated cyclic trimer concentrations have been underestimated to some

---

*There are 486 conformations for the acyclic dimer (i.e. the chain extending from carbon atom 1 to oxygen atom 6′ in *Figure 1*). In none of these conformations do terminal atoms approach to within 7 Å. Hence the probability that a dimeric chain will intramolecular cyclize is calculated to be zero. This is in agreement with Goodman and Nesbitt's observation that cyclic dimer is not present in melt equilibrates of PET.

Table 4 Calculated values of w_3 at 570K and $(\langle r^2 \rangle_0/M)_\infty$ at 303K

	$w_3{}^*$ (per cent by weight)	$(\langle r^2 \rangle_0/M)_\infty$ † [Å^2 (g mol. wt.)$^{-1}$]
Experimental values	1·4 (ref. 27)	1·0 (refs. 12 and 13)
Williams and Flory's model	0·09	0·93
General model described above with ω_1–ω_4 and δ_1–δ_9 calculated by methods of		
(i) Scott and Scheraga[21, 22]	0·45	0·55
(ii) Brant and Flory[23, 24]	0·12	0·92

*Calculated by finding the statistically-weighted fraction of the 26 244 conformations of the acyclic trimer with their ends separated by less than 3 Å. As long as r is small (so that it represents the close approach of terminal atoms) the precise value accorded to it was found to be of little consequence. Thus, the second calculated value in this column becomes w_3 = 0·53, 0·43, 0·42% for r = 2, 4, 5 Å respectively

†Unperturbed dimensions of PET were calculated by the mathematical methods described in the Appendix.

extent by neglect of the correlations between the directions of the ends of the acyclic trimer in its highly-coiled conformations[2]. Computations of the relative positions of atoms in these conformations show that such correlations are indeed present and, since termini undergoing the competitive inter-molecular condensation reaction should be randomly oriented, inclusion of this effect would result in an increase in the calculated cyclic trimer con-centrations.

When account is taken of the limitations and approximations inherent in the calculations described here, the agreement between theory and experi-ment is considered to be very satisfactory; and, in fact. the close correspon-dence between the experimental cyclic trimer concentration and the values calculated using the rotational isomeric state models supports the contention that linear chains in polymeric melts adopt disordered, random-coil con-formations[28, 29].

Department of Chemistry,
University of York,
Heslington, York,
YO1 5DD, England   *(Received 8 May 1970)*

481

REFERENCES

1 Jacobson, H. and Stockmayer, W. H. *J. chem. Phys.* 1950, **18**, 1600
2 Flory, P. J. and Semlyen, J. A. *J. Amer. chem. Soc.* 1966, **88**, 3209
3 Semlyen, J. A. and Wright, P. V. *Polymer, Lond.* 1969, **10**, 543
4 Semlyen, J. A. and Walker, G. R. *Polymer, Lond.* 1969, **10**, 597
5 Flory, P. J. *Proc. Nat. Acad. Sci., Wash.* 1964, **51**, 1060
6 Flory, P. J. and Jernigan, R. L. *J. chem. Phys.* 1965, **42**, 3509
7 Flory, P. J., Crescenzi, V. and Mark, J. E. *J. Amer. chem. Soc.* 1964, **86**, 146
8 Flory, P. J. and Williams, A. D. *J. Polym. Sci. (A-2)* 1967, **5**, 399
9 Semlyen, J. A. *Trans. Faraday Soc.* 1967, **63**, 2342
10 Nementhy, G. and Scheraga, H. A. *Biopolymers* 1965, **3**, 155
11 Carmichael, J. B. and Kinsinger, J. B. *Canad. J. Chem.* 1964, **42**, 1996
12 Williams, A. D. and Flory, P. J. *J. Polym. Sci. (A-2)* 1967, **5**, 417
13 Flory, P. J., 'Statistical Mechanics of Chain Molecules' Interscience, New York, 1969
14 Riveros, J. M. and Wilson, E. B. *J. chem. Phys.* 1967, **46**, 4605
15 Lowe, J. P. *Prog. phys. org. Chem.* 1968, **6**, 1
16 Mark, J. E. and Flory, P. J. *J. Amer. chem. Soc.* 1965, **87**, 1415
17 Mark, J. E. and Flory, P. J. *J. Amer. chem. Soc.* 1966, **88**, 3702
18 Williams, J. E., Stang, P. J. and Schleyer, P. von R. *Ann. rev. phys. Chem.* 1968, **19**, 531
19 Hirschfelder, J. O., Curtiss, C. F. and Bird, R. B., 'Molecular Theory of Gases and Liquids,' John Wiley, New York, 1964
20 Scheraga, H. A. *Adv. phys. org. Chem.* 1968, **6**, 103
21 Scott, R. A. and Scheraga, H. A. *J. chem. Phys.* 1965, **42**, 2209
22 Ooi, T., Scott, R. A., Vanderkooi, G. and Scheraga, H. A. *J. chem. Phys.* 1967, **46**, 4410
23 Brant, D. A., Miller, W. G. and Flory, P. J. *J. Mol. Biol.* 1967, **23**, 47
24 Brant, D. A., Tonelli, A. E. and Flory, P. J. *Macromolecules* 1969, **2**, 225
25 Bondi, A. *J. phys. Chem.* 1964, **68**, 441
26 Brandrup, J. and Immergut, E. H., 'Polymer Handbook,' Interscience, New York, 1966
27 Goodman, I. and Nesbitt, B. F. *Polymer, Lond.* 1961, **1**, 384
28 Flory, P. J., 'Principles of Polymer Chemistry,' Cornell University Press, New York, 1953
29 Flory, P. J. in 'Lectures in Materials Science,' W. A. Benjamin, New York, 1963

APPENDIX

Unperturbed dimensions of PET chains with triads of interdependent bonds

The general mathematical methods of Flory and Jernigan[5, 6] may be used to calculate the unperturbed dimensions of model polymer chains of any length and sequence of bonds and with interdependent bond rotational states. A considerable saving in computational time is possible for model polyamide and polyester chains where there is mutual interdependence of rotations about skeletal bonds within structural units but a total independence of rotations about bonds separated by amide or ester groups[8].

The methods of Flory and Jernigan[13] have been extended to calculate the dimensions of PET chains, whose statistical conformations are described by the general rotational isomeric state model with its triads of interdependent bond rotational states. The mean-square end-to-end distance $\langle r_x^2 \rangle_0$ of such a

chain with x repeat units and n skeletal bonds of mean-square length $\bar{l}^2$ is given by the following expression

$$\langle r_x^2 \rangle_0 = n\bar{l}^2 + 2[10 \ldots 0](\overline{\mathbf{G}}^6)^{x-1}\,(\overline{\mathbf{G}}^5)\begin{bmatrix} 0 \\ \cdot \\ \cdot \\ \cdot \\ 0 \\ l_n \\ 0 \\ 0 \\ 1 \\ 0 \\ 0 \end{bmatrix} \qquad (1')$$

where the vector $\mathbf{r}$ is defined as that between terminal oxygen atoms (i.e. oxygen atom O and oxygen atom 6" for the chain with $x = 3$ depicted in *Figure 1*). The superscript 6 of the matrix $\overline{\mathbf{G}}^6$ (which is of order 15×15) denotes the number of skeletal bonds within the repeat unit. This matrix has been normalized by division of all its elements by the partition function $\mathbf{Z}^6$ for the repeat unit, thus

$$\overline{\mathbf{G}}^6 = \mathbf{G}^6 \begin{bmatrix} \mathbf{J} & 0 & 0 \\ 0 & \mathbf{J} \otimes \mathbf{E} & 0 \\ 0 & 0 & \mathbf{J} \end{bmatrix} (\mathbf{Z}^6)^{-1} \qquad (2')$$

$\mathbf{J}$ is a 9×1 matrix with all its elements unity, $\mathbf{E}$ is the identity matrix of order 3, the symbol $\otimes$ denotes a direct product of matrices and $\mathbf{G}^6$ is the product of six generator matrices to be defined below.

$$\mathbf{G}^6 = \mathbf{G}_1\mathbf{G}_2\mathbf{G}_3\mathbf{G}_4\mathbf{G}_5\mathbf{G}_6 \qquad (3')$$

Similarly, $\overline{\mathbf{G}}^5$ for the terminal unit is given by

$$\overline{\mathbf{G}}^5 = \mathbf{G}^5 \begin{bmatrix} \mathbf{J} & 0 & 0 \\ 0 & \mathbf{J} \otimes \mathbf{E} & 0 \\ 0 & 0 & \mathbf{J} \end{bmatrix} (\mathbf{Z}^5)^{-1} \qquad (4')$$

where

$$\mathbf{G}^5 = \mathbf{G}_1\mathbf{G}_2\mathbf{G}_3\mathbf{G}_4\mathbf{G}_5 \qquad (5')$$

The generator matrices $\mathbf{G}_i$ ($i = 1\text{-}6$) are constructed as follows

$$\mathbf{G}_i = \begin{bmatrix} \mathbf{U} & (\mathbf{U} \otimes \mathbf{l}^\mathrm{T}) \, \|\mathbf{T}\| & 0 \\ 0 & (\mathbf{U} \otimes \mathbf{E}) \, \|\mathbf{T}\| & \mathbf{U} \otimes \mathbf{l} \\ 0 & 0 & \mathbf{U} \end{bmatrix}_i \qquad (6')$$

where the vector moment l_i of bond i is given by

$$l_i = \begin{bmatrix} l_i \\ 0 \\ 0 \end{bmatrix}; \quad \text{and} \quad l_i^\mathrm{T} = [l_i \quad 0 \quad 0] \qquad (7')$$

The statistical weight matrices U_i have the states of bonds $i - 2$ and $i - 1$ indexed on the rows and those of $i - 1$ and i on the columns. Thus the following statistical weight matrices take account of all the intramolecular interactions associated with rotations about the triad of interdependent bonds within a repeat unit.

$$
U_1 = \begin{array}{cc} & \begin{array}{ccc} t & t & t \\ t & g^+ & g^- \end{array} \\ \begin{array}{cc} t & t \\ t & g^+ \\ t & g^- \end{array} & \begin{bmatrix} 1 & 0 & 0 \\ 0 & 1 & 0 \\ 0 & 0 & 1 \end{bmatrix} \end{array} \tag{8'}
$$

$$
U_2 = \begin{array}{cc} & \begin{array}{cc} t & c \\ t & t \end{array} \\ \begin{array}{cc} t & t \\ g^+ & t \\ g^- & t \end{array} & \begin{bmatrix} 1 & \gamma \\ 1 & \gamma \\ 1 & \gamma \end{bmatrix} \end{array} \tag{9'}
$$

$$
U_3 = \begin{array}{cc} & \begin{array}{cc} t & t \\ t & c \end{array} \\ \begin{array}{cc} t & t \\ t & c \end{array} & \begin{bmatrix} 1 & 0 \\ 0 & 1 \end{bmatrix} \end{array} \tag{10'}
$$

$$
U_4 = \begin{array}{cc} & \begin{array}{ccc} t & g^+ & g^- \\ t & t & t \end{array} \\ \begin{array}{cc} t & t \\ t & c \end{array} & \begin{bmatrix} 1 & \sigma_1 & \sigma_1 \\ 1 & \sigma_1 & \sigma_1 \end{bmatrix} \end{array} \tag{11'}
$$

$$
U_5 = \begin{array}{cc} & \begin{array}{ccccccccc} t & t & t & g^+ & g^+ & g^+ & g^- & g^- & g^- \\ t & g^+ & g^- & t & g^+ & g^- & t & g^+ & g^- \end{array} \\ \begin{array}{cc} t & t \\ t & g^+ \\ t & g^- \end{array} & \begin{bmatrix} 1 & 0 & 0 & \sigma_2\omega_1 & 0 & 0 & \sigma_2\omega_1 & 0 & 0 \\ 0 & \omega_2 & 0 & 0 & \sigma_2\omega_3 & 0 & 0 & \sigma_2\omega_4 & 0 \\ 0 & 0 & \omega_2 & 0 & 0 & \sigma_2\omega_4 & 0 & 0 & \sigma_2\omega_3 \end{bmatrix} \end{array} \tag{12'}
$$

$$
U_6 = \begin{array}{cc} & \begin{array}{ccccccccc} t & g^+ & g^- & t & g^+ & g^- & t & g^+ & g^- \\ t & t & t & g^+ & g^+ & g^+ & g^- & g^- & g^- \end{array} \\ \begin{array}{cc} t & t \\ g^+ & t \\ g^- & t \\ t & g^+ \\ g^+ & g^+ \\ g^- & g^+ \\ t & g^- \\ g^+ & g^- \\ g^- & g^- \end{array} & \begin{bmatrix} 1 & \sigma_1\omega_2\delta_1 & \sigma_1\omega_2\delta_1 & 0 & 0 & 0 & 0 & 0 & 0 \\ \delta_1 & \sigma_1\omega_2\delta_5 & \sigma_1\omega_2\delta_6 & 0 & 0 & 0 & 0 & 0 & 0 \\ \delta_1 & \sigma_1\omega_2\delta_6 & \sigma_1\omega_2\delta_5 & 0 & 0 & 0 & 0 & 0 & 0 \\ 0 & 0 & 0 & \omega_1\delta_2 & \sigma_1\omega_3\delta_3 & \sigma_1\omega_4\delta_4 & 0 & 0 & 0 \\ 0 & 0 & 0 & \omega_1\delta_3 & \sigma_1\omega_3\delta_7 & \sigma_1\omega_4\delta_8 & 0 & 0 & 0 \\ 0 & 0 & 0 & \omega_1\delta_4 & \sigma_1\omega_3\delta_8 & \sigma_1\omega_4\delta_9 & 0 & 0 & 0 \\ 0 & 0 & 0 & 0 & 0 & 0 & \omega_1\delta_2 & \sigma_1\omega_4\delta_4 & \sigma_1\omega_3\delta_3 \\ 0 & 0 & 0 & 0 & 0 & 0 & \omega_1\delta_4 & \sigma_1\omega_4\delta_9 & \sigma_1\omega_3\delta_8 \\ 0 & 0 & 0 & 0 & 0 & 0 & \omega_1\delta_3 & \sigma_1\omega_4\delta_8 & \sigma_1\omega_3\delta_7 \end{bmatrix} \end{array} \tag{13'}
$$

where U_1 has been reduced from a 9×3 to a 3×3 matrix in order to suppress redundant rows in G_1. The statistical weight parameters γ, σ_1, σ_2,

$\omega_1-\omega_4$ and $\delta_1 - \delta_9$ are defined in *Table 1*, and the conformational partition functions for a repeat unit $\mathbf{Z}^6$ and a terminal unit $\mathbf{Z}^5$ are as follows

$$\mathbf{Z}^6 = \mathbf{U}_2\mathbf{U}_3\mathbf{U}_4\mathbf{U}_5\mathbf{U}_6\mathbf{J} \tag{14'}$$

$$\mathbf{Z}^5 = \mathbf{U}_2\mathbf{U}_3\mathbf{U}_4\mathbf{U}_5\mathbf{J} \tag{15'}$$

Thus, the conformational partition function of the acyclic trimer extending from carbon atom 1 to oxygen atom 6″ in *Figure 1*, which is required for the calculation of the cyclic trimer content of PET, is given by

$$\mathbf{Z}_{\text{trimer}} = (\tfrac{1}{2})\mathbf{Z}^6\mathbf{Z}^6\mathbf{Z}^5 \tag{16'}$$

The pseudo-diagonal matrices $||\mathbf{T}_i||$ of order $9v \times 9v$ contain the transformation matrices $\mathbf{T}_i$ for the v rotational states of bond i in diagonal array so that the indexing corresponds to that of the appropriate statistical weight matrix. Thus, for example, the super-arrays $||\mathbf{T}_5||$ and $||\mathbf{T}_6||$ are as follows.

$$||\mathbf{T}_5|| = \begin{bmatrix} \mathbf{T}_5(t) \\ & \mathbf{T}_5(t) \\ & & \mathbf{T}_5(t) \\ & & & \mathbf{T}_5(g^+) \\ & & & & \mathbf{T}_5(g^+) \\ & & & & & \mathbf{T}_5(g^+) \\ & & & & & & \mathbf{T}_5(g^-) \\ & & & & & & & \mathbf{T}_5(g^-) \\ & & & & & & & & \mathbf{T}_5(g^-) \end{bmatrix} \tag{17'}$$

$$||\mathbf{T}_6|| = \begin{bmatrix} \mathbf{T}_6(t) \\ & \mathbf{T}_6(g^+) \\ & & \mathbf{T}_6(g^-) \\ & & & \mathbf{T}_6(t) \\ & & & & \mathbf{T}_6(g^+) \\ & & & & & \mathbf{T}_6(g^-) \\ & & & & & & \mathbf{T}_6(t) \\ & & & & & & & \mathbf{T}_6(g^+) \\ & & & & & & & & \mathbf{T}_6(g^-) \end{bmatrix} \tag{18'}$$

The transformation matrix $\mathbf{T}_i$ transforms the Cartesian coordinate system of bond $i + 1$ into that of bond i, i.e. if θ_i is the bond angle supplement of bond i and ϕ_i the angle of rotation relative to the *trans* ($\phi_i = 0°$) position, and if the x_i axis lies along bond i, the y_i axis at right angles to it so as to make an acute angle with the preceeding bond and the z_i axis completes the coordinate system, then

$$\mathbf{T}_i = \begin{bmatrix} \cos\theta & \sin\theta & 0 \\ \sin\theta\cos\phi & -\cos\theta\cos\phi & \sin\phi \\ \sin\theta\sin\phi & -\cos\theta\sin\phi & -\cos\phi \end{bmatrix} \tag{19'}$$

Values for the unperturbed dimensions of PET quoted in *Table 4* were calculated using equations (1')–(19').

Stress-strain behaviour of natural rubber vulcanized in the swollen state

COLIN PRICE, G. ALLEN, F. DE CANDIA*,
M. C. KIRKHAM and A. SUBRAMANIAM

Samples of natural rubber were vulcanized in the presence of n-decane, decalin and o-chlorobenzene. The diluents were then removed, and the force–extension characteristics of the samples studied over the range $1 \cdot 1 < \alpha < 2 \cdot 0$. The elastic behaviour of the solution-vulcanized elastomers appear to be in much closer agreement with the statistical theory of elasticity than is the case for vulcanizates prepared in the dry state.

INTRODUCTION

For the case of uniaxial deformation the statistical theory of rubber elasticity predicts[1]

$$f = \nu kT \left(\langle r_i^2 \rangle / \langle r_0^2 \rangle \right) (\alpha - \alpha^{-2}) \tag{1}$$

where f is the equilibrium force per unit area of the undeformed sample, ν is the number of active chains per unit volume of the sample, T the absolute temperature, k the Boltzmann constant, $\langle r_i^2 \rangle / \langle r_0^2 \rangle$ is the so-called front factor, and the extension ratio $\alpha = L/L_i$ where L and L_i are the lengths of the sample after and before deformation. Numerous studies[2,3] have been carried out to test the validity of equation (1), the majority having been made on rubbers which had been vulcanized in the dry state. The results show that for simple extension over the range $1 \cdot 1 < \alpha < 2 \cdot 0$ there is a significant deviation from the theoretical equation, the measurements being more adequately described by the empirical Mooney-Rivlin equation

$$f = C_1 (\alpha - \alpha^{-2}) + C_2 (1 - \alpha^{-3}) \tag{2}$$

The first constant C_1 has been shown to increase with increasing crosslink density and with increasing temperature. The evidence regarding the second constant C_2 is somewhat confused, and recent experimental work[4,5] has tended to contradict earlier indications that the magnitude of C_2 was not very dependent on the conditions under which network formation occurred. One point which does appear to have been established, however, is that the observed deviation from the theoretical expression is not an experimental artefact, and is associated with the equilibrium behaviour[6] of crosslinked rubbers. It has also been shown that, on swelling the rubber, the second term in equation (2) becomes less important. In representing the effect of swelling it is convenient to modify equation (2) to the form

$$fv_r^{1/3} = C_1 (\alpha - \alpha^{-2}) + C_2 (1 - \alpha^{-3}) \tag{3}$$

---

*Permanent Address: Laboratorio Di Ricerche Su Tecnologia Dei Polimeri E Reologia, Arco Felice (Napoli), Italy

where v_r is the volume fraction of rubber in the swollen system. It is then found that to a first approximation $C_1 = (C_1)_d$ and $C_2 = v_r(C_2)_d$, where subscript d signifies values observed at $v_r = 1$.

There is as yet no satisfactory quantitative explanation for the observed deviations from equation (1) at moderate strains, although the problem has attracted a great deal of attention in recent years[7]. Many of the difficulties associated with the problem have been clearly due to the lack of basic information concerning the behaviour of C_2.

In the present study we have vulcanized natural rubber samples in the presence of varying amounts of diluent. The samples were then dried, and their stress–strain characteristics studied by the usual methods. The aim of the study was to gain a clear indication as to whether the conditions under which network formation occurred had any bearing on the relative magnitude of the two elastic constants.

EXPERIMENTAL

Crosslinking procedure

To natural rubber (lightly masticated crêpe) packed in a pyrex tube was added a solution of dicumyl peroxide in a relatively inert, high boiling point solvent: the three solvents used for this purpose were: n-decane, decalin and o-dichlorobenzene. The mixture was then either left, or stirred carefully at intermittent periods of time, until equilibrium had been reached. After all the bubbles had disappeared from the solution (this could take up to two weeks) the tube was sealed under nitrogen. Tubes in which the bubbles did not disappear after a reasonable length of time were rejected; about half of the solutions had to be rejected for this reason. The system was crosslinked by heating to 140°C for 2h, after which it was allowed to slowly cool, to room temperature. The tube was then opened at the top and a small quantity of methanol added in order to slightly de-swell the gel, so that it came away cleanly from the glass sides. On recovery the gel was extracted with benzene to remove the high boiling point solvent, catalyst residues and any uncrosslinked rubber. The rubber specimen was dried under vacuum and then its two ends were trimmed perpendicular to the principal axis. Finally stainless steel end-pieces were bonded onto the specimen using Eastman 910 adhesive.

Stress–strain measurements

The force-extension characteristics of samples 1–4 were studied in a thermostatted environment using the following simple technique. The rubber test piece was suspended vertically from a rigid steel framework by firmly clamping the upper metal end-piece, and a loading pan was attached to the lower metal end-piece. The length between two fiducial reference marks was measured to $\pm\, 0.005$ cm with a cathetometer. Measurements were made for both increasing and decreasing loads, and readings were taken only after no further movement could be detected over a period of at least 1h. The force–extension characteristics of samples 5–9 were studied using a Hounsfield

487

Model E tensile tester fitted with an environmental chamber. A much shorter time scale (approximately 4 h for a complete cycle) was adopted for these measurements; however in almost all cases hysteresis effects were found to be negligibly small. A number of preliminary measurements carried out at a series of different strain rates indicated that the relaxation times for solution-vulcanized elastomers were significantly less than those for conventional vulcanizates.

RESULTS

Stress-strain measurements within the range $1 \cdot 1 < \alpha < 2 \cdot 0$ were carried out on samples 1–9 in the dry state at 22°C. For each set of data the quantity $f/(\alpha - \alpha^{-2})$ was plotted against α^{-1}. Linear plots were obtained in each case. Calculated values of C_1 and C_2 are given in *Table 1* and three representative

Table 1 Values of C_1 and C_2 for dry samples of solution-vulcanized natural rubber

Sample	Vulcanization	ϕ_r	DCP*	C_1 (kg cm^{-2})†	C_2 (kg cm^{-2})	$\phi_r^{-2/3} C_1$
1	Decalin	0·15	3	0·51	0·00	1·78
2	Decalin	0·18	3	0·72	0·25	2·25
3	Decalin	0·22	3	1·02	0·17	2·83
4	Decalin	0·31	3	1·40	0·25	3·08
5	*n*-Decane	0·20	3	1·10	0·00	3·19
6	*n*-Decane	0·28	3	1·25	0·05	2·92
7	*n*-Decane	0·28	3	1·21	0·07	2·83
8	*n*-Decane	0·40	3	1·77	0·10	3·26
9	*o*-Dichloro-benzene	0·25	4	1·80	0·00	4·54

*Parts of dicumyl peroxide by weight per 100 parts of crêpe rubber.
†Units: 1 kg cm$^{-2} \equiv 9 \cdot 807 \times 10^4$ N m^{-2}

plots are shown in *Figure 1*. The most striking feature of the results is the magnitude of C_2 which for each sample is either very low or zero. For the purpose of comparison we give in *Table 2* some typical values (obtained some

Table 2 Values of C_1 and C_2 for samples of natural rubber vulcanized in the dry state

DCP	Cure	C_1 (kg cm^{-2})	C_2 (kg cm^{-2})
3	140°C/60 min	3·10	1·21
3	140°C/45 min	3·47	1·12

time ago in our laboratory) for samples crosslinked in the dry state in the conventional manner (compare also the data reported by Mullins[8]). Clearly the presence of a diluent during vulcanization has an important effect on the
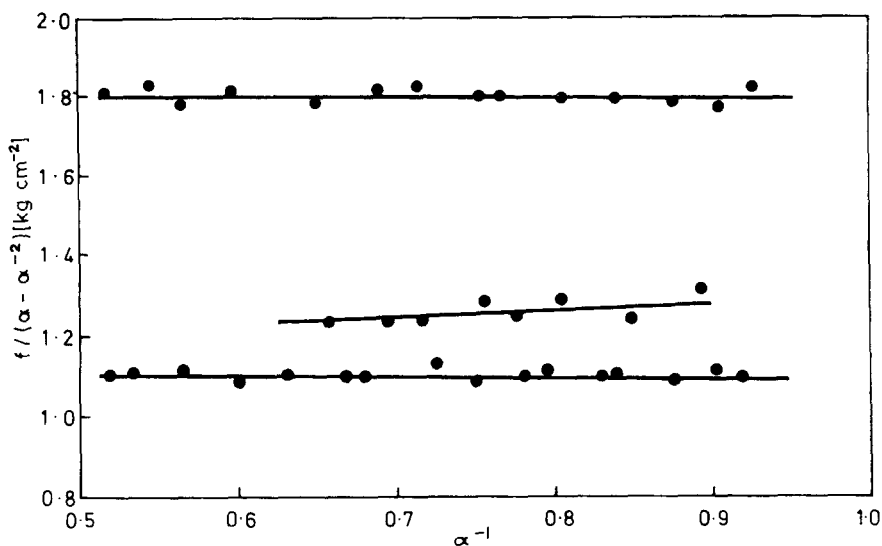
Figure 1 Mooney–Rivlin plots for three dry solution-vulcanized samples of natural rubber

elastic behaviour of the dried crosslinked rubber. For values of ϕ_r up to 0·40 (where ϕ_r is the volume fraction of rubber present during crosslinking) the magnitude of C_2 shows no sign of increasing towards the value ($\sim$ 1·0) typically observed for samples crosslinked in the dry state (see *Table 2*); it is hoped that future studies will establish over what range of ϕ_r the transition occurs.

Given in the last colum of *Table 1* are values of $\phi_r^{-2/3}C_1$ which on the basis of equation (1) can be related to the number of crosslinks per unit volume of dry rubber (see below). For a number of reasons the presence of a diluent can be expected to reduce the efficiency of the crosslinking process. However, comparison of the values of $\phi_r^{-2/3}C_1$ with the values of C_1 for conventional vulcanizates listed in *Table 2* shows that the effect is not very significant for the range of ϕ_r we have studied.

Force–extension measurements were also carried out on solution-vulcanized samples swollen to different extents by n-decane.

Plots of $f v_r^{1/3}/(\alpha - \alpha^{-2})$ against α^{-1} were found to be linear and the values of C_1 and C_2 obtained using equation (3) are given in *Table 3*.

<center>DISCUSSION</center>

Our studies show that by crosslinking natural rubber in the presence of a diluent, networks are obtained which have much lower values of C_2 (as measured in the dry state) than those found for conventional vulcanizates; for samples 1, 5 and 9 $C_2 = 0$, within the experimental uncertainty of ± 0.05 kg cm^{-2}. On swelling the solution-vulcanized networks the values of C_1, as

<center>489</center>

Table 3 Values of C_1 and C_2 for samples of
solution-vulcanized natural rubber swollen to
different extent in *n*-decane

Sample	v_r	C_1 (kg cm^{-2})	C_2 (kg cm^{-2})
6	1·00	1·25	0·05
	0·85	1·25	0·05
	0·68	1·27	−0·25
	0·51	1·27	−0·25
8	1·00	1·77	0·10
	0·77	1·74	0·10
	0·71	1·77	0·00
	0·56	1·87	−0·30

defined by equation (3), remain constant as predicted by equation (1). Values of C_2 on the other hand decrease very slightly on swelling, so that under these conditions marginally negative values are obtained. Viewing the data as a whole however it is quite clear that, for simple extension, solution vulcanized networks conform much more closely than conventional vulcanizates to equation (1). It is now highly desirable to test whether there is also good agreement with the statistical theory for other forms of strain.

It has been suggested previously[9] that low values of C_2 can be obtained if the rubber samples contain a high proportion of elastically inactive polymer which can act in a manner similar to a swelling agent. Whilst the efficiency of crosslinking. is somewhat reduced when carried out in the presence of a diluent, the reduction involved is far too small to account for the behaviour we have observed; this applies particularly in the case of samples crosslinked in the presence of only 60–80% of diluent. The most plausible explanation of the results is that the presence of a diluent during crosslinking in some way alters the actual topology of the network. It is not too difficult to see, at least qualitatively, how such differences arise. Theoretical studies of Edwards[10] predict that for concentrated polymer solutions the elastic shear modulus is proportional to $v_r{}^n$ where n becomes smaller with increasing molecular weight, approaching a limiting value of 1·5. Dynamic mechanical measurements[11] carried out on concentrated polymer solutions over the range $1 > v_r > 0.2$ broadly support the theoretical results, but give a slightly higher limiting value for n (~ 2.0). Thus there is strong evidence to suggest that the time-average number of physical constraints (i.e. entanglements) is a sensitive function of the solvent concentration. Whilst some of these constraints may be of the form in which one chain passes through a closed loop formed by a neighbouring chain, the majority are probably of a more transient nature consisting simply of tight cross-over junctions. When vulcanization takes place permanent chemical links are formed between chains. This process takes time and hence the final material has a network structure which depends upon the entire history of the process. However it can be argued that there will be built into the network a certain degree of physical entanglement which will be a function of the amount of solvent present during

the formation process. When the solvent is removed there will be an affine movement of crosslinks, so that the chains will tend to adopt a more highly coiled conformation. The average end-to-end distance for a given length of chain will be less in a dried solution-vulcanized network than in a system vulcanized in the dry state. This effect, however, should in no way add to, or detract from, the validity of equation (1) since it is adequately accounted for by the inclusion of the front term $\langle r_i^2 \rangle / \langle r_0^2 \rangle$, which will just become reduced in numerical value as solvent is removed. To a first approximation we can set $\langle r_i^2 \rangle / \langle r_0^2 \rangle = \phi_r^{2/3}$, where ϕ_r is the volume fraction of rubber present at the time of crosslinking.

It seems reasonable to conclude that the most important difference between conventional and solution-vulcanized networks lies in the degree of physical entanglement of the chains. In the classical theory of rubber elasticity physical constraints are considered effectively to be either permanent or transient. The former are treated in a manner similar to chemical crosslinks, whilst the latter are assumed to have negligible effect on the elastic properties since it is argued that their influence on average will be cancelled out. The results of the present investigation however would seem to indicate that more detailed consideration must be given to the effect of physical entanglements and overall network topology on stress–strain behaviour. The results we have reported for natural rubber clearly raise many questions and suggest some interesting future possibilities. If the behaviour we have observed for natural rubber turns out to be of a general nature it will be possible to discount many of the theories which have been put forward in recent years to account for the origin of the observed values of C_2.

Department of Chemistry,
University of Manchester,
Manchester M13 9PL

REFERENCES

1 Flory, P. J. *Trans. Faraday Soc.* 1961, **57**, 829
2 Treloar, L.R.G., 'The Physics of Rubber Elasticity', Oxford University Press, London 1958
3 Krigbaum, W. R. and Roe, R–J., *Rubber Chem. and Tech.* 1965, **38**, 1039
4 Kraus G., and Moczvgemba, G. A., *J. Polym. Sci. (A)* 1964, **2**, 277
5 Blokland, R., 'Elasticity and Structure of Polyurethane Networks', Rotterdam University Press, 1968
6 Smith, T. L. *Transactions of the Society of Rheology.* 1962, **6**, 61
7 Gordon, M., Love, J. A., and Pugh, D. *J. Chem. Phys.* 1968, **49**, 4680
8 Mullins, L., *J. appl. Polym. Sci.,* 1959, **2**, 1
9 Dunn, J. R. and Scanlan J., in 'The Chemistry and Physics of Rubber-like Substances', (Ed. Bateman), Maclarren, London, 1963, p 703
10 Edwards, S. F. *Proc. Phys. Soc.* 1967, **92**, 9
11 Yoshimura, N., PhD Thesis, University of Manchester, 1969

Note to the Editor

N.M.R. relaxation study of polymers containing para-phenylene units

G. ALLEN, M. W. COVILLE, R. M. JOHN and R. F. WARREN

We wish to report some n.m.r. work which indicates the possibility that oscillation of *para*-phenylene or substituted *para*-phenylene units about their *para* linkages supplies a relaxation process in those polymers containing these units in their main chain.

N.M.R. linewidth measurements[1], shown in *Figure 1*, for poly(2,6-dimethyl-*p*-phenylene oxide) –

I
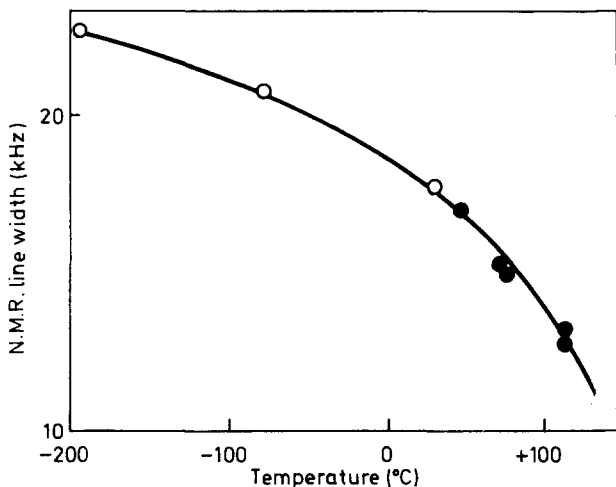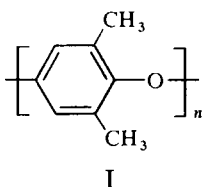
Figure 1 N.M.R. linewidth-temperature spectrum for I: ○, from ref. 2; ●, these results

extend those made by Mattes and Rochow[2]. Line narrowing is observed over an unusually wide temperature range. Spin-lattice relaxation times have also been measured for this polymer (*Figure 2*). In the T_1 spectrum the slope at low temperatures corresponds to the high temperature branch of the relaxation minimum for methyl group rotation. We assign the minimum

492

centred about 200°C to oscillation of the *para*-phenylene unit about the oxygen–oxygen axis; the high temperature side being merged with the onset of the glass transition minimum. In the $T_{1\rho}$ plot, which complements the n.m.r. wideline spectrum being measured at a frequency comparable with the n.m.r. line of the sample, this minimum has completely coalesced with the low temperature side of the glass transition minimum ($T_g = 210°C$).

We have prepared the polycyanurate II from cyanuric chloride and 2,2-*bis*-(p-hydroxyphenyl)propane:
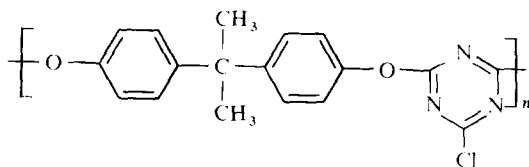
II
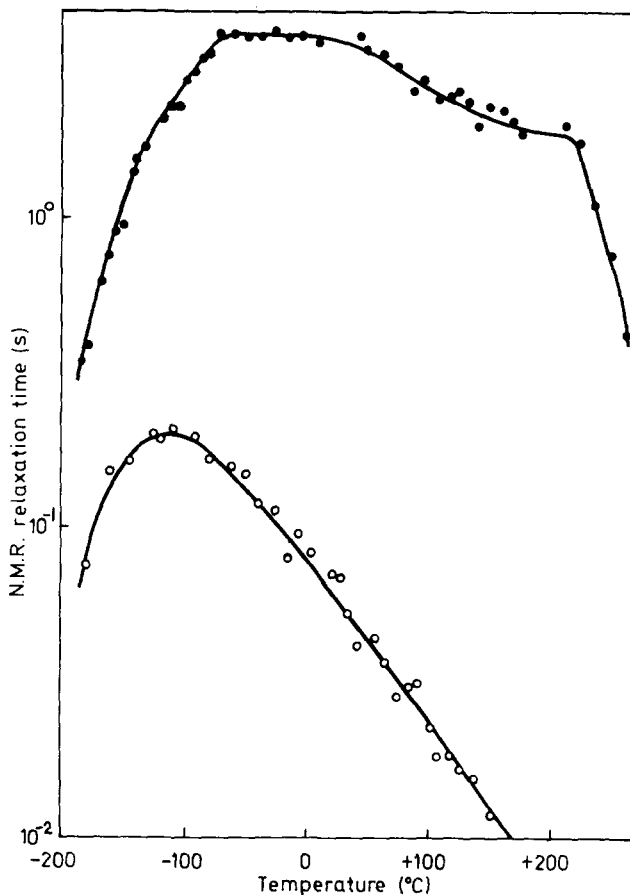
Figure 2 N.M.R. relaxation spectra for I: ●, T_1 (30 MHz); ○, $T_{1\rho}$ (25 kHz)

493

and also the polycyanurate III from cyanuric chloride and 4,4'-dihydroxy-diphenylmethane:
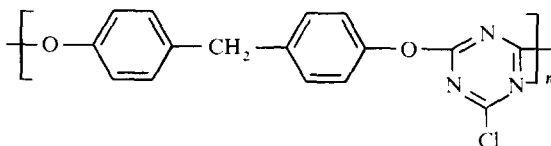
III
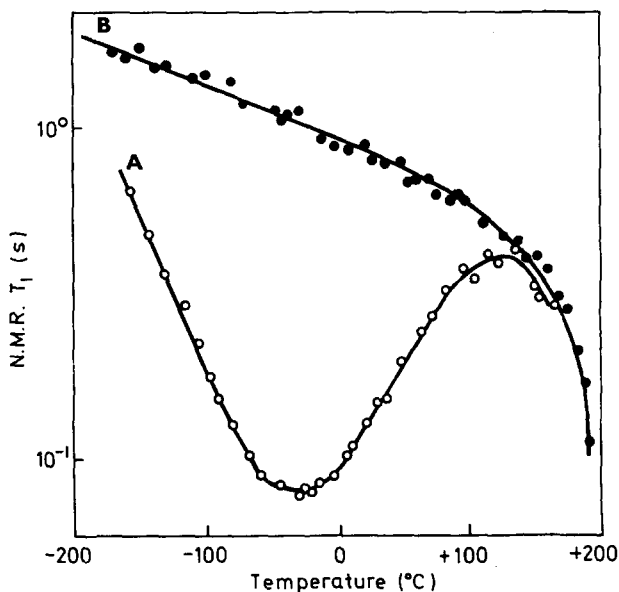
Figure 3 N.M.R. relaxation spectra for: A (O) polycyanurate II; B ($\bullet$) polycyanurate III (T_1 at 30 MHz)

Comparison of the T_1 spectrum for these compounds, (Figure 3) shows that the broad minimum observed at $-34°C$ for II is absent for III thus identifying the minimum as due to methyl group rotation. A similar T_1 spectrum to Figure 3 curve A, has also been reported in the polycarbonate of bisphenol A by McCall and Falcone[3]:

They assigned the equivalent minimum to methyl group rotation and tentatively suggested that another weak minimum may be under the high tempera-

494
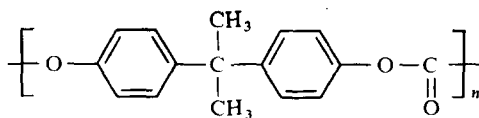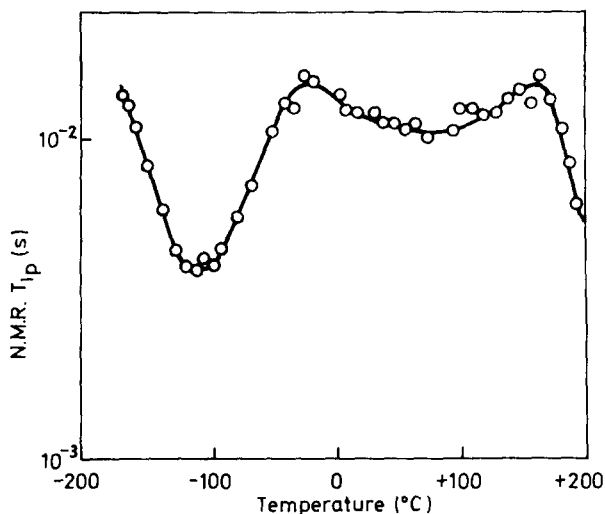
Figure 4 N.M.R. $T_{1\rho}$ spectrum for polycyanurate II at 105 kHz

ture wing of this minimum. In compound III, the slope of the T_1 temperature curve below 140°C is almost certainly the low temperature branch of a similar weak relaxation minimum which on the high temperature side has merged into the glass transition minimum. In polymer II a similar relaxation minimum occurs at about +80°C in the $T_{1\rho}$ spectrum (*Figure 4*); the −109°C minimum being the methyl group rotation. Since the glass transition relaxation minimum and the methyl group rotation relaxation minimum have been clearly identified in these compounds, we conclude that the additional weak relaxation present in the T_1 spectrum of each compound is due to phenylene group oscillation and that the thermal activation of this oscillation contributes to the line narrowing observed in compound I.

Work is presently being carried forward to further characterize this new relaxation process.

Department of Chemistry,
University of Manchester,
Manchester.

REFERENCES

1 John, R. M., MSc Thesis, Univ. of Manchester, 1968
2 Mattes, R., and Rochow, E. G. *J. Polym. Sci. (A-2)* 1966, **4**, 375
3 McCall, D. W., and Falcone, D. R. *Trans. Faraday Soc.* (Part 2) 1970, **66**, 262

Book Review

The determination of organic peroxides

by R. M. JOHNSON and I. W. SIDDIQI

Pergamon, London, 1970, 119 pp., 50s

This compact volume is one of a series of monographs dealing with organic functional group analysis and it embraces a topic of importance to all scientists who encounter either organic peroxides directly or those materials which, desirably or undesirably, become peroxidized. The title is perhaps something of a misnomer since only half the book is devoted to quantitative analytical techniques although the remaining subject matter is relevant to the detection and separation of peroxides and to the necessary understanding of their reactivity.

The first two chapters deal rather superficially with the importance of peroxides in various contexts (omitting industrial uses such as epoxidation of olefins, phenol synthesis etc.) and with general principles of structure versus reactivity. Chapters 3–8 deal in essentially a review manner with iodometric, ferrous ion, miscellaneous titrimetric, colorimetric, polarographic and spectroscopic methods for the determination of peroxides while the next four chapters are devoted to column, paper, thin-layer and gas-liquid chromatography of these materials. A final, short chapter offers advice on the choice of analytical method related to the type of peroxide, its concentration and its environment.

The text is clear and readable and free from all but a very few printing errors. On page 8 cyclohexane should read cyclohexene while on page 10 formula XI is not that of α-terpinene as stated by of p-cymene. There is some confusion between sulphide and disulphide on page 42. A few more general criticisms can be raised. The reader could be misled into thinking that the general hydroperoxidation mechanism briefly given on page 1 is applicable only to lipids. In the chapter on spectroscopic methods no mention is made of nuclear magnetic resonance spectroscopy although this is finding application as in the kinetic study of ozonide (cyclic peroxide) formation at low temperature. A statement on page 83 implies that a simple method for acetylating paper involves treatment with stearatochromyl chloride and reference 18 quoted in connection with this is incorrect in the year of the journal.

The book, however, provides a useful if generally uncritical introduction to all the important methods of peroxide analysis together with a valuable guide to chromatographic procedures and the pitfalls that can exist when these are applied to peroxides. The chapters are well endowed with summarising tables and some individual methods are described in detail. A total of some 350 references is included. The book represents excellent value for money and will be a worthwhile purchase for all who have to face the difficulties associated with the determination of organic peroxides.

D. BARNARD

496

Glass transition temperatures of crosslinked poly (isobutyl methacrylate)

Y. DIAMANT, S. WELNER and D. KATZ

The correlation between the glass transition temperatures of poly(isobutyl methacrylate) polymers crosslinked to various degrees with ethylene glycol dimethacrylate, tri- and tetraethylene glycol dimethacrylate and the degree of their crosslinking has been investigated. Based on the free volume approach a similar theoretical treatment as for the relation between T_g and the length of the polymer side chain in an uncrosslinked polymer can be used. Good agreement is found between the experimental results for the systems investigated and for data in the literature.

INTRODUCTION

SUMMARY REVIEWS regarding glass transition in polymers were prepared by Boyer[1] and Eisenberg and Chen[2] and the existing theories consider this phenomenon from the points of view of: (1) free volume; (2) thermodynamics; (3) kinetics.

We have adopted the 'free volume' approach and the glass transition temperature is assumed to be an 'iso free volume state'[3-6]. Several authors[7-11] studied crosslinked polymer systems and derived equations describing the correlation between the degree of crosslinking and the value of the polymer glass transition. Rogers and Mandelkern[12] investigated the glass transition temperatures of a homologous series of polymethacrylates in which the length of the side chain changes by a known amount from one homologue to another. Using the iso free volume theory of T_g these authors suggested an equation expressing the relation between the specific volumes of the investigated polymethacrylate above the glass transition temperature and the value of T_g. This relation is valid for the amorphous polymers in the homologous series, but fails when the straight side chain becomes long enough to form crystalline regions in the polymer. Fujita and Kishimoto[13] derived a similar, more general equation of which the Rogers and Mandelkern expression is a special case.

The general assumption in the work done by Rogers and Mandelkern was that the increase in length of the side chain in an amorphous polymer caused an increase in the ratio of the free volume to the total volume and that this lowers the T_g of the polymer. It seems to us that, in the case of a crosslinked polymer, a decrease in the degree of crosslinking and consequently an increase of the length of the network chain should have a similar effect on the value of T_g. One would expect that the Fujita and Kishimoto equation, which deals with side chains of different length in an amorphous polymer, could also be used (after suitable modification) in the case of a crosslinked polymer.

In the present work the T_g of poly(isobutyl methacrylate) crosslinked to

various degrees with ethylene, tri- and tetraethylene glycol dimethacrylate was investigated, and the results, as well as data found in previous publications were treated according to the analytical approach mentioned above.

EXPERIMENTAL

Materials

The monomers used were: *iso*butyl methacrylate (*i*-BuM), obtained from Rohm and Hass Co., and ethylene glycol dimethacrylate and tri- and tetraethylene glycol dimehacrylate (EGDM, TrEGDM, TEGDM, respectively) bifunctional crosslinking agents produced by Sartomer Resins Inc.

Polymerization

Polymer samples in the form of flat sheets were obtained by polymerization of mixtures of *i*-BuM with different amounts of EGDM, TrEGDM and TEGDM (with a small amount of benzoin as photosensitizer) between plates of Pyrex glass. The polymerization was effected by u.v. irradation (G.E. Sunlamp) for 12 h and then postcuring at 100°C for 1 h. Sol determination in the finished polymer showed less than 1 % of soluble material.

Measurements and results

(1) *Determination of crosslinking efficiency.* The crosslinking efficiency in the investigated copolymers was determined by the method used earlier by Fox and Loshaek[8]. The calculations are based on data on molar contraction of the systems, which were obtained by measurements of their specific volume before and after polymerization. An assumption is made that in the copolymer all double bonds of the vinyl compound and half the double bonds of the divinyl compound reacted to form an addition polymer: the efficiency of the crosslinking depends on the proportion of the other half of the double bonds in the divinyl compound taking part in the reaction. Accordingly the crosslinking efficiency, ϵ, will be defined by the equation

$$\epsilon = \frac{\Delta VM}{\Delta V_0 X} - \frac{1}{X} \tag{1}$$

where ΔV is the contraction of the polymer during polymerization, X is the mole fraction of the dimethacrylate and M is the average molecular weight of the monomer mixture calculated from

$$M = XM_d + (1 - X) M_m \tag{2}$$

where M_m and M_d are the molecular weights of the methacrylate and dimethacrylate respectively. ΔV_0 is a modified average value of the molar contraction of the pure monomers used in this work and is given by

$$\Delta V_0 = \frac{2X \Delta V_{0d} + (1 - X) \Delta V_{0m}}{1 + X} \tag{3}$$

where ΔV_{0m} which equals 25·45 cm³/mol is measured molar contraction of

i-BuM and ΔV_{0d} is the molar contraction of each vinyl group in the dimethacrylates and is taken as $22 \cdot 5$ cm^3/mol[10,14].

The efficiencies of crosslinking as a function of the percent of crosslinking agent in the investigated systems are plotted in *Figure 1*.
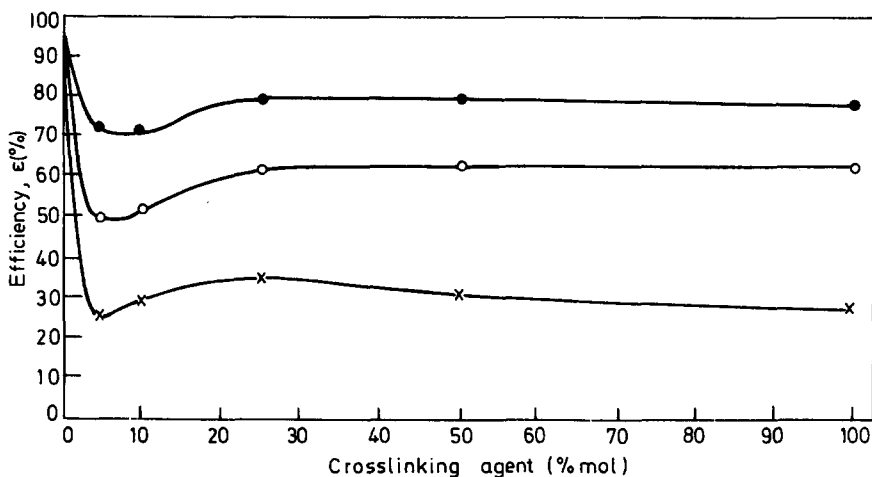
Figure 1 Efficiency of crosslinking plotted against percentage of crosslinking agent: $\times$, EGDM; $\bigcirc$, TrEGDM; $\bullet$, TEGDM

(2) *Measurements of glass transition temperature* (T_g). T_g values for the investigated polymers were determined by the method used by Eisenberg and Rovira[15] based on measurement of the change of the coefficient of thermal expansion of a sample heated at a constant rate (1 °C/min). To take these measurements strain gauges were glued on the samples and the strains occurring during the heating of the samples were measured by use of a Brüel and Kjoer strain indicator. The values of T_g obtained from these measurements are listed in *Table 1*.

Table 1 Measured and calculated data for crosslinked poly(isobutyl methacrylate)

Crosslinking agent	Conc. (% mol)	Average no. of carbon atoms in network chain	T_g (°C)	Specific volume at 46°C (cm³/g)
EGDM	0	–	46	0·968
	5	67	57	0·955
	10	32	67	0·943
	25	12	84	0·916
	50	7	107	–
TrEGDM	5	58	55	0·953
	10	28	69	0·938
	25	12	86	0·906
TEGDM	5	50	51	0·950
	10	25	54	0·938
	25	11	61	0·904
	50	10	72	0·865

DISCUSSION

The average chain length between two consecutive points of crosslinking was calculated on the assumption that the monomer units in the network structure are distributed at random and that the structure of the polymer depends on the initial molar ratio between the monomers and the efficiency of crosslinking. As we are not dealing with a point crosslink the contribution of the crosslinking monomer to the network chain, which increase with the concentration of the dimethacrylate, was taken into consideration, and the general amount of n, the number of atoms in the chain between two consecutive points of crosslinking, is given by the expression

$$n = [(2 - \epsilon)2k + 2 + (1 - \epsilon)2](1 - X) + mX \qquad (4)$$

where k is the number of monomer units between two points of crosslinking and is determined by the initial monomer ratio and m is the number of atoms between the two points of crosslinking in the dimethacrylate molecule (7, 13 and 16 for EGDM, TTEGDM and TEGDM respectively). The results of the calculations are listed in *Table 1*. When the measured values of T_g are plotted against calculated n for the investigated polymers (*Figure 2*) similar curves to those reported by Rogers and Mandelkern are obtained, although in their work n defined the number of atoms in the side chains of uncrosslinked polymers.
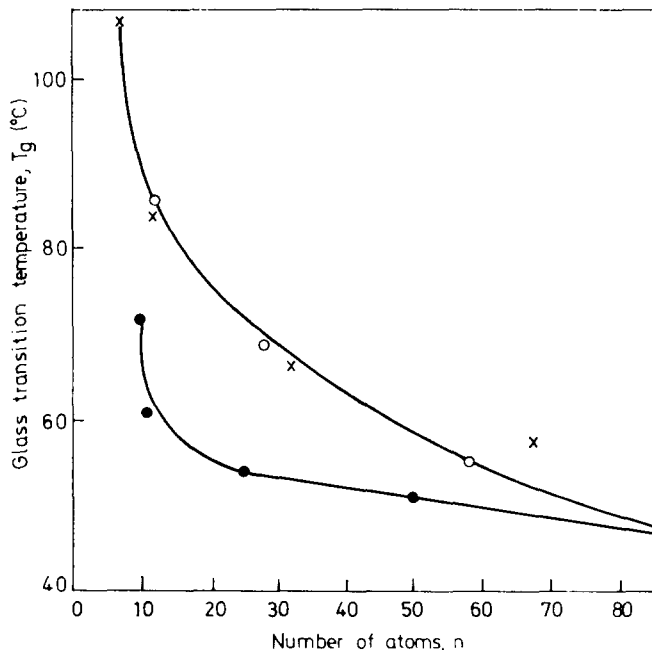
Figure 2 Glass transition temperature plotted against number of atoms between adjacent crosslinks: $\times$, EGDM; $\bigcirc$, TTEGDM; $\bullet$, TEGDM

An approach similar to the one used by Fujita and Kishimoto in the treatment of a homologous series of methacrylates was applied by us in order to develop an equation that may define the relation between T_g and the specific volume in a series of crosslinked polymers.

According to Kanig[6] the partial vibrational volume Φ^*_v is constant for all polymers at their glass transition temperature. Below T_g the volume changes are due only to the change of the vibrational volume because the total amount of holes remains almost constant and temperature independent. Therefore a_g the coefficient of thermal expansion below (T_g will be the thermal expansion coefficient of the vibrational volume.

The vibrational volume fraction at any temperature below T_g is given by

$$\Phi_v(T) = \Phi^*_v - a_g(T_g - T) \tag{5}$$

where $\Phi_v(T)$ and Φ^*_v are the partial vibrational volumes at temperatures T and T_g respectively. For any polymer (m) in a system based on the same ingredients and crosslinked to different extents the following general expression is applicable

$$\Phi(m,T) = \Phi^*_v(m) - a_g(m)\,[T_g(m) - T\,] \tag{6}$$

Assuming that the specific volume of any two polymers in the same system is related to their fractional vibrational volume, the correlation can be expressed in the following way

$$\Phi(m,T) - \Phi(1,T) = \theta[V(m,T) - V(1,T)] \tag{7}$$

where 1 denotes the reference polymer in the investigated series and θ is any function fulfilling the condition that $\theta(0) = 0$ and is characteristic for the given system. Accepting the approach suggested by Kanig for the methacrylates that

$$\Phi^*_v(m) = \Phi^*_v(1) \tag{8}$$

and substituting $T = T_g(1)$, the following expression based on equations (6) and (7) can be written

$$T_g(m) = T_g(1) - [a_g(m)]^{-1}\theta\,\{V\,[m,T_g(1)] - V\,[1,T_g(1)]\} \tag{9}$$

where (1) is the polymer with the lowest T_g in the series or in other words the T_g of the uncrosslinked polymer or the least crosslinked polymer in the series. In cases where the coefficients of thermal expansion below the glass transition temperature $a(m)$ are equal for all the polymers in the investigated series, a linear relation between $V(m,T)$ and $T_g(m)$ similar to the equation derived by Rogers and Mandelkern is obtained

$$T_g(m) = T_g(1) - \frac{\Phi^*_v - f}{a_g}\,[V(m,T) - V(1,T)] \tag{10}$$

where $T < T_g(1)$, f is the fraction of the total specific volume change that contributes to the change in the vibrational volume in going from polymer (1) to any polymer (m) in the series and Φ^*_v is the Kanig's constant and equals 0·69. It was shown[1,9] that a_g in a series of crosslinked polymers is slightly dependent on the degree of crosslinking and therefore the more general

equation (9) can be used. But because the relation between T_g and the specific volume is linear, θ must be a linear function of α_g and in the general form:

$$\theta = K\alpha_g(m) \times \Delta V(m) \qquad (11)$$

where $\Delta V(m) = V[m,T_g(1)] - V[1,T_g(1)]$ and K is a constant independent of the volume and the thermal expansion coefficient.

The experimental results obtained for the investigated systems are shown in *Figure 2* and *3*. As mentioned earlier, the plots of T_g against the number of atoms between two consecutive and adjacent points of crosslinking are very similar to the plots obtained by Rogers and Mandelkern of T_g against n for homologous series of methacrylates where n was the amount of atoms in the side chain. The plots of T_g against specific volume measured at $T_g(1)$, the glass transition temperatures of the non-crosslinked polymers in each studied system, are shown in *Figure 3*. Linear relations are obtained in all three cases: i-BuM + EGDM, i-BuM + TrEGDM and i-BuM + TEGDM and the first two lines almost coincide. It seems therefore justified to assume that
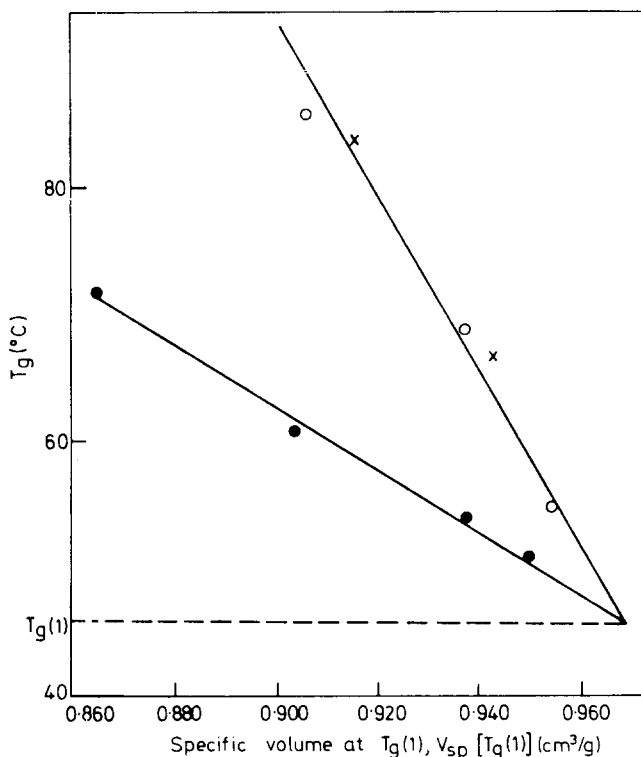
Figure 3 Glass transition temperature plotted against specific volume at $T_g(1)$ the glass transition temperature of the uncrosslinked polymer: ×, EGDM; ○, TrEGDM; ●, TEGDM

503

equations (9) and (11) can be used in order to describe the behaviour of the investigated systems.

Results reported earlier for poly(methyl methacrylate) + EGDM[16], and for rubber crosslinked by use of dicumyl peroxide[9] were plotted in the same way as the ones obtained in our investigation and are shown in *Figures 4* and *5*. Here too, when T_g was plotted against n, the plots were similar to those obtained by Rogers and Mandelkern (n was calculated for the first system from the molar percentage of the components and from efficiency of cross-linking; for the second system from the degree of crosslinking given by Mason). Plots of T_g against V_{sp} [$T_g(1)$] for the two systems are shown in *Figure 5*, with V_{sp} [$T_g(1)$] calculated from the specific volumes at reference temperatures and coefficients of thermal expansion of the polymers given by these authors. As reference temperatures, $T_g(1)$, $-71°$ and $105°$ were chosen from the work of Mason and of Loshaek, respectively. For the first system a fairly linear relation was obtained, similar to the results in our experiments; for the crosslinked rubber in a greater part of the investigated
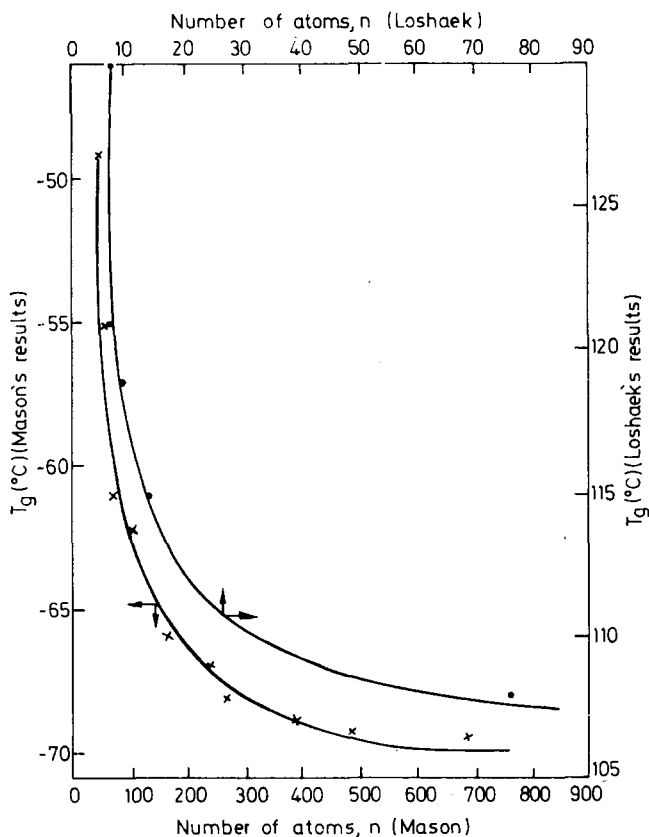
Figure 4 Glass transition temperatures plotted against number of atoms between adjacent crosslinks (plot based on results of Mason [11] and Loshaek[16])
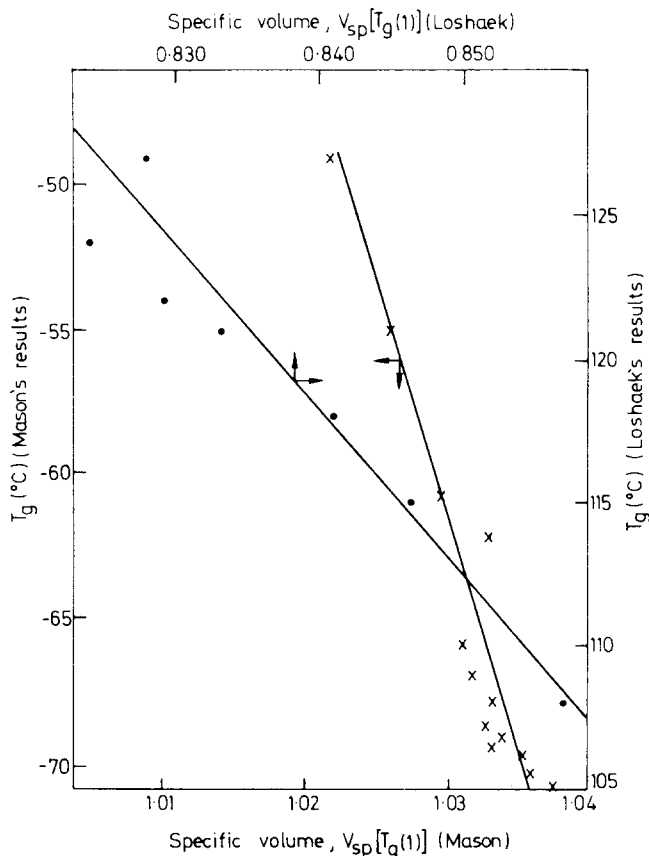
Figure 5 Glass transition temperature plotted against volume at
$T_g(1)$, the glass transition temperature of uncrosslinked polymers
(plot based on results of Mason[11] and Loshaek[16])

region a straight line was also obtained but some deviations occurred for
low degrees of crosslinking.

CONCLUSIONS

The difference in value of T_gs in the series of investigated crosslinked polymers
can be explained by changes occurring in the specific volumes of the polymers
and by consideration of the division of those changes between the vibrational
and the total volumes. The agreement between results obtained in this work
with data reported by Rogers and Mandelkern in their investigations of homo-
logous series of polymethacrylates with side chains of increasing lengths, is
probably due to the fact that the increase in density of crosslinking in polymers
described in our work does not influence seriously the interaction between the
different parts of the network because of very weak intermolecular forces.

505

In the two cases, in the one with the polymer series with increasing lengths of side chains and the other with the decreasing degree of crosslinking, an increase in the free volume of the polymer takes place this resulting in the decrease of the glass transition temperatures. Therefore a similar theoretical treatment can be used.

ACKNOWLEDGEMENTS

Scientific Department,
Ministry of Defence,
Tel Aviv, Israel   (*Received 25 June 1970*)

REFERENCES

1 Boyer, R. F. *Rubber Chem. and Tech.* (*Rubber Reviews*) 1963, **36**, 1303
2 Shen, M. C. and Eisenberg, A., 'Progress in Solid State Chemistry,' Vol. 3, Pergamon Press, Oxford and New York 1966, p 407
3 Fox, T. G. and Flory, P. J. *J. appl. Phys.* 1950, **21**, 581
4 Simha, R. and Boyer, R. F. *J. Chem. Phys.* 1962, **37**, 1003
5 Williams, M. L., Landel, R. F. and Ferry, J. D. *J. Amer. Chem. Soc.* 1955, **77**, 3701
6 Kanig, G. *Kolloid Z.* 1963, **190**, 1
7 Meares, P. 'Polymer Structure and Bulk Properties', London 1965, p 265
8 Fox, T. G. and Loshaek, S. *J. Polym. Sci.* 1955, **15**, 371
9 Mason, P. *Polymer, Lond.* 1964, **5**, 625
10 DiMarzio, E. A. *J. Res. Nat. Bur. Stand.* 1964, **68A**, 611
11 Kanig, G. *J. Polym. Sci.* 1967, **16**, p 1957
12 Rogers, S. S. and Mandelkern, L. *J. Phys. Chem.* 1957, **61**, 985
13 Fujita, H. and Kishimoto, A. *J. Colloid Sci.* 1958, **13**, 418
14 Katz, D. and Tobolsky, A. V. *J. Polym. Sci.* (*A*) 1964, **2**, 1595
15 Eisenberg, A. and Rovira, E. *J. Polym. Sci.* (*B*) 1964, **2**, 269
16 Loshaek, S. *J. Polym. Sci.* 1955, **15**, 391

Counter-current fractionation of polymers using their incompatibility*

A. ENGLERT† and H. TOMPA

It is proposed that the incompatibility of polymers could be used to produce two-phase systems suitable for liquid–liquid counter-current extraction treatment in order to achieve a sharp fractionation of a heterodisperse polymer.

The efficiency of such a procedure is examined theoretically. In order to do this, the phase diagrams of typical systems are first established on the basis of the Flory-Huggins model of polymer solutions; the results obtained are used to calculate the number of theoretical stages of a counter-current extraction column required to effect separations to given degrees of purity.

Separations under a number of typical conditions are considered; the values obtained for the number of theoretical stages required are on the whole within the limits of what is experimentally feasible. For example, it is found that 110 theoretical stages are required to separate a mixture of two polymers of chainlengths 1000 and 1100 into its two constituents in 99% purity, while a fraction with a number-average chainlength of 957 and a weight-average chainlength of 960 can be separated by two successive fractionations from a polymer with a continuous chainlength distribution and a number-average chainlength of 1000.

The results of this theoretical investigation are sufficiently favourable to justify an experimental investigation of the practical possibility of using the incompatibility of polymers to achieve sharp fractionation.

1. INTRODUCTION

CONVENTIONAL METHODS of fractionation consist essentially of fractional separation of a solution of the polymer, either by adding precipitant or by evaporating solvent. Since the two phases into which the original solution is separated are in equilibrium with each other, the individual polymer species will be distributed among them in degrees depending on the chainlength, but both phases will contain all polymer species. The distribution of chainlengths in either of the phases is thus still fairly broad, and though repeated fractionation can sharpen the distribution, no sharp separation can be achieved by single stage equilibrium processes.

Efficient separation of a polydisperse substance can only be carried out by means of a continuous, counter-current process, such as fractional distillation. A process appropriate to polymers would be counter-current liquid–liquid extraction since polymers are not volatile. This requires two immiscible liquid phases such that the solubility of the polymer in the two phases depends on its mole weight or chainlength (number of segments).

507

It is not easy to find two immiscible liquids which are both solvents for a given polymer: A. Dobry[1] has made a systematic study of possible systems, but of 289 cases of a polymer and two immiscible liquids she found only nine cases in which both liquids were solvents, and in only three of these was the polymer not all concentrated in one of the two phases. In all these cases, as well as in the previously known systems water/chloroform/poly-ethylene-oxide and water/m-cresol/poly(vinyl alcohol), the polymers were highly polar and no pairs of immiscible solvents were found for non-polar polymers. G. V. Schulz and E. Nordt[2] have in fact used the first of these systems to fractionate polyethylene-oxide. K. E. Almin[3] has made extensive studies of the fractionation of polyethylene-oxide in systems of immiscible solvents in a Craig-type apparatus; to obtain better distribution of the poly-mers between the two phases he used ternary solvent systems.

That there are not many such systems can be explained satisfactorily from existing theories of polymer solutions. In order that two liquids be immiscible, their interaction constant in a van-Laar type expression for the heat of mixing must exceed two, so that their solubility parameters must differ by more than $\sqrt{2}$. However, if a liquid is a solvent for a polymer, i.e., for a given solvent/polymer pair, the interaction constant is less than $\frac{1}{2}$, so that the solubility parameters must be within $1/\sqrt{2} = 0.7$ of each other, and even closer if one takes the contribution of entropy effects to the interaction constant into account. It is clearly impossible to find a polymer with a solubility parameter less than 0.7 different from the solubility parameters of two liquids which are themselves more than 1.4 apart.

It has occurred to us that a system of two liquid phases, both containing the polymers, can be produced by making use of the incompatibility of poly-mers; this is the well-known phenomenon that when solutions of two different polymer in the same solvent are mixed, the whole forms, in general, not one single homogeneous phase, but separates into two phases, one of which contains most of one of the polymers, the other most of the other[4]. However, both polymers are distributed between the two phases and the extent of this distribution depends on the mole weights and the concentrations; in suffi-ciently dilute solutions the two phases become identical and the whole will form one single, homogeneous phase. The concentration at the highest dilution at which phase separation can still take place can be regarded as a measure of the incompatibility of the two polymers. The incompatibility of polymers is in general not specific, in the sense that two polymers which show incompatibility in one common solvent, usually show it in all common solvents. Theories of polymer solutions show that the incompatibility of polymers is related to the unfavourable energy of interaction between their segments (see e.g. ref. 5, p 200).

Since the incompatibility of polymers produces two phases and the poly-mers are distributed among them to an extent depending on their chain-lengths, such a system can be used to effect the separation of polymers into two fractions, and since both phases are liquid, methods of counter-current liquid–liquid extraction can in principle be used to make the separation as sharp as desired.

A. Albertson[6] has already used the incompatibility of polymers to effect fractionations; however, he used the incompatibility simply to create two

508

immiscible phases between which the polymer to be fractionated is distributed. His systems were aqueous solutions and he studied polymers of biological interest.

We report here results of a theoretical study of the possibility of fractionating polymers effectively on this basis.

We imagine that a fractionation based on incompatibility is carried out in the following manner: a polydisperse polymer mixture, containing species of varying chainlengths, is dissolved with a second polymer, with which it is incompatible and which we shall call the auxiliary polymer, in a common solvent at concentrations such that phase separation takes place; the whole is subjected to a counter-current extraction treatment. The shorter species, being less incompatible, tend to accumulate in the phase containing most of the auxiliary polymer, while the longer ones will accumulate in the other phase. The sharpness of the separation will depend, under given operating conditions, and for a given system, on the number of stages of extraction and on the reflux ratio. One can say, in analogy with conventional liquid–liquid extraction, that the shorter species of the mixed polymer are 'extracted' by the auxiliary polymer phase from the other phase and we shall refer to the phase containing most of the auxiliary polymer as the 'extract' and to the other phase as the 'raffinate'.

The efficiency of a fractionation can be measured by the number of theoretical stages of counter-current extraction treatment required to effect a given separation. For the purposes of calculation we have usually assumed that the mixed polymer to be fractionated consists of two species only, of more or less similar chainlengths, and we have calculated the number of stages required to give samples of predetermined purity–usually 90% or 99%. Clearly, extraction systems containing a few hundred stages are practicable, while a resulting figure exceeding about a thousand stages would indicate the impracticability of utilizing incompatibility for the purposes of fractionation.

The methods for calculating the efficacity of counter-current extraction are well established; they require knowledge of the phase diagrams of the systems used, at the temperatures and pressures of the extraction.

The phase relationships of many-component systems can be calculated thermodynamically, in the absence of experimental data, if the free energy of mixing is known as a function of the concentrations. We have assumed that the free energy of mixing of the polymer solutions involved is given by the Flory-Huggins expression, which is well proved experimentally for solutions of non-polar polymers. It also leads to mathematical expressions which are not too involved; an important point, since the calculation of the phase diagram is sufficiently involved for any but the simplest starting formula to make the algebra very quickly unmanageable.

The system which we have considered is one consisting of four components, the solvent S, the auxiliary polymer A, and two species of the mixed polymer P. From the expression for the free energy of mixing we have calculated the phase diagrams, i.e. the critical points and the composition, of coexisting phases (section II).

From the known phase diagrams and the operating conditions of a counter-current extraction system—we shall refer to it as the 'extraction column'—

we obtained the numbers of theoretical stages by the conventional method based on the graphical representation of the phase diagram and consisting of finding the points of intersection of the so-called operating lines with the binodial surface, which is the locus of the points representing coexisting phases (section III). Since no analytical expression could be obtained for the binodial surface, these points of intersection have to be determined one by one by numerical methods and for polymers with neighbouring chain lengths, where the number of stages required is necessarily large, the method becomes impossibly laborious.

Fortunately, for the limiting case in which the relative difference in the chainlengths of the two species becomes negligible, the phase diagram shows certain peculiarities, which permits an easy evaluation of the number of stages required. This evaluation is based essentially on the hypothesis that when the relative difference in the two chainlengths is small, the distribution coefficients of the two polymer species between the two phases are, to a first approximation, constant throughout the column. We give theoretical arguments to make this hypothesis very plausible and to show that the errors involved are not large. We have used these arguments to calculate the number of theoretical stages required for the separations of polymers of chainlengths 1000 and 1100, and of chainlengths 1000 and 1010, to predetermined degrees of purity (section IV).

Further, we have examined the influence of the various parameters of the system (chainlengths of the polymers, both of the mixed polymer P and the auxiliary polymer A, temperature) on the efficiency of the fractionation and have also considered the case of a mixed polymer with a continuous distribution of chainlengths (section V.)

II. PHASE DIAGRAMS

(1) The free energy of mixing

We consider a system consisting of a solvent S and two polymers A and P; let P and A be both soluble in S, but have an unfavourable energy of interaction producing incompatibility, so that some of the mixtures S + A + P separate into two phases. We are interested in establishing the phase diagram of the quaternary system $S + A + P_i + P_j$, where P_i and P_j are two homologous polymers of different chainlengths. $P_i + P_j$ represents the mixed polymer to be separated, A the auxiliary polymer. The phase diagram can be established if the free energy of mixing is known as a function of concentration; we have assumed that this is given by the Flory-Huggins expression and its obvious extension to many-component systems (ref. 5, p 96).

We shall use in our calculation the index 1 for the solvent S, the index 2 for auxiliary polymer A and the indices 3 and 4 for the two species of the polymer P. We assume that the interaction energy between segments of P does not depend on the chainlength of P, which means

$$\chi_{34} = 0 \qquad (2.1)$$

Further, we shall assume that the segments of A and the molecules of S

are sufficiently similar for the differences between their interaction energies to be negligible, so that there are only two types of segments present; this entails

$$\chi_{12} = 0, \chi_{13} = \chi_{14} = \chi_{23} = \chi_{24} = \chi \qquad (2.2)$$

This assumption greatly simplifies the labour of calculation, but does not sacrifice any point of principle; it is not indispensable to demonstrate the essential features of fractionation by incompatibility.

With the assumptions (2.1) and (2.2), the Flory-Huggins expression reduces to

$$\Delta G/RT = \sum_i n_i \ln \phi_i + \chi(\phi_1 + \phi_2)(\phi_3 + \phi_4) \sum_i m_i n_i \qquad (2.3)$$

where n_i is the number of moles of component i, m_i its chainlength and ϕ_i its volume fraction; we shall usually assume $m_i = 1$, $m_3 < m_4$.

If χ is less than one half, P is soluble in S for all values of m_3 and m_4; if it is also well above the critical value $\chi_{23}^c = \frac{1}{2}[(1/\sqrt{m_2}) + (1/\sqrt{m_3})]$, A and P are incompatible.

The phase relationships of quaternary systems can be represented in a three-dimensional tetrahedral diagram, which is the obvious extension of the conventional representation of ternary systems on the composition triangle; the binodial surface of the system described above is shown schematically in *Figure 1*.
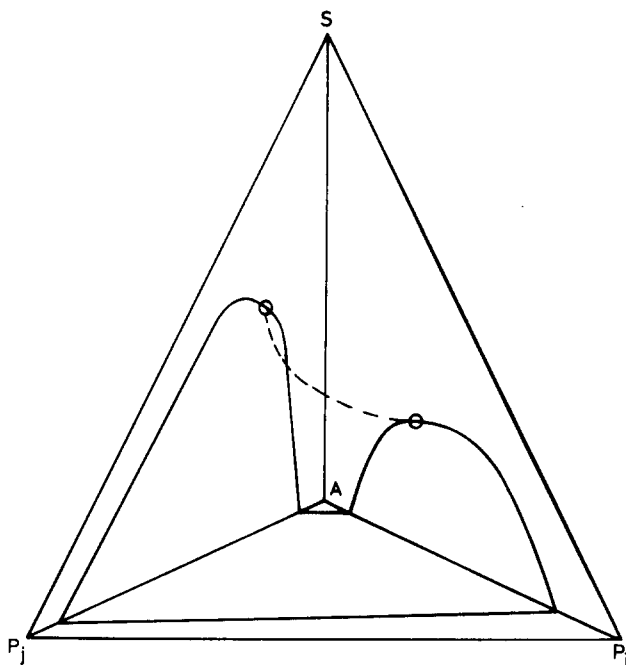
Figure 1 Schematic representation of the phase diagram of a quaternary system S + A + P, with $0.5 > \chi > \chi^c{}_{AP}$. Broken line is line of critical points

(2) Critical points

It is shown in works of thermodynamics (e.g. ref. 5, section 2.12) that for the critical point of a ternary system the following equation must be satisfied

$$\frac{\partial(S_p, G_1)}{\partial(\phi_1, \phi_2)} = 0 \tag{2.4}$$

(These equations are usually derived and expressed in terms of mole fractions x_i, but are equally valid when expressed in terms of volume fractions ϕ_i). By an obvious extension the analogous equation for quaternary systems is

$$\frac{\partial(S_p, G_1, G_2)}{\partial(\phi_1, \phi_2, \phi_3)} = 0 \tag{2.5}$$

The expressions on the left-hand sides denote the Jacobians with respect to the ϕ_i; G_i is the partial derivative of $G = \Delta G / \sum_i m_i n_i$ with respect to ϕ_i, and S_p represents the equation of the spinodial. The spinodial is the locus of the points which separate in the phase diagram, within the two-phase region, the metastable from the completely unstable region; its equation is, for ternary systems,

$$\frac{\partial(G_1, G_2)}{\partial(\phi_1, \phi_2)} = 0 \tag{2.6}$$

and analogously for quaternary systems

$$\frac{\partial(G_1, G_2, G_3)}{\partial(\phi_1, \phi_2, \phi_3)} = 0 \tag{2.7}$$

Since the critical point is always on the spinodial, (2,4) and (2.6) must be satisfied there simultaneously for ternary systems, or (2.5) and (2.7) for quaternary systems.

The critical points of our quaternary system can be obtained by an obvious extension of the method described in ref. (5), section 7.2 for ternary systems; the equation for the spinodial surface is transformed into

$$[1 - 2X(m_1\phi_1 + m_2\phi_2)][1 - 2X(m_3\phi_3 + m_4\phi_4)] = 1, \tag{2.8}$$

the second equation for the critical points into

$$m_1^2\phi_1 + m_2^2\phi_2 + \frac{m_3^2\phi_3 + m_4^2\phi_4}{[1 - 2X(m_3\phi_3 + m_4\phi_4)]^3} = 0 \tag{2.9}$$

these equations, with $\sum_i \phi_i = 1$, determine the line of critical points.

To obtain numerical values, one introduces an auxiliary variable v defined by

$$m_1\phi_1 + m_2\phi_2 = \frac{1+v}{2Xv}, \qquad m_3\phi_3 + m_4\phi_4 = \frac{1+v}{2X} \tag{2.10}$$

so that (2.8) is automatically satisfied; v is then one of the roots of the qua rtic equation

512

$$m_1 m_2 v^4 + [m_1 m_2 + m_2 m_3 + m_3 m_1 - 2\chi m_1 m_2 m_3 +$$

$$2\chi \phi_4 m_1 m_2 (m_3 - m_4)]v^3 +$$

$$+ (m_1 + m_2)m_3 v^2 - m_3^2 v - m_3^2 + 2\chi \phi_4 m_3 m_4 (m_3 - m_4) = 0 \qquad (2.11)$$

For each given value of ϕ_4, v is obtained from (2.11) and the other ϕ_1 from (2.10) and $\sum_i \phi_i = 1$. Instead of (2.11) one can use alternative expressions giving v as a function of any of the ϕ_i.

(3) Compositions of coexisting phases

The compositions of coexisting phases can be obtained from the condition that the chemical potential of any component must have the same value in both phases. We use a single prime and a double prime to distinguish the two phases and have thus

$$\mu_i' = \mu_i'' \qquad (2.12)$$

for $i = 1, 2, 3, 4$. The change of chemical potential on mixing, $\Delta\mu_i$, can be obtained by differentiating ΔG with respect to n_i; using the Flory-Huggins expression (2.3) for ΔG we obtain

$$\frac{\Delta\mu_i}{RT} = \ln \phi_i + 1 - m_i \sum_j \frac{\phi_j}{n_j} + \chi m_i (\phi_k + \phi_l)^2 \qquad (2.13)$$

where k and l are 3 and 4, respectively, for $i = 1,2$ and are 1 and 2, respectively, for $i = 3,4$. With these expressions, the four equations (2.12) give

$$\frac{1}{m_i} \ln \frac{\phi_i'}{\phi_i''} - \sum_j \frac{\phi_j' - \phi_j''}{m_j} + \chi \{(\phi_k' + \phi_l')^2 - (\phi_k'' + \phi_l'')^2\} = 0 \qquad (2.14)$$

Together with

$$\Sigma_i \phi_i' = 1, \qquad \Sigma_i \phi_i'' = 1 \qquad (2.15)$$

there are six equations for the eight unknowns ϕ_i', ϕ_i'', and determine therefore a surface in space, the binodial surface. We have not been able to deduce an analytical expression for the equation of this surface, but we have succeeded in representing it in parametric form by expressing each of the eight coordinates as a function of two parameters.

We subtract the second and third of equations (2.14) from the first and the fourth from the third and obtain

$$\frac{1}{m_i} \ln \frac{\phi_1'}{\phi_i''} - \sum_i \frac{\phi_i' - \phi_i''}{m_i} + \chi \{(\phi_3' + \phi_4')^2 - (\phi_3'' + \phi_4'')^2\} = 0$$

$$\frac{1}{m_1} \ln \frac{\phi_1'}{\phi_1''} - \frac{1}{m_2} \ln \frac{\phi_2'}{\phi_2''} = 0 \qquad (2.16)$$

$$\frac{1}{m_1} \ln \frac{\phi_1'}{\phi_1''} - \frac{1}{m_3} \ln \frac{\phi_3'}{\phi_3''} - 2\chi \{(\phi_1' - \phi_1'') + (\phi_2' - \phi_2'')\} = 0$$

$$\frac{1}{m_3} \ln \frac{\phi_3'}{\phi_3''} - \frac{1}{m_4} \ln \frac{\phi_4'}{\phi_4''} = 0$$

513

We introduce the distribution coefficients a_i defined by

$$\phi_i'/\phi_i'' = a_i \tag{2.17}$$

Then, (2.16) shows that

$$\frac{1}{m_1} \ln a_1 = \frac{1}{m_2} \ln a_2 = d_1, \qquad \frac{1}{m_3} \ln a_3 = \frac{1}{m_4} \ln a_4 = - d_3 \tag{2.18}$$

where these equations serve to define d_1 and d_3. To fix our ideas, we imagine the phase indicated by a single prime to be the extract, containing higher concentrations of S and A, and the phase indicated by a double prime to be the raffinate, containing higher concentrations of P. Then a_1 and a_2 are greater than unity, a_3 and a_4 less than unity, and the quantities d_1 and d_3 defined by (2.18) will be positive.

It is easily verified that (2.18) is a direct consequence of $\chi_{12} = 0$; introducing $A = d_1 + d_3$ and utilizing (2.15), the third of equations (2.16) becomes

$$A - 2\chi \left[(a_1 - 1)\phi_1' + (a_2 - 1)\phi_2' \right] = 0 \tag{2.19}$$

and the first

$$d_1 - \sum_i \frac{a_i - 1}{m_i} \phi_i'' - \tfrac{1}{2}A[2 - (a_1 + 1)\phi_1'' - (a_2 + 1)\phi_2''] = 0 \tag{2.20}$$

These two equations, together with (2.15), in which ϕ_i' has been substituted for from (2.17), represent four simultaneous linear equations for the ϕ_i'', in terms of a_1, a_2, a_3, a_4 as parameters; since a_2 and a_4 are by (2.18) simply related to a_1 and a_3, the ϕ_i'' can be expressed in terms of the two parameters a_1 and a_3.

To obtain the compositions of a pair of coexisting phases, one chooses a pair of values a_1 and a_3, a_1 larger than unity, a_3 less than unity, calculates a_2, a_4, d_1, d_3 from (2.18) and obtains the ϕ_i'' by solving the four simultaneous equations; the ϕ_i' are obtained from (2.17) and a check on these values is provided by (2.15).

One can easily see that not all combinations of pairs of a_1 and a_3 give physically significant values, in the sense that only values of ϕ_i' and ϕ_i'' which are all between zero and unity correspond to physical solutions. For each given value of a_1, there is an interval of values of a_3 for which the representative points lie within the composition tetrahedron, i.e. which correspond to physical solutions. The limiting values of a_3 are given by its values in the two ternary systems S-A-P, when $\phi_3 = 0$ or $\phi_4 = 0$, respectively.

(4) Phase diagrams for systems containing two nearly identical components

We shall be mostly interested in quaternary systems containing two polymer species of very similar and even nearly equal chainlengths. We have, therefore, thought it worth while to consider the special features of the phase diagrams of systems containing two identical components, e.g. two isotopes forming among themselves an ideal solution. It is evident that in a solution containing two such isotopes, the activity coefficient f of any component will

not depend on the individual amount of either isotope but only on the total of the two isotopes present and that the activity coefficients of the two isotopes will be the same.

We denote the two isotopic components by the indices m and m^* and any of the other n components by the running index i; we can then eliminate the mole fractions x_m and x_{m*} of the isotopes by the equation $x_m + x_{m*} = 1 - \sum_i x_i$, so that the chemical potentials can be written

$$\frac{\Delta\mu_i}{RT} = \ln x_i + \ln f_i \,(x_i, x_2, \ldots x_n)$$

$$\frac{\Delta\mu_m}{RT} = \ln x_m + \ln f_m \,(x_1, x_2, \ldots x_n) \qquad (2.21)$$

$$\frac{\Delta\mu_m}{RT} = \ln x_{m*} + \ln f_m \,(x_1, x_2 \ldots x_n)$$

where the f are functions of the x_i, but not of x_m or of x_{m*}. The assumption that the activity coefficients of the two isotopes are the same means $f_m = f_{m*}$.

Equation (2.21) will have the same form if mole fractions x are replaced by volume fractions ϕ, since quite generally

$$x_j = \phi_j \times g_j(\phi_i) \qquad (2.22)$$

so that

$$\frac{\Delta\mu_i}{RT} = \ln \phi_i + F_i(\phi_1, \phi_2, \ldots \phi_n)$$

$$\frac{\Delta\mu_m}{RT} = \ln \phi_m + F_m(\phi_1, \phi_2, \ldots \phi_n) \qquad (2.23)$$

$$\frac{\Delta\mu_{m*}}{RT} = \ln \phi_{m*} + F_m \,(\phi_1, \phi_2, \ldots \phi_n)$$

In the case of equilibrium of two phases

$$\ln (\phi_i'/\phi_i') = \ln a_i = F_i'' \,(\phi_1'', \phi_2'', \ldots \phi_n'') - F_i' \,(\phi_1', \phi_2', \ldots \phi_n')$$

$$\ln (\phi_m'/\phi_m'') = \ln a_m = F_m'' \,(\phi_1'', \phi_2'', \ldots \phi_n'') - F_m' \,(\phi_1', \phi_2', \ldots \phi_n') \qquad (2.24)$$

$$\ln (\phi_{m*}'/\phi_{m*}'') = \ln a_{m*} = F_m'' \,(\phi_1'', \phi_2'', \ldots \phi_n'') - F_m' \,(\phi_1', \phi_2', \ldots \phi_n')$$

whence it follows that the distribution coefficients do not depend on the volume fractions ϕ_m and ϕ_{m*}, but only on the ϕ_i, and that $a_m = a_{m*}$.

We now consider a quaternary system containing two isotopes, components 3 and 4. The two-phase boundary, the binodial surface, has two degrees of freedom and is determined by four equations of the type (2.24) together with $\sum_i \phi_i' = 1, \sum_i \phi_i'' = 1$.

Then we have the following equations

$$a_1 = a_1 \,(\phi_1', \phi_2', \phi_1'', \phi_2'')$$

$$a_2 = a_2 \,(\phi_1', \phi_2', \phi_1'', \phi_2'') \qquad (2.25)$$

$$\phi_1'' + \phi_2'' + a_3 \,(\phi_1', \phi_2', \phi_1'', \phi_2'') \,(1 - \phi_1'' - \phi_2'') = 1$$

These equations contain only the four variables ϕ_1', ϕ_2', ϕ_1'', ϕ_2''. For a given value of any one of them, say ϕ_1'', the other three are determined and are independent of the value of ϕ_3'/ϕ_4' or ϕ_3''/ϕ_4'', as are also the values of a_1, a_2, a_3, a_4.
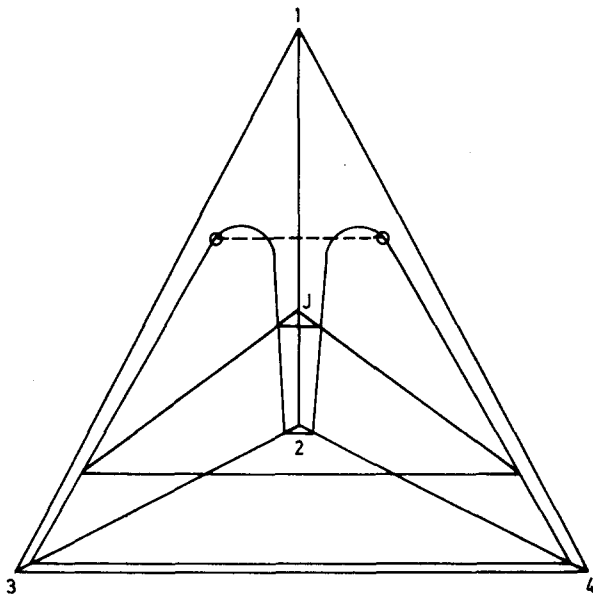
Figure 2 Schematic representation of phase diagram of quaternary system with a pair of isotopic components. Broken line is line of critical points

Figure 2 shows the composition tetrahedron and the binodial surface of such a system. The binodial surface consists of a locus of straight lines along which ϕ_1 and ϕ_2 are constant, i.e. which are parallel to the 3–4 edge of the tetrahedron. These lines intersect the faces 1-2-3 and 1-2-4 in the respective ternary phase diagrams, which are, of course, identical. The binodial surface is thus a cylinder, with generators parallel to the 3–4 edge. Each generator belongs to a particular value of a_1; phases corresponding to those represented by the points of a generator lie on another generator and these two generators lie in a plane which is parallel to the 3–4 edge and which intersects the 1–2 edge in a well-determined point J.

These considerations can be applied to quaternary systems with two polymeric components whose relative chainlength difference is small, $\Delta m = m_4 - m_3 \ll m_3$. It can be shown that in a binary mixture of two such polymers the chemical potential of either component differs from that given by the laws of ideal solutions only by a second order term in $\Delta m/m_3$: in a binary mixture containing only components 3 and 4, the chemical potential of component 3 is given by the third of equations (2.13) with $\phi_1 = \phi_2 = 0$:

$$\frac{\Delta \mu_3}{RT} = \ln \phi_3 + 1 - m_3 \left(\frac{\phi_3}{m_3} + \frac{\phi_4}{m_4} \right) \qquad (2.26)$$

516

We substitute for ϕ_3 in the logarithmic term by its value from an equation corresponding to (2.22)

$$\phi_3 = x_3 \left(\phi_3 + \frac{m_3}{m_4} \phi_4\right) \tag{2.27}$$

replace m_4 by $m_3 + \Delta m$ and develop into a series of powers of $\Delta m/m_3$; the first order terms cancel and we obtain

$$\frac{\Delta\mu_3}{RT} = \ln x_3 - \tfrac{1}{2} \left(\frac{\Delta m}{m_3}\right)^2 \phi_4^2 \tag{2.28}$$

so that the deviation from the ideal value, $\ln x_3$, is of second order of magnitude in $\Delta m/m_3$ and can be neglected. To a first degree of approximation, components 3 and 4 mix therefore ideally and the comparison of such a system with one containing two isotopic components is justifiable.

It will be shown in section IV that the quantity a_4/a_3 plays an important role in the evaluation of the efficiency of the fractionation; for small $\Delta m/m_3$ we can write

$$\frac{a_4}{a_3} = \frac{a_3}{a_3}^{m_4/m_3} = a_3^{\Delta m/m_3} = 1 + \frac{\Delta m}{m_3} \ln a_3 \tag{2.29}$$

We can show that the quantity F_m in (2.23) and therefore, according to (2.24), a_3, do not depend on ϕ_3 and ϕ_4 separately, at least up to a term of the order of magnitude of $\Delta m/m_3$: from the third of equations (2.13), ϕ_3 and ϕ_4 appear in $\Delta\mu_3$, apart from the logarithmic term, only in $\Sigma_i \phi_i/m_i$ and this can be developed as follows

$$\sum_i \frac{\phi_i}{m_i} = \frac{\phi_1}{m_1} + \frac{\phi_2}{m_2} + \frac{\phi_3}{m_3} + \frac{\phi_4}{m_4} = \frac{\phi_1}{m_1} + \frac{\phi_2}{m_2} + \frac{\phi_3 + \phi_4}{m_3} - \frac{\Delta m}{m_3} \frac{\phi_4}{m_3} \tag{2.30}$$

so that

$$\frac{\Delta\mu_3}{RT} = \ln \phi_3 + 1 - m_3 \left[\frac{\phi_1}{m_1} + \frac{\phi_2}{m_2} + \frac{1 - \phi_1 - \phi_2}{m_3} - \chi(\phi_1 + \phi_2)^2\right] - \frac{\Delta m}{m_3} \phi_4 \tag{2.31}$$

and $\ln a_3$, from (2.24), contains therefore only ϕ_1', ϕ_2', ϕ_1'', ϕ_2'' and a term $(\Delta m/m_3)/(\phi_4'' - \phi_4')$. One can show that the same holds for $\ln a_1$, so that there are lines in the binodial surface along which a_1 and a_3 are constant up to terms of the order of $\Delta m/m_3$; along these lines a_4/a_3 is thus constant up to terms of the order of $(\Delta m/m_3)^2$.

III. PRINCIPLES OF EVALUATING COUNTER-CURRENT EXTRACTION COLUMNS

We shall describe in this chapter the principles and methods which we have used to evaluate the counter-current extraction column, i.e. to determine the number of theoretical stages required to effect a given separation under
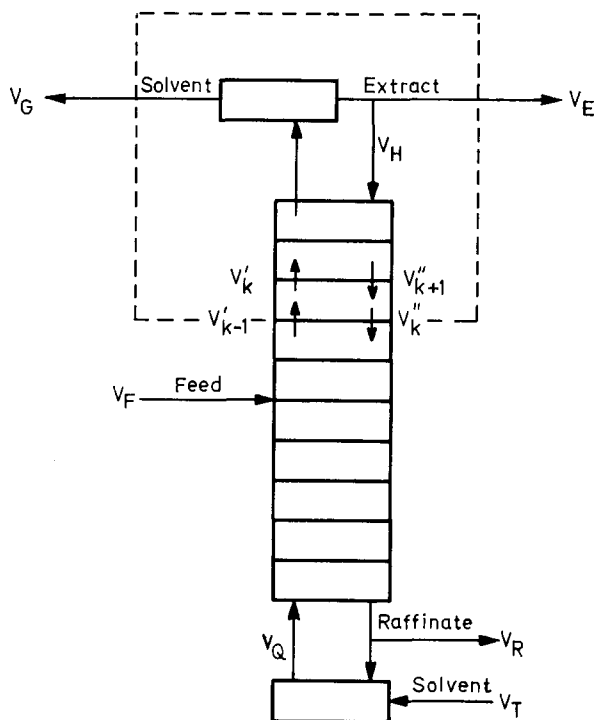
Figure 3 Schematic representation of counter-current extraction column

given conditions. The treatment is based essentially on that of Section 11 of Perry's Chemical Engineer's Handbook[7].

Figure 3 shows schematically a counter-current extraction column with reflux; there is no difference of principle between this column and a fractional distillation column. Extraction is based on the differences of solubilities of the two substances to be separated in two immiscible liquid phases. These phases move in opposite directions (counter-currently) in the column. At each stage the two phases are brought into thermodynamical equilibrium with each other, and as they progress through the column one gets enriched in one of the substances, the other in the other. The column can consist of a number of discrete stages of mixing and settling, or can provide continuous contact between the two phases moving in opposite directions. In the latter case there is a definite portion of the column which is equivalent in its effect to one theoretical stage. Reflux must be provided at either end, by returning part or all of the product issuing to the column.

We shall use the following terms and notations, adapted to our problem. The phase indicated by a single prime is the extract, the phase indicated by a double prime the raffinate. We denote the part of the column in which the extract phase accumulates polymer 3 the extract section, the other part in which the raffinate phase accumulates polymer 4 the raffinate section: they are separated by the stage on which the feed is introduced, the feed

518

stage. We number the stages in the two parts from the feed stage, running index k, calling the feed stage the first stage of the extract section, and we call the total number of stages in the two parts n_E and n_R, respectively We denote the rates of flow, expressed as volume per unit time, by V, with the appropriate index: E for extract, R for raffinate, F for feed, k for stage number k, H and Q for the reflux at the two ends, G and T for the solutions S–A (called the mixed solvent) taken off or added, respectively, at the two 'mixed-solvent separators' at the two ends. Primes and double primes are used where necessary to distinguish extract and raffinate phases; the same subscripts and superscripts are applied to the volume fractions ϕ_i, with i denoting in addition the nature of the component.

We shall derive the relevant expressions for the extract section of the column; the corresponding expressions for the raffinate section are obtained from them easily by analogy.

The required equations are obtained by taking material balances about parts or all of the column; once a stationary state has been established the quantity of each component and the total volume entering must equal that leaving.

For the section indicated by the dashed lines in *Figure 3* we obtain

$$V'_{k-1} = V''_k + V_E + V_G \tag{3.1}$$

$$V'_{k-1}\,\phi'_{i,k-1} = V''_k\,\phi''_{i,k} + V_E\,\phi_{i,E} + V_G\,\phi_{i,G} \tag{3.2}$$

Equation (3.2) holds for $i = 1, 2, 3, 4$, but one of them is redundant, since the sum of the four equations equals (3.1).

Our aim is to establish relations which allow us to obtain the compositions of the liquids on stage k if those of the liquids on stage $k - 1$ are known. Equation (3.1) and three of equations (3.2) can be regarded as four homogeneous simultaneous linear equations for the four unknowns V'_{k-1}, V''_k, V_E, V_G. Since they are known to have solutions other than the trivial "all $V = 0$", the determinant D of the coefficients, the ϕ_i, must vanish, We consider the four points P'_{k-1}, P''_k, E, G, whose coordinates are $\phi'_{i,k-1}$, $\phi''_{i,k}$, $\phi_{i,E}$, $\phi_{i,G}$, respectively; $D = 0$ means that they lie in one plane. This fact alone does not suffice to determine P''_k from the other three.

However, further conditions can be obtained from (3.1) and (3.2). E and G are given for given operating conditions of the column; we can define a point K with the coordinates $\phi_{i,K}$ from

$$(V_E + V_G)\,\phi_{i,K} = V_E\,\phi_{i,E} + V_G\,\phi_{i,G} \tag{3.3}$$

K represents the composition of the substance removed at the extract end, i.e. the sum of G and E, so that $V_K = V_E + V_G$. Equations (3.1) and (3.2) can now be written

$$V'_{k-1} = V''_k + V_K \tag{3.1'}$$

$$V'_{k-1}\,\phi'_{i,k-1} = V''_k\,\phi''_{i,k} + V_K\,\phi_{i,K} \tag{3.2'}$$

Considering (3.1') and the first two of (3.2') as three homogeneous simultaneous equations for V'_{k-1}, V''_k, V_K, we can say that since they have non-trivial solutions, the determinant of the coefficients must be zero; the same

argument can be applied to (3.1') and the first and third of (3.2'). The vanishing of these two determinants means that P'_{k-1}, P''_k, and K lie on a straight line; if the positions of K and P'_{k-1} are known, P''_k can be found since it must also lie on the binodial surface and is therefore the point of intersection of this surface and the straight line through P'_{k-1} and K. Clearly, the position of the binodial surface must be known. The point K is called the operating point and straight lines through it the operating lines; P''_k is thus found as the point of intersection of the binodial surface and the operating line through P'_{k-1}.

We have now a means of finding, at least in principle, the compositions of the two phases on all stages: from P''_k we can find P'_k as the point representing the phase coexisting with P''_k; from P'_k we find P''_{k+1} as the intersection of the binodial surface with the operating line through P'_k, and so on.

The same considerations can be applied to the raffinate phase; since the phase represented by T is added and not removed, the operating point N for the raffinate section is determined from

$$(V_R - V_T)\,\phi_{i,N} = V_R\phi_{i,R} - V_T\,\phi_{i,T} \tag{3.4}$$

N represents therefore the total liquid removed at the raffinate end.

A material balance around the whole of the column shows that the points K, N and F lie on a straight line.

The reflux ratio r_E (sometimes called the external reflux ratio) of the extract section is defined by

$$r_E = V_H/V_E \tag{3.5}$$

Taking a material balance over the top of the extract section, we obtain, remembering that E and H represent phases of identical compositions

$$V_G\,\phi_{i,G} + (V_H + V_E)\,\phi_{i,E} = V'_n\,\phi'_{i,n} \tag{3.6}$$

Substituting from (3.3), we obtain

$$V_K\,\phi_{i,K} + V_H\,\phi_{i,E} = V'_n\,\phi'_{i,n} \tag{3.7}$$

and since $V'_n = V_G + V_H + V_E = V_K + V_H$, we obtain

$$\frac{V_H}{V_K} = \frac{\phi_{i,K} - \phi'_{i,n}}{\phi'_{i,n} - \phi_{i,E}} \tag{3.8}$$

From (3.3) we obtain with $V_G = V_K - V_E$

$$\frac{V_K}{V_E} = \frac{\phi_{i,E} - \phi_{i,G}}{\phi_{i,K} - \phi_{i,G}} \tag{3.9}$$

so that

$$r_E = \frac{\phi_{i,K} - \phi'_{i,n}}{\phi'_{i,n} - \phi_{i,E}} \times \frac{\phi_{i,E} - \phi_{i,G}}{\phi_{i,K} - \phi_{i,G}} \tag{3.10}$$

The four concentration differences in this equation are proportional to the distances of the representative points KP'_n, P'_nE, EG, KG, respectively, and the value of r_E can be appreciated by considering the graphical representation of the tetrahedral diagram and the relevant points.

The same considerations can be applied to the raffinate end to obtain r_R.

If the column works under total reflux, $V_F = V_E = V_R = 0$, i.e. there is no feed and off-take and all the polymer leaving e.g. the top of the extract section as extract is returned as reflux (raffinate phase) after removal of the appropriate quantity of mixed solvent A-S, represented by G, and analogously for the raffinate end. Points K and N are then identical with G and T, respectively, and since there is no feed, G and T become identical; we call the operating point in that case J. Equation (3.10) shows that, due to the co-incidence of K and G, r_E is indeed infinite in this case.

Since the operating lines pass through J, which is a point on the 1–2 edge of the tetrahedron, the ratio ϕ_3/ϕ_4 is constant along each one of them; that is to say

$$\frac{\phi'_{3,k-1}}{\phi'_{4,k-1}} = \frac{\phi''_{3,k}}{\phi''_{4,k}} \quad (r = \infty) \tag{3.11}$$

Using (2.17) we obtain from this

$$\frac{\phi''_{3,k-1}}{\phi''_{4,k-1}} = \left(\frac{a_4}{a_3}\right)_{k-1} \times \frac{\phi''_{3,k}}{\phi''_{4,k}} \quad (r = \infty) \tag{3.12}$$

The evaluation of the number of stages required to effect a given separation, say such that $\phi_{3,E}/\phi_{4,E} = 99$ (99 % purity), proceeds in the following manner: for given F, E and R, K is chosen suitably; we assume that F represents a raffinate phase, in equilibrium with the extract on the feed stage or first extract stage P'_1; it is shown easily that this latter assumption does not introduce any errors into the evaluation. The straight line joining P'_1 and K cuts the binodial surface at P''_2, whose coexisting phase is P'_2, and so on. This procedure must be continued until a phase P'_n is reached, which is as nearly identical with E as possible; the number n gives the number of theoretical stages required in the extract section, i.e. n_E. The number of stages required in the raffinate section, n_R is obtained analogously.

A minimum value for the reflux ratio can be obtained by the following consideration: for the fractionation to be successful it is clearly necessary that P''_2 be between F and E; a limiting value of the position of K is given by a point on the tie-line passing through F, i.e. the line joining F to its coexisting phase. If the operating line becomes identical with the tie-line, P''_2 coincides with F and no advance is made. We shall call this limiting position of K, K*. As K approaches K*, the number n_E of extract stages increases beyond all bounds. The reflux ratio corresponding to K* is the minimum reflux ratio r_E*.

IV. DETERMINATION OF THE NUMBER OF THEORETICAL STAGES REQUIRED FOR FRACTIONATION

(1) Separation of polymers of chainlengths 100 and 1000

As a first case we have considered the separation of two polymer species of chainlengths 100 and 1000; we have chosen 100 for the chainlength of the auxiliary polymer A and have established the phase diagram of the system 1/100/100/1000, with $\chi = 0.4$, as described in section II.

In order to represent the points of the three-dimensional binodial surface on paper, two projections are necessary; we have chosen a perpendicular projection onto a plane parallel to the base of the tetrahedron, i.e. the 2–3–4 face, and a central projection from the vertex 1 onto such a plane. Since few of the solutions encountered contained less than 95 % S, we have chosen the plane $\phi_1 = 0.95$ as the plane of the projection. Each phase is therefore represented by two points, one which is the orthogonal projection onto this plane, i.e. the foot of the perpendicular drawn from the representative point to this plane, and one which is the intersection with this plane of the line joining the representative point to the vertex 1. It is geometrically evident that these two projections must lie on a straight line passing through the projection of the vertex, and the ratio of the distance of the two projections to the distance of the central projection from the vertex is a direct measure of the value of ϕ_1.

We have considered on such a diagram the fractionation, under conditions of total reflux, of a mixture of the two species P. Three stages of extraction lead from an extract with a polymer ratio $p = 17\,500$ (over 99·99 % purity) to a raffinate with p well below 0·01 (well over 99 % purity). The internal reflux ratio v (see next section) is about 22; the solutions used in this example contain at most 6 % total polymer A + P and have all values of a_1 near 1·02.

This example shows that under favourable conditions very efficient separations can be carried out in a small number of stages, without undue strain on the experimental conditions. We have not pursued the subject of the fractionation of this system further, but have turned our attention to the separation of polymer species whose chainlengths are fairly close to each other.

(2) Separation of polymers with neighbouring chainlengths under total reflux

We have seen in section II(4) that for systems containing two polymers of neighbouring chainlengths there are points in the binodial surface which lie in lines nearly parallel to the edge 3–4; along these lines a_1 and a_3 are approximately constant. The plane which contains the two lines representing phases ' and ", corresponding to a given value of a_1 and the corresponding value of a_3, is therefore itself parallel to the edge 3–4 and cuts the edge 1–2 in a point J. If one chooses this point as the operating point of the extraction, all operating lines will lie in this plane, and since the tie-lines also lie in the plane, the whole operation of the column will be represented by points in this plane, which we shall call the operating plane of the point J. If the point J is chosen so that the original feed composition does not lie in its operating plane, conditions in the column will quickly change so that they come to be represented by points of this plane; in a practical operation, with finite reflux, the composition on the feed stage is fixed and the operating points will be determined by the conditions at the two ends of the column such that again the conditions in the column will be approximatively given by points in their operating planes.

The calculation of the number of theoretical stages required to effect a given separation is based on (3.12), which relates the polymer ratio $p = \phi_3/\phi_4$ on one stage to that on the preceding stage. If the operation of the whole

column is represented by points of a single operating plane, a_4/a_3 is constant throughout the column, at least up to terms of the order of $\Delta m/m_3$, and we have

$$p'_n = \left(\frac{a_3}{a_4}\right) p''_n = \left(\frac{a_3}{a_4}\right)^2 p''_{n-1} = \ldots = \left(\frac{a_3}{a_4}\right)^n p_F \tag{4.1}$$

Since p''_n is practically identical with p_E, the desired value of p in the extract, we have

$$\ln p_F - \ln p_E = n \ln \frac{a_4}{a_3} = n \frac{\Delta m}{m_3} \ln a_3 \tag{4.2}$$

so that for the extract section

$$n_E = \frac{\ln p_E - \ln p_F}{(\Delta m/m_3) \ln (1/a_3)} \tag{4.3}$$

where the equation has been written in this form since a_3 is always less than unity.

We have similarly for the raffinate section

$$n_R = \frac{\ln p_F - \ln p_F}{(\Delta m/m_3) \ln (1/a_3)} \tag{4.4}$$

We should like to stress again that (4.1) is based on the assumption that a_3 and with it a_4/a_3 are constant throughout the column; in the particular case of the system 1/100/1000/1010, with $\chi = 0.4$ and for $a_1 = 1.02$, a_4/a_3 varies from 0.960261 to 0.960445 from one side of the phase diagram to the other.

It is also worth pointing out that the hypothesis of the constancy of the distribution coefficients a_3 and a_4 is based on general considerations on the chemical potentials in mixtures containing isotopic components and does not depend on the particular form of the expression for the free energy of mixing chosen.

The number of stages according to (4.3) and (4.4) is inversely proportional to the difference in the chainlengths of the two polymers to be separated. For a given value of the polymer ratio p in the feed and given values of the desired values of p in the extract and the raffinate (which are defined by the desired degrees of purity), the number of stages required to separate polymers of chainlengths 1000 and 1010 is ten times that required to separate polymers of chainlengths 1000 and 1100. The number of stages required for given values of p is determined roughly by $\Delta m/m_3$, the relative difference in the chainlengths, but it must be borne in mind that for comparative conditions a_3 changes with m_3.

We show in *Table 1* the results of our calculations for two typical systems under varying conditions; the systems chosen are 1/100/1000/1100 and 1/100/1000/1010, and we shall refer to these systems as 1000/1100 and 1000/1010, respectively. We have chosen $\chi = 0.4$ for the interaction parameter; this is a typical value for systems of non-polar polymers. *Table 1* gives the volume fractions of S, A and total P in the two phases, a quantity v to be described below and the number of stages required to obtain extracts and

raffinates of the purities quoted; these correspond to values of $p_E = 9$, 99, 999, and of $p_R = 1/9, 1/99, 1/999$, respectively. The number of stages quoted is the total number, i.e. $n_E + n_R$, and is of course independent of the polymer ratio in an assumed feed, since we have conditions of total reflux.

The quantity v, sometimes referred to as the internal reflux ratio, is the ratio of the rates of flow of the two phases, $v = V_{k-1}^1/V_k''$. Since no P is taken off, the quantity of either 3 or 4 flowing in both directions must be the same, from which one concludes

$$v = \frac{\phi_{4,k}''}{\phi_{4,k-1}'} = \frac{\phi_{3,k}''}{\phi_{3,k-1}'} = \frac{\phi_{3,k}'' + \phi_{4,k}''}{\phi_{3,k-1}' + \phi_{4,k-1}'} \tag{4.5}$$

It is easy to see that in the graphical representation v equals the ratio of the distances of the two generators representing the two phases from the point J.

Table 1 Fractionation of mixed polymers 1000/1100 and 1000/1010 in a quaternary system, $m_2 = 100$, $X = 0.4$, under conditions of total reflux

ϕ_1''	ϕ_1'	$(\phi_3'' + \phi_4'')$	$(\phi_3' + \phi_4')$	v	Number of stages $n_E + n_R$ Purity		
					90%	99%	99.9%
Polymer 1000/1100							
0.984161	0.989082	0.012064	0.004703	2.46	49	102	153
0.979848	0.989647	0.017260	0.002531	6.25	24	50	75
0.968156	0.987519	0.030188	0.000480	52.6	11	23	35
0.953706	0.982317	0.045376	0.000042	820.	7	14	21
Polymer 1000/1010							
0.983937	0.988857	0.012243	0.004851	2.52	475	993	1492
0.979650	0.989446	0.017423	0.002637	6.54	234	489	735
0.967996	0.987355	0.030330	0.000520	57.1	109	227	341
0.953558	0.982165	0.045526	0.000048	912.	64	133	200

Examination of the values quoted in *Table 1* shows that the separation of the system 1000/1100 and under certain conditions even of 1000/1010 is not beyond all possibility, at least as regards the number of theoretical stages required.

(3) Number of stages for polymers with neigbouring chainlengths under partial reflux

Under practical conditions, when there is a feed and off-takes of extract and raffinate, the column is said to operate under partial reflux. In this case the operating points K and N of the extract and raffinate sections, respectively, do no longer coincide and do not lie on the 1–2 edge of the composition tetrahedron. We shall outline the derivation of the equations for the extract section; those for the raffinate section follow from them by analogy.

The operating line of stage k passes through K, the operating point, P_k', the representative point of the extract phase on stage k, and P_{k+1}'', the repre-

sentative point of the raffinate on stage $k + 1$. The coordinates of these three points satisfy therefore the four equations

$$\frac{\phi_{i,K} - \phi''_{i,k+1}}{\phi_{i,K} - \phi'_{i,k}} = \lambda k \tag{4.6}$$

for $i = 1$ to 4. As in the case of total reflux, we want to establish a relationship between the polymer ratios p on successive stages.

Using

$$p''_k = \left(\frac{a_4}{a_3}\right)_k p'_k \tag{4.7}$$

where we mean by $(a_4/a_3)_k$ the value of the ratio a_4/a_3 on stage k and intro-ducing for any phase or stage the volume fraction of the whole of polymer P, $\phi_P = \phi_3 + \phi_4$, we obtain

$$p''_{R+1} = a_k \frac{p''_k - b_k}{c_k - p''_k} \tag{4.8}$$

where a_k, b_k, c_k are functions of λ_k, $\phi'_{P,k}$, $\phi''_{P,k+1}$, $(a_3/a_4)_k$, $\phi_{P,K}$

We shall now introduce the hypothesis used on treating the column under conditions of total reflux, that the representative points P'_k, P''_k of the two phases ' and '' lie close to two generators on the binodial surface and that the values of ϕ_1, ϕ_2, ϕ_P, a_3, a_4 are constant within quantities of the order of $\Delta m/m_3$ along the generators. The quantities a_k, b_k, c_k become independent of k and (4.8) is then a recurrence relation with constant coefficients to cal-culate p''_{k+1} from p''_k. The number n_E of the stages of the extract section is the number of steps required to arrive from p_F to p_E.

For numerical evaluation, we introduce new constants α, β, γ by writing

$$\frac{p''_{k+1} - \beta}{\gamma - p''_{k+1}} = \alpha \times \frac{p''_k - \beta}{\gamma - p''_k} \tag{4.9}$$

where α, β, γ are so chosen that the functional relationship of p''_{k+1} and p''_k given by (4.8) is the same as that given by (4.9).

Then, p_F and p_E are related by

$$\frac{p_E - \beta}{\gamma - p_E} = \alpha^n \frac{p_F - \beta}{\gamma - p_F} \tag{4.10}$$

so that

$$n = \frac{\ln\left[(p_E - \beta)/(\gamma - p_E)\right] - \ln\left[(p_F - \beta)/(\gamma - p_F)\right]}{\ln \alpha} \tag{4.11}$$

We have also derived expressions to compute the minimum reflux ratio r^*_E, but shall not give the details here.

We have calculated the number of stages required for the systems and conditions quoted in *Table 1* with values of r_E chosen somewhat arbitrarily 20–50 % above r^*_E; *Table 2* shows the values of n_E and n_R obtained, as well as r_E, r_R, r^*_E, r^*_R and n_∞, the total number of stages required at conditions of total reflux. These values show reflux ratios not very much above the

Table 2 Fractionation of mixed polymers 1000/1100 and 1000/1010 in a quaternary system, $m_2 = 100$, $X = 0.4$, under conditions of partial reflux

	Polymer 1000/1100					
	$P_F'' = 1.003, v = 6.25$			$P_F'' = 1.005, v = 52.7$		
p_E	0.111	0.010	0.001	0.111	0.010	0.001
r_E^*	7	8	8	3	4	4
r_E	11	11	11	5	5	5
n_E	20	55	82	8	22	33
p_R	0.111	0.010	0.001	0.111	0.010	0.001
r_R^*	8	10	10	5	6	6
r_R	13	13	13	7	7	7
n_R	22	55	79	10	22	33
$n_E + n_R$	44	110	161	18	44	66
n_∞	24	50	75	11	23	35

	Polymer 1000/1010			
	$p_F'' = 0.965, v = 6.55$		$p_F'' = 1.017, v = 57$	
p_E	0.111	0.010	0.111	0.010
r_E^*	86	105	38	48
r_E	143	143	65	66
n_E	179	419	80	194
p_R	0.111	0.010	0.111	0.010
r_R^*	84	105	41	50
r_R	118	143	69	69
n_R	176	419	82	188
$n_E + n_R$	355	838	162	382
n_∞	234	489	109	227

necessary minimum, and the number of stages required is not unreasonably above the number at total reflux.

We have carried out similar computations on systems with other parameters. We have compared the systems 100/101 and 10000/10100 with 1000/1010 and also 100/110 and 10000/1100 with 1000/1100 to find the effect of chainlength for systems with the same chainlength ratios, and have also used $m_2 = 1000$ and 10000 instead of 100 used in the examples given here; we have also taken different values for X in a few cases, to study the effect of temperature. We could confirm in all these cases that the essential features of the fractionation remain the same, though the numerical values change somewhat.

V. CONTINUOUS DISTRIBUTION OF CHAINLENGTHS IN THE POLYMER TO BE FRACTIONATED

Up to now we have considered the special case of solutions containing a mixture of only two polymers to be fractionated. In practice, solutions will contain polymers of species P having a wide range of chainlengths, or, putting it differently, a polymer P with a wide chainlength distribution.

Let us consider first briefly the case of a mixture of three polymer species P. To represent the phase diagram of the system S–A–P a 'pentahedron' in

four-dimensional space would be required. If the three chainlengths of P are close to each other, we can extend the argument used in section III to show that the whole operation of the column will be represented by points in one 'operating space' and that a_3, a_4, a_5 will be constant throughout. Under conditions of total reflux, (3.12) will be valid not only for the pair 3–4, but there will be an analogous equation for the pair 4–5, and so automatically also for 3–5. The total separation between extract and reflux, over n stages will be given by

$$\frac{\phi_{3,\mathrm{E}}}{\phi_{4,\mathrm{E}}} = \left(\frac{a_3}{a_4}\right)^n \frac{\phi_{3,\mathrm{R}}}{\phi_{4,\mathrm{R}}}, \quad \frac{\phi_{4,\mathrm{E}}}{\phi_{5,\mathrm{E}}} = \left(\frac{a_4}{a_5}\right)^n \frac{\phi_{4,\mathrm{R}}}{\phi_{5,\mathrm{R}}}$$

We shall illustrate the consequences of these equations in some simple numerical cases. Let $m_5 - m_4 = m_4 - m_3$, so that $a_5/a_4 = a_4/a_3$, since the logarithms of these ratios are proportional to $\Delta m = m_5 - m_4 = m_4 - m_3$. Let us assume that the number of stages are such that $(a_3/a_4)^n = (a_4/a_5)^n = 100$ and that we start with a mixture of equal parts of the three polymers, $100 + 100 + 100$. The final compositions of extract and raffinate depend on the relative amounts of the two fractions; this is of course true for separation of a mixture of two polymers as well, but there is rarely interest in considering separation of, say, an equal mixture of two species into other then two equal fractions. However, we can contemplate separation of a mixture of equal parts, $100 + 100$, into two fractions in the ratio 10:1; if $(a_3/a_4)^n = 100$, this will give an extract of $99{\cdot}78 + 82{\cdot}04$ and a raffinate of $0{\cdot}22 + 17{\cdot}96$, as against $91{\cdot}8 + 9{\cdot}2$ and $9{\cdot}2 + 91{\cdot}8$ if one separates into two equal fractions.

If the above ternary mixture is separated under these conditions into two equal fractions, they will be $99 + 50 + 1$ and $1 + 50 + 99$, respectively. However, if one wants to separate the third polymer from the first two, one would take fractions in the ratio 2:1 and they would be $99{\cdot}9 + 91{\cdot}8 + 9{\cdot}3$ and $0{\cdot}1 + 9{\cdot}2 + 91{\cdot}7$, respectively.

We consider next polymers with a continuous distribution of chainlengths. One of the most interesting and most frequent among these is the so-called exponential distribution (reference 5, section 1.3): the weight fraction of polymer with chainlengths between m and $m + dm$ is given by

$$w = \rho \, \mathrm{e}^{-\rho} \tag{5.1}$$

where $\rho = m/\bar{m}$ and $\bar{m}$ is the number-average chainlength.

We have shown that the separation of polymers with neighbouring chainlengths is given by

$$\frac{\ln (\phi_{j,\mathrm{E}}/\phi_{j,\mathrm{R}}) - \ln (\phi_{i,\mathrm{E}}/\phi_{i,\mathrm{R}})}{m_j - m_i} = n \frac{1}{m_i} \ln a_i = -k' \tag{5.2}$$

We are justified in putting the right hand side equal to a constant k', independent of i or j, since $(1/m_i) \times \ln a_i$ is constant if the free energy of mixing is given by the Flory–Huggins expression and the interaction constants do not depend on chainlength, see (2.18).

If we regard the chainlength distribution as continuous, we can transform (5.2) into a differential equation. The volume fractions ρ_E and ρ_R are then continuous functions of the chainlength m, or of ρ, and we shall find it more

527

convenient to use weight fractions w_E and w_R in the extract and raffinate polymers without solvent, so that

$$\phi_E = w_E \phi_{P,E} \qquad \phi_R = w_R \phi_{P,R} \tag{5.3}$$

If we substitute these values into (5.2) and regard $m_j - m_i$ as infinitely small, we obtain

$$\frac{d \ln (w_E/w_R)}{dm} = -k' \text{ or } \frac{d \ln (w_E/w_R)}{d\rho} = -\bar{m} k' = -k \tag{5.4}$$

This is one equation between w_E and w_R: we can obtain a second one from considerations of material balance. A material balance can be obtained in the following way: if in a column operating under total reflux there is a considerable reservoir of extract and raffinate phases, of volumes V_E and V_R, such that the volume of the column itself can be neglected, we have

$$v_E w_E + v_R w_R = w \tag{5.5}$$

where v_E and v_R are the ratios of V_E and V_R to the total volume $V_E + V_R$. We should obtain the same equation if we considered a column operating under conditions of nearly total reflux, with a very small feed and very small off-takes of volumes V_E and V_R.

The solution of (5.4) is

$$\ln w_R - \ln w_E = k (\rho - \rho^*) \tag{5.6}$$

where $-k\rho^*$ is the constant of integration; combining this with (5.5) gives us

$$w_E = \frac{\rho \, e^{-\rho}}{v_R \, e^{k(\rho-\rho^*)} + v_E}, \qquad w_R = \frac{\rho \, e^{-\rho} \, e^{k(\rho-\rho^*)}}{v_R \, e^{k(\rho-\rho^*)} + v_E} \tag{5.7}$$

The integration constant $-k\rho^*$ can be obtained from the normalization condition

$$\int_0^\infty w_E \, d\rho = \int_0^\infty \frac{\rho e^{-\rho}}{v_R \, e^{k(\rho-\rho^*)} + v_E} \, d\rho = 1 \tag{5.8}$$

Strictly speaking, equation (5.4) is only valid when there is only a narrow range of chainlengths present, since the constancy of a_i throughout the column is based on this assumption. Here we consider polymers with chainlengths from zero to infinity, however, polymers with chainlenghts far from the separation point will very quickly, over a few stages of the column, collect either in the extract or the raffinate phase and their distribution is of little interest; the primary interest is in the distribution of chainlengths near the separation point and we feel therefore justified in using (5.4) as a basis of our considerations.

The definite integral (5.8) is not of a type whose value can be expressed in terms of elementary functions and methods of approximation must be used. Integrals of this kind occur in the statistical mechanics of Fermi-Dirac distributions and their treatment had been considered extensively in that connec-

tion. If k is large, the first term in the denominator can be neglected for $\rho < \rho^*$ and the second term for $\rho > \rho^*$, and the integral can be written

$$\int_0^{\rho^*} \frac{\rho e^{-\rho}}{v_E} \, d\rho + \int_{\rho^*}^{\infty} \frac{\rho \, e^{-\rho}}{v_R e^{k(\rho - \rho^*)}} \, d\rho = 1 \qquad (5.9)$$

The integrand of the second integral is very small for large values of k and the integral can be neglected; the first integral gives

$$(1 + \rho^*) \, e^{-\rho^*} = v_R \qquad (5.10)$$

This means that ρ^* is the chainlength at which the polymer would have to be cut into two fractions in the ratio $v_E:v_R$ such that all polymer with $\rho < \rho^*$ is in one fraction and all with $\rho > \rho^*$ in the other. These are the distributions which one would get from (5.7) for $k = \infty$. For finite values of k, the distribution of the polymers with chainlengths far from ρ^* is as for $k = \infty$, but is given by (5.7) for ρ near ρ^*.

One finds that for finite values of k and ρ^* related to v_R by (5.10), the normalizing equation (5.8) is not exactly satisfied, due to the simplifications used to derive (5.10). Either ρ^* or v_R have to be changed slightly until the value of the integral in (5.8) becomes unity; in practice v_E and v_R are determined by the conditions of fractionation and ρ^* will adjust itself so that (5.8) is satisfied.

We have taken as a numerical illustration the case of a polymer with an exponential distribution of chainlengths; though the absolute value of the chainlengths does not enter the equations, we have considered $\bar{m}$ as being equal to 1000, to fix our ideas. If we choose $\rho^* = 1$, i.e. cut at $m = 1000$, we have from (5.10) $v_E = 0.2642$, $v_R = 0.7358$ as a first approximation. We have chosen $k = 100$ which corresponds to 144 theoretical stages if the distribution coefficient a is 0.5. We have calculated w_E and w_R from (5.7) and have then adjusted v_E and v_R until (5.8) was satisfied; this is the case for $v_E = 0.2604$, $v_R = 0.7396$.

Table 3 shows the values of w, $v_E w_E$ and $v_R w_R$ for different values of m, in the

Table 3 Fractionation of polymer with exponential distribution of chainlengths

$(v_E^{(1)} = 0.2604,\ v_R^{(1)} = 0.7396,\ v_E^{(2)} = 0.2373,\ v_R^{(2)} = 0.0231)$							
m	840	860	880	900	920	940	960
$10^4 w$	3626	3639	3650	3659	3666	3672	3676
$10^4 v_E^{(1)} w_E^{(1)}$	3626	3639	3650	3658	3662	3646	3494
$10^4 v_R^{(1)} w_R^{(1)}$	–	–	–	1	4	26	182
$10^4 v_E^{(2)} w_E^{(2)}$	3626	3634	3615	3421	2422	762	121
$10^4 v_R^{(2)} w_E^{(2)}$	1	5	35	237	1240	2884	3373
m	980	1000	1020	1040	1060	1080	
$10^4 w$	3678	3679	3678	3676	3673	3667	
$10^4 v_E^{(1)} w_E^{(1)}$	2657	958	167	23	3	—	
$10^4 v_R^{(1)} w_R^{(1)}$	1021	2721	3511	3653	3670	3667	
$10^4 v_E^{(2)} w_E^{(2)}$	13	1	—	—	—	—	
$10^4 v_R^{(2)} w_E^{(2)}$	2644	957	167	23	3	—	

neighbourhood of $m = 1000$. We quote $v_E w_E$ and $v_R w_R$ rather than w_E and w_R, since one can then see immediately how much of each species is in the extract and how much in the raffinate, and we have affixed a superscript (1) to indicate that these figures give the results of a first fractionation. The table shows that while the polymer with about $m = 990$ is evenly distributed among the two fractions, more than 99% of the polymer with $m = 940$ is in the extract and more than 99% of the polymer with $m = 1040$ in the raffinate.

We have also calculated the resulting distributions if one submits the extract to a second fractionation. The new extract and raffinate are given by (5.7), with $\rho e^{-\rho}$ replaced by $w_E^{(1)}$. The volumes of the new fractions, $v_E^{(2)}$ and $v_R^{(2)}$, must be determined so that a normalizing condition analogous to (5.8) is satisfied. With $\rho^* = 0.95$ we have found $v_E^{(2)} = 0.2373$ and $v_R^{(2)} = 0.0231$. The resulting values of $v_E^{(2)} w_E^{(2)}$ and $v_R^{(2)} w_R^{(2)}$ are also included in *Table 3*; the new raffinate is now a very narrow fraction, with a number-average chainlength of 957 and a weight-average chainlength of 960. 94%
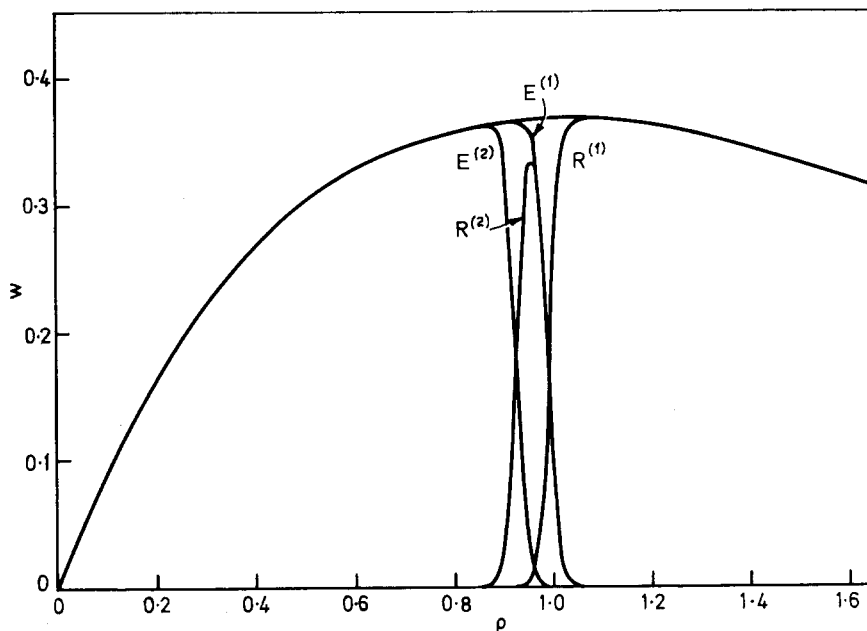
Figure 4 Weight distributions of original polymer, first extract $E^{(1)}$ and raffinate $R^{(1)}$, second extract $E^{(2)}$ and raffinate $R^{(2)}$

of the fraction have chainlengths differing less than 5% from the mean, the half-width of the distribution, i.e. the width of the distribution curve at a height equal to a half of the maximum, is 6·8% of the mean chainlength.

Figure 4 shows the distributions of the original polymer and the fractions obtained; the second raffinate is seen to approximate very closely to a Gaussian distribution (normal error distribution).

CONCLUSION

This work shows that in theory the fractionation of polymers by using the phenomenon of incompatibility is possible; since incompatibility is a general phenomenon polymers to play the rôle of the auxiliary polymer can always be found and the number of theoretical stages of an extraction column which is required to give sharp separations is within the limits of the feasible.

However, a number of difficulties can be foreseen when the ideas presented here are translated into practice. The two phases in contact are both dilute solutions in the same solvent, the difference in density is likely to be small and thus the driving force for separation is small. This implies slow settling, and the system will be very sensible to disturbances, such as mechanical vibrations, fluctuations of temperature and irregularities of flow. Very good thermal constancy and accurate control of the flow rate will be necessary.

Further, polymer solutions when stirred are very liable to form emulsions which are difficult to break and which prevent settling. This problem can only be solved individually for each polymer system, but it will probably be essential to use very gentle methods of stirring and mixing. One apparatus which satisfies this requirement is the disc extraction column (8) in which a set of vertical discs, which dip into narrow semi-cylindrical troughs, is rotated slowly about the common axis and drags a thin film of the lower phase in the troughs through the upper phase, thereby ensuring constantly renewed contact on a large surface between the phases, without necessarily breaking them up into droplets. First experiments (unpublished) confirmed that the difficulties foreseen have not been underestimated.

Union Carbide European Research Associates,
Rue Gatti de Gamond, 95
1180 Brussels, Belgium   *(Received 18 May 1970)*

REFERENCES

1 Dobry, A. *Makromol. Chem.* 1956, **18/19**, 317.
2 Schulz, G. V. and Nordt, E. *J. prakt. Chem.* 1940, **155**, 115
3 Almin, K. E. *Acta Chem. Scand.* 1937, **11**, 1541; 1959, **13**, 1263, 1278, 1287, 1293; 1964, **18**, 2051
   Svensk Papperstidn 1959, **62**, 594, 725, 801
 Almin, K. E. and Lundberg, R. *Acta Chem. Scand.* 1959, **13**, 1274
4 Dobry, A. and Boyer-Kawenoki, F. *J. Polym. Sci.* 1947, **2**, 90.
5 Tompa, H. 'Polymer Solutions', Butterworths, London, 1956

531

6 Albertsson, P.-Å. *Biochem. Biophys. Acta* 1958, **27**, 378
   Nature 1958, **182**, 709
   subsequent papers are summarized in Tiselius, A., Porath, J. and Albertsson, P.-Å.
   Science 1963, **141**, 13
   Albertsson, P.-Å. *Svensk. Kemsk. Tidskr.* 1965, **77**, 439
7 Perry, J. H., 'Chemical Engineers' Handbook', McGraw-Hill, London, 1950
8 Signer, R., Allemann, K., Köhli, E., Lehmann, W., Ritschard, W. and Meyer, H
   Chimia 1956, **10**, 95
   Dechema Monographien 1956, **27**, 32.
   Ritschard, W. J. *Helv. Chim. Acta* 1962, **45**, 1132
   Ritschard, W. J. and Tompa, H. *Helv. Chim. Acta* 1963, **46**, 1957.

Poly[benzobis(aminoiminopyrrolenines)]

D. I. PACKHAM, J. D. DAVIES and F. A. RACKLEY

A new polymer system, the poly[benzo*bis*(aminoiminopyrrolenines)] is described. The various products that may be obtained from the alkoxide catalysed condensation of pyromellitonitrile (1,2,4,5-tetracyanobenzene) and 4,4'-diaminodiphenyl ether are considered. Studies on the reactions of model compounds have helped to determine the optimum conditions for the formation of the required polymer. The experimental conditions necessary for the preparation of linear polymers of high molecular weight have been examined. Some properties of these polymers and derived products are discussed.

INTRODUCTION

WE HAVE studied in some detail the synthesis of selected polymers by the condensation of aromatic nitriles with amines. In particular we have examined the reactions of compounds containing nitrile groups in *ortho* pairs. Thus the condensation of phthalonitrile or pyromellitonitrile (1,2,4,5-tetracyano-benzene) with tetraamines where the amino groups are also in *ortho* pairs afforded oligomers and polymers containing benzimidazole units, the poly(benziminobenzimidazoles) and related products[1]. The macrocyclic polymers[2] represent a new class of polymers formed by the condensation of suitable tetranitriles (e.g. pyromellitonitrile) with *meta* and *para* diamines in a 1:2 molar ratio. Condensation of these diamines with such tetranitriles in equimolar proportions gave the linear poly[benzo*bis*(aminoiminopyrro-lenines)], I[3]. This paper describes the preparation and some properties of selected members of this series.

RESULTS AND DISCUSSION

Model compounds

The condensation of *meta* substituted diamines with diimino*iso*indoline to give macrocyclic compounds and substituted *bisiso*indolybenzene derivatives (cf VIII *Figure 1*) has been described by Elvidge *et al*[4]. Our experiments have shown that phthalonitrile will undergo similar reactions with *meta* or *para* aromatic diamines[5]. The yield and nature of the products is dependent not only on the diamines used but also the molar ratio of the reactants and the reaction conditions. In a previous publication[1] we described the condensation of *ortho* diamines with nitriles: this paper is restricted to the reactions of *meta* and *para* diamines and in particular the condensation of 4,4'-diamino-diphenyl ether with phthalonitrile and pyromellitonitrile.

In addition to the formation of the linear polymers I, the condensation of pyromellitonitrile with a diamine could lead to polymers of the type II as well as the tetracyano substituted macrocyclic compound III. From a consideration of the reactions that would afford polymers with formula I, it

533
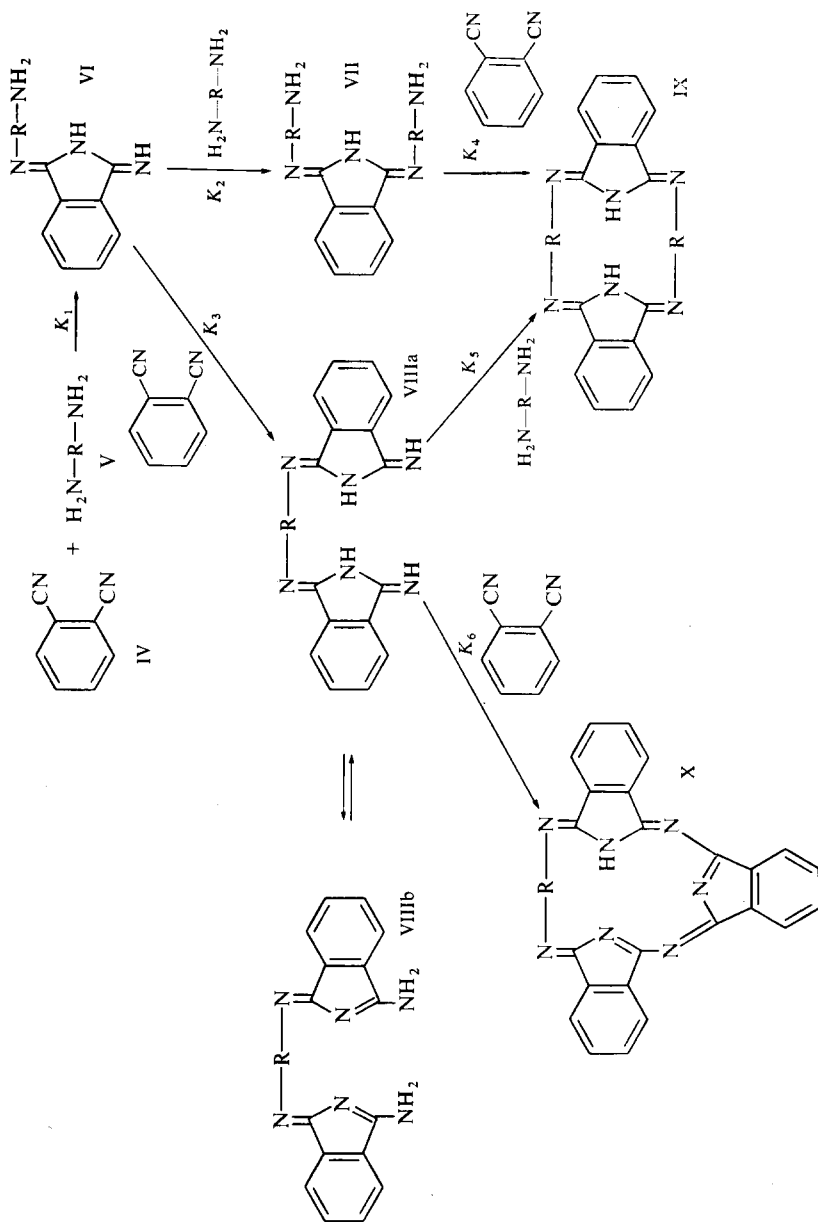
Figure 1 Reaction of phthalonitrile with a diamine
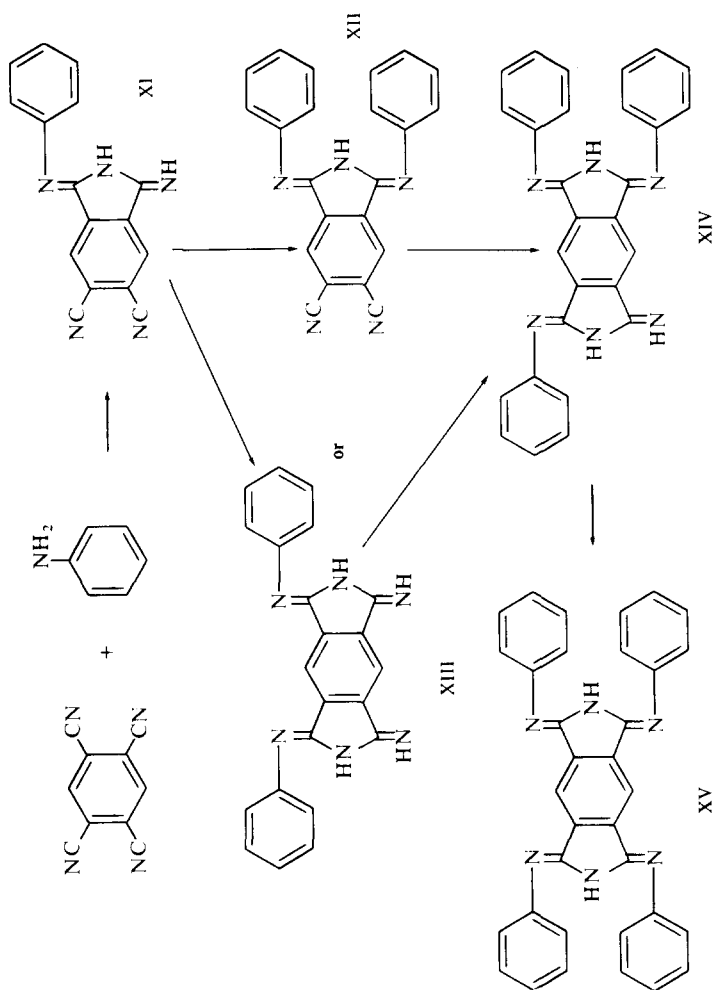
Figure 2 Reaction of pyromellitonitrile with aniline

535

may be concluded that the optimum conditions for the preparation of such polymers should be similar to the conditions necessary for the formation of the model compounds VI and VIII *Figure 1* (from phthalonitrile and a diamine) and the benzo*bis*(phenyliminopyrrolenine), XIII *Figure 2*, (from pyromellitonitrile and aniline). Under conditions where either the *bis* substituted *iso*indoline (VII) or the *bis*cyano*bis*-(phenylimino)*iso*indoline XII are obtained one might predict that the condensation of pyromellitonitrile
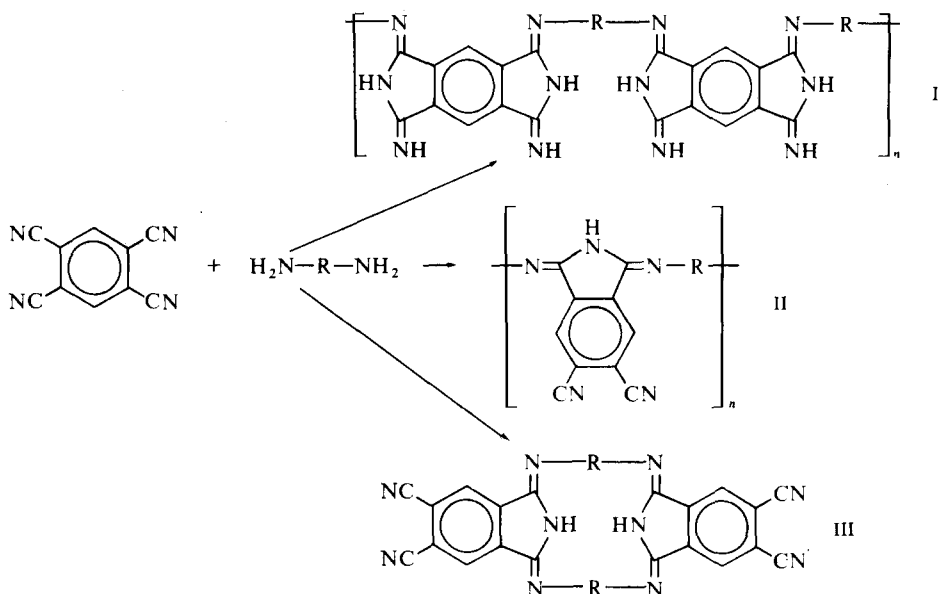
with a diamine would yield either the polymer (II) or the macrocyclic compound III. Similarly under the conditions where the condensation of aniline with pyromellitonitrile afforded tri- or tetraphenyl derivatives, the condensation of a diamine with pyromellitonitrile could yield mixtures of the crosslinked and macrocyclic polymers. We therefore studied in detail the reactions leading to the required model compounds.
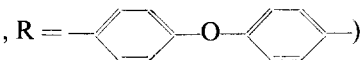
Phthalonitrile and diamines. The reaction sequence of the condensation of phthalonitrile with a diamine may be illustrated stepwise as shown in *Figure 1*. In suitable alcoholic solvents containing alkoxide catalyst, the first product we need to consider is the 1-(4'-aminophenylimino)-3-imino-*iso*indoline (VI) (where R = phenyl). The next step which is one of the deciding factors affecting the formation of the required products is dependent on the stoichiometric ratio of the reactants as well as the rate constants K_2 and K_3. According to the reaction scheme the formation of the *bis*(amino-

phenylimino)*iso*indoline (VII) should be accompanied by the evolution of ammonia, whilst no ammonia should be produced in the formation of the *bis*(di-imino*iso*indolyl)benzene (VIII). The synthesis of the macrocycle (IX) from either (VII) or (VIII) would also be accompanied by the liberation of ammonia. Thus a convenient method of following these reactions was by estimating the ammonia evolved, coupled with infra-red and mass spectrometry.

In our earlier experiments we examined in detail the condensation of phthalonitrile with 4,4'-diaminodiphenyl ether in equimolar proportions in a variety of solvents in order to obtain the macrocyclic compound in high yield. In refluxing methanol and ethanol containing alkoxide catalyst very little ammonia was evolved and the rate of formation of the macrocycle was shown to be very slow. In hydroxylic solvents at temperatures above 180°C complex mixtures were obtained. The optimum yield of macrocycle was realized by refluxing the reactants for 1–5 days in 2-methoxyethanol (b.p. 125°C).

An examination of the reaction of phthalonitrile with 4,4'-diamino-diphenyl ether in a 2:1 molar ratio in methanol, ethanol and 2-methoxy-ethanol showed that the products were dependent on the temperature and duration of the reaction. The most convenient method of studying the condensation products was to inject the total solids from each reaction into a preheated (300°C) source of an MS9 mass spectrometer. Experiments had demonstrated that under these conditions the likely products of such reactions would be vaporized and detected. It was considered that by adopting this procedure of flash vaporization the relative intensities (m/e) of the parent ions recorded on the spectra could be taken as an approximation to the concentration of the various components of the mixture.

The results obtained by this method are shown in the histograms *Figures 3* and *4*. In refluxing methanol containing sodium methoxide catalyst and with reaction times of 1–24 h the principal product was the required 1-(4'-amino-diphenyl ether imino,-3-imino*iso*indoline (VI, R = —⟨C₆H₄⟩—O—⟨C₆H₄⟩—) together with the *bis*(1-phenylimino-3-imino*iso*indolyl)ether (VIII) and a small quantity of the macrocyclic compound IX. During 24 h reflux a small amount ($\simeq 2$ mequiv/mol) of ammonia was evolved. No evidence was obtained for the formation of the *bis*(4'-aminodiphenyl ether imino)*iso*indoline (VII).

In refluxing ethanol containing sodium ethoxide catalyst the results shown in *Figure 4* were obtained. In accordance with our earlier findings, it is apparent that the formation of the macrocyclic compound is enhanced by using higher reaction temperatures. In refluxing ethanol the substituted *iso*indoline (VI) was obtained in 1 h with very little macrocycle formation. Further reaction at this temperature resulted in the formation of the *bisiso*-indolyl ether (VIII) and the macrocyclic compound, with a corresponding decrease in the yield of the derivative (VI). Again there was no evidence to suggest the formation of the *bis* substituted *iso*indoline (VII). Unless extreme care was taken to exclude water, hydrolysis of the exocyclic imino group of (VIII) occurred on prolonged heating. In refluxing 2-methoxyethanol, hydrolysis to the keto compound was even more evident.
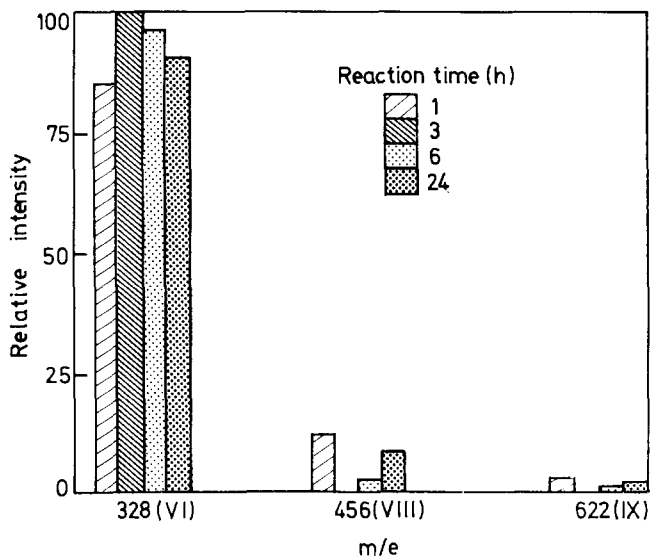
Figure 3 Products from the condensation of phthalonitrile with 4,4'-diaminodiphenyl ether in methanol
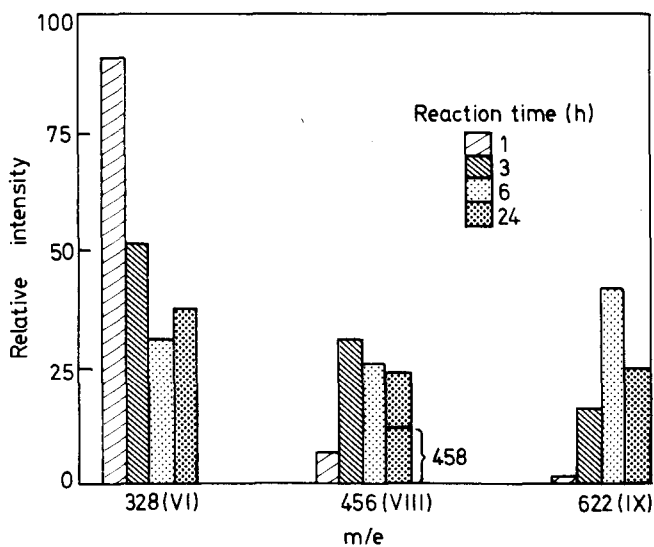
Figure 4 Products from the condensation of phthalonitrile with 4,4'-diaminodiphenyl ether in ethanol
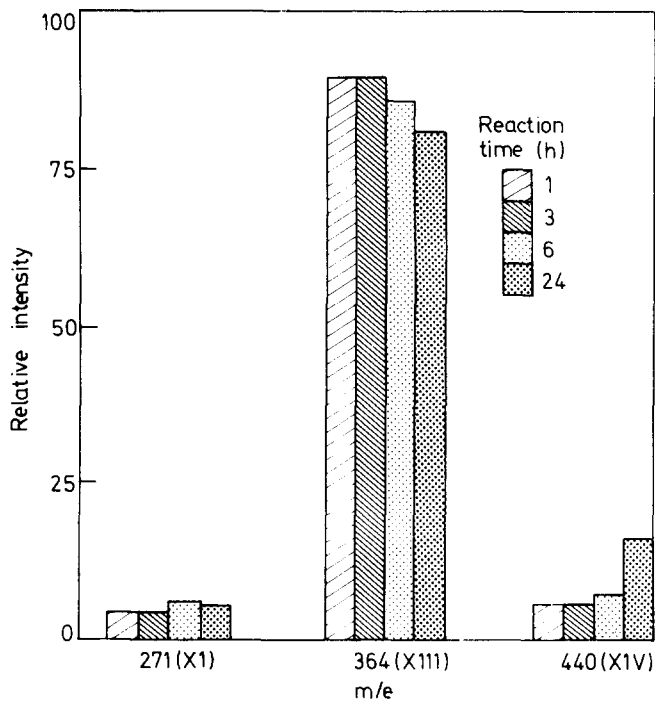
Figure 5 Products from the condensation of pyromellitonitrile with aniline in methanol
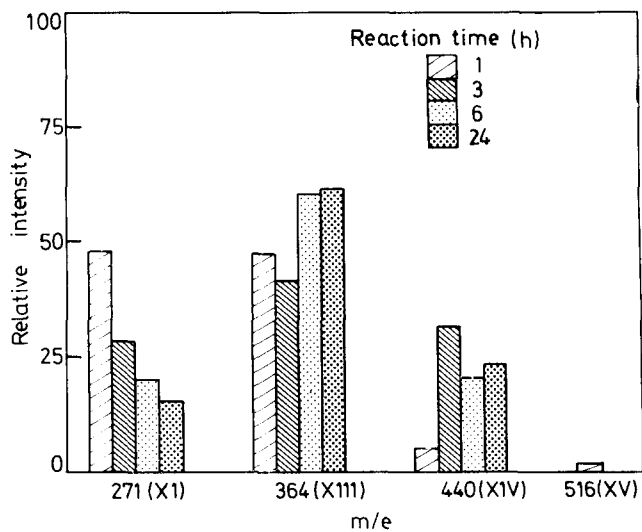
Figure 6 Products from the condensation of pyromellitonitrile with aniline in ethanol

Pyromellitonitrile and aniline. The reaction of aniline with pyromellitonitrile in a molar ratio of 2:1 was studied in methanol, ethanol and 2-methoxyethanol. The results obtained in a manner similar to the previous experiments are shown in *Figures 5, 6* and *7*. Reaction in refluxing methanol containing sodium methoxide catalyst gave as the principal product (90% yield) the required diphenyl compound (XIII). The intermediate *bis*methoxy compound was also identified. The absence of absorption in the 2240 cm^{-1} region of the infra-red spectrum ($\nu_{C \equiv N}$) coupled with elemental analysis and mass spectral analysis indicated the formation of benzo*bis*(phenylaminoiminopyrrolenine) rather than the *bis*cyano*bis*(phenylimino)*iso*indoline (XII). On prolonged reflux the yield of the triphenyl derivative (XIV) increased slightly. There was no evidence of the formation of the tetraphenyl derivative. During 24 h reflux only a trace (20 mequiv/mol) of ammonia was evolved.
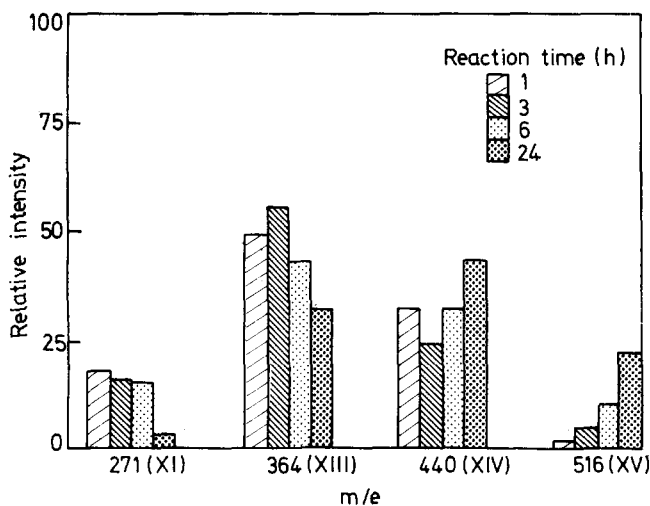
Figure 7 Products from the condensation of pyromellitonitrile with aniline in 2-methoxyethanol

The products of the reaction in refluxing ethanol containing sodium ethoxide as catalyst proved to be a mixture of the mono-, di- and triphenyl derivatives. With increasing reaction times the yield of the monophenyl derivative decreased whilst the yield of the di- and tri-phenyl derivatives increased. Even after 24 h refluxing the yield of the tetraphenyl compound was very low (~1%). The rate of formation of the diphenyl derivative was found to be much higher in methanol than in ethanol. This phenomenon was also observed in the condensation of ammonia with pyromellitonitrile.

As we previously reported[2] the condensation of aniline with pyromellitonitrile in a 4:1 molar ratio in refluxing 2-methoxyethanol for one day gave a mixture of the di-, tri- and tetraphenyl derivatives. The reaction of aniline with pyromellitonitrile in a 2:1 molar ratio in refluxing 2-methoxyethanol

containing the sodium alkoxide catalyst afforded the results shown in *Figure 7*. Reaction for one hour at 125°C gave an approximately 30% yield of the triphenyl derivative. As expected, whilst the concentration of the mono-substituted product decreased the concentration of tetraphenyl compound increased with increasing reaction time.

Polymerization

From the results of the experiments on model compounds, we can reasonably conclude that under the appropriate conditions, suitable diamines e.g. 4,4'-diaminodiphenyl ether, *m-* or *p*-phenylene diamine, should react with pyromellitonitrile to give linear polymers of the type I. Condensation of pyromellitonitrile with 4,4'-diaminodiphenyl ether in equimolar proportions in refluxing methanol, ethanol or 2-methoxyethanol containing sodium alkoxide catalyst was rapid. Dependent on the solvent, reaction temperature and the concentration of the reactants, polymer was precipitated after 20 mins to 5 hours reaction. In all cases the precipitated polymer was insoluble in the usual organic solvents.

As might be predicted from the study of the reactions of model compounds, prolonged reaction in refluxing ethanol or 2-methoxyethanol resulted in the evolution of ammonia. Only trace amounts of ammonia were detected when methanol was employed as solvent. The evolution of ammonia may be regarded as indicative of either the formation of macrocyclic units, crosslinking reactions or hydrolysis of the exocyclic imino group to the keto derivative. Unless extreme care was taken to dry the solvent, the polymers prepared in refluxing 2-methoxyethanol generally exhibited some absorption in the infra-red spectra at $\nu = 1730\,\text{cm}^{-1}$ (C=O stretch). The polymers prepared at 80° or at lower temperatures were virtually devoid of absorption in this region of the infra-red spectrum normally associated with the carbonyl group.

The precipitation of polymer could be attributed to (1) the inherent limited solubility of high molecular weight linear polymers, (2) crosslinking or (3) the high concentration of hydrogen bonding in the polymer. For the polymers prepared in methanol the degree of crosslinking and macrocycle formation should be very slight, judged by the ammonia evolved in the reactions and from the results on the model compounds. However the polymers made in refluxing methanol were difficult to mould and showed the properties normally associated with low molecular weight products. It was considered most probable that precipitation under these conditions was largely due to the inherently low solubility of the product. The polymers prepared in 2-methoxyethanol however could be moulded to give strong specimens. It was therefore concluded that the polymer remained soluble to a higher molecular weight in 2-methoxyethanol than in methanol. In all cases once the polymers had precipitated from solution they could not be redissolved.

In order to determine the optimum conditions for the preparation of soluble polymers with as high molecular weight as possible we studied in detail the condensation of pyromellitonitrile with 4,4'-diaminodiphenyl ether in 2-methoxyethanol. In particular we examined the effect of reaction
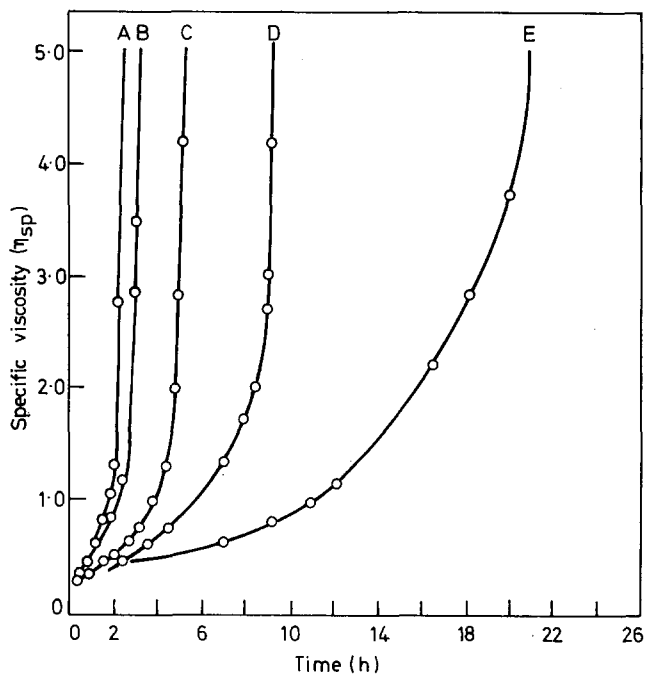
Figure 8 Condensation of pyromellitonitrile with 4,4'-diamino-diphenyl ether at various temperatures
Temperature: A, 85; B, 80; C, 70; D, 60; E, 50
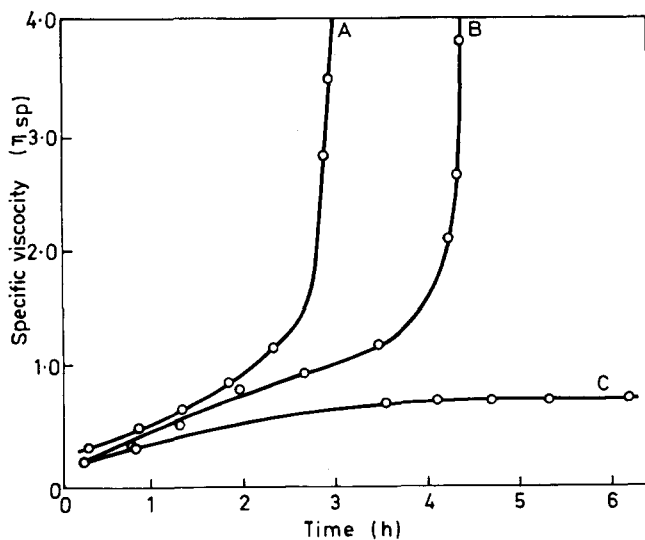
Figure 9 Condensation of pyromellitonitrile with 4,4'-diamino-diphenyl ether at 80°C
Conc. of diamine: A = 40·0 kg m^{-3}; B = 26·6 kg m^{-3}; C = 20·0 kg m^{-3}

542

temperature and the concentration of the reactants. The course of the reaction was conveniently followed by viscometry. The clear solution was placed in a viscometer tube in a constant temperature bath and the flow time periodically measured. The results obtained are given in *Figures 8, 9* and *10*. In no case was ammonia detected. Nevertheless as the reaction proceeded and the molecular weight increased, polymer precipitated from solution. Precipitation generally occurred at specific viscosities above 2. Because of the colour of the solution and the very fine particle size of the precipitated polymer the precise point of the limiting molecular weight of soluble polymer was difficult to observe.
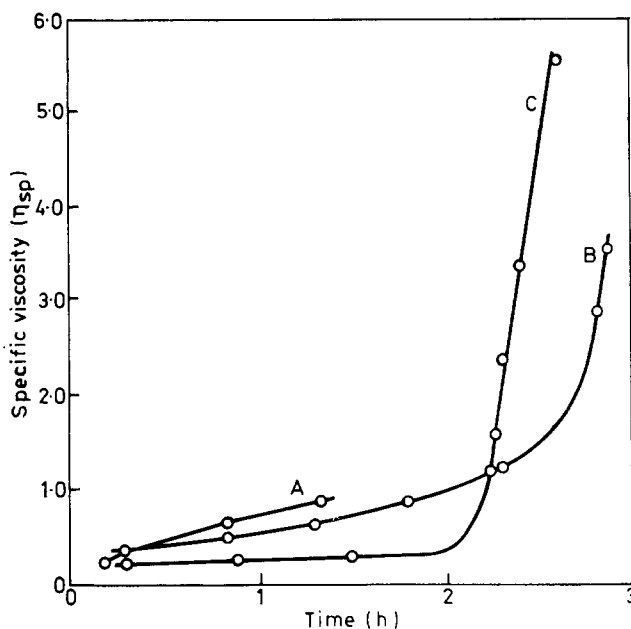
Figure 10 Condensation of pyromellitontrile with various diamines at 80°C
A, *para*-phenylene diamine; B, 4,4'-diaminodiphenyl ether; C, *meta*-phenylene diamene

As might be predicted the rate of polymerization increased with increasing temperature *Figure 8*, and increasing concentration *Figure 9*. In the temperature range 50–85°C, the rate of polymerization approximately doubled for every 10°C increase in the reaction temperature. Even at 50°C where the reaction was so slow as to require one day in order to obtain a marked increase in viscosity, the polymer still precipitated from solution. It was considered that whilst slight chain branching was feasible even under these mild conditions, precipitation of the polymer as the chain length increased (above $\eta_{sp} = 2$) was probably due to the inherent low solubility of the product in the solvents used.

A comparison of the rate of condensation of pyromellitonitrile with

meta and *para* phenylene diamine and 4,4'-diaminodiphenyl ether is shown in *Figure 10*. Some difficulty was encountered with *p*-phenylene diamine because of the low solubility of the condensation products in 2-methoxy-ethanol. After approximately 90 min reaction at 80°C, the polymers or oligomers precipitated from solution. In no case did we obtain a completely soluble polymer with very high molecular weight ($\eta_{sp} > 5$).

From the data available we conclude that the optimum conditions for preparing a high molecular weight linear polymer from pyromellitonitrile and 4,4'-diaminodiphenyl ether would be at temperatures of 65°C or less and for reaction times in excess of 8 h. Prolonged reaction times and reaction at higher temperatures would result in the formation of polymers containing branched chains and some macrocyclic units.

As with the macrocyclic polymers a reaction can be carried out simply by fusing the pyromellitonitrile and diamine together. Whilst the resultant product could be made to give approximately the correct analysis it was difficult to fabricate. The specimens obtained in this way had the appearance of highly crosslinked polymers.

Chemical Properties

In common with many other thermally stable polymers elemental analysis of these products presented some difficulty; the carbon analysis was frequently lower than that calculated. The possibility of combined solvent in the macrocyclic polymers was discussed elsewhere[2] and similar considerations might apply to the poly[benzo*bis*(aminoiminopyrrolenines)]. Prolonged drying of the polymers did not result in increased carbon analysis.
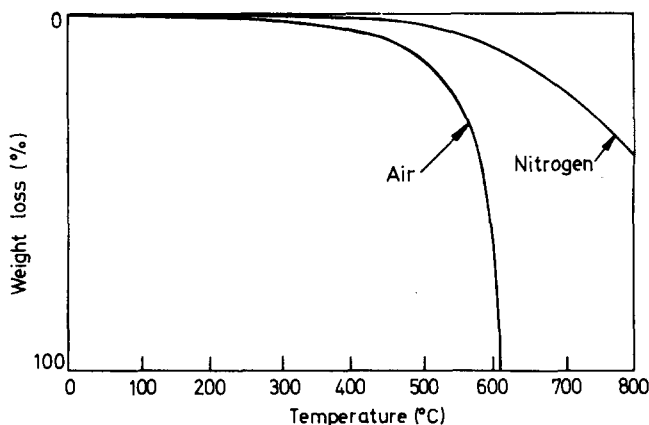
Figure 11 Thermal gravimetric analysis ($\Delta T = 15$°C/min)

The oxidative and thermal stabilities of the polymers were determined using a du Pont TGA equipment. The results of programmed heating at 15°C/min in air or nitrogen are given in *Figure 11*. In air a 10% loss in weight was recorded in the range 470 ± 20°C and in nitrogen 615 ± 20°C.

Although in some of their properties the linear polymers were similar to the

macrocyclic polymers, they were much less resistant to hydrolysis. Controlled hydrolysis of the exocyclic imino group afforded the polybenzo*bis*pyrrolenones. Further hydrolysis caused degradation of the polymer to give pyromellitic acid and diaminodiphenyl ether.

The linear polymers of this series contain reactive sites that can undergo further reactions giving rise to new polymers. The hydrolysis of the exocyclic imino group to the keto group has been mentioned. The condensation of the poly[benzo*bis*(aminoiminopyrrolenines)] with a further molecule of diamine affords the macrocyclic polymers. As it is possible to form mixed macrocyclic compounds from two different diamines[5] so it is possible to condense a dissimilar diamine with the linear polymer. Condensation of the linear polymer with aniline gave the phenyl derivatives. In the tautomeric form the exocyclic amino group will react with anhydrides to give amic acids, imides, etc. These reactions will be described elsewhere.

Electrical Properties

All of the polymers of this series were shown to be good electrical insulators in the temperature range 20–250°C[6]. In some instances at high temperatures pyrolysis of the sample occurred and the conductivity of the specimens decreased rapidly.

EXPERIMENTAL

Monomers

Phthalonitrile, aniline and the diamines were obtained from commercial sources and recrystallized or distilled before use. Pyromellitonitrile was prepared from pyromellitic dianhydride essentially by the method described by Lawton and McRitchie[7] with the modification suggested by Thurman[8].

Model Reactions

Phthalonitrile and 4,4′-diaminodiphenyl ether. A solution of phthalonitrile (3·84 g, 0·03 mol) and 4,4′-diaminodiphenyl ether (3·00 g, 0·015 mol) in methanol (75 ml) containing sodium methoxide (0·10 g) was refluxed with stirring in a stream of nitrogen. At intervals of 1, 3, 6 and 24 h an aliquot (10 ml) was removed. The solution was evaporated to dryness under reduced pressure. A sample of the resultant solid was injected into a preheated (300°C) source of an MS9 mass spectrometer. The results obtained are given in *Figure 3*. Similar experiments were also made in ethanol *Figure 4*.

Mass ratios (*m/e*) were obtained as follows:

		Found			
(a)	*m/e*	328·131	$C_{20}H_{16}N_4O$	(VI)	requires 328·132
(b)	*m/e*	456·168	$C_{28}H_{20}N_6O$	(VIII)	requires 456·170
(c)	*m/e*	622·212	$C_{40}H_{26}N_6O_2$	(IX)	requires 622·212

545

Pyromellitonitrile and aniline. A solution of pyromellitonitrile (3·56 g, 0·02 mol) and aniline (3·72 g, 0·04 mol) in methanol (100 ml) containing sodium methoxide (0·10 g) was refluxed with stirring in a stream of nitrogen. At intervals of 1, 3, 6 and 24 h an aliquot (20 ml) was removed. The solution was evaporated to dryness under reduced pressure. A sample of the resultant solid was injected into a preheated (300°C) source of an MS9 mass spectrometer. The results obtained are given in *Figure 5*. Similar experiments were also made in ethanol (*Figure 6*) and 2-methoxyethanol (*Figure 7*).

Mass ratios (m/e) were obtained as follows:

		Found			
(a)	m/e	242·079	$C_{12}H_{10}N_4O_2$		requires 242·080
(b)	m/e	271·086	$C_{16}H_9N_5$	(XI)	requires 271·086
(c)	m/e	364·144	$C_{22}H_{16}N_6$	(XIII)	requires 364·144
(d)	m/e	440·174	$C_{28}H_{20}N_6$	(XIV)	requires 440·175
(e)	m/e	516·207	$C_{34}H_{24}N_6$	(XV)	requires 516·206

The infra-red spectrum of the compound (b) showed no marked absorption in the 2240 cm^{-1} region of the spectrum associated with the nitrile group.

Polymerization reactions

Rate studies. A solution of pyromellitonitrile (1·78 g, 0·01 mol) and 4,4'-diaminodiphenyl ether (2·0 g, 0·01 mol) in 2-methoxyethanol (50 ml) containing sodium methoxyethanolate (0·05 g) was poured into a suspended level viscometer tube. The tube and contents were placed in a constant temperature bath at a predetermined temperature. After approximately 15 min the flow time was recorded. Thereafter the flow time was periodically measured. The results obtained at various temperatures are given in *Figure 8*. Similar experiments were made at different concentrations and with other diamines the results are given in *Figure 9* and *Figure 10*.

Preparation. A solution of pyromellitonitrile (7·12 g, 0·04 mol) and 4,4'-diaminodiphenyl ether (8·0 g, 0·04 mol) in methanol (150 ml) containing sodium methoxide (0·10 g) was refluxed with stirring for 16 h. The ammonia evolved (0·7 mequiv.) was swept out with a stream of nitrogen gas. The mixture was filtered hot and the insoluble polymer washed with methanol and dried at 65°C at 0·01 mmHg pressure. The product (14·8 g, 98%) was a dark red powder. Analysis: found C, 67·5; H, 4·0; N, 20·7%; $(C_{22}H_{14}N_6O)_n$ requires C, 69·9; H, 3·7; N, 22·2%; $(C_{22}H_{14}NOCH_3OH)_6$ requires C, 67·3$_n$ H, 4·4; N, 20·5%. The infra-red spectrum of the product was consistent with the proposed structure (I) and was devoid of the characteristic absorption in the 2240 cm^{-1} region normally associated with the nitrile (C≡N) group.

Division of Molecular Science,
National Physical Laboratory,
Teddington, Middlesex, UK

REFERENCES

1 Packham, D. I., Davies, J. D., and Paisley, H. M. *Polymer, Lond.* 1969, **10**, 923

2 Packham, D. I. and Rackley, F. A. *Chem. and Ind.* 1967, p 1254; *Polymer, Lond.* 1969, **10**, 559

3 Packham, D. I. and Rackley, F. A. *Chem. and Ind.* 1967, p 1566

4 Elvidge, J. A. and Linstead, R. P. *J. Chem. Soc.* 1952, p 5008

5 Packham, D. I. and Davies, J. D., unpublished work

6 Graham, J. and Packham, D. I. *Polymer, Lond.* 1969, **10**, 645

7 Lawton, E. A. and McRitchie, D. D. *J. Org. Chem.* 1958, **24**, 26

8 Thurman, J. C. *Chem. and Ind.* 1964, p 752

The acetone polymerization problem: effects of electrophilic reagents

C. L. GUIDRY and M. A. F. WALKER*

Various electrophilic reagents were used in attempts to polymerize acetone. The potential monomer was treated with Brønsted acids, Lewis acids and Friedel-Crafts systems at −78, 23 and 56°C for 24 h. No polymer formation was observed, the predominant reaction being the production of mesityl oxide, the amount of which was determined by gas chromatography.

THE POSSIBILITY of polymerizing acetone through the carbonyl group to produce a polyketal as illustrated in the following reaction

$$\begin{array}{ccc} \underset{\underset{CH_3}{|}}{\overset{\overset{CH_3}{|}}{C}}=O & \rightarrow & \left[-\underset{\underset{CH_3}{|}}{\overset{\overset{CH_3}{|}}{C}}-O-\right]_n \end{array}$$
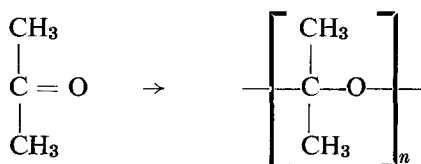
has intrigued investigators for about a decade. Several workers have actively pursued the problem since 1960[1−9] and have claimed to have produced a polymer of acetone[1−6]. Burnop[7], however, did not observe polymer formation in his attempts to reproduce the work of Okamura et al[2], Kawai[3] and Furukawa[4]. Some of Burnop's work was confirmed in our laboratory[8].

The investigations cited above used, mainly, irradiation techniques or anionic initiators. Some studies have been concerned with acetone in acidic media[7, 9−11, 15] but, with the exceptions of Burnop[7] and Kargin et al[9], were not carried out with the intent of producing polymers. Burnop did include AlCl$_3$ and TiCl$_4$ in his investigations – with no formation of polymer – and Kargin et al used ZnCl$_2$ at 200°C.

Since cationic systems have not been evaluated for polyacetone formation and since some investigators have mentioned polycondensed products[10] and polymerizing side reactions[11], it was thought advisable to determine the effect of acids in non-aqueous media upon acetone.

The present investigations extend the cationic systems to include three general types of electrophilic reagents: Brønsted acids, Lewis acids and Friedel-Crafts combinations. These were carried out at −78, 23 and 56°C. The products were analyzed by gas chromatography.

EXPERIMENTAL SECTION

Gas chromatography

For calibration, a Varian Aerograph Autoprep Model 705 with a hydrogen

---

flame detector was used with a 5 ft × 1/4 in 10% FFAP on 60/80 A/W Chromosorb W Column. The conditions were as follows: column temperature 150°C, detector and injector temperature 200°C, carrier gas flow rate (nitrogen) 300 ml/min, hydrogen flow rate 20 ml/min.

The peak areas were determined by an OTT Compensating Polar Planimeter. The component concentration used was mole percent (mol %).

Chemicals

The acetone used was 'Baker Analyzed' Reagent (99·5% pure, 0·35% water). Weissberger *et al*[12] state that acetone can be dried to about 0·05% water with Drierite and that if the water content is initially at 0·25% or less, Drierite can reduce the water content to 0·001% or less. The drying procedure was rigorous only to the extent of drying over Drierite for a minimum of 24 h.

The inorganic compounds and trifluoracetic acid were of high purity.

The organochlorides were dried over Drierite for a minimum of 24 h before using, the exception to this being acetyl chloride.

All liquids were deoxygenated by either allowing to sit in a nitrogen swept dry box for 24 h or by displacing the oxygen by a nitrogen stream.

All solids were deoxygenated by evacuating for 24 h and repressurizing with nitrogen.

The nitrogen used was 'pre-purified' and further dried by passing first through a Drierite column and then through Linde 3A molecular sieve.

Phorone, semiphorone and 2,2,6,6-tetramethyltetrahydro-γ-pyrone were prepared from triacetone dialcohol using the method of Connolly[13].

PROCEDURE

All glassware was heated at 105°C for 24 h before using.

The −78 and 23°C runs were carried out in test tubes. They were placed in the dry box after being taken from the oven and kept overnight under a flow of nitrogen. If all reagents were liquid, the tubes were stoppered with septa and cooled to −78°C under a flow of nitrogen. The acetone was added by means of a syringe. This was followed by the addition of the liquid acid. If one of the reagents was solid, then it was added in a dry box. The tube was stoppered and cooled to −78°C under nitrogen. The acetone was then added.

The 56°C runs were either carried out in beverage bottles or test tubes. In either case, the containers were treated as above. They were not, however, cooled to −78°C before addition except for the tubes which would contain BF_3 or BCl_3.

For those BF_3 and BCl_3 studies, test tubes were treated as above. After taking the stoppered tubes from the dry box, acetone was added, the tubes were cooled to −78°C and the gas was added by means of a syringe. The addition took 3–5 min. The contents were then kept at −78°C or allowed to warm up to 23°C or 56°C.

After the preparation given above, the containers were maintained at −78, 23, and 56°C for 24 h. When there was a possibility of excess pressure being developed, glass fibre sleeves were used to enclose the containers. At

the end of the reaction period, the Brønsted acids were neutralized with excess ammonia and the remainder with greater than stoichiometric amounts of water.

In each system, the Brønsted acid, Lewis acid and each Friedel-Crafts component (MCl_3 and RCl) was present in a concentration, relative to acetone, of 3 mol% except for two of the Friedel-Crafts studies. In the runs designated (*) in *Table 1*, the ethylene dichloride to acetone mole ratio was 1·95:1·00. In that designated (†), a reaction kettle was used. It was flamed out while being nitrogen swept. After cooling to room temperature, 91 ml of isopropyl chloride was added with a syringe. The vessel was further cooled to $-78°C$ and 4·9851 g of $AlCl_3$ was added. A slurry was produced. Acetone was added by means of a pressure equalization dropping funnel at the rate of 0·75 ml/min. The contents were maintained at $-78°C$ for a total of 24 h, maintaining a nitrogen sweep throughout.

Gas chromatographic analysis was performed after each reaction was completed, the percent total area determined for each component and the corresponding mol% read from the calibration curve. The data is presented in *Table 1*.

Table 1 Mole percent yields of condensation products: [acid] = [organochloride] = 3mol% relative to acetone

	Concentration (*mol %*)								
System	*Acetone*			*Mesityl oxide*			*Isomesityl oxide*		
	$-78°C$	23°C	56°C	$-78°C$	23°C	56°C	$-78°C$	23°C	56°C
HSO_3Cl	100	91	87	0	4	12	*t*	2	2
CF_3COOH	100	100	100	*t*	*t*	*t*	*t*	0	0
$H_2SO_4.0·289 SO_3$	100	94	86	*t*	5	20	0	0	0
98% H_2SO_4	100	95	90	0	3	13	0	0	0
100% H_2SO_4	100	95	93	0	3	9	0	0	0
$TiCl_4$	100	90	90	0	10	11	*t*	*t*	3
$SnCl_4$	100	91	92	0	14	10	0	*t*	0
BF_3 etherate	100	93	93	*t*	9	7	*t*	0	0
Tetraisopropyl titanate	100	100	96	*t*	*t*	3	*t*	0	0
$AlCl_3$	100	94	91	*t*	4	12	*t*	2	0
$FeCl_3$	100	94	91	0	6	11	0	0	0
$TiCl_3$	100	96	93	0	4	5	0	1	3
$SbCl_3$	100	100	100	0	0	0	0	0	0
BF_3 .	100	96	93	0	2	7	0	0	0
BCl_3	100	95	90	0	3	8	0	1	5
$AlCl_3$, ethylene dichloride	100	94	90	0	3	10	0	1	4
$AlCl_3$, CCl_4	100	94	91	0	3	5	0	1	3
$AlCl_3$, *t*-butyl chloride	100	95	90	0	2	12	0	1	3
$AlCl_3$, *i*-propyl chloride	100	95	92	0	2	9	0	2	2
$AlCl_3$, acetyl chloride	100	94	89	0	2	8	0	5	8
$AlCl_3$, ethylene dichloride*	100	95	91	0	2	8	0	1	4
$FeCl_3$, ethylene dichloride	100	94	93	0	5	9	0	0	0
$FeCl_3$, CCl_4	100	94	91	0	4	12	0	0	0
$AlCl_3$, *i*-propyl chloride†	100	—	—	0	—	—	0	—	—

t = trace, not measurable
* ethylene chloride to acetone mole ratio =1·95:1·00
† carried out in reaction kettle with acetone added dropwise to $AlCl_3$-isopropyl chloride slurry. Acetone volume = isopropyl chloride volume.

RESULTS AND DISCUSSION

No observable case of acetone polymerization was noted. With some of the AlCl$_3$ systems, there were a few instances of the formation of a gelatinous material at 23 and 56°C but the gel could be broken either by shaking or by the addition of water.

It was found that the predominant reaction was the production of mesityl oxide through an aldol-type condensation of acetone and the dehydration of the resultant diacetone alcohol.

The composition of the product mixtures obtained can be seen in *Table 1*. It will be noticed that one column is titled Isomesityl Oxide. This has been assumed rather than proven. Noller[14] states that mesityl oxide is an equilibrium mixture of two isomers, normally 91 % conjugated isomer (mesityl oxide) and 9 % non-conjugated isomer (isomesityl oxide) at 25°C. The retention time of the 'extra' peak was between mesityl oxide and diacetone alcohol and was different from those of acetone and the other standards. It was formed in over half of the systems studied, though normally in small amounts. This common factor for the various systems combined with the information above leads to the assumption that it is isomesityl oxide, but it is only an assumption. Its concentration was approximated from the percent total area.

With the exceptions of CF$_3$COOH, SbCl$_3$ and tetraisopropyl titanate, the agents generally were about equally effective in mesityl oxide production at any given temperature. No one type appears to be more or less effective than the others although the Friedel-Crafts systems at 23°C generally show a little less mesityl oxide than the Lewis and Brønsted acids. At 56°C, all appear to be roughly equal again.

Two show no activity at all. Acetone essentially remains unchanged at the three temperatures in the presence of CF$_3$COOH and SbCl$_3$. Tetraisopropyl titanate is inactive at -78°C and 23°C and only moderately active at 56°C. It is not surprising that CF$_3$COOH shows no activity since it is by far the weakest of the Brønsted acids used in the study (pK$_a$ = 0·2).

It is rather dangerous to attempt to assign relative strengths of Lewis acids, for it appears to depend on the base used for the study. Olah[15] reports a good many sequences found in the literature but SbCl$_3$ generally falls in the least active area. The data in *Table 1* support that premise. It is also said that tetraisopropyl titanate and other metal alkoxides of coordinatively unsaturated elements generally exhibit weak Lewis acid activity. This is also borne out by the present study.

The results of these investigations show that mesityl oxide production is favoured by increasing temperature. Except for traces of condensation products, acetone remains unchanged at -78°C while it progressively reacts to form mesityl oxide at 23°C and 56°C. This general finding, perhaps, favours the hypotheses of Kargin[16] and Vogl[17] that acetone can be polymerized only at or below its melting point (-95°C). Kargin[16], however, did carry out studies below the melting point with TiCl$_3$, ZnCl$_2$, and BeCl$_2$, as well as with magnesium. There was no polymer formation except for that reported in the magnesium system.

Mesityl oxide was the compound used to discuss the influence of the various electrophilic reagents but it was not the only product formed. The assumed

isomesityl oxide has already been discussed and was the only other compound formed in any measurable amount but there were traces of diacetone alcohol and phorone formed in some of the media, particularly the Brønsted acids. There was no detectable formation of 2,2,6,6-tetramethyltetrahydro-γ-pyrone, semiphorone or triacetone dialcohol, although for phorone to have been formed, one or both of the latter two must have been formed at some stage.

Chemistry Department,
Sam Houston State University,
Huntsville, Texas, 77340, USA

REFERENCES

1 Kargin, V. A., Kabanov, V. A., Zubov, V. P. and Papisov, I. M. *Doklady Akad. Nauk SSSR* 1960, **134**, 1098

2 Okamura, S., Hayashi, K. and Mori, S. *Isotopes and Radiation (Japan)* 1961, **4**, 70

3 Kawai, W. *Bull. Chem. Soc. Japan* 1962, **35**, 516; *Jap. Pat.* No. 68 16 157; *Jap. Pat.* No. 68 16 158

4 Furukawa, J. and Saegusa, T., *Makromol. Chem.* 1962, **52**, 230; with Ota, S., *Jap. Pat.* No. 20 978 (1963)

5 Wakasa, R. and Ishida, S. *Jap. Pat.* No. 18 962 (1964)

6 Miyama, H. and Kamachi, M. *J. Polym. Sci. (B)* 1965, **3**, 241

7 Burnop, V. C. E. *Polymer, Lond.* 1965, **6**, 411

8 Steward, C. W. 'The Reactions of Acetone in Anionic System', Thesis, Sam Houston State College, May, 1967

9 Kargin, V. A., Kabanov, V. A. and Zubov, V. P. *Doklady Akad. Nauk, SSSR* 1961, **140**, 122

10 Olah, G. A. (ed.), 'Friedel-Crafts and Related Reactions', Interscience, New York, 1963, pp 573, 707, 709

11 Greenwood, N. N. and Perkins, P. G. *J. Chem. Soc.* 1960, p 356

12 Weissberger, A., Proskauer, E. S., Riddick, J. A. and Toops, E. E., 'Organic Solvents', Second Edition, Interscience, New York 1955, p 382

13 Connolly, E. E. *J. Chem. Soc.*, 1944, p 338

14 Noller, C. R., 'Chemistry of Organic Compounds', W. B. Saunders, Philadelphia, 1965, p. 389

15 Olah, G.A(ed.), 'Friedel-Crafts and Related Reactions', Interscience, New York, 1963, pp 314, 853–861

16 Kargin, V. A., Kabanov, V. A. and Papisov, I. M. *J. Polym Sci., (C)* 1965, **4**, 767

17 Vogl, O. and Bryant, M. D. *Rev. Gen. Caoutchouc Plast. (Ed. Plast.)* 1965, **2**, 224

Isotactic, syndiotactic and atactic poly(2-vinylpyridine 1-oxide): relation between viscosity in aqueous solution and pH

P. F. HOLT and B. TAMAMI

The viscosity number/pH curves of aqueous solutions of mainly syndiotactic, mainly isotactic and atactic poly(2-vinylpyridine 1-oxide) do not resemble that for poly(4-vinylpyridine 1-oxide). They show minimal viscosity between pH 4 and 8 and outside this range the viscosity increases rapidly. There is probably bonding between protons of the polyvinyl chain and the N-oxide groups producing a close packed structure, this bonding being inhibited at higher concentrations of protons or hydroxyl. The curve relevant to the syndiotactic polymer shows two minima, one at either side of pH 7, which may be due to the polymer taking up two conformations, one with the N-oxide groups stacked at one side of the polymer chain, the other in which they alternate on either side. The curve relevant to the atactic polymer is approximately a composite curve derived from those of the stereospecific forms but there is also a sharp break at about pH 3.5–4 which is present in the curves of neither stereospecific form.

POLY(2-VINYLPYRIDINE 1-OXIDE) inhibits the fibrogenesis normally caused by quartz dust in the lungs of animals. The isotactic and syndiotactic forms do not behave in an identical manner[1].

Holt and Nasrallah[2] examined the change in viscosity number with pH of poly(2-vinylpyridine 1-oxide) (I) and poly(4-vinylpyridine 1-oxide) (II) as atactic polymers. They found little change in the viscosity number of the polymer (I) between pH 4 and 8.5 but there was a considerable increase at low pH and a slight decrease at high pH values. The viscosity number/pH curve for polymer (II) was very different; up to pH 3 the viscosity was constant, it increased rapidly from pH 3 to pH 9 and above pH 9 there was a slight decrease. Holt and Nasrallah deduced that bonding between a proton on the polyvinyl chain and oxygen of of the NO group in polymer (I) over the pH range 4–8.5 implied a tightly packed structure of minimal length. They confirmed this type of bonding by studies of electronic spectra and Holt and Lindsay[3] also deduced its existence from n.m.r. spectra.

I   II

553
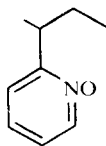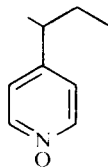
Holt and Lindsay[3] prepared the polymer (I) by a method that gave mainly the isotactic and one that gave mainly the syndiotactic type; some physical observations were made on these products. We have measured the viscosity of these two polymers, of atactic polymer (I) and of atactic polymer (II) at smaller intervals of pH than were previously used, and we find that the curves relating to the variation in viscosity of the polymer (I) are more complex than were those obtained by Holt and Nasrallah; there are considerable changes in viscosity with small variations in pH at certain pH values. The curve relevant to the atactic polymer (II) obtained by us shows none of the fine structure found in that relating to polymer (I).

To assist in the interpretation of the viscosity curves, titration curves for the two polymers have been obtained.

<div align="center">RESULTS</div>

Titration curves

Atactic polymer (II). Between pH 3 and 10 the pH changes markedly with small additions of acid (*Figure 1*). Below pH 3 the substance acts as a base and above pH 10 as an acid.
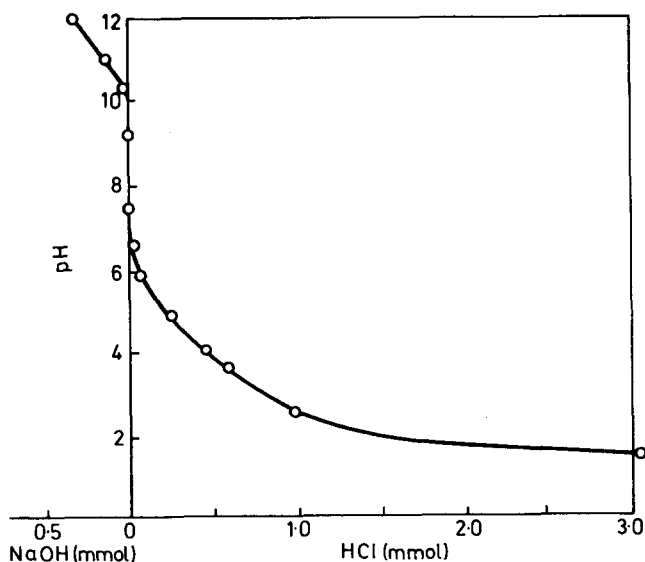
Figure 1 Titration curve of atactic poly(4-vinylpyridine 1-oxide)

Atactic polymer (I). Between pH 5 and 10 the pH changes markedly with small additions of acid or base (*Figure 2*). Below this range polymer (I) acts as a base and above it as an acid. However, between pH 3 and 6 the curve is much flatter than is that portion of the curve relevant to polymer (II).

<div align="center">554</div>
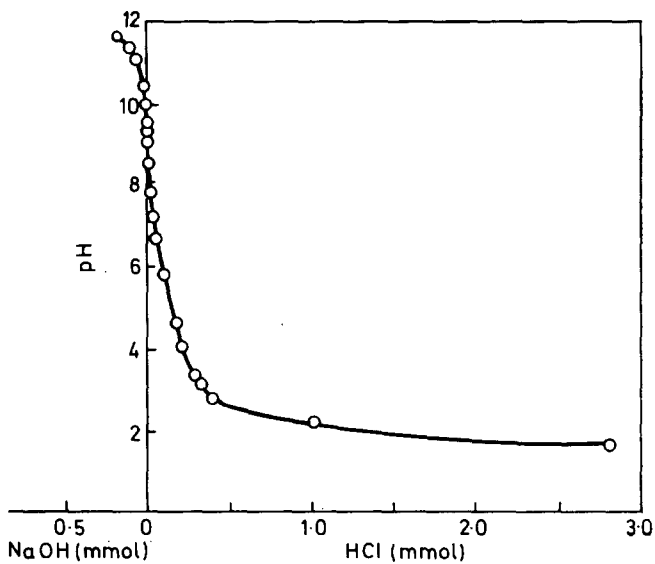
Figure 2 Titration curve of atactic poly(2-vinylpyridine 1-oxide)
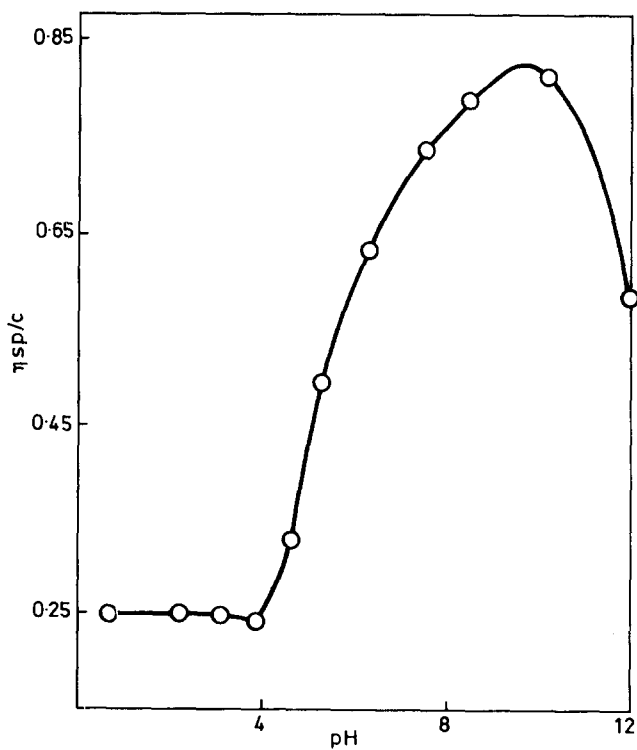
Figure 3 Viscosity/pH curve of atactic poly(4-vinylpyridine 1-oxide)

555

Viscosity/pH curves

Poly(4-vinylpyridine 1-oxide) (*II*). The form of the viscosity/pH curve (*Figure 3*) was similar to that described by Holt and Nasrallah; the viscosity varied very little with pH below pH 4 but above that pH it rose to a maximum at about pH 9. Holt and Nasrallah found the maximum at a somewhat lower pH. At higher pH values the viscosity was reduced.
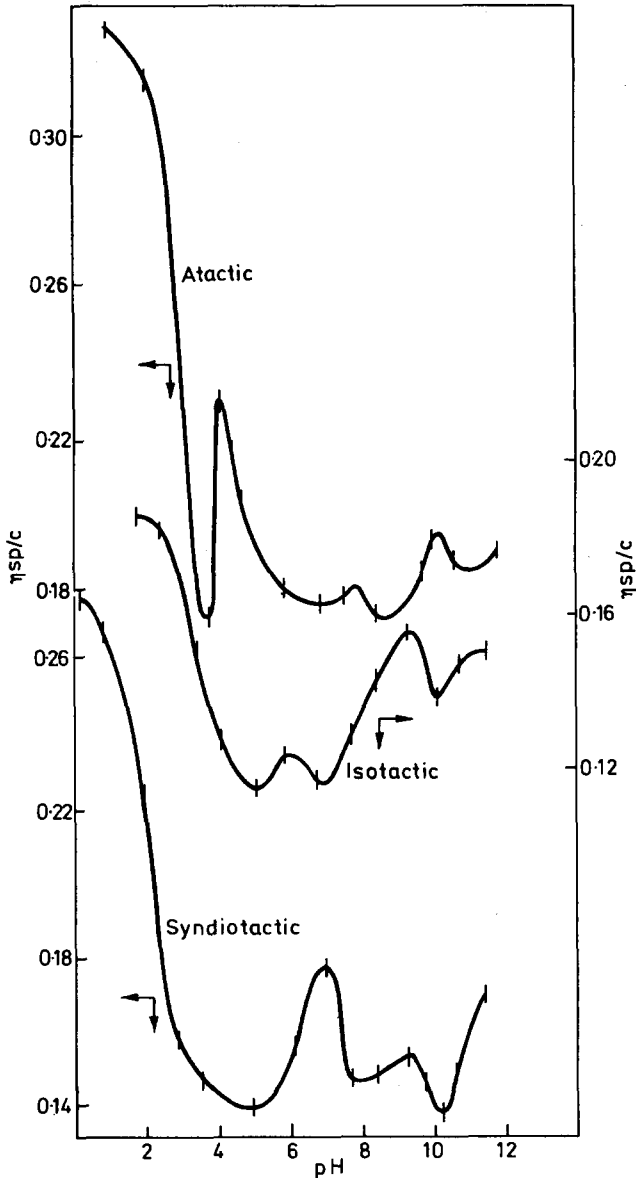
Figure 4 Viscosity curves of atactic, mainly syndiotactic and mainly isotactic poly(2-vinylpyridine 1-oxide)

Mainly isotactic poly(2-vinylpyridine 1-oxide). The viscosity is at a minimum at about pH 5 (*Figure 4*). It rises very steeply as the pH is reduced below this value. Above pH 7 the viscosity rises steeply to a maximum about pH 9, falls between pH 9 and 10 then rises again. A slight increase in viscosity to a peak at pH 6 is probably due to syndiotactic polymer (I) which is present and this may also explain the dip in the curve at pH 10.

Mainly syndiotactic poly(2-vinylpyridine 1-oxide). Below pH 5 the variation of viscosity with pH does not differ significantly from that observed for the isotactic polymer (*Figure 4*); both curves show a minimum near pH 5. Above pH 7 the viscosity of the syndiotactic polymer falls. Probably because of the effect of the isotactic moiety, there is no sharp minimum but it would appear probable that, if the polymer were completely syndiotactic, the minimum would be at about pH 9.
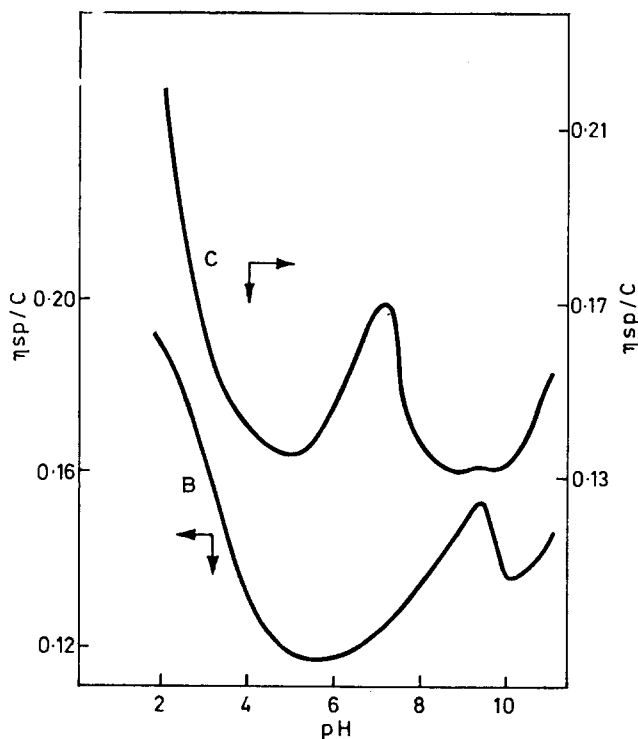
Figure 5 Viscosity curves of syndiotactic and isotactic poly(2-vinyl-pyridine 1-oxide) derived from values in *Figure 4*, assuming that each stereospecific polymer was contaminated by 10% of the other

If it is assumed that each of the partially stereospecific polymers used contained 90% of the major form and 10% of the other stereospecific form, corrected curves may be drawn (*Figure 5*). That for the syndiotactic polymer shows two definite minima at about pH 5 and 9.

557

Atactic poly(2-vinylpyridine 1-oxide). The viscosity/pH curve (*Figure 4*) shows features suggesting those in the curves relevant to the syndiotactic and isotactic polymers but they are much less definite and, in the main, the curve approximates to that published by Holt and Nasrallah[2]. There is, however, a slight rise in viscosity above pH 9 and an additional pronounced minimum at pH 3·5–4 from which the curve rises very steeply. The minimum has been confirmed by repeated measurements.

COMMENT

The pH-titration curve indicates that the atactic polymer (I) acts as a base below about pH 5 (structure III) and as an acid above about pH 10 (probably structure IV). Similarly, polymer (II) is amphoteric (structures V and probably VI). The two titration curves differ between pH 3 and 6 in that the curve relevant to polymer (I) is less steep; this may be due to the bonding shown[1,2] to exist between NO of the ring and CH of the polymer chain that must be broken to produce the structures III and IV. Holt and Nasrallah[2]
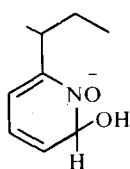
IV
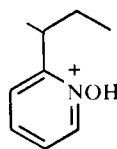
III
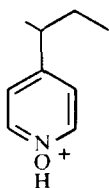
V
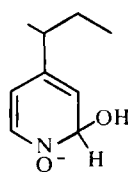
VI

and Holt and Lindsay[3] showed that the polymers do not act as polyelectrolytes at pH values near 7, since the plot of η_{sp}/c against concentration is linear, and this conforms to the titration curve.

The shape of the viscosity curve given by polymer (II) (*Figure 3*) can be explained if, as previously assumed[2], polymer chains are associated through water molecules bonded to N-oxide groups, maximally at pH values near 9. With the polyvinyl chain attached to the 4-position of the pyridine, the N-oxide groups are exposed and free to bond in this manner; steric factors would hinder the formation of such bonds when the polyvinyl chain is in the 2-position. At higher or lower pH values these bonds are broken. The titration curve shows that oxygen in polymer (II) is protonated below about

558

pH 4. The horizontal part of the viscosity curve below pH 4 probably represents the viscosity of the unassociated polymer.

The curves for the atactic, isotactic and syndiotactic forms of polymer (I) all show the same general feature; over a pH range of about 4 to 9 the viscosity is low but it increases steeply as the pH is reduced and less steeply as it is increased outside this range. The assumption that close packing of the pyridine rings due to bonding between chain hydrogen and N-oxide reduces the length of the polymer molecules between pH 4 and 9 would account for the low viscosity.

The viscosity curve of the mainly syndiotactic polymer (I) shows a definite subsidiary peak at about pH 7. This must be interpreted as meaning that the close-packed structure at pH 5 is reorientated through an expanded form to give another contracted form at pH 8–10. If intramolecular bonding of a chain proton with oxygen is assumed, models show that the syndiotactic polymer has a planar zig-zag conformation. Two such models can be made; in one the oxygen atoms are staggered on either side of the chain, in the other they are all on the same side. Perhaps the form in which oxygens are stacked on one side of the chain occurs below pH 7 where protons might be shared by the negative oxygens. It is noticeable that the minima observed on either side of neutrality have about the same value, supporting the view that at pH 5 and pH 9 pyridine rings are closely packed. The irregularities in the curve relevant to the isotactic form are less definite and it is impossible to say whether they are entirely due to the small amount of syndiotactic and atactic polymer also present. The curve in *Figure 4* would suggest, however, that a subsidiary peak occurs at pH 9–10 in the curve relating to the isotactic polymer.

It might be expected that the curve relating to the atactic polymer would approximately resemble a composite curve drawn from those of the other two forms and this is largely true. There is, however, a remarkable break at pH 3·5–4 where the viscosity is suddenly reduced. Since this feature is absent in the curves for the stereospecific polymers, it seems probable that it is due to an adjustment of the packing in the chain at the positions where a syndiotactic changes to an isotactic sequence.

EXPERIMENTAL

The mainly syndiotactic and isotactic poly(2-vinylpyridine 1-oxides) were prepared by Dr H. Lindsay by methods previously described[3]. Oxidation of the polymers was effected under conditions which give substantially complete conversion to N-oxide (Gregson and Holt[4]).

Viscosities of 0·4% polymer solutions were measured at 25 $\pm$ 0·05°C with suspended-level dilution viscometers; flow time for water approximately 137·2, 166·1 and 167·2 s used for the isotactic, atactic and syndiotactic polymers respectively. Solutions were filtered into the viscometers and were allowed to stand for 20 min before measurements were made. Each recorded viscosity represents the mean of two determinations differing by not more than 0·2 s.

The errors in determination of flow time could be $\pm$ 0·1 s This error as

reflected in viscosity values is shown as error bars in *Figure 4* but it is too small to be shown in *Figure 3*.

The pH of solutions was adjusted by adding hydrochloric acid or sodium hydroxide and the pH values were recorded by a Metrohm E 350 meter using a glass electrode. The pH was checked before and after each viscosity measurement; where a slight variation occurred the second reading was used. The error in pH determination could be ± 0.05 – too small to be shown in the curve.

The titration curves were constructed from values obtained by titrating 50 ml of a 0.03 M aqueous solution of polymer.

Department of Chemistry,
University of Reading,
Berkshire, England

REFERENCES

1 Holt, P. F., Lindsay, H. and Beck, E. G. *Brit. J. Pharmacol.* 1970, **38**, 192
2 Holt, P. F. and Nasrallah, E. *J. Chem. Soc.*, 1968, p. 233
3 Holt, P. F. and Lindsay, H. *J. Chem. Soc.*, 1969, p. 1012
4 Gregson, L. and Holt, P. F. *Makromol. Chem.* 1969, **128**, 193

560

A diaphragm test for sheet plastics

J. T. KIRKLAND, J. L. DUNCAN and R. N. HAWARD*

Circular test pieces of plastic sheet are clamped around the edge and deformed by controlled pressure acting on one side. The true stress and strain under biaxial tension in the central region of the specimen is plotted autographically using an extensometer which measures curvature and extension in the specimen and an analogue data processing unit. The deformation rate is controlled by closed loop control of the pressurizing system. Stress/strain curves under biaxial tension are compared with simple tension test results for cellulose nitrate and ABS sheet. Approximate correlation is obtained using criteria of true stress or maximum shear stress and maximum tensile strain. The advantages of this type of test compared with the uniaxial tensile test are discussed and it is shown that material which is subject to drawing in the tensile test may be tested at a controlled and measurable strain-rate in the diaphragm test. The theoretical implications of the stress/strain and stress/strain-rate characteristics under biaxial tension are discussed.

INTRODUCTION

THIS PAPER describes a test for sheet material which has not been applied previously to plastics. The test can be used to obtain the stress strain relationship for plastic sheet deformed at a constant strain-rate.

In this test, a flat circular test piece is clamped tightly around the edge and formed into a dome by the application of hydrostatic pressure on one side. In the centre of the specimen there is a region where the shape is very nearly spherical and the material deforms under a state of approximately uniform biaxial tension, i.e. the sheet is stretched equally in all directions[1, 2]. In this region stress and strain can be determined from measurements of pressure, extension and radius of curvature. Equipment is described which enables these measurements to be taken continuously during the test and also permits the test to be performed in such a way that the logarithmic strain-rate in the gauge area remains constant.

In the bulge test, the stress and strain system on a material element is quite different from that in the tensile test as is shown by the diagrams in *Figure 1*. For the purpose of this diagram we adopt the convention that the principal direction 1 is the direction (where appropriate) in which the sheet was extruded, 2 is the transverse direction and 3 the through-thickness direction (normal to the sheet surface). The element in *Figure 1a* shows the stress system in a tensile test piece whose axis was originally aligned with the extrusion direction. *Figure 1b* shows the principal stresses on an element in the gauge area of the biaxial stress or hydrostatic bulge test. The three-dimensional Mohr's circle of stress for each element is shown in *Figure 1c* and *d* and, in each case, one of the circles—a different one—is vanishingly small. The orientation of planes of maximum shear stress are shown in

Tensile test

Biaxial test
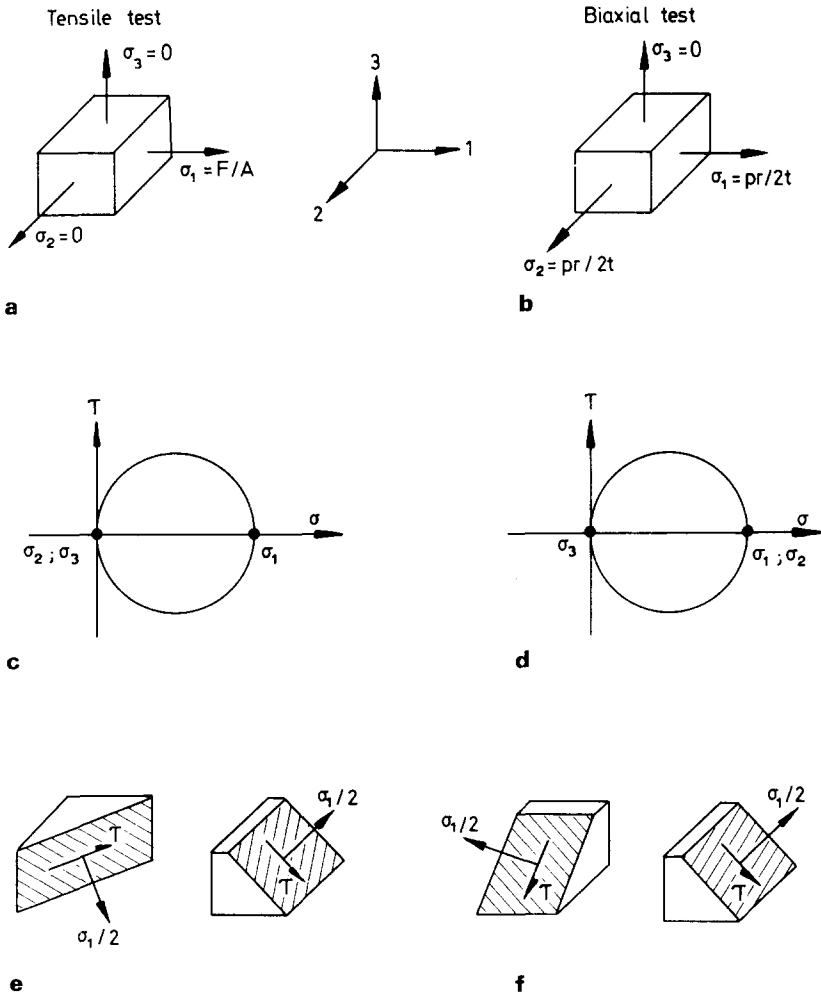
Figure 1 Comparison of stress states on an element of the sheet subjected to uniaxial and biaxial loading; (a, b) stresses on the element with the axis 3 normal to the surface; (c, d) Mohr's circle of stress; (c, f) stresses on planes of maximum shear stress

Figure 1c and d and in all cases the maximum shear stress is $\tau = \frac{1}{2}\sigma_1$ and the normal stress on a plane of maximum shear is $\frac{1}{2}\sigma_1$.

The hydrostatic bulge test is being increasingly used in testing sheet metal for a number of reasons; the principal ones are

(1) the stress/strain relation can be measured up to much larger values of total strain than in the simple tension test[2, 3]

(2) test piece preparation is simple and as measurements are made only in the middle of the test piece the results are not influenced by edge preparation or clamping

(3) in anisotropic materials, the stress/strain relation is more representative of behaviour in stretching type operations[4].

563

In testing metals in simple tension useful information can only be obtained up to the point where necking or tensile instability occurs. The limiting strain is directly related to the strain hardening characteristics of the metal and varies from a few per cent extension to about 50% at the most. In the bulge testing of metals, localised instability of this kind does not occur and necking, when it does take place is of such a diffuse nature that it extends beyond the gauge area and is imperceptible to the measuring equipment. Valid stress/strain information can be obtained right up to the point of rupture.

In tensile testing of plastics, instability is less easily analysed because of the time-dependent behaviour of the material, but necking or cold drawing is frequently observed in certain plastics[5–9]. In these materials the stress/strain relation at a given deformation rate cannot be determined by the tension test as the distribution of strain in the gauge area is not uniform. It is possible that controlled strain-rate testing of such materials could be performed using the bulge test method and in all of the bulge tests described in this paper, controlled straining right up to rupture was obtained even in a particular ABS polymer which did in certain cases neck in simple tension tests.

The true stress/strain curve for sheet metal can be obtained from the bulge test using a commercially available testing machine. This consists of a die which clamps the specimen around the edge, a hand pump to supply hydrostatic pressure to bulge the specimen, an extensometer to measure extension and curvature in the central region and a pressure gauge[10]. The test can be performed incrementally as time-dependant effects are negligible in most metals at room temperature.

In using the bulge test to determine the stress/strain relationship for plastics it is, however, necessary to control the rate of deformation. A special bulge testing machine was used which incorporates an analogue data processing unit to permit closed loop control of the loading system and autographic recording of the true stress/strain diagram. The testing machine used was built specifically for testing metals and even after some modification was not fully adapted mechanically to the testing of plastics. The object of the work was, however, to demonstrate the feasibility of testing sheet plastics by this type of test and to indicate the kind of results which would be obtained. The materials tested were plasticised cellulose nitrate and ABS sheet; these were tested at various different strain-rates and the results presented in the form of true stress/strain diagrams.

The interpretation of the test results is difficult because the relatively simple theoretical treatment of deformation of metals under combined loading is not applicable to plastics. The deformation of rubber like materials in biaxial stretching has been investigated by Flint and Naunton[11] and subsequently by Treloar[12], who has also reviewed the whole field[13]. Hopkins, et al[14] have used a similar method in testing polyethylene and a more recent paper by Hopkins and Wentz[15] emphasises some of the problems encountered when trying to compare uniaxial and biaxial tests. The implications of both Treloar's work and that of Hopkins and co-workers will be discussed later. The experimental results obtained here are compared in terms of the maximum principal stresses and strains and an indication given of the effect of strain rate in both tests and of its variation with cross-head speed in the tensile test.

THEORY OF THE BULGE TEST

When the flat circular test-piece is clamped at the edge and bulged by hydro-static pressure, a small area near the centre of the specimen, *Figure 2a* assumes the shape of part of a thin spherical shell, *Figure 2b*.

If two extensometer probes rest lightly on the sheet so as to describe the diameter D_0 of a circle at the centre of the test-piece, then after deformation the diameter of the circle becomes D, *Figure 2b* and the natural or logarithmic
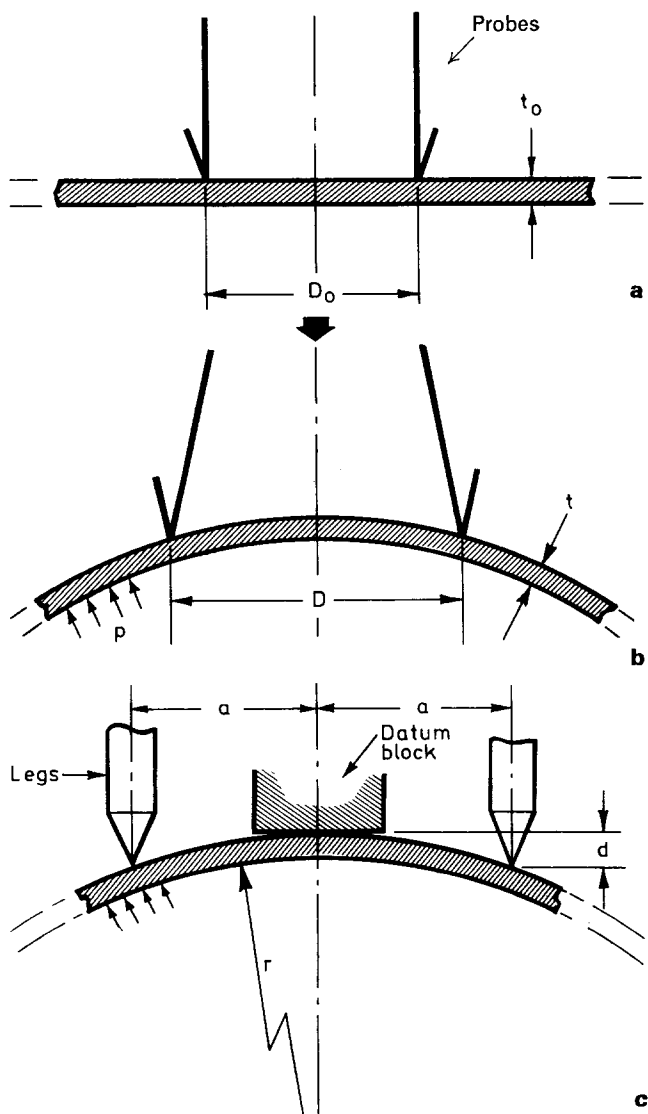
Figure 2 Schematic diagram showing (a) the undeformed sheet, (b) extension measurement and (c) curvature measurement on the bulged sheet

565

strain around the circumference of this circle is

$$\Sigma_\theta = \ln \frac{\Pi D}{\Pi D_0} = \ln \frac{D}{D_0} \tag{1}$$

If we assume a state of uniform biaxial straining at the pole, i.e. the membrane, Σ_m, is the same in all directions then

$$\Sigma_m = \Sigma_\theta = \ln \frac{D}{D_0} \tag{2}$$

Assuming that deformation occurs without change in volume the sum of the principal strains is zero, i.e.

$$\Sigma_t + \Sigma_m + \Sigma_m = 0 \tag{3}$$

where Σ_t is the thickness strain defined as,

$$\Sigma_t = \ln \frac{t}{t_0} \tag{4}$$

Combining equations (2), (3) and (4) we obtain that the initial to current thickness ratio is

$$\frac{t_0}{t} = \left(\frac{D}{D_0}\right)^2 \tag{5}$$

The radius of curvature at the pole is given by the spherometer shown in *Figure 2c*. In the bulge test equipment, this spherometer is part of the extensometer arrangement; the spherometer legs shown in *Figure 2c* are in a plane perpendicular to the extension measuring probes shown in *Figure 2b*. The radius of curvature is

$$r = (a^2 + d^2)/2d \tag{6}$$

where d is the spherometer reading.

The membrane stress is obtained using the relation for the stress in a thin spherical shell subjected to internal pressure, i.e.

$$\sigma_m = \frac{pr}{2t} = \frac{pr}{2t_0} \times \frac{t_0}{t} \tag{7}$$

where p is the hydrostatic pressure.

The membrane stress and strain at any point in the test are thus determined from measurements of p, D and d.

Recent work[16-18] has shown that the yield stress of plastics is affected by the hydrostatic stress component and may be represented by a Coulomb relationship

$$S_0 = |\tau| - \mu \sigma_n \tag{8}$$

where S_0 = critical shear stress in the plane of shear
τ = critical shear stress when $\sigma_n = 0$
σ_n = nominal tensile stress on the plane of shear

According to this concept the yield stress under biaxial tension would be the same as in simple tension. As will be seen later this proves to be approximately in accordance with our results which therefore in this case support the Coulomb relationship, though not in any critical sense.
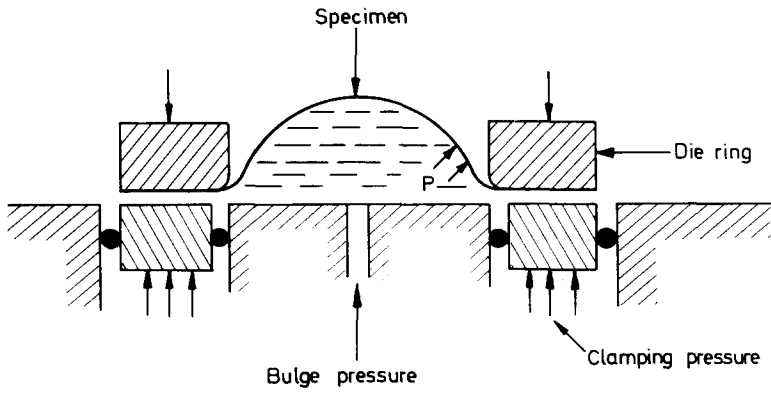
Figure 3 Schematic diagram of the clamping and bulging arrangement
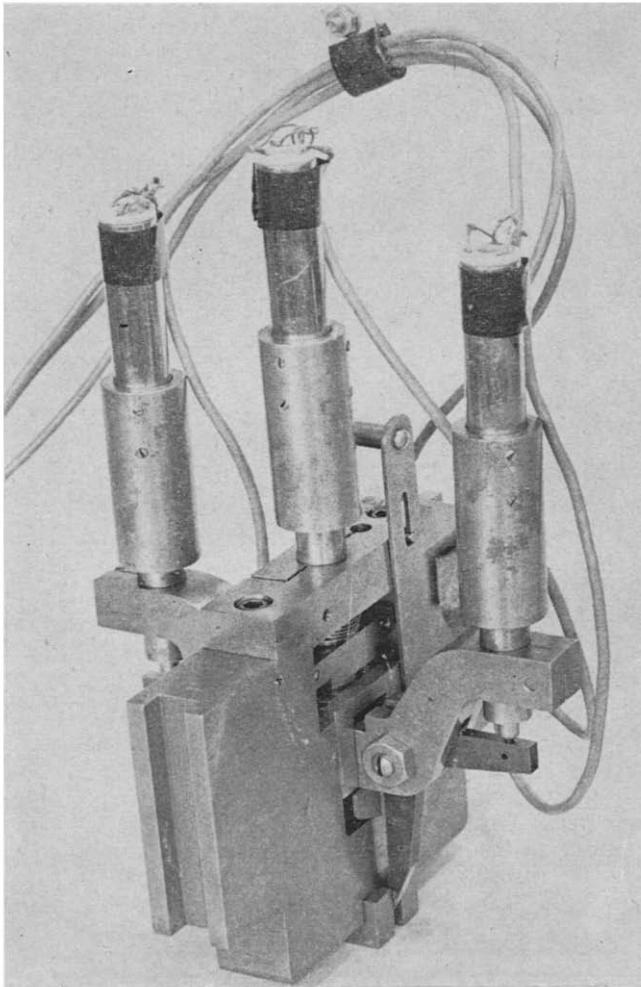
Figure 4 Photograph of the bulge test extensometer

567

EXPERIMENTAL EQUIPMENT

The sheet specimen is clamped rigidly using an annular die ring having a $4\frac{1}{2}$in* diam aperture as shown diagrammatically in *Figure 3*. The extensometer unit shown in *Figure 4* rests on the surface and rises vertically with the specimen as it deforms. Three transducers are employed to monitor the displacement of the extension probes and the spherometer legs. The transducer outputs are converted to signals proportional to radius of curvature and strain in the analogue computer unit shown diagrammatically in *Figure 5*.
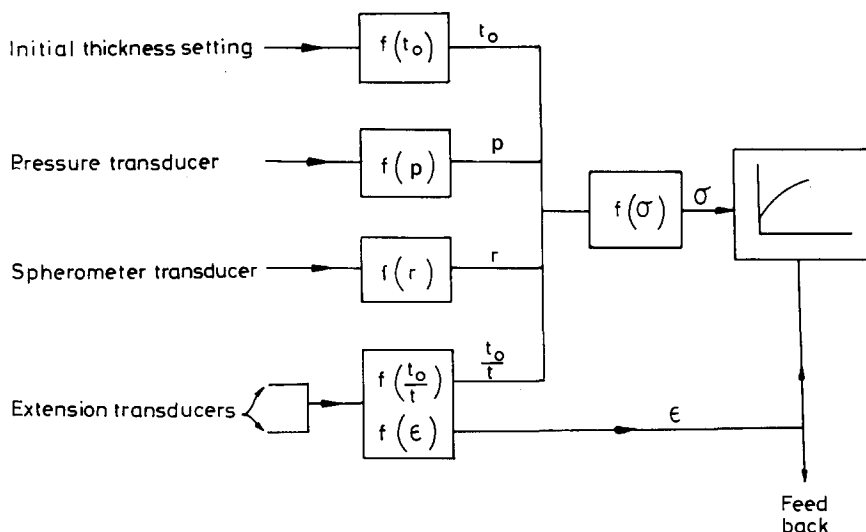
Figure 5 Block diagram of the analogue data processing unit

This unit computes these signals together with one from a pressure transducer to give outputs proportional to true membrane stress and the logarithmic thickness strain which are recorded using an X-Y plotter. The extensometer and data processing unit are described fully in Ref. 19.

The oil required to bulge the specimen is supplied from a servo-controlled intensifier unit. The feed-back signal is the computed strain signal from the analogue unit, *Figure 5*. This signal is compared with a pre-set ramp signal and the displacement of oil to the bulging diaphragm controlled by the resulting error signal. The control system of the machine is described in Ref. 20. In order to extend the range of the machine to strain-rates lower than those employed in testing metals, the command signal generator was modified. A synchronous motor and a multi-ratio gear box were used to drive a helical potentiometer. The lowest strain-rate obtainable with this system was $7.0 \times 10^{-5} s^{-1}$.

The pressure measurement system was also modified by using a much lower range pressure transducer than that used for metals.

---

*1 in $= 25.4$ mm

An overall view of the testing machine is given in *Figure 6*. This machine was designed to test metals using bulging pressures up to $6000\,lbf/in^2$* and strain-rates in the region of $0 \cdot 15\,s^{-1}$. A machine specially designed for plastics with a maximum bulge pressure of a few hundred lbf/in^2 would obviously look rather different.
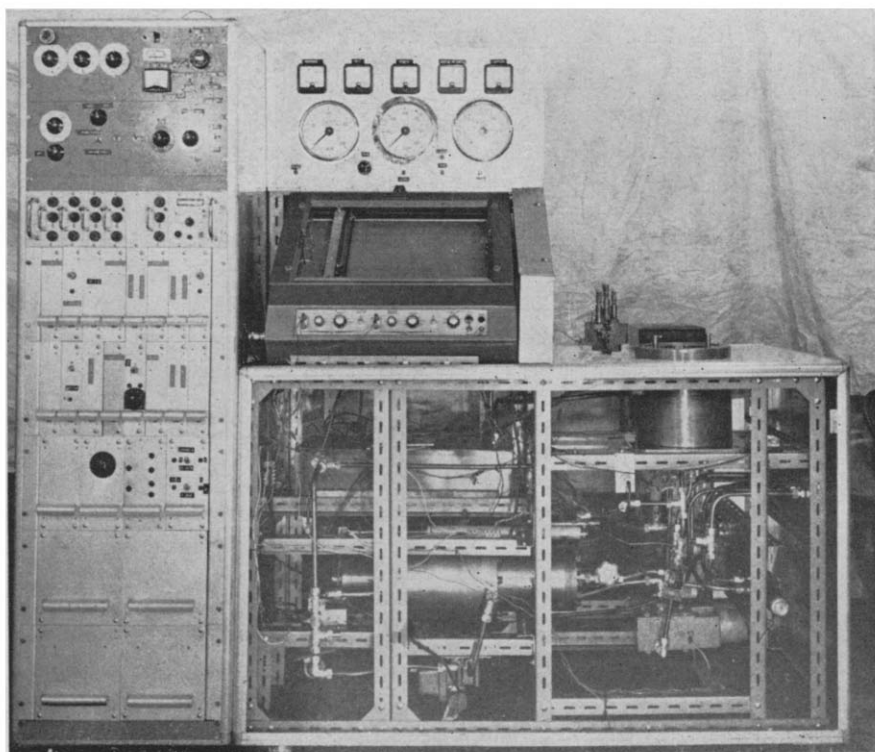
Figure 6 The autographic bulge testing machine

TEST PROCEDURE

Octagonal test pieces about $6\frac{1}{2}$ in across the flats were cut from the sheet. These were stored for a few days in a controlled atmosphere at 22°C and 50% relative humidity and then sealed between two sheets of thin polythene sheet. These precautions ensured that the water content of the sheet was constant and that the sheet was not affected by the oil used for testing.

To perform a test, the desired strain-rate and the initial thickness were set on the machine and the specimen placed in the die and clamped. The top sheet of polythene was torn off and the extensometer placed on the specimen so that the spherometer legs and extension probes rested on the surface of the specimen. The test was then started and the specimen bulged under con-

*$1\,lbf/in^2 = 6 \cdot 895\,kN/m^2$

trolled conditions up to rupture and the stress/strain curve recorded auto-graphically. The resistance offered by the polythene sheet was shown to be negligible.

The tests were not performed under thermostatically controlled temperature conditions, but measurements of both the bulging oil and air temperature near the test piece showed that throughout the tests the temperature was $20 \cdot 5 \pm 0 \cdot 5$°C.

Three or four tests were performed at each strain-rate and for cellulose nitrate sheet, tests were performed at six different strain-rates between $7 \cdot 1 \times 10^{-5}$ and $2 \cdot 1 \times 10^{-2}$ per second.

Simple tension tests were performed on the same sheet, the test piece shape is shown in *Figure 7* and these test pieces were tested at constant
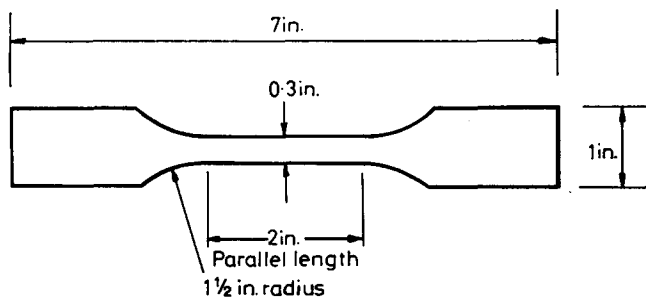
Figure 7 The tensile test piece

cross-head speed in an Instron testing machine. Extension was measured using a 1 in gauge length extensometer attached to the specimen.

A similar, although less extensive, series of tests were carried out on a commercial extruded ABS plastic sheet.

To calculate the true stress/strain diagram for the tensile tests it was assumed that straining was uniform within the gauge length and that

$$\sigma_a = \frac{F}{A_0} \frac{l}{l_0} \tag{9}$$

$$\Sigma_a = \ln \frac{l}{l_0} \tag{10}$$

In some tensile tests on the ABS plastic there was visible evidence of necking and cold drawing.

EXPERIMENTAL RESULTS

Cellulose nitrate

A typical autographic stress/strain curve obtained from the bulge test for cellulose nitrate is shown in *Figure 8*. In this diagram, the true stress in the plane of the sheet is plotted against the logarithmic thickness strain. The
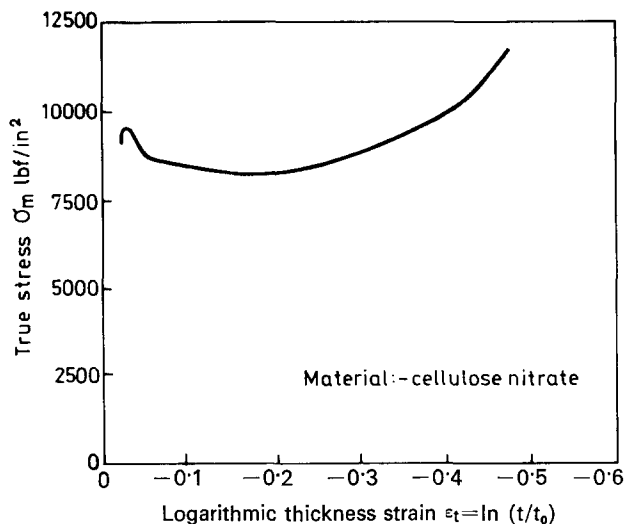
Figure 8 Typical autographic stress/strain diagram for cellulose nitrate

accuracy of the stress determination at strains less than $\Sigma_t = 0.07$ in this machine is poor. This is due partly to the errors inherent in the spherometer when the curvature of the bulge is small and partly to systematic errors in the analogue data-processing unit[15]. It is likely that the drop after first yield shown in this diagram is real, but the equipment used is not suitable for determining this drop quantitatively. The more gradual reduction in stress in the range $0.07 > \Sigma_t > 0.2$ was repeatedly observed. This effect is largest at the highest rate of strain suggesting that it might be due in part to adiabatic heating. The tests were all taken to rupture (in this case at $\Sigma_t \approx 0.48$); typically the ruptured specimen showed multiple tears radiating from the pole. Tests in which failure emanated from the point of contact of an extensometer probe were discarded.

Because of possible inaccuracies, the portion of the autographic diagrams for $\Sigma_t < 0.07$ have been deleted in all diagrams presented except for *Figure 8*.

The effect of strain-rate on the stress/strain curve in the bulge test is shown in *Figure 9*. The general stress level and also the strain at minimum stress both increase with increasing strain-rate.

The effect of strain-rate at a particular strain, $\Sigma_t = 0.15$, is shown in *Figure 10*. Each point represents the stress value obtained from the autographic diagram for a particular test. The amount of scatter between different tests performed under similar conditions can be seen from this diagram. From the slope of this line we can calculate a value of 4950 A^3 for the Eyring volume which compares with a value of 6070 A^3 previously obtained in a tensile test at 23°C. Taking into account inevitable variations between separate deliveries of cellulose nitrate sheet we regard these values as generally in line.

These particular sheets of cellulose nitrate were made by slicing blocks of
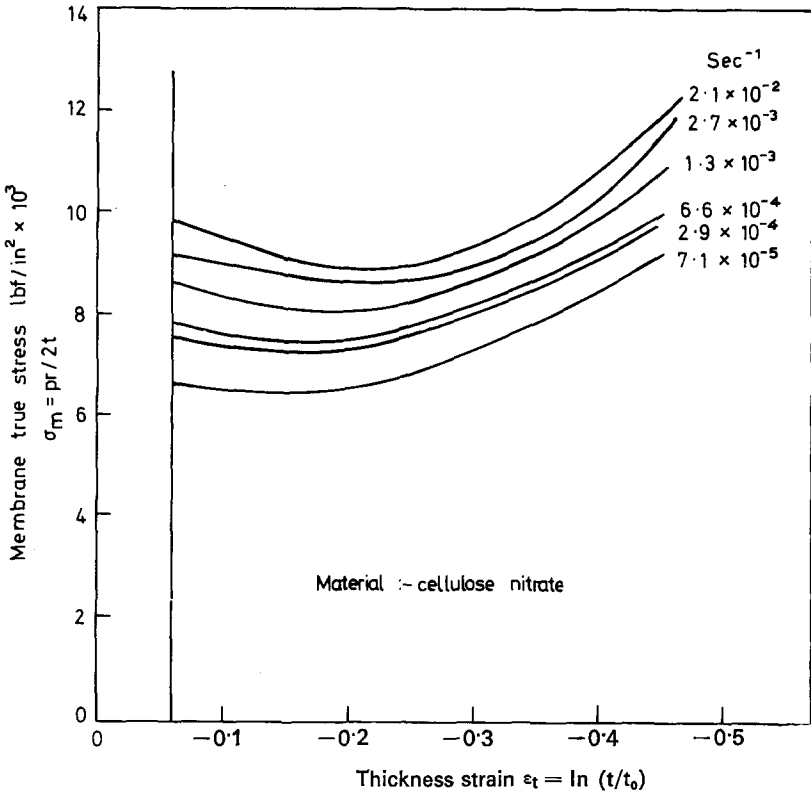
Figure 9 Stress/strain curves obtained at different strain-rates in the bulge testing of cellulose nitrate
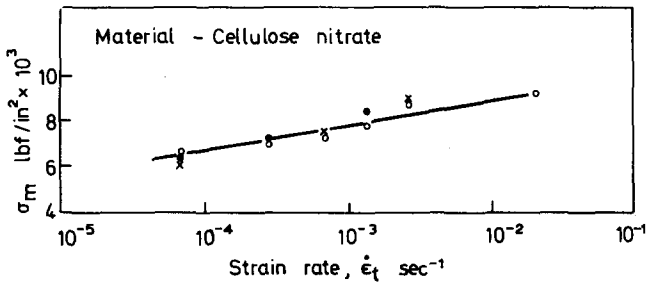
Figure 10 Stress, at a strain, $\Sigma_t = 0.15$ versus strain-rate for cellulose nitrate

compression moulded plastic. Tensile tests conducted on specimens cut in the direction of and normal to the direction of slicing showed less than 2% variation in yield stress. The true stress/strain curves derived from simple tension tests on specimens of the same orientation are shown in *Figure 11*.

The strain-rate varies during the test because of changes in gauge length. The nominal strain-rate for a test was taken as that given by
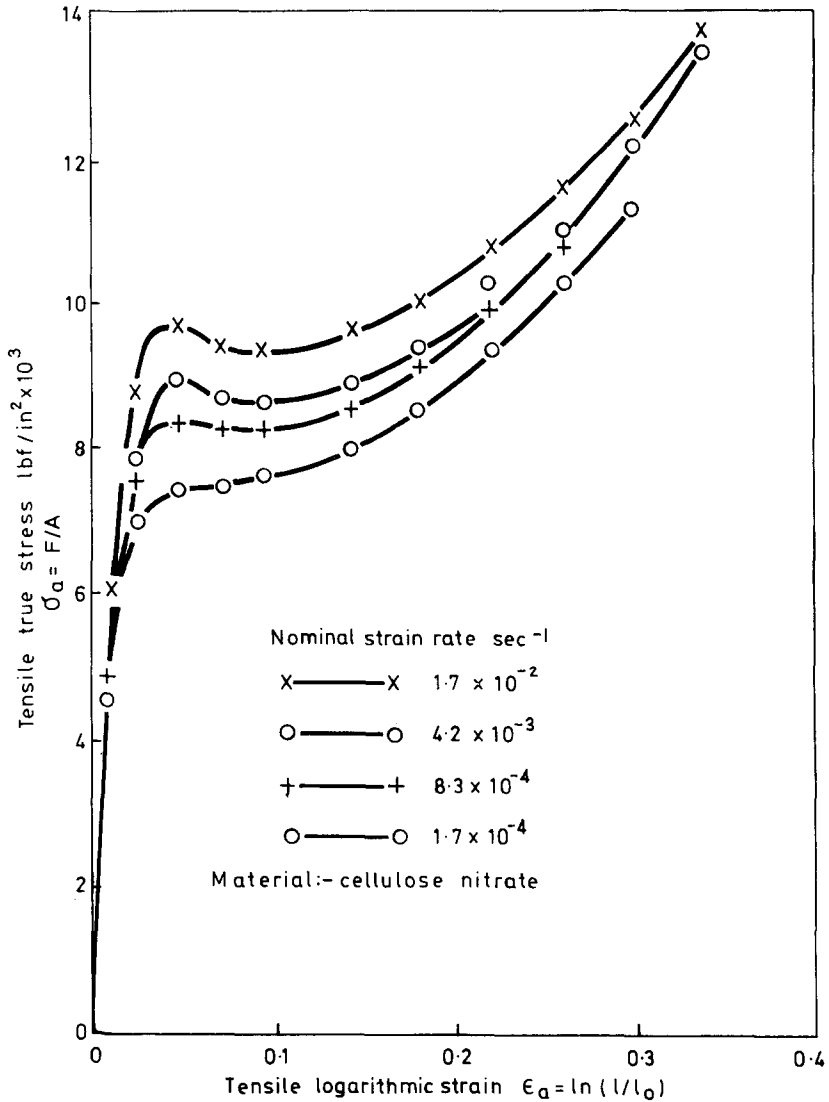
Figure 11 Stress/strain curves at different nominal strain-rates in simple tension for cellulose nitrate

$$\dot{\Sigma}_a = \frac{v}{L_0} \tag{11}$$

where v is the cross-head speed of the testing machine. This assumes that straining occurs in the parallel length L_0 and only in this length.

To investigate possible variations of strain-rate in the gauge length, tests were repeated in which a diagram of gauge length extension versus time was recorded. The mean strain-rate within the gauge length at any instant can be determined from the slope of this curve.

ABS plastic

The autographic curves for the bulge tests on ABS shown in *Figure 12* again indicate a fall in true stress after first yielding. The tendency for the stress to increase again was not so marked as in the case of the cellulose nitrate. This curve also shows the susceptibility of the particular sample to
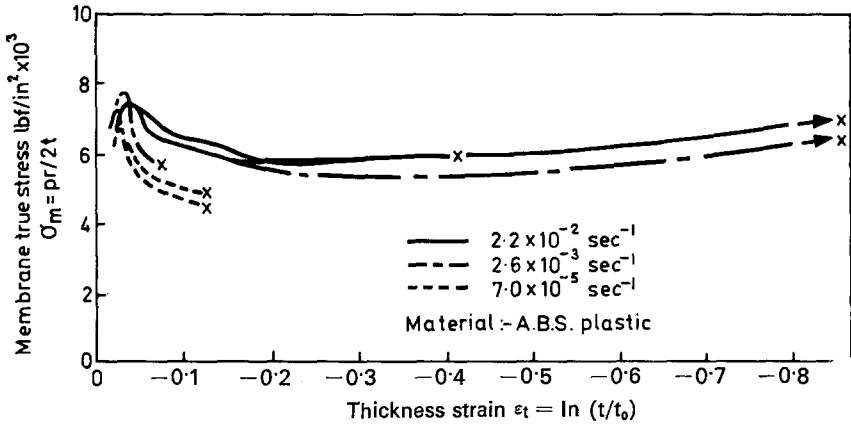
Figure 12 Stress/strain curves for ABS sheet at different strain-rates in the bulge test
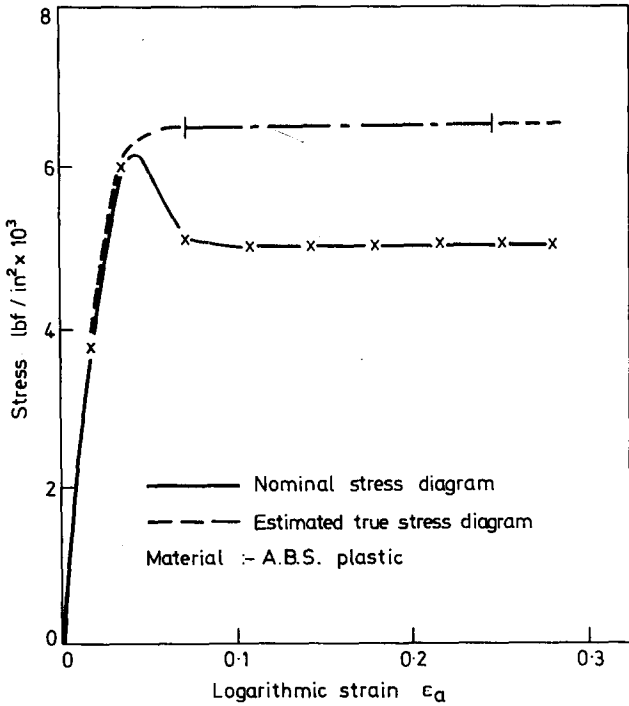
Figure 13 Estimated true stress/strain curve in simple tension, for ABS sheet

574

premature failure in tests at low strain-rates. Strains in excess of 0·8 were obtained in the higher strain-rate tests. Failure at low strain-rates was associated with a small tear not necessarily in the direction of extrusion of the sheet while at higher strain-rates the specimens split across the specimen along the direction of extrusion.

In the tensile test, failure normally occurred at strains less than 0·1; only where a constriction developed and subsequent cold drawing occurred was the strain higher. *Figure 13* shows one of these curves; the estimated true stress/strain curve for the material in the neck is indicated by the chain line.

COMPARISON OF BULGE AND TENSILE TEST RESULTS

A detailed comparison of the bulge and tensile test results is made for the cellulose nitrate sheet only.

The results of tests at approximately the same strain-rates are compared in *Figure 14a*; the numerically greatest principal stresses and strains are plotted for each test. The shape of the curves and the stress levels are reasonably similar for each test, but clearly the stress at a particular value of the numerically greatest principal strain is quite different for the two types of test.

An alternative basis is used in *Figure 14b*. In this diagram the maximum principal tensile stress is plotted against maximum principal tensile strain. For the tensile test, this curve is identical with that in *Figure 14a*. However, for the bulge test the strain and strain-rate are halved as $\Sigma_m = \frac{1}{2}\Sigma_t$. The

Figure 14a

575
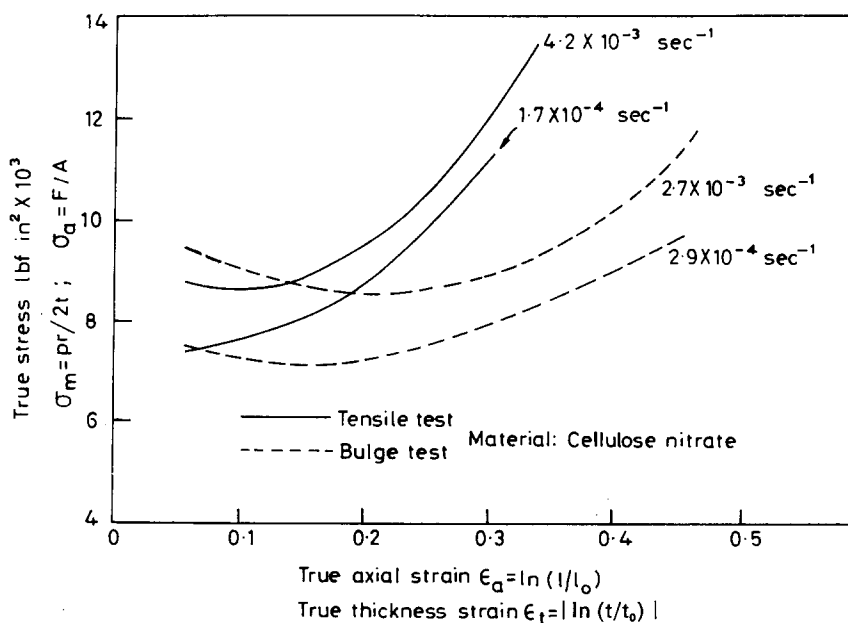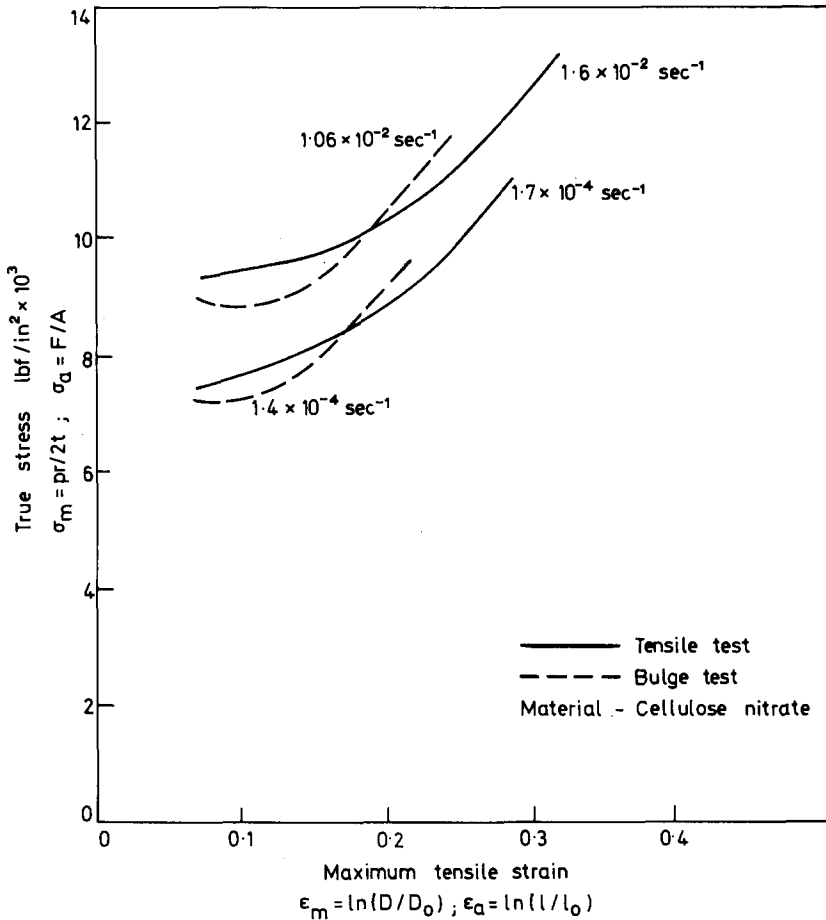
Figure 14 (a) True stress versus numerically greatest strain in the uniaxial and biaxial tests of cellulose nitrate sheet
(b) True stress versus maximum tensile strain in the unaxial and biaxial tests of cellulose nitrate sheet

correlation on this basis is improved, but the maximum tensile strain at failure is much less in the bulge test than in the tensile test.

Thus the strain hardening process (often referred to as orientation hardening[9]) in the two tests show greatest similarity when they are compared on the basis of maximum principal tensile strain. According to a theory of stress-strain curves[21] this orientation hardening[9] depends on the extensions of polymer chains between points of entanglement, and may appropriately be treated according to the theory of high elasticity[13]. If this view is right the behaviour observed should be analogous to that for rubber stretched under uniaxial and biaxial tension. Examples of this behaviour taken from the work of Trelaor[12] are illustrated in *Figure 15*. It will be seen that (apart from the higher extensibility of the rubber due to the well known greater flexibility of the rubber chain) the trends are analogous. Indeed the trend whereby the
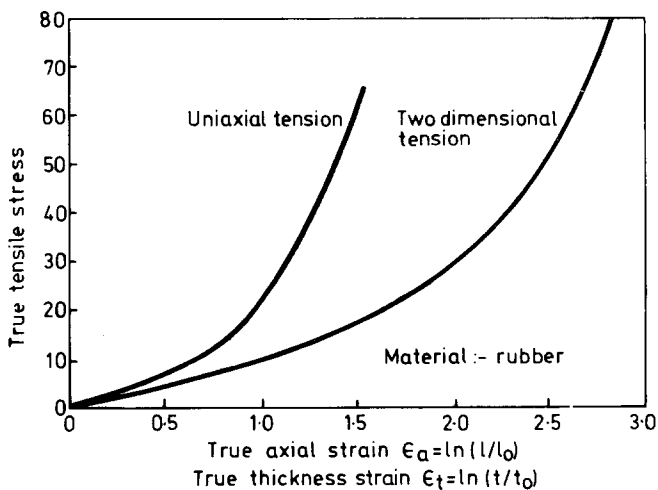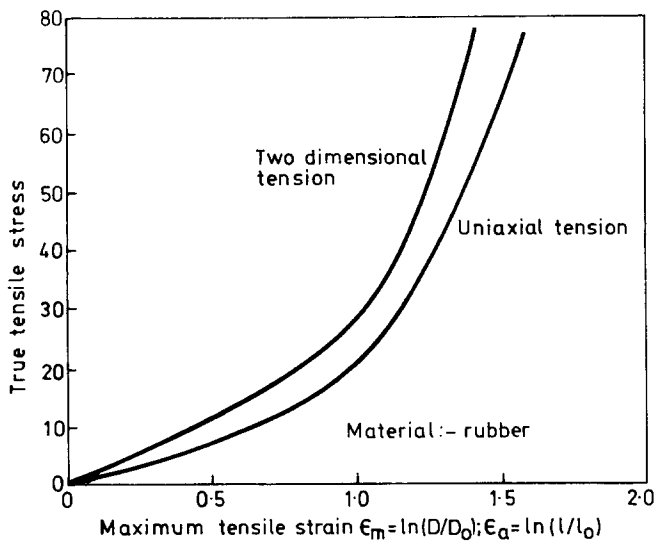
Figure 15 (a) True stress versus numerically greatest strain for rubber (from Ref. 12)

(b) True stress versus maximum tensile strain for rubber (from Ref. 12)

two dimensional tensile stress of the rubber lies above that for simple tension when plotted on a maximum tensile strain basis leads automatically to the prediction (according to the theory of Ref. 21) that the same thing should happen at the high strain end of the curve for a thermoplastic. This is actually observed. However, it should also be appreciated that this theory says nothing about fracture. It would of course be of interest to determine the relation between uniaxial and biaxial strain with other plastics. However,

577

this is not likely to be particularly easy since most other polymers either show brittle fracture in tension or necking, so that even when biaxial strain can be measured, as with certain types of polyethylene[14], it is not possible to make a direct comparison with a uniaxial test.

STRAIN RATE IN THE TENSILE TEST

As described above, the strain-rate within the gauge area in the bulge test is maintained constant by the closed-loop system; furthermore the geometry of deformation is such that non-uniform straining in the gauge area should not occur.

In the tensile test, however, only the cross-head speed is controlled. Variations in strain-rate within the gauge length can occur as a result of
1 the existence of an instability leading to the formation of a neck with or without subsequent cold drawing
2 straining extending beyond the parallel section of the specimen
3 the variation in overall length, i.e. although the nominal extension rate might remain constant the natural, or logarithmic, strain-rate would vary.

The variation in strain-rate for a typical tensile test is shown by the diagram in *Figure 16*, a true stress/strain curve from a similar test being superimposed.
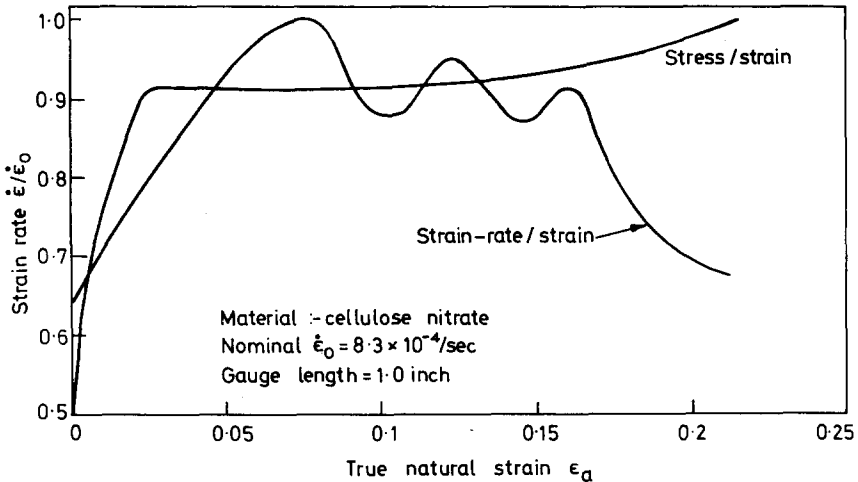
Figure 16 Variation of strain-rate with strain and the stress/strain curve for a typical tensile test on cellulose nitrate

The diagram was constructed by graphical differentiation of a gauge length/time record. The strain-rate is normalized so that unity represents the nominal initial strain-rate for the test as given by equation (11).

Graphical differentiation is a process particularly liable to error and consequently the strain-rate behaviour is not accurately given in *Figure 16*. It does indicate, however, that some straining occurs initially outside the

parallel length and that this straining is partially recovered when the load drops. Superimposed on this is the effect of decreasing strain-rate due to increasing gauge length. Whatever the cause, the variation of strain-rate during a simple tension test and constant cross head speed is clearly significant on a linear scale. On the other hand they are not large in relation to the 200 fold change in strain-rate used in *Figure 10* or to the 600 fold variation used in Ref. 21.

CONCLUSIONS

The results obtained demonstrate the feasibility of the controlled bulge testing method for determining strength properties of rigid plastic sheet material. A testing machine incorporating an extension and curvature measuring device and a closed loop hydraulic bulging system could be built specially for testing plastics and would differ only in detail from the unit described.

For the tests performed, the bulge test or controlled diaphragm test was stable and the fundamental stress/strain relations can be obtained in materials which exhibit instability or drawing in the simple tension test.

The object of this work was principally to demonstrate a new concept in testing sheet plastic in the higher strain regions. Only limited tests were performed on two different materials. For these particular materials the results obtained can be summarized as follows

1 in the bulge test the stress required to initiate large strain deformations is greater than that required to propagate the same

2 the amount of deformation obtained is related to the strain-rate, the viscous contribution appears to be similar in the two cases

3 close comparison of tensile and bulge test stress/strain curves was affected to a minor extent because of uncontrolled variations in strain-rate in the tensile tests

4 the relationship between orientation hardening in the tensile and bulge tests confirms with the qualitative predictions of a high elasticity model.

NOMENCLATURE

A_0	initial cross sectional area	$\dot{\Sigma}$	natural strain-rate
a	radius of spherometer probes	$\dot{\Sigma}_t$	thickness strain-rate
D_0	initial datum circle diameter	$\dot{\Sigma}_a$	strain-rate in uniaxial tension
D	current datum circle diameter		
d	sagitta of bulge	F	tensile load
Σ	natural or logarithmic strain	L_0	initial parallel length of
$\Sigma_{1,2,3}$	principal strains		tensile specimen
Σ_θ	circumferential strain	l_0	initial gauge length
Σ_m	membrane strain	l	current gauge length
Σ_t	thickness strain	p	pressure
Σ_a	axial strain in uniaxial tension	r	radius of curvature of bulge at pole

S_0	critical shear stress in the plane of shear	v	velocity of cross-head
t_0	initial thickness	σ	true stress
t	current thickness	$\sigma_{1,2,3}$	principal stresses
τ	critical shear stress when the normal stress on the plane of shear is zero	σ_m	true membrane stress
		σ_a	tensile true stress
		σ_n	nominal tensile stress
		μ	modulus of the material

ACKNOWLEDGEMENTS

Department of Mechanical Engineering
University of Manchester Institute of Science & Technology,
Sackville Street,
Manchester *(Received 13 July 1970)*

REFERENCES

1 Brown, Jr., W. F. and Sachs, G. *Trans of the A.S.M.E.* 1948, **70**, 241
2 Mellor, P. B. *J. Mech. Phys. Solids* 1956, **5**, 41
3 Hill, R. *Phil. Mag. Ser.* 7 1950, **41**, 1133
4 Duncan, J. L. and Johnson, W. *Int. J. Mech. Sci.* 1968, **10**, 143
5 Marshall, I. and Thompson, A. B. *Proc. Roy. Soc.* 1954, **221**, 541
6 Muller, F. H. *Rubb. Chem. Technol.* 1957, (Translated from *Kautsh. U. Gunmi*, 9, W.T. 197, 1956), **30**, 1027
7 Jackel, K. *Kolloidzschr* 1954, **137**, 130
8 Lazurkin, J. S. *J. Polym. Sci.* 1958, **30**, 595
9 Vincent, P. I. *Polymer Lond.* 1960, **1**, 7
10 Duncan, J. L. *Bull. Mech. Eng. Educ.* 1965, **4**, 29
11 Flint, C. F. and Naunton, W. J. S. *Inst. of the Rubb. Ind.* 1937, **12**, 367
12 Trelaor, L. R. G. *Trans. Faraday Soc.* 1944, **40**, 59
13 Treloar, L. R. G., 'The Physics of Rubber Elasticity', 1958, 2nd Edition, Oxford Univ. Press
14 Hopkins, I. L., Baker, W. O. and Howard, J. B. *J. Applied Phys.* 1950, **21**, 206
15 Hopkins, I. L. and Wentz, R. P. 1969, A.S.M.E. Paper No. 60-RP-14
16 Bowden, P. B. and Jukes, J. A. *J. Matl. Sci.* 1968, **3**, 183
17 Stemstein, S. S., Ongchin, L. and Silverman, A. *App. Polymer Symposia* 1968, **7**, 175
18 Murphy, B. M., Haward, R. N., and White E. F. T. (to be published)
19 Wilson, I. H. M.Sc. Thesis, 1966, University of Manchester
20 Bell, R., Duncan, J. L. and Wilson, I. H. *Proc. I. Mech. Eng.* 1965-6, **180**, (Pt. 3A)
21 Haward, R. N. and Thackray, G. *Proc. Roy. Soc.* 1968, **302**, 453

The pyrolysis of poly(vinylidene chloride) in solution

D. H. GRANT

In order to gain further information on the mechanism of pyrolytic carboniza-
tion of poly(vinylidene chloride), a study has been made of that polymer's
decomposition in a number of solvents, over the temperature range 80–304°C.
The most extensive studies have been made with N-methyl-2-pyrrolidone and
hexamethylphosphoramide. Decomposition rates are solvent dependent and
substantially higher than in the solid state reaction. Evidence is presented
that decomposition is a base catalysed dehydrohalogenation, the solvent
acting as the base. No difference in rate of decomposition was found for poly-
mer samples prepared under different conditions. Possible mechanism schemes
are discussed. Dehydrohalogenation is often accompanied by gel formation,
but conditions can be selected such that over 70% of the chlorine can be re-
moved with the polymer remaining in solution. Spectroscopic evidence is pre-
sented for some formation of aromatic structures at these high conversions.

INTRODUCTION

POLY(VINYLIDENE CHLORIDE) (PVDC) pyrolyses to eliminate hydrogen chloride
and to form a residual carbon which has a high surface area. The absorbtive
properties of these 'Saran Charcoals' have been the subject of several studies[1-5].

Since the nature of the final carbon must be related to the mechanism
of the pyrolysis reaction it is important to study the kinetics of the decom-
position. During the course of the preparation of the carbon, observations
have sometimes been made regarding the kinetics, but not in detail. In each
of these cases the study was confined to one sample of polymer, often of
unknown character or origin. An investigation of the pyrolyses of a series
of PVDC polymers of known characteristics was clearly necessary.

Studies[6] on the pyrolysis of PVDC in the solid state have shown that the
kinetics and the absorbtive properties of the resulting carbon are dependent
on the physical state of the polymer. The possibility that the rate of pyrolysis
may be determined by the rate of diffusion of hydrogen chloride out of the
semi-molten polymer is therefore a very real one. Consequently, it is prefer-
able to study the reaction in an inert solvent, to eliminate this complicating
factor. Only very few solvents are available for PVDC.

The aim of the present work was therefore to study the pyrolysis in solution
of a series of PVDC polymers, as a contribution towards an understanding of
the carbonization of PVDC.

EXPERIMENTAL

Poly(vinylidene chloride)

Five examples were examined. Sample A was supplied by Dow Chemical
Company (sample B9-1077). Nothing is known of its previous history.

581

Dow Chemical Company also supplied samples B, C, and D which were all prepared in 50% benzene/monomer mixtures. Different initiators, lauroyl peroxide (LrO₂), benzoyl peroxide (BzO₂), and 2,2'-azo-isobutyro-nitrile (AIBN) were used. In *Table 1*, their quoted concentrations are based on the monomer. Different polymerization temperatures were used, and the polymerization taken to different conversions. The absolute viscosity of 2% solutions of the polymer in *o*-dichlorobenzene at 140°C is also quoted. At this temperature the absolute viscosity of *o*-dichlorobenzene is 0·417 cps.

Table 1 Properties of polymer samples B, C, and D

| Sample | Polymerization conditions | | | | Viscosity (cps) |
	Temp. (°C)	Time (h)	Conversion (%)	Initiator (%)	
B	25	144	42·6	0·2 LrO₂ + 0·4 AIBN	1·229
C	55	24	56.8	0·6 LrO₂	0·775
D	75	16	83·3	0·6 BzO₂	0·571

Sample E was prepared as follows. Vinylidene chloride (L. Light & Co. Ltd) was washed with dilute alkali to remove inhibitor, then with water, and finally dried over sodium sulphate. This material was distilled under nitrogen, the middle fraction being collected in a vessel directely connected to a high vacuum system. With the distillation vessel maintained at −78°C, monomer was distilled twice under high vacuum finally being sealed off in a polymerization tube in the presence of 0·1 mol % AIBN. Polymerization was carried out at 50°C for 3 h. The resulting mixture of monomer and polymer was poured into absolute alcohol, and filtered. Polymer was redispersed in carbon tetrachloride to remove excess monomer and initiator and re-filtered. The process was repeated with alcohol. (Yield 15%.)

Solvents

N-Methyl-2-pyrrolidone (B.D.H. Ltd) and hexamethyl phosphoramide (a gift from Albright and Wilson Ltd) were dried over sodium sulphate and distilled under nitrogen at reduced pressure before use (b.p. 73°C at 7·5 mmHg and 96°C at 5 mmHg respectively). Other solvents were used as obtained from the usual suppliers.

Pyrolysis and analysis procedures

N-Methyl-2-pyrrolidone will only dissolve PVDC above 70°C. In this case, solutions were made up in vacuum and cooled to room temperature before being exposed to the atmosphere. These solutions do not gel for several hours. Hexamethyl phosphoramide will dissolve PVDC at room temperature.

Weighed quantities (about 100 mg) of solution of known concentration (usually about 1% w/w) were transferred by syringe into small thin-walled bulbs (0·5 ml), carefully degassed in vacuo by the usual freezing and thawing techniques and sealed off. For pyrolysis these bulbs were placed for the required length of time in a fluidized-bed bath whose temperature was controlled to ±0·2°C by a thermistor actuated relay which switches a series resistance in and out of the heating circuit. On removal, the bulbs were quenched and cleaned in distilled water.

For analysis each bulb was broken under 5 ml of an acidified solution of 1 : 1 methyl cellosolve/water. Free chloride ion in the solution was estimated by adding 100 mg mercuric chloranilate and measuring the absorbance at 530 mμ of the chloranilic acid produced, according to the method of Barney and Bertolacini[7].

Infra-red spectra

Samples of solution (1–2 ml) were pyrolysed by the normal method. Polymer was precipitated by pouring into absolute alcohol and separated by filtration or centrifugation. The Nujol mull technique was used to obtain spectra of these samples on a Unicam SP 100 spectrometer.

RESULTS AND DISCUSSIONS

When solutions of PVDC are heated in vacuum three changes occur:
(a) The solution becomes first yellow, then brown, and finally black.
(b) At some point the polymer may come out of solution as a gel or precipitate. This solid material is yellow to black depending on the solution from which it separates.
(c) Covalently bound chlorine is converted into some form which can be analysed as chloride ion.

Comparison with solid state reaction

The 'extent of reaction' is measured by the percentage of the total chlorine which is present in the form of chloride ion. A plot of extent of reaction against time is an S-shaped curve. (*Figures 1* and *2*) There is an autocatalytic phase over the first 10%, then between 10% and 30% conversion the rate remains approximately constant. Finally, the reaction slows down almost to a halt at a conversion in excess of 50%, the theoretical limit for the removal of one molecule of hydrogen chloride from every monomer unit. Previous workers studying the solid state reaction have usually claimed a first order reaction although closer inspection of reported data[8] indicate that the maximum rate is attained only after 10–15% reaction. With the present experimental conditions there is much less chance that this induction period is due to thermal lag, as has usually been assumed. Temperature dependent limiting conversions between 50% and 100% were reported by Winslow, Matreyek and Yager[9] and by Dacey and Cadenhead[10]. The shape of the curve is therefore essentially the same for both solution and solid state reactions.

It is uncertain whether the decomposition in the solid state is a true radical chain reaction, or takes place by a concerted mechanism whose transition state may be formulated with either radical or ionic contributions The former mechanism would be analogous to that proposed in some publications on the decomposition of polyvinyl chloride (PVC)[11,12], while the latter is the one proposed by Winslow, Matreyek and Yager[9]. Unless
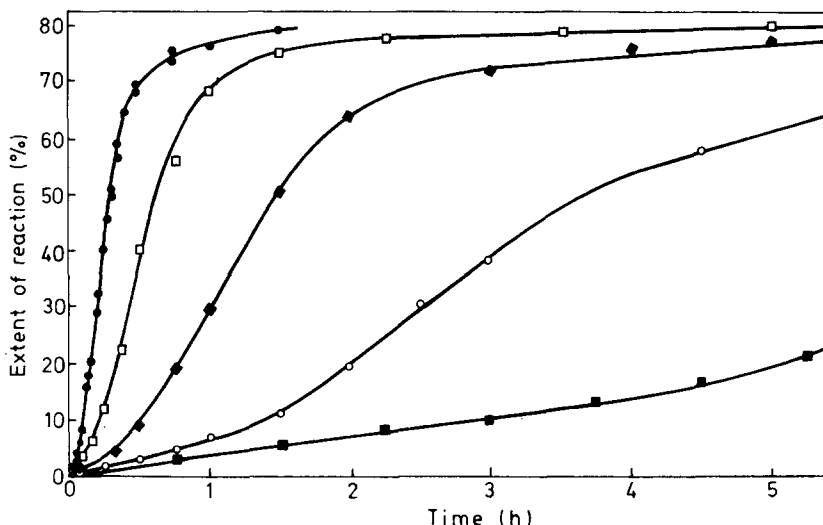
Figure 1 Pyrolysis of 1% solutions of polymer E in N-methyl-2-pyrrolidone at: ■, 90°C; ○, 100°C; ♦, 110°C; □, 120°C; ●, 130°C

there is some specific (usually inhibitory) effect the rates of radical reactions are not greatly affected by the solvent, and in fact the rates of radical decomposition of poly(methyl methacrylate)[13] and poly(α-methyl styrene)[14] are of the same order of magnitude in solution as in the solid state. On the other hand, any tendency for the reaction to proceed by a heterolytic mechanism would certainly be favoured by polar solvents, and a rate dependent on the polarity of the solvent predicted. In fact, we find that there is a major difference in the rates of reaction in the solid state and in solution. If one arbitrarily takes the time to reach 20% conversion as a measure of the rate, then at 130°C this time is about 5 days for the solid state decomposition in a nitrogen atmosphere*, 70 min in N-methyl-2-pyrrolidone, and 10 min in hexamethyl phosphoramide. The polymer is also soluble in N,N-dimethyl acetamide, dimethyl sulphoxide and *o*-dichlorobenzene. All of these are rather poor solvents and dissolve the polymer only above 100°C. The solutions gel rapidly on cooling and consequently quantitative measurements cannot be carried out by the present technique. Observation of the time taken for

* Unpublished data of D. H. Davies for reaction at 173°C with an activation energy of 36 kcal/mol.
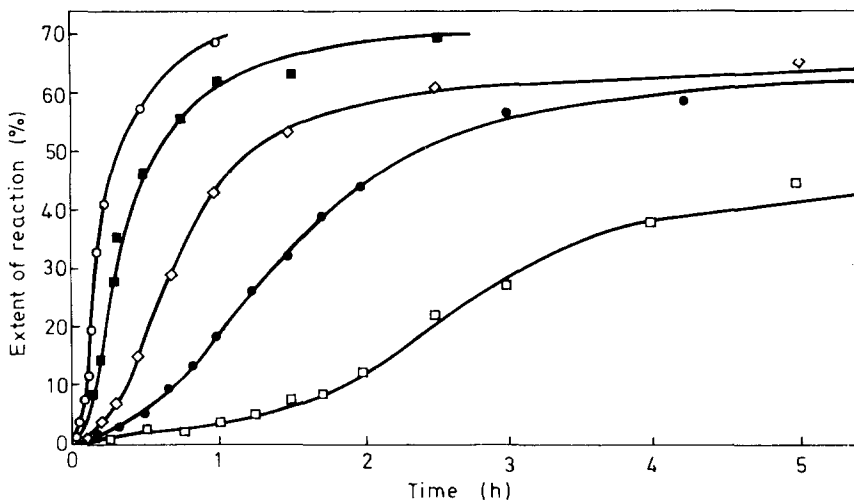
Figure 2 Pyrolysis of 1% solutions of polymer E in hexamethyl-phosphoramide at: □, 120°C; ●, 130°C; ◇, 140°C; ■, 150°C; ○, 160°C

the solution to become dark in colour do show, however, that there is a considerable difference in rate of decomposition in these different solvents, in the order: hexamethyl phosphoramide > N,N-dimethyl acetamide ∼ N-methyl-2-pyrrolidone > dimethyl sulphoxide > o-dichlorobenzene. It is concluded, therefore, that the reaction has a heterolytic mechanism in solution. Additional confirmation of this view is provided by the observation that the presence of 0·6% w/w anthracene, a known radical inhibitor[15], is without significant effect on the reaction curve.

Comparison of different solvents

Heterolytic mechanisms of dehydrohalogenation of alkyl halides in polar solvents are well established[16]. The most common is the E2 mechanism, in which the rate determining step consists of the removal of a proton by a nucleophile, particularly a base, together with the simultaneous formation of a double bond and explusion of the halogen as an ion.

$$\text{B:} \quad \text{H}-\overset{|}{\underset{|}{\text{C}}}-\overset{|}{\underset{|}{\text{C}}}-\text{X} \quad \longrightarrow \quad \text{BH}^+ \quad \overset{|}{\underset{|}{\text{C}}}=\overset{|}{\underset{|}{\text{C}}} \quad \text{X}^-$$
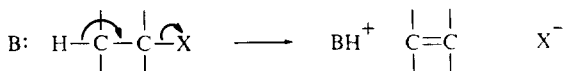
The variation in decomposition rate among the solvents may be attributed to a variation in their nucleophilic power, or basicity, i.e. their ability to interact with the hydrogen atom. Highest rates of reaction are found with amides. (N-methyl-2-pyrrolidone is reported[17] to be sufficiently basic to form a hydrochloride). The polymer does not dissolve in more strongly basic compounds such as amines, but small quantities of these, added to good solvents do not affect the solubility greatly. The considerable increase in

585
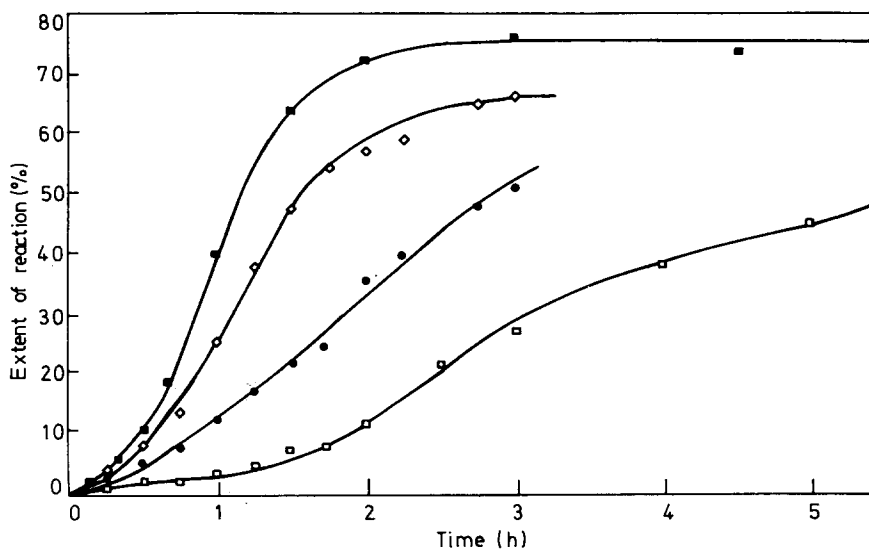
Figure 3 Pyrolysis of 1 % solutions of polymer E in N-methyl-2-pyrolidone at 120°C in presence of: □, no added pyridine; ●, 1·55 mol % pyridine; ◇, 3·08 mol % pyridine; ■, 9·16 mol % pyridine

decomposition rate caused by the addition of small amounts of pyridine to N-methyl-2-pyrrolidone is shown in *Figure 3*. N-ethyl-morpholine has a similar effect.

It is, therefore, concluded that the reaction is a base catalysed elimination, in which the solvent is acting as the base. Since the solvent concentration is so much larger than that of the solute it will be effectively constant during the reaction. This will lead to some simplification in the overall kinetics.

It has been suggested[18] that the best solvents for PVC, and therefore presumably for PVDC, are those which have:

(a) A high electron donor capacity, i.e. nucleophilic power.

(b) No steric interference for the approach of the electron donating centre to the polymer.

(c) A large bulk, to reduce interchain forces.

Clearly the first two of these are also the criteria for compounds able to act as bases in a base catalysed elimination, and it is therefore not surprising to find that the only solvents of poly(vinylidene chloride) are those which also bring about its decomposition.

Effect of solvent purity

The most extensive investigations have been carried out with N-methyl-2-pyrrolidone as solvent. In this case it was found that solvent purity has some

586

effect on the decomposition rate. Reproducible rates were only obtained when freshly distilled or vacuum-stored solvent was used. On standing in air for several days an impurity is produced which causes an increase in decomposition rate, observable as an earlier yellowing and a smoothing out of the concavity in the reaction curve.

At first, it was thought that this might indicate a radical reaction catalysed by peroxide or hydroperoxide impurities. In which case the impurity would have been expected to disappear when contaminated solvent is given a preliminary heating in vacuum to destroy any peroxides. This was not observed: the impurity effect remained.

It therefore appears more probable that the impurities are compounds more basic than N-methyl-2-pyrrolidone itself, such as the N-oxides. At concentrations at which they affect the decomposition rate these impurities cannot be detected by either infra-red spectroscopy or gas chromatography. If the solvent is deliberately oxidized by exposure to air for several hours at 100°C, then impurities can be detected by these techniques. However, it was not possible to identify any of the impurities.

Comparison of different polymer samples

Constrasting markedly with the dependence of decomposition rate on solvent and solvent purity are the results of studies where the polymer samples varied.

In samples B, C, and D molecular weights vary by at least a factor of 30. As different initiators were used, at least some of the chain ends are different. As different polymerization temperatures were used, and the polymerization taken to different conversions, these polymers should differ in the number of branched units and head to head units, if such structural irregularities exist in PVDC. All these polymers had been standing in air for several years and may have become oxidized. Consequently a fifth sample, E, was examined, which had been prepared immediately before use.

No significant difference in dehydrochlorination rate in N-methyl-2-pyrrolidone was observed with any of these five samples. Only one sample of PVDC has been examined in each of the previous publications on the solid state reaction, but unpublished data[6] show that these same five samples give approximately the same rate of dehydrochlorination when decomposed in the solid state.

In contrast PVC dehydrochlorinates at rates which are inversely proportional to the molecular weight, both in solution[19] and in solid state[11]. This has been interpreted as showing that the reaction begins at the ends of the PVC chain.

Normally runs were made with 1% solutions. More dilute solutions gave the same extent of reaction against time curve. The reaction is therefore first order, with respect to PVDC concentration, as in the case of PVC.

It must therefore be concluded that structural irregularities play only a minor part in controlling the decomposition of PVDC.

Gel formation and precipitation

Gel formation does not always occur at the same extent of reaction. Three factors are important.

587

(a) *Temperature.* As shown in *Table 2* an increase in temperature increases the extent of reaction at which gel formation is first observed.

Table 2 Effect of temperature on gel formation

Temp. (°C)	*Extent of reaction and time at which gel formation first occurs in 1% solutions of polymer sample D*	
	(1) in hexamethyl phosphoramide	*(2) in N-methyl-2-pyrrolidone*
80	4%, 4 h	–
90	11%, 3 h	–
100	22%, 2 h	–
110	(30% only), 1 h	–
120	(>75%)	3%, 1 h
130	(>75%)	18%, 1 h
140		43%, 1 h
150		69%, 2¼ h
160		(>70%)

(b) *Molecular weight.* Gel formation occurs at a lower extent of reaction with polymer of higher molecular weight. With 1% solutions in N-methyl-2-pyrrolidone at 140°C gelation occurs at 30% reaction with the high molecular weight polymer B, at 38% reaction with the intermediate molecular weight polymer C, and only slight precipitation occurs in the plateau region at 65% reaction with the low molecular weight polymer D. Polymers A and E whose position in the order of molecular weights is not known, precipitate at 20% and 43% respectively.

(c) *Concentration.* Although 1% solutions of polymer D in N-methyl-2-pyrrolidone can be heated at 150°C to about 70% reaction without any gel formation, when the concentration is increased to 5%, gel is formed after less than 25% reaction. No gel was observed at all when solutions of low concentrations (0·5% and 0·25%) of polymer B in N-methyl-2-2-pyrrolidone were heated at 140°C, although the normal 1% solutions gel at 30% reaction under similar conditions. The gelation reaction is therefore probably of higher than first order in polymer concentration.

The physical appearance of the gel varies. When formed at low temperatures it is initially clear or pale yellow and occupies the whole volume of the solution. If reaction is continued further, the gel shrinks as it darkens and finally forms a black plug in a clear liquid. At high temperatures there is partial deposition of a black solid, the amount of material deposited increasing with time.

Insolubility in polymers is often due to the presence of a crosslinked structure. In the pyrolysis of PVDC in solution, gel formation is not reversible. Gel formed at a low temperature does not re-dissolve if the temperature is subsequently raised, but instead retracts and precipitates. It is therefore likely that gelation in this case is due to the introduction of crosslinks. Since crosslink formation is an inter-chain process, one would expect it to be

second order in polymer concentration. The observed relationship between onset of gel formation, extent of reaction and concentration of polymer is consistent with this.

According to Flory[20] gel formation occurs when, on average, there is one crosslink per pair of initial polymer chains. Provided formation of crosslinks is independent of chain ends, this requires that more crosslinks have to be formed for low molecular weight polymer to form a gel than for high molecular weight polymer. The observed relationship between onset of gel formation, extent of reaction and molecular weight is consistent with this.

Since so very few crosslinks need be formed for gelation to occur, it will make negligible difference to the yield of chloride ion if the crosslinking reaction proceeds before, with, after, or without dehydrochlorination. Dehydrochlorination rate studies are therefore insensitive methods of studying the mechanism of crosslinking. Some further information regarding the nature of the degraded polymer is necessary.

Behaviour at high extents of reaction

Figure 4 shows the effect of higher temperatures on the limit of reaction. Up to 220°C there is a general drift to higher conversion with higher temperatures and longer reaction times.

The pyrolysis of 1% polymer D in N-methyl-2-pyrrolidone for 1 h at 160°C was carried out on a preparative scale to obtain sufficient pyrolysate for further studies. The pyrolysed polymer was precipitated by pouring the solution into absolute alcohol. In this case, it was possible to check the chloride analysis by weighing the reaction product. Agreement was highly satisfactory (extent of reaction by chloride ion analysis 68·4% by weight 68·9%). In this case, there was no precipitation during the reaction. After 1 h at 220°C the same polymer decomposed to 75%. In this case, about 1% of the product was deposited during the reaction.

Reactions at still higher temperatures apparently yield less chloride ion. As this is accompanied by increasing precipitation it is probable that these analyses are inaccurate due to the trapping of chloride ions within the precipitate.

The most remarkable feature of these results is that extents of reaction well beyond 50% can be obtained without gel formation. Even after precipitating in alcohol, the residue can be redissolved at room temperature in N-methyl-2-pyrrolidone. It has already been pointed out how few crosslinks would be required for gelation. One cannot therefore account for dehydrochlorination in this range by any reaction mechanism which would involve the formation of crosslinks. Such a mechanism–inter-chain Diels-Alder condensation, followed by dehydrochlorination–has been postulated for the decomposition of PVDC in the solid state[9]. It may be significant, therefore, that solid and solution pyrolysates differ in solubility. PVDC pyrolysed in the solid state develops insolubility towards N-methyl-2-pyrrolidone and hexamethyl phosphoramide at quite low extents of reaction.

Infra-red spectra

The only serious discussion, so far published, of the infra-red spectrum
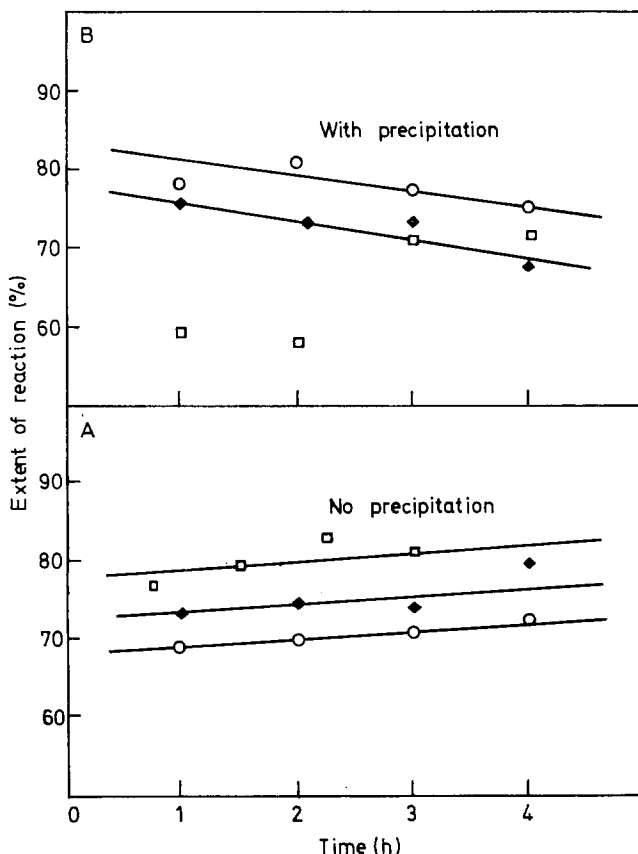
Figure 4 Pyrolysis of 1 % solutions of polymer E in N-methyl-2-pyrolidone at A: ○, 170°C; ♦, 190°C; □, 220°C (Temperatures at which there is no significant precipitation of dehydrohalogenation product.) B: ○, 240°C; ♦, 260°C; □, 304°C (Temperatures at which there is substantial precipitation of dehydrohalogenation product.)

of PVDC pyrolysed in the solid state, is that of Dacey and Barradas[21]. Spectra obtained from PVDC pyrolysed in solution do not differ significantly from these.

As in the solid state, loss of hydrogen chloride results in the decrease of all peaks attributable to –CCl₂– stretching modes.

More significant are the peaks which develop as pyrolysis proceeds.

Dacey and Barradas report the production of a doublet at 1570 and 1620 cm⁻¹. Our results show that the higher of these two frequencies, estimated here at 1635 cm⁻¹ is the initial product and that the lower frequency peak, estimated at 1580 cm⁻¹, with a shoulder at 1555 cm⁻¹ develops later, although eventually becoming the more intense. Dacey and Barradas ascribe their 1570 cm⁻¹ band to aromatic rings. One might therefore take the present results as indicating the initial formation of C=C bonds (1635 cm⁻¹) followed by aromatization. However, it must be pointed out that an equally valid

590

interpretation is that the 1635 cm^{-1} peak is due to isolated C=C bonds, and that the whole pattern of peaks, 1635, 1580 and 1555 cm^{-1} is due to a conjugated polyene system, without specifying whether it is linear or in an aromatic ring.

Somewhat better evidence for aromaticity developing in the later stages is the existence of a peak at 865 cm^{-1} which is present in polymer decomposed to a high extent of reaction. Dacey and Barradas do not discuss this peak but it is present in their reported spectra. This is the frequency expected of C—H out-of-plane deformations in a highly substituted aromatic ring. It has been used as evidence for the existence of aromatic rings in coal[22].

Like Dacey and Barradas we observed a peak at 1710 cm^{-1}, and additionally a small peak at 1950 cm^{-1}. Taken together, this is the pattern of peaks given by a highly substituted aromatic ring[23]. However, like Dacey and Barradas we cannot entirely eliminate the possibility that the 1710 cm^{-1} peak is due to a carbonyl group since, although prepared in vacuum, the sample is exposed to air at room temperature during the precipitation and preparation for infra-red analysis. It occurs irrespective of whether the pyrolysis is in N-methyl-2-pyrrolidone or in hexamethyl phosphoramide. If the 1710 cm^{-1} peak is due to carbonyl then the 1950 cm^{-1} peak alone would indicate the presence of an allene structure.

GENERAL DISCUSSION

There remain two aspects of the pyrolysis requiring further consideration. These are, the auto-catalytic nature of the rate curves, and the existence of some reaction which leads to a loss of more than 50% of the hydrogen chloride, without reaching 100% loss. In view of the unsatisfactory nature of the spectral evidence regarding the structure of the product the suggestions put forward here must be regarded as tentative.

Auto-catalysis might arise from the chloride ion produced in the reaction if it acts as a base as it is suggested to do in certain lithium chloride catalysed decompositions of PVC[24]. The major argument against this mechanism is that it is unlikely that free chloride ions exist during the solid state pyrolysis of PVDC, although the latter also shows auto-catalysis.

An isolated double bond produced in the chain is believed to have an activating influence on the neighbouring unit, making it more likely to decompose than it otherwise would. This idea has been used to explain why long sequences of conjugated double bonds causing visible coloration, are produced in the early stages of reaction. If the effect of double bonds is cumulative, a series of double bonds in conjugation having a greater activating influence than one double bond, then the reaction rate would increase with conversion until depletion of reagent caused a decrease. This would certainly explain the auto-catalysis in PVDC pyrolysis both in the solid state and in solution.

However, pyrolising PVC possesses a similar conjugation and yet does not show a similar increase in rate with conversion. Information from the study of small molecules is not available. Allyl chlorides certainly dehydrochlorinate

faster than alkyl chlorides[25] but the effect of increasing conjugation has not been determined.

If one considers the production of an isolated double bond as the initiation step, and the decomposition of a unit adjacent to a double bond as a propagation step, then the above kinetic scheme would be one in which the rate constant of propagation increased with conversion.

It has been more usual to assume that the rate constant for the decomposition reaction of a unit adjacent to a double bond is independent of conjugation length. Even with this assumption however, it is possible to have auto-catalytic rate curves. In the scheme outlined below the propagation rate constant is indeed constant, but the kinetic chain length or zip length varies with conversion.

If one defines an active centre as the combination of an unreacted unit and a reacted unit (double bond) adjacent to each other, then the above reaction steps describe the initiation and propagation of active centres along the polymer chain. Because of the head-to-tail arrangement of monomer units, reaction chain growth is likely to be unidirectional. An active centre will terminate where there is no unreacted unit adjacent to it. In principle, this could occur either at the end of the chain, or at some unit already reacted. Since the observed reaction rate is independent of molecular weight and nature of the chain ends, the zip length is smaller than the molecular chain length. (Initiation, propagation and termination of each active centre must take place over a section of the polymer which is small compared with the total length of the chain). Initiation must therefore be at random, at the normal units within the chains. Termination must be at a unit at which another active centre was initiated.

In the early stages of decomposition active centres are few, there is little termination, so that zip lengths are relatively long and the number of active centres and hence the pyrolysis rate increases with conversion. Later, steady state conditions will be reached in which initiation and termination of active centres balance and the rate of decomposition reaches a maximum. In the final stages of reaction, termination predominates, the number of active centres falls, the zip lengths become smaller and the rate of decomposition decreases. Qualitatively therefore this reaction scheme could lead to the observed auto-catalytic rate curve.

Such a scheme is consistent with the pyrolysis of PVC. There, the rate of decomposition is inversely proportional to the molecular weight due to the conjugated sequences starting, not within the chain but from the chain ends It has been suggested[19] that these ends already possess double bonds arising from chain transfer with monomer during polymerization. Consequently, there need be no new initiation steps; the number of active centres is already maximal and the rate of reaction falls off exponentially with conversion in a normal way.

Elimination of a second molecule of hydrogen chloride from a monomer unit would form an acetylenic link in the polymer chain. In the limit this would result in a poly-yne, an unusual carbon containing $-C{\equiv}C-$ repeat units. Such a polymer has been reported[26]. However, such a structure does not easily account for the reaction essentially ceasing at conversions far short of 100%.

A low limit of reaction might arise in several ways.

Due to allyl activation a conjugated sequence of double bonds will grow in one direction only. Which direction is determined by the initiation step.

```
    H   Cl  H   Cl  H   Cl
    |   |   |   |   |   |
  —C—C—C—C—C—C—
    |   |   |   |   |   |
    H   Cl  H   Cl  H   Cl
```

```
  H           Cl  H   Cl              H   Cl          H   H
  |           |   |   |               |   |           |   |
—C—C=C—C—C—C—            —C—C—C=C—C—C—
  |   |   |   |   |   |               |   |   |   |   |   |
  H   Cl  H   Cl  H   Cl              H   Cl  H   Cl  H   Cl

          ←—                                      —→

     sequence growth                         sequence growth
```
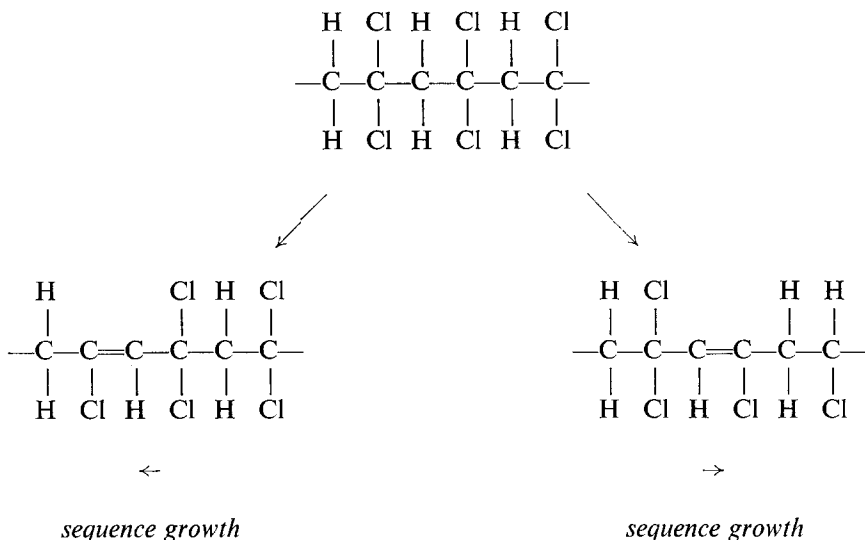
Where two such sequences start to grow in opposite directions a break in the conjugation will result, giving:

```
                  Cl
                  |
      =C—C=C—C—C=C—
        |   |   |   |   |   |
        H   Cl  H   Cl  H   Cl
```
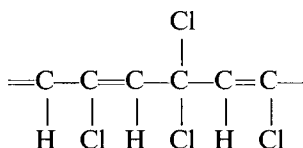
Conversion of C=C bonds to C≡C bonds would result in a structure in which chlorine atoms are isolated, having no adjacent H atoms:

```
                  Cl
                  |
     ≡C—C≡C—C—C≡C—
                  |
                  Cl
```
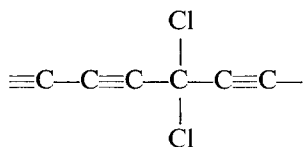
For the case of random elimination, i.e. the extreme case in which only initiation steps occur, there being no propagation due to allyl activation, one can calculate[27] that about 13% of the total chlorine would become isolated in this way. However, this is an extreme upper limit. Due to the occurrence of unidirectional propagation the limit would be reduced considerably and therefore this type of isolation is unlikely to be a significant contributing factor to the failure of the reaction to reach 100%.

Trans-elimination of hydrogen chloride occurs more readily than *cis*-elimination. There are two conformations of the monomer unit in which

2—P

hydrogen and chlorine are in the preferred *trans* or *anti* position. In these conformations the remaining portions P and P′ of the polymer chain are respectively (a) *anti* and (b) *syn* to each other. *Trans*-elimination of hydrogen chloride from these will result in structures in which the remaining hydrogen and chlorine are *trans* and *cis* respectively, and therefore differ in the ease with which further hydrogen chloride removal can occur.
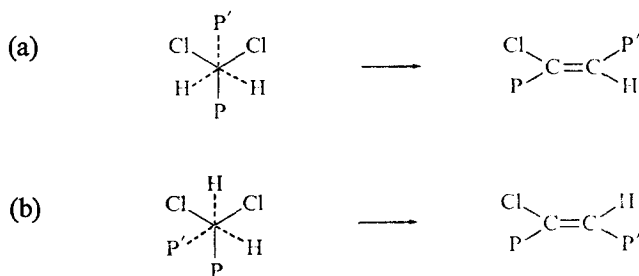
The result of process (b) is a structure in which chlorine has only *cis*-H adjacent to it. Such chlorine is effectively isolated. The failure to remove it would give rise to a low limit of reaction.

Conformation (a) exists in a planar zig-zag chain. This would not be strain free, as the most stable structure proposed by Fuller[28] for crystalline PVDC in the solid state requires some distortion from the planar zig-zag. A mixture of both conformations exists in the structure of solid PVDC proposed by Reinhardt[29]. It is possible therefore that at elevated temperatures in solution, at least some reaction may proceed by scheme (b).

Failure to detect any C≡C vibrations in the infra-red spectrum of pyrolysed PVDC is one argument against the idea that the reaction beyond 50% hydrogen chloride removal consists of formation of acetylenic bonds, together with isolation of chlorine. It is doubtful how much reliance can be placed on this observation, as the pseudo-symmetry of the structure would cause internal C≡C bonds to have only very weak stretching frequencies.

Reaction beyond removal of 50% hydrogen chloride may best be accounted for as intra-chain aromatization, by a reaction which is effectively a 1,6-elimination.
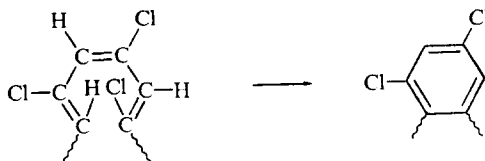
This reaction may occur directly, or by initial ring formation[30] followed by hydrogen chloride elimination, or even by acetylene formation and internal Diels-Alder addition[31].

In such a structure, each aromatic ring contains two chlorine atoms which are thus stabilized. Complete formation of this structure would, without

formation of crosslinks, result in the removal of 67% of the original chlorine, which is close to the observed extent of reaction beyond which precipitation always occurs. Finally, the 1,2,3,5-tetra-substituted aromatic ring possesses the isolated C—H bonds which would give C—H out-of-plane deformation frequencies at about 865 cm^{-1} in the infra-red spectrum.

ACKNOWLEDGMENTS

Chemistry Department
Mount Allison University
Sackville
New Brunswick
Canada

REFERENCES

1 Emmett, P. H. *Chem. Revs.* 1948, **43**, 69
2 Pierce, C., Wiley, J. W., and Smith, R. N. *J. Phys. Chem.* 1949, **53**, 669
3 Cadenhead, D. A., and Everett, D. H., Industrial Carbon and Graphite, p 272, Society of Chemical Industry, London, 1957
4 Dacey, J. R. and Thomas, D. G. *Trans. Faraday Soc.* 1954, **50**, 647
5 Culver, R. V. and Heath, N. S. *Trans. Faraday Soc.* 1955, **51**, 1569
6 Davies, D. H., Ph.D. Thesis, Bristol University, 1963
7 Barney, J. E. and Bertolacini, R. J. *Analyt. Chem.* 1957, **29**, 1187
8 Winslow, F. H., Baker, W. O. and Yager, W. *J. Amer. Chem. Soc.* 1955, **71**, 4751
9 Winslow, F. H., Matreyek, W. and Yager, W., Industrial Carbon and Graphite, p 190, Society of Chemical Industry, London 1957
10 Dacey, J. R. and Cadenhead, D. A., Proceedings of the Fourth Conference on Carbon, Buffalo, p 315, Pergamon Press, London 1960
11 Arlman, E. J. *J. Polym. Sci.* 1954, **12**, 543
12 Talamini, G. and Pezzin, G. *Makromol. Chem.* 1960, **39**, 26
13 Grant, D. H. and Bywater, S. *Trans. Faraday Soc.* 1963, **59**, 2105
14 Grant, D. H., Vance, E. and Bywater, S. *Trans. Faraday Soc.* 1960, **56**, 1967
15 Dunn, J. R., Waters, W. A. and Roitt, I. M. *J. Chem. Soc.* 1954, p 580
16 Ingold, C. K. 'Structure and Mechanism in Organic Chemistry', p 420, Bell, London, 1953
17 Heilbron, I. and Bunbury, H. M., 'Dictionary of Organic Compounds', Eyre and Spottiswoode, London, 1943
18 Adelman, R. J. and Klein, I. M. *J. Polym. Sci.* 1958, **31**, 77
19 Bengough, W. I. and Sharpe, H. M. *Makromol. Chem.* 1963, **66**, 31
20 Flory, P. J., 'Principles of Polymer Chemistry', Cornell University Press, Ithaca, New York, 1953, p 338
21 Dacey, J. R. and Barradas, R. G. *Can. J. Chem.* 1963, **41**, 180
22 Brown, J. K. *J. Chem. Soc.* 1955, p 745
23 Bellamy, L. J., 'The Infra-red Spectra of Complex Molecules', Methuen, London, 1958 p 90
24 Korshak, V. V., Sosin, S. L. and Sladkov, A. M., *J. Polym. Sci.* (*C*) 1963, **4**, 1315
25 Baum, B., and Wartman, L. H. *J. Polym. Sci.* 1958, **28**, 537
26 Roth, J. P., Rempp, P. and Parrod, J. *J. Polym. Sci.* (*C*) 1963, **4**, 1347

27 Flory, P. J. *J. Amer. Chem. Soc.* 1939, **61**, 1518
28 Fuller, C. S. *Chem. Revs.* 1940, **26**, 143
29 Reinhardt, R. C. *Ind. and Eng. Chem.* 1943, **35**, 422
30 Fonken, G. J. *Tetrahedron Letters* 1962, p 549
31 Eglington, G., Raphael, R. A. and Willis, R. G. *Proc. Chem. Soc.* 1960, p 248

Crystalline contribution to the mechanical anisotropy of uniaxially oriented polyethylene

B. E. READ and G. DEAN

The contribution from the crystalline phase to the anisotropy of the elastic modulus or compliance in uniaxially oriented polyethylene is considered. Account is taken of the orthorhombic symmetry of the crystals and their orientation distribution within the sample. Tensor components of the modulus are calculated assuming the condition of uniform strain on the crystals (Voigt average), whilst the calculation of compliance components assumes a uniform stress (Ruess average). Equations are also derived by means of which the required averages of the crystal orientation distribution may be obtained from X-ray pole figure data.

INTRODUCTION

THE ANISOTROPY of the mechanical modulus in drawn polyethylene has been interpreted by Ward and coworkers[1-3] in terms of a structural model comprising oriented aggregates of anisotropic units whose properties are those of the fully oriented polymer. Such units are transversely isotropic and their mechanical anisotropy is characterized by five independent elastic moduli or compliances[4]. This model is able to account for the variation of mechanical anisotropy with draw ratio. However, the elastic constants of the (hypothetical) structural units are not accessible from independent experiments, but are chosen from the data on the bulk polymer extrapolated to high draw ratios. In view of the known structural features of the polymer, a more realistic approach would be to consider the contributions to the modulus anisotropy both from the oriented crystalline phase, and also from the amorphous regions. The properties of each of the two phases should be obtainable from independent experiments or calculations.

Two related problems are encountered with the two-phase model namely, (a) the elucidation of the amorphous contribution to the elastic moduli, and (b) the structural arrangement of the two phases. Regarding problem (a) we note that the relatively flexible amorphous phase should have an appreciable influence on the moduli, particularly at low degrees of crystallinity. Furthermore the amorphous contribution to the modulus should depend significantly on the molecular orientation within this phase. Various optical and spectroscopic methods are available for characterizing the orientation of the amorphous regions[5]. Currently we are investigating this orientation in polyethylene, and the amorphous contribution to the modulus, by means of simultaneous stress/strain/infra-red dichroism measurements using infra-red bands originating from the amorphous phase[6]. Such studies should be aided by similar measurements on crosslinked amorphous polyethylene (at temperatures above the melting point) and with the relevant theoretical calcula-

tions of Flory and Abe[7]. Measurements of the polarization of Raman spectra might also prove useful for investigating the amorphous contribution to the modulus anisotropy, since this technique should yield averages of 2nd and 4th power functions of the segmental orientation distribution[5]. Concerning problem (b) it has been argued[8] that for undrawn polymers having degrees of crystallinity above about 50 % the crystalline phase is the continuous load carrying phase in which the amorphous regions are randomly dispersed. For highly drawn and annealed specimens a series coupling of the two phases along the draw direction may be more appropriate[9, 10]. The actual mode of coupling will, of course, depend on the detailed morphological structure of the oriented polymer, and such questions will be reserved for future study.

The purpose of this report is to present some calculations relating to the crystalline contribution to the elastic constants of uniaxially drawn polyethylene. This contribution will depend on the orientation distribution of the crystallites, which can be determined by means of x-ray pole figure measurements[11-19]. Theoretical estimates[20, 21] of the elastic constants of the polyethylene crystal suggest that a significant difference may exist between the values of the transverse constants c_{11} and c_{22}, and also between the shear constants c_{44} and c_{55} and between c_{13} and c_{23}. Furthermore, when polyethylene is stretched, the crystal a axes are initially oriented on average more perpendicular to the elongation direction than the b axes[12]. The above results suggest that the orthorhombic symmetry of the crystal should be considered when calculating the crystalline contribution to the elastic constants of the bulk sample. In the present calculations this factor is taken into account. Another main objective is to consider how the required averages of the crystal orientation distribution may be obtained from x-ray pole figure data on the known polyethylene reflections. These calculations should be applicable to our investigation of the elastic constants of drawn polyethylene using low frequency torsional and longitudinal methods and also the ultrasonic pulse technique. Attempts are also being made to produce, by high-pressure techniques, polyethylene samples containing oriented crystals in which the chains are unfolded. The present calculations should be particularly relevant to the study of the elastic properties of such materials, since extended-chain forms of polyethylene can have very high degrees of crystallinity ($\approx 95 \%$), with a consequent minimization of the amorphous contribution to the modulus.

Elastic constants of single crystals

The elastic anisotropy of a single crystal is defined in terms of the generalized Hooke's Law,[4]

$$\sigma_{ij} = \sum_k \sum_l c_{ijkl} e_{kl} \tag{1}$$

or

$$e_{ij} = \sum_k \sum_l s_{ijkl} \sigma_{kl} \tag{2}$$

where the subscripts i, j, k, l each have values of 1, 2 or 3, which are taken here to correspond to the directions of the crystal a, b and c axes respectively. The σ_{ij} and e_{kl} are tensor components of the stress and strain, respectively.

The c_{ijkl} and s_{ijkl} are 4th order tensor components of the elastic modulus and compliance, respectively.

Equations (1) and (2) are often written in the contracted forms,

$$\sigma_p = \sum_q c_{pq} e_q \qquad (3)$$

and

$$e_p = \sum_q s_{pq} \sigma_q \qquad (4)$$

respectively, where $p, q = 1, 2, 3 \ldots 6$. The p's and q's are obtained in terms of i, j, k, l by substituting 1 for 11, 2 for 22, 3 for 33, 4 for 23, 5 for 13 and 6 for 12. By definition[4], the following relations hold between the tensor and contracted forms of the elastic moduli and compliances,

$$c_{ijkl} = c_{pq} \text{ for all } p \text{ and } q \qquad (5)$$

and

$$s_{ijkl} = s_{pq} \text{ for } p, q = 1, 2 \text{ or } 3$$

$$2s_{ijkl} = s_{pq} \text{ for } p = 1, 2 \text{ or } 3 \text{ and } q = 4, 5 \text{ or } 6 \qquad (6)$$
$$4s_{ijkl} = s_{pq} \text{ for } p, q = 4, 5 \text{ or } 6$$

Noting the reciprocal relations $c_{pq} = c_{qp}$ and $s_{pq} = s_{qp}$, then it follows that in the most general case of lowest symmetry, twenty one modulus or compliance components are required to specify the elastic properties of the crystal. For crystals of orthorhombic symmetry this number reduces to nine[4], namely, c_{11}, c_{22}, c_{33}, c_{12}, c_{13}, c_{23}, c_{44}, c_{55} and c_{66} or s_{11}, s_{22}, s_{33}, s_{12}, s_{13}, s_{23}, s_{44}, s_{55} and s_{66}.

Average orientation of crystals in the bulk polymer

The orientation of a given orthorhombic crystal with respect to reference Cartesian axes within the bulk specimen is illustrated in *Figure 1*. The crystal axes are denoted by U_1, U_2 and U_3 which may be taken to coincide respectively with the a, b and c axes of the polyethylene crystal. The sample reference axes are denoted by X_1, X_2 and X_3 where, for the case of uniaxially drawn samples, the axis X_3 may be taken as the draw direction and X_1 as the normal to the sample plane (X_2X_3). The Eulerian angles θ and ϕ are the so-called polar and azimuthal angles, respectively, and define the orientation of the U_3 crystal axis with respect to the sample axes. The angle Ω specifies the rotation of the crystal around its own U_3 axis. The direction cosines between the crystal axes and the sample reference axes can be written in the following matrix forms:

$$
\begin{bmatrix}
\cos \psi_{11} & \cos \psi_{12} & \cos \psi_{13} \\
\cos \psi_{21} & \cos \psi_{22} & \cos \psi_{23} \\
\cos \psi_{31} & \cos \psi_{32} & \cos \psi_{33}
\end{bmatrix}
$$

$$
=
\begin{bmatrix}
\cos \theta \cos \phi \cos \Omega & -\cos \theta \cos \phi \sin \Omega & \sin \theta \cos \phi \\
\quad -\sin \phi \sin \Omega & \quad -\sin \phi \cos \Omega & \\
\cos \theta \sin \phi \cos \Omega & -\cos \theta \sin \phi \sin \Omega & \sin \theta \sin \phi \\
\quad +\cos \phi \sin \Omega & \quad +\cos \phi \cos \Omega & \\
-\sin \theta \cos \Omega & \sin \theta \sin \Omega & \cos \theta
\end{bmatrix} \qquad (7)
$$
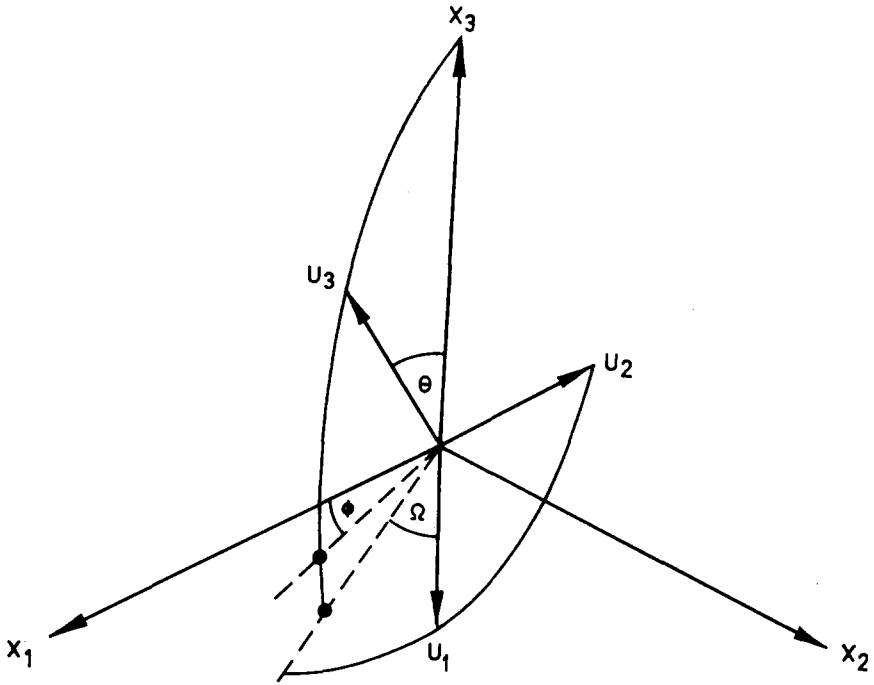
Figure 1

where ψ_{ij} is the angle between the X_i and U_j axes.

In evaluating the average orientation of all crystals within the bulk sample we consider, as usual, a distribution function $p(\theta, \phi, \Omega)$ where $p(\theta, \phi, \Omega) \sin \theta$ $d\theta \, d\phi \, d\Omega$ gives the probability of a crystal having axes lying in the angular range $\theta \to \theta + d\theta$, $\phi \to \phi + d\phi$ and $\Omega \to \Omega + d\Omega$. The distribution function is normalized such that

$$\int_{\Omega=0}^{2\pi} \int_{\phi=0}^{2\pi} \int_{\theta=0}^{\pi} p(\theta, \phi, \Omega) \sin \theta \, d\theta \, d\phi \, d\Omega = 1 \tag{8}$$

The average value of any function $f(\theta, \phi, \Omega)$ can then be written,

$$\overline{f(\theta, \phi, \Omega)} = \int_0^{2\pi} \int_0^{2\pi} \int_0^{\pi} f(\theta, \phi, \Omega) \, p(\theta, \phi, \Omega) \sin \theta \, d\theta \, d\phi \, d\Omega \tag{9}$$

Such averages are commonly referred to as orientation functions. The functions to be averaged in the present calculations are each multiples of separate functions of θ, ϕ and Ω so that,

$$\overline{f(\theta, \phi, \Omega)} = \overline{f(\theta) f(\phi) f(\Omega)} \tag{10}$$

The case of a uniaxially drawn sample corresponds to a random distribution over the azimuthal angle ϕ which may thus be taken to be independent of the distribution over θ and Ω. It follows that,

$$p(\theta, \phi, \Omega) = p(\phi) \, p(\theta, \Omega) = \frac{1}{2\pi} \times p(\theta, \Omega) \tag{11}$$

Hence from (9), (10) and (11)

$$\overline{f(\theta, \phi, \Omega)} = \frac{1}{2\pi} \int_0^{2\pi} f(\phi) \, d\Phi \int_0^{2\pi} \int_0^{\pi} f(\theta) f(\Omega) p(\theta, \Omega) \sin \theta \, d\theta \, d\Omega$$

$$= \overline{[f(\phi)]_R} \times \overline{f(\theta) f(\Omega)} \tag{12}$$

where $\overline{[f(\phi)]_R}$ is the value of $\overline{f(\phi)}$ for a random distribution over ϕ.

For an undrawn isotropic specimen the crystal orientations are randomly distributed with respect to θ, ϕ and Ω. In this case $p(\phi) = p(\Omega) = \frac{1}{2}\pi$ and $p(\theta) = \frac{1}{2}$. We thus obtain,

$$\overline{f(\theta, \phi, \Omega)} = \frac{1}{2} \int_0^{\pi} f(\theta) \sin \theta \, d\theta \times \frac{1}{2\pi} \int_0^{2\pi} f(\phi) \, d\phi \times \frac{1}{2\pi} \int_0^{2\pi} f(\Omega) \, d\Omega$$

$$= \overline{[f(\theta)]_R} \times \overline{[f(\phi)]_R} \times \overline{[f(\Omega)]_R} \tag{13}$$

Elastic constants of the bulk polymer

In evaluating the elastic constants of the anisotropic bulk polymer, account must be taken of contributions from both the crystalline and the amorphous phases. The question of main interest here concerns the structural arrangement of the two phases. For a model in which the two phases are coupled in series, the stress is uniform and the deformation or compliances of the two phases are additive. Following Nomura and coworkers[22] we may then write

$$\bar{S}_{pq} = X_c \bar{S}_{pq}^c + (1 - X_c) \bar{S}_{pq}^a \tag{14}$$

where X_c is the volume fraction crystallinity, S_{pq} is a compliance component of the bulk sample and S_{pq}^c and S_{pq}^a are the contributions to S_{pq} from the crystalline and amorphous regions respectively. The bars above the S's here indicate the averaging of contributions from all units within the respective phases. If, on the other hand, the two phases are coupled in parallel, then the strain is uniform and the moduli are additive, giving,

$$\bar{C}_{pq} = X_c \bar{C}_{pq}^c + (1 - X_c) \bar{C}_{pq}^a \tag{15}$$

where $\bar{C}_{pq}$ is a modulus component of the polymer and $\bar{C}_{pq}^c$ and $\bar{C}_{pq}^a$ are the crystal and amorphous contributions respectively. For most oriented polymers, the coupling between the two phases is probably intermediate between the series and parallel cases, as considered for example by Takayanagi[23]. The actual mode of coupling, and the related question of the amorphous contribution to the compliance or modulus components will be considered in future work. The present report concerns the evaluation of the crystal contribution to $\bar{C}_{pq}$ and $\bar{S}_{pq}$, namely the $\bar{C}_{pq}^c$ and $\bar{S}_{pq}^c$.

The calculation of $\bar{C}_{pq}^c$ and $\bar{S}_{pq}^c$ for the bulk specimen in terms of the c_{pq} or s_{pq} of the individual crystals involves 4th order tensor transformations from the crystal axes $(U_1 U_2 U_3)$ to the sample reference axes $(X_1 X_2 X_3)$. The calculations may be regarded as proceeding in two stages. Firstly the contribution to $\bar{C}_{pq}^c$ or $\bar{S}_{pq}^c$ of an individual crystal is considered, taking

account of its orientation with respect to the sample reference axes. Secondly the nett contribution from all crystals is obtained by averaging over their orientations according to equation (12). Assuming that the strain is the same on all crystals, the modulus components are additive and we obtain the so-called Voigt average,

$$\bar{C}^c_{mnop} = \sum_i \sum_j \sum_k \sum_l \overline{\cos \psi_{mi} \cos \psi_{nj} \cos \psi_{ok} \cos \psi_{pl}} \, c_{ijkl} \tag{16}$$

where m, n, o, p, i, j, k, l have values of 1, 2 or 3 ,and the bar above the direction cosines denotes averaging over all the different crystal orientations. If the stress is assumed to be the same on all crystals then the compliance constants are additive giving the Reuss average

$$\bar{S}^c_{mnop} = \sum_i \sum_j \sum_k \sum_l \overline{\cos \psi_{mi} \cos \psi_{nj} \cos \psi_{ok} \cos \psi_{pl}} \, s_{ijkl} \tag{17}$$

It is to be emphasized that the transformation represented by equations (16) and (17) must be effected by means of the tensor components c_{ijkl} and s_{ijkl}. The contracted constants c_{pq} and s_{pq} do not form the components of a tensor but can be obtained from the c_{ijkl} and s_{ijkl} by means of equations (5) and (6) respectively. Similarly $\bar{C}^c_{pq}$ and $\bar{S}^c_{pq}$ are related to the tensor components $\bar{C}^c_{mnop}$ and $\bar{S}^c_{mnop}$ by equations analogous to (5) and (6). The following results are yielded from equations (7), (12), (16) and (17).

Modulus Components

$$\begin{aligned}
\bar{C}^c_{33} = {} & \overline{\sin^4 \theta \cos^4 \Omega} \, c_{11} + \overline{\sin^4 \theta \sin^4 \Omega} \, c_{22} + \overline{\cos^4 \theta} \, c_{33} \\
& + \overline{\sin^2 \theta \cos^2 \theta \sin^2 \Omega} \, (2c_{23} + 4c_{44}) \\
& + \overline{\sin^2 \theta \cos^2 \theta \cos^2 \Omega} \, (2c_{13} + 4c_{55}) \\
& + \overline{\sin^4 \theta \sin^2 \Omega \cos^2 \Omega} \, (2c_{12} + 4c_{66})
\end{aligned} \tag{18}$$

$$\begin{aligned}
\bar{C}^c_{11} = {} & \bar{C}^c_{22} \\
= {} & \tfrac{3}{8} \overline{(1 - 2 \sin^2 \theta \cos^2 \Omega + \sin^4 \theta \cos^4 \Omega)} \, c_{11} \\
& + \tfrac{3}{8} \overline{(1 - 2 \sin^2 \theta \sin^2 \Omega + \sin^4 \theta \sin^4 \Omega)} \, c_{22} \\
& + \tfrac{3}{8} \overline{\sin^4 \theta} \, c_{33} \\
& + \tfrac{1}{8} \overline{(\sin^2 \theta \cos^2 \Omega + 3 \sin^2 \theta \cos^2 \theta \sin^2 \Omega)} \, (2c_{23} + 4c_{44}) \\
& + \tfrac{1}{8} \overline{(\sin^2 \theta \sin^2 \Omega + 3 \sin^2 \theta \cos^2 \theta \cos^2 \Omega)} \, (2c_{13} + 4c_{55}) \\
& + \tfrac{1}{8} \overline{(1 - \sin^2 \theta + 3 \sin^4 \theta \sin^2 \Omega \cos^2 \Omega)} \, (2c_{12} + 4c_{66})
\end{aligned} \tag{19}$$

$$\begin{aligned}
\bar{C}^c_{44} = {} & \bar{C}^c_{55} \\
= {} & \tfrac{1}{2} \overline{(\sin^2 \theta \cos^2 \Omega - \sin^4 \theta \cos^4 \Omega)} \, c_{11} \\
& + \tfrac{1}{2} \overline{(\sin^2 \theta \sin^2 \Omega - \sin^4 \theta \sin^4 \Omega)} \, c_{22} \\
& + \tfrac{1}{2} \overline{\sin^2 \theta \cos^2 \theta} \, c_{33} - \overline{\sin^2 \theta \cos^2 \theta \sin^2 \Omega} \, c_{23} \\
& - \overline{\sin^2 \theta \cos^2 \theta \cos^2 \Omega} \, c_{13} - \overline{\sin^4 \theta \sin^2 \Omega \cos^2 \Omega} \, c_{12} \\
& + \tfrac{1}{2} \overline{(1 - \sin^2 \theta \cos^2 \Omega - 4 \sin^2 \theta \cos^2 \theta \sin^2 \Omega)} \, c_{44} \\
& + \tfrac{1}{2} \overline{(1 - \sin^2 \theta \sin^2 \Omega - 4 \sin^2 \theta \cos^2 \theta \cos^2 \Omega)} \, c_{55} \\
& + \tfrac{1}{2} \overline{(\sin^2 \theta - 4 \sin^4 \theta \sin^2 \Omega \cos^2 \Omega)} \, c_{66}
\end{aligned} \tag{20}$$

$$\bar{C}_{13}^c = \bar{C}_{23}^c$$

$$
\begin{aligned}
= {} & \tfrac{1}{2}\,\overline{(\sin^2\theta\cos^2\Omega - \sin^4\theta\cos^4\Omega)}\,c_{11} \\
& + \tfrac{1}{2}\,\overline{(\sin^2\theta\sin^2\Omega - \sin^4\theta\sin^4\Omega)}\,c_{22} \\
& + \tfrac{1}{2}\,\overline{\sin^2\theta\cos^2\theta}\,c_{33} \\
& + \tfrac{1}{2}\,(1 - \overline{\sin^2\theta\cos^2\Omega} - 2\,\overline{\sin^2\theta\cos^2\theta\sin^2\Omega})\,c_{23} \\
& + \tfrac{1}{2}\,(1 - \overline{\sin^2\theta\sin^2\Omega} - 2\,\overline{\sin^2\theta\cos^2\theta\cos^2\Omega})\,c_{13} \\
& + \tfrac{1}{2}\,\overline{(\sin^2\theta - 2\,\sin^4\theta\sin^2\Omega\cos^2\Omega)}\,c_{12} \\
& - 2\,\overline{\sin^2\theta\cos^2\theta\sin^2\Omega}\,c_{44} - 2\,\overline{\sin^2\theta\cos^2\theta\cos^2\Omega}\,c_{55} \\
& - 2\,\overline{\sin^4\theta\sin^2\Omega\cos^2\Omega}\,c_{66}
\end{aligned}
\tag{21}
$$

$$
\begin{aligned}
\bar{C}_{12}^c = {} & \tfrac{1}{8}\,(1 - 2\,\overline{\sin^2\theta\cos^2\Omega} + \overline{\sin^4\theta\cos^4\Omega})\,c_{11} \\
& + \tfrac{1}{8}\,(1 - 2\,\overline{\sin^2\theta\sin^2\Omega} + \overline{\sin^4\theta\sin^4\Omega})\,c_{22} \\
& + \tfrac{1}{8}\,\overline{\sin^4\theta}\,c_{33} \\
& + \tfrac{1}{4}\,(3\,\overline{\sin^2\theta\cos^2\Omega} + \overline{\sin^2\theta\cos^2\theta\sin^2\Omega})\,c_{23} \\
& + \tfrac{1}{4}\,(3\,\overline{\sin^2\theta\sin^2\Omega} + \overline{\sin^2\theta\cos^2\theta\cos^2\Omega})\,c_{13} \\
& + \tfrac{1}{4}\,(3 - 3\,\overline{\sin^2\theta} + \overline{\sin^4\theta\sin^2\Omega\cos^2\Omega})\,c_{12} \\
& + \tfrac{1}{2}\,\overline{(\sin^2\theta\cos^2\theta\sin^2\Omega - \sin^2\theta\cos^2\Omega)}\,c_{44} \\
& + \tfrac{1}{2}\,\overline{(\sin^2\theta\cos^2\theta\cos^2\Omega - \sin^2\theta\sin^2\Omega)}\,c_{55} \\
& + \tfrac{1}{2}\,\overline{(\sin^2\theta + \sin^4\theta\sin^2\Omega\cos^2\Omega - 1)}\,c_{66}
\end{aligned}
\tag{22}
$$

Compliance Components

$$
\begin{aligned}
\bar{S}_{33}^c = {} & \overline{\sin^4\theta\cos^4\Omega}\,s_{11} + \overline{\sin^4\theta\sin^4\Omega}\,s_{22} + \overline{\cos^4\theta}\,s_{33} \\
= {} & + \overline{\sin^2\theta\cos^2\theta\sin^2\Omega}\,(2s_{23} + s_{44}) \\
& + \overline{\sin^2\theta\cos^2\theta\cos^2\Omega}\,(2s_{13} + s_{55}) \\
& + \overline{\sin^4\theta\sin^2\Omega\cos^2\Omega}\,(2s_{12} + s_{66})
\end{aligned}
\tag{23}
$$

$$\bar{S}_{11}^c = \bar{S}_{22}^c$$

$$
\begin{aligned}
= {} & \tfrac{3}{8}\,(1 - 2\,\overline{\sin^2\theta\cos^2\Omega} + \overline{\sin^4\theta\cos^4\Omega})\,s_{11} \\
& + \tfrac{3}{8}\,(1 - 2\,\overline{\sin^2\theta\sin^2\Omega} + \overline{\sin^4\theta\sin^4\Omega})\,s_{22} \\
& + \tfrac{3}{8}\,\overline{\sin^4\theta}\,s_{33} \\
& + \tfrac{1}{8}\,\overline{(\sin^2\theta\cos^2\Omega} + 3\,\overline{\sin^2\theta\cos^2\theta\sin^2\Omega})\,(2s_{23} + s_{44}) \\
& + \tfrac{1}{8}\,\overline{(\sin^2\theta\sin^2\Omega} + 3\,\overline{\sin^2\theta\cos^2\theta\cos^2\Omega})\,(2s_{13} + s_{55}) \\
& + \tfrac{1}{8}\,(1 - \overline{\sin^2\theta} + 3\,\overline{\sin^4\theta\sin^2\Omega\cos^2\Omega})\,(2s_{12} + s_{66})
\end{aligned}
\tag{24}
$$

$$\bar{S}_{44}^c = \bar{S}_{55}^c$$

$$
\begin{aligned}
= {} & 2\,\overline{(\sin^2\theta\cos^2\Omega - \sin^4\theta\cos^4\Omega)}\,s_{11} \\
& + 2\,\overline{(\sin^2\theta\sin^2\Omega - \sin^4\theta\sin^4\Omega)}\,s_{22} \\
& + 2\,\overline{\sin^2\theta\cos^2\theta}\,s_{33} - 4\,\overline{\sin^2\theta\cos^2\theta\sin^2\Omega}\,s_{23} \\
& - 4\,\overline{\sin^2\theta\cos^2\theta\cos^2\Omega}\,s_{13} - 4\,\overline{\sin^4\theta\sin^2\Omega\cos^2\Omega}\,s_{12} \\
& + \tfrac{1}{2}\,(1 - \overline{\sin^2\theta\cos^2\Omega} - 4\,\overline{\sin^2\theta\cos^2\theta\sin^2\Omega})\,s_{44} \\
& + \tfrac{1}{2}\,(1 - \overline{\sin^2\theta\sin^2\Omega} - 4\,\overline{\sin^2\theta\cos^2\theta\cos^2\Omega})\,s_{55} \\
& + \tfrac{1}{2}\,\overline{(\sin^2\theta} - 4\,\overline{\sin^4\theta\sin^2\Omega\cos^2\Omega})\,s_{66}
\end{aligned}
\tag{25}
$$

$$\bar{S}_{13}^c = \bar{S}_{23}^c$$
$$= \tfrac{1}{2} \overline{(\sin^2 \theta \cos^2 \Omega - \sin^4 \theta \cos^4 \Omega)} s_{11}$$
$$+ \tfrac{1}{2} \overline{(\sin^2 \theta \sin^2 \Omega - \sin^4 \theta \sin^4 \Omega)} s_{22}$$
$$+ \tfrac{1}{2} \overline{\sin^2 \theta \cos^2 \theta} \, s_{33}$$
$$+ \tfrac{1}{2} \overline{(1 - \sin^2 \theta \cos^2 \Omega - 2 \sin^2 \theta \cos^2 \theta \sin^2 \Omega)} s_{23}$$
$$+ \tfrac{1}{2} \overline{(1 - \sin^2 \theta \sin^2 \Omega - 2 \sin^2 \theta \cos^2 \theta \cos^2 \Omega)} s_{13}$$
$$+ \tfrac{1}{2} \overline{(\sin^2 \theta - 2 \sin^4 \theta \sin^2 \Omega \cos^2 \Omega)} s_{12}$$
$$- \tfrac{1}{2} \overline{\sin^2 \theta \cos^2 \theta \sin^2 \Omega} \, s_{44} - \tfrac{1}{2} \overline{\sin^2 \theta \cos^2 \theta \cos^2 \Omega} \, s_{55}$$
$$- \tfrac{1}{2} \overline{\sin^4 \theta \sin^2 \Omega \cos^2 \Omega} \, s_{66} \tag{26}$$

$$\bar{S}_{12}^c = \tfrac{1}{8} \overline{(1 - 2 \sin^2 \theta \cos^2 \Omega + \sin^4 \theta \cos^4 \Omega)} s_{11}$$
$$+ \tfrac{1}{8} \overline{(1 - 2 \sin^2 \theta \sin^2 \Omega + \sin^4 \theta \sin^4 \Omega)} s_{22}$$
$$+ \tfrac{1}{8} \overline{\sin^4 \theta} \, s_{33}$$
$$+ \tfrac{1}{4} \overline{(3 \sin^2 \theta \cos^2 \Omega + \sin^2 \theta \cos^2 \theta \sin^2 \Omega)} s_{23}$$
$$+ \tfrac{1}{4} \overline{(3 \sin^2 \theta \sin^2 \Omega + \sin^2 \theta \cos^2 \theta \cos^2 \Omega)} s_{13}$$
$$+ \tfrac{1}{4} \overline{(3 - 3 \sin^2 \theta + \sin^4 \theta \sin^2 \Omega \cos^2 \Omega)} s_{12}$$
$$+ \tfrac{1}{8} \overline{(\sin^2 \theta \cos^2 \theta \sin^2 \Omega - \sin^2 \theta \cos^2 \Omega)} s_{44}$$
$$+ \tfrac{1}{8} \overline{(\sin^2 \theta \cos^2 \theta \cos^2 \Omega - \sin^2 \theta \sin^2 \Omega)} s_{55}$$
$$+ \tfrac{1}{8} \overline{(\sin^2 \theta + \sin^4 \theta \sin^2 \Omega \cos^2 \Omega - 1)} s_{66} \tag{27}$$

Values of $\bar{C}_{66}^c$ and $\bar{S}_{66}^c$ calculated by the above procedures have been shown to be given by

$$\bar{C}_{66}^c = \tfrac{1}{2} (\bar{C}_{11}^c - \bar{C}_{12}^c) \tag{28}$$

and

$$\bar{S}_{66}^c = 2 (\bar{S}_{11}^c - \bar{S}_{12}^c) \tag{29}$$

for a random distribution over ϕ and all modulus or compliance components not given above vanish. Hence the sample is characterized by five independent moduli or compliances, as would be expected for a transversely isotropic bulk specimen. It should perhaps be emphasized that this transverse isotropy arises from the condition of a random distribution over ϕ. Furthermore the experimental observations[12, 17] that the a axis orientation function $[(3 \overline{\cos^2 \psi_{31}} - 1)/2]$ has larger negative values than the corresponding b axis orientation function in stretched polyethylene shows that $\overline{\cos^2 \psi_{31}} < \overline{\cos^2 \psi_{32}}$ or that $\overline{\sin^2 \theta \cos^2 \Omega} < \overline{\sin^2 \theta \sin^2 \Omega}$. These averages are independent of ϕ and, since they would be equal ($= \overline{\sin^2 \theta}/2$) for a random distribution over Ω, the observations show that the distribution over Ω cannot be random.

In the case where the individual crystals are transversely isotropic (i.e. hexagonal symmetry) then the nine independent elastic constants of the orthorhombic crystals reduces to five[4]. Thus if we put $c_{11} = c_{22}$, $c_{13} = c_{23}$, $c_{44} = c_{55}$, $c_{66} = (c_{11} - c_{12})/2$ and $s_{11} = s_{22}$, $s_{13} = s_{23}$, $s_{44} = s_{55}$, $s_{66} = 2(s_{11} - s_{12})$ then equations (18) to (27) above reduce to the corresponding equations of Ward[1] (which do not involve the angle Ω) for an aggregate of transversely isotropic units.

Unoriented isotropic polymer

For the unoriented polymer the crystals are randomly oriented with respect to the three angles θ, ϕ and Ω. Equations (13) and (16) then yield for the modulus components

$$\bar{C}_{11}^c = \bar{C}_{22}^c = \bar{C}_{33}^c = \tfrac{1}{5}(c_{11} + c_{22} + c_{33}) + \tfrac{1}{15}(2\,c_{12}$$
$$+ 2\,c_{13} + 2\,c_{23} + 4\,c_{44} + 4\,c_{55} + 4\,c_{66}) \qquad (30)$$

$$\bar{C}_{44}^c = \bar{C}_{55}^c = \bar{C}_{66}^c = \tfrac{1}{15}(c_{11} + c_{22} + c_{33} - c_{12} - c_{13} - c_{23})$$
$$+ \tfrac{1}{5}(c_{44} + c_{55} + c_{66}) \qquad (31)$$

$$\bar{C}_{12}^c = \bar{C}_{13}^c = \bar{C}_{23}^c = \tfrac{1}{15}(c_{11} + c_{22} + c_{33}) + \tfrac{4}{15}(c_{12} + c_{13} + c_{23})$$
$$- \tfrac{2}{15}(c_{44} + c_{55} + c_{66}) \qquad (32)$$

The compliance components follow from equations (13) and (17)

$$\bar{S}_{11}^c = \bar{S}_{22}^c = \bar{S}_{33}^c = \tfrac{1}{5}(s_{11} + s_{22} + s_{33}) + \tfrac{1}{15}(2\,s_{12} + 2\,s_{13}$$
$$+ 2\,s_{23} + s_{44} + s_{55} + s_{66}) \qquad (33)$$

$$\bar{S}_{44}^c = \bar{S}_{55}^c = \bar{S}_{66}^c = \tfrac{4}{15}(s_{11} + s_{22} + s_{33} - s_{12} - s_{13} - s_{23})$$
$$+ \tfrac{1}{5}(s_{44} + s_{55} + s_{66}) \qquad (34)$$

$$\bar{S}_{12}^c = \bar{S}_{13}^c = \bar{S}_{23}^c = \tfrac{1}{15}(s_{11} + s_{22} + s_{33}) + \tfrac{4}{15}(s_{12} + s_{13} + s_{23})$$
$$- \tfrac{1}{30}(s_{44} + s_{55} + s_{66}) \qquad (35)$$

Evaluation of crystal orientation functions from x-ray pole figure data

The x-ray pole figure technique enables the determination of the diffracted x-ray intensities as a function of the orientation of the sample with respect to the direction of the incident and diffracted beams. For a given Bragg angle, such data yields the angular distribution of the normals to the *hkl* planes with respect to the sample reference directions. Averages of the form $\overline{\cos^n \chi_{Q,hkl}}$ can thus be evaluated, where $\chi_{Q,hkl}$ is the angle between the given *hkl* plane normal and the sample reference direction Q (e.g. X_1, X_2 or X_3). For the present calculations the required averages correspond to $n = 2$ and $n = 4$ respectively.

In order to obtain the required crystal orientation functions in equations (18) to (27), we first consider the relationships between the experimentally determined $\overline{\cos^2 \chi_{Q,hkl}}$ and $\overline{\cos^4 \chi_{Q,hkl}}$ and the corresponding orientation functions for the three crystallographic axes. Following Wilchinsky[13], we take a unit vector $\mathbf{N}$ along the *hkl* plane normal and let e, f and g be the direction cosines of $\mathbf{N}$ with respect to U_1, U_2 and U_3 respectively. We then have

$$\mathbf{N} = e\mathbf{i} + f\mathbf{j} + g\mathbf{k} \qquad (36)$$

where $\mathbf{i}$, $\mathbf{j}$ and $\mathbf{k}$ are unit vectors along U_1, U_2 and U_3 respectively. If we now take $\mathbf{Q}$ as a unit vector along the sample reference direction Q, then

$$\cos \chi_{Q,hkl} = \mathbf{N} \cdot \mathbf{Q} = e\mathbf{i} \cdot \mathbf{Q} + f\mathbf{j} \cdot \mathbf{Q} + g\mathbf{k} \cdot \mathbf{Q}$$
$$= e \cos \psi_{Q1} + f \cos \psi_{Q2} + g \cos \psi_{Q3} \qquad (37)$$

where, as before, ψ_{Qi} is the angle between the sample reference direction Q and the U_i crystal axis.

Thus

$$\overline{\cos^2 \chi_{Q,hkl}} = e^2 \overline{\cos^2 \psi_{Q1}} + f^2 \overline{\cos^2 \psi_{Q2}} + g^2 \overline{\cos^2 \psi_{Q3}}$$
$$+ 2ef \overline{\cos \psi_{Q1} \cos \psi_{Q2}} + 2fg \overline{\cos \psi_{Q2} \cos \psi_{Q3}}$$
$$+ 2eg \overline{\cos \psi_{Q1} \cos \psi_{Q3}} \tag{38}$$

According to Wilchinsky[13], equation (38) is simplified by a consideration of the symmetry of the crystal unit cell. For a twofold rotation axis, then for every set of hkl planes there are equivalent planes $\overline{hk}l$, $\overline{h}k\overline{l}$ and $h\overline{kl}$. For polycrystalline materials the diffraction from these planes cannot be distinguished since they have the same spacing, the same Bragg angle and the same structure factor for scattering x-rays. The orthorhombic unit cell has three twofold rotation axes U_1, U_2 and U_3. The effect of the above multiplicity on the simplification of equation (38) can then be considered by rotating separately by 180° about U_1, U_2 and U_3 keeping e, f and g invariant and appropriately modifying the signs of the direction cosines between Q and U_1, U_2 or U_3 (equation 37). Evaluating $\cos^2 \chi_{Q,hkl}$ for each of the four equivalent orientations and averaging the resulting expressions the cross-terms vanish and equation (38) reduces to

$$\overline{\cos^2\chi_{Q,hkl}} = e^2 \overline{\cos^2\psi_{Q1}} + f^2 \overline{\cos^2\psi_{Q2}} + g^2 \overline{\cos^2\psi_{Q3}} \tag{39}$$

The orthogonality of the sample and crystal axes also results in the additional relationship

$$\overline{\cos^2 \psi_{Q1}} + \overline{\cos^2 \psi_{Q2}} + \overline{\cos^2 \psi_{Q3}} = 1 \tag{40}$$

It follows from (39) and (40) that $\overline{\cos^2 \psi_{Q1}}$, $\overline{\cos^2 \psi_{Q2}}$ and $\overline{\cos^2 \psi_{Q3}}$ can each be determined from measurements of $\overline{\cos^2 \chi_{Q,hkl}}$ on *two* different hkl reflections.

The corresponding equation for $\overline{\cos^4 \chi_{Q,hkl}}$ has not previously been considered and our derivation is based on the same procedures as for obtaining $\overline{\cos^2 \chi_{Q,hkl}}$. From equation (37) we have

$$\overline{\cos^4 \chi_{Q,hkl}} = e^4 \overline{\cos^4 \psi_{Q1}} + f^4 \overline{\cos^4 \psi_{Q2}} + g^4 \overline{\cos^4 \psi_{Q3}}$$
$$+ 6e^2f^2 \overline{\cos^2 \psi_{Q1} \cos^2 \psi_{Q2}} + 6e^2g^2 \overline{\cos^2 \psi_{Q1} \cos^2 \psi_{Q3}}$$
$$+ 6f^2g^2 \overline{\cos^2 \psi_{Q2} \cos^2 \psi_{Q3}} + 4e^3f \overline{\cos^3 \psi_{Q1} \cos \psi_{Q2}}$$
$$+ 4ef^3 \overline{\cos \psi_{Q1} \cos^3 \psi_{Q2}} + 4e^3g \overline{\cos^3 \psi_{Q1} \cos \psi_{Q3}}$$
$$+ 4eg^3 \overline{\cos \psi_{Q1} \cos^3 \psi_{Q3}} + 4f^3g \overline{\cos^3 \psi_{Q2} \cos \psi_{Q3}}$$
$$+ 4fg^3 \overline{\cos \psi_{Q2} \cos^3 \psi_{Q3}} + 12e^2fg \overline{\cos^2 \psi_{Q1} \cos \psi_{Q2} \cos \psi_{Q3}}$$
$$+ 12ef^2g \overline{\cos \psi_{Q1} \cos^2 \psi_{Q2} \cos \psi_{Q3}}$$
$$+ 12efg^2 \overline{\cos \psi_{Q1} \cos \psi_{Q2} \cos^2 \psi_{Q3}} \tag{41}$$

Equation (41) can now be simplified by symmetry considerations. As before, we rotate consecutively by 180° around the three twofold rotation axes U_1, U_2 and U_3 keeping e, f and g unchanged and modifying the signs of the $\cos \psi_{Qi}$ in equation (37). Averaging the values of $\cos^4 \chi_{Q,hkl}$ for the four

equivalent orientations, many of the cross terms vanish and equation (41) reduces to

$$\overline{\cos^4 \chi_{Q,hkl}} = e^4 \overline{\cos^4 \psi_{Q1}} + f^4 \overline{\cos^4 \psi_{Q2}} + g^4 \overline{\cos^4 \psi_{Q3}}$$
$$+ 6e^2f^2 \overline{\cos^2 \psi_{Q1} \cos^2 \psi_{Q2}} + 6e^2g^2 \overline{\cos^2 \psi_{Q1} \cos^2 \psi_{Q3}}$$
$$+ 6f^2g^2 \overline{\cos^2 \psi_{Q2} \cos^2 \psi_{Q3}} \tag{42}$$

The following relations also follow from the orthogonality equation (40)

$$\overline{\cos^4 \psi_{Q3}} = 1 - 2(\overline{\cos^2 \psi_{Q1}} + \overline{\cos^2 \psi_{Q2}}) + \overline{\cos^4 \psi_{Q1}}$$
$$+ \overline{\cos^4 \psi_{Q2}} + 2 \overline{\cos^2 \psi_{Q1} \cos^2 \psi_{Q2}} \tag{43}$$

$$\overline{\cos^2 \psi_{Q2} \cos^2 \psi_{Q3}} = \overline{\cos^2 \psi_{Q2}} - \overline{\cos^4 \psi_{Q2}} - \overline{\cos^2 \psi_{Q1} \cos^2 \psi_{Q2}} \tag{44}$$

$$\overline{\cos^2 \psi_{Q1} \cos^2 \psi_{Q3}} = \overline{\cos^2 \psi_{Q1}} - \overline{\cos^4 \psi_{Q1}} - \overline{\cos^2 \psi_{Q1} \cos^2 \psi_{Q2}} \tag{45}$$

Knowing $\overline{\cos^2 \psi_{Q1}}$ and $\overline{\cos^2 \psi_{Q2}}$ from equations (39) and (40), then it follows from equations (42) to (45) that each of the averages $\overline{\cos^4 \psi_{Q1}}$, $\overline{\cos^4 \psi_{Q2}}$, $\overline{\cos^4 \psi_{Q3}}$, $\overline{\cos^2 \psi_{Q1} \cos^2 \psi_{Q2}}$, $\overline{\cos^2 \psi_{Q1} \cos^2 \psi_{Q3}}$ and $\overline{\cos^2 \psi_{Q2} \cos^2 \psi_{Q3}}$ can be obtained from measurements of $\overline{\cos^4 \chi_{Q,hkl}}$ on *three* different *hkl* reflections.

For uniaxially drawn samples, corresponding to randomisation over ϕ, the following orthogonality relations are also obtained from equations (7),

$$\overline{\cos^2 \psi_{1i}} = \overline{\cos^2 \psi_{2i}} = \tfrac{1}{2}(1 - \overline{\cos^2 \psi_{3i}}) \tag{46}$$

$$\overline{\cos^4 \psi_{1i}} = \overline{\cos^4 \psi_{2i}} = \tfrac{3}{8}(1 - 2 \overline{\cos^2 \psi_{3i}} + \overline{\cos^4 \psi_{3i}}) \tag{47}$$

and

$$\overline{\cos^2 \psi_{1i} \cos^2 \psi_{1j}} = \overline{\cos^2 \psi_{2i} \cos^2 \psi_{2j}}$$
$$= \tfrac{1}{8} (1 + 3 \overline{\cos^2 \psi_{3i} \cos^2 \psi_{3j}} - \overline{\cos^2 \psi_{3i}} - \overline{\cos^2 \psi_{3j}}) \tag{48}$$

where $i, j = 1$, 2 or 3 and $i \neq j$. It follows from equations (46) to (48) that only one reference direction X_1, X_2 or X_3 need be considered in the subsequent calculations. Use of either of the other two reference directions will yield equivalent information. For convenience we will consider the reference direction $Q = X_3$ in the following analysis.

Polyethylene exhibits a large number of x-ray diffraction peaks[15] many of which arise from composite reflections from several *hkl* planes having similar Bragg angles. Five of the reflections give relatively well resolved peaks, and these arise from the 110, 200, 210, 020 and 211 crystal planes[15]. The 002 reflection has also been employed in recent orientation studies[3, 19], but it is very weak and not yet suitable[15] for quantitative studies using conventional equipment. Any three of the above reflections might be employed for the determination of the required orientation functions. By way of example, we will consider the use of the 200, 020 and 110 reflections.

607

200 *reflection*

For this reflection $e = 1$ and $f = g = 0$ and we obtain from equations (39) and (42)

$$\overline{\cos^2 \chi_{3,200}} = \overline{\cos^2 \psi_{31}} \qquad (49)$$

$$\overline{\cos^4 \chi_{3,200}} = \overline{\cos^4 \psi_{31}} \qquad (50)$$

020 *reflection*

In this case $f = 1$ and $e = g = 0$. Equations (39) and (42) then give

$$\overline{\cos^2 \chi_{3,020}} = \overline{\cos^2 \psi_{32}} \qquad (51)$$

$$\overline{\cos^4 \chi_{3,020}} = \overline{\cos^4 \psi_{32}} \qquad (52)$$

110 *reflection*

For this reflection we have $g = 0$ and from the data of Krigbaum and Roe[15] we obtain $e = \cos \Phi_{110} = 0.555$ and $f = \sin \Phi_{110} = 0.832$. Here Φ_{110} is the angle between the 110 plane normal and the a crystal axis. From equation (42) we obtain

$$
\begin{aligned}
\overline{\cos^4 \chi_{3,110}} &= e^4 \overline{\cos^4 \psi_{31}} + f^4 \overline{\cos^4 \psi_{32}} + 6e^2 f^2 \overline{\cos^2 \psi_{31} \cos^2 \psi_{32}} \\
&= 0.0947 \overline{\cos^4 \psi_{31}} + 0.480 \overline{\cos^4 \psi_{32}} + 1.278 \overline{\cos^2 \psi_{31} \cos^2 \psi_{32}} \quad (53)
\end{aligned}
$$

Many of the required orientation functions follow directly from equations (49) to (53)

$$\overline{\sin^2 \theta \cos^2 \Omega} = \overline{\cos^2 \psi_{31}} = \overline{\cos^2 \chi_{3,200}} \qquad (54)$$

$$\overline{\sin^2 \theta \sin^2 \Omega} = \overline{\cos^2 \psi_{32}} = \overline{\cos^2 \chi_{3,020}} \qquad (55)$$

$$\overline{\sin^2 \theta} = \overline{\cos^2 \psi_{31}} + \overline{\cos^2 \psi_{32}} = \overline{\cos^2 \chi_{3,200}} + \overline{\cos^2 \chi_{3,020}} \qquad (56)$$

$$\overline{\sin^4 \theta \cos^4 \Omega} = \overline{\cos^4 \psi_{31}} = \overline{\cos^4 \chi_{3,200}} \qquad (57)$$

$$\overline{\sin^4 \theta \sin^4 \Omega} = \overline{\cos^4 \psi_{32}} = \overline{\cos^4 \chi_{3,020}} \qquad (58)$$

$$
\begin{aligned}
\overline{\sin^4 \theta \sin^2 \Omega \cos^2 \Omega} &= \overline{\cos^2 \psi_{31} \cos^2 \psi_{32}} \\
&= 0.783 \, (\overline{\cos^4 \chi_{3,110}} - 0.0947 \overline{\cos^4 \chi_{3,200}} \\
&\quad - 0.480 \overline{\cos^4 \chi_{3,020}}) \quad (59)
\end{aligned}
$$

$$
\begin{aligned}
\overline{\sin^4 \theta} &= \overline{\cos^4 \psi_{31}} + \overline{\cos^4 \psi_{32}} + 2 \overline{\cos^2 \psi_{31} \cos^2 \psi_{32}} \\
&= 0.852 \overline{\cos^4 \chi_{3,200}} + 0.250 \overline{\cos^4 \chi_{3,020}} + 1.565 \overline{\cos^4 \chi_{3,110}} \quad (60)
\end{aligned}
$$

We also obtain with the aid of (43), (44) and (45)

$$
\begin{aligned}
\overline{\cos^4 \theta} &= \overline{\cos^4 \psi_{33}} \\
&= 1 - 2 \overline{(\cos^2 \chi_{3,200}} + \overline{\cos^2 \chi_{3,020})} + 0.852 \overline{\cos^4 \chi_{3,200}} + \\
&\quad + 0.250 \overline{\cos^4 \chi_{3,020}} + 1.565 \overline{\cos^4 \chi_{3,110}} \quad (61)
\end{aligned}
$$

$$\overline{\sin^2\theta\cos^2\theta\sin^2\Omega} = \overline{\cos^2\psi_{32}\cos^2\psi_{33}}$$
$$= \overline{\cos^2 X_{3,020}} - 0\cdot783\,\overline{\cos^4 X_{3,110}} + 0\cdot074\,\overline{\cos^4 X_{3,200}} - $$
$$- 0\cdot625\,\overline{\cos^4 X_{3,020}} \qquad (62)$$

$$\overline{\sin^2\theta\cos^2\theta\cos^2\Omega} = \overline{\cos^2\psi_{31}\cos^2\psi_{33}}$$
$$= \overline{\cos^2 X_{3,200}} - 0\cdot783\,\overline{\cos^4 X_{3,110}} + 0\cdot375\,\overline{\cos^4 X_{3,020}} - $$
$$- 0\cdot926\,\overline{\cos^4 X_{3,200}} \qquad (63)$$

$$\overline{\sin^2\theta\cos^2\theta} = \overline{\cos^2\psi_{32}\cos^2\psi_{33}} + \overline{\cos^2\psi_{31}\cos^2\psi_{33}}$$
$$= \overline{\cos^2 X_{3,200}} + \overline{\cos^2 X_{3,020}} - 1\cdot565\,\overline{\cos^4 X_{3,110}} - $$
$$- 0\cdot852\,\overline{\cos^4 X_{3,200}} - 0\cdot250\,\overline{\cos^4 X_{3,020}} \qquad (64)$$

Determination of orientation functions from coefficients of spherical harmonics

An alternative way of obtaining the required crystal orientation functions from x-ray pole figure data is based on the method of Roe and Krigbaum[14-16] for determining the crystallite orientation distribution. In this method the normalized distribution function is expressed in terms of a series of spherical harmonics. For uniaxially oriented samples in which the crystals have orthorhombic symmetry the expansion becomes[15]

$$p(\cos\theta,\Omega) = \sum_{l=0}^{\infty} A_{l0}P_l^0(\cos\theta) + 2\sum_{l=2}^{\infty}\sum_{m=2}^{l} A_{lm}P_l^m(\cos\theta)\cos m\Omega \qquad (65)$$

where $P_l^m(\cos\theta)$ is the *normalized* associated Legendre Polynomial and the summations are taken only over *even* values of the integers l and m. The coefficients A_{lm} are given by

$$A_{lm} = \frac{1}{2\pi}\int_0^{2\pi}\int_{-1}^{1} p(\cos\theta,\Omega)\,P_l^m(\cos\theta)\cos m\Omega\,d\cos\theta\,d\Omega$$

$$= \frac{1}{2\pi}\,\overline{P_l^m(\cos\theta)\,\cos m\Omega} \qquad (66)$$

In the present calculations we do not require to evaluate the complete distribution function but only the averages appearing in equations (18) to (27). From equation (66) and the definition of $P_l^m(\cos\theta)$ we obtain the following relations for the required orientation functions

$$\overline{\sin^2\theta\cos^2\Omega} = \frac{1}{3} - \frac{2\pi}{3}\left(\frac{2}{5}\right)^{\frac{1}{2}}[A_{20} - \tfrac{1}{2}(4!)^{\frac{1}{2}}A_{22}] \qquad (67)$$

$$\overline{\sin^2\theta\sin^2\Omega} = \frac{1}{3} - \frac{2\pi}{3}\left(\frac{2}{5}\right)^{\frac{1}{2}}[A_{20} + \tfrac{1}{2}(4!)^{\frac{1}{2}}A_{22}] \qquad (68)$$

$$\overline{\sin^2\theta} = \frac{2}{3} - \frac{4\pi}{3}\left(\frac{2}{5}\right)^{\frac{1}{2}}A_{20} \qquad (69)$$

609

2Q

$$\overline{\sin^4 \theta \cos^4 \Omega} = \frac{1}{5} - \frac{4\pi}{7}\left(\frac{2}{5}\right)^{\frac{1}{2}} A_{20} + \frac{2\pi}{7}\left(\frac{2}{5}\right)^{\frac{1}{2}} (4!)^{\frac{1}{2}} A_{22}$$

$$+ \frac{6\pi}{35}\left(\frac{2}{9}\right)^{\frac{1}{2}} A_{40} - \frac{2\pi}{105}\left(\frac{2}{9}\right)^{\frac{1}{2}}\left(\frac{6!}{2!}\right)^{\frac{1}{2}} A_{42}$$

$$+ \frac{2\pi}{840}\left(\frac{2}{9}\right)^{\frac{1}{2}} (8!)^{\frac{1}{2}} A_{44} \tag{70}$$

$$\overline{\sin^4 \theta \sin^4 \Omega} = \frac{1}{5} - \frac{4\pi}{7}\left(\frac{2}{5}\right)^{\frac{1}{2}} A_{20} - \frac{2\pi}{7}\left(\frac{2}{5}\right)^{\frac{1}{2}} (4!)^{\frac{1}{2}} A_{22}$$

$$+ \frac{6\pi}{35}\left(\frac{2}{9}\right)^{\frac{1}{2}} A_{40} + \frac{2\pi}{105}\left(\frac{2}{9}\right)^{\frac{1}{2}}\left(\frac{6!}{2!}\right)^{\frac{1}{2}} A_{42}$$

$$+ \frac{2\pi}{840}\left(\frac{2}{9}\right)^{\frac{1}{2}} (8!)^{\frac{1}{2}} A_{44} \tag{71}$$

$$\overline{\sin^4 \theta \sin^2 \Omega \cos^2 \Omega} = \frac{1}{15} - \frac{4\pi}{21}\left(\frac{2}{5}\right)^{\frac{1}{2}} A_{20} + \frac{2\pi}{35}\left(\frac{2}{9}\right)^{\frac{1}{2}} A_{40}$$

$$- \frac{2\pi}{840}\left(\frac{2}{9}\right)^{\frac{1}{2}} (8!)^{\frac{1}{2}} A_{44} \tag{72}$$

$$\overline{\sin^4 \theta} = \frac{8}{15} - \frac{32\pi}{21}\left(\frac{2}{5}\right)^{\frac{1}{2}} A_{20} + \frac{16\pi}{35}\left(\frac{2}{9}\right)^{\frac{1}{2}} A_{40} \tag{73}$$

$$\overline{\cos^4 \theta} = \frac{1}{5} + \frac{8\pi}{7}\left(\frac{2}{5}\right)^{\frac{1}{2}} A_{20} + \frac{16\pi}{35}\left(\frac{2}{9}\right)^{\frac{1}{2}} A_{40} \tag{74}$$

$$\overline{\sin^2 \theta \cos^2 \theta \sin^2 \Omega} = \frac{1}{15} + \frac{2\pi}{21}\left(\frac{2}{5}\right)^{\frac{1}{2}} A_{20} - \frac{2\pi}{42}\left(\frac{2}{5}\right)^{\frac{1}{2}} (4!)^{\frac{1}{2}} A_{22}$$

$$- \frac{8\pi}{35}\left(\frac{2}{9}\right)^{\frac{1}{2}} A_{40} - \frac{2\pi}{105}\left(\frac{2}{9}\right)^{\frac{1}{2}}\left(\frac{6!}{2!}\right)^{\frac{1}{2}} A_{42} \tag{75}$$

$$\overline{\sin^2 \theta \cos^2 \theta \cos^2 \Omega} = \frac{1}{15} + \frac{2\pi}{21}\left(\frac{2}{5}\right)^{\frac{1}{2}} A_{20} + \frac{2\pi}{42}\left(\frac{2}{5}\right)^{\frac{1}{2}} (4!)^{\frac{1}{2}} A_{22}$$

$$- \frac{8\pi}{35}\left(\frac{2}{9}\right)^{\frac{1}{2}} A_{40} + \frac{2\pi}{105}\left(\frac{2}{9}\right)^{\frac{1}{2}}\left(\frac{6!}{2!}\right)^{\frac{1}{2}} A_{42} \tag{76}$$

$$\overline{\sin^2 \theta \cos^2 \theta} = \frac{2}{15} + \frac{4\pi}{21}\left(\frac{2}{5}\right)^{\frac{1}{2}} A_{20} - \frac{16\pi}{35}\left(\frac{2}{9}\right)^{\frac{1}{2}} A_{40} \tag{77}$$

Roe and Krigbaum[14, 15] have devised methods for evaluating the co-efficients A_{lm} from x-ray data. Using well-resolved diffraction peaks, the required coefficients A_{20}, A_{22}, A_{40}, A_{42} and A_{44} may be obtained from equations which follow from those given by Roe and Krigbaum

$$Q_2^i = 2\pi\left(\frac{2}{5}\right)^{\frac{1}{2}} [A_{20}P_2^0(\cos \theta_i) + 2A_{22}P_2^2(\cos \theta_i) \cos 2\Phi_i] \tag{78}$$

$$Q_4^i = 2\pi \left(\frac{2}{9}\right)^{\frac{1}{2}} [A_{40}P_4^0(\cos \theta_i) + 2A_{42}P_4^2(\cos \theta_i) \cos 2\Phi_i$$
$$+ 2A_{44}P_4^4(\cos \theta_i) \cos 4\Phi_i] \qquad (79)$$

where i refers to a given hkl plane normal. θ_i and Φ_i are the polar and azimuthal angles of the ith plane normal with respect to the U_3 crystal axis, and their values have been tabulated[15] for sixteen hkl planes in polyethylene. The Q_l^i are coefficients in the expansion of the plane-normal orientation distribution $q_i(\cos \chi_i)$ which is determined from the diffracted intensities in the x-ray pole figure experiment[15]

$$q_i(\cos \chi_i) = \sum_{l=0}^{\infty} Q_l^i P_l(\cos \chi_i) \qquad (80)$$

Thus

$$Q_l^i = \int_{-1}^{1} q_i(\cos \chi_i) P_l(\cos \chi_i) \, d\cos \chi_i$$
$$= \overline{P_l(\cos \chi_i)} \qquad (81)$$

where χ_i is the angle between the ith plane normal and the sample reference direction X_3, and $P_l(\cos \chi_i)$ is the *normalized* Legendre Polynomial.

It follows from equations (78) and (79) that the coefficients A_{20} and A_{22} can be obtained from measurements on two different hkl reflections and that data on three reflections are required for the determination of A_{40}, A_{42} and A_{44}. This conclusion is consistent with the foregoing analysis. In the case of the 110, 200 and 020 reflections, we have related A_{20}, A_{22}, A_{40}, A_{42} and A_{44} to the appropriate $\overline{P_l(\cos \chi_i)}$ using equations (78), (79) and (81). After substituting in equations (67) to (77), we obtain equations identical with (54) to (64) respectively. Hence the two methods for obtaining the required orientation functions are consistent. In the latter method computer programmes may be devised which are similar to, but less complex, than those developed by Krigbaum and Roe[15]. The latter method may also be employed using overlapping diffraction peaks as described in Krigbaum and Roe's paper. However the former method seems more direct and less complex mathematically with the availability of well-resolved reflections.

Division of Materials Applications,
National Physical Laboratory
Teddington, Middlesex, UK   (*Received 26 May 1970*)

REFERENCES

1 Ward, I. M. *Proc. Phys. Soc.* 1962, **80**, 1176
2 Gupta, V. B. and Ward, I. M. *J. Macromol. Sci. (B)* 1967, **1**, 373
3 Gupta, V. B., Keller, A. and Ward, I. M. *J. Macromol. Sci. (B)* 1968, **2**, 139
4 Hearmon, R. F. S., 'An Introduction to Applied Anisotropic Elasticity', Oxford Univ. Press, 1961
5 Stein, R. S. and Read, B. E. *Applied Polymer Symposia* 1969, **8**, 255
6 Read, B. E. and Stein, R. S. *Macromolecules* 1968, **1**, 116
7 Flory, P. J. and Abe, Y. *Macromolecules* 1969, **2**, 335
8 Bondi, A. *J. Polym. Sci. (A-2)* 1967, **5**, 83

611

2Q*

9 Hosemann, R. *J. appl. Phys.* 1963, **34**, 25

10 Fischeı, E. W. *Kolloid Z.* 1969, **231**, 458

11 Wilchinsky, Z. W. *J. appl. Phys.* 1960, **31**, 1969

12 Hoshino, S., Powers, J., Legrand, D. G., Kawai, H., and Stein, R. S. *J. Polym. Sci.* 1962, **58**, 185

13 Wilchinsky, Z. W. *Advances in X-ray Analysis* (Eds. W. M. Mueller and M. Fay), Plenum Press, Denver 1963, **6**, 231

14 Roe, R. J. and Krigbaum, W. R. *J. Chem. Phys.* 1964, **40**, 2608

15 Krigbaum, W. R. and Roe, R. J. *J. Chem. Phys.* 1964, **41**, 737

16 Roe, R. J. *J. appl. Phys.* 1965, **36**, 2024

17 Fujino, K., Kawai, H., Oda, T., and Maeda, H., Proc. 4th Intern. Congr. Rheol., Providence, (1963), 1965, Part 3, p 501

18 Desper, C. R. and Stein, R. S. *J. appl. Phys.* 1966, **37**, 3990

19 Miyasaka, K. and Makishima, K. *J. Polym. Sci.* (*A*-2) 1967, **5**, 535

20 Odajima, A. and Maeda, T. *J. Polym. Sci.* (*C*) 1966, **15**, 55

21 Anand, J. N. *J. Macromol. Sci.* (*B*) 1967, **1**, 445

22 Nomura, S., Kawabata, S., Kawai, H., Yamaguchi, Y., Fukushima, A., and Takahara, H. *J. Polym. Sci.* (*A*-2) 1969, **7**, 325

23 Takayanagi, M. *Pure and Applied Chemistry* 1967, **15**, 555

Polymerization induced by gamma radiation of styrene under pressure*

G. B. GUARISE, G. PALMA, E. SIVIERO AND G. TALAMINI

The radiation-induced polymerization of styrene in both liquid and solid states has been investigated at high pressure in the temperature range 20–50°C. In the liquid phase pressure increases the polymerization rate as well as the molecular weight of the polymer in agreement with the results for chemically-initiated polymerization. In particular, activation volume and energy are consistent with literature values. When the monomer has undergone the liquid–solid transition a sudden increase in the polymerization rate takes place. However the latter falls again to negligible values for a comparatively small pressure excess above the solidification point. The mechanism of the solid-state polymerization in the high-rate region is considered in the light of existing theories.

INTRODUCTION

THE EFFECTS of high pressures on the liquid phase polymerization of styrene, proceeding both via free-radical[1–11] and ionic[12] processes have been extensively investigated. In these studies, in order to establish the pressure dependence of the propagation and termination rate constants, it was necessary to know the pressure-dependence of the rate of formation of the active centres.

The radiation-induced polymerization of styrene has been studied at ordinary pressure over a large temperature range, both below and above the melting point, in bulk and in solution. At low temperatures the liquid monomer, especially when dissolved in halogenated solvents, undergoes polymerization by an ionic mechanism[13–16]. At higher temperatures, however, this is so only when the monomer is super-dry[17–18], and, if special care is not taken to remove moisture, the polymerization occurs by a free-radical mechanism[14,16,19].

With high energy radiation used to initiate free-radical polymerization, at these temperatures, the pressure effect on the propagation and termination rate constants can be profitably investigated, as the rate of initiation is independent of pressure as well as of temperature[20].

At the same time, if the pressure is increased beyond the solidification point, the solid-phase polymerization, for which data are available at temperatures up to the normal melting point[14,21], can be investigated at higher temperatures.

EXPERIMENTAL

Materials

Styrene, supplied by Montecatini Edison SPA, was washed with 10% sodium thiosulphate solution, 10% sodium hydroxide solution and distilled water, dried with anhydrous magnesium sulphate and finally distilled three times under reduced nitrogen pressure.

Benzene, toluene and methanol, supplied by C. Erba, were distilled before use.

Apparatus

A 1/4 in diameter PTFE capsule, fitted with a conical PTFE lid, contained the monomer; it was inserted into a tungsten-carbide piston-cylinder apparatus as previously described[11]. Pressure was applied by means of a hydraulic press designed to minimise radiation attenuation.

A jacket, in which water from a thermostat circulated, surrounded the pressure cylinder; the temperature, measured with a thermocouple in close proximity to the sample, was controlled within $\pm 0\cdot1\,°C$.

Pressure calibration of the system was performed utilizing the liquid-solid transitions of carbon tetrachloride, aniline, chloroform, and carbon disulphide as given by Bridgman[22]. Uncertainty in the cell pressure value was checked to be less than 100 atm by repeated calibrations.

Volume change of the sample were measured with 2×10^{-3} mm sensitivity dial gauges symmetrically arranged with respect to the cylinder axis. The average of the two readings was taken as the piston displacement. Gauge indications were read during irradiation by means of a closed circuit television system.

Procedure

The cell which was already inserted in the pressure cylinder and brought up to the chosen temperature, was filled with monomer under nitrogen and then quickly pressurized to make it airtight. Then pressure was increased to the required value slowly, to avoid overheating which could lead to thermal polymerization[11].

If pressure is increased above the liquid-solid equilibrium value the liquid state, ('supercooled' liquid state), continues to exist till a certain excess pressure is reached. At this point a sudden pressure decrease to the equilibrium value is detected, followed by an isobaric volume change denoting the liquid-solid transition. Equilibrium pressures 3000 (20°C), 3700 (30°C), 4450 (40·5°C) and 5100 (51°C) kg cm^{-2} were obtained with this procedure.

Exposure to gamma rays of Co-60 was carried out at a dose rate of 3·2 rad s^{-1}, which was determined by means of the FRICKE solution inserted in the pressure cylinder in the radiation position. Owing to the small volume of the cylinder, several samples for each irradiation time were needed to allow the spectrophotometric determination (radiation yield $G(Fe^{3+}) = 15\cdot6$).

In the course of the irradiation the volume decrease of the sample was

followed by reading the piston displacement through the dial gauges. At the end of the run as quickly as possible, pressure was released and the PTFE cell was removed from the cylinder, weighed, and immersed in benzene. Since this procedure does not take more than 10–15 min the post-polymerization effect can be considered negligible.

The dissolved polymer was recovered by precipitation with large excess of methanol.

Assuming proportionality between volume decrement ΔV and polymerization conversion x throughout the course of the reaction, the ΔV values can be transformed into x values if the ratio $x_f/\Delta V_f$ is determined (index f refers to the final point). The ΔV values are proportional to the piston displacement Δl as in the investigated pressure ranges the piston cross section can be considered to be constant. Thus the initial fractional polymerization rate $R/[M]$ can be evaluated from the initial slope of the x time plot.

The lower limit of the investigated pressure range was chosen at about 2000 kg cm^{-2} in order to reduce error due to the pressure uncertainty, and to assure good tightness in the PTFE cell.

RESULTS AND DISCUSSION

(A) Bulk polymerization in liquid phase

Runs were carried out at 20, 30, 40·5 and 51 °C in the range of pressure corresponding to both liquid state and supercooled liquid state. The assumption of proportionality between conversion x and piston displacement Δl can be accepted in this set of experiments in view of the fact that the ratio $x_f/\Delta l_f$ found in the various runs is only slightly pressure-dependent and agrees with the corresponding values derived from the compressibility data of monomer and polymer[23]. Therefore the results can be reported in terms of conversion against time as shown in *Figure* 1 for some of the runs at 40·5 °C.

The characteristic autocatalytic behaviour is evident for $x > 0·1$; the linearity of the curves for $x < 0·1$ allows a sufficiently accurate value of the initial rate to be derived. In order to indicate the reproducibility two different runs at 3300 kg cm^{-2} are reported. The difference is negligible in the initial period and it can be ascribed to the uncertainty in the pressure value; and in the gravimetric determination of x_f, (0·2 g samples were used).

Thermal polymerization

By extending the well known scheme for the chemically initated free-radical process[24] to the polymerization induced by radiation, the following correlation can be derived for the overall rate:

$$R = (R_\gamma^2 + R_T^2)^{1/2} \tag{1}$$

R = polymerization rate; subscripts γ and T refer to radiation- and thermally-initiated polymerization respectively.
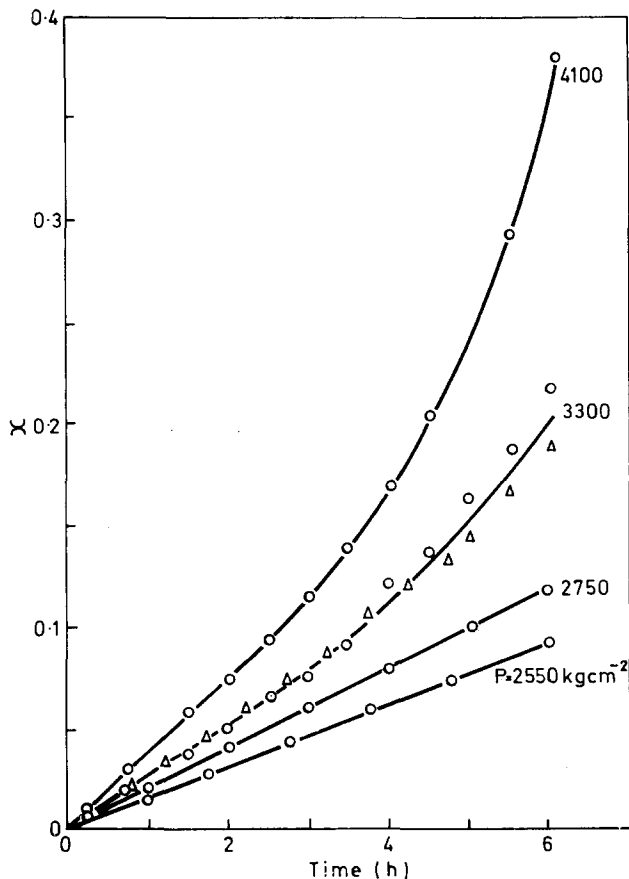
Figure 1 Rates of polymerization of styrene at 40·5⁰ in liquid phase

In equation (1) the therms R_γ and R_T are of the form:

$$R_\gamma = k_p[M](R_{i,\gamma}/k_t)^{1/2} \tag{2}$$

$$R_T = k_p(k_{i,T}/k_t)^{1/2} [M]^2 \tag{3}$$

k = rate constant; subscripts p, t, i refer to propagation, termination and initiation reactions respectively, $[M]$ = monomer concentration.

In turn, the rate of initiation induced by radiation is given by:

$$R_{i,\gamma} = 1·03 \times 10^{-12} IdG_R \tag{4}$$

$R_{i,\gamma}$ = initiation rate induced by radiation (mol $cm^{-3}s^{-1}$); d = monomer density (g cm^{-3}); I = dose rate (rad s^{-1}); G_R = radiolytic yield. For styrene $G_R = 0·69^{25}$.

Considering the above formulation it is evident that to obtain R_γ from R requires a knowledge of the contribution due to the thermal polymerization, as in equation (1). For this purpose runs were carried out without irradiation

616

of the sample. The results showed that thermal polymerization can be ignored in the explored temperature and pressure ranges. Conversions less than 3% were found at 4000 atm and 40·5°C for the usual reaction time of 6 h. This conclusion was checked by evaluation of R_T from the known values of activation volume ΔV_T^{+} and energy E_T^{+}, using the following correlations:

isothermal $\quad \Delta ln\, R_T = -\Delta V_T^{+}\, \Delta P/RT + 2\, \Delta ln[M]$ \hfill (5)

isobaric $\quad\quad \Delta ln R_T = -(E_T^{+}/R)\, \Delta(1/T) + 2\, \Delta ln[M]$ \hfill (6)

The following values were utilized: $\Delta V_T^{+} = -25\cdot8\,cm^3\,mol^{-1}$ and R_T (1 atm) $= 1\cdot27 \times 10^{-8}\,mol\ (cm^3 s)^{-1}$ at $80°C$[10]; $E_T^{+} = 21\,kcal\,mol^{-1}$[26]; $[M]/[M]_0 = 1\cdot178$ at $60°C$[27]; $[M]_0 = 8\cdot53 \times 10^{-3}\,mol\,cm^{-3}$ at $40\cdot5°C$ and
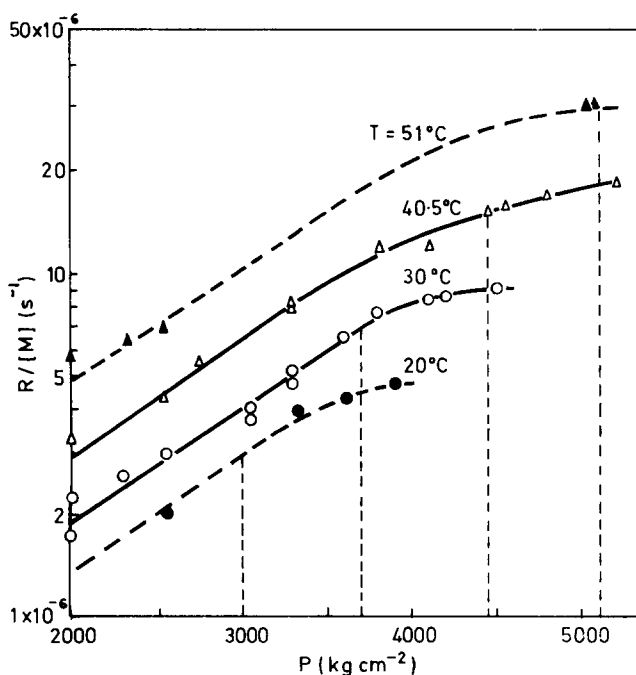
Figure 2 Pressure and temperature effects on the polymerization rate. Dashed vertical lines indicate the solidification point at the various temperatures

1 atm[28]. Then from equations (5) and (6) the value of R_T is $2\cdot78 \times 10^{-8}\,mol$ $(cm^3 s)^{-1}$ at 4000 atm and 40·5°C. Interpolation at the same pressure, of the experimental results at 40·5°C (Figure 2) gives $R = 1\cdot35 \times 10^{-7}$ and from equation (1) the value $R_\gamma = 1\cdot32 \times 10^{-7}\,mol\ (cm^3 s)^{-1}$ is obtained. The comparison of these values indicates that at least up 4000 atm and 40·5°C the thermal polymerization can be neglected, so that $R_\gamma = R$.

617

Effect of pressure on polymerization rate

The results of the liquid phase runs are shown in *Figure 2* as plots of $R/[M]$ against P. Most of them refer to the isotherms 30 and 40·5°C; a few values at 20 and 51°C are also reported for comparison. The plots indicate that the polymerization rate is an exponential function of pressure for most of the liquid region, whereas a tendency of the slope to decrease is observed at higher pressures, including the 'supercooled liquid region. In this respect it is worth noting that no discontinuity is apparent between the two regions.

In *Figure 3* the results obtained at 30°C are compared with Nicholson and Norrish's values for the polymerization of styrene photosensitized by
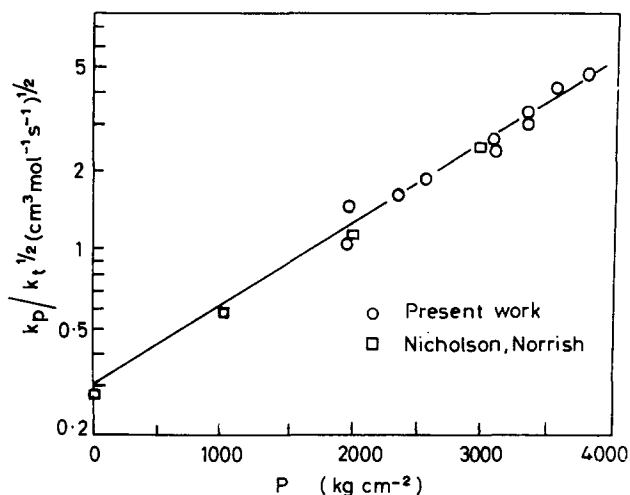
Figure 3 Comparison of $k_p/k_t^{1/2}$ values for polymerization at 30°C initiated by gamma radiation (present work) and photosensitized by benzoyl peroxide according to Nicholson and Norrish[3]

benzoyl peroxide[3]. The ratio $k_p/k_t^{1/2}$ was evaluated from the corresponding value of $R_\gamma/[M]$ and from equation (4); using density values derived from the data of the above Authors by means of the Tait equation[29], with $B = 1185$ kg cm^{-2}, $C = 0·216$.

The good agreement with Nicholson and Norrish's values supports the assumption of the same reaction mechanism in both cases. In addition, it gives *a posteriori* evidence for the negligible effect of pressure on the initiation reaction induced by gamma radiation.

The activation volume of the rate constant $k_p/k_t^{1/2}$ can be derived from[30]:

$$[\partial ln(k_p/k_t^{1/2})/\partial P]_T = -\Delta V^+/RT \tag{7}$$

The value $\Delta V^+ = -18\,\mathrm{cm^3 mol^{-1}}$ found in this case is in agreement with the corresponding value $\Delta V^+ = -19·5\,\mathrm{cm^3 mol^{-1}}$ for free-radical polymerization at 80°C in the pressure range 1–2650 atm[10].

618

Molecular weight

The intrinsic viscosity [η] in toluene at 25°C was determined for the polymer obtained at 40·5°C. From *Figure 4*, it appears that, in accordance with literature results, the molecular weight increases with increasing pressure for most of the examined pressure range, tending to constancy at higher pressure.

From the weight average molecular weight, derived from [η] = 5·21 × 10^{-5} M_w^{78} according to reference[16], an approximate value of the monomer
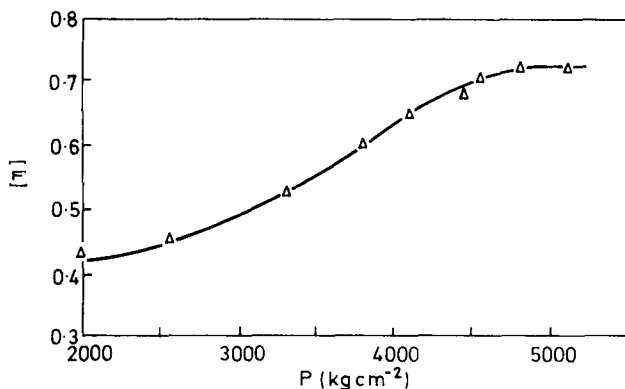
Figure 4 Intrinsic viscosity [η] (100 cm^{3}g^{-1}) of the polymers obtained at 40·5°C

transfer constant can be obtained. It appears to lie in the range from 0·7 × 10^{-4} to 0·5 × 10^{-4} with pressure change from 2000 to 4600 kg cm^{-2} and thus it compares well with the value of 10^{-4}, found at 80°C and up to 2650 atm for chemically-initiated polymerization[10].

Activation energy

Figure 5 shows the Arrhenius plot of $k_p/k_t^{1/2}$ at 2550 kg cm^{-2} for the liquid phase polymerization. From the plot the value of $\sim$7 kcal mol^{-1} is obtained, which agrees well with the value of 6·6 kcal mol^{-1} found by Matheson *et al*[31] at atmospheric pressure.

The agreement is further evidence that the polymerization in the liquid phase in the temperature range investigated, occurs by the free-radical mechanism.

(B) *Solid phase polymerization*

Runs with samples, which had passed through the liquid–solid transition, were followed dilatometrically, and were usually stopped after 6 h.

619
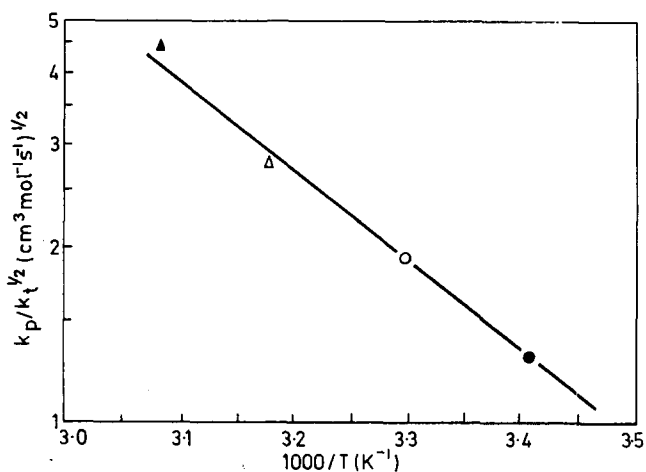
Figure 5 Arrhenius plot for the ratio $k_p/k_t^{1/2}$ at 2550 kg cm^{-2}
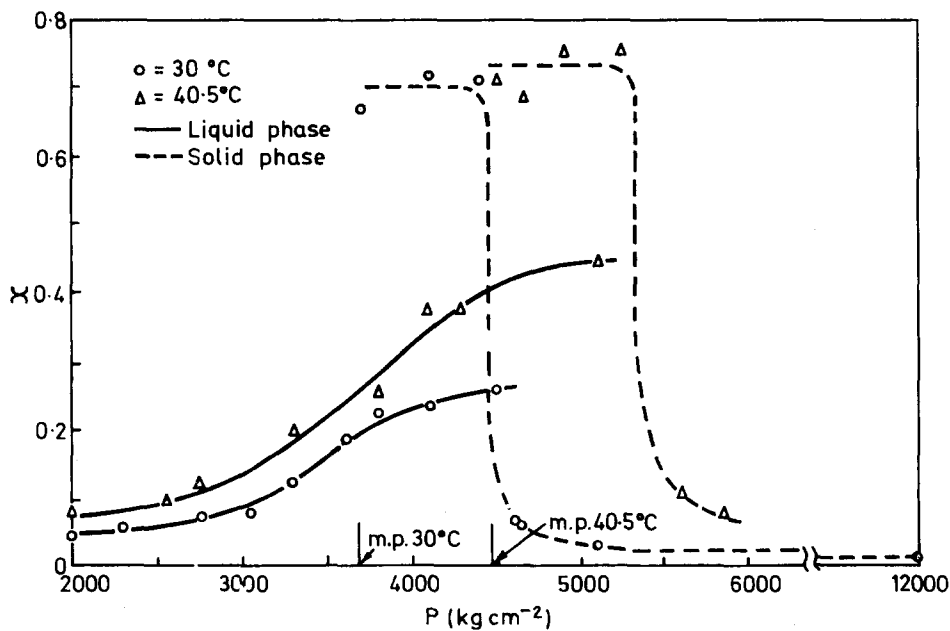
Figure 6 Pressure-dependence of polymerization conversion after 6 h irradiation at 30 and 40°C. The value at 12000 kg cm^{-2} refers to a 24 h irradiation

An indication of the influence of the physical state of the monomer on the polymerization rate is given by plots of final conversion, determined gravimetrically, against pressure for liquid, 'supercooled' and solid states. From the examples shown in *Figure 6*, a marked increase in rate appears to take place when the monomer changes from liquid to solid, followed by an equally marked decrease when a certain excess of pressure above the solidification value is attained. On the other hand no discontinuity is observed if the monomer passes from the liquid to the 'supercooled' state. A comparison of the molecular weights of the polymers obtained in the liquid and solid phases could not be made, because in the latter conditions an insoluble gel was always obtained. Higher polymerization rates in the solid phase than in the liquid phase are encountered with a number of monomers in normal pressure conditions[32], including styrene[14, 21]. Also in cases of solidification obtained by applying high pressure a similar behaviour has been observed[33].

The obvious conclusion to be drawn is that the arrangement of monomer molecules in the solid state, near the freezing point, is more susceptible to polymerization than that in the liquid state; and, in the present case, also than that in the 'supercooled' state, under similar conditions of temperature and pressure. At the same time however, it appears that a certain mobility of the monomer molecules is needed for the polymerization to occur in the solid state, as can be inferred from the high rate in the proximity of the melting point and the drastic reduction observed with further pressure increase.

In this context it may be pointed out that the 'explosive' thermally-initiated polymerization of styrene, which sets in when pressure, rapidly applied, passes through the solidification point[11], can be explained in these terms.

A better insight into the solid-state polymerization mechanism can be obtained from the shape of the dilatometric curves, although the transformation of the dilatometric data into conversion data is less accurate than in the liquid state, because of the considerably lower volume change caused by the polymerization, e.g. at $4100 \, \mathrm{kg \, cm^{-2}}$ and $30°C \, \Delta V \simeq 0.02 \, \mathrm{cm^3 \, g^{-1}}$ in solid and $\Delta V \simeq 0.08$ in liquid.

The accuracy of the dilatometric determinations was checked by comparing polymerization conversion curves, obtained dilatometrically, with a number of gravimetrically measured conversions corresponding to runs stopped at different times. From the results shown in *Figure 7*, the dilatometric curves seem to represent the conversion curves in shape with sufficient approximation, in spite of the rather large scatter of the gravimetric data. This is further supported by the thermocouple measurement of the sample temperature changes occurring during the run, also shown in *Figure 7*. A temperature increase is found to occur in the initial period, and also when the high rate sets in, while in the intermediate period a constant temperature is recorded.

Some of the dilatometric curves obtained at $40.5°C$ are shown in *Figure 8*. The relevant features are: an initial period in which a slow volume decrement

---

* Units: 1 k cal mol^{-1} $\equiv$ 4·19 kJ mol^{-1}

occurs almost linearly with time; an intermediate period characterized by nearly constant volume, and a final period in which volume rapidly decreases. The latter is not present when pressure is substantially higher than the melting point. This characteristic behaviour is also observed at the other temperatures investigated, but the length of the intermediate periods decreases as the temperature is raised (see *Figure 9*).

This form of kinetic curve has been obtained in the solid-state polymerization of other vinyl monomers[34, 35] and is in line with the general assumptions concerning the process mechanism[36, 37]. Since polymerization requires movement of monomer molecules from their lattice sites, it must be con-
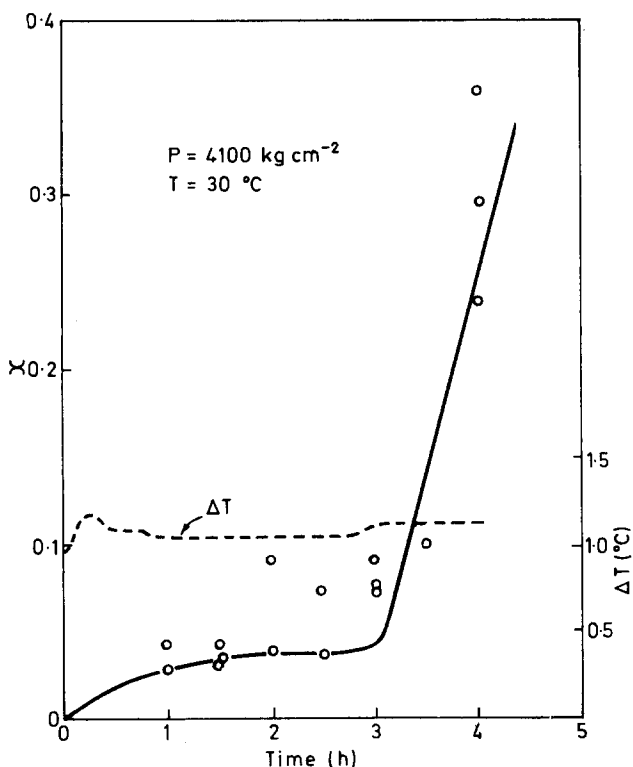
Figure 7 Polymer yield against time: continuous curve derived from the dilatometric data, assuming proportionality between piston displacement and conversion; points represents gravimetric determinations. Dashed line gives the corresponding temperature difference between sample and thermostat

sidered to occur almost exclusively at the crystal defects, where mobility is enhanced. Thus, initially, the active centres (of unidentified nature) which radiation produces homogeneously in the solid monomer, can promote polymerization only in limited portions of the crystal structure.

As irradiation is continued, new defects are progressively developed until

a critical value is attained at which the polymer formation gives rise to defect multiplication leading to a high rate of polymerization. Moreover, with increase of molecular mobility as temperature is raised smaller critical values are required and consequently the onset of acceleration occurs after shorter times. The opposite effect is conceivably to be expected from pressure increase, which may lead to polymerization suppression[38, 39], though an
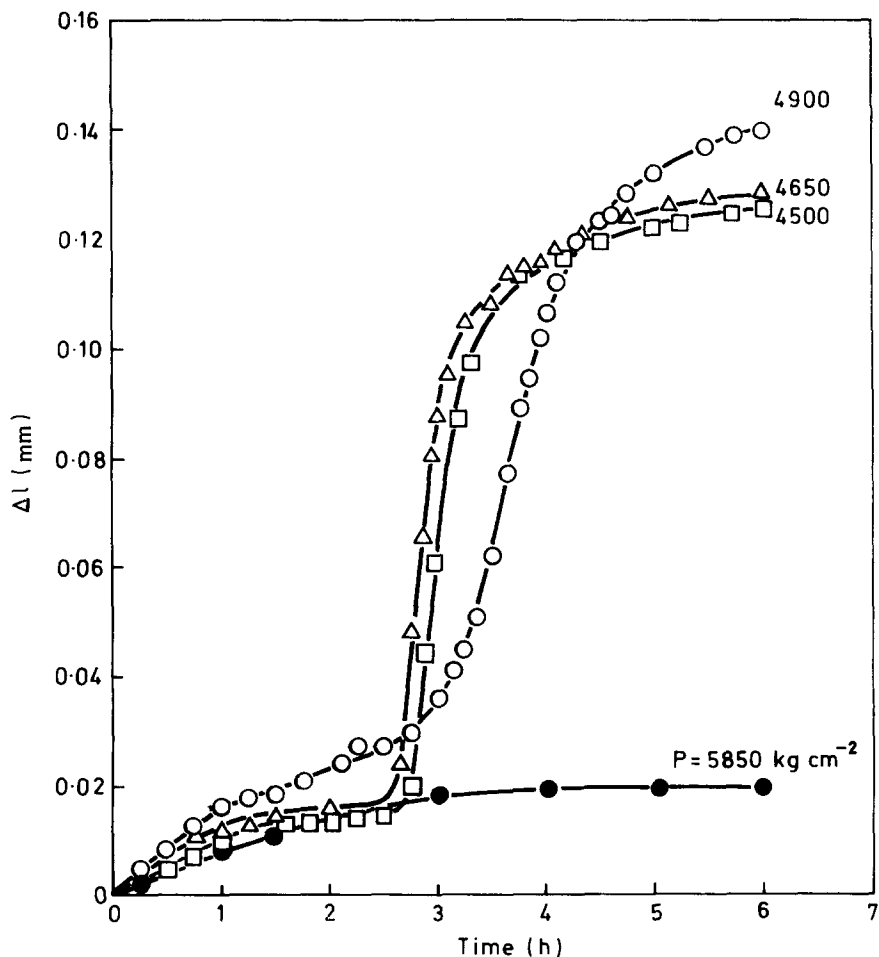
Figure 8 Pressure-dependence of the dilatometric curves for solid-state polymerization at 40·5°C

enhancement of the process is also possible, analogous to that displayed in the liquid state[40].

Several attempts have been made to describe quantitatively the kinetics of solid-state polymerization, assuming theoretical models for the propagation mechanism[37]. A treatment, based on the formation of 'hot' zones and on the 'critical' size of polymerization nuclei for thermodynamical stability[41],
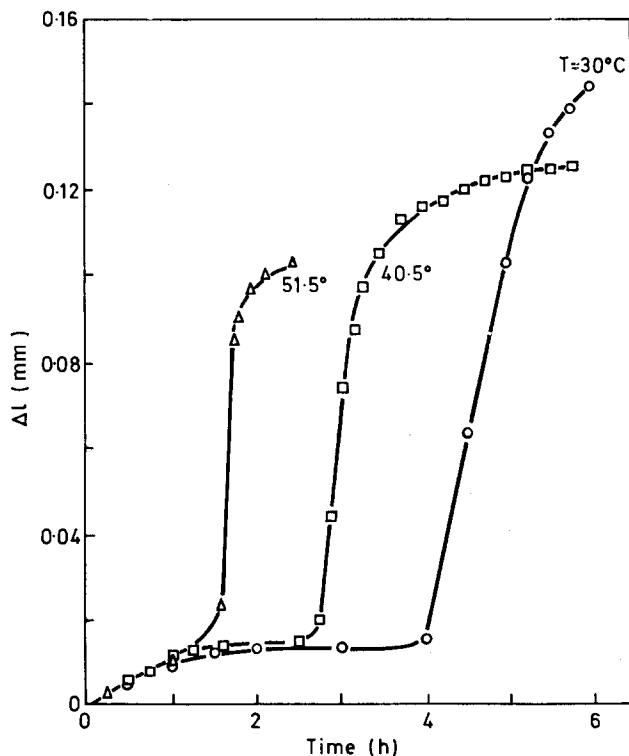
Figure 9 Temperature influence on the dilatometric curves at pressures near the melting point

leads to kinetic curves similar in shape to those of present work for an over-all process involving the successive steps: fast formation and decomposition of unstable polymer chains, annealing of unstable chains producing stable macromolecules representing 'super critical nuclei', formation and growth of 'supercritical' nuclei on crystal defects.

On this treatment, the first part of the curves represents the formation of unstable polymer which reaches a steady concentration. In the intermediate part 'supercritical' nuclei are slowly formed, and then polymerization takes place at the polymer-crystalline monomer interface with an autocatalytic character.

Istituto di Impianti Chimici e Centro di
Chimica delle Alte Temperature e
delle Alte Pressioni del CNR, Sez. I
Università di Padova;
Laboratorio di Fotochimica e Radiazioni
di Alta Energia del CNR,
Bologna, Sez. di Legnaro;
Centro di Ricerche Petrolchimiche,
Montecatini Edison,
Porto Marghera

REFERENCES

1 Gillham, R. C., *Trans. Faraday Soc.* 1950, **46**, 497
2 Merrett F. M. and Norrish R. G. W., *Proc. Royal Soc.* 1951, **A-206**, 309
3 Nicholson A. E. and Norrish R. G. W., *Disc. Faraday Soc.* 1956, **22**, 97
4 Walling C. and Pellon J., *J. Amer. Chem. Soc.* 1957, **79**, 4776
5 Walling C., *J. Polym. Sci.* 1960, **48**, 335
6 Toohey A. C. and Weale K. E., *Trans. Faraday Soc.* 1962, **58**, 2439
7 Zhulin V. M., Gonikberg M. G. and Zagorbinina V. N., *Dokl. Akad. Nauk*, 1961, **163** 106
8 Zhulin V. M., Gonikberg M. G. and Zagorbinina V. N., *Izv. An. Ser. Khim. SSSR*, 1966 827
9 Zhulin V. M., Gonikberg M. G. and Zagorbinina V. N., *Izv. An. Ser. Khim. SSSR* 1966 997
10 Guarise G. B., *Polymer, Lond.* 1966, **7**, 497
11 Guarise G. B. and Talamini G., Simposio Dinamica delle Reazioni Chimiche, CSC Vol. 5, CNR, Roma 1967, p 209
12 Zharov A. A., Berlin A. A. and Enikolopyan N. S., *J. Polym. Sci. (C)* 1967 **16**, 2313
13 Chapiro A. and Stannett V., *J. Chim. Phys.* 1959, **56**, 830
14 Amagi Y. and Chapiro A., *J. Chim. Phys.* 1962, **59**, 537
15 Sheinker A. P., Vakovieva M. K., Kristal'Nyi E. V. and Abkin A. D., *Dokl. Akad. Nauk* 1959, **124**, 632
16 Chen C. S. and Stamm R. F., *J. Polym. Sci.* 1962, **58**, 369
17 Ueno K., Hayashi K. and Okamura S., *J. Polym. Sci. (B)* 1965, **3**, 363
18 Potter R. C., Johnson C. L. and Metz D. J., *J. Polym. Sci., (A-1)* 1966, **4**, 419
19 Schneider C. and Swallow A. J., Proc. 2nd Tihany Symp. Radiation Chemistry, 1966, p 471
20 Fydelor P. J. and Charlesby A., *J. Polymer Sci. (C)* 1969, **16**, 4493
21 Chen C. S., *J. Polym. Sci.* 1962, **58**, 389
22 Bridgman P. W., *Phys. Rev.* 1914, **3**, 153; *Proc. Am. Acad. Arts Sci.* 1942, **74**, 399
23 Mazzi L., *Thesis*, Università di Padova, 1966
24 Mayo F. R., Gregg R. A. and Matheson M. S., *J. Amer. Chem. Soc* 1951, **73**, 1691
25 Chapiro A., 'Radiation Chemistry of Polymeric Systems', High Polymers Vol. XV, Interscience, New York 1962, p 131
26 Flory P. J., 'Principles of Polymer Chemistry', Cornell University Press, Ithaca, 1964, p 132
27 Weale K. E., Private communication
28 Blout E. R. and Mark H., 'Monomers', Interscience, New York 1949, p 50
29 Weale K. E., 'Chemical Reactions at High Pressures', Spon, London, 1967, p 20
30 Weale K. E., 'Chemical Reactions at High Pressures,' Spon, London, 1967, p 135
31 Matheson M. S., Auer E. E., Bevilacqua E. B. and Hart E. J., *J. Amer. Chem. Soc.* 1951, **73**, 1700
32 Chapiro A., 'Actions Chimiques et Biologiques des Radiations', (Haissinsky M. Ed.), Masson, Paris 1966, Series X, p 191
33 Brown D. W. and Wall L. A., 'Preprints of the Meeting of Am. Chem. Soc., vol. 5, Chicago 1964, p 907
34 Tüdös F., Proc. of 2nd Tihany Symp. on Radiation Chemistry, 1966, p 471
35 Országh A. and Zurakowska-Orszagh J., Proc. 2nd Tihany Symp. on Radiation Chemistry, 1966, p 583
36 Bamford C. H. and Eastmond G. C., *Quart. Rev.* 1969, **23**, 271
37 Tabata Y., 'Vinyl Polymerization', Vol. 1, part II, (Ham G. E. Ed.), Dekker, New York 1969, p 305
38 Bamford C. H., Eastmond G. C., and Ward J. C., *Proc. Roy. Soc., A* 1963, **271**, 357
39 Suzuki T., Tabata Y., Oshima K., *J. Polym. Sci. (C)* 1967, **16**, 1821
40 Tabata Y., Miyairi T., Katsura S., Ito Y. and Oshima K., Proc. Symp. on Large Rad. Sources for Ind. Process, Munich 1969, p 233
41 Papissov I. M. and Kabanov V. A., *J. Polym. Sci. (C)* 1967, **16**, 911

625

Note to the Editor

Unperturbed dimensions of poly (1-butene oxide)

C. BOOTH and R. ORME

Poly(1-butene oxide) was prepared by means of the zinc diethyl and water catalyst under conditons similar to those described for the preparation of poly(propylene oxide)[1]. Monomer was purified by fractional distillation from calcium hydride (b.p. 62·0°C at 745 mmHg), and was polymerized at 150°C in dioxan at a concentration of 3·0M with concentrations of zinc diethyl and water of 0·3M. The intrinsic viscosities in benzene at 25°C of the polymers so prepared exceeded 5 dl g^{-1} and the molecular weight distributions were very wide (similar to those found for poly(propylene oxide)[1]). Polymer samples with intrinsic viscosities near 2 dl g^{-1}, which were more suited to our purposes, were produced by ultrasonic degradation of the high molecular weight material.

Polymers were fractionated by addition of methanol to dilute solutions in benzene. Fractions comprising 5 to 10 wt% of the polymer were obtained; separation was into liquid phases. The fractions were characterized by dilute solution viscometry with good solvents benzene, *n*-butanol and hexane at 25°C, and with poor solvent *iso*-propanol at 30°C; by light scattering from solutions in hexane at 25°C; and by gel permeation chromatography of solutions in trichlorobenzene at 90°C. The methods used in viscometry and light scattering follow those described earlier[2]. Refractive index increments at 25°C for high molecular weight poly(1-butene oxide) found during this investigation are −0·040, −0·078, 0·101, 0·113 cm^3 g^{-1} for solutions in benzene, chlorobenzene, hexane and ethyl acetate respectively. Gel permeation chromatographs were analysed by use of the polystyrene standards calibration: a calibration curve for poly(1-butene oxide) was roughly parallel to the standard calibration curve.

Properties of poly(1-butene oxide) fractions are listed in *Table 1*. The

Table 1 Properties of fractions of poly(1-butene oxide)

Fraction	Weight-average molecular weight $10^{-6} \times \bar{M}_w$	Molecular weight ratio $\bar{M}_w/\bar{M}_n$	Intrinsic viscosity $[\eta]$ (dl g^{-1})			
			Benzene 25°C	Hexane 25°C	n-Butanol 25°C	i-Propanol 30°C
1	1·17	2·1	5·32	3·43	2·67	1·06
2	0·88	1·7	4·32	2·87	2·30	0·92
3	0·73	2·1	3·87	2·78	2·12	0·88
4	0·67	1·9	3·50	2·47	1·91	0·87
5	0·55	1·8	3·08	2·15	1·72	0·79
6	0·40	1·8	2·48	1·71	1·51	0·68
7	0·24	1·5	1·73	1·22	1·00	0·52
8	0·18	1·5	1·13	0·77	0·67	0·39
9	0·082	1·4	0·80	0.58	0·48	0·33
10	0·055	1·3	0·60	0·44	0·38	0·26

molecular weight distributions of the fractions are wide and vary from fraction to fraction, reflecting the inefficiency of a single stage fractionation process when applied to polymers of very wide molecular weight distribution. Accordingly the parameters of the Mark-Houwink equation

$$[\eta] = K \, \bar{M}_v^{\,v} \tag{1}$$

were evaluated from the weight-average molecular weight $\bar{M}_w$ and the molecular weight ratio $\bar{M}_v/\bar{M}_w$ (determined by gel permeation chromatography) by a method of successive approximations to parameter v. Values of K and v are listed in *Table 2*.

Values of $[\eta] \, \overline{M}_v^{-\frac{1}{2}}$ for the poor solvent are constant and yield[3] a value of $K_0 = \phi_0 \, (\overline{S_0^2}/M)^{3/2}$ of 0·11 cm^3 g^{-1}. We note that no correction for polydispersity is required since we use $\overline{M}_v$ (i.e. $\overline{M}_w^{\frac{1}{2}}$) in our evaluation of K_0.

Table 2 Mark-Houwink parameters for poly(1-butene oxide)

Solvent	v	K
Benzene, 25°C	0·75	1·59 × 10^{-4}
Hexane, 25°C	0·73	1·43 × 10^{-4}
n-Butanol, 25°C	0·69	1·96 × 10^{-4}
iso-Propanol, 30°C	0·50	1·11 × 10^{-3}

A value[4] of ϕ_0 of 42 × 10^{23} g^{-1} leads to a value of $(\overline{S_0^2}/M)^{\frac{1}{2}}$ of 0·30 Å*. Within the assumption of a Gaussian chain, the corresponding ratio for the mean square end to end distance $(\overline{r_0^2}/M)^{\frac{1}{2}}$ is 0·73 Å, and the characteristic ratio of this dimension to that of the freely jointed chain[5] is $(\overline{r_0^2/r_{0f}^2})^{\frac{1}{2}} = 1·71$. This figure compares favourably with that obtained by Kurata *et al*[6] by similar methods, and is to be further compared with the characteristic ratios for poly(ethylene oxide)[5] and poly(propylene oxide)[7] of 1·55 and 1·62 respectively.

Plots[8] of $[\eta] \, M_v^{-\frac{1}{2}}$ against $M_v^{\frac{1}{2}}$ for the good solvents are curved, after the manner found for poly(ethylene oxide)[5], and cannot be used to evaluate K_0. Attempts to use other equations[9] also proved unsuccessful.

Chemistry Department
University of Manchester   C. Booth

Science Department
Stockport College of Technology   R. Orme

* 1 Å = 0·1 nm

REFERENCES

1 Booth, C., Higginson, W. C. E. and Powell, E., *Polymer Lond.* 1964, **5**, 479
2 Allen, G., Booth, C. and Price, C. *Polymer Lond.* 1966, **7**, 167
3 Flory, P. J., 'Principles of Polymer Chemistry,' Cornell Univ. Press, Ithaca, New York, 1953
4 Pyun, C. W. and Fixman, M., *J. Chem. Phys.* 1965, **42**, 3838
5 Beech, D. R., and Booth, C. *J. Polym. Sci.*, (*A*–2), 1969, **7**, 575
6 Matsushima, M., Fukatsu, M. and Kurata, M. *Bull. Chem. Soc. Japan.* 1968, **41**, 2570
7 Allen, G., Booth, C. and Price, C., *Polymer Lond.* 1967, **8**, 397
8 Stockmayer, W. H. and Fixman, M. *J. Polym. Sci.* (*C*), 1963, **1**, 137
9 Berry, G. C., *J. Chem. Phys.* 1967, **46**, 1338

ESR study on molecular motion of peroxy radicals of polytetrafluoro-ethylene

S. Moriuchi, M. Nakamura*, S. Shimada, H. Kashiwabara and J. Sohma

Temperature variations of the line shapes of e.s.r. spectra from the peroxy radicals of polytetrafluoroethylene (PTFE) were investigated in detail and the results were quantitatively analysed based on Kneubühl's theory on the line shape. It was found that there were two kinds of rapid molecular motions, of which the correlation times were about 10^{-9} s, for the peroxy radicals of PTFE; one was the rotational motion related to the peroxy chain radical, the other was the three dimensional motion associated with the peroxy end radical. The activation energies of these molecular motions were estimated as 0·52 kcal/mol and 0·26 kcal/mol for the rotational motion and the three dimensional motion, respectively. Origins of such rapid motions were discussed in connection with the other molecular motions of polymers, which were found by other experimental methods.

INTRODUCTION

It has been established that broad-line n.m.r. is a useful experimental technique to study molecular motion of polymers[1]. Although e.s.r. is similar in principle to n.m.r., a few e.s.r. studies on molecular motion of polymers have been performed[2,3]. Successful application of e.s.r. to molecular motion of polymers supplies interesting information on molecular motion in a much shorter time range than can be obtained by the conventional techniques[4], such as mechanical or dielectric measurements or n.m.r. This is because averaging out of anisotropic parameters of e.s.r., which are usually of the order of 10^8 cps, would require a faster molecular motion than 10^{-8} s in terms of correlation time. Moreover, one can tell what parts of the polymer molecules are responsible for such rapid motion which causes changes in the e.s.r. line shape, because a radical to which the e.s.r. spectrum is ascribed can be identified by analysis of the spectrum.

Recently interesting results were reported by Siegel and Hedgpeth[5] and Iwasaki and Sakai[6] on the e.s.r. spectrum of the peroxide radical of polytetrafluoroethylene (PTFE). They found that an apparent anisotropy of the g factor of the e.s.r. spectrum of the peroxide radical of PTFE is inverted when the temperature is raised from 77 K to the room temperature. The e.s.r. spectrum observed at 77 K has the strongest peak at the higher field side and the weakest at the lower side. This means that the strongest peak corresponds to the smallest component among the three principal values of the g tensor. On the other hand the spectrum observed at the room temperature has the strongest peak at lower field, which means that the

---

* Present address: Japan Victor Co., Yokohama, Japan

strongest peak should be associated with the largest principal value of the g tensor. Iwasaki and Sakai explained the apparent inversion of the g anisotropy by assuming a rapid rotation of the radical about an axis parallel to the component of the g tensor. This explanation seemed authentic but their argument was rather qualitative and lacked a quantitative and detailed treatment. In this paper we will report the more detailed research and quantitative analyses of the temperature changes of the e.s.r. spectra of the peroxy radicals of PTFE and present information on the molecular motions of PTFE.

EXPERIMENTAL

Samples used in the experiments were Teflon film supplied by Nippon Valqua Industries, Ltd. After evacuation for 24h at 10^{-3}mmHg the samples were irradiated by γ rays from Co-60 at room temperature. The total dose was about 30 Mrad. The sample was exposed to air and heat-treated for several hours at 200°C (the sample A). The major component of the radical produced by such treatment in the sample A was the peroxy radical of the polymer chain[5, 6], (the peroxy chain radical):

$$
\begin{array}{ccc}
& \text{O·} & \\
& | & \\
\text{F} & \text{O} & \text{F} \\
| & | & | \\
-\text{C}-\text{C}-\text{C}- \\
| & | & | \\
\text{F} & \text{F} & \text{F}
\end{array}
$$
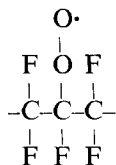
Following the treatment of Siegel and Hedgpeth[5] the scission-type radicals of PTFE were produced. The sample A was evacuated again and then irradiated with high pressure u.v. lamp (Toshiba HP-100). It has been demonstrated that scission of PTFE is caused by u.v. light and the scission radical

$$
\begin{array}{cc}
\text{F} & \text{F} \\
| & | \\
\sim\text{C}-\text{C·} \\
| & | \\
\text{F} & \text{F}
\end{array}
$$
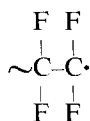
is formed[5]. The peroxy radicals of the scission type (the peroxy end radicals),

$$
\begin{array}{cc}
\text{F} & \text{F} \\
| & | \\
\sim\text{C}-\text{COO·,} \\
| & | \\
\text{F} & \text{F}
\end{array}
$$
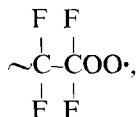
were formed by exposure of the scission radicals to air. The sample, which was treated like this and contained mainly the peroxy radical at the chain end, was named sample B. The e.s.r. spectra were taken using a JEOL X band spectrometer (Model JES-3) equipped with 100 kc modulation and the cooling system designed in our laboratory. The temperatures of the samples in the microwave cavity were controlled from 88 K to room temperature within an error of ± 1°C by the cooling system which circulated the dry

nitrogen gas through the liquid nitrogen containers. The e.s.r. spectra were observed at 77K using a dewar. The g factors were experimentally evaluated with reference to that of the Mn^{2+} ion.

RESULTS AND ASSIGNMENT

Sample A

The e.s.r. spectra observed from the sample A at room temperature and 77K are shown in *Figure 1*. Although the resolution of the X-band spectrum, which was observed at room temperature and is reproduced in *Figure 1a*, is poorer than that of the corresponding K-band spectrum obtained by Iwasaki and Sakai[6], one can reasonably separate the X-band spectrum into the two
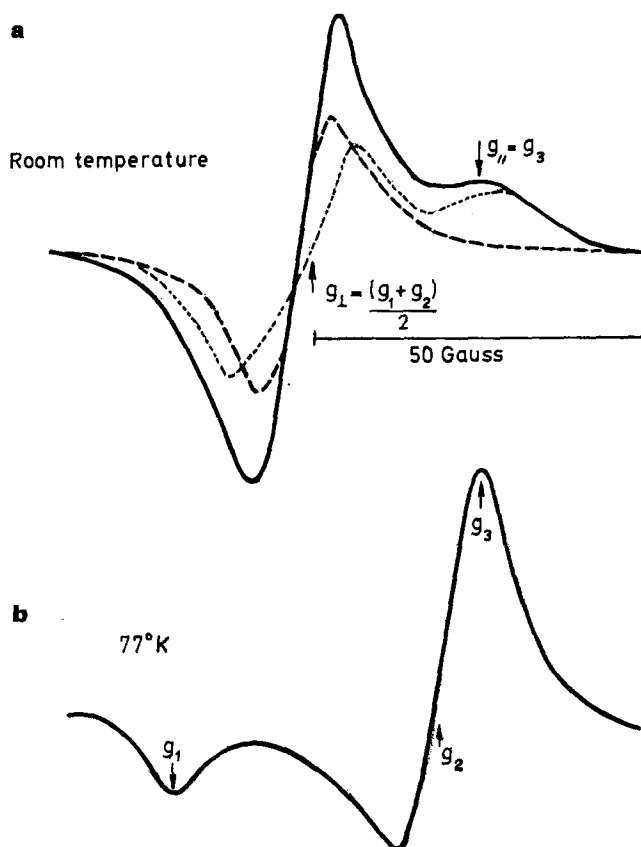
Figure 1 E.s.r. spectra of peroxy radicals in γ-irradiated PTFE. Upper pattern (a) is a spectrum observed at room temperature; the spectrum is decomposed into the two components. Lower pattern (b) is that observed at 77K. Experimentally determined values of the g factors are indicated in the figure

632

components, as shown in *Figure 1a*, by taking the Iwasaki–Sakai interpretation. The spectrum, which was observed at 77 K in the X-band and is reproduced in *Figure 1b*, has no satellite appearing in the corresponding K-band spectrum by Iwasaki and Sakai, but an anisotropic *g* tensor was concluded from the shape of the spectrum if one takes account of the Iwasaki and Sakai's results[6] and the fact that the sample was amorphous. Approximate positions corresponding to the three principal values of the *g* tensor are indicated by
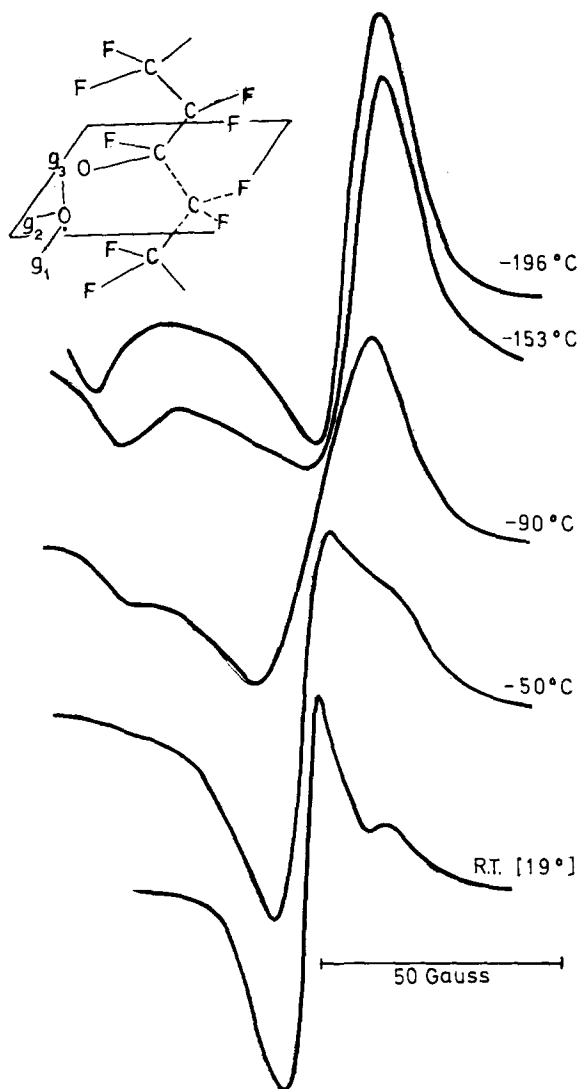
Figure 2 Temperature change of e.s.r. spectra observed from the Sample A (the peroxy chain radical). The directions of principal axis of the *g* tensor is illustrated in reference to a peroxy radical of PTFE at the upper left corner

the arrows in *Figure 2b*. The principal values were determined accurately by a computer simulation as $g_1 = 2 \cdot 0385$, $g_2 = 2 \cdot 0079$ and $g_3 = 2 \cdot 0023$, which agree well with those reported by Iwasaki and Sakai. The temperature variation of the line shapes of the peroxy chain radicals in the Sample A is represented in *Figure 2*. Although the line shapes look to be unchanged below about 120 K, the peak corresponding to g_1 shifts gradually to the
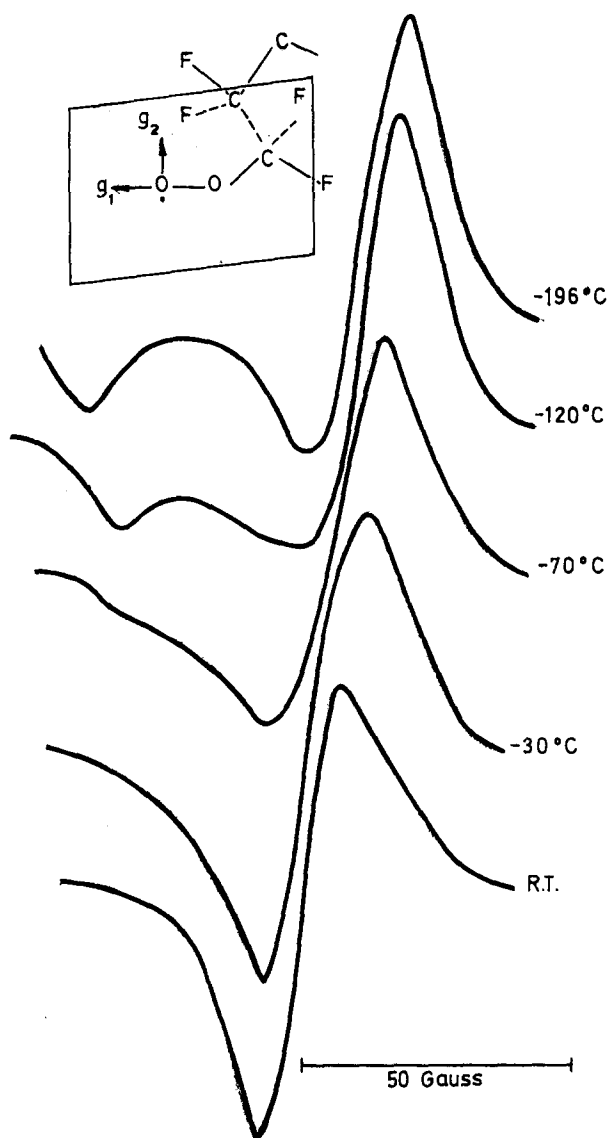
Figure 3 Temperature change of the e.s.r. spectra observed from the Sample B (the peroxy end radical). The direction of the principal values of *g* tensor is illustrated at the upper left corner

634

high field side in the temperature region above 120 K. It was found that at 223 K the peaks corresponding to g_1 and g_2 coalesced into a single line. This coalescence indicates that the g_1 and g_2 of the g tensor were completely averaged out by a rapid motion. Contrary to the coalescence of g_1 with g_2 the position of g_3 stays almost unchanged during the temperature change. By rotation about an axis the g tensor becomes axial symmetric. The averaged value of g_1 and g_2 is now the perpendicular components of the axial symmetric g factor, and the peak associated with the perpendicular component appeared strongest. Thus the strongest peak appears at the lower field side at room temperature, while the main peak is observed at the higher field at 77 K. This is the apparent inversion of the g factor. This inversion of the g factor was explained by the rotation about the axis parallel to the g_3 axis of the g tensor, as suggested by Iwasaki and Sakai[6]. That is, the rotational motion of the peroxy chain radical presumably starts at about 120 K and become so rapid at 220 K as to average out the g_1 and the g_2 components of the g tensor.

Sample B

Figure 3 illustrates how the line shapes of the peroxy end radical produced in sample B change with the increased temperatures. Although the observed line shape at 77 K appeared very similar to that observed from the sample A, the temperature variations of the spectra of the two samples were found to be quite different. The position of the main peak of the low temperature corresponding to the g_3 did not stay unchanged for the sample B but shifted gradually to the lower field side with the increased temperatures and the line shape appeared finally as a narrow singlet above 240 K. This difference in the temperature variation indicates that the molecular motion of the peroxy end radical is different from that of the peroxy chain radical and also that motion of the peroxy end radical is a three dimensional random motion which averages out the three principal values of the g tensor.

ESTIMATION OF CORRELATION TIME

A theoretical formula of averaging of an anisotropic g factor was derived by Kneubühl[7] and the average value of the g factor at a given correlation time τ was expressed by the following equation

$$\langle g^2 \rangle_{Av} = \sin^2 \beta \sin^2 \gamma \, [s + (g_1^2 - s)(2/\pi) \tan^{-1}(\tau/T_2)] +$$
$$+ \sin^2 \beta \cos^2 \gamma \, [s + (g_2^2 - s)(2/\pi) \tan^{-1}(\tau/T_2)] +$$
$$+ \cos^2 \beta \, [s + (g_3^2 - s)(2/\pi) \tan^{-1}(\tau/T_2)] \tag{1}$$

where $s = (g_1^2 + g_2^2 + g_3^2)/3$, T_2 is the spin-spin relaxation time, and β and γ are the polar coordinates of the magnetic field H in reference to a molecular fixed coordinate system. One can estimate the correlation times τs at various temperatures by using both the observed values of g_1 at the temperatures and equation (1), provided that s and T_2 are known. The quantity s, which

was above defined, was experimentally obtained from the observed principal values from the e.s.r. spectrum at 77 K. However, the experimental value of T_2 cannot be determined directly by inspection of the observed spectrum from the amorphous sample. In order to estimate the values of T_2, we carried out a computer simulation of the e.s.r. spectrum observed from an amorphous sample based on the Kneubühl theory[7]. In this simulation the line shape was assumed to be the gaussian, and the line width of the gaussian shape, which is associated with T_2, was taken as an adjustable parameter. In the *Figure 4*, the

50 Gauss
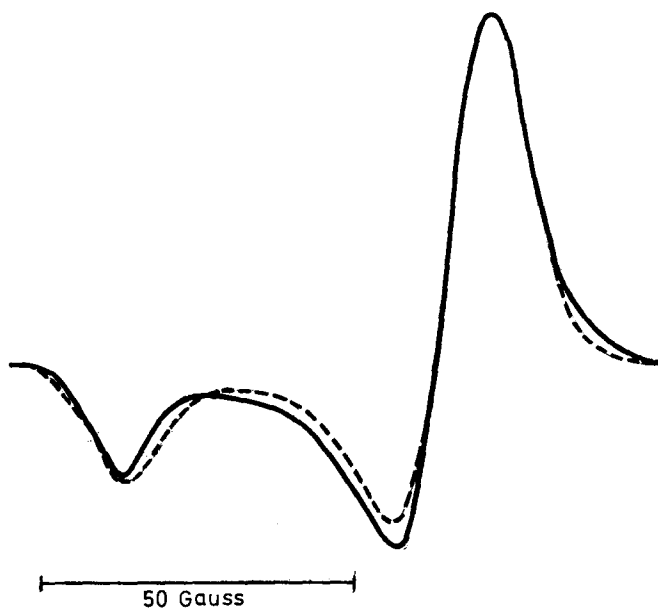
Figure 4 Comparison of the observed spectrum with the simulated one. The observed spectrum and the simulated are shown with the solid line and the dotted line, respectively. The line-width was chosen as an adjustable parameter. A gaussian curve is assumed ΔH msl = 12 Gauss

spectrum observed from the sample A at 77 K and the best fitted simulation of the spectrum are displayed. From this best fitted pattern among the trials the line width was determined as 12 G* and the experimental value of T_2 was evaluated as 3×10^{-8} s. It was found by such simulations performed at the temperatures that the best fits of the simulation were obtained with constant line width. Thus, T_2 was unvaried in the temperature range in the experiments. Using the above determined values of T_2 and s and the observed values of g factor at each temperature the correlation time τ at the temperatures was evaluated by insertion of the observed values of g at the various temperatures into the first term of equation (1).

The logarithm of the correlation time is plotted against the inverse of the

---

*1 gauss (G) $\equiv 10^4$ tesla (T)
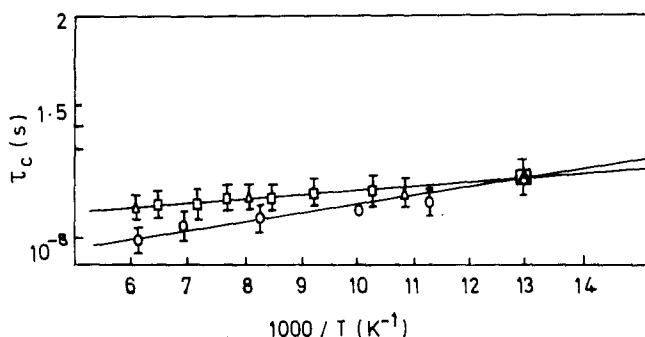
Figure 5 Arrhenius plot of the correlation times determined by averaging out of the *g* anisotropy of the e.s.r. spectra. ○, chain radical, $E = (0.52 \pm 0.12)$ kcal/mol; △ and □, end radical, $E = (0.26 \pm 0.21)$ kcal/mol

temperature in *Figure 5*. This plot is linear with the limits of experimental error. It is worth noting that the correlation time can be clearly classified into two groups depending on the type of radicals. The activation energy of the rotational motion of the peroxy chain radical was evaluated as (0.52 ± 0.12) kcal/mol and the activation energy of the three dimensional motion of the peroxy end radical is (0.26 ± 0.21) kcal/mol.

DISCUSSION

The activation energies obtained from the analyses of the peroxy radicals of PTFE are much smaller than those determined by the conventional experimental techniques in the ordinary temperature range. This discrepancy seems to be rather natural, because e.s.r. spectrum is mainly influenced by the molecular motion of small scale, such as a molecular motion of monomer size. In fact the activation energies of several hundred calories per mole are rather close to those for either the rotation of methyl radical in the simple molecule[8] or to the hindered oscillation of the methylenic group of polyethylene[9] or to the reorientation motion of the methyl group of the large side chain of the polymer[10]. These motions, the activation energy of which is smaller than 1 kcal/mol, are related to the mobilities of the smallest unit in the polymers, such as the methyl group or the methylene group. On the other hand the activation energies obtained by the conventional experimental techniques reflect the molecular motion of polymer as a whole or of several monomers even if it is called as the local mode of the motion. Since the e.s.r. is always sensitive to molecular motion of the radical to which e.s.r. spectrum is attributed, the narrowings of the spectra, from which correlation times have been evaluated, reflect the molecular motion of either the peroxy radicals or their very neighbours. The activation energy of the chain radical was found to be nearly twice as large for the end radicals. This result is quite consistent with an expectation that the chain radical is considered to be more restricted in motion but on the other hand the end radical is more mobile.

637

Ovenall[11] mentioned that the observed spectrum of irradiated PTFE was decomposed into the two components just as done in this work, but he assigned the two components to the same species of the radicals trapped in the different states of aggregation, the crystalline and the amorphous, of PTFE. The e.s.r. spectrum observed after u.v. irradiation to the sample A was the triple triplet, which is the spectrum of the scission radical,

$$\begin{array}{c} \text{F} \quad \text{F} \\ | \quad | \\ \sim\!\text{C}\!-\!\text{C}\cdot \\ | \quad | \\ \text{F} \quad \text{F} \end{array}$$
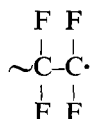
and the peroxy radical was produced by introducing air after the identification of the radical as the scission type. Therefore the peroxy radical of the sample B, from which the e.s.r. spectrum was observed as the singlet at room temperature, are apparently different species from the chain radical. The experimental procedure and the identification lead to the conclusion that the three dimensional rapid motion, which causes the narrow singlet, should be attributed not to the rapid molecular motion of the polymer chain in an amorphous state of PTFE but to the high mobility of the free end of the polymers.

It was found that the radicals produced by mechanical fracture of PTFE showed at 77 K the e.s.r. spectrum identical to what is shown as *Figure 1b*[12]. However, the temperature variation of the correlation times estimated from the radicals produced by mechanical fracture lies just on the same line of the temperature variation of the correlation time of the peroxy end radical, as shown in Δ *Figure 5*. This result strongly suggests that the peroxy radical produced by the mechanical fracture of PTFE is not the chain radical but the scission type. This means that the PTFE polymers are scissioned by the mechanical fracture just as the other polymers are[12].

ACKNOWLEDGEMENT

College of Engineering,
Hokkaido University,
Sapporo, Japan   (*Received 2 June 1970*)

REFERENCES

1 For example, Powles, J. G. *Polymer, Lond.* 1960, **1**, 219
2 Tamura, N. *J. Chem. Phys.* 1962, **37**, 479
3 Moriuchi, S., Kashiwabara, H., Sohma, J. and Yamaguchi, S. *J. Chem. Phys.* 1969, **51**, 2981

4 SAITO, N., OKANO, K., IWAYANAGI, S. and HIDESHIMA, T., 'Advances of Solid State Physics', 1963, **14**, 344
5 Siege, S. and Hedgpeth, H. *J. Chem. Phys.* 1967, **46**, 3904
6 Iwasaki, M. and Sakai, Y. *J. Polym. Sci. (A-2)* 1968, **6**, 265
7 Kneubühl, F. K. *J. Chem. Phys.* 1960, **33**, 1074
8 For example, Miyagawa, I. and Itoh, K. *J. Chem. Phys.* 1962, **36**, 2157
9 Ohnishi, S., Sugimoto, S. and Nitta, I. *J. Chem. Phys.* 1962, **37**, 1283
10 Frosini, V. and Woodward, A. E. *J. Polym. Sci. (A-2)* 1969, **7**, 525
11 Ovenall, D. W. *J. Phys. Chem. (Solids)* 1965, **26**, 81
12 Kawashima, T., Nakamura, M., Shimada, S., Kashiwabara, H. and Sohma, J., 'Report on Progress in Polymer Physics Japan', 1969, **12**, 469

The effects of contact between hydrazine solutions and some polymer materials

T. R. BOTT and G. A. R. RASSOUL

Extensive tests have been carried out on the effects of different polymer materials in extended contact with aqueous solutions containing hydrazine at temperatures up to 70°C. Estimates of the change in hydrazine content of solutions confirm that polyethylene is entirely suitable as a material of construction in contact with hydrazine solution. The results have been supported by additional tests relating to the structure. PVC was found not to be compatible with hydrazine solutions.

IT IS well known that 64% aqueous hydrazine solution can be stored for long periods without decomposition, provided that precautions are taken and correct conditions are maintained. Solutions of hydrazine are very susceptible to oxidation by the presence of atmospheric oxygen[9-11] and are capable of absorbing carbon dioxide[4, 6, 8]. Contact with some metallic surfaces can also give rise to decomposition[1-3, 7, 13]; copper and its alloys are particularly harmful in this respect.

A major industrial use, involving its affinity for oxygen, is the removal of traces of oxygen in boiler feed waters[11, 12, 18, 23, 24]. Inhibitors to reduce the tendency of hydrazine to oxidize and decompose during storage, have been given a good deal of attention. The presence of the inhibitor however may not be always tolerable in the end use of the hydrazine. Information and comment exist in the literature about the effectiveness of certain substances [8, 12, 17, 25], and with regard to the effect of some surfaces on the stability of stored hydrazine solutions.

It is of interest therefore to review the problems of storing and handling hydrazine solution in contact with polymeric materials as the material of construction with particular reference to the possibility of using polyethylene, which is readily available and reasonably priced.

EXPERIMENTAL

The object of the experiments was to contact 64% hydrazine solution with different materials of construction for long periods of time and at different temperatures.

A number of Pyrex glass cells were constructed; some minor differences existed between different batches of cells but essentially all consisted of a chamber of 200 ml* volume with facilities in some designs for suspending specimens of the test material above the 64% hydrazine solution contained

---

*1 ml $\equiv$ 1 mm^3

in the cell. Pyrex glass was chosen since a literature search had revealed that this material was considered inert to hydrazine.

In general the specimen of test material was arranged so that a large surface area was presented to the hydrazine solution. In the experiments the area of the specimen in the cell was measured and care exercised to ensure that all the surface was exposed to the solution or vapour above the solution as required by the experiment. Each sample was carefully washed with distilled water before air drying and sealing into the appropriate cell. Some of the solutions of hydrazine were modified by the addition of the alkalis potassium and sodium hydroxide to a concentration up to 16% in the final aqueous solution. In all experiments oxygen was removed from the apparatus by nitrogen (or argon) purging before the initial composition of the solution was determined. Samples could be taken by hypodermic needle passed through a rubber serum cap isolated from the cell by a glass tap. Normally the tap was kept closed during the experiment in order to isolate the serum cap from contact with hydrazine, the tap being open only for the very short sampling period.

As the tests were carried out over long periods of time (up to two years), and since temperature could possibly be an important variable it was necessary to provide a number of reliable constant temperature water baths into which the test cells containing the hydrazine solution with the material under test, could be immersed at specified different fixed temperatures. Basically the experiments involved estimating the hydrazine concentration before and after immersion.

The first task in the investigation was to establish a reliable method of estimating hydrazine concentration. The method finally adopted was the iodate titration technique. (A full account of the investigation into the analysis problem is given elsewhere[20].)

A likely product of decomposition of hydrazine is ammonia[4, 8, 14, 16, 21, 22]. Estimation of the change in ammonia in the hydrazine solution could therefore be regarded as a measure of the hydrazine decomposition. Small quantities of ammonia in solution were determined by modifications[20] of the methods of Pugh and Heynes[19] and Zuazaga and Ma[26].

Since the test specimens were to be contained for long periods in a glass cell in contact with hydrazine solution it was important to confirm that the Pyrex glass surface would indeed not affect the solution. A number of experiments therefore were conducted on test cells alone. It could be argued that the previous history of the glass surface might influence its passiveness or otherwise towards hydrazine solutions. In order to investigate the difficulty, glass cells were given different treatments and tested for activity with hydrazine solution. The treatments included

1 10% w/v K_2Cr_2O/H_2SO_4 solution

2 50% v/v HNO_3/H_2SO_4 solution

3 42% w/v KOH solution

4 3% w/v $KMnO_4$/H_2SO_4 solution

5 Washing the cell with either distilled water or dilute hydrogen peroxide solution

Contaminants in the hydrazine may not always be desirable in the end use, therefore it is important to investigate the contamination of the hydrazine solution by any potential material of construction. The detection of any compounds which could have been leached from the material of construction of the container holding the hydrazine solution was based upon the optical density measurements using an Ultrascan recording spectrophotometer (Model H999 Mark II). The solution which might possibly have contained contaminating materials was always compared with a 'blank' solution from the same 'uncontaminated' stock hydrazine 'as received'. For further comparison synthetic solutions of hydrazine containing known quantities of plasticizers, antioxidants and fillers were made and compared with the hydrazine solution after prolonged contact with the different materials of construction.

An investigation of the effect of the hydrazine on the material of construction itself is also of considerable interest. Tests here included scanning electron microscope studies of the polymer surface, changes in the wetting characteristic of the surface[5], changes observed in the transmission of polarised light and changes in the tensile strength of the specimen.

RESULTS AND DISCUSSION

The effects of glass surfaces and its treatment

The results of tests at 60°C with Pyrex glass surfaces having had the treatments already mentioned clearly indicate that provided the glass surfaces are thoroughly washed there is no effect on the stability of 64% hydrazine solution either alone or in the presence of alkalis. Pyrex glass is therefore a suitable material in which to carry out tests on the stability of hydrazine since it will not influence the results.

The effects of plastic materials

A very large number (1000) of individual experiments was carried out in order to investigate the compatibility of the materials with the aqueous hydrazine. *Table 1* contains a selection of typical results of tests on the effect of contact between polyethylene in different forms with hydrazine solution under different experimental conditions in the glass cells. The experimental data confirms that all qualities of polyethylene (e.g. thick or thin sheets, pellets or tubes; twenty-one alternative forms and qualities of the polymer were studied in all) had no influence on the stability of the hydrazine solution up to 64% either in the presence of alkali or not, and up to temperatures of 70°C. Visual observations of the polyethylene after immersion showed no apparent change in texture or colour.

The results were confirmed by some tests on the storage of the hydrazine solutions in polyethylene bottles under different experimental conditions. An interesting outcome of these 'bottle' tests was the fact that ultra violet light had little effect on the solutions contained in the bottles since the polyethylene bottle, when subjected to the ultra-violet light, absorbed an appreciable proportion of this energy. It is well known that ultra-violet light can

Table 1 The change in concentration of aqueous hydrazine solutions in contact with polyethylene samples

Form of poly-ethylene	Thickness (in)	Surface area of specimen to unit volume of solution	Caustic solution	Temp. (°C)	Exposure (days)	Hydrazine content estimate % (by iodate method)	
						Initial	Final
Pellets		8·0	–	Room	159	64·9	64·8
Sheet	0·005	0·5	–	47	44	64·2	64·0
Sheet	0·005	0·5	–	47	30	50·5	50·6
Sheet	0·005	2·0	–	36	26	64·2	64·0
Sheet	0·08	10·0	–	40	55	64·7	64·8
Sheet	0·005	0·5	10% NaOH	50	194	49·9	49·2
Sheet	0·005	2·0	14% KOH	70	7	49·2	48·9
Sheet	0·005	1·0	14% KOH	70	7	46·5	46·0
Sheet	0·02	2·0	10% NaOH	70	31	53·4	53·1
Tube	0·25 (o.d.)	1·0	8·5% NaOH	50	56	53·5	52·8

Table 2 The change in concentration of aqueous hydrazine solution in contact with samples of poly(vinyl chloride) tubes

Surface area of specimen to unit volume of solution	Temp. (°C)	Hydrazine content estimate % (by iodate method) after the specified number of days (days)												
		0	1	2	4	5	12	13	21	40	41	70	116	141
0·5	40	64·8	–	64·1	–	63·5	63·5	–	61·4	–	61·3	61·5	–	55·1
0·5	60	64·8	63·6	–	62·4	–	–	61·0	–	58·6	–	–	45·8	–

initiate the decomposition of hydrazine in solution under certain circumstances[12, 15].

Table 2 contains data obtained when the cells contained poly(vinyl chloride) (PVC) samples and hydrazine solution. The presence of free chlorine is considered to be the basic cause of the decomposition reaction; different samples of PVC decomposed the hydrazine to different extents apparently due to differences in chlorine content in the plastic material. In general the PVC changes colour in the presence of hydrazine solution (unlike polyethylene), translucent PVC usually turned to shades of orange to dark brown and black. Usually, the decrease in the hydrazine content of the solution in contact with PVC became more marked with time of contact, increase in temperature and increase in contact area. The data emphasise that PVC is not a suitable material of construction for contact with solutions of hydrazine up to 64% under conditions of storage likely to be encountered.

Table 3 details the change in hydrazine concentration with contact with

Table 3 The change in concentration of aqueous hydrazine solutions in contact with samples of different materials

Sample	Thickness (in)	Surface area of specimen to unit volume of solution	Temp. (°C)	Exposure (days)	Hydrazine content estimate % (by iodate method)	
					Initial	Final
PTFE rod	0·3 dia.	0·25	33	41	65·0	65·0
Polypropylene sheet	0·02	0·50	40	100	64·8	65·1
Nylon sheet	0·006	7·0	35	34	65·0	62·9
Nylon sheet	0·01	2·00	40	45	64·8	65·0
Cured Polyester resin sheet	0·05	1·00	32	41	65·1	60·1

some other plastic materials. Effects were observed with certain grades of nylon, and cured polyester resins. No effects were observed in the content of hydrazine solution with polytetrafluorethane (PTFE), polypropylene, and certain grades of nylon.

Contamination of the hydrazine solution by contact with plastic materials

It can be concluded from the experiments that nothing was leached from the polyethylene sample into the hydrazine solutions at temperatures up to 60°C for periods of time up to two months or at room temperature for periods up to one year. Some compounds as might be expected from the hydrazine decomposition by contact with PVC cured epoxy and polyester resins, were found in the resulting solutions as a result of leaching or reaction in the solution.

Changes in polyethylene structure in the presence of the hydrazine solutions

Comparison of samples which had been exposed to hydrazine solution with those which had not, using a scanning electron microscope and a magnification of 7500 times, revealed no striking differences. Slight variations in surface appearance were observed but these were no more than could be observed in taking samples from different points in the same polyethylene sample. It can be concluded therefore that if changes in surface appearance due to the presence of hydrazine did occur then these were no more than the differences due to circumstances in the processing of the polyethylene material. This conclusion was confirmed by comparison of samples in transmitted polarised light when again no marked differences were observed. Measurements of the wetting characteristic also suggested that there was little change in the polyethylene surfaces as a result of exposure to different hydrazine solutions over different periods of time.

Tensile tests using a standard test procedure in an Instron test machine

revealed that no changes of strength in polyethylene samples accompanied prolonged contact with hydrazine solutions.

In all the tests on the surface and structural changes in the polyethylene, long contact times (up to ninety days) and temperatures in the range of room temperature up to 60°C were employed.

CONCLUSIONS

The major conclusion from the work is that polyethylene, a reasonably cheap product, easily fabricated, is a suitable material of construction for the handling of hydrazine solutions up to 64% concentration, with, or without, added alkali, up to temperatures of 70°C.

The reasons are

(1) There is little or no decomposition of hydrazine in contact with poly-ethylene. In addition, polyethylene acts as a filter of ultra-violet light so that a solution of hydrazine is unaffected if contained in a polyethylene vessel exposed on the outside to this light

(2) The hydrazine solution is not generally contaminated by substances leached from the polyethylene

(3) The polyethylene retains its strength and material characteristics after contact with the hydrazine solutions

Other interesting points resulting from the work include

(1) Polypropylene (more expensive than polyethylene) as would be expected due to 'family' characteristics, is also suitable for contact with hydrazine solutions

(2) Hydrazine solutions are unaffected by the presence of Pyrex glass

(3) Poly(vinyl chloride) (PVC) and some other common polymer materials are not suitable as a material of construction for the handling of hydrazine solutions

ACKNOWLEDGMENTS

Department of Chemical Engineering,
The University of Birmingham, U.K.

P—2S

REFERENCES

1 Askey, P. J. *J. Amer. Chem. Soc.* 1930, **52**, 970–4
2 Audrieth, L. F. and Jolly, W. L. *J. Phys. and Colloid Chem.* 1951, **55**, 524–31
3 Audrieth, L. F. and Mohr, P. H. *Ind. Eng. Chem.* 1951, **43**, 1774–9
4 Audrieth, L. F. and Ogg, B. A., 'The Chemistry of Hydrazine', John Wiley & Sons, Inc., New York, Chapman and Hall Ltd., London 1951
5 Bott, T. R., Harvey, A. P. and Palmer, D. A. *J. appl. Polym. Sci.* 1966, **10**, 211–216
6 Brown, E. A., PhD Thesis, University of Illinois, 1947
7 Celis, J., 'Hydrazine-Water Treat. Proc. Intern. Conf.', Bournemouth, England, 26–32, 1957
8 Clark, C. C., 'Hydrazine', Mathieson Chemical Corporation 1953
9 Cuy, E. J. and Bray, W. C. *J. Amer. Chem. Soc.* 1924, **46**, 858
10 Cuy, E. and Bray, W. C. *J. Amer. Chem. Soc.* 1924, **46**, 1786–95
11 Gilbert, E. C. *J. Amer. Chem. Soc.* 1929, **51**, 2744–51
12 Hill, P., PhD Thesis, Chem. Eng. Dept., Birmingham University, 1959
13 Irrera, L. *Atti XVXII Monine Bologna Soc., Ital. Progress Sci.* 1939, **5**, 353–7
14 Leicester, J., 'Proceedings of the International Conference on Hydrazine Water Treatment', Bournemouth, England, 33–53, 1957 (Pub. 1958)
15 Moreland, C., PhD Thesis, Chem. Eng. Dept., Birmingham University, 1956
16 Olsen, E. C. *Analyt. Chem.* 1960, **32** (pt. 12), 1545
17 Pannetier, G. *Bull. Soc. Chem.* 1958, 1393–7 (France)
18 Pearson, M. A., PhD Thesis, Chem. Eng. Dept., Birmingham University 1959
19 Pugh, W. and Heynes, W. K. *Analyst* 1953, **78**, 177
20 Rassoul, G. A. R., PhD Thesis, Chem. Eng. Dept., Birmingham University 1969
21 Stones, W. F., 'Proceedings of the International Conference on Hydrazine Water Treatment', Bournemouth, England, 121–6, 1957
22 Tsitshivili, L. D. and Karkarashvili, M. V. *Trudy. Inst. Khim. im P.G. Metikishvili Akad. Nauk Gruzia S.S.R.* 1956, **12**, 101–7
23 Turner, J. M. *Elect. Light and Power* 1957, **35**, 88–93
24 Wharton, J. T., PhD Thesis, Chem. Eng. Dept., Birmingham University, 1963
25 Whiffen and Sons Ltd, 'Hydrazine and Water Treatment', Publ. by Whiffen and Sons Ltd, 1957
26 Zuazaga, T. S. and Ma, G. *Ind. and Eng. Chem.* 1942, **14**(3), 280

Studies of the polymerization and copolymerization of methacrylic anhydride

F. C. BAINES* AND J. C. BEVINGTON

Various procedures involving the use of labelled reagents have been developed for studying the behaviour of methacrylic anhydride in radical polymerizations. Studies of copolymerizations with styrene, methyl methacrylate and methyl acrylate have been correlated with studies of the initiation of homopolymerization with benzoyl peroxide; it has been shown that polar factors are prominent in the reactions of the monomeric anhydride with radicals. Tracer techniques have confirmed that there are high proportions of cyclized monomer units in homopolymers and copolymers of methacrylic anhydride.

MANY SUBSTANCES having two polymerizable groups per molecule can undergo cyclopolymerization, the intramolecular propagation

$$P\text{--}CH_2\text{--}CH\cdot \quad \longrightarrow \quad P\text{--}CH_2\text{--}CH\text{--}CH_2\text{--}CH\cdot$$
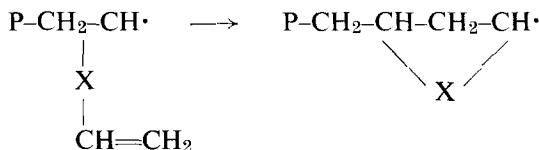
competing with the intermolecular reaction

$$P\text{--}CH_2\text{--}CH\cdot \quad + \quad CH_2\text{=}CH \quad \longrightarrow \quad P\text{--}CH_2\text{--}CH\text{--}CH_2\text{--}CH\cdot$$
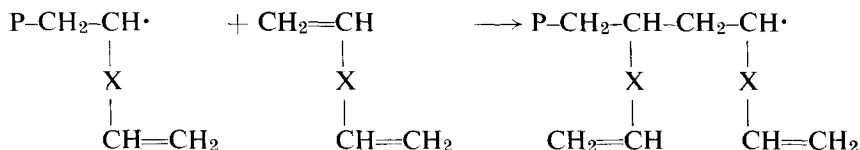
Butler and Raymond[1] performed statistical calculations, in particular for 1,6-heptadiene, showing that high degrees ($>95\%$) of cyclization would be expected only when the monomer concentration is below about $0 \cdot 10\,\text{mol/l}$.

For those symmetrical divinyl monomers where the nature of the group X leads to a ring of about six atoms, it is likely that the intrinsic reactivity of the pendant double bond is similar to that of a double bond in the monomer. On the other hand, the nature of X must determine whether the growing centre can acquire a configuration to permit the intramolecular propagation[2].

*Present address: Electrochemicals Department, E. I. Dupont de Nemours, Wilmington, Delaware, U.S.A.

It is known[3-5] that, in radical polymerizations involving methacrylic anhydride (MAA), the cyclization

$$P_n-CH_2-C(CH_3) \cdot \quad \longrightarrow \quad \begin{matrix} CH_3 & CH_3 \\ | & | \\ P_n-CH_2-C-CH_2-C \cdot \\ | & | \\ OC- O -CO \end{matrix} \quad (1)$$

with the structure:

$$\begin{matrix} P_n-CH_2-C(CH_3) \cdot \\ | \\ CO-O-OC-C=CH_2 \\ | \\ CH_3 \end{matrix}$$
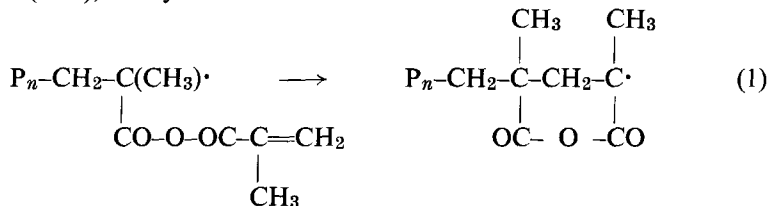
occurs very readily. This feature is considered in this paper as part of a more general examination of the behaviour of the monomer in radical polymerization. There is another distinct interest in this monomer in that its polymer can be converted to polymethyl methacrylate; cyclopolymerization leads to a polymer having a micro-structure unachievable by direct polymerization of monomeric methyl methacrylate[6].

Part of the work involving MAA concerned an examination of its reactivity towards reference radicals. For examination of the benzoyloxy radical, samples of ^{14}C-benzoyl peroxide were used to initiate polymerizations[7]; the resulting polymers were analyzed for benzoate and phenyl end-groups to permit study of the competition between the reactions

$$C_6H_5-CO-O \cdot \longrightarrow C_6H_5 \cdot + CO_2 \quad (2)$$

$$C_6H_5-CO-O \cdot + CH_2{=}C(CH_3)-CO-O-CO-C(CH_3){=}CH_2 \longrightarrow$$

$$\begin{matrix} C_6H_5-CO-O-CH_2-C(CH_3) \cdot \\ | \\ CO-O-CO-C(CH_3){=}CH_2 \end{matrix} \quad (3)$$
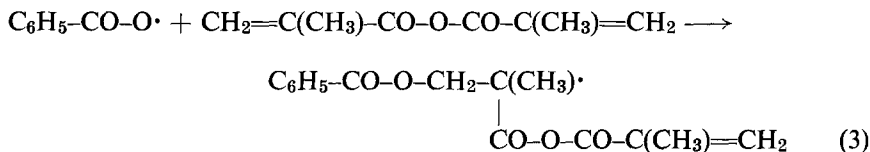
and evaluation of k_3/k_2. For investigation of the reactivity of MAA towards polymer radicals, monomer reactivity ratios were determined by an isotopic method for copolymerizations with styrene, methyl methacrylate and methyl acrylate. In a binary copolymerization with this monomer, it may be necessary to consider three types of polymer radical and six types of growth reaction in addition to reaction scheme (1). It has been shown[8] that the two radicals in reaction scheme (1) behave so similarly in copolymerization that it is possible to apply the usual treatments for binary copolymerizations without penultimate group effects. A value of e for MAA has been deduced and has been correlated with the reactivity of the monomer towards the benzoyloxy radical.

Smets et al[3] considered a competition between the intramolecular process (1) and the growth reaction

$$\begin{matrix} P_n-CH_2-C(CH_3) \cdot & + & CH_2{=}C-CO-O-CO-C{=}CH_2 \longrightarrow \\ | & & | & | \\ CO-O-CO-C{=}CH_2 & & CH_3 & CH_3 \\ | \\ CH_3 \end{matrix}$$

648

$$
\begin{array}{ccc}
CH_3 & CO-O-CO-C{=}CH_2 \\
| & | & | \\
& & CH_3 \\
| & | \\
P_n{-}CH_2{-}C{-}CH_2{-}C{-}CH_3 \\
| & \cdot \\
CO-O-CO-C{=}CH_2 \\
| \\
CH_3
\end{array}
\tag{4}
$$
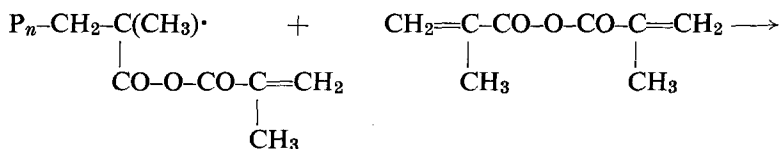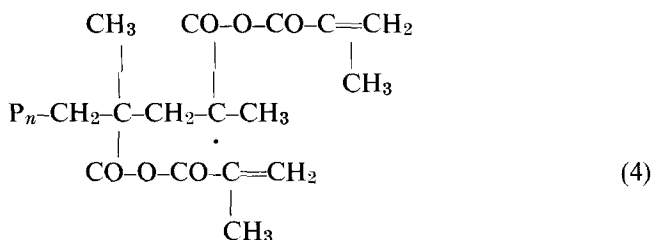
in the homopolymerization of MAA. According to a simple kinetic analysis, the molar fraction (f_c) of cyclized units is related to the concentration of monomer (m) thus

$$
\frac{1}{f_c} = 1 + \frac{2k_4 m}{k_3}
\tag{5}
$$

To find $(1/f_c)$, the pendant double bonds in a polymer were determined by bromometry. Equation (5) was not fully satisfied in that the extrapolated value of f_c for zero concentration of monomer was significantly less than unity. This result was attributed in part to experimental errors and in part to the occurrence of reactions, in addition to scheme (4), leading to carbon–carbon double bonds in the polymer. Similar results were obtained by application of the same procedure to copolymers of MAA[8].

Alternative methods have now been devised and tested for determination of f_c for homopolymers and copolymers of MAA. In general, the methods involve tracer studies of the changes in polymers brought about by hydrolysis.

Suppose that a homopolymer of MAA has labelled end-groups which are stable to hydrolysis, e.g. $(CH_3)_2C(CN)$ groups derived from ^{14}C-azoisobutyronitrile used as initiator. If the original polymer is represented as

$$
\left\{ \begin{array}{c} (CH_3)_2C(CN) \end{array} \right\}_1
\left\{ \begin{array}{c} CH_2{-}C(CH_3) \\ | \\ CO-O-CO-C(CH_3){=}CH_2 \end{array} \right\}_a
$$

$$
\left\{ \begin{array}{c} CH_2{-}C(CH_3){-}CH_2{-}C(CH_3) \\ | \qquad | \\ CO{-\!-}O{-\!-}OC \end{array} \right\}_b
$$
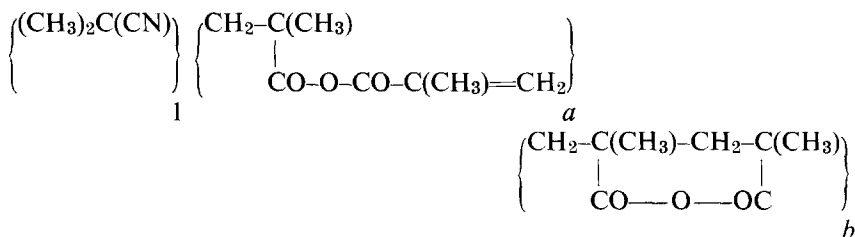
then the polymer after complete reaction can be represented as

$$
\{(CH_3)_2C(CN)\}_1 \quad \{CH_2{-}C(COOH)(CH_3)\}_{a+2b}
$$
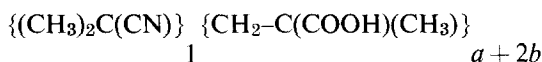
Hydrolysis must cause the specific activity of the polymer to rise because of the detachment of methacrylic units from uncyclized monomer units. If materials are assayed by gas counting, it is necessary only to consider their carbon contents so that

$$
\frac{\text{counting rate of polymer before hydrolysis}}{\text{counting rate of polymer after hydrolysis}} = \frac{a + 2b}{2(a + b)}
\tag{6}
$$

neglecting the very small contribution of the labelled end-groups to the total carbon content of the polymer. The value of f_c, equal to $b/(a + b)$, can therefore be found.

A similar procedure can be applied to a copolymer of MAA with ^{14}C-styrene. If such a copolymer is represented as $(C_8H_8)_1(C_8H_{10}O_3)_{a+b}$ where a and b are respectively the relative numbers of uncyclized and cyclized MAA units

$$\frac{\text{counting rate for copolymer}}{\text{counting rate for monomeric styrene}} = \frac{1}{1 + a + b} \tag{7}$$

After complete hydrolysis, the copolymer can be taken as

$$(C_8H_8)_1(C_4H_6O_2)_{a+2b}$$

so that

$$\frac{\text{counting rate for copolymer before hydrolysis}}{\text{counting rate for copolymer after hydrolysis}} = \frac{2 + (a + 2b)}{2 + 2(a + b)} \tag{8}$$

From equations (7) and (8), a and b can be calculated so that f_c can be found.

If a hydrolyzed copolymer of styrene and MAA were methylated with ^{14}C-diazomethane, it would be converted to a copolymer of styrene and ^{14}C-methyl methacrylate; the specific activity of this product would depend upon that of the diazomethane, the composition of the original copolymer and the relative numbers of cyclized and uncyclized MAA units. Taking the original copolymer, as before, as $(C_8H_8)_1(C_8H_{10}O_3)_{a+b}$, the final copolymer of styrene and methyl methacrylate can be represented as

$$(C_8H_8)_1(C_5H_8O_2)_{a+2b}.$$
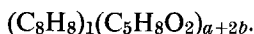
For gas counting

$$\frac{\text{counting rate of final product}}{\text{counting rate of diazomethane}} = \frac{a + 2b}{8 + 5(a + 2b)} \tag{9}$$

The value of $(a + b)$ can be deduced from data on the copolymerization of styrene and MAA; then equation (9) can be used to find a, b and f_c.

EXPERIMENTAL

Materials

Preparations of labelled initiators have been described[9, 10]. ^{14}C-methyl methacrylate and ^{14}C-methyl acrylate were made by exchange between the unlabelled monomers and ^{14}C-methanol. ^{14}C-styrene was made by destructive distillation of ^{14}C-cinnamic acid prepared from ^{14}C-benzaldehyde by the Perkin reaction. Monomeric MAA was a commercial product (Kodak Ltd). All monomers and solvents were purified by standard procedures; monomers were distilled in high vacuum immediately before use.

For preparation of ^{14}C-diazomethane, labelled methylamine was first converted to nitrosomethylurea which was then decomposed basically to give a solution of diazomethane in benzene. For assay, ^{14}C-diazomethane

was converted to ^{14}C-methyl-β-naphthoate by reaction with a suspension of β-naphthoic acid in ether; allowance was made for the substantial dilution of the active carbon.

Preparation of polymers

Polymerizations were performed in sealed dilatometers in the complete absence of air; conversions did not exceed 5%. For MAA at 60°C, 20·7% contraction was taken as equivalent to 100% polymerization; for homopolymerizations, concentrations of monomer up to 3·22 mol/l could be used without pronounced auto-acceleration.

Polymers were recovered by precipitation in methanol; after filtration almost to dryness, they were dissolved in benzene, reprecipitated in methanol, filtered off and dried in vacuum at room temperature. Filtration to dryness caused polymers containing MAA to become insoluble in benzene. Test separations established that the procedures led to complete removal from polymers of uncombined labelled monomer or labelled initiator.

Chemical treatment of polymers

Polymers were subjected to alkaline hydrolysis[11]. Samples of poly MAA (about 100 mg) were refluxed with water (75 ml) and sodium hydroxide pellets (250 mg) until the polymers dissolved. The solutions were then heated on a steam bath and concentrated hydrochloric acid was added to precipitate poly(methacrylic acid) which was filtered off and dried in vacuum (recovery, about 80%). For hydrolysis of copolymers of styrene with MAA, a little benzene was added to the system to swell the copolymers.

The method of Katchalsky and Eisenberg[12] was used for esterification of polymethacrylic acid and its copolymers with styrene. Materials were treated with ^{14}C-diazomethane in benzene until the polymer dissolved and the yellow colour persisted. The excess diazomethane was removed on a rotary evaporator. The solution of polymer was filtered through sintered glass; benzene washings of the undissolved material on the sinter were added to the filtrate which was then added slowly to excess methanol. The precipitated polymer was recovered and dried in vacuum.

Assay of labelled materials

Gas counting of carbon dioxide was used. Samples were oxidised by wet oxidation. Counting rates refer to counts per minute (corrected for lost counts and background) for a standard mass of carbon dioxide; a counting rate of 9000 corresponds to a specific activity of about 1 microcurie per g of carbon.

Polymerizations with ^{14}C-benzoyl peroxide

MAA was polymerized at 60°C in benzene with benzoyl peroxide at 1 g/l. At each concentration of monomer, one polymer was prepared with peroxide labelled in the rings (R-peroxide) and another with peroxide labelled at the

651

carboxyl carbon atoms (C-peroxide). There were indications of auto-accelera-
tion in the later stages of the polymerizations but the parallel experiments
gave very similar conversion/time plots. Values of rate of initiation and
$k_t/k_p{}^2$ were calculated from the results referring to R-peroxide. From the
counting rates of corresponding polymers and those of the peroxides, values
of the fraction x were calculated by equation (10).

$$x = \frac{\text{no. of benzoate end-groups}}{\text{sum of nos. of benzoate and phenyl end-groups}}$$

$$= \frac{\text{counting rate of C-polymer}}{\text{counting rate of R-polymer}} \times \frac{\text{counting rate of R-peroxide}}{\text{counting rate of C-peroxide}} \tag{10}$$

Results are shown in *Table 1* and *Figure 1* which gives k_2/k_1 as 0·49 l/mol.
   For comparisons of the reactivities of monomers towards the benzoyloxy
radical, methyl methacrylate ($k_2/k_1 = 0·33$ l/mol) has been used as standard[13],
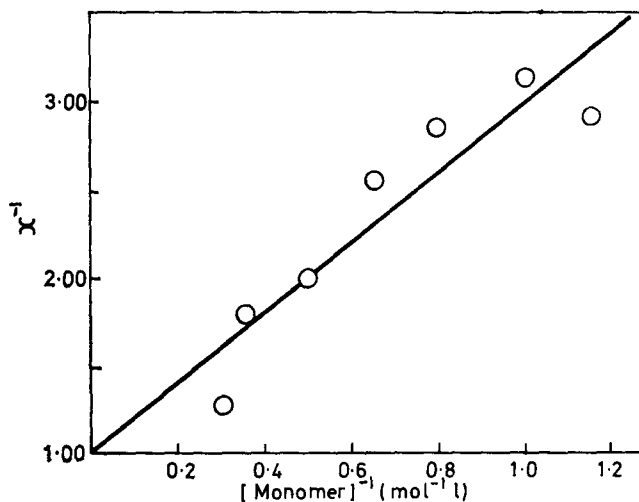
Figure 1 Nature of end-groups in poly(methacrylic anhydride)
prepared at 60°C with benzoyl peroxide as initiator and benzene as
diluent.

$x = $ (no. of benzoate end-groups)/(sum of nos. of benzoate and phenyl
end-groups)

so that the relative reactivity of MAA is 1·48. The molecule of MAA, however,
contains two identical carbon-carbon double bonds and so the relative
reactivity of one such bond can be taken as 0·74; this correction may not be
completely justified since, in a dilute solution of MAA, the double bonds are
not distributed uniformly but occur in pairs.

Table 1 Polymerizations with labelled benzoyl peroxides

Concn. of MAA (mol l^{-1})	10^5 (rate of polym.) (mol l^{-1}s^{-1})		Counting rate of polymer		10^8 (rate of init.) (mol l^{-1}s^{-1})	k_t/k_p^2 (mol l^{-1})	x
	R-per-oxide	C-per-oxide	R-per-oxide	C-per-oxide			
0·87	2·20	2·56	194	63	1·88	12·3	0·34
1·00	2·74	2·77	186	56	2·10	13·8	0·32
1·25	3·13	3·50	156	49	2·11	14·9	0·35
1·50	3·90	4·06	127	47	2·05	16·9	0·39
2·00	5·72	5·47	102	48	2·30	14·8	0·50
2·75	8·13	7·80	64	34	2·06	12·4	0·56
3·22	9·84	9·80	47	35	1·88	10·1	0·79

Counting rates for R- and C-peroxide = 281000 and 266000, respectively

Polymerizations with ^{14}C-azoisobutyronitrile

Table 2 shows results for polymerizations of MAA at 60°C in benzene with ^{14}C-azoisobutyronitrile at 0·3g/l; there were no induction periods and only slight indications of auto-acceleration.

Table 2 Polymerizations with labelled azoisobutyronitrile

Concn. of MAA (mol l^{-1})	10^5 (rate of polym.) (mol l^{-1}s^{-1})	Counting rate of polymer		10^8 (rate of init.) (mol l^{-1}s^{-1})	k_t/k_p^2 (mol l^{-1})
		before hydrolysis	after hydrolysis		
0·50	1·13	752	833	1·63	16·0
1·00	3·27	468	516	2·94	13·8
1·50	5·24	296	328	2·98	12·2
2·00	6·91	224	251	2·98	12·5
2·50	8·71	186	–	3·12	12·8

Counting rate for initiator = 1 040 000

Except at the lowest concentration of monomer, the rates of initiation correspond to those observed under similar conditions with styrene[14]. The order with respect to monomer is about 1·08, in agreement with the results shown in Table 1; the values of k_t/k_p^2 are similar for the two sets of experiments.

Using (6), the values of f_c were calculated from the counting rates of polymers before and after hydrolysis. Figure 2 shows these results and those of Smets et al[3] which refer to polymerization in cyclohexanone at 36·6°C. It is confirmed that a high proportion of MAA units are cyclized. The intercepts are clearly greater than unity; in the tracer experiments, this means

that the increases in specific activity accompanying hydrolysis are larger than might have been expected. Possible failings in the experimental procedures (such as loss of labelled end-groups, incomplete hydrolysis, and failure to remove contaminants from hydrolyzed polymers) would lead to the opposite effect. The results can be explained on the basis of the isomerization scheme (11) which was proposed by

$$
\begin{array}{ccc}
\text{CH}_3 & & \text{CH}_3 \\
| & & | \\
P_n\text{--CH}_2\text{--C}\cdot & \longrightarrow P_n\text{--CH}{=}\text{C} & \quad (11) \\
| & & | \\
\text{CO--O--CO--C(CH}_3){=}\text{CH}_2 & & \text{CO--O--CO--C(CH}_3)_2\cdot
\end{array}
$$
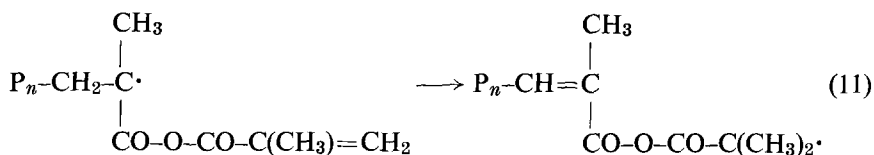
Smets et al[3] and which might be regarded as a type of 'back-biting' in competition with cyclization. If the product of scheme (11) engages in further growth, an anhydride linkage becomes incorporated in the main polymer chain; breakage of this linkage during hydrolysis would cause a section of the polymer chain to be detached leaving a residue comparatively rich in the end-groups derived from the labelled initiator.
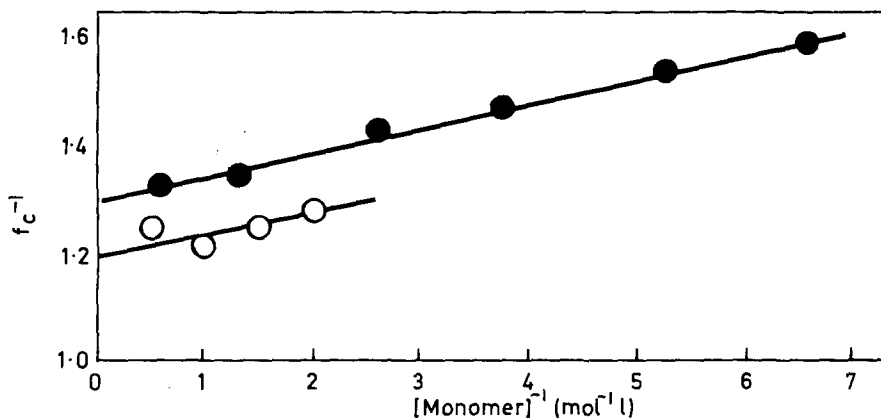
Figure 2 Dependence of fractional number (f_c) of cyclized methacrylic anhydride units upon concentration of monomer during polymerization.
○, This work; polymerization at 60°C with benzene as diluent;
●, Work of Smets et al.[3]; polymerization at 36·6°C with cyclohexanone as diluent

Copolymerizations involving methacrylic anhydride

Binary copolymerizations of MAA with labelled samples of styrene, methyl methacrylate and methyl acrylate were performed at 60° in benzene with benzoyl peroxide at 1 g/l. Contraction/time plots for systems including methyl acrylate were linear but many of those for the other comonomers showed auto-acceleration and formation of gel in the later stages.

For gas counting, a high polymer derived from MAA ($C_8H_{10}O_3$) and a

[14]C-monomer containing n carbon atoms per molecule can be represented as $(C_8)_a(C_n)_{1-a}$ so that

$$\frac{\text{counting rate of copolymer}}{\text{counting rate of labelled monomer}} = r = \frac{n(1-a)}{8a + n(1-a)}$$

$$\text{and mole fraction of MAA in copolymer} = a = \frac{n(1-r)}{n(1-r) + 8r} \qquad (12)$$

Typical results are shown in *Table 3*. Monomer reactivity ratios from Finemann-Ross plots are as follows (monomer-1 taken as MAA):
with styrene: $r_1 = 0\cdot33 \pm 0\cdot03$, $r_2 = 0\cdot10 \pm 0\cdot01$
with methyl methacrylate: $r_1 = 1\cdot70 \pm 0\cdot07$, $r_2 = 0\cdot22 \pm 0\cdot02$
with methyl acrylate: $r_1 = 4\cdot75 \pm 0\cdot15$, $r_2 = 0\cdot16 \pm 0\cdot02$
For styrene at $36\cdot6°C$, Smets *et al*[8] gave $r_1 = 0\cdot26$ and $r_2 = 0\cdot12$.

Table 3 Copolymerizations of ^{14}C-methyl methacrylate and methacrylic anhydride

Mole fraction methyl methacrylate in monomer mixture	Counting rate of copolymer	Mole fraction methyl methacrylate in copolymer
0·20	298	0·13
0·40	594	0·25
0·50	787, 740*, 771†	0·32, 0·30*, 0·31†
0·60	1005	0·39
0·70	1268	0·48
0·80	1657	0·59
0·90	2058	0·70
0·965	2809	0·87

Counting rate for monomeric methyl methacrylate = 3476; reaction mixtures contained 60% benzene by volume, except *(50%) and †(70%)

From the three values of $r_1 r_2$ and taking the values of e for styrene, methyl methacrylate and methyl acrylate as $-0\cdot8$, $0\cdot4$ and $0\cdot6$ respectively, e for MAA is found to be about $1\cdot2$; Smets *et al*[8] gave $1\cdot1$. It has been shown that the reactivities of monomers towards the benzoyloxy radical decrease as the values of e become more positive[13]; previous results suggest that a reactivity towards the benzoyloxy radical of $0\cdot74$ (that of methyl methacrylate taken as unity) might correspond to a value of about $+1$ for e, in fair agreement with the experimental result for MAA.

For comparisons of the reactivities of reference polymer radicals towards monomers, it is necessary to correct values of r_1 and r_2 and to make due allowance for the presence of two identical carbon-carbon double bonds in the molecule of MAA. To compare reactivities of monomers towards the poly(MAA) radical, the quoted values of r_1 should be halved; for comparison of the reactivity of MAA towards other polymer radicals, the values of r_2 should be doubled. These considerations do not affect calculations of e since they involve the products $r_1 r_2$.

Reactions of polymers and copolymers of methacrylic anhydride

Copolymers of MAA with ^{14}C-styrene were assayed before and after hydrolysis (see *Table 4*). Equations (7) and (8) were then used to calculate values for the ratio of the numbers of cyclized and uncyclized MAA units. *Table 4* includes a column showing the counting rate after hydrolysis calculated on the assumption that all MAA units were uncyclized. Only small changes in counting rates were caused by hydrolysis; in two cases, the counting rates were reduced so that the only conclusion to be drawn is that most of the MAA units in the copolymers were cyclized.

Table 4 Hydrolysis of copolymers of methacrylic anhydride with ^{14}C-styrene

| Counting rate of polymer | | | | |
before hydrolysis	after hydrolysis	$(a + b)$	Calc. max. counting rate for hydrolyzed copolymer	$\dfrac{b}{a + b}$
1186	1282	3·72	1960	0·8
2161	2124	1·59	3120	–
2492	2370	1·25	3450	–
2871	3018	0·95	3800	0·8

Copolymer represented as $(C_8H_8)_1(C_8H_{10}O_3)_{a+b}$ where a and b refer to uncyclized and cyclized units respectively
Counting rate for monomeric styrene = 5608

Three unlabelled homopolymers of MAA were hydrolyzed; the products were methylated with ^{14}C-diazomethane and assayed. The counting rate calculated for complete reaction was 4280; the observed values were 4130, 4116 and 4172 indicating that reaction was very nearly complete. Preliminary experiments of the same type were performed on unlabelled copolymers of MAA with styrene but the observed counting rates of the products were less than the minimum possible values calculated from (9) assuming that all MAA units were uncyclized (see *Table 5*). It can only be concluded that hydrolyses of the original copolymers were incomplete because of the heterogeneous nature of the system.

Table 5 Treatment with ^{14}C-diazomethane of hydrolyzed copolymers of methacrylic anhydride with styrene

$(a + b)$ in copolymer	Calc. counting rate for product		obs. counting rate for product
	assume $a = 0$	assume $b = 0$	
3·76	3530	3060	2960
1·25	2610	1880	2110
0·71	2010	1320	1260

See footnotes to *Table 4*
Counting rate for diazomethane = 21 400

CONCLUSIONS

(1) For radical copolymerizations at 60°C involving methacrylic anhydride (monomer–1), monomer reactivity ratios are as follows:

with styrene
$$r_1 = 0.33 \pm 0.03$$
$$r_2 = 0.10 \pm 0.01$$

with methyl methacrylate
$$r_1 = 1.70 \pm 0.07$$
$$r_2 = 0.22 \pm 0.02$$

with methyl acrylate
$$r_1 = 4.75 \pm 0.15$$
$$r_2 = 0.16 \pm 0.02$$

These results lead to a value of e of about 1·2 in agreement with Smets *et al*[8].

(2) Monomeric methacrylic anhydride is at 60°C less reactive than methyl methacrylate towards the benzoyloxy radical. Its low reactivity towards this reference radical can be correlated with the comparatively large value of e.

(3) In homopolymers of methacrylic anhydride and in its copolymers with styrene, there is a high proportion of cyclized monomer units. The results do not completely satisfy a simple reaction scheme in that the proportions of cyclized units are unexpectedly high in homopolymers prepared using low concentrations of monomer. This effect has also been reported[3] from studies involving different experimental methods.

ACKNOWLEDGEMENT

Department of Chemistry,
University of Lancaster, U.K.

REFERENCES

1 Butler, G. B. and Raymond, M. A. *J. Polym. Sci.,* (*A*) 1965, **3**, 3413
2 Corfield, G. C. and Crawshaw, A. *J. Polym. Sci.* (*A*) 1969, **7**, 1179
3 See for example, Smets, G., Hous, P. and Deval, N. *J. Polym. Sci.* (*A*), 1964, **2**, 4825
4 Jones, J. F. *J. Polym. Sci.* 1958, **33**, 7, 15
5 Butler, G. B. and Crawshaw, A. *J. Amer. Chem. Soc.* 1958, **80**, 5464

6 Hwa, J. C. H. *J. Polym. Sci.* 1962, **60**, S12
7 Bevington, J. C., 'Radical Polymerization', Academic Press, London 1961, p 41
8 Smets, G., Deval, N. and Hous, P. *J. Polym. Sci.* (*A*) 1964, **2**, 4835
9 Bevington, J. C., Melville, H. W. and Taylor, R. P. *J. Polym. Sci.* 1954, **12**, 449
10 Bevington, J. C. *Proc. Roy. Soc.* (*A*) 1957, **239**, 420
11 Bevington, J. C. and Brooks, C. S. *J. Polym. Sci.* 1956, **22**, 257
12 Katchalsky, A. and Eisenberg, H. *J. Polym. Sci.* 1951, **6**, 145
13 Bevington, J. C., Harris, D. O. and Johnson, M. *Europ. Polym. J.* 1965, **1**, 235
14 Bevington, J. C. *Trans. Faraday Soc.* 1955, **51**, 1392

Properties of polymer crystal aggregates:
Part 3. Comparison of the annealing behaviour of bulk-crystallized polyethylene with that of aggregates of polyethylene crystals

D. A. BLACKADDER and P. A. LEWELL*

The annealing of mats of aggregated polyethylene crystals was described in a previous paper. The change in properties with increasing annealing temperature was interpreted in terms of two mechanisms, each dominant over a particular temperature range. In a somewhat different sense bulk-crystallized polymer is also an aggregate of crystalline entities bound together, and a comparative study of the behaviour of a selected sample was therefore made. The results, whilst numerically different from those found for mats, confirm that the study of crystal aggregates can provide a key to the understanding of bulk-crystallized polymer in terms of microstructure.

INTRODUCTION

THE SUMMARY of the first paper[1] in this series explained that the work had two aims; besides adding to knowledge of polymer crystals it was intended to relate this knowledge to the description of bulk-crystallized polymer. As a beginning it was shown that mats of polyethylene crystals have tensile properties in the micro-strain region remarkably similar to those of bulk-crystallized polymer of comparable density. It was deduced that a common mechanism of interlamellar slip was operative. The two materials differed very greatly with respect to strain at fracture, since mats showed brittle fracture at strains of only 1 %. This difference was interpreted in terms of tie molecules between crystalline units, these tie molecules being characteristic of bulk-crystallized material[2] but absent in mats prepared from initially independent crystals. In a second paper[3], experiments were described in which mats of crystals were annealed at progressively higher temperatures, and three properties were measured to document the changes in mat structure. In the limit, a mat which had been annealed at a temperature above the melting point naturally became indistinguishable from bulk-crystallized material. Some of the results are summarized in *Figure 1*, and it is seen that the density and tensile modulus pass through a maximum for an annealing temperature of about 117°C. *In situ* thickening and partial melting respectively

---

were proposed as the dominant processes below and above this temperature.

In the present paper similar annealing experiments are reported on bulk-crystallized polyethylene, the object of the work being to interpret the observed changes in physical properties on annealing in terms of specific processes at the molecular level. The experiments again included the inhibition of these processes by irradiation in order to determine their contributions to the total annealing effect.

EXPERIMENTAL

The extent to which the properties of a given sample of polyethylene can be modified by annealing is determined by the thermal history of the sample and by its molecular constitution. Among the molecular properties the degree of branching and the $\bar{M}_w/\bar{M}_n$ ratio are particularly important. Some preliminary experiments on the three polymers, Rigidex Type 3, Rigidex Type 50 and Vestolen A6016 (as supplied in sheet form), showed that Vestolen underwent the largest density change on annealing, probably as a result of its narrow molecular weight distribution. This polyethylene was therefore selected for the subsequent experiments, on the grounds that the largest possible changes on annealing were desirable so that small effects might not go unnoticed.

The Vestolen sheet was cut into pieces of approximate dimensions 19 mm $\times$ 13 mm $\times$ 2·5 mm. These specimens were annealed for 18 h at various temperatures up to 150°C using the standard procedure described previously[3]. After annealing, the specimens were cooled to room temperature at a rate of 5°C/h. Appropriate shapes for tensile testing[1] were then cut from the annealed specimens, and the tensile modulus of each was determined at a strain rate of about $0·5 \times 10^{-6}$ s^{-1}. The maximum applied stress was about 1 MN/m^2, and the stress–strain plots were linear.

To establish the detailed pattern of density changes with annealing temperature, small cubes of polymer (edge 2·5 mm) were sealed under nitrogen in glass tubes and annealed as before[3]. The densities were then measured in a density gradient column at 25°C.

The whole testing programme was repeated using samples which had been irradiated with a dose of 40 Mrad[1].

RESULTS

For the purposes of comparison the results of the corresponding experiments on crystal mats[3] are summarized in *Figure 1*. The change in density of bulk crystallized polyethylene with annealing temperature is shown in *Figure 2* for both irradiated and unirradiated samples. The corresponding variations of tensile modulus appear in *Figure 3*.

Annealing at temperatures up to and including 75°C caused no detectable change in any specimen of bulk-crystallized polymer, and the plotted values of the density and tensile modulus for specimens annealed at 75°C are therefore effectively the values for unannealed material.
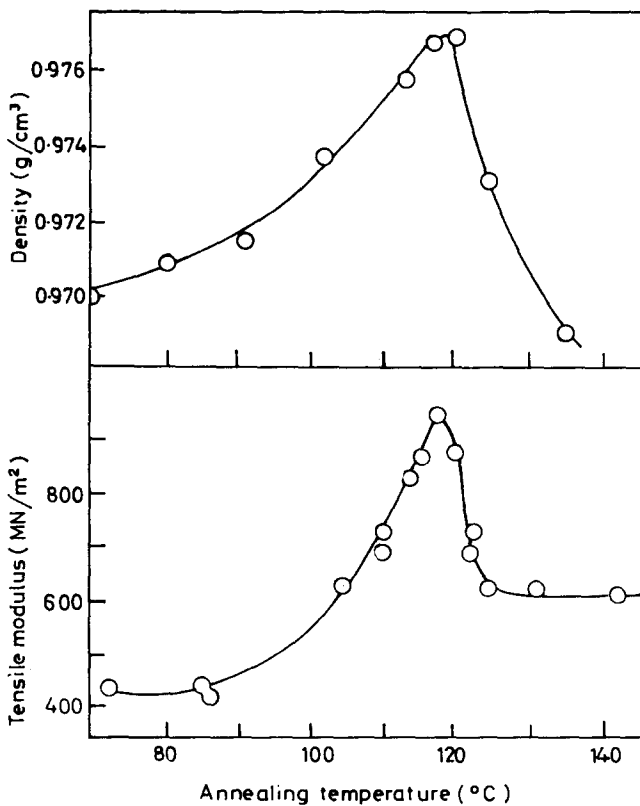
Figure 1 The variation of the density and tensile modulus of mats of agglomerated polyethylene crystals with annealing temperature[3]
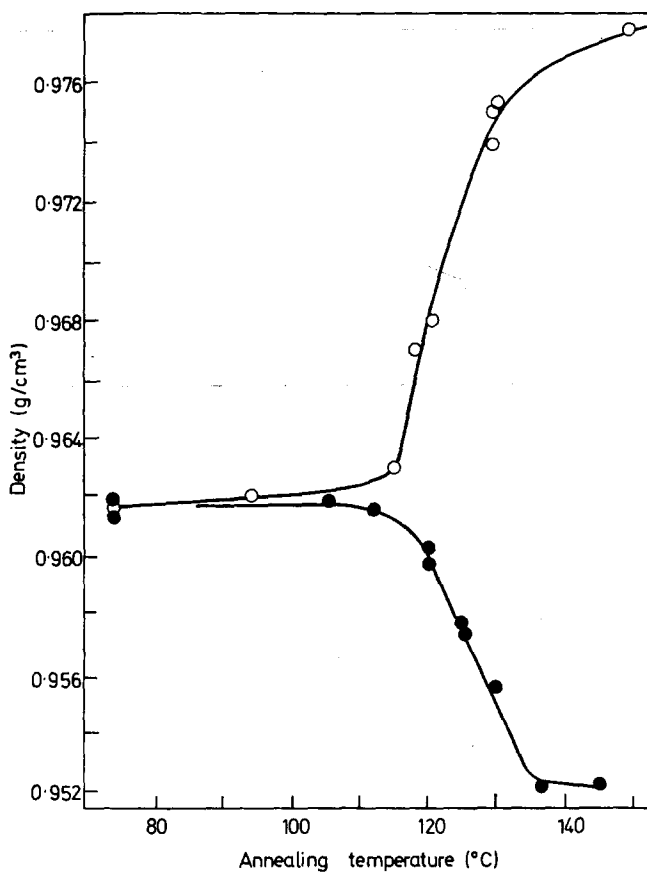
Figure 2 The variation of the density of bulk-crystallized polyethylene with annealing temperature: ○, unirradiated polymer; ●, irradiated polymer (40 Mrad)
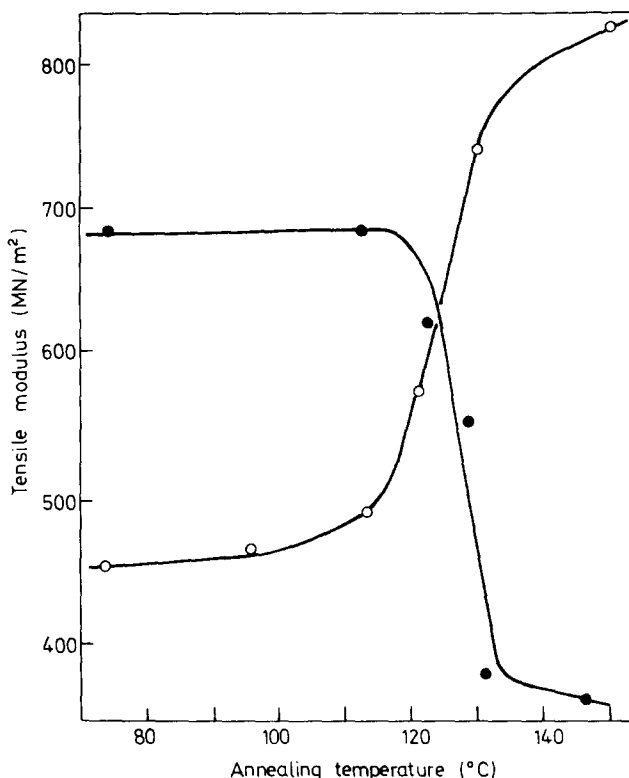
Figure 3 The variation of the tensile modulus of bulk-crystallized polyethylene with annealing temperature: ○, unirradiated polymer; ●, irradiated polymer (40 Mrad)

For unirradiated specimens the tensile modulus and density curves are of similar shape with little change in evidence for annealing temperatures below 115°C. After annealing at higher temperatures remarkable increases are observed, and both properties tend towards high limiting values for annealing temperatures in excess of 130°C. The maxima characteristic of mats (*Figure 1*) are wholly absent.

The irradiated specimens show no detectable changes on annealing at temperatures below about 115°C, but at higher temperatures a sharp decrease in both density and the tensile modulus is observed.

DISCUSSION

The fact that irradiation increases the modulus of unannealed bulk-crystallized material is consistent with the findings of other workers[4] and with the fact that mats of crystals are similarly strengthened[1]. Interlamellar slip appears to be involved, and irradiation introduces interlamellar linkages[5] which resist this kind of movement.

663

For annealing temperatures up to 115°C, the increases in density and modulus for unirradiated Vestolen were small but experimentally significant, particularly as corresponding small effects were not discernible in the irradiated samples. These observations fall neatly into the scheme proposed previously[3]. Compared with a mat of crystals, an unirradiated sample of bulk-crystallized polymer has only a very limited capacity for *in situ* thickening by which the interlamellar boundaries involved in slip processes might be strengthened. Statton's mechanism for interlamellar interlock[6] presumably operates, though to a very slight extent. After irradiation, the capacity of bulk-crystallized polymer for *in situ* thickening, small in any event, is completely suppressed. (In the case of mats a very large effect was substantially suppressed by a radiation dose of 40 Mrad.) This observation is thoroughly in accord with what is known about the close-knit structure of bulk polymer. Many molecules crystallizing from the melt are liable to be partly associated with two or more lamellae, the portions not incorporated in a lattice forming a tie which may or may not be in tension in the product when cold. Very slight *in situ* thickening would produce or increase tension in these tie molecules and the process would soon come to a halt. Molecules in mats, on the other hand, would be expected to have a considerable capacity for *in situ* thickening.

The consequences of annealing at temperatures above 115°C must be considered, bearing in mind the earlier work on mats[3]. It was there concluded that partial melting was the dominant process on annealing at the higher temperatures. The new findings, that unirradiated bulk-crystallized samples show a sharp increase in modulus and density in this region while irradiated samples show a correspondingly sharp decrease, are compatible with the postulate of partial melting.

For unirradiated bulk samples, partial melting is followed by recrystallization on cooling after completion of the annealing treatment. The state of partial disorder thus leads to an enhanced degree of crystallinity, with corresponding increases in the tensile modulus and density. Irradiated samples behave quite differently on cooling after partial melting. Instead of an increased degree of crystallinity being produced the cooled sample is actually less crystalline than it was originally, the more branched molecules resulting from irradiation crystallizing less well than the original molecules. The density and tensile modulus of irradiated samples therefore decrease on annealing above 115°C where partial melting occurs.

It should be understood that the temperature of 115°C is likely to depend on the particular polyethylene used and on its thermal history, particularly its mode of crystallization from the melt.

CONCLUSIONS

The comparison of aggregates of polyethylene crystals with bulk-crystallized polyethylene has been extended to include annealing behaviour. Experiments with irradiated samples confirm that partial melting is responsible for changes in the properties of bulk-crystallized material on annealing at temperatures above 115°C. The annealing mechanism is similar to that operating in mats

of initially discrete crystals for the same temperature range, though the physical consequences of annealing are reversed.

The annealing behaviour of bulk-crystallized samples has been found to differ from that of crystal mats in the extent to which *in situ* thickening occurs at lower annealing temperatures, prior to the onset of partial melting. This observation is related to the basic differences in molecular coordination between the two materials.

ACKNOWLEDGEMENT

University of Cambridge,
Department of Chemical Engineering,
Pembroke Street, Cambridge, England   (*Received 13 July 1970*)

REFERENCES

1 Blackadder, D. A. and Lewell, P. A. *Polymer, Lond.* 1970, **11**, 125
2 Keith, H. D., Padden, F. J. and Vadimsky, R. G. *J. appl. Phys.* 1966, **37**, 4027
3 Blackadder, D. A. and Lowell, P. A. *Polymer, Lond.* 1970, **11**, 147
4 Charlesby, A., 'Atomic Radiation and Polymers', Oxford University Press, Oxford, 1960
5 Salovey, R. and Bassett, D. C. *J. appl. Phys.* 1964, **35**, 3216
6 Statton, W. O. *J. appl. Phys.* 1967, **38**, 4149

Correlation crystallinity and physical properties of heat-treated cellulose triacetate fibres

A. M. HINDELEH and D. J. JOHNSON

Previous measurements of crystallinity in fibres of cellulose triacetate have been qualitative or semi-quantitative; in this work quantitative measurements of relative crystallinity have been made on cellulose triacetate yarn heat treated in the range 20–300°C following the x-ray diffraction method of correlation crystallinity index. The onset of crystallization is clearly marked by a transition in the crystallinity index at 172°C, and beyond this annealing temperature tenacity and crystallinity are inversely correlated. Orientation also improves with annealing temperature with a less well defined transition around 120–180°C. Initial Young's modulus increases with temperature whilst other physical properties have optimum values in the range 180–220°C. Cutting and grinding are found to have an adverse effect on the correlation crystallinity index which is in fact a measure of lattice perfection.

INTRODUCTION

THE DEVELOPMENT of crystallinity in thermally-treated cellulose triacetate fibres has been described by several workers[1], and it is well known that crystallization occurs considerably below the melting point (about 300°C). Cellulose triacetate fibres are thermoplastic and their ability to be heat set is an extremely valuable textile property, yet all previous attempts to assess crystallinity in this polymer have been qualitative or at best semi-quantitative. Several empirical indices have been proposed, based on the average angle of four major peaks in the x-ray diffraction diagram[7], or on differences between maxima and minima of prominent diffraction peaks[8,9]. These measures are completely arbitrary and must involve large errors since the diffraction diagram contains many overlapping reflections indexed by Dulmage[10] in terms of an orthorhombic unit cell. In addition these arbitrary measures cannot be applied at temperatures below 210°C where the crystallinity is poorly developed and the diffraction peaks are unresolved (see *Figure 1*).

A more reliable method of assessing crystallinity is required which will be valid for all possible heat-treatment temperatures and will take into consideration the variations in the diffraction pattern over a wide range of scattering angle. At the same time we must bear in mind recent developments in fibre science which necessitate a reappraisal of the classical two-phase crystalline—amorphous model for the structure of fibres. In particular, Hosemann's introduction of the concept of lattice disorder or paracrystallinity[11], together with an increasing need to describe some fibre properties and structural features in terms of solid-state phenomena[12–14], suggest that any measure of crystallinity will in effect be a measure of lattice order or perfection and that any absolute measure will be difficult. A relative x-ray analysis of

666
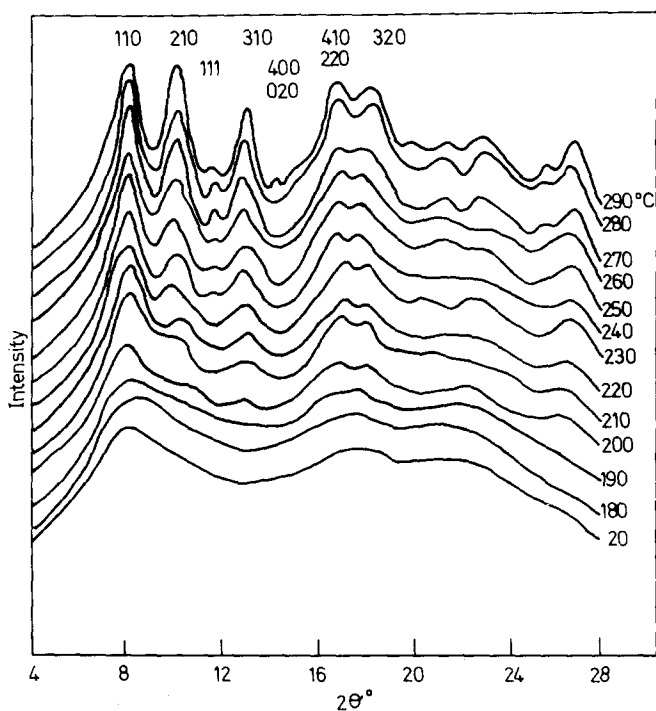
Figure 1 X-ray diffraction traces of cellulose triacetate yarn an-
nealed at different temperatures; each trace has a different base
level. Main reflections according to Dulmage[10] are indicated

crystallinity is, however, quite straightforward, especially when electronic
computation is available. This paper will therefore be concerned with a
relative assessment of crystallinity in cellulose triacetate fibres, although we
hope to return to the problem of measuring and defining absolute crystallinity
in a later publication.

METHOD

In this work the method used for assessing the crystallinity of cellulose triacetate
fibres is based on the detailed investigations of Wakelin, Virgin and Crystal[15].
The basis of the method is the x-ray scattering law termed the 'Law of Con-
servation of Intensity' by Vainshtein[16]. This law states that when x-ray
diffraction takes place, the total scatter in reciprocal space due to regions
with lattice perfection and the total scatter due to an equivalent set of
completely disordered atoms is exactly equal. Equivalent regions with inter-
mediate states of lattice order will again have exactly equal total scatter in
reciprocal space; thus lattice imperfections smooth out the oscillations of the
perfect-lattice diffraction about the random-lattice diffraction but the total
scatter remains constant (see *Figure 2*).

667
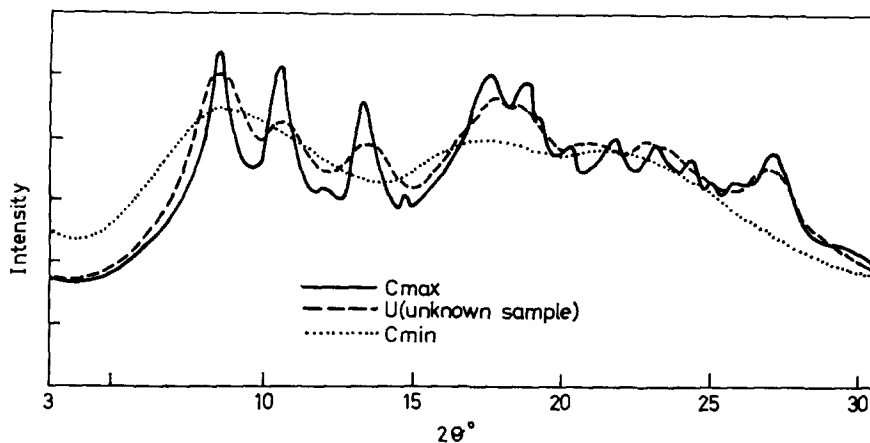
Figure 2 Normalized x-ray diffraction traces for cellulose triacetate of maximum crystallinity (C max), minimum crystallinity (C min), and unknown crystallinity (U) —— C max;
– – – U (unknown sample): . . . . . . C min.
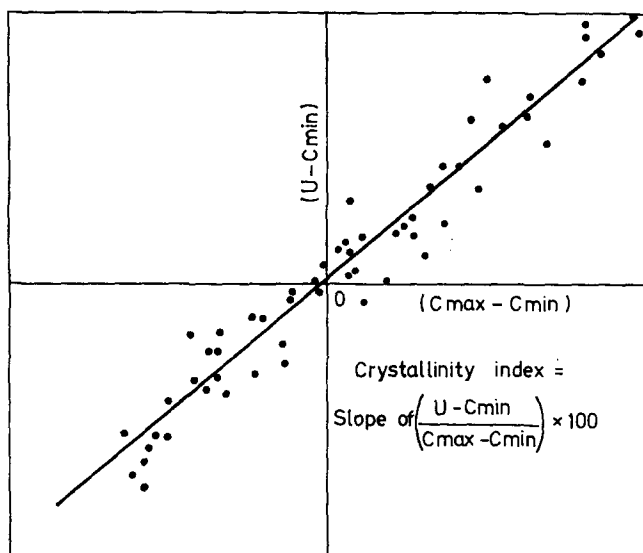
Figure 3 Typical output of normalized intensity differences together with regression line used to calculate Crystallinity Index. Crystallinity Index = Slope of (U − Cmin/Cmax − Cmin) × 100

Wakelin, Virgin and Crystal[15] made use of a crystalline standard with a relative crystallinity index of 100 and an 'amorphous' standard of crystallinity index 0. Any other specimen could then be placed on a scale within the range 0 to 100. It is arguable whether the 'amorphous' cellulosic standard was truly amorphous in the sense of having complete lattice disorder yet this does not invalidate the method. We believe it is more appropriate to term the zero-index sample, C_{min}, and the sample with index 100, C_{max}. If we refer to a

specimen of unknown lattice order as U then at incremental points on normalized diffraction traces of C_{max}, C_{min}, and U (see *Figure 2*), the intensity differences $(C_{max} - C_{min})$ and $(U - C_{min})$ can be determined. The correlation–crystallinity index can be obtained from the slope of the regression line of $(U - C_{min})$ on $(C_{max} - C_{min})$ (see *Figure 3*), thus

$$\text{Crystallinity Index, } CI = \text{slope of } \frac{(U - C_{min})}{(C_{max} - C_{min})} \times 100.$$

Because this correlation–crystallinity index makes use of differences in diffracted intensity at the same scattering angle, there is no need to correct for angular factors such as polarization incoherent scatter, or the Lorentz factor, although it may be necessary to make a correction for differences in absorption and air-scatter. We may also note that Wakelin *et al*[15] used randomized fibre specimens for diffraction analysis, but Statton[17], working with polyethylene terephthalate found it more convenient to rotate his specimens.

<div align="center">EXPERIMENTAL</div>

Heat treatment

Cellulose triacetate yarn of 150 denier 36 filaments produced by Société Rhodiaceta has been used throughout. Specimens were annealed at constant length in a nitrogen atmosphere at temperatures controlled to $\pm 1\,°C$ in the range 20–300°C for 30 min except where indicated otherwise. Extension at the annealing temperatures could be carried out by a motor-driven stretching device[18].

Physical properties

Tenacity, elongation at break, yield point, elastic recovery and initial Young's modulus were measured on an Instron Tensile Tester working with a load cell which can exert a maximum load of 2 kg. The gauge length was 10 cm and the rate of extension either 10 cm min^{-1} or 5 cm min^{-1} so that rupture occurred in about 20 s. In the case of elastic recovery and initial Young's modulus the rate of extension was 1 cm min^{-1}. Ten determinations were made for each specimen.

Orientation

High-angle x-ray diffraction photographs were recorded in a flat-plate camera with pinhole collimation (0·25 mm). Orientation measurements were made on a Joyce-Loebl microdensitometer with a polar table. Procedures were adopted to ensure that rotation was accurate about the centre, and that the optical density was within the linear range of response of the film to x-rays. The orientation parameter which was used in this study is the angular half-width at 50% amplitude of the intensity distribution curve around the 110 reflection.

Crystallinity

X-ray diffractometry was carried out with a modified Hilger and Watts Y115 diffractometer and a Y90 constant output generator. The diffractometer employs a scintillation counter whose output is fed through a single-channel pulse-height analyser to a pulse counter or, via a ratemeter, to a chart recorder. Tests showed that the apparatus gives effective monochromatization for Cu–K_α of the nickel-filtered primary beam, and that the counting response was linear in the range required.

A computer program for use on the University's KDF9 computer was written and established. Given data on scattering angle, normalized C_{max} and C_{min} intensities, and unnormalized intensities, U, for specimens of undetermined crystallinity, the program calculates the area under the scattering curve, normalizes the intensity values, then evaluates the correlation–crystallinity index and its variance by a least-squares method.

Validity of the Law of Conservation of Total Intensity

Since the method of assessing relative crystallinity by the correlation method assumes that equal masses of material with perfect lattice order (crystalline), intermediate lattice order (paracrystalline), and random lattice order
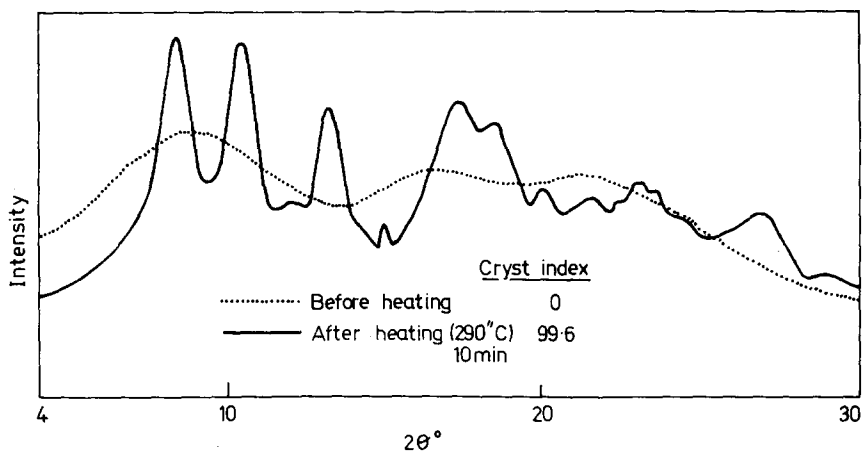
Figure 4 X-ray diffraction traces of a ground precipitate of cellulose triacetate before and after heating to 290°C

(amorphous), will give identical total scattering of x-rays under the same experimental conditions, it was felt necessary to test this assumption critically. Accordingly, a sample with a minimum ordering of the chain molecules was prepared by dissolving cellulose triacetate yarn in a mixture of 90% methylene dichloride and 10% methanol then adding petroleum ether to effect precipitation. The precipitate was dried and ground for three hours in a vibratory ball mill then pressed into a disc for x-ray analysis. The diffractometer trace is given in *Figure 4*. After annealing at 290°C for 10 min the same

disc specimen revealed crystallization of the form again plotted in *Figure 4*. Measurement of the areas under each trace in the range $3°$ to $60°$ (2θ) gave identical values within 1%. After correction of this data for air-scatter incoherent scatter, polarization and Lorentz-factor the areas agreed within 2%. Strictly the intensity data should be multiplied by $4\pi s^2$ where s is the reciprocal-lattice vector; this was tested and the agreement of the overall areas was within 3%, but the multiplication is unnecessary for routine analysis.

Selection of C_{max} and C_{min} standards

Diffractometer traces for the precipitated and ground specimens, cast film, and for a yarn specimen after melting, were compared. The ball-milled precipitate had the lowest state of crystallinity and was chosen as the zero index standard (C_{min}).

The choice of the C_{max} standard with index 100 was more difficult; specimens of annealed film, annealed precipitate and annealed yarn were considered; eventually yarn heated at $290°C$ for 10 min, then at $280°C$ for 3h, was chosen.

Uncorrected diffraction traces for the standards after normalization to equal area are given in *Figure 2*. The C_{max} standard was rotated in a plane perpendicular to the direction of the incident x-ray beam during exposure. A motor-driven rotator was built for the Y115 diffractometer[18]. The sample of annealed precipitate, which will have completely randomized crystallites was found to have a correlation crystallinity of $99\cdot6$ (see *Figure 4*). This is equivalent to the C_{max} standard within experimental error; it was considered therefore, that fibre rotation was an adequate randomization technique for the purpose of this investigation and that further randomization is unnecessary. In fact we shall show later that grinding and even cutting have an adverse effect on lattice perfection.

<div align="center">RESULTS</div>

Correlation crystallinity

A typical normalized diffractometer trace in the range $3°$ to $35°$(2θ) for an unknown sample, U, together with C_{max} and C_{min} traces are depicted in *Figure 2*; traces used for computation were in the range $3°$ to $60°$. The ordinate differences ($U - C_{min}$) and ($C_{max} - C_{min}$) together with the regression line of ($U - C_{min}$) on ($C_{max} - C_{min}$) for a specimen with unknown crystallinity are given in *Figure 3*.

Normalized diffractometer traces for rotated specimens heat treated in the range $20-290°C$ are given in *Figure 1*. It is immediately evident that methods of crystallinity measurement which rely on differences between peak maxima and minima may only be significant for specimens treated above $210°C$. The results for rotated fibre specimens annealed in the range $20-300°C$ are given in *Table 1* and *Figure 5*. The commercial yarn as produced has a CI of $6\cdot5$, annealing below $160°C$ has little effect, but above $180°C$ the onset of crystallization is rapid.

The straight line parts of the crystallization curve have been fitted by a

Table 1 Crystallinity index of heat-
treated cellulose triacetate

Temp. (°C)	CI	Temp. (°C)	CI
20	6·5	210	42·0
60	8·1	220	48·3
80	10·9	230	60·4
100	11·3	240	64·2
120	11·7	250	72·2
140	11·9	260	76·0
160	12·5	270	85·0
170	13·3	280	94·3
180	16·0	290	99·5
185	23·7	293	86·1
190	27·1	295	73·2
200	31·3	300	7·0
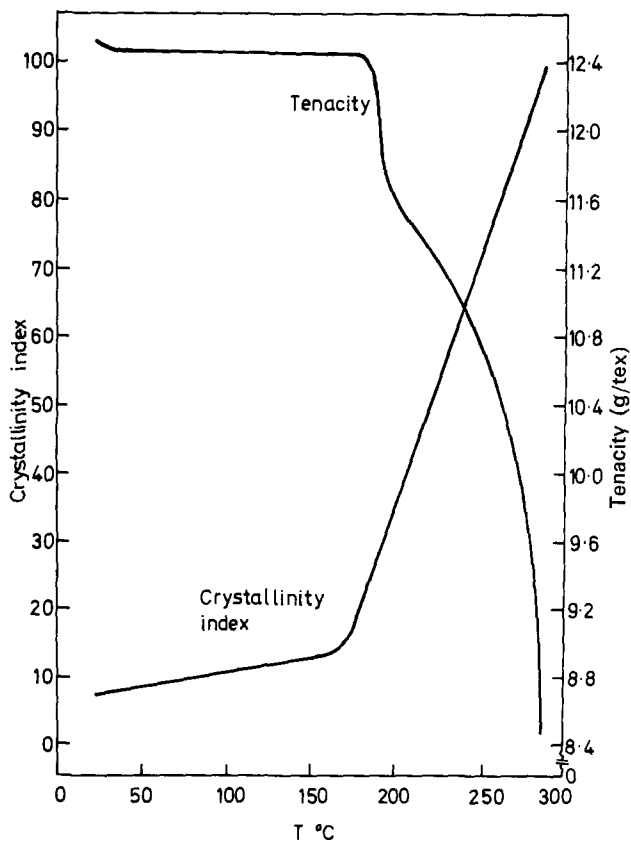
Figure 5 Crystallinity Index and tenacity of cellulose triacetate
yarn annealed at different temperatures

least-squares library program and give a transition crystallization temperature of 172°C.

After 290°C lattice disorder occurs and at 300°C the specimens melt. Gross structural changes in the region 290–300°C were studied in a Stereoscan electron microscope. At 293°C the fibres begin to stick together, at 295°C the fibre surface and cross section show blisters which suggest the evolution of gases and internal degradation, and at 300°C melting occurs.

Tensile properties

The results of tenacity measurement after annealing at different temperatures are also given in *Figure 5*. Below 185°C tensile strength remains constant, then a rapid fall off in strength occurs so that a 200°C 92% of the initial tenacity is retained, then 87% at 240°C, and 55% at 295°C. From
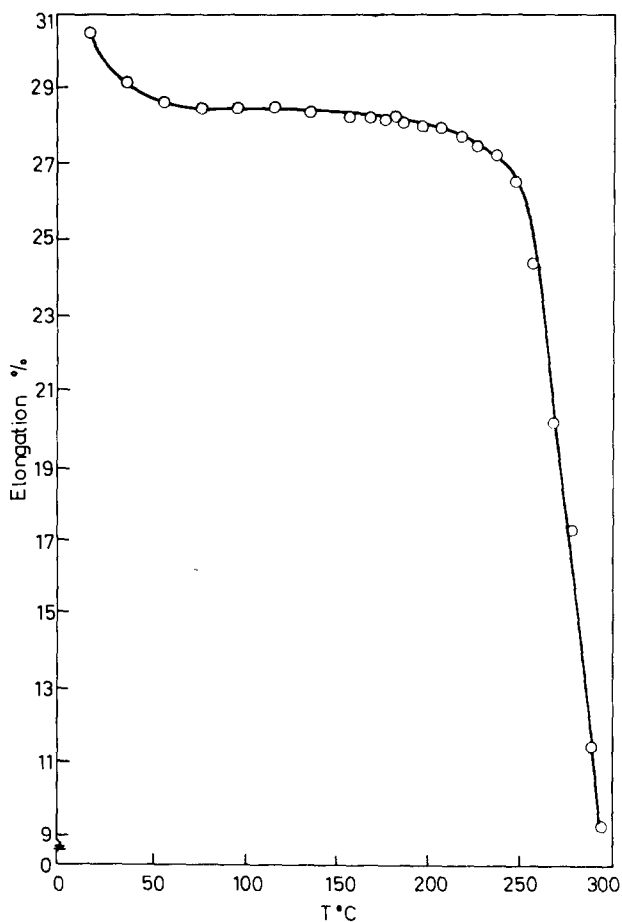
Figure 6 Elongation at break of annealed cellulose triacetate yarn

673

the curves reported by Fester and Liu[4] it can be deduced that specimens heat-set in air retain strengths of 83% at 220°C and 68% at 240°C. Evidently the use of nitrogen delays degradation due to oxidation.

The inverse relationship between tenacity and crystallinity has been observed in nylon[19], polypropylene[20] and in carbon fibres[14]; in the case of cellulose triacetate it is particularly well marked with a correlation coefficient of 0·996
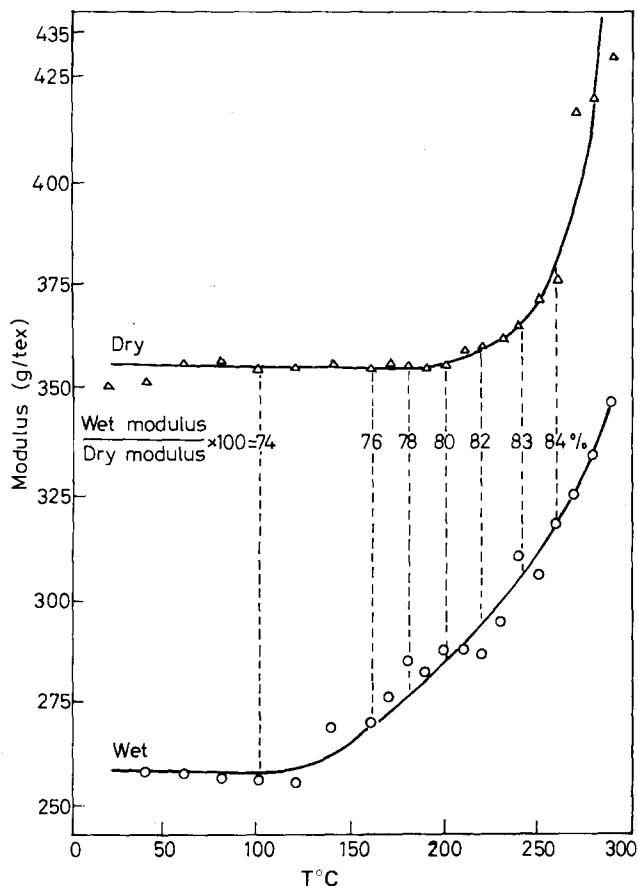
Figure 7 Initial Young's Modulus of wet and dry annealed cellulose triacetate yarn

in the range 180°C to 290°C. A second order regression equation for tenacity T (g tex^{-1}) and crystallinity index CI for the range 20°C to 290°C has been determined as:

$$T = 12 \cdot 552 - 0 \cdot 008 \text{CI} - 0 \cdot 0003 \text{CI}^2$$

Measurements of the elongation at break are given in *Figure 6*, and of wet and dry Young's modulus in *Figure 7*. Results for yield-point stress and strain are given in *Figure 8*, and for elastic recovery from 5% extension in

674

Figure 9. Although tenacity is immediately affected by crystallization the elongation at break does not suffer an appreciable fall until a heat-treatment temperature of 240°C in nitrogen; this can be contrasted with an 80% loss in elongation at break for specimens treated at 240°C in air. Evidently degradation of the disordered chains is prevented so that elongation at break
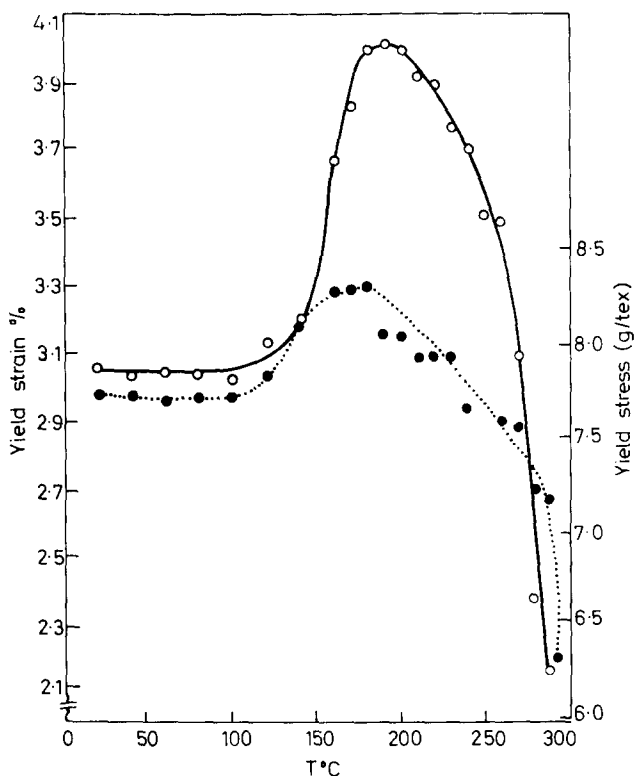
Figure 8 Yield point stress (closed circles) and strain (open circles) for annealed cellulose triacetate yarn

is maintained although the breaking stress is reduced. The initial Young's modulus increases in both the wet and dry states as crystallization proceeds. Yield stress and yield strain have optimum values in the ranges 160–200°C to 220°C respectively although the relative changes are small. Elastic recovery also reaches an optimum in the range 180–220°C.

Orientation

Orientation measurements on annealed yarn specimens are given in *Table 2* and *Figure 10*; each value is an average of three determinations on the 110 reflection for three x-ray photographs. Again a transition is observed in the region 120° to 180°C, the straight-line parts of the curve intersecting about 172°C; a further but less marked transition occurs around 200°C. Fester and
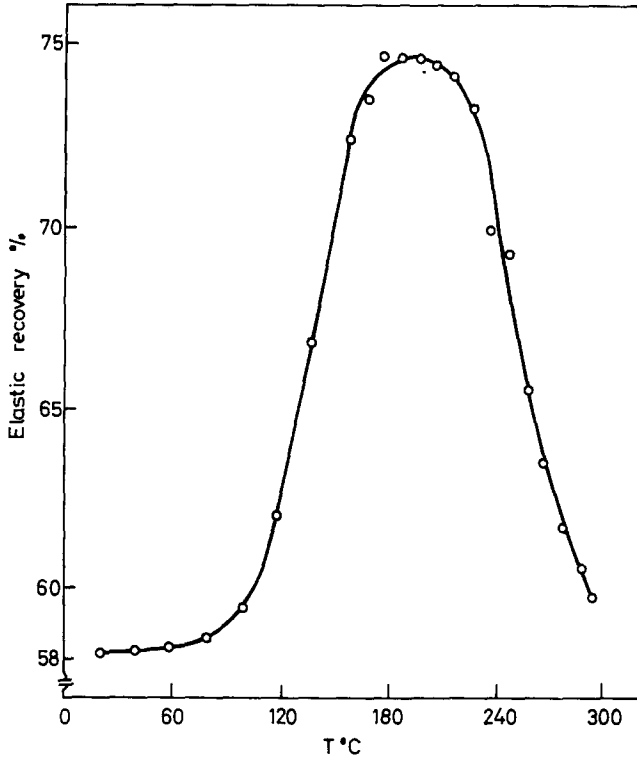
Figure 9 Elastic recovery from 5% extension of dry annealed cellulose triacetate yarn
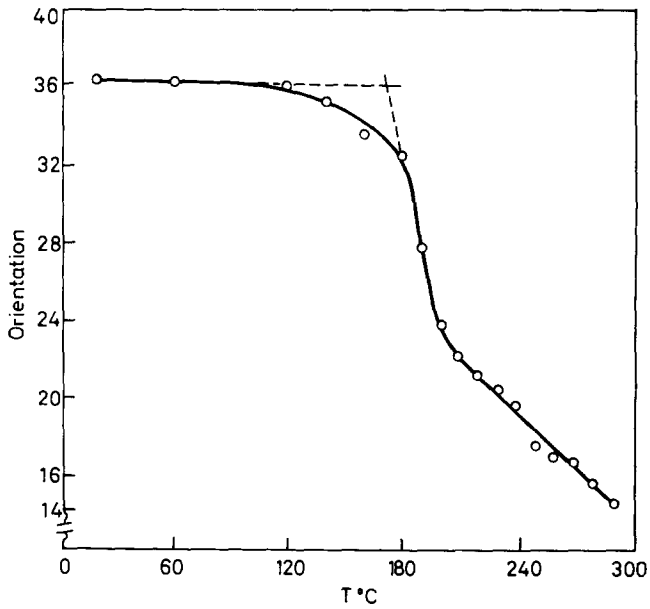
Figure 10 Angular half width at half height orientation parameter for annealed cellulose triacetate yarn

676

Table 2 Orientation of heat-treated cellulose triacetate

Temp. (°C)	Orientation (degrees)	Temp. (°C)	Orientation (degrees)
20	36·4	220	21·3
60	36·0	230	20·8
120	36·1	240	19·7
140	35·3	250	17·6
160	33·7	260	17·1
180	32·5	270	16·7
190	27·8	280	15·8
200	23·8	290	14·5
210	22·2		

Liu[4] have investigated changes in the structure of cellulose triacetate yarn by the iodine absorption method; in fact their results for both iodine absorption and dye affinity are very similar to the changes in orientation depicted here. Clearly improved crystallinity and orientation will both affect dye uptake and iodine absorption as well as physical properties in the region 180–220°C which is indeed the region where commercial heat setting is carried out.

Effect of cutting and grinding on crystallinity

We have already observed that rotation of a fibre bundle effectively randomizes the diffraction diagram; it is interesting, therefore, to check the effect of cutting and grinding on the correlation–crystallinity index of fibre specimens. Two yarn samples were chosen, one heated at 290°C, the other at 293°C. The yarn was cut into fine fragments about 1 mm in length and pressed into a disc 10 mm in diameter and 1·5 mm thick. Other specimens of yarn heat-treated at 290°C were cut into 1 mm fragments, ground in a vibratory ball mill for periods up to 3 h, then formed into discs. Rotation of the discs could be carried out during diffraction analysis. The results are given in *Table 3*. Cutting and pressing evidently results in some disordering of the crystal

Table 3 Effect of mechanical impact (vibratory ball-mill) on the crystallinity index

Sample and treatment	CI
Yarn annealed at 290°C for 10 min, sample rotated	99·5
Yarn fragmented and ball-milled	
5 min (sample rotated)	30·4
5 min (sample not rotated)	29·4
20 min (sample not rotated)	24·6
1 h (sample not rotated)	15·2
3 h (sample not rotated)	7·1

structure, with a drop in CI of about 10%. Rotation had little effect on the results and we can again assume effective randomization. Other workers have found similar changes (about 5%) in crystallinity with cotton[15] and PET[21].

Mechanical grinding is even more drastic, 5 min grinding is sufficient to reduce the correlation crystallinity index from 100 to 30, and 3 h grinding reduces it to 7. Examination of the surface topography of fibres ball-milled for 5 min indicated the occurrence of longitudinal cracks of varying length. These cracks together with the reduction in crystallinity index suggest the occurrence of disturbances in the internal structure.

Although others have noted a reduction in crystallinity on grinding[8,22-24], these are believed to be the first quantitative measures for cellulose triacetate and show that no reliance can be placed on crystallinity measurements after grinding of this nature.

A yarn specimen annealed at 290°C (CI 99·5) then ball-milled (CI 7·1), was reannealed at 290°C; the crystallinity index returned to 95·5 and gave identical total scattering within 1%, again indicating that the scattering power of the ordered and disordered crystals are equivalent.

Effect of extension on crystallinity

Specimens of cellulose triacetate yarn extended under the following conditions were investigated

(1) Yarn stretched 20% at room temperature, annealed for 30 min at 260°C, then cooled to room temperature

(2) Yarn stretched 10% at the annealing temperature of 240°C, annealed for 1 h, then cooled

(3) Yarn annealed at 270°C for 30 min, cooled to room temperature, then stretched either 5, 10 or 15%.

The effect of extension on the correlation crystallinity index is given in *Table 4*. When extension takes place before or during annealing crystallization is impeded, but when extension takes place after annealing little

Table 4 Effect of stretching on the crystallinity index of cellulose triacetate

Sample and Treatment	CI
Yarn 260°C, 30 min	
No stretch	76·0
20% stretch before annealing	49·9
Yarn 240°C, 1 h	
No stretch	64·2
10% stretch during annealing	33·4
Yarn 270°C, 30 min	
No stretch	85·0
10% stretch after annealing	80·1
15% stretch after annealing	77·9

disruption of lattice orders occurs. This disruption of lattice order has also been noted by Statton in PET[17].

The effect of extension on orientation is also given in *Table 5*. It is apparent that improved orientation does not mean improved lattice order although a cursory examination of the x-ray photographs could give the false impression that the highly oriented fibre diagram had the sharper diffraction arcs.

Table 5 Orientation of stretched cellulose triacetate

Temp. (°C)	Annealing time	Extension %	Orientation (degrees)	
			Stretching before annealing	Hot-stretch
240	1 h	0	19·7	–
		5	19·1	19·1
		10	17·0	16·6
		15	15·1	14·9
		20	12·2	12·9
		25	10·9	10·7
260	30 min	0	17·1	–
		5	16·1	16·4
		10	15·3	15·1
		15	13·4	13·3
		20	20·4	12·5
		25	10·1	10·4
290	10 min	0	14·5	–
		5	13·7	13·1
		10	11·4	11·0
		15	9·5	9·8
		20	8·5	8·8
		25	8·1	–
		40 in water	7·4	–

SUMMARY

The method of Correlation Crystallinity has revealed a definite crystallization transition in cellulose triacetate yarn at an annealing temperature of 172°C, above the crystallinity index increases sharply until 290°C where it attains a value of 100. After 290°C lattice disorder occurs. The standards chosen to define the range of crystallization were selected on a relative scale and represent the minimum and maximum attainable states of crystalline order in cellulose triacetate. A similar but less well defined transition in the region of 120–180°C occurs in orientation which improves continuously with rise in heat-treatment temperature until 290°C.

Cutting and grinding of fibres have an adverse effect on the lattice perfection as determined by this method of crystallinity measurement. Extension during annealing impedes crystallization, but after annealing extension causes little disruption of lattice order. Stretched fibres show improved orientation, but it is apparent that improved orientation, does not mean improved lattice order. Tenacity and crystallinity index are negatively correlated with a second-order regression equation in the crystallization

679

region. Initial Young's modulus improves continuously as crystallization proceeds. Others physical properties have optimum values in the region between 180°C and 220°C.

ACKNOWLEDGEMENTS

Textile Physics Laboratory
Department of Textile Industries,
University of Leeds, UK

REFERENCES

1 Baker, W. O., Fuller, C. S. and Pape, N. R. *J. Amer. Chem. Soc.* 1942, **64**, 776
2 Work, R. W. *Textile Res. J.* 1949, **19**, 381
3 Fester, W., Jellinek, G. and Liu, S. T. *Melliand Textilchemie* 1965, **6**, 153
4 Fester, W. and Liu, S. T. *Textile Praxis* 1966, **21**, 440
5 Jellinek, G. *Melliand Textilber.* 1966, **47**, 1183
6 Zaspinok, G. S., Zhegalova, N. N., Vasil'ev, B. V., Naimark, N. I. and Tarakamov, O. G. *Vysokomol Soyed (A–11)* 1969, **1**, 152
7 Stoll, R. G. *Textile Res. J.* 1955, **25**, 650
8 Sprague B. S., Riley, J. L. and Noether, H. D. *Textile Res. J.* 1958, **28**, 275
9 Veveris, G. P., Pashkevichyus, V. V. and Dobilene, A. K. *Textil. Prom.* 1967, **27**, 20
10 Dulmage, W. J. *J. Polym. Sci.* 1957, **26**, 277
11 Hosemann, R. *Polymer Lond.* 1962, **3**, 349
12 Predecki, P. and Statton, W. O. *J. appl. Polym. Sci.* (*Appl. Polymer Symposia*) 1967, **6**, 165
13 Johnson, D. J. and Tyson, C. N. *J. appl. Phys. D:* (*Appl. Phys.*) 1969, **2**, 787
14 Johnson, D. J. and Tyson, C. N. *J. appl. phys. D:* (*Appl. Phys.*) 1970, **3**, 526
15 Wakelin, J. H., Virgin, H. S. and Crystal, E. *J. appl. Phys.* 1959, **30**, 1654
16 Vainshtein, B. K. 'Diffraction of x-rays by Chain Molecules', Elsevier Publishing Co., London, 1966, p 178.
17 Statton, W. O. *J. appl. Polym. Sci.* 1963 **7**, 803
18 Hindeleh, A. M. Ph.d. Thesis, University of Leeds, 1970
19 Dismore, P. F. and Statton, W. O. *J. Polym. Sci.* (C) 1966, **13**, 133
20 Sheehan, W. C., Wellman, R. E. and Cole, T. B. *Textile Res. J.* 1965, **35**, 626
21 Johnson, J. E. *J. appl. Polym. Sci.* 1959, **5**, 205
22 Nelson, M. L. and Conrad, C. M. *Textile Res. J.* 1948, **21**, 440
23 Segal, L., Creely, J. J., Martin, A. E. and Conrad, C. M. *Textile Res. J.* 1959, **29**, 10, 786
24 Hermans, P. H. and Weidinger, A. *J. Amer. Chem. Soc.* 1946, **68**, 2547

Book Reviews

Poly(vinyl chloride)

by J. C. KOLESKE and L. H. WARTMAN

BPC Publishing Ltd., London, 1969, 50s.

This third volume of Macdonald's series of polymer monographs is particularly welcome since the number of books on poly(vinyl chloride) is surprisingly small when one considers the scientific and technological importance of the polymer. The problems posed by attempting to review the very extensive literature on poly(vinyl chloride) in such a small volume are enormous and the authors have chosen to solve them by concentrating their attention on the areas which are of interest to them. This has resulted in a rather unbalanced treatment of the subject.

The chapter dealing with the polymerization of vinyl chloride is very superficial in its approach. The description of the bulk process is sadly out of date and misleading with its suggestion that only 50% conversion can be achieved in practice. No serious attempt is made to discuss and assess modern theories of the kinetics and mechanism of either the suspension or emulsion processes.

The third chapter on the characterisation of poly(vinyl chloride) clearly shows where the authors' interests lie. This chapter is an excellent review of the literature up to 1967 on the molecular structure and particularly tacticity of the polymer. The two subsequent chapters attempt to correlate knowledge of structure with certain physical and chemical properties of poly(vinyl chloride).

Although the fourth chapter is entitled 'physical properties' much of the discussion is concerned with thermal and dynamic mechanical loss behaviour. One might have expected to have found some reference to the dielectric properties of the polymer either from the practical or theoretical point of view. The melt rheology of the unplasticized polymer is not discussed which is a pity since it would have been interesting to have read the authors' views on the effect of tacticity in the polymer chain on viscous behaviour under practical processing conditions.

The chapter on chemical properties mainly consists of a valiant attempt to make sense of the confused theories of the mechanism of thermal degradation of poly(vinyl chloride). Unfortunately the relationship between these theories and action of the various types of heat stabilizers is not discussed in detail. The authors wisely decided not to attempt any extensive description of the technology associated with the use of the polymer.

The American origin of the book becomes increasingly obvious as one reads it. Well over half the quoted references are to American work which is surprising in view of the very extensive European and Japanese literature on the subject. In discussing the physical properties and technology of the polymer the authors tend to confine their attentions almost wholly to plasticised compositions.

The book is well produced and contains few errors. Despite the price which seems a little excessive for such a slender volume it is well worth purchasing.

B. E. JENNINGS

Injection moulding of elastomers

Edited by W. S. PENN

Maclaren and Sons Ltd., London, 1969, pp. 201, £5 10s.

Activity in the injection moulding of rubber field has been higher during the last decade than at any other time in rubber industry history. This book describes the proceedings of a conference held in the Borough Polytechnic, London, 1968, on elastomer injection moulding

and consists of written papers contributed by a cross-section of authors, in the main rubber chemists, technologists and injection machine design engineers. Compounding studies covering the injection moulding characteristics possessed by a variety of elastomer classes are described by authors specialising in natural rubber, *cis*lpolyisoprene, *cis*-polybutadiene, styrene-butadiene, polychloroprene, nitrile, butyl, and silicones. Vulcanizing systems, factice, and carbon black are dealt with as separate topics. Injection machine controls, cycles, and layout are described for horizontal preplasticising screw machines and vertical transfer presses. Mould design requirements are discussed with detailed shapes and dimensions of typical runners, gates, cavity siting, and the like which should be most useful to people entering this field. A brief but very useful chapter with some fundamental aspects of elastomer injection moulding detailing the heat build-up phenomena and its mechanism which is one essential difference between thermoplastic and rubber injection moulding.

This book appears to be aimed at people active in rubber component manufacture and their raw material suppliers being written with simple descriptive terms in an easily read style. The editor's claim that it constitutes a textbook must be regarded as inaccurate since several major subject omissions are present, for example product design and manufacture, ram injection moulding and, process economics. Several chapters have no literature references qouted from which the serious reader could obtain further information. The text appears free from errors but the editing could be more precise in places. For example on page 199 the thermal conductivity of rubber is quoted without any units. The book is well produced with good quality paper and attractive binding having well presented, easily assimilated illustrations and a reasonable price.

<div style="text-align: right">CLAUDE HEPBURN</div>

An introduction to thermogravimetry

<div style="text-align: center">by C. J. KEATTCH
Heyden Sadtler (1969) 59, pp 38s</div>

This work is a short introductory text designed to present the important aspects of thermo-gravimetry, with particular emphasis on the basic principles, and the interpretation of TG curves, with illustrations from a wide range of applications.

For the potential thermogravimetry practitioner this short book serves as an extremely readable account of the thermobalance and its operation. Of particular value are the precautionary notes which draw attention to those design features and experimental parameters that are critical for the obtaining of a meaningful result. All the necessary requirements are listed but a few more positive details rather than generalisations would have been helpful. For example, the author states that the hot zone should be 'of reasonable length', granted that the necessary zone size will be governed by the actual balance used, but some specific value would have guided a worker constructing his own furnace. The precise positioning of the indicating thermocouple for the recording of a meaningful temperature (ideally the sample temperature) is not readily apparent in the experimental section of this book. The recommended use of an X_1X_2 recorder is a personal choice by the author, the X-Y recorder displaying weight as a function of sample temperature should have received equal prominence in the light of the ICTA recommendations on TG result presentation. The experimental chapters also make little reference to the use of thermogravimetric operations in the isothermal mode.

The information available from thermogravimetry and its interpretation are discussed in an easy to follow style, though in certain respects the presentation has perhaps been over simplified. Solid state reactions are discussed in relation to thermogravimetry with no comment about the possible lack of meaning to the order of reaction, particularly if concurrent reactions are involved. No emphasis is given to the possible control of the rate of decomposition by (i) the rate of progression of the reaction interface towards the centre of the sample or (ii) the rate of diffusion of volatile reaction products. In the general presentation of figures I would have liked to have seen a clearer marking of the temperature

Book Reviews

Poly(vinyl chloride)

by J. C. KOLESKE and L. H. WARTMAN

BPC Publishing Ltd., London, 1969, 50s.

This third volume of Macdonald's series of polymer monographs is particularly welcome since the number of books on poly(vinyl chloride) is surprisingly small when one considers the scientific and technological importance of the polymer. The problems posed by attempting to review the very extensive literature on poly(vinyl chloride) in such a small volume are enormous and the authors have chosen to solve them by concentrating their attention on the areas which are of interest to them. This has resulted in a rather unbalanced treatment of the subject.

The chapter dealing with the polymerization of vinyl chloride is very superficial in its approach. The description of the bulk process is sadly out of date and misleading with its suggestion that only 50% conversion can be achieved in practice. No serious attempt is made to discuss and assess modern theories of the kinetics and mechanism of either the suspension or emulsion processes.

The third chapter on the characterisation of poly(vinyl chloride) clearly shows where the authors' interests lie. This chapter is an excellent review of the literature up to 1967 on the molecular structure and particularly tacticity of the polymer. The two subsequent chapters attempt to correlate knowledge of structure with certain physical and chemical properties of poly(vinyl chloride).

Although the fourth chapter is entitled 'physical properties' much of the discussion is concerned with thermal and dynamic mechanical loss behaviour. One might have expected to have found some reference to the dielectric properties of the polymer either from the practical or theoretical point of view. The melt rheology of the unplasticized polymer is not discussed which is a pity since it would have been interesting to have read the authors' views on the effect of tacticity in the polymer chain on viscous behaviour under practical processing conditions.

The chapter on chemical properties mainly consists of a valiant attempt to make sense of the confused theories of the mechanism of thermal degradation of poly(vinyl chloride). Unfortunately the relationship between these theories and action of the various types of heat stabilizers is not discussed in detail. The authors wisely decided not to attempt any extensive description of the technology associated with the use of the polymer.

The American origin of the book becomes increasingly obvious as one reads it. Well over half the quoted references are to American work which is surprising in view of the very extensive European and Japanese literature on the subject. In discussing the physical properties and technology of the polymer the authors tend to confine their attentions almost wholly to plasticised compositions.

The book is well produced and contains few errors. Despite the price which seems a little excessive for such a slender volume it is well worth purchasing.

B. E. JENNINGS

Injection moulding of elastomers

Edited by W. S. PENN

Maclaren and Sons Ltd., London, 1969, pp. 201, £5 10s.

Activity in the injection moulding of rubber field has been higher during the last decade than at any other time in rubber industry history. This book describes the proceedings of a conference held in the Borough Polytechnic, London, 1968, on elastomer injection moulding

and consists of written papers contributed by a cross-section of authors, in the main rubber chemists, technologists and injection machine design engineers. Compounding studies covering the injection moulding characteristics possessed by a variety of elastomer classes are described by authors specialising in natural rubber, *cis*lpolyisoprene, *cis*-polybutadiene, styrene-butadiene, polychloroprene, nitrile, butyl, and silicones. Vulcanizing systems, factice, and carbon black are dealt with as separate topics. Injection machine controls, cycles, and layout are described for horizontal preplasticising screw machines and vertical transfer presses. Mould design requirements are discussed with detailed shapes and dimensions of typical runners, gates, cavity siting, and the like which should be most useful to people entering this field. A brief but very useful chapter with some fundamental aspects of elastomer injection moulding detailing the heat build-up phenomena and its mechanism which is one essential difference between thermoplastic and rubber injection moulding.

This book appears to be aimed at people active in rubber component manufacture and their raw material suppliers being written with simple descriptive terms in an easily read style. The editor's claim that it constitutes a textbook must be regarded as inaccurate since several major subject omissions are present, for example product design and manufacture, ram injection moulding and, process economics. Several chapters have no literature references qouted from which the serious reader could obtain further information. The text appears free from errors but the editing could be more precise in places. For example on page 199 the thermal conductivity of rubber is quoted without any units. The book is well produced with good quality paper and attractive binding having well presented, easily assimilated illustrations and a reasonable price.

CLAUDE HEPBURN

An introduction to thermogravimetry

by C. J. KEATTCH

Heyden Sadtler (1969) 59, pp 38s

This work is a short introductory text designed to present the important aspects of thermogravimetry, with particular emphasis on the basic principles, and the interpretation of TG curves, with illustrations from a wide range of applications.

For the potential thermogravimetry practitioner this short book serves as an extremely readable account of the thermobalance and its operation. Of particular value are the precautionary notes which draw attention to those design features and experimental parameters that are critical for the obtaining of a meaningful result. All the necessary requirements are listed but a few more positive details rather than generalisations would have been helpful. For example, the author states that the hot zone should be 'of reasonable length', granted that the necessary zone size will be governed by the actual balance used, but some specific value would have guided a worker constructing his own furnace. The precise positioning of the indicating thermocouple for the recording of a meaningful temperature (ideally the sample temperature) is not readily apparent in the experimental section of this book. The recommended use of an X_1X_2 recorder is a personal choice by the author, the X-Y recorder displaying weight as a function of sample temperature should have received equal prominence in the light of the ICTA recommendations on TG result presentation. The experimental chapters also make little reference to the use of thermogravimetric operations in the isothermal mode.

The information available from thermogravimetry and its interpretation are discussed in an easy to follow style, though in certain respects the presentation has perhaps been over simplified. Solid state reactions are discussed in relation to thermogravimetry with no comment about the possible lack of meaning to the order of reaction, particularly if concurrent reactions are involved. No emphasis is given to the possible control of the rate of decomposition by (i) the rate of progression of the reaction interface towards the centre of the sample or (ii) the rate of diffusion of volatile reaction products. In the general presentation of figures I would have liked to have seen a clearer marking of the temperature

axis, and note of the thermocouple location given. In general these sections can be read with value by even the experienced operator.

The applications are described as 'illustrative' rather than 'exhaustive'. This description is certainly correct. Greater emphasis has naturally been placed on those fields in which the author is an authority. Polymeric materials receive but scant attention being considered in one short paragraph. From the point of view of those readers interested in macromolecules the few review references quoted are all general articles. More up to date and specific reviews for polymer applications could have been afforded by reference to the excellent articles by L. Reich (Macromolecular Reviews, 1967, Vol. 1, 173; 1968, Vol.3, 49) or J. Chiu (Applied Polymer Symposia, 1966, No. 2, 25). Some of the references given to illustrate applications are far from readily accessible, being East European or Japanese in origin.

The appendix listing of the commercially available equipment may be of current value, but such a compilation must of necessity be very rapidly out of date and consequently of only limited use.

There are relatively few errors in the text; on p21, (ii) should read 'rate of weight loss upward' and not 'weight losses downward'. On p22 the point C (the inflection point of the TG curve) is incorrectly positioned on the DTG plot (Figure 4.2). The dw/dt of equation (2) (p18) should from the consistency point of view be—dW/dt or else redefined as 'rate of weight loss'.

The opening historical chapter serves little function in what is otherwise a short concise useful work which is not too expensive for individual purchase. It can be recommended to all persons considering the use of, or actively concerned with the practice of thermogravimetry.

J. S. CRIGHTON

Thermoplastics: Effect of Processing

Edited by R. M. OGORKIEWICZ

Iliffe Books Ltd, London (for the Plastics Institute), 1970, 252 pp., 80s.

This is a further addition to the Plastics Institute Monograph Series, which is designed for use by students of plastics technology and engineering. It maintains the very high standard set by the Institute.

During the past few years there has been a growing appreciation that single point data is insufficient to describe the long term properties of plastics mouldings. Coupled with this has been the recognition that commercial processing conditions may produce mouldings which deviate in properties from the ideal standards achieved in simple laboratory test specimens. This book presents a realistic picture of the factors which determine the mechanical and physical properties of plastics and the way in which they are influenced by processing parameters.

Seven leading authorities have contributed to chapters which reflect their wide knowledge of the literature available and, importantly, their first hand experience of the extrusion, calendering, injection moulding, blow moulding, rotational moulding and thermo-forming processes. The authors have kept strictly to their mandate to consider the effects of processing on the properties of thermo-plastics and have not merely outlined a process and its variables. The effects observed in the injection moulding process in particular are thoroughly discussed.

The introductory chapters discuss the basic mechanical and physical properties of plastics and the influence on these of orientation and crystallinity. The second chapter provides a succinct description of the methods used for assessing the long term performance of plastics.

The book is easy to read and is amply illustrated. It will make a useful source of information to students, technologists and engineers.

K. A. SCOTT

axis, and note of the thermocouple location given. In general these sections can be read with value by even the experienced operator.

The applications are described as 'illustrative' rather than 'exhaustive'. This description is certainly correct. Greater emphasis has naturally been placed on those fields in which the author is an authority. Polymeric materials receive but scant attention being considered in one short paragraph. From the point of view of those readers interested in macro-molecules the few review references quoted are all general articles. More up to date and specific reviews for polymer applications could have been afforded by reference to the excellent articles by L. Reich (Macromolecular Reviews, 1967, Vol. 1, 173; 1968, Vol.3, 49) or J. Chiu (Applied Polymer Symposia, 1966, No. 2, 25). Some of the references given to illustrate applications are far from readily accessible, being East European or Japanese in origin.

The appendix listing of the commercially available equipment may be of current value, but such a compilation must of necessity be very rapidly out of date and consequently of only limited use.

There are relatively few errors in the text; on p21, (ii) should read 'rate of weight loss upward' and not 'weight losses downward'. On p22 the point C (the inflection point of the TG curve) is incorrectly positioned on the DTG plot (Figure 4.2). The dw/dt of equation (2) (p18) should from the consistency point of view be—dW/dt or else redefined as 'rate of weight loss'.

The opening historical chapter serves little function in what is otherwise a short concise useful work which is not too expensive for individual purchase. It can be recommended to all persons considering the use of, or actively concerned with the practice of thermo-gravimetry.

<div style="text-align: right">J. S. CRIGHTON</div>

Thermoplastics: Effect of Processing

<div style="text-align: center">Edited by R. M. OGORKIEWICZ</div>

<div style="text-align: center">Iliffe Books Ltd, London (for the Plastics Institute), 1970, 252 pp., 80s.</div>

This is a further addition to the Plastics Institute Monograph Series, which is designed for use by students of plastics technology and engineering. It maintains the very high standard set by the Institute.

During the past few years there has been a growing appreciation that single point data is insufficient to describe the long term properties of plastics mouldings. Coupled with this has been the recognition that commercial processing conditions may produce mouldings which deviate in properties from the ideal standards achieved in simple laboratory test specimens. This book presents a realistic picture of the factors which determine the mechanical and physical properties of plastics and the way in which they are influenced by processing parameters.

Seven leading authorities have contributed to chapters which reflect their wide knowledge of the literature available and, importantly, their first hand experience of the extrusion, calendering, injection moulding, blow moulding, rotational moulding and thermo-forming processes. The authors have kept strictly to their mandate to consider the effects of pro-cessing on the properties of thermo-plastics and have not merely outlined a process and its variables. The effects observed in the injection moulding process in particular are thoroughly discussed.

The introductory chapters discuss the basic mechanical and physical properties of plastics and the influence on these of orientation and crystallinity. The second chapter provides a succinct description of the methods used for assessing the long term performance of plastics.

The book is easy to read and is amply illustrated. It will make a useful source of in-formation to students, technologists and engineers.

<div style="text-align: right">K. A. SCOTT</div>

Kinetics and mechanisms of polymerization series: Volume 2. Ring-opening polymerization

Edited by KURT C. FRISCH and SIDNEY L. REEGAN

Marcel Dekker, New York, 1969, 544 pp., £12 13s

This volume is the second of a three volume addition on kinetic and mechanistic aspects of polymerization. Its theme throughout deals with cyclic monomers. After an introductory chapter there are sections dealing with 1,2-epoxides, 1,3- and higher epoxides, cyclic formals, sulphides, amines, lactones, lactams including a chapter on N-carboxy-α-amino acid anhydrides, siloxanes and silazanes. There is also a chapter devoted to the polymerization of nitrogen-containing heterocyclics–mainly pyridine and quinoline. This variety of material has been dealt with very adequately by individual authors expert in the field. There is some variation in clarity between chapters; nevertheless, in contents the volume is a useful and up-to-date compilation of facts, theories and sources in the field of ring-opening polymerization. As such it will be of interest to practitioners rather than students in polymer science and technology, both as a source book and because of the many common mechanistic themes which emerge. Unfortunately, the price of £12 13s for the volume is so high as to detract from its general potential.

H. BLOCK

ERRATUM

We apologise for an error made in the paper 'Synthesis of branched polystyrene' by W. A. J. Bryce, G. McGibbon and I.G. Meldrum which appeared in the August, 1970 issue.

The first sentence of the last paragraph on page 402 should read as follows:
'In the reaction between living polystyrene and 1, 3, 5, trichloromethyl benzene is the coupling agent'.

GORDON RESEARCH CONFERENCES

In 1971 the Gordon Research Conferences will be held at the Miramar Hotel, Santa Barbara, California. The conference on polymers is January 25-29.

Further details can be obtained from the director, Alexander M. Cruickshank, Pastore Chemical Laboratory, University of Rhode Island, Kingston, Rhode Island 02881, USA.

Classified Contents

Author Index